SPIE

# 2012 BiOS

SPIE Photonics West

## Technical Summaries

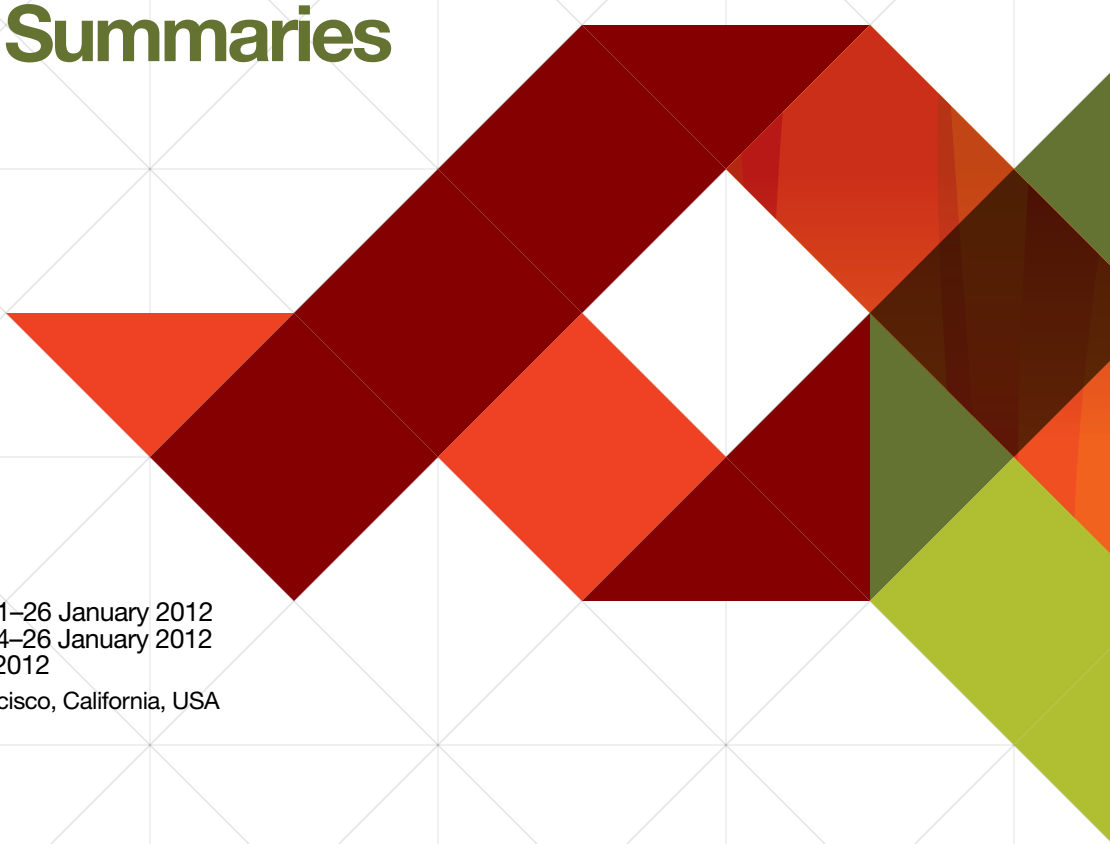

Conferences and Courses: 21–26 January 2012
Photonics West Exhibition: 24–26 January 2012
BiOS EXPO: 21–22 January 2012
The Moscone Center | San Francisco, California, USA

spie.org/pw

# SPIE thanks our technical conference sponsors

# 2012 BiOS

SPIE Photonics West

# Conference 8207A: Photonics in Dermatology and Plastic Surgery

Saturday-Sunday 21-22 January 2012

Part of Proceedings of SPIE Vol. 8207A Photonics in Dermatology and Plastic Surgery

8207A-01, Session 1

## Validation study of automated dermal/epidermal junction localization algorithm in reflectance confocal microscopy images of skin

S. Kurugol, J. Dy, Northeastern Univ. (United States); M. Rajadhyaksha, Memorial Sloan-Kettering Cancer Ctr. (United States); D. H. Brooks, Northeastern Univ. (United States)

Reflectance confocal microscopy (RCM) has seen increasing clinical application for noninvasive diagnosis of skin cancer. Identifying the location of the dermal-epidermal junction (DEJ) in the image stacks is key for effective clinical imaging. For example, one clinical imaging procedure acquires a dense stack of 0.5x0.5mm FOV images and then, after manual determination of DEJ depth, collects a 5x5mm mosaic at that depth for diagnosis. However, especially in lightly pigmented skin, RCM images have low contrast at the DEJ which makes repeatable, objective visual identification challenging. We have previously published proof of concept for an automated algorithm for DEJ detection in both highly- and lightly-pigmented skin types based on sequential feature segmentation and classification. In lightly-pigmented skin the change of skin texture with depth was detected by the algorithm and used to locate the DEJ. Here we report on further validation of our algorithm on a more extensive collection of 24 image stacks (15 fair skin, 9 dark skin). We compare algorithm performance against classification by three clinical experts. We also evaluate inter-expert consistency among the experts. The average correlation across experts was 0.81 for lightly pigmented skin, indicating the difficulty of the problem. The algorithm achieved epidermis/dermis misclassification rates smaller than 10% (based on 25x25 μm tiles) and average distance from the expert labeled boundaries of ~6.2 μm for fair skin and ~4.1 μm for dark skin, well within average cell size and less than 2x the instrument resolution in the optical axis.

8207A-02, Session 1

## Collagen crosslink status analysed in vitro using second-harmonic generation (SHG) and fluorescence lifetime imaging (FLIM)

V. Lutz, S. Puschmann, S. Gallinat, H. Wenck, K. Wittern, F. F. Fischer, Beiersdorf AG (Germany)

One of the major structural proteins in human skin is collagen. Collagen and its crosslinks are essential for the mechanical stability of the skin. Looking at extrinsically aged human skin (photo damaged skin) we find a decrease of mature collagen crosslinks. Immature crosslinks an indicator of the collagen turnover are decreasing as well in extrinsically aged skin. Hence, we assume that a certain range of mature and immature crosslinks reflect a 'good quality' of collagen in terms of photoaging.

In this study we established in vitro models of reduced crosslinking. We found that reduced collagen crosslinking resulted in a higher Second Harmonic Generation (SHG) intensity. Furthermore, we found a higher fibril diameter after crosslink reduction without an increase in collagen concentration. SHG is generated by a non-linear effect of femtosecond laser irradiation on collagen molecules. This effect might be influenced by the interspaces of the collagen molecules within the collagen fibril. From these findings the following hypothesis was introduced: reduced collagen crosslinking changes the interspace of single collagen molecules within the collagen fibril resulting in an enhanced SHG signal.

Furthermore, in this study the fluorescence lifetime (FLIM) of collagen fluorescence was found to decrease in the in vitro models of reduced crosslinking. We speculate on possible mechanisms being responsible for the decrease in lifetime.

Future in vivo measurements of the two parameters (SHG and FLIM) could lead to information about the collagen crosslink status, and therefore the status of photoaging of the skin.

8207A-03, Session 1

## The characterisation of skin lesions using two-photon excited multispectral fluorescence lifetime imaging

C. B. Talbot, Imperial College London (United Kingdom); R. Patalay, Imperial College London (United Kingdom) and Imperial College Healthcare NHS Trust (United Kingdom); Y. Alexandrov, S. Warren, I. Munro, Imperial College London (United Kingdom); H. G. Breunig, K. König, JenLab GmbH (Germany); M. A. A. Neil, P. M. W. French, Imperial College London (United Kingdom); G. W. Stamp, Imperial College Healthcare NHS Trust (United Kingdom) and The Royal Marsden Hospital NHS Trust (United Kingdom); A. Chu, Imperial College Healthcare NHS Trust (United Kingdom); C. W. Dunsby, Imperial College London (United Kingdom)

The well known strengths of multiphoton fluorescence microscopy allow for the optically sectioned subcellular imaging into scattering media such as skin and offer penetration sufficient to probe at least to the stratum basale. Fluorescence lifetime measurements of autofluorescent compounds within tissue have been shown to be associated with disease state. Therefore, the combination of fluorescence lifetime imaging (FLIM) and multiphoton imaging is an attractive technique for the in vivo diagnosis of skin lesions and detection of tumour margins.

We have previously developed a multispectral FLIM detector and a hyperspectral imager that we have integrated into the commercially available two-photon DermaInspect® tomograph for in vivo skin imaging. We now present the characterisation of over 45 skin samples, including basal cell carcinomas, naevi, melanoma imaged ex vivo, as well as in vivo normal skin. Since changes in the signature of the endogenous cellular fluorophores NADH and melanin are associated with disease state, we have chosen to perform our data analysis on a cell-by-cell basis. Double exponential decays were fitted to each cell in each of the four spectral channels and the results can be visualised on various scatter plots. For a quantitative analysis, the Kruskal-Wallis test was performed and significant differences ($p < 0.01$) were found between most diagnostic categories, indicating the substantial potential of spectrally resolved FLIM as a realistic diagnostic aid in the Dermatology clinic.

8207A-04, Session 1

## Simultaneous dual-wavelength OCT for dermatological applications

A. Alex, J. Weingast, B. Považay, B. Hofer, M. Binder, H. Pehamberger, W. Drexler, Medizinische Univ. Wien (Austria)

Optical coherence tomography (OCT) is a non-invasive, real-time biomedical imaging modality capable of providing 3-D micro-structural information of biological tissues with micron-scale resolution. The penetration depth of 1-2 mm provided by OCT is comparable to depth at which tissue biopsies are usually performed. In biological tissues such as skin, the penetration depth of OCT is mainly limited by the scattering and absorption of light. Hence light sources operating in the near infrared region extending from 700 nm to 1300 nm are usually employed for OCT imaging applications. Longer wavelength regions provide deeper penetration into tissue due to lower scattering, at the expense of reduced resolution. A dual wavelength OCT system working at 800 nm and 1300 nm was developed to combine the advantages of both wavelength regions. This system comprised two spectrometer-based frequency domain OCT systems that were combined at the sample, enabling simultaneous acquisition of dermal images at 800 nm and 1300 nm. The system was capable of acquiring images at a speed of 47,000 A-lines/s (>70 frames/s). The axial resolutions of the constituent OCT systems were 3 µm and 7 µm at 800 nm and 1300 nm wavelength regions respectively. The transverse resolution of the system was ~ 15 µm. Thus, this dual wavelength OCT system enabled access to micromorphological information from deeper regions of skin at 1300 nm and provided ultrahigh resolution images at 800 nm from superficial regions. The advantages offered by this dual wavelength OCT system can be critical in diagnosing several dermatological conditions.

8207A-05, Session 1

## Modeling of skin cooling, blood flow, and optical properties in wounds created by electrical shock

T. A. Nguyen, The Catholic Univ. of America (United States); J. W. Shupp, L. T. Moffatt, J. C. Jeng, M. H. Jordan, The Burn Ctr. at Washington Hospital Ctr. (United States); J. C. Ramella-Roman, The Catholic Univ. of America (United States)

High voltage electrical injuries may lead to irreversible tissue damage or even death. Research on tissue injury following high voltage shock is needed and may yield stage-appropriate therapy to reduce amputation rate. One of the proposed mechanisms by which electricity damages tissue is through Joule heating, with subsequent protein denaturation. Previous studies have shown that the flow of blood had a significant effect on the cooling rate of heated subcutaneous tissue. In addition, it is believed that the protein denaturation from burn effects usually cause variations in the optical properties of tissue. To assess the thermal damage in tissue, this study focused on monitoring changes of temperature and optical properties of skin areas next to high voltage wounds. The burns were created between left fore limb and right hind limb extremities of adult male Sprague-Dawley rats by a reliable 1000VDC delivery shock system. Each of four groups of rats received shock duration for 2, 4, 8 or 20 seconds. A thermal camera was utilized to record temperature variation during the exposure. The experimental results were then validated by simulation using a thermal-electric finite element model (FEM). This model is based on conductive parameters of skin and bio-heat equation in presence of blood flow. Changes of tissue perfusion and optical properties were monitored by a Laser Doppler scanning system and a high-resolution Spatial Frequency Domain Imaging system, respectively. The results of tissue temperatures from the experiment and FEM simulation, tissue perfusion and optical properties are presented and discussed.

8207A-06, Session 2

## Intelligent image analysis for image-guided hair removal and skin therapy

T. T. Lu, T. Chao, Jet Propulsion Lab. (United States)

Laser has been widely used in skin therapy such as hair removal and skin rejuvenation. Current laser hair removal products apply high energy laser on an area of the skin indiscriminately. High energy laser may cause unintentional damage on the lesion, moles, or other part of the skin in the area if the intended purpose is only to remove the hair follicles. This paper applies advanced automatic target recognition (ATR) algorithms in the digital skin images to accurately locate the hair follicles. The ATR system first performs pre-processing to enhance the contrast of the image. The system then extracts the unique features of the targets in the area and sends the features to a neural network based classify for training and recognition operations. The ATR system automatically classifies the hair, moles, or other skin lesion and provides the accurate coordinates of the intended target locations. The information can be used to guide a scanning laser to focus energy only on the hair follicles. The intended benefit would be to protect the skin from unwanted laser exposure and to provide more effective skin therapy.

8207A-07, Session 2

## Dermal reflectivity determined by optical coherence tomography is an indicator of epidermal hyperplasia and dermal edema within inflamed skin

K. G. Phillips, Y. Wang, Oregon Health & Science Univ. (United States); D. Levitz, Tel Aviv Univ. (Israel); N. Choudhury, Michigan Technological Univ. (United States); E. Swanzey, J. Lagowski, M. Kulesz-Martin, S. L. Jacques, Oregon Health & Science Univ. (United States)

Psoriasis is a common inflammatory skin disease resulting from genetic and environmental alterations of cutaneous immune responses. While numerous therapeutic targets involved in the immunopathogenesis of psoriasis have been identified, the in vivo dynamics of inflammation in psoriasis remain unclear. We undertook in vivo time course focus-tracked optical coherence tomography (OCT) imaging to noninvasively document cutaneous alterations in mouse skin treated topically with Imiquimod (IMQ), an established model of a psoriasis-like disease. Quantitative appraisal of dermal architectural changes was achieved through a two parameter fit of OCT axial scans in the dermis of the form $A(x, y, z) = \rho(x, y) \exp[-\mu(x, y)z]$. Ensemble averaging over 2000 axial scans per mouse in each treatment arm revealed no significant changes in the average dermal attenuation rate, µ, however the average local dermal reflectivity ρ, decreased significantly following 1,3, and 6 days of IMQ treatment ($p < 0.001$) in comparison to vehicle-treated control mice. In contrast, epidermal and dermal thickness changes were only significant when comparing controls and 6-day IMQ treated mice. This suggests that dermal alterations, attributed to collagen fiber bundle

enlargement, occur prior to epidermal thickness changes due to hyperplasia and dermal thickness changes due to edema. Dermal reflectivity positively correlated with epidermal hyperplasia and dermal edema. Our results suggest that dermal reflectivity as measured by OCT can be utilized to quantify a psoriasis-like disease in mice, and thus has the potential to aid in the quantitative assessment of psoriasis in humans.

8207A-08, Session 2

## Reduction of OCT image artifacts for improved imaging of skin

Y. M. Liew, R. A. McLaughlin, F. Wood, D. D. Sampson, The Univ. of Western Australia (Australia)

Optical coherence tomography (OCT) is a high resolution optical imaging modality that has been increasingly used in clinical diagnostic and research imaging of skin in vivo. It has been shown useful for the assessment of skin diseases, tumours, skin aging and treatment efficacy of laser procedures and topical agents. However, OCT suffers from significant image artifacts which can produce inaccurate and misleading scans. We have explored techniques to reduce three major types of artifact: intensity, morphological and motion artifacts. Intensity artifacts refer to A-scans with artificially reduced intensity, appearing visually as dark streaks within a B-scan. They are caused by divergence of the light beam under furrows in the skin surface, accentuated by the sudden change in refractive index between skin and the surrounding air. Morphological artifacts cause structures, such as blood vessels, to be displaced and deformed due to redirection of the OCT light beam. We demonstrate that applying either glycerol or ultrasound gel to the skin prior to imaging will reduce both intensity and morphological artifacts, and we quantify the effects of each. Both substances act by reducing the refractive index mismatch when the light beam penetrates the surface of the skin. We also demonstrate the use of image registration techniques to correct motion artifact, and propose restrictions which must be applied to the geometrical transformation used for the specific application of skin scanning.

8207A-09, Session 2

## Preclinical in-vivo evaluation of NPe6-mediated photodynamic therapy on normal vasculature

W. Moy, S. Patel, B. Lertsakdadet, R. Arora, K. Nielsen, Beckman Laser Institute and Medical Clinic (United States); K. M. Kelly, Univ. of California, Irvine School of Medicine (United States); B. Choi, Beckman Laser Institute and Medical Clinic (United States)

Port wine stain is a congenital birth-mark commonly found on the face and neck regions. It consists of abnormally-enlarged vasculature in the dermis. Current treatments typically involve use of a pulsed dye laser combined with cryogenic cooling of the skin. Yellow light, in the 585-595 nm wavelength range, is strongly absorbed by hemoglobin and can photocoagulate the targeted vasculature in a selective manner.

Currently, PDL treatment session result in varied success. Based on data from our lab and other labs worldwide, we postulate that one problem with PDL therapy is its limited efficacy in inducing acute photocoagulation of smaller vasculature. Over the past decade, we have studied the use of photodynamic therapy (PDT) as either a replacement or adjuvant treatment option to photocoagulate both small and large vasculature.

We devised a protocol that involves use of an intravascular photosensitizer (NPe6) activated by an array of light emitting diodes (wavelength = 664 ± 20 nm). To assess therapeutic efficacy, we used the mouse dorsal window chamber model and laser speckle imaging to monitor blood-flow dynamics. In this study, we defined a successful treatment outcome as achieving persistent vascular shutdown within the window, seven days following PDT treatment.

Based on our data from 20 experiments, we used dose-response analysis to identify a threshold radiant exposure to achieve a successful treatment. Our preliminary data suggest that NPe6-mediated PDT is a potential treatment option for port wine stain vasculature.

8207A-10, Session 3

## Deep skin structural and microcirculation imaging with extended-focus OCT

C. Blatter, B. Grajciar, Medizinische Univ. Wien (Austria); R. Huber, Ludwig-Maximilians-Univ. München (Germany); R. Leitgeb, Medizinische Univ. Wien (Austria)

Optical Coherence Tomography (OCT) has already become a mature biomedical imaging tool revealing high resolution subsurface structure down to a few millimeters. As such it bridges the gap between superficial microscopic imaging on subcellular level and large penetration ultrasound imaging. However there is a tradeoff in OCT between lateral resolution and depth of focus given by Gaussian optics. A way around this limitation is the use of Bessel beams: conical beams that exhibit a constant lateral extend over large depths. High sensitivity can be preserved by decoupling Bessel beam illumination from Gaussian detection with lower NA, called extended focus OCT (xf-OCT). Such scheme shares advantages with dark field microscopy, and exhibits a self-reconstruction property characteristic for Bessel beams. This is particularly useful as it avoids shadowing from surface structures such as hairs that in classical OCT obscure the structures beneath. Also, the dark field effect is beneficial since strong surface reflexes are suppressed, helping to use glass windows for fixation or as part of the applicator housing. Our OCT system is driven by a rapidly tuning swept source with 440kHz A-scan rate, and an axial resolution of 12µm. The lateral resolution is 6µm over an extended focal range of 500µm. We demonstrate in addition to standard structural imaging the capability of xf-OCT to contrast the small capillary network within the human skin in-vivo. We use this information for studying vaso-responses to hypothermia. Altered responses are an early indicator of primary or secondary vascular diseases, e.g. diabetes, or Reynauds syndrome.

8207A-11, Session 3

## Evaluation of port-wine stain treatment outcomes using multispectral imaging

R. Samatham, S. Jacques, A. L. Krol, Oregon Health & Science Univ. (United States)

Port-wine Stain (PWS) is a vascular malformation of developmental origin characterized by ectasia of superficial dermal capillaries. The flash-lamp pumped pulsed dye laser (PDL) treatment has been mainstay of PWS for the last decade. Despite the success of the PDL in significantly fading the PWS, the overall cure rate is less than 10%. The precise efficacy of an individual PDL treatment is hard to evaluate and the treatment outcome is measured by visual inspection of clinical fading. A hand-held multi-spectral imaging system was developed to image PWS before and after PDL treatment. In an NIH-funded pilot study multi-spectral camera was used to image PWS in children (2 - 17 years). Oxygen saturation (S) and blood content (B) of PWS before and after the treatment was determined by analysis of the reflectance spectra. The outcome of the treatment is evaluated during follow up visits of the patients. One of the major causes of failure of laser therapy of port-wine stains (PWS) is reperfusion of the lesion after laser treatment. Oxygen saturation and blood content maps of PWS before and after treatment can predict regions of reperfusion and subsequent failure of the treatment. The ability to measure reperfusion and to predict lesions or areas susceptible to reperfusion will help in selection of patients/lesions for laser treatment and help to optimize laser dosimetry for maximum effect. The current studies also should provide a basis for monitoring of future alternative therapies or enhancers of laser treatment in resistant cases.

8207A-12, Session 3

## In vivo multiphoton microscopy assessment of topical corticosteroid-induced skin modifications and depigmentation

E. Tancrède, H. Ait El Madani, L'Oréal Recherche & Innovation (France) and Hôpital Saint-Louis (France); A. Bensussan, Hôpital Saint-Louis (France); A. Colonna, L'Oréal Recherche & Innovation (France); A. Dupuy, l'Hôpital Pontchaillou (France); M. Bagot, Hôpital Saint-Louis (France); A. Pena, L'Oréal Recherche et Innovation (France)

The aim of this study was to assess whether multiphoton microscopy could provide new insights into the dynamics of topical corticosteroids side effects within the epidermis. For that purpose, healthy volunteers were topically treated with clobetasol propionate on a small region of the forearm under overnight occlusion for three weeks. The treated region was investigated at D0, D7, D15, D22 (end of the treatment) and D60 using the DermaInspect® medical imaging system. We visualized the skin by taking advantage of intrinsic multiphoton signals from collagen (second harmonic generation), cells and elastic fibers (two-photon excited fluorescence).

Our results show that multiphoton microscopy allows detection of corticosteroid-induced skin modifications: thinning of stratum corneum compactum and epidermis, decrease of keratinocytes size and changes in their morphology from D7 to D22. Multiphoton microscopy also enables in vivo quantitative assessment of melanin content. We observe that melanin density increasingly decreases during treatment and almost completely disappears at D22. Moreover, these alterations are reversible as they are no longer present at D60.

In conclusion, multiphoton microscopy is a convenient and powerful tool for non invasive 3D dynamical studies of skin integrity and pigmentation.

8207A-13, Session 3

## Combined fluorescence-Raman spectroscopy measurements with an optical fiber probe for the diagnosis of melanocytic lesions

A. Cosci, R. Cicchi, European Lab. for Non-linear Spectroscopy (LENS) (Italy); S. Rossari, V. De Giorgi, D. Massi, Univ. degli Studi di Firenze (Italy); F. S. Pavone, European Lab. for Non-linear Spectroscopy (LENS) (Italy)

We have designed and developed an optical fiber-probe for spectroscopic measurements on human tissues. The experimental setup combines fluorescence spectroscopy and Raman spectroscopy in a multidimensional approach. Concerning fluorescence spectroscopy, the excitation is provided by two laser diodes, one emitting in the UV (378 nm) and the other emitting in the visible (445 nm). These two lasers are used to selectively excite fluorescence from NADH and FAD, which are among the brightest endogenous fluorophores in human tissues. For Raman and NIR spectroscopy, the excitation is provided by a third laser diode with 785 nm excitation wavelength. Laser light is delivered to the tissue through the central optical fiber of a fiber bundle. The surrounding 48 fibers of the bundle are used for collecting fluorescence and Raman and for delivering light to the spectrograph. Fluorescence and Raman spectra are acquired on a cooled CCD camera. The instrument has been tested on fresh human skin biopsies clinically diagnosed as malignant melanoma, melanocytic nevus, or healthy skin, finding an optimal correlation with the subsequent histological exam. In some cases our examination was not in agreement with the clinical observation, but it was with the histological exam, demonstrating that the system can potentially contribute to improve clinical diagnostic capabilities and hence reduce the number of unnecessary biopsies.

8207A-14, Session 3

## Imaging immune response of skin mast cells in vivo with two-photon microscopy

C. Li, The Univ. of Texas at El Paso (United States); R. K. Pastila, Radiation and Nuclear Safety Authority (Finland); C. P. Lin, Wellman Ctr. for Photomedicine (United States)

Intravital multiphoton microscopy has provided insightful information of the dynamic process of immune cells in vivo. However the use of exogenous labeling agents limit its applications. There is no method to perform functional imaging of mast cells, a population of innate tissue-resident immune cells. Mast cells are widely recognized as the effector cells in allergy. Recently their roles as immunoregulatory cells in certain innate and adaptive immune responses are being actively investigated. Here we report in vivo mouse skin mast cells imaging with two-photon microscopy using endogenous tryptophan as the fluorophore. We studied the following processes. 1) Mast cells degranulation, the first step in the mast cell activation process in which the granules are released into peripheral tissue to trigger downstream reactions. 2) Mast cell reconstitution, a procedure commonly used to study mast cells functioning by comparing the data from wild type mice, mast cell-deficient mice, and mast-cell deficient mice reconstituted with bone marrow-derived mast cells (BMMCs). Imaging the BMMCs engraftment in tissue reveals the mast cells development and the efficiency of BMMCs reconstitution. We observed the reconstitution process for 6 weeks in the ear skin of mast cell-deficient Kit w-sh/w-sh mice by two-photon imaging. 3) Mast cells interactions with other immune cells in vivo. By illuminating mice ear skins with ultraviolet B with inflammatory dose, we observed skin mast cells forming cell-cell contact with migrated leukocytes following UVB induced inflammation. Our finding is the first instance of imaging mast cells in vivo with endogenous contrast.

8207A-15, Session 4

## Pulsed photothermal depth profiling of tattoos undergoing laser removal treatment

M. Milanic, B. Majaron, Jožef Stefan Institute (Slovenia)

Pulsed photothermal radiometry (PPTR) allows noninvasive determination of temperature depth profiles induced by pulsed laser irradiation of strongly scattering biological tissues and organs, including human skin. In present study, we evaluate the potential of this technique for investigational characterization and possibly quantitative evaluation of laser tattoo removal.

The study involved 5 healthy volunteers (3 males, 2 females), age 20-30 years, undergoing tattoo removal treatment using a Q-switched Nd:YAG laser. There were four measurement and treatment sessions in total, separated by 2-3 months. Prior to each treatment, PPTR measurements were performed on several tattoo sites and one nearby healthy site in each patient, using a 5 ms Nd:YAG laser at low rradiant exposure values and a dedicated radiometric setup. The laser-induced temperature profiles were then reconstructed by applying a custom numerical code. In addition, each tatoo site was documented with a digital camera and measured with a custom colorimetric system (in tristimulus color space), providing an objective evaluation of the therapeutic efficacy to be correlated with our PPTR results.

The results show that the laser-induced temperature profile in untreated tatoos is invariably located at a subsurface depth of 300 µm. In tatoo sites that responded well to laser therapy (as evidenced by colorimetric data), a significant drop of the temperature peak was observed in the profiles obtained from PPTR record. In several sites that appeared less responsive, in contrast, a progressive shift of the temperature profile deeper into the dermis was observed over the course of consecutive laser treatments.

8207A-16, Session 4

## Combination of Stokes polarized light imaging, roughness metrics, and morphological features for the detection of melanoma

P. Ghassemi, The Catholic Univ. of America (United States); T. A. Germer, National Institute of Standards and Technology (United States); J. W. Shupp, The Burn Center at Washington Hospital Ctr. (United States); S. S. Venna, M. E. Boisvert, Washington Hospital Ctr. (United States); K. Flanagan, The Burn Center at Washington Hospital Ctr. (United States); M. H. Jordan, The Burn Ctr. at Washington Hospital Ctr. (United States); J. C. Ramella-Roman, The Catholic Univ. of America (United States)

Skin cancer is the most common and most rapidly increasing form of cancer in the world specially united states. Optimal treatment of skin cancer before it reaches metastasis depends critically on early diagnosis. Usually physicians measure some outward features to diagnose malignancy of pigmented skin lesion. These are mostly morphological features like border irregularity, size, shape and also color. Also valuable information can be obtained from the analysis of skin roughness. Previously, we developed a hemispherical imaging Stokes polarimeter to monitor skin cancer based on a roughness assessment of the epidermis. In this study, Stokes images were analyzed to measure polarization properties of skin samples like principal angle of polarization ellipse and degree of polarization. A processing algorithm based on morphological operators was developed and applied on Stokes images to extract shape information. Finally, an appropriate classifier was designed to determine the type of lesion based on morphological features as well as the roughness information. Extensive calibration of the system was performed including studies on porcine skin samples. Clinical evaluation of the technique was performed on patients with benign nevi, melanocytic nevus, and normal skin.

8207A-17, Session 4

## Intense high-frequency pressure waves produced with low laser fluences

C. Serpa, G. F. F. Sá, L. G. Arnaut, Univ. de Coimbra (Portugal)

Pressure waves generated by laser pulses can permeabilize biological barriers, such as the skin or cellular membranes, with a reversibility that allows skin to recover its protective function and cells to remain viable. Doukas and co-workers [1] explored the principles of transdermal and intracellular drug delivery with pressure waves generated by laser pulses. They showed the critical relevance of generating a pressure transient with high peak pressure and high impulse. Their light-to-pressure transducers were typically 0.8 mm or 3 mm thick metal sheets or commercial plastics, respectively. However, their low energy-conversion efficiency required nanosecond laser pulses up to 10 J to affect biological barriers.

The development of materials capable of rapidly and efficiently converting the energy in a laser pulse into high-frequency broadband ultrasound, has been eluded by lack of fundamental understanding of the processes involved and by the inability to develop adequate chromophores and substrates for light-to-pressure transducers. The characteristics of the absorbing materials and their assemblage are decisive in determining the shape and amplitude of impulse transients. Based on the physics and photochemistry of light-to-pressure conversion, we disclose materials that activated by lasers with optical power densities below 10 MW/cm2 can generate broadband and high intensity ultrasound waves capable of transiently permeabilizing biological barriers.

Examples of transdermal protein delivery with our materials and portable lasers are presented. Implications for a new generation of medical devices for active skin permeation and also for diagnostics, therapeutics and imaging, are discussed.

[1] A. G. Doukas and N. Kollias, Advanced Drug Delivery Reviews 56 (2004) 559- 579.

8207A-18, Session 4

## Determination of optimal glycerol concentration for optical tissue clearing effects

E. Youn, T. Son, H. S. Kim, B. Jung, Yonsei Univ. (Korea, Republic of)

The laser scattering in tissue is significant in laser applications for diagnostic and therapeutic purposes. Many studies have been attempted to reduce light scattering effect and enhance the clinical efficacy of light-based medical devices. Optical clearing agents (OCAs) have been employed as a tool for the optical tissue clearing. The objective of this study is to investigate optimal concentration of an OCA, glycerol, so that it can be utilized for clinical diagnosis and therapeutics in dermatology. Glycerol was topically applied to avoid possible edema which has been reported to be caused by dermal injection. The effect of optical tissue clearing for different concentration of glycerol was quantitatively evaluated by using various methods. Not only optical devices including optical coherence tomography (OCT) and an integrating sphere were used to assess the enhancement of light penetration depth and refractive index matching, but also non-optical methods such as sample weight measurement and water content measurement were carried out to examine dehydration. In addition, an ultrasonic device, ultrasound biomicroscopy (UBM), was also applied to this experiment in order to investigate collagen dissociation. By determining the optimal concentration of glycerol, this study may offer a guideline regarding the use of glycerol that would result in assisting researchers and dermatologists in producing the desired diagnostic and therapeutic effects.

8207A-20, Session 5

## Evaluation of facial hyperpigmentation: comparison of fluorescence and polarization images

E. Kim, H. S. Kim, B. Jung, Yonsei Univ. (Korea, Republic of)

Various optical imaging modalities have been utilized as important tools to qualitatively and quantitatively evaluate the skin lesions due to the increment of esthetic concerns. Accurate evaluation of hyperpigmentation may be important because it is related to sun damage, inflammation, or other skin disorders. The polarization image provides surface and subsurface information of skin lesions. The fluorescent image provides various skin abnormalities such as sebum, acne and hyperpigmentation. In this study, identical facial skin region was obtained with both polarization and fluorescent images and the hyperpigmentation regions were analyzed. The results were evaluated and compared to investigate the best method for detecting hyperpigmentation regions.

8207A-21, Session 5

## Investigation of line scanning for confocal microscopy in tissue

B. A. Larson, S. Abeytunge, C. Glazowski, M. Rajadhyaksha, Memorial Sloan-Kettering Cancer Ctr. (United States)

Confocal point-scanning microscopy is being translated for clinical applications in skin cancer detection. Recent studies in generalized settings have reported that melanocytic and non-melanocytic lesion are detected with sensitivity of 92% and specificity of 69-84%, compared to specificity of 32-39% with dermoscopy. Pre-operative and intra-operative mapping of clinical margins allows precise excision of lentigo maligna- and amelanotic- melanomas and basal- and squamous-cell carcinomas. The imaging has also enabled more accurate “guided” biopsies while minimizing the otherwise large number of “blind” biopsies. Despite these advances, however, point-scanning technology remains relatively complex, expensive and confined to relatively few clinics. Line-scanning technology may offer an alternative approach to accelerate more widespread translation to the clinic.

Line-scanning, using fewer optical components, inexpensive linear-array detectors and custom electronics, may enable smaller, simpler and lower-cost confocal microscopes. A line is formed in using a cylindrical lens and scanned through the back focal plane of the objective with a galvanometric scanner. A linear CCD is used for detection. Two pupil configurations were compared for performance in imaging human tissue. In the full-pupil configuration, illumination and detection is made through the full objective pupil. In the divided pupil approach, half the pupil is illuminated and the other half is used for detection. The divided pupil configuration loses spatial and axial resolution due to a diminished numerical aperture, but the sectioning capability and rejection of background is improved. Axial response measurements and imaging in skin and oral mucosa illustrate the performance of the two configurations.

8207A-22, Session 5

## In vivo video rate multiphoton microscopy imaging of human skin

H. Wang, A. M. D. Lee, Z. Frehlick, Y. Yu, The BC Cancer Agency Research Ctr. (Canada); S. Tang, The Univ. of British Columbia (Canada); J. Zhao, The BC Cancer Agency Research Ctr. (Canada); H. Lui, D. I. McLean, The Univ. of British Columbia (Canada); H. Zeng, The BC Cancer Agency Research Ctr. (Canada)

A multi-photon microscopy system specially designed for imaging in vivo human skin at a frame rate of 27fps with a 256x256 pixel resolution was developed. In the excitation arm, the major components were a tunable (720-950nm) 80MHz femtosecond Ti:Sa laser, a scanning unit including a resonance scanner and a galvanometer scanner, a 60X (NA=1.0) long working distance water immersion objective, and a 665nm excitation long pass dichroic beamsplitter. In the detection arm, a 710nm short pass emission filter, dichroic mirrors, long pass filters, a pair of photomultiplier tubes, and a multichannel frame grabber were used. To reduce movement artifacts, a metal ring was fixed to the skin of volunteer subjects using double-sided adhesive film. The laser power incident on the skin at all wavelengths was adjusted to 40mW. The system has been tested by in vivo imaging of dorsal forearm skin of three volunteers. We could see nice cellular structures from the two-photon fluorescence (TPF) imaging channel. At 880nm excitation, elastin fibers in the TPF channel and collagen fiber bundles in the second-harmonic-generation (SHG) channel were found. In addition, integrated TPF/SHG images under 900nm excitation clearly showed papillary structure at the epidermal/dermal boundary. In summary, we believe that the high frame rate imaging capabilities provided by our optimized in vivo MPM instrument and the new integrated SHG/TPF imaging modality are unique amongst currently available systems and are necessary embodiments to the practical use of MPM in a clinical setting.

8207A-23, Session 5

## Hyperspectral imaging of bruises in the SWIR spectral region

L. L. Randeberg, Norwegian Univ. of Science and Technology (Norway); J. E. Hernandez-Palacios, Norsk Elektro Optikk AS (Norway)

Optical diagnostics of bruised skin might provide important information for characterization and age determination of such injuries. Hyperspectral imaging is one of the optical techniques that have been employed for bruise characterization. This technique combines high spatial and spectral resolution and makes it possible to study both chromophore signatures and -distributions in an injury. Imaging and spectroscopy in the visible spectral range have resulted in increased knowledge about skin bruises. So far the SWIR region have not been explored for this application. The main objective of the current study was to characterize bruises in the SWIR wavelength range, and to investigate if this technology might be feasible for age determination of bruises either as a standalone technique or in combination with visible spectroscopy or imaging. Hyperspectral images in the SWIR (900-2500nm ) and VIS (400-850nm) spectral range were collected from adult volunteers with accidental bruises of known age. The data were analyzed using spectroscopic techniques and statistical image analysis. Preliminary results from the pilot study indicate that SWIR hyperspectral imaging might be an important supplement to imaging in the visible part of the spectrum. The technique emphasizes local edema and gives a possibility to visualize bruises that cannot easily be seen in the visible part of the spectrum.

8207A-24, Session 5

## Polarization imaging for non-invasive detection of skin cancer margins

R. Samatham, S. L. Jacques, K. Lee, Oregon Health & Science Univ. (United States)

Skin cancer is most commons type of cancer in United States that occur on sun-exposed cosmetically sensitive areas like face, neck, and forearms. Surgical excision of skin cancer is challenging as more than one-third the actual margins extend beyond the clinically determined margins. Polarized light camera (polCAM) provides images of the superficial layers of the tissue with enhanced contrast which was used to image skin cancer margins. In a NIH-funded pilot study polCAM was used to image skin cancer in patients undergoing Mohs micrographic surgery for skin cancer. Polarized light imaging utilizes the polarization properties of light to create an image of a lesion comprised only of light scattering from the superficial layers of the skin which yields a characteristic “fabric pattern” of the putative lesion and the surrounding normal tissue. In several case studies conducted with a system developed for the clinic, we have found that skin cancer disrupts this fabric pattern, allowing the doctor a new means of identifying the margins of the lesion. Data is acquired before the patient underwent surgery. The clinically determined skin cancer margins were compared with margins determined by examination of the polCAM images. The true margins were provided by the dermatophathologist on examination of the frozen sections. Our initial data suggests that the contrast due to polarization changes associated with cancerous lesions can elucidate margins that were not recognized by the surgeon under normal conditions but were later confirmed by the pathologist.

8207A-25, Session 6

## Assessing human skin with diffuse reflectance spectroscopy and colorimetry

I. Seo, Y. Liu, P. R. Bargo, N. Kollias, Johnson & Johnson CPPW (United States)

Colorimetry has been used as an objective measure of perceived skin color by human eye to document and score physiological responses of the skin from external insults such as chemical irritants or UV radiation. CIE color space values (L*, a* and b*) are the most commonly used parameters to correlate visually perceived color attribute with L* for pigment, a* for erythema, and b* for sallowness of the skin. In this study, we investigated the relation of Lab color scale to the amount of major skin chromophores (oxy-, deoxyhemoglobin and melanin) calculated from diffuse reflectance spectroscopy (DRS). Thirty healthy human subjects with ages 20 years and above, skin types I-VI, were recruited for the study. DRS and colorimetry measurements were taken from the left and right cheeks, and on the right upper inner arm. The melanin content calculated from 630-700 nm range of DRS measurements was shown to correlate with the lightness of skin (L*) for most skin types.

For subjects with medium-to-light complexion, melanin measured at the blue spectrum and hemoglobin interfered on the relation of lightness of the skin color to the melanin content. The sallowness of the skin that is quantified by the melanin contribution at the blue spectrum of DRS was found to be weakly related to b* scale while strongly related to blue channel in the RGB space. This study demonstrates the importance of documenting skin color by assessing individual skin chromophores with diffuse reflectance spectroscopy, in comparison to colorimetry assessment.

8207A-26, Session 6

## Ex vivo and in vivo full-field optical coherence tomography on skin

F. Harms, E. Dalimier, B. de Poly, LLTECH SAS (France); A. Latrive, ESPCI - Institut Langevin (France); D. Salomon, Univ. Hospital of Geneva (Switzerland); A. C. Boccara, ESPCI - Institut Langevin (France) and LLTech SAS (France)

Optical Coherence Tomography (OCT) appears as an efficient technique for in-depth imaging of biological tissues, relying on interferometric selection of ballistic photons. In contrast with most of the available OCT approaches (e.g. time domain OCT or Fourier domain OCT), Full-Field OCT directly takes “en face” images using megapixels cameras and water immersion microscope objectives. En face capture gives access to high lateral and axial resolution (typically~1µm ×1µm×1µm) using medium numerical apertures.

Here we present a study evaluating Full-Field OCT as an efficient tool for high-resolution imaging and characterization of skin. Images were acquired both ex-vivo, based on a microscope configuration (Light-CT scanner - LLTech), and in-vivo, based on a needle probe arrangement.

We have imaged ex-vivo fresh specimens including healthy and pathological tissue in order to assess resolution, penetration depth, and clinical relevance of images. Pathologies such as Basal Cell Carcinoma (BCC), actinic keratosis, cheloid scars were characterized. For each specimen we have taken ~5x5mm images at different depths, a single 5x5mm image being obtained in 1 minute. Correspondence with histology allowed for the identification of microscopic features of the epidermis and dermis, on normal and pathological tissue. We have then performed in-vivo images of healthy skin using a 3µm transverse resolution FF-OCT needle probe. We show that most of the obtained images are comparable to ex-vivo ones.

The technique, due to its intrinsic high resolution en-face imaging capabilities similar to histology slides, shows eased adoptability for further development of new diagnostic devices in dermatology.

8207A-27, Session 6

## Real-time Raman spectroscopy for in vivo evaluation of skin cancers

J. Zhao, H. Zeng, The BC Cancer Agency Research Ctr. (Canada) and The Univ. of British Columbia (Canada); D. I. McLean, H. Lui, The Univ. of British Columbia (Canada) and The BC Cancer Agency Research Ctr. (Canada)

Background: Real-time Raman spectroscopy has been explored for in vivo skin cancer diagnosis in this study.

Methods: An integrated real-time Raman spectroscopic system was constructed, which is composed of a portable hand-probe and dedicated software for data processing. Both the lesional skin and its adjacent normal skin were measured. Multi-variant statistical data analysis including principal component analysis (PCA), general discriminant analysis (GDA), and partial least squares (PLS) were used for lesion classification.

Results: Over 1000 lesions have been acquired using the integrated real-time Raman spectrometer system. Five hundred and eighteen (518) cases encompassing a spectrum of skin cancers/pre cancers and benign pigmented lesions were analyzed in this study, including malignant melanoma (44), basal cell carcinoma (109), squamous cell carcinoma (47), atypical nevi (57), blue nevi (13), compound nevi (30), intradermal nevi (38), junctional nevi (34), seborrheic keratosis (114) and actinic keratosis (32). The analyses were divided into the following three classifications based on clinical interest: (1) to discriminate skin cancers and precancers from benign skin lesions; (2) to discriminate malignant melanoma from non-melanoma pigmented lesions; and (3) to discriminate malignant melanoma from seborrheic keratosis. The area under the receiver operating characteristic (ROC) curve, which is a measure of the accuracy of the diagnosis, and its 95% confidence interval (CI), was found to be 0.879 (CI: 0.829-0.929), 0.823 (CI: 0.731-0.915) and 0.898 (CI: 0.797-0.999) for the above three analyses, respectively.

Conclusion: Real-time Raman spectroscopy is a very promising technique for in vivo clinical skin cancer diagnosis.

8207A-28, Session 6

## Multiphoton tomography of tattoos

K. König, JenLab GmbH (Germany)

Multiphoton tomography of amateur and professional tattoos has been performed on volunteers. Intratissue fluorescence and SHG signals have been obtained with the femtosecond laser imaging systems DermaInspect and MPTflex providing 5D data sets. A submicron spatial resolution, a 200 picosecond temporal resolution, and 10 nm spectral resolution was achieved based on spectral fluorescence lifetime imaging. Data on the intratissue location, the size of these nano- and microparticles, and the fluorescence behaviour including fluorescence decay times will be provided.

8207A-29, Session 6

## In vivo Raman spectroscopy of the skin: advances and issues for clinical implementation

I. J. Pence, E. Vargis, Q. Nguyen, C. Patil, Vanderbilt Univ. (United States); D. Ellis, Vanderbilt Univ. Medical Ctr. (United States); A. Mahadevan-Jansen, Vanderbilt Univ. (United States)

Clinical diagnosis of malignant and benign skin lesions is often difficult because of the subjective nature of visual inspection and the potential for sampling error in biopsy. As the most common malignancy with incidence on the rise, skin cancer could be better managed with a real-time, non-destructive detection method for diagnosis and screening. Using Raman spectroscopy, we have demonstrated the potential to perform non-invasive classification of skin lesions; however, the high level of physiological and anatomical variability in benign skin can complicate optical diagnosis. A thorough understanding of benign lesion's variability both between patients and within a single patient may lead to improved diagnostic outcomes. Here, we present a fiber-optic probe-based 785nm Raman spectroscopy study of in vitro and in vivo measurements addressing practical and experimental issues associated with clinical implementation of Raman spectroscopy for real-time detection of cutaneous malignancies. In vivo measurements were made of both the lesions and adjacent or contralateral normal skin with diagnosis performed by dermatologists through visual inspection of patients prior to data collection. We report an analysis of the spectral variability of normal skin and common benign lesions made in a clinical setting along with an evaluation of system performance. System evaluation and characterization of normal and benign skin are critical first steps in the formation of a non-malignant spectral database and development of Raman spectroscopy as a reliable method for discrimination of cutaneous lesions.

8207A-30, Poster Session

## In vivo assessment of the structure of skin microcirculation by reflectance confocal-laser-scanning microscopy

K. Sugata, O. Osanai, H. Kawada, Kao Corp. (Japan)

One of the major roles of the skin microcirculation is to supply oxygen and nutrition to the surrounding tissue. Regardless of the close relationship between the micro-circulation and the surrounding tissue, there are few non-invasive methods that can evaluate both the microcirculation and its surrounding tissue at the same site. We visualized micro-capillary plexus structures in human skin using in vivo reflectance confocal-laser-scanning microscopy (CLSM), Vivascope 3000® (Lucid Inc., USA) and Image J software (National Institutes of Health, USA) for video image processing. CLSM has been introduced as a non-invasive technique to visualize the internal structure of skin at the cellular level. In addition to internal morphological information such as the extra-cellular matrix, our method reveals capillary structures up to the depth of the subpapillary plexus at the same site without any combination of different optical systems. Video images at a specific depths of the inner forearm skin were recorded. By creating frame-to-frame difference images from the video images using off-line video image processing, we obtained images that emphasize the brightness depending on changes of intensity coming from the movement of blood cells. Merging the images from different depths of the skin elucidates the 3-dimensional fine line-structure of the microcirculation. Overall our results show the feasibility of a non-invasive, high-resolution imaging technique to characterize the skin microcirculation and the surrounding tissue.

8207A-31, Poster Session

## Modeling and analytical treatment of FTIR spectra of nucleic acids and proteins in the patients with Bowen's disease

N. S. Eikje, MC Professional Ltd. (Estonia)

Qualitative and quantitative observation of the peaks for nucleic acids and proteins in FTIR spectra were performed in the patients with Bowen's disease. There were no prominent appearance of the multiplet at about 1055 cm-1 and some non-specific proteins through all pathology areas. Absence of the peaks at about 1071 and 1095 cm-1 in DNA/RNA triad was prominent in all measured patients. Based on designed modeling and analytical spectral treatment there was possible to approach common and specific features of this precancerous dermatosis.

8207A-32, Poster Session

## OCT monitoring of cosmetic creams in human skin in vivo

S. H. Han, Sogang Univ. (Korea, Republic of) and Univ. of Toronto (Canada) and Univ. Health Network (Canada); C. Yoon, Sogang Univ. (Canada); L. Conroy, A. I. Vitkin, Univ. of Toronto (Canada) and Univ. Health Network (Canada)

Optical coherence tomography (OCT) have been applied primarily for noninvasive diagnosis of human disease. Although many researches have shown that OCT can discriminate between normal and diseased tissue for diagnostics, there is another important role for OCT related to the monitoring of treatment during or after therapy. In this study, we used OCT to monitor the penetration and accumulation of cosmetic creams into human hand skin, including a cream formulation containing collagen as its primary active ingredient. Collagen is a connective tissue protein which makes up 80% of human skin. It is important for maintaining health vitality and strength of many organs. The penetration and localization / accumulation of collagen in cosmetic creams it thought to be the primary determinant of the efficacy of new collagen synthesis. Detection and quantification of collagen in cosmetic creams applied to skin may thus help predict the product's eventual efficacy in skin collagen regeneration. We hypothesize that the topically applied collagen ingredient may be detectable by OCT thru its modulation of skin scattering properties. To test this hypothesis, we used a FDML swept-source optical coherence tomography (SS-OCT) system with a sweeping range of 112 nm centered at 1310 nm, -6 dB ranging depth of 6 mm in air, axial resolution of ~8μm in tissue, and average output power of 48 mW. Two male adult volunteers participated in the study. We investigated 4 kinds of cosmetic creams, topically applied to volunteers hand's skin at same locations. One of the four cosmetic creams contained soluble collagen's as its active ingredient in cosmetic. The duration of OCT monitoring of cosmetic penetration into skin ranged from 5mins to 2hours after topical application. The results show that OCT can discriminate between a cosmetic with collagen and the other collagen-free formulations. It thus seems feasible that OCT intensity can monitor the in-vivo effects of collagen contained in a cosmetic formulation after topical skin application.

8207A-33, Poster Session

## Diagnosing basal-cell carcinoma in vivo by near-infrared Raman spectroscopy: a principal components analysis discrimination algorithm

L. Silveira, Jr., F. L. Silveira, Univ. Camilo Castelo Branco (Brazil); B. Bodanese, Univ. Comunitária da Região de Chapecó (Brazil); M. T. T. Pacheco, R. A. Zângaro, Univ. Camilo Castelo Branco (Brazil)

Raman Spectroscopy has been proposed as a tool to discriminate skin neoplastic lesions with molecular specificity. This work demonstrated the discrimination among basal cell carcinoma (BCC) and normal human skin by collecting near-infrared Raman spectra in vivo and modeling a diagnostic algorithm based on Principal Components Analysis and Mahalanobis distance (PCA/MD). A total of 15 subjects which had indication of surgery for skin cancer removal were enrolled in the study. Five spectra were obtained in the malignant lesion prior the surgery. Five spectra were also obtained in the adjacent, clinically normal skin. After tumor removal, spectra were obtained in the ex vivo fragments. The Raman spectra were measured using a compact Raman spectrometer (830 nm excitation) coupled to a fiber-optic based probe (Lambda Solutions, Inc.). Integration time was set to 20 s and laser power adjusted to 200 mW, without any burning effect in the tissue (pain). The background fluorescence was further removed by a 7th order polynomial fitting. The spectra of human skin were dominated by bands of proteins and lipids (collagen, elastin, actin, triolein, among others) in the spectral region of 400 to 1800 cm-1. By comparing the mean spectra of BCC with the normal skin, it has been found important differences in the 800-1000 cm-1 and 1250-1350 cm-1 (vibrations of C-C and amide III, respectively). PCA/MD could discriminate the spectra of both tissues with high sensitivity and specificity. Raman spectroscopy revealed differences in the biochemical constitution of BCC and normal skin in vivo, being suitable for a rapid and non-invasive skin cancer detection.

# Conference 8207B: Therapeutics and Diagnostics in Urology: Lasers, Robotics, Minimally Invasive, and Advanced Biomedical Devices

Saturday 21 January 2012

Part of Proceedings of SPIE Vol. 8207B Therapeutics and Diagnostics in Urology: Lasers, Robotics, Minimally Invasive, and Advanced Biomedical Devices

8207B-34, Session 1

## Subsurface optical stimulation of the rat prostate nerves using a continuous-wave, 1550-nm single-mode diode laser

S. Tozburun, The Univ. of North Carolina at Charlotte (United States); G. Lagoda, A. Burnett, The Johns Hopkins Univ. (United States); N. M. Fried, The Univ. of North Carolina at Charlotte (United States)

Introduction: Optical nerve stimulation (ONS) of the cavernous nerves (CN) has been previously reported in an idealized rat model in which the CN is directly visible on the prostate surface. However, successful identification and preservation of the CN's, responsible for sexual function, during prostate cancer surgery will require detecting the nerves when they are not visible, but rather covered by a thin layer of fascia. This study explores ONS in a rat CN model with a tissue layer placed over the nerve.

Methods: A 500-mW, single-mode, 1550-nm diode laser was used to stimulate the CN in continuous-wave (CW) mode in 8 rats, with a 1-mm-diameter spot from the fiber optic probe. The 1550-nm wavelength provides an optical penetration depth of ~900 microns, ~2.5 times deeper than the 1455-nm and 1870-nm lasers previously used, thus providing sufficient penetration through tissue for stimulation of the underlying CN. Fascia samples with variable thickness (~200-500 microns) were placed over the CN. ONS was measured by an intracavernous pressure response (ICP) in the rat penis. A thermal camera recorded tissue surface temperatures during stimulation.

Results: ONS was observed at threshold tissue surface temperatures of ~44 C and incident laser powers of ~53 mW. ICP signal-to-noise-ratios of 2:1 and ICP response times less than 10 s were recorded. Tissue thermal damage was not observed until temperatures above ~47 C were measured.

Conclusions: Subsurface ONS of the rat CN is feasible, as an intermediate step towards ONS of the human CN during prostate cancer surgery.

8207B-35, Session 1

## Interstitial laser coagulation of localized kidney tumor by Nd:YAG laser

O. Teodorovich, Central Clinical Hospital (Russian Federation); D. G. Kochiev, A. M. Prokhorov General Physics Institute (Russian Federation); A. V. Ivanov, N. N. Blokhin Russian Cancer Research Ctr. (Russian Federation); S. Naryshkin, Central Clinical Hospital (Russian Federation); A. Lukashev, Astelia Technologies (United States)

An Nd:YAG laser in a free running mode was used in the study of interstitial laser coagulation(ILC) on a localized kidney tumor through a puncture needle with stereotactic targeting with a help of ultrasound imaging or/and computer tomography. The laser radiation was delivered through a 600 micron bare fiber, instead of usual ITT catheter. A single time laser exposure was used to coagulate only a small fraction of tissue, while the required coagulation volume was achieved by multiple exposures.

Pre-clinical studies has been performed in vivo on a canine model. The laser operated at the output power 20W, exposure time 10s and repetition rate 100Hz. Tissue modification and healing were assessed immediately post exposure and on days 3, 7, 14 and 35. Post-exposure morphology analysis revealed that a total tissue necrosis is achieved by overlapping fractional volumes.

During 2007-2010 ILC of kidney tumors was performed on 6 patients. Tumor size varied from 5 to 20mm. One year post procedure in 2 patients tumor was fully replaced by scar tissue, in other 4 patient size and perfusion of tumor were substantially decreased but not fully disappeared, so later patients underwent recurring ILC. Then no tumor growth was found for 2 years (up to now).

ILC of localized kidney tumors is safe and efficient, it can be used as an independent method of treatment when radical treatment is not feasible; or in combination with targeted therapy.

8207B-36, Session 1

## Photoselective vaporization of prolene mesh used in female stress urinary incontinence procedures: preliminary studies using a compact, high-power red diode laser

S. B. Rosenbury, D. Burks, N. M. Fried, The Univ. of North Carolina at Charlotte (United States)

Introduction: Complications with prolene (polypropylene) mesh after surgery for female stress urinary incontinence (SUI) may require tedious surgical removal of the mesh with potential damage to healthy in-grown tissue. Lasers are currently used in other medical fields (e.g. ophthalmology) for precise, non-contact removal of non-absorbable nylon sutures, termed "laser suture lysis". This preliminary study explores selective laser vaporization and non-contact removal of prolene suture/mesh materials frequently used in SUI.

Methods: A compact, 7 W, 650-nm, continuous-wave, red diode laser was modulated to operate in long-pulse mode a pulse duration of 50-100 ms, and a 400-micrometer fiber delivered a 1.0-mm-diameter laser spot for ablation of prolene mesh samples. Red laser wavelengths have previously been shown to vaporize a variety of suture materials (e.g. polypropylene and nylon). The 650-nm wavelength was selected because absorption by water, hemoglobin, and other major chromophores in soft tissues is low, while prolene absorption is high at this wavelength. Studies were conducted on a variety of prolene suture diameters and woven prolene mesh samples with ~200-micrometer-diameter strands, embedded in tissue samples, ex vivo.

Results: Non-contact temperature mapping of the suture/mesh samples with a thermal camera was performed, demonstrating selective vaporization of the prolene material at temperatures up to ~200 C without significant thermal damage to adjacent embedded tissues which remained below ~50 C.

Conclusion: It is feasible to selectively vaporize prolene mesh materials without significant thermal damage to adjacent embedded tissue. With further development, this technique may be useful for SUI procedures requiring surgical revision.

8207B-37, Session 1

## In vitro testing of dual-mode thulium microsurgical laser

M. D. Keller, J. D. Wells, Lockheed Martin Aculight (United States)

Recently, thulium (Tm) fiber lasers have been investigated for use in place of the Ho:YAG for surgical procedures, especially in urology, because their 1.94um output is absorbed by tissue ~5 times stronger than the 2.1um of the Ho:YAG. Lockheed Martin Aculight has recently developed the first truly dual-mode Tm laser, which can be operated in either CW or in pulsed mode (rather than modulated) to produce high peak power. The goal of this study was to assess both the soft tissue ablation performance of this laser in vitro and the feasibility of using it for lithotripsy. Ablation tests were performed on liver tissue, chicken breast, and porcine skin, using a 100um or 200um delivery fiber, and operated in CW mode or pulsed (~200ns pulse widths) at 10kHz or 1kHz. Ablation efficiencies for long (3-5 minutes) exposures, and both crater size and collateral damage zones for short (3-5 seconds) exposures were determined for the different pulse modes and a range of pulse energies. In all tissues, the most energy-efficient ablation occurred for the 10kHz pulsed mode operating just above ablation threshold, while the highest mass removal rate occurred in 10kHz pulsed mode operating at max energy (2.2 mJ). In histological sections from short exposures, 10kHz pulsed exposures created slightly smaller thermal coagulation zones than energy-matched CW exposures, while 1kHz deliveries had substantially smaller thermal damage zones. In addition, using a 100um fiber, the 10kHz mode was able to fragment samples of uric acid and, to some extent, COM stones.

8207B-38, Session 2

## Prospective study on laser-assisted laparascopic partial nephrectomy

R. Sroka, G. Hennig, K. Zilinberg, W. Khoder, Ludwig-Maximilians-Univ. München (Germany)

Introduction: Developments in laparoscopic partial nephrectomy (LPN) opened a demand for surgical tools compatible with laparoscopic manipulations to make laser assisted technique safe, feasible and reproducible. Warm ischemia and bleeding during laparoscopic partial nephrectomy place technical constraints on surgeons. Therefore it was the aim to develop a safe and effective laser assisted partial nephrectomy technique without need for ischemia.

Patients and methods: A diode laser emitting light at 1318nm in cw mode was coupled into a bare fibre (core diameter 600 µm) thus able to transfer up to 100W to the tissue. After dry lab experience, a total of 10 patients suffering from kidney malformations underwent laparoscopic/ retroperitoneoscopic partial nephrectomy. Clinically, postoperative renal function and serum c-reactive protein (CRP) were monitored. Laser induced coagulation depth and effects on resection margins were evaluated. Demographic, clinical and follow-up data are presented. Using a commercial available fibre guidance instrument for lanringeal intervention, the demands on an innovative laser fibre guidance instrument for the laser assisted laparoscopic partial nephrectomy (LLPN) are summarized.

Results: Overall, all laparascopic intervention were succesfull and could be performed without conversion to open surgery. Mean operative time and mean blood loss were comparable to conventional open and laparascopic approaches. Laser assisted resection of the kidney tissue took max 15min. After extirpation of the tumours all patients showed clinical favourable outcome during follow up period. Tumour sizes were measured to be up 5cm in diameter. The depth of the coagulation on the removed tissue ranged between <1 to 2mm without effect on histopathological evaluation of tumours or resection margin. As the surface of the remaining kidney surface was laser assisted coagulated after removal. The sealing of the surface was induced by a slightly larger coagulation margin, but could not measured so far. Based on this experiences a simple and easy to use instrument described serving also for suction and rinsing.

Conclusion: This prospective in-vivo feasibility study shows that laser assisted partial nephrectomy seems to be a safe and promising medical technique which could be provided either during open surgery as well as laparascopically. This application showed good haemostasis and minimal parenchymal damage. Further investigations and development are needed for on-line detection of the remain coagulation margin. An optimised treatment equipment will support the applicability of laser assisted laparoscopic partial nephrectomy.

8207B-39, Session 2

## Tissue ablation after 120W greenlight laser vaporisation and bipolar plasma vaporisation of the prostate: a comparison using transrectal three-dimensional ultrasound volumetry

B. Kranzbühler, C. Fankhauser, O. Gross, L. J. Hefermehl, C. Poyet, R. Largo, D. Eberli, M. Müntener, H. Seifert, M. Zimmermann, T. Sulser, A. Müller, T. Hermanns, Univ. Hospital Zürich (Switzerland)

INTRODUCTION AND OBJECTIVES: Greenlight laser vaporisation (LV) of the prostate is characterised by simultaneous vaporisation and coagulation of prostatic tissue resulting in tissue ablation together with excellent hemostatis during the procedure. It has been reported that bipolar plasma vaporisation (PV) of the prostate might be an alternative for LV. So far, it has not been shown that PV is as effective as LV in terms of tissue ablation or hemostasis. We performed transrectal three-dimensional ultrasound investigations to compare the efficiency of tissue ablation between LV and PV.

Methods: Between 11.2009 and 5.2011, 48 patients underwent pure PV in our institution. These patients were matched with regard to the pre-operative prostate volume to 48 LV patients from our existing 3D-volumetry-database. Transrectal 3D ultrasound and planimetric volumetry of the prostate was performed preoperatively, after catheter removal, 6 weeks and 6 months.

RESULTS: Median prostate volume was not significantly different between the groups (45.3ml vs. 45.4ml; p=0.997). After catheter removal, median absolute volume reduction (PV 12.4ml, LV 6.55ml) as well as relative volume reduction (27.8% vs. 16.4%) were significantly higher in the PV group (p<0.001). After 6W (42.9% vs. 33.3%) and 6M (47.2% vs. 39.7%), relative volume reduction remained significantly higher in the PV group (p<0.001). Clinical outcome parameters improved significantly in both groups without relevant differences between the groups.

CONCLUSIONS: Both vaporisation techniques result in efficient tissue ablation with initial prostatic swelling. PV seems to be superior due to a higher relative volume reduction. The differences had no clinical impact after a follow-up of 6M.

8207B-40, Session 2

## Electrosurgical injuries during robot assisted surgery: insights from the FDA MAUDE database

A. Fuller, G. Vilos, S. E. Pautler, The Univ. of Western Ontario (Canada)

Introduction: The Da Vinci surgical system requires the use of electrosurgical instruments. The re-use of such instruments creates the potential for stray electrical currents from capacitive coupling and/or insulation failure with subsequent injury. The morbidity of such injuries may negate many of the benefits of minimally invasive surgery. We sought to evaluate the rate and nature of electrosurgical injury (ESI) associated with this device.

Methods: The Manufacturer and User Facility Device Experience (MAUDE) database is administered by the US Food and Drug Administration (FDA) and reports adverse events related to medical devices in the United States. We analyzed all incidents in the context of robotic surgery between January 2001 and June 2011 to identify those related to the use of electrosurgery.

Results: In the past decade, a total of 605 reports have been made to the FDA with regard to adverse events related to the Da Vinci robotic surgical platform. Of these, 24 (3.9%) were related to potential or actual ESI. Nine out of the 24 cases (37.5%) resulted in additional surgical intervention for repair. There were 4 bowel injuries of which one was recognized and managed intra-operatively. The remainder required laparotomy between 5 and 8 days after the initial robotic procedure. Additionally, there was 1 vascular injury and 4 skin burns. The remaining cases required conservative management or resulted in no harm.

Conclusion

ESI in the context of robotic surgery is uncommon but remains under-recognized and under-reported. Surgeons performing robot assisted surgery should be aware that ESI can occur with robotic instruments and vigilance for intra- and post-operative complications is paramount.

8207B-41, Session 3

## Imaging of the canine vas deferens for non-invasive laser vasectomy: comparison of optical coherence tomography and ultrasound

C. Cilip, The Univ. of North Carolina at Charlotte (United States); M. Allaf, The Johns Hopkins Univ. (United States); N. M. Fried, The Univ. of North Carolina at Charlotte (United States)

Introduction: Noninvasive laser coagulation of the canine vas deferens has recently been demonstrated, towards the development of a noninvasive vasectomy procedure. In this study, Optical Coherence Tomography (OCT) and High Frequency Ultrasound (HFUS) of the vas are compared as diagnostic tools to confirm successful laser thermal occlusion of the vas.

Methods: Bilateral noninvasive laser coagulation of the vas was performed in 10 dogs using a laser wavelength of 1075 nm, power of 9.0 W, 500-ms pulse duration, pulse rate of 0.5 Hz, and 3-mm-diameter spot. Cryogen was sprayed onto the scrotal skin to prevent burns during the procedure. An OCT system with 8-Fr probe imaged the vas with a resolution of ~20 micrometers and depth of ~2 mm. An HFUS system with 13.2-MHz transducer was also used with a resolution of ~200 micrometers and depth of ~20 mm, for comparison. Burst pressure measurements, x-ray vasography, and gross analysis of the vas were used as indicators to confirm successful closure.

Results: Both OCT and HFUS were capable of differentiating the vas from surrounding tissues. The compact OCT probe provided imaging when the vas was held close to the surface manually or with the vas ring clamp, while US provided imaging when the vas was not clamped. Doppler US helped to identify the vas and confirm normal blood flow through the testicular artery.

Conclusions: Both OCT and HFUS represent promising imaging modalities for noninvasive laser vasectomy, but with different advantages: OCT provides higher resolution but at a reduced imaging depth compared to HFUS.

8207B-42, Session 3

## Next generation of optical diagnostics for bladder cancer using probe-based confocal laser endomicroscopy

J. Liu, Y. Pan, Stanford Univ. School of Medicine (United States); S. T. Hsiao, Veterans Affairs Palo Alto Health Care System (United States); T. Chang, K. E. Mach, Stanford Univ. School of Medicine (United States); K. C. Jensen, Veterans Affairs Palo Alto Health Care System (United States); J. C. Liao, Stanford Univ. School of Medicine (United States)

Real-time imaging with confocal laser endomicroscopy (CLE) probes that fit in endoscopes has emerged as a clinically feasible technology for optical biopsy of bladder cancer. Confocal images of normal, inflammatory, and neoplastic urothelium obtained with intravesical fluorescein can be differentiated by morphologic characteristics. We compiled a confocal atlas of the urinary tract with these diagnostic criteria for use in a prospective diagnostic accuracy study. Patients scheduled for transurethral resection of bladder tumor underwent white light cystoscopy (WLC), followed by CLE, and histologic confirmation of resected tissue. Normal-appearing areas by WLC were imaged and biopsied as controls. Thus far we have imaged 165 areas in 55 patients. Initial analysis suggests CLE improves diagnostic accuracy of WLC for both cancer diagnosis and grade. Despite morphologic differences between inflammation and cancer, real-time differentiation can still be challenging. Identification of bladder cancer-specific contrast agents could provide molecular specificity to CLE. By using fluorescently-labeled antibodies or peptides that bind to proteins expressed in bladder cancer, we have identified putative molecular contrast agents for targeted imaging with CLE. We instilled these agents into bladder specimens and imaged tumor and normal urothelium. Using both an epidermal growth factor receptor (EGFR)-binding peptide and a tumor-specific antibody, we demonstrated increased fluorescent signal with CLE over areas of tumor, compared to normal areas. Thus, cancer-specificity can be achieved using molecular contrast agents ex vivo in conjunction with CLE. Future work is aimed at determining inter-observer reliability of CLE interpretation and testing of molecular contrast agents in animal models in vivo.

8207B-43, Session 3

## Monitoring of lower urinary tract function in patients with spinal cord injury using near-infrared spectroscopy (NIRS)

B. Shadgan, The Univ. of British Columbia (Canada); L. Stothers, UBC Hospital Bladder Care Ctr. (Canada); A. J. Macnab, M. Nigro, The Univ. of British Columbia (Canada)

Near infrared spectroscopy (NIRS) is a non-invasive optical method to study tissue oxygenation, hemodynamics and function by monitoring changes in the chromophore concentrations of oxygenated (O2Hb), deoxygenated (HHb) and total hemoglobin (tHb). Although feasibility of NIRS for monitoring bladder dysfunction is reported by different investigators, there is no data available in patients with neurogenic bladder dysfunction.

The purpose of this study was to assess the feasibility of NIRS in patients with spinal cord injury (SCI) during filling and emptying and to investigate the correlations of NIRS measures with simultaneous urodynamics parameters.

Methods: 10 adult paraplegic patients with neurogenic bladder dysfunction who were referred for regular urodynamics evaluation were recruited. Changes in O2Hb, HHb and tHb along with tissue saturation index (TSI%) of detrusor were monitored and recorded by a wireless NIRS system during the urodynamics evaluation. Time points of urgency and urinary leakage were marked and pattern of changes in NIRS measures were compared to standard urodynamic pressure tracings.

Results: Strong consistency between changes in NIRS-derived tHb and changes in intravesical pressure were observed during filling across the subjects. During bladder filling a gradual increase in tHb and O2Hb with minimal changes in HHb was observed. Interestingly, a drop in TSI% was detected seconds before strong urgency and urinary leakage.

Conclusions: Our preliminary data are suggesting a relationship between noninvasive NIRS measures and urodynamics parameters during bladder filling in SCI patients. Further studies are required to confirm these qualitative findings and measure them quantitatively.

8207B-44, Session 3

## Real-time bladder navigation using an advanced stereotactic system

M. Agenant, Univ. Medical Ctr. Utrecht (Netherlands); A. van Rhijn, W. Koomen, Personal Space Technologies, Inc. (Netherlands); F. Euwe, H. J. Noordmans, S. Been, R. Bosch, Univ. Medical Ctr. Utrecht (Netherlands)

During transurethral resection of bladder tumors (TURBT) a scope is placed through the urethra, inside the bladder to biopsy or resect a lesion. During this procedure the sight of the bladder wall can be impeded by bleeding from that lesion, cloudy urine caused by an infection or blue light during photodynamic diagnosis (PDD). To overcome this problem the feasibility of real-time bladder mapping using stereotactic navigational system was presented last year.

This year we present our updated device and software for real-time navigation, which are better compatible to the surgical procedure of a TURBT than neuro-navigation. It claims to overcome the problem of a rotating scope connected to a static camera and an improved calibration procedure. Pre-clinical tests in a box lined with mm paper on each wall, have shown a better accuracy and no need of interfering adjustments during the surgical procedure. With a 30º cystoscope, lesions marked at the back and base were re-located with an accuracy of about 3 mm and lesions marked at the left en right lateral wall were re-located with an accuracy of about 10 mm. About 85% of all lesions were re-located in the field of view of the camera.

The next step is evaluation in a bladder model which has been started and clinical evaluation of this newly developed system. In future, this concept of bladder navigation will lead to better (re)-recognition of suspected lesions. The result would be less recurrence and residual tumors after TURBT which leads to fewer re-surgeries. Bladder navigation will therefore be time efficient, cost effective and patient friendly.

8207B-45, Session 3

## Functional optical coherence tomography of renal cancer

D. J. Faber, Univ. van Amsterdam (Netherlands); D. M. de Bruin, Academisch Medisch Ctr. (Netherlands); K. Barwari, J. J. de la Rosette, M. Laguna, Univ. van Amsterdam (Netherlands); T. G. van Leeuwen, Academisch Medisch Ctr. (Netherlands)

The estimated overtreatment percentage of suspect renal masses (by partial nephrectomy) is 30%, due to difficult radiological differentiation between benign and malignant small renal masses and a high number of inconclusive laparoscopic biopsies. Consequently, there is a need for a fast, minimally invasive technique for in situ diagnosis of small renal masses. We hypothesize that differences in cellular organization between healthy and cancerous tissue lead to differences in optical properties that are measureable using functional optical coherence tomography. In this pilot study we quantitatively determined the attenuation coefficient of healthy and malignant renal tissue, similar to our earlier work on cardiovascular tissue and bladder cancer biopsies. Using a commercially available Santec InnerVision OCT system, in combination with a custom built imaging probe, we took in vivo images of suspect and normal just before (partial) removal of the kidney of 16 patients. Five biopsies of suspect lesions were classified benign/non-diagnostic on histopathology. Of the remaining 11 lesions that were classified as malignant, the median attenuation coefficient was 8.5 /mm (IQR 5.1-11.7). The median attenuation coefficient of normal tissue was 4.9 /mm (IQR 4.1-5.7). The present sample size is too small to justify further statistical analysis of the difference. Moreover, at present no difference between malignant and benign tissue has been found (yet) due to the small sample size.

8207B-46, Session 3

## Multimodal flexible cystoscopy for creating co-registered panoramas of the bladder urothelium

T. D. Soper, M. R. Burkhardt, M. P. Porter, E. J. Seibel, Univ. of Washington (United States)

Bladder cancer is the most expensive cancer to treat due to the high rate of recurrence. Regular cystoscopy is the gold standard for bladder cancer surveillance. The advent of fluorescence biomarkers provides an opportunity to improve sensitivity for early detection. Ideally, this fluorescence information could be combined with standard reflectance images to provide multimodal views of the bladder wall. The scanning fiber endoscope (SFE) of 1.2-mm in diameter is able to acquire wide-field multimodal video from a bladder phantom with fluorescence cancer "hot-spots". The SFE generates images by scanning red, green, and blue (RGB) laser light and detects the backscatter signal for reflectance video of 500-line resolution at 30 frames per second. We imaged a bladder phantom with painted vessels and mimicked fluorescent lesions by applying green fluorescent microspheres to the surface. By eliminating the green laser illumination, simultaneous white-light reflectance and fluorescence images can be acquired at the same field of view, resolution, and frame rate. Moreover, this multimodal video can be compiled into full panoramic images of the bladder phantom when the flexible SFE tip is steered to scan the entire synthetic urothelium. These 3D digital records are formed from stitching together hundreds of selected frames of video to form a contiguous view of the bladder phantom. The fluorescence can have exact co-registration with RGB (white-light) reflectance. The multimodal records of the entire bladder can be analyzed with computer aided diagnosis algorithms to aid the urologist determining the presence and location of recurrence.

8207B-52, Poster Session

## Could Raman spectroscopy discriminate the biochemical alterations among prostate carcinoma and benign prostate tissue? an in vitro study

L. Silveira, Jr., Camilo Castelo Branco Univ. (Brazil); K. Ramos Moreira Leite, M. Srougi, Univ. de São Paulo (Brazil); F. L. Silveira, M. T. T. Pacheco, Camilo Castelo Branco Univ. (Brazil); C. A. Pasqualucci, Univ. de São Paulo (Brazil)

Dispersive Raman Spectroscopy has been proposed as a tool to discriminate neoplastic lesions with molecular specificity. This work evaluated possible alterations in the biochemical constitution of human prostate tissues in vitro, by comparing the relative intensity of selected bands related to the tissue biochemicals in prostate carcinoma (PrCa) and benign prostate tissue fragments and developing a Principal Components Analysis discriminating algorithm. We have examined 50 prostate fragments from 10 individuals (post mortem) and 22 specimens from surgically removed PrCa, each fragment with about 3 mm2. The Raman spectrum was then measured using a compact Raman spectrometer (830 nm excitation) coupled to a fiber-optic based probe (Lambda Solutions, Inc.). Integration time was set to 50 s and laser power adjusted to 300 mW. It has been collected 3 to 5 spectra from each fragment, in different spots. Most of the samples exhibited a strong background fluorescence, which was removed by a 7th order polynomial fitting. The spectra of prostate in the region of 400 to 1800 cm-1 are dominated by bands of proteins (collagen, elastin, actin). By comparing the mean spectra of PrCa with the benign prostate tissue, we found a very small difference, mainly in the 1000-1400 cm-1 region, indicating similar biochemical constitution of benign and malignant prostate tissue. Small spectral differences among PrCa and benign tissues have been described in others in vitro studies, but not confirmed here. Principal Components Analysis could discriminate the spectra of both benign and PrCa tissues with low sensitivity and specificity.

8207B-53, Poster Session

## A systematic study of cancerous and normal prostate tissues: fractal dimensional parameter, absorption and scattering coefficients

Y. Pu, W. Wang, M. Alrubaiee, S. K. Gayen, The City College of New York (United States); M. Xu, Fairfield Univ. (United States)

The fractal dimensional parameters and optical coefficients of human cancerous and normal prostate tissues were investigated and compared in the spectral range of 750 nm - 860 nm. The scattering coefficient (us) was determined from the extinction measurements on thin prostate tissue and Beer's law. The absorption coefficient (ua) and the reduced scattering coefficient (u's) were extracted from diffusion reflection intensity measurements on thick prostate tissue. The anisotropy factor (g) was calculated using the extracted values of us and u's. The values of fractal dimension (Df) of cancerous and normal prostate tissues were obtained by fitting the power law of the wavelength dependence of u's. The numbers of scattering particles contributing to us as a function of particle size and the cutoff diameter dmax as a function of g were investigated using the fractal dimension tissue model. The cutoff diameter dmax and the most efficient diameter of scatterers in cancerous and normal tissues were determined. Results show that the cutoff diameter dmax and the most efficient diameter of normal tissue are larger than those of the cancerous tissue, which is responsible for larger scattering coefficient of normal tissue in comparison with cancerous tissue. The results are in good agreement with the change of tissue during prostate cancer evolution defined by Gleason Grade. The difference of fractal dimensional parameters and optical coefficients of cancerous and normal prostate tissues may present a potential criterion for prostate cancer detection.

8207B-54, Poster Session

## Design of catheter-based diffusing optical device for endometrial coagulation

D. Rajabhandharaks, H. W. Kang, American Medical Systems, Inc. (United States)

We describe the design, development, and evaluation of a balloon catheter-based diffusing optical device to assist in the laser coagulation of an endometrium layer for excessive menstrual bleeding (i.e. menorrhagia). Due to anatomic characteristics of uterus, synthetic fused silica was micro-machined by a CO2 laser to create a diffusing fiber tip and to distribute 532-nm laser light uniformly over the tissue surface. Optical simulation and thermal modeling were conducted to estimate the spatial distribution of irradiance and temperature increase in tissue. Various diffusing optical devices were evaluated in vitro with bovine liver. A prototype of balloon (polyurethane) catheter-based diffusing optical device was tested on caprine uterine model in vivo. Both optical simulation and in vitro liver testing demonstrated that the diffusing tip capped with glass elicited more uniform light distribution and rapid ablation, compared to a bare diffusing tip (i.e. after 1 min irradiation, coagulation thickness=2.5 mm vs. 0.7 mm respectively). Even more uniform and faster tissue coagulation (thickness=3.5 mm) as a result of rapid temperature rise was achieved with application of a polyurethane layer to the tissue. In vivo caprine studies quantified the thermal coagulation of 3.0±1.2 mm after 30 sec irradiation. Histology presented that endometrial glands with sloughed epithelial cells, atypical appearing epithelium, and interstitial edema within endometrium confirmed thermally-treated areas with no hemorrhage or necrosis in myometrial smooth muscle. Our preliminary results suggest that the catheter-based diffusing optical device can be a feasible light delivery tool to coagulate endometrial layers in an efficient and safe manner.

8207B-47, Session 4

## Short-pulsed Tm:YAG laser lithotripsy: comparative study on ablation performance with conventional Ho:YAG laser

D. Rajabhandharaks, H. W. Kang, American Medical Systems, Inc. (United States)

Urinary calculus is one of the most common urologic diseases tertiary to prostate disease and urinary tract infection. Laser lithotripsy has been well accepted as an intracorporeal treatment of urinary calculi. However, inefficient calculus removal and significant calculus movement have often remained as the unmet need in laser lithotripsy. The objective of this study was to investigate the effect on calculus fragmentation of a custom-made short-pulsed Tm:YAG laser (wavelength=2.01μm, pulse duration=0.5μs) in comparison with a conventional long-pulsed Ho:YAG laser (wavelength=2.1μm, pulse duration=350μs). Cement-based artificial calculus phantoms (similar hardness to human struvite) were used in replacement of human calculi. Removal rate and calculus retropulsion were assessed in each laser system. Fragmented calculus size of less than 3 mm was considered as removable mass and weighed to calculate removal rate. Tm:YAG fragmented the calculi into small pieces due to consecutive mechanical impacts associated with short pulses promoting calculus fragmentation via photomechanical process. However, Ho:YAG laser only drilled a hole into the phantoms throughout a relatively slower fragmentation process. Higher removal rate was observed in short-pulsed Tm:YAG laser (690mg/min vs. 0.2mg/min in Ho:YAG) because of higher water absorption coefficient of Tm:YAG (70 vs. 24cm-1 in Ho:YAG). Lastly, stone retropulsion was considerably significant in Ho:YAG laser (2~3mm) due to bubble expansion and collapse but very minimal in short-pulsed Tm:YAG. The advancement of short-pulsed Tm:YAG laser with higher absorption coefficient has the potential to improve laser lithotripsy for treating human urinary calculi.

8207B-48, Session 4

## Thulium fiber laser lithotripsy using bursts of pulse trains for enhanced stone ablation

R. Blackmon, The Univ. of North Carolina at Charlotte (United States); P. Irby, Carolinas Medical Ctr. (United States); N. M. Fried, The Univ. of North Carolina at Charlotte (United States)

Introduction: Application of bursts of short laser pulse trains has recently been shown to increase material removal for laser processing of metals. The diode-pumped Thulium Fiber Laser (TFL) is currently being studied as an alternative to the flashlamp-pumped, solid-state, Holmium:YAG laser for lithotripsy. The TFL may be electronically modulated to operate with variable parameters (e.g. pulse rate, pulse duration and duty cycle) for studying the influence of micro-pulse trains on tissue ablation. In this study, controlled bursts of TFL pulse trains are used for enhanced vaporization of urinary stones and reduction of stone charring, which causes fiber degradation.

Methods: The TFL was operated at 1908 nm, 35-mJ pulse energies, and 500-microsecond pulse duration, in bursts of 5-10 micro-pulses, and macro-pulse rates of 10-20 Hz. TFL radiation was coupled into 100-micrometer-core fibers in contact with human uric acid stone samples submerged and fixed in a saline bath. These parameters were compared with conventional macro-pulse TFL operation at 10-50 Hz.

Results: TFL operation in pulse train burst mode (5 pulses/packet, 1:1 duty cycle, and 20 Hz) resulted in a stone mass removal rate of 708 +/- 270 micrograms/s with minimal stone charring and fiber degradation, in comparison to 182 +/- 69 micrograms/s with individual pulses delivered at 50 Hz, for the same number of pulses delivered.

Conclusions: TFL pulse train bursts result in increased stone mass removal rates which, with further optimization, may approach levels comparable to high pulse energy, low pulse rate Holmium:YAG laser lithotripsy in the clinic.

8207B-49, Session 4

## 3D numerical reproduction of crack patterns, in a cylindrical sample, observed in shock wave lithotripsy

M. L. Wijerathne, M. Hori, The Univ. of Tokyo (Japan); H. Sakaguchi, Japan Agency for Marine-Earth Science and Technology (Japan)

We simulated some of the Shock Wave Lithotripsy (SWL) related experimental observations reported by Xi et al. (2001), including 3D dynamic crack propagation, with the aim of exploring the fragmentation process of kidney stones. Extracorporeal shock wave lithotripsy (ESWL) is the fragmentation of kidney stones by focusing an ultrasonic pressure pulse onto stones. Despite its wide usage, the stone fragmentation mechanisms of SWL have not been well understood. In order to accurately capture the high amplitude shear shock waves induced in stone samples, which are found to play a dominant role in fragmentation, 3D models with fine discretization are used for the simulations. For solving the resulting large scale dynamic crack propagation problem, a distributed parallel code of PDS-FEM with Tuler-Butcher type dynamic crack propagation criterion is used; PDS-FEM is chosen since it provides numerically efficient failure treatments. We simulated the transient stress waves and crack patterns in cylindrical solid samples under plane water shock waves at a normal incident to the cylinder axis. Numerically generated 3D photoelastic patterns, based on the transient stress filed, are found to be in good agreement with that of the experiment; compared only qualitatively due to lack of data. Of the numerically generated 3D crack pattern, the geometric locations of the major crack surfaces found to be closely matching those of observed in the experiment. The simulation results indicate that the high amplitude shear waves induced in the solids play a dominant role in stone fragmentation.

8207B-50, Session 4

## Effects of Holmium:YAG energy on BackStop anti-retropulsion polymer

J. Qiu, The Univ. of Texas at Austin (United States); J. M. Teichman, The Univ. of British Columbia (Canada); B. Wang, T. E. Milner, The Univ. of Texas at Austin (United States)

Holmium:YAG lithotripsy is effective for all stone compositions. However, it also can ablate metal guidewires, baskets, and anti-retropulsion devices. BackStop is a novel reverse thermosensitive polymer-based anti-retropulsion material. Response of Backstop to pulsed Ho:YAG radiation is unknown, but predicted to withstand energy better than metal based anti-retropulsion devices since BackStop retains a solid form at increased temperature. Further, a solid shape, form, and function should not be compromised even if an ablation crater may be created. This study tests the ability of BackStop polymer to withstand shape and function in response to Ho:YAG laser energy at various pulse energies. BackStop polymer can be ablated by Ho:YAG laser pulses, but still perform its function. Laser polymer interaction is characterized using fast flash imaging.

8207B-51, Session 4

## Endoscopic identification of calcium oxalate monohydrate calculi during Ho:YAG lithotripsy

R. Hamidizedah, J. M. Teichman, St. Paul's Hospital (Canada)

Prior research shows that Ho:YAG lithotripsy produces tiny dust fragments at low pulse energy (0.2J). However, calcium oxalate monohydrate (COM) stones have a high criterion threshold for ablation and may not fragment at this low pulse energy. Stone composition is rarely known until after surgery. As COM appears black under ambient light, we attempt to predict stone composition at the time of ureteroscopy by the endoscopic appearance of the stone. Any portion of the stone that appeared black under endoscopic vision was considered clinical evidence of COM. Stone analysis was conducted postoperatively (infared spectroscopy and diffraction crystallography). Seventeen consecutive stone cases were analyzed retrospectively. Twelve of 13 patients (92%) of black stones were COM by composition analysis; zero of 4 patients (0%) of non-black stones were COM, p=0.002. COM may reasonably be predicted intraoperatively by its endoscopic appearance and higher pulse energy settings employed. More sophisticated optical characterization of stone appearance may prove a useful tool.

# Conference 8207C: Optical Imaging, Therapeutics, and Advanced Technology in Head and Neck Surgery and Otolaryngology

Saturday-Monday 21-23 January 2012

Part of Proceedings of SPIE Vol. 8207C Optical Imaging, Therapeutics, and Advanced Technology in Head and Neck Surgery and Otolaryngology

8207C-300, Session 1

## Longitudinal evaluation of patients with oral potentially malignant disorders using optical imaging and spectroscopy

R. A. Schwarz, M. C. Pierce, S. Mondrik, W. Gao, M. K. Quinn, Rice Univ. (United States); V. S. Bhattar, M. D. Williams, The Univ. of Texas M.D. Anderson Cancer Ctr. (United States); N. Vigneswaran, The Univ. of Texas Dental Branch at Houston (United States); A. M. Gillenwater, The Univ. of Texas M.D. Anderson Cancer Ctr. (United States); R. R. Richards-Kortum, Rice Univ. (United States)

Dysplastic and cancerous alterations in oral tissue can be detected noninvasively in vivo using optical techniques including autofluorescence imaging, high-resolution imaging, and spectroscopy. Interim results are presented from a longitudinal study in which optical imaging and spectroscopy were used to evaluate the progression of lesions over time in patients at high risk for development of oral cancer. Over 100 patients with oral potentially malignant disorders have been enrolled in the study to date. Areas of concern in the oral cavity are measured using widefield autofluorescence imaging and depth-sensitive optical spectroscopy during successive clinical visits. Autofluorescence intensity patterns and autofluorescence spectra are tracked over time and correlated with clinical observations. Patients whose lesions progress and who undergo surgery are also measured in the operating room immediately prior to surgery using autofluorescence imaging and spectroscopy, with the addition of intraoperative high-resolution imaging to characterize nuclear size, nuclear crowding, and tissue architecture at selected sites. Optical measurements are compared to histopathology results from biopsies and surgical specimens collected from the measured sites. Autofluorescence imaging and spectroscopy measurements are continued during post-surgery followup visits. We examined correlations between clinical impression and optical classification over time with an average followup period of 4 months. The data collected to date suggest that multimodal optical techniques may aid in noninvasive monitoring of the progression of oral premalignant lesions, biopsy site selection, and accurate delineation of lesion extent during surgery.

8207C-301, Session 1

## mTHPC mediated interstitial photodynamic therapy of recurrent nonmetastatic base-of-tongue cancers: development of a new method

I. B. Tan, Het Nederlands Kanker Instituut - Antoni van Leeuwenhoek Ziekenhuis (Netherlands); B. Karakullukcu, The Netherlands Cancer Institute (Netherlands); R. L. van Veen, Erasmus MC (Netherlands); M. Witjes, Univ. Medical Ctr. Groningen (Netherlands); P. C. Levendag, H. J. C. M. Sterenborg, Erasmus MC (Netherlands)

Background. Interstitial photodynamic therapy (iPDT) can be an option in the management of locally recurrent base of tongue cancer after (chemo) radiation treatment. The purpose of the current study was to develop a technique to implant light sources into the tumor tissue.

Methods. Twenty patients with previously radiated locally recurrent base of tongue cancers who were not candidates for salvage surgery or re-radiation or refused these therapies were included in this study. The treatment planning was done on MRI. The light sources were implanted using modified brachytherapy techniques.

Results. The iPDT could be conducted in all patients without short-term complications. At 6 months, 9 patients had complete response with 4 patients still free of disease (46-80 months). Long-term complications included pharyngocutaneous fistula in 6 patients, serious bleeding in 1 patient, and cutaneous metastasis in 2 patients.

Conclusion. The initial results are encouraging. There is room for improvement to control the destructive potential of iPDT through planning and monitoring tools.

8207C-302, Session 1

## Gold nanorods for treatment of oral cancer

I. H. El-Sayed, Univ. of California, San Francisco (United States)

No abstract available

8207C-303, Session 1

## Early results of an in vivo trial of ESS in thyroid cancer

J. E. Rosen, I. D. Goukassian, O. M. A'Amar, I. J. Bigio, S. L. Lee, Boston Univ. (United States)

INTRODUCTION: Thyroid cancer is the most common endocrine malignancy. The current gold standard for diagnosis, fine-needle aspiration (FNA) biopsy, yields approximately 10-25% of indeterminate cytology results, leading to patients undergoing thyroidectomy for diagnosis. Elastic scattering spectroscopy (ESS) is a new, minimally invasive optical-biopsy technique, mediated by fiber-optic probes, which is sensitive to cellular and subcellular morphological features. We assessed the technical potential of a miniaturized in vivo ESS probe, built into an FNA needle assembly, to differentiate benign from malignant thyroid nodules.

METHODS: Under an IRB approved protocol, 15 patients in the endocrine clinic undergoing transcutaneous needle biopsy of a thyroid nodule had collection of ESS data using our novel miniaturized FNA probe. A standard operating protocol was developed and refined, including cleaning and sterilization, physician tool use, calibration and re-sterilization. Using final surgical pathology as our gold standard, data post processing and analysis was conducted to assess spectral agreement across repeated measurements.

RESULTS: A total of 225 spectra were grouped and analyzed (120 with benign, 30 with malignant and 75 from indeterminate cytology). The ESS probes demonstrated excellent reproducibility in use. Initial analysis of these preliminary data is promising, indicating distinction of spectral ESS features between malignant and benign conditions.

CONCLUSION(S): An in vivo trial of an invasive miniaturized integrated ESS biopsy probe is acceptable to patients, and collection of ESS data is feasible and reliable. With development of a disease-specific algorithm, ESS could potentially be used as an in-situ real time intra-operative diagnostic tool or as a minimally invasive adjunct to conventional FNA cytology. A larger scale clinical study is currently ongoing.

8207C-304, Session 1

## In vivo monitoring method for traumatic brain injury of mouse based on near-infrared light

W. Li, Z. Qian, X. Wang, X. Liu, Nanjing Univ. of Aeronautics and Astronautics (China)

A portable system based on near-infrared light intensity was proposed to monitor mouse model of traumatic brain injury (TBI) non-invasively. Light from a 760/850nm dual-wavelength light emitting diode is coupled to a 0.6-mm-diameter optical fiber. The collection fibers are coupled to optoelectronic detectors, which are placed in the position of 1mm and 2mm distance from the source fiber. The system consists of a constant current bias, a circuit lock-in amplifier, a PCI 6240 data acquisition card and a multi-core-processor computer. The modified Lambert Beer law was used to calculate the concentration of ΔHbO2 and ΔHb. The sensitivity matrix was defined to evaluate the effective detection region of optical probe. The model was made by intralipid solution of 20% concentration. The Nitrogen and Oxygen were added into the solution in turn. The results measured by proposed system were validated by ISS Oximeter. Five groups of TBI mouse models were built by Feeney's free-falling method. The data measured by system show after TBI the concentration of HbO2 decreased and the concentration of Hb increased. The decreased concentration of HbO2 is larger than the increased concentration of Hb. Then the changes of the concentration of HbO2 and Hb according to the development of TBI was studied. The degree of TBI in 1 hour is more severity than which in 24 hours, so the concentration of HbO2 is decreased. It can be concluded that the proposed system can be used to monitor the changes of TBI of mouse non-invasively.

8207C-305, Session 2

## High-speed digital phonoscopy images analyzed with Nyquist plots

Y. Yan, Santa Clara Univ. (United States)

No abstract available

8207C-306, Session 2

## Laser cordectomy for early glottic carcinoma

P. Chung, Dankook Univ. Hospital (Korea, Republic of)

Introduction :Laser cordectomy is very popular nowadays and become one of the treatment of choice for early glottis carcinoma. Transoral laser microsurgery has many advantages comparing conventional open surgery or radiation therapy.

Objectives: In this study, we examined the oncologic results of laser cordectomy for early glottic cancer and analyzed the prognostic impact on the survival of the several tumor-related and treatment-related factors.

Materials and methods: Patients who were diagnosed as early glottic squamous cell carcinoma (T1 or T2), treated by laser cordectomy with curative intent were analyzed. Patients with preivous radiation therapy were included. All patients had a minimum follow-up period of 5 years. (174 T1, 28 T2).

Results: Five-year overall survival and disease-free survival was 98%. Twenty two patients developed local recurrence. Total laryngectomy was done in 6 patients and laryngeal preservation rate was 97%. Recurrence was higher in the patients with anterior commissure involvement (9/39) than without anterior commissure involvement (13/163). Recurrence was higher in T1b (4/15) than T1a (13/159). Previous radiation was also highly related to the recurrence (7/20 vs 15/182). Twenty patients with local recurrence after radiation therapy were treated by salvage laser cordectomy. Of them, 7 patients developed local recurrence and 5 year disease-free survival was 57%. Complication was rare with one case of hemorrhage. Tracheotomy was not necessary in all patients.

Conclusions: Laser cordectomy for early glottic carcinoma showed high survival rate, laryngeal preservation rate and low complication rate. The prognostic factors were anterior commissure involvement, both vocal fold involvement and previous radiation therapy.

8207C-307, Session 2

## Analysis of high-speed digital phonoscopy pediatric images

R. R. Patel, Univ. of Kentucky (United States)

No abstract available

8207C-308, Session 2

## Snake based automatic tracing of vocal-fold motion from high-speed glottic images

G. Du, Y. Yan, Santa Clara Univ. (United States)

No abstract available

8207C-309, Session 2

## Endoscopic laser scalpel for head and neck cancer surgery

R. Toledo-Crow, S. Patel, M. Rajadhyaksha, S. Kirov, Y. Li, Memorial Sloan-Kettering Cancer Ctr. (United States)

Minimally invasive surgical (MIS) techniques, such as laparoscopic surgery and endoscopy, provide reliable disease control with reduced impact on the function of the diseased organ.

Surgical lasers can ablate, cut and excise tissue while sealing small blood vessels minimizing bleeding and risk of lymphatic metastases from tumors. Lasers with wavelengths in the IR are readily absorbed by water ensuring minimal thermal spread and injury to adjoining tissue, ideal for surgery near critical anatomical structures.

MIS techniques have largely been unable to adopt the use of lasers. This is partly due to the difficulty in bringing the laser into the endoscopic cavity. Hollow waveguide fibers have been adapted to bring surgical lasers to endoscopy. However, they deliver a beam that diverges rapidly and requires careful manipulation of the fiber tip relative to the target. Thus, the principal obstacle for surgical lasers in MIS procedures has been a lack of effective control instruments to manipulate the laser in the body cavity and accurately deliver it to the targeted tissue.

To overcome this limitation, we have designed and built an endoscopic laser system that incorporates a miniature dual wedge laser scanner, a video stream, and the control system for remote and /or robotic operation. The dual wedge (Risley) scanner offers the smallest profile possible for endoscopic use. Clinical specifications and design considerations will be presented together with descriptions of the device and its control system. Examples of preliminary data obtained from ex-vivo tissue samples will be shown.

8207C-310, Session 3

## Management of superficial tissue disease using PDT: non-melanomatous skin cancer

W. K. Jerjes, C. Hopper, Univ. College London (United Kingdom)

In this prospective study, 148 (86 males and 62 females) consecutive patients were referred to the UCLH Head and Neck Centre, London between 1995 to 2007 for treatment of suspicious skin lesions involving the craniofacial, torso, upper and lower limbs. The mean age was 56.3±17.1 years (Min 36, Max 72) with 95% being Caucasians.

Primary description included macules, papules and ulcers; with rolled and everted edges. Diagnosis was confirmed by either an incisional biopsy or scratch cytology. A range of pathologies was identified including actinic keratosis, basal cell carcinoma and squamous cell carcinoma. Areas included upper face, middle face, lower face, scalp, anterior and posterior chest walls and the upper and lower limbs.

The patients' main complaints were categorised into 5 parameters: pain, itchiness, bleeding, cosmetic, and fear of malignant transformation (in the case of actinic keratosis). As there is no current verified assessment of quality of life in patients undergoing photodynamic therapy the patients were asked only to report the nature of the complaint and not the severity.

All cancer patients were discussed at the UCLH Head and Neck MDT and it was agreed to offer surface illumination photodynamic therapy under local or general anaesthesia, using 5-ALA (for thin actinic keratosis and basal cell carcinoma) and mTHPC (for thicker actinic keratosis and basal cell carcinoma; also for squamous cell skin cancer).

A 60 mg/kg 5-ALA cream was applied topically 3-4 hours prior to skin illumination. mTHPC was administered at a dose of (0.05mg/kg) intravenously into the midcubital vein 48 hours prior to treatment. This would allow the agents to accumulate in the pathological area which would increase effectivity. Patients were advised to avoid direct sun light exposure for 1-2 weeks if the drug was administered intravenously to avoid systemic photosensitisation.

Shielding of the macroscopically healthy surrounding tissue was employed when indicated. For 5-ALA-PDT, a single-channel 628 nm diode laser was used for illumination. The laser light delivery fibre, with a core diameter of 400µm, was held directly above the suspect area and light was delivered. Light was then delivered from the fibres to the target tissue at 100 or 200 J/cm2 per site. For mTHPC-PDT, A single-channel 652nm diode laser was used for illumination. The laser light delivery fibre, with a core diameter of 400µm, was held directly above the suspect area and light was delivered. Light was then delivered from the fibres to the target tissue at 10-20J/cm2 per site.

Post treatment pain control is applied according to UCLH post-PDT pain protocols; NSAIDs and opiates are usually supplied if not contraindicated. Patients were discharged on the same day unless they were required to stay for other reasons (i.e. marked swelling, pain, medical reasons).

Postoperative clinical assessment was reported by the treating clinician (at ≈4 weeks). Mild-to-moderate pain at the treatment site, a recognised side effect of PDT, was reported by 24 patients of patients but was manageable with appropriate analgesia. Mild-to-moderate skin photosensitivity reactions were reported for 12 patients. The results showed excellent clinical response and cosmetic outcome.

8207C-311, Session 3

## Real-time line-scanning reflectance confocal endoscope to enhance sectioning and reduce speckle for intraoral imaging

C. Glazowski, M. Rajadhyaksha, Memorial Sloan-Kettering Cancer Ctr. (United States)

Reflectance confocal microscopy images nuclear and cellular detail in oral mucosa in-vivo. The fields of view, resolution and sectioning are comparable to standard histology. Compared to the standard point-scanning confocal microscope (PCM), a line-scanning confocal microscope (LCM) is simpler and consequently less-expensive to manufacture. For endoscopic applications, such as intraoral imaging, this allows for a smaller and lower cost device for potentially widespread clinical use. However, being confocal in only 1-dimension, the optical sectioning strength of the LCM is degraded by ~20% compared to the PCM. This sectioning performance (and thus contrast) has been successfully improved in our benchtop endoscopic LCM with a divided pupil configuration, instead of standard full pupil illumination/detection. Furthermore, speckle affects image fidelity. In our system, the detection configuration (magnification, pixel-to-resolution ratio) is optimally chosen to reduce speckle noise, thereby improving image fidelity. Imaging of a stable turbid phantom shows significant reduction in background and provides quantitative feedback to the design process. Also, the standard LCM provides en-face images of tissue and requires axial translation of the nominal focal plane through the volume of interest. A deformable-MEMs mirror is integrated for axial focus control. Preliminary images of human oral mucosa in vivo show nuclear and cellular detail and demonstrate feasibility for clinical use.

8207C-312, Session 3

## Reflectance confocal microscope for imaging oral tissues in vivo, potentially with line scanning as a low-cost approach for clinical use

G. Peterson, S. Abeytunge, Memorial Sloan-Kettering Cancer Ctr. (United States); Z. Eastman, Lucid Inc. (United States); M. Rajadhyaksha, Memorial Sloan-Kettering Cancer Ctr. (United States)

Reflectance confocal microscopy with a line scanning approach potentially offers a smaller, simpler and less expensive approach than traditional methods of point scanning for confocal microscopy in living tissues. With one moving mechanical element (galvanometric scanner), a linear array detector and off-the-shelf optics, we designed a compact (102x102x76mm) line scanning confocal reflectance microscope (LSCRM) for imaging human tissues in vivo in a clinical setting. The LSCRM may be configured with either a standard objective lens for imaging skin or with a "toothbrush-like" relay telescope for access to the human oral cavity. Custom-designed electronics, based on field programmable gate array (FPGA) logic has been developed. With 405 nm illumination and a custom-made small objective lens of numerical aperture 0.5, lateral resolution was measured to be 0.8 um (versus calculated 0.64 um). The calculated optical sectioning is 3.2 um. Preliminary imaging shows nuclear and cellular detail in human skin and oral epithelium in vivo. Blood flow is also visualized in the deeper connective tissue (lamina propria) in oral mucosa. Since a line is confocal only in one dimension (parallel) but not in the other, the detection is more sensitive to multiply scattered out of focus background noise than in the traditional point scanning configuration. Contrast and image quality as a function of scattering and aberrating properties of tissue is being investigated. Based on the results of our translational studies thus far, a simpler, smaller and lower-cost approach based on a LSCRM appears to be promising for clinical imaging.

8207C-313, Session 3

## Prospective evaluation of 110 patients following ultrasound-guided photodynamic therapy for deep seated pathologies

W. K. Jerjes, Univ. of Leeds (United Kingdom) and Leeds Teaching Hospitals NHS Trust (United Kingdom) and Univ. College London Medical School (United Kingdom); T. Upile, Univ. College Hospital (United Kingdom); C. A. Mosse, Univ. College London (United Kingdom); Z. Hamdoon, Univ. College Hospital (United Kingdom); M. Morcos, Univ. College Hospital (Canada); S. Morley, Univ. College Hospital (United Kingdom); C. Hopper, Univ. College London Hospitals NHS Foundation Trust (United Kingdom)

INTRODUCTION: Photodynamic therapy, the fourth oncological interventional modality has proved its success in the management of variety of pathologies involving the human body. Our aim in this prospective clinical study was to continue evaluating the outcome following ultrasound-guided interstitial PDT of pathologies involving the human body. Patients' reports on quality of life with clinical and radiological evaluation were the main end point parameters used to assess the outcome.

MATERIALS AND METHODS: One hundred and ten patients were referred to the UCLH Head and Neck Centre, London for treatment of various deep-seated pathologies. These included tumours in the head and neck as well as vascular anomalies of the limbs. After multidisciplinary discussion, all patients underwent interstitial photodynamic therapy (iPDT) under general anaesthesia, using 0.15mg/kg mTHPC as the photosensitising agent. Following treatment, patients were followed-up for a mean of 26 months.

RESULTS: Four out of five patients who presented with visual problems reported improvement after treatment. Also, 27/32 reported improvement of breathing. Improvement of swallowing was reported by 30/37 patients; while speech improvement was evident in 22/29 patients and 43/52 reported reduction in the disfigurement caused by their pathology. Seven out of nine patients with impeded limb function reported some degree of improvement. Clinical assessment showed that nearly half of the patients had "good response" to the treatment and 5 became disease free. Moderate clinical response was reported by 39 patients. Radiological assessment comparing radiological imaging 6-week post-PDT to the baseline showed moderate response in 45 patients and significant response in 32 patients.

CONCLUSION: This study on 110 patients with deep-seated pathologies undergoing interstitial photodynamic therapy provided further evidence that PDT is a useful modality in the management of these pathologies that are otherwise resistant to conventional treatments, and with minimal side effects.

8207C-314, Session 3

## 5-aminolevulinic acid photodynamic therapy for head and neck dysplasia

H. Quon, Johns Hopkins Univ. (United States); M. E. Putt, T. C. Zhu, J. C. Finlay, A. Dimofte, M. Mehler, K. M. Malloy, The Univ. of Pennsylvania Health System (United States); C. E. Grossman, S. Gallagher-Colombo, Univ. of Pennsylvania (United States); G. S. Weinstein, B. W. O'Malley, Jr., C. E. Rodriguez, T. M. Busch, The Univ. of Pennsylvania Health System (United States)

Background: 5-aminolevulinic acid (5-ALA) has been administered systemically for photodynamic therapy but with limited evaluation for head and neck dysplasia.

Materials and Methods: Subjects were treated with escalating light doses in combination with 60 mg/kg oral 5-ALA. After open enrollment at 50 J/cm2, subjects were randomized to either continuous or fractionated delivery of light dose at 100 mW/cm2 (basd on in-vivo light fluence). Subjects were evaluated at week 1, 2-3, 4 and 12 weeks. Toxicity and response rates were evaluated at week 4 and 12 respectively.

Results: From 11/2009-2/2011, 23/26 subjects enrolled have received light. 4 subjects re-enrolled, 2 receiving 5-ALA but no light and 2 re-enrolling with partial responses after 5-ALA-PDT. All subjects experienced in-field grade 2-3 mucositis resolving by week 4. Due to 5-ALA competing with the Jaffe assay for serum creatinine, a highly significant linear correlation between serum creatinine and plasma 5-ALA was observed in the 24 hours post treatment ($p<0.0001$). Two dose-limiting toxicities: one grade 5 toxicity (4%) in the 150 J/cm2 non-fractionated cohort and one (edema) occurred at the 200J/ cm2 fractionated cohort. At 3 months, complete response, partial response, minor - no response has been observed in 52%, 14% and 10% respectively. Of the subjects with a complete response, 63% were treated with a fractionated light schedule. One subject developed malignant transformation.

Conclusions: Preliminary analysis demonstrates that systemic 5-ALA-PDT is well tolerated and safe up to 100 J/cm2. Serum creatinine at 1 hour following oral 5-ALA administration is a good surrogate for plasma 5-ALA levels.

8207C-315, Session 3

## Quality of life of patients undergoing photodynamic therapy

W. K. Jerjes, C. Hopper, Univ. College London (United Kingdom)

Introduction: Several valuable quality of life (QoL) questionnaires have been developed and successfully used when assessing the level of function and dysfunction in cancer patients; this includes patients diagnosed and treated for head and neck cancer. These questionnaires have been used to assess outcome following the conventional treatment modalities (surgery, radiotherapy and/or chemotherapy). To date there is no questionnaire used to assess the quality of life following photodynamic therapy, and in particular in the management of head and neck pathologies.

Our aim in this prospective study was to evaluate the quality of life of a cohort of patients being treated with photodynamic therapy for various pathologies of the head and neck.

Materials and Methods: We have developed the first quality of life questionnaire for patients undergoing photodynamic therapy. The questionnaire was developed from the "University of Washington Quality of Life Questionnaire for Head and Neck Cancer Patients".

Thirty-eight patients agreed to take part in this study. The quality of life was assessed before, during and up to 3 months after photodynamic therapy. The main areas covered: Pain, Visual problems, Breathing problems, Swallowing problems, Speaking problems, Taste, Saliva, Disfigurement, Drug reactions, Skin photosensitivity, Activity of daily living, Impact on social life, Mood, Anxiety and compared to previous experience with surgery, radiotherapy, chemotherapy and/or photodynamic therapy.

Patients were also asked to highlight any major or minor concerns during this time period and asked whether the clinical information provided with regard to the treatment and light precautions were adequate?, was the treatment up to their expectations? And would they consider having photodynamic therapy again?

Results: The results from these 36-page questionnaires were statistically analysed and significant results were highlighted. Pain was the main issue in the majority of the patients, and was often described as severe in nature ($P<0.05$). Visual, breathing, speaking and swallowing problems improved significantly 22-28 days post-PDT ($P<0.001$). Taste and saliva production was not an issue for any of the patients suffering from oral and oro-pharyngeal pathologies, unlike post chemo-radiation.

Transient pain while administrating the photosensitiser was reported by 32/38 patients and skin photosensitivity was reported by 6/38 patients. Significant improvement of activity of daily living, impact on social life, mood and anxiety was reported by patients 36-42 days post-PDT ($P<0.001$).

All patients reported better overall quality of life following PDT when compared to the previous conventional modalities they have received. 35/38 patients thought that the treatment was up to their expectations and 34/38 patients would consider having the treatment again.

Conclusion: The routine application of quality of life questionnaires in head and neck patients improves information regarding how and to what extent patients feel that treatment is improving their quality of life making it possible to support patients to their real needs.

8207C-316, Session 3

## Quantifying the effects of HPV infection in the autofluorescence in the oral cavity

A. F. Zuluaga, Remicalm LLC (United States)

No abstract available

8207C-317, Session 3

## Optimization of targeted two-photon PDT triads for the treatment of head and neck cancers

C. W. Spangler, J. R. Starkey, G. Dubinina, SensoPath Technologies Inc. (United States); C. Fahlstrom, Montana State Univ. (United States); J. Shepard, SensoPath Technologies Inc. (United States)

New PDT triads have been synthesized that incorporate a tumor-killing porphyrin with large two-photon cross-section (2000 GM units) at 840 nm conjugated to a small EGFr targeting peptide and an imaging agent. They were optimized to treat FADU HNSCC xenograft tumors in SCID mice. Light and dark toxicities and PDT treatment exhibited no adverse effects. Previous experiments in human lung and breast tumors in SCID mice and phantoms indicate that the tumors can be treated directly through the skin to depths between 2 and 5 cm. Treated mice demonstrated rapid tumor regression, with some cures, in as little as 15-20 days following a single PDT treatment, with no adverse effects in the healthy tissue through which the focused laser beam passed before reaching the tumor site. Excellent healing occurred following treatment, including rapid hair re-growth over the former tumor site. The mice rapidly recovered post-PDT and could have undergone repeat PDT treatment if necessary. Not all irradiation protocols led to complete cures. Since two-photon PDT is carried out by rastering a small voxel of focused irradiation throughout the tumor it is possible that, as the treatment depth increases, fine focusing may be lost due to increased scattering, allowing some parts of the tumor to escape irradiation, and raising the possibility that tumor re-growth could be triggered by small islands of untreated cells, particularly in the rapidly growing tumor margins. We are currently developing image-guided PDT to alleviate this problem

8207C-318, Session 4

## Ultrafast laser microsurgery, simultaneous multiphoton, and SHG imaging of healthy and scarred vocal folds

M. Yildirim, O. Ferhanoglu, C. L. Hoy, The Univ. of Texas at Austin (United States); J. B. Kobler, Massachusetts General Hospital (United States); A. Ben-Yakar, The Univ. of Texas at Austin (United States)

Vocal fold scarring is one of the major causes of voice disorders and it may arise from disease like dysphonia or post-surgical wound healing. One promising treatment utilizes the injection of soft biomaterials aimed at restoring the viscoelasticity of the outermost vibratory layer of the vocal fold, superficial lamina propria (SLP). However, the density of the tissue and the required injection pressure impair proper localization of the injected material in SLP. To enhance treatment effectiveness, we are investigating a technique to ablate sub-epithelial planar voids in vocal fold tissue using ultrafast laser pulses to localize injected material.

In this paper, we present an in-depth analysis of ultrafast laser surgery parameters to create 2D planar voids below the vocal fold epithelium. Specifically, we study the effect of laser parameters, such as pulse energy (500-1300 nJ) and the number of overlapping laser pulses, on sub-epithelial void creation within porcine vocal folds at various ablation depths (70-200μm). We use a home-built, two channel nonlinear laser scanning microscope together with a high repetition rate (300 kHz - 2 MHz) ultrafast fiber laser (Raydiance Inc.) for rapidly creating and simultaneously monitoring ablations within tissue. We acquire both second harmonic generation and two-photon autofluorescence images from the tissue simultaneously. While each imaging modality shows a different tissue signature and type, together they provide a complementary view of the sub-epithelial tissue. We demonstrate deep tissue ablation and imaging of scarred hamster cheek pouches and the effects of scarring on the efficacy of laser surgery for sub-epithelium void formation.

8207C-319, Session 4

## Correlations of HSDI with other clinical voice measurements

M. Pedersen, M. Eeg, The Medical Ctr. (Denmark)

No abstract available

8207C-320, Session 4

## Analysis of mucosal wave by HSDIS and Kymography in papilloma treated with Avastin

R. M. Cruz, Santa Clara Univ. (United States); K. Izdebski, Pacific Voice and Speech Foundation (United States); Y. Yan, Santa Clara Univ. (United States)

No abstract available

8207C-321, Session 4

## High speed examination of the vocal fold activity using ultra high speed filming: presentation of 1956 archival recordings by Paul Moore and Hans von Leden

K. Izdebski, Pacific Voice and Speech Foundation (United States)

No abstract available

8207C-322, Session 5

## Microsurgery near critical structures: evaluation of temperature profile and functional outcomes following use of a flexible CO2 laser fiber

A. M. Robinson, A. J. Fishman, B. R. Bendok, C. Richter, Northwestern Univ. (United States)

Lasers have been introduced in surgery as cutting and as coagulation tools. The latter two functions are determined by the laser-tissue interactions. Laser properties include radiation wavelength, radiant power, spot size, and exposure time. Tissue properties include the absorption coefficient and heat transfer. The combinations of laser and tissue properties determine the rate of tissue heating, the area of laser effect, the amount of tissue ablated, and the amount of collateral tissue damage. Understanding the precise nature of laser tissue interaction can augment the safety margin of the surgeon employing these tools. The data provides guidelines for appropriate laser power settings for tissue ablation. When the operator is working in close proximity to the neural structures with the option that the neural structure is in the laser beam path, a laser power setting of 2 Watts or less should be employed.

8207C-323, Session 5

## In vivo measurement of differential motion inside the organ of Corti using a low-coherence interferometer system

F. Chen, D. Zha, Oregon Health & Science Univ. (United States); A. Fridberger, Karolinska Institutet (Sweden); J. Zheng, N. Choudhury, S. L. Jacques, Oregon Health & Science Univ. (United States); R. Wang, Univ. of Washington (United States); A. L. Nuttall, Oregon Health & Science Univ. (United States)

The differential motion of the organ of Corti has been expected as a result of the outer hair cell force, believed to be necessary for the cochlear amplifier. In vitro experiments have been performed to demonstrate this motion but the in vivo data was unavailable due to the technical difficulties. Using a specially-designed time-domain OCT system, we performed in vivo imaging and vibration measurement at the sensitive base of the guinea pig cochlea. This technique, for the first time, provides in vivo information about the internal vibration of the organ of Corti. At low sound level, when the cochlea is more sensitive, top surface of the organ of Corti, the reticular lamina (RL) showed tuning at a higher frequency than of the bottom surface, basilar membrane (BM) and its vibration amplitude is 2-3 times of that of the BM. Corresponding to the frequency difference, the phase of RL vibration is lead to that of the BM. Both the amplitude gain and the phase lead on RL is level dependent. This suggests that they are related to the cochlear amplification. The amplitude gain at the RL is an enhancement of the BM motion for stimulating the stereocillia. The advance in time of RL vibration can prepare proper timing of stereocillia stimulation for the cochlear amplification.

8207C-324, Session 5

## The optimal time to treat noise-induced hearing loss (NIHL) with low level laser therapy (LLLT)

C. Rhee, J. Ahn, P. Chung, M. Suh, Dankook Univ. Hospital (Korea, Republic of)

Aim: The LLLT was found to recover NIHL but the LLLT was performed immediately after the induction of NIHL. The aim of this study was to find the optimal time to recover a NIHL with LLLT.

Methods: Bilateral ears of 6 SD rats with 12 ears were exposed to noise (narrow band noise, 120 dB, 16 kHz, 6 h). Left ears of the rats were irradiated with a LLLT (830 nm, 594 J, 165 mW/cm$^2$ for 60 minutes per day) for 12 days, starting 3 days (1st group)and 7 days (2nd group)post induction of NIHL. Right ears were used as control ears. The hearing levels were measured at each frequency of 4, 8, 12, 16, and 32 kHz before and after the noise exposure and post 12th irradiations.

Results: The initial hearing levels in all frequencies before and after the noise exposure were 26.5, 24.5, 24.0, 24.0 and 24.5 dB SPL and 63.5, 64, 71.5, 73.5 and 67.5 dB SPL in 4, 8, 12, 16 and 32 kHz, respectively in 6 ears. After 12th irradiation, the thresholds of the LLLT treated left ears of the 1st group recovered significantly better (22, 30, 65, 30 and 25 dB SPL, $p<0.05$) compared to those of the untreated right ears (70, 85, 90, 80, 75 dB SPL). However, for the 2nd group, the recovery of the LLLT treated left ears (32.5, 41.3, 60.0, 57.5, and 45.0 dB SPL, $p<0.05$) was not significantly improved compared to that of the untreated right ears (25.0, 37.5, 52.5, 38.8, and 26.3 dB SPL).

Conclusion: The results of this study suggest that optimal time to treat NIHL with LLLT was within 3 days from the induction of NIHL but the hearing failed to recover if the LLLT was started 7 days post induction of NIHL.

8207C-325, Session 5

## Office-based optical coherence tomography for pre-operative assessment of middle ear pathology

J. F. Ilgner, Univ. Hospital Aachen (Germany); C. Farkas, European Laser Institute (Germany); A. Lenenbach, Fraunhofer-Institut für Lasertechnik (Germany); M. Westhofen, Univ. Hospital Aachen (Germany)

No abstract available

8207C-326, Session 5

## Three-dimensional vibration measurements of the human eardrum and middle ear ossicles

R. P. Jackson, H. Cai, Stanford Univ. (United States); S. Puria, EarLens Corp. (United States)

Why do larger mammals have an articulated malleus-incus joint? One possibility is that the mobile, saddle-shaped connection between these bones enables efficient high frequency sound conduction. Morphometric studies in our lab suggest that the malleus and incus each rotate about independent axes and interact in a way that resembles a bevel gear at high frequencies. In addition, asymmetry in the eardrum may help to "twist" the malleus, which would further amplify an energetically favorable, gear-like effect (Puria and Steele, 2010). We are investigating these potential motions through three-dimensional laser Doppler vibrometry (3DLV) and finite element modeling of the human middle ear. Here we will present the findings of our vibration measurements for fresh human temporal bones (n=4). For eardrum surface measurements, we considered both the in-plane and out-of-plane velocities of the entire eardrum in the 0.5 to 20 kHz range (SNR>20 dB). The velocity component along the focal axis approximates the out-of-plane velocity, and the two velocity components in the shared focal plane of the 3DLV lasers approximate the in-plane velocity. We found the shape, amplitude, number and position of measured eardrum surface waves in general agreement with other publications, which quantified out-of-plane motion only (e.g., Cheng et al., 2010). Though negligible at low frequency, the in-plane motion is, surprisingly, of the same order-of-magnitude as the out-of-plane motion beyond 4 kHz. The relative phase, of in-plane and out-of-plane motion is equal at low frequency, but beyond 6 kHz the in-plane significantly lags the out-of-plane motion suggesting a greater time delay. We are also applying our measurement technique to look at the relative, and possibly rotational, motion of the malleus, incus, and stapes as further evidence for a "gear" in the middle ear. [Work supported by R01 DC005960 and ARRA supplements to SP/CRS and F30DC010305 to RPJ from the NIDCD of NIH.]

8207C-327, Session 5

## Cellular-level imaging of the functional mammalian inner ear

S. Batts, E. L. M. Cheung, N. H. Blevins, G. R. Popelka, Stanford Univ. (United States); M. J. Schnitzer, Stanford Univ. School of Medicine (United States)

No abstract available

8207C-328, Session 5

## Methodology for assessment of structural vibrations in the mouse cochlea by spectral domain optical coherence tomography

S. S. Gao, Stanford Univ. School of Medicine (United States); P. Raphael, Baylor College of Medicine (United States); A. Xia, Stanford Univ. (United States); J. Park, Texas A&M Univ. (United States); E. F. Carbajal, Univ. of Houston (United States); B. E. Applegate, Texas A&M Univ. (United States); J. S. Oghalai, Stanford Univ. (United States)

Clinical diagnosis of cochlear dysfunction typically remains incomplete due to a lack of proper diagnostic methods. Medical imaging modalities can only detect gross changes in the cochlea, and non-invasive in vivo cochlear measurements are scarce. As a result, extensive efforts have been made to adapt optical coherence tomography techniques to analyze and study the cochlea. Herein, we detail the methods for measuring vibration of cochlear structures in a mouse model as a result of sound stimulus. We used spectral domain OCT with ~950 nm as the center wavelength and a bandwidth of ~80 nm. The custom spectrometer used was based on a high speed line scan camera which is capable of line rates up to 28 kHz. The signal-to-noise ratio of the system was ~90 dB. The data collection and processing software was written in LabVIEW and MATLAB. We tested whether streaming directly from the camera, writing the data to multiple hard drives in the RAID-0 configuration, and processing using the GPU shortened experiment times. We then analyzed the A-line phase noise over several hundred milliseconds and growth curves from a piezoelectric element and structures inside the mouse cochlea. We believe this is the first step towards a diagnostic device which generates vibration information of cochlear structures.

8207C-329, Session 5

## Simultaneous depth-resolved imaging of sub-nanometer scale ossicular vibrations and morphological features of the human-cadaver middle ear with spectral-domain phase-sensitive optical coherence tomography

H. M. Subhash, A. T. Nguyen-Huynh, Oregon Health & Science Univ. (United States); R. Wang, Univ. of Washington (United States); S. L. Jacques, A. L. Nuttall, Oregon Health & Science Univ. (United States)

We describe a novel method for the detection of the tiny motions of the middle ear (ME) ossicles and their morphological features with a spectral-domain phase sensitive optical coherence tomography (PS-OCT). Laser Doppler Vibrometry (LDV) and its variations are the most extensively used methods for studding the vibrational modes of the ME. However, most techniques are limited to single point analysis methods, and do not have the ability to provide depth resolved simultaneous imaging of multiple points on the ossicles especially with the intact eardrum. Consequently, the methods have the limited ability to provide relative vibration information at these points. In this study, we demonstrated the feasibility of using PS-OCT for simultaneous depth resolved imaging of both vibration information and morphological features in a cadaver human middle ear with high sensitivity and resolution. This technique has the potential to provide meaningful vibration of ossicles with a vibration sensitivity of ~0.5nm at 1KHz acoustic stimulation. To the best of our knowledge, this is the first demonstration of depth-resolved vibration imaging of ossicles with a PS-OCT system at sub-nanometer scale.

Acknowledgements

This work was supported by research grants from the National Institute of Deafness and other Communication Disorders (Grants R01DC010399, R01DC00141 and KL2RR024141).

8207C-330, Session 6

## Vocal register switch as seen by high speed digital imaging, EGG, kymography, and acoustics

K. Izdebski, Pacific Voice and Speech Foundation (United States); Y. Yan, Santa Clara Univ. (United States); G. Rust, Pacific Voice and Speech Foundation (United States); C. Cook, Pacific Voice and Speech Foundation (United States) and Santa Clara Univ. (United States) and San Francisco Conservatory of Music (United States)

No abstract available

8207C-331, Session 6

## Improvement of clinical assessment of selected mucosal vocal folds lesions using high speed digital imaging, kymography with simultaneous electroglottography and acoustics signals

K. Izdebski, Pacific Voice and Speech Foundation (United States); Y. Yan, Santa Clara Univ. (United States); R. M. Cruz, Santa Clara Univ. (United States) and Pacific Voice and Speech Foundation (United States) and Kaiser Permanente Medical Ctr. (United States)

No abstract available

8207C-332, Session 6

## Long range Fourier domain OCT for real time anatomic imaging of human upper airway

J. Zhang, J. Jing, B. J. Wong, Z. Chen, Beckman Laser Institute and Medical Clinic (United States)

Presently there are limited methods to provide structural and anatomical information on the upper airway with a relatively modest cost and without the risks of ionizing radiation. Furthermore, no currently available diagnostic tests can provide airway volumetric information in real-time for sustained time intervals. Endoscopic long range optical coherence tomography (OCT) enables ionizing free non-invasive high resolution cross-sectional optical imaging of biological tissue and can potentially address these needs. In this report, we present development and testing of a high speed long range endoscopic Fourier domain OCT (FDOCT) system capable of non-invasive real time acquisition of quantitative anatomic information about the lumen size, and shape of human upper airway. The long range FDOCT system is based on a rapid scanning wavelength swept source and can achieve an imaging rate of 100 frames/second. A rotating OCT endoscopic probe with working distance of 25 mm, outer diameter of 1.2 mm and rotating rate of 100 revolutions/second is designed to move within a stationary transparent protective biocompatible sheath with outer diameter of 3 mm. A high speed linear motor outside the endoscope is used to pull back the entire probe to create a 3-D helical scan. Parallel computing algorithms based on graphics processing unit (GPU) combined with a dual-quad-core high speed CPU processor implementing Intel hyperthreading are used to achieve real time processing and display.

8207C-333, Session 6

## Asynchrony of mucosal wave in normal subjects investigated by HSDI, Kymography, stroboscopy and and processed with Nyquist plots

Y. Yan, Santa Clara Univ. (United States); K. Izdebski, Pacific Voice and Speech Foundation (United States); R. Ward, Santa Clara Univ. (United States) and Pacific Voice and Speech Foundation (United States)

No abstract available

8207C-334, Session 6

## Confocal endomicroscopy of the larynx

T. Just, Univ. Rostock (Germany)

Beside the good image quality with the confocal laser scanning microscope (HRTII) and the Rostock Cornea Module (RCM), this technology can not be used to investigate the human larynx in vivo. To accomplish this, a rigid custom-made endoscope (KARL STORZ GmbH & Co. KG; Tuttlingen Germany) was developed. An adapter was developed to connect the scanner head of the HRTII to the rigid endoscope. With the connector, the starting plane can be set manually. To achieve optical sectioning of the laryngeal tissue (80 µm per volume scan), the scanning mechanism of the HRTII needs to be activated using a foot switch. The devices (endoscope, HRTII and connector) supply images of 400 x 400 µm and reach average penetration depths of 100-300 µm (λ/4 plate of the scanner head of the HRTII was removed). The lateral and axial resolutions are about 1-2 µm and 2 µm, respectively. In vivo rigid confocal endoscopy is demonstrated with an acquisition time for a volume scan of 6 s. Aim of this study was to differentiate pre-malignant laryngeal lesions from micro-invasive carcinoma of the larynx. 22 patients with suspicious lesions of the true vocal cords were included. This pilot study clearly demonstrates the possibility to detect dysplastic cells close to the basal cell layer and within the subepithelial space in lesions with small leukoplakia (thin keratin layer). These findings may have an impact on microlaryngoscopy to improve the precision for biopsy and to identify the margins of the pre-malignant lesion.

8207C-335, Session 7

## Virtual optical laryngoscopy

S. Luo, Y. Yan, Santa Clara Univ. (United States)

No abstract available

8207C-336, Session 7

## Preliminary subglottic stenosis imaging in a rabbit model using OCT

J. L. Lin, J. W. Boyd, B. J. Wong, Univ. of California, Irvine (United States)

Preliminary Subglottic Stenosis Imaging in a Rabbit Model Using OCT

Jennifer L Lin, MD,3, Ashley Hamamoto1, Lauren Tracey1, Andrew Heidari1, Alex Wong1, Jonathon Boyd, MD3, Zhongping Chen, MD, Brian J Wong, MD, PhD1,2,3

1Beckman Laser Institute and the Center for Biomedical Imaging, University of California, Irvine, CA 92612

2University of California, Irvine, Department of Biomedical Engineering, Irvine, California 92697

3University of California Irvine, Department of Otolaryngology, Irvine, California 92868

Abstract

Subglottic stenosis (SGS) is a severe acquired deformity of the neonatal airway that is a consequence of prolonged endotracheal intubation. Neonates are most susceptible to this disease because of the small caliber of the airway. Currently, the only way to diagnose subglottic stenosis is with surgical endoscopy. OCT (optical coherence tomography) coupled with a fiber optic probe may provide a noninvasive way to diagnose both the development and progression of subglottic stenosis by imaging the structure of this region through the endotracheal tube. This could potentially guide neonatologist in their management of the neonatal airway, and reduce the progression of this disease to severe surgical cases. We present work on a rabbit subglottic stenosis model and concurrent development of an advanced, high speed, high resolution OCT imaging system using a 3-D MEMS-based scanning probe integrated with a fiber optic probe to acquire fine and detailed anatomic data of the subglottis. This model will provide correlation between surgical endoscopy, OCT imaging and histological changes in tissue; laying a foundation for translating this work into Neonatal Intensive Care Units.

8207C-337, Session 7

## Role of the mucosal wave in voice production

D. D. Mehta, Massachusetts General Hospital (United States)

No abstract available

8207C-338, Session 7

## Miniature OCT endoscopic probe for in vivo human vocal folds imaging

G. Liu, B. J. Wong, Z. Chen, Beckman Laser Institute and Medical Clinic (United States)

We designed a miniature optical coherence tomography (OCT) endoscopic probe for in vivo imaging of human vocal folds. The probe has a small diameter (<3mm) and provides one dimension fast forward scanning capability. A PZT-based device is used for beam scanning. For in vivo human vocal folds imaging, a long working distance is preferred and a whole fiber focusing device was made for this purpose. A high speed functional swept source OCT system with an imaging speed of 100,000 A-lines per second was developed. The OCT system can provide both structure and functional information regarding the sample. The endoscopic OCT system with the designed probe offer a new way to look at the vocal folds.

8207C-339, Session 7

## Visualizations by acoustics of voice stress. Is there an optical mucosal wave correlate?

G. Demenko, M. Jastrzebska, Poznan Computing Ctr. (Poland); K. Izdebski, Pacific Voice and Speech Foundation (United States); Y. Yan, Santa Clara Univ. (United States)

No abstract available

8207C-340, Session 7

## What are we learning about neoglottic phonation from HSDI

L. Skladany, Univ. of Nevada, Reno (United States)

No abstract available

8207C-341, Session 8

## Advanced micro scanning in laryngology: implications of new advanced scanning in relation to HSDI acquired signals

M. Pedersen, The Medical Ctr. (Denmark)

No abstract available

8207C-342, Session 8

## A silent speech interface based on real time imaging of the vocal tract

L. Crevier-Buchman, Lab. Phonétique et Phonologie (France); B. Denby, Ecole Supérieure de Physique et de Chimie Industrielles (France); T. Hueber, Gipsa-lab (France); M. Cai, S. Manitsaris, Ecole Supérieure de Physique et de Chimie Industrielles (France); G. Chollet, Telecom ParisTech (France); M. Stone, Univ. of Maryland, Baltimore (United States); C. Pillot-Loiseau, Lab. Phonétique et Phonologie (France); G. Dreyfus, P. Roussel, Ecole Supérieure de Physique et de Chimie Industrielles (France)

No abstract available

8207C-343, Session 8

## Comparison of laryngeal examination visualized by fiber-optic, video-chip and high definition video chip endoscopy

J. P. Thomas, Laryngology Practice and Pacific Voice and Speech Foundation (United States)

No abstract available

8207C-345, Session 8

## Integration of flexible fiberoptic high-speed videoendoscopy with time-synchronized measures of vocal function

D. D. Mehta, D. D. Deliyski, S. M. Zeitels, Massachusetts General Hospital (United States); M. Zañartu, Univ. Técnica Federico Santa María (Chile); R. E. Hillman, Massachusetts General Hospital (United States)

No abstract available

8207C-346, Session 8

## Visual HDSI analysis of laryngeal tremor: acoustic correlates?

J. Barkmeier-Kraemer, Univ. of California, Davis (United States); K. Izdebski, Pacific Voice and Speech Foundation (United States)

No abstract available

8207C-347, Session 9

## What we can learn about hereditary dystonia from HSDI of the glottis

M. Pedersen, M. Eeg, The Medical Ctr. (Denmark)

No abstract available

8207C-348, Session 9

## Visual observations of synchronized circular breathing and glottic activity in didgeridoo performer

L. Hyde, K. Izdebski, J. C. Ross, Pacific Voice and Speech Foundation (United States)

No abstract available

8207C-349, Session 9

## Enhancement of diagnoses of allergic laryngitis using stroboscopic visual images of the vocal folds

E. Chavez,

No abstract available

8207C-350, Session 9

## Stroboscopic visualization of laryngeal mucosal wave before and after treatment for reflux: is there objective visual evidence?

J. Schloemicher-Thier, M. Weikert, Austrian Voice Institute (Austria)

No abstract available

8207C-351, Session 9

## Visualization of non-laryngeal phonation modes: a physiologic and acoustic model of alternative phonatory patterns

F. Fussi, Consultant (Italy)

No abstract available

8207C-352, Session 10

## Double-blind, randomized, intra-individual controlled feasibility trial comparing the use of 1,470 and 940 nm diode laser for the treatment of hyperplastic inferior nasal turbinates

R. Sroka, M. Havel, A. Leunig, Ludwig-Maximilians-Univ. München (Germany); P. Patel, The Univ. of Queensland School of Medicine (Australia); C. S. Betz, Ludwig-Maximilians-Univ. München (Germany)

No abstract available

8207C-353, Session 10

## Human airway structure modeling using long rang OCT

J. Jing, J. Zhang, Beckman Laser Institute and Medical Clinic (United States); M. Rubinstein, A. E. Chin Loy, B. J. Wong, Univ. of California, Irvine School of Medicine (United States); Z. Chen, Beckman Laser Institute and Medical Clinic (United States)

Modeling of the human airway requires the acquisition of a large amount of data to accurately represent the entire system. CT (computed tomography) scans are typically used to provide a slice by slice view of the airway; however the slice resolution must be limited due to the high radiation associated with CT. Long range OCT (optical coherence tomography) coupled with a fiber optic probe presents another means to acquire the same data set but with both fine slice resolution as well as with high image acquisition speeds. In this manuscript, we present work on the development of a long range OCT endoscopic probe (1.2mm OD, 25mm working distance) used in conjunction with a time domain OCT system to acquire surface structure data of the human airway. The probe is small enough to fit within the instrument channel of a fiber endoscope and by rotating and translating the probe together, 3D data sets can be acquired. We also explore using a swept source OCT system with frequency shifting techniques to double the imaging range of a typical system to acquire high speed images of the airway for use in comprehensive volumetric flow modeling throughout the airway

8207C-354, Session 10

## Thermal and mechanical processes in laser reshaping of costal cartilage for ENT

O. I. Baum, Y. M. Soshnikova, E. N. Sobol, Institute on Laser and Information Technologies (Russian Federation)

Laser reshaping of cartilage is a new effective and safe technique for correction of nasal septum and ear deformities. Costal cartilage is a most suitable natural material for transplantation. The problem is to obtain stable proper shape of cartilage implants. The objective of the work is to study reshaping of porcine costal cartilage for larynx stenosis surgery using Erbium glass fiber laser.

Porcine cartilage plates 3 mm in thickness were mechanically curved and irradiated (1) on one side (stretched or compressed) and (2) on both sides with different sequence. Irradiation was performed using a 1.56 microns laser with power varied from 1 to 2.5 W, exposure time from 5 to 20 s, spot diameter of 2.5 mm, pulse duration of 500 ms, pulse repetition rate of 1.4 Hz. For each laser setting, stable curvature radius was measured during 24 h after the experiment. Irradiated samples were analyzed by means of differential scanning calorimerty (DSC) to reveal the collagen denaturation degree.

The optimum laser setting for stable reshaping of costal cartilage without visual thermal damage of cartilage matrix was established. It is shown that (1) it is possible to use laser reshaping technique for making stable proper shape of costal cartilage, and (2) primary irradiation of compressed side followed with an irradiation of stretched side is more effective than reverse sequence of laser treatment. DSC analysis showed that thermal effect of irradiated specimens (2.58-3.79 J/g) was slightly lower that that for intact cartilage specimens and considerably lower than that for denaturation of collagen (65±5 J/g).

It is possible to use laser reshaping technique for preparation of stable cartilage implants. Nonlinear thermomechanical behavior of cartilage is experimentally revealed. The influence of irradiation sequence on curvature radius of cartilage grafts is established for the first time.

8207C-355, Session 10

## Imaging of the internal nasal valve using optical coherence tomography

A. E. Chin Loy, B. J. Wong, Z. Chen, J. Jing, Beckman Laser Institute and Medical Clinic (United States); E. Heidari, OCT Medical Imaging, Inc. (United States)

The internal nasal valve is located at the opening of the piriform aperture. The caudal end of the upper lateral cartilage, the nasal septum and the inferior turbinate forms its boundaries. The internal nasal valve represents the narrowest segment of the airway and slight adjustments of the angle can alter airflow and reduce obstructive symptoms. In Caucasian noses, the angle ranges from 10° to 15°, while Asian and Black valves may have more obtuse angles. Currently, CT scan is the technique of choice for measurement of the valve angle. This method is limited, as it does not provide real time imaging of a dynamic valve. Optical Coherence Tomography (OCT) provides real time imaging of the angle of the internal nasal valve with minimal time investment from the patient. OCT can be used in the pre- and post-operative periods as an objective measure of degree of change of the internal nasal valve without exposing the patient to ionizing radiation.

8207C-356, Session 10

## Viability of electromechanically reshaped cartilage

K. Badran, S. Hussain, C. Manuel, Univ. of California, Irvine (United States); D. E. Protsenko, B. J. Wong, Beckman Laser Institute and Medical Clinic (United States)

Background/Objective: Electromechanical reshaping (EMR) has been recently described as an alternative method for reshaping facial cartilage without the need for incisions or sutures. Assessing chondrocyte viability with a live/dead assay and confocal microscopy is well established. This study focuses on determining the viability of chondrocytes following EMR in costal cartilage.

Method: Within 48 hours of euthanasia, the harvested ears were stained under low light to prevent premature fluorescence of the dyes used. The assay uses a system of 2 fluorescent nucleic acid stains that weakly bind to DNA and RNA. A 480 nm argon laser-scanning confocal microscope (Zeiss, Göttingen, Germany) was used to image stained specimens at 10x magnification. The assay determines cell viability on the basis of cell membrane integrity, which is considered an accurate indicator of cell viability. The fraction of viable chondrocytes were qualitatively assessed and correlated with voltage, voltage application time and electric field configuration.

Results: The fraction of viable chondrocytes decreased with voltage and application time. High local electric field intensity and proximity to the positive electrode also focally reduced chondrocyte viability.

Conclusion: Viability results will aid in the optimization of EMR dosimetery and needle geometry as the parameters are adjusted to allow for the maximum amount of reshaping with the minimum amount of cell death.

8207C-357, Session 10

## Integration of flexible fiberoptic high-speed videoendoscopy with time-synchronized measures of vocal function

D. D. Mehta, D. D. Deliyski, S. M. Zeitels, M. Zañartu, R. E. Hillman, Massachusetts General Hospital (United States)

No abstract available

8207C-358, Session 10

## Software for the analysis of laryngeal imaging recordings

S. Luo, T. Jiang, N. Gu, Southeast Univ. (China); Y. Yan, Santa Clara Univ. (United States)

No abstract available

# Conference 8207D: Optical Techniques in Pulmonary Medicine

Saturday 21 January 2012

Part of Proceedings of SPIE Vol. 8207D Optical Techniques in Pulmonary Medicine

8207D-55, Session 1

## Optical techniques in pulmonary medicine

S. Lam, The BC Cancer Agency Research Ctr. (Canada)

No abstract available

8207D-56, Session 1

## Limitations of commercial time-domain optical coherence tomography in the airways

S. D. Murgu, H. G. Colt, D. S. Mukai, M. Brenner, Univ. of California, Irvine (United States)

Background and Objective: Time domain OCT systems are approved for imaging human microstructures. Bronchoscopic application of this OCT technology, however, remains uncommon. The purpose of this study was to identify the major limitations of commercial time domain OCT in the study of central airway disorders.

Materials and Methods: Commercially available time-domain OCT with front imaging and inside actuation (Niris Imaging System; Imalux Corp., Cleveland, OH) was used in 20 patients with central airway disorders who underwent rigid bronchoscopy between January 2009 and June 2011 for clinical indications at UC Irvine Medical Center (IRB # 2006-4982). OCT tomograms characteristics are illustrated to describe the shortcomings of this technology.

Results: OCT revealed a similar pattern of homogeneous light backscattering layer and absence of normal layered microstructures in patients with malignant airway tumors such as primary lung carcinoma (Fig. A) and melanoma (Fig. B), or benign tracheal disease such as severe tracheatis (Fig. C), idiopathic stenosis (Fig. D) and granulation tissue (Fig. E). There are significant motion artifacts due to cardiac and respiratory movements despite general anesthesia and positioning of the probe on the tracheal wall may be difficult (Fig. E). After laser treatment, OCT of charred tissue showed high-backscattering, reduced penetration and shadowing artifacts (Fig. F) and OCT of non-charred laser treated tissues showed a homogeneous, bright light-backscattering. The normal epithelium, mucosa and submucosa can be visualized when imaging the cartilaginous wall (Fig. G) and the posterior membrane (Fig. H) but the human tracheal and mainstem bronchial cartilage cannot be visualized in its entirety in cross section (Fig G). The low image acquisition rate does not allow real time three dimensional image reconstruction.

Conclusion: For in vivo human airway applications, currently commercially available time domain OCT is limited by: 1) inability to distinguish between benign and malignant central airway disorders; 2) compromised image quality due to laser induced charring, cardiac and respiratory motions and difficulty in positioning the probe on the tracheal wall due to front imaging feature; 3) inability to image the entire cartilage in cross section due to limited imaging depth; and 4) lack of real time three dimensional imaging from volume-based airway wall regions. Development of commercial OCT systems with faster scanning speed, producing images with much higher spatial resolution, with or without other optical or acoustic imaging modalities could overcome many of these current limitations and should be considered for airway application investigations.

8207D-57, Session 1

## Improvements to a laser Raman spectroscopy system for reducing the false positives of autofluorescence bronchoscopies

H. C. Pawluk, M. A. Short, S. Lam, A. McWilliams, D. Ionescue, H. Zeng, The BC Cancer Agency Research Ctr. (Canada)

Preneoplastic lesions of the bronchial tree have a high probability of developing into malignant tumours. Currently the best method for localizing them for further treatment is a combined white light and autofluorescence bronchoscopy (WLB+AFB). Unfortunately the average specificity from large clinical trials for this combined detection method is low at around 60%, which can result in many false positives. However a recent pilot study showed that adding a point laser Raman spectroscopy (LRS) measurement improved the specificity of detecting lesions with high grade dysplasia or carcinoma in situ to 91% with a sensitivity of 96% compared to WLB+AFB alone. Despite this success, there is still room for much improvement. One constant need is to find better ways to measure the inherently weak Raman emissions in vivo which will result in even better diagnostic sensitivity and specificity.

With this aim in mind a new generation Raman system was developed. The system uses the latest charge coupled device (CCD) with low noise, and fast cool down times. A spectrometer was incorporated that was able to measure both the low and high frequency Raman emissions with high resolution. The Raman catheter was also redesigned to include a visible light channel to facilitate the accurate indication of the area being measured. Here the benefits in the adjunct use of LRS to WLB + AFB are presented, and description of the new system and the improvements it offers over the old system are shown.

8207D-58, Session 1

## Measurements of airway wall structure by OCT: correlations with histology

P. M. Lane, A. M. D. Lee, The BC Cancer Agency Research Ctr. (Canada); T. Candido, The Univ. of British Columbia (Canada); K. Ohtani, The BC Cancer Agency Research Ctr. (Canada); R. Shalansky, The Univ. of British Columbia (Canada); A. McWilliams, T. Shaipanich, The BC Cancer Agency Research Ctr. (Canada); H. O. Coxson, The Univ. of British Columbia (Canada); C. E. MacAulay, S. Lam, The BC Cancer Agency Research Ctr. (Canada)

Optical coherence tomography (OCT) has been shown to provide high spatial and temporal resolution of human airways. It has the potential to identify the changes associated with airway diseases such as early cancer, asthma, and chronic obstructive pulmonary disease (COPD). In previous studies, we showed that early squamous cell carcinoma of the lung as imaged by OCT is associated with increased thickness of the bronchial epithelium. We also reported changes associated with airway remodeling in patients with COPD. However, the gold standard for diagnosis of these diseases is histopathology. Although changes in airway morphology have been observed and measured using OCT, a detailed comparison and correlation with histopathology has been difficult. The aim of this study is to correlate bronchial OCT images with histopathological images obtained from the identical region of the airway. This will improve the understanding of bronchial OCT imagery ultimately leading to better interpretation of disease status in the human airways. Three-dimensional (3-D) frequency domain OCT datasets were acquired from freshly excised pig and human airways before and after fixation in10% buffered formalin. Serial sections were cut from the paraffin embedded tissue blocks and matched to OCT images using anatomic landmarks. The total airway wall area, lumen area and tissue layers (smooth muscle, cartilage, etc) were manually measured using both techniques. The OCT measurements, before and after fixation, were compared to histopathology.

8207D-59, Session 1

## Volumetric optical frequency domain imaging of pulmonary pathology

L. P. Hariri, M. B. Applegate, M. Mino-Kenudson, E. J. Mark, B. E. Bouma, G. J. Tearney, M. J. Suter, Massachusetts General Hospital (United States)

Lung cancer is the leading cause of cancer-related deaths. Squamous cell (SCC) and neuroendocrine cancers typically arise in association with conducting airways, where as adenocarcinomas are more peripherally located. Tissue biopsies are often limited by small size and/or incomplete sampling. Optical frequency domain imaging (OFDI) provides large area 3-dimensional views of tissue microstructure at near-histological resolution (analogous to 4x microscopy). Recently, optical frequency domain imaging has been used bronchoscopically in vivo, but lack of correlated histopathology has limited the ability to develop imaging criteria. To assess correlated OFDI and histopathology, we performed OFDI through two approaches (bronchoscopic airway centered and pleural based parenchymal imaging) with a custom-built 2.4 French (0.8mm diameter) bronchoscopic catheter ex vivo in 47 surgical and 3 autopsy specimens. Tissue samples were marked with tissue dye to precisely correlate imaging and histological sampling locations. OFDI of normal airway allowed visualization of epithelium, lamina propria, submucosal glands, cartilage, and alveolar attachments. Carcinomas exhibited architectural disarray, loss of normal airway/alveolar structure, and rapid light attenuation. SCC showed nested architecture, while atypical glandular formation was appreciated in adenocarcinomas and mucoepidermoid carcinomas. Mucinous adenocarcinomas showed alveolar wall thickening with intra-alveolar mucin. This study is the first demonstration of volumetric OFDI with precise correlation to tissue-based diagnostics in lung pathology. With the amount of detail provided by the high resolution and vast volumes obtained, we anticipate OFDI may play a role in guiding interventional pulmonary procedures, such as CT-guided and transbronchial fine needle aspiration, and in future detection of pulmonary airway disease.

8207D-60, Session 2

## Quantitative investigation of alveolar structures with OCT using total liquid ventilation during mechanical ventilation

C. Schnabel, S. Meissner, E. Koch, Universitätsklinikum Carl Gustav Carus Dresden (Germany)

There is a lack of understanding lung tissue during mechanical ventilation on an alveolar level. Furthermore, numerical models describing the tissue behavior do not exist. With numerical models of the lung, new and more protective ventilation methods could be investigated. Our aim is to gain information about the lung behavior to develop such numerical models. We used optical coherence tomography (OCT) as a contactless and non-invasive imaging modality to acquire three-dimensional images of lung tissue with micro-scale resolution. However, OCT image quality depends on the intensity of the backscattered near-infrared light, which is caused by the change of refractive index at each air-tissue interface of alveolar structures. Hence, image artifacts lead to an incorrect imaging of the real tissue structure inside the sample. We can avoid image artifacts by using total liquid ventilation to match the refractive index inside the alveoli to the one of the surrounding tissue. In this study, we present the influence of OCT image quality on investigations of the alveolar structure for both air-filled and liquid-filled lung tissue in an in vivo animal model. Hence, we can determine quantitative differences between air-filled and liquid-filled volume changes during ventilation. By comparing air-filled and liquid-filled images obtained with OCT, we can show more detailed and realistic imaging of lung tissue by using total liquid ventilation. The knowledge of these quantitative differences can be used for further studies to achieve more precise data supporting the development of numerical models of the lung.

8207D-61, Session 2

## Modeling of light refraction to investigate the validity of alveolar shape and volume visualized by optical frequency domain imaging

C. I. Unglert, Wellman Ctr. for Photomedicine (United States) and Harvard Medical School (United States) and Air Liquide R&D Medical Gases (France); W. C. Warger II, E. Namati, Wellman Ctr. for Photomedicine (United States) and Harvard Medical School (United States); B. E. Bouma, G. J. Tearney, Wellman Ctr. for Photomedicine (United States) and Harvard Medical School (United States) and Massachusetts Institute of Technology (United States)

Accurate visualization and quantification of alveolar structure is crucial to advance our understanding of normal and diseased alveolar physiology. Optical frequency domain imaging (OFDI) has been used increasingly to study mammalian pulmonary alveoli in vivo. However, artifacts have been reported in the resultant images that greatly reduce the imaging depth and create the appearance of double walls. It has been hypothesized that these artifacts are caused by the refraction of light at the tissue-air interfaces, resulting in inaccurate representations of alveolar shapes and volumes in OFDI images.

A two-dimensional ray-tracing model was created to illustrate the refraction of light by circular objects that approximate alveolar cross-sections. The modeling results were validated with experimental OFDI images of hollow glass spheres and glass capillaries filled with various index calibration oils. Simulated images of adjacent alveolar cross-sections show the appearance of double and triple walls similar to those observed in OFDI images of excised rat lungs. Modeling several layers of alveoli suggests severe distortion of all alveoli beneath the top layer, providing a possible explanation for the limited imaging depth. Finally, the relation between air filled alveolar cross-sectional areas and different tissue refractive indices was studied. According to our results, alveolar areas as represented by OFDI are underestimated by 29% in fresh tissue and 34% in fixed tissue.

This model demonstrates that refraction may be the primary cause for artifacts and inaccurate visualization of alveolar structure in OFDI images and provides a tool to study the influence of a variety of refractive indices.

8207D-62, Session 2

## Multimodal imaging of lung tissue using optical coherence tomography and two-photon microscopy

M. Gaertner, P. Cimalla, S. Geissler, S. Meissner, C. Schnabel, Universitätsklinikum Carl Gustav Carus Dresden (Germany); W. M. Kuebler, Charité Universitätsmedizin Berlin (Germany) and Univ. of Toronto (Canada); E. Koch, Universitätsklinikum Carl Gustav Carus Dresden (Germany)

The alveolar behavior of lung tissue during breathing and ventilation is one of the main topics in the research of pulmonary mechanics. Yet, it is not known how differently sized alveoli are stabilized during their inflation and deflation. One basic stabilizing mechanism is given by extracellular matrix proteins, such as elastin and collagen. To understand the dynamic changes occurring on the alveolar level of the lung, we asked how to monitor the structure of alveoli and the density and distribution of elastic substances in a minimal-invasive model for lung dynamics. As a result, we show a combination of optical coherence tomography (OCT) and two photon microscopy (TPM) that is able to image volume changes of alveoli (with OCT) and the behavior of elastic fibers (with TPM) simultaneously. OCT visualizes three-dimensional deformations of the lung structure within a few seconds. Via image registration between OCT and TPM, the fast imaging of OCT can be assigned to the slower TPM technique. On the contrary, TPM shows functional details within the tissue, which are not accessible with OCT imaging alone. In our setup, we use ultra-short laser pulses to allow two photon excitation of elastin and second harmonic generation of collagen. Due to its fiber guided modality, the setup can be easily adjusted to bulk specimens. This allows research that is not restricted to tissue slices and makes animal studies under physiological conditions feasible. With this, a new method is introduced that opens up new insights into the behavior of microscopic lung compartments.

8207D-63, Session 2

## Four-dimensional visualization of peripheral alveolar dynamics during uninterrupted ventilation in vivo

W. C. Warger II, E. Namati, C. I. Unglert, J. E. Eckert, B. E. Bouma, G. J. Tearney, Massachusetts General Hospital (United States)

Pulmonary alveoli are spherical sacs that line and terminate the respiratory airways within the lung to provide gas exchange of oxygen and carbon dioxide with the bloodstream. While this process is crucial to sustaining life, no unifying hypothesis exists for the dynamic mechanics of alveoli during respiration. The uncertainty derives from the miniature size of alveoli (100-300 µm diameter) and the constant motion during respiration that prevent current three-dimensional imaging techniques, such as CT and MRI, from visualizing continuous alveolar dynamics in vivo. Optical techniques have provided much of the knowledge of alveolar dynamics, but these analyses have been limited to cross-sectional areas leading to uncertainty regarding their three-dimensional structure. Recently, however, optical coherence tomography (OCT) has shown promise for imaging and measuring three-dimensional volumes of peripheral alveoli. Our lab has developed a second-generation OCT technique, termed optical frequency domain imaging (OFDI), that provides significantly increased acquisition rates for in-vivo volumetric imaging. Through the development of a light-weight miniature imaging probe, we have acquired OFDI images at a rate of 1mm x 1mm x 500µm volume/second, which allows us to visualize approximately 30 alveolar air spaces continuously within living swine ventilated at 10 breaths/min. Preliminary analysis of the data shows immediate alveolar expansion upon intratracheal pressure increase and then gradual contraction upon pressure decrease with repeatable PV curves across multiple breaths. This technique provides a crucial platform to develop prognostic indicators and treatment of alveolar-based injuries and diseases through complete 4D visualization of alveolar dynamics during uninterrupted ventilation in vivo.

8207D-64, Session 3

## Optical detection and diagnosis of peripheral pulmonary lesions

A. C. Chee, Massachusetts General Hospital (United States) and Foothills Medical Ctr, Univ. of Calgary (Canada); L. P. Hariri, M. B. Applegate, C. Channick, G. J. Tearney, B. E. Bouma, M. J. Suter, Massachusetts General Hospital (United States)

Lung cancer contributes more to cancer-related death than breast, colon and prostate cancer combined. Isolated lesions are more amenable to curable therapy and there has been an increasing effort to identify high-risk individuals with resectable pulmonary nodules. However, not all pulmonary nodules are malignant and without prior histology, patients with benign lesions could be subject to needless surgery. Therefore, patients who present with peripheral pulmonary lesions (PPLs) often require tissue confirmation to guide further management. Although recent advances have improved the clinician's capacity to bronchoscopically identify peripheral lesions, there remains a gap in the ability to successfully biopsy nodules. We have developed an optical coherence tomography (OCT) probe that will fit within a 22 gauge needle and can confirm biopsy needle placement within a PPL in real-time. In this report we present the results of preliminary work using a porcine model with simulated pulmonary lesions using an agar/bromine sulphate phantom. Agar phantoms were placed via a transthoracic approach with gross localization using multidetector computed tomography. The lesions were then identified bronchoscopically with radial-probe endobronchial ultrasound and guide sheath. Using a transbronchial probe within the needle lumen, OCT images were obtained to confirm needle placement within the lesion prior to sample aspiration. Images of normal lung parenchyma were also obtained for comparative purposes. This will be the first demonstration of a bronchoscopically compatible OCT transbronchial needle probe.

8207D-65, Session 3

## In situ 3D imaging of alveoli with a 30-gauge side-facing OCT needle probe

X. Yang, D. Lorenser, R. W. Kirk, B. C. Quirk, P. B. Noble, R. A. McLaughlin, D. D. Sampson, The Univ. of Western Australia (Australia)

Many lung diseases, such as emphysema and pulmonary fibrosis, affect the structure of the alveoli and smaller airways. Histological assessment is the gold standard to evaluate such pathologies, but unsuitable for in vivo measurements of fresh tissue. Recent work has proposed the use of OCT needle probes for in situ lung imaging. It is critical to minimize the size of such probes to reduce the likelihood of pneumothorax, and minimize tissue trauma and distortion during imaging.

We have developed a side-facing OCT needle probe encased in a 30-gauge needle (outer diameter 310μm). To the best of our knowledge, this is the smallest side-facing OCT needle probe reported to date.

The focusing optics consists of no-core and GRIN fibers spliced to a length of single-mode fiber, and terminated with a gold-coated, angle-polished section of no-core fiber to perpendicularly redirect the beam. The assembly is encased within a needle, with an etched side window through which the beam is emitted.

The probe was attached to a dual-arm spectral-domain OCT system (central wavelength 836 nm, source bandwidth 50 nm). The probe was mounted on a stepper motor for rotation, and retracted with a translation stage, allowing acquisition of a cylindrical 3D data volume with dimensions 2mm x 2.7mm (diameter x length).

Multiple 3D-OCT data sets were acquired on preterm lamb lungs (excised) filled with amniotic fluid. Results demonstrated the ability to image individual alveoli and bronchioles. We observed notably less tissue distortion than in earlier work with larger 23 gauge needle probes.

8207D-66, Session 3

## High-speed three-dimensional endoscopic optical frequency domain imaging with external k-clock sampling

J. Li, J. Mo, F. Helderman, M. de Groot, J. F. de Boer, Vrije Univ. Amsterdam (Netherlands)

We present here a high speed three dimensional endoscopic optical frequency domain imaging (OFDI) system with an external uniform k-space clock for point-by-point data sampling. Such method does not require over sampling and numerical post calibration, thus can acquire k-space uniform interval data in real time. To address laser source sweep to sweep jitter a real time phase stabilization algorithm was developed to calibrate k-space sampling in consecutive A-lines to suppress fixed pattern noise and enable Doppler processing.

We introduce the design and fabrication of a miniature endoscopic catheter. A micromotor with 1 mm diameter was utilized to develop a packaged catheter with 1.6mm outer diameter. The optical focusing system was designed for a 0.5mm working distance and 10 μm spot size in air. Integrated with the OFDI system at 50 kHz A-scan rate, a 3000rpm circumferential scanning speed was achieved.

Preliminary in vitro and in vivo 3D OFDI images of biological tissues, such as human finger and porcine trachea, will be demonstrated to verify the performance of the system. Further development, such as polarization and Doppler imaging, will be integrated toward comprehensive imaging for early diagnosis of lung cancer.

8207D-67, Session 3

## Development and testing of a fiber-based rotational monocoil OCT probe for airway imaging

A. E. Heidari, OCT Medical Imaging, Inc. (United States); D. Chou, OCT Medical Imaging, Inc. (United States) and Beckman Laser Institute (United States); D. S. Mukai, Univ. of California, Irvine (United States); S. B. Mahon, Beckman Laser Institute and Medical Clinic (United States); Z. Chen, Beckman Laser Institute and Medical Clinic (United States) and Univ. of California, Irvine (United States); M. Brenner, Univ. of California, Irvine (United States) and Beckman Laser Institute, University of California, Irvine (United States); R. S. Ramalingam, OCT Medical Imaging, Inc. (United States)

Inhalation injury is a major cause of morbidity and mortality for Soldiers in modern combat. Mechanisms of inhalation injury include thermal, chemical, biological, and toxic processes, as well as secondary infectious complications. In many cases, major changes in respiratory status occur in delayed fashion following inhalation injury. However, subclinical pathophysiological changes begin to occur in airway tissues almost immediately. Therefore, accurate early detection using a minimally invasive technology with high resolution is needed to recognize the extent of early airway damage. We have developed a swept-source based high speed touch-screen Fourier domain (FD-OCT) OCT system and two small diameter fiber optic guidewire based OCT probes adaptable into either rigid or flexible bronchoscope ( 2.2mm and 1.2mm) to investigate morphological and functional airway changes following smoke and cyanide exposure in rabbits. To scan the entire inner surface of trachea or bronchus the beam is rotated 360 degree using either a distal MEMS motor or by an external motor. All probes are housed inside a monocoil with an outer disposable sheath for sterility. Results show that 3-D endoscopic FD-OCT imaging performed using all monocoil probes can detect significant increases in the thickness of the tracheal walls of the rabbit beginning almost immediately after smoke inhalation injuries similar to previous published results. This will confirm that Quantification using in-vivo 3-D endoscopic OCT using monocoil probes provide a more sensitive tool for investigation of the effectiveness of various therapeutic interventions in smoke inhalation and other airway injuries.

Supported by Army grant W81XWH-09-C-0023

8207D-68, Session 3

## Three-dimensional high-resolution imaging of lung preparations using ultramicroscopy

D. Schwenninger, C. Dassow, J. Guttmann, Univ. Hospital Freiburg (Germany)

Analysis of the pulmonary microstructure is the basis to understand the organ's mechanical function during spontaneous breathing and mechanical ventilation. But, to the authors' knowledge, there is no image-data of complete lungs with sub-alveolar resolution that allows analysis of the lungs bronchoalveolar and cardiovascular structure.

Ultramicroscopy [1] is an imaging-method that has recently been used to record the neural network of whole brains and is, thus, capable of recording three dimensional (3D) image data of any tissue, including lungs, with micrometer-resolution.

The lung-tissue is fixated, bleached and dyed with fluorescent dye. The liquid in the preparation's tissue is, then, substituted by a clearing-solution with the same optical refractive index as the tissue's protein (Spalteholz-technique). The optically transparent lung is illuminated via combination of a rod-lense and a slit-aperture producing a thin "sheet" of light. Illumination was done with the excitation-wavelength of the fluorescent dye. Hence, the images of the fluorescent tissue that were recorded only showed structures within the illuminated sheet. By stepwise moving the light sheet illumination, recording of a 3D image-stack was possible.

Preliminary results proved functionality of the method and showed that lungs are suited for this method, because substitution of liquids in the tissue is easy due to the high accessibility of the tissue via the bronchial tree. An important advantage of this method is the mechanical elasticity of the transparent tissue. This allows 3D-recordings of the same lung at different lung volumes.

References:

[1] Dodt H. et al. 2007, Nature Methods 4(4):331-336

8207D-69, Session 3

## Ultrahigh-resolution optical coherence tomography imaging of diseased rat lung using Gaussian-shaped super-continuum sources

N. Nishizawa, S. Ishida, Nagoya Univ. (Japan); M. Kitatsuji, H. Ohshima, HOYA Corp. (Japan); Y. Hasegawa, M. Matsushima, T. Kawabe, Nagoya Univ. (Japan)

We have been investigating ultrahigh resolution optical coherence tomography (UHR-OCT) imaging of lung tissues using fiber super continuum sources. The high power, low-noise, Gaussian shaped supercontinuum (SC) generated with ultrashort pulses and optical fibers at several wavelengths were used as the broadband light sources for UHR-OCT. For the 800 nm wavelength region, the axial resolution was 3.0 um in air and 2.0 um in tissue. Since the lung consists of tiny alveoli which are separated by thin wall, the UHR-OCT is supposed to be effective for lung imaging. The clear images of alveoli of rat were observed with and without index matching effects by saline. The detailed structures of trachea were clearly observed.

In this work, we investigated the UHR-OCT imaging of lung disease model. The lipopolysaccharide (LPS) induced acute lung injury / acute respiratory distress syndrome (ALI/ARDS) model of rat was prepared as the sample with disease and the UHR-OCT imaging of the disease part was demonstrated. The increment of signal intensity by pleural thickening was observed. The accumulation of exudative fluid in alveoli was also observed for two samples. By the comparison with normal lung images, we can obviously show the difference in the ALI/ARDS models.

Since the lung consists of alveolar surrounded by capillary vessels, the effect of red-blood cells (RBC) is considered to be important. In this work, ex-vivo UHR-OCT imaging of RBC was demonstrated. Each RBC was able to be observed individually using UHR-OCT. The effect of RBC was estimated with the rat lung perfused with PBS.

8207D-75, Poster Session

## Lung vasculature imaging using speckle variance optical coherence tomography

A. M. D. Lee, M. Cua, P. M. Lane, A. McWilliams, T. Shaipanich, C. E. MacAulay, The BC Cancer Agency Research Ctr. (Canada); V. X. D. Yang, Ryerson Univ. (Canada); S. Lam, The BC Cancer Agency Research Ctr. (Canada)

Architectural changes in and remodeling of the bronchial and pulmonary vasculature are important pathways in diseases such as asthma, chronic obstructive pulmonary disease (COPD), and lung cancer. However, there is a lack of methods that can find and examine small bronchial vasculature in vivo. Structural lung airway imaging using optical coherence tomography (OCT) has previously been shown to be of great utility in examining bronchial lesions during lung cancer screening under the guidance of autofluorescence bronchoscopy. Here we use a fiber optic endoscopic OCT instrument to image vasculature in the lungs.

We use a commercial fiber optic endoscopic OCT instrument for imaging. The side-looking, circumferentially-scanning probe is inserted down the instrument channel of a standard bronchoscope and manually guided to the imaging location. Multiple images are collected with the probe spinning proximally at 100Hz. Due to friction, the distal end of the probe does not spin perfectly synchronous with the proximal end, resulting in non-uniform rotational distortion (NURD) of the images. First, we apply a correction algorithm to remove NURD. We then use a speckle variance algorithm to identify vasculature.

8207D-77, Poster Session

## Optical studies of tissue mitochondrial redox in isolated perfused rat lungs

R. Sepehr, K. Staniszewski, S. Maleki, Univ. of Wisconsin-Milwaukee (United States); S. Audi, Marquette Univ. (United States); M. Ranji, Univ. of Wisconsin-Milwaukee (United States)

Objective: The mitochondrial metabolic coenzymes NADH and FAD (oxidized form of Flavoprotein Adenine Dinucleotide, FADH2) are auto-fluorescent and can be monitored using optical techniques. The fluorescence signals of NADH and FAD have been used as indicators of tissue mitochondrial redox and metabolic state in many intact organs, but their use has not been fully developed in lungs. We and others have demonstrated that the ratio of these fluorophores, (NADH/FAD), referred to as the mitochondrial redox ratio (RR), can be used to detect myocardial tissue injury due to hypoxia and ischemia in intact hearts and in vivo. We have designed a fluorometer that can be used to monitor lung surface NADH and FAD fluorescence in isolated perfused lungs and in vivo. The objective of this study was to demonstrate the ability of this fluorometer to detect change in surface NADH and FAD fluorescence in isolated perfused rat lungs in response to various metabolic inhibitors that are known to alter lung tissue mitochondrial respiratory states.

Materials and methods: Rat (Sprague-Dawley, ~300 gram) lungs were isolated and connected to a ventilation-perfusion system. At the beginning of each experiment, NADH and FAD fluorescence standards were measured to account for day-to-day variations in light intensity. Surface fluorescence was measured by placing the fiber optic probe against the pleural surface of the right lobe. Surface fluorescence NADH and FAD signals were acquired in the absence (control perfusate) and presence of rotenone (ROT, complex I inhibitor), rotenone plus potassium cyanide (KCN, complex IV inhibitor), pentachlorophenol (PCP, mitochondrial uncoupler), or PCP +KCN. The fluorometer was used in a dark room to minimize stray-light effects.

Results: The data show that rotenone, which inhibits NADH oxidation at complex I, increased NADH signal by 15%, with no effect on FAD signal. KCN, which inhibits complex IV and hence reduces the chain, increased NADH and decreased FAD signal by 33%. PCP, which oxidizes the respiratory chain, decreased NADH by 15%. The addition of KCN to PCP reversed the effects of PCP on NADH and FAD. These results demonstrate the ability of surface fluorometry to detect changes in lung tissue mitochondrial redox state in a non-destructive manner in isolated perfused lungs.

8207D-70, Session 4

## Entropy-based measures of in vivo cilia-driven microfluidic mixing derived from quantitative optical imaging

K. Chandrasekera, S. Jonas, D. Bhattacharya, M. K. Khokha, M. A. Choma, Yale School of Medicine (United States)

Motile cilia are cellular organelles that project from different epithelial surfaces including respiratory epithelium. The rotational motion of cilia generates directional fluid flow that removes harmful pathogens and particulate matter from the respiratory system. While it has been known that primary ciliary dyskinesia increases the risk of recurrent pulmonary infections, there is now heightened interest in understanding the role that cilia play in a wide-variety of respiratory diseases (e.g. cystic fibrosis, asthma). Different optical imaging technologies are being investigated to visualize cilia-driven fluid flow, and quantitative image analysis techniques are being used to generate measures of ciliary performance. Here, we demonstrate the quantification of in vivo cilia-driven microfluidic mixing using spatial and temporal measures of Shannon information entropy. Similar entropy measures previously have been used to characterize mixing driven by artificial cilia in microfabricated microfluidic systems. Using videomicroscopy, we imaged in vivo cilia-driven fluid flow generated by the epidermis of the Xenopus tropicalis embryo, an experimentally-tractable and genetically-manipulable animal model of respiratory cilia. Flow was seeded with either dyes or microparticles. Both spatial and temporal measures of entropy show significant levels of mixing, with maximum entropy measures of ~6.5 (out of a possible range of 0 to 8). Spatial entropy measures showed strong mixing near the ciliated surface, and temporal measures showed, over time, mixing throughout. Entropy measures also showed mixing “hot-spots” and “cold-spots”. In sum, entropy-based measures of microfluidic mixing can characterize in vivo cilia-driven fluid flow and hold the potential for better characterization of ciliary dysfunction.

8207D-71, Session 4

## Diffuse optical spectroscopy measurements of pulmonary physiological and metabolic effects in a lethal rabbit cyanide model

J. Lee, S. B. Mahon, D. Yoon, D. S. Mukai, B. J. Tromberg, Beckman Laser Institute and Medical Clinic (United States); M. Brenner, Beckman Laser Institute and Medical Clinic (United States) and Pulmonary and Critical Care Medicine Div. (United States)

Cyanide (CN) poisoning induces lethal histotoxic anoxia and stops aerobic cell metabolism by disabling the function of cytochrome c oxidase (CcO), terminal oxidase of the mitochondrial respiratory chain. The onset of cyanide poisoning is rapid and the presence of cyanide in blood is not easily measured by current in-vivo rapid assay technology. We have previously demonstrated that non-invasive diffuse optical spectroscopy (DOS) can be used to detect the physiologic events occurring during development of CN toxicity in an animal model. In this study, a lethal cyanide toxicity rabbit model was used to compare non-invasive in vivo DOS measurements of tissue oxy (OHb)- and deoxyhemoglobin (RHb) concentrations and CcO redox state changes with quantitative metabolic and pulmonary gas exchange parameters were measured by standard means. Toxic effects of cyanide were clearly evident by substantial decreases in blood pressure and increases in OHb and decreases in RHb concentrations, and reduction of CcO redox states seen by DOS. Lethal levels of cyanide were demonstrated by decreased O2 elimination and increased CO2 elimination in exhaled pulmonary gas analysis, decreases in bicarbonate representing an increasing metabolic acidosis as well as decreases in venous carbon dioxide and oxygen levels representing a failure of aerobic respiration. DOS measurements in combination with pulmonary and metabolic data allow more precise assessment and monitoring in cyanide toxicity in a lethal animal model.

8207D-72, Session 4

## Functional anatomic imaging by micro-optical coherence tomography reveals autoregulatory mechanisms governing mucociliary transport in mammalian respiratory epithelium

L. Liu, Wellman Ctr. for Photomedicine (United States); M. Mazur, S. B. Parker, S. Suresh, The Univ. of Alabama at Birmingham (United States); B. E. Bouma, Wellman Ctr. for Photomedicine (United States) and Harvard-MIT Health Sciences and Technology (United States); S. M. Rowe, The Univ. of Alabama at Birmingham (United States); G. J. Tearney, Wellman Ctr. for Photomedicine (United States) and Harvard-MIT Health Sciences and Technology (United States)

In mammalian respiratory airway, mucociliary clearance is an inherent part of the lung defense and the amount of mucus secretion varies depending on the stiumil, which includes bacteria, particles and chemical irritants. It is essential that mucociliary transport be adjusted in response to varying mucus loads to achieve effective lung defense.

Presently, our knowledge of the physical mechanism by which mucociliary transport is regulated in response to changes in the mucus load is limited due to the inability to visualize mucociliary interactions under natural conditions, including the extent of mucus loading. A novel imaging tool termed μOCT enables simultaneous and real-time, cellular-resolution functional anatomic imaging of ciliary motion, airway surface liquid (ASL) and periciliary layer (PCL) morphology, and mucociliary transport without altering native tissue. With μOCT imaging of respiratory epithelia, we show that that mammalian airway is actively defended by a fundamental autoregulatory mechanism in which ciliary activity and mucociliary transport is upregulated proportionally to PCL compression caused by changes in the innate mucus load experienced by surface epithelial cells ($P<0.05$). We also demonstrate that this autoregulatory response is mediated by a calcium dependent response to PCL compression induced by mucus rafts.

8207D-73, Session 4

## Assessment of smoke inhalation injury using volumetric optical frequency domain imaging in sheep models

L. P. Hariri, M. B. Applegate, J. L. Beagle, G. J. Tearney, C. A. Hales, M. J. Suter, Massachusetts General Hospital (United States)

Respiratory failure secondary to smoke inhalation injury is a serious threat to victims of house fires and explosions. Lung damage, activated by smoke gas toxins and particle components, is perpetuated by resulting inflammation with consequential epithelial disruption, bronchial obstruction due to delayed airway mucosal sloughing, bronchoconstriction, and edema. The current evaluation of smoke inhalation injury is highly subjective, integrating clinical findings with bronchoscopic assessment. New, non-invasive methods for evaluating patients at risk for inhalation injury are required to accurately assess initial damage and survey injury extent and progression over time.

Optical frequency domain imaging (OFDI) is a high resolution (<10 micron) imaging modality, providing cross-sectional images of tissue microstructure. Rapid acquisition rates allow for the generation of volumetric datasets in the upper airways within seconds. To demonstrate the potential of OFDI for detecting the airway response to smoke inhalation injury, we conducted a pilot study in sheep exposed to 10 breaths of cooled cotton smoke. OFDI imaging was conducted in the trachea/upper airways using a 1.6mm diameter OFDI catheter prior to and 30 minutes subsequent to smoke exposure. Bronchoscopic inspection of the airways after smoke exposure revealed luminal mucin accumulations. Histopathology revealed epithelial sloughing with submucosal edema with modest polymorphonuclear (PMN) infiltrate. OFDI images clearly visualized luminal mucus accumulations and epithelial disruption including sloughing. Increased submucosal signal intensity was observed, which was attributed to edema and PMN infiltrate based on prior OFDI-histopathology correlation studies. Visualization of these features using OFDI may provide a more definitive method to assess smoke inhalation injury.

8207D-74, Session 4

## Dynamic optical imaging of methacholine-induced bronchosconstriction and the response to deep inhalations in sheep

M. J. Suter, M. B. Applegate, A. Braune, V. J. Kelly, G. J. Tearney, G. Musch, T. Winkler, Massachusetts General Hospital (United States)

Asthma is a pulmonary airway disease that is characterized by both chronic and episodic airway hyperresponsiveness. At present, the pathophysiology of asthma is only partially understood, however recent studies suggest that dynamic interactions among parallel and serial pathways may play a substantial role in airway behavior and in the emergence of ventilation defects. Structural features of the tracheobronchial tree, including the lumen diameter and airway wall thickness, have been studied in vivo using computed tomography (CT) approaches in an effort to better understand the mechanisms involved in acute asthma. The limitations of CT however include the spatial and temporal resolutions, limited to approximately 0.4 mm and 330 ms in even the most advanced 64-slice CT scanners. Conversely, the spatial and temporal resolutions of optical frequency domain imaging (OFDI), a high-resolution, non-ionizing cross-sectional imaging modality, are 0.007 mm and 10 ms respectively. We are investigating the potential of OFDI for dynamically imaging the airways in sheep models of asthma. We demonstrate that the high spatial and temporal resolution of OFDI enables real-time 4D evaluation of the airway structure that is not currently possible with conventional imaging modalities. Dynamic structural alterations of the airways during tidal respiration in the normal and methacholine challenged lung, and the response of bronchoconstricted airways to deep inhalations are presented. We anticipate that information derived from these studies will provide valuable insight into the complex behavior of the normal and asthmatic lung.

# Conference 8207E: Diagnostic and Therapeutic Applications of Light in Cardiology

Saturday-Sunday 21-22 January 2012

Part of Proceedings of SPIE Vol. 8207E Diagnostic and Therapeutic Applications of Light in Cardiology

8207E-81, Session 2

## Label-free nonlinear optical microscopic comparison and quantification of type-I collagen fibrils in infarcted and adipose-derived stem-cell treated myocardium tissues

A. C. T. Ko, L. Mostaço-Guidolin, F. Wang, B. Xiang, M. S. D. Smith, National Research Council Canada (Canada); A. Major, Univ. of Manitoba (Canada); G. Tian, M. G. Sowa, National Research Council Canada (Canada)

The potential therapeutic efficacy of adipose-derived stem cells (ASCs) on infarcted hearts to improve cardiac function was recently assessed in animal models [1]. Magnetic resonance imaging and immuno-fluorescence microscopy showed that ASC-treated rat hearts have a significantly greater left ventricular ejection fraction (LVEF), LV wall thickening and higher capillary density in the infarcted border zone than did the cell-culture medium (CCM)-treated and untreated hearts. Such improvements in cardiac function observed in ASCs-treated hearts may be attributed to reduced deleterious cardiac remodeling. The latter is caused mainly by the loss of cardiomyocytes and increased production of fibrillar collagen, leading to scarring tissue formation in the infarct zone. Investigations of these changes in the extracellular matrix (ECM) will provide us with more direct evidence of tissue repair resulting from stem-cell therapy. Recently nonlinear optical microscopy (NLOM) has demonstrated its unparalleled power in visualizing structural changes associated with extracellular components in cardiovascular tissues.[2] Its label-free nature and high spatial resolution provides an ideal means to study collagen morphology in detail, and its structural correlation with other ECM components. In this study, we examine the utility of nonlinear optical microscopy in visualizing collagen fibril organization in healthy rat hearts, post-myocardial infarcted and ASCs-treated rat hearts. Not only we are able to clearly visualize the presence of thick collagen fibrils in the infarct zone, more importantly, NLOM enables us to interrogate the structural difference in collagen fibril's shape/texture between post-MI and ASCs-treated myocardium tissues. Quantitative analysis of collagen images based on a recently developed image-analysis method[3] is used to analyze NLOM images from sectioned and/or un-sectioned myocardium to enable a quantitative comparison between post-MI and ASCs-treated hearts.

[1] Wang L, et al "Adipose-derived stem cells are an effective cell candidate for treatment of heart failure: an MR imaging study of rat hearts," Am J Physiol Heart Circ Physiol. 2009 Sep;297(3):H1020-31

[2] Ko et al "Multimodal nonlinear optical imaging of atherosclerotic plaque development in myocardial infarction-prone rabbits J. Biomed. Opt. 15 020501, 2010.

[3] Mostaço-Guidolin LB et al "Evaluation of Texture Parameters for the Quantitative Description of Multimodal Nonlinear Optical Images from Atherosclerotic Rabbit Arteries," accepted, Phys. in Med. Biol.

8207E-83, Session 2

## 4D imaging of embryonic chick hearts by streak-mode Fourier domain optical coherence tomography

R. Wang, J. X. Yun, Clemson Univ. (United States); R. L. Goodwin, Univ. of South Carolina (United States); R. R. Markwald, Medical Univ. of South Carolina (United States); T. K. Borg, Univ. of South Carolina (United States); R. B. Runyan, The Univ. of Arizona (United States); B. Z. Gao, Clemson Univ. (United States)

It is well established that hemodynamics play a critical role in the development of cardiovascular structures. However, a major challenge to determining the effect of hemodynamics on cardiac morphogenesis of the heart is that the nature and magnitude of the forces generated within the developing heart are largely unknown. This is due to the lack of imaging systems that have sufficient spatial and temporal resolution to accurately capture the small scale, complex geometry, and dynamics of the beating embryonic heart.

Recently, we developed the streak-mode Fourier domain optical coherence tomography (SM-FDOCT) technique, in which an area-scan camera is used instead of a line-scan camera to record the OCT spectrum. This SM-FDOCT retains the conventional point-scanning mechanism so that the small aperture of the single-mode fiber functions as a confocal gate for rejecting multiply scattered photons. While the probe beam is scanning the sample laterally, the corresponding OCT spectrum is physically scanned on the area-scan camera using a streak scanner (in our case, a 1000-Hz resonant mirror). This technique is applied to ultrahigh-speed, non-invasive, live imaging HH19 embryonic chick hearts at a scan rate of 1,016,000 axial scans per second. The high scan rate enables the acquisition of high temporal resolution 2D datasets (1,000 frames per second or 1 ms between frames) and 3D datasets (10 volumes per second), without use of prospective or retrospective gating technique. This marks the first time that the embryonic animal heart has been 4D imaged using a megahertz OCT.

8207E-84, Session 2

## Macrophage imaging in intact atherosclerotic plaques using OCT and two-channel two-photon luminescence microscopy

T. Wang, B. Yin, M. S. Kazmi, J. Dwelle, The Univ. of Texas at Austin (United States); V. Sapozhnikova, J. Mancuso, The Univ. of Texas Health Science Ctr. at San Antonio (United States); B. Willsey, The Univ. of Texas at Austin (United States); X. Li, The Univ. of Texas Health Science Ctr. at San Antonio (United States); K. P. Johnston, The Univ. of Texas at Austin (United States); M. D. Feldman, The Univ. of Texas Health Science Ctr. at San Antonio (United States); A. K. Dunn, T. E. Milner, The Univ. of Texas at Austin (United States)

The macrophage is an important early cellular marker involved in plaque rupture and myocardial infarction. We report combined OCT and two-channel two-photon luminescence microscopy (TPLM) to image macrophages in atherosclerotic plaques using plasmonic gold nanorose as a biocompatible contrast agent. Atherosclerotic plaques were induced in the aorta of a New Zealand white rabbit subjected to a high cholesterol diet and double balloon injury. The rabbit was injected with a suspension of 30 nm diameter gold nanoroses coated with dextran. The macrophages engulfed nanorose and ex vivo plaque samples were imaged by OCT and TPLM, respectively. For OCT imaging, a high-performance computing system was used to acquire and process OCT images in real time. For TPLM, a femtosecond laser (800 nm) was used as an excitation light source. Two-photon luminescence (TPL) from the plaque samples was detected in two channels by two photomultiplier tubes (PMTs). To separate plaque fluorescence from nanorose luminescence, wavelengths shorter than 570 nm from plaque fluorescence were collected by one PMT, while wavelengths between 665 and 735 nm from nanorose luminescence were collected by another PMT. Two-channel TPLM images are merged into co-registered OCT images to show both plaque structure and composition. Results of our study suggest that combined OCT and TPLM can map the distribution of nanorose-loaded macrophages and other plaque components (e.g., elastin and lipid droplets) in response to plaque surface profile.

8207E-85, Session 3

## Miniature integrated optical coherence tomography: ultrasound probe for intravascular imaging

J. Li, Univ. of California, Irvine (United States); X. Li, The Univ. of Southern California (United States); J. Yin, Univ. of California, Irvine (United States); J. Jing, D. S. Mukai, S. B. Mahon, Beckman Laser Institute and Medical Clinic (United States); A. Edris, K. Hoang, Univ. of California, Irvine (United States); K. K. Shung, The Univ. of Southern California (United States); M. Brenner, Univ. of California, Irvine (United States) and Univ. of California, Irvine (United States); J. Narula, Univ. of California, Irvine (United States); Q. Zhou, The Univ. of Southern California (United States); P. M. Patel, Univ. of California, Irvine (United States); Z. Chen, Beckman Laser Institute and Medical Clinic (United States) and Univ. of California, Irvine (United States)

Coronary artery atherosclerosis is a major public health problem associated with high clinical morbidity and mortality. For over 20 years, intravascular ultrasound (IVUS) imaging has been a standard diagnostic tool for atherosclerosis. Recently, optical coherence tomography (OCT) with high resolution, has been applied to intravascular imaging because it enables direct imaging of tissue responses to stent implantation and thin fibrous caps, one of the key features of vulnerable atherosclerotic plaques. The combined use of OCT and IVUS is hypothesized to remarkably increase diagnostic accuracy.

Here, we report on a miniature integrated optical coherence tomography (OCT) -ultrasound (US) probe, which is small enough for imaging in human coronary arteries. The OCT probe design permits light from a single mode fiber to be focused by a 0.35-mm-diameter gradient-index (GRIN) lens and then reflected by a 0.25-mm-diameter micro prism into the sample. A 0.5mm × 0.5mm 35MHz PMN-PT side-viewing ultrasound transducer is combined with the OCT probe for ultrasound imaging. By arranging the OCT probe and US transducer sequentially, the outer diameter of the integrated OCT-US probes is decreased significantly to 0.69 mm. This miniature integrated probe simultaneously provides both OCT and ultrasound imaging. By adopting a two-channel data acquisition board, external clock and GPU parallel computing, a truly integrated OCT-US system is achieved allowing real time data acquisition, processing and display. The first in vivo imaging of a rabbit abdominal aorta, in which a lesion similar to human atherosclerosis can be easily induced, demonstrates the utility of this miniature integrated OCT-US probe.

8207E-86, Session 3

## Combining OCT and a fluorescence intensity imaging method for atherosclerosis detection

S. Liang, Beckman Laser Institute and Medical Clinic (United States) and Dalian Univ. of Technology (China); A. Saidi, J. Jing, G. Liu, Beckman Laser Institute and Medical Clinic (United States); J. Yin, J. Narula, Univ. of California, Irvine (United States); Z. Chen, Beckman Laser Institute and Medical Clinic (United States)

Atherosclerosis and cardiac disease causes over 30% of all deaths in North America. Diagnosing the most dangerous atherosclerosis, that is prone to rupture, is the most effect way to increase the chance of survival for patients who suffer from this disease. In recent years, optical coherence tomography (OCT) has become a very useful tool for intravascular imaging of the microstructure of atherosclerotic plaques, since it has high axial and transverse resolution. In addition to the microstructure information of plaques, we still need to know the biochemical characteristics that are unique for vulnerable plaques. Fluorescence molecular imaging is a standard way to examine these biochemical properties. Therefore, we integrate these two techniques together into one system. Our system is a combination of a 1310 nm swept source OCT system and a fluorescence intensity detection system. For intravascular imaging, we made an endoscope that is based on a double-clad fiber (DCF), grin lens, and a rotating beam with a MEMS mirror in front. The single-mode core of the DCF transmits both OCT light and a fluorescence excitation light; however, the multimode inner cladding is used to detect the fluorescence signal. The OCT and fluorescence imaging is synchronous and in real time. Both the OCT and fluorescence images match up well with each other in terms of the plaque lipid structure detected by OCT and a corresponding bright superficial fluorescence intensity image. In vitro results show that this is a possible method for a more accurate diagnosis of vulnerable plaques.

8207E-87, Session 3

## Translation to intravascular detection of atherosclerotic plaques using combined fluorescence lifetime and ultrasound imaging

Y. Sun, J. Liu, M. Lam, H. Xie, J. Bec, Univ. of California, Davis (United States); M. C. Fishbein, Univ. of California, Los Angeles (United States); J. M. Cannata, K. K. Shung, The Univ. of Southern California (United States); L. Marcu, Univ. of California, Davis (United States)

Detection of plaque vulnerability has critical clinical implications for patients with high risk of plaque rupture. This study aims to (1) investigate whether compositional and structural characteristics of atherosclerotic plaques can be evaluated concurrently via a bimodal technique that integrates time-resolved fluorescence spectroscopy (TRFS) and ultrasonic backscatter microscopy (UBM); and (2) develop intravascular catheters that enable integration of TRFS with intravascular ultrasound (IVUS) for subsequent deployment of this bimodal technique in patients. Experiments were conducted ex vivo with endarterectomy carotid plaque samples (20 patients, 193 distinct areas). Lesions were evaluated histopathologically and quantified as the percentage of different components. We determined that the fluorescence spectroscopic parameters at discrete emission wavelengths enhanced by the ultrasonic spectral parameters allowed for discrimination (sensitivity 82.2%, specificity 91.3%) of various compositional and pathological features associated with plaque vulnerability. The applicability of this technique to intravascular setting has been tested via a modified IVUS catheter (40 MHz transducer) combined with a side viewing optical. The resulting catheter system was validated in a pig arterial vessel. Synergistic fluorescence lifetime data and IVUS recordings during a catheter pull-back in the axial direction successfully demonstrated our ability to acquire bimodal data intravascularly and to co-register the data obtained via the two distinct modalities. Current results demonstrate the ability of the bimodal system to provide simultaneous information on both biochemistry and microstructure of arterial vessels and to improve the diagnosis of critical arterial pathologies.

8207E-88, Session 3

## Dual-modality intra-arterial imaging catheter

H. Yoo, J. W. Kim, Massachusetts General Hospital (United States); M. Shishkov, Wellman Ctr. for Photomedicine (United States); T. Morse, The Boston Univ. Photonics Ctr. (United States); R. Shubochkin, Boston Univ. (United States); J. R. McCarthy, Massachusetts General Hospital (United States); B. E. Bouma, Wellman Ctr. for Photomedicine (United States); F. A. Jaffer, Massachusetts General Hospital (United States); G. J. Tearney, Wellman Ctr. for Photomedicine (United States)

Optical frequency domain imaging (OFDI), a form of Fourier-domain optical coherence tomography (FD-OCT), acquires 3D images of the microstructure of arteries, including lipid pools, calcium, macrophages, thin fibrous caps, cholesterol crystals, thrombus, and stent struts, within a few seconds. Near-infrared fluorescence (NIRF) imaging enables intra-arterial molecular imaging, providing new biological insights into arterial inflammation in atheroma and stent-induced injury in vivo. Recently, we have developed a dual-modality intra-arterial catheter (2.4 F) that simultaneously obtains 3D OFDI microstructure and 2D NIRF molecular imaging from artery walls. A double-clad fiber is used to effectively combine two imaging modalities into a single catheter. In this study, we report a dual-modality intra-arterial imaging of stent-microthrombosis and atherosclerotic plaque in vivo. In a rabbit stent-thrombosis model, imaged with fibrin bound Cy7 NIR fluorochrome, OFDI demonstrated the microstructure of the rabbit artery, including metallic stent struts and thrombus. The simultaneously acquired NIRF images provided highly sensitive detection of the fibrin, even in some portions of the artery that did not contain clear OFDI evidence of thrombus. In a rabbit atherosclerosis model injected with a cysteine protease-activatable NIRF agent, OFDI images showed the morphological features of atherosclerotic plaque, including a highly scattering, raised, thickening of the artery wall. Co-localized NIRF demonstrated a high fluorescence signal, indicative of cysteine protease activity, at the plaque area, confirmed by immunohistochemistry. This novel catheter could open up new opportunities for understanding and management of coronary artery disease, including characterizing coronary inflammation found in plaques at risk for causing heart attacks and assessing vessel wall healing following coronary stent implantation, by simultaneously providing co-localized microstructural and biological information.

8207E-89, Session 4

## Mechanical stress on vascular wall enhances neointimal hyperplasia following stent implantation: serial explorations using optical frequency domain imaging in vivo

A. Tanaka, B. E. Bouma, M. J. Suter, B. Greenberger, K. Gallagher, Wellman Ctr. for Photomedicine (United States); D. Winsor-Hines, Boston Scientific Corp. (United States); G. J. Tearney, Wellman Ctr. for Photomedicine (United States)

Background: Several studies conducted ex vivo have suggested that mechanical stress promotes proliferation of smooth muscle cells, resulting in neointimal hyperplasia after stent implantation. We used optical frequency domain imaging (OFDI) in vivo to expand our understanding of the relationship between mechanical stress on the vessel wall and neointimal hyperplasia after stent implantation.

Methods: We implanted 10 stents in 10 coronary arteries of 4 swine. OFDI imaging was conducted at the time of stent implantation (baseline) and 28 days following stent implantation. At 28 days, the swine were sacrificed and serial histology was performed. We registered baseline, 28 day OFDI images and histology for 135 stent struts. Acquired vascular wall damage was assessed by applying Schwartz scores and analogous OFDI scores to the artery wall beneath the struts. Vascular wall kinking by the stent struts was used as a marker for mechanical stress.

Results: We found a good correlation between neointimal thickness measured by histomorphometry and OFDI ($r^2=0.91$, $P<0.001$). Both OFDI and histological assessment showed that the severity of vascular wall damage was correlated with the neointimal growth both in BMS and DES. Mechanical stress on the vascular wall was found to affect neointimal hyperplasia for DES independent of vascular wall damage.

Conclusions: OFDI can assess the vascular wall damage and mechanical stress imparted to the vessel wall in vivo. These findings suggest that OFDI could be useful for optimizing stent and deployment platform designs and stent implantation.

8207E-90, Session 4

## 3D optical coherence tomography tissue type imaging

G. van Soest, E. Regar, Erasmus MC (Netherlands); B. E. Bouma, G. J. Tearney, Wellman Ctr. for Photomedicine (United States); G. Ughi, J. D'Hooghe, Katholieke Univ. Leuven (Belgium); A. F. W. van der Steen, Erasmus MC (Netherlands) and Interuniversity Cardiology Institute of the Netherlands (Netherlands)

Background: Vulnerable plaques in the coronary circulation may rupture and cause acute coronary syndrome, such as myocardial infarction. While the histopathology of these lesions is largely known, timely identification in vivo remains a significant challenge. Reliable information on plaque composition is presently a vital missing piece in diagnostic imaging and scientific study of the disease. Tissue types in the coronary artery wall can be differentiated by their optical properties, which are accessible through analysis of the OCT signal. Strongly attenuating tissues are associated with unstable plaque types.

Methods: We acquired OCT pullbacks in 31 patients coming in for elective PCI in the Thoraxcenter, Erasmus MC, Rotterdam. OCT data were acquired with a custom-built OFDI system and catheters. OCT data were analyzed for the optical attenuation coefficient μa of artery wall tissue. The optical attenuation image was compared with interpretation of the grayscale OCT data and with clinical presentation.

Results: Pullbacks of native sections of coronary artery were successfully analyzed. The optical attenuation of coronary artery tissue was found to range from 0 to approximately 15 mm-1. Lesions that were interpreted on grayscale as being fibrous or calcified plaques had μa 8 mm-1.

Discussion: Further extensions to the model, in particular the analysis of the backscatter coefficient μb and correct treatment of multiple scattering, are the subject of current research. Progress on these issues will be incorporated in the analysis. Volumetric analysis of the data will also be discussed.

8207E-91, Session 4

## Simulation of the sunflower artifact in IV-OCT imaging of bare metal stents

S. Elahi, J. Maisano, The Univ. of Texas at Austin (United States); J. Dijkstra, Leids Univ. Medisch Ctr. (Netherlands); J. Mancuso, M. D. Feldman, The Univ. of Texas Health Science Ctr. at San Antonio (United States); T. E. Milner, The Univ. of Texas at Austin (United States)

The sunflower effect is an IV-OCT artifact observed when imaging metal stents. A phantom blood vessel was constructed from a mix of polydimethylsiloxane (PDMS) and titanium dioxide to simulate the elastic and optical scattering properties of the arterial wall. A Medtronic EndeavorR stent was deployed within the phantom vessel and high resolution Micro-CT images of the stent strut were recorded to create a three-dimensional representation that was imported into Zemax optical design software. Simulation of an IV-OCT catheter and reflection of light from the stent strut was implemented in Zemax. The IV-OCT catheter was defined in Zemax and rotation of the light beam over the stent strut was simulated. Results computed in Zemax included: 1) strut reflectivity vs. catheter angle; 2) lateral size of the strut region reflecting light into the catheter; and 3) optical pathlength of light returning to the catheter. Strut reflectivity was less than 9% of incident light and reflected light was limited to 0.7 degrees (FWHM) of catheter rotation. Lateral size of the strut region reflecting light into the catheter was less than 3.5×3.0 um2. Optical pathlength of light returning to the catheter was nearly constant with a standard deviation of 0.370 um. Since optical pathlength is nearly constant for reflections from a small-sized region on the strut, simulation results match clinical observations that the metal strut can appear in IV-OCT images as a straight line bending towards the catheter.

8207E-92, Session 4

## Conformational change in coronary artery structure assessed by optical coherence tomography in patients with vasospastic angina

A. Tanaka, B. E. Bouma, Wellman Ctr. for Photomedicine (United States); K. Shimada, Osaka City Univ. (Japan); M. Kashiwagi, T. Akasaka, J. Yoshikawa, Wakayama Medical Ctr. (Japan); G. J. Tearney, Wellman Ctr. for Photomedicine (United States)

Background: Coronary artery spasm plays an important role in the pathogenesis of ischemic heart disease. The conformational change of the arterial wall during vasospasm has not been studied in detail. The aim of this study was to investigate the conformational change of arterial structure in vasospastic lesions using optical coherence tomography (OCT).

Methods: We assessed 19 coronary arteries (10 spasm and 9 non-spasm lesions) with OCT during a provocation test for coronary spasm. An intimal bump was defined as one or more intimal projections into the lumen that disappeared after the administration of nitroglycerine (NTG). Intimal gathering was defined as a folding or gathering of the intima, resulting in multiple kinks in the luminal contour that resolved after the administration of NTG.

Results: Spasm lesions more consistently showed an intimal bump at baseline and intimal gathering during spasm compared with non-spasm lesions (spasm 80% vs non-spasm 0%, $p<0.01$, spasm 100% vs non-spasm 0%, $P<0.01$, respectively). Spasm lesions demonstrated a thicker maximum media thickness (spasm 0.24 ± 0.04 mm vs non-spasm 0.12 ± 0.03 mm, $p<0.01$) at baseline while no differences were observed after the administration of NTG (spasm 0.13 ± 0.03 mm vs non-spasm 0.13 ± 0.02 mm, $p=0.65$).

Conclusions: These results suggest that medial contraction occurs even in an asymptomatic state and facilitates the formation of an intimal bump in patients with vasospastic angina. Luminal narrowing during spasm is associated with intimal gathering without alternation of intimal area.

8207E-93, Session 5

## Automatic lipid detection in human coronary atherosclerosis using spectroscopic intravascular photoacoustic imaging

K. Jansen, A. F. W. van der Steen, Erasmus MC (Netherlands) and Interuniversity Cardiology Institute of The Netherlands - Netherlands Heart Institute (Netherlands); H. M. M. van Beusekom, J. W. Oosterhuis, G. Springeling, F. Mastik, G. van Soest, Erasmus MC (Netherlands)

Ischemic heart disease is the largest cause of death in Western countries. Most acute cardiac events are caused by the rupture of a so-called vulnerable plaque. The presence and location of lipids in atherosclerotic plaques, together with other factors such as a thin fibrous cap and dense macrophage infiltration, are associated with plaque vulnerability.

Intravascular photoacoustic (IVPA) imaging can add chemical specificity to intravascular ultrasound (IVUS) by capitalizing on tissue contrast in the optical absorption spectrum. It has the potential to identify the amount and the location of the lipid content and other constituents of coronary plaques by spectroscopic imaging. Using the pronounced peak near 1200 nm in the lipid absorption spectrum, we devised a method to automatically detect lipids in the coronary artery wall.

We performed ex-vivo IVPA measurements of atherosclerotic and healthy arteries using a combined IVPA/IVUS catheter. Co-registered IVPA/IVUS cross-sectional data were obtained at excitation wavelengths from 1180 to 1230 nm with steps of 10 nm by rotation of the catheter in 1° steps. The data were corrected for variations in the laser power output between the different wavelengths, filtered and analyzed using a peak-fitting algorithm to find the regions where the spectral IVPA data matched the peak in the lipid absorption spectrum near 1200 nm. The matching regions were color-coded and superimposed on the IVUS images. We found an excellent agreement with the lipid histology stains of the corresponding cross-sections. These results demonstrate the potential of spectroscopic IVPA imaging for spatially resolved lipid detection in atherosclerotic plaques.

8207E-94, Session 5

## High-frequency intravascular photoacoustic (IVPA) imaging for differentiating arterial wall layered structures

X. Li, The Univ. of Southern California (United States); W. Wei, Univ. of California, Irvine (United States); K. K. Shung, Q. Zhou, The Univ. of Southern California (United States); Z. Chen, Beckman Laser Institute and Medical Clinic (United States)

Arterial wall is composed of three layers: intima, media and adventitia. Differentiating the layered structures and measuring the intima-media thickness (IMT) are clinically significant for diagnosing atherosclerotic diseases. Although intravascular ultrasound (IVUS) imaging may allow the delineation of the layered structures, the imaging contrast induced by acoustic impedances of different layers is inferior, which is only a few percent for uncalcified tissues. Examination of optical absorption spectra (μa) of the arterial wall at 532nm shows that the intima and adventitia have similar μa values (10.04 and 13.29), but are twice higher than that of media (5.323). On this basis, we hypothesize that arterial three-layer structures could be better resolved by IVPA imaging at 532nm, with optical contrast and ultrasonic resolution. We introduce integrated miniature IVUS/IVPA probes that combine the capabilities of ultrasound and photoacoustic imaging for the evaluation of arterial wall layered structures. Side-looking IVUS transducer and optical fiber were arranged in parallel and integrated inside a 1.2-mm-OD polyimide tube. For the optical part, a 200-micron-core multimode fiber was used to deliver laser beams. For the ultrasound part, two types of miniature ultrasonic transducers working at 35MHz and 80MHz were fabricated for IVPA imaging. Healthy rabbit aortas were imaged ex vivo. IVPA imaging showed superior contrast over corresponding IVUS images in identifying the layered structures, and matched well with histology results. The IVPA imaging was firstly achieved at 80MHz with greatly improved resolution (35μm in axial direction). 80MHz IVPA imaging depicted the layered structures with outstanding clarity.

8207E-95, Session 5

## Combined intravascular ultrasound and spectroscopic photoacoustic imaging for detecting morphology and composition of atherosclerotic plaques

S. Y. Emelianov, The Univ. of Texas at Austin (United States) and The Univ. of Texas M.D. Anderson Cancer Ctr. (United States); B. Wang, A. B. Karpiouk, J. L. Su, D. E. Yeager, The Univ. of Texas at Austin (United States); P. Joshi, J. H. Amirian, The Univ. of Texas Health Science Ctr. at Houston (United States); S. Litovsky, The Univ. of Alabama at Birmingham (United States); K. Sokolov, The Univ. of Texas M.D. Anderson Cancer Ctr. (United States) and The Univ. of Texas at Austin (United States); R. W. Smalling, The Univ. of Texas Health Science Ctr. at Houston (United States)

The vulnerability of the atherosclerotic plaques is determined not only by their morphology but also composition and cellular activity. Therefore, comprehensive in-vivo plaque characterization is important for planning and guiding interventional procedures, monitoring treatment outcome, and understanding the pathological progression of the disease. However, most of the clinically available imaging modalities only assess the degree of stenosis. To address this clinical need, we have introduced an intravascular imaging technique - combined intravascular ultrasound (IVUS) and spectroscopic intravascular photoacoustic (IVPA) imaging. In this presentation, an overview of the latest results in IVUS/IVPA imaging of atherosclerosis will be presented, demonstrating that ultrasound-guided spectroscopic photoacoustic imaging can characterize atherosclerotic plaque composition using both endogenous and exogenous-based contrast. Specifically, IVUS/IVPA imaging has been used to concomitantly image the distribution of lipid and phagocytically active macrophages in ex-vivo atherosclerotic artery samples. Detection of lipid was performed using spectroscopic IVPA imaging of its optical absorption peaks and detection of macrophages was accomplished via imaging of plasmonic coupling of nonspecific uptake of gold nanoparticle contrast agents. Thus, the developed IVUS/IVPA imaging approach has the potential to detect the co-localization of lipid and macrophages, therefore effectively identifying the vulnerability of atherosclerotic plaques. Additionally, to demonstrate the potential for clinical use of this technique, in-vivo imaging of coronary stents deployed in a rabbit aorta using an integrated IVUS/IVPA imaging catheter is presented. Together, results indicate that combined IVUS/IVPA imaging allows for the complimentary morphological and compositional characterization of atherosclerosis.

8207E-96, Session 5

## Intracoronary Laser Speckle Imaging (ILSI) for the mechanical characterization of coronary plaques in living swine

S. K. Nadkarni, J. Toussaint, G. J. Tearney, Z. Hajjarian Kashany, Harvard Medical School (United States)

Acute myocardial infarction is caused by coronary thrombosis frequently resulting from the rupture of vulnerable plaque. Compelling evidence suggests that plaque rupture occurs when the atheroma with severely compromised viscoelastic properties fails to withstand stresses exerted upon it. We have developed a new optical technology for intracoronary use, termed ILSI that evaluates plaque viscoelastic properties, known to be intimately linked with the risk of coronary plaque rupture. In ILSI, measurements of tissue viscoelasticity are obtained by measuring the Brownian motion of light scattering particles from temporally evolving laser speckle fluctuations. Here, we describe the first in vivo studies in living swine using ILSI to characterize the mechanical properties of coronary plaques via a custom fabricated catheter and a high speed imaging console.

ILSI was conducted in three living swine using a human to swine coronary xenograft model and time-varying laser speckle patterns of coronary plaques (N=25) were obtained under physiological conditions of cardiac motion. The time constant, T, of the speckle intensity decorrelation curve was calculated to provide an index of plaque viscoelasticity and compared with Histopathological diagnosis. Our results showed that using both cardiac-gated and non-gated approaches, differences in T between lipid, fibrous and calcific plaque groups were highly significant, demonstrating that plaque viscoelasticity could be well distinguished using ILSI even under conditions of cardiac motion. Furthermore plaque T values measured in vivo demonstrated high correlation with lipid and collagen content. These studies open the exciting possibility of translating ILSI to evaluate key mechanical factors related to plaque rupture in patients.

8207E-97, Session 6

## Biochemical characterization of coronary atherosclerosis based on autofluorescence imaging

J. Park, P. Pande, S. Shrestha, F. Clubb, B. Applegate, J. A. Jo, Texas A&M Univ. (United States)

Objective: To demonstrate that autofluorescence imaging can characterize the biochemical composition of atherosclerotic plaques. Methods: Endogenous multispectral fluorescence lifetime imaging (FLIM) was performed on fresh postmortem human coronary segments. The autofluorescence emission from each pixel of the imaged plaque was quantified in terms of normalized intensity and average lifetime values. These features were then used to classify each pixel as collagen-rich or lipid-rich via Linear Discriminant Analysis. Results: A total of 58 fresh postmortem human coronary segments were imaged. From these, 23 segments, showing uniform histological characteristics, were selected to design the LDA classifier and grouped based on histopathology as: High-Collagen (n=4, plaque showing >80% of collagen content), High-Lipid (n=4, thin-cap fibroatheromas or foam-cell rich plaques) and Low-Collagen/Lipid (n=15, plaques with low content of lipids or collagen, including intimal thickening or calcification). The classifier could detect High-Collagen pixels with sensitivity/specificity of 96%/98%, High-Lipid pixels with sensitivity/specificity of 89%/99%, and the Low-Collagen/Lipids pixels with sensitivity/specificity of 99%/99% (assessed by 10-fold cross-validation). In addition, chemometric analysis of the multispectral FLIM data based on Non-Negative Factorization provided pixel estimation of the relative concentration of collagen and lipids. These approaches are allowing biochemical imaging of the plaque lumen. Conclusion: Endogenous FLIM can assess plaque composition, in particular collagen and lipids. However, since plaque morphology is not readily available from FLIM, it would be virtually impossible to identify the different types of atherosclerotic plaque. This limitation can be overcome by integrating optical coherence tomography (OCT) and FLIM, as recently demonstrated by our group.

8207E-98, Session 6

## Automated algorithm for classification of atherosclerotic plaques using depth-resolved spectral analysis of optical frequency-domain imaging datasets

C. P. Fleming, Massachusetts General Hospital (United States) and Harvard Medical School (United States); A. Tanaka, J. A. Gardecki, Wellman Ctr. for Photomedicine (United States) and Harvard Medical School (United States); P. Maurovich-Horvat, W. C. Warger II, Massachusetts General Hospital (United States) and Harvard Medical School (United States); J. E. Eckert, Wellman Ctr. for Photomedicine (United States); U. Hoffmann, Massachusetts General Hospital (United States) and Harvard Medical School (United States); B. E. Bouma, G. J. Tearney, Wellman Ctr. for Photomedicine (United States) and Harvard Medical School (United States)

Optical frequency domain imaging (OFDI) can identify key components related to plaque vulnerability but may suffer from artifacts and ambiguities that could prevent accurate identification of lipid rich regions.

We present a model of depth resolved spectral analysis for intracoronary plaque classification. Comprehensive pullback image datasets were acquired within 20 coronary arteries from 8 explant human hearts. Time-frequency analysis was used to generate depth resolved spectra of OFDI interferometric signals. A training set of registered OFDI-histology pairs (n=150) was used to develop a prediction model using quadratic discriminant analysis. Inputs to the model included attenuation, backscattering, and wavelength dependent attenuation. Model output is the probability for each pixel being assigned to lipid, calcium, fibrous, adventitial fat, or noise. The resultant spectroscopic diagnosis was compared to histological diagnosis.

Using correlated OFDI and histology images, depth resolved spectral analysis was able to classify lipid, calcium, fibrous regions, adventitial fat, and noise with significant ($p<0.001$) areas under the receiver operator characteristic curve (0.87, 0.83, 0.97, 0.89, and 0.99 respectively). Although the backscattering and attenuation coefficients were significantly different between tissue types ($p<0.001$), the addition of spectral parameters increase the classification accuracy of lipid (AUC=0.87 with spectral parameters, AUC=0.84 without) and adventitial fat (AUC=0.89 with spectral parameters, AUC=0.87 without), $p<0.05$.

We have developed a method for classification of intracoronary OFDI pullbacks. This method can increase the contrast of OFDI intracoronary images and facilitate a rapid comprehensive visualization of OFDI datasets, which can potentially improve OFDI diagnosis and/or assist in guiding therapeutic procedures.

8207E-99, Session 6

## Evaluation of intracoronary near-infrared autofluorescence spectroscopy

H. Wang, J. A. Gardecki, B. E. Bouma, G. J. Tearney, Wellman Ctr. for Photomedicine (United States)

The simultaneous acquisition of biochemical composition and morphological structure of atherosclerotic plaques provides complementary information that will likely expand our definition of plaque vulnerability.

There have been numerous arterial autofluorescence studies using UV and visible excitation that have investigated atherosclerotic plaque composition. The predominant fluorophores in this region are collagen, elastin and NADH. Here, we describe a study that evaluates the diagnostic utility of NIR excited autofluorescence (NIRAF) spectroscopy of human cadaver plaques ex vivo.

Methods: 57 plaques (44 aortic, 13 coronary) from 26 cadavers were analyzed. NIRAF data was acquired using 740nm excitation wavelength (power = 3 - 30mW) and emission was detected from 765-855 nm. Histology was read as non-necrotic core lipid, necrotic core lipid and non-lipid containing plaques. The total fluorescence intensity, fluorescence spectra, and histology were compared. Using PCA and LDA, fluorescence data was classified as necrotic core plaques or non-necrotic lipid rich plaques.

Results: Fluorescence signal intensity was higher for lipid rich plaques (5.4e7±3.5e7 counts/sec/mW for lipid and 5.1e6±1.4e6 counts/sec/mW for non-lipid, $p < 0.05$). The sensitivity of our classification algorithm for necrotic core plaque was 81% (95% confidence intervals 70.3% - 88.6%), and specificity was 83.3% (95% confidence intervals 73.3% - 90.3%).

Conclusion: These results suggest that NIRAF may be used to detect lipid rich plaques, and further differentiate necrotic core plaques from non-necrotic core lipid rich plaques.

8207E-100, Session 6

## Novel method for fast analysis of atherosclerotic plaque time-resolved fluorescence decay characteristics and accurate evaluation of plaque composition

J. Liu, Univ. of California, Davis (United States)

We report a new method for recovering the fluorescence decay characteristics from time-domain time-resolved fluorescence measurements of atherosclerotic cardiovascular tissue. Quantitative analysis of tissue fluorescence decay involves deconvolution of system impulse response function (IRF) from noise corrupted fluorescence measurements. Expansion of the IRF on orthonormal basis composed of Laguerre functions (LGF) had been demonstrated as a fast deconvolution method (due to the linear parameterization of IRF) without a priori assumption of the functional form of IRF. Previous implementation of Laguerre techniques was limited to the use of lower order LGF. The accuracy of estimating IRFs relied heavily on the choice of Laguerre scale parameters. Lower order basis set is typically insufficient for representation of IRFs with fast decay components (e.g. fluorescence of lipids). This study used higher order LGF for deconvolution of fluorescence IRFs. Overfitting due to the increased model complexity was alleviated by properly constraining the least-square deconvolution problem with a priori information on the shape of the decay profiles. This algorithm was validated on ex-vivo atherosclerotic plaques with time-resolved fluorescence spectroscopic imaging measurements. We show that higher order LGF expansion allowed for accurate recovery of tissue fluorescence with fast and slow decay characteristics and enhanced discrimination (sensitivity 80%, specificity 90%) of compositional and pathological features associated with plaque vulnerability. Furthermore, our method was significantly faster (~two order-of-magnitude) than the conventional method based on multiple exponential IRF models for simultaneous deconvolution of multiple channel measurements on systems with varieties of relaxation dynamics.

8207E-101, Session 7

## Influences on vascular wall smooth muscle cells with novel short-duration thermal angioplasty

M. Kunio, N. Shimazaki, T. Arai, Keio Univ. (Japan); M. Sakurada, Tokorozawa Heart Ctr. (Japan)

We investigated the influences on the smooth muscle cells after our novel short-duration thermal angioplasty, Photo-thermo Dynamic Balloon Angioplasty (PTDBA), to reveal the mechanism that can suppress neo-intimal hyperplasia after PTDBA. We obtained the sufficient arterial dilatations by short-duration heating (≤15s, <70°C) and low dilatation pressure (<0.4MPa) without arterial injuries in our previous in vivo studies. The smooth muscle cells, which play most important role in chronic treatment effects, are heated during PTDBA and stretch-fixed after PTDBA. To evaluate the influences on the smooth muscle cells with heating, the dead cell rate was calculated by Arrhenius equation (Arrhenius parameters: A=2.5×10^16 /s, Ea=1.17×10^5 J/mol). The calculated dead cell rate was 14.8 ± 1.9% after PTDBA (15s, 65°C, 0.35MPa). The influences on the smooth muscle cells with stretch-fixing was assessed in terms of the deformation rate of cells' nuclei and the expression of basic Fibroblast Growth Factor (bFGF) in vivo porcine study. The measured deformation rate of cells' nuclei was 1.6 ± 0.1 after PTDBA (15s, 65°C, 0.35MPa). We found that the bFGF expression after PTDBA (15s, 65°C, 0.35MPa) was inhibited 0.52 fold compared to that after the conventional balloon angioplasty (1.5MPa, 60s). The neo-intimal hyperplasia occupancy rate was measured and it was less than 20% after PTDBA (15s, 65°C, 0.35MPa) in vivo porcine study. We think that the proper decrease of smooth muscle cells with heating and the inhibition of bFGF expression with stretch-fixing may result to suppress the neo-intimal hyperplasia.

8207E-102, Session 7

## Real-time control of angioplasty balloon inflation based on feedback from ontravascular optical coherence tomography

H. Azarnoush, S. Vergnole, G. Lamouche, National Research Council Canada (Canada)

A method is proposed to achieve computerized control of angioplasty balloon inflation, based on feedback from intravascular optical coherence tomography (IVOCT). Controlled balloon inflation could benefit clinical applications, cardiovascular research, and medical device industry.

The proposed method was first experimentally tested for balloon inflation within an artery phantom. During balloon inflation, luminal contour of the phantom was extracted from IVOCT images in real-time. Luminal diameter was estimated from the obtained contour and was used in a feedback loop. Based on the estimated actual diameter and a target diameter, a computer controlled a programmable syringe pump to deliver or withdraw liquid in order to achieve the target diameter. The performance of the control method was investigated under different conditions, e.g. various flow rates and various target diameters. The results were satisfactory, as the control method provided convergence to the target diameters in various experiment.

The proposed method was then tested in a beating heart setup which provides conditions very close to in vivo conditions.

8207E-103, Session 7

## Laser-driven short-duration heating angioplasty: chronic artery lumen patency and histology in porcine iliac artery

N. Shimazaki, M. Kunio, S. Naruse, T. Arai, Keio Univ. (Japan); M. Sakurada, Tokorozawa Heart Ctr. (Japan)

Thermal angioplasty, which was proposed in 1980s, provided successful revascularization with thermal denaturation (softening) of the collagen fibers in artery media. On the other hand, several literatures suggested that the thermal angioplasty resulted in severe restenosis and abnormal artery remodeling in chronic phase caused by thermal injury in artery adventitia and outer artery surroundings. To realize the benefits of thermal angioplasty with a reduction of thermal injury in the artery adventitia and outer artery surroundings, we proposed a short-duration heating balloon angioplasty. We designed a prototype short-duration heating balloon catheter that can heat artery media to 60–70ºC within 15–25 s with a combination of laser-driven heat generation and continuous fluid irrigation in the balloon. The purpose of this study was to investigate chronic artery lumen patency as well as histological alteration of artery wall after the short-duration heating balloon dilatation with porcine healthy iliac artery.

The short-term heating balloon dilated sites were angiographically patent in acute (1 hour) and in chronic phases (1 and 4 weeks). One week after the dilatation, smooth muscle cells (SMCs) density in the artery media measured from HE-stained specimens was approx. 20% lower than that in the reference artery. One and four weeks after the dilatations, artery components in adventitia were kept normal structure without any incidence of thermal injury. Normal lamellar structure of the artery media was also maintained. We think that the local heating to artery media by the short-duration heating could maintain adventitial function and artery normal structure in chronic phase.

8207E-104, Poster Session

## Accurate measurement of systolic blood pressure by photoplethysmography

M. Nitzan, S. Akiva, O. Gleisner, E. Shalom, Jerusalem College of Technology (Israel)

The systolic blood pressure (SBP) can be measured by photoplethysmography (PPG), since the PPG pulses disappear for cuff-pressure above SBP value and reappear when the cuff-pressure decreases below SBP value.

SBP was measured simultaneously by PPG and by sphygmomanometry (Korotkoff sounds), which is generally used as reference standard for non-invasive blood pressure measurements. A PPG probe was attached to the finger distal to the cuff and the PPG signal was stored for offline analysis. The SBP value was determined as the cuff-pressure for which the PPG pulses reappeared during the cuff deflation. A second PPG sensor was attached to the second hand for confirming the PPG pulses in the finger distal to the cuff.

3 examinations were performed on each of 16 healthy subjects. In 24 examinations the difference between the two methods was lower than 3 mmHg. In 16 examinations the SBP value measured by PPG was higher than that measured by sphygmomanometry by more than 3 mmHg. In 8 examinations the SBP obtained by sphygmomanometry was higher by more than 3 mmHg.

The presence of either the PPG pulses or the Korotkoff sounds in a given cuff-pressure proves that the artery is open during systole for that cuff-pressure value. In 16 examinations there were cuff-pressure values for which the PPG pulses were detected but Korotkoff sounds were not detected, despite the open artery during systole. In these examinations the PPG-based technique was more reliable than sphygmomanometry. In 8 examinations sphygmomanometry was more accurate than the PPG-based technique.

# Conference 8207F: Optical Techniques in Neurosurgery, Brain Imaging, and Neurobiology

Saturday-Sunday 21-22 January 2012

Part of Proceedings of SPIE Vol. 8207F Optical Techniques in Neurosurgery, Brain Imaging, and Neurobiology

8207F-107, Session 1

## Raman spectroscopic imaging as complementary tool for histopathologic assessment of brain tumors

C. Krafft, N. Bergner, Institut für Photonische Technologien e.V. (Germany); B. F. M. Romeike, R. Kalff, Friedrich-Schiller-Univ. Jena (Germany); K. D. Geiger, G. Schackert, Technische Univ. Dresden (Germany); J. Popp, Institut für Photonische Technologien e.V. (Germany)

Raman spectroscopy enables label-free assessment of brain tissues and tumors based on their biochemical composition. Combination of the Raman spectra with the lateral information allows delineating tumor margins - even during surgery after coupling with fiber optic probes. This contribution presents Raman images collected from low grade brain tumors (astrocytoma grade II), high grade brain tumors (astrocytoma grade III, glioblastoma multiforme) and brain metastases. Six regions of interest in dried tissue sections encompassed high tumor cell density, low tumor cell density and regular cell density. Spectral unmixing by vertex component analysis (VCA) resolved cell nuclei in score plots and revealed the concentration of spectral contributions of nucleic acids in endmember signatures. The results correlated with the histopathological analysis after staining the specimens by hematoxylin and eosin. 32 regions of interest in non-dried tissue sections that were immersed in buffer included further features such as necrosis and hemorrhage. Here, image processing by VCA was not affected by drying artifacts such as crystallization of cholesterol. Consequently, the results represent better in vivo situations. A three-level-classification approach using support vector machines was trained to (i) perform a quality test, (ii) detect brain metastases and (iii) determine the primary tumor. The approach was applied to specimens from 17 patients with known primary tumor and 5 patients with unknown primary tumor. The results were compared with Fourier-transform-infrared images that were also acquired from the specimens.

8207F-108, Session 1

## Value of 5-aminolevulinic acid for resection of spinal tumors

G. Widhalm, B. Kiesel, Medizinische Univ. Wien (Austria); K. Novak, Medizinische Univ. Wien (Azerbaijan); G. Minchev, A. Wöhrer, C. Matula, D. Prayer, J. A. Hainfellner, E. Knosp, S. Wolfsberger, Medizinische Univ. Wien (Austria)

Objective. Incomplete neurosurgical resection of spinal tumors may lead to tumor recurrence. Currently, no clinical reliable marker is available for intraoperative visualization of spinal (residual-) tumor tissue. Recently, 5-ALA induced fluorescence-guided resection of malignant gliomas demonstrated to increase rate of complete tumor removal. So far, the value of 5-ALA in spinal tumors is unkown. The aim of our study was to assess the value of 5-ALA induced fluorescence for visualization of spinal tumors.

Methods. Neurosurgical resection was performed in 25 patients with spinal tumors between January 2009 and July 2011. 5-ALA was administered in all patients 3 hours before anaesthesia. During and at the end of tumor resection positive 5-ALA fluorescence was noted by a modified neurosurgical microscope. Histopathological tumor diagnosis was established according to the current WHO classification.

Results. Visible 5-ALA fluorescence was observed in 14/25 patients, whereas 11/25 cases were 5-ALA negative: 6/7 ependymomas (5/6 WHO grade II and 1/1 WHO grade III), 6/6 meningiomas, 1/1 glioblastoma and 1/1 ganglioglioma showed positive 5-ALA fluorescence; none of the 4 metastasis, 3 neurinomas, 2 low-grade astrocytomas and 1 hemangioblastoma showed visible 5-ALA fluorescence. In the 5-ALA positive tumor cases, positive 5-ALA fluorescence was able to identify potential residual tumor tissue at the end of resection in all patients.

Conclusion. Our study indicates that 5-ALA is a promising intraoperative marker for visualization of spinal ependymomas, meningiomas, high-grade gliomas and gangliogliomas. Intraoperative detection of potential residual tumor tissue may facilitate complete tumor resection und thus reducing the recurrence rate.

8207F-109, Session 1

## A non-contact imaging approach for quantitative ALA-induced PpIX fluorescence guided resection

P. A. Valdes, F. Leblond, K. Kolste, Dartmouth College (United States); V. L. Jacobs, Dartmouth Hitchcock Medical Ctr. (United States); B. C. Wilson, Univ. of Toronto (Canada); K. D. Paulsen, Dartmouth College (United States); D. W. Roberts, Dartmouth Hitchcock Medical Ctr. (United States)

Gliomas are the single most common primary brain tumor. Studies have shown a strong correlation between extent of resection and improved survival. In recent years, fluorescence guided resection (FGR) for brain tumors using 5-aminolevulinic acid (ALA)-induced protoporphyrin IX (PpIX) has been gaining use as a powerful surgical guidance tool to improve extent of resection. We have recently shown with use of an intraoperative spectroscopy probe that quantitative ALA-induced PpIX FGR shows significantly improved diagnostic accuracy at detecting tumor tissue compared to the state-of-the-art qualitative FGR. Here we present the development of a multi-spectral through-microscope (TM) quantitative fluorescence imaging (qFI) device compatible with modern neurosurgical microscopes, which uses a ratiometric algorithm of fluorescence/reflectance to minimize the distorting effects of tissue optical properties on the emitted fluorescence so as to quantify the absolute concentration of PpIX. We validated our TM-qFI device on tissue simulating phantoms with varying μa at the excitation wavelength λx = 405 nm and μs' at the main emission peak wavelength λm = 635 nm, as well as varying PpIX concentrations. We tested our TM-qFI device and algorithm on both a CNS-1 glioma tumor rodent model and on a case of human glioma, and observed improved detection and quantification of ALA-induced PpIX compared to the state-of-the-art approach. These results open the door to a quantitative imaging approach in ALA-induced PpIX FGR.

8207F-127, Session 1

## Fluorescence guidance during stereotactic biopsy

H. Stepp, W. Beyer, Ludwig-Maximilians-Univ. München (Germany); D. Brucker, A. Ehrhardt, S. K. Fischer, Ludwig-Maximilians-Univ. München (United States); W. Goebel, KARL STORZ GmbH & Co. KG (Germany); M. H. Goetz, MRC Systems GmbH (Germany); G. Hennig, J. Herms, Ludwig-Maximilians-Univ. München (Germany); K. Irion, KARL STORZ GmbH & Co. KG (Germany); A. Johansson, Ludwig-Maximilians-Univ. München (Germany); P. Li, MRC Systems GmbH (United States); G. Palte, Ludwig-Maximilians-Univ. München (Germany); A. Rühm, Klinikum der Univ. München (Germany); S. Sandner, Ludwig-Maximilians-Univ. München (United States)

Introduction: A stereotactic biopsy is taken to enable histopathological diagnosis of a suspected brain tumor. It is essential to i) do this safely, that is not injure a major blood vessel and ii) to obtain relevant vital material from the tumor. We are investigating the suitability of Indocyanine Green (ICG) fluorescence for blood vessel recognition and 5-aminolevulinic acid (5-ALA) induced protoporphyrin IX (PpIX) fluorescence for identification of proliferative brain tumor tissue.

Methods: A fiber-optic as well as an endoscopic approach have been studied to generate and detect both fluorescence signals. Optical tissue parameters of brain tumor have been measured by spatially resolved remission in order to determine the physiological variation range, where calibration of fluorescence signals has to be valid. PpIX concentrations in different kinds of brain tumors have been measured by chemical extraction. Preliminary equipment has been studied in optical phantoms and in a mouse model.

Results: PpIX-concentration was highest in glioblastoma tumor, ranging from 0.5 to 13.5 µM (7 pts). Optical parameters also vary considerably (at 633 nm: 0.22 mm-1 = 0.1 mm can be detected with a contrast of 2-2.5 against surrounding tissue.

Conclusion: Fluorescence detection during stereotactic biopsy might increase safety and precision of the procedure significantly.

8207F-110, Session 2

## Intraoperative laser speckle contrast imaging for monitoring cerebral blood flow: results from a 10-patient pilot study

L. M. Richards, E. L. Weber, The Univ. of Texas at Austin (United States); A. B. Parthasarathy, Boston Univ. (United States); K. L. Kappeler, St David's Hospital (United States); D. J. Fox, St. David's Hospital (United States); A. K. Dunn, The Univ. of Texas at Austin (United States)

Monitoring cerebral blood flow (CBF) during neurosurgery can provide important physiological information for a variety of surgical procedures. Although multiple intraoperative vascular monitoring technologies are currently available, a quantitative method that allows for continuous monitoring is still needed. Laser speckle contrast imaging (LSCI) is an optical imaging method with high spatial and temporal resolution that has been widely used to image CBF in animal models in vivo. In this pilot clinical study, we adapted a Zeiss OPMI Pentero neurosurgical microscope to obtain LSCI images by attaching a camera and a laser diode. This LSCI adapted instrument has been used to acquire full-field flow images from 10 patients during tumor resection procedures. The speckle images were captured with a field of view of ~2 cm x 1.5 cm at ~100 Hz. The patient's ECG was recorded during acquisition and image registration was performed in post-processing to account for pulsatile motion artifacts. For 4 patients, the speckle contrast images were co-registered with images taken under white light illumination with the Zeiss built-in color camera, which showed alignment of the anatomical vasculature and the flow images in all cases. A relative change in blood flow was observed in two patients after bipolar cautery of tissue within the field of view. The LSCI adapted instrument has the capability to produce real-time, full field CBF image maps with excellent spatial resolution and minimal intervention to the surgical procedure. Results from this study demonstrate the feasibility of using LSCI to monitor blood flow during neurosurgery.

8207F-111, Session 2

## Feasibility and methodology of optical coherence tomography imaging of human intracranial aneurysms: ex vivo pilot study

B. Vuong, C. Sun, Ryerson Univ. (Canada); T. Kiehl, Univ. Health Network (Canada); J. A. Gardecki, Wellman Ctr. for Photomedicine (United States) and Massachusetts General Hospital (United States); B. A. Standish, Ryerson Univ. (Canada); L. da Costa, Sunnybrook Health Sciences Ctr. (Canada) and Univ. of Toronto (Canada); J. V. de Morais, Hospital de Baleia (Brazil); G. J. Tearney, Wellman Ctr. for Photomedicine (United States) and Massachusetts General Hospital (United States) and Harvard-MIT Health Sciences and Technology (United States); V. X. D. Yang, Ryerson Univ. (Canada) and Univ. of Toronto (Canada)

Rupture of intracranial aneurysm is a common cause of subarachnoid hemorrhage (SAH) with potentially devastating clinical consequences. The current standard of care for management of unruptured aneurysms involves assessment of features observed under angiography along with patient risk factor evaluation. Aneurysms may undergo specific microscopic morphological changes or remodeling of the vessel wall, prior to rupture. This presents an opportunity for high-resolution imaging to be used in the management of aneurysms. Optical coherence tomography (OCT) may provide such in-vivo high-resolution imaging capability. In this pilot study, we present methods of tissue sample preparation of intracranial aneurysms in order to maintain the orientation between OCT and routine histology. We identify potential OCT imaging features, such as the presence of calcium deposits, and acute or organized thrombus, which may correlate with inflammation, fibroblast infiltration, and/or various immune responses during vessel/aneurysmal wall remodeling. Similarities in the histologic architecture of atherosclerotic plaques and aneurysms are also examined.

8207F-112, Session 2

## Feasibility of endovascular optical coherence tomography for high-resolution carotid vessel wall imaging

H. Y. Cheng, Univ. of Toronto (Canada); C. Sun, Ryerson Univ. (Canada); T. R. Marotta, J. Spears, W. J. Montanera, St. Michael's Hospital (Canada); P. R. Herman, Univ. of Toronto (Canada); A. Thind, B. K. Courtney, Sunnybrook Health Sciences Ctr. (Canada); B. A. Standish, V. X. D. Yang, Ryerson Univ. (Canada)

Atherosclerosis at carotid bifurcation represents a significant risk factor of stroke. Recent studies using non-invasive carotid vessel imaging suggest potential need of high resolution characterization of atherosclerotic carotid plaque, which may allow further risk stratification in patients with high risk plaque morphology. This study aims to demonstrate the technical feasibility of using endovascular optical coherence tomography (EV-OCT) with a distal embolic protection device to image the carotid vessel wall during carotid angioplasty and stenting, with its associated balloon dilatations. We compare 3D in-vivo porcine carotid EV-OCT images with digital subtraction angiography for vessel geometry measurement and stent apposition. We analyze vessel wall thickness and compare with conventional histology from resected carotid samples. Potential complications of carotid angioplasty and stenting, such as thrombus formation, vessel wall dissection, and stent mal-deployment, are simulated in this porcine study, and imaged using EV-OCT in real-time. Preliminary results demonstrate EV-OCT is technically feasible for carotid imaging under controlled conditions, and may be useful in the selected clinical settings.

8207F-113, Session 2

## Contrast-enhanced diffuse optical tomography of brain perfusion in humans using ICG

C. Habermehl, C. H. Schmitz, J. M. Steinbrink, Charité Universitätsmedizin Berlin (Germany)

In neurointensive care, bedside monitoring of brain perfusion is desirable to evaluate the patient's pathologic state and to guide treatment. Existing imaging modalities are not suited for constant monitoring and often require a transport of the patient.

Contrast enhanced near infrared spectroscopy (NIRS) has the potential to serve as a continuous brain perfusion monitor. It is portable, noninvasive, and can be applied continuously without adverse health effects. Previous NIRS studies of brain perfusion employed a topographic (planar) NIRS approach that contains no depth-related information and signals from superficial layers like skin can dominate the measured absorption change.

In our work we demonstrate that diffuse optical tomography (DOT) as a three-dimensional imaging modality of NIRS overcomes this major drawback and allows the clear separation of signals from intra- and extracerebral tissue. We present results from a DOT experiment with an injection of indocyanine green (ICG) that show the different bolus kinetics within the different compartments of the head. We find an early arrival of the ICG bolus in cortical layers with a fast decrease of the signal and a 2-4s delayed arrival in superficial layers. This is in good agreement with the better perfusion of brain tissue compared to skin and proves the separation of both layers. Beside the analysis of time courses we also present 3D result volumes, visualizing the earlier arrival of the bolus in the brain. To demonstrate the excellent spatial resolution, reconstructed images of blood vessel in superficial layers are presented. This work can help to promote the use of DOT for continuously monitoring patients undergoing brain trauma or stroke. It could be highly usefull to detect changes in brain perfusion in time without expensive measurements and difficult transport of the patient.

8207F-114, Session 3

## Spectral and lifetime domain measurements of rat brain tumours

B. Leh, Institut National de Physique Nucléaire et de Physique des Particules (France); D. Abi Haidar, Institut National de Physique Nucléaire et de Physique des Particules (France) and Univ Paris 7-Denis Diderot (France); K. Allaoua, Institut National de Physique Nucléaire et de Physique des Particules (France); M. Collado-Hilly, INSERM (France); I. Chebbi, SARL Nanobactérie (France); Y. Charon, Institut National de Physique Nucléaire et de Physique des Particules (France) and Univ Paris 7-Denis Diderot (France); M. Duval, Institut National de Physique Nucléaire et de Physique des Particules (France) and Univ. d'Evry Val d'Essonne (France); L. Ménard, Institut National de Physique Nucléaire et de Physique des Particules (France) and Univ. Paris 7-Denis Diderot (France); R. Siebert, Institut National de Physique Nucléaire et de Physique des Particules (France)

Nowadays, surgical intervention remains a valuable treatment for high grade glioblastoma, for many cases. The problem consists in bordering tumour sites which affects the patient's prognostic. In this context, this paper is devoted to the development of an optical probe, for future clinical application, based on fluorescence detection used for tissue characterization. After injection of tumorous cells in rat brain, the spectroscopic signal from freshly extracted brain slides is recorded. Two excitation wavelengths are used to distinguish normal from tumorous brain sites through spectral autofluorescence characteristics. The intrinsic fluorescence redox ratio derived from two primary endogenous fluorophores, reduced nicotinamide dinucleotide and oxidized flavoprotein, is studied. This autofluorescence spectral analysis is performed on fresh and paraformaldehyde fixed brain tumour tissues. The redox ratio seems to be an interesting indicator for discrimination of cancerous from healthy sites by providing information on metabolic states in pathological areas. Using the same fixed rat brain slices, fluorescence lifetime of several endogenous fluorophores are also measured with the same probe. Results suggest that lifetime spectroscopy may be a complementary modality for discrimination of cancerous from peripheral tissue.

The paper reports details of experiments and results derived from spectral and lifetime domain measurements.

8207F-115, Session 3

## Hyperthermia enhances photochemical internalization-mediated delivery of bleomycin in glioma spheroids

S. Madsen, C. Fennimore, Univ. of Nevada, Las Vegas (United States); H. Hirschberg, Beckman Laser Institute and Medical Clinic (United States)

Photochemical internalization (PCI) is a technique to improve the utilization of macromolecules (e.g. chemotherapeutic agents) in cancer therapy in a site-specific manner. The concept is based on the use of specially designed photosensitizers (e.g. AlPcS2a) which localize preferentially in the membranes of endocytic vesicles. Previous studies have shown that AlPcS2a-mediated PCI enhances the efficacy of bleomycin in human glioma spheroids. The current study was initiated to determine whether hyperthermia enhances the efficacy of PCI-mediated delivery of bleomycin in multicell glioma spheroids.

Human glioma spheroids (500 μm dia.) were established from biopsy-derived glioma cells. All experiments were conducted in a small incubator at temperatures ranging from 37 to 50 oC. Spheroids were irradiated with 670 nm laser light via an optical fiber inserted through an opening in the incubator. For each temperature investigated (45 min. heating time), spheroids were divided into 5 groups: control, dark control, bleomycin-only, photodynamic therapy (PDT), and PCI. PDT and PCI spheroids were exposed to 0.5 J cm-2 for approximately 100 s. Toxicity was evaluated from spheroid growth kinetics.

Preliminary results show that clinically relevant levels of hyperthermia (40 - 42 oC for 45 min.) enhance the efficacy of PCI-mediated delivery of bleomycin in human glioma spheroids. Although the mechanism has not been explored, the enhanced efficacy is likely due to heat-induced inactivation of DNA repair enzymes responsible for repairing bleomycin-induced DNA damage.

8207F-116, Session 3

## Quantitative measurement of cerebral blood flow during hypothermia by using time-resolved near-infrared spectroscopy

M. Fazel Bakhsheshi, M. Diop, K. St Lawrence, T. Lee, The Univ. of Western Ontario (Canada)

OBJECTIVES: Clinical trials of hypothermia therapy in asphyxiated infants have demonstrated the therapeutic potential in cerebral ischemia. A non-invasive bedside technique for monitoring of cerebral blood flow (CBF) has the potential to improve management of life-threatening neurological emergencies by detecting cerebral ischemia before brain injury occurs. We investigated using time-resolved near-infrared (TR-NIR) technique to measure local absolute CBF by a bolus-tracking method using a light-absorbing dye indocyanine green (ICG) as a flow tracer to examine the effect of cooling on CBF in new born piglet.

METHODS: Experiments were conducted on new born piglets (<3 days) that were anesthetised by isoflurane. A cannula was inserted into an ear vein for administrating of ICG. A femoral artery was catheterized to monitor heart rate and blood pressure and to intermittently collect arterial blood samples for gas (paCO2, paO2), pH and glucose analysis. Animals were placed in a prone position, and a custom-made probe holder was strapped to the head to hold the two set (TR-NIRS and DCS instruments) of emission and detection probes 2 cm apart, parasagittally, approximately 1.5 cm dorsal to the eyes. Temperature was altered by placing plastic ice bags on the surface of the piglet's body until the rectal temperature decreased to 30°C. CBF was then determined from brain ICG concentration curves as described previously [1].

RESULTS: Analysis of the ICG data resulted in estimation of CBF and cerebral blood volume (CBV) for each temperature. Table 1 presents the average physiological, optical properties and absolute values of CBF and CBV measured by TR-NIR technique.

CONCLUSION: These preliminary results suggest that CBF in new born piglets can be monitored by TR-NIR technique during hypothermia treatment. We will be validating our result against CT perfusion measurement of CBF as the next step. Diffusion Correlation Spectroscopy results will be present in the full abstract.

REFERENCES

[1]-Journal of Biomedical Engineering. 15(5) - 057004 - Sep-Oct (2010)

8207F-117, Session 3

## Enhanced gene transfection by photochemical internalization of acid transforming polypeptide micelles

H. Hirschberg, E. Shih, Beckman Laser Institute and Medical Clinic (United States); S. Madsen, Univ. of Nevada, Las Vegas (United States); Y. J. Kwon, Univ. of California, Irvine (United States)

One of many limitations for cancer gene therapy is the inability of the therapeutic gene to transfect a sufficient number of tumor cells. Cells are not prone to take up and utilize large and negatively charged macromolecules such as plasmid DNA. This necessitates the use of delivery carriers in order to overcome multiple extracellular and intracellular pathways. Among many barriers in nonviral gene delivery, cytosolic release (endosomal escape) and dissociation of nucleic acids from the carriers once arrived at their intracellular targets are crucial efficiency-determining steps We have synthesized, by self-assembling DNA with PEG-conjugated poly(ketalized serine), micelles that transform their structure in the mildly acidic endosome.

Photochemical internalization (PCI) is a photodynamic therapy-based approach for improving the delivery of macromolecules and genes into the cell cytosol. The utility of PCI to enhance delivery of a tumor suppressor gene employing acid transforming polypeptide micelles carriers was investigated in monolayers and spheroids consisting of glioma cells.

Glioma cell monolayers or spheroids were incubated in AlPcS2a followed by non-viral vectors and light treatment at 670 nm. Transfection efficiency for a plasmid construct (GFP-Luciferase-PTEN) employing either the non-viral carrier jetPEI or acid transforming polypeptide micelles was compared.

Collectively, the results suggest that AlPcS2a-mediated PCI can be used to enhance transfection of tumor suppressor genes. The results also imply that the acid-transforming PEG-polypeptide micelles are effective nonviral carriers for efficient, noncytotoxic, serum-resistant, targeted, and versatile gene delivery in vitro and in vivo and that their efficacy is significantly enhanced by PCI.

8207F-118, Session 3

## Dynamic contrast enhanced-magnetic resonance imaging (DCE-MRI) of photodynamic therapy (PDT) outcome and associated changes in the blood-brain barrier following Pc 4-PDT of Glioma in an athymic nude rat model

V. Belle, A. A. Anka, N. M. Cross, P. Thompson, E. Mott, R. Sharma, K. Gray, R. Zhang, Y. Xu, J. Sun, C. A. Flask, N. L. Oleinick, D. Dean, Case Western Reserve Univ. (United States)

Dynamic Contrast-Enhanced-Magnetic Resonance Imaging (DCE-MRI) appears to provide an unambiguous means of tracking the outcome of photodynamic therapy (PDT) in brain tumor with the photosensitizer Pc 4. The increase in Gd enhancement observed after Pc 4-PDT may be due to a temporary opening of the blood-brain-barrier, which as noted by others, may offer a therapeutic window. Methods: We injected 2.5 x 10^5 U87 cells into the brains of 9 athymic nude rats. After 8-9 days peri-tumor DCE-MRI images were acquired on a 7.0T microMRI scanner before and after administration of 150 uL Gd. DCE-MRI scans were repeated three times following Pc 4-PDT. Results: The average, normalized peak enhancement in the tumor region, approximately 30-90 seconds after Gd administration, was 1.31 times greater than baseline (0.03 Standard Error [SE]) prior to PDT and was 1.44 (0.02 SE) times baseline in the first post-PDT scans (Day 11), a statistically significant ($p \approx 0.014$, N=8) increase over the pre-PDT scans, and was 1.38 (0.02 SE) times baseline in the second scans (Day 12), also a statistically significant ($p \approx 0.008$, N=7) increase. Observations were mixed in the third post-PDT scans (Day 13), averaging 1.29 (0.03 SE) times baseline ($p \approx 0.66$, N=7). Overall a downward trend in enhancement was observed from the first to the third post-PDT scans. Discussion: DCE-MRI may provide an unambiguous indication of brain tumor PDT outcome. The initial increase in DCE-MRI signal may correlate with a temporary, PDT-induced opening of the blood-brain-barrier, creating a potential therapeutic window.

8207F-119, Session 4

## Spatial frequency domain optical imaging of neurovascular coupling in a mouse model of Alzheimer's disease

A. J. Lin, S. D. Konecky, T. B. Rice, Beckman Laser Institute and Medical Clinic (United States); K. N. Green, Univ. of California, Irvine (United States); B. J. Tromberg, Beckman Laser Institute and Medical Clinic (United States)

In this work we present an economical spatial frequency domain imaging (SFDI) platform utilizing a commercially available LED projector, camera, and off-the-shelf optical components. The fast acquisition platform is demonstrated in a neurovascular functional activation experiment in a transgenic mouse Alzheimer's model. Spatially-modulated bandpass-filtered LEDs at 530nm and 610nm, focused on an expandable field-of-view, are imaged and acquired from mouse cortex during and after forepaw stimulation. The frequency-dependent reflectance is fit to a light transport model to image light scattering and absorption within the tissue. Intrinsic chromophore concentrations of oxy- and deoxy-hemoglobin, in addition to high-contrast maps of tissue scattering were recovered. Concurrent laser speckle imaging provides co-registered blood flow maps.

While Alzheimer's disease (AD) is confirmed at time of death with brain amyloid beta (Aβ)-plaques and tau-tangles, disease diagnosis, monitoring and prognosis are very limited when the patient is alive. Our results show significant absorption and scattering contrast in Alzheimer's vs. control mice due to variations in cellular and vascular composition. Furthermore, the dynamic vascular response to forepaw stimulation may be an early biomarker for AD. If, indeed, neurovascular dysfunction plays a key role in the pathogenesis of age-related neurodegenerative diseases, further characterization of these changes will be key to understanding, staging, and potentially treating AD.

8207F-120, Session 4

## Neurosurgical hand-held optical coherence tomography (OCT) forward-viewing probe

C. Sun, Ryerson Univ. (Canada); K. K. C. Lee, Univ. of Toronto (Canada); B. Vuong, Ryerson Univ. (Canada); M. Cusimano, St. Michael's Hospital (Canada); A. Brukson, A. Mariampillai, B. A. Standish, Ryerson Univ. (Canada); V. X. D. Yang, Ryerson Univ. (Canada) and Univ. of Toronto (Canada)

A prototype neurosurgical hand-held optical coherence tomography(OCT) imaging probe has been developed to provide micron resolution cross-sectional images of subsurface tissue during open surgery. The probe has been designed based on our group's previous work on electrostatically driven optical fibers and has now been packaged into a catheter probe in the familiar form factor of the clinically accepted Bayonet shaped neurosurgical non-imaging Doppler ultrasound probes. The optical design was optimized based on ZEMAX simulation. Optical properties of the probe were tested to yield an ~20 um spot size, 5 mm working distance and a 3.5 mm field of view. The scan frequency can be increased or decreased by changing the applied voltage. Typically a scan frequency of less then 60Hz is chosen to keep the applied voltage to less than 2000V. The axial resolution of the probe was ~15 um (in air), which was determined by the OCT system. A custom-triggering methodology has been developed to provide continuous stable imaging, which is crucial for clinical utilities. Feasibility of this probe, in combination with a 1300 nm swept source OCT system was tested and images are presented to highlight the usefulness of such a forward viewing hand-held OCT imaging probe. Knowledge gained from this research will lay the foundation for developing new OCT technologies for endovascular management of cerebral aneurysms and transsphenoidal neuroendoscopic treatment of pituitary tumors.

8207F-121, Session 4

## Discriminant analysis of functional near-infrared imaging for schizophrenia diagnosis

C. Chuang, National Taiwan Univ. (Taiwan); I. Chiang, Taipei Medical Univ. (Taiwan); T. Lan, National Yang-Ming Univ. (Taiwan); C. Chen, National Taiwan Univ. (Taiwan); Y. Hsieh, C. Wang, National Chiao Tung Univ. (Taiwan); C. Lin, C. Sun, National Yang-Ming Univ. (Taiwan)

Prefrontal cortex (PFC) dysfunction in individuals with schizophrenia has been investigated by different neuroimaging methods. Functional near-infrared spectroscopy (fNIRS), a novel neurophysiological method, is being increasingly used in the investigation of frontal dysfunction in schizophrenia. Recently, low PFC activation in individuals with schizophrenia has also been evidenced during word fluency tests (WFT) and other cognitive tests by functional near-infrared spectroscopy (fNIRS). The purpose of this study was to assess hemodynamic changes and discriminant analysis in the PFC between patients with schizophrenia and healthy controls during WFT using a 52-channel fNIRS system. This study consisted of a total of 99 subjects, including 53 patients with schizophrenia and 46 age- and gender-matched healthy control subjects. The concentration change in oxygenated hemoglobin was measured in the prefrontal areas during the three versions of the WFT tasks. In the results, the healthy group showed larger activation in the right and left PFC than in the middle PFC. The schizophrenic group showed poorer task performance and less prefrontal cortex activation during all tasks compared to healthy subjects. We then performed discriminant analysis by biostatistics method using fNIRS measures as independent variables. Kolmogorov-Smirnov test was used to compare oxygenation change and k-means clustering was used to classify between schizophrenic and healthy group. As the results, the mean oxygenation changes showed a significantly difference with p-value < 0.001 in 6 channels (CH 23, 29, 31, 40, 42, 52) between schizophrenic and healthy group. Finally, 68.69% and 72.73% of the participants were correctly classified as being schizophrenic or healthy subjects with all 52 channels and 6 significantly difference channels. Our findings suggest that fNIRS measurement could be applied to discriminate patients with schizophrenia from healthy subjects.

8207F-122, Session 4

## Hyperspectral optical tomography of evoked hemodynamic activity in the rat cortex

S. D. Konecky, Beckman Laser Institute and Medical Clinic (United States); N. A. Hagen, Rice Univ. (United States); A. Mazhar, Beckman Laser Institute and Medical Clinic (United States); T. S. Tkaczyk, Rice Univ. (United States); R. D. Frostig, Univ. of California, Irvine (United States); B. J. Tromberg, Beckman Laser Institute and Medical Clinic (United States)

The connection between hemodynamic activity and neuronal function is of critical importance for both our basic understanding of brain function, as well as the study of brain pathologies including stroke and Alzheimer's disease. Yet despite intense research, the relationship between the measured signals and the underlying neuronal function remain unknown. In particular, the existence of a localized increase in the concentration of deoxy-hemoglobin caused by the oxidative metabolism of active neurons remains controversial in both the optics and fMRI communities.

We use Image Mapping Spectroscopy, a new hyperspectral imaging method we have developed, to image evoked intrinsic optical signals in the rat somatosensory cortex. We successfully image the hemodynamic response to stimulation of a single whisker simultaneously in 38 wavelengths bands from 484 nm to 652 nm at a rate of 5 Hz. We measure increases in the tissue concentrations of both oxy-hemoglobin (ctHbO2) and deoxy-hemoglobin (ctHb) within the first second after stimulus onset, indicating simultaneous oxygen consumption and re-perfusion following cortical stimulation. The mean increases in the tissue concentrations of ctHbO2 and ctHb due to stimulation were 27 +/- 20 nM and 248 +/- 80 nM respectively. Our subsequent analysis shows that 70% of the initial decrease in light intensity consistently measured in our rat model using 630 nm light results from an increase in ctHb. The use of hyperspectral imaging allowed us to supplement our quantitative analysis by visually comparing the measured spectra to the distinct spectral features of oxy- and deoxy-hemoglobin.

In addition, we use hyperspectral imaging to generate three-dimensional tomographic images of evoked hemodynamic activity in the rat cortex. This is possible because near-infrared light penetrates much more deeply into the brain than visible light. By using many wavelengths of light spanning both the visible and near-infrared (NIR), and applying tomographic imaging methods, we localize the depth in the cortex at which the evoked hemodynamic activity occurs.

8207F-123, Session 4

## Relative phase of oscillations of cerebral oxy-hemoglobin and deoxyhemoglobin concentrations during sleep in human subjects

M. L. Pierro, A. Sassaroli, Tufts Univ. (United States); P. R. Bergethon, Boston Univ. School of Medicine (United States); S. Fantini, Tufts Univ. (United States)

Near-infrared spectroscopy (NIRS) is a non-invasive optical method that provides information about cerebral tissue oxygenation, as well as deoxy-hemoglobin ([Hb]) and oxy-hemoglobin ([HbO])) tissue concentrations. A whole-night sleep study was conducted on five healthy subjects. NIRS data were collected on the right and left sides of the forehead to probe the prefrontal cortex. Polisomnography data were used to identify rapid eye movement (REM) and non-REM sleep stages. We performed a phase analysis of oscillatory components of [Hb] and [HbO] at low frequencies (0.04-0.12 Hz), respiratory frequency (~1 Hz), and cardiac frequency (~0.3 Hz). We have applied a previously proposed model based on a phasor representation to identify the contributions from blood volume and blood flow velocity oscillations to the measured relative phase of [Hb] and [HbO]. We have consistently found that [Hb] oscillations lead [HbO] oscillations at low frequencies, while the two species oscillate in phase at respiratory and cardiac frequencies. At low-frequencies, the phase lead of [Hb] with respect to [HbO] significantly changes during various sleep stages, assuming values of ~20 degrees before sleep onset, ~ 120 degrees during deep sleep (stage 4), and ~100 degrees during REM sleep. Our phasor model translates amplitude and phase measurements of [Hb] and [HbO] oscillations into amplitudes and phase measurements of blood volume and blood flow velocity oscillations, opening new opportunities for hemodynamic investigations in functional brain imaging.

8207F-105, Session 5

## Identifying brain cancers using dye-enhanced multimodal confocal imaging

D. J. Wirth, Univ. of Massachusetts Lowell (United States); M. Snuderl, Harvard Medical School (United States); S. A. Sheth, W. Curry, Massachusetts General Hospital (United States); A. N. Yaroslavsky, Univ. of Massachusetts Lowell (United States) and Massachusetts General Hospital (United States) and Harvard Medical School (United States)

Brain cancers are among the most aggressive and deadliest. Even benign tumors are associated with high morbidity and poor quality of life. Complete resection of brain tumors may improve quality of life and patient survival. The goal of this study was to evaluate multimodal confocal imaging for intraoperative detection of brain cancers. In particular, we have imaged different types of brain cancers, correlated optical images to histopathology, and evaluated the possibility of straightforward interpretation of fluorescence images in a manner similar to that of histopathology. Fresh thick specimens were obtained within several hours after surgeries. A total of 25 normal brain samples and 78 cancerous samples were studied. Of the cancerous samples there were 25 metastasis, 14 meningioma, 19 glioblastoma, 12 high grade glioma and 8 low grade glioma samples. The tissues were briefly stained in 0.05 mg/ml aqueous solution of methylene blue. Multimodal confocal images were acquired using an in house built system. Reflectance and fluorescence signals of MB were excited at 642 nm. Fluorescence emission of MB was registered between 670 and 710 nm. After imaging, all tissues were processed for H&E histopathology. Histological sections were digitized and compared side-by-side to the corresponding optical images. The results of comparison demonstrate good correlation between fluorescence images and histopathology. Reflectance images provide information on the morphology and vascularization of the specimens, complimentary to that provided by fluorescence images. Multimodal confocal approach shows promise for intraoperative brain cancer detection.

8207F-124, Session 5

## Compact fluorescence and white-light imaging system for intraoperative visualization of nerves

D. C. Gray, E. Kim, V. Cotero, P. Staudinger, S. Yazdanfar, C. Tan Hehir, GE Global Research (United States)

Fluorescence image guided surgery (FIGS) allows intraoperative visualization of critical structures, with applications spanning neurology, cardiology and oncology. An unmet clinical need is prevention of iatrogenic nerve damage, a major cause of post-surgical morbidity. Currently most procedures are performed without any form of image guidance, as available technologies lack the ability to provide nerve-specific imaging. Here we describe the advancement of FIGS imaging hardware, coupled with a custom nerve-labeling fluorophore, to bring FIGS nerve imaging closer to clinical translation.

A compact imaging system was developed to simultaneously display white light and fluorescence images for open and minimally invasive surgical procedures. The <2-kg instrument is comprised of a 405nm laser and a white light LED source for excitation and illumination, respectively, and consumer-grade cameras. The fluorescence excitation and emission characteristics were customized for an optimized derivative of our fluorophore. The imaging hardware and contrast agent were evaluated in mice during in vivo surgical procedures, through simultaneous display of reflectance and fluorescence video.

Intravenous injection of the fluorophore highlighted both central and peripheral nerves suggesting that the agent was capable of crossing the blood nerve barrier and blood brain barrier. The new contrast agent showed improved uptake by nerves, minimal binding to muscle, and high contrast in vivo.

The new fluorophore coupled with the compact imaging system demonstrates a complete image-guided surgery solution that can assist in the detection of nerves during open and minimally invasive procedures.

This study is funded by NIH grant 5R01EB011872-02.

8207F-125, Session 5

## Non-contact photoacoustic tomography and ultrasonography for brain imaging

G. Rousseau, A. Blouin, J. Monchalin, National Research Council Canada (Canada)

Photoacoustic tomography (PAT) and ultrasonography (US) of biological tissues usually rely on transducer arrays for the detection of ultrasound. Obtaining the best sensitivity requires a physical contact with the tissue using an intermediate coupling fluid (water or gel). This type of contact is a major drawback for several applications such as neurosurgery. Laser-ultrasonics is an established optical technique for the non-contact generation and detection of ultrasound in industrial materials. In this paper, the non-contact detection scheme used in laser-ultrasonics is adapted to allow probing of ultrasound in biological tissues while remaining below laser exposure safety limits. Both non-contact PAT (NCPAT) and non-contact US (NCUS) are demonstrated experimentally using a single-frequency detection laser emitting suitably shaped pulses and a confocal Fabry-Perot interferometer. It is shown that an acceptable sensitivity is obtained while remaining below the maximum permissible exposure (MPE) of biological tissues. Results obtained ex vivo with calf brain and chicken breast specimens show that sub-mm endogenous and exogenous inclusions can be detected at depth exceeding 1 cm. When fully developed, the technique could be a unique diagnostic tool in neurosurgery providing deep imaging of blood vessels, blood clots and blood oxygenation.

8207F-126, Session 5

## Full-field optical coherence tomography for intraoperative diagnosis during brain surgery?

A. Latrive, ESPCI - Institut Langevin (France) and LLTECH SAS (France); O. Assayag, ESPCI - Institut Langevin (France); F. Harms, LLTECH SAS (France); B. Devaux, Ctr. Hospitalier Sainte Anne (France); A. C. Boccara, ESPCI - Institut Langevin (France) and LLTECH SAS (France)

Optical Coherence Tomography (OCT) has proven its interest for many biomedical fields thanks to its virtual slicing and 3D imaging capability. Full-Field OCT (FFOCT) is a particular approach which directly takes “en face” 2-D images with an isotropic resolution around 1 micrometer. With such a high resolution FFOCT systems can produce images that are similar to that obtained with classical histology procedures and can thus be important tools for pathology diagnosis. One main interest of this technique is that it does not require any staining agent: it uses the backscattered light due to refractive index variations in the tissue as a source of endogenous contrast.

We have in particular shown that single myelin fibers, which have a diameter less than 1 micrometer, are clearly visible on FFOCT images. Indeed the lipid-rich myelin sheath lies in an aqueous background, thus ensuring a high contrast. Moreover we can also discriminate grey matter from white matter, and distinguish glial cells. We think that a FFOCT system placed in the operating room could be used to get a real-time diagnosis on excised samples during brain surgery, such as tumor removal surgery.

Furthermore we are developing a similar system with a rigid probe with a diameter around 2mm in order to do in vivo and in situ high-resolution imaging. Our probe could thus guide the surgeon before and during excision and ensure a more precise gesture.

8207F-128, Session 6

## Full-field optical coherence microscopy (FFOCM) is a novel technique for subcellular imaging of myenteric neurons in the gastrointestinal tract: potential role in diagnosing Hirschsprung’s disease

E. Coron, Y. Bromberg, Wellman Ctr. for Photomedicine (United States); A. Pieretti, Massachusetts General Hospital (United States); M. Mahé, INSERM (France); E. Auksorius, Wellman Ctr. for Photomedicine (United States); M. Neunlist, INSERM (France); B. E. Bouma, Wellman Ctr. for Photomedicine (United States); A. Goldstein, Massachusetts General Hospital (United States); G. J. Tearney, Wellman Ctr. for Photomedicine (United States)

Introduction: Novel non-invasive methods to assess the enteric nervous system (ENS) are needed. The goal of this study was to test and validate Full-Field Optical Coherence Microscopy (FFOCM) to characterize the ENS of the colon.

Methods: A mouse model of Hirschsprung’s disease (HD) and normal mice were used (n=10). FFOCM imaging was performed on freshly excised specimens, along the gastrointestinal tract. Stacks of images were acquired through the entire thickness of the gut using the following settings: lateral resolution 0.5µm, axial resolution 0.8µm, depth of imaging 200µm, and field of view 250µm. Then, the tissue was fixed in paraformaldehyde and imaged by confocal microscopy following staining with antibodies against PGP9.5 (for neuronal fibers) and Hu (for neuronal cell bodies).

Results: FFOCM imaging provides subcellular visualization of the full-thickness of the gut wall. Myenteric ganglia and interganglionic neurofibers can be clearly identified in normal mice. Images of the myenteric plexus were able to be acquired from the stomach, duodenum, colon, and rectum. FFOCM was then used to characterize the ENS in HD mice. Imaging revealed an important decrease of the number of ganglia in the rectum of these mice, while normal ganglia were observed proximally. Confocal microscopy of these tissues with neuronal fibers and cell bodies labeled confirmed our FFOCM observations.

Conclusions: FFOCM is a novel technique that enables full-thickness, real-time optical imaging of the ENS along the entire intestine. This technique is able to differentiate ganglionic from aganglionic colon in a mouse model of Hirschsprung’s disease.

8207F-129, Session 6

## In vivo optical microprobe imaging for intracellular Ca2+ dynamics in response to dopaminergic signaling in deep brain evoked by cocaine

Z. Luo, Y. Pan, C. Du, Stony Brook Univ. (United States)

Ca2+ plays a vital role as second messenger in signal transduction and the intracellular Ca2+ ([Ca2+]i) change is an important indicator of neuronal activity in the brain, including both cortical and subcortical brain regions. Due to the highly scattering and absorption of brain tissue, it is challenging to optically access the deep brain regions (e.g., striatum at >3mm under the brain surface) and image [Ca2+]i changes with cellular resolutions. Here, we present two micro-probe approaches (i.e., microlens, and micro-prism) integrated with a fluorescence microscope modified to permit imaging of neuronal [Ca2+]i signaling in the striatum using a calcium indicator Rhod2(AM). While a micro-prism probe provides a larger field of view to image neuronal network from cortex to striatum, a microlens probe enables us to track [Ca2+]i dynamic change in individual neurons within the brain. Both techniques are validated by imaging neuronal [Ca2+]i changes in transgenic mice with dopamine receptors (D1R, D2R) expressing EGFP. Our results show that micro-prism images can map the distribution of D1R- and D2R-expressing neurons in various brain regions and characterize their different mean [Ca2+]i changes induced by an intervention (e.g., cocaine administration, 8mg/kg., i.p). In addition, microlens images can characterize the different [Ca2+]i dynamics of D1 and D2 neurons in response to cocaine, including new mechanisms of these two types of neurons in striatum. These findings highlight the power of the optical micro-probe imaging for dissecting the complex cellular and molecular insights of cocaine in vivo.

8207F-130, Session 6

## Multichannel optical brain imaging to separate cerebral vascular, tissue metabolic, and neuronal effects of cocaine

Z. Luo, Z. Yuan, Y. Pan, C. Du, Stony Brook Univ. (United States)

Characterization of cerebral hemodynamic and oxygenation metabolic changes, as well neuronal function is of great importance to study of brain functions and relevant brain disorders such as drug addiction. Compared with other neuroimaging modalities, optical imaging techniques have the potential for high spatiotemporal resolution and dissection of the changes in cerebral blood flow (CBF), blood volume (CBV), and hemoglobing oxygenation and intracellular Ca ([Ca2+]i), which serve as markers of vascular function, tissue metabolism and neuronal activity, respectively. Recently, we developed a multiwavelength laser speckle imaging (MW-LSI) system and integrated it into a surgical microscope. Three LEDs of 530, 570 and 630nm were used for exciting [Ca2+]i fluorescence labeled by Rhod2 (AM) and measuring total hemoglobin (i.e., CBV), and deoxygenated-hemoglobin, whereas one laser of 830nm was used for laser speckle imaging to form a CBF mapping of the brain. These light sources were time-sharing for illumination on the brain and synchronized with the exposure of CCD camera for multichannel images of the brain. Our animal studies indicated that this optical approach enabled simultaneous mapping of cocaine-induced changes in CBF, CBV and oxygenated- and deoxygenated hemoglobin as well as [Ca2+]i in the cortical brain. Its high spatiotemporal resolution (0.03mm, 10Hz) and large field of view (4x5 mm2) are additional advantages for a imaging tool in brain functional study.

8207F-184, Session 6

## Optical tractography of human brain

H. Wang, J. Zhu, Univ. of Minnesota, Twin Cities (United States); B. Fischl, Massachusetts General Hospital (United States); D. A. Boas, Athinoula A. Martinos Ctr. for Biomedical Imaging (United States); T. Akkin, Univ. of Minnesota, Twin Cities (United States)

We present imaging of the ex-vivo human brain with a multi-contrast optical coherence tomography (MC-OCT). Using a polarization-maintaining fiber-based technology, the MC-OCT system is able to simultaneously generate high-resolution cross-sectional images of reflectivity, phase retardance and optic axis orientation. A cubic block of fixed human brain was mounted on a tissue slicer and imaged by MC-OCT. The imaging is repeated multiple times after removing 350 μm thick slices. En-face images of reflectivity, retardance and axis orientation are reconstructed for each slice. The contrast between the white and gray matters is small on the reflectivity images, resulting in more challenging differentiation between the structures; however, using the birefringence property of the myelin sheath, gray matter and white matter regions are clearly distinguishable in the retardance images. The slope of retardance in depth allows one to infer the inclination angle of fiber tracts in the direction orthogonal to the en-face plane, and the axis orientation information indicates the in-plane orientation. A vector space is employed to represent the 3D orientation of the fiber tracts. The 3D reconstruction of the human brain can be accomplished by stacking series of brain slices, and optical tractography can be computed by applying tracking algorithms. Furthermore, the MC-OCT technology may be useful in validating diffusion weighted MRI, and open new lines for the study of structural connections in normal and pathological brain.

8207F-226, Session 6

## Optical coherence tomography of the spinal cord: optimization of an in vivo model

A. Miriampillai, Ryerson Univ. (Canada); D. W. Cadotte, A. Cadotte, K. K. C. Lee, Univ. of Toronto (Canada); R. Kiehl, Univ. Health Network (Canada); B. C. Wilson, Princess Margaret Hospital (Canada); M. G. Fehlings, Univ. of Toronto (Canada); V. X. D. Yang, Ryerson Univ. (Canada)

Optical coherence tomography (OCT) has the combined advantage of high temporal (μsec) and spatial ( 2mm to approx. 43μm. Brief breath holds ( 40μm to 400 μm). Histology of the spinal cord was also performed for reference.

Recent advances in OCT vascular imaging have made this technology suitable for answering specific questions in neurobiology. Here we present an optimized in vivo model of the spinal cord where we address the issues of spinal cord preparation, reducing cardio-respiratory motion artifacts to achieve an optimal SNR in vascular images.

8207F-227, Session 6

## Biomechanical properties of soft tissue measurement using optical coherence elastography

M. Razani, A. Miriampillai, C. Sun, Ryerson Univ. (Canada); V. X. D. Yang, Ryerson Univ. (Canada) and Univ. of Toronto (Canada); M. C. Kolios, Ryerson Univ. (Canada)

Optical Coherence Tomography (OCT) provides images at near histological resolution, which allows for the identification of micron sized morphological tissue structures. Optical coherence elastography (OCE) measures tissue displacement and utilizes the high resolution of OCT to generate high-resolution stiffness maps. In this work, we explored the potential of measuring shear wave propagation using OCE. A swept-source OCT system was used in this study, the laser had a center wavelength of 1310 nm and a bandwidth of ~110 nm. The lateral resolution was approximately 13 μm in the samples. Acoustic radiation force was applied to two different phantoms using a 20 MHz circular (8.5 mm diameter) piezoelectric transducer element transmitting sine-wave bursts of 400 μs. The first type of phantom consisted of a 355 μm glass sphere (dark) embedded in gelatin and was used to characterize the ultrasound pushing beam. The second consisted of gelatin mixed with titanium dioxide, which provided uniform acoustic and optical scattering. The OCT signal from this second set of phantoms was used for the measurement of the shear wave speed and viscosity. For both sets of experiments phase analysis was applied to B-mode and M-mode OCT images which were obtained while ultrasound transducer was generating the “push” in the phantom. The experiments are the first step towards imaging shear wave propagation in tissue and characterization of tissue mechanical properties using OCE, with the eventual goal of developing OCE as a diagnostic tool for the assessment of pre-cancerous and cancerous lesions.

8207F-131, Poster Session

## Cortical-depth dependent cerebral hemodynamic responses to direct epidural stimulation using NIRS and ORIS

S. Lee, D. Koh, Korea Univ. (Korea, Republic of); A. Jo, H. Y. Lim, Sungkyunkwan Univ. (Korea, Republic of); Y. Jung, C. Im, Hanyang Univ. (Korea, Republic of); C. Kim, Y. Seo, Korea Univ. (Korea, Republic of); M. Suh, Sungkyunkwan Univ. (Korea, Republic of); B. Kim, Korea Univ. (Korea, Republic of)

In this study, we applied Optical Recording of Intrinsic Signal (ORIS) and Near-Infrared Spectroscopy (NIRS) alternatively to measure the hemodynamic perfusion interaction between superficial and sub cortical region when direct epidural stimulation was applied. Our result indicates that hemodynamic responses depend on the cortical depth. In deep brain, the outer layers react faster than the deeper layers to show downstream propagation of hemodynamic perfusion.

8207F-132, Poster Session

## Development of wireless-based NIRS system with cancellation of motion artifacts

C. Kim, S. Lee, D. Koh, B. Kim, Korea Univ. (Korea, Republic of)

Near-Infrared Spectroscopy (NIRS) has been widely applied in cognitive neuroscience research due to the ability to measure brain function non-invasively. However, typical commercial NIRS system made of optical fibers has considerable restriction of motion and distortion of NIRS signals Therefore, our group manufactured accelerometer imbedded wireless NIRS system to overcome the motion restriction problem. Wireless and miniaturized system was designed based on Bluetooth communication system and fPCB (flexible printed circuit board). Distortion caused by the motion of a head was reduced significantly by applying an adaptive FIR filter. We expect the system will be highly applicable in neuroscience and brain computer interface (BCI).

8207F-133, Poster Session

## Use of hypothermia in conjunction with photodynamic therapy for treatment of glioblastoma multiforme

C. J. Fisher, Univ. of Toronto (Canada); Y. Chen, B. Lai, Ontario Cancer Institute (Canada); J. H. Eubanks, Toronto Western Hospital (Canada); L. D. Lilge, Univ. of Toronto (Canada)

Malignant gliomas are invasive and difficult to treat tumours. Of this group of tumours, Glioblastoma Multiforme (GBM) is the most common and the most aggressive. Recently, ALA-PPIX mediated Photodynamic Therapy (PDT) has been examined as new treatment system for GBM. Selectivity is given by the fact that tumour tissue shows a large preferential uptake of the photosensitizer drug in the brain. This selective uptake of drug provides a significant starting point for PDT treatment of GBM. However, in a mixed treatment volume, which includes infiltrative glioma cells and normal tissue, selectivity is counteracted by the inherent sensitivity of normal tissue such that selectivity in drug uptake is abolished.

Thus, to increase the therapeutic index between neural tissue and glioma cells one needs to look at the sensitivity of either the neural tissue or glioma cells. Increasing the sensitivity of neural tissue thus becomes a promising option in increasing the therapeutic index currently seen with intracranial PDT.

The potential of adjuvant hypothermia to PDT for the treatment of GBM is investigated in an invasive micro-colonies GBM murine model and in vitro using a primary neural cell culture system. Preliminary results based on fluoro-Jade staining of apoptotic neurons in the treatment zone indicate a lower incidence of apoptotic neurons at 32C brain temperature compared to 37C, opening the possibility to increase the radiant exposure or fluence rate to achieve a higher PDT mediate resection, while avoiding post treatment neurological deficits.

8207F-134, Poster Session

## In vivo identification of brain morphology using optical coherence tomography

C. Reynolds, M. Eberle, M. S. Hsu, Y. Wang, C. M. Oh, D. K. Binder, B. H. Park, Univ. of California, Riverside (United States)

In clinical neuroscience, the goal of any imaging device is to provide accurate localization and diagnosis while causing minimal damage to the brain [1]. Depth resolved imaging with sufficient resolution is necessary for the identification of the target tissue and brain structures. Optical coherence tomography (OCT) is a minimally invasive imaging method, which combines micrometer-scale resolution with millimeter imaging depth, that has shown potential as a tissue identification and optical biopsy tool for neurological diagnosis [2].

Using OCT, we have been able to distinguish tissue layers and dominant structures of the mouse brain with in vivo experiments. The mouse brain was imaged through a thinned skull with a spectral domain OCT (SD-OCT) system based on a Michelson interferometer with a spectrometer and superluminescent diodes centered at 1310 nm. Imaging penetration depth with 25 dB of signal was 1mm. Images were acquired every 12 seconds with axial and lateral resolutions of 10 μm and 20 μm respectively. Histologic staining was performed on portions of tissue corresponding to the image location. Comparison of the images with the histologic slices identified specific physiological structures of the brain. Our results provide proof-of-principle for in vivo optical brain biopsy with high spatial resolution and unprecedented depth penetration.

1. Bizheva, K. et al. Imaging ex vivo and in vitro brain morphology in animal models with ultrahigh resolution optical coherence tomography. Journal of biomedical optics 9, 719-24(2004).

2. Fujimoto, J.G. et al. Optical coherence tomography: an emerging technology for biomedical imaging and optical biopsy. Neoplasia (N.Y., N.Y.) 2, 9-25(2000).

8207F-135, Poster Session

## Study of EEG affected by low-level laser array

J. Wu, Ming Chuan Univ. (Taiwan)

The effects of low-level laser therapy (LLLT) stimulation at the palm at the dominate alpha (α)frequency on the electroencephalogram (EEG) were investigated. The advantages of the low-level laser therapy are safe, easy to use, and low cost. Laser diode array was used as the light source in this apparatus and to radiate the palm of the tester. A laser array (6 pcs diode laser, wavelength 830nm, output power: 7mW, operation frequency: 10 Hz) was used to stimulate the palm of the tester. An eyes-open EEG data were recorded during and after LLLT stimulation. A spectral analysis of EEG was performed. The power of the  wave has been enhanced with this laser array which operated in specific frequency10Hz, significant activations were found in the parietal lobe and occipital lobe ($p<0.05$).

8207F-136, Poster Session

## In vivo measurements of FOSCAN induced fluorescence in rat brain

H. Kostron, E. Akkatuna, Univ. Hospital Innsbruck (Austria)

Objectives: To investigate a different time and does dependent schedule for FOSCAN based fluorescence in a cold lesion rat brain model.

Methods: Cold lesions were induced in 30 rats in one hemispherical cortex to measure the time and dose dependent fluorescence. MTHPC were injected via the tail vein in increasing concentrations (0,0 to 0.20 mg/ kg). The measurements were performed by a spectrometer (BIOLITEC) in vivo after slight sedation of the animals at time 0, 12, 24 and 36 hours after injection.

Results: Already at the lowest dose at 0.02 mg/kg there was a marked peak at 652 nm after 12 and 24 hours, after 36 hours no fluorescence could be detected. At 0.06 mg/ kg the ratio of emission to excitation was 1.21, at 0.08 mg/kg the ratio was 3.55 and at 0,10 mg/kg this ratio was 3.42 , respectively. Whereas the fluorescence at 36 hours was about the same for the 3 higher doses at 0.50, the ratios at 12 hours for the 3 higher doses ranged from 0.33, to 0.98, and 1.57, respectively.

Conclusion: This data show in a cold lesion model that a useful fluorescence can be achieved also at lower concentrations at shorter time intervals (id est: 0.08 mg at 24 hours). These findings can be translated into the clinical setting with shorter time -light interval and lower skin sensitivity.

# Conference 8207G: Photons and Neurons IV

Monday 23 January 2012

Part of Proceedings of SPIE Vol. 8207G Photons and Neurons IV

8207G-147, Session 1

## New applications for infrared neural stimulation

M. D. Keller, J. D. Wells, Lockheed Martin Aculight (United States)

Infrared neural stimulation (INS) has been demonstrated successfully in a number of applications, including mammalian sciatic nerve, cochlea, brain, prostate nerves, heart, and invertebrate vestibular system. In these systems, INS has shown one or more potential advantages versus electrical stimulation (ES), including the lack of a stimulation artifact, high spatial precision, and the ability to stimulate in a non-contact manner. To continue the development of INS as a complementary technology to ES, a number of new applications have been investigated recently through Lockheed Martin Aculight's program of loaning Capella infrared nerve stimulators to research labs. Among the recent efforts are stimulating the mammalian vestibular system, dorsal roots and dorsal root ganglia, somatosensory inputs to the auditory cortex, whole rabbit and leech hearts, and individual cells. Brief results from a variety of studies will be presented, indicating whether successful INS was achieved, and assessing the potential advantages or disadvantages of using INS versus ES for those applications.

8207G-148, Session 1

## Infrared light excites cells via transient changes in membrane electrical capacitance

M. G. Shapiro, The Univ. of Chicago (United States); K. Homma, Northwestern Univ. (United States); S. Villarreal, The Univ. of Chicago (United States); C. Richter, Northwestern Univ. (United States); F. Bezanilla, The Univ. of Chicago (United States)

Technologies that control the function of excitable cells with light are important for neuroscience research and the development of clinical applications. While most existing methods of optical control, such as optogenetics, require the use of genetic or chemical sensitizers, infrared (IR) light of wavelengths > 1.5um has been shown in vivo to excite neural and muscle tissue without any pre-treatment. The precise mechanism by which this occurs is unknown. Here, we reveal that IR laser pulses absorbed by water produce a rapid local increase in temperature, which transiently alters membrane electrical capacitance and produces corresponding depolarizing currents. Our data from untreated Xenopus laevis oocytes, mammalian cells and artificial lipid bilayers are consistent with an established theoretical model of double layer capacitors. This surprising mechanism is fully reversible and requires only the most basic properties of membranes common to all eukaryotes. It thus points to the potential generality of IR stimulation and avenues to further optimize and apply it.

8207G-149, Session 1

## Functional characterization of infrared neural stimulation in non-human primate cortex

J. Cayce, R. M. Friedman, E. D. Jansen, A. Mahadevan-Jansen, A. Roe, Vanderbilt Univ. (United States)

Infrared neural stimulation (INS) is an alternative to electrical stimulation in areas where contact free or high spatial precision is required to activate neural tissue. Previously, we demonstrated that focal (400um optical fiber, pulsed 1.875 um wavelength laser, 50 - 200 Hz repetition rate, 250 usec pulse width, 500 ms pulse train) INS when applied to somatosensory cortex in rats can evoke an intrinsic optical signal that is similar to that generated by tactile (paw or whisker) stimulation. Surprisingly, single unit recordings revealed INS had an inhibitory effect on neural activity in cortex. In this study, to examine whether this inhibitory effect is ubiquitous, we studied INS effects on neural response in primary somatosensory and visual cortex of non-human primates. To test whether the inhibitory effect obtained in the rat is due to recruitment of surrounding inhibitory circuits, a smaller (100um) optical fiber was used. Tactile stimulation was delivered by piezoelectric stimulators on distal digits pads; visual stimuli consisted of oriented gratings presented on a monitor. The effect of INS was studied with optical imaging of intrinsic cortical signals (hemodynamic response detected under 632 nm illumination). We found that, in both somatosensory and visual cortex, INS alone evokes intrinsic signal response at the stimulation site as well as at locations up to 1-3 mm away from the stimulation location, consistent with activation of loci connected to the INS activation site. Additionally, when INS is coupled with sensory stimulation, it enhanced the sensory evoked intrinsic signal. Importantly, in contrast to the rat, INS had an excitatory effect on neuronal firing. Although currently, we cannot exclude species specific differences, we hypothesize the smaller optical fiber size provided focal stimulation without recruiting inhibitory surround circuits. We will further evaluate this hypothesis by testing different sized optical fibers in the monkey. Cortical INS thus provides a means to study both excitatory and inhibitory circuits within cerebral cortex and could prove to be a powerful method for functional tract tracing in vivo and study of cortical circuits underlying behavior.

8207G-150, Session 1

## Selective, high-optrode-count, artifact-free stimulation with infrared light via intrafascicular Utah Slanted Optrode Arrays

G. A. Clark, S. L. Schister, N. M. Ledbetter, D. J. Warren, F. Solzbacher, The Univ. of Utah (United States); J. D. Wells, M. D. Keller, Lockheed Martin Aculight (United States); S. M. Blair, L. W. Rieth, P. R. Tathireddy, The Univ. of Utah (United States)

Here we present the first use of intrafascicular infrared nerve stimulation (IRNS) with Slanted Optrode Arrays (USOAs) to produce highly selective, artifact-free stimulation of peripheral nerves.

USOAs utilize technology previously developed for Utah Slanted Electrode Arrays (USEAs). The 100 USOA optrodes penetrate directly into the nerve and closely abut nerve fibers, thus providing multiple, independent, focal sites of stimulation.

This early-generation USOA contained optrodes of 0.5 to 1.5 mm length, spaced 400 um apart in a 10 x 10 grid (Abaya et al., this meeting). A 400-um diameter optical fiber from a Lockheed Martin Aculight Capella laser source delivered light to individual USOA optrodes (wavelength 1873 nm, 5-ms stimulus pulse, ~1-2 mJ at optrode). We recorded evoked nerve compound action potentials (CAPs) with a USEA and cuff electrode, plus CAPs from multiple hindlimb muscles.

We explicitly compared extraneural and intrafascicular IRNS. Extraneural IRNS invariably failed to evoke a response. In contrast, after USOA implantation into the sciatic nerve, intrafascicular IRNS evoked relatively strong and highly selective, optrode-specific responses. IRNS not only differentially activated muscles innervated by different nerve branches (e.g., tibialis anterior and gastrocnemius), but also different muscles innervated by the same nerve branch (e.g., gastrocnemius and soleus). Further, there were no observable stimulus artifacts, thereby allowing adjacent electrical recordings.

Multiple improvements remain to be implemented. Nonetheless, these initial results indicate that intrafascicular IRNS via USOAs may provide a more efficient, highly selective, high-optrode-count means of activating PNS axons, plus greater access to interior nerve fibers.

8207G-151, Session 1

## Cochlear infrared neural stimulation in the chronically deaf guinea pig

A. I. Matic, C. Richter, Northwestern Univ. (United States)

Infrared neural stimulation (INS) has been investigated as a means of stimulating spiral ganglion cells in the cochlea. In contrast to previous studies in which most of the data were acquired from animals that were acutely deafened, here we present data in which the cochlea was chronically deaf. We characterize the spatial and temporal patterns of neuronal activity to irradiation of the cochlea. To chronically deafen the guinea pig, one transtympanic dose of neomycin (~200µl, 20mM) was administered in the left cochlea under sedation. The guinea pigs were allowed to wake up and survive for ~4 weeks. For the recordings, a multichannel electrode was placed in the central nucleus of the right inferior colliculus (ICC). ICC neural activity was recorded in response to INS of spiral ganglion neurons. Data analysis included spatial tuning curves (STCs), peri-stimulus histograms (PSTHs), and entrainment. Data show similar results and patterns to previously collected data in acutely deafened guinea pigs. Spatial tuning curves were narrow. PSTHs show latencies of the neural response to be ~4.9 - 5.4 ms. Neurons were entrained to the stimulus up to ~200Hz stimulation rate.

8207G-152, Session 2

## Perturbing biomechanical forces in the developing heart tube with optical pacing

L. M. Peterson, M. T. McPheeters, L. M. Barwick, S. Gu, M. Watanabe, A. M. Rollins, M. W. Jenkins, Case Western Reserve Univ. (United States)

Mechanically-transduced signaling is crucial for normal cardiac development. Although a host of perturbation techniques have suggested that altered blood flow can lead to congenital heart defects, previous perturbations were gross manipulations (vessel ligation, conotruncal banding, etc.) that are difficult to control for probing the delicate mechanisms of mechanotransduction. We have utilized a pulsed laser operating at 1851 nm to noninvasively lock the heart rate of embryonic quails to the pulse frequency of the laser. By employing optical coherence tomography (OCT), we can measure the degree and location of perturbations to biomechanical forces and develop optical pacing protocols that allow us to investigate mechanotransduction pathways. Here, we developed an optical pacing protocol that increased regurgitant flow in the location of future valve development. The resultant shear forces on the endocardium were measured with 4-D OCT. Both the spatial and temporal extent of the regurgitant shear stress was increased significantly during optical pacing (50% above intrinsic heart rate), while forward blood flow remained comparable between sinus and paced beating. Regurgitant flow has been linked with valve development and precise perturbations may allow one to determine the role of hemodynamics in valvulogenesis.

8207G-153, Session 2

## Novel hardware development for infrared neural stimulation

M. D. Keller, J. D. Wells, Lockheed Martin Aculight (United States); M. Dummer, M. Hibbs-Brenner, Vixar Inc. (United States)

Infrared neural stimulation (INS) was initially studied using a free electron laser and then a Ho:YAG laser. Lockheed Martin Aculight (LMA) and Vanderbilt University then collaborated to develop a portable, rugged bench-top laser known as the Capella. While the Capella is a valuable tool for acute studies, chronic studies and eventual implants require smaller, more complex devices. To that end, LMA has developed the tri-pack, a wirelessly controlled, battery-powered, wearable unit for chronic stimulation studies in large animal models (e.g. cat). Individual control of each of three laser stimulators allows real-time control of all laser parameters, including power, repetition rate, pulse width, and wavelength. A low noise physiological monitoring system allows for remote recording. All data (stimulation inputs and recorded outputs) are time stamped, sorted, saved, and easily accessible from a GUI. A breakaway interface connector allows for attachment/detachment of various optical fiber-based implantable light delivery systems with up to 3 channels.

The realization of INS in implantable neural prostheses requires a compact and efficient optical source. One attractive candidate is the vertical cavity surface emitting laser (VCSEL), which can provide high conversion efficiency, narrow beam divergence, and a very small form factor. While VCSELs are commercially available below 1000 nm, the longer wavelengths desired for nerve stimulation have taken much longer to develop. In a partnership with LMA, Vixar, Inc. has developed 1860nm VCSELs emitting more than 10mW of power from a single aperture, demonstrating the potential to achieve power and efficiency levels needed for implantable devices.

8207G-154, Session 2

## Optical characterization of the Utah Slant Optrode Array for intrafascicular infrared neural stimulation

T. V. F. Abaya, M. Diwekar, S. M. Blair, P. R. Tathireddy, L. W. Rieth, F. Solzbacher, G. A. Clark, The Univ. of Utah (United States)

We present an early-generation Utah Slant Optrode Array (USOA) for infrared (IR) neural stimulation. Intrafascicular IR stimulation with the early prototype in the cat sciatic nerve produced highly selective and artifact-free responses, which outperformed extraneural IR stimulation (Clark et al., this meeting) We characterized the light delivery and loss mechanisms of the device in order to facilitate design optimization. Fabrication of the USOA takes advantage of the extensive research in the development of the Utah Slant Electrode Array (USEA). An undoped (20 ohm-cm) c-Si (100) substrate was used to produce a 10x10 array of optrodes with lengths from 0.5um to 1.5um in a 400um pitch. This substrate was able to transmit IR (wavelength > 1.1um ) with negligible absorption losses.

Transmission with different fiber core diameters, apertures and coupling interfaces was investigated. Fibers were aligned to the array backside using windows in an aluminum layer or DRIE holes positioned at the base of the optrodes. At 1550nm, transmittance for a butt-coupled 50um multimode fiber in air was 16%, which decreases by about 1% as the fiber core diameter is doubled. When the interface becomes a higher index medium of n=1.7, transmission improved by as much as 2x for smaller core fibers. An interface with n=1.45 matching that of the fiber index yielded 21% efficiency, which agreed well with ray tracing simulations. Output power dependence on electrode length and shank taper angle were also studied.

Analysis reveals that Fresnel reflection at the backside, scattering loss, and the losses due to the shank geometry are the primary loss mechanisms in the system. Anti-reflection coatings were implemented and are expected to improve the optrode efficiency.

8207G-155, Session 2

## Identifying and controlling sources of variability in hybrid opto-electrical neural stimulation

A. R. Duke, Vanderbilt Univ. (United States); H. Lu, M. W. Jenkins, Case Western Reserve Univ. (United States); E. D. Jansen, Vanderbilt Univ. (United States); H. Chiel, Case Western Reserve Univ. (United States)

Electrical techniques have served as the standard for neural activation and monitoring due in part to reliable performance, tunable parameters and successful clinical track record. New technologies now address one of the main potential drawbacks of electrical stimulation - unwanted current spread that fundamentally limits selectivity. These not only include improved nerve cuffs and electrode arrays, but also novel optical methods of neural activation, such as infrared neural stimulation (INS). A primary advantage of INS, whereby transient pulses of infrared light evoke neural activity, is improved selectivity with extraneural stimulation. However, in some applications the clinical utility of INS may be limited by the risk of thermal damage, as well as design constraints that restrict the size of implantable laser sources. To circumvent the limitations of both electrical stimulation and INS while maintaining their respective advantages, we have developed a novel hybrid stimulation modality. With hybrid stimulation sub-threshold electrical and optical stimuli are delivered simultaneously such that they combine to achieve neural activation. However, feasibility studies showed large amounts of variability in the performance of this technique. Here we present factors that contribute to this variability, as well as overall performance, and describe how to improve the reproducibility of hybrid stimulation. A comparative physiology approach was taken by identifying common trends in both an invertebrate and vertebrate neural system. Some of the factors identified include relative location of the optical and electrical stimuli, strength of the optical stimulus, polarity of the electrical stimulus and variability in the underlying electrical stimulation threshold.

8207G-156, Session 2

## Neuron absorption study and mid-IR optical excitations

D. Guo, X. Chen, S. Vadala, J. Leach, F. Choa, Univ. of Maryland, Baltimore County (United States); B. Bewley, C. S. Kim, J. Meyer, U.S. Naval Research Lab. (United States)

Neuron optical excitation can provide non-contacting tools to explore brain circuitry and durable stimulation interface for heart beats and visual as well as auditory sensory neuron stimulation. To obtain accurate absorption spectrum of live neurons, we scanned neuron transmission spectrum when they are in serum-containing cell culture medium and normalize it by subtracting out the absorption spectrum alone, with the same optical set-up. To achieve this we use GaAs wafers for windows of serum and neuron containing chambers. Other window materials are either water resolvable or not bio-compatible. GaAs wafer with thin oxide coating has the best results up to 18 μm. The normalized absorption spectrum of cultured neurons shows that the main neuron absorption peaks are close to 3000 nm to 6000 nm. In the 1400- 2500 nm region, there is a smaller absorption peak near 1450 nm. This result is consistent with the fact that neuron cells contain a large percentage of water. With the help of recent developed Mid-IR laser sources including quantum cascade laser (QCL), interband cascade laser (ICL) and Sb-based lasers; we are able to cover the source emission wavelength from 2 μm to 20 μm. By using chalcogenide fibers and applying appropriate laser power and pulse repetition rate, we can effectively deliver MIR photons to the excitation site without introducing significant heating. Pulsed Mid-IR lasers near 1500 nm and 3000 nm were prepared for neuron excitations. Cultured neurons are prepared on electrical circuits. Results will be reported in the meeting.

8207G-157, Session 3

## Parametric evaluation of calcium waves evoked by infrared neural stimulation

J. Cayce, Vanderbilt Univ. (United States); M. Bouchard, Columbia Univ. (United States); E. D. Jansen, Vanderbilt Univ. (United States); E. M. Hillman, Columbia Univ. (United States); A. Mahadevan-Jansen, Vanderbilt Univ. (United States)

Infrared neural stimulation (INS) has been well characterized stimulate peripheral nerves; however the application of INS to stimulate central nervous system structures has only recently been demonstrated. Intrinsic imaging of INS evoked responses revealed intrinsic optical signals which had similar magnitudes and durations to intrinsic optical signals evoked by natural stimuli (i.e. tactile stimulation). Surprisingly, single unit recordings revealed inhibition of spontaneous activity in response to INS. Previous studies by our group indicate that INS evokes a slow propagating calcium wave with a time course lasting 10 to 20 seconds. In this study, calcium dye imaging was employed to examine the parametric space associated with INS evoked calcium signals. INS was performed in the somatosensory cortex corresponding to the forepaw, hindpaw, and barrelfield cortex. Repetition rate, radiant exposure, stimulation duration, pulse width, spot size, and wavelength were assessed by varying each parameter separately. In general, INS was performed at 1.875 um, a repetition rate of 200 Hz, a pulse width of 250 us, a stimulation duration of 500 ms, a spot size of 400 um, and a consistent radiant exposure for each tested parameter with only the experimental parameter being varied. Optical images were collected at 30 Hz for 30 secs under 470 nm illumination light to excite the calcium dye. A 500 nm longpass filter was used to collect emitted light. The resulting images were compared for signal amplitude, spatial precision, and temporal precision between different laser parameters.

8207G-158, Session 3

## Design and implementation of an optical coherence tomography-based optical electrode for non-contact neural recording

M. S. Islam, M. R. Haque, C. M. Oh, Y. Wang, B. H. Park, Univ. of California, Riverside (United States)

Neural activity is generally characterized by generation and propagation of action potentials. It has been known for several decades that these action potentials are associated with rapid transient structural and optical changes in neurons. Although electrical recording is the most common method, there are often cases where bringing an electrode into contact with a nerve is difficult or even impossible (such as in the retina). The objective of this work is to take the advantage of phase-resolved optical coherence tomography in detecting very small thickness changes and develop a minimally invasive non-contact optical tool for recording these action potentials. In our experiments, the lateral compound eye of horseshoe crabs (Limulus polyphemus) is stimulated with light and activity in its optic nerve is monitored over time both optically and electrically (as a control method). One set of optically recorded data (raster scanning) have been used to generate 2D cross-sectional images and 3D volume reconstruction of the nerve sample. Another set of optically recorded data (only point scanning) has been used for phase-resolved measurements and these results have shown good correlation with electrical recording. A cold block system has been used to control the temperature around nerve and temporarily block/unblock the neural activity. The recorded data have confirmed this switched deactivation and reactivation of action potential propagation. Current and future works involve improving system accuracy and evaluate it in different controlled conditions. We believe that these experimental results will serve as basic groundwork for future experiments using the developed optical electrode.

8207G-159, Session 3

## The influence of source-detector separation on NIRS signal correction

A. J. Berger, Univ. of Rochester (United States); J. Goodwin, Univ. of Rochester (United States) and Queensland Univ. of Technology (Australia); C. Gaudet, Univ. of Rochester (United States)

Near infrared spectroscopy (NIRS) of the human brain, performed noninvasively using source and detector fibers, can monitor hemodynamic responses to stimuli. To study such responses, one must minimize contributions from unrelated brain activity and from scalp hemodynamics. One strategy is to regress against NIRS signals recorded from “off-target” head regions, displaced vertically or laterally (or both) from the regions expected to exhibit a localized response. Previous studies have shown that regressing NIRS time series against dedicated “short-separation” recordings can significantly improve activation-related signals. In this study, we directly compare (a) two different short-separation distances and (b) the use of single versus globally-averaged short-distance recordings.

A hexagonal grid of 24 sources and 21 detectors (13 mm nearest-neighbor spacing) was augmented with three detector fibers placed 6 mm from selected source fibers. Volunteers wearing the probe over their occipital cortex received visual stimulation (reversing radial checkerboard) for 10-second intervals, interspersed with varying recovery periods. NIRS recordings were regressed three ways: against single 6-mm time series, against single 13-mm time series, and against the global average of all 13-mm time series.

All methods of regression produced better results than doing no regression at all, in agreement with previous studies. Global 13-mm regression appears to be more beneficial than single 6-mm regression. Greater distance between the off-target region and the region of interest tends to worsen the 6-mm correction. Recommendations for future NIRS probe designs will be presented based upon these and similar observations.

8207G-160, Session 3

## Neural imaging in songbirds using fiber optic fluorescence microscopy

F. Nooshabadi, G. Hearn, T. Lints, K. C. Maitland, Texas A&M Univ. (United States)

The song control system of juvenile songbirds is an important model for studying the developmental acquisition and generation of complex learned vocal motor sequences, two processes that are fundamental to human speech and language. To understand the neural mechanisms underlying song production, it is critical to characterize the activity of identified neurons in the song control system when the bird is singing. Neural imaging in unrestrained singing birds, although technically challenging, will advance our understanding of neural ensemble coding mechanisms in this system. We are exploring the use of a fiber optic microscope for functional imaging in the brain of behaving and singing birds in order to better understand the contribution of a key brain nucleus (HVC) to temporal aspects of song motor control We have constructed a fluorescence microscope with LED illumination, a fiber bundle for flexible transmission of fluorescence excitation and emission light, a ~2× GRIN lens at the distal tip, and a CCD for image acquisition. The fiber bundle microscope has 2 µm resolution, 375 µm field of view, 200 µm working distance, and 1 mm outer diameter. As an initial characterization of this setup, neurons in HVC were imaged using the fiber optic microscope after injection of qdots or fluorescent retrograde tracers into efferent song nuclei. A Lucid Vivascope confocal microscope was used to confirm the imaging results in anesthetized birds and fixed brain tissue. Long-term imaging of the activity of these neurons in juvenile birds during singing will lead us to a better understanding of the central motor codes for song and the central mechanism by which auditory experience modifies song motor commands to enable vocal learning and imitation.

8207G-161, Session 3

## Neural correlates of contour detection in the primary visual cortex revealed with voltage-sensitive dye imaging

H. Slovin, Bar-Ilan Univ. (United States)

Contour integration is an important intermediate stage of object recognition, in which single elements belonging to an object boundary are perceptually linked and segmented from a noisy background. The neuronal mechanisms underlying this effect are still not well understood. Here we studied the spatio-temporal patterns of activation and synchrony among neuronal population in the primary visual cortex (V1) during contour detection. We used voltage-sensitive dye imaging (VSDI) that enables to measure neuronal population activity at high spatial and temporal resolution. Two monkeys were trained on a contour discrimination task and were presented with one out of two images: (1) a circled contour (circle composed of Gabors elements) embedded in a noisy background (randomly oriented and positioned Gabors) (2) a similar noisy pattern without the contour. The monkeys had to discriminate between the two images. Shortly after stimulus onset, the VSDI signal increased in area V1 at the retinotopic sites corresponding to the contour and background elements. Although the time course of activation was similar in the contour and non-contour conditions shortly after stimulus onset, the synchronization pattern was different. In the contour condition, circle activated sites tended to synchronize more among themselves and less with background activated sites. At later times, the time course of the VSDI signal in the contour condition deviated, and showed a transient decrease in amplitude, reaching a minimum approximately 250 ms after stimulus onset. This dynamics was characterized with a distinct synchronization pattern: the background activated sites were more synchronized among themselves and less with circle activated sites. These complementary patterns of synchronization and activation patters may mediate the process of contour integration and segregation from background.

8207G-162, Session 4

## Multi-plane two photon microscopy for high speed 3D neuroimaging

E. M. Hillman, L. Grosberg, B. Chen, Columbia Univ. (United States); U. Klibaite, P. T. Galwaduge, Columbia Univ. (USA)

No abstract available

8207G-163, Session 4

## Plasticity in the visual cortex: interactions between synapses and microglia

A. Majewska, Univ. of Rochester (United States)

Rapid changes in neuronal response properties occur in the visual cortex as a result of imbalances in binocular vision during the critical period. In order to understand the underlying changes in synaptic morphology during critical period plasticity we combined intrinsic signal imaging of brain function with in vivo two-photon microscopy of individual cortical neurons labeled with GFP using viral vectors. We found that closing one eye led to a very rapid change in cortical responses and surprisingly an equally rapid loss of dendritic spines. Opening the deprived eye reversed both the structural and functional changes. This suggests that functional changes are mediated by a very fast remodeling of synapse structure and network connectivity. Additionally, we are exploring extracellular signaling mechanisms that may regulate both functional and structural synaptic changes and the involvement of microglia-synapse interactions in modulating plasticity. Microglia are highly dynamic in the non-injured brain and remodel the extracellular matrix as they navigate through the neuropil. Their rapid contacts with dendritic spines are accompanied by changes in spine shape and are altered by the visual envionment. Hence rapid remodeling of synapses, which underlies plastic changes in the cortex, may be facilitated by dynamic microglia-synapse interactions.

8207G-164, Session 4

## Optically imaging intrinsic signals produced by intracortical microstimulation reveals the circuitry of cortical networks

R. M. Friedman, A. A. Brock, O. A. Gharbawie, I. Stepniewska, J. H. Kaas, A. Roe, Vanderbilt Univ. (United States)

Intracortical microstimulation (ICMS) has been used to generate sensations, alter percepts, and study the functional organization of the brain. Here we report on the correspondence of functional maps within primate visual, motor and somatosensory cortical areas to neural activation patterns, observed with the optical imaging of intrinsic signals (OIS), evoked by ICMS.

In anesthetized monkeys cortical areas were functionally mapped with OIS using tactile or visual stimuli or by recording motor evoked responses (under ketamine/xylazine anesthesia). Subsequently, an electrode was placed in a functional domain for ICMS (bipolar, 0.4 ms pulses, 30-300 μA, 250 or 300 Hz, 30 to 500 ms duration) and OIS (632 nm illumination).

Activation surrounding the electrode was accompanied by areas of activation that crossed interareal borders. For instance, ICMS in VI produced activation within V2 stripes. ICMS within the hand region of area 3b produced activation in somatotopically corresponding areas in area 1. ICMS in primary motor and premotor cortex activated corresponding motor eliciting areas in posterior parietal cortex and visa-versa. In summary, activation patterns evoked by ICMS reveal the functional connectivity of different areas of cortex. With ICMS and OIS our long term goals are to reveal intra- and inter-areal cortical networks which underlie sensation and perception.

8207G-165, Session 4

## Subthreshold and suprathreshold cortical lateral interactions revealed by optical imaging

Y. Fregnac, Ctr. National de la Recherche Scientifique (France)

No abstract available

8207G-166, Session 4

## What hemodynamics can and cannot tell us about local neural activity

A. Das, Columbia Univ. (United States)

Brain imaging is based on measuring not neural activity but rather, brain hemodynamics - local changes in blood volume, blood flow and oxygenation. These hemodynamic signals are understood to reliably report local neural activity. In particular, it is typically assumed that the hemodynamics follow uniformly from local neural responses, with increases in neural activity causing local deoxygenation in the blood which then drives fresh oxygenated blood into the activated regions of the brain. However, the neurophysiology of brain imaging has primarily been studied in anesthetized animals. Neural and hemodynamic responses have rarely been compared in alert subjects to understand how these signals relate to each other in individuals engaged in a behavioral task.

By recording with electrodes while simultaneously imaging hemodynamic signals in alert behaving monkeys, we find a complex relationship between hemodynamics and neural activity. This complexity is evident at two levels. First we find that when the animals are engaged in a systematic visual task, the hemodynamic signal recorded from their primary visual cortex (V1) contains a strong task-related component in addition to visually evoked responses. This task-related component is a novel anticipatory signal that dilates local arteries and brings in fresh blood ahead of an expected visual trial. Unlike the visually driven signal, this task-related component is independent of visual input or measurable local neural activity, whether spiking or local field potential (LFP). This signal is intimately connected with the level of the animal's engagement in a task: it entrains to any trial period that the animal is willing to entertain and switches rapidly from correct to error trials. We speculate that this task-related signal may result from distal neuromodulatory inputs into visual cortex. Next, we find that even the visually evoked hemodynamic signal is not driven by deoxygenation in the blood per se. Rather, it is likely driven by a process that occurs in parallel, roughly anticipating the local demand before it leads to any blood deoxygenation. These findings should lead to a better appreciation both of the multiple neural mechanisms underlying brain hemodynamics and the causal relationships linking neural activity and blood flow.

8207G-167, Session 5

## Axonal regeneration of cultured mouse hippocampal neurons studied by an optical nano-surgery system

F. Difato, H. Tsushima, M. Pesce, Istituto Italiano di Tecnologia (Italy); A. Guiggiani, Univ. degli Studi di Firenze (Italy); F. Benfenati, A. Blau, Istituto Italiano di Tecnologia (Italy); M. Basso, Univ. degli Studi di Firenze (Italy); M. Vassalli, Consiglio Nazionale delle Ricerche (Italy); E. Chieregatti, Istituto Italiano di Tecnologia (Italy)

During development, the axons of neurons in the mammalian central nervous system lose their ability to regenerate after injury. In order to study the regeneration process, we developed a system integrating an optical tweezers and a laser dissector to manipulate the sample. A sub-nanosecond pulsed UVA laser was used to inflict a partial damage to the axon of mouse hippocampal neurons at early days in vitro. Partial axonal transections were performed in a highly controlled and reproducible way without affecting the regeneration process. Force spectroscopy measurements during and after the ablation of the axon were performed by optical tweezers with a bead attached to the neuronal membrane. Thus the release of tension in the neurite could be analyzed in order to quantify the inflicted damage. After dissection, we monitored the viscoelastic properties of the axonal membrane, the cytoskeleton reorganization, and the dynamics of the newly formed growth cones during regeneration. In order to follow cytoskeleton dynamics in a long time window by tracking a bead attached to the neuron, we developed a real-time control of the microscope stage position. Axonal regeneration was documented by long-term (24-48 hours) bright-field live imaging using an optical microscope equipped with a custom-built cell culture incubator.

8207G-168, Session 5

## Repair of damage and stimulation of growth cone response following laser- induced sub-axotomy

T. Wu, S. K. Mohanty, V. Gomez-Godinez, L. Liaw, Beckman Laser Institute and Medical Clinic (United States); J. Miotke, R. Meyer, Univ. of California, Irvine (United States); M. Berns, Beckman Laser Institute and Medical Clinic (United States)

Understanding how axonal growth cones respond to localized axonal damage and possibly play a role in the healing process is very important for the understanding of the repair of neurological damage. The laser microbeam provides a unique opportunity to induce highly localized and controlled damage on various parts of the axon, thus allowing for the study of the response of the growth cone to the localized damage. By generating controlled sub-axotomy injury (using the 532 nm, 12 ns pulse of a Nd:YVO4 laser) on retinal ganglion axons derived from goldfish retina explants, we demonstrate the response of near-by axonal growth cones to the damage. The damaged axons underwent a localized decrease in thickness (“thinning”) without detectable rupture of the cell membranes as assayed by fluorescent dye analysis and transmission electron microscopy. In addition, using the fluorescent dye Rhodamine 123 mitochondrial transport along the axonal cytoskeleton was observed to stop at the damage site to recover over several minutes. Within seconds of damage-induction nearby neuronal growth cones extended filopodia toward the injury and were often observed directly contacting the damaged site. Redirection (turning) of the growth cone towards the injured axonal site was also observed. Repair of the laser-induced axon damage was evidenced by recovery of the axon thickness at the lesion site as well as the restoration of mitochondrial transport.

8207G-169, Session 5

## Enhancement and probing of neuronal growth using optical tweezers

S. K. Mohanty, The Univ. of Texas at Arlington (United States)

Trapping and manipulation of cells and intra-cellular objects using optical tweezers has led to non-contact determination of physical (viscoelastic, viscosity) as well as physiological (motility, force etc) properties important for maintenance of cellular structures and associated functions. Further, intra-cellular transport using spatially-modulated optical tweezers has enabled guidance and enhancement of neuronal growth. Dependency of this effect on cell-type and laser wavelength as well as pulsed vs cw conditions, will be presented. In order to understand the mechanism behind enhancement of neuronal growth by optical tweezers based method, correlation spectroscopy was employed. The measured intra-cellular diffusion of actins was found to depend on optical tweezers actuation. In addition to enhancement of growth rate, optical tweezers was employed for measurement of force exerted by neuronal growth cone under normal and stimulated condition. The talk will describe advancements and state-of-the-art use of optical tweezers for neuronal growth and guidance.

8207G-170, Session 5

## Impact of nanosecond pulsed electric fields on primary hippocampal neurons

C. C. Roth, General Dynamics Information Technology (United States); J. A. Payne, G. J. Wilmink, B. L. Ibey, D. R. Dalzell, Air Force Research Lab. (United States)

Nanosecond pulsed electric fields (nsPEF) cause repairable damage to plasma membranes through the creation of nanopores. These nanopores enable passage of small ions, but remain impermeable to larger molecules like propidium iodide. Previous work found thresholds for pore formation in non-excitable cell lines, such as CHO-K1 and GH3, using both fluorescent microscopy and whole cell electrophysiology. Interestingly, these nanopores appear to last for minutes, suggesting that formation of such pores in excitable cells could lead to prolonged action potential inhibition. In this paper, we explored the sensitivity of primary hippocampal neurons to nsPEF using a whole cell patch technique coupled with fluorescent microscopy to detect formation of nanopores in the plasma membrane. We determined the threshold for nanopore formation in primary hippocampal neurons across three distinct nsPEF parameters (pulse width, amplitude, and number of pulses). Understanding of such thresholds will guide future studies to determine if nsPEF can in-fact inhibit action potentials without causing irreversible damage.

8207G-171, Session 6

## Shining new light on optogenetics

S. K. Mohanty, L. Gu, The Univ. of Texas at Arlington (United States); T. Li, Univ. of Electronic Science and Technology of China (China)

Since development of optogenetic stimulation paradigm, there has been several attempts to red shift the excitation maximum of the efficient blue-sensitive opsins. While there has been some success at the cost of altered light-activation kinetics, near-infrared optogenetic probe will be ideal for in-depth cell-specific stimulation of excitable cells in an organ. However, single-photon near-infrared optogenetics based stimulation may limit precise probing and modulation of in-vivo neural circuits. In contrast, by virtue of non-linear nature of ultrafast light-matter interaction, high spatial precision in optogenetic activation can be achieved in addition to inherent cellular specificity and temporal resolution provided by the opsins. Here, we report use of non-linear optogenetics for stimulation of neurons in-vivo in mouse models. Advantage of using non-linear optogenetics for probing neuronal circuitry in retina and sub-cellular stimulation will also be presented. Further, we will introduce Bessel beam for in-depth non-linear optogenetic stimulation. The effectiveness of the non-diffracting optogenetic Bessel beam over classical Gaussian beam in a layered mouse-brain geometry will be demonstrated using Monte Carlo (MC) simulation. The effects of wavelength, beam size, and NA of the beam on the photon fluence distribution in 3D neuronal tissue will be presented. The large propagation distance, characteristics of Bessel beam is better suited for in-depth single as well as two-photon optogenetic stimulation.

8207G-173, Session 6

## Optogenetic stimulation of the auditory nerve

V. H. Hernandez, G. Hoch, M. Bartels, Georg-August-Univ. Göttingen (Germany); G. Vogt, C. Garnham, MED-EL Deutschland GmbH (Germany); G. J. Augustine, Duke Univ. (United States); N. Strenzke, T. Moser, Georg-August-Univ. Göttingen (Germany)

When hearing fails, electrical stimulation of spiral ganglion neurons (SGNs) by cochlear implants (CIs) enables hearing in a majority of deaf subjects. However, frequency resolution in current CIs is poor and might be improved by optical stimulation. Here we employed the light-gated ion channel, channelrhodopsin-2 (ChR2), to render SGNs sensitive to blue light. Optical stimulation of ChR2-expressing SGNs by a light emitting diode (LED) activated the auditory pathway in hearing mice and in mouse models of acute and chronic human deafness. Optogenetic auditory brainstem responses (oABR) had a threshold of 1.9 µJ/mm2. oABR amplitude encoded changes in irradiance over more than one order of magnitude. oABR had a minimum latency of approximately 3 ms and were present up to stimulus rates of 70 Hz. Telemetric activation of oABR was achieved by implanting a light emitting diode (µ-LED) stimulator in mice. In summary, optogenetic stimulation of the auditory nerve is feasible.

8207G-184, Session 6

## Two-photon control of neurons with optogenetics and caged neuromodulators

D. Peterka, A. M. Packer, R. Yuste, Columbia Univ. (United States)

Two-photon microscopy has revolutionized neuroscience by allowing long term, high resolution imaging of structure and function in the brain.

Unfortunately, many of the method's advantages, such as a small excitation volume, have made it difficult to use non-linear excitation to control activity using either conventional caged compounds, or more recently, optogenetics. However, tremendous progress has been made in the understanding and development of these tools, and they can now be used to control neural activity with single cell precision.

Additionally, the coupling of these tools with advanced microscopies, such as spatial light modulator (SLM) based microscopes that can shape the incoming two-photon laser beam into nearly arbitrary excitation patterns, allows for the simultaneous imaging or photostimulation of different regions of a sample with three-dimensional precision at high frame rates. We demonstrate the functionality of this system in brain slices by activating multiple neurons simultaneously, in two- and three-dimensions.

8207G-174, Session 7

## Imaging voltage in electrically excitable cells

J. Kralj, D. Hochbaum, A. Douglass, D. Maclaurin, V. Venkatachalam, A. E. Cohen, Harvard Univ. (United States)

Microbial rhodopsin proteins transduce light into changes in membrane potential. We engineered microbial rhodopsins to run backward: to transduce changes in membrane potential into light. The endogenous fluorescence of some microbial rhodopsins is exquisitely sensitive to membrane potential, and responds to changes in potential in less than 0.5 ms. Upon expression of these voltage indicators in E.coli, we observed "blinking" of the cells, indicating that E. coli generate electrical spikes reminiscent of action potentials. The electrical spiking is correlated with active efflux of cationic organic molecules. We also imaged electrical activity in neurons and cardiomyocytes, achieving single-spike detection in both cases.Microbial rhodopsins are a new class of environmentally sensitive fluorescent proteins that emit in the near infrared, are highly photostable, and have no homology to GFP or to any other fluorescent indicator.

8207G-175, Session 7

## Targeted modulation of retinal cell subtypes to restore visual function in the rd10 mouse model of blindness

R. M. Stewart, ; M. M. Doroudchi, Eos Neuroscience Inc. (United States)

Previous work established retinal expression of Channelrhodopsin-2 (ChR2), an algal cation channel gated by light, could be genetically targeted to restore physiological and behavioral visual responses in otherwise blind rd1 mice. However, developing a viable ChR2-based human therapy must meet several key criteria: 1) ChR2 targeted expression must be cell-specific, robust, and long-term, 2) ChR2 must provide long-term and continuous therapeutic efficacy, and 3) both viral vector delivery and ChR2 expression must be safe. Here, we demonstrate the development of a clinically relevant therapy for late stage retinal degeneration using ChR2. We achieved specific and stable expression of ChR2 in ON bipolar cells using a recombinant adeno-associated viral vector packaged in a tyrosine-mutated capsid. Targeted expression lead to temporally precise ChR2-driven electrophysiological ON responses in postsynaptic retinal ganglion cells and significant improvement in visually guided behavior for multiple models of blindness up to 10 months post injection. Light levels to elicit visually guided behavioral responses were within the physiological range of cone photoreceptors. Finally, chronic ChR2 expression was non-toxic, with transgene biodistribution limited to the eye. No measurable immune or inflammatory response was observed following intraocular vector administration using. Together, these data indicate that virally delivered ChR2 can provide a viable and efficacious clinical therapy for photoreceptor disease-related blindness. Currently, we are using promoter-driven expression to introduce light-sensitive genes into photoreceptor, retinal pigmented epithelial, and bipolar ON cell types to improve complex vision in visually impaired mice.

8207G-176, Session 7

## A 3-D waveguide array for optogenetic control of neural circuits in the brain

A. N. Zorzos, J. Scholvin, E. S. Boyden, MIT Media Lab. (United States)

A key feature of neural circuits in the mammalian brain is their 3-dimensionality and geometric complexity. The ability to optically drive or silence neural activity in complex shaped brain circuits for milliseconds to seconds at a time would enable analysis of the time-resolved contribution of specific neural circuits, and specific neural activity patterns, to behaviors and pathological states. However, the ability to manipulate neural circuits in their geometric complexity still requires significant innovation, to confront the dense and difficult matter of the brain. Recently we developed a new kind of thin implantable probe for light delivery into the brain, which comprises many parallel waveguides, each terminating at a different point along the length of the probe (Zorzos et al., 2010). This probe is capable of independently delivering light to multiple targets along the probe axis, thus enabling versatile optical control of sets of distributed brain targets along a linear axis. We now present a novel 3-D neuromodulation array which is a 2-D array of many individual such 1-D probes, held in a custom microfabricated holder and connected to an computer-controlled light source array consisting of a laser and digital micromirror device (DMD). We demonstrate its use in the living mammalian brain to modulate neural dynamics in 3-D neural circuits. Such a device may enable new kinds of experiment, and may serve as prototype optical neural control prosthetics, which may be of use in the treatment of intractable brain disorders.

8207G-177, Session 7

## Implantable optrode design for optogenetic visual cortical prosthesis

N. Dong, X. Sun, Southeast Univ. (China); P. Degenaar, Newcastle Univ. (United Kingdom)

The rise of optogenetic neural stimulation has opened new opportunities for neuroprosthesis. Of particular interest are retinal prosthesis, brain pacemakers and visual cortical prosthesis. The latter necessitates an efficient delivery of light into the cortex. New forms of photosensitizing channelrhodopsin are reducing the required light intensities for stimulation, but implantable systems need to be highly efficient. Such efficiency calls for low loss in the transmission path, high coupling efficiency between the optic delivery system and optical emitter, as well as emitting efficiency from the light emitting diode. In this paper, we perform simulations as to the best strategy to attachment of optrode structures to Gallium Nitride-μLED arrays so as to maximize the efficiency of light delivery to the target neural tissue.

We use a combination of Monte Carlo and ray tracing simulations to calculate the coupling efficiency from LED into optical waveguide. Then we use diffuse reflection and Kubelka-Munk scattering theory to analyze the output power density on penetration into tissue. The simulations are performed for different shapes and dimensions of optrode devices and refractive indices. We assume that neurons photosensitized with either wild type channelrhodopsin or more advanced versions such as CatCh respectively require 1mW/mm2 and 0.1 mW/mm2 to generate action potentials. Given that the LED efficiency is non-linearly and inversely proportional to its radiance, we simulate for the total efficiency of the combined LED-optrode system.

Our results show that it is feasible to connect optrode elements and GaN- μLED arrays for cortical stimulation and describe the optimisation requirements.

8207G-178, Session 7

## All-optical control of neuronal function via optical delivery of light-sensitive proteins and optogenetic stimulation

A. Villalobos, L. Gu, S. K. Mohanty, The Univ. of Texas at Arlington (United States)

While pulsed laser beams have been used for stimulation of neurons, precise cellular specificity of the optical stimulation is achieved by photo-sensitization of genetically targeted cells. Till date, the process of optogenetic-sensitization primarily involves use of viral vectors. In rare occasions, electroporation has been used. Here, we report an all-optical method by use of pulsed laser beam for delivery of genes, encoding optogenetic probes, to spatially-targeted cells and optogenetic stimulation. Use of laser microbeam alone and in combination with nanoparticles enabled highly precise spatially-patterned delivery of optogenetic probes, as confirmed by expression of conjugated fluorescent protein. Light-activation of opsin-expressing cells was confirmed by calcium-imaging and electrophysiology. The laser assisted expression of optogenetic probes in spatially-targeted regions will help in better understanding of the neuronal circuitry. Laser parameters and scope for efficient laser-based delivery of opsins into various organs will be presented. The light based non-viral method for allowing expression of opsins in a spatially-controlled manner and subsequent optogenetic stimulation will allow faster screening of the opsins in efficiently modulating neuronal function.

8207G-179, Poster Session

## Polarization-dependent responses of fluorescent indicators partitioned into myelinated axons

I. Micu, C. Brideau, P. K. Stys, Univ. of Calgary (Canada)

Myelination, i.e. the wrapping of axons in multiple layers of lipid-rich membrane, is a unique phenomenon in the nervous systems of both vertebrates and invertebrates, that greatly increases the speed and efficiency of signal transmission. In turn, disruption of axo-myelinic integrity underlies disability in numerous clinical disorders. The dependence of myelin physiology on nanometric organization of its lamellae makes it difficult to accurately study this structure in the living state. We expected that fluorescent probes might become highly oriented when partitioned into the myelin sheath, and in turn, this anisotropy could be interrogated by controlling the polarization state of the exciting laser field used for 2-photon excited fluorescence (TPEF). Live ex vivo myelinated rodent axons were labeled with a series of lipohilic and hydrophilic fluorescenct probes, and TPEF images acquired while laser polarization was varied at the sample over a broad range of ellipticities and orientations of the major angle [see Brideau, Micu & Stys, abstract this meeting]. We found that most probes exhibited strong dependence on both the major angle of polarization, and perhaps more surprisingly, on ellipticity as well. Lipophilic vs. hydrophilic probes exhibited distinctly different behavior. We propose that polarization-dependent TPEF microscopy represents a powerful tool for probing the nanostructural architecture of both myelin and axonal cytoskeleton in a domain far below the resolution limit of visible light microscopy. By selecting probes with different sizes and physicochemical properties, distinct aspects of cellular nanoarchitecture can be accurately interrogated in real-time in living tissue.

8207G-180, Poster Session

## Quantitative characterization of peripheral nerve structural features using optical coherence tomography

M. C. Oliveira, M. S. Islam, Univ. of California, Riverside (United States); F. P. Henry, Harvard Medical School (United States); J. F. de Boer, Vrije Univ. Amsterdam (Netherlands); B. H. Park, Univ. of California, Riverside (United States)

Here we present the application of multi-functional spectral domain optical coherence tomography for detailed quantification of features in peripheral nerve imaging. Using intensity- and polarization-sensitive OCT, we have acquired high resolution cross sectional images of 5 mm sections of rat sciatic nerve in vivo. In a few cases, nerves were excised and attached to a micrometer to investigate the effects of non-damaging amounts of stretch on the nerve. All image data sets were also reconstructed in 3D, allowing for a more thorough analysis of the structural features of peripheral nerves.

We quantitatively distinguished the sciatic nerve from the surrounding muscle tissue using the extinction coefficient and birefringence, calculated from intensity and polarization images respectively, of each tissue. Our results show that the sciatic nerve has a higher extinction coefficient and lower birefringence compared to the surrounding muscle. Additionally, we determined the epineurium thickness and birefringence of the interior of the sciatic nerve for un-stretched and stretched nerves to determine whether there is a change in epineurial thickness or axonal birefringence with stretch. The 3D reconstructions were used to quantify the frequency of Fontana's bands for un-stretched and stretched nerves, as a measure of the amount of stretch a nerve is experiencing. Our results show a decrease in the number of bands per millimeter for stretched nerves compared to un-stretched nerves. Our results show that the epineurium thickness remains unchanged as the nerve is stretched. Most notably, we report no change in birefringence between the two tension states of the nerve.

8207G-181, Poster Session

## Fiber-array based optogenetic prosthetic system for stimulation therapy

C. Cote, L. Gu, S. K. Mohanty, The Univ. of Texas at Arlington (United States)

Treatment of neurological disorders requires stimulation of specific cell types in multiple regions of the brain. Recent advent of optogenetics has enabled reversible activation of genetically-targeted neuronal cells using low intensity blue light with high temporal precision. In order to activate multiple regions of the brain in 3D, we report development of a prosthetic comprising of array of fibers coupled to independently-controllable LEDs. This design avoids direct contact of LEDs with the brain tissue and thus does not require electrical and heat isolation, which can non-specifically stimulate and damage the local brain regions. The intensity, frequency, and duty cycle of light pulses from each fiber in the array was controlled independently using an in-house developed LabView based program interfaced with a microcontroller driving the individual LEDs. While the temporal profile of the light pulse was controlled by varying the current driving the LED, the beam profile emanating from each fiber tip could be sculpted by microfabrication of the fiber tip. Control of neural activity in the mice cortex transfected with channelrhodopsin-2 using the fiber-array based prosthetic is evaluated from recordings made with tungsten microelectrodes using Plexon multichannel acquisition processor. We will present the design and construction of the implantable fiber optic array based prosthetic and demonstrate its ability for spatio-temporal stimulation of targeted neurons at arbitrary 3D locations within the brain.

8207G-182, Poster Session

## Quantitative study of peripheral nerve myelination using polarization-sensitive optical coherence tomography

Y. Wang, B. H. Park, Univ. of California, Riverside (United States)

Histopathology can be used in a laboratory setting to accurately yield the degree of myelination. In a normal clinical setting where an inherently destructive technique is not feasible, nerve viability is typically determined using a nerve conduction test, which yields functional grading but not a quantitative measure of myelination. Optical coherence tomography (OCT) is a minimally-invasive technology capable of rapid two- and three-dimensional imaging of subsurface tissue structure. Polarization sensitive-OCT (PS-OCT) additionally utilizes the polarization state of that light to determine the light polarization changing properties of a sample, such as its endogenous form birefringence. A preliminary study was performed by the research group using a crush injury model of the rat sciatic nerve. Crush injury was applied on rat sciatic nerve on the right leg and left leg was left as control, with weekly examinations of PS-OCT imaging, walking track analysis and histology performed from 1 week to 4 weeks post injury. The results of this pilot study showed a reduced birefringence after injury and increased birefringence during nerve regeneration from 1 week to 4 weeks post injury. The amount of optically determined birefringence correlates better with sciatic function index derived from walking track analysis than myelin thickness. This is especially true during Wallerian degeneration, where the optical signal properly ignores myelin debris that can artificially inflate measures of histological myelin thickness.

8207G-183, Poster Session

## The microdibi project

M. Genovese, Istituto Nazionale di Ricerca Metrologica (Italy)

In this poster we will present a project finaced by Piedmont region (Italy) and finalised to the realization of functional devices for cellular bio-sensing based on nanodiamonds. The main features of the final devices will be briefly summarized.

Firstly, we envisage an active diamond-based cellular substrate, that can simultaneously stimulate and detect a range of signals (chemical, optical, electrical) to and from neuroendocrine cells, in a fully bio-compatible environment for the cellular system under test. Such a device can be realized by fully exploiting the peculiar properties of diamond: optical transparency, bio-compatibility, chemical inertness, accessibility to a conductive graphite-like phase; properties that will be further explored and tested during the project.

The diamond bio-sensor will be based on the following basic components:

• buried conductive paths (fabricated by MeV ion implantation in defined paths) will contact the neuronal cells surface and enable their electrical stimulation, as well as the electrical collection of their action potential signal via a voltammetric measurement, or the quantal release of bio-molecules by means of amperometric measurement;

• buried microfluidic channels (fabricated by selectively etching graphitized sub-superficial paths) will locally deliver specific drugs for the chemical stimulation of the cells;

• waveguiding structures based on either the sculpting of the bulk material into three-dimensional structures, or on the formation of specific regions characterized by different refractive index.

This innovative diamond-based biosensor will present several advantages with respect to the current cellular sensing devices: namely, the possibility of integrating a series of different interfacing structures (microchannels, conductive paths, waveguides) in a single device which is fully bio-compatible and optically transparent, thus allowing the ability to simultaneously collect and stimulate a range of different signals (chemical, electrical and optical) while being able to monitor the system of interest through a standard microscope with back illumination of the active substrate.

# Conference 8207H: Optics in Bone Surgery and Diagnostics

Saturday 21 January 2012

Part of Proceedings of SPIE Vol. 8207H Optics in Bone Surgery and Diagnostics

8207H-137, Session 1

## Optical coherence tomography for the identification of musculoskeletal structures of the spine

K. Beaudette, Ecole Polytechnique de Montréal (Canada); M. Strupler, Sainte-Justine Mother and Child Univ. Hospital Ctr. (Canada) and Ecole Polytechnique de Montréal (Canada); F. Benboujja, C. Aubin, C. Boudoux, Ecole Polytechnique de Montréal (Canada) and Sainte-Justine Mother and Child Univ. Hospital Ctr. (Canada)

Scoliosis is a complex 3D deformation of the spine that, for severe cases, requires corrective surgery. Most surgical approaches involve very invasive procedures and massive instrumentation resulting in the fusion of instrumented vertebrae. Several alternative techniques involving minimally invasive surgery (MIS) are currently under investigation. One of these consists in inserting small staples directly on the vertebrae's growth plates to locally induce corrective growth. Endoscopic identification and precise localization of growth plates are of paramount importance to ensure the success of the intervention. This study aims at assessing the potential of optical coherence tomography (OCT) as a guiding system for MIS of the spine.

In the past, we presented in vivo OCT images of spinal structures (intervertebral tissues, vertebrae, growth plates) acquired with a custom-made handheld probe during open surgery on a porcine model. In order to refine our understanding of the OCT contrast of spinal structures and optimize the imaging parameters for future clinical studies, we performed further ex vivo comparisons between OCT (using two different wavelengths) and histological sections. Volumetric data sets (~5mmx5mmx3mm) of fresh porcine samples were acquired using a swept-source OCT system ($\lambda 0$=1325nm, $\Delta\lambda$=100nm, $\Delta z$=12µm) and a spectrometer-based OCT system ($\lambda 0$=930nm, $\Delta\lambda$=100nm, $\Delta z$=7µm). All samples were then marked with India ink and processed for histology. For each musculoskeletal tissue, OCT images showed distinctive features that have been correlated to histology. This study will provide surgeons with characteristic markers to precisely localize growth plates on in vivo images and will enable the use of OCT as a guiding tool during MIS for the correction of scoliosis.

8207H-139, Session 1

## Polymer-capped fiber optic Raman probe for in vivo non-invasive Raman tomography and spectroscopy

P. I. Okagbare, M. D. Morris, Univ. of Michigan (United States)

As advances in fiber optic probe design move Raman spectroscopy into the clinic, there remain important practical problems. Most in-vivo applications employ specialized fiber optic probes. Much effort has been devoted to minimizing Raman and fluorescence background from fiber. Less attention has been paid to the need to generate reference Raman signals proportional to delivered laser power without direct measurement of tissue albedo. Knowledge of laser power is needed for quantification of changes in tissue composition. The need is especially acute in diffuse Raman tomography, where accurate modeling of light transport through the tissue is required for accurate reconstruction of subsurface features.

We describe a fiber optic probe that incorporates a transparent polymer cap at the end of each excitation fiber. As laser light propagates through the cap it generates Raman bands whose intensity can directly measure power delivered to the tissue of interest. Our first implementation uses a fluorinated ethylene-propylene copolymer (FEP) cap that is attached to the ferrule at the distal (delivery) end of each excitation fiber. FEP is transparent and functions as a waveguide with only a small insertion loss, about 5%. Importantly, there are few overlaps between the Raman bands of FEP and the bands of tissue constituents. The cap increases the diameter of the structure in contact with the specimen, but with extensive photon diffusion this makes little difference in performance. We will present latest non-invasive bone spectroscopy results with the calibrator. We will also discuss other materials and prospects for incorporation of refractive elements.

8207H-140, Session 1

## Photoacoustic diagnosis of early osteoporotic bone loss and density variations

B. Lashkari, A. Mandelis, Univ. of Toronto (Canada)

Over the past two decades, osteoporosis has been recognized among the most serious public health problems. Fortunately with the growing awareness of osteoporosis, new treatments have been developed for the prevention of fracture. At the same time, there is a rapid improvement in diagnostic methods. In this study biomedical photoacoustics (PA) is applied to the analysis of bone mineral concentration. The PA signal depends on optical as well as mechanical properties of the object and therefore has the potential to provide higher sensitivity to density variation compared with standard diagnostic methods, like ultrasound. A laser source with 850 nm wavelength and three different ultrasonic transducers with resonance frequencies in the range 1 to 5 MHz were employed. The CW or frequency-domain (FD) PA radar method was utilized with linear frequency modulation chirps to provide temporal gating control over the transmitted signal and higher sensitivity in the detected signal. The laser intensity was set below the safety standards for skin exposure. The preliminary studies showed adequate optical absorption by cortical bone to generate measurable PA signals and the transmission of laser light through this layer. Experiments are focused on detection and evaluation of PA signal from in-vitro animal cortical bones with and without trabecular sublayer. The trabecular layer is then diluted by chemical etching and differences in the PA signals are discussed.

8207H-141, Session 1

## Bone-demineralization diagnosis in a bone-tissue-skin matrix using the pulsed-chirped photothermal radar

S. Kaiplavil, A. Mandelis, Univ. of Toronto (Canada)

Aiming at non-invasive and non-ionizing early bone-osteoporosis diagnostics, we have recently introduced a pulsed-chirped photothermal radiometry (PTR) radar with improved depth resolving capability compared to harmonic modulation techniques for the same energy of exposure. Preliminary results revealed that this PTR radar could identify the subsurface features of bone with fat and skin overlayers with a total thickness ~3 mm, much deeper than conventional frequency-scanned PTR. In practice, the PTR detection mechanism between the bone and skin surface is mostly conductive, not radiative, due to the strong infrared absorption by water in tissue. The radar parameters have been optimized to identify the maximum soft tissue thickness that could be probed within the Maximum Permissible Exposure (MPE) safety ceiling. A matrix comprising goat bones with cortical and trabecular layers, chicken breast and pig skin has been prepared with pre- and post demineralized (acid etched) bone samples. Results of optimal radar data show that output cross-correlation peak delay time, amplitude and half-width are sensitive to the state of bone etching, thus enabling a clear screening methodology for demineralized bones from healthy ones, all being buried in skin-soft tissue overlayers. For extending PTR radar depth resolution to the case of bones with thicker tissue overlayers, a problem of high practical significance, alternate thermal-wave detection schemes bypassing the limitations of PTR detection will be discussed.

8207H-142, Session 2

## Raman spectroscopy: a powerful tool for monitoring unusual bone mineral in diseased or damaged bone

M. D. Morris, Univ. of Michigan (United States)

We will describe important cases of bone disorders in which mineral whose composition, orientation and/or crystallinity differ subtly and in some cases dramatically from those characteristic of healthy bone. These differences can be used to assess health of bone tissue and to monitor progress of therapeutic interventions. In healthy human bone, the mineral is a poorly crystalline carbonated apatite. Mineral composition and crystallinity vary with tissue age, but within a generally defined range. For example, in newly mineralized tissue, the mineral has a high monohydrogen phosphate content and very low crystallinitly. Similar composition changes are encountered during fracture healing and can be used to follow progress from unmineralized callus to integrated bone. In many genetic defects of the skeleton the matrix is disordered, and with it, disordered mineral may be formed. Invading bacteria may form biofilms with low local pH, leading to mineral dissolution and abiotic precipitation of calcium phosphates that different from the normal bone mineral. In osteoradionecrosis, poorly vascularized bone tissue results from radiation induced cell death. The fibrotic matrix that forms supports an undercarbonated and highly crystalline apatitic mineral. X-ray techniques report calcium content and, in the case of computed tomography, architectural features, but contain no other direct composition information. Raman spectroscopy is therefore a powerful complement and may become a preferred methodology in many cases. We will illustrate these prospects using examples from our own laboratory. and report fiber status of specialized optic probes and measurement protocols to implement them

8207H-143, Session 2

## Validating in vivo Raman spectroscopy of bone in human subjects

F. W. Esmonde-White, K. A. Esmonde-White, M. D. Morris, Univ. of Michigan (United States)

Raman spectroscopy can non-destructively measure properties of bone related to mineral density, mineral composition, and collagen composition. Raman spectroscopy has been widely used for assessing both fresh and embedded specimens of bone extracted from animals and humans. Several studies have shown that Raman spectroscopy can further be used to non-invasively measure the properties of bone through the skin in animal and human subjects. While both ex vivo and in vivo measurements have been demonstrated with animal models, correlations between the properties measured through the skin and on the exposed bone have only been reported for human cadavers. In this study, we examine human subjects and compare measurements taken transcutaneously, on surgically exposed bone, and on recovered bone fragments according to an IRB-approved protocol. The Raman spectrum of bone is first measured transcutaneously (in vivo) in a pre-operative visit. Next, the exposed bone is measured in vivo during anterior cruciate ligament (ACL) repair surgery. Finally, a specimen of bone recovered during the normal surgical procedure is examined by microspectroscopy (ex vivo). A commercially available Raman spectrograph and optical probe operating at 785 nm excitation are used for the in vivo measurements. In addition to the Raman results for the transcutaneous and exposed bone measurements, important instrumentation requirements for Raman spectroscopy during surgery will be discussed.

8207H-144, Session 2

## Thermal coherence tomography: a depth-selective thermophotonic radar imaging technique for demineralization diagnosis in hard dental and bone tissues

N. Tabatabaei, A. Mandelis, Univ. of Toronto (Canada); M. Dehghany, K. H. MIchaelian, Natural Resources Canada (Canada)

Photothermal diagnostic methodologies have received much attention in recent years as potential tools for early dental caries diagnosis. Progress in bone loss diagnosis has not been as rapid due to excessive absorption of the water content in overlying tissues. The major advantage of these modalities is the intrinsically high contrast associated with light-tissue interactions. Dental enamel and cortical/trabecular bone are optically turbid media, therefore when light enters the hard tissue it scatters and gets absorbed along its path. Photons are selectively absorbed and/or scattered in abnormal tissues rather than in the surrounding healthy areas. The optical energy conversion to heat features extremely low background signal and high sensitivity to defects or pathology. The significance of early caries detection is that it can be arrested well before cavitation. Similarly, early diagnosis of bone loss can be used to treat osteoporosis effectively. Thermophotonic imaging uses intensity-modulated laser excitation to generate a thermal-infrared photon field inside hard tissue samples. The subsequent infrared emission is captured by a mid-infrared camera and is then processed using Radar matched-filter signal processing algorithms to reveal defects and early caries in human teeth, and to probe the cortical-to-trabecular interface of goat bone samples. This presentation will introduce a depth-selective imaging approach, thermal coherence tomography, as a promising candidate of superior thermophotonic contrast and sensitivity to carious lesions in teeth and will also explore our first studies of the cortical/trabecular interface zone of artificially etched goat bones, with a view to resolving trabecular bone density variations. Furthermore, a comparison between polarized Raman spectroscopy and thermophotonic imaging will be presented to show the enhanced sensitivity of this method to early caries detection.

8207H-145, Session 2

## Raman spectroscopy of bone metastasis

K. A. Esmonde-White, J. Sottnik, Univ. of Michigan Medical School (United States); M. D. Morris, Univ. of Michigan (United States); E. T. Keller, B. J. Roessler, Univ. of Michigan Medical School (United States)

Raman spectroscopy of bone has been used to characterize chemical changes occurring in diseases such as osteoporosis, osteoarthritis and osteomyelitis. Metastasis of cancer into bone causes changes to bone quality that are similar to those observed in osteoporosis, such as decreased bone strength, but with an accelerated timeframe. In particular, osteolytic (bone degrading) lesions in bone metastasis have a marked effect on patient quality of life because of increased risk of fractures, pain, and hypercalcemia. We used Raman spectroscopy to examine bone from two different mouse models of osteolytic bone metastasis. Raman spectroscopy measures physicochemical information which cannot be obtained through standard biochemical and histological measurements. This study was reviewed and approved by the University of Michigan University Committee on the Care and Use of Animals. Two mouse models of prostate cancer bone metastasis, RM1 (n=3) and PC3-luc (n=4) were examined. Tibiae were injected with RM1 or PC3-luc cancer cells, while the contralateral tibiae received a placebo injection for use as controls. After 2 weeks of incubation, the mice were sacrificed and the tibiae were examined by Raman microspectroscopy ( =785 nm). Spectroscopic markers corresponding to mineral stoichiometry, bone mineralization, and mineral crystallinity were compared in spectra from the cancerous and control tibiae. X-ray imaging of the tibia confirmed extensive osteolysis in the RM1 mice, with tumor invasion into adjoining soft tissue and moderate osteolysis in the PC3-luc mice. Raman spectroscopic markers indicate that osteolytic lesions are less mineralized than normal bone tissue, with an altered mineral stoichiometry and crystallinity.

8207H-146, Session 2

## Stem cell treated osteogenesis imperfecta bone imaged using Raman spectroscopy

K. Cloyd, M. Hedegaard, M. Vanleene, P. Guillot, S. Shelfelbine, M. M. Stevens, Imperial College London (United Kingdom)

Osteogenesis Imperfecta is a genetic disorder in which affected persons experience varying levels of bone fragility due to an inability to produce normal amounts and/or quality of type I collagen. Transplantation of healthy stem cells provide potential treatment options which have been previously suggested1 however further research is needed to determine the interaction between the stem cells and the recipient. This study investigated Osteogenesis Imperfecta mice (oim), treated prenatally with human stem cells, using bio-Raman micro-spectroscopy to determine the biomolecular differences of the bone matrix between oim, oim with a stem cell treatment (oim+IUT), and wild type mice(WT) 2. Raman spectra were taken from the cortical cross-sections of the mice femurs in a band of frequencies including the peaks attributed to apatite crystals and proteins associated with the bone mineral matrix. Further univariate and multivariate statistical analysis has been applied to extract information on the variances between experimental groups. Raman analysis shows distinct differences in the bone matrix between males and females receiving the same treatment. Oim in comparison to WT showed a higher mineral to protein ratio potentially attributed to a decrease in collagen content. Oim+IUT mice in comparison to oim displayed a higher carbonate to phosphate ratio and a possible increase in carbonate substitution in females and a sharper apatite peak in males suggesting a more crystalline matrix. These and other results from Raman analysis provide insight into how a stem cell treatment would affect the bone matrices of patients suffering from Osteogenesis Imperfecta.

1. Guillot PV et al. Blood. 2008;111(3):1717-1725.

2. Vanleene M et al. Blood, 2011, 117: 1053-1060.

# Conference 8208: Lasers in Dentistry XVIII

Sunday 22 January 2012
Part of Proceedings of SPIE Vol. 8208 Lasers in Dentistry XVIII

8208-01, Session 1

## Comparison of Er,Cr:YSGG laser versus open flap debridement in periodontal pocket therapy: a clinical study

M. Gupta, A. K. Lamba, F. Faraz, S. Tandon, K. Chawla, D. K. Koli, Maulana Azad Institute of Dental Sciences (India); A. Bhardwaj, Private Practitioner (India)

ABSTRACT

Background - Traditional periodontal open flap debridement (OFD) results in reduced pocket depth, attachment loss, gingival recession and post-operative pain and discomfort. The quest to overcome these shortcomings led to research over Er,Cr:YSGG laser assisted pocket therapy (ELAPT). This study was designed to evaluate and compare the clinical outcomes of ELAPT versus OFD.

Methods - 15 patients having probing depth of ≥5mm and ≤8mm at 2 sites were selected. Test sites (group 1) were treated by ELAPT and control (group 2) by OFD. Clinical parameters were recorded at baseline, 3 and 6 months and included Plaque index (PI), Gingival index (GI), Modified Sulcular Bleeding Index (mSBI), Pocket probing depth (PD), Clinical attachment level (CAL) and Gingival recession (GR).

Results - Both treatments produced reduction in PI, GI, mSBI and PD, increase in GR, and gain in CAL at 3 and 6 months. The mean gain of CAL in group 1 at 3 and 6 months (1.60±0.78 & 1.80±0.63) was similar ($p>0.05$) to the value of group 2 (1.93±0.88 & 2.00±0.54). GR increased significantly ($p<0.05$) only in group 2 at 3 and 6 months (1.80±0.56 & 1.87±0.64) compared to group 1 (0.50±0.68 & 0.57±0.74).

Conclusion - ELAPT compared with OFD results in similar CAL gains with less GR and significant reductions in PD, GI and mSBI and may be considered as an alternative to the surgical therapy for pockets ranging from 5-8mm.

8208-02, Session 1

## Effects of the new 940 diode laser treatment combined with scaling and root planing in the reduction of periodontal pockets: an in vivo study

A. Fallah, Iran Dental Laser Academy (Iran, Islamic Republic of)

Objective: This study compared the effect of 940 Diode laser + scaling and root planing (SRP) versus SRP alone in the reduction of periodontal pockets.

Method: Twenty-four patients were included in the study with 144 random teeth divided in 2 equal groups (each 72 teeth) - control (SRP) and experimental (SRP with laser treatment). There was 4 dental treatment sessions every 7 days and one last assessment session at the 28th day. In both group and in all 4 treatment sessions, the complete SRP with ultrasound techniques and Gracy curettage was performed. In experimental group, we used 940nm diode laser with 1.5W, continuous mode, and 3 mm/sec sweeping motion from the depth of pocket upward to the margin. The whole laser process was done twice with a 2 minutes gap. The same laser process was performed as sham for the control group during the treatment sessions. PPD and BOP were determined before and 28 days after the treatment.

Results: The PPD values at the end of the treatment were lower than the baseline values. The results also showed significant improvement from laser+ SRP group to SRP alone group.

Conclusion: The present data suggest that periodontal pocket treatment with either 940 Diode laser + SRP or SRP alone results in statistically significant improvements in the clinical parameters. The combination of 940 Diode laser irradiation in the gingival sulcus and SRP, was significantly better as compared to SRP alone.

8208-03, Session 1

## In-vivo gingival sulcus imaging using full-range, complex-conjugate-free, endoscopic spectral domain optical coherence tomography

Y. Huang, K. Zhang, The Johns Hopkins Univ. (United States); W. Yi, Seoul National Univ. Dental Research Institute (Korea, Republic of); J. U. Kang, The Johns Hopkins Univ. (United States)

Frequent monitoring of gingival sulcus will provide valuable information for evaluating the presence and severity of periodontal disease. Optical coherence tomography, as a 3D high resolution high speed imaging modality could provide information for pocket depth, gum contour, gum texture, gum recession simultaneously. In this work a handheld forward-viewing miniature resonant fiber-scanning probe was evaluated for real-time in-vivo gingival sulcus imaging. The system is based on full-range, complex-conjugate-free, real-time endoscopic SD-OCT achieved by accelerating the data processing using a graphics processing unit architecture. Preliminary results showed a real-time in-vivo imaging at 33 fps with an imaging range of lateral 2 mm by depth 1.5 mm. Gap between the tooth and gum area was clearly visualized.

8208-04, Session 1

## Subgingival calculus detection by swept-source optical coherence tomography

Y. Hsieh, National Chiao Tung Univ. (Taiwan); Y. Ho, S. Lee, National Yang-Ming Univ. (Taiwan); C. Lu, Industrial Technology Research Institute (Taiwan); C. Jiang, National Formosa Univ. (Taiwan); C. Chuang, National Taiwan Univ. (Taiwan); C. Wang, National Chiao Tung Univ. (Taiwan); C. Sun, National Yang-Ming Univ. (Taiwan)

we demonstrate a method that can be applied to subgingival calculus detection in dentistry. Moreover, the refractive index of dental calculus was measured in experiment. The dental calculus shows different optical and image properties to the caries. In Fig. 9, we can find that the dental calculus shows different optical and image properties to the caries. The caries reveals lower group delay and destroys the tooth structure inwardly. On the other hand, the calculus shows stronger group delay and do not affect the tooth structure because the calculus always deposits on the tooth surface. The different features can be observed in OCT images. Figure 9(e) shows the small volume of calculus still reveals the same property of strong group delay. Therefore, the difference between caries and calculus can be diagnosed by OCT imaging directly. In clinical diagnoses, the method presents advantages when compared to conventional X-ray imaging. X-ray imaging is radioactive and cannot observe the calculus on the buccal or lingual surface of the tooth. However, OCT imaging can overcome these two drawbacks. For further study, an oral probe will be developed instead of the sample arm for in vivo measurement.

8208-05, Session 1

## Er,Cr:YSGG laser: a new treatment modality for lower lip mucocele

K. Chawla, M. Gupta, A. K. Lamba, F. Faraz, S. Tandon, D. K. Koli, Maulana Azad Institute of Dental Sciences (India); A. Bhardwaj, Private Practitioner (India)

Mucoceles are benign, mucus containing cystic lesions of the minor salivary glands. They are not true cysts since most of them lack an epithelial lining. These lesions occur most commonly in the lower lip. They are caused by trauma, orthodontic devices or biting habits. This report presents a case of a 22 year old male with a 3 mm mucocele on the lower lip. This lesion was removed using an Er,Cr:YSGG laser. Local infiltrative perilesional anesthesia was applied (12 mg of 2% lidocaine with epinephrine 1:100.000). The anesthetic was not infiltrated directly into the lesion to avoid compromising the biopsy. The lip was then everted with digital pressure to increase the lesions prominence. The laser application was done with 600 µm sapphire tip, 1.5 W power, 13% air and 9% water in noncontact mode. A circular incision was made around the lesion to obtain a proper biopsy sample. Irradiation of the mucocele was avoided and it was lasered around to obtain the lesion in one piece. Once the lesion had been removed, the operation field was wiped with sterile gauze soaked in 1% normal saline solution. A laser bandage was applied with 0.5 W power with air and water switched off. The healing was uneventful and no suture or analgesic was required. The histopathological report confirmed the presurgical diagnosis. No relapse was observed till one year after surgery.

8208-06, Session 2

## Bond strengths evaluation of laser ceramic debonding

T. Dostálová, Charles Univ. in Prague (Czech Republic); H. Jelinkova, J. Sulc, Czech Technical Univ. in Prague (Czech Republic); P. Michalik, Charles Univ. in Prague (Czech Republic); M. Nemec, M. Fibrich, Czech Technical Univ. in Prague (Czech Republic); M. Miyagi, Sendai National College of Technology (Japan)

Ceramic brackets can lead to problems such as enamel tear outs or pain at removal because of their low fracture resistance and high bond strengths. Laser systems can be used to eliminate those problems mainly during bracket debonding. The principle of bracket debonding is to degrade the adhesive resin strength connecting the tooth and bracket. The aim of our study was to analyze the laser radiation effect during brackets debonding to compare shape and size enamel adhesive resin area and bracket surface. The laser system was a longitudinally diode-pumped Tm: YAP laser operating at 1997 nm. The flat enamel structure and bracket surface were evaluated in scanning electron microscope. The digital force gauge FMI-230C5 measured the actual bond strength to simulate practical situation in vivo. After laser irradiation the bracket can easily be removed without cracks. In previous studies it was confirmed that Tm: YAP microchip laser radiation with power: 1W; time: 60 second; spot size - 3 mm has direct influence on the adhesive resin strength connecting the tooth and bracket. The microcracks in enamel and the thickness of adhesive resin layer significantly decreased bond strength during bracket debonding. Metal component inside bracket limited laser effect. The diode-pumped Tm: YAP laser operating at 1997 nm might be an effective clinical way to reduce the shear bond strengths of orthodontic ceramic brackets.

8208-07, Session 2

## Shear bond strength of a self-etch adhesive to caries-affected dentin after caries removal by Er:YAG laser

Z. Zhan, Fujian Normal Univ. (China); W. Wu, Fujian Medical Univ. (China); H. Zhao, X. Zhang, Fujian Normal Univ. (China); S. Lin, Fujian Medical Univ. (China); S. Xie, Fujian Normal Univ. (China)

Nowadays, Er:YAG laser has been considered as a most promising alternative to traditional mechanical instruments for cavity preparation and caries removal. Moreover, more and more studies had focused on the bond strength of adhesive systems to normal enamel or dentin prepared by Er:YAG laser and influencing factors. However, little is known about the bond strength of caries-affected dentin after caries removal by Er:YAG laser. The purpose of this study was to evaluate the shear bond strength of a self-etch adhesive to caries-affected dentin after caries removal by Er:YAG laser and analyze the resin-dentin interface. The caries-infected dentin of human molars were removed by Er:YAG laser with energy density of 20 J/cm2 and pulse repetition rate of 20 Hz. The conventional bur was used as control group. After bonding procedures, specimens were subjected to shear bond strength test and the adhesive interface was examined by laser confocal scanning microscope (LCSM). The result showed that Er:YAG laser could effectively remove dentin caries. There was no statistical difference in shear bond strength between two groups and the adhesive interface created on laser-irradiated dentin surface presented similar features to that on bur-ground surface.

8208-08, Session 2

## Relationship between nondestructive OCT evaluation of resins composites and bond strength in a cavity

T. A. Bakhsh, Tokyo Medical and Dental Univ. (Japan) and King Abdulaziz Univ. (Saudi Arabia) and Global Ctr. of Excellence (Japan); A. Sadr, Tokyo Medical and Dental Univ. (Japan) and Globl Ctr. of Excellence (Japan); Y. Shimada, Tokyo Medical and Dental Univ. (Japan); J. Tagami, Tokyo Medical and Dental Univ. (Japan) and Global Ctr. of Excellence (Japan); Y. Sumi, National Ctr. for Geriatrics and Gerontology (Japan)

Objectives: Formation of microgaps under the composite restorations due to polymerization stress and other causes compromise the adhesion to the dental substrate and restoration durability. However, the relationship between cavity adaptation and bond strength is not clear. In this paper, we introduce a new testing method to assess cavity adaptation by swept-source optical coherence tomography (SS-OCT) and microtensile bond strength (MTBS) in the same class-I cavity.

Methods: Round class-I cavities 3 mm in diameter and 1.5 mm in depth were prepared on 10 human premolars. After application of Tokuyama Bond Force adhesive, the cavities were filled by one of the two techniques; incremental technique using Estelite Sigma Quick universal composite or flowable lining using Palfique Estelite LV with bulk filling using the universal composite. Ten serial B-scan images were obtained throughout each cavity by a hand-held SS-OCT probe (Panasonic Health Care, Japan) for each specimen at a center wavelength of 1310 nm. Significant peaks in the signal intensity were detected at the bonded interface of the cavity floor and to compare the different filling techniques. The specimens were later cut into beams (0.7×0.7 mm) and tested to measure MTBS at the cavity floor.

Results: Flowable lining followed by bulk filling was inferior in terms of cavity adaptation and MTBS compared to the incremental technique ($p<0.05$, t-test). The adaptation (gap free cavity floor) and MTBS followed similar trends in both groups.

Conclusion: Quantitative assessment of dental restorations by OCT can provide additional information on the performance and effectiveness of dental composites and restoration techniques. It may potentially become an essential clinical monitoring tool for the assesment of bonded composite restorations.

This study was supported by Global Center of Excellence and King Abdulaziz University.

8208-09, Session 2

## Assessing ex vivo dental biofilms and in vivo composite restorations using cross-polarization optical coherence tomography

No abstract available

8208-10, Session 3

## Particle characteristics of different materials after ultra-short pulsed laser (USPL) irradiation

J. Meister, F. Schelle, P. Kowalczyk, M. Frentzen, Rheinische Friedrich-Wilhelms-Univ. Bonn (Germany)

The exposition with nano particles caused by laser application in dental health care is an open discussion. Based on the fact that nano particles can penetrate through the mucosa, the knowledge about the particle characteristics after irradiation with an USPL is of high importance. Therefore the aim of this study was to investigate the particle characteristics, especially the size of the ablated debris after USPL irradiation.

The irradiation was carried out with a USP Nd:YVO4 laser having a center wavelength at 1064 nm. Based on the pulse duration of 8 ps and a pulse repetition rate of 500 kHz the laser emits an average power of 9 W. The materials investigated were dental and dental restorative materials (composite and amalgam), ceramic and different metals (gold, aluminium). The samples were irradiated with a power density of 318 W/cm^2 at distances of 5, 10, 15 and 20 mm. The debris were collected on an object plate. REM pictures were used for analysis of the ablation debris.

Depending on the irradiated material, we observed different kinds of structures: vitreous, flocculent and pellet-like. The mean particel sizes were in the order 10x10 up to 30x30 µm^2. In addition a cluster of ablated matter (nanometer range) distributed over the whole irradiated area was found. With increasing distances the cluster structure reduces from multi-layer to mono-layer clusters.

Particle sizes in the micrometer and the nanometer range were found after irradiation with an USPL. The nano particles create a cluster structure which is influenced by increasing distances.

8208-11, Session 3

## Modeling distributed feedback GaAs/AlGaAs lasers in dentistry

M. Shih, Univ. of Florida (United States)

Distributed-feedback gallium-arsenide-based lasers with metal-gratings can generate stable wavelength at 980nm for applications in dentistry. This model uses the periodic optical waveguide method to calculate the coupling coefficient, which is a key parameter of laser performance. This model shows how the optical, geometrical, and material parameters depending on each other and how they affect the coupling coefficients in the laser waveguides. Numerical results compare the coupling coefficients of 980 nm lasers with those of 810 nm lasers. The modeling process including results, discussions, and physical interpretations helps to design and analyze lasers for more clinical and research applications in dentistry.

8208-12, Session 3

## Investigations on the potential of a novel diode pumped Er:YAG laser system for dental applications

K. Stock, F. Hausladen, R. Hibst, Univ. Ulm (Germany)

Pulsed Er:YAG lasers are well established in dentistry for variety of indications. These lasers are pumped by a flashlamp, typical mean powers are up to about 8W, and pulse repetition rates can reach 100Hz. Recently, a novel diode pumped Er:YAG laser system (Pantec Engineering AG) becomes available with a mean laser power up to 15W and a pulse repetition rate up to 1kHz.

The aim of the presented study is to investigate the effect of this laser system on dental hard tissue at various irradiation parameters, particularly at repetition rates exceeding 100 Hz.

For reproducible experiments, firstly an appropriate set-up was realized with a beam delivery and focusing unit, a computer controlled translation stage with sample holder, and a shutter unit. It allowed to move the sample (dentin or enamel slides of extracted human teeth) with a defined velocity while irradiation by various laser parameters. A water spray served to moisten the sample surfaces. After irradiation, the craters were analyzed by light microscopy and a 3D measurement system regarding to the ablation quality, the crater geometry, the ablation efficacy, and the thermal side effects.

The results show the typical rough surface in dentin and enamel in the ablation area. The craters are slightly cone shaped with sharp edges on the surface. Water cooling is essential to prevent thermal injury. The ablation efficacy in dentin is comparable to literature values of the flashlamp pumped Er:YAG laser.

In conclusion these first experiments with the diode pumped Er:YAG laser system on dental hard tissue demonstrate its ability for use in dentistry.

8208-13, Session 3

## Hyperspectral laser-induced autofluorescence imaging of dental caries

M. Bürmen, A. Fidler, F. Pernuš, B. Likar, Univ. of Ljubljana (Slovenia)

Dental caries is a disease characterized by demineralization of enamel crystals leading to the penetration of bacteria into the dentine and pulp. Early detection of enamel demineralization resulting in increased enamel porosity, commonly known as white spots, is a difficult diagnostic task. Laser induced autofluorescence was shown to be a useful method for early detection of demineralization. The existing studies involved either a single point spectroscopic measurements or imaging at a single spectral band. In the case of spectroscopic measurements, very little or no spatial information is acquired and the measured autofluorescence signal strongly depends on the position and orientation of the probe. On the other hand, single-band spectral imaging can be substantially affected by local spectral artefacts. Such effects can significantly interfere with automated methods for detection of early caries lesions. In contrast, hyperspectra imaging effectively combines the spatial information of imaging methods with the spectral information of spectroscopic methods providing excellent basis for development of robust and reliable algorithms for automated classification and analysis of hard dental tissues. In this paper, we employ 405 nm laser excitation of natural and artificial caries lesions of various degrees. The autofluorescence signal is acquired by a state-of-the-art hyperspectral imaging system consisting of a high-resolution Acousto-Optic Tunable Filter (AOTF) and a highly sensitive Scientific CMOS camera in the spectral range from 500 nm to 900 nm. The results are compared to the sensitivity and specificity of near-infrared hyperspectral imaging methods employed in the existing studies on early detection of dental caries.

8208-14, Session 3

## Spectrally enhanced image resolution of tooth enamel surfaces

L. Zhang, L. Y. Nelson, J. H. Berg, E. J. Seibel, Univ. of Washington (United States)

Short-wavelength (405-nm) laser illumination of intricate dental topography produced enhanced image detail of the enamel surface using a threadlike scanning fiber endoscope (SFE). Video frames acquired at 405-nm were compared to longer wavelengths of 444, 532, and 635-nm after compensating for wavelength-dependent illumination spot size differences. Enhanced clinical detail for occlusal surfaces of extracted teeth is more apparent using 405-nm illumination. Scattering and absorption coefficients for a Monte Carlo model of light propagation in dental enamel for 405 nm were scaled from published data at 532-nm and 633-nm. The value of the scattering coefficient used in the model was scaled from the coefficients at 532-nm and 633-nm by the inverse third power of wavelength. Simulations showed that the penetration depth of short-wavelength illumination is localized close to the enamel surface, while long-wavelength illumination travels much further and is backscattered from greater depths. Therefore, images obtained using short wavelength laser are not contaminated by the superposition of light reflected from enamel tissue at greater depths. The dental caries process on the occlusal surface begins on the lateral cusp slopes where the progression of the caries process is not visible with typical broadband light sources, but is discernible with the 405 nm light source. Hence, the SFE with short-wavelength illumination may make it possible to visualize surface manifestations of phenomena such as demineralization, thus better aiding the clinician for the detection of early caries.

8208-15, Session 4

## Evaluation of cross-polarized near-infrared hyperspectral imaging for early detection of dental caries

P. Usenik, M. Bürmen, A. Fidler, F. Pernuš, B. Likar, Univ. of Ljubljana (Slovenia)

Despite major improvements in dental healthcare and oral hygiene, dental caries remains one of the most prevalent oral diseases and represents the primary cause of oral pain and tooth loss. The initial stages of dental caries are characterized by demineralization of enamel crystals and are difficult to diagnose. Near-infrared (NIR) hyperspectral imaging is a new promising technique for detection of early changes in the surfaces of carious teeth. This noninvasive imaging technique can characterize and differentiate between sound tooth surface and initial and advanced tooth caries. The absorbing and scattering properties of dental tissues reflect in distinct spectral features, which can be measured, quantified and used to accurately classify and map different dental tissues. Specular reflections from the tooth surface, which appear as bright spots, mostly located around the edges and the crests of the teeth, act as a noise factor which can significantly interfere with the spectral measurements and analysis of the acquired images, degrading the accuracy of the classification and diagnosis. Employing cross-polarized imaging setup can solve this problem, however has yet to be systematically evaluated, especially in broadband hyperspectral imaging setups. In this paper, we employ cross-polarized illumination setup utilizing state-of-the-art high-contrast broadband wire-grid polarizers in the spectral range from 900 to 1700 nm for hyper-spectral imaging of natural and artificial carious lesions of various degrees. The classification results obtained for a standardized set of lesions by employing cross-polarized illumination setup are systematically compared to the corresponding classification obtained for a non-polarized illumination setup.

8208-16, Session 4

## Longitudinal assessment of subsurface artificial root caries lesions by optical coherence tomography in comparison with transverse microradiography

A. Sadr, S. Nakashima, Y. Shimada, J. Tagami, Tokyo Medical and Dental Univ. (Japan); Y. Sumi, National Ctr. for Geriatrics and Gerontology (Japan)

We previously demonstrated that a swept-source optical coherence tomography system (SS-OCT) without polarization-sensing could quantitatively estimate the progress of cavitated dentin lesions in vitro. The purpose of the current study was to investigate the ability to estimate the lesion development in non-cavitated dentin lesions with a surface layer. Bovine root dentin specimens were subjected to different periods of demineralization (1 to 14 days). Cross-sectional images of the specimens before and after the demineralization were captured by SS-OCT at 1310 nm center wavelength. Following each period, the specimens were cut into sections for transverse microradiography (TMR) and correlations between SS-OCT data and TMR parameters were examined. TMR images of the specimens showed subsurface lesions ranging 100 to 400 μm in lesion depth (LD) and 1,000-5,000 vol% μm in mineral loss (ΔZ). SS-OCT images showed a boundary suggesting the lesion front. Reflectivity increased with demineralization progress. A strong correlation was found between the boundary depth from the lesion surface and LD. Integrated dB values from the lesion surface to the boundary depth before and after the demineralization (RD and RS, respectively) were calcualted. There was a significant positive relationship between ΔZ and RD; but not between ΔZ and ΔR, where ΔR=RD-RS. A clear indication of surface layer thickness was not found on OCT images. In conclusion, SS-OCT system could provide quantitative estimation of caries progress in artificial subsurface dentin lesion in terms of lesion depth. Further studies are needed to investigate whether other parameters of the dentin lesion with surface layer could be determined by this technique. Study supported by GCOE at TMDU and NCGG.

8208-17, Session 4

## Monitoring tooth demineralization using a cross polarization optical coherence tomographic system with an integrated MEMS scanner

D. Fried, Univ. of California, San Francisco (United States)

No abstract available

8208-18, Session 4

## Transmission of 1064-nm laser radiation during ablation with an ultra-short pulse laser system (USPL)

F. Schelle, J. Meister, B. Oehme, M. Frentzen, Rheinische Friedrich-Wilhelms-Univ. Bonn (Germany)

During ablation of oral hard tissue with an USPL system a small amount of the incident laser power does not contribute to the ablation process and is being transmitted. Since the centre wavelength of our laser system is at 1064 nm, the transmitted light could for example be absorbed by hemoglobin inside the dental pulp, leading to severe side effects. The aim of this study was to assess the transmission during ablation and to deduce possible risks for the patient.

The study was performed with an Nd:YVO4 laser, emitting pulses with a duration of 8 ps at a wavelength of 1064 nm. A repetition rate of 500 kHz and an average power of 9 W were chosen to achieve high ablation efficiency. The transmission through slices of mammoth ivory and dentin with a thickness of 2 mm and 5 mm was measured with a power meter, placed directly beyond the samples. The effect of the transmitted light on blood was assessed in two steps. First a basin filled with pork blood was irradiated with a laser power corresponding to the measured transmission. In a second step the basin was placed beyond a specimen, which was then ablated with an average power of 9 W.

Transmission during ablation of 2 mm mammoth ivory slices was about 4 % of the incident laser power. The transmitted power caused coagulation of the blood. Given these circumstances the use of ultra short laser pulses could lead to severe side effects for the patient.

8208-19, Session 4

## Minimally invasive treatment of carious dentin with a nanosecond pulsed laser at 5.8 μm wavelength

K. Ishii, M. Saiki, Osaka Univ. (Japan); K. Yoshikawa, K. Yasuo, K. Yamamoto, Osaka Dental Univ. Hospital (Japan); K. Awazu, Osaka Univ. (Japan)

[Background] In clinic, Er:YAG laser and Er,Cr:YSGG laser have already realized the optical drilling of dental hard tissue. Although the selective excavation of carious dentin for minimal intervention is required, conventional lasers lack the ability to discriminate carious tissue only because they use the laser tissue interaction derived from a strong absorption of water. Based on the absorption property of carious dentin, which has a characteristic absorption bands called amide 1 and amide 2, a wavelength range around 6 μm is a candidate for selective excavation. Our group has already observed the difference of ablation depth between demineralized and normal dentin (selective excavation) in the wavelength range from 5.75 to 6.60 μm. Also this study has showed the effectiveness of 5.8 μm. Objective of this study is to determine optimal irradiation parameters of selective excavation by using 5.8 μm. [Material and Method] Bovine dentin demineralized by soaking in lactic acid solution was used as a carious dentin model. A nanosecond pulsed laser with a wavelength of 5.8 μm was obtained by difference-frequency generation technique. The laser delivers 5 ns pulse width at a repetition rate of 10 Hz. After irradiation, morphological change and measurement of ablation depth was observed with a scanning electron microscope and a confocal laser microscope, respectively. [Results] In 5.8 μm wavelength, high ablation efficiency with a low thermal side effect was observed. This effect was observed at average power density around 20 W/cm2. [Conclusion] 5.8 μm wavelength provides a selective excavation technique for minimal intervention.

8208-20, Poster Session

## Comparison of soft tissues effects of 810, 940 and 980-nm diode lasers for dentistry

R. M. Verdaasdonk, A. van der Veen, M. Verleng, Vrije Univ. Medical Ctr. (Netherlands); V. Lemberg, D. Boutoussov, BIOLASE Technology, Inc. (United States)

Diode lasers are becoming more established in dentistry especially to perform soft-tissue surgery and to kill bacteria at areas that are difficult to reach. These lasers are available at various wavelengths in the near infrared and each are ascribed to have unique tissue effects.

In this study, the tissue effects of diode lasers at 810, 940 nm (Biolase) and 980 nm (Sirona) were compared under controlled conditions in tissue simulating clinical settings using special close up imaging and thermal imaging techniques.

Tissue with either high blood content (liver) or low blood content (pale muscle) was irradiated at 4 W for 10 seconds from a 300 µm bare fiber positioned in contact with the surface (clean or pre-carbonized tip). The dynamic tissue effects underneath the surface were imaged through a glass window on the side of the tissue sample. The progression of coagulation and carbonization/ablation front were followed in time.

In liver, only 810 nm created instant tissue carbonization/ablation (ascribed to higher blood absorption) while similar effects were delayed at 980 nm (ascribed to a higher water absorption). In pale muscle, all the wavelengths only induced coagulation. The 940 nm wavelength has a low absorption dip for both blood and water, resulting a deep tissue penetration without carbonization. When the tip was precarbonized, the tissue ablation started within 1 second for all wavelengths.

With a pre-carbonized fiber tips all diode laser wavelengths work effectively for tissue cutting/ablation. The 940 nm diode laser seems unique for deep tissue penetration and hence sterilization without uncontrolled carbonization.

8208-21, Poster Session

## Relationship between Refractive Index and Mineral Content of Enamel and Dentin using OCT and TMR

I. Hariri, A. Sadr, Y. Shimada, S. Nakashima, J. Tagami, Tokyo Medical and Dental Univ. (Japan); Y. Sumi, National Ctr. for Geriatrics and Gerontology (Japan)

Objective: Optical Coherence Tomography (OCT) has been used for imaging dental caries lesions. Early demineralization influences interaction of light with tissue and may alter optical path length and therefore refractive index (n). The aim of this work was to investigate relationship between n and mineral content (MC) of enamel and dentin using OCT and transverse microradiography (TMR). It was hypothesized that an accurate measurement of the changes in n after demineralization and remineralization may provide quantitative information on mineral loss or gain.

Material and Method: Resin-embedded bovine enamel and dentin surfaces were partitioned into three regions; sound, demineralized and remineralized. The latter two were subjected to demineralization and de/remineralization solutions for 2-months. 300-µm slabs were prepared, polished and placed on a metal plate in order to obtain transverse B-scans by SS-OCT at each lesion depth where n was calculated. The specimens were further polished for TMR analysis and MC calculations.

Results: n ranged 1.52 to 1.65 in enamel, and 1.44 to 1.56 in dentin. Significant correlation ($p<0.001$) was found between n and MC after demineralization and remineralization in enamel ($r = 0.8947$ and 0.9245) and dentin ($r = 0.9245$ and 0.8962), respectively. However, the linear regression parameters were different among the groups.

Conclusions: A highly positive correlation was demonstrated between MC and n for enamel and dentin. MC in remineralized samples corresponds to higher n values, perhaps due to different crystalline structure after remineralization. Supported by GCOE and JSPS.

8208-22, Poster Session

## Tooth structure analyzing by use of Stokes formalism and Mueller matrix

Y. Hsieh, National Chiao Tung Univ. (Taiwan); Y. Ho, S. Lee, National Yang Ming Univ. (Taiwan); C. Chuang, National Taiwan Univ. (Taiwan); C. Wang, National Chiao Tung Univ. (Taiwan); C. Sun, National Yang-Ming Univ. (Taiwan)

This work focuses on tooth polarization feature analysis. A tooth cross-section sample including enamel and dentin are used in a transmission polarization analyzing measurement. Experiment data are plot into one-dimension figure. All the tooth structures are analyzed by Stokes formalism and Mueller matrix. By analyzing Mueller matrix, the retardence and diattendance of structures are observed and described mathematical. An obviously polarization changing can be measured around the dentin enamel junction (DEJ) since the structure difference between enamel and dentin.

A bleached tooth is also measured to observe the side effect of bleaching. The polarization property of DEJ is changed after bleaching and the structure may be destroyed.

This method provides a non-invasive method to observe the changing of tooth structure including enamel, dentin and DEJ. It is also a preliminary study of our polarization sensitive optical coherence tomography (PS-OCT). A further study and 2-D images reconstructing will be analyzed in PS-OCT.

8208-23, Poster Session

## Treatment of an aberrant intraoral hair with Er,Cr:YSGG laser: a case report

M. Gupta, A. K. Lamba, F. Faraz, S. Tandon, K. Chawla, D. K. Koli, Maulana Azad Institute of Dental Sciences (India); A. Bhardwaj, Private Practitioner (India)

Occurrence of hair in the oral cavity is an extremely rare phenomenon. In personal communication, we have never seen or heard of hair being detected in the oral cavity. Even Julia Pastrana, the famous “Bearded Lady” of the 1800s, had no record of oral hair, although her entire body was covered with hair. She suffered from excessive gingival hyperplasia, but apparently no hair existed within the mouth. A thorough review of literature reveals only four reported cases of oral hair. The present case was a young man who on oral examination revealed a single black hair on floor of the mouth near the lingual frenulum. The hair was removed using Er,Cr:YSGG laser. Topical anaesthetic gel was applied to the operation field. The laser application was done with 600-µm sapphire tips, 1.5 W power, 13% air and 9% water in noncontact mode to remove the hair along with the follicle.It seems that this ectopic phenomenon maybe a mutation in the tissues. Whatever the cause, this phenomenon is extremely rare. Therefore, its etiology is unclear, but we can treat this problem with various modalities, ie, excision with a scalpel, electrosurgery, radiosurgery, or lasers. In our case, we used lasers because of less patient discomfort, better hemostasis, less postoperative discomfort, and better healing.Because of the extreme rarity of such cases, it is interesting as well as important to report and further study their relevance.

8208-24, Poster Session

## Management of denture-induced epulis fissuratum with Er,Cr:YSGG laser: a case report

D. K. Koli, M. Gupta, M. Verma, A. K. Lamba, K. Chawla, Maulana Azad Institute of Dental Sciences (India); A. Bhardwaj, Private Practitioner (India)

Epulis fissuratum refers to tissue growth into the oral cavity, located over the alveolar ridges or the soft tissues of the vestibular sulcus. Trauma and irritation are important aetiological factors for epulis fissuratum and lesions arise in areas of persistent mucosal injury. This report presents a case of a 68-year old male patient with two soft tissue hyperplastic growths seen in the buccal vestibule in the lower anterior region.On examination of the oral cavity the patient was completely edentulous and wearing dentures since 7 years. Two soft tissue hyperplastic growths were seen in the buccal vestibule in the lower anterior region (approx. 1cm ×3cm on left side and 1cm×2cm on right side).These lesions were removed using an Er,Cr:YSGG laser. A pulsed Er,Cr:YSGG laser was used for epulis dissection with the following settings: 2.5W power, 15% water, 20% air, and 20 Hz frequency. No sutures were given. A laser bandage was applied using 0.5W power with air and water turned offThe healing was uneventful and no suture or analgesic was required. The histopathological report confirmed the presurgical diagnosis. No relapse was observed till one year after surgery.The Er,Cr:YSGG laser is a very precise ablation instrument that offers certain advantages. It is strongly absorbed by water and causes minimal damage to the adjacent tissues, especially the underlying muscle layers. Due to minimal trauma to the adjacent tissues, postoperative healing was favourable, with very little scar formation. Postoperative bleeding in the case reported was minimal. No sutures were placed after the excision, as the denatured proteins serve as a natural wound dressing. In this case there was little contraction and scarring.The technique presented in this paper was easily executable and allowed a better prediction of the surgery results.

8208-25, Poster Session

## Diffusion analysis of one photosensitizer in bovine teeth using fluorescence optical imaging

D. Jacomassi, A. Rastelli, S. Pratavieira, V. Bagnato, Univ. de São Paulo (Brazil)

Photodynamic antimicrobial therapy (PACT) promotes bacterial death as a result of the photosensitization of microbial components, because the photosensitizer (PS) shows an affinity for bacterial walls and can be photo-activated to cause the desired damage. In Dentistry, the PACT has been used for different applications; one example is dental caries treatment. However, bacteria in dentine may be less susceptible to PACT as a result of limited penetration of the photosensitizer and of limited light propagation through dentine structures. Then, the purpose of this study was to evaluate the diffusion of one PS on dentine structures by means of fluorescence optical imaging. Three bovine incisors were used to obtain dentine cavities with 1, 2 and 3 mm depth. Photogem solution at 0.5 g/l was used as PS. After the cavity preparation, 20 ul of PS solution was placed on the top surface of the floor of the cavity. Using a fluorescence imaging system with excitation at 400 nm and a high-pass filter, the images were captured using a color CCD camera. The images were analyzed using MatLab and the diffusion of PS was observed.

8208-26, Poster Session

## Optical characterization of one dental composite resin using bovine enamel as reinforcing filler

J. Tribiolli, D. Jacomassi, A. Rastelli, S. Pratavieira, V. Bagnato, C. Kurachi, Univ. de São Paulo (Brazil)

The use of composite resins for restorative procedure in anterior and posterior cavities is highly common in Dentistry due to its mechanical and aesthetic properties that are compatible with the remanescent dental structure. Thus, the aim of this study was to evaluate the optical characterization of one dental composite resin using bovine enamel as reinforcing filler. The same organic matrix of the commercially available resins was used for this experimental resin. The reinforcing filler was obtained after the gridding of bovine enamel fragments and a superficial treatment was performed to allow the adhesion of the filler particles with the organic matrix. Differents optical images as fluorescence image were performed to compare the experimental composite with the human teeth. The fluorescence image was obtained using a lamp with an optical filter to irradiate the sample at 400 nm and the fluorescence was captured by a high resolution color RGB Bayer filter CCD camera with a simple objective lens. The present experimental resin shows similar optical properties compared with human teeth.

8208-27, Poster Session

## All in one: Er,Cr:YSGG periodontal laser therapy

A. Bhardwaj, Private Practitioner (India); M. Gupta, D. K. Koli, K. Chawla, Maulana Azad Institute of Dental Sciences (India)

Modern laser technology has resulted in treatments that are less traumatic and more comfortable for patients. Lasers present an opportunity for general practitioners to treat certain periodontal conditions and they enable treatment with fewer complications. This also presents an opportunity for dentists to focus on the more complex treatments.various abnormalities such aberrant intra-oral hair, mucocele, gingival hyperplasia, high frenal attachment, periodontal pocket lining removal, epulis excision can easily be performed and result in high levels of patient comfort and tolerance.Although the state of periodontics is undergoing a paradigm shift, the advent of new laser technology provides periodontists and general practitioners with an instrument that allows minimally invasive, more comfortable treatment within the standard of care. The treatment capabilities involve the successful and effective treatment of traditional procedures, such as gingivectomies, frenectomies, soft tissue lesions; advanced procedures, such as functional or cosmetic crown lengthening; and site-specific therapies for residual periodontal conditions.

8208-28, Poster Session

## Low-level laser intensity improves propulsive appliance effects on condylar cartilage

A. C. Ribeiro Figueiredo, F. C. A. dos Santos II, L. R. Capelletti, Sr., M. V. B. Galdino, Sr., R. V. Araújo, Sr., M. R. Marques, Univ. Federal de Goias (Brazil)

Mandibular propulsive appliance (MPA) stimulates cell proliferation and gene expression on mandible condylar cartilage (Marques et al., 2008). However, its association with low level laser therapy (LLLT) is unknown. This study evaluated the effects of LLLT associated to MPA on mandibular condyle. Twenty Wistar rats were divided into four groups. Group I received any treatment. Group II was bilaterally irradiated on temporomandibular joint with 10 J/cm2 low level laser (680nm, 40mW and 10s) on alternate days. Group III used the propulsive appliance for ten hours daily and Group IV used the appliance daily and was irradiated on alternate days. After 15 days the animals were killed by lethal doses of anesthetics. The condyles were fixed in Methacarn solution and decalcified in 4.13% EDTA solution for 30 days. Seriate saggital 5 µm-thick sections were stained by the hematoxilin-eosin method. Morphological and morphometric analyses were performed to measure the length and the height of the mandibular condyle, the thickness of the condilar cartilage and the bone mass. Results were expressed as mean ± standard deviation (one-way ANOVA, Tukey´s post-test.) The appliance increased all measures compared to the control group, except bone mass. Alone, LLLT had no effects on all measures, however, the association of the appliance with the LLLT increased condilar cartilage and bone mass significantly compared to the others groups. These results suggest that LLLT improves the effects of mandibular propulsive appliance in the condylar cartilage growth and formation of bone mass. Financial support: National Institute for Optics and Photonics (INOF).

8208-29, Poster Session

## Image-guided laser ablation of occlusal caries using a rapidly swept CO2 laser operating at 9.3-µm

K. H. Chan, D. Fried, Univ. of California, San Francisco (United States)

No abstract available

8208-30, Poster Session

## Remineralization of root caries monitored using cross polarization optical coherence tomography

C. L. Darling, H. Kang, D. Fried, Univ. of California, San Francisco (United States)

No abstract available

8208-31, Poster Session

## An investigation of acid-etching CO2 laser ablated enamel surfaces using cross polarization optical coherence tomography

B. Nahm, K. H. Chan, H. Kang, C. L. Darling, D. Fried, Univ. of California, San Francisco (United States)

No abstract available

8208-32, Poster Session

## Nondestructive monitoring of the repair of occlusal caries lesions using cross polarization optical coherence tomography

H. Kang, C. L. Darling, D. Fried, Univ. of California, San Francisco (United States)

No abstract available

8208-33, Poster Session

## Monitoring demineralization and remineralization in occlusal surfaces using optical coherence tomography and near-IR Imaging

C. M. Buehler, C. L. Darling, D. Fried, Univ. of California, San Francisco (United States)

No abstract available

8208-34, Poster Session

## Imaging secondary caries lesions with cross polarization optical coherence tomography

R. Lee, D. Fried, C. L. Darling, Univ. of California, San Francisco (United States)

No abstract available

# Conference 8209: Ophthalmic Technologies XXII

Saturday-Sunday 21-22 January 2012

Part of Proceedings of SPIE Vol. 8209 Ophthalmic Technologies XXII

8209-01, Session 1

## In vivo multiphoton imaging of the cornea in control and diabetic rats

G. Latour, L. Kowalczuk, Ecole Polytechnique (France); M. Savoldelli, Univ. Paris Descartes (France); J. Bourges, Univ. Paris Descartes (France) and INSERM (France); I. Gusachenko, K. Plamann, Ecole Polytechnique (France); F. Behar-Cohen, Univ. Paris Descartes (France) and INSERM (France); M. Schanne-Klein, Ecole Polytechnique (France)

Multimodal multiphoton microscopy is an efficient method for obtaining virtual biopsies in unstained corneas. In particular, fibrillar collagen, that composes corneal stroma, exhibits strong Second Harmonic Generation (SHG) signals. In this study, we evaluated hyperglycemia-induced effects in the corneas of diabetic rats by combining in vivo confocal reflectance microscopy, multiphoton microscopy and transmission electron microscopy (TEM). This correlative imaging approach showed that SHG images reveal corneal abnormalities in diabetic rats with an excellent contrast. Striated collagen fibrils clearly appeared in TEM images in the same region of the Descemet's membrane as SHG signals in multiphoton images. SHG imaging was also performed in ex vivo human corneas and consistently showed similar SHG structures. These observations were confirmed by TEM using the same correlative imaging approach as in diabetic rat corneas. Finally, we performed in vivo multiphoton imaging of anesthetized rats and successfully observed the same structures in the Descemet's membrane. It demonstrates that in vivo multiphoton cornea imaging could provide a diagnosis of hyperglycemia-induced corneal abnormalities.

We also developed polarization-resolved SHG microscopy to obtain complementary information about the orientation of the fibrils in the stroma since SHG epidetected images do not directly reveal the fibrillar structure of the collagen lamellas. We successfully retrieved the orientation of the fibrillar domains in the whole cornea thickness using a specific image processing. This technique was also demonstrated in vivo. It opens the way for further biomedical studies using in vivo multiphoton imaging of structural abnormalities in corneal stroma.

8209-02, Session 1

## In vivo assessment of the acute effect of sodium iodate toxicity on photoreceptor-RPE layer complex in a rat retinal model with UHROCT

S. Hariri, A. Akhlagh Moayed, Univ. of Waterloo (Canada); S. Boyd, Univ. of Toronto (Canada); K. Bizheva, Univ. of Waterloo (Canada)

A high speed, high resolution 1060nm SD-OCT system was used to image and quantify acute, time-varying changes in the rat retina morphology associated with administration of retinotoxin Sodium Iodate (NaIO3). Images acquired from the same location in the rat retina prior and post injection of NaIO3 show for the first time in-vivo progressive morphological changes (a low reflectivity band) in the photoreceptor-RPE complex over the first 12 hours post injection. It is hypothesized that the low reflectivity band corresponds to cell swelling or fluid influx between the retina and the choroid.

8209-03, Session 1

## Measurement of pulsatile total blood flow in the rat retina with ultrahigh-speed spectral/ Fourier domain OCT

W. J. Choi, Massachusetts Institute of Technology (United States); B. Baumann, Massachusetts Institute of Technology (United States) and Tufts Univ. (United States); A. C. Clermont, E. P. Feener, Joslin Diabetes Ctr., Harvard Medical School (United States); J. S. Duker, Tufts Medical Ctr. (United States); J. G. Fujimoto, Massachusetts Institute of Technology (United States)

We present a novel approach to measure total retinal arterial blood flow and pulsatility in rats using ultrahigh-speed Doppler OCT. The axial blood velocity is measured in an en-face plane by scanning a raster pattern, and the flow is calculated by integrating over the vessel area. This avoids the need to measure the Doppler angle. Since flow is measured in the central retinal artery, the area of scanning can be extremely small. Combined with ultrahigh-speed, this approach enables high volume acquisition rates necessary for pulsatile total flow measurement without any modification in the OCT system optics. Since the normal heart rate in rats is about 4 times faster than in humans and the axial blood velocity in the central retinal artery is very fast, an OCT system with high axial scan rate is desired to avoid phase wrapping. An ultrahigh-speed spectral / Fourier domain OCT system at 840nm with an axial scan rate of 244kHz was developed. At 244kHz the nominal axial velocity range that could be measured without phase wrapping was +/-37.7mm/s. However, because only the central retinal artery was measured, the maximum axial velocity that could be unwrapped without ambiguity was 75.4mm/s. By repeatedly scanning a small area centered at the central retinal artery with high volume acquisition rates, pulsatile flow characteristics, such as systolic, diastolic, and mean total flow values, were measured. Measurements can be entirely automatic as only the central retinal artery is used for calculation. This method should be useful for investigation of small animal models of ocular diseases.

8209-04, Session 1

## Effects of intraocular pressure on retinal and optic nerve head blood flow in rats determined by optical coherence tomography/optical microangiography

Z. Zhi, Univ. of Washington (United States); W. Cepurna, E. Johnson, J. Morrison, Oregon Health & Science Univ. (United States); R. Wang, Univ. of Washington (United States)

Perfusion of the retina, choroid and optic nerve head (ONH) is critical to the development and progression of various ocular diseases, including glaucoma. Hence, the development of non-invasive methods for assessing blood flow of these structures is important for both patient care and research. As a variation of Spectral-domain optical coherence tomography (SDOCT), Optical microangiography (OMAG) is capable of generating 3D dynamic perfusion images of tissue microcirculation. When combined with phase-resolved analysis method, it produces Doppler OMAG (D-OMAG) for quantitative and directional blood flow imaging. Recently, it was refined into ultra-high sensitive OMAG (UHS-OMAG) with the capability of imaging capillary vessels down to 4 μm/s level. The combined use of D-OMAG and UHS-OMAG to provide simultaneous 3D angiography and quantitative measurement of blood flow in rat retinal blood vessels has recently been described. In this study, we present the first use of 1300 nm light source OMAG for imaging rodent eye with enhanced penetration depth. Reduction of ocular blood flow caused by elevated intraocular pressure (IOP) may contribute to the glaucoma progression. Hence, we applied OMAG to image and measure the effect of acute IOP elevation on retinal and optic nerve head (ONH) perfusion in the rat eye. We demonstrate the ability of OMAG to image the vascular anatomy of the rat retina, ONH and surrounding choroid and demonstrate the effects of acutely elevated IOP on this anatomy. Quantitative measurements of the effect of elevated IOP on rat retinal vasculature and ONH perfusion as determined by this technique are presented.

8209-05, Session 1

## Ultrahigh-speed swept-source/Fourier-domain OCT imaging of the rodent retinal structure and blood flow

J. J. Liu, Massachusetts Institute of Technology (United States); B. Baumann, Massachusetts Institute of Technology (United States) and Tufts Univ. (United States); B. M. Potsaid, Massachusetts Institute of Technology (United States) and Thorlabs, Inc. (United States); M. F. Kraus, Massachusetts Institute of Technology (United States) and Friedrich-Alexander-Univ. Erlangen-Nürnberg (Germany); I. Grulkowski, Massachusetts Institute of Technology (United States) and Nicolaus Copernicus Univ. (Poland); A. C. Clermont, E. P. Feener, Harvard Medical School (United States); J. Hornegger, Friedrich-Alexander-Univ. Erlangen-Nürnberg (Germany); J. S. Duker, Tufts Medical Ctr. (United States); J. G. Fujimoto, Massachusetts Institute of Technology (United States)

Recent advances in swept-source / Fourier domain OCT technology enables in vivo ultrahigh speed 3D imaging, offering a promising technique for rat and mouse retinal imaging. We performed imaging of the rodent retina at 100,000 axial scans per second with ~5 μm resolution using ultrahigh speed swept-source / Fourier domain OCT technology. Three-dimensional OCT (3D-OCT) data sets are acquired. Imaging at 1050nm wavelengths provides enhanced penetration into ocular structures. Ultrahigh speed imaging enables high pixel density 3D-OCT data with minimal eye motion artifacts. Image processing methods such as image registration can reduce residual motion artifacts and improve signal to noise ratio. The ultrahigh speed axial scan rate enables detection of high flow velocities. Doppler OCT provides non-invasive in vivo quantitative measurements of retinal blood flow properties and may benefit studies of diseases such as glaucoma and diabetic retinopathy. We demonstrated detailed visualization and quantification of retinal structure and blood flow, which can allow repeated non-invasive measurements to track disease progression. Ultrahigh speed imaging using swept-source / Fourier domain OCT promises to enable novel protocols for measuring small animal retinal structure and physiology. Furthermore, this non-invasive imaging technology is a promising tool for monitoring disease progression in rat and mouse models to characterize ocular disease pathogenesis and response to treatment.

8209-06, Session 1

## In vivo quantification of microglia dynamics with a scanning laser ophthalmoscope in a mouse model of focal laser injury

C. Alt, C. P. Lin, Wellman Ctr. for Photomedicine (United States)

Microglia are the resident immune cells of the central nervous system and play a crucial role in maintaining neuronal health and function. Their dynamic behavior, that is, the constant extension and retraction of microglia processes, is thought to be critical for communication between microglia and their cellular neighbors, such as neurons, astrocytes and endothelial cells of the vasculature. Here, we investigate the dynamics of retinal microglia in vivo under normal conditions and in response to focal laser injury of blood vessel endothelial wall.

We have developed a scanning laser ophthalmoscope specifically for mouse retinal imaging that allows retinal microstructure, such as the processes of microglia and retinal vasculature, to be visualized. In order to generate focal laser injury, a laser photocoagulator was adapted to the SLO. An acousto-optic modulator chopped pulses from a continuous wave laser. A tip-tilt-scanner was used to direct the laser beam into a blood vessel of interest under SLO image guidance. Mild coagulation was produced using millisecond-long pulses.

Microglia react dynamically to focal laser injury of blood vessel endothelial walls. Under normal conditions, microglia soma remain stationary and the processes probe a territory of their immediate environment. In response to local injury, process movement velocity approximately doubles and amplitude increases several fold within minutes after injury. Moreover, the previously unpolarized process movement assumes a distinct directionality towards the injury site, indicating signaling between the injured endothelial cells and the microglia. In vivo retinal imaging is a crucial tool for understanding the dynamic behavior of retinal cells.

8209-07, Session 2

## A new principle for remote continuous monitoring of intraocular pressure variations

I. Margalit, Y. Beiderman, Bar-Ilan Univ. (Israel); A. Skaat, M. Belkin, Tel Aviv Univ. Goldshleger Eye Research Institute (Israel); R. Tornow, Universitätsklinikum Erlangen (Germany); V. M. Vicente Mico, J. Garcia, Univ. de València (Spain); Z. Zalevsky, Bar-Ilan Univ. (Israel)

Purpose: We demonstrate a new principle and technology for high-precision, non-contact remote measurement and continuous monitoring of intra-ocular pressure (IOP).

Methods: A photonic device comprising of a laser, a fast camera and a computer was tested on rabbit's eyes for continuous remote monitoring of the IOP. The device is based on recording and analysing the secondary speckle patterns trajectories produced by reflection of an illuminating laser beam from the iris or the sclera. To verify the working principle of the device, the rabbits' IOP was varied by elevating or lowering an infusion bag connected by a needle inserted into the vitreous cavity. The IOP variations changes the speckle distributions reflected from the rabbit's iris or sclera, both tissues serving as a transducer element of the sensing system.

Results: The alterations in the speckle patterns induced by varying the infusion bag's altitude were recorded and analysed. These data showed a good correlation and sensitivity in relation to the bag's altitude and hence presumably with the IOP (5% estimated error) for the best experimental configuration.

Conclusions: We have presented the first demonstration of a new photonic device have been performed on rabbits and which is indicating that laser speckle analysis may become an inexpensive technology for precise non-contact measuring and monitoring IOP.

8209-08, Session 2

## Image diversity, shape modification with accommodation, dynamical change with accommodation, and age dependence of the ciliary body imaged by optical coherence tomography

K. Shimizu, N. Satou, A. Igarashi, M. Nakanishi, Kitasato Univ. (Japan); A. Goto, Canon Inc. (Japan); D. Choi, R. Yoshimura, H. Hiro-Oka, H. Furukawa, Kitasato Univ. (Japan); K. Ohbayashi, Kitasato Univ. School of Medicine (Japan)

For investigation of accommodation and presbyopia, we imaged the ciliary body and its dynamics with OCT. We used a discretely-swept frequency-comb SS-OCT system operating in the wavelength region 1561 nm - 1639 nm lasers. Extensive measurements of the ciliary body of volunteer Asian's natural eyes have been carried out. In the case of a subject with an implantable contact lens (ICL), the surface of the ICL was clearly imaged, verifying the support by the ciliary sulcus. We demonstrate "diversity" of ciliary body OCT images. A series of 22 cross-sections of the ciliary body separated by 0.18 mm was imaged. For the case of subject was 39 years old male subjects, typical ciliary body OCT images with distinct closed boundary were observed as well as images which have no clear enclosure boundary. The image diversity and its relation to ciliary body anatomy shall be discussed. For observation of modification due to accommodation change, measurements were done in the dark asking a subject to gaze illuminated fixation targets placed at near and far distances. For a subject of 29 years old male, the thick ciliary body and elongated iris were observed under accommodation. Under the relaxed state, the remarkable thinning of the ciliary body and shortening of the iris were confirmed. On the contrary, for a volunteer subject of 79 years old male, no substantial change of the ciliary body thickness was observed. Dynamical changes of the ciliary body modification were video imaged. Both directions between accommodation and relaxation were imaged at a rate of 0.1 frames per second. Movies shall be shown.

8209-09, Session 2

## Volumetric ocular anterior segment biometry using OCT registration and refraction correction techniques

I. Grulkowski, Massachusetts Institute of Technology (United States) and Nicolaus Copernicus Univ. (Poland); M. F. Kraus, Friedrich-Alexander-Univ. Erlangen-Nürnberg (Germany) and Massachusetts Institute of Technology (United States); B. Potsaid, Massachusetts Institute of Technology (United States) and Thorlabs Inc. (United States); B. Baumann, Massachusetts Institute of Technology (United States) and Tufts Univ. (United States); D. Huang, Oregon Health & Science Univ. (United States); J. Hornegger, Friedrich-Alexander-Univ. Erlangen-Nürnberg (Germany); J. G. Fujimoto, Massachusetts Institute of Technology (United States)

Optical coherence tomography (OCT) can provide depth-resolved images of anatomical features of the anterior segment of the eye with a resolution of a few microns. Ophthalmic biometry is useful in diagnosis of corneal diseases as well as monitoring surgical outcome. However, reliable OCT based ocular biometry suffers from optical distortions due to light refraction and motion artifacts. We show that the latter can be minimized using 3-D motion correction and registration techniques. In our approach, two or more 3-D volumes with orthogonal orientation of the fast scanning axis are acquired, and multiple motion corrected 3-D datasets can be merged to improve signal-to-noise ratio and image quality.

We demonstrate measurement of ocular biometric parameters of the anterior eye using 3-D OCT motion corrected data and 3-D refraction correction algorithms. A dewarping algorithm based on three-dimensional ray tracing was developed. Custom automated software enabled generating thickness and surface maps such as: topography, pachymetry, elevation, mean curvature and power. Results acquired using raster scan pattern and registration technique were compared, and repeatability was assessed.

To conclude, raster scanning and 3-D data motion correction combined with ocular biometry software which corrects for refractive distortion enables accurate and comprehensive anterior segment mapping. Access to 3-D ophthalmic biometric data of the anterior eye promises more sensitive detection of central and peripheral abnormalities in the anterior segment.

8209-10, Session 2

## Quantitative corneal refractive power measurements utilizing distributed scanning SDOCT

R. P. McNabb, F. LaRocca, S. Farsiu, A. N. Kuo, J. A. Izatt, Duke Univ. (United States)

Corneal keratometry and topography are currently the primary methods for clinically assessing corneal shape. These placido ring-based methods accurately measure the curvature of the anterior surface of the cornea while calculating the total power of the cornea by assuming a constant ratio between the anterior and posterior surfaces of the cornea. This power calculation fails however when the ratio between surfaces can no longer be considered constant, notably in subjects who have undergone laser refractive surgery. Spectral domain optical coherence tomography (SDOCT) could potentially overcome this limitation by offering the capability to acquire full tomographic information of both anterior and posterior surfaces. A major limitation, however, is the corruption of data by low spatial frequency subject motion during the time required to obtain a volumetric image. We have developed a novel scanning approach based on the spatial distribution of individual A-scans across the cornea during a volume acquisition, thus encoding subject motion into high spatial frequencies which are then removed by spatial filtering. We report on a preliminary patient study comparing the measured anterior and posterior corneal curvature and the calculated corneal power acquired using distributed scanning OCT (DSOCT) to both corneal topography and Scheimpflug photography in normal subjects. The repeatability for the measured radius of curvature of both anterior and posterior surfaces using DSOCT was comparable to those of both topography and Scheimpflug photography. The calculated power repeatability variability was comparable to the 0.25D resolution of clinical refraction.

8209-11, Session 2

## Design and validation of a quasi real-time global aberrometer: the EyeMapper

C. Fedtke, K. Ehrmann, D. Falk, B. Holden, Brien Holden Vision Institute (Australia)

Since the discovery that peripheral refraction can influence eye growth, its fast and accurate measurement has become of considerable relevance. Based on the aberrometry principle, a new clinical instrument, the EyeMapper, was developed that performs quasi real-time global refraction measurements of the human eye.

This paper focuses on the optical and mechanical design of the EyeMapper and its validation. ZEMAX design software (Zemax Development Corporation) was used for the optical design and the tolerancing analysis. CAD Software (SolidWorks Dassault Systèmes SolidWorks Corporation) was employed for the mechanical instrument design. The optical design consists of five optical sub-systems. The most distinctive sub-system is the deflection system, which permits rapid measurements (0.6s) by steering the interrogation beam across the visual field, ranging from -50° to +50° in 10° steps. Other features of the EyeMapper are the pupil imaging paths through the deflection system, providing pupil images from different observation angles for improved lateral and axial pupil alignment and a movable fixation target determining the accommodation stimulus response function. The entire optical system can be rotated around its main optical axis to provide three dimensional power maps of the eye.

The EyeMapper was cross-validated against a conventional aberrometer and an autorefractor using two methods. Firstly, a physical model eye with a pivoting and translating reflective surface, simulating the peripheral and central retina, was measured. Secondly, the right eyes of 10 participants were measured across the horizontal meridian. Overall, the EyeMapper showed good agreement and improved repeatability when compared to the two other instruments.

8209-12, Session 3

## Biological engineering of retinal disease: needs for technology

R. Ali, Univ. College London (United Kingdom)

No abstract available

8209-13, Session 4

## The effect of (micro-) saccades on the image quality of ultrawide-field multimegahertz OCT data

T. Klein, W. Wieser, R. J. André, C. M. Eigenwillig, R. Huber, Ludwig-Maximilians-Univ. München (Germany)

Involuntary eye motion during fixation directly affects OCT datasets. Hence, the total acquisition time is usually restricted such that the probability of undistorted images is sufficiently high. For this reason, the fundus area covered by retinal OCT is either sparsely sampled or it is small compared to standard clinical imaging modalities such as fundus cameras and scanning laser ophthalmoscopes. With the advent of MHz Fourier domain mode-locked (FDML) lasers operating in the 1050nm wavelength range, densely sampled three-dimensional tomograms over 70° external field of view have been acquired within a few seconds. We analyzed ~50 three-dimensional OCT datasets acquired at 684kHz and 1.37MHz line rate and observed a significant probability for motion artifacts in the en-face projections. Nevertheless, the line rate is approaching a regime where most motion artifacts can be corrected in post-processing. For example, our recently implemented 6.4MHz system has an angular scan speed of 150°/s for the slow axis. This is higher than the 100°/s of the fastest microsaccades - thus dense sampling is always maintained. Hence, in contrast to slower systems, no information is lost, even in the case of fastest eye motion during data acquisition. Additionally, due to the high speed, large datasets can be acquired faster than the average time between two microsaccades. We will discuss various motion correction approaches that benefit from these high line rates.

8209-14, Session 4

## Heartbeat phase-coherent Doppler optical coherence tomography

T. Schmoll, R. A. Leitgeb, Medizinische Univ. Wien (Austria)

We equipped a Doppler OCT (DOCT) system with a pulse-oximeter and acquired multiple DOCT volumes, while recording the pulse synchronously. Information of the pulse phase was used to recombine tomograms in order to receive pulse phase coherent DOCT volumes. These volumes were used to evaluate the blood flow within individual vessels, as well as the total retinal blood flow over a full heart beat cycle. We believe that such quantitative information of retinal blood flow and the ability to monitor dynamic processes over time holds great potential to gain a better understanding of retinal physiology and patho-physiology in-vivo.

8209-15, Session 4

## Feature-based registration of cone photoreceptor images from AO-OCT volumes using iterative Delaunay triangulation

S. Lee, O. P. Kocaoglu, R. S. Jonnal, Q. Wang, D. T. Miller, Indiana Univ. (United States)

Cone photoreceptors are the most imaged cell in the living retina with adaptive optics (AO) retina cameras. While successful, a continuing bottleneck remains the registration of cone images acquired at different times. Cone registration typically requires identification of thousands of individual cones, each essentially identical in appearance, yet uniquely distorted by eye motion. Eye motion artifacts are particularly problematic for scanning systems such as optical coherence tomography (OCT). Intensity-based registration methods, which most commonly incorporate cross-correlation similarity metrics, have been applied successfully to cone registration. However, the linearity in these block-based matching schemes is not well suited for correction of high-order motion artifacts that can be present in cone images, especially OCT images. As an alternative approach, we propose a novel feature-based algorithm that is tailored to registering cone images acquired with an OCT system that incorporates adaptive optics. For this approach, cone centers in en face view are automatically detected using customized spatial and spectral filters followed by morphological operations. With feature points comprised of cone centers, Delaunay triangles are iteratively built to associate neighboring cones. Thin-plate-spline is then applied to register each cone based on its local image coordinates.

8209-16, Session 4

## Automatic segmentation of closed-contour features in ocular images using graph theory and dynamic programming

S. J. Chiu, A. Mittal, C. Bowes Rickman, C. A. Toth, J. A. Izatt, S. Farsiu, Duke Univ. (United States)

We previously developed a generalized framework based on graph theory and dynamic programming (GTDP) to segment layered structures in ocular SDOCT images. However, aside from layered structures, there is a need for automatically segmenting closed-contour features in ophthalmic images, such as cysts seen on retinal SDOCT images. In this work, we present an extension of our generalized GTDP framework for segmenting closed-contour ocular features. Our algorithm is based on the observation that with an appropriate transform, closed-contour features in the Cartesian domain are represented as lines in a pseudo-polar domain. While a simple polar transform is suffice to map a circle into a line, the pseudo-polar transform includes an extra flattening step required to map general closed-contour shapes into lines. The parameters for flattening can be attained from a pilot estimate of the feature of interest. Once the closed-contour feature is flattened, our previous GTDP method is used to segment the object as if it were a layered structure. Finally, we apply an inverse transform to map the segmented line into the Cartesian domain. To improve upon segmentation accuracy, we have included an additional sparse representation-based image enhancement step, which further separates the anatomy of interest from noise and outliers. Preliminary results attest to the effectiveness of the proposed technique to segment cystoid spaces seen on SDOCT images of pediatric retina and RPE cells seen on confocal fluorescence microscopy images of flat-mounted retina.

8209-17, Session 4

## Automated detection and counting of keratocytes in human corneal stroma from ultrahigh-resolution optical coherence tomograms

A. Karimi, A. Wong, K. Bizheva, Univ. of Waterloo (Canada)

A novel approach to automatic detection and counting of keratocyte cells from UHROCT images of the human cornea acquired in-vivo is presented. The method utilizes despeckling and thresholding followed by second order moment analysis to identify the highly reflective features in corneal stroma that most likely correspond to reflections from keratocyte nuclei. Cell density distribution analysis carried on a number of 3D volumes of corneal OCT images showed increased cell density in the anterior stroma and almost constant density in the mid and posterior stroma. These results correlate very well with previous research conducted with confocal microscopy.

8209-18, Session 4

## Spatial dewarping of ocular posterior segment SDOCT data

A. N. Kuo, R. P. McNabb, C. A. Toth, J. A. Izatt, Duke Univ. (United States)

SDOCT data is conventionally displayed in a rectangular form inconsistent with the geometry of posterior segment SDOCT scanning; this inconsistency could in turn affect quantitative morphometric analysis of features in the images. To better reflect actual posterior segment morphology, we developed algorithms to de-warp adult retinal SDOCT images based on models of posterior segment scanning geometry.

Two algorithms were developed for retinal image dewarping: a simple analytical and a more rigorous, ray-traced numerical algorithm. In both algorithms, ocular biometry data (corneal curvatures, anterior chamber depth, and axial lengths) were used to customize the models for the imaged subject.

After dewarping with the algorithms, posterior segment images appeared fan shaped consistent with posterior segment scanning geometry. As a general measure of morphology across the image, retinal curvature values from the dewarped images were closer to expected values. In contrast, the original retinal images were flatter than expected values by an order of magnitude.

Interestingly, results from the simpler analytical algorithm compared favorably with those from the more rigorous numerical algorithm. The analytical algorithm requires far less information about the SDOCT system and can be broadly applied to any system if the scan width and minimal ocular biometric data are known.

These algorithms provide the basis for more accurate clinical morphometric analyses of imaged posterior segment structures, particularly metrics reliant on the true spatial morphology across the image such as curvature and topography of surfaces.

8209-19, Session 5

## Visualization of parafoveal capillary network by high-speed swept source optical coherence tomography with volumetric registration and averaging

Z. Wang, Z. Yuan, C. Reisman, Q. Yang, C. Chang, K. Chan, Topcon Medical Systems, Inc. (United States)

As a potential indicator for early diagnosis of several retinal diseases, such as diabetes, the parafoveal capillary network has attracted much research attention. While recent developments in adaptive optics OCT, ultrahigh sensitive optical microangiography, and ultrahigh resolution OCT have enabled the visualization of capillary network, the observation of microscopic structure can be adversely affected by motion artifacts which cause blurring, and speckle noise that degrades the image contrast. As a way for improvement, we have developed a post processing technique that combines a volume registration and averaging method with an automatic layer segmentation algorithm to render the capillary network. In the present feasibility study, up to 5 volumes (256x256x885 voxels) acquired with a high-speed (100KHz) 1050nm swept source OCT prototype were registered and averaged. Each B-frame of the averaged volume was then segmented with an automated dual-scale segmentation algorithm to extract a thin layer of approximately 10um at the INL/OPL boundary to create a projection image that portrays the capillary network. Our preliminary study with healthy subject eyes showed that the capillary network could be visualized across the entire field of view (3x3 mm2). With the recent availability of ultra-high speed OCT, the present volumetric registration and averaging technique may provide a promising method to acquire high quality volumetric OCT images for the observation of microscopic structures.

8209-20, Session 5

## Flow velocity assessment in retinal microvasculature with joint spectral and time domain OCT

I. M. Gorczynska, D. Ruminski, M. Szkulmowski, D. Szlag, M. Sylwestrzak, A. A. Kowalczyk, M. D. Wojtkowski, Nicolaus Copernicus Univ. (Poland)

We have developed a method allowing for quantitative assessment of blood flow in retinal microvasculature. This technique uses segmented scanning of the object implemented with a fast oscillating mirror introduced to the sample arm of a spectral/Fourier domain OCT apparatus. Joint Spectral and Time domain OCT method is used to simultaneously generate structural and flow images. The method utilizes Doppler frequency shifts detection to assess the axial component of the flow velocity. We will demonstrate application of the slow flow measurement method to two- and three-dimensional quantitative imaging of blood flow in the retinal microvasculature. We will compare the results with qualitative imaging of retinal capillaries utilizing intensity variation analysis methods.

8209-21, Session 5

## Choroidal imaging by one-micrometer dual-beam Doppler optical coherence angiography with adjustable velocity range

F. Jaillon, S. Makita, Y. Yasuno, Univ. of Tsukuba (Japan)

Optical coherence tomography has proven in the last two decades its clinical value for imaging the eye by providing 3D non-invasive in vivo biopsy of the anterior eye segment and retina. OCT provides structural information given by the backscattered intensity, and it also gives access to flow information using Doppler signal. One micrometer wavelength has enabled this technique to probe deeper into the choroid. Exploring the choroid is essential since early stages of many retinal pathologies, such as age related macular degeneration (AMD) and central serous chorioretinopathy (CSC), are associated with the abnormalities of choroidal circulation. Imaging techniques providing early detection of these abnormalities are thus necessary to dispense efficient treatments. Conventional technique to retrieve vasculature structure is done by phase-resolved Doppler method. One drawback of phase-resolved Doppler technique is that as the acquisition rate is increased, the flow sensitivity is diminished. Therefore vessels with low velocity are not measurable. We therefore present one-micrometer dual-beam optical coherence angiography (OCA) for choroidal vasculature imaging. The two probing beams are utilized to enhance the flow sensitivity. A particular feature of this system is the adjustable time delay between the two probe beams. This allows changing the measurable velocity range of moving constituents such as blood without alteration of the scanning protocol. It is shown that acquiring images with different velocity ranges, in other words with different beam separations, provides a more complete vasculature representation. This method may be valuable for pathological choroid characterization.

8209-22, Session 5

## Using ultrahigh sensitive optical microangiography to achieve comprehensive depth-resolved microvasculature mapping for human retina

L. An, Univ. of Washington (United States)

This paper presents comprehensive and depth-resolved retinal microvasculature images within human retina achieved by a newly developed ultrahigh sensitive optical microangiography (UHS-OMAG) system. Due to its high flow sensitivity, UHS-OMAG is much more sensitive to tissue motion due to the involuntary movement of human eye and head compared to the traditional OMAG system. To mitigate the motion induced artifacts on final imaging results, we propose a new phase compensation algorithm in which the traditional phase-compensation algorithm is repeatedly used to efficiently minimize the motion artifacts. Comparatively, this new algorithm demonstrates at least 8 to 25 times higher the motion tolerability, critical for the UHS-OMAG system to achieve retinal microvasculature images with high quality. Furthermore, the new UHS-OMAG system employs a high speed line scan CMOS camera to capture 500 A-lines for one B-frame at 400 Hz frame rate. With this system, we performed a series of in vivo experiments to visualize the retinal microvasculature in humans. Two featured imaging protocols are utilized. The first is of the low lateral resolution and a wide field of view , whilst the second is of the high lateral resolutionand a narrow field of view (1.5×1.2 mm2 with single scan). The great imaging performance delivered by the proposed system suggests that UHS-OMAG promises a useful alternative for retinal microvasculature imaging in the clinical diagnosis of vision diseases that have vascular involvement, for example diabetic retinopathy and age-related macular degeneration.

8209-23, Session 5

## Differential intensity contrast swept source optical coherence tomography for human retinal and choroidal vasculature visualization

R. Motaghiannezam, S. E. Fraser, California Institute of Technology (United States)

The importance of retinal and choroidal vasculature visualization is inevitable in diagnosing various eye diseases. Color fundus photography and fluorescein angiography have served as the gold standard methods for retinal vasculature network visualization. Deeper choroidal vessels imagining has also been realized by Indocyanine green angiography. However, the 2-D nature of these imaging techniques limits their applications for providing depth information and/or deep choroidal blood vessels visualization. To meet the need for 3D retinal and choroidal vasculature assessment without the use of fluorescent dye injection, Doppler optical coherence tomography (D-OCT) and phase contrast (PC)-OCT have been proposed as motion sensitive methods. However, D-OCT and PC-OCT are sensitive to phase instability of the system and environment by relying on the phase information. Thus, there is a need for OCT methods which do not rely on the phase information and highlights only motion with the required sensitivity through the retina and choroid for microvasculature visualization.

To exploit deep penetration, superior sensitivity in depth, and less reliance on the phase stability of the system and environment, we extend the swept-source OCT to human retinal/choroidal vasculature imaging at 1060 nm by capturing differential intensity variance (DIV) data from not only the retina but the inner choroid as well. The vasculature was identified as regions of motion by creating DIV tomograms: multiple B-scans of individual slices through the retina were collected and the variance of the intensity differences was calculated. DIV captured the small vessels and the meshwork of capillaries associated with different inner retina layers in en face images over 4 mm2 without the need for phase information and compensation algorithm. To depict regions of motion in the choroid, the depth-integrated DIV en face images were generated by summing DIVs over 25 micrometers thickness located at the inner choroid. Results of DIV and differential phase variance (DPV) methods were also compared for foveal avascular zone (FAZ) visualization.

8209-24, Session 5

## Investigation of exudative macular diseases by high-penetration Doppler optical coherence angiography

Y. Hong, S. Makita, Univ. of Tsukuba (Japan); M. Ju, B. Lee, Gwangju Institute of Science and Technology (Korea, Republic of); M. Miura, Tokyo Medical Univ. (Japan); Y. Yasuno, Univ. of Tsukuba (Japan)

High-penetration Doppler optical coherence angiography (HP-D-OCA) was developed based on 1-μm swept-source optical coherence tomography (SS-OCT), in order to substitute conventional invasive angiographic modality, indocyanine green angiography (ICGA).

For the correct Doppler shift frequency estimation, phase error induced by random spectral shift of SS-OCT is numerically canceled. Phase difference between an A-line which is under the spectral-shift compensation and a reference A-line is obtained. The differentiated phase of a signal close to the zero-delay, which is mainly created from reference beam, would possess a phase slope, and this phase slope is equivalent to the amount of the spectral shift relative to the reference A-line. Linear fitting with weights proportional to the signal intensity is applied to obtain the phase slope. Then phase difference by spectral shift of entire spectrum is compensated by multiplying the inverted phase slope. Succeeded inverse Fourier transform yields spectral-shift compensated spectrum. Standard Fourier domain OCT processing is then applied to obtain a phase-stabilized OCT image, and phase difference between adjacent A-lines is calculated for the Doppler OCT image.

Choroidal vasculature and bidirectional blood flow images of three eyes of 3 cases of polypoidal choroidal vasculopathy (PCV) and 1 eye of 1 case of type-2 choroidal neovascularization (CNV) were examined by HP-D-OCA and compared with ICGA images. Abnormal choroidal vaseculature and blood flow were identified from the depth resolved cross-sectional OCT and Doppler OCT images. Good agreement of vasculature including abnormal choroidal vessels between ICGA and Doppler imaging is observed.

8209-25, Session 5

## Ultrahigh-speed wide-field angiography

C. Blatter, T. Schmoll, Medizinische Univ. Wien (Austria); T. Klein, W. Wieser, C. M. Eigenwillig, R. Huber, Ludwig-Maximilians-Univ. München (Germany); R. Leitgeb, Medizinische Univ. Wien (Austria)

Assessment of the retinal and choroidal vascularisations is of important diagnostic benefit for ocular diseases such as age-related macular degeneration. The current gold standard for their visualization is fluorescein angiography. We present a potential non-invasive alternative to image blood vessels based on functional Fourier Domain OCT. Speckle variance is a technique for imaging vascularisation by calculating changes between successive intensity tomograms. High lateral sampling is required to obtain good contrast between flow and static tissue. For OCT to compete with the field of view and resolution of angiography, ultrahigh-speed imaging has to be introduced. Moreover, to reduce motion artifacts to a minimum and to improve the patient comfort, the acquisition time has to be restricted to a few seconds. We employ Fourier domain mode locking (FDML) swept source technology that offers high quality imaging at an unprecedented A-scan rate of up to 1.4 MHz. We present visualization of retinal vascularisation over large field of view as large as 30° acquired in a few seconds. The use of up to 1.4MHz A-Scan rate allows for single recording of the full field of view without the need of image stitching. High lateral sampling is maintained which permits resolving the vessel network down to the capillary level.

8209-26, Session 6

## Swept source OCT with air puff chamber for corneal dynamics measurements

K. M. Karnowski, Nicolaus Copernicus Univ. (Poland); D. Alonso-Caneiro, Nicolaus Copernicus Univ. (Poland) and Queensland Univ. of Technology (Australia); B. J. Kaluzny, A. A. Kowalczyk, M. D. Wojtkowski, Nicolaus Copernicus Univ. (Poland)

We present a novel method and instrument for imaging and measurement of the human corneal dynamics during deformation induced by air stream. Swept source OCT setup combined with air puff system allows to collect multiple A-scans in time (M-scan) at the center of the air puff which induces cornea deformation. Dynamics behavior of the anterior and posterior corneal surfaces as well as anterior lens surface is observed. It is driven by the biomechanical properties of the cornea as and its intraocular pressure. A set of controlled clinical measurements are performed to shown potential applicability of the method to further understand the eye biomechanics and intraocular pressure measurements. Results for healthy eyes measured at baseline conditions and after IOP reducing treatment are compared to IOP changes measured with commercially available tonimeter. Closer look at displacement plots and its correlation with IOP changes and/or cornea biomechanical properties are presented. Limitations and possibilities of the new apparatus are discussed.

8209-27, Session 6

## Estimation of surface wave propagation in mouse cornea

R. K. Manapuram, F. M. Menodiado, P. Truong, K. V. Larin, Univ. of Houston (United States)

In this paper we report the capability of phase stabilized swept source optical coherence tomography (PhS-SSOCT) for real-time measurements of surface mechanical wave propagation in mouse cornea in-situ. The wave propagation was measured in the mice cornea of different ages attributing to the different stiffness. The measurements were performed by inducing very low amplitude cylindrical waves and measuring the wave amplitudes attenuation at spatially distributed points using a phase-sensitive analysis of OCT signals. Obtained results indicate that the damping of the wave amplitude was different in the mice cornea of different age (and presumably of different stiffness). Results also suggest that PhS-SSOCT is capable of measuring the changes in the wave amplitude as small as 0.03 μm that allowed the measurements with a very low amplitude excitation wave, thus making the method minimally invasive. Therefore, this method could potentially be used to assess tissue biomechanical properties and to reconstruct 3-D stiffness maps of the cornea.

8209-28, Session 6

## Spatially resolved Brillouin spectroscopy for in vivo determination of the biomechanical properties of the crystalline lens

O. Stachs, S. Reiss, R. F. Guthoff, H. Stolz, Univ. Rostock (Germany)

The confocal Brillouin spectroscopy is an innovative measurement method, which allows the non-invasive determination of the rheological properties of materials. Their application in ophthalmology offers the possibility to determine in vivo the deformation properties of sections of transparent biological tissue such as the cornea or the lens with spatial resolution. This seems to be a promising approach concerning the current presbyopia research. Due to the spatially resolved detection of the viscoelastic lens properties a better understanding of the natural aging process of the lens and the influences of different lens opacities on the stiffness is expected. From the obtained spectral data the relative protein levels, the relative refractive index profile and the relative density profile within the lens tissue can be derived additionally. A measurement setup for confocal Brillouin microscopy based on spectroscopic analysis of spontaneous Brillouin scattering signals by using a high-resolution dispersive device is presented. First in vitro test results on animal and human lenses and a first in vivo measurement are presented and evaluated concerning their rheological significance. The developed design already satisfies the requirements of the laser protection class 2, which are possible in vivo measurements on the human eye. Thereby it seems that in vivo measurements on the eye are possible.

8209-29, Session 6

## Quantitative RNFL attenuation coefficient measurements by RPE-normalized OCT data

K. A. Vermeer, Rotterdam Ophthalmic Institute (Netherlands); J. Van der Schoot, Rotterdam Ophthalmic Institute (Netherlands) and Rotterdam Eye Hospital (Netherlands); H. G. Lemij, Rotterdam Ophthalmic Institute (Netherlands); J. F. de Boer, Rotterdam Ophthalmic Institute (Netherlands) and Vrije Univ. Amsterdam (Netherlands)

We demonstrate significantly different scattering coefficients of the retinal nerve fiber layer (RNFL) between normal and glaucoma subjects. In clinical care, SD-OCT is routinely used to assess RNFL thickness for glaucoma management. In this way, the full OCT data set is conveniently reduced to an easy to interpret output, matching results from older (non-OCT) instruments. However, OCT provides more data, such as the signal strength itself, which is due to backscattering in the retinal layers. For quantitative analysis, this signal should be normalized to adjust for local differences in the intensity of the beam that reaches the retina. In this paper, we introduce a model that relates the OCT signal to the attenuation coefficient of the tissue. Our model incorporates the RNFL and the retinal pigment epithelium (RPE) and allows calculation of the RNFL attenuation coefficient by assuming constant RPE scattering properties. The resulting equation for the attenuation coefficient depends on the ratio of measured summed RNFL and RPE signals and on the thickness of the RNFL. Three-dimensional images of one eye of each of ten normal and eight glaucomatous subjects were acquired with a Spectralis OCT (Heidelberg Engineering, Germany) system. For every A-line, the attenuation coefficient was calculated according to the model, resulting in normalized RNFL attenuation coefficient maps. These maps showed local defects matching those found in thickness maps derived from the same OCT images. The average (normalized) RNFL attenuation coefficient of a fixed band around the optic nerve head was significantly lower in glaucomatous eyes than in normal eyes (3.0 mm-1 vs. 4.9 mm-1, $P<0.01$, Mann-Whitney test).

8209-30, Session 6

## Extraction of the optical attenuation coefficient of human corneal stroma from UHROCT tomograms

S. Zaboli, P. W. Fieguth, K. Bizheva, Univ. of Waterloo (Canada)

The optical clarity of the human cornea is indicative of its health and normal or abnormal function and could serve as a marker in studies of corneal pathologies. We propose an automated algorithm for the extraction of the optical attenuation coefficient of human corneal stroma from UHROCT tomograms. The algorithm corrects for the spatial variations in the image contrast induced by the corneal curvature, the imaging field curvature, and the focus of the imaging beam. The stromal attenuation coefficient is calculated using Beer-Lambert's law. Preliminary results show good correlation with previous studies using low resolution OCT or confocal microscopy.

8209-31, Session 6

## Does near infrared radation used for remote control, sensing and diagnotics cause cumulative damage in the lens?

P. G. Söderberg, Z. Yu, K. Galichanin, N. Talebizadeh, Uppsala Univ. (Sweden); K. Schulmeister, Seibersdorf Labor GmbH (Austria)

No abstract available

8209-32, Session 7

## Restorative retinal photocoagulation

D. V. Palanker, Y. M. Paulus, P. Huie, Stanford Univ. School of Medicine (United States); L. Leung, Stanford Univ. (United States); B. Jones, The Univ. of Utah (United States); A. Sher, Univ. of California, Santa Cruz (United States)

Retinal photocoagulation is an effective therapy for proliferative retinopathies and macular edema. However, the standard burns produce detrimental side effects such as scotomata, decreased night vision, and scarring that expands over time and leads to additional loss of visual field.

We have observed that in small lesions with selective coagulation of photoreceptors avoiding inner retinal damage the photoreceptors from adjacent untreated areas shift into the lesion over time, restoring continuity of the photoreceptor layer.

To verify whether migrating photoreceptors rewire to the local inner retinal neurons we applied two methods: electrophysiology using multielectrode array (MEA) and AGB marker of neural activity.

MEA recording from the retinal ganglion cells (RGCs) demonstrated that non-sensitive regions, corresponding to the lesions, significantly decreased at one week, and completely disappeared after 2 months in smaller (200um) lesions, while some scotomata over larger lesions (400um) remained. The number of responding RGCs above the lesions was initially reduced by approximately a factor of 3, and was restored to the original level after 2 months. AGB marker has demonstrated that signaling in the inner nuclear layer within 200um lesions was reduced 2 days after photocoagulation but was restored to normal level after 2 months. These results demonstrate for the first time a phenomenon of restorative retinal plasticity: rewiring of migrating photoreceptors to the inner retinal neurons restoring functional retinal circuitry. This process can significantly improve retinal laser therapy by avoiding its common detrimental side effects such as scotomata and scarring, especially important for treatment in the macula.

8209-33, Session 7

## Precise and fast creation of LASIK flaps with nanosecond laser pulses from a compact 150 kHz UV laser system

N. Linz, S. Freidank, S. Eckert, Univ. zu Lübeck (Germany); K. Schlott, Medizinisches Laserzentrum Lübeck GmbH (Germany); S. Faust, S. Schwed, SCHWIND eye-tech-solutions GmbH & Co. KG (Germany); A. Vogel, Univ. zu Lübeck (Germany)

We present a new technique of precise and rapid flap dissection in refractive surgery (LASIK) using a UV nanosecond microchip laser. The precision of cuts in porcine cornea performed by 355-nm, 1-µJ pulses is better than with IR femtosecond laser pulses focused at the same NA because focus diameter and length are only one third of the values at 1064 nm. The cutting speed at 150 kHz laser repetition rate is similar to that achieved with commercial state-of-the-art fs laser systems.

To optimize the novel technique, we investigated the quality of the flap cut and the corresponding cutting time for different parameter sets consisting of laser pulse energy, application patterns, and point to point distance of the individual laser spots. The minimum laser pulse energy required for an easy detachment of the flap was determined for each parameter set. A safety assessment was performed using ray tracing software and temperature calculations.

The compact UV microchip laser system emits laser pulses with a duration of 0.7 ns, 355 nm wavelength and 150 kHz repetition rate. The scanning optics produces a diffraction limited spot size (below 1 µm) in the cornea. LASIK flaps of 9.5 mm diameter with 90-130 µm thickness were produced in porcine cornea. During flap dissection, the central cornea was applanated by a removable suction device. The cutting pattern (spiral or meander) was documented by video. The cutting performance was evaluated by scanning-electron microscopy and histology.

The generation of the flap bed lasted less than 10 s. A homogeneous, smooth, and very thin bubble layer in the cornea was achieved at laser pulse energies below 1 µJ. The flaps could be lifted easily without any tissue bridges, and both the electron microscopy and histology show a smooth flap bed. Reproducibility of flap thickness is excellent. The radiant exposure for cutting the flap bed is below 2 J/cm$^2$, slightly better than for most fs LASIK systems. This value is well below the thresholds for photochemical damage of the retina, UV-induced cataract formation, and endothelial cell damage.

The cutting performance of the new UV nanosecond laser system surpasses the precision of current IR femtosecond laser systems with comparable laser pulse energies because of the shorter focus length that allows a cutting between or within individual cornea lamella. The scanning system allows for the cutting of flaps, lenticels and incisions for the insertion of intracorneal rings and implants.

8209-34, Session 7

## A miniature forward-imaging optical coherence tomography (OCT) probe

K. M. Joos, J. Shen, Vanderbilt Univ. (United States)

Purpose: Optical coherence tomography (OCT) has had a tremendous global health impact upon the current ability to diagnose, treat, and monitor multiple eye diseases. We propose that a miniature forward-imaging OCT probe can be developed for real-time ocular imaging.

Methods: A miniature 25-gauge forward-imaging probe was designed and developed to use with an 850 nm spectral-domain optical coherence tomography (SDOCT) system (Bioptigen, Inc. Durham, NC). Imaging parameters were determined. Ocular tissues were examined with the miniature OCT probe.

Results: A miniature SDOCT probe was developed with the scanning driver within the hand piece. The SDOCT fiber-scanning probe transmitted power of 800 µW. The scanning range was 3 mm when the probe tip was held 5 mm from the tissue surface. The axial resolution was 6 µm and the lateral resolution was 30-60 µm. The 25-gauge forward-imaging probe was used to image cellophane tape, eyelid skin, cornea, conjunctiva, sclera, iris, anterior lens, anterior chamber angle, retina, retinal tear, retinal detachment, optic nerve head, optic nerve sheath, and extraocular muscle. Images obtained from the miniature probe appeared similar to images from a 3 mm scanning range of a commercial large handheld OCT probe (Bioptigen, Inc. Durham, NC).

Conclusions: A miniature 25-gauge probe was developed that is capable of SDOCT forward-imaging within the eye. It has the future potential to guide real-time intraocular surgery.

8209-35, Session 7

## Intraoperative optical coherence tomography (iOCT) for ophthalmic surgery

M. Müller, UniversitaetsKlinikum Schleswig-Holstein (Germany); E. Lankenau, Opto Medical Technologies GmbH (Germany); P. Steven, UniversitaetsKlinikum Schleswig-Holstein (Germany); M. Krug, E. Acidereli, Opto Medical Technologies GmbH (Germany); S. Oelckers, Moeller-Wedel GmbH (Germany); S. Grisanti, UniversitaetsKlinikum Schleswig-Holstein (Germany); R. Birngruber, G. Hüttmann, Univ. zu Lübeck (Germany)

Optical coherence tomography (OCT) has become one of the main diagnostic options in ophthalmology. However, applications in OCT are not restricted to diagnosis. Coupled to a surgical microscope intraoperative OCT (iOCT) can visualize tissue structures during the surgical procedure.

A newly developed OCT camera which adapts to different surgical microscopes is presented. Central working wavelength is 840nm, depth range 5.2 mm and lateral field of view changes bewtween 5 mm and 30 mm depending on the magnification of the microscope. Lateral and depth resolution are better than 25 µm and 15 µm, respectively. The OCT camera works at an acquisition speed of 10000 A-scans/s. Optical pathlength and focus position are automatically corrected, when changing between anterior or posterior segment of the eye or when changing the magnification. For a clinical evaluation the OCT-camera was adapted to a MOELLER-WEDEL Hi-R 900 surgical microscope which was equipped with the MOELLER-WEDEL EIBOS.

The OCT-Camera enabled real-time OCT imaging of anterior and posterior segment surgery. Intraoperative images of different pathologies such as epiretinal membranes, macular holes and vitreomacular traction were possible with good quality. Cataract corneal incisions, trabeculectomy flap and corneal sutures are shown online. A pilot study with 9 patients demonstrated the possibility of simultaneously real-time OCT imaging of catheterization of Schlemm's canal. Preparation of Descemet's window was analyzed in real-time and reconstructed in 3D and 2D over time. Descemet's window could be visualized in high-resolution after surgical preparation.

Our results suggest that iOCT has the potential to become a new technological tool in different applications in ocular surgery

8209-36, Session 7

## Phase-resolved optical frequency-domain imaging for the evaluation of retinal pigment epithelium and choroid transplantation surgery

B. Braaf, E. J. T. van Zeeburg, K. A. Vermeer, V. A. D. P. Sicam, Rotterdam Ophthalmic Institute (Netherlands); J. C. van Meurs, The Rotterdam Eye Hospital (Netherlands); J. F. de Boer, Rotterdam Ophthalmic Institute (Netherlands)

Retinal pigment epithelium (RPE) and choroid transplantation surgery is used as a last resort to restore the vision of patients with exudative age-related macular degeneration (AMD). The success of this surgery is highly dependent on the survival of the transplanted tissues and therefore on revascularization and reperfusion occurrence. Phase-resolved optical frequency domain imaging (PR-OFDI) is a non-invasive optical technique to measure tissue perfusion with high resolution and is potentially an excellent tool to evaluate transplantation surgery. A high-speed (100 kHz) high-resolution (6.5 µm) OFDI system at 1-µm was developed to image the posterior segment of the human eye. A post-processing algorithm was implemented to resample all interference fringes to the exact same wavenumber space to obtain phase-resolved measurements. Bi-directional blood flow was detected by calculation of the difference in phase for subsequently measured A-lines with 86% beam-overlap. The blood perfusion of transplanted RPE and choroid tissues was imaged in an AMD patient six weeks after treatment. Blood flow was located within the transplanted tissue slab just below the RPE within several vessels. Intensity images show that this flow originates from a network of parallel vessels that is characteristic for the location where the transplanted tissue slab was obtained. The observed blood flow indicates (partial) reperfusion and gives therefore a good indication of successful surgery. This shows that PR-OFDI has the potential to evaluate transplantation surgery in the posterior segment of the human eye.

8209-37, Session 8

## Optimization of CSLO design

F. LaRocca, A. Dhalla, S. Farsiu, Duke Univ. (United States); J. A. Izatt, Duke Univ. (United States) and Bioptigen Inc. (United States)

The confocal scanning laser ophthalmoscope (CSLO) is an important imaging tool capable of producing high contrast images by raster scanning and detecting backscattered light through a confocal pinhole. One of the guiding principles behind the design of the CSLO is the inversion of the allocation of pupils, according to Gullstrand's principle. Conventional fundus cameras typically illuminate the retina only around a central pupillary collection aperture in order to eliminate unwanted corneal reflections. Alternatively, the CSLO illuminates the retina with a narrow collimated beam pivoting through the pupil plane. We describe a simple optical CLSO design optimized in ZEMAX to balance resolution and throughput while minimizing common imaging artifacts such as lens and corneal reflections. We follow through with an experimental setup from which we obtain high SNR retinal images demonstrating complete artifact removal. In addition, we investigate the relationship between retinal image sharpness and the times-diffraction-limited spot size. We obtained preliminary experimental results with trends confirmed by theoretical calculations.

8209-38, Session 8

## Ophthalmic OCT imaging with new ultrahigh-speed MEMS tunable VCSEL light source technology

B. M. Potsaid, Massachusetts Institute of Technology (United States); J. Y. Jiang, Thorlabs Inc. (United States); V. Jayaraman, Praevium Research, Inc. (United States); M. F. Kraus, Friedrich-Alexander-Univ. Erlangen-Nürnberg (Germany); D. Huang, Oregon Health & Science Univ. (United States); J. Hornegger, Friedrich-Alexander-Univ. Erlangen-Nürnberg (Germany); A. E. Cable, Thorlabs Inc. (United States); J. G. Fujimoto, Massachusetts Institute of Technology (United States)

This paper demonstrates new wavelength swept light source technology, MEMS tunable VCSELs, for ophthalmic OCT imaging. The VCSEL achieves a combination of ultrahigh sweep speeds, wide spectral tuning range and extremely long coherence length, which cannot be simultaneously achieved with other OCT light source technologies. The VCSEL can be driven to sweep at imaging speeds ranging from 100kHz to 1MHz over a 110nm range centered at ~1310nm. The micron-scale cavity length of the VCSEL enables single mode operation without mode hopping. Consequently, the coherence length of the laser is extremely long and has been measured to be much larger than 25mm in air. The OCT sensitivity roll-off vs. imaging depth performance with the VCSEL is far superior to other swept source laser technologies used in swept source OCT as well as in spectral / Fourier domain detection. We demonstrate imaging of the anterior eye in normal human subjects. Images obtained at 100kHz axial scan rate demonstrate a long imaging range extending from the cornea to beyond the posterior lens surface. Minimal motion artifacts are visible in dense 3D data sets and comprehensive structural information from the entire corneal surface, iris and crystalline lens is available, which promises to aid in diagnosing disease, as well as improving refractive surgery. Near term future work will also include demonstration of a prototype 1050nm VCSEL for retinal imaging. Results from this study suggest that VCSEL light source technology has unique and powerful advantages for the next generation of ophthalmic instrumentation.

8209-39, Session 8

## Comparison of MEMS-based handheld OCT scanner with commercial OCT system in corneal and retinal evaluation

S. I. Sayegh, EYE Ctr. (United States); W. Jung, Univ. of Illinois at Urbana-Champaign (United States); J. Kim, Kyungpook National Univ. (Korea, Republic of); D. T. McCormick, AdvancedMEMS (United States); Z. Hubler, E. J. Chaney, Univ. of Illinois at Urbana-Champaign (United States); C. N. Stewart, Blue Highway, LLC (United States); S. A. Boppart, Univ. of Illinois at Urbana-Champaign (United States)

Purpose: To discuss the imaging capability of a hand-held MEMS-based OCT scanner in evaluating the anterior and posterior segment of the eye for a variety of pathologies and following surgical interventions and compare its performance to that of a commercial system.

Methods: A handheld MEMS-based scanner developed to enable fast 3-D OCT imaging, along with co-registered video-based imaging is used. It is originally designed to be multifunctional and has interchangeable tips for tissue site specific imaging of the eye, ear, skin, and oral mucosa, a compact control unit, and a user-friendly interface. In this presentation we evaluate its performance and present results relating exclusively to eye imaging both in the anterior and posterior segments.

In the posterior segment we present cases of posterior uveitis, diabetic macular edema, neovascular membranes in macular degeneration and vitreomacular traction and epiretinal membranes both prior to and following surgical intervention. In the anterior segment we also present corneal imaging prior to and following LASIK surgery. Automatic segmentation using a fast three layer algorithm is also demonstrated.

Results: The performance and clinical value of the hand-held scanner is comparable to that of the commercial system.

Conclusion: It is desirable and often possible to obtain the relevant clinical information relating to the anterior and posterior segments in healthy and pathological states of the eye using a hand held portable OCT scanner.

8209-40, Session 8

## Extended depth optical coherence tomography with an optical switch for ocular biometry

M. Ruggeri, Bascom Palmer Eye Institute (United States) and Univ. of Miami (United States); C. De Freitas, S. Uhlhorn, Bascom Palmer Eye Institute (United States); F. Manns, Bascom Palmer Eye Institute (United States) and Univ. of Miami (United States); J. Parel, Bascom Palmer Eye Institute (United States) and Univ. of Miami (United States) and Vision Cooperative Research Ctr. (Australia)

Non-invasive imaging of ocular structures and quantitative assessment of biometric parameters is essential for diagnosis and treatment of disorders that affect the human eye. Fourier Domain OCT (FD-OCT) offers high axial resolution, high sensitivity, fast imaging speed and 3D imaging of ocular structures. The axial range of the current FD-OCT implementations must be extended if biometry of the human eye along its entire axial length, which is about 24mm, is required. We developed an SD-OCT system that obtains quantitative information of the entire eye by sequentially recording 3 frames that cover the anterior segment and the retina. The eye was imaged with 3 consecutive frames recorded at different depths that cover the anterior segment and the retina. Each frame had an axial length of 10mm (in air). An optical switching method was implemented to record the 3 frames. The switch uses a mirror mounted on a galvanometer scanner that rapidly switches the reference beam between 3 delay lines with calibrated optical path length difference, allowing the 3 frames to be recorded within 75ms. The 3 frames were precisely combined in a single OCT image and processed with a ray-tracing algorithm for correcting image distortions and obtain biometric information. This study demonstrates the feasibility of whole-eye biometry by acquiring multiple frames without the need for dynamic focusing. Combined with a distortion correction algorithm, the system provides measurements of the radius of curvature of the anterior and posterior surface of cornea and lens, intraocular distances and ocular axial length.

8209-41, Session 8

## High contrast, eye-tracked optical coherence tomography of retinal and choroidal pathologies at 800/1060 nm

B. Považay, Medizinische Univ. Wien (Austria); M. Esmaeelpour, Medizinische Univ. Wien (Austria) and Ludwig Boltzmann Institute for Retinology (Austria); C. Bloch, D. Fechtig, Medizinische Univ. Wien (Austria); I. Böttcher, Heidelberg Engineering GmbH (Germany); A. Unterhuber, B. Hofer, Medizinische Univ. Wien (Austria); S. Binder, Ludwig Boltzmann Institute for Retinology (Austria); R. Engelhardt, Heidelberg Engineering GmbH (Germany); W. Drexler, Medizinische Univ. Wien (Austria)

Following the success of motion stabilized high sensitivity optical coherence tomography (OCT) at the common 800 nm wavelength band a novel device is presented that alternatively combines standard or ultrahigh axial resolution (UHR) imaging at 880±27 nm/800±70 nm (<8/<3 µm) with enhanced penetration tomography at 1060 nm (70/110 nm, corresponding to <9/<5 µm). Hardware-based suppression of speckle and an extension of the dynamic range due to registration and averaging of multiple tracked exposures significantly improved the image quality of tomograms. Enhanced penetration through cataract as well as into the subretinal tissue of the choroid and sclera by 1060 nm technology can be well quantified and contrasted with the lower penetrating but higher resolving UHR OCT technology at 800 nm by acquisition of the signals at exactly equal imaging conditions. Spectral, penetration and contrast differences are compared and used as a means of contrast enhancement. The clinical significance of these methods is evaluated especially with diseases that deteriorate the transmissivity of the fundus, but also for mapping deeper choroidal vessels in emmetropic or hyperopic subjects, where the choroid usually obscures the structure of the bulbus formed by the rigid scleral shell. The analysis of a range of subjects with diabetic retinopathy, glaucoma and macular disease and the correlation is presented. With this technology it becomes possible to directly associate changes in the choroidal morphology with subtle structural modifications in the retina.

8209-42, Session 9

## Detection of inter- and intrafibrillar corneal stroma modifications by the analysis of polarization-modulated second-harmonic generation micrographs

F. Ratto, P. Matteini, Istituto di Fisica Applicata Nello Carrara (Italy); R. Cicchi, Univ. degli Studi di Firenze (Italy); F. Rossi, Istituto di Fisica Applicata Nello Carrara (Italy); D. Kapsokalyvas, F. S. Pavone, Univ. degli Studi di Firenze (Italy); R. Pini, Istituto di Fisica Applicata Nello Carrara (Italy)

The fibrillar order of certain connective tissues is vital for their biological function, as it happens in the case of the corneal stroma and its refractive properties. However the inter- and intra-fibrillar relationships behind this orderly architecture may become modified by circumstances such as e.g. thermal treatments and damages. Relevant examples of thermal treatments of the cornea include its laser bonding during e.g. penetrating keratoplasty, which proves superior to conventional suturing, especially when temperature is kept within 55-60°C. This range was found to induce functional fibrils misalignment and tissue adhesion, without collateral impairment of intra-fibrillar relationships such as collagen denaturation. Indeed collagen denaturation begins slightly above 60°C and may significantly delay the post-op recovery. Unfortunately the identification of ideal conditions, which is just below the onset of collagen denaturation, is hardly possible on visual inspection.

Here we propose the use of second harmonic generation (SHG) microscopy to investigate both the inter- and intra-fibrillar configuration of connective tissues with a regular architecture. Stacks of polarization-modulated SHG micrographs of corneal specimens were analyzed by an extension of the theoretical models from the recent literature. This extension holds potential for a complete three dimensional retrieval of the fibrils orientations and accounts for both the effective misalignment and inner conformation of the collagen molecules which contribute to the SHG signal intensity. Finally we discuss issues and future perspectives before the use of this approach for clinical applications such as the evaluation of thermal treatments of ophthalmic tissues.

8209-43, Session 9

## Ocular biometric factors affecting to scleral birefringence

M. Yamanari, Univ. of Tsukuba (Japan); S. Nagase, Tokyo Medical Univ. (Japan); S. Fukuda, K. Ishii, Y. Lim, Univ. of Tsukuba (Japan); M. Miura, Tokyo Medical Univ. (Japan); T. Oshika, Y. Yasuno, Univ. of Tsukuba (Japan)

Biomechanical property of sclera takes an important role for myopia and glaucoma. Previous studies have reported that the scleral biomechanics is likely related to the arrangement of collagen fiber bundles and diameter of collagen fibrils with microscopic observations ex vivo. Although these studies have relied on microscopic observations of sclera ex vivo, it has been difficult to investigate them in vivo. Since the birefringence of collagen fiber is assumably related to the scleral microscopic properties, polarization-sensitive optical coherence tomography (PS-OCT) is suitable for indirect investigation of scleral microstructure in vivo. We show our pilot study of birefringence measurement for healthy human eyes using PS-OCT and the relationship with standard ocular biometric parameters (spherical equivalent, axial eye length, and intraocular pressure (IOP)).

In our preliminary study with 19 healthy human eyes, birefringence of sclera and IOP had statistically significant negative correlation, but spherical equivalent and axial eye length did not show statistically significant correlations with birefringence. Considering the known anatomy of sclera, the correlation between birefringence and IOP might imply the directional deformation of sclera by IOP. The depth profiles of birefringence showed that birefringence of episclera increased along the depth, indicating that its loose connective tissue was more organized near the sclera. In sclera, B-scan images of scleral birefringence showed nonuniform distribution, suggesting that organization of collagen fiber bundles and collagen fibril diameter have regional differences.

Scleral birefringence measurement by PS-OCT would be able to provide us detailed properties of sclera and implication to mechanisms of the diseases.

8209-44, Session 9

## Birefringence measurement of retinal nerve fiber layer using AO-PS-OCT: a comparison with PS-OCT

Q. Wang, Indiana Univ. (United States); B. Cense, Utsunomiya Univ. (Japan); O. P. Kocaoglu, R. S. Jonnal, S. Lee, Z. Liu, D. T. Miller, Indiana Univ. (United States)

Birefringence of the retinal nerve fiber layer (RNFL) has been suggested a sensitive indicator of tissue health, with changes reported to precede clinically detectable vision loss. A leading method to measure RNFL birefringence is polarization-sensitive optical coherence tomography (PS-OCT), which measures simultaneously the layer's double pass phase retardation (DPPR) and thickness.

Recently, we have extended birefringence measurements of this layer to that of individual retinal nerve fiber bundles (RNFBs) by combining PS-OCT with adaptive optics (AO-PS-OCT). While successful, our bundle measurements resulted in noticeably higher birefringence than RNFL measurements reported in the literature using PS-OCT. One explanation is that PS-OCT measures an average effect across RNFBs and the surrounding glial tissue, while AO-PS-OCT - due to its higher lateral resolution - individuates the two tissues enabling just the bundles to be measured. To test this hypothesis, we measured birefringence at several different retinal locations in the same eye with PS-OCT and AO-PS-OCT. With AO-PS-OCT, birefringence measurements were made of individual RNFBs and the full RNFL. Additional measurements were made at different times to assess repeatability. A T-test and ANOVA analysis compared quantitatively the measurements. The results support the hypothesis that birefringence of individual RNFBs is higher than that of the RNFL (bundles plus glial). In this study, birefringence was approximately two times higher (~0.5 deg/μm for RNFBs; ~0.25 deg/μm for RNFL)

8209-45, Session 9

## Polarization-sensitive optical coherence tomography for in vivo phase retardation measurements of basal laminar deposits

B. Cense, Utsunomiya Univ. (Japan); Q. Wang, S. Lee, L. Zhao, J. Papay, D. T. Miller, A. E. Elsner, Indiana Univ. (United States)

The presence of basal laminar deposits beneath the retina pigment epithelium is a risk factor for the development of age related macular degeneration. These deposits contain birefringent materials, making them potentially detectable with polarization-sensitive optical coherence tomography (PS-OCT). To investigate this possibility, the retina of 20 subjects were imaged with PS-OCT. A volumetric data set (100 x 1000 A-scans) was taken in 4.4 s. Data were obtained without the use of dilation drops. Using the Stokes vectors of the photoreceptors as a reference, the double pass phase retardation (DPPR) angle was calculated. At approximately 60 μm below the photoreceptors, the DPPR induced by the basal laminar deposits was retrieved. By using the photoreceptors as a reference, DPPR contamination of birefringence in the cornea, nerve fiber layer and Henle's fiber layer was avoided. As predicted, results varied significantly across subjects. For example, the eye of one subject with known retinal pathology contained a large area of elevated double pass phase retardation, with retardation values up to 180º, while another subject without pathology had values close to 0º. These results were confirmed in a second experiment. These measurements provide a new biomarker to monitor the build up of basal laminar deposits in patient eyes and the effect of medication.

8209-46, Session 9

## Wide-field high-definition polarization sensitive optical coherence tomography of the retina

M. Pircher, S. Zotter, E. Götzinger, Medizinische Univ. Wien (Austria); H. Yoshida, F. Hirose, Canon Inc. (Japan); M. Bolz, C. Vass, U. Schmidt-Erfruth, C. K. Hitzenberger, Medizinische Univ. Wien (Austria)

We present results of an improved polarization sensitive optical coherence tomography instrument. The imaging speed of the instrument is increased to 70k A-lines per second using a custom designed single camera spectrometer. This speed enables to record 3D data sets of the human retina with a large field of view (~40°x40°) within a few seconds and reduces image artifacts due to eye motion. From the 3D data sets, en-face images of retardation and optic axis orientation are obtained, showing the distribution of the retinal nerve fiber layer and Henle's fiber layer. Additionally, the reproducibility of polarization sensitive measurements is tested in healthy volunteers.

8209-54, Poster Session

## Effect of dehydration in the UV transmittance of "in vitro" corneas

V. A. Cacciacarro Lincoln, L. Ventura, S. J. Faria e Sousa, M. M. Makiyama Mello, Univ. de São Paulo (Brazil)

In ophthalmology the research using "in vitro" corneas are an excellent model for studies of new ophthalmologic procedures, enabling the analysis of effectiveness, performance and even safety parameters of the procedure. In this work we studied four "in vitro" human corneas preserved in OPTISOL-GS, with initial average pachymetry of 542 microns and a post-mortem average of 6 days. Each cornea was removed from the container of conservation and cleaned with saline solution to remove excess of OPTISOL-GS. The corneas were placed in a support aligned with an ultraviolet source of 3mw/cm2 and an optical fiber positioned under the support near the back of the cornea. The UV transmittance spectrums in the region of 360-370nm were captured by the emission of UV source for 3 seconds. These spectrums were captured every 5 minutes in a total of 60 minutes, producing 13 spectrums per cornea. The initial average transmittance measured was 73% and up to 50 minutes there were no significant differences. In the last 10 minutes we observe a decrease in UV transmittance around 4%, probably indicated by dehydration and wrinkling of the cornea tissue. The final average pachymetry was 421 microns and the UV transmittance after the 60 minutes was 69%. Therefore we can suppose that the UV transmittance of corneas "in vitro" is invariant over a period of up to 60 minutes, even with the thickness decrease, since the material that absorbs in the UV region remains intact and only water loss occurs.

8209-55, Poster Session

## A prototype for measurements in visible light transmittance of sunglasses

M. M. Makiyama Mello, V. A. Cacciacarro Lincoln, L. Ventura, Univ. de São Paulo (Brazil)

The measurements of the transmittance of ultraviolet and infrared radiation through sunglasses are standard requirements for certification of these lenses. According to international standards, the electromagnetic spectrum relative to UV (100 - 400nm) and IR (700-1400nm) must be protected according with the lens category. The categories are in a scale of 0 to 4, according to the amount of visible light transmitted through the sunglasses. This test becomes important because the pupil dilates and contracts according to the intensity of light that reaches the eye, protecting it when exposed on a sunny day since the pupil contraction helps to block the UV rays. The major problem with the sunglasses without adequate protection is precisely the inhibition of this natural capacity of the eye, reducing the intensity of only visible part of the electromagnetic spectrum and causing dilation of the pupil, while there is no proportional protection from UV rays. An opto-electronic set up was assembled in this work, using LEDs as lighting sources , covering from 380nm to 780nm; a sensor for visible light; and an electronic circuit to control the signal, providing results and user interface. The prototype had an accuracy of 0.1% for transmission; resolution of 0.1% and correlation factor of r = 0.9982 compared to CARY 5000 - Varian spectrophotometer.

8209-56, Poster Session

## Spectroscopic measurements during the corneal collagen cross linking procedure for in vitro human corneas

L. Ventura, V. A. Cacciacarro Lincoln, S. J. Faria e Sousa, M. M. Makiyama Mello, Univ. de São Paulo (Brazil)

The transmittance of UVA light through the human preserved cornea of over 400µm thickness during the corneal collagen cross-linking procedure has been measured spectroscopically. The 25 corneas, (average thickness of 570 µm), preserved in OptisolGS, were washed with saline, desepithelization was performed, and the cornea was laid on the lid of a Chiron Ophthalmics corneal storage chamber. Immediately under the endothelium, a 600 µm core diameter UV-VIS optical fiber was fixed in a 3mm hole and then connected to a spectrophotometer to detect the amount of delivered UVA light on the endothelium. Current procedure protocol was performed, i.e., one drop of riboflavin 0.1%, 400 mOsm, was applied on the naked cornea, every 5 minutes (total of 12 drops). The UV irradiation (365±5 nm, 3mW/cm2, 1.51 mW, 5.405 J/cm2) was performed after 30 min of instillation for an additional 30 min. The average transmittance of the desepithelized cornea without Riboflavin is 65.8%'; after the 1st drop of Riboflavin, transmittance is 51.4%; after 2nd drop, 46.1%; after 3rd drop, 41.9% ; after 4th drop, 38.7%; after 5th drop, 35.9%; after 6th drop 33.6% ; after 7th drop, 31.0%; after 8th drop; 28.8%; after 9th drop, 27.2%; after 10h drop, 25.4%; after 11th drop, 23.9%; and finally after 12th drop, 22.5%. The average transmittance in terms of energy during the 30 min irradiation procedure fluctuated from 0.930 to 0.675mW/cm2, well beyond the currently accepted rabbit corneal endothelium safety limit for cytotoxic level of 0.36 mW/cm2.

8209-57, Poster Session

## Does tropicamide affect choroidal blood flow in humans? a laser Doppler flowmetry study

N. Palanisamy, Univ. degli Studi di Modena e Reggio Emilia (Italy); C. E. Riva, Univ. of Lausanne Medical School (Switzerland); L. L. Rovati, Univ. degli Studi di Modena e Reggio Emilia (Italy); M. Cellini, C. Gizzi, E. Strobbe, E. C. Campos, Univ. degli Studi di Bologna (Italy)

The measurement of blood flow in the ocular fundus is of scientific and clinical interest. Investigating ocular blood flow in the choroid may be important to understand the pathogenesis of numerous ocular diseases, such as glaucoma or age-related macular degeneration (AMD). Laser Doppler flowmetry (LDF) was applied to measure mean velocity, volume and flux of red blood cells in the tissues of human eye. Its main application lies in the possibility of assessing alterations in blood flow early in the course of diseases. The purpose of the present study was to investigate the effect of pupil dilatation with one drop of 1% tropicamide on blood flow in the foveal region of the choroid of the human fundus. The blood flow parameters were measured in 12 eyes during 30 minutes (one measurement every 3 minutes) after the application of the drop. Since the flow parameters depend on the scattering geometry, which itself may change as the pupil dilates, an artificial pupil of 4mm in diameter was placed in front and close to the eye. Following the administration of tropicamide the mean pupil diameter increased during the 30 min of measurements from 3.3 mm to 8.1 mm ($P<0.0001$). In comparison to the baseline values, the data shows no significant changes in mean velocity, volume and flow of red blood cells following the application of tropicamide.

Keywords

Laser Doppler flowmetry, tropicamide, mean blood velocity, flux of red blood cells, choroidal blood flow, artificial pupil

References

[1] Robinson F, Petrig BL, Sinclair SH, Riva CE, and Grunwald JE: Does topical phenylephrine, tropicamide or proparacaine affect macular blood flow? Ophthalmology 1985, 92, 1130-1132.

[2] Riva CE, Geiser M, Petrig BL. Ocular blood flow assessment using continuous laser Doppler flowmetry. Acta Ophthalmol. 2010, 88, 622-629.

[3] Riva CE, Harino S, Petrig BL and Shonat RD. Laser Doppler flowmetry in the optic nerve. Exp. Eye. Res. 1992, 55, 499-506

[4] Logean E, Geiser MH and Riva CE. Laser Doppler instrument to investigate retinal neural activity induced changes in optic nerve head blood flow. Optics and Lasers in Engineering 2005; 43; 591-602.

8209-58, Poster Session

## An ophthalmic instrument to detect nano and micro-aggregates in blood flow

S. Cattini, L. L. Rovati, R. Salvatori, A. M. Gatti, Univ. degli Studi di Modena e Reggio Emilia (Italy)

An ophthalmic instrument for innovative analyses of the eye microcirculation is presented.

Thanks to the transparency of the ocular media, eyes are a natural observation window for non-invasive measurements. The proposed system allows investigations of the presence of nano- and micro-aggregates in the blood flow of the fundus, thus allowing diagnoses when the presence of such aggregates is associated to specific diseases or verifying the impact of nanoparticles injection in Nanomedicine.

Moreover, nanoparticles play an increasingly important role in medical research, e.g. as drug delivery vehicles and contrast/therapeutic agents. However, the physiology of the dispersion of such nanoparticles inside the human body is quite complex and not easily predictable. Therefore, our system may represent an instrument to gain further insight on such dynamics and by their quantification a prognostic tool.

Based on an ad-hoc modified ophthalmic microscope, the developed measuring system performs a diffusing wave spectroscopy (DWS) analysis of the radiation back-scattered from the ocular media. The temporal fluctuations of the detected signal reveal motion of aggregates and changes in the optical properties of the investigated media.

Preliminary tests, performed injecting a bolus of 20nm diameter Au-nanoparticles in the ear vein of soft-anesthetized New-Zealand rabbits, demonstrate the applicability of the proposed measuring-system. Even thought the ocular fundus is known to be a complex scattering and absorbing medium, our system has been shown to be able to detect both the crossing of nano- micro-aggregates carried by the blood flow in the ocular fundus after the injection and the subsequent physiological recovery.

8209-59, Poster Session

## ‘All-Laser’ endothelial corneal transplant in human patients

F. Rossi, Istituto di Fisica Applicata Nello Carrara (Italy); L. Menabuoni, A. Malandrini, A. Canovetti, I. Lenzetti, U.O. Oculistica - Ospedale Misericordia e Dolce (Italy); R. Pini, Istituto di Fisica Applicata Nello Carrara (Italy)

Femtosecond laser sculpturing of corneal tissue is commonly used for the preparation of endothelial flaps. Diode laser welding of ocular tissues is a procedure that enables minimally invasive suturing of tissues. The combination of these laser based techniques results in a new approach to minimally invasive ophthalmic surgery, such as in endothelial corneal transplant (or endothelial keratoplasty - EK). In this work we present the “all laser” EK performed in human subjects. 24 pseudophakic patients with bullous keratopathy underwent EK: the femtosecond laser was used to prepare the 100 µm thick and 8.5 mm diameter donor Descemet endothelial flap. After staining the stromal layer of the donor flap with a liquid ICG solution, the donor flap was inserted in the recipient eye by the use of the Busin injector. Then, the endothelial layer was laser-welded to the recipient eye (10 laser spots around the periphery of the flap), in order to reduce the risk of postoperative dislocation of the transplanted flap. A transplanted flap engraftment was observed in all the treated eyes. The staining procedure used to perform laser welding also enabled to evidence the stromal side of the donor flap, so as the flap was always placed in the right side position. The endothelial cells counts in both the laser-welded flaps and in a control group were in good agreement. The proposed technique is easy to perform and enables the reduction of postoperative endothelial flap dislocations.

8209-60, Poster Session

## Extracting diagnostic information from optical coherence tomography images of diabetic retinal tissues using depth-dependent attenuation rate and fractal analysis

D. Cabrera DeBuc, Bascom Palmer Eye Institute (United States)

The sensitivity of optical coherence tomography (OCT) images to classify diabetic morphology is tested by two classification methods. The first method is based on finding the attenuation coefficients for the OCT signal that propagates through various regions of the retinal tissues. The second method uses a wavelet algorithm to calculate the fractal dimension (FD) in the regions of interest identified in the images. Stratus OCT data from diabetic patients with and without early retinopathy were analyzed using a custom-built software that facilitates the extraction of 7 cellular layers of the retina (RNFL, GCL+IPL, INL, OPL, ONL+IS, OS, RPE) on OCT images. Scattering increased for all the layers (except in the RNFL, INL and OPL). Fractal dimension increased for all the layers (except the GCL+IPL). The highest AUROC values estimated for the FD were observed for GCL+IPL. The maximum discrimination value for FD of 0.80 (SE =0.05) for the GCL+IPL complex was obtained at a FD $\leq$ 1.56. At this value, the sensitivity for the GCL+IPL complex was 65.1% with a specificity of 76.3%. No advantage was found for the method using depth-dependent attenuation rate. The fractal method provided a better sensitivity when compared to the OCT signal attenuation method. We demonstrate that by analyzing the OCT signal using fractal analysis we are able to differentiate diabetic patients with and without early retinopathy. The use of fractal analysis for classification of diabetes-induced retinal damage in OCT clinical data could potentially provide additional diagnostic information for early detection and progression of DR.

8209-61, Poster Session

## Prospects of the vision correction under non-ablative laser radiation

E. N. Sobol, Institute on Laser and Information Technologies (Russian Federation); A. V. Bolshunov, Research Institute of Eye Diseases, RAMS (Russian Federation); O. I. Baum, A. Omelchenko, Institute on Laser and Information Technologies (Russian Federation)

The aim of the paper is to present two novel approaches allowing cornea reshaping and increase of water permeability of eye trabecula using thermo-mechanical effect of pulse repetitive laser radiation. The first technique is based on the essential property of cornea - temporal thermo plasticity. Experiments were performed in vitro with eyes of pigs, rabbits, cadavers, and also in-vivo with rabbit eyes using an Erbuim glass fiber laser of 1.56 microns in wavelength with pulse duration of 200 -500 ms, pulse repetition rate 0.5-1.5 Hz, variable power 0.6-4.5 W.

The maximal change of eye refraction obtained was of 7 diopters. The advantages of the new approach are provided by the following factors (1) noninvasive and potentially reversible nature of exposure on the cornea and sclera, (2) minimal exposure on the central zone of the cornea, (3) availability of a feed back control system that prevents denaturation and damage of the cornea, (4) possibility of a repeated procedure.

The second technique is based on the nondestructive heterogeneous laser heating allowing alteration in porous system of biological tissues and increase water permeability in the sclera and the zone of angle of anterior chamber of the eye. The laser settings were established to provide the substantial increase of water permeability of eye trabecular zone without tissue coagulation. That can be used as a basis for an effective technology of glaucoma treatment.

8209-62, Poster Session

## Efficient outer retina cellular simulation

A. N. Azar, A. C. Parker, K. Tseng, The Univ. of Southern California (United States)

The retina's massive number of cells, graded potential responses and various connectivity patterns create a scalability challenge for retinal modelers. The human's retina contains over one hundred million cells with complex interconnectivity patterns that include feedforward, feedback and lateral connections across the retinal systems. This will lead to a continuous process of cell state computations, and "broadcasting" the newly computed states to other cells challenging modeling a scalable retinal system. We propose to solve the problem by applying an enhanced event-driven algorithm to simulate a bio-inspired cellular-level scalable outer retina. We chose an event-driven simulation strategy because, with an efficient approach, it can be much faster than a time-driven simulation. We propose several novel simulation acceleration strategies for the original event-driven algorithm and show the trade-offs of the retinal simulation speed and accuracy. The simulation input is a video sequence of images, and the simulation produces the bipolar cells outputs. We model the outer part of the retina including the cones, horizontal cells and bipolar cells. We consider the non-uniform distribution of the retinal cells, and carry out the cell-to-location assignment efficiently using log-polar mapping and sparse matrices. We carry out simulations to illustrate various retinal visual functionalities including horizontal cell spatial averaging, and bipolar cell edge detection. The simulator can be used by retinal prosthesis modelers to determine various design parameters in their prosthetic chips like the least number of needed cones to create facial recognition.

8209-63, Poster Session

## Reflectometry technique for characterizing human tear film

H. Lu, M. R. Wang, J. Wang, M. Shen, Univ. of Miami (United States)

Healthy condition of tear film is very crucial to support normal eye functions. The disorder of tear flow may cause the lack of lubrication for the ocular surface, leading to Dry Eye Syndrome (DES). In its most severe case, DES may develop to recurrent corneal erosion or secondary infection with complication of vision loss. In-vivo measurement of the tear film thickness and most importantly of the tear film break up process in human eyes is one of the most attractive research subjects due to its importance to the effective clinical diagnosis of DES. Although several methods are currently available to characterize in-vivo tear film, their applications are hindered by either inefficient resolution or too complicated operation for clinical use. Based on prior successful measurement of water film thickness and thinning dynamics on soft contact lens, in this paper, we report a fiber based optical reflectometry method combined with an auxiliary scanning system for fast alignment, specifically designed for in-vivo tear film evaluation in human eyes. We measured tear film thickness, tear film thinning dynamics, and tear film breakup thickness on a model eye with artificial tears. The fiber based optical reflectometer is robust, compact, easy to handle, and is capable of very high thickness measurement resolution. These features will definitely have a significant impact to the dry eye diagnosis and treatment.

8209-65, Poster Session

## Portable retinal imaging for eye disease screening using a consumer-grade digital camera

E. S. Barriga, VisionQuest Biomedical, LLC (United States); A. V. Larichev, Lomonosov Moscow State Univ. (Russian Federation); G. Zamora, P. Soliz, VisionQuest Biomedical, LLC (United States)

The development of affordable means to image the retina is an important step toward the implementation of eye disease screening programs. In this paper we present the i-RxCam, a low-cost, hand-held, retinal camera for widespread applications such as tele-retinal screening for eye diseases like diabetic retinopathy (DR), glaucoma, and age-related ocular diseases. Existing portable retinal imagers do not meet the requirements of a low-cost camera with sufficient technical capabilities (field of view, image quality, portability, battery power, and ease-of-use) to be distributed widely to low volume clinics, such as the offices of single primary care physicians serving rural communities.

The i-RxCam uses a Nikon D3100 digital camera body. The camera has a CMOS sensor with 14.8 million pixels. We use a 50mm focal lens that gives a retinal field of view of 45 degrees. The internal autofocus can compensate for about 2D (diopters) of focusing error. The light source is an LED produced by Philips with a linear emitting area that is transformed using a light pipe to the optimal shape at the eye pupil, an annulus. To eliminate corneal reflex we use a polarization technique in which the light passes through a nano-wire polarizer plate. This is a novel type of polarizer featuring high polarization separation (contrast ratio of more than 1000) and very large acceptance angle (>45 degrees). The i-RxCam approach will yield a significantly more economical retinal imaging device that would allow mass screening of the at-risk population.

8209-66, Poster Session

## Toward optical coherence topography

S. I. Sayegh, Y. Jiang, EYE Ctr. (United States)

Commercial OCT systems provide pachymetry measurements and multiple section of a corneal map are available but typically not used to full advantage. Full corneal topographic information of anterior and posterior corneal surfaces for use in cataract surgery and refractive procedures is a desirable goal and would add to the usefulness of anterior and posterior segment evaluation. With the advent of toric intraocular lenses, a full evaluation of corneal astigmatism is necessary for cataract surgery planning. Similarly a full evaluation of corneal topography, both anterior and posterior, prior to LASIK is a must, to optimize results and avoid the risk of corneal ectasia. While substantial progress has been made towards obtaining "average" central corneal power via optical coherence tomography (D Huang), power in different meridians and full topographic information are still missing. This is usually reported to be due to eye movements. Decentration in addition to eye movements turn out to be a crucial contributors to errors in the computation of curvature. We analyze the role of centration, eye movements and develop a model that takes into account both the device and the eye dynamics and allows for the formulation of criteria for obtaining reliable topographic data within ¼ of a diopter. The use of a commercial system to obtain topographical maps illustrates the limitation and promise of this approach.

8209-67, Poster Session

## Toward the development of a low-cost laser Doppler module for ophthalmic microscopes

S. Cattini, L. L. Rovati, Univ. degli Studi di Modena e Reggio Emilia (Italy)

A low-cost, small-size and easy to use laser Doppler module for fundus blood flow measurements is proposed. The proposed instrument may provide important clinical information such as the investigation of possible vessel occlusions provided by surgical treatments (i.e. photocoagulation).

The measuring system is based on a self-mixing laser diode Doppler flowmeter (SM-DF) that we previously describe [1]. Reduced costs, easy implementation and small size represent the main features of SM-DF. Moreover, SM-LD technique offers the advantage to have the excitation and measurement beams spatially overlapped, thus overcoming the alignment difficulty due to limited optical aperture of the pupil.

The proposed low-cost optoelctronic module may be easily integrated into a commercial ophthalmic microscope, thus adding flow measurement capability to standard visual inspection of the fundus.

Thanks to an on-board DSP-microcontroller, the optoelectronic module directly estimates the blood flow; USB connection and an ad-hoc developed user-friendly software interface allow displaying the result on a personal computer.

Preliminary test performed on a mechanical eye model demonstrate the applicability of the system.

Bibliography: [1] Cattini, S., Salvatori, G., Rovati, L., “Self-mixing laser velocimeter for retinal blood flow measurements,” Proceedings of SPIE Vol. 6426, 642611 (2007).

8209-68, Poster Session

## Corneal tissue ablation using 6.1 µm quantum cascade laser

Y. Huang, J. U. Kang, The Johns Hopkins Univ. (United States)

High absorption property of tissues in the IR range ($\lambda > 2$ µm) results in effective tissue ablation, especially near 3 µm due to the strong water absorption. In the mid-infrared range, wavelengths of 6.1 µm and 6.45 µm falls into the absorption bands of the amide protein groups Amide-I and Amide-II, respectively, which also coincide with the deformation mode of water at 6.1 µm. This coincidence makes 6.1 µm a highly effective ablation band that promises minimum collateral damages to the surrounding tissues compared to 3 µm band. In this work, we performed bovine corneal ablation study in-vitro using high-power pulsed 6.1µm quantum cascade laser (QCL). Quantum cascade laser has the advantages of low cost, compact size and tunable wavelength, which makes it a great alternative to other Mid-IR light sources for medical applications. Preliminary results show that with a peak-optical power of 250 mW, 5 ms pulse width and 100 Hz frequency, effective corneal stroma craters were achieved. Future study will focus on optimizing the control parameters of QCL to attain precise control of corneal tissue ablation.

8209-69, Poster Session

## Test and design of a high-spatial and temporal resolution aberrometer

B. Emica, S. Meimon, ONERA (France); G. Chenegros, Observatoire de Paris à Meudon (France); J. Conan, T. Fusco, ONERA (France); M. Paques, Ctr. Hospitalier National d’Opthalmologie des Quinze-Vingts (France)

The design of robust Adaptive Optics systems (AO) requires to characterize spatially and temporally the aberrations. Thus, it is of importance to have an instrument able to measure the aberrations at high spatial and temporal resolutions. The high spatial resolution is necessary to have an extended modal decomposition of aberrations, to characterize finely the pupil irradiance and to quantify aliasing and fitting errors. The high temporal resolution is necessary to discriminate and analyze the evolution of very fast phenomena contributing in the aberration dynamics. Fast pupil movement, tear film and accommodation are among the contributors. These characterizations are essential, however, hardware constraints make it difficult to obtain high spatial and temporal resolutions on a single detector. We have therefore designed a new aberrometer composed of two synchronized instruments that allows to perform such measurements. Each instrument is composed of an eye pupil imager and a wavefront sensor. The first instrument studies the spatial distribution of pupil irradiance and aberrations by synchronizing a high definition eye pupil imager and a 32x32 lenslets wavefront sensor measuring the aberrations. The second instrument studies the temporal dynamics of the aberrations by synchronizing, at 300Hz, an eye pupil imager, recording the pupil position, and a low order wavefront sensor measuring the aberrations.

Preliminary results have been obtained on the first instrument. The integration of the second instrument is in progress. Data will be recorded and analyzed on various healthy and pathological subjects in the coming months. An overview of the results will be presented at the conference.

8209-70, Poster Session

## In vivo imaging of the fast intrinsic optical signal (fIOS) in chicken retina with functional UHROCT

A. Akhlagh Moayed, S. Hariri, V. Choh, K. Bizheva, Univ. of Waterloo (Canada)

A high speed, ultra high resolution SD-OCT system, operating in the 1060nm wavelength range was used to record in-vivo fast Intrinsic Optical Signals (fIOSs) due to visual stimulus from healthy chicken retina. The OCT system provided 3.5µm axial resolution and about 5 µm lateral resolution in the chicken retina and ~99 dB sensitivity at 1.6 mW power of the imaging beam. Data acquired with this system clearly shows fIOSs signals in different layers of the retina resulting from the visual stimulation. Correlation of the data with ERG recordings shows clear synchronicity between the fIOS and ERG recordings.

8209-47, Session 10

## LCoS-based adaptive optics visual analyzer in white light

E. Fernández, P. M. Prieto, P. Artal, Univ. de Murcia (Spain)

Vision should be tested under natural conditions for obtaining realistic information. Natural conditions include binocular vision and white-light or polychromatic illumination. In this direction, the performance of an adaptive optics (AO) system using a Liquid Crystal on Silicon (LCOS-Pluto, Holoeye Photonics, Germany) correcting device under white-light illumination has been investigated in this work. The purpose is characterizing how phase wrapping and chromatic dispersion of the LCOS affect the performance of aberration correction or manipulation for visual oriented applications. The visual simulator or analyzer (Voptica, Spain) incorporates AO technology for the manipulation of aberrations. With this instrument, subjects can undergo visual testing, while aberrations are being measured and manipulated, ideally under white-light illumination. Zernike polynomials up to the 5th order were objectively estimated with a Hartmann-Shack wavefront sensor, and also under the white light, after being generated by the correcting device. Comparison across wavelengths is presented. In all cases, for the range of use in the human eye, chromatic degradation was below the natural chromatic aberration of the eye. Differences across wavelengths at the tails of the spectrum were typically inferior to 10%. The practical significance of such discrepancy decreases when the spectral response of the human visual system is taken into account. Subjective measurements of different visual functions in real patients, as visual acuity and contrast sensitivity were performed under polychromatic illumination demonstrating the feasibility of the technique. The presented technology offers the possibility of realistic visual testing, with the ability of manipulating wavefronts in the entire visible range.

8209-48, Session 10

## Adaptive optics line scanning ophthalmoscope: recent progress

R. D. Ferguson, D. X. Hammer, D. P. Biss, E. Plumb, Physical Sciences Inc. (United States); C. A. Toth, M. McCall, Duke Univ. Medical Ctr. (United States)

Physical Sciences Inc. (PSI) made significant progress toward the development of a Compact Adaptive Optics Line Scanning Ophthalmoscope for retinal imaging in the past year. The device combines line scanning ophthalmoscopy (LSO), invented at PSI and used in several commercial clinical ophthalmic imagers, with AO components for correction of ocular aberrations and high resolution imaging of retinal cells. We have recently completed design and fabrication of an improved prototype clinical AOLSO imager. The system was assembled on a 30×45 cm optical plate that is mounted vertically in a light-tight housing attached to a standard slit lamp stand for clinical deployment. The primary components are an ALPAO 97-actuator deformable mirror (DM) for wavefront compensation, a Hartmann-Shack wavefront sensor (HS-WS), an e2-v linear detector (LD) for imaging, and a new scanning assembly. An LCD-based fixation target is also included. Retinal and pupil conjugates are relayed with pairs of spherical mirrors. The front spherical mirror closest to the eye is a 10-cm mirror that allows rapid, automated mapping of the macula with a unique dual-scanning assembly. We describe other unique AOLSO design features made possible by the line-scanning configuration and present preliminary imaging results in human subjects. We are also evaluating preliminary wavefront-sensorless AO control algorithm, and are developing automated clinical analysis software in preparation for an upcoming pilot clinical study at Duke Eye Center.

8209-49, Session 10

## Patient retinal imaging with adaptive optics-assisted optical coherence tomography

K. Sudo, Utsunomiya Univ. (Japan); K. Kurokawa, K. Sasaki, S. Makita, Y. Yasuno, Univ. of Tsukuba (Japan); T. Yatagai, B. Cense, Utsunomiya Univ. (Japan)

With the introduction of new OCT engines that operate at high acquisition rates, retinal image quality is limited by the number of photons returning from the eye. One way around this problem is to improve the light efficiency collection by using a larger beam size and adaptive optics. We quantified the performance of a low-cost AO-OCT design (45 cm x 25 cm x 25 cm footprint) built around a MEMS deformable mirror (5.5 µm mechanical stroke, 4.95 mm effective diameter) and tested the instrument on patient eyes (age related macular degeneration, diabetes, glaucoma). Preliminary measurements with a 3.4 mm beam on a human eye and on a model eye demonstrated that diffraction-limited performance can be achieved for aberrations as large as ~1.3 µm wavefront RMS. For a 3.4 mm beam at 840 nm, this is equivalent to approximately 3 D of defocus. An increase of 30 dB in dynamic range was observed in the OCT data obtained from the model eye, comparing the dynamic range in images before and after AO operation.

8209-50, Session 10

## Large-field of view lens-based adaptive optics scanning laser ophthalmoscope

F. Felberer, J. S. Kroishamer, C. K. Hitzenberger, M. Pircher, Medizinische Univ. Wien (Austria)

We present a novel adaptive optics scanning laser ophthalmoscope that is based on lenses instead of mirrors. Because of the lower aberrations introduced by the lenses a wider scanning field (up to 5°) is enabled that is only limited by the isoplanatic angle of the eye. Large field of view images of the cone mosaic of healthy volunteers are presented together with densely sampled images of the foveal cones. This design might be useful in order to build more compact adaptive optics scanning laser ophthalmoscope instruments.

8209-51, Session 10

## In vivo imaging of inner retinal cellular morphology with adaptive optics/optical coherence tomography: limitations and challenges

R. J. Zawadzki, UC Davis Medical Ctr. (United States); S. M. Jones, Lawrence Livermore National Lab. (United States); D. Y. Kim, UC Davis Medical Ctr. (United States); L. A. Poyneer, Lawrence Livermore National Lab. (United States); A. G. Capps, UC Davis Medical Ctr. (United States); S. S. Olivier, Lawrence Livermore National Lab. (United States); J. S. Werner, UC Davis Medical Ctr. (United States)

Recent progress in retinal image acquisition techniques, including optical coherence tomography (OCT) and scanning laser ophthalmoscopy (SLO), combined with improved performance of adaptive optics (AO) instrumentation, has resulted in improvement in the quality of in vivo images of cellular structures in the outer layers of the human retina. Despite the significant progress in imaging cone and rod photoreceptor mosaics, visualization of cellular structures in the inner retina has been achieved only with extrinsic contrast agents. In this paper we describe the main limiting factors in visualizing inner retinal cells and the methods we implemented to reduce their effects on images acquired with AO-OCT. These include improving the system point spread function (AO performance), reduction of motion artifacts (retinal motion tracking), and speckle pattern reduction (temporal and spatial averaging). Results of imaging inner retinal morphology and the improvement offered by the new UC Davis AO-OCT system with novel image processing will be presented.

8209-52, Session 10

## Optic nerve head features measured with a multimodal adaptive optics system

D. X. Hammer, R. D. Ferguson, D. P. Biss, M. Mujat, N. V. Iftimia, A. H. Patel, E. Plumb, Physical Sciences Inc. (United States); G. Wollstein, L. Kagemann, H. Ishikawa, Z. Nadler, J. S. Schuman, Univ. of Pittsburgh Medical Ctr. (United States)

The multimodal adaptive optics (AO) retinal imaging system simultaneously acquires high resolution, high magnification aberration-corrected en-face scanning laser ophthalmoscope (SLO) and cross-sectional optical coherence tomography (OCT) images. The OCT channel is a spectrometer-based Fourier domain OCT imager with a 1-µm illumination source specifically designed for enhanced depth penetration into the optic nerve head (ONH). In addition to the OCT and SLO channels, the multimodal AO system also uses a wide field line scanning ophthalmoscope (LSO), an integrated retinal tracker (RT), and an LCD-based fixation target (FT). Recent upgrades include real-time GPU-based OCT processing (<4 µs/A-line processing rate) and simultaneous dual-deformable mirror control. Both the SLO and OCT channels can resolve cone photoreceptors close to the fovea and individual nerve fiber bundles near the ONH. In clinical testing underway, we compare the differences in ONH features such as nerve fiber bundle density, lamina cribrosa boundaries and pores, and ONH vessel flow rates between normal and glaucomatous eyes.

8209-53, Session 10

## Adaptive optics optical coherence tomography for measuring phase and reflectance dynamics of photoreceptors

O. P. Kocaoglu, R. S. Jonnal, S. Lee, Q. Wang, Z. Liu, D. T. Miller, Indiana Univ. (United States)

Optical coherence tomography with adaptive optics (AO-OCT) is a noninvasive method for imaging the living retina at the microscopic level. We used AO-OCT technology to follow changes in cone photoreceptor outer segment (OS) length and reflectance. To substantially increase sensitivity of the length measurements, a novel phase retrieval technique was demonstrated, capable of detecting changes on a nanometer scale. We acquired volume videos of 0.65˚x0.65˚ retinal patches at 1.5˚ temporal to the fovea over 75 minutes. Volumes were dewarped and registered, after which the cone intensity, OS length, and phase difference signal were tracked over time. The reflections from inner segment/OS junction (IS/OS) and posterior tips of OS (PTOS) showed significant intensity variations over time. In contrast, the OS length did not change, as measured directly from the intensity images, expectedly so, due to the small axial changes (~100 nm/hour) that are known to occur over 75 minutes are well below our system's axial resolution (3 microns). Such small changes, however, were detectable with our phase retrieval technique. The PTOS-IS/OS phase difference signal for the same cones showed significant variation, suggesting real sub-wavelength changes in OS length of 183 and 123 nm/hr for the two cones followed. These length changes are thought to be due to the normal renewal process of the cone OS. The phase difference measurements were strongly correlated among A-lines within the same cone (0.65 radians standard deviation) corresponding to length change detection capability of 31 nm, or ~100 times smaller than the axial resolution of our system.

# Conference 8210: Optical Methods for Tumor Treatment and Detection: Mechanisms and Techniques in Photodynamic Therapy XXI

Saturday-Sunday 21-22 January 2012

Part of Proceedings of SPIE Vol. 8210 Optical Methods for Tumor Treatment and Detection: Mechanisms and Techniques in Photodynamic Therapy XXI

8210-01, Session 1

## Determinants of autophagic cell death after PDT

D. H. Kessel, Wayne State Univ. (United States)

Photodynamic therapy (PDT) is a process that can induce apoptosis, autophagy or both depending on the cell phenotype. Studies involving the murine 1c1c7 hepatoma indicated that where singlet oxygen is the predominant primary reactive oxygen species (ROS) formed during PDT, apoptosis represents a death pathway while autophagy is cytoprotective. In other cell lines where apoptosis is unavailable, there is evidence that suppressing autophagy can promote survival after PDT. In 1c1c7 cells, when PDT results in formation of only superoxide radical and hydrogen peroxide, we observed a very strong autophagic response that eventually led to the appearance of an apoptotic morphology and loss of viability. In contrast, a 1c1c7 subline in which autophagy was inhibited was found to be markedly resistant to photodamage initiated by ·O2- and H2O2. These studies indicate that autophagy can be a pathway to cell death where an atypical pattern of ROS formation occurs.

8210-02, Session 1

## Topical delivery of preformed photosensitizer for photodynamic therapy of cutaneous lesions

N. L. Oleinick, M. E. Kenney, M. Lam, T. S. McCormick, Case Western Reserve Univ. (United States); K. D. Cooper, Case Western Reserve Univ. (United States) and Univ. Hospitals Case Medical Ctr. (United States); E. D. Baron, Case Western Reserve Univ. (United States) and Univ, Hospitals Case Medical Ctr. (United States)

Photosensitizers for photodynamic therapy (PDT) are most commonly delivered to patients or experimental animals via intravenous injection. After initial distribution throughout the body, there can be some preferential accumulation within tumors or other abnormal tissue in comparison to the surrounding normal tissue. In contrast, the photosensitizer precursor, 5-aminolevulinic acid (ALA) or one of its esters, is routinely administered topically, and more specifically, to target skin lesions. Following metabolic conversion to protoporphyrin IX, the target area is photoilluminated, limiting peripheral damage and targeting the effective agent to the desired region. However, not all skin lesions are responsive to ALA-PDT. Topical administration of fully formed photosensitizers is less common but is receiving increased attention, and some notable advances with selected approved and experimental photosensitizers have been published. Our team has been examining topical administration of the phthalocyanine photosensitizer Pc 4 to mammalian (human, mouse, pig) skin. Pc 4 in a desired formulation and concentration was applied to the skin surface at a rate of 5-10 uL/cm(2) and kept under occlusion. After various times, skin biopsies were examined by confocal microscopy, and fluorescence within regions of interest was quantified. Early after application, images show the majority of the Pc 4 fluorescence within the stratum corneum and upper epidermis. As a function of time and concentration, penetration of Pc 4 across the stratum corneum and into the epidermis and dermis was observed. The data can help explain observed variability in the response of human skin cancers to PDT with topically administered Pc 4 and suggest further improvements.

8210-03, Session 1

## Nanoconstructs for combinations based on PDT and oncogenic inhibitors

T. Hasan, Wellman Ctr. for Photomedicine (United States)

Molecular responses to cancer treatment can be complex due to the multifaceted structure of cancer tissues and the varied reactions and intricate interactions of individual components to a given treatment. Treatments might destroy cancer cells or inhibit their growth potential, at the same time stimulating molecular responses that support metastases, growth of surviving cancer cells and angiogenesis. These observations have led to a widespread acceptance of combinations as the preferred mode of cancer therapeutics where several oncogenic pathways are inhibited. But the clever synchronization of these survival pathways by injured or surviving cancer cells makes the timing of delivery of multiple inhibitors critical. Nanotechnology provides an exciting opportunity to develop multi-functional constructs carrying a targeting moiety, high payloads of more than one drug, and an imaging agent. Our laboratory has focused on the use of nanoconstructs for developing rational combinations where the PDT agent and multiple inhibitors of oncogenic pathways may be delivered simultaneously for most optimal outcomes, while the imaging agent allows for dose treatment monitoring. This presentation will discuss some of the promises and challenges of this approach.

8210-04, Session 2

## Whole-body or local hypothermia enhances the tumor-imaging and phototherapeutic potential of photosensitizers

A. Srivatsan, E. Repasky, A. Sen, R. K. Pandey, Roswell Park Cancer Institute (United States)

Despite advances in therapeutic interventions, clinical response rates in cancer therapy have not dramatically improved in the last few decades. Head and neck (H&N) cancers account for 6% of all the malignancies and are the seventh most common cause of cancer-related death in the United States. Photodynamic therapy (PDT) is one of the methods being established for management of H&N cancer, possessing advantages of localized treatment without long-term systemic effects with lesser morbidity and traumaticity compared to surgical intervention. Hyperthermia is considered as an attractive complimentary modality for cancer therapy. It has been shown that minimal tissue hyperthermia (whole body or local, < 400C) increases blood flow, which yields higher concentrations of the chemotherapeutic agents with improved efficacy.

Results from our new preclinical in vivo experiments demonstrate improved treatment response to PDT when mild local or systemic hyperthermia is combined with phototherapy. This novel combination produced significantly improved tumor-uptake of HPPH (a chlorophyll derivative currently under multicenter clinical trials) in mice Colon 26 tumors with enhanced PDT efficacy. We observed that mild hyperthermia increases blood flow, and reduces tumor interstitial fluid, which results in the higher concentrations of HPPH needed for more effective treatment outcome. The utility of this approach for enhanced tumor-imaging and therapy will be discussed.

8210-05, Session 2

## Targeting stromal influences in pancreatic cancer with photodynamic therapy

J. P. Celli, I. Rizvi, I. Massodi, M. Glidden, Massachusetts General Hospital (United States); S. P. Pereira, Univ. College London (United Kingdom); T. Hasan, Massachusetts General Hospital (United States)

Pancreatic ductal adenocarcinoma is a lethal disease that is often unresectable by the time of diagnosis and is typically non-responsive to chemo- and radiotherapy, resulting in a five year survival of only 3%. Tumors of the pancreas are characterized by a dense fibrous stroma rich in extracellular matrix proteins, which plays a poorly understood role in tumor growth and therapeutic response. Indeed, while the use of therapeutics that target the stroma is an emerging paradigm in the clinical management of this disease, it is unclear to what extent the characteristically rigid stroma of pancreatic tumors acts as a mechano-sensitive signaling partner, or merely a physical barrier for drug delivery. Here we use 3D in vitro co-cultures of pancreatic cancer cells and normal human fibroblasts as model system to study tumor-stroma interactions in the ECM-rich hypovascular pancreatic tumors. Leveraging these models along with optical techniques for quantification of tumor microrheology and high-content quantitative interrogation of growth and therapeutic endpoints we examine the role of verteporfin-based photodynamic therapy (PDT) for targeting tumor-stroma interactions in pancreatic tumors. This imaging-based platform comprises a unique system to quantify PDT-induced structural and mechanical changes in multicellular 3D tumors and shed new light on the role of PDT for treatment of this otherwise lethal disease.

8210-06, Session 2

## In vitro 3D tumor model-based screen of EtNBS derivatives to optimize PDT of hypoxic tumor environments

O. J. Klein, B. Bhayana, Wellman Ctr. for Photomedicine (United States); Y. J. Park, KAIST (Korea, Democratic Peoples Republic of); C. L. Evans, Wellman Ctr. for Photomedicine (United States)

The lack of oxygen known as hypoxia is a major source of treatment resistance in all cancers. Hypoxia is thought to be linked to the development of aggressive and metastatic cancer phenotypes, and is a major factor in the poor survival of patients with late-stage cancers. To improve the survival of these patients, it is imperative to create new therapeutic tools that target and specifically kill hypoxia-protected cells. In prior in vitro studies using a 3D model of ovarian cancer, we have found that the cationic, primarily Type-I photosensitizer EtNBS selectively homes into the acidic and hypoxic tumor microenvironments known to be resistant to many therapies. PDT with EtNBS in this model system was found to be effective by inducing widespread apoptosis in hypoxic tumor regions, making the photosensitizer a promising candidate. It is possible, though, that a more optimized functional form of EtNBS exists that might provide even greater efficacy. To this end, we developed a series of side-chain functionalized derivatives, including alcohol, amine, thiol, and ester functional groups. These EtNBS derivatives were each tested using an extensive screening protocol involving monolayer PDT cytotoxicity studies, subcellular localization experiments, 3D model time-lapse uptake imaging, and high-content, high-throughput image-based PDT efficacy studies in the 3D metastatic ovarian cancer model. We observed a range of uptake patterns and efficacies in the tumor model, and determined optimal derivatives for hypoxia-targeted photodynamic therapy. In a continuation of this study, successful derivatives were also encapsulated in nanoparticles, with the goal of improving photosensitizer delivery and therapeutic efficacy.

8210-07, Session 2

## Coupling photodynamic therapy with EGFR inhibition improves therapeutic benefit in human tumor xenografts

S. Gallagher-Colombo, J. Miller, A. L. Maas, S. L. Carter, M. Yuan, T. M. Busch, Univ. of Pennsylvania (United States)

Numerous cancers express high levels of the epidermal growth factor receptor (EGFR), whose activation initiates signaling events critical for tumor progression. Inhibitors of EGFR, such as erlotinib (a small molecule inhibitor) and cetuximab (a monoclonal antibody) are currently being used as therapeutics for lung, colon and head and neck cancers. Recent studies also report enhanced therapeutic benefit in animal models of bladder, ovarian, and head and neck cancers when coupling photodynamic therapy (PDT) with EGFR inhibition. The goal of this study is to evaluate the potential benefits of EGFR inhibition in combination with PDT in tumor models specific to histologies being examined in clinical trials of PDT at our institution. Using human tumor xenografts, including those of ovarian adenocarcinoma (OVCAR-5) and head and neck squamous cell carcinoma (SQ20B), we examined the efficacy of combining PDT with erlotinib or cetuximab. The best outcomes, measured as recurrence-free survival for 3 months, were found in animals treated with erlotinib and PDT. BPD-PDT of OVCAR-5 tumors led to a 10% cure rate that was improved to 50% by adding erlotinib to the treatment regimen; likewise, erlotinib improved the cure rate in SQ20B xenografts to 50% compared to 0% with PDT alone. These studies serve to identify clinically feasible schedules that combine PDT with EGFR inhibition and demonstrate that the combined modality approach improves outcome in several tumor models. Ongoing studies examine the effects of erlotinib on the molecular and physiologic tumor microenvironment to elucidate the mechanisms by which it serves to augment PDT response.

8210-08, Session 2

## Assessing heterogeneity and PDT response in head and neck lesions with diffuse optical spectroscopies

D. J. Rohrbach, W. Mo, N. Rigual, E. Tracy, K. Keymel, M. T. Cooper, H. Baumann, B. W. Henderson, U. Sunar, Roswell Park Cancer Institute (United States)

Photodynamic therapy (PDT) has recently shown potential for the treatment of head and neck cancer. For improved PDT efficacy, there is a need for quantitative tools that can monitor PDT. Here, we present initial results from a Phase I clinical trial of 2-1[hexyloxyethyl]-2-devinylpyropheophorbide-a (HPPH)-mediated PDT in head and neck cancer. We used a custom probe that combined diffuse correlation spectroscopy (DCS), diffuse reflectance spectroscopy (DRS) and diffuse fluorescence spectroscopy (DFS) for quantification of blood flow, blood volume, blood oxygenation and HPPH fluorescence. Non-invasive measurements were acquired before and after treatment from three sites in the oral cavity: lesion, periphery and normal. Our initial results from 5 patients indicate significant differences in these parameters between the lesion and periphery pre-treatment. We also observed significant inter- and intra-lesion heterogeneity before and after PDT. Our results suggest diffuse optical spectroscopies may provide important physiological parameters related to treatment effectiveness and patient outcome.

8210-09, Session 3

## A real-time treatment guidance system for pleural PDT

T. C. Zhu, X. Liang, J. Sandell, J. C. Finlay, A. Dimofte, K. A. Cengel, J. S. Friedberg, S. M. Hahn, E. Glatstein, The Univ. of Pennsylvania Health System (United States)

Intrapleural photodynamic therapy (PDT) has been used as an adjuvant treatment with lung-sparing surgical treatment for mesothelioma. In the current intrapleural PDT protocol, a moving fiber-based point source is used to deliver the light and the light dose are monitored by 7 detectors placed in the pleural cavity. To improve the delivery of light dose uniformity, an infrared (IR) camera system is used to track the motion of the light sources. A treatment planning system uses feedback from the detectors as well as the IR camera to update light fluence distribution in real-time, which is used to guide the light source motion for uniform light dose distribution. We have reported previously the success of using IR camera to passively monitor the light fluence rate distribution. In this study, the real-time feedback has been implemented in the current system prototype, by transferring data from the IR camera to a computer using OpenIGTLink at a rate of 20 Hz, and by calculation/displaying using Matlab. A dual-correction method is used in the feedback system, so that fluence calculation can match detector readings. The calculation model is further improved by including scattering light. In this method, real-time light fluence correction and short-interval accumulative light fluence correction are applied to the navigation feedback system to give a correct light fluence rate calculation according to the detector readings. Preliminary data from a phantom showed superior light uniformity using this method. Light fluence uniformity from patient treatments is also shown using the improved dose model.

8210-10, Session 3

## Light dose verification for pleural PDT

J. Sandell, X. Liang, T. C. Zhu, The Univ. of Pennsylvania Health System (United States)

The ability to deliver uniform light dose in Photodynamic therapy (PDT) is critical to treatment efficacy. Current protocol in pleural PDT uses isotropic detectors placed at discrete locations within the pleural cavity to monitor light dose throughout treatment. While effort is made to place the detectors uniformly through out the cavity, measurements at selective points does not guarantee an overall uniform measurement of delivered dose. A real-time infrared (IR) tracking camera is in development to better deliver and monitor a more uniform light distribution during treatment. It has been shown previously that there is good agreement between fluence calculated using IR tracking data and isotropic detector measurements for direct light in phantom experiments. This study presents the results of an extensive phantom study which uses variable, patient-like geometries and optical properties (both absorption and scattering) in conjunction with IR tracking system. Position data of the treatment is collected from the IR navigation system while concurrently light distribution measurements are made using the aforementioned isotropic detectors. These measurements are compared to fluence calculations made using data from the IR navigation system to verify our light distribution theory is correct and applicable in patient-like settings. The verification of this treatment planning technique is an important step in bringing real-time fluence monitoring into the clinic for more effective treatment. Support by P01 CA-87971/CA/NCI and NIH training grant 5T32CA009677-19

8210-11, Session 3

## Characterization of tissue optical properties for prostate PDT using interstitial diffuse optical tomography

X. Liang, T. C. Zhu, Univ. of Pennsylvania (United States)

Photodynamic therapy (PDT) is an important treatment modality for localized diseases such as prostate cancer. In prostate PDT, light distribution is an important factor because it is directly related to treatment efficacy. During PDT, light distribution is determined by tissue optical property distributions (or heterogeneity). In this study, an interstitial diffuse optical tomography (iDOT) method was used to characterize optical properties in tissues. Optical properties (absorption and reduced scattering coefficients) of the prostate gland were reconstructed by solving the inverse problem using an adjoint model based on diffusion equation using a modified matlab public user code NIRFAST. In the modified NIRFAST method, linear sources were modeled for the reconstruction. Cross talking between absorption coefficients and reduced scattering coefficients were studied to have minimal effect, and a constrained optical property method (set either absorption coefficient or reduced scattering coefficient to be homogeneous) is also studied. A prostate phantom with optical anomalies was used to verify the iDOT method. The reconstructed results were compared with the known optical properties, and the spatial distribution of optical properties for this phantom was successfully reconstructed.

8210-12, Session 3

## Photoacoustic imaging of intravenously injected photosensitizer in rat burn models for efficient antibacterial photodynamic therapy

Y. Tsunoi, Keio Univ. (Japan); S. Sato, H. Ashida, National Defense Medical College (Japan); M. Terakawa, Keio Univ. (Japan)

For efficient photodynamic treatment of wound infection, a sensitizer must be distributed in the whole infected tissue region, for which in vivo depth profile monitoring of a sensitizer is necessary. In this study, we applied photoacoustic (PA) imaging to visualize the depth profile of an intravenously injected sensitizer density in rat burn models. In burned tissue, pharmacokinetics is complicated, since vascular occlusion takes place in the injured tissue, while vascular permeability increases due to the thermal invasion. First, we used Evans Blue (EB) as a test drug to examine the feasibility of the PA imaging. An EB solution was intravenously injected into a rat deep dermal burn model. B-scan PA imaging was performed on the wound with 532-nm and 610-nm optical pulses for visualizing vasculatures and sensitizer, respectively. Just after the injection, the distributions of vascular signal and sensitizer signal spatially coincided well, showing a sensitizer inside the blood vessels. Afterwards, the peaks of the sensitizer signal were spatially broadened and then the signal profile got diffused in several hours, indicating vascular permeation and diffusion of EB molecules. Twelve hours after the injection, the sensitizer signal clearly appeared even in the zone of stasis, while no signal was detected in the subsurface region. The PA imaging was also performed for an actual sensitizer, sulfonated phthalocyanine, and its permeation and diffusion were visualized. However, the signal level and time course were different from those of EB. In conclusion, PA imaging is useful to observe sensitizer density profile for photodynamic bacterial inactivation.

8210-31, Poster Session

## Control of burn wound sepsis in rats by methylene blue-mediated photodynamic treatment

H. Hasegawa, Keio Univ. (Japan); S. Sato, D. Saitoh, N. Shinomiya, H. Ashida, National Defense Medical College (Japan); M. Terakawa, Keio Univ. (Japan)

Control of wound sepsis is an important challenge in traumatology. However, the increase in drug-resistant bacteria makes this challenge considerably difficult in recent years. In this study, we attempted to control burn wound sepsis in rats by photodynamic treatment, which has been reported to be effective against some drug-resistant bacteria. A 20% total body surface area full-thickness burn was made in rat dorsal skin, and five days after injury, a suspension of Ps. aeruginosa (ATCC 27853) was applied to the wound surface. Six hours after infection, a methylene blue (MB)-dimethyl suloxide solution was applied to the wound surface. Two hours later, the wound was illuminated with a 665-nm light emitting diode panel for 30 min. The light intensity on the wound surface was in the range of 3-4 mW/cm2 due to the element-by-element variation, the corresponding total light dose being 5.4-7.2 J/cm2. This treatment was performed daily for one week and thereafter, the numbers of bacteria in the blood and liver were counted based on colony forming assay. The numbers of bacteria of the treated group were one to two orders of magnitude less than those of the sham control group, showing a certain level efficacy. However, optimization of the treatment conditions is needed for improvement. Penetration depth of a sensitzer in the tissue, which was estimated to be 0.2 - 0.3 mm by the present surface delivery, should be increased. Combination of transvascular delivery with the surface delivery would be an effective approach, which also enables systemic photodynamic treatment.

8210-32, Poster Session

## Thermography for early detection of cancer

J. Kim, H. Choi, S. Ryu, M. Kook, G. Kim, G. Kim, K. Chang, Korea Basic Science Institute (Korea, Republic of)

Cancer is increasing fast nowadays through all over the world. Early diagnosis of cancer is a desirable subject as it can significantly improve the patient's chances of survival. In most cases the cancer is diagnosis using MRI, CT, PET. But, there are several disadvantages associated with high cost, low sensitivity and specificity, and health risks from radioactive. For that reason, significant efforts are being invested to improve the current imaging system.

Thermography can offer some advantages. Chief among these are the contact free and low cost for detect cancer. But thermography has some disadvantages associated with low sensitivity for small tumors.

In this research develops non contact, safe, high sensitivity, and low cost infrared imaging technique. Experiments were performed using lock in thermography with a small amount of magnetic nanoparticle(MNP) and radiofrequency generator. As a result, highly sensitive infrared thermography can a small amount of MNP be detected by the technique.

8210-34, Poster Session

## Maximizing fluence rate and field uniformity of light blanket for intraoperative photodynamic therapy

M. Goodwin, T. C. Zhu, J. C. Finlay, The Univ. of Pennsylvania Health System (United States)

The light blanket is designed with a system of cylindrically diffusing optical fibers which are spirally oriented. This 25x30 cm rectangular light blanket is capable of providing uniform illumination during intraoperative photodynamic therapy. The flexibility of the blanket proves to be extremely beneficial when conforming to the anatomical structures of the patient being treated. Previous tests of light distribution from the blanket have shown significant loss of intensity with the length of the fiber. This can be improved through the use of an optical adaptor which will be able to match the numerical aperture of the laser source to the numerical aperture of the blanket fiber; thus transmitting a higher percentage of light. Initial scans with an isotropic detector have also shown 'hot spots' of significant intensity at the corners of the blanket. The diffusing optical fibers have heightened leakage when bent (e.g. at the corners of the blanket) and create hot spots which compromise the homogenous fluence rate of the blanket. We address this through a custom-built partially-transmitting filter. The resulting emission distribution is uniform and provides sufficient power for clinical photodynamic therapy.

8210-35, Poster Session

## Photodynamic therapy is conservative approach for treatment of lymphangioma

A. A. Sultan, Univ. College London (United Kingdom); Z. Hamdoon, K. Karavidas, G. B. Bottini, Univ. College Hospital (United Kingdom); D. Muhammad Rashed, Univ. College London (United Kingdom); J. Lee, S. Morley, C. Hopper, Univ. College Hospital (United Kingdom)

A Conservative Approach for Treatment of Lymphangioma

A. A. Sultan (1,2,3), K. Karavidas(1), D. Muhammad Rashed(1,2), Y. Lee(1), S. Morley(1), C. Hopper(1,2,3)

1University College Hospital, London, UK

2Eastman Dental Institute, University College London, London, UK

3National Medical Laser Centre, Division of Surgery and Interventional Science, University College London, London, UK

Introduction: Lymphangiomas are lymphatic malformations which effect any age and any site in body; however 90% of disease effect children less than 2 years old and occur in the head and neck region. Treatment of lymphatic malformations involving the head and neck region remain to be challenging for aesthetic, function, vital structures and facial growth preservation reasons. We present two case reports of young children with treated oral lymphangioma using photodynamic therapy.

Materials and Methods: (case 1) 3 year old female child with unilateral facial, right cheek, lymphangioma and 7 year old male child (case 2) with tongue lymphangioma were referred to our clinic. A photosensitiser, 0.15 mg/kg Foscan (mTHPC), was given intravenously with four days drug light interval. Intra oral ultrasound guided interstitial photodynamic therapy used to treat the cheek lesion while the tongue lymphangioma illuminated by microlense fibre. 652 nm diode laser used to supply 20 J from each fibre. The lesions were evaluated by clinical examination and MRI or US scans.

Results: Case 1: Clinical examination after 3 months after treatment showed dramatic reduction in the size of the lesion and this confirmed with ultrasound. Lesion dimensions were reduced by 50% at 3 months with no affects on the surrounding vital structures such as the facial nerve.

Case 2: complete treatment response of a tongue lymphangioma was observed 8 weeks after the treatment.

Conclusion: Photodynamic therapy could be a valuable treatment for head and neck vascular and lymphatic malformations especially in young children where preservation of nerve function is so important. As these conditions are hard to completely eradicate, therapy must be repeatable and also allow normal growth. PDT offers just this possibility.

8210-36, Poster Session

## Double-excitation technique: eliminating tissue auto-fluorescence from in vivo PPIX measurements

S. Torosean, Dartmouth College (United States); J. Axelsson, B. W. Pogue, Thayer School of Engineering at Dartmouth (United States)

An Ultrasound coupled handheld-probe-based optical fluorescence tomography system has been in development for the purpose of quantifying the production of Protoporphyrin IX (PPIX) in Basal Cell Carcinoma (BCC) in vivo. The design couples fiber-based spectral sampling of protoporphyrin IX fluorescence emission with high frequency ultrasound imaging, allowing thin-layer fluorescence intensities to be quantified. The optical data are obtained by sequential excitation of the tissue with a 633nm laser, at four source locations and five parallel detections at each of the five interspersed detection locations. This method of acquisition permits fluorescence detection for both superficial and deep locations in ultrasound field. The optical boundary data, tissue layers segmented from ultrasound image and diffusion theory are used to estimate the fluorescence in these layers. To improve the recovery of the fluorescence signal of PPIX, eliminating tissue auto-fluorescence is of great importance. We propose the integration of an additional laser source at a wavelength just off of the excitation peak, namely at 637 nm. This is integrated into the hardware of the system, and provides a background signal allowing subtraction of the endogenous tissue auto-fluorescence spectrum from the fluorescence spectrum, specific for each subject under study. This system upgrade increases the sensitivity and precision of the fluorescence tomography system, paving the way for a more accurate photosensitizer dosimetry and better understanding of drug delivery to the malignant tissue in the course of photodynamic therapy (PDT).

Support:

This work has been funded by NIH Program Project P01CA84203.

8210-37, Poster Session

## Evaluating primary human ovarian cancer using a targeted multimodal theranostic agent

T. W. B. Liu, J. M. Stewart, Univ. of Toronto (Canada) and Ontario Cancer Institute (Canada); J. Chen, Ontario Cancer Institute (Canada); J. Shi, Univ. of Toronto (Canada); T. D. MacDonald, Univ. of Toronto (Canada) and Ontario Cancer Institute (Canada); B. C. Wilson, B. G. Neel, G. Zheng, Ontario Cancer Institute (Canada)

Ovarian cancer is the most frequent cause of death from gynecological cancer. Greater than 70% of patients are diagnosed with advanced stages of this disease, which has an associated 5-year survival rate of less than 30%. Conversely, the 5-year survival rate of patients diagnosed with stage I ovarian cancer is over 90%. The relationship between the stage at presentation and survival rate in ovarian cancer indicates a need to improve detection of early stage disease. Folate receptor targeted diagnostics and therapeutics have gained momentum in the past decade as the folate receptor is highly expressed in a variety of epithelial cancers, particularly ovarian cancer. We have constructed a porphyrin-peptide-folate (PPF) agent that has shown preferential accumulation in tumour tissues with tunable near infrared fluorescence and high folate receptor specificity and delivery efficiency. In addition to the fluorescent and photodynamic capabilities of porphyrins, they are also excellent metal chelators forming highly stable metallo-complexes making porphyrins efficient radioisotope delivery vehicles. Of particular interest is copper-64 (64Cu) as Cu-porphyrins are exceedingly stable to demetallation, have patient-tested non-toxicity, comparable 64Cu half-life with porphyrin pharmacokinetics and 64Cu-chelation does not alter the biodistribution of its host porphyrin. Here, we demonstrate the potential of PPF in selectively detecting (optical and PET imaging) and treating (photodynamic therapy) primary human ovarian cancer in SCID murine models. Not only may early detection of ovarian cancer be clinically feasible, PPF possesses fluorescence image-guidance capabilities for surgical debulking and PET imaging for treatment planning.

8210-38, Poster Session

## Photodynamic therapy: diagnostic and treatment applications

I. M. Ndhundhuma, Council for Scientific and Industrial Research (South Africa) and Univ. of Johannesburg (South Africa); H. Abrahamse, Univ. of Johannesburg (South Africa)

Photodynamic Therapy: Diagnostic and Therapeutic Applications

I.M. Ndhundhuma1,2 and H. Abrahamse2

1CSIR, NLC-Biophotonics Group, Pretoria, South Africa, 2Laser Research Centre, University of Johannesburg, Doornfontein, South Africa

Although pathologic examination remains the gold standard for diagnosis, cancer has the potential to be diagnosed through minimally invasive approaches because of its cutaneous location. A pathologist's ability to detect cutaneous cancers in their earliest form has been amplified. However, the problem with skin biopsies are that a pathology report is highly dependent on the quality of the biopsy that is submitted and when it is performed incorrectly, and without appropriate clinical information, a pathologist's interpretation of a skin biopsy can be severely limited. As current approaches are refined and new techniques are developed, the improved ability to diagnose and treat cancer will enhance reaching the goal of reducing cancer mortality rates.

Photodynamic therapy (PDT) has been established as a selective treatment modality for some medical indications during the last three decades1. Photodynamic diagnosis (PDD), a fluorescence based technique defined from the photodynamic therapy principle, involves a combination of a fluorescent tumor-localizing photosensitizer (PS) with light and is currently under investigation as an early cancer detection tool2. Considerable evidence has indicated that a suitable PS for PDT or PDD should selectively and preferably localize in tumor cells rather than in normal surrounding cells3. In this study, a laser scanning confocal microscope (LSCM) was used to compare fluorescence localization of hypericin, a naturally occurring photosensitizer, in normal (fibroblasts) and cancerous skin cells (squamous cell carcinoma). A higher uptake and fluorescence localization of hypericin in cancer cells was observed.

References

1. Dougherty T, Gomer C, Henderson B, Jori G, Kessel D, Korbelik M, Moan J and Peng Q 1998 Photodynamic Therapy Journal of the National Cancer Institute 90 (12) 889

2. Moghissi K, Stringer M R, Dixon K 2008 Fluorescence photodiagnosis in clinical practice Photodiagnosis Photodyn Ther 5 235

3. Huang Z, Xu H, Meyers A D, Musani A I, Wang L, Tagg R, Barqawi A B, Chen Y K 2008 Photodynamic therapy for treatment of solid tumors - potential and technical challenges, Technol Cancer Res Treat 7(4) 309

8210-39, Poster Session

## Optimization of parameters in photodynamic therapy to kill p. aeruginosa with 809-nm diode laser and indocyanine green

N. Topaloglu, S. Yüksel, M. Gülsoy, Bogaziçi Üniv. (Turkey)

The emergence of antibiotic resistant bacteria causes significant increase in deaths due to infections around the world. Nowadays, it could be impossible to find appropriate antibiotics to treat some bacterial strains, especially multidrug resistant types. Therefore, there is an urgent need to develop new and safe treatment techniques for multidrug resistant bacteria associated morbidity and mortality. In this study, Photodynamic Therapy was used to destroy these kinds of bacteria with near infrared light and Indocyanine Green. Different wavelengths of lasers mostly in the visible spectrum have been investigated for Photodynamic Therapy; however near infrared lasers have been used in very few studies. The main motivation to test photodynamic therapy with near infrared light and indocyanine green is that the near infrared laser (around 800-nm) has more penetration depth in the biological tissue than the other lasers have. Therefore it is supposed that it will show more antibacterial effect. And also indocyanine green has a very low toxicity and an FDA-approved drug. This study investigated optimum parameters for PDT with 809-nm laser and Indocyanine green (ICG) to kill P. aeruginosa strain (ATCC 27853) in vitro. We were able to optimize the laser power and ICG concentration to non-toxic levels and achieved 99% decrease in bacterial load with 240 J/cm2 laser light and 150 µg/ml ICG concentration. This study demonstrates that PDT with near-infrared light and ICG can be powerful and non-hazardous treatment strategy for untreatable pathogens.

8210-40, Poster Session

## Modeling stromal determinants of ovarian cancer growth and response to PDT-chemotherapy combinations

I. Rizvi, J. P. Celli, S. R. Anbil, S. A. Elrington, I. Massodi, Massachusetts General Hospital (United States); U. Gurkan, U. Demirci, Brigham and Women's Hospital (United States); T. Hasan, Massachusetts General Hospital (United States)

The complex biology, significant treatment-related toxicities, and persistently poor outcomes associated with residual ovarian carcinomatosis underscore the need for sophisticated screening tools to identify more effective therapeutic strategies. Among the critical determinants of ovarian cancer growth and treatment response is communication between tumor cells and stromal components such as endothelial cells. Clinical samples of peritoneal malignancies, including ovarian metastases, as small as 1mm show evidence of vascularity that may lack functionality. The role of endothelial cells as signaling partners that influence growth and confer treatment resistance in ovarian cancer remains poorly understood. Motivated by these observations and questions, we investigate the impact of incorporating endothelial cells into a 3D model for micrometastatic ovarian cancer previously developed in our laboratory. We leverage the rapid, quantitative image analysis capabilities of this platform to characterize the growth dynamics of heterocellular ovarian micronodules and generate comprehensive dose response matrices to establish the interaction of chemotherapeutic cocktails commonly used to manage ovarian cancer. To enhance the efficacy of these multi-line chemotherapy regimens, combinations with Verteporfin-based photodynamic therapy are evaluated with the goal of reducing tumor volume and viability at the treatment site and mitigating tumor attachment and growth at secondary sites from cells under flow conditions.

8210-41, Poster Session

## Histological differences between orthotopic xenograft pancreas models affect verteporfin uptake measured by fluorescence microscopy and spectroscopy

K. S. Samkoe, Dartmouth Hitchcock Medical Ctr. (United States); J. A. O'Hara, Dartmouth Medical School (United States); A. Chen, M. E. Isabelle, Dartmouth College (United States); P. J. Hoopes, Dartmouth Medical School (United States); T. Hasan, Wellman Ctr. for Photomedicine (United States); B. W. Pogue, Dartmouth College (United States)

No abstract available

8210-42, Poster Session

## Tissue photosensitizer dosimetry using spectrally-resolved fluorescence for pre-clinical and clinical verteporfin-PDT of pancreatic cancer

M. E. Isabelle, Dartmouth College (United States); S. C. Davis, Thayer School of Engineering at Dartmouth (United States); Z. Li, Dartmouth College (United States); J. A. O'Hara, Dartmouth Medical School (United States); K. Samkoe, Thayer School of Engineering at Dartmouth (United States); P. J. Hoopes, Dartmouth Medical School (United States); S. Pereira, Univ. College Hospital (United Kingdom); C. A. Mosse, Univ. College London (United Kingdom); T. Hasan, Massachusetts General Hospital (United States); B. W. Pogue, Thayer School of Engineering at Dartmouth (United States)

PDT mediated with verteporfin is currently being investigated to treat pancreatic cancer in patients who are not surgical candidates1. Clinically, interstitial light delivery is administered through a fiber, via percutaneous needle implantation guided by ultrasound and/or verified by CT. Tumor response to PDT is based on photosensitizer (PS) dose, light dose, light dose rate and the timing of light application following PS injection. However, studies2,3 have shown that even when matching administered PDT treatment parameters such as drug dose and light level, there can be significant inter-patient variation in tissue damage post-PDT, and this has been primarily attributed to imprecise PS concentration at the target tissue site4.

In order to achieve optimal tumor response from PDT without causing major damage to surrounding tissue, it would be advantageous to measure the PS concentration in the target tissue just prior to light application. From these measurements, the clinician can adapt the light application dose to the measured target tissue PS concentration (i.e. insufficient target tissue PS concentrations compensated by higher light doses and vice versa.) in order to provide an optimal light dose for each patient.

In our animal studies, we are using CCD-based in-vivo fluorescence dosimetry to assess accumulated PS levels (verteporfin) in situ. Measurements are taken from leg muscle, buccal mucosa and tumor tissue locations one hour after injection of the photosensitizer. Real-time subtraction of background autofluorescence and ratiometric analysis is performed on the raw data to extract out only the photosensitizer fluorescence and therefore concentration. Using a pre-measured calibration data set of varying concentrations for verteporfin in tissue phantoms composed of intralipid and whole blood, it was possible to accurately assess the local concentration of the photosensitizer at these different tissue locations.

In the clinical studies being performed at UCL Hospital in which Verteporfin-PDT treatment is being given to patients with pancreatic cancer, the dosimetry system is being used to assess PS concentration the pancreatic tumor tissue prior to interstitial light dose treatment. The goal here is to determine whether the dosimetry system can accurately and efficiently be used clinically by evaluating the measured local tissue PS concentration to treatment outcome (area of necrosis established). The results of this study will determine the need for fluorescence dosimetry to individualize PDT treatment for patients based on local tissue PS concentration.

[ ] VERTPAC - phase I trial of verteporfin photodynamic therapy for locally advanced cancer of the pancreas. Trials and research. CancerHelp UK. Accessed on: April 20th 2010. http://www.cancerhelp.org.uk/trials/a-trial-of-verteporfin-photodynamic-therapy-for-locally-advanced-cancer-of-the-pancreas

[2] Braichotte DR, Savary JF, Monnier P, van den Bergh HE. Lasers Surg Med. 1996;19(3):340-346.

[3] Grosjean P, Savary J, Wagnières G, Mizeret J, Woodtli A, Theumann J, et al. Lasers in Medical Science. 1996 Dec 28;11(4):227-235.

[4] Zhou X, Pogue BW, Chen B, Demidenko E, Joshi R, Hoopes J, Hasan T. International Journal of Radiation Oncology Biology Physics. 2006; 64(4): 1211-1220.

8210-13, Session 4

## The role of bone marrow derived cells in photodynamic therapy responsiveness

C. J. Gomer, Children's Hospital Los Angeles (United States) and Univ. of Southern California (United States)

Photodynamic therapy (PDT) continues to be used in the clinical treatment of a variety of solid tumors. This procedure is effective but it has not yet received an appropriate level of acceptance, support, or use. Methods to further enhance the differential photosensitization of malignant tissue could lead to increased clinical acceptance and use of PDT. We hypothesize that PDT induces prosurvival responses within the tumor microenvironment that negatively modulates overall treatment effectiveness. Specifically, the re-establishment of functioning blood vessels following PDT can lead to tumor recurrences and therefore targeted approaches to block post-treatment angiogenesis and vasculogenesis are clinically relevant avenues of investigation. Our laboratory continues to investigate the role(s) of bone marrow derived cells that infiltrate tumor tissue following PDT. Contributions of cells from the monocyte/macrophage and the endothelial cell lineages are being examined in the context of how these cells and factors released from these cells contribute to post-PDT survival and growth in tumor xenograft models. An update of our results will be presented.

8210-14, Session 4

## Microendoscopy guided photodynamic therapy of ovarian cancer

B. Q. Spring, A. O. Abu-Yousif, X. Zheng, T. Hasan, Massachusetts General Hospital (United States)

We are developing photodynamic therapy (PDT) of metastatic ovarian carcinoma (OvCa) to overcome the poor therapeutic index of current modalities and to address chemoresistant disease. A key challenge is the micronodular and multifocal nature of OvCa tumors disseminated throughout the peritoneal cavity. A multifunctional photoimmunoconjugate targets OvCa cells for fluorescence detection and for selective PDT of the tumors with minimal damage to the neighboring tissues. For image-guidance, a custom-built fluorescence microendoscope (FME) enters the body via a catheter to enable minimally invasive, in vivo microscopy. The FME was applied to determine optimal parameters for PDT and for monitoring treatment response.

8210-15, Session 4

## Mechanistic studies on thiaza and thioxa-based type 1 photosensitizers

R. Rajagopalan, Covidien (United States); T. Lin, R. Loomis, J. Wei, Washington Univ. in St. Louis (United States); A. R. Poreddy, A. Karwa, B. Asmelash, R. B. Dorshow, Covidien (United States)

Photosensitizers operate via two principal mechanisms: Type 1 and Type 2. In Type 1 process, the excited photosensitizer may interact directly with the tissues, produce reactive intermediates such as free radicals, nitrenes, etc. through photofragmentation, or generate secondary reactive oxygen species via collision of these reactive intermediates with molecular oxygen. We have prepared and tested several thiaza and thioxa compounds that are designed to operate via Type 1 process. Exposure of these compounds in the presence of UVA or UVB light resulted in cell death in a dose- and time-dependent manner. However, the cell viability activity of these photosensitizers varied substantially depending on the molecular structure. In order to explain the observed differences among the photosensitizers, ESR and ultrafast laser flash photolysis studies were undertaken. The results show that all the compounds generated copious free radicals upon photoexcitation. Laser flash photolysis studies indicated a substantial difference in the electronic spectra between the active and inactive compounds. These results of these studies and possible mechanism will be presented.

8210-17, Session 5

## Development of photodynamic therapy for pancreatic cancer

K. K. Wang, Mayo Clinic (United States)

Pancreatic cancer is one of the most deadly malignancies in humans. Life expectancy after diagnosis is typically less than one year. The purpose of these studies was to develop PDT for use in pancreatic cancers. This involved a series of studies:

1) Testing of pancreatic cell lines for susceptibility to HPPH mediated PDT. These studies demonstrated that pancreatic cell lines are as susceptible to PDT as esophageal cell lines.

2) Assessment of HPPH concentration in vitro using a fluorescence spectroscopy device that can be placed through an endoscope to assess concentration within the mucosa. The correlation of the degree of fluorescence with the concentration of drug in tissue phantoms was r=0.9 including after addition of blood components.

3) Development of a through the scope photoradiation device that can photoradiate the tumor under direct visualization. This was created and can uniformly radiate an area of approximately 1 cm without thermal effects.

Conclusions: We believe that PDT using HPPH is feasible for the palliation of pancreatic carcinoma.

8210-18, Session 5

## Qualitative and quantitative differences in the toxicity of HPPH-mediated PDT with a 24 versus 48-hour drug light interval: moving from the bedside to the bench and back

K. A. Cengel, Univ. of Pennsylvania School of Medicine (United States); S. Yendamuri, T. Demmy, Roswell Park Cancer Institute (United States); M. Culligan, The Univ. of Pennsylvania Health System (United States); M. Schofield, D. Smith, S. Punekar, D. Sterman, J. Stevenson, T. M. Busch, E. Glatstein, S. M. Hahn, J. S. Friedberg, Univ. of Pennsylvania School of Medicine (United States)

In this study, we have evaluated the toxicity of pleural HPPH-mediated PDT as an intraoperative adjuvant to lung-sparing, macroscopically complete surgical resection for patients with malignant pleural dissemination. The PDT dose was increased by either shortening the drug light interval or increasing the light dose. To date, 18 patients with pleural dissemination of malignancy limited to one hemithorax (14 MPM, 4 carcinoma metastatic to pleura) have been treated at 5 dose levels. In 17 patients treated with a 48h drug light interval, DLT was observed in two of six subjects treated at the 45J/cm2 light dose in the form of cardio-pulmonary complications with onset of toxicity at 3 and 14 days post-surgery/PDT. One patient treated at a 24h drug light interval and 15 J/cm2 light dose experienced DLT in the form of systemic edema-related complications beginning within hours after the surgery/PDT. In preliminary studies of PDT therapeutic index using ectopic murine AB12 mesothelioma tumors, a similar level of cure rate could be achieved in mice by a 2-2.5-fold increase in light dose with 48h as compared to 24h drug light interval. However, at these light doses, the animals treated with 48h drug light interval experienced a delayed onset of edema with significantly less skin damage. Thus, HPPH-mediated PDT can be safely combined with surgical resection with a 48h drug light interval and the present results suggest that the therapeutic index of intraoperative, pleural HPPH-mediated PDT may be more favorable with a 48h versus 24h drug light interval.

8210-19, Session 5

## Activation of p53-mediated apoptosis in squamous cell carcinoma tumors in vivo, during combination treatment with 5-fluorouracil and ALA-photodynamic therapy

E. V. Maytin, S. Anand, K. Rollakanti, N. Brankov, K. Iyer, The Cleveland Clinic (United States)

We are interested in ways to improve the effectiveness of photodynamic therapy (PDT) in which aminolevulinic acid (ALA) drives the synthesis of the intracellular photosensitizer, protoporphyrin IX (PpIX). In previous work, we showed that PpIX levels are significantly enhanced by a combination approach in which Vitamin D or methotrexate (MTX) are given for several days prior to ALA. Here, we report that 5-fluorouracil (5-FU) preconditioning of deep A431 tumors in nude mice (squamous carcinoma cells implanted subcutaneously) causes a significantly enhanced PDT response, via mechanisms that involve elevated p53 levels and apoptosis. After giving 5-FU (intraperitoneal, 300 mg/kg, daily for 3 days) and ALA (4 hours), PpIX levels detected in tumor frozen sections by confocal microscopy equaled or exceeded PpIX levels induced by pretreatment with MTX. The 5-FU preconditioning inhibited DNA synthesis (reduction in Ki67 labeling), and stimulated cellular differentiation (increase in E-cadherin staining). Because 5-FU is known to cause damage-related upregulation of p53 as a result of misincorporation of the fluoronucleotide into RNA and DNA, we examined levels of p53 and related molecules in the tumors by immunostaining. After 5-FU preconditioning, p53 was strongly upregulated, as were the downstream target molecules p21 (cip-1/waf-1) and p27 (cyclin dependent kinase inhibitor 1B; kip-1). Levels of p19/Arf (which regulates MDM2 stability) were not altered. Following ALA-PDT, TUNEL-labeling (apoptosis) was selectively and significantly increased in the 5-FU preconditioned tumors, relative to unconditioned controls. Overall, these data suggest that a sequence-specific combination regimen with 5-FU and ALA-PDT offers therapeutic promise.

8210-20, Session 6

## Light dose mapping in pancreatic PDT trial VERTPAC to compare with volume of necrosis in treatment outcome

B. W. Pogue, M. Jermyn, S. C. Davis, Thayer School of Engineering at Dartmouth (United States); S. Mosse, M. Huggett, S. P. Pereira, Univ. College London, National Medical Laser Ctr. (United Kingdom); T. Hasan, Wellman Ctr. for Photomedicine (United States)

Accurate light dose modeling is a critical part of understanding PDT treatment effect, yet in many cases the treated tissue is so complex and the uncertainty of the tissue optical properties is so high, that the simulations can be meaningless. In this work, the methodology for dosimetry calculations in pancreas cancer PDT was developed. High resolution diagnostic pre-treatment scans were used for tissue segmentation of the pancreas and tumor for light dose modeling, but with the location of the treatment diffuser fiber needing to be determined from lower resolution interventional scans. The interventional scans were used to verify the percutaneous needle placement during the procedure, and so the location of the treatment fiber was extracted from these and rigidly mapped onto the higher resolution diagnostic scans, using anatomic fiducials. The diagnostic scans provide the sequence of contrast agent imaging, which is used to verify where major blood vessels are located and to map these into the absorption coefficients of the optical diffusion simulation. This methodology for simulating the light delivery was developed for the first time and evaluated to determine the effect of the neighboring major vessels upon the light distribution. Here simulations were used to estimate the deposited dose, and the 3D map used to determine correlation with photosensitizer dosimetry at the site of the treatment fiber, and to the treatment outcome in terms of volume of necrosis as seen on the 4-day post treatment contrast CT scan.

8210-21, Session 6

## Induction of cutaneous phototoxicity after photodynamic therapy by over-exposure to CRT and LCD monitor: a simulation study

T. Lei, S. Pendyala, L. Scherrer, Z. Huang, Univ. of Colorado Denver (United States)

Cutaneous phototoxicity induced by over-exposure to cathode ray tube (CRT) monitor has been reported but the light emission profiles of CRT monitors have not been fully studied yet. The aim of this study was to investigate the light emission profiles of CRT and liquid crystal display (LCD) monitor and their implication in potential cutaneous phototoxicity after photodynamic therapy (PDT). CRT and LCD color monitor (17 inches) were used as model monitors. Pre-recorded video game and movie streams were played back on each screen for a time period of 10 min. Light emission profiles of both monitors including fluence and wavelength distributions were recorded at 18 inches away from the centre of the monitor screen (imitating facial exposure) and the surface of computer keyboard (imitating hand exposure), respectively. The wavelength distribution profiles matched the absorption peak(s) of commonly used PDT photosensitizers. This study confirms that the over-exposure of the skin directly to the CRT or LCD color monitors after the topical or systemic administration of a photosensitizer is a risk factor that in combination with the residual photosensitizer in the skin tissues can induce cutaneous phototoxicity. Post PDT light restriction in patient warning should include the avoidance of over-exposure to any bright color monitors.

8210-22, Session 6

## A compact laparoscope type radiation source for the pin-point cancer treatment using a femtosecond laser

N. Kawashima, Kinki Univ. (Japan)

Focusing a femto-second laser (1 mJ/pulse repetition 1 kHz) on a special tape, a strong radiation consisting of the electron beam ~ 200 keV and X-rays ~ 6.4 keV(5 %) has been generated. It has been verified that the radiation source is sufficient to kill the cancer cells and to show the DNA laddering structure in the in-vivo test using cancer cells.

More test implanting the cancer under the skin of mouse and irradiating the laser-generated radiation on the deseased area, we have shown its clear powerful therapeutic capability. about 80 % of mice irradiated, their cancer almost disappeared. For further clinical test use, a compact laparoscope-type unit mounted on an articulated arm has been constructed and it can generate the necessary amount of radiation dose.

8210-23, Session 6

## Influence of the photosensitizer photobleaching in the propagation of light during photodynamic therapy

I. Salas-García, F. Fanjul-Vélez, N. Ortega-Quijano, J. L. Arce-Diego, Univ. de Cantabria (Spain)

Photodynamic Therapy (PDT) is an optical treatment modality used in several clinical fields to destroy malignant tissues. It consists on the administration of a photosensitive substance which is activated by the posterior irradiation of the tumoral area. As a consequence reactive oxygen species are produced. Nowadays there are fixed clinical PDT protocols that make use of a particular optical dose, photosensitizer amount and drug-light interval. However the treatment response varies depending on the type of pathology and the patient. In order to adjust current dosimetry to get an optimal treatment outcome, the development of accurate predictive models has emerged as the ideal tool to achieve new personal protocols. Several attempts have been made in this way although the influence of the photosensitizer distribution on the optical parameters has not been taken into account till this moment. We present a first approach to predict the spatial-temporal variation of the absorption coefficient during the photodynamic process applied to a dermatological disease taking into account the photobleaching of a topical photosensitizer. The model presented also takes into account an inhomogeneous initial distribution of the photosensitizer, the propagation of light in the biological media and the evolution of the molecular concentrations of different components involved in the photochemical reactions. The obtained results permit us to investigate how the depletion of the photosensitizer during the photochemical reactions affects to the light propagation in the target tissue.

8210-24, Session 7

## Selectivity of Amphinex® based bleomycin photochemical internalization in the Syrian hamster cheek pouch tumour model

A. A. Sultan, T. Wang, J. H. Woodhams, Univ. College London (United Kingdom); A. Jay, Univ. College Hospital (United Kingdom); K. Berg, Oslo Univ. Hospital (Norway); A. Høgset, PCI Biotech AS (Norway); A. J. MacRobert, S. G. Bown, C. Hopper, Univ. College London (United Kingdom)

Selectivity of Amphinex® based bleomycin photochemical internalization in the Syrian hamster cheek pouch tumour model

Ahmed A. Sultan 1,2,3, Julie Tzu-Wen Wang 1, Josephine Woodhams 1, , Amrita Jay 3, Kristian Berg 4, Anders Høgset 5, Alexander MacRobert1, Stephen G. Bown 1,3, Colin Hopper 1,2,3

1National Medical Laser Centre (UK), Division of Surgery and Interventional Science, University College London, London, UK

2Eastman Dental Institute (UK), University College London, London, UK

3University College Hospital (UK), London, UK

4Oslo University Hospital, Oslo, Norway

5PCI Biotech

Introduction: Photochemical internalisation (PCI) is a technology which involves releasing therapeutic molecules into the cell cytosol using a sublethal photochemical treatment with the photosensitiser Amphinex®. Tumour selectivity was observed clinically in some patients in a phase I clinical trial. To study this, further experiments were undertaken on squamous cell carcinomas transplanted into the hamster cheek pouch.

Material and methods: Biodistribution of TPCS2a (Amphinex®, PCI Biotech AS, Norway) in the normal and cancerous hamster cheek pouch was studied using fluorescence microscopy and spectroscopy after i.p injection of 1 mg/kg. ImageJ software was used to measure the fluorescence uptake and to determine the optimum drug light interval for preferential uptake in tumour tissue.

PDT and PCI treatments were carried out using 0.5 mg/kg Amphinex® administered i.p. 96 hours before light with bleomycin, (60,000 IU/kg) given 2hours before illumination (laser 652nm, 100mW/cm2, 15 J/cm2 ), lowest doses to give detectable effect from PDT alone, to tumour and surrounding normal mucosa were assessed. The response was assessed macroscopically and microscopically at day 4 using tissue damage scale (Borle et al, 2003).

Results: Selectivity of Amphinex® uptake was greatest 96h after administration (2:1 tumour:normal). Histologically, PCI demonstrated selective damage in the cancer; adjacent illuminated normal mucosa was left intact (minimum inflammatory cell infiltration in underlying connective tissue). Also PCI demonstrated a synergistic necrotic effect in comparison with PDT alone.

Conclusion: PCI may be able to produce selective necrosis of cancer with a minimal effect on the surrounding normal tissues.

8210-25, Session 7

## Photodynamic therapy of pleurally disseminated non-small cell lung carcinoma in an orthotopic murine model

C. E. Grossman, S. Pickup, A. Durham, E. P. Wileyto, M. E. Putt, T. M. Busch, Univ. of Pennsylvania (United States)

Photodynamic therapy (PDT) for disseminated malignancies of the thoracic surfaces is a challenging application with substantial clinical potential. By using orthotopically-propagated tumors, a more relevant pre-clinical and biological model compared to their heterotopic counterparts can be exploited to study such human diseases. We therefore employed a murine orthotopic model to evaluate PDT of pleurally disseminated non-small cell lung carcinoma (NSCLC). Twelve days after intrathoracic injection of H460 cells into nude mice, multinodular disseminated disease limited to the bilateral thoracic cavity was detected. At this timepoint, HPPH-mediated PDT was delivered interstitially with a 1-cm cylindrical diffusing fiber (150 mW/cm, 661-nm) and successfully reduced tumor mass by >2-fold at fluences of 50-200 J/cm. PDT effect (pre- vs. post-treatment) within an individual animal was assessed using magnetic resonance imaging (MRI), after demonstrating a linear relationship existed between extracted tumor mass and imaged tumor volume ($r2 \geq 0.8$). An abrogated increase in tumor volume was observed in mice five days after PDT (compared to control-treated animals, $p = 0.04$). Interestingly, this PDT-associated reduction in tumor burden was uniform, without any spatial predominance. Normal tissue damage, consisting of edema, fibrin deposition, and neutrophil infiltration within the lung parenchyma was identified by histopathology 24 hours after PDT. This occurred concomitantly with an acute systemic inflammatory response consisting of thrombocytopenia, anemia, and neutrophilia in the blood. Our findings establish a feasible and effective intracavitary PDT regimen in a pre-clinical model of disseminated NSCLC and support additional studies to improve clinical outcomes of this aggressive disease.

8210-26, Session 7

## Accurate dosimetry for monitoring response to photodynamic therapy

M. Seetamraju, R. S. Gurjar, R. Myers, Radiation Monitoring Devices, Inc. (United States); T. Hasan, Wellman Ctr. for Photomedicine (United States); D. E. Wolf, Radiation Monitoring Devices, Inc. (United States)

Photodynamic therapy (PDT) for treatment of cancer and other conditions, involves the interplay between three main variables - photosensitizer (PS), molecular oxygen and NIR light. During PDT, it is unclear whether variances in either irradiance, the amount of PS or oxygen are the sources of varying treatment responses in animals of the same treatment group. This suggests that it is very important to develop a more accurate, complete, and reliable dosimetry technique, by monitoring all three PDT variables in order to determine an optimized dose that will lead to improved treatment efficacy. The currently used explicit dosimetric techniques for PDT fail to take into account tissue variability between individuals and the dynamically changing local tissue oxygenation and have not resulted in reliable correlation with treatment outcome.

We have developed an implicit dosimetric method for PDT that is proportional to the amount of PS and molecular oxygen present in the surrounding tissue and directly related to the quantum yield of singlet oxygen generated during PDT. Experiments performed with the PDT drugs; Benzoporphyrin Derivative monoacid ring A (BPD-MA) and Protoporphyrin IX (PpIX), showed that their transient NIR emission signatures exhibited long-lived weak luminescence whose lifetime and intensity varied as a function of the oxygenation level of the solution. We show that these parameters correlate with oxygenation in the tissue and offer a better algorithm to determine PDT dose. This approach uses the same tools presently available for PDT, making it attractive to health professionals, without increasing treatment cost or instrument complexity.

8210-27, Session 7

## Photodynamic therapy for the management of leukoplakia and oral lichen planus using methylene blue

C. Pravada, Sathyabama Deemed Univ. (India); E. Ingle, J. Vadivel, D. Koteeswaran, Meenakshi Ammal Dental College & Hospital (India); W. P. Savarimuthu, G. Bharanidharan, P. R. Aruna, Anna Univ. Chennai (India); C. Muralikrishna, Advanced Ctr. for Treatment, Research & Education in Cancer (India); S. Ganesan, Anna Univ. Chennai (India)

In this study, methylene blue-mediated photodynamic therapy (MB-PDT) was used as a possible alternative method for the treatment of Oral Lichen planus (OLP) and Oral Leukoplakia (OL).6 patients with 15 OLP lesions and 14 patients with 20 OL lesions were enrolled in the study. The patients were irradiated using xenon arc lamp filtered at $\lambda$=630nm, with a light exposure dose of 120J/cm2. Lesions were evaluated pre and post and at follow-up sessions by changes in signs and symptoms scores, and size of lesions. There was a statistically significant decrease in size, sign and symptom score after treatment and at follow-up session. The details of the results will be discussed.

8210-29, Session 7

## Singlet oxygen dosimetry modeling for photodynamic therapy

X. Liang, T. C. Zhu, Univ. of Pennsylvania (United States)

Photodynamic therapy (PDT) is an important treatment modality for cancer and other localized diseases. In addition to PDT dose, singlet oxygen concentration is used as an explicit PTD dosimetry quantity, because singlet oxygen is the major cytotoxic agent in photodynamic therapy, and the reaction between singlet oxygen and tumor tissues/cells determines the treatment efficacy. Singlet oxygen concentration can be obtained by the PDT model, which includes diffusion equation for the light transport in tissue and macroscopic kinetic equations for the generation of the singlet oxygen. This model was implemented using finite-element method (FEM) by COMSOL. In the kinetic equations, 5 photo-physiological parameters were determined explicitly to predict the generation of singlet oxygen. The singlet oxygen concentration profile was calculated iteratively by comparing the model with the measurements based on mice experiments, to obtain the apparent reacted singlet oxygen concentration as an explicit PDT dosimetry quantity. Two photosensitizers including Photofrin and Verteporfin, were tested using this model to determine their photo-physiological parameters and the reacted singlet oxygen concentrations.

8210-30, Session 7

## Binding potential can determine tumor epidermal growth factor receptor status in response to photodynamic therapy in pancreatic cancer

K. S. Samkoe, Dartmouth Hitchcock Medical Ctr. (United States); K. M. Tichauer, Thayer School of Engineering at Dartmouth (United States); J. Gunn, Thayer School of Engineering at Dartmouth (USA); T. Hasan, Wellman Ctr. for Photomedicine (United States); B. W. Pogue, Dartmouth College (United States)

Verteporfin photodynamic therapy (PDT) for the treatment of pancreas cancer (PCa) is showing promise as a therapy for patients with unresectable tumors. Measured changes in tumor volume are the conventional indicator for tumor status post-therapy and, as such, magnetic resonance (MR) imaging was investigated to assess in vivo tumor status at 48-hours post-PDT in a xenograft orthotopic PCa mouse model. Total tumor and vascular volumes were determined pre- and post-PDT using T2-weighted and gadolinium-enhanced contrast MR imaging. Although an overall decrease in vascular volume was observed, inflammation in the PDT-treated tissues caused an apparent increase in total tumor volume making it difficult to determine the tumor status. Recent alternative approaches to monitoring tumor status exploit the overexpression tumor-specific cell-signaling receptors (e.g., epidermal growth factor receptor (EGFR)) that cause increases in tumor growth, replication and invasiveness. In general, these approaches involve injecting a molecular imaging agent targeted to the receptor of interest and then imaging the in vivo distribution of the agent after some interval. The idea then is that locations of image contrast represent the tumor volume. Aside from tumor volume, image contrast has the potential to indicate tumor receptor status; however, the contrast can be skewed by the enhanced permeability and retention effect and agent delivery (i.e., hemodynamics), as well as the inflammation that occurs after PDT, and is therefore unable to accurately quantify targeted agent binding. Recently, we have demonstrated a novel method of quantification where an EGFR targeted and non-targeted agent are administered and imaged simultaneously. Computational analysis of the uptake curves provides the binding potential (BP), a unit-less measure of both receptor density and ligand binding affinity. Here we monitor orthotopic PCa response to interstitial verteporfin PDT (1mg/kg, 20J/cm) using three methods: Gd-MRI, fluorescence contrast imaging and BP determination to elucidate the most promising method to establish tumor status post-PDT.

# Conference 8211: Mechanisms for Low-Light Therapy VII

Saturday 21 January 2012

Part of Proceedings of SPIE Vol. 8211 Mechanisms for Low-Light Therapy VII

8211-01, Session 1

## Penetration of light into living tissue

L. Hode, Swedish Laser-Medical Society (Sweden); P. Jenkins, Irradia USA (United States); J. Tunér, Dala Dental (Sweden); T. Hode, Immunophotonics, Inc. (United States)

At some time or another in every young scientist's formative years, he or she has experimented by shining a flashlight through their fingers or, even more fun, up their own nose, to discover that the flashlight's white light not only penetrates through their appendages but also glows red on the other side, thus leading them to the conclusion that some light, but not all, can pass through tissue. Now our young scientist is older and more learned, and she understands that living tissues are a highly-complex, dynamic turbid medium, the optical properties of which are defined by varying rates of absorption, scattering, transmission and reflection. She also knows that different imaging techniques, such as optical coherence tomography (OCT), laser doppler flowmetry and transmissive laser speckle imaging (TLSI), rely upon an understanding of these complex optical properties. Penetration of living tissue - the subject of this particular discussion - depends on parameters like wavelength, intensity, polarization and coherence of the light source, tissue compression and those of the tissues themselves, like pigmentation, fibrotic structure, hydration and composition, in addition to more obvious factors such as hair and clothes. In a series of experiments we study how different forms of light penetrate into different forms of tissue, and we discuss a dynamic interference that follows changes in this medium due to microscopic movements of scattering particles in real time. We further relate the performance of the algorithm to the measured timescale of the changes in the speckle pattern created in a volume of laser-irradiated tissue, and analyze our experiment in the light of laser phototherapy.

8211-02, Session 1

## Mechanisms for low level light therapy - what's new?

M. R. Hamblin, Y. Huang, S. K. Sharma, Wellman Ctr. for Photomedicine (United States)

It is accepted that photons are absorbed in the mitochondria of cells and lead to increase of mitochondrial metabolism resulting in more electron transport, increase of mitochondrial membrane potential, and more ATP production. Intracellular calcium changes are seen that correlate with mitochondrial stimulation. The situation with two other intermediates is more complex however: reactive oxygen species (ROS) and nitric oxide (NO). Evidence exists that low levels of ROS are produced by low-level light that can be beneficial to cells by (for instance) activating NF-kB. However high fluences of light can produce large amounts of ROS that can damage the cells. Furthermore cells that are under oxidative stress have their elevated levels of ROS reduced by low dose light. NO signaling in response to light is less well understood but several reports have shown NO is released.

8211-03, Session 1

## LLLT biphasic dose response: update

J. D. Carroll, THOR Photomedicine Ltd. (United Kingdom)

It is well established that if an LLLT light source is of insufficient irradiance or irradiation time then there is no response. If the irradiance is too high or irradiation time is long then the response may be inhibited. Somewhere in between is the optimal combination of irradiance and time for stimulation. This dose response often likened to the biphasic response known as "Arndt-Schulz Law" or the more credible term known as Hormesis. The phenomena is not new, it was first reported at least 30 years ago by Andre Mester however it seems to be poorly recognised by the LLLT academic community. This presentation will be an update on dose, dose rate effects, beam measurement, calculations, an improved 3D dose model, the dose "sweet spot", possible explanations for this phenomenon and how it might best be exploited clinically.

8211-04, Session 1

## Red laser attenuation in biological tissues: study of inflammatory process and pigmentation influence

C. P. Sabino, M. Simões Ribeiro, I. T. Kato, D. T. Meneguzzo, R. A. Prates, Instituto de Pesquisas Energéticas e Nucleares (Brazil)

Several studies indicate that low level laser therapy (LLLT) accelerates the healing process, however, for a determined pathology, dosimetry remains difficult to be established.

To understand the tissue optical properties under different conditions is extremely relevant since the dose delivered to the target tissue is known to be critical. The skin pigmentation influence on the laser attenuation is not yet well established on different mice lineages or human ethnical groups, making the dose problematic. Along the same line, inflammatory processes may cause similar problems since the tissues in this condition change their optical properties due to inflammatory cell accumulation. This work evaluated the attenuation pattern of a HeNe laser ($\lambda$=632.8 nm) using ex vivo skin samples from Balb/C and C57BL/6 mice under inflammatory stages induced in their left paw by local carrageenan inoculation. The right healthy paw was used as the control group. The samples were placed between two microscope slides, and a CCD camera was placed orthogonal to the beam path. The intensity distribution of the scattered light was photographed in grayscale and analyzed by ImageJ software. Our findings suggest that even slight differences of the epithelial pigmentation could result in a relevant dose loss delivered to the deeper tissues. The increase of the inflammatory cell density in the connective tissue indicated a highly scattering area also resulting in a dose loss for the deeper tissues when compared to control group.

8211-05, Session 2

## Study of the characteristics of a irradiation experimental setup on fibroblast like cell cultures

T. D. Magrini, A. R. dos Santos, H. da Silva Martinho, Univ. Federal do ABC (Brazil)

Low Level Laser Therapy is based on laser irradiation with the aim of tissue repair. But some review papers [1] have highlight that there are some controversial in the results that exist because of the irradiation way. This work is dedicated to quantify and qualify characteristics of an experimental setup done for irradiation of cultured cells. One knows that the profile intensity of the laser is in the Gaussian form, so this setup was done based on a spatial filter to homogenize the intensity like a plateau profile. It was composed of 2 plan-concave lenses 150 mm of focal distance, pinhole of 0.23 mm diameter and a bi-concave lens. The delivered light power was verified with a power- meter. A 45° mirror deflects the light beam to the individual cells well plate. The light intensity distribution was checked through CCD camera placed perpendicular to the beam. The exit signal of the CCD was analyzed by Image J software. The net delivered power within the well was calculated from the radial intensity distribution. Experiments with fibroblast like cells were done with five different configurations (different profile intensities) of the setup to verify the corresponding effects of the light intensities on the cells viability. Differences on the cells were also verified by IR spectroscopy and in cell cycle by flow citometry. Our previous results show that there are differences in the proliferation of irradiated and not irradiated fibroblasts.

[1] De Haan R. J. et al., Laser Med. Sci., 17(2), 110-134 (2002).

8211-06, Session 2

## Antimicrobial activity of new porphyrins of synthetic and natural origin

G. V. Gyulkhandanyan, Institute of Biochemistry (Armenia); R. K. Ghazaryan, Yerevan State Medical Univ. (Armenia); M. Paronyan, Institute of Biotechnology (Armenia); G. Ulikhanyan, Armenian Pharmaceutical Association (Armenia); A. Gyulkhandanyan, Institute of Biochemistry (Armenia); L. Sahakyan, Yerevan State Medical Univ. (Armenia)

Currently photodynamic inactivation (FDI) of microorganisms by photosensitizers is one of the most promising directions for the destruction of antibiotic resistance microorganisms. Photosensitizers (PS) are the natural or synthetic origin dyes, mainly porphyrins. The concept of photodynamic inactivation follows the same principles as for the photodynamic therapy (PDT) of tumors: non-toxic dyes, porphyrins, can be localized in/on cells, activated by light, generate singlet oxygen and free radicals that are toxic to target cells (microorganisms). PDI has been successfully used against Gram (+) microorganisms, but most of the PS on Gram (-) bacteria acts weakly. The purpose of this study was the synthesis of new porphyrins and metalloporphyrins, as well as their purification from a natural source (from chlorophyll of nettle) and their testing against Gram (+) and Gram (-) microorganisms. We have synthesized more than 100 new cationic porphyrins and metalloporphyrins with different functional groups (hydroxyethyl, butyl, allyl, methallyl) and metals (cobalt, iron, copper, zinc, silver and other); from the nettle have also been purified pheophytin (a+b) and pheophytin (a) and have synthesized their Ag-and Zn-metalloporphyrins. It was found that in the dark (cytotoxic) mode, the most highly efficiency against microorganisms showed Ag-metalloporphyrins of both types of porphyrins (synthetic and natural). It was determined that in photodynamic mode the most highly efficiency for destruction of microorganisms has a new cationic metalloporphyrin Zn-TBut4PyP: 0.4-0.75 mkg/ml for Gram (+) and about 2 mkg/ml for Gram (-) microorganisms.

8211-07, Session 2

## Effects of LED or laser phototherapy on bone defects grafted with MTA and irradiated with laser or LED light: a comparative Raman spectroscopic study

A. L. B. Pinheiro, L. G. P. Soares, A. F. S. Barbosa, Univ. Federal da Bahia (Brazil); L. Silveira, Jr., Univ. do Vale do Paraíba (Brazil)

We studied peaks of calcium hydroxyapatite - CHA on defects grafted with MTA, treated or not with Light Emitting Diode - LED or IR Laser. 54 rats were divided in 6 groups each subdivided into 3 subgroups (15,21,30d). LED (λ850 ± 10nm) or IR Laser (XXX) were applied over (LED) or in 4 points around the defect at 48 h intervals for 15 days. Raman readings were taken at the surface of the defect. There were no statistically significant differences between non-irradiated subjects on regards the CHA peaks. On the other hand, there were statistically significant differences between the Group Clot and LED, Clot and Laser, and Clot and MTA + Laser (T test, $p = 0.01$, $p = 0.02$, $p = 0.003$). There were no significant differences between Group MTA and MTA + LED ($p=0.2$) but significant differences were seen between Groups MTA and MTA + Laser ($p=0.01$). Significant differences were also observed between Groups LED and Laser ($p < 0.001$) and between Groups MTA + LED and MTA + Laser ($p=0.009$). MTA, due to its characteristics, seemed to be directly affected by the light. However, the use of either phototherapy positively affected bone healing similarly as observed on different studies using other biomaterials. The overall analysis of our results indicated that the use of either light source resulted in a better, more advanced, and of quality bone repair.

8211-08, Session 2

## Chromophore absorbance change quantification in tissue during low-level light therapy

D. Huynh, C. J. Fisher, C. Chung, Ontario Cancer Institute (Canada); L. Qian, Univ. of Toronto (Canada); L. Lilge, Ontario Cancer Institute (Canada)

Low Level Light Therapy (LLLT) has been implicated to be able to stimulate tissue to promote healing and pain reduction. One of the potential pathways stimulated by LLLT lies in the electron transport chain, where the light irradiation can induce a change in the biochemical reactions within the cell. The aim of this study is to assess the feasibility of exploiting low level light irradiation as a diagnostic tool to determine tissue physiology, in particular in quantifying the changes in redox states of Cytochrome C as a result of a biochemical reaction due to LLLT. To achieve this goal a multi-wavelength approach is used by examining changes in the absorption of Cytochrome C, first in an in vitro model and verified ex vivo in rat brain tissue. Brain tissue is known to have a high metabolic activity, therefore making it an appropriate tissue type for this investigation. Laser irradiation at 633nm or 808nm is used to stimulate the targeted tissue to induce a LLLT effect. A second light source at 525nm or 550nm is used to measure the absorption changes of Cytochrome C through diffuse transmittance. Absorption changes in the redox states of Cytochrome C can be quantified as it is known that the difference in absorption of reduced and oxidized state Cytochrome C maximized at 525nm and 550nm.

8211-09, Session 3

## In vivo studies of LLLT for traumatic brain injury

M. R. Hamblin, W. Xuan, Q. Wu, Y. Huang, S. K. Sharma, L. Huang, Wellman Ctr. for Photomedicine (United States)

Low-level laser (or light) therapy (LLLT) is attracting growing interest to treat both stroke and traumatic brain injury (TBI). The fact that near-infrared light can penetrate into the brain allows non-invasive treatment to be carried out with a low likelihood of treatment-related adverse events. It is proposed that red and NIR light is absorbed by chromophores in the mitochondria of cells leading to changes in gene transcription and upregulation of proteins involved in cell survival, antioxidant production, collagen synthesis, reduction of chronic inflammation and cell migration and proliferation.

We developed two different models of TBI in; a closed head weight drop and an open skull controlled cortical impact (CCI). Transcranial laser therapy consisting of a single exposure 4-hours post TBI to 36 J/cm2 of various lasers was delivered to the closed head model. 810-nm or 660-nm laser significantly improved neurological severity score in TBI up to 4-weeks post TBI. Laser therapy at 730-nm or 980-nm was ineffective. We then examined the effect of 0, 1, 3, and 14 daily laser treatments in the CCI model. 1 laser Tx gave a significant improvement while 3 laser Tx was even better. Surprisingly 14 laser Tx was no better than no treatment. Histological studies at necropsy suggested that the cortical lesion was repaired by neural progenitor (stem) cells from the subgranular layer of the dentate gyrus and the subventricular zone of the lateral ventricle, possibly stimulated by the laser. Transcranial laser therapy is a promising treatment for acute (and chronic TBI) and the lack of side-effects and paucity of alternative treatments encourages early clinical trials.

8211-10, Session 3

## Effects of polarization in low-level laser therapy of spinal cord injury in rats

T. Ando, Keio Univ. (Japan); S. Sato, H. Kobayashi, H. Nawashiro, H. Ashida, National Defense Medical College (Japan); M. R. Hamblin, Wellman Ctr. for Photomedicine (United States) and Harvard Medical School (United States) and Harvard-MIT Health Sciences and Technology (United States); M. Obara, Keio Univ. (Japan)

Low-level laser therapy (LLLT) is a novel promising approach to treat the spinal cord injury (SCI). Since nerve fibers have optical anisotropy, photon migration in spinal tissue might be affected by the polarization. However, the effect of polarization on the efficacy of LLLT has not been elucidated. In this study, we investigated the effect of polarization on the near-infrared LLLT. Rat spinal cord was exposed and injured with a MASCIS impactor device. The lesion site was treated with an 808-nm diode laser beam, which was transmitted through a polarizing filter to control the polarization, immediately after injury and daily for 5 consecutive days. The laser power at the injured spinal cord surface was 25 mW and the dosage per day was 9.6 J/cm2 (spot diameter, 2 cm; irradiation duration, 1200 seconds). Functional recovery was assessed daily by an open-field test. The results showed that the locomotive function of SCI rats that were irradiated with linear-polarized laser parallel to the spinal column (group 1) was significantly improved at 5 days after SCI ($P < 0.05$), as compared to those treated with perpendicularly aligned polarization (group 2). Average scores of the control group (SCI alone) and treated groups 1 and 2 were 6.8, 11.2 and 8.9, respectively, at 14 days after injury ($n = 7 - 8$). Although more detailed examination will be needed, the observation suggests that polarization plays an important role for healing injured spinal cords by using a low-level near-infrared laser beam.

8211-11, Session 3

## Control of anoxic depolarization in rat brain by near-infrared laser irradiation and its monitoring by intrinsic optical signal imaging

S. Kawauchi, S. Sato, Y. Uozumi, H. Nawashiro, M. Ishihara, M. Kikuchi, National Defense Medical College (Japan)

In brain ischemia or hypoxia, spreading depolarization is a key event associated with brain tissue survival. After onset of ischemia/hypoxia, impairment of energy metabolism causes ischemic/anoxic depolarization (AD), which increases energy demand, leading to ATP depletion and thus acute neuronal death. In a peri-infarct penumbra region, AD-like peri-infarct depolarization leads to energy failure and expanded infarction. Therefore, control of depolarization may prevent tissue death due to ischemia/hypoxia. We previously performed intrinsic optical signal imaging of a rat brain during hypoxia and observed that AD-related light-scattering waves were focally generated in the bilateral outermost regions in the cortex and spread toward the midline; the behavior of scattering waves correlated with survival of rats. In the present study, we examined whether near-infrared laser irradiation can control AD in rat brains using the same imaging technique. Transcranial 808-nm laser irradiation was performed for the left hemisphere at 7.5 mW/cm2 before (30 min) and during hypoxia. The time point for the scattering wave generation was significantly delayed ($4.8 \pm 2.4$ s) in the irradiated hemisphere than in the non-irradiated hemisphere ($n=4$). The coverage of the scattering wave, i.e., volume of AD, in the irradiated hemisphere was significantly smaller than that in the non-irradiated hemisphere (39-73% of the non-irradiated hemisphere's coverage at 10-30 s after scattering wave generation). These results suggest that near-infrared light can delay and reduce anoxic depolarization, which is probably due to increase in the cerebral ATP by near-infrared laser irradiation.

8211-12, Session 3

## Healing effect of low-level laser therapy (LLLT) on bone fracture

C. Rhee, Dankook Univ. Hospital (Korea, Republic of); H. Park, Dankook Univ. (Korea, Republic of); J. Ahn, Dankook Univ. Hospital (Korea, Republic of)

Aim: To evaluate the effect of LLLT on healing of bone fracture using two different wavelengths LD lasers. Methods and materials: Guinea pigs were divided into the control, 632 nm, and 830 nm groups. Fourteen animals into control group, 16 animals into 632 nm group, and 16 animals into 830 nm group, were assigned. Right femurs of all animals were fractured and fixed with intramedullary nails. Then, animals in 632 nm and 830 nm groups were irradiated with each responsible laser q 2 days for 3 weeks and 6 weeks. All animals in 3 groups were examined grossly, X-rayed, and examined by histology. The animals in each group were sacrificed at 3 weeks and 6 weeks. The gross, radiologic, and histologic findings were assessed by the modified Zorlu Scoring System. Results: The gross and radiologic findings showed significantly better callus formation at the both laser groups compared to the control group at 3 weeks. The significantly more enhanced osteoblastic proliferation in histologic examination was noted in both laser groups compared to the control group at 3 weeks. The results of Zolu scoring showed significantly higher scoring in both laser groups comparing to the control group at 3 and 6 weeks. The Zolu scoring also showed higher score in 830 nm group compared to 630 nm group. Conclusion: LLLT using 632 and 830 nm LD laser appears to accelerate healing of bone fracture.

8211-18, Poster Session

## Coherence and speckle in photomedicine and photobiology

Z. Zalevsky, Bar-Ilan Univ. (Israel); M. Belkin, Tel Aviv Univ. (Israel)

Using light to biostimulate a cell is common approach in Low Level Laser Therapy (LLLT). The growing acceptance of incoherent light sources (such as light emitting diodes i.e. LEDs) in phototherapy continues to debate on the value of coherence in achieving beneficial results with light. Some scientists argue that the spatial coherence of lasers is not useful in LLLT since according to the first law of photochemistry light must be absorbed to induce a chemical reaction and therefore the intensity of the illumination rather than its phase (which determines the coherence of light) plays the critical role. Others claim that coherence of laser light is not lost when the light enters tissues and thus it affects the measured outcome.

The purpose of this paper is to clear up those issues while supporting the claim that lasers have no preference over LEDs since they lose their coherency once penetrating into biological tissues. The paper provides a brief explanation to non-professionals or to scientists that do not come from physics related background, on the meaning of coherence of light as well as the physics behind the generation of speckle patterns, and the relation of those terms to photomedicine and photobiology.

8211-19, Poster Session

## Mechanism study on mitochondrial fragmentation under oxidative stress caused by high-fluence low-power laser irradiation

S. Wu, South China Normal Univ. (China)

Mitochondria are dynamic organelles that undergo continual fusion and fission to maintain their morphology and functions, but the mechanism involved is still not clear. Here, we investigated the effect of mitochondrial oxidative stress triggered by high-fluence low-power laser irradiation (HFLPLI) on mitochondrial dynamics in human lung adenocarcinoma cells (ASTC-a-1) and African green monkey SV40-transformed kidney fibroblast cells (COS-7). Upon HF-LPLI-triggered oxidative stress, mitochondria displayed a fragmented structure, which was abolished by exposure to dehydroascorbic acid, a reactive oxygen species scavenger, indicating that oxidative stress can induce mitochondrial fragmentation. Further study revealed that HF-LPLI caused mitochondrial fragmentation by inhibiting fusion and enhancing fission. Mitochondrial translocation of the profission protein dynamin-related protein 1 (Drp1) was observed following HF-LPLI, demonstrating apoptosis-related activation of Drp1. Notably, overexpression of Drp1 increased mitochondrial fragmentation and promoted HF-LPLIinduced apoptosis through promoting cytochrome c release and caspase-9 activation, whereas overexpression of mitofusin 2 (Mfn2), a profusion protein, caused the opposite effects. Also, neither Drp1 overexpression nor Mfn2 overexpression affected mitochondrial reactive oxygen species generation, mitochondrial depolarization, or Bax activation. We conclude that mitochondrial oxidative stress mediated through Drp1 and Mfn2 causes an imbalance in mitochondrial fission-fusion, resulting in mitochondrial fragmentation, which contributes to mitochondrial and cell dysfunction.

8211-20, Poster Session

## Photodynamic action on microorganisms using iron oxide Fe2O3 nanoparticles and LED blue (405 nm) light

E. S. Tuchina, P. O. Petrov, M. V. Kulikova, V. I. Kochubey, V. V. Tuchin, N.G. Chernyshevsky Saratov State Univ. (Russian Federation)

Iron oxide (Fe2O3) nanoparticles are widely used in chemical and biomedical research because of its photocatalytic and magnetic properties.

The goal of this study was to evaluate the sensitivity of microorganisms to the action of LED blue (405 nm) light after treatment of their cells with Fe2O3 nanoparticles.

Iron oxide (Fe2O3) nanoparticles are widely used in chemical and biomedical research because of its photocatalytic and magnetic properties.

The goal of this study was to evaluate the sensitivity of microorganisms to the action of LED blue (405 nm) light after treatment of their cells with Fe2O3 nanoparticles.

The bacterial strains used in this study were Staphylococcus aureus 209 P (standard strain), Staphylococcus simulans and Dermabacter hominis (isolated from the pus of patients with maxillary sinusitis). Cultures were grown on dense brain-heart infusion medium and incubated at 37°C.

As blue light source LED with spectrum maxima at 405 nm (31.5 mW/cm2) was taken. The light exposure was ranged from 5 to 30 min. Fe2O3 nanoparticles with average size about 8 nm in concentration 0.005% were used.

The account of results was provided by calculation of colony forming units (CFU) in 24 hrs after light exposure.

Reduction of CFU number of S. aureus incubated with nanoparticles occurred in the range of 3 - 82%. The observed reduction of the CFU number of S. simulans was not depending on the duration of light exposure. Using Fe2O3 nanoparticles and blue light led to a same, but more pronounced effect: after 10 min-exposure the reduction of CFU was on 72%. Reduction of the CFU number of D. hominis, incubated with Fe2O3 nanoparticles, with variation of exposure time from 5 to 30 min occurred in the range of 80 - 91%.

8211-21, Poster Session

## Effectiveness of the use of LLLT on disorders of the maxillofacial region

L. G. P. Soares, C. Montagn Carvalho, A. M. C. Marques, M. C. T. Cangussú, A. L. B. Pinheiro, Univ. Federal da Bahia (Brazil)

Several clinical and experimental studies have shown the effectiveness of LLLT as a non-invasive, painless, and off good acceptance treatment by patients. We studied the use of LLLT in the treatment of disorders of the maxillofacial region at the Laser Center of the Federal University of Bahia between 2003-2010. 298 (70.81% female, ~ 50.5 years old whom fulfilled the inclusion criteria of complete 12 sessions and have no other treatment) patient's files were reviewed and statistical analysis performed. For pain cases, a visual analog scale was used prior treatment and at the end of 12 sessions. Diode Lasers (λ780nm, λ830nm, λ660nm, 30/40mW, spot~3mm) were used for treatment.. TMJ pain (43.3%), trigeminal neuralgia (23.2%), paresthesia (16.8%), mucositis (7%), Bell´s palsy (5%) and dentin hypersensitivy (4.7%) were treated. The mean dose per session was 17.92J/cm2 and the mean treatment length was 25 sessions. Most of patients were treated with IR laser (67.45%) and 14.77% used the association of red and IR laser. At the end of treatment, 70% of the patients were asymptomatic or had improved. The best results of asymptomatic patients were achieved in cases of mucositis and trigeminal neuralgia when compared to TMJ and bell´s palsy (p=0.02). Among the pathologies treated the total dose and the number of sessions presented statiscally significant difference (p=0,01 and p=0,00 respectively). Patients with trigeminal neuralgia required more treatment sessions (40.5) and higher doses (64.6 J/cm2) than other pathologies. LLLT was effective in the treatment of diseases of the maxillofacial region.

8211-22, Poster Session

## Evaluation of photodynamic antimicrobial therapy (PACT) against promastigotes form of the Leishmania (Viannia) braziliensis: in vitro study

A. F. S. Barbosa, Univ. Federal da Bahia (Brazil); S. L. Galdino, Univ. Federal de Pernambuco (Brazil); M. Barral Netto, Fundacao Oswaldo Cruz (Brazil); I. da Rocha Pitta, Univ. Federal de Pernambuco (Brazil); B. B. Sangiorgi, Fundacao Oswaldo Cruz (Brazil); N. A. Correia, A. L. B. Pinheiro, Univ. Federal da Bahia (Brazil)

Leishmaniasis is a complex disease that affects more than 12 million people in 88 countries worldwide. Leishmania (Viannia) braziliensis is the most common species in the Americas and the most important causative agent of cutaneous and mucocutaneous leishmaniasis in Brazil. The therapeutic arsenal routinely employed to treat patients with leishmaniasis is limited and unsatisfactory. For cutaneous leishmaniasis, pentavalent antimonials are the first line therapeutic scheme recommended by World Health Organization. These compounds are highly toxic, poorly tolerated and their effectiveness highly variable. In this work, we demonstrate a technique with, so far, unknown disadvantages. We aimed to verify the effectiveness of PACT in vitro, as a new technique for the treatment of Leishmaniasis. We used a semiconductor laser (λ = 660nm, 40mW, 4.2J/cm2, CW) associated to phenothiazine's derivatives (5 and 10 µg/ml, TBO, Methylene Blue or Phenothiazine) on the promastigotes form of Leishmania braziliensis in a single session. Viability of the parasites was assessed in quadruplicates of each group. The samples were removed and analyzed in a hemocytometer 72h after PACT. We found an important decrease in the number of viable parasites on all treated groups in comparison to their controls. Our results demonstrated significant percentage of lethality (above 95%). The 99.23% of lethality was achieved with 10 µg/ml of TBO. No lethality was seen on groups treated with laser or with the compounds separately. Our results are promising and indicative that the use of PACT may be a powerful treatment of leishmaniasis when compared to already available ones.

8211-23, Poster Session

## Effect of non-homogenous thermal stress during sub-lethal photodynamic antimicrobial chemotherapy

S. Dehipawala, N. Gadura, T. Holden, S. Dehipawala, R. Hong, D. Kokkinos, G. Tremberger, Jr., D. Lieberman, T. D. Cheung, Queensborough Community College (United States)

Pathogens could be inactivated via a light source coupled with a photosensitizing agent in photodynamic antimicrobial chemotherapy (PACT). This project studied the effect of non-homogenous thermal stress on cell colony. The non-homogeneity could be controlled by iron oxide nano-particles doping in porous glassy substrates such that each cell would experience tens of hot spots when illuminated with additional light source. The substrate non-homogeneity was characterized by Atomic Force Microscopy, Transmission Electron Microscopy and Extended X-Ray Absorption Fine Structure at Brookhaven Synchrotron Light Source. Laboratory cell colonies on non-homogenous substrates exhibit induced thermal stress complementing sub-lethal PCAT treatment with the reduction of cell vitality. The studied pathogens included E. coli, Staphylococcus aureus, and Pseudomonas aeruginosa. Non-pathogenic microbes Bacillus subtilis and Mycobacterium smegmatis were also studied for comparison. The results show that sub-lethal PACT could be effective with additional non-homogenous thermal stress.

8211-24, Poster Session

## GaAlAs laser therapy on neuropathic pain in rats

C. Na, Y. Lee, D. Youn, C. Choi, Dongshin Univ. (Korea, Republic of); S. Lee, Y. Moon, S. Jeong, Gwangju Institute of Science and Technology (Korea, Republic of); W. Kim, Dongshin Univ. (Korea, Republic of)

In the past 30~40 years many studies have reported the efficiency of low level laser therapy(LLLT) as a treatment for diverse diseases and injuries We have studied the effects of GaAlAs(808 nm) LLLT and acupuncture treatment(AT) at BL40 on neuropathic pain in rats induced by lumbar spinal nerve 5 ligation. To produce the model of neuropathic pain, under isoflurane 2.5% anesthesia, the lumbar spinal nerve 5 was ligated by 6-0 silk thread. After neuropathic surgery, we examined if the animals exhibited the behavioral sign of allodynia. The allodynia was assessed by stimulating the medial malleolus with von Frey filament and acetone. Three weeks after the neuropathic surgery, GaAlAs(808 nm) low level laser and acupuncture was inserted at BL40 once a day for 6 days. We examined the withdrawal response of neuropathic rats' legs by von Frey filament and acetone stimulation. And also we examined c-Fos, nociceptin and nociceptin receptor in the midbrain central gray of neuropathic rats. The GaAlAs(808 nm) low level laser therapy and acupuncture at BL40 decreased the withdrawal response of mechanical allodynia that assessed with von Frey filament in LLLT group on 5 and 6 times and with acetone in AT group and LLLT on 6times. The LLLT and acupuncture at BL40 decreased the c-Fos protein expression in AT and LLLT groups. The 808 nm LLLT and acupuncture at BL40 decreased the nociceptin protein and nociceptin receptor protein in LLLT group. We have noticed that GaAlAs(808 nm) LLLT and acupuncture at BL40 decreased mechanical allodynia in the model of neuropathic pain. c-Fos, nociceptin and nociceptin receptor expression in the central gray of that group was also decreased. This study can be used as a basic resource on a study and a treatment of pain.

8211-25, Poster Session

## The effect of the photobiomodulation in the treatment of Bell's palsy: clinical experience

A. M. C. Marques, F. Colombo, C. Montagn Carvalho, G. Paraguassu, J. A. Sousa, L. G. P. Soares, E. Magalhães, M. C. T. Cangussú, A. L. B. Pinheiro, Univ. Federal da Bahia (Brazil)

The Bell's palsy is a sudden unilateral facial paralysis of unknown etiology that causes a complete loss of facial mimics. It is known that light therapies may improve the regeneration of damaged nerves. We aimed to assess the effectiveness use of the use of λ780nm, λ 660nm laser, and λ850nm LED in the treatment of facial paralysis. 15 patients suffering from Bell's palsy were submitted to light treatment at the Laser Clinic of the School of Dentistry of the UFBA between 2005 and 2010. 11 patients were treated with IR laser, one with red laser and 3 with IR LED. Protocol was carried out at 48 h intervals and patients assessed weekly. No other treatment was prescribed during the treatment. At the end of 12 sections, 12 patients were fully recovered and 3 (IR laser) showed no response. The use of IR laser or LED was effective on treating Bell's palsy, but the association with the physiotherapy and medications is important.

8211-26, Poster Session

## Efficacy of the photodynamic antimicrobial therapy (PACT) with the use of methylene blue associated with the λ660nm laser in Leishmania (Leishmania) amazonesis: in vitro study

A. M. C. Marques, Univ. Federal da Bahia (Brazil); G. M. Pires-Santos, E. Alves, Research Ctr. Gonçalo Moniz (Brazil); S. C. Oliveira-Sampaio, J. S. Monteiro, A. F. S. Barbosa, Univ. Federal da Bahia (Brazil); M. Azevedo-Silva, M. A. Vannier-Santos, Research Ctr. Gonçalo Moniz (Brazil); A. L. B. Pinheiro, Univ. Federal da Bahia (Brazil)

Leishmaniasis is a major public health problem in many countries. The parasite that causes this disease has a high prevalence. The usual therapeutics is based on the use of pentavalent antimonials compounds. This study aimed to assess the effects of Photodynamic Antimicrobial Therapy (PACT) on promastigotes forms of Leishmania (Leishmania) amazonesis in vitro. The promastigotes of L. (L.) amazonensis were pre-incubated with methylene blue (MB) at different concentrations, for 5 minutes, were photoactivated by λ660nm laser (2.4 J /cm²; 40mW) and then incubated at 26 ° C for 24 hours. After this period, the amount of parasites was determined by colorimetry and they were analyzed by SEM. The promastigotes treated with PACT showed inhibition of cell proliferation at concentrations of 5 e 0.625µg/mL, compared to the control group. The structural changes produced in the cells were: two flagella, formation of 'blebs', deformation of the cell body and cells tap, while no change was seen in this control. The observed changes in the microtubule network of the parasite might be indicative of the induction cell death. However, free radicals generated during the procedure might also cause the degradation of several molecules present on the parasite causing changes at cellular level. These changes are not the only targets of phototherapy involved in the processes of cell death. The use of PACT in L. (L.) amazonesis was effective and our results may help the understanding of the mechanism of the parasites´ death treated with this technique using MB as a photosensitizer.

8211-13, Session 4

## A novel role of iNOS gene expression in the anti-inflammatory and tissue protective mechanisms of 905 nm superpulsed laser therapy

A. Mandel, Theralase, Inc. (Canada); L. Lilge, Ontario Cancer Institute (Canada)

We hypothesized that up regulation of iNOS gene expression is playing a role in the initiation of the anti-inflammatory and tissue protective mechanisms of 905 nm superpulsed laser therapy (SPLT). In the present study, the iNOS expression before and after SPLT (TLC-1000, Theralase Inc., Toronto, Canada; with pulse wave mode: 50Wcm-2, 200 nsec (10kHz) pulses) were evaluated in the zymozan-induced arthritis model, in knee joints of old (30 weeks) FVB/N-Tg (iNOS-luc) mice. The level of iNOS expression in the treatment group remains significantly ($p<.041$) lower than in the control group. In older animals, the low level of iNOS activity was reversed by SPLT to control; level control (6.97+/-2.7) and treated older animals (6.61+/- 4.1), respectively. The restored level of iNOS represents a normal level of iNOS gene expression in the same strain of young (10 weeks) mice injected with zymozan. Moreover, this up regulation of iNOS directly correlated with a moderate amount of inflammation and fibrin deposition in the joint space, indicating that the SPLT could modulate inflammation and tissue damage via iNOS mediated pathway. Nitric oxide synthase (iNOS) catalyzes the oxidation of L-arginine through a five electron reduction, ending with formation of L-citrulline and subsequent production of ·NO. The results indicate that iNOS mediated pathway plays a significant role in the mechanisms of 905 nm SPLT. The lack of iNOS expression may cause significantly enhanced inflammatory reactions and contribute to the overall tissue damage, perhaps due to suppression of ·NO production. SPLT is able to balance the lower propensity to mount iNOS expression in this study.

8211-14, Session 4

## Pulsed versus CW low-level light therapy on osteoarticular signs and symptoms in patients with limited scleroderma (CREST syndrome)

D. Barolet, Opusmed Inc. (Canada) and McGill Univ. (Canada)

Limited cutaneous systemic sclerosis (lcSSc) was formerly known as CREST syndrome in reference to the associated clinical features: Calcinosis, Raynaud's phenomenon, Esophageal dysfunction, Sclerodactyly, and Telangiectasias. The transforming growth factor beta (TGF-ß) has been identified has a major player in the pathogenic process, while low level light therapy (LLLT) has been shown to modulate this cytokine superfamily. The primary objective of this study was to assess the efficacy of millisecond pulsing vs. continuous wave mode (CW) LLLT treatment on osteoarticular symptoms and signs associated with lcSSc. Patients were three times per week over 4 weeks, using a sequential pulsing mode on one elbow, and a CW mode on the other. Efficacy assessments included inflammation, symptoms, pain, and health scales, patient satisfaction, clinical global impression, and adverse effects monitoring. Significant functional and morphologic improvements following LLLT treatment were observed with best results seen with the pulsing mode. Therapy was generally well tolerated. The cascade of events leading to photobiomodulatory effects are thought to be initiated by the antenna molecule mitochondrial cytochrome c oxidase. Respiration in the mitochondria can be inhibited by nitric oxide (NO) binding to cytochrome c oxidase which competitively displaces oxygen and affect cell metabolism. Excess NO binding is associated with inflammatory processes, cell damage and apoptosis. Light absorption dissociates NO, allowing cellular respiration to resume and normalization of cell activity, ultimately triggering biomolecular processes. Short and intermittent light emission might enhance NO dissociation therefore augmenting mitochondrial energy production and cellular activity.

8211-15, Session 4

## Enlightenment and light

D. D. Patthoff, Academy of Laser Dentistry (United States)

In the beginning of the age of enlightenment (or reason), philosophy, science, and theology stemmed equally from the same pens. Inventors and entrepreneurs noted and measured different characteristics of light and redirected the use of lenses beyond the heat lens. Within decades, microscopes, telescopes, theodolites, and many variations were well known.

These advances changed and expanded the nature of science, subsequent technology, and society.

Ethicists exploring enlightenment thinking are currently noting that goods and oversights built into enlightenment language remain imbedded within it.

Its hidden defects are not limited to philosophy; science and technology, consequently, are restrained, as are their organizational communities, and society. This overlooked history of ethics and metaphysics needs inclusion within the study, exploration, education and use of lasers. Without it, the kind of research and literature, that will give light based medicine the place it now needs in our world, will be hard to generate

8211-16, Session 4

## No urge to purge

E. D. Laser, Consultant (United States)

Keywords: Bulimia, bulimia nervosa, LLLT, low-level light therapy, hypnosis, eating disorder, CBT.

No Urge to Purge : Treating Bulimia with Hypnosis and Low-Level Light Therapy

Bulimia nervosa is a life-threatening disorder characterized by recurrent episodes of binge eating followed by self-induced vomiting or other compensatory methods (i.e. excessive exercise, fasting, the consumption of laxatives or diuretics, etc.) aimed at preventing weight gain (Agras, 1989; Fairburn, 1986; Freeman, 1988). According to most sources, the bulimic is intensely afraid of weight gain and exhibits persistent dissatisfaction with body and appearance, as well as a significant distortion in the perception of the size and shape of the body (Bossert, 1989; Walsh, 1997; Wilson, 1986).

Clinical trials combining hypnosis and psychotherapy in treating bulimia nervosa have produced mixed results. Many sources support the efficacy of cognitive-behavioral psychotherapy (CBT) in the treatment of people with bulimia nervosa in both group and individual settings (Agras, 1989; Bossert, 1989; Fairburn, 1986; Wilson, 1986) with results that are at most modest. However, even in those cases, the trial qualities vary and their sample sizes have often been too small to prove reliable (Loeb, 2000).

In certain studies, bulimic patients have been more hypnotizable than controls and have scored higher on a self-report scale of dissociative experiences (Covino, 1994; Esplen, 1998; Vanderlinden, 1995), with self-help proving as equally effective as one-on-one or group treatments (Durand, 2003). In most instances, a series of treatments are necessary to produce a favorable result, and even in those cases, the patient often returns to his or her bulimic tendencies after treatment ends (Loeb, 2000; Torem, 1992; Thackwray, 1993).

While traditionally used to relieve chronic and acute pain, low-level (or cold) laser therapy is the application of a single wavelength of red and near-infrared light (600-1000nm) over injuries or lesions (Baxter, 1991; Kreisler, 2002). The painless, non-toxic, non-thermal treatment is without side effects and often complements traditional therapies. (Basford, 1989; Baxter, 1991; Sakurai, 2000).

In LLLT, a laser directs biostimulative light energy at the cellular level to mitochondria - the “engines” of the cells, in that they are responsible for generating cellular energy - which the cells convert into chemical energy, in turn promoting natural healing and pain relief (Baxter, 1991). Through this process, LLLT has been clinically documented to increase the speed, quality, and tensile strength of tissue repair through this process of photobiostimulation. Additionally, the application of LLLT treatment is believed to enhance fibroblast function (Kreisler, 2002), the structural framework comprising human connective tissue that play a central role in the process of wound healing. Indeed, several studies attribute LLLT with producing anti-inflammatory and pain attenuation (Ceccherelli, 1989; Mizokami, 1991).

In this report, we describe how hypnosis combined with low-level laser therapy produced a complete cessation in purging episodes for a 14-year bulimic patient. The patient’s name was changed to protect her privacy

8211-17, Session 4

## Aculaser therapy for the treatment of cerebral palsy

S. Anwar, Anwar Shah’s First C.P. and Paralysis Clinic and Research Ctr. (Pakistan)

A single, open and non comparative study was conducted at Anwar Shah Trust for C.P. & Paralysis in collaboration with the Departments of Neurology and Neurosurgery, Children Hospital Lahore, Pakistan to evaluate the effects of ACULASER THERAPY in childern suffering from Cerebral Palsy (C.P.) and associated Neurological Disorders like epilepsy, cortical blindness, spasticity, hemiplegia, paraplegia, diplegia, quadriplegia, monoplegia, sensory-neural deafness and speech disorders. In all 500 children were treated and the data was gathered during a period of 4 years from December 2006 till December 2010. These children were further classified according to the type of C.P. (spastic, athetoid, mixed) they suffered from and associated Neurological Disorders.

This article shows results in C.P. childern who were treated with ACULASER THERAPY for a minimum of 08 weeks and more or had minimum of 15 treatment sessions and more. This article also shows that those childern who were given a break in the treatment for 1 month to 1 year did not show any reversal of the signs and symptoms.

Analysis of the data showed that out of 342 children with Spasticity and Stiffness 294 showed marked improvement showing 87% success rate, out of 252 children with Epileptic fits, there was a significant reduction in the intensity, frequency and duration of Epileptic fits in 182 children showing 72% success rate, out of 96 children with Cortical Blindness 60 children showed improvement accounting for 63% efficacy rate, out of 210 children with Hearing Difficulties, 126 showed marked improvement accounting for 60% improvement rate, out of 380 children with Speech Disorders 244 showed improvement reflecting 64 % improvement rate, out of 192 children with Hemiplegia 142 showed improvement in movement, tone and power accounting for 74% improvement rate, out of 152 children with Quadriplegia 104 showed improvement in gross and fine motor functions showing 69% success rate and out of 106 children with Paraplegia of lower limbs 88 showed improvement in weight bearing, standing and movement accounting for 76% improvement rate.

Key Words: Cerebral Palsy, Aculaser therapy, Laser acupuncture, CP Childern, Cortical blindness, Epilepsy, Spasticity, Stiffness, Sensory neural deafness, Speech disorders, Hemiplegia, Quadriplegia, Paraplegia.

# Conference 8212: Frontiers in Biological Detection: From Nanosensors to Systems

Saturday-Sunday 21-22 January 2012

Part of Proceedings of SPIE Vol. 8212 Frontiers in Biological Detection: From Nanosensors to Systems IV

8212-01, Session 1

## Stretchable and shapeable nanomembranes for biological detection on and off the chip

O. G. Schmidt, Leibniz-Institut für Festkörper- und Werkstoffforschung Dresden (Germany)

Stretchable magnetoelectronic devices based on thin nanomembranes are wrapped around millifluidic channels to perform in-flow detection of magnetic particles, which can be conveniently attached to cells.

To downscale this approach, highly strained nanomembranes out of GMR layer stacks are rolled-up on-chip to integrate sensitive magnetic sensors into microfluidic channels. Rolled-up nanotech is fully

integrative and can include almost arbitrary materials and material combinations. We create optofluidic sensors to detect single cells and functionalize the inner walls of transparent rolled up microtubes to study in great detail cell division in

2D confined space. The final goal is to generate a fully integrative multifunctional lab in a single tube, which can be mass produced on a single chip by common semiconductor fabrication techniques.

In addition, off-chip rolled-up micro- and nanotubes are used as multifunctional jet engines that autonomously move around in fluids and transport/deliver cargo. These engines can be remotely controlled by magnetic fields and switched on/off by light control.

They reach remarkably high relative speeds and can be as small as a few hundred nanometers. They can transport and detect cell material and isolate organic material from compley media. Ultra-small autonomous systems with both physical as well as biochemical functionalties are envisioned.

8212-02, Session 1

## Polymer-coated surface enhanced Raman scattering (SERS) gold nanoparticles for multiplexed labeling of chronic lymphocytic leukemia cells

C. M. MacLaughlin, N. Mullaithilaga, G. C. Walker, Univ. of Toronto (Canada); C. Wang, Mount Sinai Hospital (Canada)

Gold nanoparticles of 60 nm diameter were used in the development of surface enhanced Raman scattering (SERS) particles. A library of SERS tags was created using various classes of Raman-active dyes. The SERS particles were subsequently coated with 5kDa poly(ethylene glycol) to impart stability in addition to sites for functionalization of the nanoprobes to either research grade or therapeutic monoclonal antibodies. SERS nanoparticle stability has been evaluated both during storage, and in in vitro biological conditions. Multiplexed cell surface labeling was accomplished by simultaneously targeting SERS probes to several cell surface proteins of interest in the diagnosis of chronic lymphocytic leukemia (CLL). The efficacy and specificity of cell surface targeting by SERS nanoparticles were assessed using Raman spectroscopy, Raman imaging, dark field microscopy, and flow cytometry.

8212-03, Session 1

## Lipid-encapsulation of surface enhanced Raman scattering (SERS) nanoparticles and targeting to chronic lymphocytic leukemia (CLL) cells

S. Y. Ip, C. M. MacLaughlin, Univ. of Toronto (Canada); N. Mullaithilaga, Mount Sinai Hospital (Canada); M. Joseph, Univ. of Toronto (Canada); S. Wala, C. Wang, Mount Sinai Hospital (Canada); G. C. Walker, Univ. of Toronto (Canada)

Commercially available 60 nm diameter gold nanoparticles were coated with a bilayer composed of a ternary mixture of lipids. The versatility of the lipid coating was demonstrated by the incorporation of three classes of Raman-active species: Electrostatically associated, lipophilic, and lipid-conjugated dyes. The lipid layer was characterized by transmission electron microscopy (TEM), UV-Vis absorption, and dynamic light scattering. The SERS spectrum of the three dye species was confirmed by Raman spectroscopy. UV-Vis and Raman spectra indicate that lipid-encapsulated particles are stable in water and phosphate buffered saline for at least one month. Furthermore, specific targeting of lipid-encapsulated Au nanoparticles to patient-derived chronic lymphocytic leukemia (CLL) cells was demonstrated. Targeting was achieved using lipid-conjugated antibody fragments, and demonstrated using Raman spectroscopy, Raman imaging, and darkfield microscopy.

8212-04, Session 1

## A novel nano-enhanced evanescence technique (NEET) for integrated microfluidic biochemical detections in micro-total analysis systems

A. Chandrasekaran, M. Packirisamy, Concordia Univ. (Canada)

Photonic sensing techniques offer have several advantages for implementation in integrated microfluidic Micro-Total Analysis Systems (mTAS) and Lab-on-a-Chip (LOC) devices. Among several sensing techniques, Evanescent wave detection which is used for sensing any chemical or biological activity that takes place on the surface of the waveguide, is very sensitive to the identification of the presence or activity or reactions of chemical and biological specimens present in the bio-optical interaction zone, due to the direct interaction of the biological specimens with the optical field. Other advantages of using evanescence based biochemical detections include immunity to electromagnetic interferences, feasibility of instantaneous detections, ability to carry out time based reaction studies etc. But surprisingly, this detection technique has not been explored for applications in mTAS and LOC devices. Also, as seen with other hybrid integrated optical-microfluidic systems, it is important to improve the sensitivity of evanescence based biodetection, which will be useful for detection of very low concentration of chemical and biological specimens upon the integration of the evanescence system with microfluidics.

In this work, a novel method of Nano-Enhanced Evanescence detection Technique (NEET) is proposed for integration with the Micro-Total Analysis System for the detection of active chemical and biological specimen. This technique includes the integration of nanoparticles on the surface of the waveguide which would thereby facilitate better bio-optical interaction, between the evanescent field of light and the chemical/ biological substrates. The NEET principle has been validated through Finite Difference Time Domain studies and the experimental results show that the proposed technique is highly suitable for applications in Micro-total Analysis Systems.

8212-05, Session 1

## Specific detection of protein aggregates with a Bloch surface wave sensor

V. Paeder, Ecole Polytechnique Fédérale de Lausanne (Switzerland); M. Kolympadi Markovic, Univ. of Neuchâtel (Switzerland); V. Musi, L. Hvozdara, Ecole Polytechnique Fédérale de Lausanne (Switzerland); R. Neier, Univ. of Neuchâtel (Switzerland); H. P. Herzig, Ecole Polytechnique Fédérale de Lausanne (Switzerland)

The key role of protein conformational changes in numerous degenerative diseases is nowadays a subject of thorough interest [1]. The misfolding and aggregation of specific proteins has been recognised as the cause of widespread diseases such as Alzheimer's or Parkinson's. The aggregation process yields fibrillar structures known as amyloid fibrils. In the case of Alzheimer's, recent studies pointed out the toxicity of prefibrillar forms of aggregates appearing in the early stages of aggregation [2]. The ability to distinguish early aggregation events is hence of prime importance.

We recently demonstrated a detection scheme for protein aggregation using a Bloch surface wave (BSW) sensor made of a periodic stack of silicon oxide and silicon nitride layers [3]. The detection principle relies on the optical density changes caused by the interaction of oligomeric aggregates with the sensor silicon nitride surface and by the precipitation of large aggregates. As such, the sensitivity of this label-free detection scheme is limited by the moderate affinity of protein oligomers with the sensor surface.

In this paper, we present a comparison of several surface modification schemes (HMDS, thioflavin-T, antibodies) enabling the enhanced detection of Alzheimer's amyloid beta 1-42 with a BSW sensor. The efficiency of each scheme in detecting the early aggregation events is discussed. It is shown that an appropriate choice of functionalisation allows the sensor to selectively detect aggregation at an early stage. These results highlight the interest of BSW sensing as a candidate tool for the early diagnosis of degenerative diseases.

[1] P.T. Lansbury and H.A. Lashuel, "A century-old debate on protein aggregation and neurodegeneration enters the clinic," Nature 443, 774-779 (2006)

[2] S. Baglioni et al, "Prefibrillar amyloid aggregates could be generic toxins in higher organisms," J Neurosci 26, 8160-8167 (2006)

[3] V. Paeder et al, "Detection of protein aggregation with a Bloch surface wave based sensor", Sens Act B 157, 260-264 (2011)

8212-06, Session 2

## The potential of back-scattering interferometry for use in diagnostics

D. J. Bornhop, A. Kussrow, I. Olmsted, C. S. Enders, Vanderbilt Univ. (United States); D. Cox, A. Castro, R. Ballard, Ctrs. for Disease Control and Prevention (United States)

The ability of BSI to perform fast, inexpensive, highly sensitive, and label-free binding measurements using minimal sample volume makes the technique highly attractive as a potential field-deployable or point-of-care diagnostic tool. BSI is a unique and universal platform technology capitalizing on a simple optical train to measure refractive index (RI) changes within a microfluidic channel. Femtomolar sensitivity and compatibility with complex matrices sets BSI apart from other optical biosensing methods. BSI detects changes in RI that accompany changes in conformation and solvation state of molecules which occur upon binding. All binding interactions generate such changes, so BSI works with species of widely divergent masses and types without artificial labels, at femtomolar levels. We will show that BSI is Assay Agnostic enabling detection schemes that are based on protein-protein, DNA-DNA, protein-small molecule, aptamer-protein, aptamer-small molecule and proteins or nucleic acids to virtually any molecule, all without the need for tagging or chemical derivatization in any way. The ability of BSI to perform fast, inexpensive, highly sensitive, label-free, free-solution binding measurements using minimal sample volume makes the technique highly attractive as a diagnostic tool. The potential of a multiplexed version will be discussed that would enable multiple disease diagnoses to be performed in a plug-and-play manner, on a few drops of sample. Our goal is to dramatically enhance the abilities of physicians to monitor therapeutic efficacy and to tailor treatment to patients on an individual basis.

8212-07, Session 2

## Resonant porous silicon microcavity for enhanced detection of protease activity in chronic wound fluid

S. Pace, F. S. H. Krismastuti, Flinders Univ. (Australia); B. Farrugia, T. Dargaville, Queensland Univ. of Technology (Australia); N. H. Voelcker, Flinders Univ. (Australia)

Porous silicon (pSi), thanks to its spongiform structure, can efficiently host many organic molecules dispersed in solutions having proper chemical affinity. The synthesis of pSi-based photonic structures for bio-sensing applications has been widely investigated in the last years. Fluorescence emission of organic dyes embedded in pSi can be efficiently enhanced if a photonic structure like a Fabry-Pérot resonator is employed as a host solid matrix. In this work, we present a system to monitor the activity of the matrix metalloproteinases (MMP), a family of zinc ion-containing proteolytic enzymes. MMPs are know to be involved in wound repair, playing an important role in extracellular matrix degradation, growth factor activation and immune system regulation. The enzyme substrate, with a specific peptide sequence recognized and cleaved by the MMPs, is coupled with a fluorophore and a quencher (DABCYL-GABA-Pro-Gln-Gly-Leu-Glu(EDANS)-Ala-Lys-NH2), and is covalently bound to the nanostructured surface of pSi. When active MMP enzymes cleave the Gly-Leu bond, proximity-based fluorescence energy transfer between EDANS and the DABCYL quencher is switched off, causing EDANS dye fluorescence, which is enhanced by the resonant microcavity properly tuned at emission wavelength of the hosted dye. With such a system, low MMP concentration can be detected thanks to the enhancement effect of the resonant microcavity, enabling the quantification of MMPs present in a media real time.

8212-08, Session 2

## Highly sensitive anisotropic porous silicon-based optical sensors

J. Álvarez, Univ. de València (Spain); P. Bettotti, N. Kumar, Univ. degli Studi di Trento (Italy); I. Suárez, D. Hill, J. Martínez-Pastor, Univ. de València (Spain)

Porous Silicon (PSi) has unique properties for sensing due to a morphological structure that presents tunable pore sizes for selective molecule infiltration and a large surface area/volume ratio that can be chemically modified for selective capture of target analytes. Moreover its low cost fabrication process and compatibility with microfabrication technologies make highly integrated low cost sensors possible. PSi made from (110) silicon presents high birefringence values for normal incidence light. PSi made from (100) silicon has no birefringence for normal incidence light, but its birefringence increases with sample tilt angle up to similar values of (110) PSi. These birefringence values are very sensitive to the presence of different substances inside the PSi pores. In this work, we report on the modeling, fabrication and characterization of PSi from (110) and (100) surface oriented silicon for optical sensing. First based on the modified Bruggeman method, the birefringence and sensitivity of the fabricated membranes are obtained as a function of the fabrication parameters such as porosity and pore sizes, and external effects such as the pores surface oxidation. Thereafter we report on the fabrication of several PSi membranes from (110) and (100) surface oriented silicon, with different pore diameters and thicknesses. Using a polarimetric setup the birefringence and sensitivity of the fabricated samples are determined; a bulk refractive index sensitivity of 1245nm/RIU comparable to the 1525 predicted by our model is reported. To the best of our knowledge this is the first time such a measurement scheme has been used for liquids in PSi

8212-09, Session 2

## Photonic crystal microcavity engineering and high-density biopatterning for chip-integrated microarray applications

W. Lai, The Univ. of Texas at Austin (United States); S. Chakravarty, Omega Optics, Inc. (United States); Y. Zou, R. T. Chen, The Univ. of Texas at Austin (United States)

Photonic crystal (PC) microcavities, with ultra-small mode volumes and high quality (Q) factors have found diverse applications in light emission, chip integrated optical communications and label-free sensing. While Q ~ 1million has been demonstrated in freely suspended membranes, the reduced refractive index contrast when PC microcavities are immersed in phosphate buffered saline (PBS), a typical ambient for biomolecules, reduces Q by more than 2 orders of magnitude. In PC waveguide (PCW) coupled drop resonance type PC microcavity sensors (typically L3 type PC microcavity with a row of 3 air holes removed), due to reduced refractive index contrast in PBS, the Q of the resonance mode that couples to the PCW is reduced. We investigate by simulations and experiment, multiple resonant modes of multiple PC microcavities that couple to a single PCW guided mode in PBS in the efficient coupling slow light guiding region. Geometries for high Q and large resonance wavelength shift in PBS are investigated. In addition, although PC microcavities can be densely integrated on chip, current bio-patterning methods impose fundamental engineering limits to the minimum spacing between individual microcavity sensor elements, when fabricating a microarray chip where each resonator is coated with its unique biomolecule to measure target biomolecule-probe biomolecule specific conjugate binding. We show that ink jet printing allows a minimum spacing of 50 microns between PC microcavities. High throughput microarray measurement is demonstrated by simultaneous interrogation of binding events on all PC microcavities coupled to a single PCW.

8212-10, Session 2

## Experimental demonstration of application of ring-down measurement approach to microcavities for biosensing

M. I. Cheema, A. G. Kirk, McGill Univ. (Canada); S. Mehrabani, A. M. Armani, The Univ. of Southern California (United States); A. A. Hayat, F. Vanier, Y. Peter, Ecole Polytechnique de Montréal (Canada)

Resonant micro-cavities with ultra high quality factors (Q~10^8-10^9) have a great potential for ultra sensitive bio-sensing as a single photon will interact with a sample many times. Until now, most work on micro-cavity biosensors has been based on measurement of the resonant frequency shift induced by binding of biomarkers to a cavity. However, there are two aspects of this approach which impede practical applications: 1) Intensity fluctuations of the light source add noise; and 2) Due to the very high Q of the silica micro-cavity, high field intensities are produced, resulting in large thermal effects at resonance which result in thermally induced shifts in resonant frequency. We hypothesize that these two issues can be overcome by the application of the ring down measurement approach to the micro-cavity in a biosensor and thus high sensitivity and better noise tolerance can be achieved without requiring very high resolution spectroscopic equipment. A finite element model of silica toroidal micro-cavity immersed in water has already been shown to verify the feasibility of a micro-cavity ring down biosensor [1, 2]. Here we report our preliminary experimental results that demonstrate the application of ring down measurement approach to micro-cavities for sensing refractive index changes in water.

References

[1] M. Imran Cheema, and Andrew G. Kirk. “Application of ring down measurement approach to micro-cavities for bio-sensing applications”, SPIE BIOS, San Francisco, Jan 2011.

[2] M. Imran Cheema, and Andrew G. Kirk. “Implementation of the perfectly matched layer to determine the quality factor of axisymmetric resonators in COMSOL”, COMSOL conference, Boston, Oct 2010

8212-11, Session 3

## Optofluidics in bio-chemical analysis

X. Fan, Univ. of Michigan (United States)

Optofluidics organically integrates microfluidics and photonics and is an emerging technology in biological and chemical analysis. In this talk, I will overview the recent studies in bio-chemical sensing applications of optofluidics. Particularly, I will report the research progress in my lab in developing various optofluidic devices, including optofluidic ring resonator label-free sensors, optofluidic Fabry-Pérot cavity flow-through label-free sensors, microfluidic laser based intra-cavity sensors, and optofluidic Surface-Enhanced Raman Spectroscopy (SERS) based sensors, as well as on-column optical detectors for micro-gas chromatography. These devices take advantage of superior fluidic handling capability and high sensitivity, and can be used in detecting various biological and chemical analytes in either liquid or vapor phase.

8212-12, Session 3

## Demonstration of optical-force assisted particle transport to an optical biosensor

A. Heiniger, B. L. Miller, P. M. Fauchet, Univ. of Rochester (United States)

Detection of single biological molecules is necessary for research, clinical, and defense applications. However, accepted methods are typically costly and require processing of the biological sample in a central laboratory. Therefore, a drive is underway to produce cheap, portable labs-on-a-chip that guarantee rapid detection of a single particle, if present in the input sample. Typical optical biosensing systems consist of a microfluidic layer, for transporting the input sample on-chip, fabricated atop a photonic layer, for particle detection. Detection of single sub-micrometer particles has been demonstrated using on-chip optical resonators, but a minimum particle concentration is necessary to ensure that a single particle randomly diffuses to the micrometer-scale resonator in a given time. Our goal is to reduce this minimum detectable concentration, ultimately to the limit of a single particle in the input volume. One method for improving the minimum detectable concentration is directed transport of particles to the sensing area. Here we look to optical forces for the particle delivery mechanism. In resonators, there is a buildup of optical intensity as resonant light makes multiple round trips, and optical forces attract dielectric particles to these high intensity regions. We perform experiments to measure the minimum target particle concentration that can be detected by a two-dimensional photonic crystal resonator using various optical powers and fluid flow speeds. We find that optical forces can lower the minimum detectable concentration by an order of magnitude or more. We also explore the impact of various geometrical system parameters, like resonator size and channel size.

8212-13, Session 3

## Optoelectronic tweezers for medical diagnostics

C. Kremer, S. Neale, A. Menachery, M. Barrett, J. M. Cooper, Univ. of Glasgow (United Kingdom)

Optoelectronic Tweezers (OET) allows the spatial patterning of electric fields by the selected illumination of a photoconductive surface. This has many applications for medical diagnostics demonstrated here with work towards diagnosing Human African Trypanosomiasis (HAT).

HAT, also known as African sleeping sickness, results from infection of a single celled parasite that spends most of its life cycle in the blood of the host. Diagnosing trypanosomiasis remains a challenge as it is necessary to visually confirm the presence of the parasite in a blood sample, which is difficult due to the extremely low levels of parasitemia. Concentrating the parasites to increase their density with respect to the erythrocytes in the blood sample is an essential part of the diagnostic process.

OET allows the manipulation of micro particles and cells by creating non-uniform electrical fields that then produce dielectrophoretic forces (DEP, the force between the dipole induced in a particle and an electric field gradient). The field pattern is reconfigurable by changing the light pattern focused onto a photoconductive element of the device. This provides real time control over the position of the particles being trapped.

The DEP force can be tuned through varying the frequency of the applied electric field or the conductivity of the surrounding medium. In this work we show that we can use a set of conditions that allows the attraction of the parasites and the repulsion of blood cells in the same sample making this a powerful tool to concentrate the parasites for optical detection.

8212-14, Session 3

## Optofluidic surface-enhanced Raman spectroscopy with nanoparticle-functionalized flow-through nanohole capillary

Y. Guo, M. K. Khaing Oo, X. Fan, Univ. of Michigan (United States)

Surface-enhanced Raman scattering (SERS) has emerged as a powerful analytical technique for direct detection of chemical and biological analytes because of high sensitivity, selectivity and rapid response. Here we propose and develop a novel optofluidic SERS structure, i.e., nanoparticle-functionalized flow-through nanohole capillary. This unique platform provides many advantages. First, its 3-dimensional (3-D) structure, similar to porous silicon, porous aluminum membranes, polymer monoliths, and photonic crystal fibers (PCFs), provides large surface area for the deposition of noble nanoparticles or nanoclusters to achieve high SERS intensity. Second, it has well-defined flow-through channels. It provides robust and controllable nanoparticle immobilization like PCF, but much higher nanoparticle density due to multiple nanoholes, and also enables fast and convenient analyte delivery for real-time, online detection. Third, the well-defined nanohole capillary can also confine and transmit light along the longitudinal direction, accumulating more SERS signal like PCFs. Fourth, it is easy to integrate with other sensing platforms, such as label-free biosensors, to provide comprehensive information on molecular interaction. Moreover, the nanohole capillary can be mass-produced easily and cost effectively using the fiber drawing method.

In this report, we will explore the operation of the optofluidic SERS system, discuss the immobilization of gold naoparticles or/and nanoclusters onto the flow-through capillary consisting of thousands of nanoholes, and characterize its sensitivity with ultra-low concentration Rhodamine 6G.

8212-24, Poster Session

## Morphological change monitoring of CMV infected tobacco leaf in vivo by optical coherence tomography

C. Lee, S. Lee, S. Han, H. Jung, J. Kim, S. H. Choi, H. Lee, Kyungpook National Univ. (Korea, Republic of)

CMV is one of the dangerous viruses at various plants such as a cucumber, a tobacco , and so on, which can cause serious damage in plant harvest. In spite of the enormous decline of the production of agriculture, there is no exit an adaptable method to screen the viral-diseases immediately. Conventional methods, such as a destructive biological or serological method, require significant effort and time. In this study, we verified a novel application of optical coherence tomography (OCT) to monitor the morphological change of a cucumber mosaic virus (CMV) infected tobacco leaves inner structure in vivo during a fifteen-day period. As comparing with the normal seeds, we can observe difference of the distance between the epidermal layer and the palisade parenchyma layer in CMV infected tobacco leaves. Histological study was performed for comparison and demonstrated close correlation with the OCT image analysis. Our results indicate that OCT shows potential as a tool to noninvasively reveal the morphological changes of the tobacco leaves infected by CMV and a frontier modality to differentiate the infected crop in real time screening.

8212-26, Poster Session

## Classification of bacteria by analysis of Fresnel diffraction patterns of bacteria colonies

I. B. Buzalewicz, A. Suchwalko, H. Podbielska, Institute of Biomedical Engineering and Instrumentation (Poland)

The early detection and classification of bacteria is an important problem in life science, health safety and food protection, due to the presence of the bacteria in the environment and its resistance against ordinary antibacterial chemicals. The proposed optical system designed for classification of bacteria species is based on the forward light scattering by bacteria colony. The analysis of light diffraction has a significant advantage: it does not required the special preparation of bacteria colonies. In the presented paper the optical system with converging spherical wave illumination for classification of bacteria species, is proposed. It allows for compression of the observation space to the finite region, observation of Fresnel patterns, diffraction pattern scaling and low level of optical aberrations, which don't possess other optical configurations. According to our knowledge, it is the first attempts to use such optical system to investigate the light diffraction by bacteria colonies. Based on the scalar theory of diffraction the complex physical model of light transformation by bacteria colonies in designed system, is presented. Obtained experimental results have shown that colonies of specific bacteria species generate unique diffraction signatures. It is possible to control the scale of obtained Fresnel pattern by changing the location of the sample respectively to the location of transforming lens. To determine the unique features of bacteria colonies diffraction patterns the image processing analysis was proposed. It was demonstrated that Fresnel patterns can be use for classification of following species: Escherichia coli, Salmonella enteritidis, Staplyococcus aureus, Proteus mirabilis and Citrobacter freundii.

8212-27, Poster Session

## Impedance spectroscopy of food micotoxins

O. I. Bilyy, R. Y. Yaremyk, Ivan Franko National Univ. of L'viv (Ukraine); I. Y. Kotsyumbas, State Scientific-Research Control Institute of Veterinary Preparations and Fodder Additives (Ukraine)

A new analytical method of high-selective detection of mycotoxins in food and feed are considered. A method is based on optical registration the changes of conduct of the electric polarized bacterial agents in solution at the action of the external gradient electric fields. Measuring are conducted in integrated electrode-optical cuvette of the special construction, which provides the photometric analysis of forward motion of the objects registration in liquid solution under act of the enclosed electric field and simultaneous registration of kinetics of change of electrical impedance parameters solution and electrode system. In the process of measuring functional dependences of coefficient of polarization of the set types of toxins and their mobility in solution at the different gain-frequency characteristics of the enclosed electric field, degree of agglomeration, photometric changes of solution. In basis of the offered method principle of the active use of a priori information is stopped up about the investigated objects, mathematical models of variants of co-operation, kinetic analysis and design of result measured curves. World-modeling is saved in a renewal database and can be modified and complemented in a prospect. On the whole the process of management of measuring and processing of data it is planned to realize on the basis of conception of the open intellectual systems in which there is modification of database in certain moments of time, that equivalent to perception the system of new content.

8212-28, Poster Session

## Quantitative analysis of OCT signal for virus-infected gourd seed distinction

C. Lee, S. Lee, S. Han, H. Jung, J. Kim, Kyungpook National Univ. (Korea, Republic of)

Optical coherence tomography (OCT) can be utilized to reveal the cross-sectional structure of the sample with a micrometer resolution. And, it also can be used to acquire the optical property of the samples that do not show the critical layers. In this study, we have verified the agricultural industry application of OCT to the quantitative analysis of the gourd seeds distinction between the infected seeds and the normal seeds by acquiring optical interference signal intensity inner structure and optical attenuation coefficients of the samples. As a result of the experiment, there was a 23 % OCT intensity signal decrease in the infected seeds when we compared with the normal ones. The optical attenuation coefficient in infected seeds was 2.9±0.09 mm−1, whereas, in the normal case, 3.4±0.12 mm−1 was observed. The quantitative analysis showed a strong and significant correlation compared with the microscopic pictures of cross-sectioned seeds.

8212-29, Poster Session

## Detection of pancreatic biomarkers by gallium nitride-based high electron mobility transistor

C. Tsai, W. Hsu, S. Jian, K. Cheng, S. Hsieh, H. J. Wang, L. Tu, National Sun Yat-Sen Univ. (Taiwan)

Gallium nitride based high electron mobility transistors (GaN-HEMT) are good candidate for biological detection due to their high stability in reactive environment, such as chemical/physiological solutions, not easy to be damaged by static electricity, and simple to be fabricated. Furthermore, the conducting two-dimensional electron gas is close to the surface (~30 nm) and is very sensitive to the changes of surface charges due to the binding of biological molecules. In this work, AlGaN/GaN films grown on c-plane sapphire were used as the conduction channel of the GaN-HEMTs. The GaN-HEMTs were fabricated by photolithography process. The as-fabricated GaN-HEMTs were then used as biosensors to detect the biomarkers, such as CA19-9. The detection limit, selectivity, and reliability were analyzed and discussed.

8212-15, Session 4

## Microflow cytometer for optical analysis of phytoplankton

J. P. Golden, N. Hashemi, J. S. Erickson, F. S. Ligler, U.S. Naval Research Lab. (United States)

Analysis of the intrinsic scatter and fluorescence profiles of marine algae can be used for general classification of organisms based on cell size and fluorescence properties. We describe the design and fabrication of a Microflow Cytometer on a chip for characterization of phytoplankton. The Microflow Cytometer measured distinct side-scatter and fluorescence properties of Synechococcus sp., Nitzschia d., and Thalassiosira p. Measurements were confirmed using the benchtop Accuri C6 flow cytometer. The Microflow Cytometer proved sensitive enough to detect and characterize picoplankton with diameter approximately 1 um and larger phytoplankton of up to 80 um in length. The wide range in size discrimination coupled with detection of intrinsic fluorescent pigments suggests that this Microflow Cytometer will be able to distinguish different populations of phytoplankton on unmanned underwater vehicles. Reversing the orientation of the grooves in the channel walls returns the sample stream to its original unsheathed position allowing separation of the sample stream from the sheath streams and the recycling of the sheath fluid.

8212-16, Session 4

## Microflow cytometer with 3D hydrodynamic focusing

G. Testa, R. Bernini, Consiglio Nazionale delle Ricerche (Italy)

This paper reports a micro flow cytometer for fluorescence detection of particles/cells at two different wavelengths fabricated in Polymethylmethacrylate (PMMA). In the proposed device the analysis of particle/single cells can be carry out by exploiting a three-dimensional (3D) hydrodynamic focusing of a liquid sample. The hydrofocusing is achieved simultaneously in both directions in a single step by combining the central channel with two pairs of deeper channels orthogonally connected to it. The device was made up by two halves of PMMA bonded together with part of the channels milled into each halve by direct micromilling. In order to simplify the fabrication, all the channels have the same width. Since the two focusing channels have the same dimension and the same flow rate, only one sheath inlet is necessary. With a suitable choice of the height ratio between the lateral and central channel, it is possible to obtain a circular sample stream located in the center of the channel regardless of the flow rate ratio of the sample and sheath liquid (FR). Moreover, by simply varying the flow rate ratio FR it is possible to reduce considerably the width of the central stream. This aspect offers great flexibility since the device permits to analyze particles/cells of very different size. The detection system comprises a pair of optical fibers orthogonally aligned with the flow stream. The scheme offers the possibility to carry out not only fluorescence, but also scattering analysis in each measurement simultaneously.

8212-17, Session 4

## Demonstration of a microfluidic polarimeter

R. P. Rajan, A. Ghosh, Indian Institute of Science (India)

We demonstrate a microfluidic device capable of detecting optically active or chiral samples with very high sensitivity. Traditional methods of detection, such as optical rotation are not suitable for miniaturization, since, the magnitude of the rotation of polarization scales down linearly with the optical path length of the device. Since the origin of optical activity is due to difference of refractive indices between the two circularly polarized states of light, it is possible to detect chiral media by measuring the dependence of the angles of refraction on the polarization state of the incident light. This however is a weak effect and hence requires sensitive optical detection schemes, based on multiple polarization modulation. The present method can be scaled down and is therefore more suitable for applications involving small sample volumes. In this report, we demonstrate a “microfluidic polarimeter” that can measure the optical activity arising out of sub-microliter volumes of a common chiral liquid (sugar in water). Our method is sensitive enough to be extended to measurements of physiological blood-glucose levels, which is of great importance to the pharmaceutical industry.

8212-18, Session 4

## Highlights of biosensing program at NSF

A. Simonian, National Science Foundation (United States)

The Biosensing Program supports innovative, transformative, and insightful investigations of fundamental problems with broad long term impact and applications that require novel use of bio-inspired engineering principles and sophisticated devices to meet the engineering and technology needs of the nation. The program is targeting research in the area of the monitoring, identification, and/or quantification of biological phenomena and will support potential technological breakthroughs that exist at the intersection of engineering, life science, and information technology.

Projects submitted to the Program must advance both engineering and life sciences. Projects in the program may range from single investigator to multi-investigator collaborative research efforts.

The development of these novel principles and devices will require highly collaborative interactions between engineers, life scientists, and experts in nanotechnology, biomaterials, bioinformatics, and the chemical and physical sciences. The program recognizes the important role of education and workforce development specifically relevant to the multidisciplinary nature of the area of biosensing. Interdisciplinary teams are essential and must be fostered from discovery to application.

8212-19, Session 5

## Lensless microscopy and sensing on a chip

A. Ozcan, Univ. of California, Los Angeles (United States)

Computational microscopy modalities are becoming quite powerful due to constantly increasing performance of opto-electronic components, computers as well as digital reconstruction algorithms. Therefore we have unique opportunities today to create new digital imaging and sensing architectures that significantly improve our microscopic analysis and sensing capabilities when compared to their analog counterparts.

As part of this broad research theme, our group at UCLA has recently created various lensfree on-chip imaging modalities including partially-coherent lensless holographic microscopy and tomography for field-use, cell-phone microscopy for telemedicine applications, lensfree fluorescent imaging over an ultra-wide field-of-view using compressive sampling, and lensfree incoherent on-chip imaging and sensing based on nano-structured plasmonic surfaces. In this presentation, we will review the basics of these emerging computational microscopy and sensing techniques and demonstrate their applications to e.g., high-throughput imaging and automated counting of blood cells, monitoring of HIV+ patients and detection of waterborne parasites towards rapid screening of water quality. Further, we will also discuss lensfree implementations of various other on-chip imaging modalities on the same platform such as pixel super-resolution imaging, holographic opto-fluidic microscopy and tomography. And finally, we will demonstrate lensfree on-chip imaging of fluorescently labeled cells over an ultra wide field-of-view of >8cm2, which could be especially important for rare cell analysis (e.g., detection of circulating tumor cells), as well as for high-throughput screening of DNA/protein micro-arrays.

These recent developments could enable new imaging and sensing architectures that are especially suitable for telemedicine as well as high-throughput biomedical imaging and screening applications in resource limited environments.

8212-20, Session 5

## Integrated optical sensor array for biochemical multiparameter analysis

D. Pergande, P. Lützow, H. Heidrich, Fraunhofer-Institut für Nachrichtentechnik Heinrich-Hertz-Institut (Germany)

Integrated optical refractometric waveguide sensors have already been shown to feature high sensitivity and fast response rate at low cost by full-wafer fabrication. Multiparameter detection is required for reliable biochemical analysis with low false-positive rates.

We have demonstrated the ability to analyze a multiple of miniaturized bus-integrated sensor elements at high sensitivity from the superimposed complex overall spectrum by individual frequency modulation of optical microring resonators (MRR) fed by a single bus waveguide.

The diverse sensor elements can be coated with biochemically selective adlayers (e.g., antibody molecules) to specifically promote the accumulation of target molecules on the MRR surface. Adhesion of target molecules results in an increase of the MRR resonance frequencies which can be measured at high sensitivity with picometer accuracy. Readout of each of the MRR from the complex overall spectrum is performed by using phase sensitive lock-in detection to filter out the individual and selective response to external stimuli.

We fabricated test arrays with 12 MRR elements based on silicon nitride material, each element integrated with a platinum heater electrode for thermo-optical modulation of the microcavity. A clear readout of the individual MRR by using a tuneable laser source is accomplished in a simple and reliable manner via lock-in detection despite strong overlap of the individual resonances.

With our first results, we point out the large potential for multiplexed label-free detection of diverse bio molecular compounds. Due to the miniaturization of the MRR arrays the realization of portable sensor systems will be feasible.

8212-21, Session 5

## Differential diffractive reflectance modulation sensing

N. Kumawat, G. R. Prashanth, M. M. Varma, Indian Institute of Science (India)

We have fabricated a reflectance based sensor which relies on the diffraction pattern generated from a bio-microarray where an underlying thin film structure enhances the diffracted intensity from protein monolayers. The zero order diffraction represents the background signal and the higher orders represent the phase difference between the array elements and the background. By taking the differential ratio of the first and zero order diffraction signals we get a quantitative measure of molecular binding while simultaneously rejecting common mode fluctuations. We improved the signal-to-noise ratio by an order of magnitude with this ratiometric approach compared to conventional single channel detection. In addition, we use a lithography based approach for fabricating microarrays which results in spot sizes around 5 micron diameter unlike the 100 micron spots from inkjet printing and is therefore capable of a high degree of multiplexing. We will describe our work on the real-time measurement of adsorption kinetics of charged polymers and single stranded DNA using this system with a current noise floor of less than 10 pm without any signal averaging. The lack of moving parts for point scanning of the microarray and the differential ratiometric measurements using diffracted orders from the same probe beam allows us to make real-time measurements in spite of noise arising from large thermal or mechanical fluctuations in the fluid sample above the sensor surface. Further, the lack of moving parts leads to considerable simplification in the readout hardware permitting the use of this technique in compact point of care sensors.

8212-22, Session 6

## Xerogel-nanocrystallite hybrids for optical sensing

F. V. Bright, Univ. at Buffalo (United States)

Sol-gel processing is widely used to create low-k materials, thermal insulations, and stationary phases in the separation sciences. Xerogels, porous sol-gel derived materials formed by solvent evaporation at or near ambient conditions, are also attractive platforms for chemical sensor development. Over the past 20 years our research group has devoted significant time and effort to elucidate the chemistry within amorphous silica-based xerogels as a means to intelligently guide the development of useful xerogel-based materials for use in areas ranging from chemical sensors to anti-fouling coatings. More recently we have been coupling amorphous silica-based xerogels to photoluminescent nanocrystalline materials (e.g., silicon quantum dots and porous silicon) as a way to create analyte-responsive nanoscopic sensors. The speaker will summarize his research team's pathway to developing hybrid silica-silicon nanosensors.

8212-23, Session 6

## Design of a gel electrophoresis device with an integrated transmitter/receiver system for power delivery and data communication: toward a wireless lab-on-chip

P. J. R. Roche, K. Greig, Y. Wang, M. C. K. Cheung, A. G. Kirk, V. P. Chodavarapu, McGill Univ. (Canada)

Gel electrophoresis systems are still operated with gel bed and power sources that consume laboratory space, in addition imaging methods using UV lamps and digital cameras do not constitute a portable analysis method. Microfluidics has made a contribution towards the miniaturisation of biomolecule separation, from gel filled channels, micro-pillar arrays and conventional capillary channel electrophoresis. The challenge remaining in miniaturisation is decoupling the separation method from un-miniaturised power sources, pumps and optical readout systems required to drive microfluidics that are physically the exact opposite of miniaturisation. In this study, the power to drive electrophoretic separation and LED excitation of fluorescently labelled biomolecules achieved by conversion of RF signal to DC voltage. Fluorescence detected by the blue enhanced 12 photodiode (individual PD size 2x1mm) array and signal was communicated wirelessly back to the RF reader connected to a laptop. The inclusion of a voltage regulator enables the control of electrical field (V/cm) over the separation chip to allow different forms of electrophoresis applied filled agarose filled channels or a capillary is possible. To lower the field strength required for gel electrophoresis, the dielectric of the agarose was altered by addition of gold nanoparticles (12nm diameter) and loading was optimised by impedance spectroscopy. The future directions towards multiple systems powered by a common RF source and a common data analysis node such as a laptop equipped with an RF reader are considered.

8212-25, Session 6

## Nano-sensing with a silica micro-toroid

T. Lu, Univ. of Victoria (Canada)

No abstract available

# Conference 8213: Optical Coherence Tomography and Coherence Domain Optical Methods in Biomedicine XVI

Monday-Wednesday 23-25 January 2012

Part of Proceedings of SPIE Vol. 8213 Optical Coherence Tomography and Coherence Domain Optical Methods in Biomedicine XVI

8213-01, Session 1

## Non-invasive optical imaging of true capillary blood flow within microcirculatory tissue beds using supercontinuum light source

Z. Zhi, R. Wang, Univ. of Washington (United States)

In this work, we present the utilization of supercontinuum light source to achieve ultra-high resolution and ultra-high sensitive optical microangiography (OMAG) imaging of microcirculations within tissue beds in vivo. After passing through a special designed optical filter with a bandwidth of 120 nm centered on 800 nm, the output light source is coupled into an optic-fiber based OMAG system that provides a measured axial resolution of ~3.2 μm over a ranging distance of 2 mm. Within this ranging distance, the system gives an averaged signal to noise ratio of 87 dB and a sensitivity roll-off of 7 dB. We demonstrate the capability of the system to visualize detailed microvascular perfusion map, including the single red blood cells within the capillaries, by imaging the mouse ear flap in vivo. We also demonstrate its capability for in vivo human skin microcirculation imaging with ultra-high resolution and sensitivity.

8213-02, Session 1

## High-resolution three-dimensional vasculature imaging by adaptive optics optical coherence angiography

K. Kurokawa, K. Sasaki, S. Makita, Y. Yasuno, Univ. of Tsukuba (Japan)

We developed adaptive optics optical coherence angiography (AO-OCA) for non-invasive, high-resolution, and three-dimensional investigation of retinal and choroidal vasculatures. Simultaneous intensity and Doppler imaging was used for the investigation.

The system is based on our custom-built AO SD-OCT. The SD-OCT sub-system uses an InGaAs camera driven with a line-rate of 91,911 line/s (Sensors Unlimited, Inc., NJ). In the AO sub-system, the dichroic mirror was used to split probe and beacon beams. This modification improved the signals for AO and SD-OCT sub-systems.

The Doppler signals are obtained from the phase-differences between the adjacent B-scans, where the time-separation of 1.4 msec. The Doppler artifacts were corrected by a histogram method. The power of Doppler shift was used for the visualization.

After taking multiple volumes, volume registration was performed semi-automatically.

As a result, the obtained photoreceptor mosaic showed the successful performance of the volume registration.

In the retina, two layers of capillary beds were observed at the top and bottom boundaries of the inner nuclear layer. Between two capillary beds, there were intermediate capillaries. The density of capillaries around a venule were higher than that around an arteriole. This is consistent with the anatomy.

In the choroid, we segmented into 4 depth layers for en-face visualization. Higher correlation between the intensity and Doppler was observed at the deeper position of choroid. This may indicate their complex, dense and non-layered structure at the close to the RPE. Three-dimensional investigation would provide better understanding of vasculature and micro-vasculature function, even they are complex in structure.

8213-03, Session 1

## In vivo human retinal and choroidal vasculature visualization using differential phase contrast swept source optical coherence tomography at 1060 nm

R. Motaghiannezam, S. E. Fraser, California Institute of Technology (United States)

Recent studies suggest the importance of imaging the retinal and choroidal vasculature networks in diagnosing various eye diseases such as age-related macular degeneration and diabetic retinopathy. Color fundus photography and fluorescein angiography have served as the gold standard methods for imaging the retinal vasculature network. Indocyanine green angiography extends such imaging to the deeper choroidal vessel. However, the 2-D nature of these imaging techniques limits their applications for providing depth information and/or deep choroidal blood vessels visualization. To meet the need for 3D retinal and choroidal vasculature assessment without the use of invasive fluorescent dye injection, optical coherence tomography (OCT) has emerged as an attractive depth-resolved imaging technology. By collecting multiple depth scans of the same retinal loci, it is possible to calculate the phase shift or phase variance needed for Doppler OCT (D-OCT) and differential phase contrast (DPC)-OCT, respectively. D-OCT captures the regions of high-velocity blood flow, such as in major vessels. However, the limited phase sensitivity and small time separation between A-scans limit the ability of D-OCT to capture slow flow in retinal capillaries or deep flows such as the choroidal circulation. To enhance sensitivity to the smaller signals expected from the microvasculature, the DPC-OCT method has been demonstrated by increasing the time separation between two depth scans and relying on the acquired phase of spectral domain (SD)-OCT signals for contrast.

To combine both deep penetration and superior sensitivity in depth for improving DPC-OCT at 800 nm, we extend the swept source (SS)-OCT to retinal/choroidal vasculature imaging at 1060 nm with the needed phase sensitivity and scan speed to capture phase variance data from not only the retina but the inner choroid as well. Motion contrast was achieved by phase difference measurements between two successive B-scans and removing one of the inherent phase error sources in SS-OCT (timing-induced phase error). DPC was implemented for assessing the retinal microvasculature at three different depths and regions of motion in the inner choroid. Two different DPC approaches were tested: power Doppler phase shift (PDPS) and differential phase variance (DPV). Direct comparisons of DPV and power Doppler phase shift (PDPS) methods revealed better visualization of the foveal avascular zone (FAZ) in DPV en face images.

8213-04, Session 1

## Phase-stabilized optical frequency domain imaging for the measurement of choroidal blood flow

B. Braaf, K. A. Vermeer, V. A. D. P. Sicam, J. F. de Boer, Rotterdam Ophthalmic Institute (Netherlands)

In optical frequency domain imaging (OFDI) the measurement of interference fringes is not exactly reproducible due to small instabilities in the swept-source laser and other optical components. The resulting variation in wavenumber sampling makes phase-resolved detection and the removal of fixed-pattern noise challenging in OFDI. In this paper this problem is solved by a new post-processing method in which interference fringes are resampled to the exact same wavenumber space using a simultaneously recorded calibration signal. This method is implemented in a high-speed (100 kHz) high-resolution (6.5 µm) OFDI system at 1-µm and is used for the removal of fixed-pattern noise artifacts and for phase-resolved blood flow measurements in the human choroid. The system performed close to the shot-noise limit (<1dB) with a sensitivity of 103.5 dB for a 1.7 mW sample arm power. The phase-stability of the OFDI system was measured to be limited by the SNR of the sample and calibration signal. Consequently, the suppression of fixed-pattern noise artifacts was shown up to 39.0 dB which effectively removed all artifacts from the OFDI-images. The clinical potential of the system is shown by the detection of choroidal blood flow in a healthy volunteer. Phase-resolved OFDI imaging showed a different part of the choroidal vasculature existing of smaller vessels located directly below the retinal pigment epithelium compared to the large choroidal vessels that were seen with intensity based OFDI imaging. The visualization of a different part of the choroidal vasculature by phase-resolved OFDI is potentially interesting in the evaluation of pathology.

8213-05, Session 1

## Measurement of blood flow in 3-D based on intensity information analysis of OCT data

D. Ruminski, I. M. Gorczynska, M. Szkulmowski, D. Bukowska, M. D. Wojtkowski, Nicolaus Copernicus Univ. (Poland)

We propose an alternative OCT data processing method to visualize and assess retinal microcirculation. This robust method uses only intensity information to investigate the blood flow in retinal blood vessels in 3 dimensions.

Data from eye measurements were acquired with Fourier domain OCT laboratory setup using high speed custom designed spectrometer, fiber based Michelson interferometer and Ti: Al2O3 laser as a light source.

We present scanning protocols and new method of quantitative flow measurement based on OCT images. We will present evaluation of this method by utilizing standard ,,optical flow" algorithms applied to 3-D OCT data. Proposed method is suitable for estimating velocity in strongly scattering micro-particles and can be successively applied for assessment of retinal microcirculation. Advantage of proposed method is the simplicity of algorithm and ability to detect small capillaries without requirement of high oversampling.

8213-06, Session 1

## Intensity vs. phase-variance optical coherence tomography for visualization of human retinal capillary networks: comparative study

D. Y. Kim, UC Davis Medical Ctr. (United States); J. Fingler, California Institute of Technology (United States); J. S. Werner, UC Davis Medical Ctr. (United States); D. M. Schwartz, Univ. of California, San Francisco (United States); S. E. Fraser, California Institute of Technology (United States); R. J. Zawadzki, UC Davis Medical Ctr. (United States)

We evaluate two methods to visualize human retinal micro-circulation in vivo with standard intensity-based optical coherence tomography (OCT) and phase-variance optical coherence tomography (pvOCT). En face projection views created from the same volumetric data set of the human retina using both data processing methods are created and compared. Additionally we used support vector machine (SVM) based semi-automatic segmentation to separate two retinal layers and to generate en face projection views from these layers. The segmented layers include: first, from the nerve fiber layer to the outer nuclear layer, and second, from the ganglion cell layer to the outer nuclear layer. In order to evaluate these two methods, we compare capillary density of the retinal vasculature images processed from two techniques and fluorescein angiography (FA).

8213-07, Session 2

## Handheld OCT probe for advanced diagnostics in primary care medicine

W. Jung, Univ. of Illinois at Urbana-Champaign (United States); J. Kim, Kyungpook National Univ. (Korea, Republic of); D. T. McCormick, AdvancedMEMS (United States); C. T. Nguyen, Z. Hubler, E. J. Chaney, Univ. of Illinois at Urbana-Champaign (United States); S. I. Sayegh, EYE Ctr. (United States); M. Novak, Carle Foundation Hospital (United States); C. N. Stewart, Blue Highway, LLC (United States); S. A. Boppart, Univ. of Illinois at Urbana-Champaign (United States)

We demonstrated a new type of handheld OCT probe which is able to not only image various tissues, but also provide convenient imaging functions for use in the primary care clinical environment. The handheld OCT probe utilized a 2-axis MEMS scanner for compactness, and interchangeable lens mounts for imaging various tissue sites such as the cornea, retina, tympanic membrane, and the skin. The size of the probe body was 11.5 cm (height) × 7.7 cm (width) × 4.5 cm (depth), and a 3.5 inch display was mounted on the probe body for efficient diagnostic procedures. During acquisition of OCT images, real-time OCT and video images are shown both on the computer monitor and the small display. Our device also has the function of data sonification in order to indicate the distance between probe and tissue. We integrated the handheld probe with a portable cart-based spectral-domain OCT system. Under IRB-approved protocols, normal human volunteers and those with various pathologies were recruited in order to evaluate the use and performance of our handheld OCT probe.

8213-08, Session 2

## Real-time three-dimensional dynamic imaging of airways reactivity using optical coherence tomography

J. Xi, R. Yung, W. Mitzner, R. Brown, X. D. Li, The Johns Hopkins Univ. (United States)

Precise quantitative measurement of lower airways' normal structure and structural changes in disease states is essential for both diagnosis and treatment of a multitude of pulmonary diseases, including asthma, bronchitis, bronchiectasis, and chronic obstructive pulmonary disease (COPD). In this study, we investigated the feasibility of a high-speed swept-source optical coherence tomography (SS-OCT) system along with a miniature side-viewing catheter to dynamically assess structural changes of the bronchus in response to in vivo real-time bronchoconstriction mimicking asthma. Changes of luminal area and wall thickness can be clearly identified by OCT in real time. Results demonstrated the potential of the catheter-based SS-OCT system for diagnosis of pulmonary diseases and dynamic assessment of treatment effects in real time.

8213-09, Session 2

## Volumetric optical frequency domain imaging of pulmonary pathology

L. P. Hariri, M. B. Applegate, M. Mino-Kenudson, E. J. Mark, B. E. Bouma, G. J. Tearney, M. J. Suter, Massachusetts General Hospital (United States)

Lung cancer is the leading cause of cancer-related deaths. Squamous cell (SCC) and neuroendocrine cancers typically arise in association with conducting airways, where as adenocarcinomas are more peripherally located. Tissue biopsies are often limited by small size and/or incomplete sampling. Optical frequency domain imaging (OFDI) provides large area 3-dimensional views of tissue microstructure at near-histological resolution (analogous to 4x microscopy). Recently, optical frequency domain imaging has been used bronchoscopically in vivo, but lack of correlated histopathology has limited the ability to develop imaging criteria. To assess correlated OFDI and histopathology, we performed OFDI through two approaches (bronchoscopic airway centered and pleural based parenchymal imaging) with a custom-built 2.4 French (0.8mm diameter) bronchoscopic catheter ex vivo in 47 surgical and 3 autopsy specimens. Tissue samples were marked with tissue dye to precisely correlate imaging and histological sampling locations. OFDI of normal airway allowed visualization of epithelium, lamina propria, submucosal glands, cartilage, and alveolar attachments. Carcinomas exhibited architectural disarray, loss of normal airway/alveolar structure, and rapid light attenuation. SCC showed nested architecture, while atypical glandular formation was appreciated in adenocarcinomas and mucoepidermoid carcinomas. Mucinous adenocarcinomas showed alveolar wall thickening with intra-alveolar mucin. This study is the first demonstration of volumetric OFDI with precise correlation to tissue-based diagnostics in lung pathology. With the amount of detail provided by the high resolution and vast volumes obtained, we anticipate OFDI may play a role in guiding interventional pulmonary procedures, such as CT-guided and transbronchial fine needle aspiration, and in future detection of pulmonary airway disease.

8213-10, Session 2

## Studying limb formation defects in mouse model of human diseases with OCT

K. V. Larin, Univ. of Houston (United States); I. V. Larina, M. E. Dickinson, P. Overbeek, Baylor College of Medicine (United States)

Congenital abnormalities of limbs are among the most common birth defects. These include missing or extra fingers or toes, abnormal limb length, and abnormalities in patterning of bones, cartilage or muscles. Optical Coherence Tomography (OCT) is a 3-D imaging modality, which can produce high-resolution (~8 μm) images of developing embryos with an imaging depth of a few millimeters. Here we demonstrate the capability of OCT to perform 3D imaging of limb development in normal embryos and mouse model with congenital abnormalities. Obtained results suggest that OCT technique is a promising tool to analyze internal structure and external appearance of the embryonic limb in mammalian models of congenital defects.

8213-11, Session 2

## Assessment of collagen changes in ovarian tissue by measuring optical scattering coefficient from OCT images

Y. Yang, T. Wang, N. C. Biswal, Univ. of Connecticut (United States); X. Wang, M. Sanders, M. Brewer, Univ. of Connecticut Health Ctr. (United States); Q. Zhu, Univ. of Connecticut (United States)

Optical scattering coefficient from ex-vivo unfixed normal and malignant ovarian tissue was quantitatively measured by fitting optical coherence tomography (OCT) A-line signals to a single scattering model. 1097 average A-line measurements at a wavelength of 1310nm were performed at 108 sites obtained from 18 ovaries. The average scattering coefficient obtained from normal group consisted of 833 measurements from 88 sites was 2.41 mm-1 (±0.59), while the average coefficient obtained from malignant group consisted of 264 measurements from 20 sites was 1.55 mm-1 (±0.46). The malignant ovarian tissue showed significant lower scattering than the normal group ($p < 0.001$). Using a threshold of 1.90 mm-1, a sensitivity of 76% and a specificity of 80% were obtained. The area under the receiver operating characteristic curve (AUC) is 0.877. The amount of collagen which is the main scattering source in ovarian tissue was analyzed from the tissue histological sections stained with Sirius Red. The average collagen area fraction (CAF) obtained from normal group was 48.4% (±12.3%), while the average CAF obtained from malignant group was 11.4% (±4.7%). Statistical significance of the collagen content was found between the two groups ($p < 0.001$). These results demonstrated that quantitative measurement of optical scattering coefficient from OCT images could be a potential powerful method for ovarian cancer detection and diagnosis.

8213-12, Session 2

## Fourier domain OCT imaging of American cockroach nervous system

J. Wyszkowska, I. M. Gorczynska, D. Ruminski, K. Karnowski, A. A. Kowalczyk, M. Stankiewicz, M. D. Wojtkowski, Nicolaus Copernicus Univ. (Poland)

In this pilot study we will demonstrate results of structural Fourier domain OCT imaging of the nervous system of Periplaneta americana (American cockroach). The purpose is to develop OCT apparatuses enabling examination of the insect neural system structure and to develop methods of sample preparation and handling during the OCT imaging experiments. We have performed imaging in the abdominal nerve cord excised from the American cockroach. For this purpose we have developed two OCT apparatuses: a spectral OCT system operating at 820nm and a swept source OCT system using a laser with a central wavelength of 1040nm. We will compare structural images obtained with these setups. We will discuss the applicability of OCT technique for imaging of nervous system of the American cockroach as well as the suitability of this insect model for further development of functional OCT methods.

8213-13, Session 3

## Probing single cone photoreceptor functionality to green light stimulus with combined SLO/OCT

S. Zotter, M. Pircher, E. Götzinger, T. Torzicky, M. Bonesi, C. K. Hitzenberger, Medizinische Univ. Wien (Austria)

We present a cellular resolution SLO/OCT system which is capable of imaging the human cone photoreceptor mosaic with a volume frame rate of 40Hz. We use a resonant scanner operating at 4kHz and a Basler sprint CMOS camera operating at 200kHz in order to achieve such a high volume frame rate. Individual cone photoreceptors can be tracked over a measurement period of up to 1 second and their response to green light stimulus can be investigated over time. By taking advantage of the 3D OCT data, we are able to measure the relative optical outer segment length changes which correspond to the length differences between inner/outer segments junction and end tips of the cone photoreceptors. This technique allows us to observe changes in the outer segment optical length with sub wavelength resolution. Various measurement protocols with different green light stimulation periods, ranging from flicker stimulation to no stimulus light given, were performed. The results show that the majority of the observed photoreceptors stay in their initial state if no green stimulation light is applied, whereas a significant change in the optical path length of the outer segment can be observed 25ms after every stimulus that was applied.

8213-14, Session 3

## Instrument tip-tracking ophthlamic intrasurgical SDOCT

J. V. Migacz, P. Hahn, R. V. O'Connell, C. Thomas, Z. Moustafa, C. Wang, S. J. Chiu, Duke Univ. (United States); L. Dai, U.S. Army Research Office (United States); C. A. Toth, J. A. Izatt, Duke Univ. (United States)

Intraoperative guidance of ophthalmic surgery using spectral-domain optical coherence tomography (SDOCT) holds promise for real-time visualization of delicate and translucent tissues during intrasurgical maneuvers. This approach provides faster feedback to the surgeon improving surgery speed and success. Similar systems under development operate at relatively low speeds employing current-generation clinical scanners with ~20k A-scans/sec, thus real-time volumetric imaging of the entire field-of-view of interest to the surgeon is impractical. Even with conversion to higher speed scanning, real-time complete volumetric imaging is unlikely due to limited computation hardware and limited light exposure during surgery. However, essential real-time feedback for the surgeon may be obtained over a reduced field of view by tracking the OCT imaging location to the tip of the surgical instrument in use. Such tracking could be used for either direct real-time imaging of single B-scans or small volumes at the instrument tip. In this submission, we introduce such a system that is provide fast, relevant, OCT imaging to the surgeon can be readily modified to match his or her surgical style. This system uses a clinical SDOCT system at 850nm and we demonstrate here its operation in simulated surgery of an animal eye.

8213-15, Session 3

## Ultrahigh speed spectral domain OCT for retina imaging at half megahertz A-line capturing rate

L. An, Oregon Health & Science Univ. (United States); T. Shen, R. Wang, Univ. of Washington (United States)

In this paper, we demonstrate a newly built ultrahigh speed spectral domain optical coherence tomography system (SDOCT) for ophthalmology applications. Through precisely controlling two high speed line scan CMOS cameras, the SDOCT system could achieve half megahertz A-line scan rate. And simultaneously, the proposed system could maintain both high axial resolution (~9 m) and acceptable depth range for retina imaging (~2.5 mm). It is worth emphasizing that two scanning protocols were designed for in vivo applications. The first one aimed to achieve isotropic dense sampling and super-fast scanning speed (~0.72 second for one 3D data set) for retina imaging. The ultrafast scanning speed (700 Hz B-frame rate) could contribute to eliminate most of the motion artifacts during the in vivo applications, while the isotropic dense sampling (500 A-lines within 4 mm on both directions) could enable two directional average for simultaneously enhancing the image signal to noise ratio and maintaining the resolution. The second protocol was designed to scan the retina in a large field of view, which captured 1200 A-lines within ~10 mm scanning range on both X and Y directions to provide overall information about the retina status. Using RPE layer as a reference, the captured original 3D data was flattened on both X and Y directions to be further explicitly evaluated through the depth resolved en face fundus images. The presented great performance suggested that the proposed newly built SDOCT has good potential in clinical diagnosis applications.

8213-16, Session 3

## Visible light optical coherence tomography for in vivo imaging the spectral contrasts of the retinal nerve fiber layer

X. Zhang, S. Jiao, The Univ. of Southern California (United States)

The ultimate goal of the study is to provide an imaging tool to detect the earliest signs of glaucoma before clinically visible damage occurs to the retinal nerve fiber layer (RNFL). Studies have shown that the optical reflectance of the damaged RNFL at short wavelength (<560nm) is reduced much more than that at long wavelength, which provides spectral contrasts for imaging the earliest damage to the RNFL. To image the spectral contrasts we built a dual-band spectral-domain optical coherence tomography (SD-OCT) centered at 808nm (NIR) and 415nm (VIS), respectively. The light at the two bands was provided by the fundamental and frequency-doubled outputs of a broadband Ti: Sapphire laser. The depth resolutions of the NIR and VIS OCT systems are 4.7μm and 12.2μm in the air. The system was applied to imaging the rat retina in vivo. Significantly different appearances between the OCT cross sectional images at the two bands are observed. The experimental results showed that the dual-band OCT system is feasible for imaging the spectral contrasts of the RNFL.

8213-17, Session 3

## Towards digital holographic imaging of the eye using a partially coherent light source

A. S. G. Singh, T. Schmoll, Medizinische Univ. Wien (Austria); B. Javidi, Univ. of Connecticut (United States); R. Leitgeb, Medizinische Univ. Wien (Austria)

In this paper, we explore the feasibility of using digital holography for ophthalmic imaging. Digital holography allows full control over the propagating wavefront and might therefore open up new possibilities for ophthalmic imaging. We discuss challenges of building a holographic system that can be used for holographic imaging of the eye and special requirements in ophthalmic imaging. We present the experimental setup and our attempts to deal with various challenges such as the reflex that is produced by the apex of the cornea. Preliminary results using a resolution test target are presented. In-vivo imaging is discussed and possibilities of aberration compensation are presented.

8213-18, Session 3

## Adaptive optics-assisted optical coherence tomography using a single small stroke deformable mirror

K. Sudo, Utsunomiya Univ. (Japan); K. Kurokawa, K. Sasaki, S. Makita, Y. Yasuno, Univ. of Tsukuba (Japan); T. Yatagai, B. Cense, Utsunomiya Univ. (Japan)

Optical coherence tomography (OCT) is a non-invasive method for three-dimensional imaging of the human retina in vivo. With the introduction of new OCT engines that operate at high acquisition rates, retinal image quality is limited by the number of photons returning from the eye. One way around this problem is to improve the light efficiency collection by using a larger beam size and adaptive optics. We quantified the performance of a low-cost AO-OCT design (45 cm x 25 cm x 25 cm footprint) built around a MEMS deformable mirror (5.5 µm mechanical stroke, 4.95 mm effective diameter). Preliminary measurements with a 3.4 mm beam on a human eye and on a model eye demonstrated that diffraction-limited performance can be achieved for aberrations as large as ~1.3 µm wavefront RMS. For a 3.4 mm beam at 840 nm, this is equivalent to approximately 3 D of defocus. An increase of 30 dB in dynamic range was observed in the OCT data obtained from the model eye, comparing the dynamic range in images before and after AO operation.

8213-19, Session 3

## Multicolor, integrated light stimulator for in vivo imaging of intrinsic optical signals in light-stimulated chicken retina with functional UHR-OCT

A. Akhlagh Moayed, S. Hariri, V. Choh, K. Bizheva, Univ. of Waterloo (Canada)

A multi-color light stimulator was designed and integrated with the imaging probe of a functional UHR-OCT (fUHR-OCT) system for measuring the intrinsic optical signals (IOS) from visually stimulated retina. The stimulator utilizes 4 LEDs, from which light is projected onto the retina to form a uniformly illuminated spot with precisely controlled intensity and duration of the visual stimulus. The fUHR-OCT system operates at ~1060 nm and provides 3.5 µm axial resolution in biological tissue and 11 µs time resolution. Consistent and reproducible, the IOS signals were observed with the modified fUHR-OCT system from all major retinal layers of the chicken retina in vivo.

8213-20, Session 3

## Adaptive optics - optical coherence tomography system for in-vivo imaging of the mouse retina

Y. Jian, A. Issaei, Simon Fraser Univ. (Canada); R. J. Zawadzki, UC Davis Medical Ctr. (United States); M. V. Sarunic, Simon Fraser Univ. (Canada)

Adaptive Optics (AO) is increasingly being used to improve the lateral resolution in human retinal imaging with techniques such as Optical Coherence Tomography (OCT), Scanning Laser Ophthalmoscopy (SLO), and fundus photography. In this report, we investigate integration of AO with Fourier Domain (FD) OCT for in vivo retinal imaging in mice. The mouse eye has a numerical aperture roughly twice that of humans, but the small size of the eye and the highly curved surfaces of the refractive elements of the cornea and crystalline lens makes high-resolution retinal imaging challenging. We have integrated a Hartmann-Shack wavefront sensor and deformable mirror into the sample arm of a FDOCT interferometer customized for small animal retinal imaging. A plano-concave lens was placed in soft contact with the mouse's eye to cancel refraction (and refractive errors) at the mouse's cornea, and also to facilitate mouse alignment for imaging. A short focal length objective lens was placed at the pupil plane conjugated with the wavefront sensor to focus the light on the retina. The broad band NIR light used for FDOCT was also used for the wavefront sensing. A benefit of this approach is that the wavefront sensing and FDOCT imaging are generated from the same focal plane. The estimated spot size on the mouse retina (based on Gaussian beam calculations) was ~3 micrometers. Representative B-scan images of the mouse retina acquired with FDOCT are presented with and without the Adaptive Optics.

8213-21, Session 4

## MEMS tunable VCSEL light source for ultrahigh speed 100kHz - 1MHz axial scan rate and long range centimeter class OCT imaging

B. M. Potsaid, Massachusetts Institute of Technology (United States); V. Jayaraman, Praevium Research, Inc. (United States); J. G. Fujimoto, Massachusetts Institute of Technology (United States); P. J. S. Heim, Covega Corp. (United States); J. Y. Jiang, A. E. Cable, Thorlabs Inc. (United States)

We demonstrate ultrahigh speed Swept Source / Fourier domain OCT imaging with record imaging depth ranges at imaging rates from 100kHz to 1MHz with new MEMS-tunable vertical-cavity surface-emitting laser (VCSEL) light source technology. The VCSEL is optically pumped at 980nm and a low mass electrostatically tunable mirror enables high speed wavelength tuning centered at ~1310nm with ~110nm of tunable bandwidth. The technology can be scaled to operate in wavelength regimes from 800nm to 1500nm. The micron-scale cavity length of the VCSEL enables single mode operation without mode hopping. Consequently, the coherence length of the laser can be extremely long. Measurements indicate a coherence length of much greater than 25mm, which allows direct optical clocking of the A/D converter without requiring electrical frequency doubling techniques. Linearization of the frequency sweep combined with the ability to use both the forwards and backwards sweeps gives high duty cycle and efficient utilization of A/D bandwidth. Commonly available 400-500MSPS A/D converters can be used to obtain long OCT imaging range with the VCSEL source. Sampling at higher rates enables extremely long centimeter range imaging with very low OCT sensitivity roll-off. OCT imaging of biological and non-biological samples at speeds of 100kHz - 1MHz axial scan rate are demonstrated. The results of this study suggest that MEMS based VCSEL swept light source technology has unique characteristics of wide tuning bandwidth, adjustable sweep repetition rates and record long coherence lengths, suggesting that VCSELs will be a critical technology for future ultrahigh speed and long depth range OCT imaging.

8213-22, Session 4

## Dispersion compensated megahertz FDML laser for imaging the anterior segment

W. Wieser, T. Klein, Ludwig-Maximilians-Univ. München (Germany); D. C. Adler, LightLab Imaging LLC (United States); F. Trépanier, TeraXion Inc. (Canada); C. M. Eigenwillig, S. Karpf, Ludwig-Maximilians-Univ. München (Germany); J. M. Schmitt, LightLab Imaging LLC (United States); R. Huber, Ludwig-Maximilians-Univ. München (Germany)

We present a 1300nm Fourier domain mode locked (FDML) laser for optical coherence tomography (OCT) application at 1.57 MHz scan rate with greatly improved coherence length. By reducing the dispersion in the fiber delay line of the FDML laser, the coherence length and hence the available imaging range is more than doubled compared to previously published MHz-FDML setups, reaching a 6dB sensitivity roll-off at >4.5mm imaging depth. We demonstrate OCT imaging of the anterior segment of the human eye. At 1GHz detection bandwidth, scan range and imaging depth can be traded off by adjusting the sweep range.

8213-23, Session 4

## Coherence length extension of Fourier-domain mode locked lasers

D. C. Adler, LightLab Imaging LLC (United States); W. Wieser, Ludwig-Maximilians-Univ. München (Germany); F. Trépanier, TeraXion Inc. (Canada); J. M. Schmitt, LightLab Imaging LLC (United States); R. A. Huber, Ludwig-Maximilians-Univ. München (Germany)

Fourier domain mode locked (FDML) lasers provide a desirable combination of high sweep rate, broad tuning range, and high output power for use in optical coherence tomography (OCT) systems. However, presently-known FDML lasers at 1300nm have relatively short coherence lengths, limiting the size of samples that can be imaged. Furthermore, FDML lasers produce only one useable sweep direction per filter drive period, necessitating the use of bulky and complex external buffering stages if high duty cycle laser output is required. Here we overcome these limitations by incorporating advanced dispersion compensation modules (DCMs) into the cavity, resulting in significant extension of FDML coherence lengths at wavelengths of 1310 nm and sweep rates up to 200 kHz.

The DCMs incorporate two chirped fiber Bragg gratings, the grating pair being designed to correct both normal and anomalous dispersion around 1310 nm.

The DCMs substantially eliminate group velocity dispersion (GVD) in the long fiber cavity, doubling the coherence length of the light source to > 21 mm. Removal of GVD allows the roundtrip time of light in the FDML cavity to be simultaneously matched for all wavelengths in the sweep, resulting in a spectrally-invariant coherence length. Unlike previously-known FDML lasers, this novel design provides uniform axial resolution over the entire imaging range, which is an important criterion for OCT imaging systems. An additional benefit of GVD removal is that the properties of the forward and backward sweeps become nearly identical, enabling high duty cycle operation without the use of external buffering stages.

8213-24, Session 4

## Polarization maintaining buffered Fourier domain mode-locked swept source for optical coherence tomography

J. Zhang, J. Jing, P. Wang, Z. Chen, Beckman Laser Institute and Medical Clinic (United States)

A polarization maintaining buffered Fourier domain mode-locked (FDML) swept source at center wavelength of 1310 nm for multiplying the scanning rate of FDML swept source was demonstrated. The scanning rate of the buffered FDML swept source was doubled without sacrificing the output power of the swept source by combining two orthogonally polarized outputs with a polarization beam combiner (PBC). The stability of the swept source was improved significantly because the polarization state of the laser beam inside the cavity is maintained without any polarization controllers. With the linear polarization states of the output laser beam, the buffered FDML swept source is also ready to be used in a PSOCT system. The swept source is capable of a tuning range of more than 150 nm at a 102 kHz sweeping rate. An FDOCT system was developed with the built swept source.

8213-25, Session 4

## Comb spacing-swept multi-wavelength source for deeper OCT imaging

S. Park, J. S. Park, C. Kim, Pusan National Univ. (Korea, Republic of)

As optical coherence tomography (OCT) has been realized with Fourier-domain OCT scheme, such as swept-source (SS) OCT and specral-domain (SD) OCT, for the various applications of biomedical imaging and industrial surface inspection, the research issue is focused on the enhancement of depth region of the target sample. It has been hard to get a high sensitivity point spread function (PSF) at the deeper depth over ~ 5 mm of sample in FD-OCT system because the finite coherence length of swept source outpout or the finite number of CCD pixels limits the roll-off characteristics of dynamic range, respectively. Though the time-domain OCT provides a relatively longer length of PSF depth, there is a critical limitation that time-domain OCT requires to move the reference arm of the interferometer to receive the interferogram by changing the optical path length difference.

In this research we propose a novel light source of comb spacing-swept multi-wavelength source based on polarization differential delay line (PDDL) and Piezoelectric transducer (PZT). Various types of multi-wavelength source have been mainly studied for the wavelength-division multiplexing (WDM) optical communication and the improved energy efficiency of spectrally sampled source.

Except the light source part, the proposed OCT interferometer setup is same with the SS-OCT system, which does not employ either a free space spectrometer or reference path scanning. The signal processing method for depth profiling is similar with TD-OCT to acquire the deeper depth information, however it is not necessary to scan the reference path to induce a interferogram because the interference is generated from the inside of light source.

8213-26, Session 4

## Broadband Fourier domain mode-locked laser for optical coherence tomography at 1060 nm

S. Marschall, Technical Univ. of Denmark (Denmark); T. Klein, W. Wieser, B. R. Biedermann, Ludwig-Maximilians-Univ. München (Germany); C. Pedersen, Technical Univ. of Denmark (Denmark); R. A. Huber, Ludwig-Maximilians-Univ. München (Germany); P. E. Andersen, Technical Univ. of Denmark (Denmark)

Optical coherence tomography (OCT) in the 1060 nm range is interesting for in vivo imaging of the human posterior eye segment (retina, choroid, sclera) due to low absorption in water and good penetration through the retinal pigment epithelium. Rapidly tunable light sources, such as Fourier domain mode-locked (FDML) lasers, enable the acquisition of densely sampled 3D datasets covering a wide field of view. However, semiconductor optical amplifiers (SOAs) - the typical gain media for swept sources - for the 1060 nm band available until now could only provide relatively low output power and bandwidth.

We have implemented an FDML laser using a new SOA featuring broad gain bandwidth and high output power. The output spectrum coincides with the wavelength range of minimal water absorption, making the light source ideal for OCT imaging of the posterior eye segment. With moderate SOA current (270 mA) we achieve 93 nm total sweep range and 12 µm depth resolution in air. By modulating the current, we can optimize the output spectrum and thereby improve the resolution to 8 µm in air (~6.5 µm in tissue). The average output power is higher than 20 mW. Both sweep directions show similar performance; hence, both can be used for OCT imaging. This enables a depth scan rate of 350 kHz without buffering the light source output.

8213-27, Session 4

## Dual-wavelength-swept active mode locking laser for multiband OCT imaging

H. Lee, C. Kim, M. Jeong, Z. Chen, Pusan National Univ. (Korea, Republic of)

This paper shows experimentally dual wavelength swept property with active mode locking (AML) method. Unlike conventional wavelength swept laser, AML wavelength swept laser does not require any wavelength selecting filter in the cavity. The cavity has two free spectral ranges (FSRs) depend on dual path configuration. This wavelength swept laser can be useful for dual-band swept source optical coherence tomography (OCT) imaging.

8213-28, Session 4

## A monolithic semiconductor laser with long coherence length for fast and inexpensive optical coherence tomography

J. R. Ensher, P. Boschert, K. Featherston, J. Huber, M. Crawford, M. Minneman, Insight Photonic Devices (United States); C. Chiccone, D. Derickson, California Polytechnic State Univ., San Luis Obispo (United States)

We demonstrate a new swept-wavelength laser for optical coherence tomography using a monolithic semiconductor device with no moving parts. The laser is based on a vernier-tuned Distributed Bragg Reflector (VTDBR) structure. We show 50nm wavelength sweeps centered at 1590nm, operated at 200Hz sweep repetition rates, with peak output power of 10mW. Using a test interferometer, we demonstrate point-spread functions with 45-55dB dynamic range. We also show high coherence length > 40mm at up to 200kHz sweep rates. The laser system has wavelength calibration to set an electronic sample trigger clock (an electronic k-clock) that denotes equal optical frequency intervals during the sweep. The laser tuning mechanism is all-electronic, which makes the laser highly adjustable and programmable. We demonstrate a controlled, flat power vs. wavelength profile, programmable sweep rates with the same device, and an adjustable duty cycle of up to 95%. Because the laser is a monolithic semiconductor structure based on reliable, wafer-scale processes, the cost of the laser will decrease rapidly in volume production. We will also present an update of our development of lasers capable of 100nm sweeps at 200kHz, centered at 1570nm and 1310nm, with output powers approaching 30mW.

8213-85, Poster Session

## Using surface wave to assess mechanical properties of skin and skin diseases as measured by phase-sensitive OCT

C. Li, G. Guan, Univ. of Washington (United States); Z. Huang, Univ. of Dundee (United Kingdom); R. Wang, Univ. of Washington (United States)

Mechanical properties of skin are important tissue parameters that can aid disease diagnosis and treatment, since most of the skin disease can cause the skin elasticity disorder. This paper presents a method that combine phase sensitive spectral domain optical coherence tomography (PS-OCT) imaging system and surface wave method to evaluate the mechanical properties of soft tissues, especially skin. In this study, PS-OCT acts as a tool to measure the surface wave generated by impulse stimulation from a home-made shaker, and provides the images for the geometry information of sample surface. Experiments are carried out on single and double-layer agar-agar phantoms, of different concentrations and thickness, and on human skin and at the sites of the forearm and the palm in vivo. In addition, we carried on a skin disease case study on ex vivo chicken breast to mimicking malignant melanoma (MM). For each experiment, the surface wave phase velocity dispersion curves were calculated, from which the elasticity of each layer of the sample was determined. It is demonstrated that the experimental results agree well with theoretical expectations. This study provides a novel combination of PS-OCT technology with a mechanical impulse surface wave stimulation that can be used to non-invasively evaluate the mechanical properties of skin and soft tissues, and may offer potential use in clinical situations.

8213-86, Poster Session

## Discretely swept optical coherence tomography system using super-structure grating distributed Bragg reflector lasers at 1561-1639 nm

D. Choi, R. Yoshimura, H. Hiro-Oka, H. Furukawa, Kitasato Univ. (Japan); A. Goto, Canon Inc. (Japan); N. Satou, A. Igarashi, M. Nakanishi, K. Shimizu, Kitasato Univ. (Japan); K. Ohbayashi, Kitasato Univ. School of Medicine (Japan)

A swept source optical coherence tomography (SS-OCT) system was developed by combined use of discretely swept two super-structure grating Bragg reflector (SSG-DBR) lasers; L--band (1.561-1.601um) and L+-band (1.598-1.639um). The instantaneous output frequency of these lasers is determined by a few injection currents, which are scanned following look up tables. Methods to make the look up tables for stepwise noise free scanning, to eliminate stitching noises associated with abrupt change of the injections currents and to concatenate the two lasers seamlessly are described. Techniques to reduce optical aliased noise in this frequency comb SS-OCT are also explained. A system sensitivity of 127 dB was observed, compared to the theoretical shot noise limited sensitivity of 132 dB at an A-scan rate of 3.1 kHz and with a sample illumination power of 9.4 mW. The sensitivity roll off of less than 1 dB and a nearly constant resolution of 16 um were observed within the principal region of 12 mm depth range. A dynamic range of as large as 80 dB was attained near the zero optical path length difference, decreasing to 57 dB as the depth increased in the principal region. Enhanced image penetration depths were demonstrated for a few samples; intralipid, skin, a tooth and anterior segment of the eye.

8213-87, Poster Session

## Depth profile absorber concentration reconstruction using photothermal optical coherence tomography

R. Reif, G. Guan, R. Wang, Univ. of Washington (United States)

Non-invasive measurements of drug concentrations as a function of depth in biological tissues may have implications in diagnosing, monitoring and treating several diseases, such as cancer. In this study, we present a photothermal optical coherence tomography system (PT-OCT) which contains a pump laser and a phase sensitive spectral domain optical coherence tomography system (OCT). The pump laser (808 nm modulated at 400 Hz, 50.8mW) is used to increase the temperature of the optically absorbing drug inside the tissue, known as a photothermal effect. This increase in temperature causes a change in the optical pathlength (OPL) which can be detected by the phase sensitive OCT system (1310 nm). An analytical model that describes the depth dependent changes in OPL induced by the pump laser has been developed. The model is derived theoretically and the coefficients are empirically determined using solid homogeneous agar gel phantoms. It is demonstrated that the OPL increases linearly as a function of depth for small values of the product of the depth times the attenuation coefficient. The OPL is insensitive to scattering values typically found in biological tissues. The accuracy of the model and the inversion algorithm were investigated and validated by reconstructing the depth dependent tissue absorber concentration in solid double layered phantoms. To our knowledge, this is the first reconstruction of the concentration of an absorber as a function of depth on solid tissues based on PT-OCT.

8213-88, Poster Session

## Imaging of breast cancer tumor margins with an OCT needle probe

R. A. McLaughlin, A. Curatolo, B. Y. Yeo, K. M. Kennedy, B. C. Quirk, R. W. Kirk, D. Lorenser, The Univ. of Western Australia (Australia); B. A. Wood, PathWest Lab. Medicine WA (Australia); A. G. Bourke, Sir Charles Gairdner Hospital (Australia); C. M. Saunders, D. D. Sampson, The Univ. of Western Australia (Australia)

This paper presents the use of a side-facing OCT needle probe for the assessment of breast cancer tumor margins. The OCT needle probe comprises lengths of no-core and GRIN fibers, fused to a length single mode fiber and encased within a 23-gauge needle. The beam was deflected at 90 degrees by a polished copper mirror positioned within the needle, and passed through a small window etched into the needle wall. Fresh human breast tumor specimens were imaged as the OCT needle probe was retracted across the tumor margin, and images were validated against a histological gold-standard. Images showed a clear distinction between areas of malignant and healthy tissue, and features such as individual blood vessels were identified.

8213-89, Poster Session

## High resolution long imaging range SSOCT system based on a multi-spectral band Fourier domain mode-locked swept source

J. Zhang, P. Wang, J. Jing, Z. Chen, Beckman Laser Institute and Medical Clinic (United States)

A broad band narrow line-width Fourier domain mode-locked (FDML) swept source at center wavelength of 1310 nm utilizing multi-spectral bands coherently fused with a phase processing technique was demonstrated. A dual spectral band fiber Fabry-Perot filter in the cavity of the FDML swept source selects two wavelengths simultaneously. The interference signals in two spectral bands are separated into two channels for detection thru the use of WDM couplers and then coherently fused with a phase analysis approach. The scanning ranges within each spectral band are 55 nm and 54 nm, respectively. The total scanning range by coherently fusing multiple bands is more than 100 nm. The axial resolution of the system is measured to be 9.6 μm with imaging range of more than 6 mm.

8213-90, Poster Session

## Frequency-domain coherence-gated Shack-Hartmann wavefront sensor

J. Wang, A. G. Podoleanu, Univ. of Kent (United Kingdom)

In the present report we investigate the possibility of narrowing the depth range of a physical Shack-Hartmann wavefront sensor (SH-WFS) using coherence gating (CG) in spectral domain. We have already demonstrated a time-domain low coherence interferometry (LCI) set-up, capable of generating similar Shack-Hartmann spots pattern to that delivered by a conventional SH-WFS and capable of eliminating stray reflections. Hereby we present another approach by employing a wavelength tuneable light source to obtain SH spot patterns with a narrow coherence gate in a 3D volume without any axial scanning. Signal noise ratio measurements are compared to conventional SH-WFS and previous time-domain setup (TD-CG/SH-WFS). This novel technique has the potential of providing depth resolved wavefront aberration information, which can guide better correction in adaptive optics assisted ophthalmology imaging and confocal imaging instruments.

8213-91, Poster Session

## Automated three-dimensional registration of intra-vascular optical coherence tomography images for the clinical evaluation of stent implantation over time

G. Ughi, T. Adriaenssens, Katholieke Univ. Leuven (Belgium); M. Larsson, Royal Institute of Technology (Sweden); C. Dubois, P. Sinnaeve, M. Coosemans, W. Desmet, J. D'Hooghe, Katholieke Univ. Leuven (Belgium)

Intravascular optical coherence tomography (IV-OCT) is a catheter based high resolution imaging technique able to visualize in-vivo the inner wall of the coronary arteries and implanted devices with an axial resolution below 20µm. IV-OCT is typically used in several clinical trials aiming to quantify the vessel response to stent implantation over time. However, image analysis is currently performed manually and corresponding images over time are spatially registered through a very labor intensive and subjective procedure. We present an automated method for the registration of IV-OCT datasets. Stent struts are segmented through consecutive images and three-dimensional models of the stents are created for both the datasets to be registered. The two models are set in approximate registration through an automatic initialization procedure and an iterative closest point algorithm is subsequently applied. To correct for non-uniform rotational distortions and other potential acquisition artifacts, registration is consecutively refined on a local level. The algorithm was validated by using an in-vitro experimental setup based on a polyvinyl-alcohol gel tubular phantom. The registration error was quantified through the use of markers resulting in a mean translation error of 0.14mm (pullback direction) and a mean rotation error of 7.3°. These results suggest that the proposed methodology can be used for automated registration of in-vivo data. Such a tool would be able to give unique insights about vessel healing pathophysiology and reaction to stent implantation testing the performance of new generation of intracoronary devices and different drugs.

8213-92, Poster Session

## Motion-insensitive optical coherence tomography based microangiography

T. Chi, C. Lee, C. Wu, H. Tseng, Y. Kiang, C. Yang, C. Chiang, National Taiwan Univ. (Taiwan); M. Tsai, Chang Gung Univ. (Taiwan)

Because it can provide important information of blood flow in living bio-tissue, optical Doppler tomography (ODT) has become an attractive technique in the development of the optical coherence tomography (OCT) technology. However, unless three-dimensional OCT scanning or other approaches are used, it is usually difficult to obtain the real blood flow speed due to the missing information of blood flow direction in two-dimensional OCT scanning. On the other hand, without the information of blood flow speed, the distribution of blood vessels or the blood vessel density in a living tissue is important information for understanding the tissue condition, particularly around a tumor. For such a micro-angiography application, OCT scanning and the related ODT image-processing techniques have shown to be quite useful. In processing OCT scanning images, the suppression of the phase noise caused by motion artifacts is an important issue. The phase noise seriously degrades the processed micro-angiography and ODT images. Several methods have been proposed for suppressing such phase noise. However, those methods are generally not so effective. In this paper, we propose an alternative imaging process procedure for effectively suppressing the phase noise due to motion artifact. In particular, we can effectively suppress the phase noise due to the inherent motion pattern of a stepping motor, which is usually used for building an OCT scanning probe.

8213-93, Poster Session

## Resolution improvement in dual-band OCT by filling the spectral gap

P. Cimalla, M. Gaertner, J. Walther, E. Koch, Universitätsklinikum Carl Gustav Carus Dresden (Germany)

A method for axial resolution improvement in dual-band optical coherence tomography (OCT) is presented. The spectral domain dual-band OCT system is illuminated by a supercontinuum laser light source and allows simultaneous imaging at 800 nm and 1250 nm with two synchronized spectrometers. In order to improve the resolution to a value achievable with a spectrum from the beginning of the short band to the end of the long band, several methods were compared. A simple FFT of the data of both spectral bands with intensity zero in the spectral gap results in high amplitude side bands and therefore is not useful for resolution improvement. In spite of the missing data in the spectral gap, the data from the two bands can be transformed by a Fourier transformation using non equidistant sample points. This method is based on a calculation using a Vandermonde matrix. Simulations show that this method copes well with small spectral gaps but produces pronounced imaging artifacts with larger spectral gaps. Similar results were achieved using the Lomb transformation. Performing short-time Fourier transformation on the spectral data shows that the phase of the signal varies slowly with spectral position in the center of a feature while it varies strongly at the edges. Using this approach, the signal strength for the complete spectrum can be estimated. This approach was trimmed and tested with data of a single band omitting a part of the spectrum. Afterwards, this method was applied to dual-band data resulting in higher resolution with only little artifacts.

8213-94, Poster Session

## Partially coherent reconstruction for optical coherence tomography

M. L. Villiger, G. J. Tearney, B. E. Bouma, Wellman Ctr. for Photomedicine (United States)

Optical Coherence Tomography (OCT) and other coherent imaging systems, especially in reflection mode, are flawed by speckle. The ability to resolve two point objects is no longer an unambiguous function of the distance they are separated, but changes periodically in function of the precise spatial arrangement. In this work, we analyze the coherent image formation of OCT, which gives access to the amplitude and phase of the scattered field, with the formalism of partially coherent imaging. Instead of using all available spatial frequencies to improve resolution, partially coherent systems use part of this information for averaging and suppressing speckle. Here we analyze this tradeoff and find that the speckle contrast can be suppressed by a factor of sqrt(2) in hand with a loss of resolution by the same factor. We use this approach to reconstruct tomograms in a partially coherent fashion. The formalism of partially coherent imaging is convenient tool to assess the notion of resolution and speckle suppression, and could help to guide future efforts in the development of algorithms or optical system design.

8213-95, Poster Session

## High-speed spectroscopic OCT around 1550 nm based on dual-band swept laser source

R. Zhu, J. Xu, C. Zhang, K. K. Y. Wong, E. Y. Lam, The Univ. of Hong Kong (Hong Kong, China)

Spectroscopic OCT (SOCT) has been demonstrated to be a powerful tool for the classification of different tissue types. Even though the two-spectrometer-based Fourier-domain spectroscopic OCT saves the computational cost, the speed is still limited. On the other hand, a swept laser can dramatically improve the sweep rate. In order to further increase the imaging speed in spectroscopic OCT, it is essential to enhance the sweeping wavelength range of the conventional FDML swept-source by a dual-band swept-source as we demonstrate here.

In our experimental setup, optical parametric amplifier (OPA) was used to generate the dual-band swept-source. A time-multiplexing architecture was developed to combine the two wavelength bands from OPA. Sweeps with different wavelength ranges were separated in time domain. By this time-multiplexing technique, the dual-band swept laser can be easily assembled in typical swept-source OCT system utilizing single-band detecting configuration.

The SOCT imaging was finally performed at the anterior segment of a fish eyeball using this high speed dual-band swept laser source. Comparing with the spectrometer based configuration, this system improves the speed by a factor of 40. The SOCT which combines the advantages of the two wavelengths enhances the structure contrast in comparison with OCT image generated by single band. The color that mapped by different bands in SOCT can be used for tissue classification and water content measurement.

8213-96, Poster Session

## Wide tuning range wavelength-swept laser at 1020 nm for ultra-high resolution FD-OCT

S. Lee, H. Song, M. Jung, S. Kim, Electronics and Telecommunications Research Institute (Korea, Republic of)

In this study, we demonstrated a wide tuning range wavelength-swept laser at 1020 nm with a single semiconductor optical amplifier (SOA) for ultra-high resolution Fourier-domain optical coherence tomography (FD-OCT). The wavelength-swept laser was constructed on the external line-cavity with Littman configuration. To obtain a wide wavelength tuning range, we adjusted a temperature of a thermoelectric (TE) cooler in an SOA mount. Our swept laser had a tuning range of 142 nm and - 3 dB bandwidth of 121.5 nm at a scan speed of 18 kHz. In addition, the averaged optical power was measured to be 8.2 mW. When our swept laser was used in the FD-OCT system, the measured axial resolution was 4.0 um in air corresponding to 2.9 um in tissue (n = 1.35).

8213-97, Poster Session

## Gold nanocages with enhanced scattering as OCT contrast agents

Y. Chen, J. Xi, J. Li, J. Mavadia, The Johns Hopkins Univ. (United States); J. C. Ramella-Roman, The Catholic Univ. of America (United States); X. D. Li, The Johns Hopkins Univ. (United States)

We report the synthesis and optical characterization of structured gold nanocages with a scattering-dominated cross-section, which serves as potential contrast agent with enhanced scattering for OCT imaging around 800 nm. We characterized the optical properties of gold nanocages with an SPR of ~780 nm using a tissue phantom and confirmed with integrated sphere measurements, furthermore we demonstrated contrast enhancement for OCT imaging of mouse liver and tumor in vivo by ~2.4 dB after intravenous injection. To the best of our knowledge, this is the first demonstration of scattering dominant OCT contrast agents based on gold nanoparticles which have a large backscattering cross-section as well for OCT contrast enhancement.

8213-98, Poster Session

## Microfluidics analysis of blood using spectral and time domain optical coherence tomography

D. Bukowska, M. Szkulmowski, I. M. Gorczynska, A. A. Kowalczyk, M. D. Wojtkowski, Nicolaus Copernicus Univ. (Poland)

In this paper we present a microfluidic system to investigate the flow behavior of blood using Spectral and Time domain Optical Coherence Tomography. The key idea is to propose a novel method for measurement of rheological parameters of the blood using simple device with geometry similar to natural blood capillaries network to get a qualitative and quantitative understanding of what kind of flows we might expect and what is the nature of flow in vessels with thickness comparable to cell size.

Since the Doppler OCT techniques have already enabled imaging of biological flow in large vessels, the reconstruction of velocity maps of the capillary network still provides a challenge. In the flow maps of capillary network randomly varying Doppler signal is observed. There may be few hypotheses that could explain the observed effects. One possible explanation is that blood in such small vessels cannot be treated as optically homogenous medium anymore since the vessel diameter is already similar to that of individual red blood cells. Different blood constituents may flow with different, varying velocities which results in random Doppler signal. Moreover in small capillaries the hematocrit is extremely low. Under all of these conditions Doppler OCT may be inaccurate in blood flow measurements. Investigation of blood flow in microchannel device can help to answer the question if Doppler OCT is accurate to flow measurement in small vessels or not.

8213-99, Poster Session

## Limited effect of phase modulation amplitude on polarization-sensitive optical coherence tomography measurements with continuous polarization modulation

Z. Lu, D. K. Kasaragod, S. J. Matcher, The Univ. of Sheffield (United Kingdom)

We report for the first time (to our knowledge) that the measured phase retardance, relative optic-axis orientation and diattenuation of a sample are independent of the Bessel functions of the first kind of the order of 0 and 1 evaluated at the set phase modulation amplitude by using polarization-sensitive optical coherence tomography with continuous polarization modulation (CPM-PS-OCT). This discovery has fundamental importance for clinical CPM-PS-OCT devices and systems development by simplifying the instrumentation significantly. This makes it possible to remove the electro-optical modulator (EOM) calibration process, and use any phase modulation amplitude when the EOM is not saturated at any point without affecting the measurement.

8213-100, Poster Session

## Lateral resolution improvement in oversampled optical coherence tomography images assuming weighted multiscatterer contributions

E. Bousi, C. Pitris, Univ. of Cyprus (Cyprus)

A novel method for lateral resolution improvement of Optical Coherence Tomography (OCT) images, which is independent of the focusing of the delivery optics and the depth of field, is presented. This method was inspired by radar range oversampling techniques. It is based on the lateral oversampling of the image and the estimation of the locations of the multiple scatterers which contribute to the signal. The information in the oversampled images is used to estimate the locations of multiple scatterers assuming each contributes a weighted portion to the detected signal, the weight determined by the location of the scatterer and the point spread function (PSF) of the system. A priori knowledge of the PSF is not required since optimization techniques can be employed to achieve the best possible enhancement of the image resolution. Preliminary results of such an approach on laterally oversampled OCT images have shown that it is possible to achieve a two-fold lateral resolution improvement. Moreover by performing deconvolution with the new improved PSF the lateral resolution can be further improved by another factor of two for a total of 4x improvement. Such improvement can be significant, especially in cases where the Numerical Aperture (NA) of the delivery optics is limited, such as, for example, in the case of ophthalmic imaging where the optics of the eye itself limit the lateral resolution.

8213-101, Poster Session

## Brownian motion quantification of micro- and nanoparticles using phase resolved Doppler Optical coherence tomography

C. S. Kim, W. Qi, J. Zhang, Beckman Laser Institute and Medical Clinic (United States); Y. J. Kwon, Univ. of California, Irvine (United States); Z. Chen, Beckman Laser Institute and Medical Clinic (United States)

Micro and nanoparticles have been synthesized and characterized for potential biomedical applications, and it is crucial to characterize their sizes. The current modality used to characterize the particle size, dynamic light scattering (DLS), does not provide imaging function. In this presentation, we report the development of phase resolved Doppler OCT, a technique combining Doppler velocimetry with optical coherence tomography (OCT), for imaging and quantification of particle size. This is achieved by measuring the spectral bandwidth of the Doppler frequency shift due to Brownian motion of particles in colloidal solution. Various sizes of micro- and nanoparticles were prepared and spectral bandwidths of Doppler frequency shift for each size of particles were quantified with a spectral domain OCT system. The results showed the spectral bandwidth of the Doppler frequency shift was inversely proportional to the diameter of the micro- and nanoparticles.

8213-102, Poster Session

## Correction of phase-error for phase-resolved k-clocked optical frequency domain imaging

J. Mo, J. Li, J. F. de Boer, Vrije Univ. Amsterdam (Netherlands)

Phase-resolved optical frequency domain imaging (OFDI) has emerged as a promising technique for blood flow measurement in human tissues. Phase stability is essential for this technique to achieve high accuracy in flow velocity measurement. In OFDI systems that use k-clocking for the data acquisition, phase-errors occur due to jittering in the data acquisition electronics. We present a statistical analysis of jitter represented as point shifts of the k-clocked spectrum. We demonstrate a real time phase-error correction algorithm for phase-resolved OFDI. A 50 KHz wavelength-swept laser (Axsun Technologies) based balanced detection OFDI system was developed centered at 1310 nm. To evaluate the performance of this algorithm, a stationary gold mirror was employed as sample for phase analysis. The results show that the algorithm can effectively correct the jittering-induced phase errors in real-time.

8213-103, Poster Session

## High-speed polarization sensitive optical coherence tomography for retinal diagnostics

B. Yin, B. Wang, The Univ. of Texas at Austin (United States); K. Vemishetty, J. Nagle, National Instruments Corp. (United States); S. Liu, T. Wang, H. Rylander III, T. E. Milner, The Univ. of Texas at Austin (United States)

We report design and construction of an FPGA-based high-speed swept-source polarization-sensitive optical coherence tomography (SS-PS-OCT) system for clinical retinal imaging. Clinical application of the SS-PS-OCT system is accurate measurement and display of thickness, phase retardation and birefringence maps of the retinal nerve fiber layer (RNFL) in human subjects for early detection of glaucoma. The FPGA-based SS-PS-OCT system provides three incident polarization states on the eye and uses a bulk-optic polarization sensitive balanced detection module to record two orthogonal interference fringe signals. Interference fringe signals and relative phase retardation between two orthogonal polarization states are used to obtain Stokes vectors of light returning from each RNFL depth. We implement a Levenberg-Marquardt algorithm on a Field Programmable Gate Array (FPGA) to compute accurate phase retardation and birefringence maps. For each retinal scan, a three-state Levenberg-Marquardt nonlinear algorithm is applied to 360 clusters each consisting of 100 A-scans to determine accurate maps of phase retardation and birefringence in less than 1 second after patient measurement allowing real-time clinical imaging-a speedup of more than 300 times over previous implementations. We report application of the FPGA-based SS-PS-OCT system for real-time clinical imaging of patients enrolled in a clinical study at the Eye Institute of Austin and Duke Eye Center.

8213-104, Poster Session

## Estimating external beam radiation damage of the esophagus in mice using endoscopic OCT

D. M. de Bruin, Academisch Medisch Ctr. (Netherlands); M. van Herk, A. Gasparini, J. J. Sonke, Netherlands Cancer Institute (Netherlands); T. G. van Leeuwen, D. J. Faber, Academisch Medisch Ctr. (Netherlands)

A dose-limiting side effect of radiation therapy in lung cancer patients is radiation damage of the esophagus. In order to balance the risk of damage versus the risk of local treatment failure, detailed knowledge of the effect of esophageal radiation is paramount. To gain knowledge of the local dose-effect relation for esophageal radiation damage, optical coherence tomography (OCT) is used in-vivo in mice after precision irradiation of small parts of the esophagus using computed tomography (CT) guided irradiation. These pilot experiments warrant a start of a similar study in lung cancer patients being treated with external beam radiotherapy.

The used Swept Source OCT (1310 nm, 20 µm in air) system is employed with an endoscopic rotational probe which is pulled back after insertion internally at a speed of 10 mm/s, while an outer tube remains in place. The entire mouse esophagus (~5 cm) is scanned in less than 6 seconds in 3D. At ~2 mm imaging depth, the trachea is clearly visible, and is used to localize the OCT volume in 3D. Subsequently, OCT scans are manually registered with cone-beam CT data, normally used for irradiation planning. Hereafter, the delivered dose can be correlated with the local effect is the esophagus. The apoptotic effect induced by irradiation is believed to induce time dependent optical changes which can be measured with OCT. For this study, the OCT data of several irradiated mice will be analyzed qualitatively and quantitatively on changes of back scattering (µb) and attenuation (µoct) as function of delivered dose.

8213-105, Poster Session

## Evaluation of polypyrrole nanoparticles as an absorptive contrast agent for optical coherence tomography imaging beyond 1 micron

K. Au, Z. Lu, S. J. Matcher, S. P. Armes, The Univ. of Sheffield (United Kingdom)

There is considerable interest in developing exogenous contrast agents for use with OCT imaging. Both noble-metal nanoparticles and molecular dyes such as indocyanine-green have been evaluated. Metal nanoparticles can generate scattering contrast if they are sufficiently large or absorptive contrast if they are smaller than about 100 nm. However current agents have a number of inferior optical properties including low overall extinction coefficients in the case of metal nanoparticle suspensions or an unadvantageous peak absorption wavelength in the case of ICG.

In this paper we report on the evaluation of a polymer-latex comprising nanoparticles of the electrically conductive polymer polypyrrole. We demonstrate a strong and reproducible absorption spectrum extending beyond 1.3 microns and also demonstrate a latex with 2% solids fraction displaying over 400 OD cm-1 of absorption at 1.3 microns. Liquid phantoms of intralipid and water are imaged by OCT with varying amounts of added polypyrrole and changes in the

extinction coefficient are quantified.

8213-106, Poster Session

## Speckle reduction in swept source optical coherence tomography images with slow-axis averaging

O. Tan, Y. Li, Y. Wang, Casey Eye Institute (United States); M. F. Kraus, Massachusetts Institute of Technology (United States) and Univ. Erlangen-Nuremberg (Germany); J. J. Liu, Massachusetts Institute of Technology (United States); B. Potsaid, Massachusetts Institute of Technology (United States) and Thorlabs Inc. (United States); B. Baumann, J. G. Fujimoto, Massachusetts Institute of Technology (United States); D. Huang, Casey Eye Institute (United States)

Space compounding was used to improve signal noise ratio and reduce speckle in optical coherence tomography (OCT) images. Among space compounding methods, frame averaging of repeated line scans was widely used for its ease of implementation. However, the motion between repeated lines becomes too small to disrupt speckle correlation between B-scans with an ultrahigh speed OCT system. Therefore traditional frame-averaging technique is not effective in suppressing speckle when the OCT scan speed is very high. This problem could be solved by averaging frames acquired at slightly different locations. The optimized scan range could be decided according to the spot size of the laser beam, the smoothness of the boundary, and the homogeneity of the tissue. In this study we presented a method to average frames obtained within a narrow range along the slow-axis. A swept-source OCT with 100,000 Hz axial scan rate and 20 micron spot diameter was used to scan the retina in vivo. A series of narrow raster scans (0-50 micron along the slow axis) were tested. Each scan contained 20 frames evenly distributed in the scan range. The frame rate was 417 HZ. Only frames with high correlation after rigid registration were used in averaging. The result showed that the contrast-to-noise ratio (CNR) increased with the scan range but the edge reservation was the best with a scan range of 15 micron. The optimal tradeoff in CNR and edge preservation was between 0.5 to 1 spot diameter for slow-axis averaging.

8213-107, Poster Session

## Quantitative comparison of wavelength dependence on penetration depth and imaging contrast for ultrahigh-resolution optical coherence tomography using supercontinuum sources at five wavelength regions

S. Ishida, N. Nishizawa, Nagoya Univ. (Japan)

We have been investigating ultrahigh resolution optical coherence tomography (UHR-OCT) using fiber based supercontinuum (SC) sources. It is necessary for UHR-OCT to innovate the technology that can achieve the high penetration depth. To realize ultrahigh resolution and high penetration depth simultaneously, it is necessary to choose the proper wavelength to maximize the light penetration and enhance the image contrast at deeper depths. Recently, we have demonstrated the wavelength dependence of penetration depth and imaging contrast for ultrahigh-resolution OCT at 0.8 um, 1.3 um, and 1.7 um wavelength ranges. In this paper, in addition to these wavelengths, we used SC source at 1.06 um and 1.55 um, and we have investigated the wavelength dependence of ultrahigh resolution OCT in terms of image contrast and penetration depth from the scattering coefficient and water absorption of samples. All supercontinuum sources used in this study were constructed in our group. Using these sources, we have developed OCT systems for each wavelength and the ultrahigh longitudinal resolutions of 3.6 - 7.7 um in air were realized at each wavelength region. The obtained sensitivities were more than 95 dB for all wavelength regions. We have investigated the pig trachea as water contained samples, tooth as low water contained samples, and so on with all wavelength systems. From OCT images, we have confirmed the enhancement of image contrast and decreased ambiguity of deeper epithelioid structure at longer wavelength region. From OCT signals, we have confirmed lower scattering coefficient of low water contained samples at longer wavelength region.

8213-108, Poster Session

## Megahertz processing rate for Fourier domain optical coherence tomography using a graphics processing unit

Y. Watanabe, D. Kamiyama, Yamagata Univ. (Japan)

We developed ultra high-speed processing of FD-OCT images using a low-cost graphics processing unit (GPU) with many stream processors to realize highly parallel processing. The processing line rates of half range FD-OCT and full range FD-OCT were 1.34 MHz and 0.7 MHz for a spectral interference image of 1024 FFT size × 2048 lateral A-scans, respectively. A was our OCT system achieved display rate of 22.5 frames per second for processed full range images (1024 FFT size × 2048 lateral A-scans), which is eventually limited by the acquisition rate of an InGaAs line scan camera (1024 pixels, 47kHz).

8213-109, Poster Session

## Quantitative comparison of hardware architectures for high-speed processing in optical coherence tomography

B. E. Applegate, Texas A&M Univ. (United States); D. Schmidt, K. Vemishetty, National Instruments Corp. (United States)

Several factors are spurring the development of hardware and software to accomplish high-speed processing of spectral interferograms for Optical Coherence Tomography (OCT): The emergence of ultrahigh speed systems capable of lines rates in excess of a megahertz and the push to utilize OCT in clinical settings (e.g. surgery) where real-time feedback is imperative. The two most prevalent hardware architectures incorporate either a Field Programmable Gate Array (FPGA) or a Graphics Processor Unit (GPU) to perform the necessary calculations. While GPUs nominally have faster clock-speed the fact an FPGA can be pipelined makes a direct comparison based simply on system specifications difficult. The question is further complicated when one considers transfer times across the Host bus as well as the different bit-sizes required in algorithms running on each architecture. We have undertaken an effort to make a direct comparison of the two architectures on the same host with similar code in order to control for host communication and consider the total time from digitization to rendering of the image on the Host. In addition to making quantitative comparisons between the two architectures we hope to derive useful benchmarks that will inform the design of an optimal high-speed processing system. Preliminary results indicate that the FPGA has a marked advantage in the linear interpolation operation while the GPU has an advantage for the FFT operation. Likewise, while the total computation time on the GPU is much faster (1.4 MHz A-line rate), when the time from digitization to rendering is measured, the FPGA outperforms the GPU by ~35% for a 1024X2048 (16-bit) frame acquired at 250 MS/s.

8213-110, Poster Session

## Improvement of the coherence length of a 200 kHz swept light source driven by a KTN deflector

S. Yagi, NTT Photonics Labs. (Japan); K. Naganuma, NTT Advanced Technology Corp. (Japan); T. Imai, Y. Shibata, J. Miyazu, M. Ueno, Y. Okabe, NTT Photonics Labs. (Japan); Y. Sasaki, K. Fujiura, NTT Advanced Technology Corp. (Japan); M. Sasaura, K. Kato, NTT Photonics Labs. (Japan); M. Ohmi, M. Haruna, Osaka Univ. (Japan)

We are developing a new light source for the swept-source OCT, that is, an external-cavity LD equipped with a KTN electro-optic deflector. Being free from mechanical resonance, our 1.3-μm laser exhibits 100-nm wavenumber-linear scanning range up to 200-kHz under a ±300 V deflector driving voltage. However, since our light source has suffered from short coherence length of only 1.2 mm, we have tried to improve it by sharpening the filter selectivity of the grating. According to a semi-empirical equation we have derived, the instantaneous line width is proportional to the filter's bandwidth to the 2/3 power, where the filter's bandwidth is mostly deteriorated by a KTN's lens power. At high frequencies, injected electrons in the KTN crystal are trapped in defects, which cannot realign according to the alternating external field. The trapped electrons generate a cylindrical convex lens in KTN crystal via KTN's second order electro-optic effect, where its lens axis displaces in proportion to the instantaneous external field. Although the lens power deteriorates the coherence length via broadening the filter function of the grating, the lens power is easily compensated by adding a cylindrical concave lens because the lens power is independent of the external field as long as the electrons distribute symmetrically across the KTN. By measuring the grating's filter function, it is improved to 1.8 nm by adding a cylindrical concave lens from 5 nm of uncompensated one, although it's still worse than 1.5 nm of not-electron-injected one.

8213-111, Poster Session

## Estimation of vibration amplitude in Fourier domain optical coherence tomography interferometric signals from Doppler spectrum

M. D. Wojtkowski, D. Alonso-Caneiro, Nicolaus Copernicus Univ. (Poland); B. F. Kennedy, The Univ. of Western Australia (Australia); K. Karnowski, Nicolaus Copernicus Univ. (Poland); D. D. Sampson, The Univ. of Western Australia (Australia) and Microscopy (Australia); M. Szkulmowski, Nicolaus Copernicus Univ. (Poland)

Recently a number of imaging modalities using Optical Coherence Tomography have shown the ability to estimate the motion parameters, which can provide further quantitative information about the physical properties of the sample. For example dynamic elastography OCT measures the elastic properties of different biological samples while applying a vibrational motion. This information can be extracted by phase-sensitive FdOCT techniques. However, there is also possibility to analyze time dependent Doppler spectrum of the interferometric signal. In this contribution we show a method to extract information about the vibration or motion amplitude from Doppler spectrum. Combination of Fourier and Time domain detection enables to broaden the effective bandwidth for time dependent Doppler signals, which in turn allows for using more orders of Bessel functions to calculate the vibration amplitudes without ambiguity.

8213-112, Poster Session

## Enhanced optical clearing of skin in vivo and OCT in-depth imaging

X. Wen, Britton Chance Ctr. for Biomedical Photonics (China) and Key Lab. of Biomedical Photonics of Ministry of Education (China); S. L. Jacques, Oregon Health & Science Univ. (United States); V. V. Tuchin, N.G. Chernyshevsky Saratov State Univ. (Russian Federation); D. Zhu, Britton Chance Ctr. for Biomedical Photonics (China) and Key Lab. of Biomedical Photonics of Ministry of Education (China)

The strong optical scattering of skin tissue makes it very difficult for optical coherence tomography (OCT) to achieve deep imaging in skin. Optical clearing technique has shown great potential to improve in-depth optical imaging by making skin tissue transparent with optical clearing agents (OCA). But for skin application of OCA, the strong barrier effect of stratum corneum makes it very hard for OCAs to penetrate into dermis. In this work, a new combine of chemical penetration enhancer and physical massage was used to improve the optical clearing effect on in vivo rat skin. Significant optical clearing of in vivo rat skin sites was achieved within 15 min by topical application of an optical clearing agent, a chemical enhancer and physical massage. All three components were needed to achieve a 3-fold increase in the OCT reflectance signal from a 300 μm depth.

8213-113, Poster Session

## Self-assembled quantum dot based swept laser source for optical coherence tomography applications

N. Peyvast, D. Childs, N. Krstajic, Z. Lu, S. J. Matcher, The Univ. of Sheffield (United Kingdom); D. Livshits, A. Shkolnik, I. Krestnikov, Innolume GmbH (Germany); R. Hogg, The Univ. of Sheffield (United Kingdom)

Fourier domain swept laser optical coherence tomography (OCT) permits rapid morphological tissue imaging by providing higher signal to noise ratio in comparison with time domain OCT. Because of moderate absorption and low scattering, wavelengths between 1100nm to 1300nm are attractive for skin imaging since this range can penetrate deeply into the tissue. GaAs based quantum dot (QD) materials allow the ready access of this spectral region exploiting inhomogeneous QD distributions and state-filling to realize broad spectral bandwidth sources. QD semiconductor optical amplifiers (SOAs) driven to very high current densities exploiting state-filling effects have realised external cavity lasers >200nm tuning ranges, raising the opportunity for ultra-broadband swept laser sources.

In this work, we describe preliminary OCT imaging using a QD SOA based swept laser operating in the ~1200nm region with a 3dB bandwidth of ~90nm. We discuss how this swept laser system can be engineered for either broader bandwidth or higher powers. This is achieved in our case by utilising multiple SOAs. We discuss how pairs of identical SOAs can be used in different configurations to marginally enhance spectral bandwidth. We go on to discuss how two SOAs of different wavelength bands can be combined. By combining InP based quantum well (QW) and GaAs based QD SOAs we are able to demonstrate >150nm bandwidth swept laser with ~mW level output powers centered at ~1270nm.

8213-114, Poster Session

## Enhancement of the signal-to-noise ratio at depths in Fourier-domain optical coherence tomography

A. Bradu, Univ. of Kent (United Kingdom); P. Bouchal, Brno Univ. of Technology (Czech Republic); A. G. Podoleanu, Univ. of Kent (United Kingdom)

We present a Fourier domain optical coherence tomography set-up built around an optical configuration that exhibits Talbot bands. To produce Talbot bands, the two interferometer beams, object and reference are laterally shifted in their way towards the diffraction grating. This allows attenuation of mirror terms and optimization of the sensitivity profile. We imaged the human skin in-vivo, and quantified the profile of the sensitivity profile in tissue by measuring the ratio between the strengths of signals originating in the reticular dermis and in the stratum corneum for different values of the lateral shift of the two interfering beams.

8213-115, Poster Session

## Phase-sensitive optical coherence microscopy for detection of neural activity

R. Ansari, G. Hüttmann, A. Schweikard, Univ. zu Lübeck (Germany)

Non-invasive detection of neural activity in a network of neurons, spatio-temporally resolved to individual cells activity, has always been a challenge in Neuroscience. Over past few decades, many different approaches have been reported for optical detection of neural activity, most of which involve measuring transient changes in intrinsic optical properties of tissue accompanied with an action potential, such as absorption, scattering1, birefringence2 and cell membrane displacement3. More recently, two-photon ca2+ imaging has been reported for neuronal population imaging4. However, ca2+ imaging requires staining of the tissue, which not only affects the tissue dynamics but also reduces its lifetime. In this study, we propose to investigate the dynamics of neural retina with phase-sensitive optical coherence microscopy, where the phase component of the signal is sensitive to the transient spatio-temporal changes of refractive index on cellular level.

Optical coherence microscopy (OCM) allows sharp optical sectioning of biological tissue by virtue of its compound confocal and coherence gating. The light source is a superluminescence diode (105nm FWHM, centered at 930nm. Superlum Ltd., Ireland.) with an axial resolution of ~3.6um in air. For high phase stability, source beam is scanned through the beamsplitter using X-Y galvanometer scanner unit (Cambridge Technology, U.S.A) and an identical pair of 0.8 NA, water immersion objectives are used in both arms of interferometer, providing lateral spatial resolution of ~1um. The phase stability of the setup is 0.5mrad, corresponding to optical path length sensitivity of 37pm axially. High speed line scan camera (Basler sprint, 140k) allows up to 200k Ascans/sec.

References

1. Stepnoski et al. Proc. Natl. Acad. Sci., USA. 88, 9382-9386 (1991)

2. Cohen et al. J. Physiol. 203, 489-509 (1969)

3. Akkin et al. Optics Express. 12(11), 2377-2386 (2004)

4. Grewe et al. Biomedical Optics Express. 2(7), 2035-2046 (2011)

8213-116, Poster Session

## Detailed software design of an ultraparallel ultrahigh speed SD-OCT for real-time 4D display at 12 volume/second

H. Hiro-oka, D. Choi, K. Shimizu, Kitasato Univ. (Japan); K. Ohbayashi, Kitasato Univ. School of Medicine (Japan)

As optical coherence tomography (OCT) becomes a powerful diagnostic modality, speed-up of the A-scan rate is required for high quality imaging without motion artifacts and for real-time movie display. We have been developing ultrafast SD-OCT system capable of A-scan rates at a few tenth of MHz and recently succeeded in upgrading to perform real time 4D movie display. In our ultrafast SD-OCT systems, dual optical de-multiplexers are used for spectral dispersion, which enables simultaneous parallel detection of the interference fringe at 320 frequencies in linear k-space without a need for re-scaling. The A-scan rate in this architecture is determined by the speed of DAQs, which is in this case 50MHz. All these features favor real-time 4D movie display. For distributed parallel preprocessing of the interference fringe, such as background subtraction, apodization, and FFT, we used FPGAs installed in the DAQ boards. The bottleneck of the real-time data processing in our system is the traffic speed from the parallel DAQ system to PC, in the latter real-time data processing for 4D display is performed using GPUs. Details of the system architecture and software algorithm are presented as well as display of OCT movies at a rate of 12 volume/second.

8213-117, Poster Session

## High-power sweeping semiconductor light sources at 840 nm with up to 100 nm tuning range

V. Shidlovskii, S. D. Yakubovich, S. Ilchenko, A. Lobintsov, M. V. Shramenko, Superlum (Russian Federation)

Tunable/swept lasers of NIR spectral range 800-900 nm with a high output power are of a great interest as light sources for the next generation of OCT systems including full-field ones. Two types of MOPA tunable/swept systems, in which semiconductor laser with Acousto-Optic Tunable Filter (AOTF) in an external ring PM fiber cavity was used as a Master Oscillator (MO), will be reported. The main advantage of AOTF as an intracavity spectral filter is a very high accuracy and reproducibility of wavelength tuning and a possibility for a “liner k” sweep. Earlier, we reported ~60 nm tuning with output power of 1-3 mW in an external cavity laser based on a quantum well (QW) AlGaAs SOA and AOTF. Changing to a ring cavity with optimized output coupler and using of a new modified QW SOA at 840 nm allowed us to extend tuning range of a laser to ~100 nm at 1 mW output power and to almost 70 nm when output power was increased to 10 mW, with a sweeping rate of 10,000 nm/s and instantaneous linewidth of 0.04 nm. Such a swept source may be of a self-standing interest, at least for a certain full-filed OCT systems. Usage of a spectrally-matched single-mode (4 mm stripe) or tapered (50 mm output aperture) SOAs for power boosting of MO to 50 mW in PM fiber and to 500 mW in free space, with a tunability of 60 nm and 40 nm, correspondently, will be reported, too. Finally, a possibility for using of new SOAs in fast swept sources will be discussed.

8213-118, Poster Session

## Non-local sparse reconstruction of OCT images

C. Liu, Beijing Univ. of Posts and Telecommunications (China); A. Wong, K. Bizheva, P. W. Fieguth, Univ. of Waterloo (Canada); H. Bie, Beijing Univ. of Posts and Telecommunications (China)

The resolution in corneal OCT imaging is an important parameter which determines the size of the smallest features that can be visualized. In this paper, we propose a non-local approach to the reconstruction of sparsely-sampled OCT images. An iterative strategy is introduced for minimizing non-local total variation in the spatial domain, subject to data fidelity constraints in the k-space domain. The novel algorithm was tested on human corneal images, acquired in-vivo with an UHR-OCT system, demonstrate the effectiveness of the proposed approach in reconstructing from a limited number of camera pixels.

8213-119, Poster Session

## Complex conjugate term manipulation in optical frequency-domain imaging using the time-frequency distribution

N. Lippok, S. Coen, P. M. F. Nielsen, F. Vanholsbeeck, The Univ. of Auckland (New Zealand)

Optical coherence tomography (OCT) is an established and successful imaging technology that enables high resolution, cross-sectional imaging in biological tissues. In Fourier Domain-OCT, the depth information is retrieved by performing a Fourier transform of the spectrally detected signal leading to an ambiguity between positive and negative delays from the zero-path position. This can result in mirror artifact in the images and is referred to as depth degeneracy or complex conjugate ambiguity. Most methods to remove or reduce this ambiguity are based on phase shifting techniques and require two frames per image and additional optical components in the setup. Here, we propose two numerical methods that use the dispersion imbalance present in the optical setup. Using time-frequency projections, the first method manipulates a small amount of dispersion to have a similar affect on the conjugate complex term as large dispersion. The energy of the mirror term is spread without changing the true signal. The second method shows how we can use the time-frequency distribution to filter the mirror terms for a pre-configured depth range about zero path length.

8213-120, Poster Session

## Flow velocity analysis by joint spectral and time domain optical coherence tomography (STdOCT) and phase-resolved Doppler OCT

J. Walther, E. Koch, Universitätsklinikum Carl Gustav Carus Dresden (Germany)

Several techniques of flow velocity analysis in spectral domain optical coherence tomography (SD OCT) were recently proposed. To enable high sensitivity blood flow imaging, the question of which method is favorable for quantitative flow velocity measurement becomes apparent. In this research, we compare two different implementations for flow quantification in SD OCT - the recently presented joint spectral and time domain optical coherence tomography (STdOCT) and the widely used phase-resolved Doppler OCT (DOCT). While STdOCT analyzes the time-resolved interference fringe spectra by using a two-dimensional fast Fourier transformation (2D FFT) to determine the Doppler frequency shift, DOCT directly calculates the phase difference at each depth position of adjacent depth scans (A-scans). To avoid biased flow velocity profiles, we present initially two complex algorithms for both STdOCT and DOCT. For STdOCT, the amplitude of the broadened Doppler frequency shift is calculated using the complex analytical signal as a result of the second FFT instead of detecting the maximum intensity signal. The averaged Doppler phase shift in DOCT is also determined in the complex plane to weight the phases with the signal amplitude. The comparison of both methods was achieved experimentally using a well-known flow phantom model. There, we found that the unbiased complex STdOCT and the complex phase-resolved DOCT result in equivalent velocity profiles of the flow phantom used.

8213-121, Poster Session

## Dynamic analysis of mental sweating and the peripheral vessels for the activity of the autonomic nervous system by optical coherence tomography

M. Ohmi, D. Takada, Y. Wada, M. Haruna, Osaka Univ. (Japan)

Optical coherence tomography (OCT) has been developed intensively for clinical diagnoses in ophthalmology. Besides the clinical application, OCT is a powerful tool to detect physiological functions of sweat glands and peripheral vessels, as recently proposed and demonstrated by the authors' group. In particular, we discussed in detail mental sweating where mental or physical stress was applied to a volunteer to accelerate excess sweating. When a sound stress was used, we found internal mental sweating without ejection of excess sweat to the skin surface, which was used for evaluation of activity of the sympathetic nerve. Furthermore, we demonstrated dynamic OCT observation of the small artery of a human finger in response to sound stress. It was found that the small artery contracts and expands in response to sound stress while it continues pulsation in synchronization with the heartbeat.

Both mental sweating and the peripheral vessels reflect the activity of the sympathetic nerve of the autonomic nervous system (ANS). The sympathetic nerve is also known as a values of the LF/HF (low frequency / high frequency) of the heart rate variability (HRV). In this paper, we demonstrate simultaneous measurement of dynamics of mental sweating of the eccrine sweat glands and the peripheral vessels of a human finger by SS-OCT for the activity of the ANS. In the experiment, the Kraepelin test as a continuous stimulus was applied to the volunteer to discuss in detail the dynamics of the physiological function of such small organs in response to the HRV.

8213-122, Poster Session

## Swept-source OCT using programmable laser

G. Lamouche, S. Vergnole, National Research Council Canada (Canada); Y. Kim, B. Burgoyne, A. Villeneuve, Jr., Genia Photonics Inc. (Canada)

New results are presented for a fully programmable picosecond laser source based on a dispersion-tuned actively mode-locked fiber laser that was introduced last year. The programmable laser is unique in that it offers complete tailoring of the wavelength sweep. This programmability is achieved through especially developed electronics. In SS-OCT, one can select the sweep range, the sweep rate, all this with a linear in k-space sweep. The output is delivered through a single mode polarization maintaining fiber. The source design is discussed and new SS-OCT results are presented.

In this experiment, we used a CFBG with 10 psec/nm dispersion (100 nm bandwidth, 1520-1620 nm). The EOM was driven by a 150 psec pulse from the electronic pulse generator circuit at a repetition rate of 75 MHz which is the third harmonic frequency of the PL cavity. The small signal gain of the SOA is 25 dB. Polarization maintaining fiber was used with all the optical components and the cavity. Signal from the cavity is amplified by erbium-doped fiber amplifier (EDFA) before final output. In this paper, we didn't implement any gain flattening scheme for the EDFA. Fig. 1(b) shows the typical optical spectrum of the PL. Asymmetric spectrum shape represents the nonlinear response of SOA. Full width at half maximum (FWHM) is 0.03 nm.

8213-123, Poster Session

## Optical coherence tomography based angle-resolved backscattering studies on bovine tendon and cartilage

D. K. Kasaragod, Z. Lu, S. J. Matcher, The Univ. of Sheffield (United Kingdom)

Optical coherence tomography (OCT) is a non-invasive tool to obtain structural information of scattering biological tissues. Various attempts are made to study the optical properties of tissues to differentiate normal from diseased tissues using OCT. In this study, we report a comparative study carried on the angle-resolved backscattering on bovine tendon and articular cartilage samples using an OCT based system. We observe an isotropic scattering profile in articular cartilage whereas tendon shows anisotropic scattering profile. We put forward a hypothesis of different size and type of the scatterers involved in the two tissues for this observation. A model based on Rayleigh-Gans (RG) approximation, which is equivalent to first order Born approximation is being used here to account for the experimental results obtained.

8213-124, Poster Session

## Linear in-wavenumber optical spectrum registration in SD-OCT

P. A. Shilyagin, V. M. Gelikonov, G. V. Gelikonov, Institute of Applied Physics (Russian Federation)

The spectrometer non equidistance and material dispersion influence can be presented as the nonlinearity of the phase of modulation of optical spectrum by interference between reference wave and reflected from mirror in object arm one. The equation for $\phi(k,z)$ corresponds to a surface in (k,z) space. Using it directly, it is possible to reconstruct OCT images without any profile widening, but this operation needs a high number of calculations. To decrease the number of calculations the surface can be divided on a number of parts in z or k directions. For both cases two algorithms were developed and investigated.

It is shown, that k-algorithm is more sensitive to order of segmentation, then z-one. This fact results in arising of artifacts around the peaks, illustrating reflector posotion. Increasing a number of segments one can eliminate this artifacts, but it will result in increasing of calculations. Moreover using of the correction algorithms increases signal component by 3 dB for maximal observing depth. This way the depth degeneration of signal is decreased and comes to 6 dB at depth about 2 mm.

8213-125, Poster Session

## Concentrically symmetric hollow core interferometer for common path optical coherence tomography

Y. Zhang, E. Pienkowski, T. Wei, X. Lan, H. Xiao, Missouri Univ. of Science and Technology (United States)

A hollow core, concentrically symmetric, beam splitting, Michelson interferometer for common-path, Fourier-domain Optical Coherence Tomography has been demonstrated and analyzed. The key component of the system is a compact, small diameter probe composed of a collimating lens, hollow core beam splitting tube, and a focusing lens. The beam splitting tube is created by sputter coating the distal endface of a finely polished thick wall capillary tube with a highly reflective gold layer. Light from a coherent source is coupled into the tube. Part of the light travels through the wall of the tube is reflected by the distal endface forming a reference arm and part passes through the hollow core to be backscattered by the sample material forming a sample arm. To demonstrate the functionality and utility of the probe, cross-sectional and volumetric images of various samples have been obtained. Some advantages of this system include a small probe diameter and an easily adjustable working distance.

8213-126, Poster Session

## High-speed spectral-domain optical coherence tomography with dual detection of the retina and the cornea

H. Jeong, B. Kim, Korea Univ. (Korea, Republic of)

Optical coherence tomography (OCT) is a promising medical imaging modality that can noninvasively provide cross-sectional images of microstructures within biological tissues. Recent development of OCT has shifted its emphasis on the frequency domain (FD) techniques based on either a spectrometer (spectral-domain OCT, SD-OCT) or a frequency-swept laser source (swept-source OCT, SS-OCT) thanks to the dramatically improved sensitivity and fast imaging speed over the conventional time-domain (TD) OCT. Due to high image acquisition speed, it enables 2-D or 3-D fast cross-sectional imaging with high resolution. To date, OCT has become a well accepted clinical imaging tool for diagnosis of retinal disease including layer's thickness change, retinal pigment epithelium detachment (PED), macular degeneration, glaucoma, macular edema, and diabetic retinopathy in ophthalmology. Recently, it has been also applied to clinical imaging of anterior segment. Spectral domain OCT techniques demonstrated the first applicability in diagnosis of cornea disease and monitoring of postoperative healing process. Furthermore, possible applications such as contact lens fit and its movement on the eye surface were represented by video-rate and three-dimensional imaging.

In this study, to the best of our knowledge we first designed and fabricated a novel spectral domain OCT with dual detection of retina and cornea simultaneously via customized ultrahigh speed optical switch made of solid-state electro-optic material. Broadband SLD with a FWHM of 64nm centered at 830nm was used as a source. Measured axial resolution and sensitivity was 5μm and 104.9 dB near at zero depth, respectively. The entire imaging depth was doubled to 12mm with off-pivot full range technique.

8213-127, Poster Session

## New method for suppressing the mirror image in Fourier-domain optical coherence tomography

C. Wu, T. Chi, C. Lee, Y. Kiang, C. Yang, C. Chiang, M. Tsai, National Taiwan Univ. (Taiwan)

Suppression of mirror image in Fourier-domain (FD) optical coherence tomography (OCT) is an important research topic for improving the image quality. The mirror image appears in an FD-OCT image due to the incomplete information for inverse Fourier transform based on a single A-mode scan. Among several proposed approaches, the BM-scan method based on a certain phase shift mechanism has been widely used for mirror image suppression. In this method, the real spectral signals of a 2-D image are first Hilbert transformed along the B-mode scan direction to give the complex spectral signals, which can lead to mirror image suppression after a Fourier transformation. In this paper, we demonstrate an alternative approach of mirror image suppression based on galvanometer scanning for producing a phase shift along the B-mode scan. In this situation, the phase shifts between two neighboring A-mode scans of the real and mirror image signals are mutually reversed. Our approach utilizes this property for differentiating the real image from the mirror one. This approach can be applied to an FD-OCT system with any other phase shift mechanism. It has the advantage of shorter process time, when compared with the aforementioned BM-scan method. Also, because our mirror image suppression process is a "localized" operation of OCT signals, we can select any A- and B-mode ranges for process to further save computer time.

8213-128, Poster Session

## Single-shot full complex spectrum spectrometer-based OCT with a single-line photodiode array

P. A. Shilyagin, V. M. Gelikonov, G. V. Gelikonov, A. A. Moiseev, Institute of Applied Physics (Russian Federation)

Spectral domain optical coherence tomography (SD-OCT) is based on measuring of optical spectrum of sum of two interfering waves: the reference one and the backscattered from the object one. Because of the obtained spectrum is the real function of optical frequency, the reconstructed by Fourier transformation image has mirror-symmetrical structure relative to zero of path-difference. Some methods of eliminating of the mirror artifacts, obtained for SD-OCT, are based on consecutive obtaining of spectral components with different phase shift between reference and object waves. The simultaneous obtaining of full complex spectrum makes possible eliminating the influence of Doppler phase shifts of moving scatterers in the object. The simultaneous obtaining of quadrature interference components in spectrometer-based OCT was proposed by using polarization optics.

The first interferometer for simultaneously observing of interference with different phase shifts between interfering waves was described in 1926 by Kennedy, R. J.. The relative phase difference between two parts of one beam was obtained by a short step. Unfortunately, using of this setup for observing broad spectra, which is necessary for OCT, will result in arising of mirror artifacts.

An efficient technology of simultaneous obtaining of quadrature spectral components of interference signal in spectrometer-based OCT, proposed in 2011 by our group, has a disadvantage, was swown by using of a dual line array for record both qudrature components of optical spectrum.

We propose polarization optics free SD-OCT setup with achromatic phase shifting and simultaneous obtaining of quadrature interference components using an ordinary single-line linear photodiode array.

8213-129, Poster Session

## Optical coherence tomography imaging for ex-vivo endoscopic laryngeal cancer screening using a forward-viewing resonant fiber optic scanning endoscope

R. C. Cernat, Univ. of Kent (United Kingdom); Y. Y. Zhang, The Johns Hopkins Univ. (United States); A. Bradu, Univ. of Kent (United Kingdom); T. Tatla, Northwick Park & St. Marks Hospitals (United Kingdom); P. J. Tadrous, Northwick Park Hospital (United Kingdom); X. D. Li, The Johns Hopkins Univ. (United States); A. G. Podoleanu, Univ. of Kent (United Kingdom)

A miniature endoscope probe for forward viewing in a 47 kHz swept source optical coherence tomography (SS-OCT) configuration was developed. The work presented here is an intermediate step in our research towards endoscopic laryngeal cancer screening. The endoscope probe consists of a miniature tubular lead zirconate titanate (PZT) actuator, a single mode fiber (SMF) cantilever and a GRIN lens, with a diameter of 2.4 mm. The outer surface of the PZT actuator is divided into four quadrants that can be driven by two pairs of electrodes (X and Y). When sinusoidal waves of opposite polarities are applied to one electrode pair, the PZT tube will bend transversally with respect to the two corresponding quadrants, and the fiber optic cantilever will be displaced perpendicular to the PZT tube. The cantilever's resonant frequency was found experimentally as 47.03 Hz. With the GRIN lens used, a lateral resolution of ~ 13 μm is expected. 2D en face spiral scanning pattern was achieved by adjusting the phase between the pairs of X and Y electrodes drive close to 90 degrees.

8213-130, Poster Session

## Parametric study of femtosecond inscription of micro-structures for OCT artifact fabrication

J. Rasakanthan, G. C. B. Lee, M. Dubov, Aston Univ. (United Kingdom); P. D. Woolliams, National Physical Lab. (United Kingdom); K. Sugden, Aston Univ. (United Kingdom)

As the optical coherence tomography (OCT) becomes widespread use in medical field, validation and characterisation of the system becomes important. A reference (gold) standard is required to quantitatively measure the performance between difference systems. Additionally, the performance degradation of the system over time must be monitored.

In this report, the properties of the femtosecond inscribed structures from three different systems were analysed for making suitable OCT characterisation artifacts.

This work studies the microstructures produced by three different femtosecond inscription systems as calibration artifacts. Two of the systems use Ti:Sapphire and both operate at a central wavelength of 800nm. The repetition rates are 11MHz and 1kHz and the pulse durations 50 and 110fs respectively. The third system is Nd:YAG s-pulse HP laser (change to type of laser), operates at the centre wavelength of 1026nm with100kHz repetition rate and has ~500fs pulse duration.

Highly focused ultra-short pulse produce localised modification in the bulk of the material. Depending on the regime the structures can be stress damage, micro-cracks or refractive index change. A parameter test sample was inscribed inside the bulk of transparent materials. The parameters energy, speed of translation and depth of the inscription were varied. The samples were characterised using an optical microscope together with QPm software and a swept source OCT system. Factors affecting the artifact performance that relate to the fabrication laser will be discussed.

8213-131, Poster Session

## Linewidth of swept laser source

H. Omran, D. Khalil, Ain Shams Univ. (Egypt)

A swept wavelength laser source is currently an essential element for many biomedical applications especially for low coherence tomography and imaging. For such application, the main interest is to have a wide wavelength tuning range while the source could be a multi longitudinal mode source which means a source with a relatively wide spectral range. We may even claim that the increase of the source line width could be of interest to reduce the coherent noise that results from multiple reflections within the sample. On the other hand, the linewidth is limited by the required spectral resolution that nearly determines the examined penetration depth in the sample. For these reasons the engineering of the swept laser source linewidth has a special interest on both the academic and industrial levels. In this work we study the factors affecting this parameter. A ring fiber laser source based on EDFA and a Fabry-Perot resonator is used for this purpose. With this setup a swept source with a linewidth of 0.1 nm is obtained over a tuning range of about 47 nm limited by the spectral gain of the EDFA amplifier used. The factors affecting the source linewidth are then examined and experimental results are compared to theoretical predictions.

8213-29, Session 5

## Measurement and perturbation of embryonic cardiac dynamics using optical coherence tomography and optical pacing

L. M. Peterson, M. T. McPheeters, L. M. Barwick, S. Gu, A. M. Rollins, M. W. Jenkins, Case Western Reserve Univ. (United States)

Several studies have shown that altering blood flow early in development leads to congenital heart defects. In these studies the perturbations to hemodynamics were very gross manipulations (vessel ligation, conotruncal banding, etc.) that would be inappropriate for probing the delicate mechanisms responsible for mechanically-transduced signaling. Also, these perturbations lacked feedback from a monitoring system to determine the exact degree of alteration and the location of its effect. Here, we employed optical pacing (OP) to alter the heart rate in quail embryos and optical coherence tomography (OCT) to measure the resultant shear forces on the endocardium. OP is a new technique utilizing pulsed 1.851 μm infrared laser light to noninvasively lock the heart rate to the pulse frequency of the laser without the use of exogenous agents. To measure shear stress on the endocardium, we extended our previous OCT algorithms to enable the production of 4-D shear maps. 4-D shear maps allowed easy observation of the spatial and temporal distribution of shear stress. Employing both OCT and OP, we were able to develop perturbation protocols that increase regurgitant flow and greatly modify the oscillatory shear index (OSI) in a region of the heart tube where future valves will develop. Regurgitant flow has been linked with valve development and precise perturbations may allow one to determine the role of hemodynamics in valvulogenesis.

8213-30, Session 5

## Simultaneous high-resolution morphological and biochemical optical imaging of atherosclerosis

P. Pande, J. Park, S. Shrestha, F. Clubb, B. Applegate, J. A. Jo, Texas A&M Univ. (United States)

Motivation: Improving the understanding of atherosclerotic plaque development will require in-vivo monitoring of morphological and biochemical changes accompanying plaque formation. Objective: To develop a novel technology for high-resolution morphological and biochemical imaging of atherosclerotic plaques. Methods: Optical Coherence Tomography (OCT) generates high-resolution 3D images of plaque morphology. Endogenous Fluorescence Lifetime Imaging Microscopy (FLIM) characterizes plaque biochemical composition. Both methods rely on intrinsic optical characteristics of the plaque, thus contrast agents are not required. A multimodal OCT/FLIM system was built to generate morphological and biochemical maps of the plaque, composed of a high-resolution (10-20 microns) structural volumetric image superimposed with a luminal lipid map. Results: Fresh postmortem human coronary segments were imaged and included: intimal thickening (IT; n=11), pathological IT (PIT; n=14), PIT infiltrated with foam cells (FC-PIT, n=20), thin cap fibroatheroma (TCFA, n=1), and calcification (CA, n=12). FLIM allowed detecting collagen-rich plaques (PIT) with sensitivity/specificity of 96%/99%, lipid-rich plaques (TCFA, FC-PIT) with sensitivity/specificity of 89%/99%, and plaques with low collagen/lipids content (IT, CA) with sensitivity/specificity of 99%/99%. OCT could not distinguish PIT from FC-PIT, but when including the FLIM lipid map, this was possible. FLIM could not distinguish FC-PIT from TCFA or PIT from CA, but when including the OCT volume, this was possible. Conclusion: The developed technology enables the characterization of plaque morphology and biochemistry with micron resolution and identification of most types of atherosclerotic plaques. An intravascular OCT/FLIM system for in vivo imaging is currently being developed and will represent a powerful tool to study mechanisms of atherosclerosis.

8213-31, Session 5

## Classification of atherosclerotic plaques using depth resolved spectral analysis of optical frequency domain imaging datasets

C. P. Fleming, A. Tanaka, Massachusetts General Hospital (United States) and Harvard Medical School (United States); J. A. Gardecki, Massachusetts General Hospital (United States); P. Maurovich-Horvat, W. C. Warger II, Massachusetts General Hospital (United States) and Harvard Medical School (United States); J. E. Eckert, Massachusetts General Hospital (United States); U. Hoffmann, Massachusetts General Hospital (United States) and Harvard Univ. (United States); B. E. Bouma, G. J. Tearney, Massachusetts General Hospital (United States) and Harvard Medical School (United States)

Currently, lipid rich plaques are identified within OCT/OFDI images as a signal poor region with diffuse boundaries. We have chosen to attempt to improve OCT/OFDI discrimination by analyzing the spectral signature of the acquired data. We present the use of spectroscopic optical coherence tomography for automated plaque classification through morphological and depth resolved spectrosocopic analysis of OFDI images.

Imaging was conducted with our clinical OFDI system and catheters. Comprehensive pullback image sets were acquired from 20 coronary arteries from 8 explant human hearts. Time-frequency analysis was used to generate depth resolved spectra of averaged axial scans. A training set of registered OFDI-histology pairs (n=150) was used to develop a prediction model using quadratic discriminant analysis. Inputs to the model included attenuation, backscattering, and wavelength dependent attenuation. Model output was the probability for each pixel being assigned to lipid, calcium, fibrous, adventitial fat, or noise.

Using correlated OFDI and histology images, depth resolved spectral analysis was able to classify lipid, calcium, fibrous regions, adventitial fat, and noise with significant ($p<0.001$) areas under the receiver operator characteristic curve. Although the backscattering and attenuation coefficients were significantly different between tissue types ($p<0.001$), the addition of spectral parameters increase the classification accuracy of lipid (AUC=0.87 with spectral parameters, AUC=0.84 without) and adventitial fat (AUC=0.89 with spectral parameters, AUC=0.87 without), $p<0.05$.

8213-32, Session 5

## In vivo intracardiac OCT imaging through percutaneous access: towards image guided radio-frequency ablation

H. Wang, W. Kang, T. Carrigan, A. P. Bishop, M. Arruda, A. M. Rollins, Case Western Reserve Univ. (United States)

Complete catheter-tissue contact and permanent tissue destruction are essential for efficient radio-frequency ablation (RFA) during cardiac arrhythmia treatment. Current methods of monitoring lesion formation are indirect and unreliable. We aim to develop optical coherence tomography (OCT) as an imaging guidance tool for RFA. The purpose of this study is to evaluate the feasibility of using an OCT catheter to image endocardial wall in active beating hearts through percutaneous access. This is a critical step toward image guided RFA in a clinical setting.

A cone-scanning forward-viewing OCT catheter was advanced into active beating hearts through percutaneous access in four swine. The OCT catheter was steered by an introducer to contact the endocardial wall. Images were then acquired at 10 frames per second with an axial resolution and lateral resolution of 15 μm. We report the first in vivo intracardiac OCT imaging through percutaneous access with a thin and flexible OCT catheter. We are able to acquire high quality OCT images in active beating hearts, observe the polarization-related artifacts induced by the birefringence of myocardium and readily evaluate catheter-tissue contact. In conclusion, it is feasible to acquire OCT images in beating hearts through percutaneous access. The observations indicate that OCT could be a promising technique for in vivo guidance of RFA.

Acknowledgments

The project was supported by the Wallace H. Coulter Foundation and by the National Institutes of Health (HL085939, HL083048, RR1246, CA114276) and the National Science Foundation (NSF IIP-0917940). The content is solely the responsibility of the authors and does not necessarily represent the official views of the National Institutes of Health.

8213-33, Session 5

## Advances in a fully integrated intravascular OCT-ultrasound system for cardiovascular imaging

J. Jing, Beckman Laser Institute and Medical Clinic (United States); J. Li, J. Yin, Univ. of California, Irvine (United States); X. Li, The Univ. of Southern California (United States); J. Zhang, Beckman Laser Institute and Medical Clinic (United States); K. Hoang, P. M. Patel, Univ. of California, Irvine School of Medicine (United States); Q. Zhou, The Univ. of Southern California (United States); Z. Chen, Univ. of California, Irvine (United States) and Beckman Laser Institute and Medical Clinic (United States)

Intracoronary optical coherence tomography (OCT) and intravascular ultrasound (IVUS) are two popular techniques for the detection and determination of atherosclerosis. IVUS allows visualization of plaques while also providing a large penetration depth to determine plaque volume. Intracoronary OCT provides the ability to capture microscopic features associated with high risk plaque. Traditionally to utilize the benefits of both modalities, separate probes and systems had to be used one at a time to image a vessel. We present work required to create a combined OCT IVUS system capable of simultaneous imaging to detect atherosclerotic plaques. A novel integrated probe of size 0.69 mm OD featuring sequential placement of components was created to acquire co-registered images within small coronary vessels. By utilizing commercial graphics processing units (GPUs) real time visualization of acquired data is possible up to a maximum 48 frames per second per channel. In vitro studies on human coronary artery samples as well as in vivo studies in rabbits and pigs show various plaque buildups in both OCT and IVUS images which match histology results, demonstrating the capabilities of the system.

8213-34, Session 5

## Three-dimensional volumetric quantification of fibrous caps using intravascular optical coherence tomography

Z. Wang, Case Western Reserve Univ. (United States); D. Chamie, H. Bezerra, Univ. Hospitals of Cleveland (United States); D. L. Wilson, Case Western Reserve Univ. (United States); M. A. Costa, Univ. Hospitals of Cleveland (United States); A. M. Rollins, Case Western Reserve Univ. (United States)

The rupture of thin-cap fibroatheroma (TCFA) accounts for most acute coronary events. Optical Coherence Tomography (OCT) is able to identify TCFA and quantify the fibrous cap (FC) thickness in vivo. Conventional analysis measuring the thinnest part of the cap is subject to inter-observer variability and does not capture the 3-D morphology of the lesion. We aim to provide a solution for automated segmentation that will allow volumetric analysis of FC. A total of 323 images were analyzed from 14 lipid rich lesions. FC boundary was automatically segmented based on the intensity difference between the cap and the underlying lipid plaque, and attenuation of OCT signals using a dynamic programming algorithm. The thickness at every point of the cap was quantified. FC surface area and volume can be quantified in addition to the minimum cap thickness. The segmented boundaries obtained by the automated method were compared against 3 experienced OCT analysts. The mean absolute difference (MAD) between the automated method and human analysts of FC thickness at each point was 26.6μm. This was slightly less than the MAD between human analysts. The proposed automated method is as accurate as expert human analysts and provides a more comprehensive volumetric quantification of FC.

8213-35, Session 6

## Multiple blood flow imaging modes by ultrahigh speed dual-beam Doppler optical coherence angiography

S. Makita, F. Jaillon, Univ. of Tsukuba (Japan); B. Cense, Utsunomiya Univ. (Japan); Y. Yasuno, Univ. of Tsukuba (Japan)

Ultrahigh speed acquisition of optical coherence tomography enables several imaging applications. High-speed three-dimensional imaging shows morphology with less motion artifact, high-dense volumetric imaging enables to visualize fine morphology, and four dimensional imaging enables to investigate dynamics in 3D.

On the other hand, Doppler optical coherence tomography has been applied to depth-resolved cross-sectional blood flow imaging. However, the requirement of multiple sampling at the same location increase the total acquisition time.

In this study, we demonstrate multiple blood flow imaging modes of ultrahigh speed dual-beam-scan Doppler optical coherence angiography.

Polarization-multiplexed dual-beam spectral-domain optical coherence tomography was used.

Light from a source which has 840 nm central wavelength and 50 nm bandwidth (FWHM) were divided into two polarization states to obtain two OCT signals.

The acquisition rate of 123,000 lines/s enables high-dense or high-speed volumetric blood flow imaging.

Phase-resolved blood flow images of the posterior part of in vivo human eye were obtained.

High-dense volumetric imaging (2048 x 256 lines) revealed the high-definition micro-vasculature of capillary-level vessels.

Because of dual-beam method, low-dense sampling is allowed for blood flow imaging. 4D flow imaging of 1.18 vol./s visualizes three-dimensional vasculature and dynamic change of blood flow.

A new beam scanning pattern allows 4D flow imaging with high flow sensitivity. Volumetric flow imaging consists from 256 x 256 lines and takes 1.18 vol./s with the observation time for blood flow of 2.5 ms is available. Multiple 3D fine micro-vasculature images can be obtained within a few seconds.

8213-36, Session 6

## Real-time, angle-insensitive total axial flow measurement using transversal scanning Doppler OCT

H. C. Hendargo, A. Dhalla, J. A. Izatt, Duke Univ. (United States)

Measurement of total retinal blood flow using Doppler optical coherence tomography (DOCT) has potential clinical utility for monitoring disease progression in diabetic retinopathy and glaucoma. Quantifying blood flow velocities and volumes with conventional DOCT requires knowledge of the Doppler angle, which requires either additional hardware (such as in dual-angle Doppler measurement) or significant post-acquisition signal/image processing which is susceptible to patient motion artifacts. Recently, a novel technique for integrative, completely angle-insensitive DOCT flow measurement normal to a given en-face sample plane of interest was introduced. This technique was adapted for total retinal blood flow measurement by volumetric imaging of the entire optic nerve head, followed by software extraction of an en-face plane intersected by all retinal vessels. However, this approach suffers from the inefficiency that an entire retinal volume is acquired while only a single en-face plane is required. While Fourier-domain OCT systems deliver the axial dimension essentially for free, nonetheless even relatively fast, densely sampled swept-source OCT systems still have volume acquisition times long compared to the time scale of interesting retinal vascular dynamic processes, such as pulsatility. On the other hand, transversal scanning OCT (TSOCT) is capable of rapidly acquiring en-face images with demonstrated imaging rates up to 40 Hz. Here, we introduce the use of Doppler TSOCT for fast (10Hz) total axial flow measurement, with anticipated applications for real-time monitoring of total retinal blood flow.

8213-37, Session 6

## Strain rate measurement of embryonic chick heart in vivo using spectral domain optical coherence tomography

P. Li, Univ. of Washington (United States); X. Yin, L. Shi, S. Rugonyi, Oregon Health & Science Univ. (United States); R. Wang, Univ. of Washington (United States)

During the cardiac development, the cardiac wall and the blood flow actively interact with each other, and determine the biomechanical environment to which the embryonic heart exposes. Previously, the biomechanical environment of the development beating heart is characterized based on the velocity measurement of blood flow. And then the biomechanical environment, such as shear rate and shear stress, is deduced from the velocity of blood flow. The directly radial strain rate measurement of the myocardial wall provides a new entry point to study this biomechanical environment. By employing two identical spectrometers that capture two adjacent A-scans with a flexible and precisely controlled time interval in SDOCT, an ultrafast line scan rate (~184 kHz) is realized. With 256 A-line for a B-frame, 580 B-frames per second can be achieved. The radial strain rate measurement can be conducted by analyzing the phase shift between the repeated B-frames with high signal-to-noise ratio based on the phase-resolved tissue Doppler OCT (tissue-DOCT) technology. Additionally, because of the improved line scan rate, the maximal measurable Doppler velocity of blood flow is increased, which is desirable because of the fast blood flow in the beating heart. The ability to simultaneously and independently characterize the cardiac wall and the blood flow provides a powerful potential to better understand the interaction between these two cardiac tissues, which is of great importance to understand the biomechanics of cardiac development.

8213-38, Session 6

## Real-time speckle variance swept-source optical coherence tomography using a graphics processing unit

K. K. C. Lee, Univ. of Toronto (Canada) and Ryerson Univ. (Canada); A. Mariampillai, J. X. Yu, B. A. Standish, V. X. D. Yang, Ryerson Univ. (Canada)

Advances in swept source laser technology continuing increase the imaging speed of swept-source optical coherence tomography (SSOCT) systems and thus the speed at which volumetric imaging can be obtained. These fast imaging speeds are ideal for microvascular detection schemes, such as speckle variance (SV), where interframe motion can cause severe imaging artifacts and loss of vascular contrast. However, full utilization of the laser scan speed is hindered by the computationally intensive signal processing required by SSOCT and SV calculations when implemented on a serially-oriented central processing unit (CPU). Alternatively, commercial graphics processing units (GPU) are optimized for parallel data processing, and have recently been adapted to accelerate processing speeds in several biomedical imaging modalities. These advances in both laser and GPU technology have enabled our team to develop a high-speed SSOCT imaging platform capable of real-time SV processing, display and saving at 120,000 lines per second. The system utilizes a polygon-based short cavity ring laser at 60kHz, where buffering and amplification is performed to double the A-scan rate of the laser. The laser has a total output power of ~50mW, a 3dB bandwidth of 105nm and a coherence length of ~3mm. The complete SSOCT signal processing including λ-to-k spectral resampling, fast Fourier transform (FFT) and post-FFT (structural and SV) processing were all implemented on the GPU. Real-time intraoperative spinal cord imaging in rats will be demonstrated, where microvascular changes will be monitored at 224 frames per second (512 x 512) without the implementation of gating or post-processing.

8213-39, Session 6

## Simultaneous in-vivo structural and functional assessment of the microcirculation using correlation mapping optical coherence tomography (cmOCT)

J. G. Enfield, E. Jonathan, Univ. of Limerick (Ireland); M. J. Leahy, National Univ. of Ireland, Galway (Ireland)

Various diseases have been shown to induce both functional and structural changes in the microcirculation. Detection of these changes can provide an early indicator of pathological conditions. A number of techniques have thus been developed that enable study of the microcirculation. Recently, correlation mapping optical coherence tomography (cmOCT) has been demonstrated to conveniently produce, high resolution maps of the microcirculation in vivo that clearly follow the accepted anatomical structure in a non-invasive non-contact manner.

In this paper we propose that cmOCT can enable both structural and functional characterization of the microcirculation simultaneously. We demonstrate that cmOCT can visualize the structural changes that occur within the microcirculation during tissue regeneration with capillary level resolution in a non-invasive manner. We also demonstrate that cmOCT is capable of assessing the functional health of the microcirculation through tracking the response of the microcirculation to a post occlusive reactive hyperemia, the characterization of which, provides an indicator of vascular dysfunction.

8213-40, Session 6

## Intensity-based modified Doppler variance algorithm dedicated for phase instable optical coherence tomography systems

G. Liu, D. Chou, W. Jia, W. Qi, B. Choi, Z. Chen, Beckman Laser Institute and Medical Clinic (United States)

Traditional phase-resolve Doppler method demonstrates great success for in-vivo imaging of blood flow and blood vessel. However, the phase-resolved methods always require high phase stability of the system. During phase instable situations, the performance of the phase-resolved methods will be degraded. We propose a modified Doppler variance algorithm that is based on the intensity or amplitude value. Performances of the proposed algorithm are compared with traditional phase-resolved Doppler variance and color Doppler methods for two phase instability systems. The proposed algorithm demonstrates good performances without phase instability induced artifacts.

8213-41, Session 7

## All-fiber optically based catheter system for simultaneous endoscopic optical coherence tomography and fluorescence imaging

J. Mavadia, J. Xi, X. D. Li, The Johns Hopkins Univ. (United States)

An all-fiber-optically based balloon catheter for simultaneous fluorescence imaging and optical coherence tomography has been designed and implemented. With the use of double clad fiber we were able to deliver excitation light for both optical coherence tomography and fluorescence while collecting the OCT signal through the single-mode core and fluorescence emission through the large inner cladding. The performance of this small yet robust multimodal catheter has been demonstrated on tissue phantom, ex vivo pig esophagus and mouse tumor imaging.

8213-42, Session 7

## Ultra-thin 30-gauge needle probe for minimally invasive 3D optical coherence tomography

D. Lorenser, X. Yang, R. W. Kirk, B. C. Quirk, R. A. McLaughlin, The Univ. of Western Australia (Australia); D. D. Sampson, The Univ. of Western Australia (Australia) and Ctr. for Microscopy, Characterisation and Analysis (Australia)

We present the smallest published side-viewing needle probe for optical coherence tomography (OCT). Ultra-thin dimensions suitable for minimally invasive imaging of small animals or delicate organs are achieved by using a simple all-fiber probe design incorporating an angle-polished and reflection-coated fiber tip reflector which is limited in size only by the fiber cladding diameter, allowing it to be inserted into a 30-gauge hypodermic needle (diameter 0.31 mm). The distal focusing optics consist of fusion-spliced sections of no-core and gradient-index fiber. An additional section of no-core fiber at the end of the probe is angle-polished at 45 degrees and coated with Cr/Au via thermal vacuum deposition to form the beam deflector. The probe beam profile is measured and simulated using ray-matrix theory. The beam acquires astigmatism as it exits the curved interface formed by the fiber cladding but when immersed in water our simulation shows that the astigmatism ratio decreases from 4.4 to 1.8. This allows us to obtain a depth of field of 700 µm in biological tissue with elliptical beam diameters below 30 µm in this entire range. The probe was interfaced with an 840-nm spectral domain OCT system and 3D images of saline-filled lamb lungs were acquired using a rotation/pullback scanning mechanism. Extensive alveolar networks and airways can be resolved in the images. The results demonstrate that the probe is capable of generating OCT images of biological tissue with good resolution over a depth range of ~600 µm, which is consistent with our probe beam characterisation.

8213-43, Session 7

## Preclinical study on breast cancer using full-field optical coherence tomography

O. Assayag, Ecole Supérieure de Physique et de Chimie Industrielles (France); M. Antoine, Hôpital de Paris (France); B. Sigal-Zafrani, Institut Curie (France); F. Harms, LLTECH SAS (France); A. Burcheri, Ecole Supérieure de Physique et de Chimie Industrielles (France); B. de Poly, LLTECH SAS (France); A. C. Boccara, Ecole Supérieure de Physique et de Chimie Industrielles (France) and LLTech SAS (France)

We present a preclinical evaluation of FFOCT technology for determining malignancy or not of breast tissue using a large field, very high resolution LightCT scanner. The scanner offers a 2µm(axial) , 1µm (lateral) resolution, and an image of 1,5cm² is obtained in less than 7 minutes. In this study we proved the safety of the technique on breast tissue by showing the non-alteration of the morphological aspect of the tissue and the immunophenotypic characteristics of the lesions. The aspect of the basic structures of the breast tissue such as the galactophorous ducts, the lobules, the adipocytes and various types of fibrous tissue was defined on the images. Then, we established a list of criteria that have to be verified in order to classify the tissue as malignant or normal/benign. The criteria are related to the size and shape of the fat cells, the aspect of the fibrous tissue and the presence or not of foci of carcinomatous cells. Different types of invasive carcinomas (nodular and stellate) were recognized as well as benign lesions such as fibroadenomas or carcinoma in situ. Following these criteria, 70 to 75 Light-CT images were reviewed by breast pathologists and were classified in two categories: malignant and normal or benign. Light CT images were reviewed first, the classification was given on the images only, and then confirmed with histological sections observation. Analysis of corresponding HES sections yielded a sensitivity of 97%/ 90% and a specificity of 74%/77% for each pathologist involved in the study respectively.

8213-44, Session 7

## Catheter designs for magnetomotive optical coherence tomography

J. S. Kim, Beckman Institute for Advance Science and Technology (United States); D. Li, A. Ahmad, Beckman Institute for Advance Science and Technology (United States) and Univ. of Illinois at Urbana-Champaign (United States); S. G. Adie, Beckman Institute for Advance Science and Technology (United States); S. A. Boppart, Beckman Institute for Advance Science and Technology (United States) and Univ. of Illinois at Urbana-Champaign (United States)

Optical fiber-based catheters for OCT have been used to perform high-resolution cross-sectional imaging in clinical and research applications. Magnetomotive OCT (MM-OCT) is a functional extension of OCT which utilizes magnetic nanoparticles (MNPs) that are modulated by an external magnetic field for contrast enhancement and for elastography to assess the structural and viscoelastic properties of the surrounding tissues. To demonstrate MM-OCT for cardiovascular imaging applications, we prepared protein-shell microspheres (2-5 micron in diameter) filled with MNPs plus vegetable oil and functionalized with RGD peptides to target the $\alpha v$ 3 integrin receptors that are known to be overexpressed in atherosclerotic lesions. For future intravascular imaging applications, there is a need for a catheter-based MM-OCT system for the in-vivo detection of microspheres targeted to the endothelial cells of blood vessels. In this study, we developed and investigated the performance of MM-OCT catheters. One MM-OCT catheter design consists of an iron-core solenoid wrapped around a standard optical fiber-based catheter for OCT intravascular imaging system. Optimal parameters (i.e., number of turns, geometry, and core material) of the solenoid-based MM-OCT catheter were investigated by using numerical simulations (COMSOL Multiphysics Inc software). A plastic vessel phantom filled with iron-oxide-containing microspheres was used to demonstrate the performance of our solenoid-based OCT catheter. Preliminary results with phantoms demonstrate successful magnetomotive signal detection using spectral-domain OCT with magnetic fields generated at the distal end of our catheter. These results demonstrate the potential for a catheter-based MM-OCT intravascular imaging system. Further studies are being carried out to explore the possibility of incorporating our MM-OCT catheter for the early detection of atherosclerotic lesions using targeted microspheres in an in-vivo atherosclerotic rabbit model.

8213-45, Session 7

## Cellular resolution imaging using a full-field optical coherence tomography endoscopic probe

A. Latrive, A. C. Boccara, ESPCI - Institut Langevin (France) and LLTech (France)

Optical Coherence Tomography (OCT) has proven its interest for many biomedical fields thanks to its virtual slicing and 3D imaging capability. Full-Field OCT (FFOCT) is a particular approach which directly takes “en face” 2-D images with an isotropic resolution around 1µm. With such a high resolution FFOCT systems can produce images that are similar to that obtained with classical histology procedures and can thus be important tools for pathology. This is why we worked on combining the interest of an endoscopic setup with a needle probe with the performances of FFOCT.

The principle of our endoscopic FFOCT setup is based on the coupling of two distinct interferometers under incoherent illumination: one is external to the probe, and one is placed at the distal end of the probe in contact with the tissue to image. The distal interferometer is common-path: interferences occur between the reference beam reflected at the tip of the probe and light backscattered by structures at each depth within the tissue. The advantage compared to scanning system is that it does not require any advanced miniaturized mechanical systems at the tip of the probe, which are likely to increase the diameter as well as the cost of the probe. Our simple design is well-suited for in situ imaging.

On a setup with a 150 mm long and 2 mm wide GRIN-based probe we achieve axial and lateral resolutions of 1.8 µm and 3.5 µm, and a sensitivity of -80dB. We present ex vivo images obtained on fixed human breast tissue showing adipocytes and connective tissue, and in vivo images on human skin up to depths around 200 µm revealing the different cell and tissue structures of each layer.

8213-46, Session 7

## Optical frequency domain imaging as a diagnostic method and interactive tool for marking-guided biopsy in patients referred for screening or surveillance of Barrett’s esophagus

M. Gora, M. J. Suter, Massachusetts General Hospital (United States); E. Coron, Massachusetts General Hospital (United States) and Institute of Digestive Diseases (France); K. Gallagher, G. Y. Lauwers, Massachusetts General Hospital (United States); B. E. Bouma, Massachusetts General Hospital (United States) and Massachusetts Institute of Technology (United States); N. S. Nishioka, Massachusetts General Hospital (United States); G. J. Tearney, Massachusetts General Hospital (United States) and Massachusetts Institute of Technology (United States)

Barrett’s esophagus (BE) is a disease of the esophagus, which can undergo dysplastic progression, ultimately leading to the development of esophageal adenocarcinoma (EAC). The current approach for screening, i.e. upper gastrointestinal (GI) endoscopy is limited by the requirement of sedation, cost, and risk of sampling errors while performing biopsies of the distal esophagus.

Optical frequency domain imaging (OFDI) is a technique allowing high-resolution imaging of semi-transparent objects. It has been shown that it can be successfully used in clinical practice for imaging of the Barrett’s esophagus. Volumetric OFDI imaging reduces the potential for sampling errors, but there is still a need for guiding the endoscopist to the region of interest to perform biopsies or interventional therapy.

In this presentation, we will show the results of OFDI imaging of the distal esophagus as a diagnostic method as well as an interactive tool to perform laser marking-guided biopsies in patients undergoing screening or surveillance endoscopy for BE. Firstly, in order to validate the OFDI technique for screening and surveillance of BE, we have enrolled 106 patients in a clinical study. 10 cases will be used as a training set. 80 cases will be analyzed to assess the sensitivity and specificity of the method. Secondly, in order to reduce the risk of biopsy sampling error, we tested the feasibility of performing laser marking of the regions of interest based on OFDI images, during the same procedure, in 10 patients.

8213-47, Session 7

## Image guided 3D OCT for early diagnosis of carcinoma in situ of the bladder

H. Ren, K. Park, Stony Brook Univ. (United States); K. Shroyer, W. C. Waltzer, Stony Brook Univ. Medical Ctr. (United States); Y. Pan, Stony Brook Univ. (United States)

We compare the efficacies and potential limitations of surface imaging modalities, e.g., white light (WL), fluorescence (FC) and 3D optical coherence tomography (3D OCT) for early diagnosis of bladder carcinoma in situ (CIS). SV40T transgenic mice were employed as the rodent carcinogenesis model to closely mimic human bladder CIS. Our results show that the low diagnostic sensitivities and specificities of WL and FC for early CIS were significantly enhanced by quantitative 3D OCT to 95.0% and 90.0%, suggesting the value of image-guided 3D OCT for future clinical diagnosis of CIS in vivo.

8213-48, Session 7

## Elastic and optical tomography for the intraoperative diagnosis of tumors

A. Burcheri, A. Nahas, A. C. Boccara, Ecole Supérieure de Physique et de Chimie Industrielles (France)

FFOCT method is limited by nature of the contrast in biological tissues and often leads to incomplete information for a definitive diagnosis. Similarly to what has been done with ultrasound, extracting the elasticity of specimens would provide a necessary additional contrast. This approach is also known in the OCT community as “optical coherence elasticity”.

We present a method of mapping and quantifying tissue mechanical properties (static or dynamic) at micron-scale resolution with full field optical coherence tomography (FFOCT). Material employed were a piston in a sample holder inducing several levels of load on the sample. With this simple setup installed on a FFOCT-Light-CT scanner, we managed to get a displacement map image correlation in 2-D.

In addition to our FF-OCT maps we started to set a static elastography approach in order to get a multi-parameter image analysis that could complement histopathology diagnostics. To get all the information contained in our stacks of images we intend to develop programs of 3-D correlation in order to overlay en-face views of tissue properties maps.

8213-49, Session 8

## Multi-MHz FDML OCT: snapshot retinal imaging at 6.7 million axial-scans per second

T. Klein, W. Wieser, R. J. André, C. M. Eigenwillig, R. A. Huber, Ludwig-Maximilians-Univ. München (Germany)

We demonstrate the acquisition of densely sampled wide-field 3D OCT datasets in 0.3s - two million axial OCT scans of the human retina. This performance is achieved with a multi-MHz Fourier domain mode-locked (FDML) laser source operating at 1050nm. A two-beam setup doubles the 3.35MHz laser sweep rate to 6.7MHz, which is 16x faster than any non-FDML source used for retinal OCT. The “snapshot” acquisition time offers a broad range of benefits including a high probability of undistorted datasets. A detailed analysis of system performance, applications and the ultimate speed limits of flying-spot confocal retinal OCT will be presented.

8213-50, Session 8

## Optical amplification of the signal and performance of the ultrafast spectral domain optical coherence tomography at an A-scan rate of 12.5 MHz in a wavelength region of 1300 nm

D. Choi, H. Hiro-Oka, K. Shimizu, Kitasato Univ. (Japan); K. Ohbayashi, Kitasato Univ. School of Medicine (Japan)

For the optical biopsy application of optical coherence tomography (OCT), faster methods are required to reduce the inspection time and motion artifacts. A criterion to satisfy the purpose is an endoscopic-OCT method capable to display volumetric tomography continuously in real-time at a rate of video movie like conventional endoscopes. For the purpose, we have been developing ultra-fast spectral domain (SD) OCT systems at a few tenths MHz A-scan rate. In this work, characterization of a newly developed ultra-fast SD-OCT system at a wavelength range of 1300 nm reported. For spectral dispersion, we used 320-channel arrayed wave guides (AWGs) which enable separated parallel optical fiber output at each wavelength. A-scan rate is determined by the speed of the 50 MHz 12-bit A/D converters. Because we averaged four A-scans in most of cases, the effective A-scan speed was 12.5 MHz. A resolution of 27 micrometers, depth range of 3.98 mm, and sensitivity roll off of 3 dB within the principal region were confirmed. We introduced a semiconductor optical amplifier (SOA) to enhance the signal. Due to RIN, the maximum sensitivity was limited to 78 dB without the SOA. With the SOA, we could increase the sensitivity up to 94 dB. This sensitivity enabled imaging of biological tissues in a reasonable S/N ratio. Selected examples of movies are shown such as miosis dynamics, real-time 3D movie example of moving tissues, and real-time virtual cutting of tissues.

8213-51, Session 8

## Dual-depth SSOCT for simultaneous complex conjugate resolved anterior segment and conventional retinal imaging

A. Z. Dhalla, T. Bustamante, H. C. Hendargo, R. P. McNabb, A. N. Kuo, J. A. Izatt, Duke Univ. (United States)

We present a novel OCT system design that employs polarization encoding to image both the anterior segment and the retina. The design can be implemented to allow for either rapidly switched sequential or simultaneous imaging of the anterior and posterior segment of a patient eye with no adjustment of the sample arm optics. The temporal encoding scheme of the dual depth imaging system (i.e. sequential versus simultaneous imaging) depends only on the implementation of the reference arm and sampling electronics. This design is a significant step toward whole-eye human OCT, which would enable customized ray-traced modeling of patient eyes to improve refractive surgical interventions and to eliminate optical artifacts in retinal OCT diagnostics. We demonstrated the feasibility of such a system by acquiring images of the anterior segments and retinas in healthy human volunteers.

8213-52, Session 8

## Streak-mode Fourier domain optical coherence tomography

R. Wang, J. X. Yun, Clemson Univ. (United States); X. Yuan, Nankai Univ. (China); R. L. Goodwin, Univ. of South Carolina (United States); R. R. Markwald, Medical Univ. of South Carolina (United States); B. Z. Gao, Clemson Univ. (United States)

In conventional FD-OCT, the A-scan rate is limited by the line-scan cameras. A state-of-the-art area-scan camera can achieve a higher data-acquisition rate than a line-scan camera can. Thus, using high speed area-scan cameras allows for the development of a megahertz OCT. Here, we report streak-mode Fourier domain optical coherence tomography (SM-FDOCT), a technique in which an area-scan camera is used instead of a line-scan camera to record the OCT spectrum. This SM-FDOCT retains the conventional point-scanning mechanism so that the small aperture of the single-mode fiber functions as a confocal gate for rejecting multiply scattered photons. While the probe beam is scanning the sample laterally, the corresponding OCT spectrum is physically scanned on the area-scan camera using a streak scanner, in our current case, a 1000 Hz resonant scanner. Pixels of the camera are illuminated by the OCT spectrum row by row in correspondence with each A-scan at different lateral positions.

SM-FDOCT is theoretically compared with the conventional FD-OCT, and the effect of the streak-scanning is numerically analyzed. 1,016,000 Hz A-scan is achieved with a sensitivity of ~ 95 dB. To demonstrate the dynamic imaging capability, our SM-FDOCT is used to image the heart outflow tract (OFT) of HH19 stage chick embryos at 1000 frames/s B-scan rate. 4D imaging embryonic chick hearts is achieved with this method. The results have demonstrated that this technique has the potential for multimegahertz OCT imaging. Due to its high temporal resolution, it is suitable for cross-sectional imaging high speed dynamic biomedical processes.

8213-53, Session 8

## Dispersion encoded full-range swept source OCT at 1060 nm

B. Hofer, Medizinische Univ. Wien (Austria); L. Wang, Katholieke Univ. Leuven (Belgium); B. Hermann, R. Werkmeister, B. Povazay, A. Alex, W. Drexler, Medizinische Univ. Wien (Austria)

Diversity in measurements must be introduced in order to remove the complex conjugate in frequency domain optical coherence tomography (FD-OCT). The bulk dispersion mismatch between reference and sample arm offers a systematically simple diversity mechanism. The associated dispersion encoded full range (DEFR) scheme allows for iterative reconstruction of full range tomograms with largely reduced complex conjugate terms. Here, we investigate how DEFR can be used in conjunction with swept source OCT at 1060 nm. Anterior and posterior segment in vivo imaging of human subjects is demonstrated. Real time processing can be achieved by porting the iterative algorithm to GPU based massively parallel processing.

8213-54, Session 8

## Depth-ambiguity free or polarization sensitive optical frequency domain imaging using the Pancharatnam-Berry phase

N. Lippok, S. Coen, R. Leonhardt, P. M. F. Nielsen, F. Vanholsbeeck, The Univ. of Auckland (New Zealand)

Optical Coherence Tomography (OCT) is a well established imaging modality, allowing one to perform in vivo and non invasive biopsies to up to several millimeters deep in tissue. Spectral Domain OCT (SD-OCT) yields a depth ambiguity caused by the Fourier transform of a real function that will always be Hermitian, and therefore consists of symmetric positive and negative depth terms leading to image distortion. In order to remove the depth ambiguity we applied the Pancharatnam's phase by using a Fresnel rhomb and a linear polarizer. We show analytically how this simple configuration allows for a constant and instantaneous $\pi/2$ phase shift, therefore offering single-frame full-range OCT images. The method proposed here is highly wavelength independent, due to the reduced number of components compared to other proposed techniques, making it the ideal procedure for a high-resolution system. Experimentally, we achieved a 45 dB reduction in the complex conjugate term for a bandwidth of 80 nm at a central wavelength of 1550 nm in a swept source OCT configuration. Furthermore, the Pancharatnam's phase can be used to perform single frame polarization sensitive OCT (PS-OCT) measurements. PS-OCT systems traditionally need two orthogonally polarized detection channels to calculate the birefringence of the sample. Here, the detection scheme for the Pancharatnam's phase allows one to retrieve three independent parameters such as two intensities and an interferometric phase shift. Using the Newton-Raphson method, these parameters offer an estimate of the Jones vector of the sample.

8213-55, Session 8

## Influence of image detectors on the signal fall-off in spectral domain optical coherence tomography systems

M. Hagen-Eggert, Univ. zu Lübeck (Germany); P. Koch, Thorlabs GmbH (Germany); G. Hüttmann, Univ. zu Lübeck (Germany)

The influence of the performance of different image detectors on the depth dependent sensitivity fall off (roll-off) in spectral domain optical coherence tomography (SD-OCT) is investigated. We present a method for characterization of the roll-off of SD-OCT systems via modulation transfer function (MTF) analysis. The MTF of different image sensors was measured in a newly developed experimental setup, which projects sinusoidal interference gratings with different spatial frequencies on the image detector. Therefore, the cameras under test were illuminated by two coherent beams which were derived from a single-mode laser diode source. The signal contrast was detected by calculating the power spectrum of the modulation contrast of the interference pattern. In order to calculate an overall roll-off, the results of the MTF measurements were combined with simulations of the theoretical limited MTF due to diffraction, aberration and sampling of a SD-OCT spectrometer. The results are compared with roll-off measurements of the corresponding commercially available SD-OCT system. The discrepancy between our roll-off simulation and the roll-off measurement is less than 2 dB at Nyquist frequency. Furthermore, it is shown that the depth dependent sensitivity loss due to the MTF of the image detectors is the main contribution to the roll-off of the SD-OCT system. The characterization of SD-OCT systems via MTF analysis gives a detailed insight to the contribution of the spectrometer components to depth dependent sensitivity degrading effects and shows possibilities for improvements in a SD-OCT systems design.

8213-56, Session 8

## Multiple-depth en face optical coherence tomography using active recirculation loops in the non-stationary state

J. A. Rogers, A. Bradu, A. G. Podoleanu, Univ. of Kent (United Kingdom)

We demonstrate the use of recirculating delay lines in both the object and reference paths of an interferometer in the non-stationary state. It is demonstrated that modulation of active gain in each arm may be used to control the optical power that interrogates multiple paths at the same time. This is achieved by opening and closing the loops using both the acousto-optic frequency shifters and modulation of the SOA drive current to maintain the roundtrip gain in the loops at 1. Using this concept, simultaneous interrogation of ten depths in a sample at 75 microns apart is demonstrated, with much less attenuation from one recirculation to the next than we previously reported. Broadening of the correlation function was seen as expected due to narrowing of the linewidth of circulating light due to repeated amplification in the SOA gain medium.

8213-57, Session 9

## Simultaneous dark-bright field swept source OCT for ultrasound detection

C. Blatter, B. Grajciar, B. Hermann, Medizinische Univ. Wien (Austria); R. Huber, Ludwig-Maximilians-Univ. München (Germany); W. Drexler, R. Leitgeb, Medizinische Univ. Wien (Austria)

We introduce a swept source FDOCT imaging system that allows measuring simultaneously the reflected light and scattered light (bright field) and the scattered light only (dark field) in two different channels through separate Gaussian and Bessel detection. We show that this system can be applied to gain contrast information from the sample if reflected light is discarded so that both channels can be used for imaging. It is the result of different lateral PSF as well as detection with different angles. If specular reflection is present, the dark field channel, remained unaffected, is used for OCT imaging while the other one allows for the reflex measurement with high SNR. It can be used to obtain knowledge about the sample time evolution for phase or vibration analysis. Based on this configuration, we provide a proof-of principle study for resolving US pulse trains with high temporal resolution on reflecting surfaces. High speed swept source OCT offers in fact a time resolution for sampling the spectra of up to 1GHz. This time resolution is apt for monitoring oscillations of ultrasound waves that manifest as phase variations of the spectral interference pattern. A windowed FFT across the spectral phase allows to directly access those changes and to temporally resolve the pulse train. This has been demonstrated in-vitro with a chicken breast sample. This scheme potentially provides a novel all optical detection scheme for the combination of OCT with photoacoustic imaging.

8213-58, Session 9

## Optimizing magnetomotive contrast of SPIO-labeled platelets for thrombosis imaging in optical coherence tomography

A. L. Oldenburg, D. Spivak, F. Tsui, The Univ. of North Carolina at Chapel Hill (United States); T. Fischer, The Univ. of North Carolina at Chapel Hill School of Medicine (United States)

Rehydratable, lyophilized (RL) platelets loaded with superparamagnetic iron oxides (SPIOs) provide magnetomotive imaging contrast to sites of vascular damage, including thrombosis complicating atherosclerosis and hemorrhage. Magnetomotive optical coherence tomography (MMOCT) contrasts SPIO-platelets based on their nanoscale, magnetically-induced motion. Magnetomotion is tracked using a phase-sensitive, spectral-domain OCT system. We report improvements in the SPIO loading of RL platelets by a factor of 4.5, which leads to concomitant improvements in their magnetic and magnetomotive contrast properties. SQUID magnetometry shows that the effective magnetic domain size in the improved SPIO-RL platelets is increased by more than a factor of 3, as evidenced by an increased blocking temperature in temperature-dependent scans, and increased magnetic susceptibility in field-dependent scans. This enhancement may be attributed to interparticle magnetic interactions between SPIOs when packed into platelets. Agarose tissue phantoms prepared with SPIO-RL platelets at a fixed iron concentration show that the improved SPIO-RL platelets provide 3dB enhancement in MMOCT contrast at a 4.5-fold lower concentration of 3.1E8 platelets/mL. Extrapolation from these results suggests a sensitivity limit of 2.2E8 platelets/mL, or only 0.23% by volume, when incorporated into a blood clot. In previous work, SPIO-platelets have been shown to specifically adhere to sites of vascular damage in porcine arteries ex vivo and provide MMOCT contrast. This may lead to new methods for detecting internal bleeding and monitoring the formation of blood clots using infused SPIO-platelets.

8213-59, Session 9

## Conformal laser therapy

M. L. Villiger, D. L. Arruda, M. Shishkov, B. J. Vakoc, G. J. Tearney, B. E. Bouma, Wellman Ctr. for Photomedicine (United States)

Thermal coagulation of the esophageal epithelium represents a promising treatment to revert Barrett's esophagus into normal squamous epithelium. To improve the efficacy of such treatment and avoid complications, the thermal injury profile should be conformed to a specific anatomical boundary. The high resolution cross-sectional images of endoscopic optical frequency domain imaging (OFDI) have proved efficient for diagnosis and can be utilized for treatment planning by defining a local target depth for thermal ablation. Here, we investigate a possible strategy for intervention by combining a scanned therapy laser beam to induce thermal injury with a collinear OFDI channel to control the injury depth. Using the strong variation of water absorption close to 1.9 μm, the penetration and resulting treatment depth can be accurately tuned by changing the wavelength of a Thulium fiber laser. Similar depth control is achieved by combining two discrete wavelengths with independent power tuning, with the benefit of higher speed. In the OFDI monitoring channel, the scanning of the combined treatment and monitoring beams produces primarily a structural signal. The conformational change induced by the thermal coagulation however results in an additional Doppler-like signal that can be extracted from the structural background. This provides a measure of the instantaneous treatment depth, which is used to control the tuning of the treatment laser. We present depth-controlled injury during linear pullbacks in the swine esophagus in vivo.

8213-60, Session 9

## In vivo measurement of differential motion within the organ of Corti under sound stimulation using optical coherence tomography

N. Choudhury, Michigan Technological Univ. (United States); F. Chen, D. Zha, A. Fridberger, Oregon Health & Science Univ. (United States); R. Wang, Univ. of Washington (United States); S. L. Jacques, A. L. Nuttall, Oregon Health & Science Univ. (United States)

Hearing in mammals, depend on an amplifying motion which hypothetically uses force from outer hair cells (OHC) motility to enhance sound induced vibration of the organ of Corti of cochlea. In this hypothesis the differential motion among key structures in this organ and the timing of the OHC force generation is essential for cochlear amplification to occur. However, currently used techniques fail to provide accurate measurement beyond the first surface. Therefore, in vivo nanomechanics of the organ of Corti has remained hidden from the researchers.

Using a time domain optical coherence tomography (TD-OCT) system which allows us to make vibration measurements we were able to measure differential motion of two functionally important surfaces, namely, basilar membrane and reticular lamina. In order to record differential motion between RL and BM, we have developed a TD-OCT based system that provides both in vivo images and vibration measurements of the organ of Corti of guinea pigs.Since,the system provided a structural image and the location of vibration measurement was also known, we could compare with the known morphology of the organ of Corti and ascertain the identity of our measurement location. Using this TD-OCT system we have observed sub-nanoscale (>0.3nm) displacements from various surfaces (RL and BM) of the organ of Corti under pure-tone sound stimulation (~19KHz). In this report, we show that there is differential motion between BM and RL by noting: a) larger amplitude of displacement in RL over BM and b) a phase lead of RL over BM.

8213-61, Session 9

## Measuring the vibrational response of the mouse ear using coherently interleaved optical coherence tomography

R. L. Shelton, Texas A&M Univ. (United States); S. S. Gao, J. S. Oghalai, Stanford Univ. (United States); B. E. Applegate, Texas A&M Univ. (United States)

Optical coherence tomography (OCT) has recently seen increased applications for imaging the morphology and function of the middle and inner ear. Spectrometer based Fourier domain OCT is well suited to making vibratory measurements due to its excellent phase sensitivity, which can be used to measure the small periodic mechanical motions of the ear; however, the speed of the CCD line-scan camera in the spectrometer severely limits the measurable frequency range. We have developed a technique that enables interrogation of the entire mouse auditory spectrum (4 - 90 kHz) using a standard, low-noise, CCD line-scan camera. This technique takes advantage of the fact that the small mechanical motions inside the ear are periodic in nature, by phase-locking the camera trigger to the acoustic stimulation. The technique employs a spectrometer based OCT system and an algorithm that coherently interleaves multiple time windows to increase the effective sampling rate, enabling much higher frequency response measurements.

The algorithm was evaluated first on a piezo element as a proof of concept demonstration. Frequency vibrations up to three times the Nyquist rate of the spectrometer were accurately measured. The algorithm was then used to measure the tympanic membrane of a freshly sacrificed mouse. A speaker placed within 12 inches of the mouse stimulated the membrane and the system was used to measure the frequency response. Using a spectrometer setup with a Nyquist frequency of 11.9 kHz vibratory measurements up to 40 kHz were made on the tympanic membrane, limited only by the 35 kHz frequency cutoff of the speaker. Artifacts inherent to the algorithm are investigated and discussed.

8213-62, Session 9

## Spectral and time domain OCT - a tool for optimal imaging of biological samples

M. Szkulmowski, I. M. Gorczynska, D. Szlag, M. D. Wojtkowski, Nicolaus Copernicus Univ. (Poland)

Spectral and Time domain OCT (STdOCT) is a data analysis scheme proposed for sensitive Doppler imaging. In this work we show that it has an additional feature: tomograms prepared using STdOCT have the same or better signal to noise ratio (SNR) and contrast to noise ratio (CNR), than tomograms prepared using standard spectral OCT processing with averaging of A-scans moduli. Relevant simulations and experimental results are presented. Images of human retina prepared with two different techniques are shown.

8213-63, Session 10

## Imaging of photothermal tissue expansion via phase sensitive Optical Coherence Tomography

H. Spahr, L. Rudolph, H. H. Müller, R. Birngruber, G. Hüttmann, Univ. zu Lübeck (Germany)

Phase sensitive Optical Coherence Tomography enables the measurement of thermal expansion in laser irradiated material with high spatial and temporal resolution. This could be utilized for a non-invasive mapping of the retinal absorbance by measuring thermal responses, i.e. the thermal expansion due to absorption of light, to slight irradiation. A subsequent observation of the cooling behavior that is mainly determined by the amount of nearby blood flow could possibly reveal the local perfusion. Both quantities are of high clinical and scientific relevance. The possibilities of quantitative investigations with high axial and lateral resolution are demonstrated by imaging the reversible thermal expansion in laser irradiated bilayer and multilayer silicone phantoms: Irradiation of phantoms with laterally or in-depth varying absorbance causes an accordingly varying phase shift. To convert this phase shift distribution into a 3D displacement vector field, first of all the 2pi phase ambiguity has to be removed by 1D or 2D phase unwrapping algorithms. After that, an estimate of the underlying physical quantity of interest, the change in optical path length and therefore longitudinal displacement, is possible. Under certain symmetry conditions, knowledge of just the longitudinal component is sufficient to estimate the local expansion, which is the divergence of the 3D displacement vector field. Finally, a quantitative correlation between the thermal expansion and the underlying evolution of temperature distribution has to be elaborated.

8213-64, Session 10

## Ultrahigh speed swept source / Fourier domain polarization sensitive optical coherence tomography

B. Baumann, Massachusetts Institute of Technology (United States) and Univ. of Pittsburgh Medical Ctr. (United States); W. J. Choi, Massachusetts Institute of Technology (United States); B. M. Potsaid, Massachusetts Institute of Technology (United States) and Thorlabs Inc. (United States); D. Huang, Oregon Health & Science Univ. (United States); J. S. Schuman, Univ. of Pittsburgh Medical Ctr. (United States); J. S. Duker, Tufts Medical Ctr. (United States); J. G. Fujimoto, Massachusetts Institute of Technology (United States)

Polarization sensitive optical coherence tomography (PS-OCT) is a functional extension of OCT that enables imaging with additional contrast based on the light polarizing properties of a sample. Here, we present PS-OCT based on ultrahigh speed swept source / Fourier domain OCT at 1050nm at 100kHz axial scan rates using single mode fiber optics and a multiplexing approach. Unlike previously reported multiplexing PS-OCT schemes, the method presented here does not require active polarization modulating devices, but relies on a passive polarization delay unit. This decreases system cost and avoids sophisticated synchronization requirements. The polarization delay unit was implemented in the sample beam path in order to illuminate the sample with two different polarization states simultaneously. The orthogonal polarization components for the depth-multiplexed signals from the two input states were detected using a polarization sensitive detection unit. PS-OCT images were computed using Jones calculus.

3D PS-OCT imaging was performed in the human retina and various biological samples using the ultrahigh speed OCT system. The high imaging speed enabled the acquisition of virtually motion artifact free volumetric data sets within less than one second. In addition to standard OCT images, PS-OCT images were generated using contrast based on birefringence and depolarization. Enhanced tissue discrimination as well as quantitative measurements of sample properties were enabled using the additional contrast and information contained in the PS-OCT images.

8213-65, Session 10

## Automated measurement of choroidal thickness by polarization sensitive optical coherence tomography

T. Torzicky, E. Götzinger, M. Pircher, S. Zotter, M. Bonesi, C. K. Hitzenberger, Medizinische Univ. Wien (Austria)

In our current work we are using a polarization sensitive optical coherence tomography (PS-OCT) system with a central wavelength of 1060 nm, for acquiring intensity, retardation and degree of polarization uniformity (DOPU) images of retina, choroid and sclera in vivo. Based on the acquired images a segmentation algorithm for identifying the retinal pigment epithelium (RPE) and the choroidal-scleral interface, in order to measure the choroidal thickness, was developed. The segmentation of the RPE was done by using the DOPU images, which show the depolarizing characteristics of the RPE clearly. For identifying the border between choroid and sclera the retardation images were used, where the birefringence of the sclera is well shown. The images segmented with our algorithm show segmentation of the choriodal-scleral interface and the RPE and allow automated calculation of choroidal thickness.

8213-66, Session 10

## Absolute measurement of subnanometer scale vibration of cochlear partition of an excised guinea pig cochlea using spectral-domain phase-sensitive optical coherence tomography

H. M. Subhash, Oregon Health & Science Univ. (United States)

measurement of absolute vibration parameters from different locations within the mammalian organ of Corti is crucial for understanding the hearing mechanics such as how sound propagates through the cochlea and how sound stimulates the vibration of various structures of the cochlea, namely, basilar membrane (BM), recticular lamina, outer hair cells and tectorial membrane (TM). In this study we demonstrate the feasibility a modified phase-sensitive spectral domain optical coherence tomography system to provide subnanometer scale vibration information from multiple angles within the imaging beam. The system has the potential to provide depth resolved absolute vibration measurement of tissue microstructures from each of the delay-encoded vibration images with a noise floor of ~0.3nm at 200Hz.

8213-67, Session 10

## Automated detection of chorio-scleral interface using polarization-sensitive optical coherence tomography

L. Duan, M. Yamanari, Y. Yasuno, Univ. of Tsukuba (Japan)

Since the practicability of back-scattered intensity optical coherence tomography (OCT) is limited in segmentation of chorio-scleral interface (CSI) segmentation for low contrast as well as absence of anatomical or histological evidence , a polarization sensitive optical tomography based automated algorithm is presented for CSI detection. The birefringent properties of choroid and sclera have a clear difference. The birefringent properties measured by polarization sensitive OCT (PS-OCT) can be utilized as a contrast source for segmentation of this two layers.

This algorithm consists of two steps: the rough segmentation of the two tissues in step-1, and accurate determination of CSI in step-2. In step-1, the choroid and sclera is generally distinguished by a Gaussian mixture model using local birefringence image, and segmentation with low precision is performed for CSI detection. Successively, the linear fitting is applied to the phase retardation in both choroid and sclera in each A-lines, and the CSI is determined as the cross-point of the two phase retardation slope lines. Finally, a median filter is employed to smooth the boundary obtained in step-2.

This segmentation algorithm is successfully applied to PS-OCT images acquired from a normal eye, and reasonable result is automatically obtained. Since the CSI is defined by the different birefringent property of the choroid and the sclera the subjective segmentation error existing in manual segmentation is relevantly avoided. This automated segmentation algorithm also offers possibility to full automatic and highly accurate volumetric assessment of choroidal thickness.

8213-68, Session 10

## Polarimetry noise analysis and compensation in polarization sensitive optical coherence tomography

E. Z. Zhang, B. J. Vakoc, Massachusetts General Hospital (United States) and Harvard Medical School (United States)

High noise levels in fiber-based polarization-sensitive optical coherence tomography (PS-OCT) have broadly limited its clinical utility. In this study we investigate two system noises that limit performance in PS-OCT: signal to noise ratio (SNR) and polarization mode dispersion (PMD). Using both analytical methods and empirical studies, we show that small levels of PMD commonly induced by single-mode fiber and discrete optical components are a dominating source of noise in fiber-based PS-OCT systems. As it is very challenging if not impossible to entirely avoid PMD in fiber-based system, a PMD compensation method is proposed to measure and compensate PMD in the instrumentation during post-processing.

8213-69, Session 11

## Optical coherence microscopy for deep tissue imaging of the cerebral cortex with intrinsic contrast

V. J. Srinivasan, H. Radhakrishnan, Massachusetts General Hospital (United States); J. Y. Jiang, S. Barry, A. E. Cable, Thorlabs Inc. (United States)

In vivo optical imaging techniques have recently emerged as important tools for studying neurobiological development and pathophysiology. In particular, two-photon microscopy has proved to be a robust and highly flexible method for in vivo imaging in highly scattering tissue. However, two photon imaging typically requires extrinsic dyes or contrast agents, and imaging depths are limited to a few hundred microns. This paper demonstrates and validates Optical Coherence Microscopy (OCM) for in vivo imaging of neuronal cell bodies, capillaries, and cortical myelination up to depths of ~1.3 mm in the rat cortex. Lamina-specific features are demonstrated. Imaging does not require addition of dyes or contrast agents, and is achieved through intrinsic scattering contrast and image processing alone. Imaging depths are 2.5-3x higher than those achieved by two-photon microscopy. We also demonstrate in vivo, quantitative measurements of optical properties (index of refraction and scattering properties) in the cortex, which also show lamina-specific behavior. We show that these techniques enable direct visualization of cellular morphological changes during depolarization and repolarization and may provide novel optical markers of cell viability.

8213-70, Session 11

## Structural and functional imaging of the pathology of Alzheimer's disease in a mouse model using extended-focus optical coherence microscopy

A. Bouwens, T. Bolmont, C. Pache, P. C. Fraering, T. Lasser, Ecole Polytechnique Fédérale de Lausanne (Switzerland)

The accumulation of amyloid-β (Aβ) peptides in cerebral plaques and blood vessels is a pathological hallmark of Alzheimer's disease (AD). High-resolution optical imaging of cerebral Aβ plaques in the living mouse brain currently requires the use of fluorescent labeling. The influence of labeling on the formation and maintenance of Aβ plaques is however largely unknown. We present extended-focus optical coherence microscopy (xfOCM) as a technique capable of imaging cerebral Aβ plaques in and ex vivo, without the use of exogenous contrast agents. Therefore, xfOCM imaging precludes any possible bias caused by labeling.

We have constructed an xfOCM instrument tailored to small animal research. The use of a Bessel-like illumination beam provides a uniform, high lateral resolution (1.3 µm) over an extended depth of field (400 µm) into the mouse brain. A small craniotomy and a glass window allow repeated imaging of the cortex of anesthetized wild type and AD model mice. Three-dimensional xfOCM images of the AD brain structure clearly reveal Aβ plaques. In addition to the acquisition of structural images, xfOCM provides high-resolution functional images of blood perfusion in the AD mouse brain simultaneously. The interesting link between blood perfusion and the deposition of Aβ plaques around blood vessels can therefore be studied without exogenous contrast agents.

A label-free investigation of the disease development necessitates imaging of the same region of brain tissue at several time-points. We demonstrate a method that uses the vascular network as a reference for registration of the label-free images.

8213-71, Session 11

## Sub-cellular resolution imaging of coronary arteries and respiratory mucosa using micro-optical coherence tomography (µOCT)

L. Liu, Massachusetts General Hospital (United States) and Harvard Medical School (United States); J. A. Gardecki, Massachusetts General Hospital (United States); B. E. Bouma, Massachusetts General Hospital (United States) and Massachusetts Institute of Technology (United States) and Harvard Medical School (United States); G. J. Tearney, Wellman Ctr. for Photomedicine (United States) and Harvard Medical School (United States) and Massachusetts Institute of Technology (United States)

We have developed a novel imaging technique termed micro-OCT (µOCT) which obtains images with a resolution of 2 µm × 2 µm × 1 µm (x, y, z) in tissue. We used the µOCT system to image fresh human coronary arteries prosected from explant (donor) hearts, and demonstrate that µOCT provides anatomical microstructures of coronary arterial wall including endothelial cells, leukocytes, platelets and fibrin, macrophages, smooth muscle cells, cholesterol crystals, micro-calcifications and superficial calcium, bare metal stents and drug eluting stents, and stents pathology. We also imaged cultured human bronchial epithelial (HBE) cells, and freshly explanted swine tracheas, and show that µOCT provides video-rate functional live motion capture of respiratory mucosa physiology including ciliary activity, airway surface liquid (ASL) and periciliary liquid (PCL) layer morphology at the sub-cellular level. We also show that µOCT enables real-time measurement of ASL and PCL depth, CBF, MCT and glandular mucus extrusion in epithelia derived from normal subjects and subjects infected by cystic fibrosis (CF) airway disease.

8213-72, Session 11

## Interferometric synthetic aperture microscopy with virtual adaptive optics aberration correction

S. G. Adie, B. W. Graf, A. Ahmad, P. S. Carney, S. A. Boppart, Univ. of Illinois at Urbana-Champaign (United States)

Interferometric synthetic aperture microscopy (ISAM) reconstructs the scattering potential of a sample with spatially invariant resolution. The reconstruction algorithms take into account the incident beam profile, the beam scan pattern, the physical model of light sample interaction, and subsequent light collection by the system. In practice, aberrations may influence the beam profile, particularly at higher NA, when ISAM is expected to provide maximum benefit over optical coherence microscopy. In our previous work, we showed that modest amount of spherical aberration produces artifacts in the far-from-focus point-spread function. We present a method for post-acquisition aberration compensation for OCT and ISAM, incorporating space-invariant and space-variant aberration correction. Since the raw spectral-domain data is an invertible transform of the complex scattered field, post-acquisition numerical correction of specific pupil plane aberrations is possible using the corresponding Zernike polynomials. We demonstrate space-invariant aberration correction in 3D data of a silicone tissue phantom with sub-resolution titanium dioxide scatterers, acquired with a highly astigmatic sample beam, with the recovery of space-invariant of (focal plane) resolution after ISAM reconstruction. Space-variant aberration correction is explored through simulations and experiment. This virtual adaptive optics method enables post-acquisition aberration correction, and thus does not require adaptive optics hardware.

8213-73, Session 11

## Combined two-photon microscopy and optical coherence tomography for in vivo tissue imaging

B. Jeong, H. Nam, M. S. Jang, T. Wang, J. Doh, B. Yang, M. H. Jang, K. H. Kim, Pohang Univ. of Science and Technology (Korea, Republic of)

The combination of two-photon microscopy (TPM) and optical coherence tomography (OCT) is useful in conducting in-vivo tissue studies, because they provide complementary information regarding tissues. In the present study, we developed a new combined system using separate light sources and scanners for individually optimal imaging conditions. TPM used a Ti-Sapphire laser and provided molecular and cellular information in microscopic tissue regions. Meanwhile, OCT used a wavelength-swept source centered at 1300 nm and provided structural information in larger tissue regions than TPM. The system was designed to do simultaneous imaging by combining light from both sources. TPM and OCT had the field of view values of 300 µm and 800 µm on one side respectively with a 20x objective. TPM had resolutions of 0.47 µm and 2.5 µm in the lateral and axial directions respectively, and an imaging speed of 40 frames/s. OCT had resolutions of 5 µm and 8 µm in lateral and axial directions respectively, a sensitivity of 97dB, and an imaging speed of 0.8 volumes per second. This combined system was applied to image small intestine of mouse models ex-vivo. Molecular, cellular, and structural information of the tissues were visualized using the proposed combined system.

8213-74, Session 11

## Quantifying sub-diffractional tissue mass density correlation function by spectroscopic optical coherence tomography

J. Yi, J. D. Rogers, I. R. Capoglu, A. J. Radosevich, Y. Stypula, Northwestern Univ. (United States); H. K. Roy, NorthShore Univ. HealthSystem (United States); A. Taflove, V. Backman, Northwestern Univ. (United States)

Abbe's diffraction limit has hindered the exploration of sub-wavelength biological features. Although novel methods have been developed to break this limit, nanometer features within intact tissue is still inaccessible. Here we report a label-free approach to quantify sub-diffractional tissue mass density correlation function by spectroscopic optical coherence tomography which can localize spectrum from an interrogated volume. Under a modified Born approximation, this localized spectrum is free of the diffraction limit and is associated with physical tissue structure (three dimensional refractive index correlation function). Moreover, the real-time three dimensional imaging capability with millimeter penetration depth promises an excellent modality for in vivo applications. Rigorous simulation and phantom designs verified the sub-diffractional accuracy of the approach. A tissue study reveals that in situ biological structures are most likely organized in a fractal manner and the mass fractal dimension can be quantified at the length scale of sensitivity from about 40nm to 0.8μm.

8213-75, Session 11

## High resolution holoscopy

G. L. Franke, Univ. zu Lübeck (Germany); D. Hillmann, Thorlabs GmbH (Germany) and Medizinisches Laserzentrum Lübeck (Germany); T. Claußen, C. Lührs, P. Koch, Thorlabs GmbH (Germany); G. Hüttmann, Univ. zu Lübeck (Germany)

Holoscopy, a new imaging approach combining holography and Full-Field Fourier-Domain Optical Coherence Tomography (OCT), has been presented recently. Holoscopy provides a depth-invariant lateral resolution and therefore overcomes a known limitation of Fourier-Domain OCT, where the lateral resolution and the sensitivity degrade outside of the focal plane. The degradation depends on the Rayleigh length and the corresponding numerical aperture (NA) of the optical setup. Therefore, the advantage of holoscopy becomes especially significant at high NAs. High lateral resolutions within the Rayleigh length can be achieved with Optical Coherence Microscopy, but for measurements over a depth range larger than the Rayleigh length axial scanning has to be implemented. This becomes unnecessary with holoscopy. So far, only low NA (= 0.07) measurements with holoscopy were performed. With a setup based on a Michelson interferometer an axial resolution comparable to standard OCT systems and a depth-invariant lateral resolution has been achieved. We present a high resolution holoscopy setup based on a Mach-Zehnder interferometer. The implementation of a swept source based on a Ti:sapphire laser provides us with a broad bandwidth spectrum, while the optical design is adapted to provide high NA. This setup allows us to obtain simultaneously ultra-high axial and depth-invariant lateral resolutions and sensitivities over a depth range significantly larger than the Rayleigh length of the setup.

8213-76, Session 11

## Development and dynamics of 3D mammary epithelial-stromal co-cultures using optical coherence tomography

R. K. Chhetri, A. C. Sullivan, The Univ. of North Carolina at Chapel Hill (United States); M. A. Troester, The Univ. of North Carolina at Chapel Hill (United States) and Lineberger Comprehensive Cancer Ctr. (United States); A. L. Oldenburg, The Univ. of North Carolina at Chapel Hill (United States) and 4Biomedical Research Imaging Ctr. (United States)

The human mammary gland consists of an intricate network of cells in a complex, heterogeneous microenvironment. The interactions between mammary epithelial cells (MECs) and stromal fibroblasts have been shown to regulate tumorigenesis, where MEC malignancy results in and is promoted by the activation and transformation of stromal fibroblasts. 3-dimensional co-cultures of MECs and fibroblasts in a Matrigel-collagen I matrix offer a stable model that recapitulates several aspects of mammary glandular tissues in vivo. A majority of imaging tools currently used to study such co-cultures require fixing and staining, which may perturb the native architecture and prevent longitudinal study. Optical Coherence Tomography (OCT) offers a non-invasive method to monitor the morphologyand dynamics of such co-cultures. We show that OCT provides excellent visualization of acinar structures formed by MECs in 3D co-culture, which exhibit hollowed centers similar to mammary ducts in vivo. Using OCT, we performed a longitudinal study of live co-cultures to monitor the morphological changes of acini and adjacent fibroblasts. OCT image stacks (4 x 4 x 1.5mm) of normal and pre-malignant MECs in co-culture are acquired at 2 and 4 weeks with an ultrahigh-resolution (12 x 12 x 3μm) spectral-domain OCT system. We also demonstrate the ability to measure motility in the co-cultures, defined as the decorrelation time of the local OCT signal when monitored at 1 kHz. We find that the motility of acini are significantly higher when live compared to fixed, and expect that motility may correlate with long-term migratory potential in future studies.

8213-77, Session 12

## Anterior segment and retinal 3D-OCT motion correction using image registration and orthogonal scan patterns

M. F. Kraus, Friedrich-Alexander-Univ. Erlangen-Nürnberg (Germany) and Massachusetts Institute of Technology (United States); I. Grulkowski, Massachusetts Institute of Technology (United States) and Nicolaus Copernicus Univ. (Poland); B. M. Potsaid, Massachusetts Institute of Technology (United States) and Thorlabs Inc. (United States); B. Baumann, Massachusetts Institute of Technology (United States) and Tufts Univ. (United States); J. S. Schuman, Univ. of Pittsburgh Medical Ctr. (United States); J. S. Duker, New England Eye Ctr. (United States); D. Huang, Oregon Health & Science Univ. (United States); J. G. Fujimoto, Massachusetts Institute of Technology (United States); J. Hornegger, Friedrich-Alexander-Univ. Erlangen-Nürnberg (Germany)

Optical Coherence Tomography (OCT) has become a clinical standard for detection and tracking of ocular pathology through its ability to perform non-invasive micron scale imaging of the anterior and posterior parts of the eye. However, since 3D-OCT sequentially records A-Scans over multiple seconds, motion of the eye caused for example by heartbeat or by saccadic motion leads to distortions and discontinuities in the acquired volume data. We present a software based motion correction method using multiple 3D-OCT raster scan volumes with orthogonal fast scan axis. A global objective function is optimized in a multi resolution scheme to estimate and subsequently correct for object motion in three dimensions and on a per A-Scan basis. Imaging experiments were performed on various OCT systems both for retinal as well as anterior segment imaging. Results indicate that the method achieves very good results in correcting motion. Motion artifacts caused by transverse and axial motion can be corrected. For anterior segment imaging the potential issue of moving parts in the iris is avoided by excluding the iris from the data used to estimate motion. Also, quantitative assessment of nerve fiber layer thickness reproducibility around the optic nerve head indicates improved reproducibility through our motion correction method. In conjunction with high speed OCT systems and subsequent quantitative measurement extraction these methods promise to improve image quality in OCT and allow for more accurate measurements of ocular structure which could enable earlier diagnosis of both anterior and posterior ocular pathology.

8213-78, Session 12

## Holoscopy image reconstruction

D. Hillmann, Thorlabs GmbH (Germany) and Medizinisches Laserzentrum Lübeck GmbH (Germany); G. L. Franke, Univ. zu Lübeck (Germany); C. Lührs, T. Claußen, P. Koch, Thorlabs GmbH (Germany); G. Hüttmann, Univ. zu Lübeck (Germany) and Medizinisches Laserzentrum Lübeck GmbH (Germany)

Holoscopy provides the means to acquire three-dimensional tomograms with nearly depth-invariant sensitivity and resolution by combining holographic techniques with Fourier-domain optical coherence tomography (FD-OCT). Digital holograms are acquired for a number of different wavelengths and numerically reconstructed to a common layer inside the sample. Subsequent FD-OCT signal processing can then be applied to obtain depth discrimination. The sample will be imaged sharply in the chosen focus layer but resolution will degrade rapidly a few Rayleigh lengths away. Due to the holographic nature of the technique, the numerical reconstruction can be repeated for various foci until the complete sample is imaged with sufficient resolution. However, when going to higher lateral resolutions the Rayleigh length decreases rapidly and thus this reconstruction procedure needs to be repeated more often. We demonstrate a new numerical approach for an effective, parallel reconstruction of all sample layers which decreases the computational time by several orders of magnitude for high lateral resolution holoscopy.

8213-79, Session 12

## Morphological image analysis for classification of gastrointestinal tissues using optical coherence tomography

P. B. García-Allende, Helmholtz Zentrum München GmbH (Germany) and Imperial College London (United Kingdom); I. Amygdalos, H. Dhanapala, R. D. Goldin, G. B. Hanna, D. S. Elson, Imperial College London (United Kingdom)

Optical coherence tomography (OCT) is an optical technique based on low-coherence interferometry that provides noninvasive, subsurface, high-resolution imaging of biological microstructure, whose main application has traditionally been ophthalmology. However, new OCT applications are emerging and they aim at “optical biopsy” in areas such as cardiology, skin imaging and gastroenterology, where it could decrease sampling error and increase yield, and ultimately even eliminate the need for tissue sampling. This would solve the limitation of current clinical management for patients with gastrointestinal diseases for example in terms of the reduced tissue fraction sampled during standard endoscopic examinations.

Computer-aided diagnosis of ophthalmic diseases using OCT relies on the extraction of thickness and size measures from the OCT images, but such defined layers are usually not observed in nonopthalmic OCT imaging, and cellular resolution is difficult to achieve, especially in an endoscope format. In this regard, texture analysis of OCT images has shown promising results but it requires the determination of appropiate regions of interest to compute the textural features. We propose a two-step methodology to overcome this problem. OCT images are first segmented in the axial direction in an automated manner according to intensity. Aftewards, a morphological analysis of the segmented OCT images is employed for quantifying the features that serve for tissue classification. Reliable discrimination of freshly-excised specimens of gastrointestinal tissues is reported showing that the approach surpasses the previous textural algorithms and, therefore, it is feasible for gastrointestinal tissue classification in the clinical setting.

8213-80, Session 12

## Hybrid FPGA and GPU acceleration of optical frequency domain angiography computation

W. C. Y. Lo, Harvard Medical School (United States) and Wellman Ctr. for Photomedicine (United States) and Massachusetts General Hospital (United States); H. Tang, Tianjin Univ. (China) and Wellman Ctr. for Photomedicine (United States) and Massachusetts General Hospital (United States); E. Z. Zhang, Wellman Ctr. for Photomedicine (United States); B. E. Bouma, Harvard Medical School (United States) and Wellman Ctr. for Photomedicine (United States) and Massachusetts General Hospital (United States); B. J. Vakoc, Wellman Ctr. for Photomedicine (United States)

Optical frequency domain imaging (OFDI) has shown promise in numerous clinical and preclinical applications. At current acquisition rates, the OFDI system can only process ~10-20% of the acquired data in real-time on latest-generation CPUs, necessitating high-throughput storage devices and lengthy post-processing. This is particularly burdensome in angiographic imaging which acquires larger datasets and requires more extensive processing. Although the current OFDI angiographic (OFDA) imaging system utilizes a highly optimized, multi-threaded library for signal and image processing (Intel IPP library), less than 10% of the raw data is processed in real-time.

To solve this problem, we developed a hybrid approach to accelerate OFDA image reconstruction and processing. Our new platform combines field programmable gate arrays (FPGAs) and graphics processing units (GPUs) for real-time image reconstruction. Highly customized hardware was created on the FPGA for basic signal processing common to both our OFDI and OFDA systems, while the GPU was reserved for advanced, application-specific image reconstruction algorithms. To process the interferogram data continuously at a high speed on the FPGA, a fast demodulation method and a pipelined, streaming I/O FFT algorithm were incorporated into the design. To reduce the development time and maximize the flexibility of the GPU code, the NVIDIA Performance Primitives (NPP) library was used. In this presentation, we will describe the design of this computational platform and quantify its performance relative to CPU-based solutions. Currently, our hybrid platform supports real-time interferogram processing at a clock rate of 220 MHz and angiogram reconstruction at a processing rate of ~182 fps.

8213-81, Session 12

## Joint spectral and time domain processing applied to optical coherence elastography

B. F. Kennedy, K. M. Kennedy, The Univ. of Western Australia (Australia); K. M. Karnowski, M. Szkulmowski, M. D. Wojtkowski, Nicolaus Copernicus Univ. (Poland); D. D. Sampson, The Univ. of Western Australia (Australia)

Elastography is an imaging technique in which contrast is based on variations in the mechanical properties of tissues. It was initially applied to Ultrasound and magnetic resonance imaging (MRI). Its application to optical coherence tomography (OCT) is known as optical coherence elastography (OCE). OCE allows detection of the mechanical properties of tissue with at least an order of magnitude higher spatial resolution than can be obtained using other imaging modalities. We present a new optical coherence elastography (OCE) processing technique. In this technique, spectral and time domain OCE (STd-OCE), two Fourier transforms are performed. The first, in the frequency domain, allows depth information to be obtained. The second, in the time domain allows the Doppler spectrum to be measured. For a vibrating sample, the Doppler spectrum consists of discrete spectral lines separated by the oscillatory frequency and weighted by Bessel functions. We measure sample vibration amplitude by analyzing the spread of the Doppler spectrum. We compare STd-OCE to phase-sensitive OCE and demonstrate that STd-OCE is superior in measuring the vibration amplitude. We also present results from a bilayer phantom.

8213-82, Session 12

## Graphics processing unit-based ultra-high-speed real-time multidimensional Fourier domain optical coherence tomography

K. Zhang, J. U. Kang, The Johns Hopkins Univ. (United States)

Compared to the conventional image-guided interventions (IGI) using modalities such as MRI, X-ray CT and US, optical coherence tomography (OCT) has much higher spatial resolution and therefore possesses a great potential for applications in a wide range of microsurgeries. For a clinical interventional imaging system, high-speed image acquisition, reconstruction and visualization are all essential. While the acquisition speed of Fourier domain optical coherence tomography (FD-OCT) has satisfied the real-time multi-dimensional imaging requirement, current FD-OCT systems generally suffers from shortcomings in the last two stages.

This work describes a series of novel graphics processing unit (GPU) based image reconstruction and visualization methods we developed for realizing ultrahigh speed, real-time FD-OCT: Several GPU based algorithms including high-speed linear/cubic interpolation, gridding-based non-uniform fast Fourier transform (NUFFT), numerical dispersion compensation, and multi-GPU implementation were developed to improve the point spread function, SNR roll-off, and stability of the system. Full-range complex-conjugate-free FD-OCT was also implemented on the GPU architecture to double the imaging range and to improve SNR. The maximum processing speed of >3.0 Giga-Voxel/second (>6.0 Mega-A-scan/second of 1024 FD-OCT) was achieved using the latest GPU module from NVIDIA. The GPU-based volume rendering enabled real-time 4D (3D+time) FD-OCT imaging, and a 5 volume/second 4D FD-OCT system was demonstrated via in vivo tissue imaging.

These GPU technologies were highly effective in circumventing the well-known imaging reconstruction and visualization bottlenecks exist among current ultra-high speed FD-OCT systems and could open the door to realize interventional OCT imaging for applications in guiding microsurgery.

8213-83, Session 12

## Digital refocusing in optical coherence tomography

A. A. Moiseev, G. V. Gelikonov, P. A. Shilyagin, D. A. Terpelov, V. M. Gelikonov, Institute of Applied Physics (Russian Federation)

The problem of restoration Optical Coherence Tomography (OCT) images, acquired with tightly focused probing beam, in out-of-focus region for improving lateral resolution of the OCT has been discussed. In this work we show similarity between data acquisition in OCT and Digital Holography (DH). The algorithm of digital refocusing has been proposed. After the refocusing at several depths, focus fusion have been performed to obtain micrometer scale resolution in the whole investigated volume. Proposed methods have been applied to the simulated as well as to experimental OCT data, acquired with tightly focused scanning beam to restore micrometer lateral resolution in the whole investigated volume.

8213-84, Session 12

## Graphics processing unit based dispersion encoded full-range frequency domain OCT

L. Wang, Cardiff Univ. (United Kingdom) and Katholieke Univ. of Leuven (Belgium); B. Povazay, Medizinische Univ. Wien (Austria); J. A. Guggenheim, Cardiff Univ. (United Kingdom); W. Drexler, B. Hofer, Medizinische Univ. Wien (Austria)

The technique of dispersion encoded full range (DEFR) frequency-domain optical coherence tomography (FD-OCT) and its enhanced version, fast DEFR, use the dispersion mismatch between sample and reference arm to double the imaging depth range by iteratively suppressing complex conjugate artifacts. Previously, the computational complexity of DEFR prevented its application in fields where real-time visualization or large volumetric datasets are needed. A graphics processing unit (GPU) with hundreds of processing cores provides highly parallel computation capability to FD-OCT in which processing for each A-line is identical and independent. In this paper, we adopted GPUs to accelerate DEFR, thereby significantly improving reconstruction speed by a factor of ~100 with respect to CPU based processing. A maximum display line rate of ~21 k-lines/s for 2048 points/A-line using 10 iterations of the fast DEFR algorithm has been successively achieved, sufficient for real-time visualization in situ.

# Conference 8214: Advanced Biomedical and Clinical Diagnostic Systems X

Sunday-Tuesday 22-24 January 2012

Part of Proceedings of SPIE Vol. 8214 Advanced Biomedical and Clinical Diagnostic Systems X

8214-01, Session 1

## A compact fluorescence and white light imaging system for intraoperative visualization of nerves

D. C. Gray, E. Kim, V. Cotero, P. Staudinger, S. Yazdanfar, C. Tan Hehir, GE Global Research (United States)

Fluorescence image guided surgery (FIGS) allows intraoperative visualization of critical structures, with applications spanning neurology, cardiology and oncology. An unmet clinical need is prevention of iatrogenic nerve damage, a major cause of post-surgical morbidity. Currently most procedures are performed without any form of image guidance, as available technologies lack the ability to provide nerve-specific imaging. Here we describe the advancement of FIGS imaging hardware, coupled with a custom nerve-labeling fluorophore, to bring FIGS nerve imaging closer to clinical translation.

A compact imaging system was developed to simultaneously display white light and fluorescence images for open and minimally invasive surgical procedures. The <2-kg instrument is comprised of a 405nm laser and a white light LED source for excitation and illumination, respectively, and consumer-grade cameras. The fluorescence excitation and emission characteristics were customized for an optimized derivative of our fluorophore. The imaging hardware and contrast agent were evaluated in mice during in vivo surgical procedures, through simultaneous display of reflectance and fluorescence video.

Intravenous injection of the fluorophore highlighted both central and peripheral nerves suggesting that the agent was capable of crossing the blood nerve barrier and blood brain barrier. The new contrast agent showed improved uptake by nerves, minimal binding to muscle, and high contrast in vivo.

The new fluorophore coupled with the compact imaging system

demonstrates a complete image-guided surgery solution that can assist in the detection of nerves during open and minimally invasive procedures.

This study is funded by NIH grant 5R01EB011872-02.

8214-02, Session 1

## Tracking ophthalmic drugs in the eye using confocal fluorescence microscopy

K. K. Buttenschoen, J. M. Girkin, Durham Univ. (United Kingdom); D. Daly, Lein Applied Diagnostics Ltd. (United Kingdom)

We report on the development of a non-invasive instrument based on scanning confocal microscopy for tracking inherently fluorescent drugs and measuring spatial features in the anterior chamber of the eye. The new instrument incorporates all features of the initial instrument [1] with the addition of fluorescence detection from within the anterior chamber of the eye. We have measured the diffusion of Fluorescein with high time resolution within a cuvette, an artificial eye and perfused bovine eyes. Results will be presented that demonstrate the capability of the instrument to accurately measure the concentration and the location of the fluorescent drug over a given period of time along the optical axis of the eye with an axial resolution of 60 µm and temporal resolution of 1 ms. We show that the instrument has high sensitivity and can measure concentrations of < 1µM/l of compounds having a quantum yield as low as 0.01 with high specificity for the compound of interest over competing background signals. The role of the instrument in assessing the efficiency of any inherently fluorescent ophthalmic drug as well as monitoring other medication that might produce fluorescent compounds in the eye will be discussed. We furthermore believe that the instrument might also be capable of monitoring certain bodily processes which have an impact on the compounds present in the eye.

[1] Buttenschön K.K., Girkin J.M., Daly D. Development of a low-cost confocal instrument to measure the axial dimensions of components in the anterior section of the eye. Clinical Optometry. 2010; 2010(2):67-72

8214-03, Session 1

## Novel compact endoscope design for simultaneous wide-field multispectral fluorescence lifetime imaging (FLIM)

S. Cheng, J. M. Jabbour, K. Maitland, J. A. Jo, Texas A&M Univ. (United States)

Fluorescence Lifetime Imaging (FLIM) offers a noninvasive approach for characterizing the biochemical composition of biological tissue. In recent years, there has been an increasing interest in the application of multispectral FLIM for clinical diagnosis. A few flexible endoscope designs have been proposed to facilitate wide-field FLIM imaging of internal tissue. These designs, however, usually use two separate optical channels for illumination and imaging, resulting in large diameter endoscope probes. Moreover, multispectral imaging is performed sequentially by interchanging optical filters in the emission path, resulting in long acquisition time. A novel compact endoscope design for simultaneous multispectral wide-field FLIM imaging is presented here. Wide-field FLIM was implemented using a time-gated approach with a high-speed ICCD. The endoscope consisted of a single imaging bundle (1.1mm diameter, 10,000 fibers) suitable for transmitting both in the UV (excitation) and VIS (fluorescence emission). Simultaneous multispectral imaging was accomplished in two steps. First, the fluorescence emission was separated into different spectral components through a series of dichroic mirrors and filters. Then, each spectral image was focused onto distinct regions of the ICCD through a set of mirrors and a large aperture lens. The current system has three customizable spectral channels, resolution of ~25 um, field of view of ~2 mm in diameter, and working distance of ~5 mm. Acquisition times as short as 1 s can be achieved. The system was validated in-vitro, by imaging endogenous fluorophores (NADH, FAD and collagen), and in-vivo by imaging hamster cheek pouch epithelial tissue.

8214-05, Session 2

## Plasmonic coupling interference: a new approach for cancer diagnostics using SERS detection

H. Wang, T. Vo-Dinh, Duke Univ. (United States)

No abstract available

8214-06, Session 2

## Estimation of diffuse reflectance spectrum from RGB values by the synthesis of new colors for tissue measurements

Q. Liu, S. Chen, Nanyang Technological Univ. (Singapore)

There has been an increasing interest in the development of robust techniques for the estimation of diffuse reflectance spectra from RGB values, which have been explored in a variety of applications such as the archiving of fine art paintings and skin cancer diagostics. Wiener estimation has been widely used for this purpose because of its fast operation. However, it has been reported that a simple set of RGB values is not sufficient to accurately recover the diffuse reflectance spectrum because of the underdetermined nature of the problem that seeks the mapping from three data points to a few hundred data points.

A new method is presented for the accurate estimation of diffuse reflectance spectra from RGB values based on Wiener estimation. In this method, the original RGB values are combined with a set of synthetic optical filters to generate another three values corresponding to new colors by using the system matrix. A new Wiener matrix can then be created with the original RGB values and the new color values, which will yield more accurate estimation of diffuse reflectance spectra because of the new color information incorporated from the system matrix. This method is tested on both tissue phantoms and human skin. The results show that the proposed method could improve the accuracy in estimated diffuse reflectance spectra significantly, especially when the Wiener estimation with the original RGB values does not work well.

8214-07, Session 2

## Design, validation, and implementation of a diffuse reflectance spectroscopic imaging system for tissue absorption and scattering

J. Y. Lo, S. Dhar, M. Brooke, B. Yu, Duke Univ. (United States); T. F. Kuech, Univ. of Wisconsin-Madison (United States); N. M. Jokerst, N. Ramanujam, Duke Univ. (United States)

Diffuse reflectance spectroscopy has been previously explored as a promising method for providing real-time visual maps of tissue composition to help surgeons determine breast lumpectomy margins and to ensure the complete removal of a tumor during surgery. We present the simple design, validation, and implementation of a compact and cost effective spectroscopic imaging system for the application of breast tumor margin assessment, but also with the potential for use in applications for other organ sites in which quantitative tissue spectral imaging would be useful. Our new system consists of a broadband light source with bandpass filters for illumination and a fabricated custom 16-pixel photodiode imaging array with a low-noise, integrating transimpedance amplifier for the detection of diffuse reflectance. To select the bandpass filters in the system, we have used a genetic algorithm for wavelength optimization. We validate the use of this wavelength selection method for breast tissue, and we provide a platform for which the method can be used to design systems for other tissue sites with different absorbers. The overall system prototype has an estimated signal to noise ratio of greater than 35 dB and is characterized and validated in tissue-mimicking phantoms. Clinical implementation of the system will be shown on breast tissue specimens. We show proof-of-concept for performing fast, wide-field spectroscopic imaging with a simple, inexpensive design. The strategy also allows for the scaling to higher pixel number and density in future iterations of the system.

8214-08, Session 2

## Diffuse reflectance imaging system for spatial mapping of tissue optical properties

S. F. Bish, Y. Wang, X. Zhang, J. W. Tunnell, The Univ. of Texas at Austin (United States)

Diffuse reflectance spectroscopy provides a noninvasive means to determine tissue optical properties and has been used as a diagnostic tool for early cancer detection in several organ sites including the skin, cervix, and oral cavity. Until recently, these measurements were made on a single point of tissue. To expand on these point measurements, we have developed a diffuse reflectance spectroscopy imaging (DRSI) system capable of acquiring wide field optical property maps of tissue. This system uses a white light source and a 16 channel photomultiplier tube to simultaneously acquire 16 wavelength bands per image, with a resolution of approximately half the source-detector separation, currently adjustable from 150μm-500μm. These DRSI images were post processed with Least Squared Support Vector Machine (LS-SVM) regression in order to obtain optical property maps of reduced scattering and hemoglobin concentration. Samples used to train the machine came from an empirically derived look-up-table inverse model for optical property estimation. Currently, we can achieve total imaging times of less than 5 seconds depending on image size and the number of averaged frames. To demonstrate the capability of our system, we imaged ex vivo healthy and bruised porcine epithelium in the band of 480-635nm. The optical property maps for healthy tissue showed no contrast due to hemoglobin presence, while the maps for scarred tissue showed scattering and absorption contrast in regions of bruised tissue. Here, we have presented the initial prototype of our diffuse reflectance imaging system, demonstrating the potential for imaging tissues in vivo.

8214-09, Session 2

## Discrimination of selected species of pathogenic bacteria using near-infrared Raman spectroscopy and principal components analysis

L. Silveira, Jr., Univ. Camilo Castelo Branco (Brazil); H. E. Giana, Lab. Oswaldo Cruz (Brazil); F. S. de Siqueira Oliveira, Univ. Estadual Paulista (Brazil)

In microbiological routine analysis, the identification of bacteria species are based on the observations on the morphology and biochemical reactions which present limitations, such as the time to perform the biochemical tests and often need of combination of several methods for proper identification. An approach based on near-infrared Raman spectroscopy techniques has been proposed for identification of different microorganisms involved in bacterial urinary tract infections. Spectra were collected directly from different bacterial colonies (Gram negative: E. coli, K. pneumoniae, P. mirabilis, P. aeruginosa, E. cloacae and Gram positive: S. aureus and Enterococcus sp.) grown in standard culture medium (agar) using a dispersive Raman spectrometer with fiber probe (Lambda Solutions, Inc., 830 nm excitation, 300 mW power). After fluorescence background removal and normalization, spectra were submitted to Principal Component Analysis and Mahalanobis distance (PCA/MD) algorithm for group discrimination. It has been found that the mean Raman spectra of different bacterial species exhibit similar bands, being the S. aureus well characterized by strong bands related to carotenoids. PCA/MD could discriminate Gram positive bacteria with high sensitivity and specificity using PC2 and PC3. PCA/MD could discriminate the Gram negative bacteria with good sensitivity and specificity using PC4 and PC5. These results indicated the possibility of using Raman spectroscopy associated to discrimination by PCA and Mahalanobis distance algorithm for grouping bacteria species according to spectral similarities.

8214-10, Session 2

## Effect of hormonal variation on in vivo high-wavenumber Raman spectra improves cervical precancer detection

S. Duraipandian, Z. Huang, W. Zheng, National Univ. of Singapore (Singapore); J. Ng, J. J. H. Low, I. A, National Univ. Hospital (Singapore) and National Univ. of Singapore (Singapore)

Raman spectroscopy is a unique analytical probe for molecular vibration and is capable of providing specific spectroscopic fingerprints of molecular compositions and structures of the biological tissues. The aim of this study is to improve the classification accuracy of cervical precancer by characterizing the variations in the normal high wavenumber (HW - 2800-3700cm-1) Raman spectra arising from the menopausal status of the cervix. A rapid-acquisition NIR Raman spectroscopic system was used for in vivo tissue Raman measurements at 785 nm excitation. Individual HW spectrum was measured with a 5s exposure time from both normal and precancer tissue sites of 15 patients recruited. The acquired Raman spectra were stratified based on the menopausal status of the cervix before the data analysis. Significant differences were noticed in Raman intensities of prominent band at 2924 cm-1 (CH3 stretching of proteins) and the broad Water Raman band (in the 3100-3700 cm-1 range) with a peak at 3390 cm-1 in normal and dysplasia cervical tissue sites. Multivariate diagnostic decision algorithm based on principal component analysis and linear discriminant analysis (PCA-LDA) was utilized to successfully differentiate the normal and precancer cervical tissue sites. By considering the variations in the Raman spectra of normal cervix due to the menopausal status, a diagnostic accuracy of 91% can be achieved. By incorporating this information before the statistical analysis, we can significantly improve the diagnostic accuracy of cervical precancer using Raman spectroscopy.

8214-44, Poster Session

## The cervical cancer detection system based on an endoscopic rotary probe

Y. Yang, H. Zhao, Z. Qin, F. Gao, Tianjin Univ. (China)

To get the optical diffuse tomographic image of the cervix, a novel endoscopic rotary probe is designed and the frequency domain measurement system is developed.

In the optical diffuse tomographic imaging of the cervix, an endoscopic probe is needed and the detection of light at different separation to the irradiation spot is necessary. To simplify the system, only two optical fibers are adopted for light irradiation and collection, respectively. Two small stepper motors are employed to control the rotation of the incident fiber and the detection fiber, respectively. For a position of source fiber, the position of the detection fiber is changed from -90O to 90O to the source fiber. Then, the position of the source fiber is changed to another preconcerted position, and the detection fiber is rotated from -90O to 90O relative to the source fiber. To get the efficient irradiation and collection of the light, a gradient-index (GRIN) lens is connected at the head of the optical fiber. The other end of the GRIN lens is cut to 45O. With this design, light from optical fiber is reflected to the cervix wall that is perpendicular to the optical fiber or vice versa. Concerning the cervical size, the external diameter of the endoscopic probe is made to 20mm.

A frequency domain (FD) near-infrared diffuse system is developed aiming at the detection of early cervical cancer, which modulates the light intensity in radio frequency and measures the amplitude attenuation and phase delay of the diffused light using heterodyne detection.

Phantom experiment results demonstrate that the endoscopic rotary scan probe and the system perform well in the endoscopic measurement.

8214-45, Poster Session

## Fluorescence yield and lifetime tomography from time-resolved transmittances of a breast tumor phantom

Y. Lu, W. Zhang, L. Wu, F. Gao, H. Zhao, Tianjin Univ. (China)

In optical tumor detection region, there has been recently a considerable interest in simultaneously reconstructing yield and lifetime distributions of fluorescent imaging agents inside a pathologic tissue, since combined monitoring of these two parameters provides a potential means of in vivo interrogating quantitative and environmental information of specific molecules, as well as accessing interactions among them. This paper describes the structure of a multi-channel time-correlated single photon counting (TCSPC) system for early breast tumor detection and how we use it to reconstruct the distribution of fluorescent parameters. By using a normalized Born appropriation algorithm, the proposed examination scheme in a transmission mode is experimentally validated to achieve simultaneous reconstruction of the fluorescent yield and lifetime distributions with reasonable accuracy. The performance of the instrument will be proved by using two targets be of different fluorescent agents embedded in solid phantom for image reconstruction.

8214-46, Poster Session

## Prokaryotic expression and polyclonal antibody preparation of autophagy-related gene ATG5 in arabidopsis

W. L. Chen, J. Zhou, South China Normal Univ. (China)

Objective: Arabidopsis autophagy-related gene Atg5 was cloned in Escherichia coli DH5αand expressed in Escherichia coli BL21, followed by development of its polyclonal antibody.

Methods: RT-PCR was performed to amplify gene Atg5 from Arabidopsis, then the gene was subcloned into prokaryotic expression vector pET32a and transformed to E.coli BL21. After induced expression, the transformed Escherichia coli BL21 was collected to perform SDS-PAGE and Western blot ,in order to identify the specific expression and bioactivity of protein Atg5 respectively. The identified and purified protein was used to immunize rabbits, whose serum was then separated for anti-Atg5 polyclonal antibody extraction. Then the antibody was identified by Western blot.

Results: Atg5 gene was successfully cloned from Arabidopsis. And the expressed Atg5 protein, obtained from transformed BL21, has supposed molecular mass and bioactivity. Bioactive purified Anti-Atg5 polyclonal antibody was obtained from rabbit serum.

Conclusion: Anti-Atg5 polyclonal antibody was successfully prepared and can be used for autophagy analysis in the following experiments.

8214-47, Poster Session

## A multichannel time-resolved system for fluorescence diffusion optical tomography

W. Zhang, F. Gao, L. Wu, Y. Lu, W. Ma, H. Zhao, Tianjin Univ. (China)

A prototype time-domain 32 channels dual-modality system based on the time-correlated single-photon counting (TCSPC) technique has been constructed for the research of diffuse fluorescence-optical breast tomography methodology, aiming at enhancing the reliability of breast diffuse optical tomography (DOT). The system employs two pulsed light sources, 32 source fibers and 32 detection channels, working separately for acquisition of the temporal distribution of light emerging from the tissue surface. The light sources are provided by high power pico-second diode lasers, and an optical switch directs light sources to the object through one of 32 source fibers. The light signals from the object are collected by a time-resolved system. Every 8 detection fibers switch to a single channel which consists of a collimator, a filter wheel, and a TCSPC module. Finally, the performance and efficiency of this system are examined by the image reconstructions of optical parameters, as well as fluorescent yield and lifetime in turbid media, such as a solid phantom.

8214-48, Poster Session

## Axial accuracy correction for FDK algorithm in digital tomosynthesis imaging

H. Miao, H. Zhao, F. Gao, Tianjin Univ. (China)

Abstract Among the early period of the medical imaging diagnosis, digital tomosynthesis imaging (DTS) has been thoroughly investigated for clinical applications and it holds a significant clinical role in medical diagnosis field. As a novel medical imaging technique, digital tomosynthesis imaging can provide us with the confidence to distinguish the overlapping lesion tissue and make the exact lesion-localizing. In digital tomosynthesis imaging, FDK (Feldkamp-Davis-Kress) reconstruction algorithm is widely employed to reconstruct a series of the coronal images, for it spends less reconstruction time and provides higher reconstruction quality. However, digital tomosynthesis imaging cannot meet the accurate reconstruction condition. And the inherent characteristics of FDK reconstruction algorithm definitely results in the accuracy attenuation along the rotation axis in the digital tomosynthesis images. This accuracy attenuation can be described as a hatlike function. In this paper, a reciprocal-cosine function weighted correction method was introduced to compensate this axial accuracy attenuation in digital tomosynthesis images. To evaluate the correction effect to the accuracy attenuation, a digital tomosymthesis imaging system was designed and built up. Then an anthropomorphic breast phantom was reconstructed using and without using the weighted correction method. Upon the comparison between the corrected images and the non-corrected images, the results demonstrate that the correction method can effectively correct the axial accuracy attenuation in digital tomosynthesis reconstructed images.

8214-49, Poster Session

## Toward surface analysis on diabetic feet soles to predict ulcerations using photometric stereo

C. Liu, F. van der Heijden, Univ. Twente (Netherlands); J. van Netten, Hospital Group Twente (Netherlands)

Diabetic foot ulceration is a major complication for patients with diabetes mellitus. Approximately 15% to 25% of patients with Type I and Type II diabetes eventually develop feet ulcers. If not adequately treated, these ulcers may lead to foot infection, and ultimately to total (or partial) lower extremity amputation, which means a great loss in health-related quality of life. The incidence of foot ulcers may be prevented by early identification and subsequent treatment of pre-signs of ulceration, such as callus formation, redness, fissures, and blisters. Therefore, frequent examination of the feet is necessary, preferably on a daily basis. However, self-examination is difficult or impossible due to consequences of the diabetes. Moreover, frequent examination by health care professionals is costly and not feasible. The objective of our project is to develop an intelligent telemedicine monitoring system that can be deployed at the patients' home environment for frequent examination of patients feet, to timely detect pre-signs of ulceration. The current paper reports the preliminary results of an implementation of a photometric stereo imaging system to detect 3D geometric abnormalities of the skin surfaces of foot soles. Using a flexible experimental setup, the system parameters such as number and positions of the illuminators have been selected so as to optimize the performance with respect to reconstructed surface. The system has been applied to a dummy foot sole. Finally, the curvature on the resulting 3D topography of the foot sole is implemented to show the feasibility of detecting the pre-signs of ulceration using photometric stereo imaging. The obtained results indicate clinical potential of this technology for detecting the pre-signs of ulceration on diabetic feet soles.

8214-50, Poster Session

## A novel technique for x-ray source size determination based on wavelet transformation

Z. Zhou, F. Gao, H. Zhao, L. Zhang, Tianjin Univ. (China)

For in-line phase contrast imaging, the effect of source size swamps the fine phase contrast fringes, often making them almost undetectable. A few works have been conducted to enhance the quality of phase-contrast images by partial deconvolution of the finite source effects. The results for mitigating source size effect and improving phase-contrast visibility depended greatly on the accuracy of source size determination. One novel approach to retrieve the source size based on correctly acquisition of the measured phase contrast image and the propagated ideal image. If the Fourier transform of the measured phase contrast image was divided by the Fourier transform of the propagated ideal image, the Fourier transform of an estimation of source distribution function was obtained. However, this method depended on the assumption on low noise level of acquired images, which would be difficult to implement in practical system. In this study, source size determination was implemented based on appropriate wavelet band of the measured phase contrast image and the propagated ideal image. The results showed that our method obtained better source size estimate by accepting an increase in the overall image noise.

8214-51, Poster Session

## Fiber-based full-field optical coherence tomography

H. J. Ma, S. S. Lee, Chosun Univ. (Korea, Republic of); B. I. Lee, S. Hann, Korea Photonics Technology Institute (Korea, Republic of); E. Choi, Chosun Univ. (Korea, Republic of)

We present fiber-based full-field optical coherence tomography(FF-OCT) using optical fiber coupler and reflection-type optical delay line. Optical beam split from SLD source through the optical fiber coupler is collimated by a pair of fiber-pigtailed collimator and fed into bulk-optic probing head to illuminate the light beam over a sample. The probing head including the pair of collimators and bulk-optic beam splitter acts as interferometer although conventional reference mirror is not used. Optical path difference is also adjusted with the reflection-type optical delay line before launching the probing head. Mechanically actuated parts for depth scanning and phase stepping were separately implemented before the bulk-optic interferometer. Since all control parts in this interferometer is placed separately with the probing head, function of probing head is only collection of reflected optical signal and bypassing the reference beam. This configuration can prevent vibration-sensitive performance degradation of optical signal that is a critical disadvantage of FF-OCT. Another advantage of the configuration is enabled to make compact probe. This probing head can also include a dispersion compensator such as plate or prism pair. By using fiber-based FF-OCT setup, we demonstrate imaging performance for biological sample with demonstrating imaging results of colon tissues. From obtained images, the healthy, intermediated and cancerous state can be distinguished clearly. The proposed configuration can provide high potential of FF-OCT in practical diagnostic application.

This research was supported by Basic Science Research Program through the National Research Foundation of Korea(NRF) funded by the Ministry of Education, Science and Technology (No. 2010-0024886).

8214-52, Poster Session

## Low-cost/high-accuracy transcutaneous bilirubin meter for neonatal jaundice using laser diodes or LEDs

M. Hamza, Mansoura Univ. (Egypt); M. H. Sayed El-Ahl, Military Medical Academy (Egypt); A. M. Hamza, National Research Ctr. (Egypt); A. M. Hamza, Y. M. Hamza, Tabarak Children's Hospital (Egypt)

Globally , neonatal jaundice is a major cause of newborn death and disability.The burden of brain injury due to jaundice remains a well recognized threat in many countries in the world.To prevent kernicterus in newborn infants , it is important to detect jaundice in its early stages. The accuracy and precision of the results obtained from conventional bilirubin meters have undesirable variability. The authors present the theory , design and operating principles of a new transcutaneous bilirubin meter using laser diodes or LEDs with incorporation of four wavelengths to make no allowance for melanin or skin maturity. The choices of wavelengths follow the principles of optical bilirubinometry. Our new low-cost / high-accuracy transcutaneous bilirubin meter can help to avoid the potential errors associated with the clinical estimation of bilirubin levels.

8214-53, Poster Session

## Bacterial biofilm disruption using laser-generated shockwaves

A. Navarro, Jr., Z. D. Taylor, Univ. of California, Los Angeles (United States); A. Z. Matolek, VA Greater Los Angeles Healthcare System (United States); A. Weltman, V. Ramaprasad, S. Huang, Univ. of California, Los Angeles (United States); D. O. Beenhouwer, D. A. Haake, UCLA School of Medicine (United States); V. Gupta, W. S. Grundfest, Univ. of California, Los Angeles (United States)

Bacterial biofilms inhibit antibiotic therapy and prolong infections in surgical and traumatic wounds. These infections are a burden on the healthcare industry where surgical site infections occur in 2 out of 100 surgical procedures. The goal of this study is to explore the use of laser-generated shockwaves to delaminate the biofilm and destroy bacteria utilizing in vitro models.

Methods: A system was built to test the efficacy of laser generated shockwaves on bacterial viability of two species of S. epidermidis: 1) FDA strain PCI 1200 (ATCC 12228) and 2) RP62A (ATCC 35984) undergoing laser generated shockwaves. The system uses a Q-switched, ND:YAG pulsed laser operating with a 2-6 ns pulse duration at a wavelength of 1.064 μm that ablates aluminum-coated fused glass over a 3 mm spot size. Bacterial strains were grown on acrylic slides as a model for implant materials. The shockwave from the glass slide was coupled to the bacteria on the acrylic surface using a thin layer of growth medium. After irradiation a quantifiable fluorescence live/dead assay was used to assess bacterial viability.

Results: Increasing energy fluences from 14.1 J/cm2 to 135.8 J/cm2, resulted in bacterial reduction from 20% to 70% over controls with one pulse of irradiation.

Conclusion: This method could be adapted for the treatment of bacterial-infected wounds or materials where biofilms play a significant role.

8214-11, Session 3

## Field-portable reflection and transmission microscopy based on lensless digital holography

M. Lee, O. Yaglidere, A. Ozcan, Univ. of California, Los Angeles (United States)

We report a field-portable lensless dual-mode holographic microscope that can image specimens in both transmission and reflection geometries using in-line transmission and off-axis reflection holography, respectively. This cost-effective dual-mode holographic microscope weighs ~200grams with dimensions of 15cm x 5.5cm x 5cm. Based on digital in-line holography, the transmission microscope on this platform achieves a sub-pixel lateral resolution of $\leq$ 2 um over a wide field-of-view (FOV) ~24 mm2. Although it provides several advantages such as simplicity, cost-effectiveness, and ease of operation, in-line transmission geometry in general is not suitable to image dense or spatially connected objects such as tissue slides since the reference in-line wave gets distorted causing aberrations in reconstruction of such objects. To overcome this challenge, on the same cost-effective and field-portable assembly we also built a lensless reflection mode microscope based on digital off-axis holography. As a result of the reduced space-bandwidth product of the off-axis geometry compared to its in-line counterpart, the imaging FOV of our reflection mode is reduced to ~9 mm2, while still achieving a similar sub-pixel resolution of $\leq$ 2 um. We evaluated the performance of this compact dual-mode lensless microscope by imaging a US-air force resolution test target, various micro-particles and a histopathology slide corresponding to human skin tissue. Since it provides a compact, cost-effective, and light-weight microscopy interface, this dual-mode lensless holographic microscope might find use in resource limited settings and field applications involving e.g., global health challenges.

8214-12, Session 3

## Cellular pattern recognition discriminates normal skin from melanoma in non-invasive confocal imaging

A. Swerdlin, E. Simpson, S. Jacques, D. S. Gareau, Oregon Health & Science Univ. (United States)

The screening of melanocytic lesions (moles) for the presence of melanoma is a critical diagnostic that is expensive and invasive. Reflectance mode confocal imaging solves these problems while maintaining cellular resolution but interpretation of the data remains somewhat inconsistent among human reviewers. The reproducible human terminology thus far for biological features in confocal images is insufficient to fully exploit the diagnostic value, so we propose automatic pattern recognition image processing for morphometry of normal and pathological skin. Normal traits that are of diagnostic value and are observable in the superficial window of confocal penetration include the presence of a regularly organized spinous keratinocyte matrix on an underlying smooth basal keritinocyte layer. Computational identification of the dark nuclei in spinous keratinocytes (chromatin filaments: little scattering versus cytoplasm: high scattering) and bright structure of pigmented basal keratinocytes (melanin provides contrast) yields two distinct regions: basal and super-basal. These two independent computational algorithms yield complementary regions in the majority of data sets but overlap or leave gaps in roughly 20% of clinical cases. Ongoing work aims to improve discrimination or narrow the gap, respectively. Improved accurate discrimination of microanatomical regions will yield a better diagnostic map to evaluate morphology for cancer detection as well as cosmetic evaluation.

8214-14, Session 3

## Comparing combined Raman spectroscopy: in vivo confocal microscopy related to age and location in human skin

M. A. Mackanos, C. Patil, Vanderbilt Univ. (United States); C. L. Arrasmith, Montana State Univ. (United States); C. Paras, Vanderbilt Univ. (United States); D. L. Dickensheets, Montana State Univ. (United States); A. Mahadevan-Jansen, Vanderbilt Univ. (United States)

Skin cancer is the most common cancer in the United States, with a rising rate of incidence; however, it can be curable if detected early. The best clinical practices require physicians to screen large areas of skin, identify suspicious lesions, perform biopsies, and wait for the pathology for diagnosis. However, identification of lesions can be subjective, biopsy is invasive, and pathological analysis is time consuming and costly. The potential of novel optical techniques such as Raman spectroscopy and in vivo confocal microscopy to perform rapid, non-invasive “optical biopsy” has been widely touted; however, these methods suffer limitations. The biochemical sensitivity of Raman spectroscopy facilitates classification of lesions with high accuracy; however it is unable to relate lesion microstructure. Confocal microscopy can image tissue microstructure but lacks molecular specificity. The two methods can be combined in a single instrument to provide for in vivo analysis without the need for a biopsy. We will demonstrate using a Raman spectroscopy - in vivo confocal microscope system to perform image guided acquisition of Raman spectra and biochemical identification of features in confocal images related to both patient age as well as the body location. We report the performance of a clinical system for performing Raman spectroscopy - in vivo confocal microscopy of the skin, and the results of an ongoing pilot study demonstrating the systems feasibility for diagnosing lesions. Images and spectra acquired from non-cancerous lesions at varying locations from a patient profile with a large age range using the clinical instrument will be presented.

8214-04, Session 4

## Determining limitations of protoporphyrin IX for resolving depth of tumors during fluorescence-guided neurosurgery

K. Kolste, P. A. Valdes, K. D. Paulsen, Thayer School of Engineering at Dartmouth (United States); D. W. Roberts, Dartmouth Hitchcock Medical Ctr. (United States); F. Leblond, Thayer School of Engineering at Dartmouth (United States)

Intra-operative fluorescence imaging for brain tumor resection currently utilizes a blue light ($\lambda \approx 405$nm) source to excite the Soret band of the molecule protoporphyrin ix (PpIX) following systemic administration of the precursor aminolevulenic-acid (ALA). In order to image fluorescence several millimeters beneath the brain surface, use of a red light source ($\lambda \approx 635$nm) is considered to exploit the dramatic decrease of hemoglobin absorption in the red and near-infrared part of the spectrum.

The development of a neurosurgical microscope is presented where an adapter has been designed allowing multi-spectral charged-coupled device (CCD)-based fluorescence detection with interference filters to be achieved during brain surgery using a free optical port on a commercial microscope. Studies were completed on a depth-resolved tissue phantom containing locations to insert PpIX at depths ranging from 0-20 mm, in increments of 1 mm. The PpIX concentrations tested range from 0.1-10.0 µg/mL dissolved in dimethyl sulfoxide (DMSO) as this is a typical range found in gliomas during clinical trials of fluorescence-guided surgery. This study will be used to determine the limitations of this system as it relates to the concentration sensitivity as a function of depth. This information will be used to increase surgeon’s confidence that tumor resection is complete when the pre-operative magnetic resonance image (MRI) and blue light fluorescence indicate complete resection.

8214-15, Session 4

## Haematic pH sensor for extracorporeal circulation

L. Ferrari, P. Fabbri, L. L. Rovati, F. Pilati, Univ. degli Studi di Modena e Reggio Emilia (Italy)

The present work deals with the study and the realization of an optical sensor for measuring haematic pH during extracorporeal circulation. It consists of a chemical sensing element in contact with the blood, an interrogation optical head to externally probe the sensing element and the front-end electronics to collect and process the information of interest.

The fluorescein methacrylate, whose fluorescence intensity depends on the pH of the solution in contact with it, is used as indicator. Different polymeric matrices were tested since the sensor needs to satisfy important requirements: high robustness towards blood flow, high sensitivity, long lifetime and fast response time.

The design of the optical head and front-end electronics has taken into account: (i) the need of the fluorescein to be excited by a proper radiation, i.e. wavelength, (ii) the low intensity of the green light emitted by the sensing element and (iii) the low signal to noise ratio of the signals of interest. The optical head has been realized fixing in the same plastic block a blue interrogation LED and two photodiodes, one used to monitor the power of the LED and one to collect the fluorescence of the chemical sensing element. The lock-in technique has been exploited to recover the information of interest.

The developed system was firstly tested on water, then on in-vitro cow blood and finally on an in-vivo animal model. It has shown a linear behavior in the haematic range of interest with a mean error lower than 0.01 degree of pH.

8214-16, Session 4

## In vivo dynamic breast tumor oxygenation imaging for assessing response to neoadjuvant chemotherapies

S. Jiang, B. W. Pogue, M. Jermyn, K. E. Michaelsen, Dartmouth College (United States); T. E. Frazee, P. A. Kaufman, W. A. Wells, R. M. diFlorio-Alexander, Dartmouth Hitchcock Medical Ctr. (United States); K. D. Paulsen, Dartmouth College (United States)

Increases in the arterial blood partial pressure of oxygen (PO2) and carbon dioxide (PCO2) cause vasoconstriction and vasodilation in tumors, respectively. Thus a study was completed imaging tumors while manipulating both arterial blood PCO2 and PO2, as a test to see if this would allow a direct assessment of the tumor aggressiveness and resistance to antineoplastic therapies. In this pilot clinical study, imaging was done during neoadjuvant chemotherapy breast cancer treatment, applying a consistent stimulation to each subject. For the inhaled stimulation, a specialized sequencer and breathing circuit were used to prospectively target and sustain end-tidal pO2 and pCO2 independently of each other. Dynamic vascular changes in the breast were imaged by a frequency domain NIR tomographic system with 30 seconds time resolution. By analyzing the resulting images from the normal subjects under different arterial blood PCO2 and PO2 manipulation sequences, the optimum sequences for obtaining the maximum tissue vascular and oxygenation changes has been fund. The results of a particular normal subject case show the maximum changes of deoxy-hemoglobin, oxygen saturation, oxy-hemoglobin, and total hemoglobin are 20%, 9%, 7% and 3%, respectively. By using the same manipulation sequence, a cancer patient under neoadjuvant chemotherapy has been imaged at the different time points during the treatment cycles and the oxygenation changes of two invasive ductal carcinoma masses in the same breast have been monitored and compared. We expect to see similar pathological and clinical responses to the chemotherapy in these tumor regions after the full course of treatment is completed.

8214-17, Session 4

## Measuring the mechanical properties of blood clots using resonant acoustic spectroscopy with optical vibrometry

G. Wu, A. Wolberg, A. L. Oldenburg, The Univ. of North Carolina at Chapel Hill (United States)

Blood clot elastic modulus (CEM) correlates with various hemostatic and thrombotic disorders and may be an important diagnostic parameter in cardiovascular diseases. We present a novel method of CEM measurement named resonant acoustic spectroscopy with optical vibrometry (RASOV). RASOV is accomplished by applying a frequency-swept magnetic field on a metallic sheet sitting on the top of a clot sample, and monitoring the resulting surface displacement with optical coherence tomography (OCT) to acquire the mechanical resonance spectrum of the clot. Nanoscale (10 nm) displacement resolution and 40 microsecond temporal resolution is afforded by phase-resolved OCT. Using RASOV, we measured the resonance frequencies of clots with varied fibrinogen and thrombin concentrations. CEM were computed from the resonance frequencies with knowledge of the boundary conditions. Results showed an approximately linear relationship between CEM and fibrinogen content within a concentration range from 0.5 to 6 mg/mL fibrinogen. A doubled CEM was observed with increased thrombin concentration from 5 to 25 nM. In addition, we theoretically show that two independent linear elastic properties (i.e., Young's modulus and Poisson's ratio) of a homogenous material can be measured by performing RASOV on the material using at least two different boundary conditions. From these two properties, any other linear elastic property (e.g., shear modulus) can then be computed. This resonance-based method has the potential for higher accuracy, speed, and smaller sample volume than current methods for CEM analysis, which may be relevant for monitoring risk of thrombosis and bleeding during and after surgery.

8214-18, Session 4

## Comparison of performance of commercial vessel imaging systems in a tissue phantom

H. J. Noordmans, N. Cuper, Univ. Medical Ctr. Utrecht (Netherlands); R. M. Verdaasdonk, Vrije Univ. Medical Ctr. (Netherlands)

Puncture of veins to draw blood is a problem in ~15 % of young children and groups of adults (obese, diabetics etc). Recently, various imaging systems have become available to enhance the visibility of the veins.

In this study, 3 commercial systems were compared in performance regarding vein contrast in relation to depth using a tissue phantom. The 'Accuvein' and 'Veinviewer' project a false color image of the vein structure on the skin reconstructed from IR light scattered and reflected from the skin surface. The 'Vasculuminator' acts like an augmented vision system showing the vein structure on a small screen positioned above the puncture site using transluminated IR light.

The systems were tested on (1) an increasing number of diffusing sheets put on a USAF test target and (2) a silicone skin phantom embedding a canal of 3 mm diameter filled with black ink going from the surface into the depth at a shallow angle. Images were captured with a digital camera and analyzed.

While the 'Accuvein' and 'Veinviewer' could not resolve any detail on the USAF target after resp. 1 and 3 diffusing sheets, the 'Vasculuminator' was still able to resolve half of the objects.

In the silicone phantom the 'Accuvein' and 'Veinviewer' showed the 3 mm 'vein' almost 2x bigger and more blurry almost independent of the depth. The 'Vasculuminator' showed the 'vein' sharp at the surface and going gradually diffuse into the depth providing a good depth perspective.

All vein viewing systems showed large structures up to 5 mm depth, while the Vasculuminator also resolved smaller structures with higher contrast.

8214-19, Session 5

## Multimodality 3D imaging for histology 3D reconstruction

Y. Yagi, M. Onozato, P. A. Bautista, M. Mino-Kenudson, Massachusetts General Hospital (United States)

Using whole slide images of the serial sections of a tissue specimen it is possible to provide a 3D visualization of the histology slides. There are now demands to interface between 3D imaging of histology slides with other imaging modalities such as CT scanning, endoscopy and TEM. The interface between these imaging modalities has the potential to bring about new discoveries in Medicine. In this work we report progress in the 3D reconstruction of histology images. In our previous work, there were issues with regards to missing spaces between serial section slices, which occurred regardless of how thin or how uniform we cut the tissue specimens. To minimize the occurrence of missing spaces, we instead collected the data for the 3D reconstruction from the fixed tissues. Then for information of the missing spaces in the 3D reconstructed histology images, we used MicroCT (Skyscan) and an Optical Frequency Domain Imaging (OFDI), which is in its prototype stage yet, to provide the relevant information. The correlations between these 3D imaging modalities have been shown using a lung cancer tissue. These correlations provided us with better understanding on the value of 3D imaging of histology slides.

8214-20, Session 5

## Multispectral image enhancement by spectral shifting

P. A. Bautista, Y. Yagi, Massachusetts General Hospital (United States)

A multispectral enhancement method that preserves that natural color of the background pixels was previously proposed. In such method, the band for enhancement was identified from the spectral residual-error of the objects of interest. The spectral residual-error is determined by taking the difference between the original spectrum of the pixel and its estimate using m<<N principal components in principal component analysis (PCA). However, for stained histopathology images where staining variations do exist even among tissue slides stained with the same chemical stain, this band for enhancement could vary. In this work, we introduced a modification to the previously proposed multispectral enhancement method such that the band for enhancement could be specified independently.In the proposed modification, the original spectral transmittance of the pixels at each band are shifted by the product between the spectral residual-error coefficient of the pixel and the weighting factor assigned by the user to each band. In this approach, the band for enhancement is independent from the spectral residual-error configuration of the multispectral pixel. In the experiment we utilized multispectral images of H&E stained liver tissue. Results of the experiments show that the proposed modification delivers consistent enhancement results regardless of the staining condition of the image.

8214-21, Session 5

## Multidepth imaging by chromatic dispersion confocal microscopy

C. Olsovsky, R. L. Shelton, M. Saldua, O. Carrasco-Zevallos, B. Applegate, K. Maitland, Texas A&M Univ. (United States)

Confocal microscopy has shown potential as an imaging technique to detect early signs of cancer. Imaging cellular features throughout the depth of epithelial tissue can provide useful information for diagnosis. However, the current in vivo axial scanning techniques for confocal microscopy are cumbersome, time-consuming, and restrictive when attempting to reconstruct volumetric images acquired in breathing patients. Chromatic Dispersion Confocal Microscopy (CDCM) exploits severe longitudinal chromatic aberration in the system to axially disperse light from a supercontinuum source and, ultimately, spectrally encode high resolution images along the depth of the object. Hyperchromat lenses are designed to have severe and linear longitudinal chromatic aberration, but have not yet been used in confocal microscopy. We use a hyperchromat lens in a stage scanning confocal microscope to demonstrate the capability to simultaneously capture information at multiple depths without mechanical scanning. A PCF fiber pumped with a 830nm wavelength Ti:Sapphire laser was used as a broadband source, and a spectrometer was used as the detector. The chromatic aberration and magnification in the system give a focal shift of 125μm after the objective lens and an axial resolution of 5.2-7.6μm over the wavelength range from 600nm to 775nm. A 400x400x100μm^3 volume of pig cheek epithelium was imaged in a single X-Y scan. Nuclei can be seen at several depths within the epithelium. The capability of this technique to achieve simultaneous high resolution confocal imaging at multiple depths may reduce imaging time and motion artifacts and enable volumetric reconstruction of in vivo confocal images of the epithelium.

8214-22, Session 5

## Stroboscopic illumination scheme for seamless 3D endoscopy

N. T. Clancy, D. Stoyanov, G. Yang, D. S. Elson, Imperial College London (United Kingdom)

Intraoperative 3D imaging during minimally invasive surgery (MIS) is possible using structured lighting and has applications in the quantification of tissue morphology. However, projection schemes containing various patterns and colours can be disruptive to the surgeon's field of view.

In this paper, a stroboscopic system is proposed in which structured lighting and white light images are interleaved in a high-speed camera acquisition so that the patterned light is not perceived and has a limited effect on white light viewing. A beam chopper synchronised with the camera provides a means of switching rapidly between the two lighting modes while operating above the flicker frequency of human vision (35-42 Hz).

Structured lighting is provided by an optical fibre-based probe developed in our lab and suitable for use in endoscopic biopsy channels. This probe uses spectral encoding to provide a unique pattern of projected features that can be read with a standard colour camera for robust triangulation of 3D information.

The ratio of structured lighting frames to white light was varied by altering the rotation speed and the blade width. It was possible to use varying exposure times between frames, allowing simultaneous display of normal and structured light images as well as recording high dynamic range images of the coloured pattern. A number of clinicians were asked to navigate using the system within a MIS abdominal trainer in order to evaluate which was the most seamless operating mode.

Possible applications of this work include classification of polyp morphology as an indicator of pathology.

8214-23, Session 5

## Recent advances in optical chemo/biosensing for biomedical applications at IFAC-CNR

F. Baldini, A. Giannetti, F. Senesi, C. Trono, Istituto di Fisica Applicata Nello Carrara (Italy)

Optical sensors for medical diagnostics can be classified in three main classes: i) invasive sensors, with the sensor entering the human body using suitable catheters/tubing; ii) minimally invasive sensors, which limit their contact with the human body, for example to the tissue, and iii) not invasive sensors, which has no contact with the human body and the measurement is performed on biological samples drawn from the patient. In this area, at IFAC is active since many years. The recent activity was focused on i) the design and development of a novel miniaturized pH sensor tip for continuous monitoring in gastroesophageal apparatus; ii) the use of microdialysis approach to measue metabolites and in particular pH in the adipose tissue and iii) the development of a multianalyte bioassay for the detection of sepsis biomarkers (C-reactive protein, procalcitonin and neopterin) by means of a fluorescence-based bioanalytes. Last results achieved in these areas will be presented.

8214-24, Session 6

## Optical sensor system for continuous non-invasive monitoring of total hemoglobin concentration in real time in patients in the clinical environment

E. Lewis, Univ. of Limerick (Ireland); U. Timm, Univ. of Rostock (Germany) and Univ. of Limerick (Ireland); G. Leen, Univ. of Limerick (Ireland); J. Kraitl, H. Ewald, Univ. of Rostock (Germany); D. McGrath, Univ. of Limerick (Ireland); G. Shorten, A. Broderick, Cork Univ. Hospital (Ireland)

A non-invasive optical sensor system for the in vivo measurement of total haemoglobin based on a study of patients undergoing cardiac surgery is reported. The authors have developed a novel developed optical sensor system uses three wavelengths of light for the measurement of Total Haemoglobin (Hb) concentration, Oxygenated Haemoglobin (SpO2) and pulse. This non-invasive multi-spectral measurement method is based on radiation of near monochromatic light, emitted by Light Emitting Diodes (LED) in the range of 600nm to 1400nm, through an area of skin on the finger or on the ear. The optical sensor utilises 3 LEDs and a single wavelength sensitive photodetector which are mounted in a compact clip worn on the finger or ear of the patient. The photoplethysmographic signals are processed in a microcontroller unit connected to the finger clip and worn on the arm of the patient. The resultant signals are transmitted wirelessly to a clinical base station where they are displayed, recorded and stored for further clinical analysis. The novel development offers a robust method for real time measurement of total haemoglobin in actual patients in the clinical environment. Results are presented from a series of clinical tests undertaken with patients undergoing cardiac surgery involving cardiopulmonary bypass at Cork University Hospital (CUH), Ireland and are compared to simultaneously measured 'gold standard' in-vitro methods of haemoglobin concentration.

8214-25, Session 6

## New technique for easy registration of visual (multispectral) and thermal images to evaluate tissue perfusion

R. M. Verdaasdonk, B. Kunnen, L. Vink, A. van der Veen, Vrije Univ. Medical Ctr. (Netherlands); H. J. Noordmans, J. Klaessens, Univ. Medical Ctr. Utrecht (Netherlands)

Tissue health can potentially be determined from the degree of perfusion. Low of high local perfusion might be a sign of e.g. flow obstruction, infections, wound or tumour. Multi-spectral imaging techniques, looking at specific wavelengths in the visible and near IR range, can provide information on tissue structure and colour. Thermal imaging shows the heat dissipation at the tissue surface as an indicator of tissue perfusion or inflammation. Combining visual and thermal images can contribute to more qualitative and quantitative information. However, due to a lack in contrast in thermal images, the registration on visual images is difficult. Therefore, synthetic netting was placed on the tissue surface to superpose a grid that could be visualized with both imaging modalities and made image registration less complicated.

This new combined imaging method was applied in a clinical setting on patients suffering from open wounds on their legs to obtain better understanding of the local perfusion conditions. Provoked events by temporary blocking the blood flow to the extremities provided dynamic information. Sterilized disposable netting was placed over the wound without discomfort for the patient. The thermo camera and visual camera (with small band LED illumination) were placed close to each other to obtain images simultaneously with minimum parallax. The images could be registered automatically with dedicated software. Learning how to interpret the patient images, it would be possible to discriminate between blood flow and inflammations and quantify tissue perfusion. Visual (multi-spectral) and thermal images can easily be combined introducing an artificial contrast by a netting to obtain a better understanding of local tissue perfusion.

8214-26, Session 6

## Non-invasive surface and tomographic imaging of breast cancer using a hand-held optical device

S. J. Erickson, M. Roman, J. Gonzalez, Florida International Univ. (United States); R. Kiszonas, Univ. of Miami, Sylvester Comprehensive Cancer Ctr. (United States); C. Lopez-Penalver, Advanced Medical Specialities (United States); A. Godavarty, Florida International Univ. (United States)

Breast cancer affects 1 in 8 women in the U.S. and early diagnosis is essential to reduce the mortality rate of the disease. Hand-held optical imaging devices are currently developed by several research groups as a noninvasive and non-ionizing method towards clinical imaging of breast cancer. The devices developed to date are typically utilized towards spectroscopic imaging via reflectance-based measurements. Additionally, a couple of devices have been used to perform 3D tomography with the addition of a second modality (e.g. ultrasound). In our Optical Imaging Laboratory, we have developed a hand-held optical device that is unique in its ability to perform rapid 2D imaging and 3D tomography (without the use of a second modality). Herein, diffuse optical imaging studies are performed in breast cancer subjects. All studies are IRB approved and written informed consent was obtained from all subjects. For these studies, the subject lay in a recliner chair and both breast tissues were imaged with the hand-held optical device which uses 785 nm laser source and an intensified CCD camera-based detector. Preliminary results demonstrate the ability to image invasive ductal carcinoma and lymphatic spread, as compared to the patient's medical records (e.g. x-ray, ultrasound, MRI). Multiple imaging studies with a subject undergoing chemotherapy demonstrated the potential to monitor response to treatment. Currently, studies are carried out to tomographically determine the 3D location of the tumor(s) in breast cancer subjects using the hand-held optical device.

8214-27, Session 6

## Development and evaluation of a light-emitting diode endoscopic light source

N. T. Clancy, R. Li, Imperial College London (United Kingdom); K. Rogers, Univ. of Glamorgan (United Kingdom) and Cymtec Ltd. (United Kingdom); P. Driscoll, Cymtec Ltd. (United Kingdom); P. Excell, Glyndwr Univ. (United Kingdom); R. Yandle, Cymtec Ltd. (United Kingdom); G. B. Hanna, Imperial College London (United Kingdom); N. Copner, Univ. of Glamorgan (United Kingdom) and Cymtec Ltd. (United Kingdom); D. S. Elson, Imperial College London (United Kingdom)

Light-emitting diode (LED) based endoscopic illumination devices have been shown to have several benefits over arc-lamp systems. LEDs are energy-efficient, small, durable, and inexpensive, however their use in endoscopy has been limited by the difficulty in efficiently coupling enough light into the endoscopic light cable. We have demonstrated a highly homogenised lightpipe LED light source that combines the light from four Luminus LEDs emitting in the red, green, blue and violet using innovative dichroics that maximise light throughput. The advantage of the light source is related to the method of spectrally combining light from highly divergent incoherent sources that have a Lambertian intensity profile to provide illumination matched to the acceptance numerical aperture of a liquid light guide or fibre bundle.

The LED light source was coupled to a standard laparoscope and performance parameters (power, luminance, colour temperature) were compared with a xenon lamp. Although the total illuminance from the endoscope was lower than a Xenon lamp, we found that the variation in colour rendering that could be achieved via adjusting the relative intensities of the LEDs created changes in the contrast image of biological tissues. The inclusion of a violet (wavelength < 420 nm) wavelength LED enabled fluorescence images to be acquired with application in photodynamic diagnosis using protoporphyrins IX, a diagnostic indicator in bladder cancer detection. The LED light engine has also been evaluated in a minimally invasive surgery box trainer and during surgery and is a new key technology for robust and flexible illumination.

8214-28, Session 6

## An in-vitro cell system for studying molecular mechanisms of action associated with low intensity focused ultrasound

M. Babakhanian, Univ. of California, Los Angeles (United States) and Ctr. for Advanced Surgical and Interventional Technology (United States); R. Fan, Univ. of California, Los Angeles (United States) and Ctr. for Advanced Surgical and Interventional Technology (CASIT) (United States); A. P. Mulgaonkar, R. S. Singh, Univ. of California, Los Angeles (United States) and Ctr. for Advanced Surgical and Interventional Technology (United States); M. O. Culjat, Univ. of California, Los Angeles (United States) and Ctr. for Advanced Surgical and Interventional Technology (United States) and Univ. of California, Los Agneles (United States); S. Danesh, L. Toro, Univ. of California, Los Angeles (United States); W. S. Grundfest, Univ. of California, Los Angeles (United States) and Ctr. for Advanced Surgical and Interventional Technology (United States); W. P. Melega, Univ. of California, Los Angeles (United States)

Focused ultrasound has long been proposed as a noninvasive means to reversibly modulate the function of the central nervous system. Recent studies using low intensity focused ultrasound (LIFU) in the brains of rodents have demonstrated that ultrasound can safely and reversibly target structures in the brain to modulate cortical activity and to reduce the severity of epileptic seizures. However, both underlying molecular mechanisms that drive this LIFU-induced neuromodulation and ultrasound parameters leading to neuromodulatory effects are not well defined. Accordingly, we have developed an in-vitro ultrasound assay system to efficiently conduct multiple parameter sweeps and determine their effects on different types of cells grown in culture. An array of 12 piezoelectric transducer elements was incorporated into a fixture that matches the layout of a well plate. Water coupling was maintained between the fixture and the well plate, such that acoustic energy is transmitted through the flat bottom of each well with minimal cross-talk into neighboring wells. The transducer array was wire-bonded to a PCB board, with a switch allowing for individual element control via a function generator. Sonication of the cells in the well plate is performed upon selecting appropriate ultrasound parameters (pulse duration, frequency, intensity, and total energy delivered), and the well plate is then inserted into a plate reader to observe the effect of the ultrasound stimulation for a given assay. Identification of molecular mechanisms underlying LIFU efficacy and ultrasound parameters using this high throughput approach is expected to lead to new avenues of clinical applications for the treatment of neurological and psychiatric illnesses.

8214-29, Session 6

## Optical measurements of microvascular circulatory function in the foot for detection of peripheral neuropathy

G. Zamora, E. S. Barriga, VisionQuest Biomedical, LLC (United States); S. Luan, V. Checkh, P. H. Heintz, M. R. Burge, The Univ. of New Mexico (United States); P. Soliz, VisionQuest Biomedical, LLC (United States)

The purpose of this research is to quantify functional signals in the microvascular circulation of the plantar in response to cold stimulus provocation. The objective is to detect dysfunction associated with preclinical signs of peripheral neuropathy. Our device is based on thermal and spectral technologies that can be easily adopted for both a clinical environment and a telescreening setting. This device will make an important contribution toward meeting the needs of an underserved population, diabetics.

Eighty-two thousand amputations are performed annually on diabetics in the US. Studies have shown that 5% of diabetic patients will develop a foot ulcer in a given year. Fifteen percent of diabetics will undergo amputation sometime in their lives. Foot pathology accounts for 25% of all hospital stays among diabetics, and the cost of foot disorder diagnosis and management are estimated at $10.9 billion dollars annually. Current methods to assess peripheral neuropathy are subjective, prone to inter- and intra-operator variability, and not appropriate for preclinical or early detection.

Our experiments on normal controls and diabetics assess the temperature recovery time characteristics due to cold provocation to the foot (plantar). Under a controlled environment, the plantar was cooled to 15 degrees C below the body temperature and thermal and spectral images were continuously acquired for 300 s after removal of the cold provocation. Statistically significant differences between normal controls and diabetics were found for rate of recovery and initial temperature.

8214-30, Session 6

## An all fiberized portable cytometer for cellular and molecular biology analysis in space and other remote environments

O. Mermut, C. Riviere, S. Leclair, INO (Canada); M. Fortin, Handyem (Canada); G. Dubeau-Laramee, D. Provencal, L. Y. Cohen, Canadian Space Agency (Canada)

In remote environments such as space, infrastructure like the International Space Station (ISS) offers the possibility of maintaining microorganisms, cells, and tissues. However, the ISS does not possess the instrumentation and facilities required to perform modern analytical molecular biology tests. One of the most versatile analytical instruments in molecular biology is a flow cytometer. Conventional cytometers are in many aspects limited from operating in such remote and difficult environments. They are not robust enough to withstand vibration and shocks during launch, and are payload and footprint limited. Furthermore flow cytometers would be restricted for use in ISS due to their need for manipulation by highly qualified personal.

We present here a new fiber optic based compact and portable flow cytometer technology (Microflow-1) being developed towards in situ medical diagnostics in future manned space flights. At the core of this fully fiberized technology is a specially designed and engineered square optical fiber. A square hole is transversally bored through this fiber by laser micromachining. A capillary is fitted into that hole to flow analyte within the square fiber cross-section for detection and counting. Since the interrogation of fluorescence and scattering is done entirely through a fiber optic flow cell, there is an advantage of autoalignment (in fabrication) eliminating the need for on-site optical alignment as with conventional bulk optics. The technology is uniquely and inherently compatible with remote environments such as space, due to its fiber optic sheathless configuration and hence minimized need for on-site opto-fluidics management and manipulation.

8214-31, Session 6

## Clinical study for spectral diagnosis of in vivo melanoma and non-melanoma skin cancer diagnosis

L. Lim, B. Nichols, The Univ. of Texas at Austin (United States); N. Rajaram, Duke Univ. (United States); J. S. Reichenberg, The Univ. of Texas Medical Branch (United States); M. R. Migden, The Univ. of Texas M.D. Anderson Cancer Ctr. (United States); J. W. Tunnell, The Univ. of Texas at Austin (United States)

Diffuse optical spectroscopy (DOS), laser induced fluorescence spectroscopy (LIFS) and Raman spectroscopy (RS) can provide noninvasive interrogation of tissue morphology and function. The goal of this study was to determine the diagnostic capability of a multi-modal Spectral Diagnosis (SD) for in vivo non-invasive disease diagnosis of melanoma and non-melanoma skin cancer.

We acquired in vivo spectra from 137 lesions in 76 patients. Corresponding biopsies were acquired from each site and classified using standard histopathology as malignant melanoma (MM), pigmented lesion (PL), basal cell carcinoma (BCC), actinic keratosis (AK), and squamous cell carcinoma (SCC). Spectra were analyzed using principal component analysis. Using 3 diagnostically relevant principal components (PC), we built leave-one-out logistic regression classifiers for melanoma and non-melanoma. The 3 PCs were chosen using forward stepwise regression analysis and verified by surveying every combination of the top PCs from all modalities. Classification results were compared to histopathology of the lesion.

Sensitivity and specificity for classifying MM vs. PL (12 lesions vs. 17 lesions) was 1/0.94, Normal vs. BCC (22 lesions vs. 22 lesions) was 0.95/0.95, and AK vs. SCC (14 lesions vs. 24 lesions) was 1/0.57. In all cases, a combination of PCs from multiple modalities provided the best diagnostic performance. Raman PCs accounted for several wavenumber regions (e.g. amide 1 and amide 3) and peaks (e.g. CH2). DOS PCs accounted for reflectance intensity and absorption differences between pathologies. This study demonstrated that SD has potential to aid in both melanoma and non-melanoma skin cancer diagnosis.

8214-32, Session 7

## Toward a real-time core-needle biopsy assessment with full-field OCT

A. Burcheri, Ecole Supérieure de Physique et de Chimie Industrielles (France); V. Servois, B. Sigal-Zafrani, Institut Curie (France); A. C. Boccara, Ecole Supérieure de Physique et de Chimie Industrielles (France) and LLTech SAS (France)

Radiologists perform core needle biopsies under the guidance of low-resolution imaging techniques such as ultrasound or CT scans.

To assess whether relevant material is biopsied, an accurate and fast ex-vivo technique would be a first step before in-vivo optical biopsies. A technique offering a morphological assessment similar to histopathology could therefore provide an aid for targeting highly suspicious tissues during the procedure.

En-face visualization of high resolution OCT data provides the advantage of safely acquiring a large unitary field of view of 1mm2 with micron-scale resolution without any staining or particular tissue preparation.

A compact full-field OCT system using a Light-CTTM scanner has been tested under routine clinical conditions at Institut Curie, Paris.

The compact instrument provides a lateral resolution of ~1µm, which is equivalent to medium power microscopy and with an axial sectioning of 1µm in comparison to confocal microscopy.

At this resolution, the image acquisition and display took less than 5 minutes and less than 15 minutes for the overall process on a large surface of 10x10 mm2.

16 specimens from 13 patients have been examined from different organs. Imaging results include kidney, lung and breast tissues.

Characteristic features of malignancy have been identified, such as stroma shape, contrast and cell size. We present the imaging technique along with digital pathology features specific to micron-scale Full-Field OCT imaging.

8214-33, Session 7

## In-vitro observation of induced cartilage-degeneration progression by Fourier-domain OCT

U. Marx, R. Schmitt, Fraunhofer-Institut für Produktionstechnologie (Germany); B. Rath, S. Nebelung, M. Tingart, C. Lüring, Universitätsklinikum Aachen (Germany)

Optical Coherence Tomography (OCT) as emerging clinical diagnostic imaging technology for dermatology and other semitransparent tissues has shown high potential in monitoring and evaluating the inner structure of articular cartilages. Since novel therapies for the limitation of cartilage degeneration in early stages of osteoarthritis are available, the early minimal invasive diagnosis of cartilage degradation is clinically essential for further treatment options. With the advancing performance and thus diagnostic opportunities of 3D-OCT devices, we carried out a systematic study by monitoring arthrotic alterations of porcine osteochondral explants that are mechanically induced under continual pressure or traumatic impaction. As for in-vitro tomographic imaging we utilized two OCT devices, a Thorlabs Telesto Fourier Domain FD-OCT device with 92KHz A-scan rate and 1325nm as central wavelength and a self-developed FD-OCT device at 840nm central wavelength. This allows the comparison in image contrast and optical penetration of cartilage tissue between these two spectral bandwidths. For further analysis, the OCT tomograms are characterized qualitatively regarding the inner tissue structure and quantitatively regarding the tissue absorption parameters. Therefore, we are developing image processing algorithms for the automated inline monitoring of cartilage tissue. A scoring system for 3D-monitoring allows the characterization of the probe volume regarding the morphological structure and tissue compactness by processing the C - scan data. In a second step, the probes are histologically, biochemically and molecularbiologically analysed regarding their specific arthrosis parameters and correlated with the OCT - data and scoring.

8214-34, Session 7

## Office-based multifunctional anterior eye segment optical coherence tomography

Y. Lim, M. Yamanari, Y. Hong, S. Makita, Univ. of Tsukuba (Japan); M. Miura, Tokyo Medical Univ. (Japan); Y. Yasuno, Univ. of Tsukuba (Japan)

Functionally extended optical coherence tomography (OCT) technologies, such as Doppler OCT and polarization sensitive OCT (PS-OCT) have been extensively utilized in posterior eye imaging to assess blood flow and to discriminate ocular tissues based on their birefringence properties. However, only limited number of studies of these technologies was demonstrated on anterior eye. The purpose of the paper is to demonstrate the potential applications of a multi functional OCT, i.e., Doppler polarization-sensitive OCT (DPS-OCT), for anterior eye segment.

The DPS-OCT is an extension of our custom made office based PS-OCT, which has been successfully utilized to volumetrically visualize birefringent tissues in a large number of clinical cases, such as pterygium, bleb in trabeculectomy, and keratoconus. The DPS-OCT employed in this study possesses an axial resolution of 9.2 μm in tissue, and perform a volumetric scan of the eye within 10 s.

A healthy in vivo human eye was measured by the DPS-OCT. A single scan provides three-dimensional polarization insensitive intensity, bi-directional flow, Doppler power, and phase retardation images simultaneously. Volumetric structure of cornea, iris, conjunctiva and sclera were observed in the intensity image. Three-dimensional vasculature and blood flow were visualized by power Doppler and bi-directional flow tomographies. Birefringence characteristics of sclera and trabecular meshwork were recognized in the phase retardation images. The results showed that the DPS-OCT may have potential to identify blood vessels and discriminate fibrous tissues in abnormalities, such as scarring and inflammation. A large scale study will be conducted to show the potential applications of the DPS-OCT.

8214-35, Session 7

## Dual-wavelength photothermal (DWP) OCT for in vivo depth-resolved measurement of oxygen saturation (SaO2) in murine brain arterioles

R. V. Kuranov, The Univ. of Texas Health Science Ctr. at San Antonio (United States); A. B. McElroy, S. M. S. Kazmi, The Univ. of Texas at Austin (United States); J. W. Kiel, The Univ. of Texas Health Science Ctr. at San Antonio (United States); A. K. Dunn, The Univ. of Texas at Austin (United States); T. Q. Duong, The Univ. of Texas Health Science Ctr. at San Antonio (United States); T. E. Milner, The Univ. of Texas at Austin (United States)

Microvasculature hemoglobin oxygen saturation (SaO2) is important in progression of various pathologies. Non-invasive depth-resolved measurement of SaO2 levels in tissue microvasculature may provide early biomarkers and a better understanding of the pathophysiological processes allowing improved diagnostics and prediction of disease progression. We develop and validate Dual-Wavelength Photothermal Optical Coherence Tomography (DWP-OCT) to measure hemoglobin oxygenation saturation (SaO2) in vivo in a murine brain. Arterioles with diameters between 25-35 μm were investigated in six mice. The microvessels were excited with intensity modulated light at 770 nm and 800 nm simultaneously and the induced nanometer range optical pathlength variations due to hemoglobin absorption were recorded with Phase-Sensitive OCT. Ratio of optical pathlength amplitudes induced by 770 nm and 800 nm laser excitation was used to calculate SaO2 levels. Absorption of oxygenated and de-oxygenated hemoglobin at 800 nm is nearly equal while at 770 nm absorption coefficient of deoxygenated hemoglobin is approximately two times greater than of oxygenated hemoglobin. The 770 nm and 800 nm wavelength light was intensity modulated at 400 Hz and 380 Hz, respectively, to independently measure pathlength modulation amplitude in the microvessels at each excitation wavelength. Different SaO2 levels in the murine brain arterioles were achieved by varying oxygen flow in the N/O2 breathing mixture of the animal. DWP-OCT SaO2 was linearly correlated with pulse oximeter systemic SaO2 measurements, with an averaged difference below 6%. Development and validation of the ability of DWP-OCT to measure non-invasively SaO2 levels in the murine brain microvasculature is demonstrated.

8214-36, Session 8

## Live OCT display on an intraoperative surgical microscope featuring augmented reality

K. Kim, C. Lee, H. Jung, U. Jung, N. Jo, J. Kim, Kyungpook National Univ. (Korea, Republic of); H. Kim, Kyungpook National Univ. Hospital (Korea, Republic of)

Conventional ophthalmic surgical microscope is usually utilized to observe enlarged images of the eye during a surgical operation. However, it has a limitation to distinguish the axial layers in retinal tissue because of the contrast differences in retinal layers. To compensate this problem, an operator usually use the surgical implements such as an intraocular mirror, however, this method requires the incision of the tissues. In this study, we developed an intraoperative Optical Coherence Tomography probe which was mounted in an ophthalmic surgical microscope. By using an augmented reality feature and GPU programming, we could display OCT's cross-sectional images simultaneously with microscope images through the ocular lens in real-time display at over 100 frames/sec (1024 pixels x 500 pixels). Owing to the development, surgeons can continuously monitor the operation and live OCT images of the operation site without change of viewing. Also the augmented feature can support the surgeon decision by displaying surgical guide lines on the microscope's ocular lens. The augmented OCT displaying is switchable with the surgeon's intention. The experimental result contains application of the system in an animal surgical environment. From the performance, we can expect that the developed surgical OCT probe can provide a noble application as a surgical assistant tool.

8214-38, Session 8

## In vivo measurements of local hemoglobin absorption in the dermal microcirculation by low-coherence spectroscopy

N. Bosschaart, D. J. Faber, T. G. van Leeuwen, M. C. G. Aalders, Univ. van Amsterdam (Netherlands)

Spectroscopic determination of tissue optical properties can offer a fast and painless alternative to invasive clinical diagnostic procedures such as drawing of blood. For instance, the absorption coefficient of the dermal microcirculation is directly related to the hemoglobin concentration, which provides information on blood volume, hematocrit and oxygen saturation. The currently clinically applied optical spectroscopic techniques have limited ability to measure the optical properties in a confined volume such as the dermal microcirculation, since they lack exact control over the size and depth of the probed tissue volume.

Spectroscopic techniques that have potential for highly localized optical property measurements are low-coherence interferometry based techniques such as low-coherence spectroscopy (LCS), but their performance has not yet been tested in vivo. Previously, we have shown that we can use LCS to quantitatively obtain the absorption μa, scattering μs and backscattering μb coefficients between 480 - 700 nm from the attenuation coefficient μt of homogeneous turbid media. In this study, we show that we can use low-coherence spectroscopy to measure the local μt and μa in optically inhomogeneous media. By controlling both the size and location (lateral and depth position) of the measurement volume (as small as 300 x 100 μm, width x depth), we investigate the ability of LCS to retrieve the absorption coefficient of an Intralipid-dye phantom, covered by light attenuating layers that vary in thickness and scattering. Finally, we use LCS to measure the μt and μa of the epidermis and the dermal microcirculation in vivo.

8214-13, Session 9

## Tri-modal confocal margin screening for the presence of residual squamous cell carcinoma in Mohs surgical excisions

A. Bar, N. Snavely, N. Chen, S. Jacques, D. S. Gareau, Oregon Health & Science Univ. (United States)

The screening of skin cancer from the margin of excised specimens may be done with confocal microscopy to save time and cost over the gold standard histopathology. However, diagnostic accuracy requires sufficient contrast. Reflectance mode enables detection of large (>500um) nodular tumors. Enhanced nuclear contrast with acridine orange fluorescence mode additionally enables detection of tiny (<50um) basal cell carcinomas. Here, we present a novel combination of three modes to detect squamous cell carcinoma (SCC). For accurate screening of SCC, more than just the nuclear detail (that, alone, accurately detects heavily nucleated BCCs) is required. Eosin fluorescence (excited with 532nm laser light), reflectance and acridine orange fluorescence enable contrast for cytoplasm, collagen and nuclei respectively. Amalgamating these signals in a digital staining algorithm where the collagen and cytoplasm appear pink and the nuclei appear purple replicates the appearance of traditional hematoxylin and eosin staining, and therefore may be translated into the clinic rapidly.

8214-39, Session 9

## Rapid confocal imaging of large areas of excised tissue with strip mosaicing

S. Abeytunge, B. A. Larson, Y. Li, Memorial Sloan-Kettering Cancer Ctr. (United States); E. Seltzer, Livingston High School (United States); B. Parks, New York Univ. School of Medicine (United States); R. Toledo-Crow, M. Rajadhyaksha, Memorial Sloan-Kettering Cancer Ctr. (United States)

Tumor removal is guided by the examination of pathology prepared concomitantly during surgery. The total preparation time during Mohs surgery in skin is one to several hours per excision, head-and-neck surgery is several hours, and breast cancer surgery is days. Confocal mosaicing microscopy offers a way to examine large areas of tissue with nuclear-level resolution directly on fresh excisions.

We previously reported a confocal microscope that images 12x12 mm2 of tissue by constructing a mosaic in nine minutes. With our newer technique called strip-mosaicing, 10x10 mm2 is imaged in three minutes. We report further advances to reduce the time to approximately one minute.

In our confocal microscope a polygon mirror scans a line on the tissue (x-axis) and a stepper motor-driven stage translates the tissue in the orthogonal (y-axis) direction to acquire an image strip. Each strip is 457 um x 10 mm which gives a x:y aspect ratio of 1:21. Thirty-one adjacent image strips were stitched with 15% overlap on each edge to complete the x direction scan of ~10 mm. A synchronizing mechanism minimizes the mismatch between any two strips along y-axis. A newly-developed fixture flattens and holds the tissue during imaging.

Mosaics of skin excision from Mohs surgery clearly show nuclear and cellular morphology of basal cell carcinomas differentiated against normal skin, with excellent correlation to pathology. Preliminary analysis suggests that a strip mosaic of 2.5 cm x 2.5 cm may be generated in approximately six minutes for use in diverse surgical settings.

8214-40, Session 9

## Large-area reflectance confocal microscopy for intraoperative lumpectomy margin assessment

D. Kang, E. F. Brachtel, B. L. Smith, Massachusetts General Hospital (United States); J. H. Lee, KAIST (Korea, Republic of); B. E. Bouma, G. J. Tearney, Massachusetts General Hospital (United States)

Lumpectomy followed by radiation therapy is a standard surgical treatment for patients with early stage breast cancer. However, surgically-removed tissues show positive margins upon postoperative histologic analysis in as many as 50% of the lumpectomy patients. In such cases, patients are required to undergo additional surgeries, resulting in increased patient morbidity and procedure costs. Spectrally encoded confocal microscopy (SECM) is a high-speed reflectance confocal microscopy technology that can achieve 10 to 100 times faster image acquisition speed than conventional confocal microscopy systems. By utilizing the high image acquisition speed, SECM can be utilized to image entire lumpectomy specimens and provide accurate margin status during surgery. The capability of assessing margin status intraoperatively with SECM can enable surgeons to acquire tumor-free margins during the initial surgery, reducing the needs for additional surgeries. Here, we report results from a preliminary study of imaging large areas of surgically-removed breast tissues with an SECM benchtop system. Large area SECM images (4 mm by 2 mm to 5 mm by 4mm) of 27 breast tissues were shown to visualize architectural and cellular features similar to those used in histologic analysis: SECM images of normal breast tissues clearly visualized benign glands with cellular details; low-grade invasive ductal carcinoma showed small glands invading stroma in a disorganized fashion; and high-grade invasive carcinoma exhibited poorly differentiated tumor cells with little stroma. We also describe automatic image processing algorithms that can differentiate benign and malignant regions for fast margin status determination.

8214-41, Session 9

## Photoacoustic detection of induced melanoma in vitro using a mouse model

S. K. Gupta, K. K. Bhattacharyya, J. R. Newton, T. P. Quinn, J. A. Viator, Univ. of Missouri-Columbia (United States)

Metastasis is a life threatening complex physiological phenomenon that involves the movement of cancer cells from one organ to another by means of blood and lymph. An understanding about metastasis is extremely important to device diagnostic systems to detect and monitor its spread within the body. For the first time we report rapid detection of the induced circulating metastatic melanoma in mice in vitro using photoacoustic flowmetry.

A new photoacoustic flow system was developed, that employs photoacoustic excitation coupled with an ultrasound transducer capable of detecting the presence of individual, induced mouse melanoma cells (B16/F10) within the circulating system in vitro. A preliminary study was performed that could detect 5, 10, 20 and 50 cells in 5 microliter detection volume in the stationary set up. For animal studies, tumor was induced in mice by injecting mouse melanoma cells through tail vein into the C57BL/6 mice. A luciferase based in vivo bioluminescence imaging is performed to confirm the tumor load and multiple metastases in the tumor-induced mice. 1ml of blood obtained through cardiac puncture of the induced metastasized mice was treated to lyse the red blood cells (RBC) and enriched, leaving the induced melanoma in the peripheral blood mononuclear suspension (PBMC). A photoacoustic flowsystem coupled with an ultrasound transducer is used to detect the circulating metastatic melanoma cells from the enriched cell suspension.

8214-42, Session 9

## Optical color-coding for automated detection of skin cancers

A. N. Yaroslavsky, Univ. of Massachusetts Lowell (United States)

Optical techniques provide real-time information on tissue spectral response and morphological appearance. However, in most cases multimodal interrogation is required for definitive identification of pathology. At the same time, interpretation of multiple gray scale images has proven to be challenging for pathologists and surgeons, who are trained to work with thin hematoxylin and eosin (H&E) stained sections. In this contribution we report an algorithm for automated construction of a diagnostic color-coded image using multimodal optical images for facilitating optical biopsy of skin cancers. Methylene blue stained fresh thick cancerous skin specimens were utilized for the study. Multispectral reflectance, fluorescence and fluorescence polarization images were simultaneously acquired using a multimodal confocal microscope. Quantitative database of the optical images of skin components was created. For the obtained combinations of pixel value distributions, pseudo-color was assigned to each tissue type, effectively accomplishing phenomenological segmentation of the images. The resulting color-coded images correlated well with corresponding H&E histopathology. The developed algorithm based on phenomenological comparative analysis allowed for successful differentiation of the normal and cancerous skin structures. The developed technique holds the potential to simplify image analysis and enable automated detection of skin pathology.

8214-43, Session 9

## Optical biopsy on breast tissue using Light-CT: toward OCT-based diagnosis in pathology

F. Harms, LLTECH SAS (France); O. Assayag, A. Burcheri, ESPCI - Institut Langevin (France); M. Antoine, Hôpital de Paris (France); B. Sigal-Zafrani, Institut Curie (France); B. de Poly, LLTECH SAS (France); A. C. Boccara, ESPCI - Institut Langevin (France) and LLTECH SAS (France)

In contrast with most of the available OCT approaches (e.g. time domain OCT or Fourier domain OCT), Light-CT directly takes “en face” images using megapixels cameras and gel or water immersion microscope objectives of medium numerical apertures, allowing for high lateral and axial resolution (typically~1µm×1µm×1µm). After stitching a grid of acquired images, Light-CT gives access to the architecture of the tissue, for both macroscopic and microscopic structures, in a non-invasive process, which makes the technique particularly suitable for applications in pathology.

Here we present the results of a pre-clinical study on breast tissue, and its use to define new criteria for the diagnosis of breast cancer. We have imaged 120 specimens of freshly excised breast tissue coming from 24 patients, on both healthy tissue and different histological types of carcinoma. For each specimen we have taken 10x10mm Light-CT images at 4 different depths, a single 10x10mm Light-CT image is obtained in 2,5 minutes. Histology has been possible on 100% of the specimens. Microscopic features such as lobules, vessels, adipocytes, microcalcifications, fibrous stroma, were easily recognizable and correlated with histology.

Reading criteria based on Light-CT images have been identified, mainly linked to the assessment of particular cellular structures such as adipocytes and fibrous stroma. Also research directions for further image processing have been identified by clinicians. As a result, blind diagnosis conducted on the Light-CT images by 2 pathologists leaded to an evaluation of a sensitivity of 94% and a specificity of 76%.

# Conference 8215: Design and Quality for Biomedical Technologies V

Saturday-Sunday 22-23 January 2011

Part of Proceedings of SPIE Vol. 8215 Design and Quality for Biomedical Technologies V

8215-01, Session 1

## Scanning nonlinear endomicroscopy technology and potential applications

X. D. Li, The Johns Hopkins Univ. (United States)

We report the recent advances in developing a fully integrated and all-fiber-optic scanning endomicroscope of an ~2mm diameter, capable of performing real-time nonlinear optical imaging of biological tissues. The ultimate goal of this research is to miniaturize a bench-top scanning laser microscope down to a flexible scanning endomicroscope, and thus enable various in vivo applications and clinical translation of the nonlinear microscopy technology. The key building blocks of the endomicroscope consists of a customized double-clad fiber (DCF) for single-mode delivery of femtosecond excitation light to and multimode collection of the nonlinear signal from the sample, a tubular piezoelectric actuator for high-speed 2-dimentional beam scanning, and a miniature lens for focusing the excitation light and collecting the nonlinear optical signal. Special considerations were given to: (1) the design of the DCF which improved the signal-to-noise ratio of the endomicroscope by more than 100 fold; (2) a customized microlens of an ~1.5mm diameter, 0.8NA, and superb achromaticity over a broad spectrum which significantly improved the nonlinear signal collection efficiency by more than 10 fold; and (3) a high-speed fiber-optic scanner that can operate either in a spiral or Lissajous scanning pattern of which the hysteresis can be conveniently corrected. A compact depth scanner which is based on shape-memory alloy and easy to be integrated to the endomicroscope, will also be discussed. Representative two-photon fluorescence and SHG imaging results of biological tissues for cancer and preterm-birth detection and other potential applications will be presented.

8215-02, Session 1

## OCT-based freeze-drying microscopy

M. Mujat, Physical Sciences Inc. (United States); K. Greco, Univ. of Connecticut (United States); K. L. Galbally-Kinney, R. D. Ferguson, N. V. Iftimia, D. X. Hammer, P. A. Mulhall, W. J. Kessler, Physical Sciences Inc. (United States); M. J. Pikal, Univ. of Connecticut (United States)

The purpose of this research was to develop a laboratory tool that provides 3D product structural information during freeze drying and product collapse temperature Tc in a product/container format typically used during laboratory and manufacturing scale freeze drying. The development of biological drugs requires product formulations that must be lyophilized to produce stable products that are stored in vials and can be reconstituted for patient use. The most critical process design parameter is the temperature at which the product undergoes structural collapse during primary drying - Tc. Freeze drying below Tc is necessary to insure elegant appearance, low residual water content, and good storage stability and reconstitution characteristics. Accurate determination of Tc enables the design of efficient, economical drying processes that results in a high quality pharmaceutical product. We use optical coherence tomography (OCT) as a high-resolution optical imaging technique for providing structural images of frozen and drying drug formulation samples during freeze drying in an instrumented, single vial, bench top freeze dryer. OCT is the optical analog of ultrasound. Cross-sectional imaging with resolutions of 5-10 µm can be achieved. During this program we have demonstrated the application of OCT for imaging the 3D structure of product formulations freeze dried in standard product vials. This OCT-based freeze-drying microscope (OCT-FDM) provides product collapse temperature data in a container of practical significance, a vial that is used during laboratory and manufacturing scale freeze drying overcoming the limitation of current FDM systems which interrogate thin film product samples.

8215-03, Session 1

## Interferometer for measuring the dynamic surface topography of a human tear film

B. C. Primeau, J. E. Greivenkamp, The Univ. of Arizona (United States)

The anterior refracting surface of the eye is the thin tear film that forms on the surface of the cornea. Following a blink, the tear film quickly smooths and normally becomes irregular after 10 seconds. This irregularity can affect comfort and vision quality. An in vivo method of characterizing dynamic tear films has been developed using a near-infrared phase-shifting interferometer. This interferometer continuously measures light reflected from the tear film, allowing sub-micron analysis of the dynamic surface topography. Movies showing the tear film behavior can be generated along with quantitative metrics describing changes in the tear film surface. This tear film measurement allows analysis beyond capabilities of typical fluorescein visual inspection or corneal topography and provides better sensitivity and resolution than shearing interferometry methods.

The interferometer is capable of identifying features in the tear film much less than a micron in height with a spatial resolution of about ten microns over a 6 mm diameter. The collected surface topographies are analyzed with both traditional optical metrics such as RMS surface deviation and aberration coefficients along with a custom analysis routine used to identify early indications of tear film breakup.

This paper presents the interferometer design of the tear film interferometer along with the considerations that must be taken when designing an interferometer for on-eye diagnostics. Discussions include accommodating eye movement, design of null optics for a range of ocular geometries, and laser emission limits for on-eye interferometry in general.

8215-04, Session 1

## Visualization of mucosal vasculature with narrow-band imaging: a theoretical study

Q. Wang, U.S. Food and Drug Administration (United States); D. Le, U.S. Food and Drug Administration (United States) and The Catholic Univ. of America (United States); A. Agrawal, U.S. Food and Drug Administration (United States); J. C. Ramella-Roman, The Catholic Univ. of America (United States); J. Pfefer, U.S. Food and Drug Administration (United States)

Narrow band imaging (NBI) is a spectrally-selective reflectance imaging technique that is rapidly increasing in popularity as an adjunctive approach to endoscopic detection of mucosal abnormalities such as neoplastic lesions. While numerous clinical studies in tissue sites such as the esophagus, oral cavity and lung indicate the efficacy of this approach, it is not well understood from a theoretical perspective. In this study, we performed Monte Carlo simulations to elucidate the factors that affect NBI device performance. The model geometry involved a two-layer turbid medium based on mucosal tissue optical properties and embedded cylindrical, blood-filled vessels at varying diameters and depths. The effect of implementing a realistic camera detection geometry was simulated. Specifically, we studied the effect of wavelength (415, 540 nm and white light), numerical aperture and blood vessel diameter (10-200 micron) and depth (50-500 micron) on vessel contrast. Our results provide quantitative evaluation of the two mechanisms that are commonly believed to be the primary components of NBI: the increased contrast provided by hemoglobin absorption peaks and the difference in penetration depth produced by the decrease in scattering with increasing wavelength.

8215-06, Session 2

## Monitoring of biofilm formation on different material surfaces of medical devices using hyperspectral imaging method

D. Kim, U.S. Food and Drug Administration (United States); M. S. Kim, U.S. Dept. of Agriculture (United States); J. Hwang, National Institute of Standards and Technology (United States)

Contamination of the inner surface of indwelling (implanted) medical devices by microbial biofilm is a serious problem. Some microbials such as Staphylococcus aureus form biofilm that lead to potentially life-threatening infections. Other types of medical devices, for example bronchoscopes and duodenoscopes, account for the highest number of reported endoscopic infections where microbial biofilm is one of the major causes of these infections. We applied a hyperspectral imaging method to detect biofilm contamination on the surface of four most common materials used for medical devices. Such materials include stainless steel, titanium, stainless-steel-titanium alloy, and plastic. The potential uses of the hyperspectral imaging technique to investigate surface-dependent biofilm properties such as growth pattern, growth speed, and the degree of attachment will be discussed.

8215-07, Session 2

## Comparison of the measurements of an experimental endoscope tester with the Dovideq MDE endoscope test system for two hospitals

H. J. Noordmans, Univ. Medical Ctr. Utrecht (Netherlands); M. W. Nelisse, UMC Utrecht (Netherlands); M. de Braak, B. Dommerholt, DOVIDEQ medical BV (Netherlands); H. van den Brink, Univ. Medical Ctr. Utrecht (Netherlands)

Last years results were presented from an experimental endoscope test system to guarantee the optical quality of rigid endoscopes in clinical practice by measuring the illumination pathway using a white LED and photo cell and the viewing pathway using a LCD generated test pattern and high resolution camera. This year we compare the experimental test system with the prototype DOVIDEQ medical MDE endoscope test system. By determining the distortions introduced by defects in the endoscope using a test pattern, this MDE system is able to measure overall light transmission, sharpness, color constancy and image alignment. This MDE system was introduced in the sterilization department of the Sint Jansdal clinic in Harderwijk, the Netherlands, from May to June 2011.

In this comparison, it appeared that the MDE system is more user-friendly and can yield a result in 30 s as opposed to 3 minutes with the experimental system. The MDE system yields more parameters for the lense quality but does not have a fiber transmission measurement yet. The MDE system showed to be stable over two month period, with little variations due to environmental factors like room temperature and moisture. A quick lesson learned during these measurements was that the cover glasses should be dried after cleaning as otherwise debris would settle during sterilization impinging light transmission.

The use of a test bench to monitor the optical quality of endoscopes over time shows to be a valuable investment that will contribute to the quality of patient treatment. In the coming year the prototype will be extended with a fiber transmission measurement, a particle scan and a broken lens detection system.

8215-08, Session 2

## Numerical comparison of thermal damage threshold from pulsed and scanned laser in a measurement aperture

D. Kim, U.S. Food and Drug Administration (United States)

The optical radiation hazard of scanning light sources has been evaluated using pulsed light source criteria because pulse parameters which give equal energy to a scanning light source can be determined based on the energy delivered through a measurement aperture. However, a pulsed light source is temporally dynamic but spatially stationary, while a scanning light source is temporally stationary but spatially dynamic, thus their actual damage to the tissue needs further study. In this study, numerical analysis based upon a melanin granule lattice model was adapted to investigate the equivalence of scanning and pulsed light sources through a measurement aperture based on their damage threshold in pigmented retinal layer. The analysis showed that the damage threshold was not equal between two different light sources. The inequality was due to the dynamic contribution from irradiated regions to the temperature rise. For the proper evaluation of optical radiation hazard from medical optical devices with scanning light sources, a dynamic thermal process should be considered.

8215-09, Session 2

## Automated model-based calibration of imaging spectrographs

M. Kosec, Sensum d.o.o. (Slovenia); D. Tomaževic, Sensum d.o.o. (Slovenia) and Univ. of Ljubljana (Slovenia); F. Pernuš, B. Likar, Univ. of Ljubljana (Slovenia) and Sensum d.o.o. (Slovenia)

Hyper-spectral imaging has gained recognition as an important non-invasive research tool in the field of biomedicine. Among the variety of available hyper-spectral imaging systems, systems comprising an imaging spectrograph, lens, wide-band illumination source and a corresponding camera stand out for the short acquisition time and good signal to noise ratio. The individual images acquired by imaging spectrograph-based systems contain full spectral information along one spatial dimension. Due to the imperfections in the camera lens and in particular the optical components of the imaging spectrograph, the acquired images are subjected to geometric and spectral distortions, resulting in scene dependent nonlinear spectral degradations and spatial misalignments which need to be corrected. However, the existing correction methods require complex calibration setups and a tedious manual involvement, therefore, the correction of the distortions is often neglected. Such simplified approach can lead to significant errors in the analysis of the acquired hyper-spectral images. In this paper, we present a novel fully-automated method for correction of the geometric and spectral distortions in the acquired images. The method is based on automated non-rigid registration of the reference and acquired images corresponding to the proposed calibration object incorporating standardized spatial and spectral information. The obtained transformation was successfully used for sub-pixel correction of various hyper-spectral images, resulting in significant improvement of the underlying classification and multivariate hyper-spectral image analysis results. It was found that the proposed calibration is highly accurate and suitable for routine use in applications involving either diffuse reflectance or transmittance measurement setups.

8215-10, Session 2

## Optical fibers with polyimide coatings for medical applications

A. A. Stolov, B. Slyman, D. A. Simoff, A. S. Hokansson, R. S. Allen, J. Earnhardt, OFS (United States)

Key properties of polyimide-coated optical fibers, unaged and exposed to various harsh environments, were investigated. The main intent was to model extreme conditions that can be encountered in medical applications of the fibers. A fiber designed by OFS showed good strength and was able to withstand exposure to extreme heat and humidity, multiple autoclave cycles, extended water soak and immersion in organic solvents. Similar fibers offered by other suppliers displayed shortcomings in some of the tested properties.

8215-11, Session 3

## Calibration and validation of chemical imaging spectrometry for clinical use

M. Litorja, National Institute of Standards and Technology (United States)

Multispectral and hyperspectral imaging of readily accessible health biomarkers such as hemoglobin oxygenation and bilirubin are currently being used in the clinic in a variety of devices. The different spectral deconvolution algorithms used to extract quantitative information about the concentration and distribution of these compounds in vivo cannot be evaluated properly without the use of laboratory-bench validation methods. This work describes standards currently used for laboratory medical devices such as blood oximeters and blood analyzers and how these can be extended towards in vivo imagers where sampling does not have the benefit of prior chemical purification methods. The differences in the optical configuration used in blood chemistry analyzers vs that by in vivo chemical imagers will be discussed and uncertainties that arise simply from this difference. In this work we describe the correlation of oxygen saturation values from spectral data with independent concurrent dissolved oxygen measurement. This also describes work on validation of spectra-based in vivo bilirubin assessment.

8215-12, Session 3

## Standard test methods for established medical imaging modalities and their implications for optical coherence tomography

J. Pfefer, A. Agrawal, A. Beylin, U.S. Food and Drug Administration (United States)

Standardized approaches for assessing device performance have a wide range of benefits such as improved ability to reliably and objectively compare device performance and provide quality assurance during research studies or clinical use. The adoption of field-wide consensus techniques can facilitate innovation and reduce the time and cost required for development, validation and regulatory approval. International standards documents detailing benchtop image quality assessment techniques are well established for imaging modalities such as MRI, CT and ultrasound, whereas few exist for optical diagnostic techniques. We have reviewed numerous standards for established medical imaging techniques and analyzed the general characteristics employed (e.g., resolution), as well as the specific, tissue-phantom-based test methods and figures of merit used to evaluate image quality. We have identified common themes from these documents that can be incorporated in development of tests for assessment of image quality in optical coherence tomography systems. This work also has relevance to a wide range of imaging techniques under development in biomedical optics which would benefit from standardized performance assessment methods.

8215-53, Session 3

## Challenges in manufacturing optical tissue phantoms: an industrial perspective

J. Bouchard, I. Noiseux, O. Mermut, INO (Canada)

Optical tissue phantoms can serve many needs encountered in the translation path between fundamental research and clinical acceptance. Each of these needs call for a different set of requirements on the phantom design. Earlier stage research will require the phantom to reproduce adequately the measurement challenges of the intended application. Phantoms used during the final verification and validation phase of a medical device seeking FDA clearance will focus more on stability, repeatability and traceability. Developing and producing phantoms meeting those quality requirement is a challenging task. Unlike MRI or CT, Optical technologies will not reach clinical practice as versatile multipurpose imaging platforms but as a collection of application specific instruments. This variety in the instrumentation and the way they will interact with the human body translates in very diverse requirements for phantoms. This presentation will illustrate the challenges imposed by this diversity of requirements with real life examples from a commercial phantom production. Solutions to overcome the diversity challenge through standardization will be proposed.

8215-54, Session 3

## Report on a recent workshop: Standards for Phantoms for the Performance Evaluation and Validation of Optical Medical Imaging Devices

J. Hwang, National Institute of Standards and Technology (United States); R. J. Nordstrom, National Cancer Institute (United States)

Phantoms for optical medical imaging provide a critical tool for independent assessment of biophotonic imaging systems for benchmarking performance and ensuring data consistency across multiple instruments, and their use as tools for the evaluation and validation of optical imaging devices has been demonstrated. For further use of phantoms for biomedical optical devices' regulatory clearance and quality assurance, their physical properties need to be accurately known and fabricated to the same quality according to the rigorous material and measurement standards. In a recent international workshop in November 2011, experts from government agencies (NIH, FDA, NIST, NPL, NRC etc.) and several universities and industries presented perspectives to address important issues on the material and measurement standards of phantoms such as phantom material composition, performance standards, and phantom-based test methods in the several key optical measurement platforms. This talk summarizes the key outcome of this workshop.

8215-13, Session 4

## Primary care imaging using a handheld OCT-video scanner

S. A. Boppart, Univ. of Illinois at Urbana-Champaign (United States)

Primary Care Medicine, including Family Practice and Pediatrics, has traditionally relied on physical exam skills and simplistic instruments for critical disease screening, diagnostic decision making, monitoring, and referral to medical specialists. The otoscope and ophthalmoscope are two historical and ubiquitous instruments that largely only illuminate and magnify tissue surfaces in the ear and eye, respectively. We have developed a new Primary Care Imaging system integrating optical coherence tomography (OCT) and video imaging with these instruments in a handheld scanner and portable system to advance the screening, diagnostic, and monitoring capabilities in primary care, and to more effectively manage and refer patients based on quantitative data.

This Primary Care Imaging system with a MEMS-based handheld scanner and interchangeable tips enables high-resolution real-time 3-D OCT imaging of the multiple tissue sites commonly examined during primary care outpatient exams including the eyes, ears, oral and nasal mucosa, skin, and cervix. Our initial focus is on two increasingly prevalent diseases encountered in the primary care office, namely otitis media (middle ear infections) and diabetic retinopathy.

With an increasing reliance on effective primary care patient management for the expected increase in numbers of patients, new advanced screening, diagnostic, and quantitative technologies and instruments are needed in the outpatient primary care clinic for the early detection of disease, for quantitative monitoring of disease progression or regression, and for more efficient and evidence-based referrals to specialists. This Primary Care Imaging system addresses this critical need, and for the first time, brings advanced diagnostic imaging technology to the primary care office.

8215-14, Session 4

## Clinical dissemination of near-infrared fluorescence imaging using the FLARE imaging system

S. Gioux, N. J. Durr, A. Stockdale, C. J. Cross, Y. Ashitate, J. V. Frangioni, Beth Israel Deaconess Medical Ctr. (United States)

Image-guided surgery using near-infrared (NIR) fluorescence imaging has increased rapidly; however, worldwide dissemination is needed to validate this technique as standard of care. To achieve this goal, we created a novel FLARETM imaging system design that was optimized for surgery and complies with all applicable safety regulations. A custom FPGA controls 1 color and 2 NIR CCD sensors and is capable of acquisitions at up to 140 frames per second, with integration times from 1 us to 10 s. Moreover, the FPGA preprocesses all images and controls the focus lens motor to permit fast and accurate focusing. A custom-made 15x macro-zoom focusing objective lens permits precise imaging from 400 to 1000 nm at working distances between 12 and 18 inches. Light from a high power custom source integrating both NIR and visible wavelengths is propagated using fiber bundles and arranged in a multiple sources pattern over the patient to allow for efficient illumination. All elements are contained within a 22 x 22 x 37 inches cart using standard rack mounts and universal power supplies. The imaging head can be positioned anywhere in space using an articulated arm. All design processes, testing, and validation procedures have been documented, and the device optimized for robustness and ease of fabrication. This novel FLARETM system has been validated preclinically and translated to the clinic. Our next goal is to file approvals for clinical use in the United States and Europe. This study lays the foundation for large-scale dissemination of NIR fluorescence-guided surgery.

8215-15, Session 4

## Fluorescence goggle device for intraoperative oncologic imaging

Y. Liu, A. Bauer, W. J. Akers, G. P. Sudlow, K. Liang, T. Charanya, S. Mondal, J. P. Culver, S. Achilefu, Washington Univ. in St. Louis (United States)

We have developed a wireless fluorescence goggle device for intraoperative oncologic imaging. With our system design, the surgeon can directly visualize the fluorescence information from the eyepieces in real time. The fluorescence state of diseased tissues from molecular contrast agents can guide the surgeons to find lesions that may be otherwise neglected. In addition, the goggle device is directly worn by the surgeon without the need for additional monitor, which can improve coordination and the surgical accuracy. The device is further equipped with wireless communication capability, where the images can be transmitted to remote site for further analysis and medical advising. It can be applied to standard care in the conventional hospital settings, telemedicine, and point-of-care. We have applied this device in several oncologic imaging applications. In conjunction with targeting fluorescent dyes, the goggle device can successfully detect small nodules or metastases that are not obvious to the naked eye. This can improve surgical outcomes and reduce cancer recurrence. In addition, the ability to clearly visualize the functional status of lesions can enhance surgical decisions and improve surgical margins, thereby reducing the amount of healthy tissues resected. Furthermore, the cost of prototype goggle device is significantly lower than existing and emerging intraoperative imaging instruments. Thus, it holds great potential to be applied to a wide range of medical settings, both in advanced medical centers and under-resourced regions.

8215-16, Session 4

## Visualization technique for air flows in a live operating room in view of infection prevention

R. M. Verdaasdonk, R. van den Berg, A. van der Veen, Vrije Univ. Medical Ctr. (Netherlands); H. J. Noordmans, Univ. Medical Ctr. Utrecht (Netherlands)

Infections can be a serious complication after surgery. In an operating room (OR), a laminar flow of clean air is creating in the operating field to prevent contaminations. However, people, obstructions and equipment can interfere with the ideal air flow in the OR.

In this study, a technique has been developed to visualize air flows in a live OR setting. Using a large 35 cm diameter concave mirror with a 200 cm focal length, a Schlieren setup was constructed with a spatial filter (knife edge) to achieve an enormous contrast enhancement to visualize small variations in air density induced by temperature differences. To avoid interference from the normal OR lighting, a bright 810 nm LED was used as point light source for the Schlieren setup and images were obtained with a NIR camera with a 780 nm filter blocking the light from the environment.

The NIR Schlieren setup showed significant disturbance of the laminar flow of clean air above the operation table depending on the position of the operating lamp. Looking at the air flow around various instruments that are standard in the OR, air turbulence over 1 m distance was visible created by the cooling vent. When these vents are directed to the ground or into the operation field the flow of clean air, intended to prevent infections, could easily be disrupted.

The near IR Schlieren setup can be used in a live operation room to study air flows and is a useful instrument to investigate potential sources for infection.

8215-18, Session 5

## Parallel 3D confocal/OCM imaging system with adaptive objective lens

G. Li, Univ. of Missouri-St. Louis (United States)

Rapid, noninvasive high-resolution en-face three-dimensional (3D) imaging with a constant resolution along the depth is of great significance in general biomedical diagnostic applications. It is also extremely important to achieve parallel wide-field imaging in the transverse directions and dynamic focusing in the longitudinal direction with no moving components for live cell imaging where dynamic behaviors inside cells need to be recorded in real time for better understanding of the cell functions. Here we report a novel parallel confocal/fluorescence 3D microscopic imaging system without mechanic scanning by introducing electro-optic adaptive objective lens for depth scanning and reconfigurable digital micro-mirror device as point source array and pinhole array. Such a confocal imaging system is further used as the object arm for a full-field optical coherence microscopy. The focal length of the adaptive lens can be tuned from infinity to  25 mm, and the depth scanning range of the whole dynamic objective lens is 1mm. The field of view in the object plane is about 1mm  1mm. The system shows high optical performance through the total imaging depth. The modulation transfer function at the frequency of 250lp/mm is above 0.3 and the focused spot size in the whole field is about 2 micron or less. Detailed design and experimental results will be shown.

8215-19, Session 5

## An afocal beam relay for laser XY scanning systems

D. Kessler, Kessler Optics & Photonics Solutions, Ltd. (United States)

Two dimensional beam deflection is often required in medical laser scanning systems such as OCT or confocal microscopy. Commonly two linear galvo mirrors are used for their large apertures and scan angles performance. The galvos are placed at the vicinity of the scan lens entrance pupil with a “displacement distance” separating them. This distance limits the scan fields and/or reduces the effective aperture of the scan lens. Another option is to use a beam relay, and relay one glavo onto the other. However, beam (or pupil) relays are notoriously complicated, expensive and can add significant aberrations.

This paper discusses a simple, all reflective, diffraction limited, color corrected, beam relay, capable of large scan angles and large deflecting mirrors.

The design is based on a unique combination of an Offner configuration with a Schmidt aspheric corrector. It allows significantly larger scan field as compared with scanners using galvos separated by the displacement distance.

Design examples for 15 mm diameter pupil ad 50 degrees optical field are shown.

The design details and performance are presented as well as different possible configurations for use in high performance microscopic systems.

8215-20, Session 5

## Instrumentation considerations for measurement of early-arriving photons in diffuse fluorescence tomography

N. Valim, M. Niedre, Northeastern Univ. (United States)

The high degree of photon scatter in biological tissue remains a major challenge for imaging resolution in diffuse fluorescence tomography. Time-gated detection of early-photons (EPs) from a pulsed laser source has been shown to yield significant reduction in photon scatter compared to quasi-continuous wave (CW) photons. Recently we showed that measurement of EPs reduced the width of instrument imaging photon density sensitivity functions (PDSFs) by 40-60% versus CW photons over a range of conditions relevant for small animal imaging. However, Monte Carlo simulations predicted better improvement than was experimentally observed at very early-time gates. To better understand this discrepancy, in this work we studied the impact of instrumentation on EP measurements including the system temporal impulse response function (TIRF), instrument measurement geometry and the detected photon count rate (DPCR).

We experimentally measured time-dependent instrument PDSFs between a pulsed laser and a photomultiplier-tube array operated in photon counting mode as we have done previously. We first modulated the instrument TIRF by coupling multimode optical fibers (up to 20 m) to the system on source and detector sides. Our results indicate that increasing the system TIRF from 161 to 393 ps increased the PDSF width by ~15% at early-time gates, thereby imaging performance. Decreasing the DPCR by an order of magnitude had a similar effect. Conversely, modulating source-detector geometry did not cause significant changes in the relative PDSF width at early times. These considerations are important in the design of future time-resolved small animal fluorescence tomography instruments based on EP detection.

8215-21, Session 5

## Comparison of divided-pupil and full-pupil configurations for line-scanning confocal microscopy of skin

Y. G. Patel, C. A. DiMarzio, Northeastern Univ. (United States); M. Rajadhyaksha, Memorial Sloan-Kettering Cancer Ctr. (United States)

Point-scanning and line-scanning confocal microscopy have proven successful for imaging of human skin, providing resolution and optical sectioning that shows nuclear and cellular detail in vivo. Point-scanning offers superior resolution, optical sectioning and image quality, while line-scanning offers a simpler and lower cost alternative for potential translation into widespread clinical use. However, analysis based on a Fourier optics model shows that the sectioning with line-scanning may be significantly improved with pupil engineering. Instead of the standard full pupil, a divided pupil configuration offers improved sectioning that may compete with point-scanning for clinically useful imaging. To confirm our modeling results experimentally, we developed a bench-top line-scanning confocal microscope, using 10 optical components and a CMOS linear-array detector, for imaging skin. The bench-top system contains pupil planes in the transmitter and receiver paths, so we can test in a full pupil or divided pupil configuration. Theoretical optical sectioning and lateral resolution for line-scanning full pupil configuration are 0.34μm & 0.20μm, respectively, and 0.46μm & 0.38μm for divided-pupil configuration. This shows good agreement to point-scanning full-pupil system measurements of 0.51μm & 0.23μm, respectively. Imaging of skin ex vivo with the divided pupil demonstrates sufficient resolution and contrast to observe nuclear and cellular detail and improved sectioning, compared to that seen with the full pupil.

8215-22, Session 5

## Development of low-cost webcam-based biomedical monitoring system over a network for real-time physiological assessment

S. Hu, V. Azorin-Peris, Loughborough Univ. (United Kingdom); C. Papin, Univ. Paris-Sud 11 (France); S. Yu, A. Karki, R. Kalawsky, R. Summers, Loughborough Univ. (United Kingdom)

This study presents a non-contact biomedical monitoring system consisting of physiological signal processing algorithm, and a low cost webcam to real-time capture physiological signals over a network. The work demonstrates the live acquisition of physiological signals verified by the calculated heart rate, photoplethysmographic pulsatile waveform, and respirations. Also we explored the capability of remotely monitoring the captured data, demonstrated in this study through the data being stored and accessed on a shared work space by multiple computers. The results are shown by one computer constantly acquiring data, processing this data and saving it to a workspace, while another computer monitors the changes made to the saved data and calculating the end results. The study presents potential possibilities of using remote monitoring of physiological data to allow long distance medical diagnosis readily available, to monitor physiological signals for security purposes and the use of remote monitoring on portable technology for mobile monitoring.

8215-23, Session 6

## Hyperspectral projection of a skin flap animal model for use as a digital tissue phantom

D. Allen, S. W. Brown, J. P. Rice, J. Hwang, M. Litorja, National Institute of Standards and Technology (United States); R. X. Xu, Ohio State Univ. (United States)

Hyperspectral imaging provides a means to acquire quantitative information from burns and wounds without physical contact. Anticipated wide-spread use of hyperspectral imagers in the clinic will require common performance validation metrics in order to establish confidence in measurements by different hyperspectral imagers. One challenge in testing optical instruments using biological samples is the sample variability over time. Physical phantoms provide an artificial substitute for real tissue and serve to reduce sample variability. The shortcoming of physical phantoms is the inability to fully represent reality both spectrally and spatially. NIST has been developing a hyperspectral image projector that can project both spatially and spectrally realistic scenes. When the scene projected is that of biological tissue, the scene is termed a digital tissue phantom (DTP). With the DTP, scenes are projected into the imager under evaluation, providing a realistic substitute for real patient images (or common instrument performance validation platform). Since the DTP is of a digital nature, there are no degradation issues over time and the same platform can provide a wide variety of application-specific sets of images. For a reference DTP, we collected hyperspectral datacubes of a skin flap model using a pig over three days. The spectral signatures were correlated to clinical measurements in order to develop a scale for oxyhemoglobin concentration. The datacube of the skin flap model was projected using the DTP and measured with a calibrated reference hyperspectral imager. Differences between the original and projected datacubes will be quantified and a rudimentary measurement uncertainty budget developed. This demonstration of the ability to accurately project complex medical scenes is the first step in the longer term goal of developing common, accepted medical hyperspectral imager performance validation metrics.

8215-24, Session 6

## Multispectral imaging approach for simplified non-invasive in vivo evaluation of gingival erythema

T. Eckhard, E. M. Valero, J. L. Nieves, Univ. of Granada (Spain)

Ginigval health state assessment plays a key role in early detection of common diseases like gingivitis and periodontitis. We have previously developed an initial low-cost image acquisition set-up using standard photographic equipment that allows an objective evaluation of visual signs of gingival inflammation in clinical environment [Eckhard et al., Proc. Int. Color Assoc., 2011]. In this study, we present a new and simple approach for quantifying gingival erythema on a pixel-by-pixel bases using multispectral imaging techniques and image processing tools.

Erythema can quantitatively be evaluated by measuring the level of oxygenation and the amount of blood in the gingival capillary net. These parameters can be estimated indirectly by computing ratios between two bands of spectral reflectance of gingival tissue [Douven et al., Proc. SPIE 3914, 2000]. Obtaining reflectance spectra by conventional spectroscopy is not useful in this case because erythema can exhibit a strong spatial variation. A very interesting alternative is mulispectral imaging, because it measures reflectance curves for each pixel of an image. Zakian et al. [Zakian et al., J. Biomed. Optics 13(5), 2008] use a commercial multispectral dental color assessment system and a complex image processing workflow for erythema assessment, which requires evaluation by image processing experts. We propose a more simple approach to obtain a spectral ratio from only two intensity images acquired with multiplexed LED illumination at 460nm and 630nm peak wavelength and a digital camera. We also propose an algorithm for automatic mapping of erythema which is easy to use by any dental health care professional. The main advantage of our method is the simplicity, accessibility and low-cost of the biomedical imaging technique proposed.

8215-25, Session 6

## Hyperspectral imaging and analysis of subcellular substances in single cells

J. Y. Lee, National Institute of Standards and Technology (United States); F. Tokumasu, National Institute of Standards and Technology (United States) and National Institute of Health (United States); D. Samarov, D. Allen, M. Litorja, National Institute of Standards and Technology (United States); D. Sackett, R. Nossal, National Institute of Health (United States); J. Hwang, National Institute of Standards and Technology (United States)

We present a confocal hyperspectral imaging and analysis technique to analyze subcellular substances in single cells. Hyperspectral imaging is a spectral analysis technique which is non-invasive and suitable for investigating tissue samples. Here, we focus on two intracellular substances, cytochrome c and hemoglobin, which are important endogenous biological chromophores. Cytocrhome c is a small heme protein confined in the intermembrane space in mitochondria. It is a component of the electron transport chain and is also involved in apoptosis. Hemoglobin is an oxygen-carrying heme protein present in erythrocytes. Hyperspectral data cubes were collected by a confocal hyperspectral microscope system equipped with a white light laser and acousto-optic beam splitter (AOBS). The data were analyzed by algorithms based on a spectral angle mapper. We extracted unique spectral signatures (i.e. endmembers) for cytochrome c, a few subtypes of hemoglobin, such as oxyhemoglobin and methemoglobin, and for scattering from cell membranes. We built intracellular maps of the distribution of substances of interest using abundances of specific endmembers. In addition, we performed a reflectance measurement to understand the backscattering signatures of subcellular substances and organelles. The developed imaging and analysis technique enables label-free molecular imaging of endogenous biomarkers in single cells and ultimately may be applied in vivo as well.

8215-26, Session 6

## Intercomparison of EMCCD- and sCMOS-based imaging spectrometers for biomedical applications in low-light conditions

J. E. Hernandez-Palacios, Norsk Elektro Optikk AS (Norway); L. L. Randeberg, Norwegian Univ. of Science and Technology (Norway); T. Løke, Norsk Elektro Optikk AS (Norway); T. Skauli, Norwegian Defence Research Establishment (Norway)

Imaging techniques for a spectroscopic characterization of biological tissue are frequently limited by the amount of light available for analysis. Increasing acquisition times to collect more light may induce irreversible changes or damages on some samples. Hyperspectral imaging offers flexibility that makes it an interesting tool for optical diagnostics. It provides means for characterizing large biological samples with microscopic spatial resolution and a narrow spectral sampling interval. The use of a highly sensitive detector is required for overcoming the limitations imposed by working with biological samples and to detect weak light signals. For this study we have built and compared the performance of two imaging spectrometers using state of the art sensors for low light environments: an electron-multiplying CCD (EMCCD) and a scientific CMOS (sCMOS). Both systems have been designed to detect weak fluorescence signals, delay bleaching of fluorophores and prevent photo-damage. The imagers work within the VNIR spectral region (400 nm - 900 nm) with spectral sampling less than 4 nm. The resulting images have scene pixel sizes less than 25 µm and a FOV larger than 25 mm. The systems have been tested side by side measuring the diffusion of a fluorescent tag in tissue samples. The advantages and limitations of each approach are emphasized. The benefits of a dedicated low light system are stressed by comparison to standard hyperspectral imaging technology.

8215-27, Session 6

## Characterization and modeling of the spatially and spectrally varying point-spread function in hyperspectral imaging systems for computational correction of axial optical aberrations

Ž. Špiclin, M. Bürmen, F. Pernuš, B. Likar, Univ. of Ljubljana (Slovenia)

Spatial resolution of hyperspectral imaging systems with a broad spectral range can be substantially limited due to axial optical aberrations that originate from wavelength-induced index-of-refraction variations of the imaging optics. Even though spatial resolution can be largely improved by using adaptive optics, some residual blurring can still remain present in the spectral images and thus reduce contrast of fine image details. Moreover, the spatial resolution can vary significantly both with respect to the acquisition wavelength and the position within each spectral image. Variations of the spatial resolution can be effectively characterized as part of the calibration procedure by modeling the point-spread function (PSF) of the hyperspectral imaging system. The recovered PSF model can then be used in the image deconvolution methods to improve the spatial resolution of the spectral images. We recover the PSF model from the spectral images of a geometric caliber, which consist of intersecting line patterns. From individual line segments between the line intersections, the PSF model was obtained by a non-parametric estimation procedure that uses orthonormal series representation of the PSF. The estimated coefficients of the orthonormal series representation were then linked in the spatial and spectral coordinates so as to fully characterize the PSF of a hyperspectral imaging system. Tests were performed on a hyperspectral imaging system that uses acousto-optic tunable filter in the visible and near-infrared spectral range. The results demonstrate that the spatial resolution of the acquired spectral images can be significantly improved using the recovered PSF and image deconvolution methods.

8215-28, Poster Session

## On the spectral sensitivity calibration of fluorescence spectrometers: extension to the NIR, polarization, and grating effects

S. Fore, PicoQuant Photonics North America, Inc. (United States); S. Tannert, P. Kapusta, A. Glatz, U. Ortmann, F. Koberling, R. Erdmann, PicoQuant GmbH (Germany)

Reliable and traceable correction of recorded emission spectra is an important and unfortunately often overlooked procedure. For example measuring quantum yields, calculating Stokes shifts or discussing the shape of emission bands is meaningless without taking into account the wavelength and polarization plane dependent sensitivity of the complete detection system.

Recording correct emission spectra without excitation and emission polarizers assumes completely depolarized emission. However, this is a strong assumption, not always valid for fluid solutions and certainly invalid for solid samples. Therefore, to record the true emission spectra the grating polarization bias has to be avoided by the proper use of polarizers.

We present data illustrating that correction factors vary widely for different emission polarization states, and different gratings in the same monochromator. Therefore, a single sensitivity correction curve is not applicable for all measurements. With the existing emission standards for the visible range obtaining all required correction curves is feasible. However, with the advent of new, far-red sensitive photomultipliers (sensitive up to 900nm), new calibration standards are necessary.

8215-29, Poster Session

## A new phototherapy unit for neonatal hyperbilirubinemia using computer controlled laser diodes or LEDs

M. Hamza, Mansoura Univ. (Egypt); M. H. Sayed El-Ahl, Military Medical Academy (Egypt); A. M. Hamza, National Research Ctr. (Egypt); A. M. Hamza, Y. M. Hamza, Tabarak Children's Hospital (Egypt)

In this paper the authors introduce the theory, design and operating principles of a new phototherapy unit for neonatal hyperbilirubinemia. The new phototherapy unit provides combined monitoring and therapy for newborn infants with hyperbilirubinemia using laser diodes or LEDs. The operation of the new phototherapy unit is under control of the computer unit which receives periodic informations from the transcutarneous monitoring sensors. The informations obtained from the sensors help to achieve the control of serum bilirubin away from critically high level and to stop treatment when a reasonably safe level is reached. The setting of these levels will vary according to the risk factors of each individual case. The new portable phototherapy unit can allow the treating physician to avoid over or under treatment of jaundiced neonates and is therefore expected to provide widespread clinical application in addition to safe, easy to use and cost effective home phototherapy of neonatal hyperbilirubinemia.

8215-30, Poster Session

## The evaluation model of the physiological lag parameter between the glucose concentration in blood and the glucose concentration in interstitial fluid

T. Shi, D. Li, Y. Ji, K. Xu, Tianjin Univ. (China)

In recent years, using the detection of interstitial fluid glucose concentration to realize the real-time continuous monitoring of blood glucose concentration gets more and more attention, because for one person, the relationship between blood glucose concentration and interstitial fluid glucose concentration satisfies specific rules. However, the glucose concentration in interstitial fluid is not entirely equal to the glucose concentration in blood and has a physiological lag because of the physiological difference of cells in blood and interstitial fluid. Because the clinical diagnostic criteria of diabetes are still blood glucose concentration, the evaluation model of the physiological lag parameter between the glucose concentration in blood and the glucose concentration in interstitial fluid should be established. The physiological difference in glucose molecules uptake, utilization, and elimination by cells in blood and interstitial fluid and the diffusion velocity of glucose molecule from blood to interstitial fluid will be induced to the mass transfer model to express the physiological lag parameter. Based on the continuous monitoring of glucose concentration in interstitial fluid, the project had studied the mass transfer model to establish the evaluation model of the physiological lag parameter between the glucose concentration in blood and the glucose concentration in interstitial fluid. We have preliminary achieved to evaluate the physiological lag parameter exactly and predict the glucose concentration in blood through the glucose concentration in interstitial fluid accurately.

# Conference 8216: Multimodal Biomedical Imaging VII

Saturday-Sunday 21-22 January 2012

Part of Proceedings of SPIE Vol. 8216 Multimodal Biomedical Imaging VII

8216-01, Session 1

## Wide-field optical tomography

X. Intes, Rensselaer Polytechnic Institute (United States)

No abstract available

8216-02, Session 1

## Multimodal fluorescence DOT-SPECT/CT for in vivo sentinel lymph node imaging

M. Solomon, Washington Univ. in St. Louis (United States); R. E. Nothdruft, W. J. Akers, K. Liang, Washington Univ. School of Medicine in St. Louis (United States); B. Xu, Washington Univ. in St. Louis (United States); S. Achilefu, J. P. Culver, Washington Univ. School of Medicine in St. Louis (United States)

Multimodal optical imaging can combine of structural information from well established clinical techniques with the newer functional and molecular contrast provided by optical methods such as fluorescence diffuse optical tomography (FDOT). However, multimodality imaging presents challenges. Hardware integration requires compatibility of all the parts in one platform for accurate co-registration of multimodal 3D images. One of the main challenges in combining imaging modalities is determining how to merge the information from multiple technologies into a single imaging output, as each modality is sensitive to a different set of tissue properties and have disparate reporting strategies. Here, we demonstrate the feasibility of combining our fiber-based video-rate fluorescence DOT with preclinical NanoSPECT/CT system (Bioscan, Inc.) for concurrent optical and nuclear imaging of sentinel lymph node (SLN). In addition, we synthesized monomolecular multimodal agents (MOMIAs) based on a near-infrared dye, cypate, radiolabeled with 111In for simultaneous acquistion of data with the combined nuclear-DOT imaging plotform. The multimodal imaging agent, 111In-Cypate, is injected intradermally in the forepaw of rats for concurrent data acquisition with FMT-SPECT/CT platforms immediately after injection and at 30 minutes after injection. The fiber-based video-rate fluorescence DOT imaging system is composed of a grid of alternating 12 sources (785nm and 830nm LDss) and 13 detectors. To maintain high temporal sampling, the system simultaneously acquires ratio-metric data by measuring frequency encoded fluorescent emission and reference transmission light levels at each detector through individualized bandpass filter optimized for fluorescence emission. The data is then reconstructed using the normalized Born approach with a 3D finite element model derived from an anatomical CT image of a rat for accurate light propagation modeling. Fluorescence and radioactivity from the 111In-cypate is localized in spatially coincident region with each platform in the area of the axillary LN corresponding to the side of the injection. Multimodal fluorescent DOT has the potential to become a powerful and practical tool for a broad array of imaging applications, ranging from sentinel lymph node mapping to monitoring cancer therapy progress.

8216-03, Session 1

## Heat-sensitive microbubbles for therapeutic margin assessment in liver ablation surgery

J. X. Huang, C. Schmidt, R. X. Xu, The Ohio State Univ. (United States)

Thermal ablation treats tumors by localized deposition of thermal energy that causes protein denaturation and coagulation necrosis. However, many cancer ablation processes are still considered highly investigational because of the poor process control, the incomplete destruction of residual cancer cells, and the damage to surrounding normal tissue structures. We fabricated heat-sensitive microbubbles for intra-procedural assessment of ablation margins. The microbubbles encapsulate low boiling point perfluorocarbon compounds and fluorescence dyes in a poly (lactic-co-glycolic acid) (PLGA) shell. The biodistribution of HSMs in a domestic pig after intravenous injection was quantified by MS-LC testing. The technical feasibility of HSM-assisted ablation margin assessment was demonstrated in vivo in a pig model. After ventral midline laparotomy, the liver of the pig was ablated by a radiofrequency ablation system at 250W for 5 minutes. The propagation of the ablation margin was monitored by ultrasound and compared with photographic imaging. After ablation, the tissue was dissected for fluorescence microscopic imaging. Our experiment demonstrated the technical feasibility of intra-procedural ablation margin assessment by HSM-assisted ultrasound imaging.

8216-04, Session 1

## Multimodality imaging using double clad fiber challenges and solutions

E. Hamidi, H. Yoo, H. Wang, J. A. Gardecki, P. Vacas-Jacques, M. Rosenberg, M. Shishkov, B. E. Bouma, G. J. Tearney, Wellman Ctr. for Photomedicine (United States)

Multimodality imaging techniques can be an invaluable diagnostic and investigational tool in clinical medicine. As an example, co-registered optical frequency domain imaging (OFDI) and near infrared fluorescence (NIRF) imaging can enable better understanding of coronary artery disease by providing microstructural and molecular information underlying this disease. For a multimodality imaging in vivo, a catheter should be ideally as small as possible while providing transmission channels for both modality signals. More specifically we utilize a double clad fiber (DCF) in the catheter where the single-mode core transmits the OFDI light while the multimode inner cladding is used to excite and receive NIRF. In the rotary junction, which is utilized to mechanically scan the catheter in a helical pattern OFDI and NIRF light are coupled through free space resulting in finite cross channel isolation. However, the optical coupling between core and inner cladding, and, as a result, cross channel isolation, is also dependent upon fiber bending. Here we study the cross channel isolation and how this can degrade the OFDI performance. Our investigations demonstrate that the OFDI light collected via the fiber's inner cladding in the form of multimode light can couple into single-mode fiber receiver of the OFDI system at the rotary junction and be detected as multimode interference. In order to combat this crosstalk, we propose a miniaturized spatially wavelength selective filter at the rotary junction to isolate the channels and improve the quality of OFDI images.

8216-05, Session 1

## PH-sensitive fluorescence detection by fluorescence diffuse optical tomography

J. Li, F. Gao, L. Duan, L. Zhang, H. Zhao, Tianjin Univ. (China)

Intracellular pH plays many critical roles in cell and tissue activities, such as proliferation and apoptosis, multidrug resistance, etc. Monitoring pH changes inside living cells is also important for studying biochemical information about the surroundings. So PH-sensitive fluorescence imaging has merited great interest lately for near-infrared fluorescence diffuse optical tomography - the efficient small animal imaging tool. We present a two-dimensional image reconstruction method for time-domain fluorescence diffuse optical tomography, which employs the analytical solution to the Laplace-transformed time-domain photon-diffusion equation to construct the inverse model and introduces a pair of real-domain transform-factors to effectively separate the fluorescent yield and lifetime parameters from the algebraic reconstruction technique solutions to the resultant linear inversions. By use of a specifically designed a multi-channel time-correlated single photon counting system and a normalized Born formulation for the inversion, the proposed scheme in a circular domain is experimentally validated using small-animal-sized cylindrical phantoms that embed several PH-different fluorescent targets made from 1%-Intralipid solution and PH-sensitive fluorescence dye, where the time-resolved excitation and fluorescence signals are measured on the boundary. The results show that the approach retrieves the positions and shapes of the targets with a reasonable accuracy and achieves PH-sensitive quantitative reconstruction of the fluorescent yield.

8216-06, Session 1

## Mammogram-based diffuse optical tomography

H. Chiang, J. Yu, L. Chen, National Central Univ. (Taiwan); M. Pan, Tung Nan Institute of Technology (Taiwan); M. Pan, National Central Univ. (Taiwan); S. Sun, TaoYuan General Hospital (Taiwan)

The study aims at developing an optical measurement module incorporated with an X-ray mammographic system to obtain diffuse optical imaging (DOI) for detecting breast tumors. Two goals steer the study: (1) to reduce radiation exposure by using only one mammogram, instead of two, as structure information to compute optical-coefficient images for breast tumor detection; and (2) to enhance sensitivity and specificity of tumor detection through the use of functional DOI. A dual-direction scanning device to project illuminated near infrared light with multiple-channel switching for both sources and detectors was designed and constructed. The module operates to compress phantoms by two compression plates in order to reduce the distance between sources and detectors for enhancing the signal to noise ratio of measurements and obtaining more reliable data. A dual-direction projection scheme is employed to obtain double information that can benefit image reconstruction; moreover, a half pitch shift of a channel span between downward and upward light illumination through an XY translation table is arranged to avoid acquiring redundant data. For a dual-modality imaging scheme, a suspected region or more are first circled from a mammogram, and the plane in the sagittal view including that suspected region is to be optically scanned for subsequent image reconstruction. Three types of initial guess were proposed, verified and compared to locate the depth of tumors. The proposed computation scheme was validated by using designated cases including various size, contrast and location of inclusions to background, and also a phantom made of fat, lean meat and bone. As a comparison, both simulation and experiments were performed to reconstruct functional optical-coefficient images. Mean square errors were used for the quantitative evaluation on all reconstruction images.

8216-07, Session 2

## In vivo quantification of human dermal skin aging using SHG and autofluorescence

S. Puschmann, C. Rahn, H. Wenck, S. Gallinat, F. F. Fischer, Beiersdorf AG (Germany)

There are visible changes during skin aging. In the extracellular matrix these changes referred to as intrinsic aging (skin areas not exposed to sunlight) and extrinsic aging can be measured using various methods, such as subjective clinical evaluation, histology and molecular analysis. In this study we developed a new parameter for the non-invasive quantitative determination of dermal skin aging utilizing a five-dimensional intravital tomography (5D-IVT). This device, also known as 5D - multi-photon laser scanning microscopy, is a powerful tool to investigate (photo)aging-associated alterations in vivo.

Structural alterations in the dermis of extrinsically aged (chronically sun-exposed) and intrinsically aged (sun-protected) human skin were recorded utilizing the collagen-specific second harmonic generation (SHG) signal and the elastin-specific autofluorescence (AF) signal. Recording took place in young and elderly volunteers. The resulting images were processed in order to gain the elastin percentage and the collagen percentage per image. Then, the elastin - to - collagen ratio (ELCOR) was calculated. With respect to volar forearm skin, the ELCOR parameter significantly increased with age. In elderly volunteers, the ELCOR value calculated for the chronically sun-exposed temple area was significantly augmented compared with the sun-protected upper arm area.

Based on 5D-IVT we introduce the ELCOR parameter as a new means to quantify age-associated alterations in the extracellular matrix of in vivo human skin. This novel parameter is compared to the currently used “SHG to AF aging index” of the dermis (SAAID).

8216-08, Session 2

## Multimodal full-field optical coherence tomography on biological tissue: toward all optical digital pathology

F. Harms, B. de Poly, LLTECH SAS (France); A. C. Boccara, ESPCI - Institut Langevin (France) and LLTECH SAS (France)

Optical Coherence Tomography (OCT) is an efficient technique for in-depth optical biopsy of biological tissues, relying on interferometric selection of ballistic photons. Full-Field Optical Coherence Tomography (FF-OCT) is an alternative approach to Fourier-domain OCT (spectral or swept-source), allowing parallel acquisition of en-face optical sections. Using medium numerical aperture objective, it is possible to reach an isotropic resolution of about 1x1x1 µm. After stitching a grid of acquired images, FF-OCT gives access to the architecture of the tissue, for both macroscopic and microscopic structures, in a non-invasive process, which makes the technique particularly suitable for applications in pathology.

Here we present a multimodal approach to FF-OCT, combining two Full-Field techniques for collecting a backscattered endogeneous OCT image and a fluorescence exogeneous image in parallel.

Considering pathological diagnosis of cancer, visualization of cell nuclei is of paramount importance. OCT images, even for the highest resolution, usually fail to identify individual nuclei due to the nature of the optical contrast used. We have built a multimodal optical microscope based on the combination of FF-OCT and Structured Illumination Microscopy (SIM). We used x30 immersion objectives, with a numerical aperture of 1.05, allowing for sub-micron transverse resolution. Fluorescent staining of nuclei was obtained using specific fluorescent dyes such as DAPI or acridine orange. We present multimodal images of healthy and pathological breast tissue at various scales.

This instrumental development paves the way for improvements of standard pathology procedures, as a faster, non sacrificial, operator independent digital optical method compared to frozen sections.

8216-09, Session 2

## Combined macroscopic FLIM and microscopic reflectance confocal microscopy for epithelial imaging

J. M. Jabbour, S. Cheng, J. A. Jo, K. C. Maitland, Texas A&M Univ. (United States)

Simultaneous biochemical and morphological imaging of epithelial tissue may have potential to improve cancer diagnosis. Here we present a bench-top optical imaging system design combining low-resolution and large field of view (FOV) biochemical fluorescence lifetime imaging (FLIM) with high-resolution and small FOV morphological reflectance confocal microscopy (RCM). Multispectral FLIM will be implemented in scanning-mode adopting a direct-pulse recording approach using a solid-state pulsed laser (355nm, 1ns FWHM, 100kHz) for excitation, and a MCP-PMT coupled to a 1.5GHz digitizer for time-resolved acquisition (250ps temporal resolution). The FLIM module will have an expected lateral resolution of ~100μm, a FOV of ~9mm in diameter, a working distance of ~30mm, and a frame rate >1Hz. In the RCM module, 1064nm CW laser light is raster scanned by a resonant mirror and a galvanometer scanner, with a line scan of 8khz and a frame rate of 15Hz. The RCM module will have expected lateral and axial resolutions of ~0.9μm and ~4μm, respectively, and a FOV of ~0.45mm in diameter.

To register the FOV of both imaging modalities, the two modules will be placed back to back and a computer controlled motorized stage will be used to translate the sample between them, so that the RCM FOV will coincide with the center of the FLIM FOV. The multimodal system will be validated by imaging hamster cheek pouch epithelial tissue. The long-term goal is to integrate macroscopic FLIM and microscopic RCM into a handheld probe for in vivo precancer evaluation of oral mucosa.

8216-10, Session 2

## Optical characters and texture maps of skin and the aging mechanism by use of multiphoton microscopy and optical coherence tomography

S. Wu, H. Li, X. Zhang, Fujian Normal Univ. (China)

Cutaneous aging is a complicated biological process affecting different constituents of skin, which can be divided into two types: the chronological aging and the photo-aging. The two cutaneous aging processes often co-exist accompanying with each other. The effects are often overlapped including changes in epithelium and dermis. The degeneration of collagen is a major factor in dermal alteration with aging. In this study, multiphoton microscopy (MPM) with its high resolution imaging and optical coherence tomography (OCT) with its depth resolved imaging were used to study the anti-aging dermatology in vivo. It was attempted to make the optical parameter and texture feature to evaluate the process of aging skin using mathematical image processing. The links among optical parameter, spectrum and texture feature in collagen with aging process were established to uncover mechanism of aging skin.

8216-11, Session 2

## Combined SECM and OCT using a dual-band wavelength-swept laser

E. De Montigny, N. Goulamhoussen, D. Banville, Ecole Polytechnique de Montréal (Canada); M. Strupler, Sainte-Justine Mother and Child Univ. Hospital Ctr. (Canada) and Ecole Polytechnique de Montréal (Canada); C. Boudoux, Ecole Polytechnique de Montréal (Canada) and Sainte-Justine Mother and Child Univ. Hospital Ctr. (Canada)

Spectrally encoded confocal microscopy (SECM) and optical coherence tomography (OCT) are two high resolution imaging techniques that have shown great potential for medical diagnosis in the fields of ophthalmology, gastroenterology and laryngology. OCT enables three-dimensional visualization of tissues in depth with good morphological contrast while confocal microscopy provides high resolution en face images with subcellular features. In order to take advantage of the complementary information and orthogonal views offered by these two techniques, we have developed a combined instrument capable of producing simultaneous OCT-SECM images in real time and without crosstalk. A novel dual band (780 nm and 1310 nm) polygon-based wavelength swept laser provides simultaneous wavelength scanning for SECM and swept-source OCT, respectively. Slow scanning (for 2D imaging) was performed using a translation stage to simulate endoscopic imaging using a rotating probe.

The respective wavelengths were chosen because the shorter 780nm ($\Delta\lambda$=30nm) wavelength laser increases the resolution in SECM while the 1310nm ($\Delta\lambda$=65nm) wavelength laser augments tissue penetration in the OCT system. Both modalities share a 40X 0.65NA microscope objective for co-registration, but the objective pupil was under-filled by the OCT beam to obtain a longer Rayleigh range. A dichroic mirror combines the different wavelengths. Axial resolutions of 5 μm and 17 μm and lateral resolutions of 1.2 μm and 10 μm were respectively measured in SECM and OCT using a USAF 1951 target. This setup is also compatible with spectrally encoded fluorescence imaging as the 780 nm band could excite NIR fluorophores.

8216-12, Session 3

## Compression-induced changes in breast hemodynamics

D. R. Busch, Univ. of Pennsylvania (United States); R. Choe, Univ. of Rochester Medical Ctr. (United States); W. Baker, Univ. of Pennsylvania (United States); T. Durduran, ICFO - Institut de Ciències Fotòniques (Spain); M. A. Rosen, Hospital of the Univ. of Pennsylvania (United States); A. G. Yodh, Univ. of Pennsylvania (United States)

Diffuse Optical Spectroscopy and Tomography utilize optically-detectable contrasts in total hemoglobin content, blood oxygen saturation, and other chromophores to detect and classify breast cancer. Breast tissue is deformable, permitting simplified measurement geometries. However, several groups have shown that deforming the breast may effect the very contrasts DOT/DOS utilizes to identify and classify cancerous lesions. Furthermore, external deformation or compression may have significant effects on blood flow, thus complicating the interpretation of contrast agent uptake, irrespective of imaging modality.

We have therefore applied Diffuse Correlation Spectroscopy, a diffuse optical technique new to medical imaging, to directly measure microvascular hemodynamics during parallel-plate compression. This geometry is similar to that typically used in cranio-caudal X-Ray mammographic imaging. Our initial study of 15 subjects using transmission DOS and DCS showed significant changes in the microvascular blood flow (-65+/-21) and volume (-47+/-16) during ~15% change in plate separation. In our current study, we have expanded our study population, improved our instrumentation, and increased the range of applied force to better quantify compression-induced hemodynamic changes.

These results have implications for measurements of contrast agents injected intravenously, irrespective of imaging modality. Additionally, studies focused on therapy monitoring across days and weeks should account for fluctuations in tissue properties due to variable compressions. Future work will explore the possibility of using compression to enhance the optical contrast of breast cancer, under the hypothesis that the often-chaotic vascular structure found in tumors will have different responses to pressure perturbations than healthy tissue.

8216-13, Session 3

## Multi-modality monitoring of response to rapamycin in colorectal neoplasia with optical-MR imaging

T. D. Wang, Univ. of Michigan (United States)

No abstract available

8216-14, Session 3

## Quantification of the cortical contribution to the NIRS signal over the motor cortex using concurrent NIRS-fMRI measurements

L. Gagnon, M. A. Yucel, M. Dehaes, R. J. Cooper, K. L. Perdue, Massachusetts Institute of Technology (United States); J. Selb, D. A. Boas, Massachusetts General Hospital (United States)

Near-Infrared Spectroscopy (NIRS) measures the hemodynamic response occurring at the surface of the cortex. Large pial veins are located above the surface of the cerebral cortex. Previous compartmental microscopic studies have shown that following activation, these veins exhibit oxygenation changes but their volume stays constant. The back-reflection geometry of the NIRS measurement makes the signal very sensitive to these superficial pial veins. As such, the NIRS signal measured contains contributions from both the cortical region as well as the pial vasculature. In this work, the cortical contribution to the NIRS signal was investigated in two ways. We first used Monte Carlo simulations on a realistic numerical volume constructed from both anatomical and angiographic MRI images. In a second step, we used a biophysical model of the fMRI signal together with simple linear regression to estimate the cortical contribution to the NIRS signal from two distinct multimodal data sets acquired over the motor cortex of human subjects during a finger tapping task. Results from simulations matched very well with the in vivo results. We found that 19% of the NIRS signal originated from the cortical region while the other 81% was due to pial vein washout. We finally showed that correcting the NIRS data to take into account the pial vein washout is important in the computation of the Cerebral Metabolic Rate of Oxygen (CMRO2) from multimodal NIRS-fMRI recordings.

8216-15, Session 3

## Temperature-modulated fluorescence tomography

Y. Lin, Univ. of California, Irvine (United States); R. B. Dalvi, InnoSense LLC (United States); M. T. Ghijsen, G. Gulsen, Univ. of California, Irvine (United States)

One of the main barrier in wide-spread use of fluorescence tomography is its low spatial resolution due to strong tissue scattering. Here we demonstrate a new technique, namely temperature-modulated fluorescence tomography (TM-FT), which combines sensitivity of fluorescence imaging with focused ultrasound resolution. The key elements of this technique are the temperature sensitive ICG loaded pluronic nanocapsules and low intensity focused ultrasound (LIFU). While conventional fluorescence tomography measurements are acquired, the tissue is irradiated using LIFU beam to produce a local hot spot, in which the temperature increases nearly 5K. Actually, the LIFU beam is scanned over the probed medium during optical data acquisition. The fluorescence emission signal measured by the optical detectors varies drastically when the hot spot overlays onto the location of the nanocapsules. The small size of the focal spot (~1mm) allows imaging the distribution of these temperature sensitive agents with not only high spatial resolution but also high quantitative accuracy using a proper image reconstruction algorithm. Accordingly, this technique is called temperature modulated fluorescence tomography (TM-FT). A phantom study confirms that 3 mm diameter fluorescence object embedded 2 cm deep in a turbid medium is recovered successfully with high quantitative accuracy.

8216-16, Session 3

## In vivo 3D image reconstruction from limited view projection fluorescence molecular signals by means of registration with x-ray computed tomography

K. Radrich, A. B. F. Ale, V. Ermolayev, V. Ntziachristos, Helmholtz Zentrum München GmbH (Germany) and Technische Univ. München (Germany)

Fluorescence Molecular Tomography (FMT) is an imaging modality that reconstructs fluorescence biodistribution in small animals, using diffuse optical measurements. A major current advance is the combination of FMT with anatomical imaging modalities, to improve FMT performance. The information of the inner structures of an animal can be employed both in the forward model for allocation of different optical properties to different tissue types, and in the inverse problem as prior information in the regularization term.

We aim to show herein that this kind of hybrid imaging approach can significantly improve the reconstruction quality and accuracy, yielding a more accurate FMT method in-vivo. This work relates to currently disseminated FMT systems, using limited projection scans, and can be employed to enhance their performance. To demonstrate the effectiveness of the approach, we co-registered data sets from phantoms and mice consecutively measured with a limited view projection FMT device and an X-ray CT with the aid of an imaging cartridge providing fiducial markers. Living mice bearing different tumor model types were imaged after administration of targeted near infrared fluorescence probes. The XCT volume was segmented and used as functional and structural prior information to guide the reconstruction. We studied the relative improvements imparted by the use of prior information in the FMT forward and inverse problem, under different implementation schemes and parameters and showcase an optimal implementation that brings optimal imaging accuracy, while demonstrating significant improvements over the stand alone method.

8216-17, Session 3

## Cerenkov emission spectroscopy during radiation therapy treatment to plan fractionation

B. W. Pogue, Thayer School of Engineering at Dartmouth (United States)

No abstract available

8216-18, Session 3

## Fluorescence-enhanced optical tomography and nuclear imaging system for small animals

I. Tan, Y. Lu, C. D. Darne, J. C. Rasmussen, B. Zhu, A. Azhdarinia, The Univ. of Texas Health Science Ctr. at Houston (United States); S. Yan, A. Smith, Siemens Medical Solutions USA, Inc. (United States); E. M. Sevick-Muraca, The Univ. of Texas Health Science Ctr. at Houston (United States)

Near-infrared (NIR) fluorescence is an alternative modality for molecular imaging that has been demonstrated in animals and recently in humans. Fluorescence-enhanced optical tomography (FEOT) using continuous wave or frequency domain photon migration techniques could be used to provide quantitative molecular imaging in vivo if it could be validated against "gold-standard," nuclear imaging modalities, using dual-labeled imaging agents. Unfortunately, developed FEOT systems are not suitable for incorporation with CT/PET/SPECT scanners because they utilize benchtop devices and require a large footprint. In this work, we developed a miniaturized fluorescence imaging system installed in the gantry of the Siemens Inveon PET/CT scanner to enable NIR transillumination measurements. The system consists of a CCD camera equipped with NIR sensitive intensifier, a diode laser controlled by a single board compact controller, a 2-axis galvanometer, and RF circuit modules for homodyne detection of the phase and amplitude of fluorescence signals. The performance of the FEOT system was tested and characterized. A mouse-shaped solid phantom of uniform optical properties with a fluorescent inclusion was scanned using CT, and NIR fluorescence images at several projections were collected. The method of high-order approximation to the radioactive transfer equation was then used to reconstruct the optical images. Dual-labeled agents were also used on a tumor bearing mouse to validate the results of the FEOT against PET/CT image. The results showed that the location of the fluorophore obtained from the FEOT matches the location of tumor obtained from the PET/CT images. Besides validation of FEOT, this hybrid system could allow multimodal molecular imaging (FEOT/PET/CT) for small animal imaging.

8216-19, Session 3

## Time-reversal optical tomography: detecting and locating extended targets in a turbid medium

B. Wu, W. Cai, The City College of New York (United States); M. Xu, Fairfield Univ. (United States); S. K. Gayen, The City College of New York (United States)

Time Reversal Optical Tomography (TROT) is developed to locate extended target(s) in a highly scattering medium, and retrieve their optical strength and size. The approach uses Diffusion Approximation of Radiative Transfer Equation for light propagation along with Time Reversal (TR) Multiple Signal Classification (MUSIC) scheme for signal and noise subspaces for non-iterative determination of target location. A MUSIC pseudo spectrum is calculated using the eigenvectors of the TR matrix T, whose poles provide target locations. Based on the pseudo spectrum contour, retrieval of target size is modeled as an optimization problem, using a "local contour" method. The eigenvalues of T are related to optical strengths of targets. It was found that only the same number of eigenvectors and eigenvalues as the number of targets from the signal subspace associated with the source and detector arrays are needed to extract the optical strength of each target. The efficacy of TROT to obtain location, size, and optical strength of one absorptive target at different positions and of different sizes, and two absorptive targets with different separations, all for different noise levels was tested using simulated data. Target locations were always accurately determined. Error in optical strength estimates was small even at 20% noise level. Target size and shape were more sensitive to noise. Similar results were obtained for scattering targets. Results from simulated data demonstrate high potential for application of TROT in practical biomedical imaging applications. The research is supported in part by USAMRMC.

8216-20, Session 3

## Towards single snapshot multispectral skin assessment

J. Spigulis, D. Jakovels, L. Elste, Univ. of Latvia (Latvia)

A novel skin assessment technology based on logical comparative analysis of the image single-pixel RGB signal values at multi-wavelength illumination is under development. It opens the possibility to obtain multi-spectral imaging information from a single-shot RGB image data set. The first results obtained with color masks, skin chromophore phanthoms and in-vivo skin will be presented.

8216-21, Session 3

## Co-axial electrohydrodynamic atomization for multimodal imaging and image-guided therapy

T. Si, L. Jia, G. Li, X. Yin, Univ. of Science and Technology of China (China); L. Zhang, R. X. Xu, The Ohio State Univ. (United States)

Many microfabrication processes have been explored for encapsulating drugs, genes, antibodies, and contrast agents in biodegradable microparticles for the applications of multimodal imaging and image-guided therapy. However, commonly used processes such as double emulsion are limited by their low encapsulation rate, large size distribution, and potential damage of antibody/gene bioactivity. To overcome these limitations, we fabricated multifunctional microparticles using a coaxial electrohydrodynamic atomization process. The process setup consisted of a customized co-axial needle, a high-voltage power supply, two syringe infusion pumps, a particle collection reservoir, and process monitoring accessories. The instability of coaxial jet flow in electric fields was studied systemically by linear stability analysis based on the classical normal mode method. Different flow modes and their breakup mechanisms were identified mathematically and verified experimentally. The contributing factors to flow instability, such as electrical intensity, electrical conductivity, flow rate, and interfacial tension, were studied mathematically and tested experimentally. Our work provides a quantitative guidance to optimize the co-axial electrohydrodynamic atomization process for the enhanced particle size distribution, high productivity, and large drug-loading efficiency.

8216-22, Session 3

## Combined three-dimensional computer vision and epi-illumination fluorescence imaging system

D. S. Gorpas, D. Yova, K. Politopoulos, National Technical Univ. of Athens (Greece)

There has been an intense scientific interest during the last few years in the field of fluorescence molecular imaging. However, most of the reported methods and systems for the fluorophore distributions reconstruction highlight the need for three-dimensional information of the surface geometry. The scope of this manuscript is to introduce a novel epi-illumination fluorescence imaging system, which has been enhanced with a binocular machine vision system for the translation of the inverse problem solution to the global coordinates. The epi-illumination fluorescence imaging system consists of a structured scanning excitation source, which increases the spatial differentiation of the measured data, and a telecentric lens, which through its orthographic acquisition increases the angular differentiation. On the other hand, the binocular system is based on the projection of a structured light pattern on the inspected area for the solution of the correspondence problem between the stereo pair images. The functionality of the system has been evaluated on tissue phantoms, presenting 0.067±0.004 mm three-dimensional surface reconstruction accuracy, as resulted from the mean Euclidean distance between the three-dimensional position of the real world points and those reconstructed from the system, and more than 80% accuracy for the reconstruction of the fluorophore distributions, as resulted from the absolute mean relative error between the actual fluorophores distribution and the outcome of the inverse problem solution. The inverse problem was confronted with a dual coupled radiation transfer equation and diffusion approximation model and the construction of a database, filled with numerous synthetic fluorescence images.

8216-23, Poster Session

## Single-pass construction of the Jacobian matrix for fluorescence diffuse optical tomography using a perturbation Monte Carlo method

X. Zhang, Duke Univ. (United States)

Image formation in fluorescence diffuse optical tomography is critically dependent on construction of the Jacobian matrix. For clinical and preclinical applications, because of the highly heterogeneous characteristics of the medium, Monte Carlo methods are frequently adopted to structure the Jacobian matrix. Conventional Monte Carlo methods typically compute the Jacobian by multiplying the optical density fields originated from the source at the excitation wavelength and the detector at the emission wavelength, respectively. Nonetheless, this approach assumes that the source and the detector in Green's function are reciprocal, which is invalid in general. This assumption is particularly questionable in small animal imaging, where the mean free path length of photons is typically only one order of magnitude smaller than the representative dimension of the medium. We propose a new method that does not rely on the reciprocity of the source and the detector by tracing photon propagation entirely from the source to the detectors. This algorithm used a perturbation Monte Carlo method to account for the differences in optical properties of the medium at the excitation and the emission wavelengths. Compared to conventional Monte Carlo methods, the proposed method is more valid in reflecting the physical process of photon transport in diffusive media and is more efficient in constructing the Jacobian matrix for densely sampled configurations. Image reconstructions using the proposed method achieved favorable results compared to those using conventional methods.

8216-24, Poster Session

## Near-infrared brain volumetric imaging for neurodegenerative diseases diagnosis: a feasibility study based on Monte Carlo simulation

C. Chuang, National Taiwan Univ. (Taiwan); T. Lan, National Yang-Ming Univ. (Taiwan); C. Chen, National Taiwan Univ. (Taiwan); Y. Hsieh, C. Wang, National Chiao Tung Univ. (Taiwan); C. Lin, C. Sun, National Yang-Ming Univ. (Taiwan)

Brain atrophy is an irreversible brain disease that causes problems with cognitive and memory functions in many diseases, such as mild cognitive impairment (MCI), Alzheimer disease (AD), multiple sclerosis, schizophrenia, alcoholism, and dementia, etc. The quantitative assessment of brain volumetric changes is becoming an important consideration in monitoring the clinical outcome and treatment effects. The reason is because recent considerable advances in neuroimaging and computer technology have allowed the study of brain volumetric changes in vivo, which could provide an accurate, reproducible, and quantitative measure for assessing brain volumetric changes. In this paper, we offer an approach of three-dimensional (3D) brain modeling with image segmentation processes from in vivo MRI T1 data, in order for a comparison of diffuse optical signal among normal, aged and AD subjects with different characterization of brain volumetric changes. To our knowledge, this is the first study to show the structural monitoring for brain volumetric changes detection by using near-infrared diffuse optical imaging via various source-detector separations. Although the penetration depth of near-infrared light is limited by strong scattering in human brain, our simulation result indicates that optical method still allows detecting the volumetric changes of cerebral cortex with brain atrophy that caused the concomitant expanded CSF volume with the white matter and gray matter degeneration, especially in interhemispheric fissure of prefrontal cortex. Because the expanded CSF volume offers light guiding channels, our optical measurement could be a great tool to detect brain volumetric changes for patient-oriented neurodegenerative diseases diagnosis.

8216-25, Poster Session

## Hybrid light transport model-based bioluminescence tomography reconstruction for early gastric cancer detection

X. Chen, J. Liang, Xidian Univ. (China); H. Hu, Fourth Military Medical Univ. (China) and Xijing Hospital (China); X. Qu, Xidian Unv. (China); D. Yang, D. Chen, S. Zhu, J. Tian, Xidian Univ. (China)

Gastric cancer is the second cause of cancer-related death in the world, and it remains difficult to cure because it has been in late-stage once that is found. Early gastric cancer detection becomes an effective approach to decrease the gastric cancer mortality. Bioluminescence tomography (BLT) has been applied to detect early liver cancer and prostate cancer metastasis. However, the gastric cancer commonly originates from the gastric mucosa and grows outwards. The bioluminescent light will pass through a non-scattering region constructed by gastric pouch when it transports in tissues. Thus, the current BLT reconstruction algorithms based on the approximation model of radiative transfer equation are not optimal to handle this problem. To address the gastric cancer specific problem, this paper presents a novel reconstruction algorithm that uses a hybrid light transport model to describe the bioluminescent light propagation in tissues. The radiosity theory integrated with the diffusion equation to form the hybrid light transport model is utilized to describe light propagation in the non-scattering region. After the finite element discretization, the hybrid light transport model is converted into a minimization problem which fuses an l1 norm based regularization term to reveal the sparsity of bioluminescent source distribution. The performance of the reconstruction algorithm is first demonstrated with a digital mouse based simulation with the reconstruction error being 1.38mm. An in situ gastric cancer-bearing nude mouse based experiment is then conducted. The primary result reveals the ability of the novel BLT reconstruction algorithm in early gastric cancer detection.

8216-26, Poster Session

## Bimodal BLT source reconstruction based on adjoint diffusion equations

Y. Hou, J. Liang, X. Qu, D. Chen, S. Zhu, J. Tian, Xidian Univ. (China)

The ultimate goal of medical imaging is to obtain anatomic, functional and molecular information at various levels in tissues, organs, and whole body in vivo, thus exploring solutions to early disease diagnosis, drug development and therapy evaluation. Both miniaturized versions of clinical diagnostic modalities (such as CT, MRI, PET/SPECT and ultrasound) and new emerging modalities (including optical tomography, photoacoustic tomography, etc), have been applied in characterizing the animal model of human disease, as well as developing and screening of new drugs. However, each single modality has its own advantages and limitations. Multimodal imaging is an obvious approach to make overall arrangements for sensitivity and resolution. In this contribution, we report a homebuilt hybrid imaging system consisting of bioluminescence tomography (BLT) and micro-CT, and propose an improved source reconstruction method based on adjoint diffusion equations (ADEs). Compared with conventional methods based on constrained minimization problem (CMP), ADEs-based method replaces expensive iterative computation with solving a group of linear ADEs. Micro-CT is employed to gain 3D volume information, and BLT is used for collecting bioluminescent light on animal surface. Given surface flux density, internal source power density and photon fluence rate can be efficiently determined in one step. Both 2D numerical and 3D physical experiments are designed and performed to evaluate our bimodal BLT/micro-CT system and this novel source reconstruction method. The relevant results demonstrate that both accuracy and efficacy are improved when a priori structural information acquired with micro-CT is incorporated to BLT reconstruction.

8216-27, Poster Session

## Visualization of subcutaneous veins using modulated hyperspectral imaging

J. Katrasnik, F. Pernuš, B. Likar, Univ. of Ljubljana (Slovenia)

Visualization of subcutaneous veins is very difficult with the naked eye, but important for diagnosis of medical conditions and different medical procedures such as catheter insertion and blood withdrawal. Moreover, recent studies showed that the images of subcutaneous veins could be used for biometric identification. For all these applications high contrast images of subcutaneous veins are most useful. However, they are difficult to acquire with current imaging technologies. The majority of existing vein imaging systems based on CMOS or CCD cameras and near infrared illumination cannot acquire high resolution images with depth information. We propose a new method for high contrast imaging of veins with an Acousto-Optic Tunable Filter (AOTF) based hyperspectral imaging system utilizing structured illumination in the near infrared spectral range. Varying the spatial frequency of the structured illumination pattern allows one to control the depth sensitivity inside a turbid medium. Hyperspectral images of the object corresponding to different depths underneath the surface are going to be obtained by using a special reconstruction method based on numerical differentiation of spectral images acquired at different spatial frequencies of the illumination pattern. From these images, spectra of structures underneath the skin surface can be easily obtained. Matching these spectra to the reference vein spectrum will result in high contrast, high resolution, three dimensional images of subcutaneous veins.

8216-28, Poster Session

## Improvement of blood perfusion signal in brain cortex by using depth selective filtering method

H. Kawamoto, M. Fujii, Sophia Univ. (Japan)

Functional near-infrared spectroscopy (fNIRS) is neuroimaging technology which measures absorption changes in near-infrared light and enables us to monitor blood flow in the brain. By using multiple source and detector pairs attached on scalp, we can produce 2-D topographic image of brain activity in real time.

For imaging algorithm, commercially available NIRS devices adopt a simple back-projection method, however, they cannot distinguish the perfusion changes at different depth. Thus, the data are contaminated by skin perfusion. To suppress the disturbing signals from superficial skin layer, we have been proposed depth selective filtering method based on inverse problem.[1] Using the photon diffusion approximation in homogeneous medium.

In this study, we report the experimental result of human forehead by using ten CW source and eight detector. The influence of the surface blood flow was suppressed by applying the depth selective filtering method to the measured data of 30mm distance and 15mm distance. The subjects were instructed to perform an n-back working memory task.

8216-29, Poster Session

## GPU-accelerated Monte Carlo simulation for fluorescence modeling in turbid medium

X. Yi, W. Chen, L. Wu, W. Ma, W. Zhang, J. Li, X. Wang, F. Gao, Tianjin Univ. (China)

In biomedical optics, the Monte Carlo (MC) simulation is widely recognized as a gold standard for its high accuracy and versatility. However, in fluorescence regime, due to the requirement for tracing a huge number of the consecutive events of an excitation photon migration, the excitation-to-emission convention and the resultant fluorescent photon migration in tissue, the MC method is prohibitively time-consuming, especially when the tissue has an optically heterogeneous structure. To overcome the difficulty, we present a parallel implementation of MC modeling for fluorescence propagation in tissue, on the basis of the Graphics Processing Units (GPU) and the Compute Unified Device Architecture (CUDA) platform. By rationalizing the distribution of blocks and threads a certain number of photon migration procedures can be processed synchronously and efficiently, with the single-instruction-multiple-thread execution mode of GPU. We have evaluated the implementation for both homogeneous and heterogeneous scenarios by comparing with the conventional CPU implementations, and shown that the GPU method can obtain significant acceleration of about 20-30 times for fluorescence modeling in tissue, indicating that the GPU-based fluorescence MC simulation can be a practically effective tool for methodological investigations of tissue fluorescence spectroscopy and imaging.

8216-30, Poster Session

## A high-sensitive diffuse fluorescence tomography system with CT-analogous scanning mode

X. Wang, J. Li, X. Yi, L. Wu, W. Ma, W. Zhang, Tianjin Univ. (China); F. Gao, Tianjin Univ. (China) and Tianjin Key Laboratory of Biomedical Detecting Techniques and Instruments (China)

Diffuse fluorescence tomography (DFT) provides spatial distributions of fluorescence parameters by measuring fluorescence signals of probes or agents that are targeted to interior specific molecules or tissues. The potential applications of DFT can be found in drug development and early tumor diagnosis. This work proposes a CT-analogous mode of DFT, where the imaging chamber is impinged by collimated beam from a fiber-coupled laser diode and the resultant fluorescence re-emissions on the opposite side, i.e., the so-called “projections”, are collected by eight detection fibers placed from 101.25° to 258.75° perspectives opposite to the incidence that are then successively filtered out into a photon-counting channel for quantification. By rotating the imaging chamber or phantom at an angular, the system acquires the “projections” of surface-emitted fluorescence under different perspectives as a CT system does. This ease of acquiring a large data-set enables realization of high-quality imaging. Pilot experiments on phantoms with Cy5.5-target embedded have validated the efficacy of the proposed method.

8216-31, Poster Session

## CT-analogous method for high-resolution fluorescence molecular tomography

J. Li, F. Gao, F. Li, L. Zhang, H. Zhao, Tianjin Univ. (China)

In vivo biomedical imaging using near-infrared light must overcome the effects of highly light scattering, which limit the spatial resolution and can affect contrast recovery. The high-resolution, sensitive and quantitative fluorescence optical imaging tool is urgent need for the applications in drug development and early tumor diagnosis. We present a CT-analogous method for fluorescence molecular tomography (FMT) of small animal models for significantly improving the resolution of FMT which is limited to about 5-10% of the diameter of the tissue being imaged. The method combines FMT with fan beam computed tomography using early photons of time-domain optical signals, and is suitable for two dimensional imaging of small size biological models. By use of a normalized Born formulation for the inversion, the algorithm is validated using full time-resolved simulated data for 2D phantom that are obtained from a hybrid finite-element-finite-time-difference photon diffusion modeling, and its superiority in the improvement of the spatial resolution is demonstrated, in comparison with the featured-data algorithm for image reconstruction in time-domain FMT based on diffused photons.

8216-32, Poster Session

## Investigations on shape-based reconstruction method for diffuse fluorescence tomography of breast cancer

L. Wu, Y. Lu, W. Zhang, X. Yi, W. Ma, J. Li, X. Wang, H. Zhao, F. Gao, Tianjin Univ. (China)

A common difficulty for the traditional methods of diffuse fluorescence tomography (DFT) reconstruction is that only a small amount of measurements can be used to recover an image with a large number of pixels, not only leading to expensive computational cost but also likely resulting in an unstable solution prone to be affected by the measurement noise. In this paper, we propose a shape-based approach to DFT reconstruction, which aims to simultaneously recover the smooth boundaries of the tissue regions and the constant fluorescent coefficients within them.

In our protocol, the FDA-approved Indocyanine Green (ICG) agent is used as the fluorophore. Tumor-to-normal ICG contrast is assumed to be two-to-four-fold higher than the hemoglobin-absorption and scattering ones. The fluorescence excitation and detection are accomplished by a multi-channel time-resolved measurement system based on the time-correlated single photon counting (TCSPC) technique. The results have demonstrated that the proposed shape-based approach is able to simultaneously reconstruct the shapes and the constant fluorescent properties of the target regions.

8216-33, Poster Session

## Time-domain diffuse fluorescence tomography of CT-analogous scheme: an experimental validation

F. Gao, P. Zhu, Tianjin Univ. (China)

Non-contact scheme is becoming prevalent to diffuse fluorescence tomography (DFT) since it facilitates instrumentation as well as simplifies experimental procedure. Although non-contact DFT generally uses a CCD camera as the detector to achieve high throughput of the data collection, a fiber-based implementation can make full use of the high-sensitive, time-resolved detection techniques, and also achieve a spatial sampling of high density with a CT-scanning mode. This paper presents a fiber-based, non-contact scheme of the time-domain DFT that combines a time-correlated single photon counting technique and a CT-analogous configuration. A pilot validation of the methodology is performed for two-dimensional scenarios using experimental data. The result convinces the community of the potential of the proposed scheme in improving the image quality.

8216-34, Poster Session

## A time-domain noncontact fluorescence tomography system for breast cancer diagnosis

H. Zhao, H. Guo, T. Wang, F. Gao, Tianjin Univ. (China)

A time domain noncontact fluorescence tomography system and the corresponding reconstruction algorithm towards the early diagnosis of breast cancer are developed. The time domain system based on the time-correlated single photon counting technique is adopted to provide both the high sensitivity in detection and good capability in multi-parameter reconstruction. Comparing to the conventional contact measurement mode, the noncontact system with light scanning can provide more measurement data for improving the spatial resolution of the images. The performance and efficacy of the system is evaluated with measurements on solid phantoms. For the phantom with single fluorescent target, the fluorescence yield and lifetime were simultaneously reconstructed with good quality. For the phantom with two fluorescent targets, the targets with the center-to-center separation of 20mm and the edge separation of 15mm can be distinguished. Measurements also show that the reconstructed yields are linear to the concentration of the fluorescence dye. The results demonstrated the potential of the system in the in vivo diagnosis of the early breast cancer.

8216-35, Poster Session

## Fluorescence-guided diffusion optical tomography based on wavelet transform and singular value decomposition

L. Zhang, W. Zhang, F. Gao, J. Li, H. Zhao, Tianjin Univ. (China)

Diffuse optical tomography (DOT) is a noninvasive method to image the optical properties of tissue and has potential application for optical mammography based on endogenous tissue contrast. At present, the main application barriers of DOT are low spatial resolution, quantitativeness and have not sufficient specificity to distinguish between malignant and benign tumors based on intrinsic optical properties. Fluorescent contrast agents have been considered as a means to enhance tumor detection and characterization. The injected fluorescent agents such as Indocyanine Green (ICG) may preferentially accumulate in diseased tissue because of increased blood flow from neovascularization. As a result of using exogenous fluorescent agents, the specificity and the contrast of DOT can be greatly enhanced and thus facilitate early diagnosis.

By incorporating the merits of FDOT and DOT, we present a scheme for fluorescence guided diffusion optical tomography to reconstruct the fluorescence parameters (yield and lifetime) and optical parameters (absorption and reduced coefficients) using time-resolved data. In this method, the fluorescence parameters were reconstructed at first based on discrete wavelet transform to efficiently improve the spatial resolution and computational efficiency, then the fluorescence images were segmented into background and targets regions by the binary image segmentation strategy to guide and constrain the diffusion optical tomography reconstruction. Due to reducing the reconstruction region of interest, the singular value decomposition was applied to in DOT to improve the reconstruction quality. To validate the proposed method, the numerical simulation was performed.

8216-36, Poster Session

## Development of multimodal microscope combined with confocal imaging and two-photon imaging

W. Chun, D. Do, D. Gweon, KAIST (Korea, Republic of)

Multimodal analysis is essential to improve reliability of analysis results and attractive due to anticipation of innovative results in biochemical researches. Multimodal imaging technology which acquires various images simultaneously for the same interest area plays an important role in the process to synthesize biological information from the images. In this paper, confocal microscope obtaining reflection and fluorescence light signal and two-photon microscope dealing with nonlinear optical signal are operated in the unified platform by sharing scanning mechanism. Reflection light signal, fluorescence signal and nonlinear optical signal at the same focal point are detected through separate channels; these signals are converted into multichannel images respectively with scanning information. Optical system used commonly is customized to satisfy entire requirements for those imaging technologies instead of using commercial microscope platform. Especially relay optics between the scanner and objective lens is designed to compensate chromatic aberration for broadband wavelength region. Wavelength region of used light in the microscope includes fluorescence region (400 nm ~ 750 nm), reflection light region (830 nm) and ultrafast light wavelength region (800 ~ 1000 nm), covering from NUV to IR. The microscope system is designed considering future combination with other imaging techniques and expected to be base platform to complete comprehensive analysis tool through continuous upgrade. The developed system is verified through multichannel images acquisition experiment and comparison discussion.

8216-37, Poster Session

## Orientational characterization of fibrillar collagen in histopathological samples by SHG microscopy and Mueller polarimetry

N. Ortega-Quijano, Univ. de Cantabria (Spain); B. H. Haj Ibrahim, S. Bancelin, M. Schanne-Klein, Ecole Polytechnique (France); A. Nazac, CHU Bicêtre (France); P. Dokladal, E. Decencière, Ecole Nationale Supérieure des Mines de Paris (France); J. L. Arce-Diego, Univ. de Cantabria (Spain); A. De Martino, Ecole Polytechnique (France)

Collagen fibrils confer strength and mechanical resistance to biological tissues. A variety of pathological processes modify the collagen organisation, provoking deterioration in the tissue biomechanics. Therefore, the study of collagen 3D architecture can reveal valuable information about the pathological state of collagenous tissues.

In this work, we focus on genital prolapse, which consists in an abnormal displacement of female pelvis organs from their usual anatomic position. One of the main factors that contribute to the development of a prolapse is the deterioration of the collagen fibrillar network. The aim of this work is to characterize the 3D distribution of collagen fibrils in order to evaluate its potential implications for genital prolapse diagnosis.

To achieve this objective, post-operative histological samples from the vagina anterior wall are measured by two optical techniques, namely second harmonic generation (SHG) microscopy and Mueller microscopic polarimetry. SHG microscopy enables direct visualization of the 3D distribution of collagen fibrils within the tissue, but it requires a complex and expensive multiphoton microscope. On the contrary, Mueller microscopic polarimetry is a cheap and easy technique, but advanced image analysis is required to visualize the collagen fibrils and to obtain their orientation within the tissue. Correlation of both techniques has been evaluated in various aspects to confirm that Mueller microscopic polarimetry is a valuable technique for orientational mapping of fibrillar collagen. The influence of several experimental parameters like tissue thickness, histological sample orientation and measurement wavelength is discussed. Finally, the main characteristics observed in normal and pathological samples are presented.

8216-38, Poster Session

## Examination of a demyelinated fiber by action-potential-encoded second-harmonic generation

X. Chen, Z. Luo, H. Yang, Y. Huang, S. Xie, Fujian Normal Univ. (China)

Axonal demyelination is a common phenomenon in the nervous system in human. Conventional measured approaches such as surface recording electrode and diffusion tensor imaging, are hard to fast and accurately determine the demyelinated status of a fiber. In this study, we first presented a mathematical model of nerve fiber demyelination, and it was combined with second harmonic generation(SHG) technique to study the characteristics of action-potential-encoded SHG and analyze the sensitivity of SHG signals responded to membrane potential. And then, we used this approach to fast examine the injured myelin sheaths resulted from demyelination. Each myelin sheath of a fiber was examined simultaneously by this approach. The results showed that fiber demyelination led to observable attenuation of action potential amplitude. The delay of action potential conduction would be markedly observed when the fiber demyelination was more than 80%. Furthermore, the normal and injured myelin sheaths of a myelinated fiber could be distinguished via the changes of SHG signals, which revealed the possibility of SHG technique in the examination of a demyelinated fiber. Our study shows that this approach may have potential application values in clinic.

8216-39, Poster Session

## Combined intravascular photoacoustic and ultrasound imaging of atheromatous human artery

W. Wei, Univ. of California, Irvine (United States); X. Li, Q. Zhou, The Univ. of Southern California (United States); Z. Chen, Beckman Laser Institute and Medical Clinic (United States)

Intravascular ultrasound (IVUS) is mature imaging modality to diagnose blood vessel disease. Based on the intrinsic optical absorption, intravascular photoacoustic (IVPA) works as a complementary method to IVUS. In this paper, We develop a miniature intravascular probe combined photoacoustic and ultrasound imaging. The optical components and ultrasound transducer were integrated to achieve internal illumination. Healthy human artery and atheromatous human artery were imaged ex vivo, which demonstrates the imaging ability of the multi-functional probe and illustrate its clinical potential.

8216-40, Poster Session

## Quantitative measurements and longitudal study of retinal autofluorescence in the ABCA4 knockout mouse using the combined optical coherence tomography and scanning laser ophthalmoscopy

A. Issaei, L. Szczygiel, N. Hossein-Javaheri, M. Young, Simon Fraser Univ. (Canada); L. L. Molday, R. S. Molday, The Univ. of British Columbia (Canada); M. V. Sarunic, Simon Fraser Univ. (Canada)

Optical Coherence Tomography (OCT) and Scanning Laser Ophthalmoscopy (SLO) are complimentary retinal imaging modalities. We are investigating multimodal cSLO/OCT imaging of a mouse model of Stargardt's Macular Dystrophy which is characterized by retinal degeneration and accumulation of toxic autofluorescent lipofuscin deposits. The purpose of this research is to quantify lipofuscin accumulation over time in the retinal pigmented epithelium of the ABCA4 knockout mouse eye using non-invasive optical measurement of retinal autofluorescence. Fluorescent intensity measurements were performed on ABCA4 knockout mice and wild type controls. Lipofuscin accumulation was measured using a customized fluorescence confocal Scanning Laser Ophthalmoscope (f/cSLO) with 532nm excitation beam. The fluorescent intensity data was standardized against a fluorescent reference and compared at each time-point. Additionally, Optical Coherence Tomography, which is a depth-resolved structural imaging technique, was used to provide information on the retinal cell layers. Structural changes corresponding to retinal degeneration were quantified by measuring the thickness of the Outer Nuclear Layer (ONL). We verified the results from f/cSLO and OCT with standard histology.

8216-41, Poster Session

## Simultaneous dual-band rapidly wavelength-swept laser for real-time endoscopic imaging

N. Goulamhoussen, Ecole Polytechnique de Montréal (Canada); M. Strupler, Sainte-Justine Mother and Child Univ. Hospital Ctr. (Canada) and Ecole Polytechnique de Montréal (Canada); E. De Montigny, Ecole Polytechnique de Montréal (Canada); C. Boudoux, Ecole Polytechnique de Montréal (Canada) and Sainte-Justine Mother and Child Univ. Hospital Ctr. (Canada)

We present a dual band rapidly tunable swept laser simultaneously sweeping wavelengths in the 780 nm and 1310 nm bands. It consists of two separate swept sources using a single polygon for wavelength selection. The simultaneity of the two lasers is obtained by using different facets of the same rotating polygonal mirror in their respective wavelength filters. The polygon's high rotational speed enables a repetition rate of up to 30 kHz, allowing real-time biomedical imaging. The 780 nm source can be tuned between 761 and 798 nm with a single mode fiber output power of 54 mW, while the 1310 nm centered source has a 70 nm wide spectrum with an output power of 20 mW.

This novel scheme allows for synchronous imaging at two different wavelengths to obtain images with different contrast of the same section of a biological sample. Combining both bands could permit tissue oxygenation maps, since the absorption coefficient ratio of oxy-hemoglobin versus deoxy-hemoglobin inverts at 800 nm.

Finally, we show that this laser can be used to create a multimodal imaging system, combining OCT at 1310 nm with spectrally encoded confocal microscopy (SECM) at 780 nm. This multimodal setup allows subcellular resolution imaging with SECM of the first 250 µm of the sample, combined with the lower resolution but millimeter penetration depth of OCT.

# Conference 8217: Endoscopic Microscopy VII

Sunday-Monday 22-23 January 2012

Part of Proceedings of SPIE Vol. 8217 Endoscopic Microscopy VII

8217-02, Session 2

## Fluorescence-based SMC and OCT endoscope

R. A. Wall, J. K. Barton, The Univ. of Arizona (United States)

Optical coherence tomography (OCT) is a non-invasive, interferometric imaging technique capable of imaging up to 2 mm deep in highly scattering tissue. We have previously shown the benefit of combining OCT with other endoscopic imaging modalities. Surface-magnifying chromoendoscopy (SMC) has gained wide-ranging application for early detection of colorectal cancer and its precursors and has shown its ability to discriminate stained normal colonic crypt structure from aberrant crypt foci (ACF), which have been considered an early event in colorectal carcinogenesis.

Our new design is a side-viewing SMC-OCT endoscope 2 mm in diameter that is capable of high contrast crypt visualization, molecular imaging, and cross-sectional microstructure imaging in vivo in the mouse colon. Light for the fluorescence-based SMC system is relayed with a 0.72 mm clear aperture, 30,000 element fiber bundle. OCT is delivered in separate, single mode fibers. The distal optics consist of a gradient-index (GRIN) lens-spacer-annulus system. The GRIN lens and spacer were designed to provide a magnification of 1 at a working distance of 1.58 mm specific to the side-viewing nature of the endoscope, necessary to image the sample through a 0.23 mm thick outer glass envelope as well as an aluminized right-angle prism fixed to the distal end of the GRIN lens assembly. The resulting 1:1 SMC imaging system is theoretically capable of 125 lp/mm resolution across a 0.70 mm field of view. Preliminary testing of the endoscopic system indicates that optical specifications are met.

8217-03, Session 2

## Development of a wide-field SERS imaging endoscope

P. McVeigh, Univ. of Toronto (Canada); R. Mallia, I. Veilleux, Univ. Health Network (Canada); B. Wilson, Univ. of Toronto (Canada) and Univ. Health Network (Canada)

A large body of literature has demonstrated that Raman spectroscopy can be a powerful adjuvant to white light endoscopy in terms of characterising dysplastic tissue, determining tumour margins, or performing optical biopsy of suspicious polyps. In these applications, however, Raman monitoring has always been restricted to a small point focus within the endoscopist's field of view. The addition of a Surface Enhanced Raman Scattering (SERS) based contrast agent allows for the possibility of molecularly specific imaging through the use of targeting moieties such as antibodies/peptides, and the corresponding increase in Raman signal intensity may permit widefield Raman imaging instead of point measurement. Widefield SERS imaging through an endoscope must still overcome the hurdles associated with endogenous Raman measurements: strong background tissue autofluorescence, fluorescence/Raman generated within the endoscopic components, and very low signal levels overall.

Here we report on the design and testing of a prototype widefield SERS imaging system based on a fiber optic bronchoscope using a tuneable filter for Raman signal selection. The SERS contrast agents employed consist of gold nanoparticles encoded with a Raman-active dye and made specific for lung adenocarcinoma tissue through the use of an anti-Epidermal Growth Factor Receptor (EGFR) antibody. By exploiting the extremely narrow character of the SERS spectral peaks we demonstrate a facile method of background fluorescence rejection which may be implemented at video rates. The system has been tested on xenograft tumour samples and properties such as maximum tissue penetration and minimum detectable nanoparticle quantity determined in a standardized fashion.

8217-04, Session 2

## Self-interference fluorescence microscopy

M. de Groot, J. F. de Boer, Vrije Univ. Amsterdam (Netherlands)

We will present Self Interference Fluorescence Microscopy (SIFM), a novel technique that allows 3D fluorescence imaging by self interference depth localization. Because the technique does not require mechanical depth scanning it is ideally suited for incorporation into small endoscopes. The technique is based on the principle of self-interference: by presenting the fluorescent photons with two alternative optical paths they are forced to interfere with themselves. Alternating constructive and destructive interference modulates the detected fluorescence spectrum. The phase of this spectral modulation uniquely determines the depth location of the fluorescent source. We demonstrate that 120 independent depths can be distinguished over the full depth-of-field and we quantify the dependence of the localization accuracy on the signal to noise ratio and the numerical aperture. The accuracy of the technique will be validated by a direct comparison between 3D image stacks obtained with SIFM and standard confocal microscopy. We will show 3D images of microvasculature in excised mouse lungs.

Early cancer diagnosis can be greatly improved by employing fluorescent labels that selectively target tumors. However, effective endoscopic imaging tools are needed to optimally exploit the potential of these markers. Depth resolved imaging of fluorescence will aid in the determination of the extent of invasion of a tumor in the underlying tissue in real time during intervention. The potential integration with OCT will provide both depth resolved tumor location and information about the surrounding tissue architecture. This could improve the effectiveness of therapy and response monitoring.

8217-05, Session 2

## Compact clinical high-NA multiphoton endoscopy

M. Weinigel, H. G. Breunig, P. Fischer, M. Kellner-Hoefer, R. Bückle, K. König, JenLab GmbH (Germany)

Multiphoton imaging methods are excellent for non-invasive imaging of living tissue without any need of additional contrast agents. The increasing demand for endoscopic techniques forced the development of multiphoton endoscopes for imaging of areas with reduced accessibility like chronic wounds. Gradient index (GRIN) lenses can miniaturize the bulky distal focusing optics of conventional tomographs into a diameter of less than 1.6 mm and a numerical aperture (NA) of 0.8.

To enable the examination of wound healing processes we combined a high NA clinical multiphoton endoscope with existing multiphoton tomographs like the DermaInspect® and the MPTflex®.

8217-06, Session 3

## Spectrally encoded flow cytometry for high-resolution microscopy of flowing blood cells in vivo

L. Golan, D. Yeheskely-Hayon, L. Minai, D. Yelin, Technion-Israel Institute of Technology (Israel)

Blood counting is a common clinical test that measures the number and properties of various cells in the blood for diagnosing a wide range of disorders. Currently, cell counting is often performed by ex vivo flow cytometry of a patient's blood sample, although in vivo cytometry of blood cells would, in many cases, provide an immediate, more reliable clinical indication and highlight rapid changes in blood composition. Several techniques for in vivo flow cytometry which require fluorescent labeling are useful mostly for research applications, but would be too invasive for clinical use. Stain-free reflectance confocal microscopes are more suitable for patient imaging, but their limited speed and bulky scanning mechanisms often prevent their use as point-of-care medical devices. By replacing mechanical scanning with spectral encoding, spectrally encoded flow cytometry (SEFC) images reflectance from flowing cells to form an effective two-dimensional confocal image of blood cells, using a scan-free hand-held miniature probe.

In this work, we demonstrate in vivo SEFC of blood flow in the oral mucosa of a human volunteer. The shape, size and flow velocity of red blood cells were clearly resolved, and subcellular features of white blood cells enabled differentiation between different cell types. Potential applications for an SEFC system with a compact, scan-free probe include online noninvasive monitoring of patients during routine and critical care, reducing cost, pain, risk of infections, and increasing diagnosis accuracy and speed.

8217-07, Session 3

## Esophageal endoscopic probe optics for spectrally encoded confocal microscopy

D. Kang, P. Pal, R. W. Carruth, S. Schlacter, B. E. Bouma, G. J. Tearney, Massachusetts General Hospital (United States)

Spectrally encoded confocal microscopy (SECM) is a high-speed reflectance confocal microscopy technology that diffracts different wavelengths of light to distinct locations on the sample. With SECM, images can be acquired 10-100 times faster than video rate using a rapid wavelength-swept source and a large-bandwidth photodetector that are located outside of the patient. The high imaging speed of SECM makes it possible to automatically image entire luminal organs, such as the distal esophagus, by helical scanning of the probe optics. To be utilized for in vivo human imaging, the probe optics needs to simultaneously satisfy the following technical requirements: small probe size for comfortable insertion of the probe, high NA for cellular imaging, and large field-of-view (FOV) for shortening the imaging time. In this paper, we present a new optics design for the SECM endoscopic probe. A custom aspheric singlet (NA = 0.5; clear aperture = 1.8 mm) was designed and used as the objective lens. A 1144-lpmm grating and a wavelength-swept source (central wavelength = 1290 nm; bandwidth = 140 nm) were used for spectral encoding, achieving a FOV of 360 μm with the custom objective lens. The focal plane of the objective lens was tilted relative to the luminal surface of the sample to obtain three-dimensional information over a depth of 88 μm. With the high repetition rate of the swept source, 100 kHz, the SECM endoscopic probe can obtain comprehensive confocal images over the entire distal esophagus with a representative length of 5 cm within 4 minutes.

8217-08, Session 3

## High-speed spectrally encoded confocal microscopy

S. Schlachter, Wellman Ctr. for Photomedicine (United States) and Harvard Medical School (United States); D. Kang, P. Pal, R. W. Carruth, K. Woods, B. E. Bouma, G. J. Tearney, Wellman Ctr. for Photomedicine (United States)

Spectrally Encoded Confocal Microscopy (SECM) is a high-speed, label-free imaging technique that shows great promise for clinical implementation. However, there are still several challenges associated with transitioning SECM from the lab bench to the patient bedside.

Specifically, those challenges include: (1) developing a catheter-based imaging platform that provides sub-micron positioning accuracy in-vivo and (2) increasing the speed of acquisition such that a diagnostically significant area of tissue can be imaged in a reasonable amount of time.

We have addressed the second of these challenges by using a high-bandwidth InGaAs APD combined with an ultra-low-noise amplifier and high-speed ADC, controlled through custom written software. In addition we have developed a wavelength-swept laser source capable of operating at 100kHz.

Using this new instrument we have acquired SECM images at rates in excess of 30 megapixels per second. This is several times faster than any existing reflectance confocal microscopy method, and corresponds to a full HD video frame rate of over 15 fps. A one square-centimeter section of tissue can be imaged with one-micron resolution in well under ten seconds. Combined with the imaging catheter described elsewhere, this advance has enabled the first demonstration of SECM as an in-vivo clinical tool.

8217-09, Session 3

## Spectrally encoded confocal microscopy using a multi-mode, large-core optical fiber

P. Pal, D. Kang, S. Schlachter, R. W. Carruth, B. E. Bouma, G. J. Tearney, Massachusetts General Hospital (United States)

Spectrally encoded confocal microscopy (SECM) is a high-speed reflectance microscopy modality based on the confocal selection of light reflected from the sample. An appropriate diffractive optical element, along with a focusing objective, is employed for interrogating distinct transverse locations on the sample with various wavelengths generated by a multi-wavelength source (such as a wavelength-swept or a broadband source), thus encoding one dimension of spatial information in the optical spectrum. In this paper, we investigate the performance of a commercially available optical fiber (Thorlabs' SM2000) as an illumination/detection conduit with a view to lower speckle contrast of images. This fiber is slightly multi-moded (~7 modes) within our spectral operating region (1320 ± 35 nm) with a core that is ~34% larger than a standard single-mode fiber (Corning's SMF28). We compare the two fibers in terms of resolution, signal collection efficiency, and speckle noise. Although the use of a larger illumination aperture compromises on lateral resolution (~9% reduction) as well as the optical sectioning (which reduces by ~17%), our preliminary measurements show that the use of the SM2000 fiber results in an approximate 20% enhancement of the signal collection and an ~18% reduction in the speckle contrast of the images owing to its larger core size and subsequent multimode nature. In addition, the SM2000 fiber also demonstrates a lower background due to reflections related to the Rayleigh scattering within the fiber itself, which, in conjunction with the aforementioned characteristics, show the potential of this fiber for use in compact probes for SECM.

8217-10, Session 4

## Endoscopic probes for combined optical frequency domain imaging and laser ablation therapy

D. L. Arruda, M. Shishkov, M. L. Villiger, B. J. Vakoc, G. J. Tearney, B. E. Bouma, Wellman Ctr. for Photomedicine (United States)

The integration of minimally-invasive, high-resolution, optical imaging techniques, such as optical frequency domain imaging (OFDI), with laser ablation therapy in a single endoscopic probe presents an exciting new paradigm in the diagnosis and treatment of epithelial diseases. This methodology, termed conformal laser therapy, involves pre-treatment structural mapping using OFDI to define the disease boundary followed by controlled laser ablation therapy in order to accurately match the depth of therapy with the depth of disease. Although many of the component technologies are available, realization of a clinically-viable conformal laser therapy system requires the development of novel endoscopic probes to access epithelial tissues within the body.

Here, we present a novel, double-clad fiber-based endoscopic probe for delivery of conformal laser therapy to the distal esophagus. Two optical channels are housed within a protective sheath that is pressed against the esophageal wall with an inflatable balloon. One channel delivers an OFDI imaging signal via SMF-28 fiber to a distal imaging head for pre-treatment screening. The other channel delivers a co-registered OFDI monitoring signal (1310nm, single mode) with laser therapy radiation (1850nm, 2-5W, multimode) to a more distal imaging head via the core and cladding of a double clad fiber, respectively. Imaging is performed by rapidly acquiring sequential A-lines while the imaging heads are linearly translated at a rate that is comparable to helical, volumetric scanning. Probe design, ZEMAX modeling, bench-level testing, and preliminary results from a study of in vivo porcine esophagus are presented.

8217-11, Session 4

## Endoscopic probe for in vivo and in situ cellular imaging using full-field optical coherence tomography

A. Latrive, A. C. Boccara, ESPCI - Institut Langevin (France) and LLTech (France)

The Full Field OCT technique has proven its good performances in imaging of biological tissue samples. However such a bulky system is not suited for hardly accessible areas of the body and can only be used for imaging of ex vivo pieces. In order to perform an in situ minimally invasive optical biopsy one requires a millimeter-size system such as an endoscopic probe.

Here we present an endoscopic cellular imaging system adapted from the Full-Field OCT principle.

Our approach is to couple two different interferometers. A Michelson-type interferometer is placed after the light source and is used for spectral modulation. A Fizeau common-path interferometer is formed at the distal end of the probe. The probe has a fixed focalization depth within the sample, but a variable scan depth set by the processing interferometer. The advantage of this technique is that all moving parts are exterior to the entirely passive probe. Thus there are no constraints on its size and diameter, allowing designing a very simple and miniature probe.

Our first rigid probe is based on a Graded-Refractive-INdex (GRIN) lens assembly with a diameter of 2 mm and a length of 150 mm. It achieves an axial resolution in tissue of 1.8 µm, a transversal resolution in tissue of 3.5 µm, and a sensitivity of -80dB. Ex vivo images on human breast samples show cellular details such as adipocytes. In vivo images on human skin reveal the different layers of the epidermis up to the junction with the dermis where we can recognize epithelial cells and collagen fibers.

8217-12, Session 4

## Autoregulation of ciliary beat frequency in swine oviduct ex vivo: a micro-optical coherence tomography study

L. Liu, Wellman Ctr. for Photomedicine (United States); B. E. Bouma, Wellman Ctr. for Photomedicine (United States) and Harvard-MIT Health Sciences and Technology (United States); S. M. Rowe, The Univ. of Alabama at Birmingham (United States); G. J. Tearney, Wellman Ctr. for Photomedicine (United States)

The importance of fluid transport by motile cilia to human reproduction has long been recognized. However, the mechanisms by which ciliary beat frequency is regulated through the physical interactions between cilia and gametes and embryos, and their collective influence on the tubal transport efficiency are not clearly understood. Our poor understanding of these processes is in part due to the lack of an investigational tool for visualizing the ciliary motion and dynamic interactions. We have recently developed a novel microscopic technique termed µOCT micro-OCT which provides cross-sectional images of ciliary motion and mocuciliary transport in real-time. In order to test whether or not autoregulatory mechanisms drive ciliary function, artificial mechanical stimulation (glass beads mimicking gametes) was applied to freshly explanted swine fallopian tube epithelium bathed in Krebs solution at 37 degree C. Bead transport, ciliary morphology, and beat frequency was monitored using µOCT in real-time. Cilia height decrease was observed where cilia were in contacted with the bead, and ciliary beat frequency was upregulated by 13.5% with a mean cilia height decrease of 1 +/- SEM µm ($P < 0.05$). Further deformation caused ciliary beat frequency to decrease by 4% ($P = 0.42$), 28% ($P<0.005$), and 49% ($P<0.005$) at cilia height decrease of 2 µm, 3 µm, and 4 µm respectively. We conclude that ciliary beat frequency in swine fallopian tube is autoregulated through a mechanism that senses cilia height decrease in response to external mechanical stimulation.

8217-13, Session 4

## Endoscopic spectral domain optical coherence tomography of murine colonic morphology to determine effectiveness of chemopreventive and chemotherapeutic agents in colorectal cancer

S. LeGendre-McGhee, P. F. Rice, J. Klein, A. Luttman, J. K. Barton, The Univ. of Arizona (United States)

Optical coherence tomography (OCT) is a minimally-invasive imaging modality capable of tracking the development of individual colonic adenomas. As such, OCT can be used to evaluate the mechanisms and effectiveness of chemopreventive and chemotherapeutic agents in colorectal cancer models. This study evaluated $\alpha$-difluoromethylornithine (DFMO) and sulindac for chemoprevention and chemotherapy using mice treated with the carcinogen azoxymethane (AOM). 39 A/J mice were included in the study, comprising two experimental groups (chemoprevention and chemotherapy) subdivided into four therapy groups (No Drug, DFMO, Sulindac, DFMO/Sulindac). 30mm lateral images of each colon at eight different rotations were obtained at five different time points using a 2mm diameter spectral domain OCT endoscopy system centered at 890nm with 3.5µm axial resolution in air and 5µm lateral resolution. Images were visually analyzed to determine number and size of adenomas. Gross photos of the excised colons and histology provided gold standard confirmation of the final imaging time point. Preliminary results show that 100% of mice in the No Drug group developed adenomas over the course of the chemoprevention study. Incidence was reduced to 71.43% in mice given DFMO, 85.71% for Sulindac and 0% for DFMO/Sulindac. In the chemotherapy study, treatment with DFMO and/or sulindac did not regress existing adenoma but appeared to slow the formation of new adenoma. Discrete adenoma size did not vary significantly between experimental groups. Additional studies are currently under way to verify these results.

8217-14, Session 4

## Characterization of sub-squamous intestinal metaplasia (SSIM) pre- and post-radio frequency ablation using three-dimensional optical coherence tomography

C. Zhou, T. Tsai, H. Lee, Massachusetts Institute of Technology (United States); M. Figueiredo, T. Kirtane, VA Boston Healthcare System (United States); Y. K. Tao, O. A. Ahsen, Massachusetts Institute of Technology (United States); D. C. Adler, J. M. Schmitt, LightLab Imaging LLC (United States); Q. Huang, VA Boston Healthcare System (United States); J. G. Fujimoto, Massachusetts Institute of Technology (United States); H. Mashimo, VA Boston Healthcare System (United States)

Radiofrequency ablation (RFA) allows broad and superficial ablation of dysplastic Barrett's esophagus (BE). Standard random four-quadrant pinch biopsy with inherently limited sampling area and depth is likely to under-diagnose patients with sub-squamous intestinal metaplasia (SSIM) that may have potential for dysplastic progression. We used endoscopic 3D optical coherence tomography (3D-OCT) probe passed through the working channel of a standard endoscope to evaluate the presence, size and distribution of SSIM in 31 short segment BE patients treated with RFA at the Boston VA Medical Center. Among them, 23 patients were imaged before complete eradication (CE) of BE, 20 patients were imaged after CE (12 patients were imaged both pre- and post CE). The prototype 3D-OCT system acquires a 20mm x 8mm x 2mm data set with a 5µm axial resolution and 15µm transverse resolution within 20s. This clearly revealed laminar propria / muscular mucosa in the esophagus of all patients, indicating sufficient imaging depth for the evaluation of SSIM. SSIM was identified near the squamous-columnar junction (SCJ) in 83% (19/23) of patients before CE, and in 70% (14/20) of patients after CE. The size of the SSIM was not changed before and after CE. And, most of the SSIM was observed within 3mm from the SCJ. In conclusion, we demonstrate in vivo characterization of SSIM using 3D-OCT, which is a promising technique for evaluating RFA treatment efficacy of BE.

8217-15, Session 5

## Wide-field near-infrared fluorescence endoscope for real-time in vivo imaging

Z. Liu, S. J. Miller, B. Joshi, T. D. Wang, Univ. of Michigan (United States)

Early detection and prevention of colorectal cancer is currently performed with screening colonoscopy where polypoid adenomas are identified and removed. However, non-polypoid adenomas incur a significant miss rate, and may confer a higher risk for malignancy. Improvements in image contrast and resolution for visualizing these pre-malignant lesions may result in reduced mortality and better outcomes. Molecular probes that generate near-infrared (NIR) fluorescence can be used to target disease with high specificity on wide-field endoscopic imaging with reduced autofluorescence background. A NIR endoscope with resolution of 15.6  m at a distance of 3 mm is developed using laser excitation at ex = 671 nm for real time imaging of Cy5.5-labeled peptides. We have previously selected specific peptides using phage display technology. Target (QPIHPNNM) and control (YTTNKH) peptides are conjugated with Cy5.5 using solid phase chemistry. The peptides at a concentration of 100 µM are topically administered to the colon of CPC;Apc mice that are genetically engineered to spontaneously develop adenomas. After a 5 minute incubation period followed by rinsing of the unbound peptide, the fluorescence images collected demonstrate individual dysplastic crypts. Regions-of-interest defined around the adenoma and from adjacent normal appearing mucosa are used to measure the average target-to-background ratio (T/B), which is 3.42 ± 1.30 (n = 8) and 1.88 ± 0.38 (n = 9) for the target and control peptides, respectively, p = 0.007. We demonstrate a novel endoscope that performs real time imaging of colonic dysplasia in vivo with single crypt resolution using a highly-specific NIR fluorescent-labeled peptide.

8217-16, Session 5

## Development of a miniature fibre-based rotary interstitial probe for live deep brain structures fluorescence imaging

J. Crépeau, Y. De Koninck, D. Côté, Univ. Laval (Canada)

A major challenge related to deep brain imaging is to limit the damage caused by the probe while imaging enough tissue to provide good context to the user. This is particularly critical since brain biopsies are rarely possible. Using an en face configuration, the field of view scales with the probe size, thus also with damage.

To work around this problem, we developed a fluorescence rotary interstitial probe inspired from OCT side-viewing probes. Through the juxtaposition of a short piece of Graded-Index fibre and a 48° prism at the end of a single-mode fibre, laser light is focussed on the side of the endoscope. To form an image, the probe turns quickly around its axis (6000rpm) while it is being pulled up slowly by a piezometer. The optical guide is inserted into a 31-gauge stainless steel needle (300µm outer diameter). The first prototype is optimized for fluorescence excitation at 633nm.

The cylindrical symmetry offers several important advantages compared to other endoscopic methods. The first is a better contextual setting of images. It is also possible to image repeatedly with this system, because the probe does not damage the tissue moving back and forth.

We present the development and optical characterization of our fluorescence imaging system. We also present its performances in fixed and live brain tissue. Finally, its inflammatory effect in vivo is assessed.

8217-18, Session 5

## Targeted detection of murine colonic dysplasia in vivo with flexible multispectral scanning fiber endoscopy

B. Joshi, S. J. Miller, Univ. of Michigan (United States); C. Lee, Univ. of Washington (United States); A. Gustad, Univ. of Michigan (United States); E. J. Seibel, Univ. of Washington (United States); T. D. Wang, Univ. of Michigan (United States)

Novel targeted imaging using specific molecular probes has potential to impact diagnosis and treatment of cancer transformation in the digestive tract. Gastrointestinal cancers are heterogeneous and can over express several gene targets that can be imaged simultaneously on endoscopy using multiple probes. In the present work, we have utilized the colon adenoma as a model for detecting pre-malignant mucosa to demonstrate the use of a multi-spectral scanning fiber endoscope for wide-field fluorescence detection. Excitation at 440, 532 and 635 nm was delivered into a single-mode fiber, and fluorescence was collected by a ring of multi-mode fibers placed around the periphery of the instrument. Peptides were selected with phage display technology using the CPC; Apc mouse model of spontaneous colonic dysplasia. Validation of peptide specificity was performed on flow cytometry and in vivo endoscopy. The peptides KCCFPAQ, AKPGYLS, and LTTHYKL were labeled with 7-Diethylaminocoumarin-3-carboxylic acid (DEAC), 5-Carboxytetramethylrhodamine (TAMRA), and CF633, respectively. Separate droplets of KCCFPAQ-DEAC, AKPGYLS-TAMRA, and LTTHYKL-CF633 were distinguished at concentrations of 100 and 1 μM. Separate application of the fluorescent-labeled peptides demonstrated specific binding to colonic adenomas in vivo. Images were quantified by selecting the regions-of-interest from both normal and dysplastic mucosa. The average target/background ratios were 1.71±0.19 and 1.67±0.12 for KCCFPAQ-DEAC and AKPGYLS-TAMRA, respectively. Administration of these two peptides together resulted in distinct spatial patterns of binding in the blue and green channels. Specific binding of two or more peptides can be distinguished in vivo using a novel multi-spectral endoscope to localize colonic dysplasia on real-time wide-field imaging.

8217-26, Poster Session

## 2D resonant in-plane MEMS scanner for dual-axes confocal microendoscope

H. Li, Z. Qiu, Z. Liu, C. C. Rhee, K. Oldham, K. Kurabayashi, T. D. Wang, Univ. of Michigan (United States)

We have developed a high-fidelity, two-dimensional (2D) comb driven resonant in-plane MEMS scanner (RIMS) to perform en-face XY-plane lissajous-pattern scanning for our miniature (OD 5mm) dual axes confocal fluorescence microscope. Combined with a thin-film PZT actuator for z-axis focusing, this RIMS device will be used to collect vertical cross-sectional (XZ-plane) and 3D volumetric imaging in tissue. Based on the parametric resonance driving mechanism, this new 2D MEMS scanner can achieve large oscillation angles (+/-12° optical defection angle degree for both the inner and outer axes at low driving voltage (<60V), corresponding to 800×800 um2 FOV) with a tunable frequency bandwidth close to resonance. On the inner (fast) axis (3.2 kHz), a gold-coated movable silicon plate mirror (30 um thickness, 90% reflectivity at 785 nm) consists of two reflection surfaces connected to each other via an intermediate plate. A gimbaled frame structure on the outer axis(1.1kHz) includes flexure beams on four-bar bridge piers to connect the inner mirror plate to the frame, and comb fingers on complementary sides of the reflective mirror plate and the gimbal frame. Within the 3×3 mm2 chip die, both the outer axis gimbal frame and the inner axis mirror plate have backside structural enhancement islands which provide stronger mechanical structure and reduce deformations during dynamic motion. A “four-mask, three-step deep reactive-ion etching (DRIE)” SOI process has been developed for fabricating the RIMS devices. A during-process protection layer and dry release with laser dicing have been implemented to achieve high device yield (>80%) on 4-inch wafers.

8217-27, Poster Session

## Study of tactile endoscope using silicone rubber membrane based on image processing

K. Yamada, Osaka Univ. (Japan); H. Takahashi, Osaka City Univ. (Japan); T. Nagakura, K. Ishihara, Y. Ohno, Osaka Univ. (Japan)

NOTES is a remarkable endoscope technology which puts an endoscope in the body from the nature aperture. Endoscopic mucosal resection (EMR) has been widely used to treat cancer. Endoscopic submucosal dissection (ESD) allows en bloc resection for intramucosal tumors and reduces local recurrence. In the field of Robotic surgery, the da Vinci and ZEUS are very famous Robotic Surgical Systems. The system seamlessly translates the surgeon’s hand, wrist and finger movements into precise, real-time movements of surgical instruments inside the patient. However, there are big common problems in robotic surgeries. Especially, most serious problem is without having sense of touch, when the surgeon touches any organs using the clamp. Examination by touch is very important technology which senses the stiffness of organ.

We have developed a tactile endoscope using silicone rubber membrane based on image processing. This system consists of silicone rubber membrane, image sensor and illumination system. A surface of the Silicone rubber membrane has any patterns which made by nanotechnology. This pattern is deformed by pressing tissue such as cancer and so on. The deformed pattern is captured by image sensor and is analyzed by image processing.

In this paper, we use the silicone rubber membrane marked both sides with etching technology. These patterns are evaluated by test bed system. We produced evaluation system. The evaluated pattern used on evaluation system. Also, we compared results on evaluation system to computer simulation results. We confirm the effectiveness of evaluation results.

8217-19, Session 6

## Correction of astigmatism in endoscopic OCT for esophageal and coronary imaging

T. Wang, Erasmus MC (Netherlands); A. F. W. van der Steen, Erasmus MC (Netherlands) and Interuniversity Cardiology Institute of The Netherlands (Netherlands); G. van Soest, Erasmus MC (Netherlands)

Endoscopic optical coherence tomography (EOCT) is widely used in biomedical analysis of hollow organs, specifically in the coronary and esophagus circulation. The EOCT catheter generally contains an optical fiber, terminated by a rotating assembly which focuses the light and directs it towards the wall of the organ under investigation, to perform optical scanning and collect backscattering light. The catheter optics is commonly encased in a protective transparent plastic tube. The tube can also act as a negative cylindrical lens, which diverges the light beam along azimuthal direction of the catheter. The beam becomes astigmatic, which will lead to a decrease in transverse resolution and image contrast

In this report, we will numerically analyze this astigmatism for standard catheter designs, and discuss the methods of correction, applicable to esophageal and coronary imaging. For esophageal imaging, as a result of astigmatism, the spot size will be 200μm along azimuthal direction at the focus plane, whereas the ideal beam waist is 20 μm. To maintain image quality, the light beam could be refocused to the focus plane by setting a curved mirror or prism to adjust the divergence angle of light beam. For coronary imaging, the flushing liquid that is used to displace blood aggravates the problem: the spot size approximately doubles along the azimuthal direction and irradiance peak value is reduced by a factor two at the focus plane. In order to handle this situation, another method based on matching refractive indices is described and shown to successfully restore a round beam.

8217-20, Session 6

## Transnasal OFDI catheter for unsedated gastrointestinal imaging

M. Gora, Wellman Ctr. for Photomedicine, Massachusetts General Hospital (United States); E. Coron, Wellman Ctr. for Photomedicine, Massachusetts General Hospital (United States) and Univ. Hospital, Nantes (France); K. Gallagher, Wellman Ctr. for Photomedicine, Massachusetts General Hospital (United States); B. E. Bouma, G. J. Tearney, Wellman Ctr. for Photomedicine, Massachusetts General Hospital (United States) and Harvard-MIT Health Science and Technology (United States)

Barrett's esophagus (BE) is a metaplastic disorder that can undergo dysplastic progression, leading to esophageal adenocarcinoma. Upper endoscopy is the standard of care for screening for BE, but this technique has a relatively low diagnostic accuracy and high cost due to the requirement of conscious sedation.

Optical frequency domain imaging (OFDI) is a high-speed imaging modality that generates cross-sectional images of tissues with a resolution <10 μm sufficient for detecting microscopic tissue architecture. It has been demonstrated that, in combination with a balloon-centering catheter, this method enables BE diagnosis over the entire distal esophagus. At the present time, however, all balloon OFDI procedures have been conducted in conjunction with sedated upper endoscopy.

In order to reduce the cost of the BE screening procedure, we have developed a transnasal OFDI catheter that enables imaging of the esophagus without requiring patient sedation. Our goal was to design a catheter that centers the optics while exerting a minimal effect on tissue surface topology. We have fabricated a wire-based transnasal device in which a set of wires is deployed to center the probe. The outer diameter of the transnasal catheter is less than 16 French (5.34 mm), which is one of the standard sizes for transnasal feeding tubes. The use of the wire-centering mechanism enables sufficient flexibility for the transnasal catheter to be passed through the nasal tract. We have tested the mechanical and optical performance of the new wire-based design in swine esophagus and ileum ex vivo. Imaging was sufficient for diagnosis in many portions of the specimen, while other areas were out of focus. We are continuing to improve the catheter design to enable comprehensive imaging of the esophagus; the next generation catheter will be tested in swine in vivo.

8217-21, Session 6

## Wide-field of view OCT needle probe

B. C. Quirk, R. W. Kirk, P. B. Noble, R. A. McLaughlin, D. D. Sampson, The Univ. of Western Australia (Australia)

Recent work has demonstrated that OCT needle probes are able to acquire high resolution images deep in tissue. However, the field of view of a rotating probe is restricted by the small penetration depth of near-infrared light, typically only 1-2mm. Thus, the overall volume of tissue probed is smaller than desirable for many applications. We have developed an enclosed, linear-scanning OCT needle probe to address this issue. The focusing optics consists of no-core and GRIN fiber spliced to a length of single-mode fiber, all encased within a 22 gauge needle. The beam was deflected at 90 degrees by a polished copper mirror positioned within the needle, and passed through a small window etched into the needle wall. The internal needle was then encased within a larger, enclosing needle, etched with a long lateral slit through which the beam could pass. The internal needle was driven linearly over a range of 12mm by a connecting rod attached to a rotating wheel. Each rotation allowed the acquisition of a 12mm x 2mm B-scan (lateral x axial). Excised, preterm lamb lungs (fresh, not fixed) were imaged during inflation and deflation with saline, and the movement of individual alveoli and larger macroscopic features were simultaneously observed

8217-22, Session 6

## Scanning fiber optic endomicroscope with precise focal-spot localization

K. Murari, W. Liang, Y. Y. Zhang, J. Xi, X. D. Li, The Johns Hopkins Univ. (United States)

Endomicroscopes use miniature beam scanners to move the focal spot in spiral, Lissajous or raster patterns on the sample. Accurate image reconstruction requires knowledge of the spot location in time in order to correlate the measured optical signal to its origin. Physical kinematic models in conjunction with electrical drive waveforms can be used to predict the spot position. However, imprecise manual assembly of the scanners limits the utility of these models.

Measuring the spot position continuously during the scan is the most direct technique for optimal reconstruction. Typical spot sizes and dwell times in microns and microseconds respectively make this a challenging prospect. Analog techniques such as quadrant detectors and lateral effect detectors offer limited accuracy and bandwidth. CMOS or CCD based sensors lack the required frame rate.

We propose a technique for directly imaging the spot position on a 6.4-μm-pixel CCD array using an acousto-optic modulator (AOM) to strobe the excitation light. Strobing permits exposure times under 100 ns with an equivalent frame rate of over 10 million frames/second. We use this to effectively freeze the imaging beam position in time and build up a lookup table of (x,y,t) triplets with (x,y) being the Cartesian coordinates of the beam spot at time t. Sub-pixel spatial accuracy was achieved by focusing the beam to about 30 μm in diameter and calculating the centroid of the resultant region. Experimental results are shown for spiral and Lissajous scans from a multiphoton and an OCT endomicroscope equipped with a piezoelectric fiber-optic resonant scanner.

8217-23, Session 7

## Confocal microlaparoscope for imaging the fallopian tube

T. Wu, R. Schafer, A. R. Rouse, A. F. Gmitro, Univ. of Arizona (United States)

Recent evidence suggests that epithelial ovarian cancer may originate in the fimbriated end of the fallopian tube. Unlike many other cancers, poor access to the ovary and fallopian tubes has limited the ability to study the progression of this deadly disease and to diagnosis it during the early stage when it is most amenable to successful therapy. We have previously reported on a rigid confocal microlaparoscope (CLM) system that is currently undergoing a clinical trial to image the epithelial surface of the ovary. In order to gain in vivo access to the fallopian tubes we have developed a new confocal microlaparoscope with an articulating distal tip. The new articulating instrument builds upon the technology developed for the existing CLM. It has an ergonomic handle fabricated by a rapid prototyping printer, with four control buttons. While maintaining compatability with a 5 mm trocar, the articulating distal tip of the instrument consists of a 1.2 mm diameter bare fiber bundle catheter with automated dye delivery for fluorescence imaging. This small and flexible catheter design should enable the CLM system to image early stage ovarian cancer arising inside the fallopian tube. Early ex-vivo imaging results of human fallopian tube tissue will be presented. These high quality images are similar to that obtained from the epithelial surface of ovaries with the clinical CLM system.

8217-24, Session 7

## Vertical cross-sectional imaging by handheld dual-axes confocal microscope

Z. Qiu, Z. Liu, C. C. Rhee, H. Li, K. Oldham, K. Kurabayashi, T. D. Wang, Univ. of Michigan (United States)

We have demonstrated vertical cross-sectional imaging using a near infra-red (NIR) handheld dual-axes confocal microscope, which is based on a novel scanning and actuation mechanism. The microscope is fully packaged and sealed, encasing a 1D resonant in-plane MEMS scanner (RIMS) and a translational piezoelectric micro-motor. The RIMS device, fabricated by a 3-mask SOI MEMS technology, utilizes a parametric resonance mechanism. With low driving voltage (40 Vpp square waveform), this scanner can achieve a large scanning angle (+/- 5.4 mechanical degrees) with a tunable frequency bandwidth close to the resonant frequency (~3kHz). The dumb-bell shaped mirror (2.71 mm length, 650 um width) surface is coated by Au/Cr to enhance the optical reflectivity (>90% at 785 nm). The imaging probe housing is made by a hybrid method, including 3D-printing polymer structure (Viper™ SLA® system) and aluminum metal components, in which a dedicated package for the scanner and precise optical alignment are implemented. In this scaled down NIR fluorescent imaging instrument, a large field-of-view (600 um by 400 um) can be achieved in the XZ-plane with sub-cellular axial resolution and deep tissue penetration (z-axis) at a 2 Hz frame rate. This view shows directly the relationship among tissue micro-structures as they vary with depth in the epithelium, and is the preferred view of pathologists allowing for real time histopathology to be performed in vivo. For characterization of the vertical cross-sectional imaging instrument, we also have demonstrated a novel structured 3D phantom design with micro-fluidic channel array using ICG dye for contrast.

8217-25, Session 7

## Novel peptide for in vivo confocal imaging of neoplasia in the esophagus

M. B. Sturm, B. Joshi, D. K. Turgeon, H. D. Appelman, T. D. Wang, Univ. of Michigan (United States)

Esophageal adenocarcinoma (EAC) is deadly gastrointestinal cancer with steadily rising incidence in the U.S. Barrett's esophagus, a precursor lesion, can develop in patients with acid reflux. Endoscopic surveillance of high-grade dysplasia (HGD) in Barrett's patients has aided in the early detection of EAC. Dysplastic changes and early cancer are often difficult to identify on white light endoscopy. Fluorescent-labeled peptides that are specific for early cancer can be used to guide tissue biopsy during endoscopy to increase the rate of detection. Few cell surface targets are known for HGD and they lack homogeneity in disease detection. We aim to select, characterize and validate a peptide that binds specifically to early esophageal neoplasia. Using phage display on cultured cells, our lab generated an esophageal cancer binding peptide as a specific molecular probe for in vivo confocal imaging. The fluorescent-labeled peptide ASYNYDAGGGSK-FITC demonstrated specific binding on bound phage counts, ELISA, flow cytometry, competitive inhibition, and fluorescence microscopy. Stereomicroscopy of n=13 specimens showed the fluorescence intensity (mean±SEM) in 1 mm intervals classified as squamous (n=73), metaplasia (n=142), and neoplasia (n=88) was 424±21, 504±25, and 829±37 arb units, respectively. On confocal microscopy of n=23 specimens, increased fluorescence intensity was qualitatively observed on the high grade dysplasia and EAC specimens. In a phase I clinical trial, we present in vivo imaging results (n=13) of the topically applied peptide with the 1000x Cellvizio flexible confocal miniprobe. No adverse toxicity was observed. Peptide imaging agents may have promise for targeting specific detection of early esophageal cancer during endoscopy.

# Conference 8218: Optical Fibers and Sensors for Medical Diagnostics and Treatment Applications XII

Sunday 22 January 2012

Part of Proceedings of SPIE Vol. 8218 Optical Fibers and Sensors for Medical Diagnostics and Treatment Applications XII

8218-01, Session 1

## Investigation of tapered silver/silver halide coated hollow glass waveguides for the transmission of CO2 laser radiation

C. M. Bledt III, J. A. Harrington, Rutgers, The State Univ. of New Jersey (United States); S. Kino, Y. Matsuura, Tohoku Univ. (Japan); J. M. Kriesel, Opto-Knowledge Systems, Inc. (United States)

This study focuses on the theoretical and practical infrared radiation propagation properties of gradually tapered silver / silver iodide coated Hollow Glass Waveguides (HGWs). Tapered HGWs with inner diameter ranging from 300 μm to 650 μm at an approximate rate of 1.5 μm/cm were fabricated and optimized for low-loss transmission of carbon dioxide laser radiation at an emission wavelength of 10.6 μm. The theoretical losses in these silver / silver iodide coated tapered HGWs involving the propagation of light along the waveguide in the direction of increasing diameter as well as in the direction of decreasing diameter are presented. Theoretical calculations used in this study are based on ray-optics analysis. Experimental loss measurements are likewise presented, along with spatial beam profiling, and compared with theoretical values. The experimental bending losses of the tapered HGWs are thoroughly studied and are compared with those measured and expected values for constant bore size silver / silver iodide HGWs involving bore sizes ranging from 300 to 700 μm. Further practical analysis of tapered HGWs includes their mode propagating and high-order mode filtering properties.

8218-02, Session 1

## Microsphere chain fiber tips for multimode filtering of erbium:YAG laser beam during contact tissue ablation

T. Hutchens, A. Darafsheh, The Univ. of North Carolina at Charlotte (United States); H. S. Ying, The Johns Hopkins Univ. (United States); V. N. Astratov, N. M. Fried, The Univ. of North Carolina at Charlotte (United States)

Introduction: Ophthalmic laser surgery may benefit from use of more precise fiber delivery systems. In this study, chains of sapphire microspheres integrated into a hollow waveguide are used for Erbium:YAG laser (wavelength=2940 nm) ablation studies in contact mode with ophthalmic tissues, ex vivo. The Er:YAG laser's short optical penetration depth, highly diverging beam after the contact surface, and small spot diameters achieved with this probe may provide precise tissue removal with limited thermal damage.

Methods: One, three, and five chain structures consisting of ~300-micrometer-diameter sapphire spheres were assembled inside a 5-cm-long hollow waveguide, which in turn was attached to the distal tip of a flexible, 150-micrometer-core-diameter germanium oxide trunk fiber. Porcine corneas were used as a simple model for preliminary laser tissue ablation studies. Histologic analysis of ablation crater depth, width, and thermal damage was conducted.

Results: One, three, and five microsphere chains provided FWHM spot sizes of 67, 32, and 30 μm, respectively, in air, with a peak intensity drop of ~25% for each higher order sphere configuration. Single 100-microJoule pulses with a 300-μs duration produced ablation craters with average full widths ranging from 60-90 micrometers, depths of 20-40 micrometers, and thermal damage zones of 20-30 micrometers.

Conclusions: Microsphere chains produced spatial filtering of the multimode Er:YAG laser beam and fiber providing small spot diameters in contact mode for precise tissue ablation. With further probe development, this approach to mid-IR laser tissue ablation may provide an alternative to mechanical tools for surgical dissection/removal of delicate ophthalmic tissues.

8218-03, Session 1

## Uniform polymer-film formation in 100-μm-bore hollow fiber for Er:YAG laser transmission

K. Iwai, M. Suzuki, Sendai National College of Technology (Japan); M. Miyagi, School Corp. of Tohoku Gakuin (Japan); Y. Shi, Fudan Univ. (China); Y. Matsuura, Tohoku Univ. (Japan)

Flexible 100-μm-bore hollow fibers were developed for Er:YAG laser delivery.The hollow fiber was inner-coated with silver and dielectric layers to enhance the reflectivity at an objective

wavelength band.A dielectric layer is formed by using a liquid-phase coating technique.Micro-tube pump with an inner diameter of 300-μm is newly used to flow polymersolution through the ultra-thin silver

hollow fiber with a constant speed.Fabrication process and transmission properties of the ultra thin polymer-coated silver hollow fiber were discussed.The loss for the 100-μm-bore size, 10-cm-length polymer-coated silver hollow fiber was 1.4 dB at the wavelength of 2.94 μm.

8218-04, Session 1

## Silica hollow-core photonic crystal fibres for mid-infrared applications

A. Urich, R. R. J. Maier, D. P. Hand, Heriot-Watt Univ. (United Kingdom); J. Knight, B. J. Mangan, Univ. of Bath (United Kingdom); J. D. Shephard, Heriot-Watt Univ. (United Kingdom)

In this work we present silica hollow core photonic crystal fibres (HC-PCF) with guidance from 2.6μm up to 3.6μm. The bandgap of these fibres can be controllably scaled and therefore tailored to a specific wavelength of interest e.g. for a specific biomedical application or laser wavelength. As light is confined inside the hollow core with a very small overlap of the guided E-M wave with the fibre material, the high intrinsic loss of silica at these mid-infrared wavelengths can be overcome. The band gap effect is achieved by a periodical structure made out of air and fused silica. As silica is bio-inert, chemically stable and mechanically robust, these fibres have potential advantages over other multi-component, non-silica optical fibres designed to guide in this wavelength regime. These fibres have a relatively small diameter, low bend sensitivity and single-mode like guidance which are ideal conditions for delivering laser light down a highly flexible fibre. Consequently they provide a potential alternative to existing surgical laser delivery methods such as articulated arms and lend themselves to endoscopy and other minimally invasive surgical procedures. In particular, we present the characterisation and performance of these fibres at 2.94 μm, the wavelength of an Er:YAG laser. This laser is widely used in surgery since the wavelength overlaps with an absorption band for water which results in clean, non cauterised cuts. However, the practical implementation of these types of fibres for surgical applications is a significant challenge. Therefore we also report on progress made in developing hermetically sealed end tips for these hollow core fibres to avoid contamination and the launching of laser light into the fibre. This work ultimately prepares the route towards a robust, practical delivery system for this wavelength.

8218-05, Session 1

## Motion artifact handling of forehead photoplethysmograms using a self-mixing interferometric motion reference

R. Wijshoff, M. Mischi, Technische Univ. Eindhoven (Netherlands); A. Van der Lee, P. Woerlee, P. Aelen, N. Lambert, Philips Research (Netherlands); R. Aarts, Technische Univ. Eindhoven (Netherlands)

It is foreseen that photoplethysmography will be applied in ambulatory settings in the near future to measure a patient's heart rate and blood oxygenation. To perform accurate measurements in ambulatory settings, the motion robustness of photoplethysmography has to be improved. Therefore, the aim of this research is to reduce the optical motion artifacts in photoplethysmograms (PPGs).

Motion of the PPG sensor with respect to the skin causes optical motion artifacts in the PPGs. Therefore it has been hypothesized that measuring motion of the sensor with respect to the skin provides a reference that can be used to handle these optical motion artifacts. To measure the sensor motion with respect to the skin, a laser diode configured as an interferometer has been attached to a commercially available forehead PPG sensor. Sensor motion is obtained from the laser's monitor signal, since the laser's monitor diode measures the Doppler signals in the laser cavity that result from motion with respect to the skin.

Measurements are performed on five healthy volunteers with the customized forehead sensor to investigate whether sensor motion can be used to handle the optical motion artifacts. Forehead PPGs and relative sensor motion are measured while the volunteers are walking on a treadmill. A reference for the subject's heart rate is obtained by a simultaneous ECG measurement. The correlation between the relative sensor motion and the motion artifacts is investigated. Results are presented from a signal processing scheme in which motion artifacts are reduced using sensor motion as an artifact reference.

8218-06, Session 1

## Picoliter-volume glucose concentration microsensor based on miniature abrupt-tapered Mach-Zehnder interferometer

Z. Feng, T. Yang, N. Chen, Y. Chen, National United Univ. (Taiwan); Y. Chang, National Changhua Univ. of Education (Taiwan)

We construct ultracompact fiber Mach-Zehnder interferometers (FMZIs) by introducing two micro-abrupt-tapers in a cladding-reduced highly Er/Yb codoped fiber (Fibercore: DF1500Y). We demonstrate that a glucose solution of 72 picoliter is sufficient to shift the resonant dips for 0.8 nm under a concentration variation of 100 mg/dl. The total length of the FMZI is as short as 197.9 um as shown in Fig. 1(a). The spectral responses of FMZI are shown in Fig. 1(b). Fig. 1(a) is taken with a 1000  CCD microscope. The FMZI is fabricated by chemical-etching the cladding of DF1500Y using tiny hydrofluoric acid within a local area before irradiated by the CO2 laser beam. The diameter of the depressed cladding of DF1500Y is 46.3  m while waist diameter of an abrupt taper is about 28.3 m and 34  m, respectively. In our measurement, a drop of 72 picoliter glucose solution with different concentrations (100 mg/dl and 200 mg/dl) is respectively applied to be trapped at one micro-abrupt-taper of the FMZI while a white light comprising superluminescent diodes spanning 1250-1650 nm is launched into the FMZI. The micro abrupt taper can convert part of the core mode into cladding modes and, consequently, the optical path length difference between the core mode and the excited cladding mode is changed with the index variations of the applied liquid. The miniature FMZI presented here is ultracompact, simple, cost-effective, and promising in precision microsensing for the specimen with an ultraminute quantity or in a space-limited situation such as intra-cell sensing.

8218-07, Session 2

## Raman spectral imaging using hollow flexible fiber bundles

T. Tomiyama, T. Katagiri, Y. Matsuura, Tohoku Univ. (Japan)

A flexible fiber bundle based on the hollow optical fiber is developed for remote Raman spectral imaging. The fiber bundle is fabricated by coating silver film on the inner surface of a borosilicate glass poly-capillary tubing formed by the stack-and-draw technique. The minimum bending radius of the fiber bundle (1 mm outer diameter,187 pixels ) is about 40 cm, and the loss for incoherent near infrared light is 1 dB/cm. A Raman spectral image of a sample made of TiO2 and CaCO3 is obtained by combining fabricated fiber bundle and the line-scan imaging system.

8218-08, Session 2

## Silver/polystyrene coated hollow glass waveguides for the transmission of visible and infrared radiation

C. M. Bledt III, J. A. Harrington, Rutgers, The State Univ. of New Jersey (United States)

This study involves the use of polystyrene dielectric thin films in silver coated Hollow Glass Waveguides (HGWs) for broadband transmission of visible and infrared radiation. Polystyrene is an attractive material for use as a dielectric thin film in HGWs due to its relatively low refractive index nearing the optimal refractive index of n = 1.414 for use as a single dielectric thin film in HGWs. Furthermore, its non-toxicity, low cost, and chemical inertness add to its beneficial use as a transparent thin film at both visible and infrared wavelengths. Its broadband transparency allows for its use as a dielectric film in HGWs extending from infrared wavelengths to down to visible wavelengths. The functional properties of polystyrene coated HGWs optimized for broadband transmission are presented, including FTIR spectroscopy, optical attenuation measurements, and spatial beam profiling. The design for the optimization of deposited polystyrene thin films in HGWs based on desired transmission wavelength range is presented.

8218-09, Session 2

## Lifetime prediction for 405-nm single-mode delivery systems for therapeutic laser applications

C. P. Gonschior, K. Klein, Technische Hochschule Mittelhessen (Germany); E. J. Seibel, M. R. Kirshenbaum, Univ. of Washington (United States); T. Sun, City Univ. London (United Kingdom)

Near-UV laser light is used for soft tissue treatment for several years now. In first applications the light was delivered directly from the laser, but for in vivo treatment more flexibility was needed. Multi-mode fibers can be used to achieve a high output power coupled from multi-mode lasers and if fiber bundles are used the power can be increased additionally. But the power density on the treated tissue does not rise proportionally, because of the larger spot. A better ablation can be achieved with a Gaussian beam profile coming from a single-mode fiber. Higher beam quality and higher intensity from a small single-mode core produce power densities in the order of kW/cm² in a focus spot smaller than 100 µm. If the laser therapy is used with the scanning fiber endoscope, treatment in between imaging spirals can be employed and only a single fiber is required. 405 nm laser-induced fluorescence may be able to produce both wide-field fluorescence imaging and laser therapy in a single laser. However additional wavelengths combiners and dual-clad couplers are necessary for multi-wavelength reflectance imaging requiring increased input power to compensate for the losses of these devices. This leads to very high intensities at the fiber coupler and as shown before damage will occur at this interface. Differences in damage rate due to differently treated fiber end-faces will be discussed. We suggest a new loss mechanism which is basal for the end-face damage and show miscellaneous methods to reduce the occurring damage and enhance the system lifetime.

8218-10, Session 2

## Image-guided intervention in the human bile duct using scanning fiber endoscope system

E. J. Seibel, Univ. of Washington (United States); J. A. Jo, Texas A&M Univ. (United States); C. D. Melville, R. S. Johnston, C. R. Naumann, M. D. Saunders, Univ. of Washington (United States)

Bile duct cancers are increasing in frequency while being difficult to diagnose. Currently available endoscopic imaging devices used in the biliary tree are low resolution with poor image quality, leading to inadequate evaluation of indeterminate biliary strictures. However, a new ultrathin and flexible cholangioscope system has been successfully demonstrated in a human subject. This mini-cholangioscope system uses a scanning fiber endoscope (SFE) as a forward-imaging guidewire, dimensions of 1.2-mm diameter and 3-m length. Full color video (500-line resolution at 30Hz) is the standard SFE imaging mode using spiral scanning of red, green, and blue laser light at low power. Image-guided operation of the biopsy forceps was demonstrated in healthy human bile ducts with and without saline flushing. The laser-based video imaging can be switched to various modes to enhance tissue markers of disease, such as wide-field fluorescence and enhanced spectral imaging. In parallel work, biochemical discrimination of tissue health in pig bile duct has been accomplished using fiberoptic delivery of pulsed UV illumination and time-resolved autofluorescence spectroscopic measurements. Implementation of time-resolved fluorescence spectroscopy for biochemical assessment of the bile duct wall is being done through a secondary endoscopic channel. Preliminary results indicate that adequate SNR levels (> 30 dB) can be achieved through a 100 micron fiber, which could serve as an optical biopsy probe. The SFE is an ideal mini-cholangioscope for integration of both tissue and molecular specific image contrast in the future. This will provide the physician with unprecedented abilities to target biopsy locations and perform endoscopically-guided therapies.

8218-11, Session 2

## Infrared spectral imaging by hollow-optical fiber bundle

C. Huang, S. Kino, T. Katagiri, Y. Matsuura, Tohoku Univ. (Japan)

A system for endoscopic spectral imaging in the infrared that has potential capability for early detection of tumor and diagnosis of arterial sclerosis is developed. The system includes an FT-IR spectrometer with an infrared focal-plane array and a bundle of thin, hollow-optical fibers. High-speed Fourier transfer calculation and image processing enable remote observation of spectral images in the infrared. In the preliminary experiment, an image of lipid in lean tissue is observed by detecting absorption band of cholesterol.

8218-12, Session 2

## TBD

I. Gannot, Tel Aviv Univ. (Israel)

No abstract available

8218-13, Session 3

## Small-diameter hollow waveguides based on silver-clad stainless steel tube for infrared laser light transmission

A. Hongo, M. Ohkawa, N. Shiina, S. Sato, Hitachi Cable, Ltd. (Japan)

We fabricated hollow waveguides based on a silver-clad stainless steel tube for delivery of infrared laser light such as Er-YAG and CO2 laser light. The inside wall of the silver-clad layer was polished to a mirror-smooth state. A thin AgI layer was formed by iodination of the inner surface of the silver layer to enhance reflection of the propagating infrared light at the inner wall of the hollow waveguide. The inner and outer diameters of the waveguide are 0.4 and 0.6 mm, respectively. Since this type of metallic hollow waveguide has high mechanical strength and heat resistance, the waveguide hardly breaks or melts. Moreover, it has such small diameter that it can be bent flexibly. We experimentally fabricated a 1-m long hollow waveguide with inner AgI layer 0.24 um thick, which is optimum thickness for Er-YAG laser light transmission. The transmittance of Er-YAG laser light was 64 % under straight conditions. In this measurement, we used an Er-YAG laser source producing multi-mode oscillation (M2 ≒ 12). The Er-YAG laser light was launched into the waveguide by using an incident CaF2 lens with a focal length of 50 mm. By optimizing the thickness of the inner AgI layer according to the propagating light, CO2 laser light can be also transmitted effectively though the hollow waveguide.

8218-14, Session 3

## Effects of high humidity and high temperature on failure of optical fiber for high-power delivery

X. Sun, J. Li, OFS (United States)

Large core silica optical fiber has been successfully used for delivering high power laser for medicine. In a typical medical application, the fiber will experience high power laser, tight bends, and high humidity. Therefore its mechanical strength under these conditions is essential. In our previous studies, we have investigated the failures of several types of step-index optical fibers using lasers at various wavelengths (532 nm, 755 nm, 1064 nm and 2140 nm) in tight bends. We have shown that the polymer cladding/coating plays an important role in the failure rate. By improving the polymer coating/cladding, failure rate of the fiber under bend and high power can be reduced and the reliability of fibers significantly improved. In this study, we further examine the performance of the fiber after its treatment in a high humidity and high temperature condition similar to that in an autoclave. High temperature and high humidity may change the properties of the polymer coating. Specifically, we will study the transmitted laser power, far filed pattern and failure rates of different optical fibers (as-received and after humidity-temperature treatment samples) using a two point bend tester and a high power pulsed laser at 1064 nm.

8218-15, Session 3

## Metal-assisted guided-mode resonance device for biosensing

S. Lin, W. Chen, J. Chang, National Central Univ. (Taiwan)

The guided mode resonance (GMR) device has been applied to biosensing since its resonance wavelength was found sensitive to the refractive index. A conventional GMR device is composed with a subwavelength grating and a planar waveguide. The GMR device reflects a specific wavelength by choosing a proper grating period and waveguide thickness. The GMR phenomenon shows a narrow stop band in the transmission spectrum. However, the sensitivity of GMR biosensor is one order lower than surface plasmon resonance (SPR) biosensor.

In this study, a metal buffer layer is added at the rear of the GMR device. The metal buffer layer terminate the resonance wave penetrating into the substrate, thus, the resonance wave extend to the other side of the device (usually the analytes). According to the simulations, the sensitivity of metal assisted guide mode resonance (MaGMR) sensor is 4-fold higher than the conventional GMR sensor.

8218-16, Session 3

## Multilayer silver/dielectric thin-film coated hollow waveguides for sensor and laser power delivery applications

C. M. Bledt III, J. A. Harrington, Rutgers, The State Univ. of New Jersey (United States); J. M. Kriesel, Opto-Knowledge Systems, Inc. (United States)

Hollow Glass Waveguides (HGWs) incorporating single dielectric thin film designs deposited on silver coated silica hollow waveguides have been used for low-loss transmission of infrared radiation in the 2 - 14 micrometer region. Silver iodide has traditionally been the material of choice as a dielectric thin film in HGWs, with other dielectric thin film materials such as cadmium sulfide and lead sulfide being used as well. The incorporation of multilayer stacks of alternating low and high refractive index dielectric thin films in HGWs has been theoretically shown to further reduce the optical attenuation. Theoretically, lower losses are achieved when the refractive index contrast of the two thin film materials used is high and the number of films incorporated in the HGW film structure increases. This study involves the practical design of multilayer dielectric stacks in HGWs, with lead sulfide and cadmium sulfide as high refractive index materials and polystyrene, cadmium sulfide, and zinc sulfide as low refractive index materials. The design, optimization, and processing methodology for achieving low-loss multilayer dielectric stacks in HGWs at desired infrared wavelengths is discussed. Characterization of multilayer dielectric coated HGWs includes FTIR spectroscopy, optical attenuation measurements, and optical beam profiling. The loss dependency of dielectric coated HGWs on the particular thin film materials used and number of dielectric layers incorporated is thoroughly studied and compared with both losses attained for single dielectric coated HGWs as well as those predicted by theory.

8218-17, Session 4

## Microtapered long-period fiber gratings for application to a radiation dosimeter

Y. Han, H. Kim, Hanyang Univ. (Korea, Republic of); Y. Ji, Korea Institute of Radiological & Medical Sciences (Korea, Republic of)

We have fabricated periodically micro-tapered long-period fiber gratings (MT-LPFGs) by using a micro-tapering technique for application of a radiation dosimeter. The fundamental core mode can be coupled to the cladding mode by tapering an optical fiber periodically, which produces resonant peaks in transmission spectrum. The periodic refractive index modulation of MT-LPFGs results from the residual stress and the densification of the silica induced by heating and elongation processes in the micro-tapering technique. Since MT-LPFGs do not depend on glass photosensitivity that is required for UV-induced fiber gratings such as fiber Bragg gratings (FBGs) and conventional long-period fiber gratings (LPFGs), MT-LPFGs can be fabricated with any types of optical fibers, such as photonic crystal fiber or rare-earth-doped fiber without photosensitivity. If the optical fibers are exposed to radiations, their optical properties are changed due to the formation of color centers and the modification of the glass matrix depending on the doping materials. Therefore, radiation sensitivities of MT-LPFGs can be adjusted by selecting suitable optical fibers with different doping materials. The MT-LPFGs with the total length of 2 cm and the period of ~1300 nm was fabricated by using germanosilicate single-mode optical fibers and the effect of gamma radiation on the transmission characteristics of the MT-LPFGs is investigated. As the MT-LPFGs were irradiated with 1.25-MeV 60Co gamma rays, the resonant wavelength was linearly shifted to longer wavelengths. The resonant wavelength shift of 1.1 nm was observed for total dose of 500 Gy at dose rate of 2Gy/min. Consequently, the radiation-induced refractive index change resulted in the resonant wavelength shift of the MT-LPFGs, and the radiation sensitivity of the proposed MT-LPFG was estimated to be 2.2 pm/Gy, which is much higher than that of the FBGs (0.3 pm/Gy). It should be noted that the linear sensitivity of the MT-LPFGs is different from that of UV-induced LPFGs that are insensitive gamma radiation due to the effect of UV-radiation, which eliminates the precursors of gamma radiation-induced color centers in the process of grating writing.

8218-18, Session 4

## Design and fabrication of hollow fiber-based Raman tweezers for bioparticle measurement

Y. Morisaki, T. Katagiri, Y. Matsuura, Tohoku Univ. (Japan)

The optical trapping is useful to suppress random motions of particles when one analyzes a single particle in solutions. Recently, this technique has been combined to Raman spectroscopy and applied for the analysis of bioparticles such as blood cells and bacteria. In this report, we design and fabricate a flexible fiber Raman tweezers which consist of the hollow optical fiber and a high-index lens. The Raman measurement of optically trapped single red blood cell using fiber Raman tweezers is demonstrated.

8218-20, Session 4

## Real-time bio(chemical)sensing with clad etched fiber Bragg grating

G. R. Prashanth, S. B. Nanjunda, S. Asokan, M. M. Varma, Indian Institute of Science (India)

Fiber bragg grating (FBG) sensors have been extensively used for strain and temperature sensing where the grating pitch is modified by these variables leading to a shift in the Bragg wavelength. By etching the clad region and exposing the core of the FBG, we increased the interaction of the guided optical mode with the surrounding medium and consequently increased the refractive index sensitivity of our FBG sensors by more than two orders of magnitude compared to cladded FBGs, enabling their use in bio(chemical) sensing. We functionalized the exposed core region of these FBG sensors with polyelectrolytes, which are charged polymer species which can electrostatically adsorb proteins, DNA and other biological entities. By monitoring the Bragg wavelength shift of two etched FBGs in a differential manner, we studied the adsorption kinetics of sequential multilayer deposition of alternately charged polyelectrolytes with good temporal resolution and refractive index sensitivity in the range of 10^-5 RIU. We have shown that these polyelectrolyte layers respond to several variables such as pH, presence of ions and so on permitting their measurement with the FBG sensor. In addition, we have shown that proteins can be immobilized on these polymer layers and retain their activity and therefore can be used in various biosensing applications. Unlike conventional biochip based sensors, this fiber based biosensing platform is capable of real-time in-vivo sensing via an endoscope or similar instrument. We will present our work on developing various applications, such as the ones described above, of FBG sensors functionalized with polyelectrolyte mutlilayers.

8218-21, Session 4

## Highly birefrengent terahertz hollow fiber: design, fabrication, and experimental characterization

X. Tang, Y. Shi, Fudan Univ. (China)

Dielectric-coated metallic hollow fibers have been identified as an efficient means of delivering terahertz hollow waves. Elliptical cross section is introduced to achieve high birefringence in dielectric-coated metallic hollow fibers. By use of finite element method, effective refractive indices of the two polarizations of the HE11 mode, the modal power fraction in the air core and the birefringence of the fiber are presented. Owing to the high reflectivity of the inner coatings, more than 99% of the fundamental mode power can be confined in the air core. Emphasis is put on the optimization of the fiber geometry to lower the transmission loss and to increase the birefringence. It is found that a desirable ellipticity of the air core is around 3. For a given wavelength and a fixed ellipticity, both the birefringence and the transmission loss are inversely proportional to the cube of the fiber bore-size. Polymer coated silver hollow fibers with elliptical bores are fabricated by coating the inner face of elliptical tubes with layers of silver (Ag) and COP (cyclic olefin polymer). The elliptical supporting tubes are obtained by squeezing the round capillaries in transversal direction. The loss and birefringence properties are experimentally characterized.

8218-22, Session 5

## Highly efficient excitation and detection of whispering gallery modes in a dye-doped microsphere using a microstructured optical fiber

K. J. Rowland, A. Francois, T. Monro, The Univ. of Adelaide (Australia)

A platform for the excitation of Whispering Gallery Modes (WGMs) has been demonstrated using a dye-doped microsphere positioned onto the tip of a microstructured optical fiber with a suspended, micron scale, core. With this configuration, we have shown that both the excitation and collection efficiency of the WGMs modulated fluorescence spectra of the dye are greatly improved compared to a more conventional (objective coupling) excitation and collection scheme; an overall efficiency increase by a factor of 200 is demonstrated. It is also shown, by using the fibre-attached microsphere in a dip sensor configuration, that positioning the resonator onto the fiber tip does not impact its sensitivity, providing a compact and robust architecture for applications such as localized in-vivo/vitro biosensing.

8218-23, Session 5

## Label-free DNA biosensor based on double tilted fiber Bragg grating

A. Candiani, M. Sozzi, A. Cucinotta, S. Selleri, R. Veneziano, R. Corradini, R. Marchelli, Univ. degli Studi di Parma (Italy); P. Childs, S. Pissadakis, Foundation for Research and Technology-Hellas (Greece)

Double Tilted Fiber Bragg Gratings (DTFBGs) are a very powerful fiber optic device for biosensing applications, due to their high sensitivity. The presence of the two tilted Bragg gratings induces the formation of interference fringes in the Bragg, ghost and higher order cladding modes, visible in the transmission spectrum of the fiber. By analyzing the change of the interference fringe visibility of the ghost mode (related to the refractive index changes on the fiber surface) it is possible to detect the presence of a biomolecular layer; thus avoiding the use of labeled DNA strands. The fringe visibility is calculated via Fourier analysis of the transmission spectra.

In the present work a DTFBG has been inscribed in a standard photosensitive optical fiber. Subsequently the external surface of the optical fiber has been modified by covalent linking of peptide nucleic acid (PNA) probes. DNA molecules, complementary to the PNA probes, have been linked to the fiber cladding itself. Experimental measurements show a well defined change in visibility for a 10 nM DNA solution. The visibility modulation has been observed in different experiments on the same fiber, at the same concentration, proving good reliability and reproducibility of the results, suggesting that a re-use for several measurements is possible. Tests have been also made using a 10 nM mismatched DNA solution, containing a single nucleotide polymorphism, showing high selectivity of the sensor.

8218-24, Session 5

## Miniature fiber optic force sensor for vitreoretinal microsurgery based on low-coherence Fabry-Pérot interferometry

X. Liu, I. Iordachita, R. H. Taylor, J. U. Kang, The Johns Hopkins Univ. (United States)

Vitreoretinal surgery requires delicate manipulation of retinal tissue. However, tool-to-tissue interaction forces in the order of sub-millinewton are usually below human sensory threshold. A surgical force sensor (FS) compatible with conventional surgical tools may significantly improve the surgery outcome by preventing tissue damage.

We designed and built a miniature FS for vitreoretinal surgery using a fiber optic common-path phase-sensitive spectral domain optical coherence tomography system (CP-PS-SD-OCT) where the distal end of the fiber probe forms a low-finesse Fabry-Pérot (FP) cavity between the cleaved tip of the lead-in single mode fiber and the polished surface of a stainless steel rod. The lead-in fiber and the stainless steel rod are bonded together by a 6-layer Nitinol flexure which deforms proportionally to the force exerted to the FS and thus changes the length of the FP cavity in the order of nano meter. The fabricated FS has an outer diameter of 0.8mm which enables us to integrate it into a 18- gauge surgical tool such as a forceps or a surgical needle.

To accurately measure the change of the FP cavity length, the cavity is interrogated by the fiber optic CP-PS-SD-OCT operating at 840nm. The phase extracted from the interferometric signal varies proportionally as the cavity length change. Experimental results show that the phase-sensitive measurement leads to a displacement sensitivity as high as 50pm.

We have conducted calibration experiments which shows that our FS responses linearly to force in axial direction with force sensitivity better than 0.25 millinewton.

8218-25, Session 5

## Dispersive Fourier transform using few-mode fibers for real-time and high-speed spectroscopy

Y. Qiu, C. Zhang, K. K. Y. Wong, K. K. Tsia, The Univ. of Hong Kong (Hong Kong, China)

Dispersive Fourier transform (DFT) is a powerful technique for real-time and high-speed spectroscopy. In DFT, the spectral information of an optical pulse is mapped into time using group velocity dispersion (GVD) in the dispersive fibers with an ultrafast real-time spectral acquisition rate (>10 MHz). Typically, multi-mode fiber (MMF) is not recommended for performing DFT because that the modal dispersion, which occurs simultaneously with GVD, introduces the ambiguity in the wavelength-to-time mapping during DFT. Nevertheless, we here demonstrate that a clear wavelength-to-time mapping in DFT can be achieved by using the few-mode fibers (FMFs) which, instead of having hundreds of propagation modes, support only a few modes. FMF-based DFT becomes appealing when it operates at the shorter wavelengths e.g. 1-μm range - a favorable spectral window for biomedical diagnostics, where low-cost SMFs and high-performance dispersion-engineered fibers are not readily available for DFT. By employing the telecommunication SMFs (e.g. SMF28), which are in effect FMFs in the 1-μm range as their cut-off wavelength is ~1200 nm, we observe that a 20-nm wide spectrum can be clearly mapped into time with a GVD as high as -0.33 ns/nm and a loss of ~2 dB/km at a spectral acquisition rate of 20 MHz. Moreover, its larger core size than the high-cost 1-μm SMFs renders FMFs to exhibit less nonlinearity, especially high-power amplification is implemented during DFT to enhance the detection sensitivity without compromising the speed. Hence, FMF-based DFT represents a cost-effective approach to realize high-speed DFT-based spectroscopy particularly in the biomedical diagnostics spectral window.

8218-26, Session 5

## Optimal design for hollow fiber inner-coated by dielectric layers with surface roughness

B. Sun, X. Tang, Y. Shi, Fudan Univ. (China); K. Iwai, Sendai National College of Technology (Japan); M. Miyagi, School Corp. of Tohoku Gakuin (Japan)

Hollow fibers have found applications in high power and ultra-short pulse laser light delivery, gas sensing, Raman detection and wide band spectroscopy. Single dielectric layer coated metallic hollow fiber has been studied for many years and achieved low-loss property and high durability. However, it has an additional loss caused by bending. One of the most effective methods to reduce the bending loss and transmission loss is to deposit multiple dielectric layers. It has been reported that several different kinds of metallic multilayer fibers were proposed and fabricated successfully. However, they all observed that the measured loss is much larger than the theoretical calculations. This is because transmission characteristics of the multilayer fiber are more dependent on surface roughness of dielectric films.

In this paper, we theoretically discuss the influence of film roughness on the optimal design for the multilayer hollow fiber. Comparisons of fibers with smooth and rough films are made and discussed in detail. The optimal design for film thickness, inner radius, the number of layers and refractive indices is presented. It is shown that surface roughness changes the optimum thickness of each layer. The layer with higher refractive index has a greater influence on the transmission loss than that of the lower refractive index. The optimum number of layers exists when the films are rough. The calculation results are useful for structure design, material selection and further fabrication of metallic multilayer hollow fiber when considering imperfections in film coating techniques.

8218-27, Session 5

## Dy:PbGa2S4 laser radiation and its delivery by hollow waveguide

H. Jelinkova, M. Nemec, Czech Technical Univ. in Prague (Czech Republic); M. Miyagi, K. Iwai, H. Takaku, Sendai National College of Technology (Japan); M. Doroshenko, T. Basiev, A. M. Prokhorov General Physics Institute (Russian Federation); V. Badikov, D. V. Badikov, Kuban State Technological Univ. (Russian Federation)

The mid-infrared radiation generated by bulk Dy:PbGa2S4 laser working at the room temperature was characterized and for its delivery the special type of COP/Ag hollow waveguide was used. The coherent pumping of Dy:PbGa2S4 laser was performed by flashlamp pumped Er:YLF laser with 1.73 um wavelength. The compact 60 mm long Dy:PbGa2S4 laser oscillator worked in free-running regime with the repetition rate 1.8 Hz. The output energy was 3.1 mJ in 80 us long pulse at 4.3 um wavelength. The space structure was close to Gaussian.

The goal of the presented study was the preliminary investigation of the mid-infrared Dy:PbGa2S4 radiation delivery possibility by the cyclic olefin polymer and silver coated hollow glass waveguide. The length of waveguide was 103 cm and the inner diameter was 700 μm. The thickness of the polymer inner layer was calculated and manufactured for the optimal 4 um radiation transmission. Mid-infrared laser radiation was guided into waveguide by the CaF2 lens with the focal length 55 mm. The characterization of delivered 4.3 μm radiation was provided. It was observe that the space structure is changing essentially which follows from the transmission principle of the hollow waveguide. As conclude the delivery system for 4.3 μm mid-infrared Dy:PbGa2S4 laser radiation was investigated for the first time.

8218-28, Session 6

## Characterization of atherosclerotic plaque depositions in vivo by fiber optic Raman spectroscopy and ex vivo by FTIR imaging

C. Matthäus, S. Dochow, C. Krafft, Institut für Photonische Technologien e.V. (Germany); A. Lattermann, Friedrich-Schiller-Univ. Jena (Germany); B. R. Brehm, Universitätsklinikum Jena (Germany); J. Popp, Institut für Photonische Technologien e.V. (Germany)

The combination of Raman and infrared spectroscopy with conventional light microscopy enables analyzing the biochemical composition of atherosclerotic plaques without markers in a non-destructive way. Arterial plaque-depositions that are mainly composed of proteoglycans, triglycerides, cholesterol, cholesterolester and calcium apatite were induced in rabbits by high cholesterol diet. Thin sections were prepared and studied in transmission mode using a FTIR imaging spectrometer with a 64×64 focal plane array detector (Agilent, USA). A small diameter (1 mm) fiber optic probe with one excitation and 11 detection fibers (Emvision, USA) was coupled to a Raman spectrometer (Kaiser Optical Systems) to study excised arteries ex vivo and rabbit arteries in vivo. For data analysis and image reconstruction multivariate algorithms such as vertex component analysis (VCA) were applied. The individual plaque components were spectroscopically identified. The IR and Raman spectra indicate variations in the composition of these plaques. Furthermore, spectroscopic imaging shows the plaque distribution and compositions in a more quantitative manner than traditional staining techniques. The results are in good agreement with the histopathology and demonstrate how IR and Raman spectroscopy can complement standard histopathologic tools.

8218-29, Session 6

## Spectral ATR-sensor with variable pass lengths

K. Klein, C. P. Gonschior, Technische Hochschule Mittelhessen (Germany)

Using new light-sources together with selective mode-excitation, the spectral light-guidance of meridional and skew modes in different step-index fibers was studied. Due to the polymer cladding materials, the numerical aperture of silica-based fibers (HCSF) has been increased significantly. Therefore, the maximum propagation angle in these fibers can be increased significantly;

Because the penetration depth of ATR-sensors depends on the propagation angle, different shaped ATR-sections of interaction with removed cladding have been realized. With the new approach, the pass length in the active ATR-section can be adjusted using different meridional rays/modes. However, low mode conversion in the light-transporting section of the HCSF is required.

After discussing the spectral properties of the HCS fibers, the absorption of selected liquids/substances surrounding the light-guiding core will be shown in dependence of the wavelengths. Especially, the possibilities to change from low to high propagation angles including the excitation and detection system will be discussed. Finally, the impact to sensor applications on different fields will be shown, too.

8218-30, Session 6

## Behavior of polymer cladding materials under extremely high temperatures

T. E. Clark, SSCP USA (United States); S. Chang, SSCP Co., Ltd. (China); J. Oh, SSCP Co., Ltd. (Korea, Republic of)

Polymer claddings with various low refractive indices for use with silica core fibers were developed. Applications for fibers with these claddings include fiber lasers and transmission of high power lasers in surgery. For many applications, the possibility of operating fibers under high temperatures for extended durations is desirable. In another publication the results of testing a polymer cladded silica core fiber at 150 ºC for 6400 hours were given, along with 5000 hours of testing polymer films under the same conditions. The results at 150 ºC were encouraging, with little additional loss measured during the run. In this paper we demonstrate results of much more severe heating, at 270 ºC, for periods of up to 10 hours, on cladding materials with indices ranging from 1.374 to 1.397 (at 852 nm). During this heating, significant changes in Young's modulus, refractive index, yellowing, weight, hardness, strength, elongation and glass transition temperature (Tg) were observed, although some changes were much less than others. While these polymers cannot function at 270ºC for long periods, it is possible to expose them for much shorter periods of time without significant damage. Such polymers have been successfully jacketed with materials extruded at high temperatures (including Tefzel®) for a few minutes without harm. It may be that a sensor, fiber laser or other fiber device could function in these temperatures for periods up to an hour without the coating changing beyond the ranges required for operation.

8218-31, Session 6

## Fiber optic based heart-rate and pulse pressure shape monitor

D. Kokkinos, S. Dehipawala, M. Musa, G. Tremberger, Jr., T. Holden, D. Lieberman, T. D. Cheung, Queensborough Community College (United States)

Macro-bending fiber optic based heart-rate and pulse pressure shape monitors have been fabricated. Study of fiber bending loss and its stability and variations is very important especially for sensor designs based on optical fiber bending. The objective was to measure the heart rate and pulse pressure shape during physical activities. Wavelengths from 1300 nm to 1500 nm have been used with fabrication based on multimode fiber, single mode fiber, and photonic crystal fiber. The smallest studied curvature would demand the use of single mode standard and photonic crystal fibers. The collected data series show high quality suitable for random series analysis. Fractal property of optically measured pulse pressure data has been observed to correlate with physical activity. The application to real time measurement of blood vessel stiffness with this optical non-invasive device will be discussed.

8218-32, Session 6

## Force sensing microforceps with integrated fiber Bragg grating for vitreoretinal surgery

X. He, M. Balicki, J. U. Kang, P. Gehlbach, J. Handa, R. H. Taylor, I. Iordachita, The Johns Hopkins Univ. (United States)

Vitreoretinal surgery is the most technically demanding ophthalmologic discipline. One of the main technical challenges in vitreoretinal surgery is the lack of force sensing since the movements required for dissection fall below the human sensory threshold. Previously, a 2-degree-of-freedom (DOF) force sensing instrument with a surgical pick was developed and tested. However, a more commonly used instrument for vitreoretinal surgery is the forceps, with which a surgeon can easily grasp and delaminate the membrane.

We have designed, fabricated and calibrated a novel 20-gauge microsurgical instrument with a 2-DOF force sensing forceps. Three Fiber Bragg Grating (FBG) sensors are integrated into the customized Alcon forceps tip. The redundant sensor configuration provides good temperature compensation. The calibration data show that the tool can guarantee a force resolution of 0.25 mN.

In order to test the functionality and performance, the forceps was evaluated in an inner shell membrane peeling experiment with chicken embryos as well as in in-vivo rabbit experiments. The instrument has demonstrated the capability of being applied in the clinical environment, with consistent force measurements. The force exerted in the inner shell membrane peeling is between 5 to 15 mN, while the force to tear the retinal membrane in in-vivo experiments is about 5 to 10 mN. The development of the microsurgical 2-DOF force sensing forceps tool has shown that the fabrication process is feasible and reliable, and can be used to develop a future 3-DOF force sensing tool.

8218-33, Session 6

## Portable fiber optic ballistocardiogram sensor for home use

Z. Chen, J. T. Teo, S. H. Ng, X. Yang, Institute for Infocomm Research (Singapore)

Heart failure is a growing problem in the world. This problem affects more than five million Americans and takes hundreds of thousands of lives each year. A substantial number of heart failure hospitalizations may be reduced by monitoring outpatients at home. This has led some companies to develop monitoring devices for heart failure outpatients at home. One promising monitoring method is the use of the ballistocardiogram (BCG) which measures the reaction force on the body due to cardiac ejection of blood. This method requires no electrodes to be attached to the patient. It is “contact free” method in between body skin and sensor. Some research has shown that BCG signals are valuable, particularly for evaluating myocardial strength. The amplitude of BCG signals is an accurate sign of degrading cardiac health.

In the past two years, we have developed microbend sensor technology for breathing rate and heart rate measurements. Breathing sensing technology has been successfully transferred to a company for product development. In this paper, however, we propose and demonstrate a highly sensitive fiber optic microbend sensor for BCG recording. The sensor is embedded inside cushion. It is portable, small, light and low cost device. High quality and repeatable BCG signals can be obtained by using this device which allows patients at home to monitor their cardiovascular health. The measured BCG waveforms qualitatively matched the ones in the existing literatures. Comparison with ECG and waveforms from SpO2 will also be given.

8218-34, Session 6

## A prospective for new mid-infrared medical endoscopy using mid-infrared chalcogenide glass fibres

A. B. Seddon, The Univ. of Nottingham (United Kingdom)

Chalcogenide glasses potentially provide a solution for mid-infrared medical endoscopy. Chalcogenide glass fiberoptics could underpin new mid-infrared medical endoscopic systems for real-time molecular sensing, imaging and analysis of tissue and for fiber laser surgery at new mid-infrared wavelengths. These ideas are developed in this paper and the current status of chalcogenide glass photonics is surveyed.

8218-19, Poster Session

## An implantable fiber optic surface plasmon resonance glucose sensor utilizing fiber grating for temperature compensation

P. Wu, D. Li, J. Yang, R. Zhu, K. Xu, Tianjin Univ. (China)

Continuous blood glucose monitoring is a very efficient and important way to control blood glucose level of diabetes. An implantable fiber optic surface plasmon resonance sensor for continuous blood glucose monitoring is presented. As the temperature drift plays a great effect in practical measurement, fiber grating is utilized for temperature compensation to improve measurement accuracy. The sensor is based on surface plasmon waves with fiber cladding modes excited by the grating written in the fiber core. The fiber optic surface plasmon resonance glucose sensor is theoretically analyzed. The parameters such as the length of sensor, diameter of the core and cladding, thickness of Chrome (adhesive layer) and gold film are simulated. The impact of temperature on the refractive index of optical fiber, metal film and measured medium is calculated. The parameters of long period fiber grating and blazed grating is analyzed and simulated, such as length, period and angel of inclination. The factors influencing the grating resonance peak including the refractive index of the medium and ambient temperature are also simulated, and appropriate cladding mode has been found. The structural parameters of the sensing probe are optimized through the calculation and simulation of optical fiber optic and fiber grating, and the experimental results demonstrate the rationality of the structure. The refractive index resolution of sensor is estimated to reach 10-6 RIU and the measuring limit of glucose concentration is able to be 10mg/dL.

# Conference 8219: Biomedical Vibrational Spectroscopy VII: Advances in Research and Industry

Saturday-Sunday 21-22 January 2012

Part of Proceedings of SPIE Vol. 8219 Biomedical Vibrational Spectroscopy V: Advances in Research and Industry

8219-01, Session 1

## Combining optoacoustics and resonance Raman spectroscopy for quantification of biomolecules in situ

M. Wollweber, Leibniz Univ. Hannover (Germany)

Resonant enhancement in Raman spectra of specific molecules is a technique to select and enhance the vibrational fingerprint of target molecules. 'Amplification' of a specific Raman spectrum or specific components therein may be by several orders of magnitude. This allows to detect their fingerprint even at low concentrations or in fluorescent environment without external signal enhancement. We use this approach to identify carotenoids of the antioxidant network in human skin in vivo. Quantification of the carotenoids relies on knowledge about attenuation of excitation light and Raman signal on their way through the skin. To calculate this attenuation, the optical properties of the sample have to be known. This is very difficult for highly individual and inhomogeneous tissue like human skin. If this cannot be measured however, comparison between individuals is virtually impossible and even for different skin sites of the same subject only relative results may be given. We use optoacoustics to probe the optical properties of the investigated skin area parallel to the Raman measurements. To the best of our knowledge, this is the first time that optoacoustics and vibrational spectroscopy are combined in one sensor. The combination of these two techniques allows identification and quantification of specific molecules in living human skin.

8219-02, Session 1

## High-throughput Raman and surface-enhanced Raman microscopy

W. Shih, J. Qi, Univ. of Houston (United States)

Raman spectroscopy enables us to visualize cellular biochemical make up beyond expressive structural information without the need for staining, fixation or metallization. In biosensing context, surface-enhanced Raman spectroscopy provides much higher sensitivity on the per molecule basis compared to normal Raman spectroscopy. However, these techniques currently are limited by throughput and thus are typically implemented as a point measuring tool, rather than an imaging tool. To make Raman microscopy a more versatile tool in both cellular imaging and sensing, we have advanced in both imaging instrumentation and SERS substrate engineering. Based on parallel acquisition, we have developed high-throughput Raman imaging techniques that perform 100X faster than traditional point-scan method. We have also engineered novel plasmonic substrates for large-area SERS imaging and sensing. We have employed IC fabrication techniques to make a high-density SERS substrate directly on 1 in2 coverslip and demonstrated enhancement factor ~106 and uniformity better than 20%.

We present our results on high-throughput chemical imaging of colonial microalgae Botryococcus braunii to reveal spatial distribution of intra-cellular and extra-cellular chemical constituents such as carotenoids, chlorophyll, lipids and hydrocarbons. We also show that our system enables single bacteria counting over a large area (104 μm2). We have also employed our system to perform large area uniformity characterization of the SERS substrate recently developed by us.

8219-03, Session 1

## Multifocal laser tweezers Raman spectroscopy for high-throughput functional analysis of red blood cells

R. Liu, N. Satake, D. L. Matthews, J. Chan, NSF Ctr. for Biophotonics Science and Technology (United States)

Populations of biological cells are almost always heterogeneous in function and fate. To understand the variability of cells, it is vital to measure quantitatively and dynamically the molecular processes that underlie cell-fate decisions in single cells. Micro-Raman spectroscopy is an attractive analytical method for single cell analysis because of its capability to quantitatively examine the biochemical composition of individual cells noninvasively and to monitor, in real-time, cellular dynamics. The combination of laser tweezers with micro-Raman spectroscopy, namely Laser Tweezers Raman Spectroscopy (LTRS) facilitates the Raman spectroscopic investigation of cells in suspension by immobilizing the cells during the Raman acquisition and improving the signal to noise ratio. Large-scale single cell analysis using LTRS, in which the dynamics of many cells need to be sampled simultaneously and continuously, is impeded by the low analytical throughput of current LTRS technology. To address these limitations, we report on the development and characterization of a multifocal laser tweezers Raman spectroscopy (M-LTRS) technique for parallel Raman spectral acquisition of multiple individual biological cells by combining 1D and 2D optical tweezers arrays with micro-Raman spectroscopy. In addition, high-throughput functional analysis of the oxygen carrying capacity of different types of red blood cells (RBCs), such as sickle, adult, and fetal RBCs, is made feasible by observing the cellular behavior under different trapping powers in the M-LTRS scheme.

8219-04, Session 1

## Ultralow-frequency Stokes and anti-Stokes Raman spectroscopy at 785 nm with volume holographic grating filters

J. T. Carriere, F. Havermeyer, Ondax, Inc. (United States)

We report the first results of ultra-low frequency Stokes and anti-Stokes Raman spectra at 785nm showing clearly resolved frequency shifts down to 10cm-1 from the excitation line, using commercially available ultra-narrow band notch and ASE suppression filters, and a single stage spectrometer. Near infra-red (NIR) wavelengths are of particular interest for Raman spectroscopy due to the reduced fluorescence observed for most materials. Previously reported attempts at producing ultra-low frequency Raman spectra with holographically written grating filters for the most commonly used NIR wavelength of 785nm were unsuccessful. Ultra-narrow line notch filters must be very well matched to the wavelength of the laser to be effective. If the filters have any manufacturing errors or the laser wavelength is unstable, incomplete suppression of the Rayleigh scattered light will overwhelm the Raman signal.

Recent improvements have enabled Raman spectra to be taken at 785nm for several typical materials. Two ultra-narrow line notch filters formed as volume holographic gratings (VHGs) in glass with individually measured optical densities of 4.5 were used to block the Rayleigh scattered light from a matched VHG wavelength stabilized laser. Five discrete peaks below 100cm-1 were simultaneously observed for Sulfur in both the Stokes and anti-Stokes regions at 28, 44, 52, 62, and 83cm-1. With no degradation in filter performance over time and extremely narrow spectral transition widths of less than 10cm-1, this relatively simple system is able to make ultra-low frequency Stokes and anti-Stokes Raman measurements at a fraction of the size and cost of traditional triple monochromator systems.

8219-05, Session 1

## Mid-IR laser-based vibrational circular dichroism spectroscopy

M. Pfeifer, Fraunhofer-Institut für Physikalische Messtechnik (Germany); S. Lüdeke, Univ. of Freiburg (Germany); P. Fischer, Fraunhofer-Institut für Physikalische Messtechnik (Germany)

Most biological and many pharmaceutically active molecules are chiral. Optical methods provide a direct means of distinguishing the enantiomers of a chiral molecule in solution, and have become a valuable tool in determining the stereochemistry of chiral molecules. The differential response to left and right circularly polarized light in absorption (circular dichroism) is particularly useful for determining the absolute configuration of a chiral molecule. Furthermore Vibrational Circular Dichroism (VCD) in the mid-infrared provides a characteristic band pattern and has therefore become one of the key methods for the determination of the absolute configuration of pharmaceutically active chiral compounds and natural products. Dramatic advances in the accurate computation of VCD spectra facilitate the unambiguous identification of the chiral enantiomers. One difficulty in VCD spectroscopy, however, is the strong infrared absorption of most solvents. Traditional VCD instrumentation therefore limits the study of (bio)molecules to selected spectral regions and solvents. We present the first VCD spectra recorded with a tunable mid-infrared quantum cascade laser (QCL). Because QCLs can have at least four orders of magnitude more power than thermal IR light sources, we were able to successfully record VCD spectra in strongly absorbing solvents, including spectra of L-proline in water with optical densities of up to 3.5. A number of applications are discussed.

8219-07, Session 1

## Transmission versus reflection diffraction gratings for detector array based spectrometers

R. Pawluczyk, A. Rohani, P&P Optica Inc. (Canada)

Traditionally scanning spectrometers with rotating reflection gratings, collecting light from a narrow spectral band, were used; resulting in inefficient Raman spectrum registration process. Development of large CCD or CMOS arrays allows for simultaneous collection of light in the entire spectral range of interest. Currently for this application, especially in the visible range, two technical solutions are used. One is based on blazed Surface Relief (SR) gratings and the other on Volume Phase Holographic gratings (VPH). While in an ideal and optimal configuration both kinds of gratings could demonstrate comparable maximum efficiencies, in real applications, due to spatial limitation of SR gratings (drop of efficiency when operated off Littrow mount), VPH gratings in conjunction with refractive optics provide significant gain in collected light and simultaneously produce better optical performance over large detector array resulting in higher photometric dynamic range. In this paper the advantage of spectrometers using VPH gratings over those utilizing an SR grating is demonstrated by comparison of two Raman spectrometers, one designed using a VPH grating and the other using an SR grating.

8219-08, Session 2

## Analyzing near infrared scattering from human skin to monitor changes in hematocrit

J. Chaiken, B. Deng, J. Goodisman, Syracuse Univ. (United States); G. Shaheen, R. J. Bussjager, LighTouch Medical, Inc. (United States)

The leading preventable cause of death, world-wide, civilian or military, for all people between the ages of 18-45 is undetected internal hemorrhage. Autonomic compensation mechanisms mask changes such as e.g. hematocrit fluctuations that could give early warning if only they could be monitored continuously with reasonable degrees of precision and relative accuracy. Probing tissue with near infrared radiation (NIR) simultaneously produces remitted fluorescence and Raman scattering (IE) plus Rayleigh/Mie light scattering (EE) that noninvasively give chemical and physical information about the materials and objects within. We model tissue as a three-phase system: plasma and red blood cell (RBC) phases that are mobile and a static tissue phase. In vivo, any volume of tissue naturally experiences spatial and temporal fluctuations of blood plasma and RBC content. Plasma and RBC fractions may be discriminated from each other on the basis of their physical, chemical and optical properties. Thus IE and EE from NIR probing yield information about these fractions. Assuming there is no void volume in viable tissue, or that void volume is constant, changes in plasma and RBC volume fractions may be calculated from simultaneous measurements of the two observables, EE and IE. In a previously published analysis we showed the underlying phenomenology but did not provide an algorithm for calculating volume fractions from experimental data. Here we present a simple analysis that allows continuous monitoring of fluid fraction and hematocrit (Hct) changes by measuring IE and EE, and apply it to some experimental in vivo measurements.

8219-09, Session 2

## Multivariate analysis methods for spectroscopic blood analysis

M. F. G. Wood, A. Rohani, R. Ghazalah, R. Pawluczyk, P&P Optica Inc. (Canada)

Every year millions of blood tests are ordered to diagnosis or monitor various diseases and conditions, however, the complexities of these measurements restrict them to a laboratory setting making blood tests both expensive and slow. Accordingly, advancements in the methods for blood testing could potentially both reduce medical costs and accelerate patient care. P&P Optica has developed and currently produces patented high performance spectrometers employing non-scanning volume phase holographic transmission gratings. With this technology as a platform, P&P Optica is developing a spectrometer-based system for rapid reagent-free blood analysis. Currently, both Raman and NIR spectroscopy are being explored as potential methods. However, either measured spectrum contains the signals from all analytes present in blood, thus complicating the analysis. This necessitates the use of methods to extract the specific information from the measured spectrum for each analyte, such that their concentrations can be determined. This multivariate calibration can be accomplished using statistical techniques from the field of chemometrics. The use of advanced multivariate techniques is being explored for simulated Raman and NIR signals from a blood serum model to determine their respective sensitivity and specificity. In addition, methods of combining and regressing both signals are also being explored to determine if a combined approach offers an advantage. Future work will focus on experimentally confirming the results of this simulation study and further refining the approach.

8219-10, Session 2

## Univariate and multivariate methods for chemical mapping and imaging of cervical cancer cells

S. Duraipandian, W. Zheng, Z. Huang, National Univ. of Singapore (Singapore)

Visualization of cells and subcellular organelles are carried out using currently available microscopy methods such as electron microscopy, cryoelectron microscopy, and fluorescence microscopy. These methods require external labeling using fluorescent dyes and extensive sample preparations to access the subcellular structures. However, Raman micro-spectroscopy provides a non-invasive, label-free method for imaging the cells and for cancer detection at cellular level with sub-micrometer spatial resolution. The scope of this paper is to image the biochemical/molecular distribution in the cell induced by cancerous changes. Raman map data sets were acquired from the human cervical carcinoma cell lines (HeLa) after fixation, using 785 nm excitation wavelength. The individual spectrum was recorded by raster-scanning the laser beam over the sample with 1μm step size and 10s exposure time. Images revealing nucleic acids, lipids and proteins (phenylalanine, amide I) were reconstructed using univariate methods. In near future, the small pixel to pixel variations will also be imaged using different multivariate methods (PCA, clustering (HCA, K-means, FCM)) to determine the main cellular constitutions. The hyper-spectral image of cell was reconstructed utilizing the spectral contrast at different pixels of the cell (due to the variation in the biochemical distribution) without using fluorescent dyes. Normal cervical squamous cells will also be imaged in order to differentiate normal and cancer cells of cervix using the biochemical changes in different grades of cancer. Based on the information obtained from the pseudo-color maps, constructed from the hyper-spectral cubes, the primary cellular constituents of normal and cervical cancer cells were identified.

8219-11, Session 2

## Thinking outside the black box regime: an alternate chemometric prediction framework for minor component quantification in biological Raman spectroscopy

N. C. Dingari, I. Barman, J. W. Kang, R. R. Dasari, Massachusetts Institute of Technology (United States)

Raman spectroscopy is a powerful spectroscopic technique for noninvasive and real time diagnosis of biological samples due to its excellent molecular specificity and lack of sample preparation requirements. However, due to its low signal levels, the valuable information available in Raman spectra is often hidden in the tissue spectra. Extracting pure spectra of the analyte of interest, which is often a minor component, is challenging, especially due to the presence of a large fluorescence background. Here we incorporate a self-modeling curve resolution method based on seminal entropy minimization concepts to provide quantitative concentration information after extraction of pure component spectra from a set of mixture Raman spectra. We show that this method works well even for highly non-linear cases such as those introduced by tissue turbidity or changes in temperature. To validate this application, spectral resolution was performed on Raman spectroscopic data of highly overlapping mixture spectra containing blood analytes. We illustrate the application in simulated Raman spectroscopic data and physical tissue model data. We envision that this application will introduce a new pathway into previously intractable areas of analyte prediction replacing the conventional black-box applications of multivariate chemometric schemes. The latter, while of substantive use in a wide spectrum of applications, often result in apparently functional models based on spurious correlations in the training dataset and consequently can never be successfully used in prospective prediction. Using this new framework, we anticipate that such a hurdle can be overcome in a number of biological applications including Raman spectroscopy-based non-invasive blood glucose detection.

8219-12, Session 2

## Singlet oxygen induced advanced glycation end product photobleaching of in vivo human fingertip autofluorescence

B. Deng, A. Simental, P. S. Lutz, Syracuse Univ. (United States); G. Shaheen, LighTouch Medical, Inc. (United States); J. Chaiken, Syracuse Univ. (United States)

Nonenzymatic glycation and oxidation of ubiquitous proteins in vivo leads to irreversible formation of advanced glycation end products (AGEs). Due to their relatively long half life and low clearance rate AGEs tend to accumulate within static tissues and the circulatory system. Spectra obtained using 830 nm near-infrared (NIR) excitation suggest that the so-called "autofluorescence" from all tissues has a finite number of sources but the fact that senior and diabetic subjects produce more detectable emission than other members of the general population suggests that a significant portion of the total autofluorescence from all sources originates from AGEs. Using pentosidine generated in a reaction mixture as described by Monnier as representative, an in vitro study unveiled a very similar fluorescence and photobleaching pattern as observed for autofluorescence in vivo. A series of oxygen and argon purging experiments on the pentosidine-generating reaction mixture suggests that pentosidine is a singlet oxygen sensitizer and secondary reactions between the pentosidine itself and/or other fluorophores and the photosensitized singlet oxygen explain the observed photobleaching. Ab initio Gaussian calculations on pentosidine and related structures verify the existence of a low-lying triplet excited state required for the sensitization of ground state oxygen. A commercially available product known as singlet oxygen sensor green (SOSG) that specifically serves as a singlet oxygen detection reagent confirms the generation of singlet oxygen from NIR radiated pentosidine trimixture. This study provides one definite chemical mechanism for understanding in vivo human skin autofluorescence and photobleaching.

8219-36, Session 2

## Assessing the performance of spectroscopic models for cancer diagnostics using cross-validation and permutation testing

G. R. Lloyd, J. C. Hutchings, C. A. Kendall, N. Stone, Gloucestershire Hospitals NHS Foundation Trust (United Kingdom)

Abstract: Multivariate classifiers (such as Linear Discriminant Analysis, Support Vector Machines etc) are known to be useful tools for making diagnostic decisions based on spectroscopic data. However, robust techniques for assessing their performance (e.g. by sensitivity and specificity) are vital if the application of these methods is to be successful in the clinic. In this work the application of repeated cross-validation for estimating confidence intervals for sensitivity and specificity of multivariate classifiers is presented. Furthermore, permutation testing is presented as a suitable technique for estimating the probability of obtaining the observed sensitivity and specificity by chance. Both approaches are demonstrated through their application to a Raman spectroscopic model of gastrointestinal cancer.

8219-13, Session 3

## Classification of Raman spectra of single cells with autofluorescence suppression by modulated wavelength excitation

S. Dochow, N. Bergner, C. Krafft, Institut für Photonische Technologien e.V. (Germany); J. H. Clement, Universitätsklinikum Jena (Germany); M. Malizu, R. F. Marchington, K. Dholakia, Univ. of St. Andrews (United Kingdom); J. Popp, Institut für Photonische Technologien e.V. (Germany)

Raman spectroscopy is a non-invasive technique that has great potential in the biomedical field for label-free discrimination between normal and tumor cells based on their biochemical composition. Depending of the excitation wavelength, the purity of the cell suspension or the optical elements in the light path, high autofluorescence often swamps the weaker Raman signals. Modulated wavelength Raman spectroscopy has recently been shown to suppress autofluorescence background. This contribution applies this approach to a model system of circulating tumor cells that consists of leukocytes from patients' blood, acute myeloid leukemia cells (AML-OCI3), and breast tumor cells BT20 and MCF7. The laser excitation wavelength of 785 nm was modulated with a frequency of 40 mHz by 0.6 nm. The excitation power was 14 mW and 40 spectra were accumulated with an exposure time of 5 seconds each. These spectra were used as input for a principal component analysis to calculate modulated Raman spectra. Altogether 840 spectra were collected at several days to compensate day-to-day variations of the system and the progressive fixation of cells. After principal component analysis the first ten principal components were used as input for classification by a support vector machine. A ten fold cross validation of independent test spectra gave 93.3% accuracy for cancer vs. healthy cells and 81.2% accuracy for the recognition of the cell type. These values are similar to previous classification of Raman spectra of these cells after drying, in laser tweezers and in a microfluidic chip.

8219-14, Session 3

## Effect of photodynamic therapy on single cancer cells studied by integrated Raman and angular scattering microscopy

D. W. Shipp, S. Mitra, T. H. Foster, A. J. Berger, Univ. of Rochester (United States)

Integrated Raman and angular scattering microscopy (IRAM) combines two non-labeling light scattering techniques. Raman spectroscopy reveals chemical information about the sample while angular (or elastic) scattering measures the size of scattering particles within tens of nanometers. When applied to single cells, IRAM extracts concentration levels of various molecules (e.g. proteins, lipids, nucleic acids, etc.) as well as the sizes of mitochondria and other organelles (such as lysosomes or granules). These parameters can be monitored for several hours as the cells remain in stable living conditions.

While much is known about the effects of photodynamic therapy (PDT) on tumors, most of that information is gained by studying the behavior of large populations of cells. Individual cells may present a variety of chemical, structural, and temporal responses to PDT treatment. Knowing the details of single cells' responses can paint a more detailed picture of the response of a whole tumor.

In this study, IRAM tracks the chemical and morphological changes in individual EMT6 cancer cells as they progress through PDT treatment. The same cells are measured before and after photoactivation of the PDT agent protoporphyrin IX. Because treatment occurs on the microscope stage, IRAM can measure the response of cells in the first minutes after the treatment begins to take effect. The cells are measured in an incubated, nutrient-rich environment, allowing measurements to continue for several hours. The latest results of this ongoing study will be discussed.

8219-15, Session 3

## Raman study of power-dependent oxygenation state transition of red blood cells in a single-beam optical trap

R. Liu, L. Zheng, D. L. Matthews, N. Satake, J. Chan, NSF Ctr. for Biophotonics Science and Technology (United States)

Optical tweezers have become widely used for the manipulation and analysis of individual biological cells. A simple and most commonly used configuration is the single beam optical trap in which a tightly focused laser beam optically immobilizes individual cells within the laser focus. The perturbative effect of an optical trap operating under such a tight focusing condition on the function and biochemistry of a live cell is often a concern, with photoinduced damage typically being a primary focus. Mechanically induced biochemical changes, however, have not been as extensively studied, even though it is known that optical forces are imposed on a biological cell by a single beam optical trap that are often strong enough to modify its shape. Herein, we report that a red blood cell (RBC) in a single beam optical trap transitions from an oxygenated to a partially deoxygenated state with increasing trapping power using laser tweezers Raman spectroscopy (LTRS). Continuous switching between the two states is possible by repeatedly cycling between low and high trapping powers. Alterations in the hemoglobin conformation and interactions due to cell folding in the trap are proposed to be responsible for the transition. This study demonstrates that mechanically induced biochemical changes by optical forces need to be considered when applying single beam optical tweezers for cell analysis. In addition, preliminary results show that LTRS holds promise as a functional assay to characterize normal, sickle and fetal RBCs based on their biochemical response to the forces of a single beam optical trap.

8219-16, Session 3

## Raman spectroscopy of fiber-optically manipulated cells

N. Cardenas, The Univ. of Texas at Arlington (United States); I. Barman, Massachusetts Institute of Technology (United States); B. Black, The Univ. of Texas at Arlington (United States); N. C. Dingari, R. R. Dasari, Massachusetts Institute of Technology (United States); S. K. Mohanty, The Univ. of Texas at Arlington (United States)

Raman spectroscopy of single cells has the ability to non-invasively characterize their patho-physiological condition, by virtue of its chemical specificity, and therefore has significant use in disease diagnosis as well as in screening the effect of drugs on these cells. However, owing to the considerable time required for point-by-point spatial Raman mapping, analysis of cells in suspension often necessitates their immobilization, which mars the principal advantage of performing Raman spectroscopy - namely its non-invasive nature. Furthermore, such fixing protocols can change the intrinsic properties of the cells (due to a change in the physico-chemical environment) leading to potentially spurious inferences. While integration of Raman spectroscopy with optical tweezers has enabled some intrinsic measurements, it is limited by the depth at which such analysis can be performed due to the low working distance of high NA microscope objectives employed in optical tweezers. Here, we report Raman spectroscopy of cells, in suspension, immobilized by fiber optic trapping that can be achieved at relatively large sample depths. With single fiber optical tweezing, we could trap cells at depths as large as a few centimeters. Further, for tomographic Raman spectroscopy, the optically trapped cell was rotated at a controlled rate. The possibility of using the same fiber for both trapping/stretching and Raman spectroscopy will also be presented. The approach presented in this talk is broad and general enough to address a variety of cellular investigations, ranging from red blood cell measurements in normal and infected cells to investigations of malignant eukaryotic cell characteristics.

8219-17, Session 3

## Raman spectroscopic analysis of human tissue engineered oral mucosa constructs (EVPOME) perturbed by physical and biochemical methods

M. D. Morris, A. Ganguly, M. Raghavan, S. Kuo, J. H. Cole, C. L. Marcelo, S. E. Feinberg, Univ. of Michigan, Ann Arbor (United States); K. Izumi, Niigata Univ. (Japan)

We show the application of near-infrared (785 nm) Raman spectroscopy to in-vitro monitoring of the viability of a tissue engineered construct, human ex vivo produced oral mucosa equivalent (EVPOMEs), during their production. During the two-week fabrication period EVPOME may encounter thermal, chemical or biochemical stresses that could cause failure of EVPOME to function effectively, rendering the affected constructs useless. We identify Raman metrics that can be used to distinguish between viable and compromised constructs. We previously investigated spectral changes that result when elevated temperature is used to stress the constructs. We now report spectral changes resulting when chemical (calcium ion) and biochemical (rapamycin) agents are used to stress the constructs. These stress protocols allow us to identify Raman signatures for viable/compromised constructs that will be useful over a wide range of conditions encountered during the fabrication process. We used non-linear data mining techniques to uncover a set of Raman metrics that best distinguished between viable and compromised constructs. Using these multidimensional analyses, we successfully identified sets of spectroscopic metrics with discriminatory power that also met criteria for practical implementation: intense bands, minimal spectral interference and a spectral interval of 400 cm-1 or less. We discuss measurement challenges arising from local stress and non-uniform thickness of both the AlloDerm® substrate and the cultured constructs, as well as sampling protocols to overcome such problems.

8219-18, Session 4

## In vivo Raman spectroscopy methods for oral cancers diagnosis

S. P. Singh, A. Deshmukh, P. Chaturvedi, C. M. Krishna, Advanced Ctr. for Treatment, Research & Education in Cancer (India)

Oral squamous cell carcinoma is the most common cancer among males and accounts for 30 to 40% of total cancer burden in India. Conventional diagnosis suffers from limitations of being invasive, subjective and time-consuming. Raman spectroscopy based methods due to non interference of water are ideal for in vivo applications. In the present study we have recorded in vivo Raman spectra from contralateral normal and suspected buccal mucosal sites of 50 subjects, under clinical supervision, using fiber-optic probe coupled HE-785 spectrometer. Spectra were recorded on buccal mucosa as per teeth positions with an average exposure time of 3 seconds. A total of 264 and 190 spectra from normal and tumor sites, respectively, were recorded. Spectral features of normal suggested more lipids while proteins were high in tumor indicated by amide III and broad features in amide I region. 1200-1800 cm-1 region was explored for classification using LDA. Standard models were developed using 125 normal and 129 tumor spectra from 25 subjects. Two separate clusters with an efficiency of ~97% were obtained. Leave-one-out cross-validation also yielded ~89% efficiency. Further, standard model was validated with remaining 139 normal and 61 tumor spectra as test data and prediction efficiency of 83% and 95%, respectively was observed. Studies involving precancerous lesions are ongoing. Findings of the study indicate that Raman spectroscopic methods in combination with appropriate multivariate tool can be used for objective, noninvasive and rapid diagnosis of oral cancers.

8219-20, Session 4

## Online detection of malignant lesions in vivo in the upper gastrointestinal tract using image-guided Raman endoscopy

M. S. Bergholt, W. Zheng, L. Kan, National Univ. of Singapore (Singapore); K. Y. Ho, M. Teh, National Univ. of Singapore (Singapore) and National Univ. Hospital (Singapore); K. G. Yeoh, National Univ. of Singapore (Singapore); J. B. Y. So, National Univ. of Singapore (Singapore) and National Univ. Hospital (Singapore); Z. Huang, National Univ. of Singapore (Singapore)

Raman spectroscopy is a vibrational analytic technique sensitive to the changes in biomolecular composition and conformations occurring in tissue. With our most recent development of near-infrared (NIR) Raman endoscopy integrated with diagnostic algorithms, in vivo Raman tissue diagnosis (optical biopsy) during clinical gastrointestinal endoscopy has been realized under multimodal wide-field imaging (i.e., white- light reflectance (WLR), narrow-band imaging (NBI), autofluorescence imaging (AFI)) modalities guidance.

A selection of 177 patients who previously underwent Raman endoscopy (n=2510 spectra) was used to render two distinct models for esophageal and gastric cancer diagnosis based on partial least squares - discriminant analysis (PLS-DA). The Raman endoscopy technique was validated prospectively on 4 new gastric and esophageal patients for in vivo tissue diagnosis.

High quality in vivo Raman spectra can be acquired and evaluated in real-time within 0.5 sec during clinical endoscopic examinations. Significant differences in Raman spectra between normal and neoplastic tissue are observed reflecting the pathological transformation associated with carcinogenesis (e.g., increased protein synthesis and elevated DNA content). The Raman endoscopic technique developed could prospectively identify esophageal cancers in vivo with a sensitivity of 88.9% (8/9) and specificity of 100.0% (11/11) and gastric cancers with a sensitivity of 77.8% (14/18) and specificity of 100.0% (13/13).

This study demonstrates for the first time the image-guided Raman endoscopy can become a clinical tool for realizing in vivo diagnosis of malignancies in the esophagus and gastric at the molecular level.

This study demonstrates for the first time the image-guided Raman endoscopy can become a clinical tool for realizing on-line in vivo diagnosis of malignancies in the esophagus and gastric at the molecular level.

8219-21, Session 4

## Rapid intra-operative analysis of human brain tumor tissue with infrared spectroscopy

A. L. Stelling, Technische Univ. Dresden (Germany); M. Kirsch, K. D. Geiger, O. Uckerman, Univ. Hospital, Technische Univ. Dresden (Germany); H. Cramm, G. Steiner, Technische Univ. Dresden (Germany)

Intra-operative assessment of brain tumor margins continues to be an active area of clinical research, as tumor borders are altered during neurosurgery from the pre-operative images. This work investigated the suitability of infrared spectroscopy for inter-operative use as a fast, chemically based method for delineating brain tumor borders.

Excised brain tumor tissue was investigated during surgery. Infrared spectra could be obtained from wet tissue within minutes after removal from the patient. Parallel histopathological diagnoses were obtained by a board certified neuropathologist. Various tumor pathologies were examined with infrared spectroscopy. Epileptic human tissue was also investigated to serve as a non-tumor control. To determine how water loss influences the infrared spectrum of freshly excised brain tissue, and to control for the effects of water in the patient spectra, additional studies were performed in a mouse model. These experiments examined the effect of air drying on freshly excised mice brain tissue.

The differences observed between tumor and non-tumor tissues may arise from higher levels of RNA present in freshly excised tissue. RNA in particular is known to degrade within minutes after excision. This work both highlights the importance of acquiring the infrared spectra within ten minutes after removal from the brain, and demonstrates the high clinical potential of infrared spectroscopy for rapid intra-operative analysis.

8219-37, Session 4

## Assessment of fibre-optic near-infrared Raman spectroscopy for diagnosis of early oesophageal neoplasia

L. M. Almond, J. C. Hutchings, C. A. Kendall, J. Day, N. Shepherd, Gloucestershire Hospitals NHS Foundation Trust (United Kingdom); H. Barr, N. Stone, Gloucestershire Royal Hospital (United Kingdom)

No abstract available

8219-22, Session 5

## Raman spectroscopy of bone infections in diabetic foot wounds

K. A. Esmonde-White, Univ. of Michigan Medical School (United States); F. W. Esmonde-White, K. Flannagan, Univ. of Michigan (United States); C. Holmes, Univ. of Michigan Medical School (United States); M. D. Morris, Univ. of Michigan (United States); B. J. Roessler, Univ. of Michigan Medical School (United States)

Diabetic osteomyelitis is an infectious complication of diabetic foot ulcers that can affect any foot bones and is a major risk factor for foot amputation. Current clinical imaging methods of detecting osteomyelitis, such as x-ray or MRI, are inadequate as these methods can only detect the late-stage changes such as severe demineralization and tissue edema. We hypothesized that Raman spectroscopy can be used to determine the chemical composition of bone infected by diabetic osteomyelitis to provide an early marker of bone infection. This pilot clinical study was approved by the University of Michigan Institutional Review Board. Bone fragments containing cortical and cancellous bone were removed from non-healing foot ulcers of study participants as part of their treatment for diabetic osteomyelitis. Bone fragments were examined by Raman microspectroscopy (785 nm) and fiber-optic Raman spectroscopy (830 nm). Raman spectra of bone fragments from diabetic osteomyelitis patients were compared to clinical imaging (x-ray or MRI), microbiology and pathology results. Unexpectedly, Raman spectra of infected bone fragments contained bands from non-apatitic minerals. Because non-apatitic minerals cannot be measured by clinical tests, Raman identification of their presence may be a useful marker of diabetic osteomyelitis. An in vitro study of bone cocultured with bacteria commonly found in deep foot wound cultures, including Escherichia coli and Staphylococcus aureus, is currently underway to support our clinical findings.

8219-23, Session 5

## Transcutaneous monitoring of steroid-induced osteoporosis with Raman spectroscopy

J. R. Maher, H. A. Awad, A. J. Berger, Univ. of Rochester (United States)

Although glucocorticoids are among the most frequently prescribed anti-inflammatory agents used in the treatment of the painful symptoms associated with rheumatoid arthritis, extended exposure to this steroid hormone is the leading cause of iatrogenic osteoporosis, leaving patients susceptible to fractures at reported rates of 30-50%. In addition, bone mineral density, the current standard indicator for diagnosing osteoporosis, is a fairly poor predictor of fracture risk in glucocorticoid-treated patients.

Recently, vibrational spectroscopic techniques have been utilized to exploit biochemical differences between osteoporotic and normal bones in order to predict fracture risk. Specifically, Raman spectroscopy has been used to generate predictions of biomechanical strength in the bones of both glucocorticoid- and placebo- treated mice. In this presentation, we report the results of ongoing research in our laboratory towards the clinical translation of this technique.

Transcutaneous acquisition of Raman signatures from bone remains one of the primary obstacles to achieving successful noninvasive clinical translation of this technique. While others have reported the transcutaneous extraction of Raman spectra from the bones of mice, rats, chickens, canines, and humans, the spectra extracted in these studies were not used for subsequent predictions of fracture risk or pathologic diagnoses. Many of these studies used spatially offset Raman spectroscopy, along with multivariate techniques such as band-target entropy minimization, in order to extract the Raman spectrum of the underlying bone. We will discuss additional strategies for the transcutaneous acquisition of spectra from the tibiae of mice that are of sufficient quality to generate accurate predictions of fracture risk.

8219-24, Session 5

## Development of Raman spectroscopy for discrimination of inflammatory bowel disease

I. J. Pence, D. Balikov, D. Schwartz, X. Bi, A. Herline, A. Mahadevan-Jansen, Vanderbilt Univ. (United States)

Inflammatory bowel disease (IBD), including ulcerative colitis (UC) and Crohn's disease (CD), affects nearly 2 million Americans, and the incidence is increasing worldwide. It has been established that UC and CD are distinct forms of IBD and require different medical care. Currently, the distinction made between UC and CD is based upon inexact clinical, radiological, endoscopic, and pathologic features. A diagnosis of indeterminate colitis occurs in up to 15% of patients when UC and CD features overlap and cannot be differentiated. In these patients, diagnosis relies on long term follow up based on success or failure of existing treatment and recurrence of the disease. Thus, there is need for a tool that can improve the sensitivity and specificity for fast, accurate and automated diagnosis of IBD. Here we present fiber optic probe-based Raman spectroscopy as a novel diagnostic tool for IBD. This in vitro study of excised fresh frozen colon biopsy samples with UC (N=43) and CD (N=21) aims to characterize spectral signatures of UC and CD. Samples are correlated with tissue pathology markers and optimal collection parameters for detection have been identified. The collected spectra presented are processed and analyzed using multivariate statistical techniques to identify spectral markers and discriminate UC and CD. Development of spectral markers for each disease type is a necessary first step in the development of real-time, accurate and automated in vivo detection of IBD during colonoscopy procedures.

8219-25, Session 5

## High-resolution mid-infrared imaging for disease diagnosis

M. J. Walsh, D. Mayerich, Univ. of Illinois at Urbana-Champaign (United States); A. Kajdacsy-Balla, Univ. of Illinois at Chicago (United States); R. Bhargava, Univ. of Illinois at Urbana-Champaign (United States)

Histopathology is the gold standard for evaluating the presence and severity of most cancers. Unfortunately, the manual nature of histopathologic recognition leads to low throughput analysis, delays in decision-making and errors. Here, we report on the evaluation of an automated means for accurate histologic recognition using Fourier Transform infrared (FT-IR) spectroscopic imaging. This method does not require dyes or probes and dispenses with human input but relies on the inherent biochemistry of unstained tissue coupled with computational approaches to provide histologic information. Results demonstrate that infrared (IR) imaging is capable of accurate segmentation of cell types and disease subtypes that can potentially become competitive with that attained by conventional histopathological analyses.

Advances in high resolution IR imaging have demonstrated the ability to resolve cell types and tissue structures that are not readily identifiable using conventional transmission FT-IR. The identification and chemical characterization of these features may be critical for accurate staging and diagnosis of cancers. Advances in IR instrumentation to provide high resolution IR images include Attenuated Total Reflectance (ATR) FT-IR (1.56x1.56μm) and using a 74X objective coupled with an IR microscope (diffraction limited). Examples of high resolution IR imaging will be presented from breast, prostate and colon tissues with clinically important cell types and tissue structures examined.

8219-26, Session 5

## Raman spectroscopy: an effective method of detecting biochemical changes of the pregnant cervix

E. Vargis, C. N. Webb, K. Williams, K. Bennett, J. Reese, Vanderbilt Univ. (United States); A. Al-Hendy, Meharry Medical College (United States); A. Mahadevan-Jansen, Vanderbilt Univ. (United States)

Preterm birth is the second leading cause of neonatal mortality and can lead to a myriad of complications like delayed development, cerebral palsy and hemorrhage. Currently, there is no way to accurately predict preterm labor, making its prevention and treatment virtually impossible. While there are some at-risk patients, over half of all preterm births do not fall into any high-risk category. This study seeks to predict and prevent preterm labor by using Raman spectroscopy to detect changes in the cervix during pregnancy and prior to delivery. Since Raman spectroscopy has been used by many research groups to detect cancers and other malignancies in vivo in organs like the cervix and skin, it follows that spectra from the cervix will significantly change over the course of pregnancy. Previous studies have shown that fluorescence decreased during pregnancy and increased during post-partum exams to pre-pregnancy levels. Similarly, we believe significant changes will occur in the Raman spectra obtained during the course of pregnancy. In this study, Raman spectra from the cervix of pregnant mice and women will be acquired. Specific changes that occur due to cervical softening or changes in hormonal levels will be observed to understand how Raman spectra can be utilized to determine the likelihood that a female mouse or a woman will give birth.

8219-27, Session 5

## Vibrational Raman spectroscopic signature from skin and other biofluids in autism spectrum disorder (ASD): biomarkers in early diagnosis and prevention

N. DeSilva, T. Sultan, Washington Univ. in St. Louis (United States)

For prevention of ASD in children, we need to understand the cellular events that underlie the disease at the molecular level. If we know that specific molecular changes constitute an early signature of ASD, or what molecular changes may predispose a child to that disease, then we can take definite steps to target treatment or even prevent the disease from developing in the first place. Thus we hypothesize that the vibrational Raman signature specified by Raman 'fingerprint' (RPF) analysis can function as ASD biomarker and affords us one of the best analytical strategies that could be used in vivo and non-invasively to diagnose and prevent ASD. Basically in this study we will focus our attention on the skin tissue and other biofluids of the ASD children to accentuate the importance of Raman specroscopy to the realm of the presymptomatic treatment modality (prevention) through the use of ASD biomarkers. ASD has been diagnosed as a developmenal brain disorder that is currently monitored by the observation of core behavioral symptoms. As with many neurodevelopmental disorders, brain dysfunction may precede abnormal behavior by a time lapse of months or years. Thus the importance of biomarkers become apparent to detect children either with or 'at risk' for ASD during early development and avoids reliance only on diagnosis based on behavioral observations. It is critical that we enhance methods for detecting ASD earlier in life, so that early intervention is possible. This study is based on the Raman spectral analyis of skin and other biofluids (plasma, urine,etc) of ASD children compared to age-matched controls. Skin is the largest human organ comprising about one sixth of total body weight. It serves as the barrier to the outside environment with well defined functions of anti-infectivity, protection from water loss and UV radiation, production of vitamin D, regulation of body temperature and also regulate overall body metabolism. Thus human skin is a highly efficient self-repairing barrier that could be used as a physiological indicator of health and disease. In this study underlying skin molecular structure is related to its function by the Raman spectroscopic analysis of major bio-molecules of proteins and lipids. Of the skin structural components, only the epidermal stratum corneum (ESC) will be examined in this study (later studies will focus on the dermal and subcutaneous tissues). Of special importance to ESC are the ceramide lipids and proteins such as keratins. We have examined the Raman shifts of the mid-frequency RPF region ( 1000 to 2000 cm-1) and the high frequency (RHF) region of 2500-3200 cm-1. The data indicate significant changes may occur in Raman shifts of both these regions in vivo evaluations of skin samples of ASD children compared to controls.

8219-28, Session 5

## Toward minimally invasive, continuous glucose monitoring in vivo

C. Vrancic, N. Gretz, N. Kröger, S. Neudecker, A. Pucci, W. Petrich, Ruprecht-Karls-Univ. Heidelberg (Germany)

Diabetes mellitus is a disorder of glucose metabolism and it is one of the most challenging diseases, both from a medical and economical perspective. People with diabetes benefit from a frequent or even continuous monitoring of the blood glucose concentrations. The continuous approach presented takes advantage of the observational nature of biomedical vibrational spectroscopy in contrast to chemical reactions which consume glucose and which inherently may adverse immune reactions. The particular technique employed here is based on the high sensitivity of mid-infrared transmission spectroscopy where strong vibrational bands of glucose can be monitored at wavelengths around 10µm.

The strong absorption of water in this spectral region was mitigated by the use of quantum cascade lasers and very short interaction path lengths of about 20µm. Various sensor concepts have been explored. In one of the concepts, the interaction of mid-infrared radiation with glucose is established within a miniature measurement cavity, formed by a gap between two silver halide fibers. Using this setup a noise-equivalent concentration of 0.5mg/dL was achieved during in-vitro experiments with an integration time as short as 5s. Furthermore, potential interfering substances were analyzed with the result that within normal physiological ranges no substance caused a significant disturbance of the glucose sensitivity. Biocompatibility testing supplemented the research towards in-vivo applicability.

Considering further improvements concerning production process, robustness and cytotoxicity of the sensor, the results of initial in-vivo experiments will be presented.

8219-38, Session 6

## Raman chemical imaging of explosive-contaminated fingerprints for forensic attribution

A. W. Fountain III, A. Tripathi, E. D. Emmons, P. G. Wilcox, J. A. Guicheteau, D. K. Emge, S. D. Christesen, U.S. Army Edgewood Chemical Biological Ctr. (United States)

Raman chemical imaging (RCI) has been used to detect and identify explosives in contaminated fingerprints. Bright-field imaging is used to identify regions of interest within a fingerprint, which can then be examined to determine their chemical composition using RCI and fluorescence imaging. Results are presented where explosives in contaminated fingerprints are identified and their spatial distributions are obtained. Identification of explosives is obtained using Pearson's cosine cross correlation technique using the characteristic region (500-1850 cm-1) of the spectrum. This study shows the ability to identify explosives non-destructively so that the fingerprint remains intact for further biometric analysis. Prospects for forensic examination of contaminated fingerprints are discussed.

8219-39, Session 6

## Infrared microscopy for forensic applications: an emerging technology aided by fundamental optical theory

R. Bhargava, Univ. of Illinois at Urbana-Champaign (United States); B. J. Davis, Creare Inc. (United States); T. van Dijk, Vrije Univ. Amsterdam (Netherlands); P. S. Carney, Univ. of Illinois at Urbana-Champaign (United States)

Infrared spectroscopic imaging combines the spatial specificity of optical microscopy with the molecular selectivity of vibrational spectroscopy. While infrared spectroscopy and point microscopy have been used for forensic analyses, imaging represents a rapid and comprehensive mode for forensic problems. As an example, we first discuss application of Fourier transform infrared (FT-IR) spectroscopic imaging for latent print analysis. Oils and skin can be visualized easily from spectral absorbance using appropriate vibrational modes. Fingerprints from different times and people can easily be separated, further, using chemometric techniques. The spatial specificity of the technique leads enhanced spectral sensitivity when a material of interest can be localized. We demonstrate the extraction and identification of particulate trace evidence within prints. The explosive, RDX, is detected and quantified using spectral analysis. We also demonstrate the facile detection of other trace evidence such as fibers. Fibers, by themselves, form a very important class of forensic interest. Their analysis by IR imaging, however, is not straightforward and has traditionally required destructive sample preparation. Recording spectral data from fibers is actually a subset of a major analytical challenge in forensic science, hair product development, in advanced fiber-reinforced composites and in the textile industry is understanding molecular events in intact samples. Unfortunately, spectra are distorted by optical effects (namely scattering, focusing and diffraction) in fibers to the point that directly-recorded spectra are analytically useless. A rigorous theory is presented for IR absorption microspectroscopy by using Maxwell's equations to model beam propagation. Focusing effects, material dispersion and the geometry of the sample are accounted to predict spectral response for fibers. As a consequence, an algorithm that enables the recording of accurate spectral data from cylindrical objects that have physical dimensions of the order of the wavelength of light is formulated. In summary, the combination of new technology and new theoretical understanding presents a new opportunity to make forensic analyses significantly more powerful with infrared imaging.

8219-40, Session 6

## Raman spectroscopy offers a great potential for nondestructive confirmatory identification of body fluid traces

V. Sikirzhytski, A. Sikirzhytskaya, G. McLaughlin, A. Afnan, Univ. at Albany (United States); I. K. Lednev, Univ. of Pittsburgh (United States)

Raman spectroscopy is a technique that is increasing in popularity among the different disciplines of forensic science. Some examples of its use today involve the identification of drugs, lipsticks, and fibers, as well as paint and ink analysis. The theory behind Raman spectroscopy is based on the inelastic scattering of low-intensity, nondestructive laser light by a solid, liquid or gas sample. Very little or no sample preparation is needed, and the required amount of material tested with a Raman microscope can be as low as several picograms or femtoliters. A typical Raman spectrum consists of several narrow bands and provides a unique vibrational signature of the material. Typically, nonresonance Raman spectroscopic measurements do not damage the sample. The stain could be tested on the field and still be available for further use in the laboratory for DNA analysis. A portable Raman spectrometer is a reality now that should allow the identification at the crime scene.

We report here on the development of a new method for identification of body fluid traces using Raman spectroscopy combined with advanced statistics.2, 3 Dry traces of semen, vaginal fluid, sweat, saliva, and blood were analyzed using confocal Raman microscopy with a 785-nm excitation.4-6 It was found that dry samples of these body fluids are intrinsically heterogeneous. We proposed and developed a library of multidimensional Raman spectroscopic signatures that allowed differentiating the traces of body fluids with high confidence. In addition, traces of human and animal blood could be distinguished.7, 8 Overall, this preliminary study demonstrates the great potential of Raman spectroscopy for nondestructive, confirmatory identification of body fluids for forensic purposes.

This project was supported by Award No. 2009-DN-BX-K196 awarded by the National Institute of Justice, Office of Justice Programs, U.S. Department of Justice. The opinions, findings, and conclusions or recommendations expressed in this publication are those of the authors and do not necessarily reflect those of the Department of Justice.

8219-41, Session 6

## Forensic science perspectives for blood identification with Raman scattering

S. J. Boyd, S. Seashols, Virginia Commonwealth Univ. (United States); D. Ye, Rensselaer Polytechnic Institute (United States); M. F. Bertino, Virginia Commonwealth Univ. (United States)

In forensic science, Raman scattering is frequently employed to identify fibers, textiles and controlled substances, but it is seldom employed to identify body fluids such as blood. This is somewhat surprising since Raman scattering is a sensitive and non-destructive technique which could potentially be useful for crime scene investigation. We have therefore compared Raman scattering of blood with other detection techniques using forensic science criteria. Specifically, we have focused on:

• False positives. An array of substances and body fluids which are commonly encountered at the crime scene were analyzed. The spectra of these substances could be easily discriminated from human blood, with the exception of blood from other mammals. Most important, substances that give false positives with other techniques (e.g., bleach for Luminol) did NOT yield false positives when analyzed with Raman scattering.

• Ease of use. Little or no sample preparation was required for Raman scattering and acquisition times were on the order of minutes. For comparison, the current identification techniques are immunochromatographic in nature and require one hour incubation before sample analysis, and are not as sensitive as the Raman technique. Thus, Raman scattering is more suited for rapid, confirmatory analysis at the crime scene or in the laboratory.

• Non-destructiveness. Samples could be exposed for up to four hours to the laser used for data collection without degrading the DNA. The laser had a wavelength of 532.1 nm and the power at the sample was about 3 mW.

• Dilution Limits. Raman scattering from blood has a dilution limit on the order of 1:250, which is comparable to that of presumptive techniques used in field work. The current screening methods of luminol and fluorescein are quite sensitive and comparable to Raman scattering, but are known to give false positive results with a vast number of substances other than blood. By using surface enhanced Raman scattering (SERS), dilutions on the order of 1:100,000 could be measured, and be absolutely confirmatory for blood.

These features of Raman scattering from blood are very attractive for forensic science. Perspective applications of Raman spectroscopy of blood in the crime laboratory and in the field will be discussed.

8219-29, Poster Session

## Identification of paracoccidioides brasiliensis by gold nanoprobes

L. J. Raniero, M. L. Castilho, M. A. G. Cardoso, R. A. Canevari, A. A. Martin, Univ. do Vale do Paraíba (Brazil)

Paracoccidioides brasiliensis (Pb) is a thermal dimorphic fungus and causal agent of the paracoccidioidomycosis. Epidemiological data shows that mainly its incidence is concentrated in Central and South America countries, been larger the cases registered in Colombia, Brazil and Venezuela. The histopathological similarity with others fungal infection makes the diagnosis of Pb more complicate. Therefore, the aim of this work was find the positive and negative test of Pb using gold nanoprobes as a new tool for Pb detection. Nanoparticles of gold were synthesized by reduction of gold chloride by sodium citrate. This results of this procedure is a wine-red solution with a maximum of absorption in the range of ~520-530nm. A specific Pb sequence of oligonucleotide was bonded to the nanoparticles, which maintain the wine-red colour. The results show a colour change from red to blue for negative diagnostic and unchanged for positive test. The H-bond interaction of DNA with the complementary DNA keeps strands together and form double helical structure, keeping the colloid stability. However to uncomplimentary DNA the nanoprobes merge into a cluster, changing the light absorption.

8219-30, Poster Session

## A rheumatoid arthritis study by Fourier transform infrared spectroscopy

C. S. Carvalho, A. C. A. Silva, T. J. P. S. Santos, A. A. Martin, Univ. do Vale do Paraíba (Brazil); L. E. C. Andrade, Univ. Federal de São Paulo (Brazil); L. J. Raniero, Univ. do Vale do Paraíba (Brazil)

Rheumatoid arthritis (RA) is a systemic inflammatory disease of unknown causes. The pathology of the disease process often leads to the destruction of joint's protective cartilage and ankylosis of the joints. RA affect approximately 0.5-1.5% of the world's population between the ages of 40 and 60. The difficulties in clinical diagnosis of RA are essentially due to the complexity of this disease. Most cases of RA are unfortunately only identified in the advanced stages. The main purpose of this work is to determine the biochemical differentiation of sera between normal and RA patients by infrared spectroscopy (FT-IR). The human sera from 39 healthy donors and 39 rheumatics donors were collected and analyzed by FT-IR using a Perkin Elmer Spotligh 400 system. The results show significant spectral variations with $p < 0.05$ in regions corresponding to protein $\delta$ (NH), lipids $\nu$as (CH2) and immunoglobulins. The technique of latex agglutination for the polystyrene covered with human immunoglobulin G and PCR (protein c-reactive) was performed for confirmation of possible false-negative results within the groups, facilitating the statistical interpretation and validation of the technique.

8219-31, Poster Session

## Biochemical differentiation of mycelium and yeast forms of paracoccidioides brasiliensis by Fourier transform infrared spectroscopy

M. L. Castilho, G. M. Alves de Abreu, T. G. F. Matos, Univ. do Vale do Paraíba (Brazil); C. B. L. Campos, Univ. Federal de São Paulo (Brazil); A. A. Martin, L. J. Raniero, Univ. do Vale do Paraíba (Brazil)

Paracoccidioides brasiliensis the etiological agent of paracoccidioidomycosis, is a dimorphic fungus existing as micelia in the environment (or at 25°C in vitro) and as yeast cells in the human host (or at 37°C in vitro). Epidemiological data has shown a uniform distribution among Central and South America countries, but the most cases registered are from Colombia, Brazil and Venezuela. The fungus diagnoses can be complicated due to similar histopathological pattern with other fungal infection and symptoms are also similar to other diseases. Besides morphology, mycelia and yeasts also display molecular and biochemical features that distinguish each of them. The most prominent difference between both forms is probably the cell wall polysaccharyde, being beta-1, 3-glucan usually found in mycelia and alpha-1, 3-glucan found in yeasts, but a plethora of other differences have already been described. In this work we performed a Fourier Transform Infrared Spectroscopy (FTIR) analysis to compared yeasts and mycelia from P. brasiliensis and found additional biochemical differences. The analysis of the spectra showed that differences were distributed in chemical bonds of proteins, lipids and carbohydrates.

8219-32, Poster Session

## Bucal microbiology analyzed by infrared spectroscopy (FT-IR)

G. M. Alves de Abreu, G. R. Oliveira, S. Khouri, P. P. Favero, L. J. Raniero, A. A. Martin, Univ. do Vale do Paraíba (Brazil)

Rapid microbiological identification and characterization are very important in dentistry and medical areas. Oral pathogens are directly linked to cases of endocarditis, premature delivery, low birth weight of newborns and loss of organ transplants beyond dental diseases. The FT-IR spectroscopy has been applied successfully in recent years for the identification and characterization of pathogenic microorganisms due to their fast and objective results, as well as, high specificity and applicability. In this study we have used strains of oral pathogens Aggregatibacter actinomycetemcomitans ATCC 29523, Aggregatibacter actinomycetemcomitans JP2 and Aggregatibacter actinomycetemcomitans clinical isolate from the human blood and measured by using a FT-IR Perkin Elmer Spotlight 400. This study was performed in triplicate, under controlled conditions of temperature, time and medium environment. A total of 75 spectra for each strain were obtained by using the method of stamping in ZnSe window. Biochemical analyses were performed to study the differences between organisms of the same species after culturing for 10 hours. This cultivation time is significantly reduced in comparison to 48-72 hours from the conventional grown. Significant spectra differences were found among each organism allowing the identification and characterization of each bacterial species. Vibrational modes in the regions of 1038 $cm^{-1}$, 1060 $cm^{-1}$, 1100 $cm^{-1}$, 1312 $cm^{-1}$, 2928$cm^{-1}$ were used in this differentiation. The identification and classification of each strain were performed by cluster analysis presenting a 100% of strains separation. We demonstrated that FT-IR could be used to decrease the identification time compared to the traditional methods.

8219-33, Poster Session

## Gold and silver nanostructures for SERS

M. Pokhrel, G. A. Kumar, B. G. Yust, D. K. Sardar, The Univ. of Texas at San Antonio (United States)

SERS is a surface-sensitive detection technique that enhances the Raman scattering plasmon resonance signal with the modification of size, shape and surface of a material. Due to plasmon at the surface, the absorption and scattering of electromagnetic radiation by metallic nanoparticles are strongly enough. Gold and Silver nanorods, nanostars, and nanoflowers with suitable aspect ratios can absorb and scatter strongly in the NIR region. In this present work, we are interested to study these multi shape metal nanoparticles theoretically and experimentally to see their application for surface enhanced Raman spectroscopy. These structures will be modeled based on the image obtained from SEM and TEM. The nanostructure properties as substrates for SERS will be investigated and compared with respect to shape and size. Preliminary study has shown that silver and gold nanoflowers/nanostars can be synthesized by using seed-mediated, surfactant-directed synthesis

8219-34, Poster Session

## Study of aggressiveness prediction of mammary adenocarcinoma by Raman spectroscopy

R. Andrade Bitar, Univ. Federal do ABC (Brazil); A. A. Martin, Univ. do Vale do Paraíba (Brazil); H. da Silva Martinho, Univ. Federal do ABC (Brazil); L. N. Z. Ramalho, Univ. de São Paulo (Brazil); A. R. S. Junior, Univ. Federal do ABC (Brazil); L. J. Raniero, Univ. do Vale do Paraíba (Brazil); F. Silva Ramalho, Univ. de São Paulo (Brazil)

Raman spectroscopy has been widely used for biomedical application and, results published to date, have shown it excellent potential to distinguish normal from neoplastic tissues with high specificity and sensitivity. Although there are many articles focused on in vivo or ex vivo Raman analysis of cancer tissue for cancer diagnosis, to the best of our knowledge its potential to predict the aggressiveness of tumor has not been fully explored yet. Therefore, the aim of this study was explores the capability of Raman spectroscopy in providing an indication of the aggressiveness of a tumor.

In this work Raman spectra in the 500 to 1800 cm-1 wavenumber region of ex vivo breast tissues of both healthy mice (normal, N=5) and mice with induced mammary gland tumors (abnormal, N=15) were measured and associated to matrix metalloproteinase-19 (MMP-19) immunohistochemical exam. It was possible to verify that normal breast, benign and adenocarcinomas lesions, including the subtypes (cribriform, papillary and solid) could have their aggressiveness associated with changes in the vibrational Raman bands. By using MMP-19 exam was possible to classify the samples by malignant graduation in accordance to the classification results of Principal Component Analysis (PCA), Cluster Analysis (CLA) and Linear Discriminant Analysis with cross-validation (LDA) algorithm applied to all Raman spectra. The proportion of correct classification for all groups was 66.7% for cribriform, 86.7% for cribriform-papillary and 31.6% for papillary samples. This result lead us to conclude that this algorithm and the predictors used for this analysis were able to identify the adenocarcinomas “++”, therefore, the less aggressive ones. These preliminary results suggest that Raman spectroscopy has the potential to contribute to an accurate and early prediction of tumor behavior extending beyond it ability to diagnose benign and malignant lesions.

8219-35, Poster Session

## Low cost substrates for Raman spectroscopy

O. J. Cornell, R. Bhargava, Univ. of Illinois at Urbana-Champaign (United States); B. G. Clay, bioMérieux Industry (United States); R. Robinson, bioMérieux, Inc. (United States)

Raman spectroscopy is a standard research tool for the evaluation of biological specimens. In order to simplify the analysis of the spectra, substrates such as fused silica and calcium fluoride are used. These substrates have poor Raman spectra so that the task of separating the biological sample spectra from the substrate is straight forward. However, these crystal substrates can be expensive causing issues to the researcher such as limited sample archival and budget issues.

Metal substrates have been shown to be effective for Raman substrates, but implementations to-date have not resulted in low-cost substrates. In addition, metal substrates offer advantages in Raman signal improvement. We describe several methods for the synthesis of a low-cost metal substrate and analyses for determining the minimum thickness of metal that is required. We will present test data from microbiological samples to demonstrate substrate effectiveness.

# Conference 8220: Optical Biopsy X

Tuesday-Wednesday 24-25 January 2012

Part of Proceedings of SPIE Vol. 8220 Optical Biopsy X

8220-01, Session 1

## Screening prostate cancer using a portable near infrared scanning imaging unit with an optical fiber-based rectal probe

Y. Pu, W. Wang, G. Tang, Y. Budansky, M. Sharonov, The City College of New York (United States); M. Xu, Fairfield Univ. (United States); S. Achilefu, Washington Univ. School of Medicine in St. Louis (United States); J. A. Eastham, Memorial Sloan-Kettering Cancer Ctr. (United States); R. R. Alfano, The City College of New York (United States)

A portable near infrared scanning polarization imaging unit with an optical fiber-based rectal probe, namely Photonic Finger (PF), was designed, developed and was designed and developed o locate the 3D position of abnormal prostate site inside normal prostate tissue. The scanning polarization imaging acquires experimental data by sequentially scanning a polarized illuminating light beam at different areas of a prostate gland through rectum, and recording the distribution of light intensity backscattered from the prostate using a CCD camera. An inverse algorithm, Optical Tomography using Independent Component Analysis (OPTICA) was improved particularly to unmix the signal from targets (cancerous tissue) embedded in a turbid medium (normal tissue) in the backscattering imaging geometry. Two steps were achieved: (1) synthesizing a “clean” background image of the host medium numerically; and (2) marching the propagation of the scattered light from target to the surface until matching the retrieved independent component. PF combined with OPTICA were used to detect the three dimensional (3D) positions of cancerous prostate tissue covered by large pieces of normal tissues. This research will provide a noninvasive optical imaging technique for detecting and 3D locating cancerous sites in prostate. Therefore, PF introduces a new criteria/indicator for prostate cancer screening in addition to the conventional examinations to enhance the accuracy of diagnosing prostate cancers.

8220-02, Session 1

## Angular domain spectroscopic imaging for breast cancer margin assessment after lumpectomy

F. Vasefi, Lawson Health Research Institute (Canada); M. Najiminaini, Simon Fraser Univ. (Canada); A. Chamson-Reig, M. Brackstone, Lawson Health Research Institute (Canada); B. Kaminska, Simon Fraser Univ. (Canada); J. J. L. Carson, Lawson Health Research Institute (Canada)

Purpose: To determine the feasibility of transillumination hyperspectral imaging for delineation of ex-vivo breast tumor margins after lumpectomy procedures.

Material and methods: A novel optical spectroscopic tool (Angular Domain Spectroscopic Imaging, ADSI) was assembled from a collimated broadband light source, a silicon micro-machined micro channel array to select the ballistic and quasi-ballistic (snake) photons, and a pushbroom spectrometer. ADSI generates hyperspectral shadowgrams containing two dimensional spatial maps of spectral information for objects in the field of view. The performance of the ADSI system was evaluated in the near infrared region (650 nm to 900 nm). Pixel-by-pixel correlation analysis was performed on the spectral data. Analysis was performed on the zero order transmission spectra and the first derivative of the transmission spectra.

Results: The spectroscopy imager was able to measure up to 1 cm × 1 cm area of ex-vivo fresh breast tissue (sliced and slightly compressed to ~ 2 mm thickness) with spatial resolution of 200 µm. Spectral data were obtained from 2 patients with invasive Ductal Carcinoma In Situ (DCIS) and 2 patients with normal tissue. Correlation analysis revealed measurable differences between regions were DCIS was known to be present compared to regions of normal tissue.

Conclusion: We have developed a hyperspectral transillumination imager which mostly accepts weakly-scattered photons to form hyperspectral shadowgrams. The correlation analysis results suggested that ADSI is feasible for thin tissue samples such as those obtained during lumpectomy procedures.

8220-03, Session 1

## Diffuse reflectance imaging: a tool for guided biopsy

J. L. Jayanthi, S. Narayanan, Ctr. for Earth Science Studies (India); S. Manju, Government Dental College, Thiruvananthapuram (India); G. U. Nisha, Ctr. for Earth Science Studies (India); V. T. Beena, Government Dental College, Thiruvananthapuram (India)

The major clinical challenge is to precisely locate the biopsy site in a clinically suspecting indurated lesion. Dips due to oxygenated hemoglobin absorption has been noticed at 545 and 575 nm in the diffusely reflected white light spectra and intensity ratio R545/R575 has been found suited for early detection of oral precancers. A multi-spectral diffuse reflectance (DR) imaging system has been developed consisting of an EMCCD camera and a liquid crystal tunable filter (LCTF).

A clinical trial was conducted on patients with lesions in the lateral/dorsal/ventral surface of the tongue, as per ethically approved protocol (IEC/C/28-A/2010/DCT). Study population consisted of 24 patients with suspecting leukoplakia lesions in the oral cavity and 25 healthy volunteers having no oral cavity lesions, as control.

Monochrome images are recorded sequentially on the camera by positioning the LCTF at 545 and 575 nm. A computer generated algorithm converts the ratio image R545/R575 into false colours based on the severity of the disease. Tissue biopsies were taken from the malignant sites identified by imaging.

Among the 24 patients studied, 13 were squamous cell carcinomas and 11 were pre-malignant lesions as per the histopathology report. A sensitivity of 100% and a specificity of 91% was obtained for discriminating SCCs from pre-cancers. For discriminating healthy lesions from pre-caners the study yielded 100% diagnostic accuracy. The results show that DR imaging can be used as an effective clinical tool when visual inspection fails to identify the exact location for a biopsy.

8220-04, Session 1

## Statistical image analysis of neo-adjuvant chemotherapy monitoring with diffuse optical tomography

D. R. Busch, Univ. of Pennsylvania (United States); R. Choe, Univ. of Rochester (United States); S. Pathak, Univ. of Pennsylvania (United States); T. Durduran, ICFO - Institut de Ciències Fotòniques (Spain); W. Guo, M. A. Rosen, A. G. Yodh, Univ. of Pennsylvania (United States)

Diffuse Optical Tomography (DOT) provides 3D images of hemoglobin concentration, blood oxygen saturation, and optical scattering coefficients in deep tissues. We have applied this technique to image breast cancers, but the images are sometimes plagued by artifacts. This is of especial concern when monitoring changes in serial imaging in a cancer during a months-long course of neo-adjuvant chemotherapy. Nevertheless, the DOT data sets are rich in information (spatial, spectral and even temporal) and provide functional information on tissue, while X-Ray and Ultrasound provide primarily structural information. We have previously developed a statistical image analysis technique, based on the hypothesis that each tissue type will have a `chromophore signature' across a population after the data is suitably normalized between individuals. The approach enables us to reduce 3D reconstructions of total hemoglobin concentration, blood oxygen saturation, and tissue scattering coefficient into a 3D probability of malignancy map, which in turn enables volumetric tissue segmentation into `normal' and `cancerous' regions.

We have now applied this technique to create probability maps from serial DOT imaging during the course of neo-adjuvant chemotherapy. With these probability maps, we can calculate probability of malignancy isosurface volumes and compared the results to clinical radiology. Our initial results suggest that this statistical analysis of DOT data provides quantitative information on therapeutic effects during neo-adjuvant chemotherapy, without lengthy interpretation by an expert reader.

This research further advances automatization of DOT image interpretation through the development of Optical Computer Aided Diagnosis (CAD).

8220-05, Session 1

## Quantification of scattering and absorption coefficients of oral mucosa with hyperspectral imaging and Monte Carlo modeling

H. Pi, Y. Li, T. Tseng, H. Chen, C. Chen, K. Sung, National Taiwan Univ. (Taiwan)

Quantitative spectroscopy is increasingly used to obtain diagnostically relevant information of tissue for early detection of epithelial cancer. Recently, we reported accurate quantifications of the reduced scattering coefficient and absorption coefficient of two-layered tissue models by obtaining spatially-resolved reflectance spectra with a hyperspectral imaging system in contact probe geometry and simultaneously fitting the spatio-spectral data with an inversion procedure based on multi-layered scaling Monte Carlo forward modeling. In this paper we report the results of experimentally validating the method with solid two-layered tissue mimicking phantoms, followed by quantification of the optical properties of oral mucosa in vivo. Compared with our previously published results, the computational efficiency of the inversion procedure is improved and an oblique illumination and detection probe design is used to increase the sensitivity of the measured reflectance to the scattering coefficient of the top layer representing the epithelium. The bottom layer representing the lamina propria is assumed to be semi-infinite and homogeneous with the effective blood vessel diameter as a free parameter to be determined. To validate the performance of the proposed method we compare our results with independent quantification of the scattering and absorption coefficients of individual phantom layers by using double integrating spheres and the adding-doubling inversion method. The optical properties of the epithelium and the lamina propria at non-keratinized sites of the oral mucosa are obtained from normal volunteers with a hand-held flexible probe. The potential of using the hyperspectral imaging-based method to capture inhomogeneous tissue optical properties is also investigated.

8220-06, Session 1

## Analysis of soft tissue near-infrared spectra under dynamic pressure effects

B. Cugmas, F. Pernuš, B. Likar, Univ. of Ljubljana (Slovenia)

Near-infrared spectroscopy is a useful tool in many biomedical areas, for example, in cancer diagnostics, monitoring blood glucose concentration, monitoring tissue oxygenation and others. While measuring, it is normal to place a probe against the tissue and record a spectrum. Light pressure is regularly applied on the tissue and consequently tissue optical properties change. Changes can be seen in spectra and they can cause wrong interpretation of the data. Pressure effects on diffuse reflectance spectroscopy of different soft tissues have been reported by few researches. Mostly, visible light and human skin samples were used. Applying mentioned conditions, diffuse reflectance decreases with higher pressure. On the contrary, physiological parameters, representing scattering and absorption due to hemoglobin and oxygen saturation, are not simply correlated with pressure. Many parameters also vary when applying constant pressure for a longer duration. Variations are most likely tissue specific, therefore they can be also used as extra information in diagnostic applications. Pressure effects were studied in vivo and in vitro on different soft tissues, which are frequently the objects of interest in veterinary science, with a commercial near-infrared spectrometer. While continuously varying pressure, tissue spectra were acquired and subsequently analyzed. The purpose is to identify the dependence of spectral variations on probe pressure for each individual tissue type. For achieving that we also implemented continuous spectral measurements when pressure was staying at fixed amplitude.

8220-07, Session 2

## Pump-probe imaging of melanoma

W. S. Warren, Duke Univ. (United States)

Melanoma is one of the few cancers where mortality continues to rise (slowly), and it is unquestionably a serious concern; however, over the last several decades, the diagnosis rate based on histopathology has risen more than twenty times faster than the mortality rate. Numerous studies have concluded that the problem is that the diagnostic criteria, developed in an era when thick lesion biopsies were the norm (and when most of those lesions were fatal), are probably not appropriate for thin lesions. In effect, the "gold standard" of histopathology is probably not correctly predicting clinical outcome. As a result, it is likely there is significant overcalling of melanoma, but the precise extent of the problem is unknown.

Over the last two years we have demonstrated that a modified microscope can extract useful chemical information from existing histopathology slides-even ones that are already fixed and stained with hematoxylin and eosin (H&E) as in common practice (see for example Sci Transl Med. 2011;3(71):71ra15 and Biomed Opt Express. 2011;2(6):1576-83.) The chemical information is the spatial distribution of eumelanin and pheomelanin, the two different pigments in skin, which arise from different biochemical pathways. Our work has shown that both the bulk eumelanin content and the morphology do change significantly as we progress from dysplasic nevi to melanoma. Thus we believe we can improve the histopathology gold standard in diagnosis of melanoma, eliminating thousands of false negatives and false positives per year and saving many millions of dollars in healthcare costs.

8220-08, Session 2

## Time-resolved optical biopsy spectroscopy of normal, benign, and malignant tissues

V. Masilamani, King Saud Univ. (Saudi Arabia); J. Secor, B. B. Das, The City College of New York (United States); M. Al Salhi, King Saud Univ. (Saudi Arabia); S. Bint Amer, King Faisal Specialist Hospital & Research Ctr. (Saudi Arabia); D. Rabah, K. Farhat, Princess Johara Al-Ibrahim Ctr. for Cancer Research (Saudi Arabia); R. R. Alfano, The City College of New York (United States)

Histopathological examination is the gold standard to discriminate between benign and malignant growth of tissues. But this is invasive and stressful. Hence many non-invasive techniques such as CT, MRI, PET, etc are employed, each with certain advantages and disadvantages. In this respect optical diagnosis is quite promising, since it employs non-ionizing radiation like light or laser, which could be delivered through optical fiber to reach any part of the body.

This paper reports results of time resolved emission spectra of 24 excised tissue samples (normal control=12; benign=3 and malignant=9) of breast and prostate tissues, employing a 390 nm, 100 femtosecond, Ti- Sapphire laser pulses.

The fluorescence decay times were measured using streak camera and fitted for double exponentials with reliability of 97%. Our results showed distinct differences among the three sets. The fast and slow emission lines (with amplitude in parenthesis)were:- for Normal tissues: Major Fast component= 124±10 Ps (A1= 73726), Minor Slow component = 1177±210 Ps (A2= 5251), for benign tissues: Major Fast component= 60±15 Ps (A1= 15281), Minor Slow component = 773±111 Ps (A2= 1176) and for malignant tissues: Major Fast component= 42±8 Ps (A1= 1076),Minor Slow component = 610±58 Ps (A2= 188)

8220-09, Session 2

## Fluorescence lifetime techniques for tissue diagnosis: challenges and solutions

L. Marcu, Univ. of California, Davis (United States)

Fluorescence lifetime provides a powerful means for retrieving information about biochemical, functional and structural changes in fluorescent bio-molecular complexes in tissues and cells. Such changes can result from either pathological transformation or therapeutic intervention. Thus fluorescence lifetime-based techniques can play an important role in medical diagnosis. We developed time-resolved fluorescence spectroscopy and imaging techniques that utilize label-free fluorescence lifetime contrast to research, detect, and monitor in vivo biochemical features that are relevant for diagnosis of cancer and cardiovascular diseases. This presentation overviews clinically-compatible fluorescence lifetime instrumentation developed in our laboratory, design solutions for dynamic measurement of fluorescence lifetime from tissues, studies demonstrating the diagnostic potential of this optical technique, and challenges in clinical translation of this technology. We present results demonstrating that intrinsic fluorescence signals provide useful contrast for intravascular characterization of vulnerable atherosclerotic plaques and for intra-operative delineation of primary brain tumors and oral carcinomas. In addition, we present recent efforts concerning the integration of fluorescence lifetime techniques with other imaging methods that permit acquisition of complementary diagnostic information. This includes development of hybrid systems that allow for visual reconstruction of tissue microanatomy using ultrasound backscatter microscopy.

8220-10, Session 3

## Clinical requirements for optical imaging in medical robotics

J. Sorger, Intuitive Surgical, Inc. (United States)

Surgical robotics relies heavily on data collection, transmission and display technologies. Novel acquisition and visualization techniques have the ability to provide physiologic information not typically available at the bedside, enhancing the surgeon's senses. The stability of a robotic platform has enabled and will continue to drive various forms of augmented reality. The presentation will focus on the challenges surrounding the integration and presentation of such material in addition to providing insight into how new technologies are tested and prototyped in an industry setting.

8220-11, Session 3

## In vivo imaging of bladder cancer using prototype endoscope-adaptable system providing parallel RGB and NIR autofluorescence image acquisition

S. G. Demos, Lawrence Livermore National Lab. (United States); M. C. Jacobson, R. W. deVere White, UC Davis Medical Ctr. (United States)

In this paper we describe a prototype instrument that we developed to simultaneously conduct ordinary visual endoscopy together with NIR autofluorescence imaging via parallel image acquisition. The two images are recorded concurrently, without the need to switch back and forth between imaging modes, and the instrument interfaces with an ordinary endoscope. For our initial investigation using this instrument, we conducted an in vivo pilot study of bladder tumors to build on our previous work with NIR autofluorescence of bladder cancer using ex vivo specimens and define the current limitation for further development of the system. This study was conducted in 21 patients undergoing transurethral resection of bladder tumors at UC Davis Medical Center. After the tumor and the region of interest were initially defined via standard video cystoscopy, the standard coupler and video camera enabling the conventional RGB imaging were detached from the cystoscope and were replaced by the coupler and image preserving fiber bundle of the prototype system. The input of the cystoscope's light guide was detached from the conventional light source and coupled to the illumination assembly of the prototype system. The system was then used to capture RGB and NIR AF images of the region of interest while these images were displayed in separate adjacent monitors which guided the operator. The entire process of connecting the prototype system to the cystoscope, acquiring the in vivo data and, reverting to the regular RGB camera was accomplished within a time window of about 2 minutes.

8220-12, Session 3

## Correction for melanin absorption in a two-layer skin model using an artificial neural network in the spatial frequency domain

D. Yudovsky, A. J. Durkin, Univ. of California, Irvine (United States)

Monitoring of tissue blood volume and oxygen saturation using biomedical optics techniques has the potential to inform the assessment of tissue health, healing, and dysfunction. These quantities are typically estimated from the contribution of oxyhemoglobin and deoxyhemoglobin to the absorption spectrum of the dermis. However, estimation of blood related absorption in superficial skin can be confounded by the strong absorption of melanin in the epidermis. Furthermore, epidermal thickness and pigmentation varies with anatomic location, race, gender, and degree of disease progression. Therefore, a method is desired that decouples the effect of melanin absorption in the epidermis from blood absorption in the dermis for a large range of skin types and thicknesses.

We present a technique for decoupling the effect of melanin absorption in the epidermis from blood absorption in the dermis for a large range of skin types and thicknesses. An artificial neural network was used to map input optical properties to spatial frequency domain diffuse reflectance of two layer media. The neural network model was applied to mutli-layered tissue phantoms and in vivo human skin. We were able to independently probe the optical properties of the epidermis and dermis, and thus remove the effects of melanin on the oximetry signal.

8220-13, Session 3

## An intraoperative probe combining positron detection and OCT imaging for ovarian cancer detection and characterization

Y. Yang, T. Wang, N. C. Biswal, P. D. Kumavor, Univ. of Connecticut (United States); X. Wang, M. Karimeddini, J. Vento, M. Sanders, M. Brewer, Univ. of Connecticut Health Ctr. (United States); Q. Zhu, Univ. of Connecticut (United States)

Ovarian cancer has the lowest survival rate of the gynecologic cancers because it is predominantly diagnosed in the late stages due to the lack of reliable symptoms and efficacious screening techniques. A novel hybrid intraoperative probe based on OCT and positron detection has been developed and evaluated for its potential role in detecting and characterizing ovarian tissue. The dual-modality device could simultaneously map the local activities of 18F-FDG uptake, image local morphological changes and measure optical scattering coefficient of ovarian tissue. Ten patients were recruited to the study and a total of 18 normal, abnormal and malignant ovaries were evaluated ex-vivo using this device. 1097 scattering coefficient measurements were performed at 108 sites obtained from these ovaries. Positron count rates of 7.5/8.8-fold higher were found between malignant and abnormal/normal ovaries. OCT imaging of malignant and abnormal ovaries revealed many detailed morphologic features. The average scattering coefficient obtained from normal group consisted of 833 measurements from 88 sites was 2.41 mm-1 (±0.59), while the average coefficient obtained from malignant group consisted of 264 measurements from 20 sites was 1.55 mm-1 (±0.46). The malignant ovarian tissue showed significant lower scattering than the normal group ($p < 0.001$). Using a threshold of 1.90 mm-1, a sensitivity of 76% and a specificity of 80% were obtained. These initial results have demonstrated that our novel hybrid imager has great potential for ovarian cancer detection and characterization.

8220-14, Session 3

## Evaluating limb ischemia using a non-invasive multimodal spectroscopic system

R. Luthra, N. J. Crane, Naval Medical Research Ctr. (United States); E. A. Elster, Naval Medical Research Ctr. (United States) and Walter Reed National Medical Ctr. (United States) and Uniformed Services Univ. Health Sciences (United States)

Casualties in Operation Iraqi Freedom (OIF) and Operation Enduring Freedom (OEF) have experienced a high rate of extremity injuries with nearly ubiquitous diffuse tissue damage and compromised local circulation and are often associated with overt vascular injury. These injuries include traumatic amputations, open fractures, crush injuries, and, acute vascular disruption. Delayed repair of critical blood vessels with these types of injuries has been common, given the nature of the environment and the limitation of surgical techniques in theater. Direct consequences of vascular damage are tissue ischemia and compartment syndrome leading to hypoxia and ultimately necrosis requiring amputation. Current methods of assessing limb perfusion are either invasive, suffer from high variability or provide extremely localized information. An improved assessment of global and regional perfusion is necessary for timely and accurate treatment of major extremity trauma, and reducing the number and extent of amputations.

In this study, we examine the use of 3-CCD (3 charge-coupled device) imaging, infrared imaging, Raman spectroscopy, near-infrared and visible reflectance spectroscopic imaging in a multimodal and concurrent fashion for the non-invasive measurements of tissue oxygenation and perfusion in large animals and humans. Ideally, this will allow for the determination of viable of damaged tissue which can ultimately imapctthe tissue environment for wound healing. In turn, this can provide objective indicators for physicians deciding between limb salvage versus amputation.

8220-15, Session 3

## Fluorescence anisotropy characterization of oral tissues

S. Shanmugam, Anna Univ. Chennai (India); D. Koteeswaran, Meenakshi Ammal Dental College & Hospital (India); K. Muthuvelu, Stanley Medical College and Hospital (India); G. Bharanidharan, P. R. Aruna, Anna Univ. Chennai (India); C. Muralikrishna, Advanced Ctr. for Treatment, Research & Education in Cancer (India); S. Ganesan, Anna Univ. Chennai (India)

The changes in fluorescence and scattering properties can occur in the early stages of cancer development. Therefore, optical techniques, such as fluorescence and reflectance spectroscopy, can be useful in probing the events occurring in the early stages of cancer development. In this study, the feasibility of utilizing the fluorescence anisotropy measurements was attempted to detect the changes that occurs during the transformation of normal state to cancerous state. In vitro fluorescence anisotropy measurements were made for thirty oral carcinoma patients and compared with twenty normal counterparts. The anisotropy value of tryptophan was 0.397±0.055 for normal whereas 0.612±0.124 for oral cancer patients and the anisotropy value of collagen was 0.278±0.154 for normal whereas 0.542±0.072 for oral cancer patients. The details of result will be discussed.

8220-16, Session 3

## Fibre optic fluorescence spectroscopy for monitoring fish freshness

J. Wu, S. Chu, T. Hsiao, H. Hu, National Chiao Tung Univ. (Taiwan)

Fish freshness is the major concern for consumer purchasing. Therefore, many different sensing technologies system have been developed for monitoring freshness now. The fluorescence spectra of such as lipid oxidation, tryptophan and NADH products have been distinguished the stages of fish freshness and assumed as an index of fish freshness. However, the factors of freshness are too complicated to select a compound as freshness so we want to measure broad wavelengthes fluorescence spectra to search the best range for detecting the freshness of fish. In this study, we selected Cobia ( Rachycentron canadum ), which are widely used in sashimi and other delicacies. We use a portable Y-type fibreoptic fluorescence spectroscopy measurement system to evaluate the freshness of meat. This system included a CERMAX xenon lamp, a H10 monochromator, a MicrHR180 spectrometer, a R928 photomultiplier tube (PMT), a Y-type optical fiber, and a general commercial desktop. The sliced fish samples were excited by specific wavelength of light and emitted respective fluorescence signals. The signals were sent back through the fiber bundle, and then split by the MicrHR180 spectrometer and eventually acquired by PMT for detecting. Our results showed that the ratio of fluorescent intensity, which F480 nm/Fexci+50 nm was belong with the range of collagen type I and type V characteristic spectra, was positive correlated to the frozen time by hours. It was a strong approach to be a potential index for differentiating the fish freshness during delivery process. Besides, the different pattern results of dorsum and abdomen were shown in this study. In the further, fibreoptic fluorescence spectroscopy could be a way not only to measure and quantify the freshness of different fish body but also to verify the level of taste.

8220-17, Session 3

## Compact Stokes shift and fluorescence spectroscopic diagnostics ratiometer unit with no moving parts for cancer detection

L. A. Sordillo, Y. Budansky, R. R. Alfano, The City College of New York (United States)

Stokes shift spectroscopy (S3) measures differences in wavelength maxima of absorbed and emitted photons corresponding to vibrational relaxation and energy decreases in emitted photons. A compact device with no moving parts which uses this technique for identification of biomolecules within cancerous tissue samples is presented. This ratiometer unit measures the effect of the emission and absorption spectra of key native organic biomolecules by using multiple wavelength LEDs coupled to an optical fiber and wavelengths in the ultraviolet to blue-green range (280nm-520nm). Light from a LED travels through an optical fiber probe at a fixed wavelength to the potentially cancerous tissue. The sample is excited and emits radiation where emission spectra and the intensity at the Stoke shift is displayed and recorded. This Stokes shift difference between excitation and emission peak maxima generally ranges from 10nm to 150nm. From a single scan done in seconds, extensive information on the tissue state can be obtained. Through this optical biopsy approach, the multiple peaks obtained are used to identify the biomolecules in the tissue, giving an optical fingerprint. Biomolecules such as tryptophan, collagen, and NADH are easily identified. This new approach allows for the extraction of information not obtained from excitation or fluorescence spectroscopy. This S3 ratiometer device can be used as part of the evaluation to determine whether a lesion is benign or malignant, for determining the presence of residual cancer after surgery, to locate margins during surgery or radiation, or assess for recurrence making second biopsies unnecessary. This technique may also allow identification of histologic sub-types, potentially resulting in more individualized therapies.

8220-18, Session 3

## Spectral grading and Gleason index of malignant prostate tissue using optical biopsy fluorescence and Stokes shift

M. Al Salhi, V. Masilamani, King Saud Univ. (Saudi Arabia); D. Rabah, K. Farhat, Princess Johara Al-Ibrahim Ctr. for Cancer Research (Saudi Arabia); C. Liu, Y. Pu, R. R. Alfano, The City College of New York (United States)

Gleason index is the most common method for grading the virulence of prostate malignancy and is based on the pathological assessment of morphology of the tissues. Since this involves invasive excision of the tissue, we are working on a new, non-invasive, procedure for spectral diagnosis of prostate malignancy.

In this preliminary in vitro study, we have analyzed 27 tissue samples (normal control =8: benign=9: malignant =10) by Fluorescence Emission Spectra (FES) and Stokes' Shift Spectra (SSS).

FES was done with excitation at 300nm, 325nm, and 400 nm; SSS was done with wavelength offsets of 70nm and 20 nm; In addition diffuse reflectance spectra ($\Delta\lambda$=0 nm in SSS) were also taken.

The results showed that there were distinct differences in the spectral features of normal, benign and malignant sets; but the contrast between Normal and Malignant is greater than that between Normal and Benign. Among the 10 malignant samples, there is a good parallelism between spectral parameters and Gleason Index. This indicates the promising potential of native fluorescence spectroscopy for non-invasive tissue diagnosis of prostate malignancy.

8220-19, Session 4

## Terahertz imaging of nonmelanoma skin cancers

C. S. Joseph, Univ. of Massachusetts Lowell (United States); A. N. Yaroslavsky, Univ. of Massachusetts Lowell (United States) and Massachusetts General Hospital (United States); V. A. Neel, Massachusetts General Hospital (United States); T. M. Goyette, R. H. Giles, Univ. of Massachusetts Lowell (United States)

Continuous wave terahertz imaging has the potential to differentiate between nonmelanoma skin cancers and normal skin. Contrast between cancerous and normal tissue in transmission mode has already been demonstrated using a continuous wave terahertz system. The aim of this experiment was to interrogate fresh samples of nonmelanoma skin cancers using a continuous wave terahertz source. A CO2 optically pumped far-infrared molecular gas laser was used for illuminating the tissue at 3 frequencies, 1.6 THz, 1.4 THz and 584 GHz. The reflected and transmitted signals were detected using liquid helium cooled silicon bolometers. Fresh skin cancer specimens were obtained from Mohs micrographic surgeries. The samples were processed and imaged within 24 hours after surgery. To enable simultaneous reflectance and transmittance imaging the samples were sectioned horizontally and 240 µm thick sections were imaged in the terahertz system. Hematoxylin & Eosin (H&E) histology was processed on adjacent 10 µm sections for comparison. During imaging skin specimens were hydrated in pH balanced saline solution. The terahertz reflection and transmission images were found to correlate well with each other and with sample histology. Reflectance continuous wave terahertz imaging has potential for noninvasive detection of nonmelanoma skin cancers during surgeries.

8220-20, Session 4

## Breast biopsy guidance with OCT: an in vivo study in a mouse model of breast cancer

N. V. Iftimia, M. Mujat, D. X. Hammer, Physical Sciences Inc. (United States)

We present the development and preliminary in vivo testing of a breast biopsy guidance system based on optical coherence tomography (OCT). A special biopsy gun that integrates an OCT probe within the plunger of a regular 10-20 ml syringe was designed, fabricated, and tested in vivo in a mouse model of breast cancer. The OCT signal is analyzed by a custom-designed algorithm that runs in a GPU card and the information related to the tissue-type present at the needle tip is conveyed in real-time to biopsy physician. Preliminary data suggest that this technology could help the clinician to more objectively decide when to perform an aspirate and thus it might increase the diagnostic yield of current fine needle biopsy procedures. The detailed description of the instrument and its preliminary testing on an animal model of breast cancer will be discussed.

8220-21, Session 4

## Use of Mueller polarimetric imaging for early detection of uterine cervix cancer

A. Pierangelo, S. Manhas, M. R. Antonelli, T. Novikova, A. De Martino, Ecole Polytechnique (France); A. Benali, P. Validire, H. Cohen, Institut Mutualiste Montsouris (France); A. Nazac, CHU Bicêtre (France)

Ex-vivo cone biopsies (conisations) were analyzed using a multispectral Mueller polarimetric imaging. These conisations are typically 2 cm diameter samples extracted from uterine cervix when biopsy under colposcopy shows the presence of malignant or pre malignant zones. Cervical cancer is preceded by a pre-cancerous tissue transformation, named Cervical Intraepithelial Neoplasia (CIN). If the disease is treated at this stage the patient survival rate is about 95%. Other, non-malignant lesions (ectropion, inflammation, parakeratosis) are often present and make the visual detection of CIN very difficult. Our preliminary results show that Mueller polarimetry is a valuable tool to detect abnormal zones and to distinguish malignant from non-malignant diseases.

For short wavelengths (500-550nm) malignant zones are less depolarizing than healthy ones. This difference decreases for longer wavelengths (600-700nm). This behavior can be explained in terms of light penetration depth that is less for shorter wavelengths due to the strong absorption of haemoglobin. In malignant zones (due to the increasing of cellular density and vascularisation) light beam interacts prevalently with malignant cells in the epithelial tissue for shorter wavelengths, while longer wavelengths probe also the strongly depolarizing deeper connective tissues. In contrast, in healthy zones the light beam interacts with the epithelium and deeper connective tissue for all wavelengths. Birefringence is observed for all wavelengths in healthy zones when parakeratosis (ordered fibrous structure) is present on the epithelium. These results pave the way to develop an optical tool for early cancer detection with higher sensitivity and specificity than those of classical colposcopy.

8220-22, Session 4

## Advances in optogenetics

K. Deisseroth, Stanford Univ. (USA)

No abstract available

8220-23, Session 5

## Discovery in translation: near-infrared fluorescence imaging

E. M. Sevick-Muraca, The Univ. of Texas Health Science Ctr. at Houston (United States)

When translating brand new imaging modalities into human studies, one can expect new discoveries. Owing to high photon count rates, near-infrared fluorescence offers exquisite sensitivity and high temporal resolution. Herein, we present some new “glimpses” of human physiology provided in translational studies of normal subjects and in persons with lymphatic disorders.

8220-24, Session 5

## Multimodal optical imaging for detecting breast cancer

R. Patel, Univ. of Massachusetts Lowell (United States); A. Khan, UMass Memorial Medical Ctr. (United States); D. J. Wirth, Univ. of Massachusetts Lowell (United States); M. Kamionek, R. Quinlan, UMass Memorial Medical Ctr. (United States); A. N. Yaroslavsky, Univ. of Massachusetts Lowell (United States)

Delineation of cancer margins at the time of surgery is a problem of major importance in surgical oncology. The goal of this study was to evaluate the feasibility of wide-field and high-resolution multimodal optical imaging, including, polarization, reflectance, and fluorescence for detecting breast cancer margins. Fresh thick breast tissue specimens were collected following surgeries, stained with 0.05 mg/ml aqueous solution of methlylene blue and imaged using wide-field and high resolution confocal systems. In total, 16 samples were investigated, including 10 ductal carcinomas, 4 lobular carcinomas, 1 intracystic papillary carcinoma, and 1 colloid carcinoma. Wide-field reflectance polarization images were taken at 9 wavelengths between 390 nm and 750 nm. Wide-field fluorescence polarization images were excited at 640 nm and registered between 660 nm and 750 nm. High resolution confocal reflectance and fluorescence images were excited using 642 nm laser with fluorescence images registered between 670 nm and 710 nm. After imaging, the specimens were processed for H&E paraffin embedded histopathology. Histological slides were digitized and compared side-by-side with the multimodal wide-field and high-resolution optical images to evaluate correlation of tumor margins and cellular morphology, respectively. The results of the study demonstrate that all the specimens investigated produced high contrast wide-field reflectance and fluorescence polarization images. Dark sections in reflectance images in the spectral range between 577 nm and 680 nm, and bright areas in fluorescence polarization images grossly correlated with tumor regions in their respective histopathology. Fluorescence confocal imaging enables cellular resolution and facilitates analysis of microscopic morphology of tissue in the manner similar to histopathology. Wide-field high-resolution optical imaging shows promise for intraoperative delineation of breast cancers.

8220-25, Session 5

## A dual-modality imaging approach to early diagnosis of cancer in a hamster cheek pouch model

P. Pande, S. Shrestha, J. Park, J. A. Jo, Texas A&M Univ. (United States); I. Gimenez-Conti, J. L. Brandon, The Univ. of Texas M.D. Anderson Cancer Ctr. (United States); B. E. Applegate, Texas A&M Univ. (United States)

It is known that both biochemical and morphological changes accompany the transition from normal to neoplastic tissue. Yet most optical techniques investigated so far as potential screening and diagnostic tools for cancer have largely concentrated on detecting one or the other. We have taken a multimodal approach for early cancer detection which integrates Optical Coherence Tomography (OCT) with multi-spectral Fluorescence Lifetime Imaging (FLIM). This approach enables the simultaneous interrogation of both sets of biomarkers. For this study, we have used Syrian hamster cheek pouch model of epithelial cancer. As a part of the imaging protocol we have successfully imaged 52 male Syrian hamsters (20 control, 32 treated) using a multimodality OCT/FLIM system developed by our group that is capable of a maximum A-line rate of 59 KHz for OCT and a pixel rate of up to 30 KHz for FLIM. In order to provide a qualitative assessment of the high-resolution OCT data we describe texture analysis methods to quantify tissue morphology that includes nonstationary texture analysis methods like Gabor filters and descriptive methods like Laws and Walsh filtering. Similarly, for multi-spectral FLIM data, in addition to the standard intensity and lifetime features we describe a new set of features based on hyperspectral unmixing that quantify the relative abundance of different fluorescent species present in the tissue. We also present a statistical classification algorithm that uses the derived morphological and biochemical features to perform tissue classification that is capable of distinguishing between normal, pre-malignant and malignant oral tissue.

8220-26, Session 5

## Monitoring the morphochemistry of laryngeal carcinoma by multimodal imaging

T. Meyer, Friedrich-Schiller-Univ. Jena (Germany); C. Krafft, Institut für Photonische Technologien e.V. (Germany); O. Guntinas-Lichius, Universitätsklinikum Jena (Germany); B. Dietzek, Friedrich-Schiller-Univ. Jena (Germany); J. Popp, Institut für Photonische Technologien e.V. (Germany)

Multimodal nonlinear imaging constitutes a contemporary approach to investigate the morphochemistry of complex samples in a noninvasively and label free. Here we discuss our recent success in jointly using various nonlinear microspectroscopic approaches such as coherent anti-Stokes Raman scattering (CARS), two-photon fluorescence (TPF) and second-harmonin generation (SHG) to study the chemical composition of surgically removed tissue sections from laryngeal carcinoma. In particular we will show how multimodal nonlinear imaging in combination with linear microspectroscopy, i.e. single-photon fluorescence or Raman scattering can be employed to study the structural and chemical development of disease formation as well as to monitor the clinically important aspect of tumor boundary detection.

Financial support of the European Union via the Europäischer Fonds für Regionale Entwicklung (EFRE) and the “Thüringer Kultusministerium (TKM)” (Projects: B714-07037, B578-06001, 14.90 HWP) and via the European network of excellence P4L (Photonics4Life) as well as financial support by the German Ministry for Science and Education is highly acknowledged.

8220-27, Session 6

## Profiling wound healing with wound effluent: Raman spectroscopic indicators of infection

N. J. Crane, R. Luthra, Naval Medical Research Ctr. (United States); E. A. Elster, Naval Medical Research Ctr. (United States) and Walter Reed National Medical Ctr. (United States) and Uniformed Services Univ. of Health Sciences (United States)

The care of modern traumatic war wounds remains a significant challenge for clinicians. Many of the extremity wounds inflicted during Operation Enduring Freedom and Operation Iraqi Freedom are colonized or infected with multi-drug resistant organisms, particularly Acinetobacter baumannii. Acinetobacter baumannii is a gram-negative nosocomial pathogen with a capacity for forming antimicrobial resistant biofilms, which can be resistant to host defense as well as traditional antibiotic treatments. Biofilm formation and resistance to current treatments can significantly confound the wound healing process. Overtreatment of infections with broad spectrum antibiotics can result in an increased number of multi-drug resistant organism strains, such as with Acinetobacter baumannii. Thus, accurate strain identification and targeted drug administration for the treatment of wound bioburden has become a priority for combat casualty care.

In this study, we use vibrational spectroscopy to examine wound exudates for bacterial load. Inherent chemical differences in different bacterial species and strains make possible the high specificity of vibrational spectroscopy. The use of vibrational spectroscopy has the potential to offer improved objective assessment of combat wounds, resulting in faster healing times, decreased infection rates, and decreased local and systemic complications of injury.

8220-28, Session 6

## Fluorescence emission and excitation spectroscopic characterization of blood plasma protein

P. R. Aruna, S. Shanmugam, Anna Univ. Chennai (India); K. Muthuvelu, Stanley Medical College and Hospital (India); G. Bharanidharan, Anna Univ. Chennai (India); D. Koteeswaran, Meenakshi Ammal Dental College & Hopsital (India); C. Muralikrishna, Advanced Ctr. for Treatment, Research & Education in Cancer (India); S. Ganesan, Anna Univ. Chennai (India)

Native fluorescence spectroscopy has been widely considered in the characterization of metabolic and pathological conditions of cells and tissues at the molecular level. In this work, it is aimed to compare the emission and excitation spectroscopic characterization of protein present in blood plasma to discriminate the normal subjects from the diseased one. Based on the discriminant analysis, it is found that the fluorescence emission spectra of tryptophan resulting a specificity of 81.3%, whereas the sensitivity to correctly classify cervical cancerous subjects is found to be 58.7%. From the excitation spectra the specificity and sensitivity was 87.5% and 100 % respectively. The details of result will be discussed

8220-29, Session 6

## Synchronous luminescence spectroscopic characterization of urine of normal and cancerous patients

R. Ramu, Y. Manoharan, Anna Univ. Chennai (India); K. Muthuvelu, Stanley Medical College and Hospital (India); D. Koteeswaran, Meenakshi Ammal Dental College & Hopsital (India); T. T., Dr. Rai Memorial Cancer Institute (India); G. Bharanidharan, P. R. Aruna, Anna Univ. Chennai (India); C. Muralikrishna, Advanced Ctr. for Treatment, Research & Education in Cancer (India); S. Ganesan, Anna Univ. Chennai (India)

Urine is one of the diagnostically important bio fluids, as it has different metabolites in it, where many of them are native fluorophores. There may be a variation in the distribution and the physiochemical properties of the fluorophores during any metabolic change and pathologic conditions. Fluorescence spectroscopy has been considered as a tool to characterize the fluorophores present in the urine. This is because, it is sensitive even at trace level and has many complementary techniques. Among these, the synchronous luminescence technique is a powerful tool, as it is possible to analyse multicomponents in single spectrum and it is possible to obtain resolved emission spectrum without much of photobleaching of fluorophores. In this study, we aimed at characterising the urine of both normal and patients with confirmed cancer using synchronous luminescence spectroscopy. Attempts were also made to discriminate the cancer patients from normal subjects. The details of synchronous luminescence spectral signatures between normal and cancer patients and its statistical significance will be discussed.

8220-30, Session 6

## Time-resolved fluorescence spectroscopic characteristics of normal and cancerous blood

Y. Manoharan, U. Kanniappan, Anna Univ. Chennai (India); J. Vadivel, Meenakshi Ammal Dental College & Hopsital (India); S. Suresh, Arignar Anna Memorial Cancer Hospital (India); D. Koteeswaran, Meenakshi Ammal Dental College & Hopsital (India); K. Muthuvelu, Stanley Medical College and Hospital (India); C. Pravada, Sathyabama Deemed Univ. (India); G. Bharanidharan, P. R. Aruna, Anna Univ. Chennai (India); C. Muralikrishna, Advanced Ctr. for Treatment, Research & Education in Cancer (India); S. Ganesan, Anna Univ. Chennai (India)

Many attempted to study native fluorescence spectroscopy of tissues and blood in the discrimination of cancer from normal. Data reported that there is a possibility of discriminating the normal from cancer with excellent statistical significancy, using both fluorescence emission and excitation spectroscopy. However, still the reasons for the altered spectral signature between normal and pathologically confirmed tissues are not clear. The excited state kinetics of fluorophores provides the reason for altered emission, as the life time of fluorophore is highly sensitive to micro environmental changes. In this context, an attempt was made to study the excited state kinetics of tryptophan and endogenous porphyrin present in both normal and cancerous blood to verify whether there is any photo physical changes occur or not. The decay characteristics of amino acid, tryptophan and endogenous porphyrin present in blood plasma of normal subjects and cancer patient and the statistical significancy between them will be discussed.

8220-31, Session 7

## Novel ratiometric imaging techniques and 280-nm-excited autofluorescence for improved visualization of adenocarcinoma in human colon specimens

T. Renkoski, L. Graves, U. Utzinger, V. L. Tsikitis, N. S. Rial, P. Tiwari, H. Gavini, B. Banerjee, The Univ. of Arizona (United States)

Better visualization is needed of “flat” and often-missed neoplastic lesions of the colon. A prototype spectral imager was applied to 22 fresh human colon resections, and macroscopic autofluorescence (AF) images were collected including AF excited with 280-nm light (AF280). Narrowband crossed polarization reflectance (REF) images were also collected. Decreased AF280 intensity was observed from adenocarcinomas compared to the surrounding normal mucosa. This result, likely due to hemoglobin absorption in hypervascular tumor regions, was opposite that predicted by previous work on isolated colonocytes. Utilizing additional AF images excited with longer wavelengths (AF320, AF340, AF440), we investigated a variety of novel ratiometric imaging combinations to achieve optimal lesion visualization. Arithmetic combinations of AF images were formulated using knowledge of the underlying endogenous fluorophores tryptophan, collagen, NADH, and FAD. Many of the formulated ratio images proved to be useful in correcting for heterogeneity in optical properties. We compare the novel ratiometric images to previously published techniques including AF divided by REF, redox, and oxygenation imaging ratios. Among the results: Combinations of AF images that included AF280 were more effective than those from which AF280 was omitted. Correction of AF280 images by reflectance was most effective using our longest REF wavelength, 555 nm. No exogenous contrast agent is used in the method, and phototoxicity concerns should be reduced recognizing that penetration of 280-nm light is restricted to surface epithelial cells, which are soon-to-be shed and replaced. This ratio imaging technique has great potential for use in an advanced colonoscope to detect flat lesions.

8220-32, Session 7

## Time-resolved picosecond fluorescence spectroscopy for cancer detection in human breast tissues

Y. Pu, The City College of New York (United States); A. Pradhan, Indian Institute of Technology Kanpur (India); G. Tang, C. Liu, B. B. Das, R. R. Alfano, The City College of New York (United States)

Time-resolved fluorescence spectroscopy from normal breast tissue, benign and malignant breast tumors were measured at emission band of 340 nm using 100 fs ultrafast laser pulse of 310nm. Fluorescence relaxation decay parameters were extracted from the measured spectroscopy. The differences of time-resolved spectra of normal tissue, benign and malignant tumor, including their profiles, decay time and relation between the amplitude were observed. The malignant tumor can be separated from non-malignant tissue using slow decay time and the ratios of amplitude of fast components over the slow components. The fast decay time of normal breast tissue is higher than that of benign tumor. The differences between the decay times and amplitude ratios of slow and fast components can be explained that the presence of tryptophan in different proportions in cancerous and noncancerous tissues and the different environments in normal and abnormal tissues. It is known that the fluorescence yield at 340 nm arises from tryptophan and its residues. The decay times are strongly influenced by their microenvironments, such as different pH values and proximity of charged groups to the fluorophores. Different pH value sometimes results in larger nonradiative energy losses. The large s for malignant tissue suggest more nonradiative processes in benign breast tissue.

The work about the time-resolved measurements and analysis make it possible to detect small changes in the environment of tissues. The studies of molecular structure changes and the underlying dynamics, fluorescence lifetime analysis may provide a potential technique for medical diagnostic purpose.

8220-33, Poster Session

## Improving the accuracy of quantifying epithelial scattering coefficient in a two-layered tissue model by using a beveled fiber bundle probe

H. Chen, Y. Li, H. Pi, C. Chen, K. Sung, National Taiwan Univ. (Taiwan)

Diffuse reflectance spectroscopy has been widely used to interrogate the scattering and absorption coefficients of turbid media and has the potential to noninvasively detect epithelial dysplasia which is a precursor of many cancers. We recently developed a hyperspectral imaging-based system with an imaging fiber bundle to measure spatially-resolved reflectance spectra and quantify optical properties of both numerical and physical two-layered tissue models. To improve the sensitivity of the measured reflectance intensity to the optical properties of the epithelium, we propose to use a beveled fiber bundle whose end surface is flush with the surface of the specimen to be measured. In comparison with the more frequently used design in which the source and/or detection fibers are tilted to point toward each other, our proposed probe geometry facilitates miniaturization of the probe for endoscopic applications. We implement a fast scaling Monte Carlo (MC) method for the sensitivity study. The MC code is also used in conjunction with an iterative curve fitting algorithm to extract the optical properties of two-layered tissue models from two-dimensional spatio-spectral reflectance data. Results of both the MC simulation and physical model experiments show increased sensitivity to changes in the epithelial scattering coefficient and improved accuracy of quantifying the epithelial optical properties. The proposed method is a viable option to improve noninvasive detection of dysplasia and early cancer in stratified squamous epithelium.

8220-34, Poster Session

## Optical spectroscopic characteristics of lactate and mitochondrion as new biomarkers in cancer diagnosis: understanding Warburg effect

C. Liu, X. H. Ni, Y. Pu, Y. L. Yang, F. Zhou, R. Zuzolo, W. Wang, The City College of New York (United States); V. Masilamani, King Saud Univ. (Saudi Arabia); A. Rizwan, Weill Cornell Medical College (United States); R. R. Alfano, The City College of New York (United States)

Cancer cells display high rates of glycolysis even with oxygen and mostly in the hypoxia condition. Warburg proposed this effect of altered metabolism in cells more than 80 years ago. It is considered as a hallmark of cancer. Optical spectroscopy can be used to explore this effect.

Pathophysiological studies indicate that mitochondria are enlarged and increase in number in cancer cells. Warburg observed that cancer cells tend to convert most glucose to lactate regardless of the presence of oxygen. Previous observations show increased lactate in breast cancer lines.

The focus of this study is to investigate the relative content changes of lactate and mitochondria in human breast cancerous and normal tissues using optical spectroscopic techniques.

The optical spectra were obtained from 30 cancer and 25 normal samples of breast tissues and four model components (fat, collagen, lactate and mitochondrion) using fluorescence, stokes shift and Raman spectroscopy. The basic biochemical component analysis model (BBCA) and a set of algorithm were used to analyze the spectra.

Our preliminary analyses of fluorescence spectra show the content changes of lactate and mitochondria in cancerous and normal tissues. The lactate and mitochondrion concentrations are evaluated in cancerous tissue suggesting a correlation between the lactate and mitochondrion, and increase contribution trend from cancerous tissue.

Our findings indicate that optical spectroscopic techniques may be used to understand Warburg effect. Lactate and mitochondrion content changes in tumor studied using optical spectroscopy may be used as a prognostic marker in clinic applications.

# Conference 8221: Optical Interactions with Tissue and Cells XXIII

Monday-Wednesday 23-25 January 2012

Part of Proceedings of SPIE Vol. 8221 Optical Interactions with Tissue and Cells XXIII

8221-01, Session 1

## Optical and laser treatments: What now? What next?

R. R. Anderson, Massachusetts General Hospital (United States)

No abstract available

8221-02, Session 1

## Nanoparticle supported laser-tissue-soldering for closure of natural orifices for transluminal endoscopic surgery

M. Frenz, S. Bogni, Univ. Bern (Switzerland); A. Schönbächler, Bern Univ. Hospital (United States); U. Pieles, Bern Univ. Hospital (Switzerland); M. Reinert, I. Vaytai, Bern Univ. Hospital (United States); M. Ortner, Univ. Hospital Zürich (United States); B. Dallamagne, Les Hôpitaux Univ. de Strasbourg (France)

No abstract available

8221-03, Session 1

## Optical and thermal effects of diode lasers in tissues at 810, 940, and 980 nm with clean and coated fiber tips

R. M. Verdaasdonk, A. van der Veen, M. Visser, Vrije Univ. Medical Ctr. (Netherlands); V. Lemberg, D. Boutoussov, BIOLASE Technology, Inc. (United States)

Diode lasers are available at various wavelengths in the near infrared and each are ascribed to have unique tissue effects. In this study, the tissue effects of diode lasers at 810, 940 nm (Biolase) and 980 nm (Sirona) were compared under controlled conditions in tissues simulating clinical settings using special close up imaging and thermal imaging techniques.

A transparent model tissue with a IR absorber and biological tissue with either high blood content (liver) or low blood content (pale muscle) was irradiated at 4 W for 10 seconds from a 300 µm bare fiber positioned 2 mm above or in contact with the surface (clean or carbon coated tip). The progression of coagulation and ablation were followed in time imaging subsurface through a window from the side. Tissue ablation started only after a short delay in liver at 810 and 980 nm in both contact (< 1s) and non-contact (<5s) mode. In all other condition, the tissue was only coagulated. When the tip was carbon-coated, the tissue ablation started within 1 second. The initial beam distribution from a clean tip could be visualized using thermal imaging in both the transparent model tissue and biological tissue showing the influence of scattering.

The 940 nm diode laser seems unique for deep tissue penetration inducing coagulation without uncontrolled carbonization. Carbon- coated fiber tips work effectively at all diode laser wavelengths for tissue cutting.

8221-04, Session 1

## Comparison of excimer laser angioplasty with long-wavelength laser angioplasty

V. Mosallanejad, Kerman Graduate Univ. of Technology (Iran, Islamic Republic of); M. H. Z. Goharrizi, Shahid Bahonar Univ. of Kerman (Iran, Islamic Republic of); M. Hajjafar, Arjomand Hospital (Iran, Islamic Republic of); A. Bahrampour, Sharif Univ. of Technology (Iran, Islamic Republic of)

Common Excimer laser angioplasty (ETCA) uses a 308 nm Excimer laser to vaporize the coronary plaque. There are two problems for this method which still exist. Although the thermal problem is solved by choosing short wavelengths, the high absorption of UV by DNA and proteins in the vessel wall cells produces restenosis. The water high absorption coefficient in UV region causes bubble formation and it will cause deformations in the vein. The laser pulse duration is in the order of several ten nanoseconds. It is possible to remove tissues by plasma mediated ablation in the long wavelength. By choosing a proper laser parameter the precise ablation could be possible. Numerical method is applied for determining of optical breakdown threshold for different materials in coronary plaque for long wavelength irradiation. Comparison between thresholds and breakdown threshold in water has shown that the contact ablation regime is more efficient. The swallowing side effects have been considered for different pulse duration in the contact regime. The delivered energy density to medium is key factor for the study of undesirable side effects for internal vessel laser surgeries. In this study the comparison of ETCA is done with long wavelength laser angioplasty.

8221-05, Session 1

## Assessment of thermal lensing in ocular media using an articial eye

E. L. Weber, The Univ. of Texas at Austin (United States) and Consortium Research Fellows Program (United States) and Air Force Research Lab. (United States); M. Rickman, TASC, Inc. (United States); A. K. Dunn, The Univ. of Texas at Austin (United States); R. J. Thomas, Air Force Research Lab. (United States)

High energy lasers operating in the near-infrared region are steadily becoming popular for use in a variety of applications, and thus a complete understanding of their safety is required. In recent years, studies have shown that thermal lensing significantly impacts damage thresholds in ocular media by utilizing indirect confocal imaging techniques to visualize the effect in an artificial eye; however, a minimum threshold of effect has yet to be determined. Therefore, a new fiber based imaging system has been incorporated into a modified artificial eye for direct measurement of the thermal lensing effect induced by an infrared laser, 1319 nm, to quantify the threshold for effect. The response of a visible beam, 632 nm, was observed with respect to various exposures of the infrared light under different power levels and exposure durations. Infrared irradiance levels of 225, 450, 625, 900, 1200, 1500, and 1800 mWcm-2 were used with exposure durations of 0.25s, 0.50s, 0.75s, 1s, and 2s in order to observe the optimal level of radiant energy needed to blur the visible beam at the retinal plane. Results suggest that deformation of the visible beam begins at irradiance levels of 600 mWcm-2 with significant blurring (10 times larger than the original size) at 1500 mWcm-2 for exposure durations longer than 0.75s. Results will be discussed in the context of exposure limits for safety and related ocular damage thresholds.

8221-06, Session 2

## Fundamental study on photodynamic therapy for atrial fibrillation: effect of photosensitization reaction parameters on myocardial necrosis in vitro

E. Ogawa, A. Ito, T. Arai, Keio Univ. (Japan)

We studied necrotic cell death effect on myocardial cells with photosensitizer existed outside the cells varying photosensitization reaction parameters widely in vitro. We have developed non-thermal ablator with the application of the photosensitization reaction for atrial fibrillation. Since laser irradiation is applied shortly after the photosensitizer injection, the photosensitization reaction is induced outside the cells. The interaction for the myocardial cells by the photosensitization reaction is not well understood yet on various photosensitization reaction parameters.

Rat cardiomyocytes were cultured in 96 well plates for 7 days. The photosensitization reaction was applied with talaporfin sodium (NPe6) and the semiconductor laser of 663nm wavelength. The average drug light interval was set 8 mins. The photosensitizer concentration and laser fluence were varied from 5 to 40 μg/ml and 1.2 to 60 J/cm2, respectively. The well bottom was irradiated by the red laser with irradiance of 293 mW/cm2. The photosensitizer fluorescence was monitored during the photosensitization reaction. The alive cell rate was measured by WST assay after 2 hours from the irradiation.

In the case of 10μg/ml of the photosensitizer concentration, the cells were almost alive even thought 60 J/cm2 of the laser fluence was applied. In the 15 μg/ml case, the alive cell rate was almost linear relation to the photosensitizer concentration and laser fluence. We obtained that the threshold for cell necrosis on the photosensitizer density was around 15 μg/ml with 20 J/cm2 of the laser fluence. This threshold on the photosensitizer density was similar to the reported threshold for cancer therapy.

8221-07, Session 2

## NF-kB activation as a laser biomarker of injury using a transgenic mouse model

G. M. Pocock, Air Force Research Lab. (United States); A. R. Boretsky, M. Motamedi, The Univ. of Texas Medical Branch (United States)

Nuclear factor-kB (NF-kB) is a family of heterodimeric transcription factors that regulates the expression of genes controlling cellular response to inflammation, immune response, and apoptosis. Stimuli that activate NF-kB include oxidative stress, injury, and ischemia. The expression kinetics and protein localization of NF-kB after laser induced injury to the retina and skin would provide a better understanding of the laser exposure levels at which the tissue becomes “stressed” and may be useful to detect sub-threshold laser damage that may or maynot manifest as a visible lesion. In this study, we use a transgenic mouse strain (cis-NF-kB-EGFP)that expresses enhanced green fluorescent protein (EGFP) under the transcriptional control of the NF-kB promoter to study the response of the retina and skin to laser damage.

8221-08, Session 2

## Biomedical effect in vivo photodissociation of blood oxyhemoglobin

M. M. Asimov, B.I. Stepanov Institute of Physics (Belarus); R. M. Asimov, Sensotronica Ltd. (Belarus); A. N. Rubinov, B.I. Stepanov Institute of Physics (Belarus)

Oxygen plays a key role in energy production for aerobic cell metabolism. The concentration of oxygen is critical for normal cell metabolism and it should be delivered during blood microcirculation in adequate amount for it normal functioning.

Reduction the volume of blood microcirculation in biological tissue (ischemia) or decreasing the concentration of oxyhemoglobin in arterial blood induces hypoxia. Improving tissue oxygenation and elimination of local hypoxia remains as an actual problem in modern medicine.

In this report new approach in solving the problem of elimination local tissue hypoxia based on biophotonics of laser-induced photodissosiation of blood oxyhemoglobin is discussed. The results of in vivo investigation of laser-induced photodissosiation of oxyhemoglobin in cutaneous blood vessels and its application for tissue oxygenation are presented. Significant increasing tissue oxygen concentration directly at irradiating zone by light or laser radiation is obtained. The efficiency of laser-induced tissue oxygenation is comparable with the method of hyperbaric oxygenation (HBO) at the same time gaining advantages in local action.

In order to make phototherapy and laser therapy methods really efficient one has to control the oxygen concentration in tissue keeping it at the necessary level. This goal could be reached by the use of laser-induced photodissociation of oxyhemoglobin in tissue blood vessels. Laser-induced enrichment of tissue oxygenation stimulates cell metabolism and allows develop new effective methods for laser therapy as well as phototherapy of pathologies where elimination of local tissue hypoxia is critical.

New method of optical “dosimetry” for laser and phototherapy based on using the changes in oxygen concentration as feedback signal to optimizing therapeutic effect of laser radiation is proposed.

Different biomedical applications the effect of light and low intensity laser radiation on gas exchange in biological tissue are discussed.

8221-09, Session 2

## Optical modulation of astrocyte network using ultrashort pulsed laser

J. Yoon, T. Ku, K. Chong, S. Ryu, C. Choi, KAIST (Korea, Republic of)

Astrocyte, the most abundant cell type in the central nervous system, has been one of major topics in neuroscience. Even though many tools have been developed for the analysis of astrocyte function, there has been no adequate tool that can modulate astrocyte network without pharmaceutical or genetic interventions. Here we found that ultrashort pulsed laser stimulation can induce label-free activation of astrocytes as well as apoptotic-like cell death in a dose-dependent manner. Upon irradiation with high intensity pulsed lasers, the irradiated cells with short exposure time showed very rapid mitochondria fragmentation, membrane blebbing and cytoskeletal retraction. We applied this technique to investigate in vivo function of astrocyte network in the CNS: in the aspect of neurovascular coupling and blood-brain barrier. We propose that this noninvasive technique can be widely applied for in vivo study of complex cellular network.

8221-10, Session 2

## Effect of femtosecond laser radiation on morphofunctional state of neoplasm in vitro

D. Arslanova, T. Gening, Ulyanovsk State Univ. (Russian Federation); A. Sysolyatin, A. M. Prokhorov General Physics Institute (Russian Federation); T. Abakumova, V. Svetukhin, I. Antoneeva, Ulyanovsk State Univ. (Russian Federation)

In the experiments on rat ascitic ovarian tumors the effect of femtosecond laser radiation provided by the Erbium fiber laser with the pulse duration of 82 fs, peak power - 6,0±0,3 kW, average power - 1,26±0,15 mW and wavelength λ - 1,55 μm has been studied. The radiation has been performed at the average intensity of 0,027±0.002 mW/cm2 and peak intensity - 0,129±0,02 kW/cm2 at two expositions under femtosecond laser radiation of 600 and 900 s. The membrane topology and rigidity of the cancer cells have been estimated with the Atomic -force microscopy. The viability and apoptosis have been evaluated for the cancer cells. Free-radical processes and antioxidant enzyme activity have been studied in cancer cell lysate. It is established that the femtosecond laser radiation in vitro dose-dependently increases the activity of the “Lipoperoxidation- antioxidation” system in neoplasm, enhances the apoptosis, decreases the viability, and changes cancer cell membrane rigidity.

8221-11, Session 3

## Femtosecond and nanosecond laser nanosurgery: new perspectives for controlled nonlinear energy deposition exemplified on ophthalmic surgery

N. Linz, S. Freidank, X. X. Liang, S. Eckert, Univ. zu Lübeck (Germany); S. Faust, S. Schwed, SCHWIND eye-tech-solutions GmbH & Co. KG (Germany); A. Vogel, Univ. zu Lübeck (Germany)

Using a novel experimental technique that detects transient laser effects as small as 50 nm [1], we demonstrate that low-density plasmas and nanoeffects can be produced not only using ultra-short laser pulses but also, in a much more cost-effective way, by means of temporally smooth nanosecond pulses of short wavelengths [2]. We also show that luminescent plasmas of high energy density are formed when tightly focused femtosecond pulses of > 100 nJ pulse energy are focused into transparent materials, and determine plasma pressure and temperature [3]. Controlled nonlinear energy deposition with widely tunable energy densities is, hence, possible in a large part of the parameter space spanned by wavelength (UV to IR) and pulse duration (fs to ns). Only ns breakdown at IR wavelengths is intrinsically characterized by an abrupt jump from ‘no absorption’ to brightly luminescent, dense plasma. The tunability opens exciting perspectives for laser material processing, precision manufacturing, and surgery of cells and tissues.

We demonstrate the tuning of nanosecond laser effects from nanoeffects to larger, disruptive effects on various examples ranging from bubble formation in water through photoporation of cells and cavitation in corneal tissue to the creation of refractive index changes or voids in glass.

8221-12, Session 3

## Effect of microsecond pulse length and tip shape on explosive bubble formation of 2.78 μm Er,Cr;YSGG and 2.94 μm Er:YAG laser

R. M. Verdaasdonk, M. Verleng, A. van der Veen, Vrije Univ. Medical Ctr. (Netherlands); V. Lemberg, P. Pham, W. Landgraf, D. Boutoussov, BIOLASE Technology, Inc. (United States)

Erbium lasers are mostly used in dermatology and dentistry for either superficial and precise ablation of soft tissue or hard tissue cutting. With new fiber systems becoming available to transmit wavelengths around 3 μm, there is a growing interest in using of Erbium lasers in a water environment like urology, ENT, neurosurgery and new/improved applications in dentistry.

In this study, the dynamics of explosive bubble formation in water was investigated in relation to absorption at 2.78 μm (Er,Cr;YSGG) and 2.94 μm (Er:YAG), pulse length from 20 - 150 μs and fiber tip shape (flat or tapered).

Using time delayed high speed μs flash imaging, sequences of the dynamics of exploding and imploding bubbles between 10 - 300 μs were assembled for pulse energies from 10 to 50 mJ. The characteristic shape and size of the bubbles were determined in relation to time.

Increasing the pulse length, the bubble shape changed from smooth surface spherical to rough surface elongated.

Increasing the pulse energy, the length of the bubble protruding from the fiber increased (‘digging deeper through the water’) with a smaller effect for the width. For tapered shaped tips, the bubble shape was almost spherical with an optically transparent surface. There was no significant difference in bubble shape comparing 2.78 and 2.94 μm at the same settings.

The spherical shaped vapor bubbles with smooth (transparent) surface, induced by Erbium lasers at shorter pulse length or tapered fiber shapes, are expected to be more forceful for creating mechanical effects in both hard and soft tissues.

8221-14, Session 3

## Temperature measurement during Laser Brain Ablation by Thulium fiber Laser

B. Tunç, M. Gülsoy, Bogaziçi Üniv. (Turkey)

The aim of the study was to find a relationship between laser power, exposure time, ablation efficiency and temperature increase during laser brain ablation by Thulium fiber laser. The thermal effects of the 1940-nm Tm-fiber laser on the brain tissue was also investigated in terms of ablation efficiency and histological analysis. These experiments are very important in order to model temperature increase-ablation efficiency during lasing with different power and exposure time. 4-5 mm coronal sections were taken from lamb brains. Laser was applied at cortical and subcortical tissue with 0-0.1 mm distance, in both continuous and pulsed modes with 200 mW, 400 mW and 600 mW which were chosen by a predosimetric study. In continuous and pulse mode doses were changed with exposure time and on-off cycle respectively, in order to achive the tissue to absorb same energy. During lasing temperature increases were recorded by a thermoprobe (thermoprobe is a system which a 300 micrometer fiber was embedded into a thermocouple). The radius of ablation and coagulation for each laser application was recorded by a microscope. By calculating ablation efficiency (100xablation/calculation radius) the appropriate laser doses were determined for both cortical and subcortical tissue. The maximum ablation efficiency for cortical tissue in continuous mode was found for 200 mW and in pulsed mode was found for 400 mW and for subcortical tissue maximum ablation efficiency was found for 200 mW in both continuous mode and pulsed mode. Temperature increases showed a significant difference for continuous and pulse mode operating systems and effect the ablation efficiencies.

8221-15, Session 3

## Optical properties measurement of the laser-ablated tissues for the combined laser ablation with photodynamic therapy

N. Honda, K. Ishii, K. Awazu, Osaka Univ. (Japan)

To beyond the limits of photodynamic therapy (PDT) treatment depth about 3 mm, the combination of PDT and laser ablation which reduces tumor mass is researched. However, the influence of laser ablation on PDT procedure is unknown. The clinical outcome of PDT may be improved by the accurate knowledge about the light distribution within tissue. Optical properties (absorption coefficient; μa, scattering coefficient; μs, anisotropy factor; g, refractive index, etc.) of tissues help us realizing a light propagation through the tissue. The aim of this study is acquisition of the knowledge of light propagation within tissue with the optical properties of the tumor tissue performed laser ablation. This study compared the optical properties of CO2 laser irradiated tumor tissue and non-irradiated tumor tissue. The optical property of the tumor tissue after laser ablation was evaluated using a double integrating sphere setup and an algorithms based on the inverse Monte Carlo method in the wavelength range from 350 to 1000 nm. After laser ablation, the carbonization of tissue surface was observed. And, the reduced scattering coefficient of the laser ablated tissue increased. These results indicate that the PDT treatment depth after laser ablation might decrease. For making accurate estimation of the treatment depth of the combined therapy, the optical properties of the laser ablated tissue are important.

8221-16, Session 4

## Microtensile test of electrochemically aligned collagen fibres on MEMS device under SHG microscope

K. Yoshiki, N. Goami, T. Namazu, S. Inoue, Univ. of Hyogo (Japan)

Collagen fibres provide mechanical strength to biological tissues. When mechanical stress is applied, a cell enzymatically degrades and restructures the collagen fibres to relieve the stress in the extracellular matrix around the cell. For quantitative research of this mechanism, visualization of stress distribution in collagen fibres is essential. We demonstrated quantitative measurement of stress in collagen fibres by second-harmonic generation (SHG) microscopy and a micro tensile test device manufactured by MEMS process. The collagen molecule is an ampholyte and forms bundles spontaneously under the conditions of pH 7. Based on this behavior, electrochemically aligned collagen fibres were fabricated under a pH gradient generated between parallel electrodes after application of DC voltage in the collagen solution.

Our micro tensile test device, which manufactured by MEMS process consists of two opposite translation arms. One of the arms have spring for measurement of the force applied to collagen fiber, and interdigitated electrode for calibration of stiffness of the spring. We calculated exact constant of the spring from weight and resonance frequency of the arm when we applied AC oscillation signal. We gripped an electrochemically aligned collagen fiber between the electrode, and performed tensil tests. We observed tensile test and

Simultaneously, the intensity of SHG light emitted from the collagen fibre excited by a femtosecond pulsed laser was measured at the transmission and reflection sides. The dependence of SHG intensities and stress will provide us a database for converting SHG micrograph to stress distribution.

8221-17, Session 4

## Monitoring micrometer-scale deformation of collagenous tissues under controlled mechanical strain using SHG microscopy

Y. Goulam Houssen, Ecole Supérieure de Physique et de Chimie Industrielles (France); I. Gusachenko, S. Bancelin, G. Latour, V. Tran, J. Allain, M. Schanne-Klein, Ecole Polytechnique (France)

The relationship between microscopic macromolecular organization and macroscopic biomechanical properties is a general concern about collagenous tissues. Tendon is a unidirectional model system in that respect. It is a highly structured tissue mainly composed of type I collagen that forms fibrils of around 200 nm diameters. These fibrils assemble into fibers that further form fascicles with a crimped pattern. This hierarchical organization is responsible for the biomechanical properties of the tissue.

We combined a multiphoton microscope with a mechanical traction device to monitor simultaneously the fibrillar collagen architecture at microscopic scale using endogenous second harmonic generation (SHG) signals and the strain-stress relationship at macroscopic scale [1]. We analyzed the stress-strain relationship versus the crimp morphology during multiple loading cycles with continuous SHG imaging. We observed that cyclic stretch/relaxation at increasing strains leads to a shift of the toe region accompanied by an increase of the crimp spatial period. Our data confirm that the toe region is due to the straightening of the crimps, and that the linear region is due to sliding of the fibrils. This supports the notion that the mechanical behavior of a tendon fascicle relies on its microstructure remodeling that is reversible on long time-scales.

Our new biomechanical device can be readily generalized to other mechanical assays and to any other bidimensional tissue, such as skin. It should bring new valuable information to biomechanics of microstructured tissues.

[1] Goulam Houssen et al, J. Biomechanics 44, 2047-2052 (2011)

8221-18, Session 4

## Photomechanical targeting of transvascular drug delivery

S. Sato, National Defense Medical College (Japan); K. Oyama, Japan Self-Defense Force (Japan); T. Akiyama, Keio Univ. (Japan); H. Nawashiro, National Defense Medical College (Japan); M. Terakawa, Keio Univ. (Japan)

Transvascular drug delivery is a golden standard in pharmacotherapeutics, where a drug is delivered to lesion sites based on enhanced permeability and retention (EPR) effect in many cases. However, the selectivity and efficiency of this type of delivery are often insufficient. In this study, we examined the use of photomechanical waves (PMWs) to transiently enhance the permeability of blood vessels in the target tissues in rats. As a test drug, Evans blue (EB) was injected into a tail vein, and thereafter a light-absorbing material (black rubber disk) was placed on the dorsal skin, tibial muscle and brain surface in a cranial window. The rubber disk was irradiated with a nanosecond laser pulse (3 mm in diameter, 532 nm) to induce a PMW. Four hours later, the target tissues were extracted after perfusion fixation and observed by fluorescence microscopy. We observed intense EB fluorescence in all the target tissues; the fluorescence was distributed not only in the intracellular spacings but also in the cells, i.e., fibroblasts, muscle cells and neurons or glias respectively in the skin, tibial muscle and brain. This indicates that EB molecules were leaked out from the vessels and delivered into the surrounding cells; blood-brain barrier (BBB) was opened in the brain. No histological damage was observed at peak pressures of <135 MPa for skin, <130 MPa for muscle and <100 MPa for brain. These findings show that an intravenously injected drug can be selectively delivered to the target tissue by applying photomechanical waves.

8221-19, Session 4

## Human teeth model using photoacoustic frequency response

Y. H. El-Sharkawy, Cairo Univ. (Egypt)

In this paper, a novel photo-acoustic technique modality utilizing a frequency- modulated Q-switch Nd:YAG laser at 1064 nm and coherent frequency domain signal processing is introduced for impulse and frequency responses of biological tissues. We present a photoacoustic technique to monitor the temporal behavior of temperature and pressure in an excised sample of human teeth after either a single laser pulse or during multiple laser pulses at pulse repetition frequencies (PRF) from 5 Hz to 100 Hz.

Knowledge of the dynamic characteristics of structural elements often means the difference between normal and abnormal tissue. The determination of the resonance characteristics of structures is termed “modal analysis.”

The results of our study suggest that it is possible to identify the impulse, frequency response and resonance modes of simplified human teeth. This data provided a powerful tool to differentiate between normal and decay teeth.

8221-20, Session 4

## Photomechanical model of tooth enamel ablation by Er-laser radiation

A. Belikov, K. V. Shatilova, A. Skrypnik, R. Vostryakov, National Research Univ. of Information Technologies, Mechanics and Optics (Russian Federation)

The photomechanical model of ablation of human tooth enamel is described in this work. It takes into account the structural peculiarities of enamel: free water in the enamel pores or cracks. We consider the photomechanical destruction of the enamel prisms of hydroxyapatite by the pressure of water heated by laser radiation. Water begins to put pressure on the wall of the hydroxyapatite, because the coefficient of volume expansion of water is larger than the coefficient of volume expansion of the hydroxyapatite. Normal and shear stresses appear in the wall of the hydroxyapatite. Wall is destroyed when the maximum stress exceeds ultimate strength of hydroxyapatite. The air-blast appears due to the pressure gradient inside and outside of the pore. First we calculated the force which leads to the normal and tangential stresses which exceed the failure threshold of hydroxyapatite wall. Then we determined the energy needed to water heating which leads to expansion of water and the appearance of destructive force. Than the removal efficiency was calculated as the ratio of removal volume to energy needed for removal this volume. This model takes into account attenuation by the Lambert Beer law when radiation passes through the tissue and the fact that the tissue removal occurs when a unit volume of water was heated to the critical temperature. Decreasing logarithmic dependence of the enamel removal efficiency on the energy density was obtained as a result of the calculations. The shape of this function follows the shape of the experimental curve. It should be noted that our photomechanical model allows us to more accurately calculate the absolute values in compare with the previously described “blow off” model, which shows the logarithmic dependence too.

8221-50, Poster Session

## Simulation the temperature increase in porcine cadaver iris during direct illumination by femtosecond laser pulses

H. Sun, Univ. of California, Irvine (United States); N. Hosszufalusi, Semmelweis Univ. (Hungary); E. Mikula, Univ. of California, Irvine (United States); T. Juhasz, LenSx Lasers, Inc. (United States)

PURPOSE: To model of the laser exposure of the iris during laser corneal surgery, we simulated the temperature rise in porcine cadaver iris using direct illumination by the femtosecond laser.

METHODS: The temperature increase induced by a 60 kHz FS60 Laser (AMO Inc., Santa Ana, CA) in porcine cadaver iris was simulated using COMSOL (Comsol Inc., Burlington, MA) finite element software. The simulation data was compared with measured temperature increase in ex vivo experiment using porcine cadaver iris. In addition we also simulated the typical clinical settings for other types of femtosecond lasers (150 kHz iFS Advanced Femtosecond Laser; FEMTEC system; and VisuMax system).

RESULTS: Temperature increases up to 2.45 °C (corresponding to 2 μJ and 24 seconds of illumination) and to 1.23 °C (corresponding to 1 μJ and 24 seconds of illumination) in the porcine cadaver iris based on the simulation for 60 kHz FS60 Laser showing a little variation in temperature profile compared with specimens for the same laser energy illumination in the ex vivo experiment (2.30 ± 0.14 °C; 1.20 ± 0.15 °C, respectively). Our simulation data for the other types of femtosecond lasers indicate the similar range of the temperature increase.

CONCLUSIONS: Simulation results indicate that using the commercial 60 kHz FS60 Laser at typical clinical energy settings (1 μJ laser pulse energy and 24 second procedure time), the temperature increase in the iris does not exceed 1.23 °C and therefore, does not present a safety hazard to it. Our simulation data also suggest that the other femtosecond lasers could be considered safe if the total laser energy used for the procedures are similar in magnitude presented in this study.

8221-51, Poster Session

## Optical study of aligned collagen fiber matrix as anisotropic biological substrate

C. Guo, Columbia Univ. (United States)

Our research is focused on the optical study of aligned collagen fiber formation and its application as an anisotropic biological substrate. Two straightforward techniques have been developed to align collagen fibers in one direction, which is a useful extracellular matrix (ECM) model to study cellular behaviors. The first technique requires only collagen solution, surface-modified magnetic beads and a small magnetic field. The collagen gels are imaged with confocal reflectance microscopy, allowing the entire gelation procedure to be recorded. The degree of alignment is quantitatively assessed using MatLab image analysis programs that permit the identification of fiber shape, position and angular distribution. Rheology and microscopy experiments together suggest that alignment results from bead coupling to, and entrainment and entrapment in collagen fibrils during their assembly into fibers that form a sample-spanning gel. C6 glioma cells and NIH 3T3 cells are successfully imbedded in such a matrix. Such a biological system is monitored by confocal reflectance microscopy and also differential interference contrast microscopy (DIC). The second technique, which requires only collagen solution and directional mechanical forces, achieves excellent collagen fiber alignment without the use of magnetic beads. Cancer cells are also successfully embedded in such an aligned collagen matrix. By confocal reflectance microscopy, different layers of collagen fibers surrounding a single cell are imaged and analyzed. This anisotropic biological substrate has many potential uses, such as study of cancer cell growth, metastasis, development and differentiation.

8221-52, Poster Session

## Optical parameters of turbid media in a new kinetic light propagation model: extraction from diffuse reflectance measurements

A. V. Lappa, A. Kulikovskiy, A. N. Kulikovskiy, T. A. Makarova, Chelyabinsk State Univ. (Russian Federation)

A new method for nondestructive evaluation of optical properties of turbid media (biological tissues, first of all) is presented in this work. The method refers to the spatially resolved diffuse reflectance techniques. There are three significant features in our method: a new light propagation model, new characteristics for measurement, a new technique for inverse problem solving.

Our model is kinetic one (bases on radiation transport equation), it allows correct consideration of processes dependent on photon directions (reflection and refraction on boundaries, angular aperture of optical fibers, and so on) in contrast to diffusion, P1, and some other non-kinetic approximations. Besides refractive index the model includes only 2 optical parameters of media: conventional absorption coefficient ua and some model scattering coefficient us* (not reduced scattering coefficient). The suggested method is intended to evaluate these two parameters only.

The method uses a probe with 3 optical fibers: one illumination and two reading fibers. As the measured quantities to extract the parameters we suggest to use two ratios: Q1=D1/S and Q2=D2/D1, where D1, D2 - detector indications from the reading fibers, S - from the illumination one.

The technique of parameters determination includes preliminary calculations of Q1, Q2 at different ua, us* in sufficiently broad range (i.e. calculation of functions q1(ua,us*)) with the original algorithm using the Green function approach, the similarity transformation, and a special non-analog correlated technique of the Monte Carlo method. Media parameters are found as numerical decision of equation system: q1(ua,us*)=Q1, q2(ua,us*)=Q2, where Q1,Q2 - measured values.

A series of test experiments on tissue phantoms showed good performance of the proposed method.

8221-53, Poster Session

## Optical properties measurement of laser coagulated tissues with double integrating sphere and inverse Monte Carlo technique in the wavelength range from 350 to 2100 nm

K. Awazu, N. Honda, T. Nanjo, K. Ishii, Osaka Univ. (Japan)

In laser medicine, the accurate knowledge about the optical properties (scattering coefficient; μs, absorption coefficient; μa, anisotropy factor; g) of laser irradiated tissues is important for the prediction of light propagation in tissues, since the efficacy of laser treatment depends on the photon propagation within the irradiated tissues. Thus, it is likely that the optical properties of tissues at near-ultraviolet, visible and near-infrared wavelengths will be more important in the future due to more biomedical applications of lasers will be developed. For improvement of the laser induced thermotherapy, the optical property change during laser treatment should be considered in the wide wavelength range. For estimation of the optical properties of the biological tissues, the optical properties measurement system with a double integrating sphere setup and an inverse Monte Carlo technique was developed. The optical properties in normal chicken muscle tissue were determined in the native state and after laser coagulation using the optical properties measurement system in the wavelength range from 350 to 2100 nm. After laser coagulation, the reduced scattering coefficient of the tissue increased. And, the optical penetration depth decreased. For improvement of the treatment depth during laser coagulation, a quantitative procedure using the treated tissue optical properties for determination of the irradiation power density following light penetration decrease might be important in clinic.

8221-54, Poster Session

## Fundamental research in laser Doppler method for cerebral blood flow measurement

H. Nagano, M. Fujii, F. Taiki, Sophia Univ. (Japan)

Our research is aiming to develop feasible blood perfusion monitor by using analyzing fluctuation of light intensity from laser light through diffusive tissue. To access the realistic system, we designed an experimental system using a single mode solid-state laser source and APDs with optical fibers, and performed preliminary experiments. For this experiment an agar diffusive phantom containing polystyrene particles adjusted reduced scattering coefficient of 0.2 mm^-1 wad prepared. In this phantom glass flow tubes filled with diluted soymilk were embedded to imitate blood perfusion.The detecting fibers were positioned with the distance of 5mm, 10mm, 15mm and 20 mm from the source fiber on the phantom, and the flow glass tubes were set with the depth of 5mm, 10mm, 15mm and 20mm from the phantom surface respectively. This preliminary experiment shows that flow velocity change in class tube up to 15mm depth was appear as power spectrum change.

8221-55, Poster Session

## Analysis of bacterial growth by spectroscopy and laser reflectometry

R. Gallegos, M. C. Peña-Gomar, G. Viramontes-Gamboa, Univ. Michoacana de San Nicolás de Hidalgo (Mexico)

This work presents a preliminary study on an experimental analysis of the lactobacillus bacterial growth in liquid medium with and without the presence of silver nanoparticles. The study aims to quantify the bactericidal effect of nanoparticles. Quantification of bacterial growth at different times was analyzed by spectroscopy UV/visible and laser reflectometry near the critical angle. From these two techniques the best results were obtained by spectroscopy, showing that as the concentration of silver nanoparticles increases, it inhibits the growth of bacteria, it only grows 63% of the population. Regarding Laser Reflectometry technique, the variation of reflectance at an angle near the critical angle is measured in real time. The bacteria are placed in a container where the total internal reflection is done. The observed results in a short time are reasonable, since they indicate a gradual growth of the bacteria and the stabilization stage of the population. But at long time, the observed results show trends and abrupt changes caused by the effect of temperature. The bacteria were isolated from samples taken from commercial yougurth, and cultured in MRS broth at pH 6.5, and controlled with citric acid and constant temperature of 32 °C. Separately, silver nanoparticles were synthesized at 3 ° C from aqueous solutions of 1.0 mM silver nitrate and chemically reduced with sodium borohydride to 2.0 mM, with magnetic stirring. The particles thus obtained have average dimensions of 12 nm ± 2 nm. In the beginning the experiments bacteria is inoculated in 70 mL liquid medium RMS with 30 mL of silver nanoparticles at different concentrations.

8221-56, Poster Session

## Delayed photolysis of liposomes: a strategy for the precision timing of bolus drug release using ex vivo photochemical sensitization

R. T. Kozikowski, B. S. Sorg, Univ. of Florida (United States)

Chemotherapy is a standard treatment for metastatic cancer. However drug toxicity limits the dosage that can safely be used, thus reducing treatment efficacy. Drug carrier particles, like liposomes, can help reduce toxicity by shielding normal tissue from drug and selectively depositing drug in tumors. Over years of development, liposomes have been optimized to avoid uptake by the Reticuloendothelial System (RES) as well as effectively retain their drug content during circulation. As a result, liposomes release drug passively, by slow leakage, but this uncontrolled drug release can limit treatment efficacy as it can be difficult to achieve therapeutic concentrations of drug at tumor sites even with tumor-specific accumulation of the carriers.

Lipid membranes can be photochemically lysed by both Type I (photosensitizer-substrate) and Type II (photosensitizer-oxygen) reactions. It has been demonstrated in red blood cells (RBCs) in vitro that these photolysis reactions can occur in two distinct steps: a light-initiated reaction followed by a thermally-initiated reaction. These separable activation steps allow for the delay of photohemolysis in a controlled manner using the irradiation energy, temperature and photosensitizer concentration. In this work we have translated this technique from RBCs to liposomal nanoparticles.

To that end, we present in vitro data demonstrating this delayed bolus release from liposomes, as well as the ability to control the timing of this event. Further, we demonstrate for the first time the improved delivery of bioavailable cargo selectively to target sites in vivo.

8221-57, Poster Session

## Incoherent source angular domain imaging through complex three-dimensional scattering structures

R. Cheng, G. Chiang, G. Chapman, Simon Fraser Univ. (Canada)

Scattering of photons in biological imaging is a known factor of degrading image resolution and quality. Angular Domain Imaging (ADI) is a technique which utilizes the angular distribution of photons to filter out multiple-scattering photons and accept only photons with small angular deviation from their original trajectories. The advantage of ADI is that it does not require a high optical quality, coherent, or pulsed source to acquire quality image. Initial experiments with Spatialfrequency Filter (SFF) ADI on simple liquid scattering test phantom showed good results as it can image through media with scattering ratio (SR) of 106:1. Previous work with complex 3D aquatic species eliminated scattering but showed optical interference patterns from the coherent laser sources. With SFF ADI, our target is to image through a complex 3D scattering structure with multilayer of different refractive indices and scattering coefficient from an Intralipid-infused polymer/agar, and a small species called Branchiostoma lanceolatum, a lancelet that is 5-8cm long and ~5mm thick. To remove interference, several narrow wavelength-band LEDs were used as illumination sources with one peaks at 630nm and the other peaks at 415nm. The LEDs are collimated and illuminates the 3D structure/lancelet in a water-filler container while a SFF removes the scattered photons before the imager. This allows us to reduce the optical interference and to study the impact of switching from coherent laser source into an incoherent narrow wavelength-band source. Hence, it allows us to investigate the enhancement of imaging the internal structures using the incoherent narrow wavelength-band source.

8221-58, Poster Session

## Determine the optical properties of fibrous biological tissue using anisotropic diffuse model

A. S. Shuaib, G. Yao, Univ. of Missouri-Columbia (United States)

We compared the isotropic and anisotropic diffuse models in retrieving the optical properties in fibrous samples from time-resolved reflectance measurements. A Monte Carlo model was used to simulate light propagation in a fibrous tissue consisting of aligned cylinders and spherical particles. Using the anisotropic diffuse model, the reduced scattering coefficients for both cylinder and background can be derived from a single time-resolved reflectance measured perpendicularly to the fiber direction in media with small fibers. Using isotropic diffuse solution, these parameters can be derived from two measurements as following. The background reduced scattering coefficient is calculated by applying the isotropic diffuse fitting to the time-resolved reflectance measured along the fiber direction; whereas the summation of the reduced scattering coefficients of the background and cylinders can be derived by fitting the isotropic diffuse model to the measurements perpendicular to the fiber direction. The simulation results indicate that the derived optical properties are correct only for fibrous samples with small fiber diameter. For large fiber diameters, the reduced scattering coefficient of fibers needs to be corrected by fiber-size dependent factor.

8221-59, Poster Session

## Optical diffusion property of cerumen from ear canal and correlation to metal content measured by synchrotron x-ray absorption

T. Holden, S. Dehipawala, E. Cheung, P. Schneider, S. Dehipawala, G. Tremberger, Jr., D. Kokkinos, D. Lieberman, T. D. Cheung, Queensborough Community College (United States)

Human (and other mammals) would secret cerumen (ear wax) to protect the skin of the ear canal against pathogens and insects. The studies of biodiversity of pathogen in human include intestine microbe colony, belly button microbe colony, etc. Metals such as zinc and iron are essentials to bio-molecular pathways and would be related to the underlying pathogen vitality. This project studies the biodiversity of cerumen via its metal content and aims to develop an optical probe for metal content characterization. The optical diffusion mean free path and absorption of human cerumen dissolved in oil have been measured in standard transmission measurements with green and red laser sources. EXFAS and XANES have been measured at Brookhaven Synchrotron Light Source for the determination of metal contents. The results show that a calibration procedure can be used to correlate the optical diffusion parameters to the metal content, thus expanding the diagnostic of cerumen in the study of human pathogen biodiversity without the regular use of a synchrotron light source.

8221-60, Poster Session

## Protection and sensitization of benign and malignant cells against photochemical stress by a naturally occurring compound

Y. Lee, N. Kumar, The Univ. of Texas Health Science Ctr. at San Antonio (United States); R. D. Glickman, The Univ. of Texas Health Science Ctr. at San Antonio (United States) and The Univ. of Texas at San Antonio (United States)

Certain phytonutrients are known to confer skin protection and immunosuppression against radiation damage resulting from photochemical stress reactions in biological systems. The radiation-induced oxidative stress can lead to cellular destruction as well as radio-resistance mediated by endogenous molecules. To identify whether ursolic acid reduces radiation-induced damage in benign cells and promotes apoptosis of malignant cells, we investigated the molecular mechanisms of radiation-cell interaction. UV-VIS light and γ-rays were employed to investigate the efficacy of ursolic acid in altering cellular viability by the modulation of p53, Nrf-2 and NF-κB p65 signaling. The cellular effects of UV-VIS radiation exposure can lead to DNA breakage and cellular apoptosis. Bromodeoxyuridine staining for DNA synthesis, and 2',7'-dichlorofluorescin liquid chromatography for assessing free radical generation, were used to characterize the ability of ursolic acid to modulate the cell cycle and inhibit oxidative reactions of retinal pigment epithelium (hTERT-RPE). UV-VIS induced cell death of human skin melanoma cells (CRL-11147™, the ATCC No.) was markedly facilitated by ursolic acid pretreatment. Ursolic acid also strongly increased the level of p53 and decreased the level of phosphorylated p65 in skin melanoma cells. In addition, the inhibitory effect of ursolic acid on Nrf2 activation appears to be correlated with the increase of oxidative stress in hTERT-RPE cells. These findings indicate that ursolic acid may beneficially increase radiosensitivity of tumor cells while potentiating a photoprotective effect on benign cells through the differential inactivation of NF-κB and activation of p53. Ursolic acid, having few adverse side effects, may thus be a useful adjunct in tumor radiotherapy.

8221-61, Poster Session

## Terahertz spectroscopy of dry, hydrated, and thermally-denatured biological macromolecules

D. Lipscomb, J. E. Grundt, Air Force Research Lab. (United States); I. Echchgadda, National Academy of Sciences (United States); B. L. Ibey, M. A. Kuipers, H. T. Beier, R. J. Thomas, G. J. Wilmink, Air Force Research Lab. (United States)

Terahertz time-domain spectroscopy (THz-TDS) is an effective technique for probing the intermolecular and collective vibrational modes of biological macromolecules at THz frequencies. To date, few spectroscopic studies have been performed on hydrated biomolecular samples. Since water is required for protein folding and function, valuable information can be gained by investigating their optical properties while in native conformation. In this study, we used a THz-TDS system to measure the absorption coefficients and refractive indices for water and collagen in dry, hydrated, and thermally-denatured states. The system uses optical rectification for THz pulse generation and free-space electro-optical sampling for detection. Broadband THz pulses were generated by pumping nonlinear Zinc telluride (ZnTe) crystals with femtosecond optical pulses from a Ti:sapphire laser (800 nm, 80 MHz, 12 nJ/pulse). Our data show that variations in temperature and pH directly affect the optical properties of dry, hydrated and thermally-denatured collagen. Structural conformation and degree of interfacial water content may contribute to variations seen in the optical properties of collagen.

8221-62, Poster Session

## MicroRNA-mediated stress reponses in human cells exposed to terahertz radiation

C. Z. Cerna, General Dynamics Advanced Information Systems (United States); J. E. Grundt, Air Force Research Lab. (United States); I. Echchgadda, National Academy of Sciences (USA); B. L. Ibey, G. J. Wilmink, Air Force Research Lab. (United States)

MicroRNAs (miRNAs) are a recently discovered class of regulatory RNA species that suppress protein synthesis. Emerging data suggest that miRNAs play a central role in development, proliferation, cellular stress response (CSR), and other fundamental cellular processes. In this study, we examined the miRNA expression profiles for human Jurkat cells exposed to Terahertz (THz) radiation. Analyses were also performed for positive controls with matched temperature-time profiles (44°C for 40 minutes). Cells were irradiated using an optically pumped THz source with the following exposure conditions (2.52 THz, 636 mWcm-2, durations: 30, 40, and 50 minutes). miRNA expression profiles were measured using the latest Affymetrix microarray genechip that provides the most comprehensive coverage for miRNAs in the Sanger registry. The data show that for each THz exposure group ($p<0.05$) 45 or more miRNAs were differentially expressed. We validated microarray expression profiles with qPCR and found results to be comparable. Interestingly, the magnitude of expression for several miRNA targets increased linearly with the duration of THz exposure. These results indicate that cells express a specific group of miRNAs when exposed to THz radiation. Future studies will be performed to determine if other cell lines express these miRNAs when exposed THz radiation.

8221-21, Session 5

## Cutting-edge terahertz technology and prospect of its application

M. Tonouchi, Osaka Univ. (Japan)

Recent rapid progress of technological innovation in "opto" and "nano" science stimulates the THz research to extend in various fields such as ICT, biology, NDE, security, quality control of food and agricultural products, environmental monitoring, ultrafast computing, and novel science. This paper reviews such over-all THz technology[1].

Main THz Application is classified into two categories, sensing and ICT. THz spectroscopy is advanced analytical technology for various materials. One can expect that the unprecedented sensing capabilities are available for many research fields such as biology, pharmacy, medical science, industrial NDE, material science, environment monitoring, security, astronomy, and basic science. ICT also covers a wide range of applications such as wireless communication, high-speed data processing, etc. Besides, synergy effect of such research will bring forth many other applications such as biometrics using THz camera, massive sensor network, selective communications, and new others.

In this review, we introduce recent progress of terahertz science and technology and its future prospect. High power THz source and sensitive THz sensor/camera will bring brake through in many researches such as nonlinear response of the matters. Temporal trace in femtosecond time scale of low energy dynamics of excited matters also opens new many research fields in bio/chemical studies as well as solid state physics. We will also give attractive examples for bio/chemical sensing applications such as Redox reaction imaging, Immune-Assay, cell imaging, THz-micro-TAS, and so on.

[1] M.Tonouchi, "Cutting-edge terahertz technology," Nature Photonics 1, 97 - 105 (2007).

8221-22, Session 5

## Breast cancer tissue diagnosis at terahertz frequencies

E. Pickwell-MacPherson, Hong Kong Univ. of Science and Technology (Hong Kong, China); A. Fitzgerald, V. Wallace, The Univ. of Western Australia (Australia)

Our previous terahertz spectroscopy study of human breast tissues from 20 patients has found that the refractive index and absorption coefficient of breast cancer are consistently higher than those of the healthy fibrous and adipose tissues. Although the difference between the tumor and adipose tissue properties is very large, the difference between the fibrous tissue and cancer properties is more subtle. If terahertz imaging is to be used in the future to identify these tissues in a clinical environment then it is important that the terahertz properties of fibrous tissue and breast cancer tissues can be reliably distinguished.

One proposed approach to using terahertz imaging for breast cancer detection is to perform reflection geometry imaging in vivo intra-operatively, enabling the surgeon to check that the margins are clear of tumor in real-time. To ascertain the potential reliability of this approach we use the spectroscopy properties of excised tissues to simulate the reflected terahertz response functions in vivo. The impulse response function arises due to the fundamental tissue properties - namely both the refractive index and absorption coefficient. Previously we have looked at the refractive index and absorption coefficient separately to characterize tissues. In this work we investigate their combined effects and identify parameters from the simulated reflected impulse response functions and corresponding spectroscopic properties to improve our ability to distinguish between the fibrous and cancer tissues in the breast.

8221-23, Session 5

## Feasibility demonstration of frequency domain terahertz imaging in breast cancer margin determination

S. K. Yngvesson, Univ. of Massachusetts Amherst (United States)

In breast conservation surgery, the surgeon attempts to remove malignant tissue with a surrounding margin of healthy tissue. Subsequent pathological analysis must determine if the margins are clear of malignant tissue, a process that typically requires at least one day. Only then can a determination about possible follow-on surgery be made, with undesirable consequences in terms of healthcare cost and undue emotional stress.

It has been shown that terahertz images of breast specimens can accurately differentiate between breast carcinoma and normal fibroglandular and adipose tissue. That study employed the “Time-Domain Spectroscopy (TDS)” technique. We are instead developing a new technique, “Frequency-Domain Terahertz Imaging (FDTI)”.

In a joint UMass/Amherst - UMass Medical School/Worcester (UMMS) project we are investigating the feasibility of the FDTI technique for terahertz reflection imaging of breast cancer margins by employing an existing THz gas laser system source to produce mechanically scanned images of several different phantom materials. Despite several years of TDS work, few examples of THz images of specimens of biological origin are known; this talk will present many new such examples performed with FDTI. We have demonstrated that reflection coefficients as low as 1-2 % can be measured, and are presently ready to begin imaging thin (2 mm) specimens cut from lumpectomies performed at UMMS; these will be discussed in the talk. Finally, we will describe how we envision that FDTI can be transitioned into a very compact, inexpensive CMOS THz camera for use in the operating room, something that is not feasible using TDS techniques.

8221-24, Session 5

## Terahertz molecular imaging using nanoparticles

J. Son, The Univ. of Seoul (Korea, Republic of)

The use of terahertz (THz) imaging as a modality of medical imaging techniques for diagnosing cancers is feasible[1]. However, it cannot be used for clinical trials because of its low sensitivity, which is insufficient for clearly differentiating cancerous tumors from healthy tissues, and some other drawbacks.

These problems can be solved by using nanoparticle (NP) probes as contrast agents for THz imaging. NP probes can be delivered to or targeted toward tumors, organs, or cells by various techniques. When NPs are irradiated with a near-infrared (NIR) laser beam, a cell’s ambient temperature increased because of the resonance of surface plasmon polaritons. This temperature rise changes the optical properties of the cell’s water, e.g., the absorption and refractive index much at THz frequencies because water molecules show a characteristic resonance at frequencies around 6 THz. Therefore, the THz absorbance and reflectance change dramatically by the NIR irradiation of NPs[2].

On the basis of this principle, molecular imaging using THz waves was demonstrated, and factors such as sensitivity, resolution, and quantification property were characterized. As an example of medical diagnosis, a THz molecular imaging (TMI) technique was used for characterizing cancerous tumors and measuring the distribution of NP drug delivery to organs in vivo and ex vivo[3].

For the early clinical adaptation of the TMI technique, human-approved (by USFDA) iron oxide NPs, originally designed for magnetic resonance imaging (MRI), were adopted for in vivo imaging of cancers. The TMI results were compared with MRI results and showed a good agreement.

REFERENCES

[1] Son, J.-H., “Terahertz electromagnetic interactions with biological matter and their applications,” J. Appl. Phys. 105(10), 102033 1-10 (2009).

[2] Oh, S. J., Kang, J., Maeng, I., Suh, J.-S., Huh, Y.-M., Haam, S. and Son, J.-H., “Nanoparticle-enabled terahertz imaging for cancer diagnosis,” Opt. Express 17(5), 3469-3475 (2009).

[3] Oh, S. J., Choi, J., Maeng, I., Park, J. Y., Lee, K., Huh, Y.-M., Suh, J.-S., Haam, S. and Son, J.-H., “Molecular imaging with terahertz waves,” Opt. Express 19(5), 4009-4016 (2011).

8221-25, Session 5

## A new chirped-pulse THz method for rapid detection of gas and condensed phase material properties

D. F. Plusquellic, E. Gerecht, K. O. Douglass, J. Scherschligt, Z. Ahmed, S. G. Chou, National Institute of Standards and Technology (United States)

A new chirped-pulse THz spectrometer will be discussed for performing high-speed (sub-us) phase-coherent broadband measurements at frequencies up to 1 THz. The sensitivity and speed of the method have been first demonstrated for detection of trace gases in direct absorption and by free induction decay in the region from (0.53 to 0.62) THz. Chirped pulses that are linear in frequency, spanning 10 MHz repetition rates and mixed with a MW signal from a phase-locked synthesizer. The upper sideband of the mixed signal (typically between 10 GHz to 12 GHz) is filtered (YIG) to reduce out-of-band spurs to less than 50 dB and used to drive a x48 (x24 or x72) amplifier multiplier chain (AMC). The output power of the AMC is ~1 mW (30 mW or 300 uW). The output beam is coupled into a 25 m long White cell and detected using a sub-harmonic heterodyne detector (mixAMC) operating at x24 (x12 or x36). The IF signal is detected directly on the oscilloscope. The AMC and mixAMC have been specially adapted to enable rapid response to < 1 us frequency changes of the driving MW signals permitting access to any portion of the multiplier range. Each chirped pulse can be signal averaged directly in the time domain for any length of time in order to improve the signal-to-noise ratio. At the Doppler limited resolution of 5 MHz, an absorption line is phase coherently excited in less than 2 ps.

8221-26, Session 6

## The unexplored avenues of human skin: electromagnetic properties in the sub-THz band

Y. Feldman, A. Puzenko, P. Ben Ishai, The Hebrew Univ. of Jerusalem (Israel); A. Caduff, The Hebrew Univ. of Jerusalem (Israel) and Biovotion AG (Switzerland); A. J. Agranat, The Hebrew Univ. of Jerusalem (Israel)

Studies of the morphology of the skin by optical coherence tomography revealed that the tips of the sweat ducts that conduct the sweat from the gland to the pore at the surface of the skin, have a helical structure. This, together with fact that the tips are embedded in the epidermis which has a comparatively low dielectric constant, gave rise to the supposition that at sub-THz frequencies the response of the ducts should be similar to that of low Q helical antennas, provided a fast enough current mechanism exists in the ducts.

This supposition was substantiated by a series of simulations, which showed that the spectral response of the ducts indeed coincides with the analytical prediction of antenna theory. In particular it was found that the strongest spectral response appeared at approximately the predicted frequencies (240 GHz and 380 GHz) for the respective normal and axial modes of the helical structure of similar dimensions to the ducts.

Consequently it was further suggested that the electromagnetic response of the skin in the sub-Terahertz region should manifest the level of activity of the perspiration system. This was verified in series of experiments in which it was shown that changes in the electromagnetic reflection from the skin at sub THz frequencies in response to physiological and mental stresses is strongly correlated with the respective changes in the pulse rate and the systolic blood pressure.

Initial findings indicate that changes in the electromagnetic reflection appear also in response to emotional excitation, which is phasic in nature.

8221-27, Session 6

## Terahertz techniques for human skin measurement

K. Kawase, Nagoya Univ. (Japan) and RIKEN (Japan); S. Hayashi, RIKEN (Japan)

We are developing novel THz techniques for human skin measurement. Firstly, a high-resolution tomographic imaging was demonstrated using a reflection-type terahertz time-domain spectroscopy. The wideband spectrum of the generated terahertz waves provided high-axial resolution of 5um leading to tomographic imaging of multilayered skin structure. Secondly, we report on the measurement of stratum corneum using metallic mesh. The dielectric constant of the metallic mesh surface changed after the stratum corneum was attached. When the lipid among the skin cells was dissolved by chloroform, the change was confirmed in the transmission spectra. These suggest that the metal mesh sensor can be used to measure compositional variation of human skin by observing its transmission property. Thirdly, we are studying the possible sweat duct helical antenna at THz region on the human skin. It is known fact that human beings are the only creatures that possess helically shaped sweat duct. Prof. Feldman reported that the sweat ducts in human skin, filled with electrically conductive sweat, act like an array of tiny helical antennas that pick up radiation at around 90 GHz. We measured the reflection spectrum of palm using TDS and a resonance was observed around 200GHz by heating hand using a drier. The resonance relaxed back towards its initial curve 20 minutes after heating, then the resonance reappeared by heating again. Fourthly, we are also studying non-thermal effects of THz/MMW radiation on human skin cells at power levels well below 1uW/cm2. Detailed information will be shown at the conference.

8221-28, Session 7

## Long-range hydration effect of lipid membrane studied by terahertz time-domain spectroscopy

K. Tanaka, M. Hishida, Kyoto Univ. (Japan)

Water is essential for life. Although the importance of water for bio-materials have been investigated for long, even the amount of hydration water at the surface of biomolecules have not been defined. In the past studies, the hydration states of solutes were observed by NMR or neutron scattering from the viewpoint of dynamics of water molecules. Despite picosecond time scale of the collective dynamics of bulk water, these methods have measured that only in nanosecond time scale and have defined only the strongly perturbed water as the hydration water. However, it is expected that much more slightly perturbed water exist near the solute surfaces.

To define the hydration state precisely including slightly perturbed water, we have used terahertz time-domain spectroscopy, with which picosecond dynamics of water can be measured. From the change in the dielectric response of rotational dynamics of water by the hydration effect, we can evaluate the amount of hydration water. For the sample, phospholipid bilayer is used, which is the basic structure of biomembrane. By comparing the terahertz results with the structural information of the lipid/water system obtained by X-ray scattering, it is concluded that there is a long-range hydration layer on the surface of lipid membrane on up to 4-5 water layers (1 nm), which is 5 time as much as that in previous reports. Our results indicates that the hydration water is important for the self-assembly of biomolecules because its length scale is comparable to that of some interactions such as van der Waals interaction.

8221-29, Session 7

## High-resolution THz spectroscopy of nucleic-acid biomolecules and crystals

E. Brown, Wright State Univ. (United States)

Biomolecules exhibit low-lying vibrational modes in the THz region which can be detected in transmission given a strong molecular dipole moment and a spectrometer of adequate sensitivity. The nucleic acids are particularly interesting because of applications like label-free gene assay, bio-agent detection, etc. Sample preparation and THz coupling are of paramount importance because of the strong absorption by liquid water in physiological solutions, and the scattering by bio-compatible sample holders. This paper will summarize work to date on short strands of small-interfering (si) RNA (15-to-23 bp), low-MW DNA (200 bp), and Lambda-phage DNA (48.5 kbp) suspended in SiO2 nanofluidic channels. We have measured surprisingly strong (absorbance ~0.8) and narrow (~10 GHz FWHM) signatures in the 800-GHz-to-1.1-THz region, especially in si-RNA, and we have identified a common absorption band for all the nucleic-acid species around 840 GHz, which has been utilized for monitoring the effect of electrophoretic control by the nanofluidic chips. To reduce the effect of liquid water and explore the vibrational nature of DNA in biomolecular architectures, we have also measured the THz transmission through single-crystal DNA (13-mer oligonucleotide grown by the hanging drop method). Because of their limited size (~100 micron), DNA crystals pose a challenge to THz spectroscopy that we are addressing with an evanescent-mode waveguide-coupling technique

8221-30, Session 7

## Using terahertz radiation for the non-contact control and selective stimulation of biological responses

G. J. Wilmink, J. E. Grundt, Air Force Research Lab. (United States); C. Cerna, I. Echchgadda, National Academy of Sciences (United States); C. C. Roth, General Dynamics Advanced Information Systems (United States); D. Lipscomb, M. L. Doroski, J. A. Payne, B. L. Ibey, Air Force Research Lab. (United States)

Water molecules near the surface of biomolecule (i.e., interfacial, hydration, or biological water) play a central role in the folding and function of proteins and carbohydrates. Interfacial water molecules create dynamical hydration shells, which extend up to 20 Å from the surface of a biomolecule. The properties of interfacial water are known to differ considerably from those of bulk water, and recent data shows that water's second solvation shell exhibits appreciably higher absorption than bulk water at frequencies ranging from 2.3-2.7 THz. In this study we hypothesized that human cells exposed to 2.52 THz radiation may activate a cellular response that is considerably different than cells exposed to matched bulk heating. To test this hypothesis, human cells were irradiated with a molecular gas THz laser (2.52 THz, 636 mWcm-2, durations: 5-50 minutes). Viability was assessed using MTT assays, and gene expression was evaluated using mRNA and miRNA microarrays, qPCR, and Luminex protein assays. Bioinformatics software was employed to discover unique putative biomarkers and to determine the intracellular signaling pathways activated exclusively by THz-exposed cells. The microarray, qPCR, and protein assay data showed that THz radiation induced the transcriptional activation of genes associated with cellular proliferation, inflammation, transcriptional activation, and chaperone protein stabilization. These results provide evidence that 2.52 THz radiation triggers a biological response in human cells that is not observed in bulk-heated cells. These findings suggest that THz radiation may be useful means for the non-contact control and selective stimulation of desirable biological responses in human cells.

8221-31, Session 8

## Influence of optical properties on sampling depth of laser speckle contrast imaging

A. K. Dunn, The Univ. of Texas at Austin (United States)

No abstract available

8221-32, Session 8

## Depolarization of light in biological tissues: affect the polarization state by flow and estimation of flow rates

D. Fixler, Z. Zalevsky, Bar-Ilan Univ. (Israel)

Recently in phototherapy the use of diodes and broadband light devices instead of lasers was suggested for economical and practical reasons. It has been argued that lasers have no preference over diodes since they lose their coherency and polarization once penetrating into biological tissues. However, this point has never been experimentally proven. In this talk we, for the best of our knowledge, have for the first time experimentally validated the conditions that affect the polarization state of light when laser illumination is propagated through a biological tissue with and without a flow. We will show experimentally validated that the tissue thickness almost does not change the polarization for relatively low reduced scattering coefficient while there is no flow. Furthermore, the flow velocity highly affects the polarization. In additional we will present physical modeling as well as by experimental validation showing that illuminating a flow in a medium with linear polarized light and measuring the change in the polarization state at the output of the medium can be highly correlated to the direction and rate of the flow through that medium. By inspecting the change in the spatial shape of the spot of light, in addition to the change of the polarization state versus different integration times, we are able to fully extract the direction and rate of the flow.

8221-33, Session 8

## Parametric imaging of tissue pathology based on optical properties measured with optical coherence tomography

B. R. Klyen, L. Scolaro, D. D. Sampson, The Univ. of Western Australia (Australia)

Measurement of the optical properties of biological tissue using optical coherence tomography (OCT) can be used to differentiate tissue types. Its utility has previously been demonstrated in characterizing atherosclerotic plaques, monitoring engineered tissue matrices and measuring substrate concentrations in blood.

Here we evaluate the use of parametric OCT imaging based on measurement of optical properties to enhance tissue classification and identify pathology for two new applications. The first is identification of cancer in axillary lymph nodes and in breast tissue, with the aim of improving surgical intervention. The second is detection of inflammation and necrosis in skeletal muscle tissue of the mdx mouse model of human muscular dystrophy, aimed at improving pre-clinical studies of potential therapies for the disease.

We conducted 3D-OCT imaging of ex vivo biological tissue samples, calibrated and corrected to account for system modulations due to the confocal gate and depth scanning of the reference arm. A single-scattering model of OCT is used, with a least squares linear regression applied to the corrected log reflectance profiles, to extract the attenuation coefficient $\mu$ and local reflectivity $\rho$ from the 3D-OCT data.

We will demonstrate enhanced classification of tissue types based on attenuation coefficients measured using OCT. We will present parametric images of the optical properties extracted from ex vivo human axillary lymph nodes and breast tissue, and ex vivo mouse skeletal muscle tissue, validated by co-located histopathology. This work will demonstrate that obtaining optical properties enhances the ability of OCT to characterize tissue types and identify pathology.

8221-34, Session 8

## Fast computation of optical coherence tomography signal using an importance sampling-based Monte Carlo method

I. T. Lima, Jr., A. Kalra, North Dakota State Univ. (United States); H. E. Hernández-Figueroa, Univ. Estadual de Campinas (Brazil); S. S. Sherif, Univ. of Manitoba (Canada)

Computer simulations of light transport in multi-layered turbid media are an effective way to theoretically investigate light transport in tissue, which can be applied to the analysis, design and optimization of optical coherence tomography (OCT) systems. We present a computationally efficient method to calculate the diffusive reflectance due to ballistic and quasi-ballistic components of photons scattered in turbid media, which represents the signal in optical coherence tomography (OCT) systems. Our importance sampling based Monte Carlo method enables the calculation of the OCT signal with less than one hundredth of the computational time required by the conventional Monte Carlo method. It also does not produce a systematic bias in the statistical result that is typically observed in existing methods to speed up Monte Carlo simulations of light transport in tissue. This method can be used to assess and optimize the performance of existing OCT systems, and it can also be used to design novel OCT systems.

8221-35, Session 8

## A hybrid method for fast Monte Carlo simulation of diffuse reflectance from a multi-layered tissue model with tumor-like heterogeneities

C. Zhu, Q. Liu, Nanyang Technological Univ. (Singapore)

We present a novel method that combines a multi-layered scaling method and a perturbation method to speed up the Monte Carlo simulation of diffuse reflectance from a multi-layered tissue model with tumor-like heterogeneities. The proposed method consists of two steps. In the first step, a set of photon trajectory information generated from a baseline Monte Carlo Simulation is utilized to scale the exit distance and exit weight of survival photons for the multi-layered tissue model. In the second step, the similar photon trajectory information and the scaling result obtained from the first step are employed to estimate diffuse reflectance from the multi-layered tissue model with tumor-like heterogeneities using the perturbation Monte Carlo method. Our method is demonstrated to be able to shorten simulation time significantly. Furthermore, it is applicable to a much broader range of optical properties and tissue models compared to the scaling or perturbation method alone.

8221-36, Session 9

## Coherent Raman scattering for localized thermal mapping

H. T. Beier, Air Force Research Lab. (United States); G. D. Noojin, TASC, Inc. (United States); B. A. Rockwell, Air Force Research Lab. (United States)

Coherent Raman scattering (CRS) spectroscopy is explored as a tool for obtaining localized intra-cellular temperature measurements. A single femtosecond oscillator is used to pump a photonic crystal fiber to provide a broadband Stokes pulse. The CRS signals from the broad OH-stretching modes between 3250 and 3550 1/cm are recorded for water at different temperatures. The shapes of these two modes are shown to correlate with water temperature. As a multi-wave process, excitation is limited to only the focal volume giving inherent spatial resolution that allows for mapping of the thermal profile. The local variation of temperature across cells are mapped so that the localized thermal response from directed energy exposure can be obtained. As these exposures typically have some thermal component to their effect on cells, it is important to have a means of specifically characterizing the thermal effects. The thermal portion can then be decoupled from the other effects from the directed energy source so that the non-thermal components are better characterized.

8221-37, Session 9

## Extracting scattering coefficient and anisotropy factor of tissue using optical coherence tomography

N. Choudhury, Michigan Technological Univ. (United States); S. L. Jacques, Oregon Health & Science Univ. (United States)

Determination of tissue optical properties is important for applications of light in both diagnostic and therapeutic medicine. Determining tissue optical properties will lead to better design of optical diagnostic tools, improvement in laser therapy, photo dynamic therapy dosimetry, drug pharmacokinetics, etc. Some of the experimental techniques used to determine optical properties include: integrating sphere, frequency domain diffused reflectance, time-domain diffuse reflectance, spatially resolved steady state diffuse reflectance, etc. Each of these techniques has its own advantages and disadvantages. Non-contact determination of optical properties using optical coherence tomography (OCT) has also been proposed before, but these OCT methods only provide total optical attenuation coefficient, mut, instead of scattering coefficient, mus, and anisotropy factor, g. We have developed a theoretical model for OCT signal using Monte Carlo simulation that allows us to fit values extracted from the OCT signal, namely, reflectance, rho, and the total optical attenuation coefficient, mut, to obtain optical properties of tissue (mus and g). Since OCT signal as a function of depth falls faster than it should because of the focusing effect of the lens, we employ focus tracking to obtain our images which helps us to determine mut more accurately. In order to obtain reflectance, rho, the OCT signal is converted into the unit of reflectance by using a glass-oil interface as a calibration standard. Using this method we have extracted optical properties of different tissue types, e.g., skin, muscle, liver, and brain of mouse.

8221-38, Session 9

## Study of Fourier transform infrared spectra of cockroach nervous tissue and chitin

V. H. Ghadage, Baburaoji Gholap College (India); G. R. Kulkarni, S. V. Bhoraskar, Univ. of Pune (India)

Fourier Transform Infrared Spectroscopy (FTIR) is a very sensitive tool which is capable of providing strong insight on structural and functional changes in lipids and proteins induced by laser radiation.

In the present work cockroach nervous tissue and chitin from tibia region and are irradiated with Nd: YAG laser (λ= 1064 nm, Power =150mW) via fiber optics (Numerical aperture=0.22, diameter = 8 μ). Nd: YAG laser exposure time is varied from 10 sec to 50 sec for nervous tissue and chitin.FTIR (Fourier Transform Infra Red spectra) of cockroach nervous tissue and chitin are compared before and after laser irradiation. The FTIR spectrum of non irradiated cockroach nervous tissue shows clearly the peaks due to O-H (Carboxylic acid), C=O (Amide I), C=C (Aromatic), N=0 (Nitro), C-H (Alkenes), CH (Aromatics). FTIR Spectra of non irradiated cockroach chitin clearly shows O-H (Carboxylic acid), C=O (Carbonyl stretch), C=C (Aromatic), N=O (Nitro), C-O, (anhydrides), C-H (Alkenes stretch) group.

FTIR spectra of laser radiated nervous tissue from cockroach tibia and chitin shows significant changes in transmittance for O-H, C=O, C=C, C-H, N=O, C-O and C-H groups. The percentage transmittance increases for O-H, C=C group for exposure time 10sec, 40sec and 50 sec for nervous tissue. The percentage transmittance increases for O-H, C=C group for exposure time 10sec, 20sec, 30sec and 40 sec for chitin. The study shows clearly that FTIR spectroscopy of nervous tissue can reveal the interactions between infrared laser light and nervous tissue.

8221-39, Session 9

## Optical parameters of embedded abnormalities in tissues as determined by Monte Carlo simulation

J. B. Jeeva, M. Singh, VIT Univ. (India)

The measurement of diffuse reflected or backscattered radiation provides information about the structural variation of the tissues. For the construction of tissue phantoms, the heart, adipose and spleen tissues of goat were selected. The tissue phantom of size 30x30x30mm of heart tissue is constructed with adipose, the high scattering tissue, and spleen, the high absorbing tissue, as compared to heart, are introduced to simulate the scattering and absorbing abnormalities. The size of the embedded tissues is 2x2x1mm. These are placed at locations (0,0,2), (0,0,4) and (0,0,6). The measuring probe is also modelled with one source fiber and four detector fibers separated by 2mm from each other along x direction. The probe model is made to move over the top (x,y) surface of the tissue slab starting from top left to right end. The probe scans over an area of 15mm x 10mm on the top surface of the tissue phantoms. At each position of the probe Monte Carlo simulation of photon propagation in the tissue medium is carried out. The backscattered photons received by the detecting fibers are stored in separate files for respective positions. For detection of adipose and spleen tissues surface profiles of backscattered radiations are drawn. This study shows that the backscattered intensity is increased and decreased depending on the embedded adipose and spleen, respectively, as measured by the detectors placed at 2mm, 4mm, 6mm away from the source fiber. This effect is also observed in the images constructed by measurement of backscattered fraction at various locations on the surface.

8221-40, Session 9

## Analysis of the influences of biological variance, measurement error, and uncertainty on retinal photothermal damage threshold studies

D. Wooddell, C. Schubert-Kabban, R. Hill, Air Force Institute of Technology (United States)

Exposure limits for directed energy sources are derived from a compilation of known injury thresholds taken primarily from animal models and simulation data. The summary statistics for these experiments are given as exposure levels representing a 50% probability of injury, or ED50, and fiducial limits. These fiducial limits define the confidence interval for the ED50 and are greatly impacted by the variance of the data collected. As such, a relatively high variance can lead to wider confidence intervals and, in turn, negatively impact the quality of safe exposure limits for laser radiation by creating a larger than optimal safety cushion.

Using sensitivity analysis in a first principles simulation, we examine the most significant variance inducing factors for visible and near-infrared wavelength exposures and their impacts on ED50 levels from the photothermal damage perspective. Better understanding of experimental variance will allow for less aggressive safety cushions for exposure limits and improve directed energy research methodology.

8221-41, Session 10

## Optical property change of blood on an optical window boundary by 660-nm band laser irradiation

M. Takahashi, A. Ito, T. Arai, Keio Univ. (Japan)

We studied an optical interaction at on optical window boundary until blood charring occurrence. This interaction may occur at contact laser irradiation (660 nm band, CW) via a laser catheter in heart cavity. We previously reported that pre-charring optical behavior may be detected by diffuse-reflected-light power time-history. The aim of this study is to measure absorption coefficient (μa) and reduced scattering coefficient (μ's) to explain this pre-charring optical behavior. A blood model (rabbit red blood cells 2-4 after donation in saline with hematocrit of 40%, 1 mm in thickness) sandwiched between 2 glass plates to simulate the interface between blood and optical window was used. A double integrating sphere system was constructed. The red laser beam (660 nm band) was irradiated to the sandwiched blood model. Fourty W/cm2 in irradiance was used to set the maximum irradiance during irradiation via the laser catheter in vivo. μa and μ's at red laser wavelength were measured continuously until blood charring occurrence. Inverse adding doubling method was utilized to analyze measured data to obtain μa and μ's. Continuous μa increase of 5-10% from the initial value until charring was observed. μ's decrease of 8-10% during 15-30 s before charring following broad peak was obtained. We think these μa and μ's changes may explain the pre-charring optical behavior detected by the diffuse-reflected-light power time-history in our reported study.

8221-42, Session 10

## Determining light distribution in human head using 3D Monte Carlo simulations

C. Böcklin, D. Baumann, J. Fröhlich, ETH Zurich (Switzerland)

Near Infrared (NIR) extinction measurements can be used to determine the cerebral haemodynamics of adult patients. A novel device generation allows for the parallel intra- and transcranial measurement of cerebral blood volume and blood flow. However, it is necessary to have an accurate numerical model to be able to interpret and verify the measurement data. The key point of this numerical model is to attain a full 3D light intensity map of the whole area of interest.

The modeling of light propagation for the transcraniel measurements is complex, as the light is crossing several tissue types with very distinct optical properties. Light propagation in such turbid media can, in principle, be described by the Radiative Transport Equation (RTE). The RTE can, however, not be solved in a closed form.

Therefore, a fully 3D Monte-Carlo simulator has been developed to obtain a statistical solution of the RTE. It allows to produce intensity maps for arbitrary 3D structures, as for example the human head. Two different schemes are implemented in the 3D Monte-Carlo simulator, the single photon method and the photon packet method. Both methods are validated against two widely used analytical approximations of the RTE, the Beer-Lambert law for largely absorptive media and the Diffusion Equation for primarily scattering media. The choice of the grid dimensions and spacing of the intensity map along with the number of simulated photons prove to be crucial to reproduce the RTE accurately.

8221-43, Session 10

## Monte Carlo simulation of fluorescence imaging of microvasculature

M. A. Davis, A. D. Estrada, A. Ponticorvo, A. K. Dunn, The Univ. of Texas at Austin (United States)

Lately, in-vivo fluorescence imaging in the microvasculature has become popular method in the neuroimaging community for evaluating both structural and functional parameters in the brain. However, to our knowledge, no one has evaluated these methods to determine where the fluorescence, or phosphorescence, is coming from in the tissue using a realistic in-vivo model. We employed a novel 3D fluorescence Monte Carlo method and created a set of tissue geometries with which to evaluate fluorescence origination. We evaluated the accuracy of a homogeneous tissue assumption in the cerebrum and found that it cannot accurately predict depth penetration due to the large difference between intra- and extravascular absorption. Additionally, several illumination and detection methods were evaluated to study the effect of imaging technique on fluorescence signal origination. We found that a localized illumination source with a small detector can strongly emphasize surface vessels, while using a wide-field illumination method with a small detector can allow for the integration of signal from a large amount of vasculature. We also found that the excitation wavelength can be selected to restrict signal to a single vessel. Wavelengths around the absorption peaks of oxy- and deoxy-hemoglobin allowed for the signal to be restricted to the vessel targeted, while near infrared wavelengths tended to easily penetrate the vessel and generate fluorescence from deeper into the tissue.

8221-44, Session 10

## Fluorescence angular domain imaging of skin tissue phantoms using intralipid-infused solids

R. Cheng, M. Phang, R. Thomas, N. Pfeiffer, G. Chapman, B. Kaminska, Simon Fraser Univ. (Canada)

Optical imaging through biological tissue has the significant problems of scattering which degrades the image resolution and quality. Research has shown that Angular Domain Imaging (ADI) improves image quality by filtering out the scattered light in the biological tissue images based on the angular direction of photons. The advantage of this technique is that it is independent of the wavelength, coherent, pulse, or duration compared to OCT or time domain. This allows us to couple ADI with conventional fluorescence imaging technique. Previous work was creating test media by varying Intralipid/water concentration to produce different scattering levels. This showed difficulties in producing a consistent scattering medium in liquid states. Hence, ideally we want a reusable solid medium which has a stable scattering characteristic. Our target is to investigate fluorescence ADI on skin with cancerous collagen tissue where healthy collagen fluoresces while the cancerous collagen tissue does not. To mimic the characteristic of skin, a solid scattering medium over a patterned fluorescence material with non-emitting structures is created. We used a solid agar medium, or a transparent polymer, infused with Intralipid at different concentrations, as the scattering medium. The solid media with similar scattering characteristic of skin (μs = 20cm-1, g = 0.85) is placed on top of a fluorescence plastic (415nm excitation, ≈ 580nm emission) which is patterned by strips of non-emitting structures (200-400μm). Using 2D collimated matrix with acceptance angles of 5.72° on top of the solid scattering medium, these non-emitting structures are detectable at shallow scattering tissue depth (1-2mm).

8221-45, Session 10

## Evaluation of fast avalanche photodiode detectors for early photon diffuse fluorescence tomography

M. J. Niedre, R. Duross, Northeastern Univ. (United States)

Small animal diffuse fluorescence tomography has great potential as a pre-clinical research tool, but the achievable resolution is limited by the high-degree of light scatter in biological tissue. It is well understood that light scatter between a source and detector pair can be effectively reduced by measurement of so-called “early-photons” (EPs) from a pulsed laser source. We have recently shown that measurement of EPs can reduce detected photon scatter by 40%-60% compared to un-gated photons using a well-designed time-resolved DFT instrument but that Monte Carlo propagation models indicate that higher degrees of improvement are theoretically possible. To better understand this, we studied instrumentation effects of EP measurements and showed that these are practically limited primarily by i) the instrument temporal impulse response function (TIRF), and ii) the maximal signal level at the detector.

In this presentation we describe a new time-resolved diffuse fluorescence tomography instrument that addresses these limitations. In particular, the key technical features of our system are, i) a set of fast avalanche photodiode detectors with rapid TIRFs operating in photon counting mode, ii) a femto-second pulsed laser source, and iii) “pulse-picking” technology to allow high pulse energies but low average power at the sample. We demonstrate that our instrument has an overall TIRF of about 50 ps and can tolerate high detected fluences without damage. This allows measurement of EPs with 70-80% reduction in scatter compared to ungated photons with corresponding improvement in tomographic imaging resolution. We also report on ongoing in vivo validation studies in mice.

8221-46, Session 10

## Angle-resolved spectroscopy: a tissue-mimicking phantom study

Y. Zhang, Simon Fraser Univ. (Canada); F. Vasefi, A. Chamson-Reig, Lawson Health Research Institute (Canada); M. Najiminaini, B. Kaminska, Simon Fraser Univ. (Canada); J. J. L. Carson, Lawson Health Research Institute (Canada)

Angular Filter Array (RAFA) is a novel optical filter consisting of a radially-distributed series of micro-machined channels with a focal length of a few millimeters. It filters photons passing through the focal point according to the propagation direction and can be used to couple angularly-filtered photons to a camera or imaging spectrometer. It has proven to be capable of collecting the angular distribution and the spectral information of photons simultaneously and non-invasively, which allows angle-resolved spectroscopic measurement of a turbid medium. To explore the feasibility of using this device to characterize the optical abnormalities in human tissues, we tested the performance of an angle-resolved RAFA-based spectroscopy system to detect absorption targets embedded within a tissue-mimicking phantom. The body of the phantom was made of 0.1% Intralipid™/agarose gel (7 mm in thickness) and the targets were spherical (1.5 mm in radius) and contained 10 μM Indocyanine Green (ICG). The illumination source was a broadband near infrared (NIR) collimated beam which was projected on to the surface of the phantom in a trans-illumination configuration. Photons were angularly filtered by the RAFA and spectrally resolved by a pushbroom spectrometer. The experimental results confirmed that RAFA preferentially filtered photons that carried information on the embedded targets. The results suggested that the angle-resolved spectroscopy by RAFA has potential for detection of optical abnormalities in biomedical samples.

8221-63, Session 10

## CUDA-MPI-FDTD implementation of Maxwell’s equations in general dispersive media

M. R. Zunoubi, Kirtland Air Force Base (United States); J. A. Payne, Air Force Research Lab. (United States); W. P. Roach, Kirtland Air Force Base (United States)

In recent years, a great deal of effort has been expended to understand the interaction of High Peak Power (HPP) electromagnetic (EM) waves as well as focused Gaussian beams on biological tissues since it is important to accurately determine the EM dose delivered to biological targets during RF exposure while understanding the nature of optical wave interaction with tissues is equally important since it aids with the development of optical diagnostic techniques which in turn, are capable of evaluating the tissue pathology very rapidly and noninvasively. Owing to its ease of implementation and a broad range of capabilities and applications, the Finite-Difference Time-Domain (FDTD) technique has been widely employed to analyze the interaction between the HPP EM waves and focused optical beams with biological cells. However, many practical applications require simulation of realistic scenarios that could require hundreds of millions of FDTD voxels resulting in prohibitively expensive computational models. Traditionally, a computer cluster has been used to circumvent this problem which itself needs a relative large space, is expensive, requires occasional maintenance, and is shared among various research teams. Alternatively, researchers have recently focused on implementing the FDTD on multiple Graphic Processing Units (GPUs) which possess inherent attributes for parallel computing. In this research, we present the first CUDA-MPI-FDTD implementation of Maxwell’s equations in general dispersive media that uses the MPI API to synchronize the operation of GPUs and their corresponding CPUs. Practical results will be presented along with a measure of speedup factors achieved when using multiple GPUs.

# Conference 8222: Dynamics and Fluctuations in Biomedical Photonics VII

Saturday-Monday 21-23 January 2012

Part of Proceedings of SPIE Vol. 8222 Dynamics and Fluctuations in Biomedical Photonics IX

8222-01, Session 1

## Phase singularities in speckle patterns for investigating tissue dynamics and flow

S. J. Kirkpatrick, K. Khaksari, D. Thomas, Michigan Technological Univ. (United States); D. D. Duncan, Portland State Univ. (United States)

Optical phase singularities, alternatively known as optical vortices or wavefront dislocations, are locations in a scattered optical field where the intensity of the field is exactly zero and the phase is undefined. The number density, lifetime, and other statistics of these singularities offer versatile methods for assessing motion, flow, and dynamics in biological tissues and structures. In this presentation, we will present our method for locating phase singularities in dynamic speckle patterns that is based on identifying points where the path integral of the phase gradient over a closed four-pixel loop is non-zero. We will further discuss how the number density and other statistics of the phase singularities can be used in time-integrated speckle patterns to gain information regarding flow and dynamics of biological tissues. This presentation will present both simulated and experimental data that demonstrate a strong relationship between the number of pseudo-optical vortices and the decorrelation behavior and contrast of laser speckle patterns. Further elucidation of these relationships should open new avenues in investigating dynamic systems using optical vortex metrology. In particular, these findings should prove to be useful in advancing biomedical applications of laser speckle contrast analysis and other investigations into flow and motion in both ordered and un-ordered dynamic systems.

8222-02, Session 1

## Experimental comparison of perfusion imaging systems using multi-exposure laser speckle, single-exposure laser speckle, and full-field laser Doppler

O. B. Thompson, E. R. Hirst, Industrial Research Ltd. (New Zealand); J. Bakker, F. Salomonsson, Perimed AB (Sweden); C. Kloeze, E. Hondebrink, W. Steenbergen, Univ. Twente (Netherlands)

A variety of laser Doppler and laser speckle systems have been constructed by various groups and companies, for commercial sale and for research. All rely on the same physical phenomenon - the dynamic laser speckle pattern generated by illuminating tissue with coherent light - but differ in details of system design, operation and analysis. We present a comparison between measurements made with three systems: a multi-exposure laser speckle system built at Industrial Research Ltd, a commercial single-exposure laser speckle system developed by Perimed AB (PSI NR) and the full-field laser Doppler camera built by the University of Twente (TOPcam). We compare the response to changing flows, and the sensitivity to movement artefacts, of all three systems.

The systems are found to produce similar results for a variety of in-vivo and in-vitro measurements. Multi-exposure speckle shows some advantages in information gained and insensitivity to static speckle, at the cost of increased complexity and measurement time.

8222-03, Session 1

## Multi-exposure laser speckle perfusion imaging for retinal blood flow

E. R. Hirst, M. K. Andrews, O. B. Thompson, Industrial Research Ltd. (New Zealand)

Measurements of flow in retinal vessels will be presented and compared with in vitro measurements on whole blood in capillaries ranging from 25 to 200-micron diameter. The viewing angle of the capillaries and their range of size allows size-dependent effects to be investigated when estimating flow within actual vessels.

Retinal measurements show a pulse effect. When this is removed by synchronisation, multi-exposure measurements show that in both cases the spectral signature of vessel flow differs from that of non-directed tissue perfusion. Unlike scattering in dermal tissue, photons in retinal vessels must return by multiple scatter from moving Red Blood Cells, whose motion is directed. The capillary measurements show that the speckle frequencies present are dependent on the flow speed, but are not affected by the viewing angle. Speckle estimates of flow in retinal vessels, which are necessarily made close to 90deg to the flow, are therefore possible.

8222-04, Session 1

## Optical viscometry of biological fluids using laser speckle rheology

Z. Hajjarian Kashany, S. K. Nadkarni, Harvard Medical School (United States)

Alterations in the viscosity of biological fluids, such as blood, plasma, synovial and cerebro-spinal fluids, are associated with numerous pathological conditions. Currently available techniques for viscosity measurement are predominantly limited to conventional mechanical testing, which involves straining the sample in a cup and rod tool and measuring induced stress. Due to manipulation during mechanical testing, the sample is susceptible to shear thinning or stress hardening which may confound the viscosity assessment. Moreover, the requirement for large sample volumes complicates assessment of biological fluids. Laser speckle rheology (LSR) is a new non-contact, optical technique we are developing that is capable of measuring the dynamic viscosity of fluids, requiring small sample volume.

In LSR, light from a Helium-Neon (632 nm) source is focused within a couvette containing the sample and time varying laser speckle patterns are captured using a high speed CMOS camera. The speckle pattern is temporally modulated by the thermal Brownian motion of scattering particles within the sample. Thus, speckle fluctuations are exquisitely sensitive to viscoelastic properties of the medium. By calculating speckle intensity decorrelation and applying the Stokes-Einstein equation, linear frequency dependent viscous modulus G”($\omega$) is extracted.

The LSR approach is validated by measuring viscous modulus of test solutions (dilutions of Glycerol, Visipauqe, and Dextran 40), and swine, sheep, and rabbit blood. LSR measurements of G”($\omega$) demonstrate a highly significant, strong correlation with conventional mechanical viscometry results for the test samples ($R=0.99$, $p< 0.0001$) and animal blood samples ($R=0.92$, $p < 0.0004$). These results reveal the invaluable potential of LSR as a tool for viscometry of bio-fluids, requiring only a sub-milliliter sample volume.

8222-05, Session 1

## Optical speckles of blood proteins embedded in porous glassy substrate

T. Holden, P. Schneider, S. Dehipawala, N. Gadura, S. Dehipawala, D. Kokkinos, G. Tremberger, Jr., D. Lieberman, T. D. Cheung, Queensborough Community College (United States)

Blood proteins could be embedded in porous glassy substrate with 100 nm pores. The embedding principle is based on blood cell dehydration with the destruction of the cell membrane, and reconstitution and centrifuge could yield a suitable solution for doping into a porous glassy medium. The doped glassy substrate speckle pattern under laser illumination could be used to characterize the protein size distribution. Calibration with the distributions obtained via atomic force microscopy would result in an optical procedure for the characterization of a blood sample. Wavelength dependence studies, red versus green, have been modeled with Monte Carlo simulation of non-Gaussian speckle correlation. The protein sizes in the red blood cells show a wider distribution as compared to the protein size in the white blood cell. Comparison to chlorophyll doping in porous glassy substrate will be discussed.

8222-06, Session 1

## Evaluation of algorithms used in tissue perfusion assessment using fast analytical calculation of laser Doppler signals

S. Wojtkiewicz, A. Liebert, Institute of Biocybernetics and Biomedical Engineering (Poland); H. Rix, Univ. de Nice Sophia Antipolis (France); R. Maniewski, Institute of Biocybernetics and Biomedical Engineering (Poland)

We have developed a new method of fast simulation of power spectral density of laser Doppler (LD) signal. The method is based on superposition of analytically calculated Doppler shift probability distributions derived for assumed light scattering phase function. We have validated the method by comparison of the analytically calculated spectra with results of Monte Carlo (MC) simulations. For semi-infinite, homogenous medium and single Doppler scattering regime, our method describes the LD spectra with the same accuracy as the MC simulations. Analytical calculation of LD signal in time domain, its spectra and furthermore perfusion index can be performed for any assumed speed distribution of moving particles, refractive index of the medium, anisotropy factor of light scattering on moving particles, laser light wavelength, LD signal sampling frequency, cut-off frequencies of low- and high-pass filters implemented in the LD instrument and signal to noise level.

The presented fast method of Doppler spectra calculation can be used as a tool for evaluation of signal processing algorithms used in LD method and/or for development of new algorithms of LD flowmetry and imaging. Fast simulations of laser Doppler signal in time domain and its frequency spectrum can be utilized in applications in which a knowledge of LD photocurrent is required, e.g. in development of detectors for tissue microperfusion monitoring or in measurements of LD autocorrelation function for perfusion measurements.

8222-07, Session 1

## Dual-wavelength endoscopic laser speckle contrast imaging system for indicating tissue blood flow and oxygenation

L. Song, D. S. Elson, Imperial College London (United Kingdom)

Endoscopic monitoring of haemodynamic and oxygenation changes is important in both the study of tissue function and in the diagnosis and treatment of disease. We previously reported an endoscopic laser speckle contrast analysis system (ELASCA) that could generate images of a fluid flow speed through a leached fibre image guide. In this paper we introduce dual-wavelength illumination into ELASCA so that it can not only indicate changes in blood flow but also the oxygenation state of the tissue. In this system two lasers at wavelengths of 660 nm and 830 nm were directed through an endoscopic probe in two polarization maintaining fibres. This system was firstly tested on human fingers by occluding the blood flow to induce changes in the blood flow and the oxygenation status. Sequences of 200 speckle images with a 1 ms exposure time were recorded over a period of 21 seconds when the occlusion was applied and after it was released. The speckle contrast was calculated by using a window of 7*7 pixels. The experimental results show that this system could detect the change of blood flow as well as indicating oxygen state. These parameters were observed to change on a fast scale and can monitor both the heart beat and respiration. The change of the mean intensity followed the respiration cycle and the contrast fluctuated at the frequency of the cardiac pulsation. This instrument is being evaluated in endoscopy to monitor blood flow changes in the bowel.

8222-09, Session 3

## Illuminating tissue dynamics with real-time optoacoustic tomography

V. Ntziachristos, Helmholtz Zentrum München GmbH (Germany)

No abstract available

8222-10, Session 3

## In vivo label-free photoacoustic flow cytometry of circulating clots

E. I. Galanzha, M. Sarimollaoglu, D. A. Nedosekin, V. P. Zharov, Univ. of Arkansas for Medical Sciences (United States)

No clinically relevant method has yet been developed for the rapid detection of circulating clots (termed also thrombi) which may lead to heart attacks and strokes which cause most deaths in the world. Indeed, commonly used troponin tests, creatine kinase (CK) or CK-MB markers do not appear in the peripheral circulation until at least four hours after the onset of infarction (i.e., too late to use the preventive drugs), and do not directly address the formation of clots. We introduce photoacoustic (PA) and photothermal (PT) techniques to detect circulating clots in the entire blood volume with their high-spatial resolution. This method is label-free, non-invasive, and provides real-time dynamic monitoring of clot composition (white, red and mixed clots), size and number/min by analyzing PA/PT signal shape, width, and rate. The capability of our technology was demonstrated in a mouse model of myocardial infarction and human blood samples. Our clinically relevant noninvasive diagnostic platform using robust, portable inexpensive photoacoustic devices attached to the wrist or neck, may provide a precedent for in vivo blood testing focusing on the earliest detection and prediction of heart attacks and strokes; as well as real-time control of therapy efficacy by counting circulating clots as a main therapeutic target.

8222-11, Session 3

## Absolute flow velocity measurement using spectral-domain optical coherence tomography

Z. Zhi, R. Wang, Univ. of Washington (United States)

Absolute blood flow velocity measurement in vivo is of great interest for clinical applications. In this work, we achieved measurement of the absolute velocity of particle-flow by simultaneously obtained axial and transverse components without knowing Doppler angle using spectral domain optical coherence tomography (SDOCT). The axial and transverse components of the velocity were derived from the phase and amplitude of the captured SDOCT signal, respectively. Phase-resolved Doppler OCT is a well-developed method for axial flow velocity measurement. Recently, SDOCT has been proposed to measure the transverse particle-flow velocity using an autocorrelation method by our group. In that work the flow direction was adjusted perpendicular to the sample beam to achieve a negligible effect of Doppler angle on transverse flow. However, in real situation when we measure the absolute velocity of blood flow, the vessel orientations are randomly distributed and in most cases are not ideally perpendicular to the probing beam. Thus, we need to evaluate this method for measuring the transverse blood flow velocity under different Doppler angles. Here we demonstrate that the transverse flow velocity measurement is free of Doppler angle which enables us to measure absolute velocity from the independent axial and transverse components. The proposed method is experimentally verified using an intralipid flow phantom. We also test it for in vivo blood flow velocity measurement and the volumetric blood flow rate of arteries before and after a bifurcation is verified in a mouse ear.

8222-12, Session 3

## Dual-mode label-free methodology for non-invasive imaging of blood and lymphatic vessels

V. Kalchenko, Weizmann Institute of Science (Israel); I. Meglinski, Univ. of Otago (New Zealand); Y. Kuznetsov, A. Harmelin, Weizmann Institute of Science (Israel)

We report a dual-mode methodology for non-invasive imaging of blood and lymph vessels by using Dynamic Light Scattering (DLS) technique. Along with the ability to obtain free-label images of lymph and blood vascular bed current approach is lead to be promising in non-invasive studies of functional vascular density and monitoring of blood and lymph flow.

8222-13, Session 3

## Optical coherence tomography in quantifying the permeation of human plasma lipoproteins in vascular tissues

M. G. Ghosn, Baylor College of Medicine (United States); M. Mashiatulla, Univ. of Houston (United States); V. V. Tuchin, N.G. Chernyshevsky Saratov State Univ. (Russian Federation) and Univ.of Oulu (Finland); J. D. Morrisett, Baylor College of Medicine (United States); K. V. Larin, Univ. of Houston (United States)

Atherosclerosis is the most common underlying cause of vascular disease, occurring in multiple arterial beds including the carotid, coronary, and femoral arteries. Atherosclerosis is an inflammatory process occurring in arterial tissue, involving the subintimal accumulation of low-density lipoproteins (LDL). Little is known about the rates at which these accumulations occur. Measurements of the permeability rate of LDL, and other lipoproteins such as high-density lipoprotein (HDL) and very low-density lipoprotein (VLDL), could help gain a better understanding of the mechanisms involved in the development of atherosclerotic lesions. The permeation of VLDL, LDL, HDL, and glucose was monitored and quantified in normal and diseased human carotid endarterectomy tissues at 20°C and 37°C using optical coherence tomography (OCT). The rates for LDL permeation through normal tissue at 20°C was (3.16 ± 0.37) ×10-5 cm/sec and at 37°C was (4.77 ± 0.48) ×10-5 cm/sec, significantly greater ($p<0.05$) than the rates for diseased tissue at these temperatures ((1.97 ± 0.34) ×10-5 cm/sec and (2.01 ± 0.23) ×10-5 cm/sec, respectively). The observed results support previous suggestions of an enhanced transport mechanism specific to LDL. This study effectively uses optical coherence tomography to measure the rates of permeation of vascular tissue by the range of naturally occurring lipoproteins.

8222-14, Session 3

## Wavelet-based multifractal analysis of laser biopsy imagery

J. Jagtap, Indian Institute of Technology Kanpur (India); S. Ghosh, Univ. of KwaZulu-Natal (South Africa); P. K. Panigrahi, Indian Institute of Science Education and Research Kolkata (India); A. Pradhan, Indian Institute of Technology Kanpur (India)

In this work, we report a wavelet based multi-fractal study of images of dysplastic and neoplastic HE-stained human cervical tissues captured in the transmission mode when illuminated by a laser light (He-Ne 632.8nm laser). It is well known that the morphological changes occurring during the progression of diseases like cancer manifest in their optical properties which can be probed for differentiating the various stages of cancer. Here, we use the multi-resolution properties of the wavelet transform to analyze the optical changes. For this, we have used a novel laser imagery technique which provides us with a composite image of the absorption by the different cellular organelles. As the disease progresses, due to the growth of new cells, the ratio of the organelle to cellular volume changes manifesting in the laser imagery of such tissues. In order to develop a metric that can quantify the changes in such systems, we make use of the wavelet-based fluctuation analysis. The changing self-similarity during disease progression can be well characterized by the Hurst exponent and the scaling exponent. Due to the use of the Daubechies' family of wavelet kernels, we can extract polynomial trends of different orders, which help us characterize the underlying processes effectively. In this study, we observe that the Hurst exponent increases as the cancer progresses. This measure could be used to relatively differentiate the different stages of cancer which could lead to the development of a novel non-invasive method for cancer detection and characterization.

8222-15, Session 3

## Mitosis detection in 3D tissue culture using tissue dynamics spectroscopy

R. An, K. Jeong, J. J. Turek, D. D. Nolte, Purdue Univ. (United States)

Mitosis is the most dramatic phase in the cell cycle, especially during telophase and cytokinesis. For single cells and cell monolayers, there are precise microscopic techniques that capture the physiological changes during mitosis. However, cellular physiology in 2D cell monolayers is not representative of three-dimensional tissues, and for that reason cell-based assays are currently shifting away from monolayers into three dimensional tissue culture. But in 3-D tissue, for example tumor spheroids, light signals are obscured by the high background of diffusely scattered light, and mitosis cannot be detected inside using conventional microscopic techniques. In this work, we introduce Tissue Dynamics Spectroscopy (TDS) that can detect mitosis up to 1 mm deep inside living tissue by capturing depth-gated dynamic speckle from a tumor spheroid using coherence-gated digital holographic imaging [1]. Fluctuation spectrograms of the dynamic speckle depend on cell shape changes, membrane undulations and organelle movements. By using these fluctuation spectral responses as functional fingerprints, we can identify mitosis events from different voxels inside tumor spheroids and generate 3-D mitosis maps for tumor spheroids. We show that for proliferating tumor spheroids, mitosis events only occur within the proliferating shell, but not in the hypoxic core. We also compare results when anti-cancer drugs are applied to arrest, release and synchronize mitosis. These results demonstrate the applicability of TDS to early drug discovery. The technique also has potential for malignancy diagnosis and developmental biology studies.

[1] Jeong, K., J.J. Turek, and D.D. Nolte , Speckle fluctuation spectroscopy of intracellular motion in living tissue using coherence-domain digital holography, JBO 030514-1 2010 Vol. 15(3)

8222-48, Session 3

## Dual-beam optical coherence tomography system for quantification of flow velocity in capillary phantoms

S. M. Daly, E. Jonathan, Univ. of Limerick (Ireland); M. J. Leahy, National Univ. of Ireland, Galway (Ireland) and National Biophotonics and Imaging Platform (Ireland) and Royal College of Surgeons (Ireland)

The analysis of light interactions with tissue performs a non-invasive ‘optical biopsy’ morphologically and functionally, both of diagnostic and pathological importance. However, many techniques commonly employ point scanning and thus are not optimised for time-evolution studies as signals are acquired at different times.

There exists a myriad of methods aimed towards measuring values of flow velocity within media. However, every technique contains limitations or trade-offs which must be compensated for in order to utilise the technique in a practical manner. Notably, the Doppler functionality has been the predominant force in velocity estimation in recent times. However, it is necessary (as dictated by its theoretical formulation) that the (Doppler) angle between the incident beam and the flow vector must be precisely known before an exact value of fluid flow velocity can be calculated. In many applications, however, it is difficult to estimate the Doppler angle accurately when complex flow geometries are embedded in highly scattering media.

Optical Coherence Tomography (OCT) is an imaging technique which performs cross-sectional imaging in materials by measuring the magnitude of backscattered light from within a sample, as a function of the optical delay times. The subject of this study pivots upon the design and development of an in-house spectral domain OCT system with dual beam configuration for velocity estimation. The proposed method operates by simultaneous illumination and measurement from two planes in one acquisition. By measuring the temporal variations of light intensity at two points a known distance apart, transit times may be deduced thereby yielding velocity values irrespective of vessel tortuosity.

8222-49, Session 3

## Identifying brain cancers using dye-enhanced multimodal confocal imaging

D. J. Wirth, Univ. of Massachusetts Lowell (United States); M. Snuderl, Harvard Medical School (United States); S. A. Sheth, W. Curry, Massachusetts General Hospital (United States); A. N. Yaroslavsky, Univ. of Massachusetts Lowell (United States)

Brain cancers are among the most aggressive and deadliest. Even benign tumors are associated with high morbidity and poor quality of life. Complete resection of brain tumors may improve quality of life and patient survival. The goal of this study was to evaluate multimodal confocal imaging for intraoperative detection of brain cancers. In particular, we have imaged different types of brain cancers, correlated optical images to histopathology, and evaluated the possibility of straightforward interpretation of fluorescence images in a manner similar to that of histopathology. Fresh thick specimens were obtained within several hours after surgeries. A total of 25 normal brain samples and 78 cancerous samples were studied. Of the cancerous samples there were 25 metastasis, 14 meningioma, 19 glioblastoma, 12 high grade glioma and 8 low grade glioma samples. The tissues were briefly stained in 0.05 mg/ml aqueous solution of methylene blue. Multimodal confocal images were acquired using an in house build system. Reflectance and fluorescence signals of MB were excited at 642 nm. Fluorescence emission of MB was registered between 670 and 710 nm. After imaging, all tissues were processed for H&E histopathology. Histological sections were digitized and compared side-by-side to the corresponding optical images. The results of comparison demonstrate good correlation between fluorescence images and histopathology. Reflectance images provide information on the morphology and vascularization of the specimens, complimentary to that provided by fluorescence images. Multimodal confocal approach shows promise for intraoperative brain cancer detection.

8222-50, Session 3

## Dye-enhanced optical imaging for delineating breast cancer margins

R. Patel, Univ. of Massachusetts Lowell (United States); A. Khan, Univ. of Massachusetts Medical School (United States); D. J. Wirth, Univ. of Massachusetts Lowell (United States); M. Kamionek, ; R. Quinlan, Univ. of Massachusetts Medical School (United States); A. N. Yaroslavsky, Univ. of Massachusetts Lowell (United States)

Delineation of cancer margins at the time of surgery is a problem of major importance in surgical oncology. The goal of this study was to evaluate the feasibility of wide-field and high-resolution multimodal optical imaging, including, polarization, reflectance, and fluorescence for detecting breast cancer margins. Fresh thick breast tissue specimens were collected following surgeries, stained with 0.05 mg/ml aqueous solution of methlylene blue and imaged using wide-field and high resolution confocal systems. In total, 19 samples were investigated, including 12 ductal carcinomas, 5 lobular carcinomas, 1 intracystic papillary carcinoma, and 1 colloid carcinoma. Wide-field reflectance polarization images were taken at 9 wavelengths between 390 nm and 750 nm. Wide-field fluorescence polarization images were excited at 640 nm and registered between 660 nm and 750 nm. High resolution confocal reflectance and fluorescence images were excited using 642 nm laser with fluorescence images registered between 670 nm and 710 nm. After imaging, the specimens were processed for H&E paraffin embedded histopathology. Histological slides were digitized and compared side-by-side with the multimodal wide-field and high-resolution optical images to evaluate correlation of tumor margins and cellular morphology, respectively. The results of the study demonstrate that all the specimens investigated produced high contrast wide-field reflectance and fluorescence polarization images. Fluorescence confocal imaging enables cellular resolution and facilitates analysis of microscopic morphology of tissue in the manner similar to histopathology. Wide-field high-resolution optical imaging shows promise for intraoperative delineation of breast cancers.

8222-51, Session 3

## Application of multiphoton tomography for safety assessment of ZnO nanoparticles used in cosmetic products

J. M. Lademann, Charité Universitätsmedizin Berlin (Germany); K. König, M. Kellner-Hoefer, H. G. Breunig, JenLab GmbH (Germany); W. Werncke, Max-Born-Institut für Nichtlineare Optik und Kurzzeitspektroskopie (Germany); M. C. Meinke, A. Patzelt, W. Sterry, M. E. Darvin, Charité Universitätsmedizin Berlin (Germany)

ZnO nanoparticles (NPs) are commonly used as UV filters in commercial sunscreen products. Their penetration into the skin is controversially discussed in the literature. In the present in vivo study, penetration of ZnO NPs (30 nm in size) into the human skin was investigated by multiphoton tomography. Based on the non-linear effects of a second harmonic generation (SHG) and hyper-Rayleigh scattering (HRS), the distribution of ZnO NPs in the horny layers of the epidermis, as well as the furrows, wrinkles and orifice of the hair follicles was analyzed. This method permitted to distinguish between the particular and dissolved forms of Zn. A detection limit of 0.16 µg/cm2 was estimated.

Taking advantage of this sensitivity, it was clearly shown that ZnO NPs penetrate only into the outermost layers of stratum corneum, furrows and in the orifices of the hair follicles and do not reach the viable epidermis.

8222-16, Session 4

## Intraoperative functional mapping of eloquent brain cortex for minimizing post-operative neurological deficit

S. A. Sheth, C. Kwon, S. Bourne, E. N. Eskandar, Massachusetts General Hospital (United States); A. N. Yaroslavsky, Univ. of Massachusetts Lowell (United States)

One of the chief tenets of neurosurgery is avoiding damage to eloquent brain regions. Due to anatomical variability of the brain, intraoperative mapping of eloquent function is imperative within each individual patient. Functional MRI can provide a gross indication of functional localization prior to surgery, but is unreliable for intraoperative mapping. In this presentation, we address clinical feasibility of an imaging technique, optical polarization imaging (OPI), designed to provide rapid, high-resolution maps of human cortical function. OPI combines the advantages of optical intrinsic signal imaging, which has been used to study functional architecture in animals, and polarized light imaging, a technique used for the superficial imaging. The changes in hemoglobin concentration and oxygenation during hemodynamic response to neural activity change light reflectance from cortical surface. By filtering reflected light at various wavelengths, we capture different aspects of the hemodynamic response. Imaging at an isosbestic wavelength of hemoglobin measures changes in local cerebral blood volume (CBV). Imaging at other wavelengths follows changes in local tissue oxygenation. Using a pair of CCD cameras and linearly polarizing filters, we obtained temporal sequences of multi-spectral reflectance images and assessed functional architecture of the brain during surgeries. CBV maps provided the best localization of eloquent brain regions. Our results demonstrate the utility of optical imaging techniques during neurosurgical procedures for minimizing iatrogenic neurological injury.

8222-17, Session 4

## Real-time, non-invasive assessment of human hematocrit

D. D. Duncan, Portland State Univ. (United States); D. Fischer, J. Myers, NASA Glenn Research Ctr. (United States)

The human health effects of space flight (weightlessness, radiation) are diverse and variable in terms of severity. Because of this, there is need for a continuous non-invasive means of monitoring specific indicators of health as a component of a comprehensive health maintenance program. Additionally, there is need for such monitoring in the case of trauma. One indicator of health status is hematocrit (HCT), the fractional volumetric ratio of red blood cells (RBCs).

Scanned Doppler systems are commonly used for assessing blood velocity throughout the heart and vasculature system, and for generating tomographic images and 3-D reconstructions. The technology has been demonstrated safe, practical, and completely non-invasive. Recent measurements have demonstrated the direct relationship between acoustical attenuation and the HCT of whole blood: for frequencies less than 20MHz, attenuation is dominated by absorption. An issue that complicates the interpretation of acoustic measurement of hematocrit, however, is that the RBC fractional volume is high enough that nearest neighbor scatter effects are significant. Moreover, these nearest neighbor effects, commonly described in terms of a pair distribution function, depend upon blood flow shear rates. These effects are seen most strongly in the backscatter cross-section.

We present the theoretical foundation for the measurement concept, describe a reference-free experimental implementation that obviates the shear-rated dependence of the backscatter cross-section, discuss the requisite signal processing algorithms, and show results of a series of in vitro experiments on pulsatile flows for a variety of hematocrits using blood mimicking fluids.

8222-18, Session 4

## Ultrahigh-resolution image of human skin using optical coherence tomography/optical microangiography

Z. Zhi, R. Wang, Univ. of Washington (United States)

As a non-invasive imaging technique, Optical coherence tomography (OCT) has the capability to perform “optical biopsy” in situ in real time with micro-scale resolution, which has previously demonstrated potential for use in dermatology. There are two goals for this study. One is to improve the resolution approaching cellular level (~1 um) which is designated as Ultra-High Resolution OCT (UHR-OCT) to resolve the structure of skin better. This requires utilization of light sources with broad bandwidth. In this study, we developed an UHR-OCT by coupling a supercontinuum light source into the system. With a bandwidth of 120 nm centered on 800 nm, the UHR-OCT system provides a measured axial resolution of ~2.4 μm in tissue. Until now, more and more evidences suggest that vascular abnormalities may play crucial role in many dermatologic diseases, such as psoriasis, port wine stain, and skin cancer. To better understand the vascular involvement in skin conditions, the other goal of this study is to apply Ultra-High Sensitive OMAG (UHS-OMAG) scanning protocol and algorithm onto the UHR-OCT system to achieve ultra-high resolution, ultra-high sensitivity imaging of 3D microcirculations within skin tissue beds in vivo. The system has an unprecedented sensitivity to slow blood flow (down to 10 μm/s) and a lateral resolution of 5.8 μm, we were able to show true capillary level microvasculature map of skin. Finally, we will introduce a new idea for 3D segmentation of the epidermis and dermis by combining the structure and microvasculature image.

8222-19, Session 4

## In vivo 3D multifunctional imaging of human corneal-scleral limbus with spectral-domain optical coherence tomography

P. Li, T. Shen, M. Johnstone, R. Wang, Univ. of Washington (United States)

Pathologically and clinically, the corneal-scleral limbus is an important transitional zone from the cornea to the sclera and conjunctiva, covering corneal arcades, palisades of Vogt, rich vascular network and aqueous outflow system. Optical coherence tomography (OCT) is a powerful, noninvasive, 3D real-time imaging technique with high resolution and enough imaging depth of up to the entire anterior eye segment. Integrating with the ultrahigh sensitive optical microangiography algorithm, we demonstrate that our multi-functional anterior segment OCT system is capable of visualizing the microstructure and microvasculature of the corneal-scleral limbus and providing the quantitative biometrics of the anterior angle in the human eye. The results show our anterior segment OCT can be a useful tool for the investigation of corneal-scleral limbus, especially for the diagnosis and treatment of glaucoma.

8222-20, Session 4

## In vivo spectral and fluorescence imaging microscopy of tumor microvessel blood supply and oxygenation changes following vascular targeting agent treatment

J. A. Lee, D. W. Siemann, R. T. Kozikowski, B. S. Sorg, Univ. of Florida (United States)

The formation of new microvasculature is essential for a tumor mass to grow. Vascular targeting agents (VTAs), including anti-angiogenic drugs and vascular disrupting agents, aim to either inhibit new vasculature growth or destroy existing vasculature, respectively. Because the mechanisms for anti-angiogenic drugs and vascular disrupting agents are complementary, analysis of these drugs used together is under investigation for the enhanced treatment of tumors in comparison to each treatment alone. The preclinical evaluation of the effects of VTAs on tumor growth in small animal models is vital for the development of effective drugs for clinical use. In vivo hyperspectral imaging microscopy of hemoglobin saturation has been used previously to investigate the efficacy of VTAs through analysis of tumor microvessel oxygenation after drug administration. Combining this imaging modality with first-pass fluorescence angiographic imaging can give additional important information about the vessel morphology and blood flow changes that occur after VTA treatment, thus elucidating the relationship between microvessel structure changes and oxygenation. In this study, we report the combined use of hyperspectral and first pass fluorescence angiographic imaging to examine the relationship between vessel morphology and oxygenation of human renal carcinomas (Caki-1 tumors) in mice following a combination treatment of vascular disrupting agent, OXi4503, and anti-VEGF angiogenesis inhibitor, Avastin. Imaging of the tumors is completed before treatment as well as in the days following treatment.

8222-21, Session 4

## Clinical Evaluation of Psoriasis using Optical Coherence Tomography and Raman Spectroscopy

M. O’Connell, Univ. of Limerick (Ireland)

In clinical practice, the Psoriasis Area and Severity Index (PASI) score is used to quantify the extent of the disease, and evaluate its response to treatment. It is widely considered to be a slow, non-sensitive, and highly subjective procedure giving impetus to the development of objective, validated instruments for its assessment. Several such instruments have been, and continue to be developed to provide an assessment of the severity of the skin lesions. To this end, we report upon the simultaneous use of a compact Raman spectrometer and Optical Coherence Tomography (OCT) system. Whilst recent efforts using a combined system have been promising, the operating centre wavelengths of the configuration limit the penetration depth for in vivo studies. Thus the Raman spectrometer demonstrates an operating centre wavelength in the 1 micron range. The latter yields the biochemical specificity of an affected area whilst the former provides high resolution wide-field images required for a more comprehensive evaluation. Together they offer a synergistic and more complete evaluation for the clinical diagnosis, assessment and treatment of psoriasis in a non-invasive, non-contact, rapid manner.

8222-22, Session 4

## OCT and 4D microcirculation imaging

M. J. Leahy, National Univ. of Ireland, Galway (Ireland) and National Biophotonics and Imaging Platform (Ireland) and Royal College of Surgeons (Ireland)

Leeuwenhoek's high NA lens elucidated Harvey's theory that blood passes from arterial to venous side via the microcirculation. TV provided a basis for video microscopy and the laser led to laser Doppler and laser speckle blood perfusion imaging. For 50 years physical sciences publications have been approximately 5% of all publications mentioning the microcirculation. After 2007 that has jumped to more than 20% indicating that something exciting is happening in the development of microcirculation tools. This is the arrival of 3D and 4D imaging at clinically relevant speeds and depths. Recently clinically relevant high resolution imaging of the microcirculation has become available in research labs [1]. These new microscopes are based on optical coherence tomography and photoacoustic microscopy. The authors have recently developed a number of techniques for imaging the microcirculation in 2D (TiVi) [2] and 3D (cross-correlation OCT and an absorption-based tomographic system) [3,4] which we hope will provide imaging at clinically useful speeds and depths. This paper will discuss new and highlight the challenges which currently prevent 3D microcirculation imaging at sub-second speeds.

1. Microcirculation Imaging. (Wiley-VCH), Leahy, M.J. editor, 2011.

2. O'Doherty, J., McNamara, P.M., Fitzgerald, B.W. and Leahy, M. J., Dynamic microvascular responses with a high speed TiVi imaging system J. Biophotonics 1-5 (2010).

3. Jonathan, E. Enfield, J., and Leahy, M.J. 2010. Correlation mapping method for generating microcirculation morphology from optical coherence tomography (OCT) intensity images. J. Biophotonics (published online 17 December 2010).

4. McNamara, P.M., Jonathan, E., O'Connell, M. and Leahy, M. J. Development of an absorption-based tomographic system for mapping the human microvasculature, SPIE BiOS Photonics West 2011 Oral, Proceedings of SPIE [7898 49].

The authors would like to acknowledge the support of the IRCSET (Irish Research Council for Science, Engineering & Technology) for funding this project. This research was also supported by the National Biophotonics Imaging Platform (NBIP) Ireland funded under the Higher Education Authority PRTLI Cycle 4, co-funded by the Irish Government and the European Union - Investing in your future.

8222-23, Session 6

## Functional imaging of freshly isolated pancreatic islets using glucose-evoked intrinsic optical signal response

X. Yao, W. Cui, X. Wang, Y. Li, W. Zhang, R. Lu, The Univ. of Alabama at Birmingham (United States)

Diabetes has become a global epidemic. It is well known that beta-cell dysfunction is at the center of all major forms of diabetes. In intact islets, beta-cells are coupled together as a network for effective glucose regulated insulin release. Better understanding of diabetes associated beta-cell dysfunctions requires simultaneous imaging of many beta-cells functioning together. Optical methods, such as calcium fluorescence imaging, have been explored for high resolution study of glucose-evoked beta-cell activities in intact islets. However, loading of fluorescence dyes into the center part of intact islets is difficult, and photo-toxicity of fluorescence dyes may render the islets for long term observation. Intrinsic optical signal (IOS) imaging has been established for noninvasive monitoring of stimulus-evoked physiological responses in the retina and other neural tissues. Here, we demonstrate the feasibility of functional IOS imaging of freshly isolated (but intact) pancreatic islets. Rapid near infared (NIR) imaging of rat and human islets disclosed fast IOSs with time courses comparable to previously reported electrophysiological response and insulin dynamics correlated with the glucose stimulation. Comparative investigation of donor human islets demonstrates the feasibility of IOS identification of normal and diseased islets. Our experiments indicate that IOS imaging can provide a high resolution method for advanced study of diabetes associated beta-cell dysfunctions, which may lead to improved prevention and diagnosis of diabetes. Moreover, without any requirement of exogenous biomarkers, IOS imaging also promises a noninvasive method for high-throughput functional screening of donor islets prepared for transplantation.

8222-24, Session 6

## 3-dimensional absorption-based chromophore mapping

P. M. McNamara, E. Jonathan, Univ. of Limerick (Ireland); M. J. Leahy, National Univ. of Ireland, Galway (Ireland) and National Biophotonics and Imaging Platform (Ireland) and Royal College of Surgeons (Ireland)

Numerous planar imaging methods for mapping the human microvasculature exist. In medical diagnostics, tomography is preferred over surface imaging for the reason that biological organs are 3-dimensional in nature. The aim of this work is to create a novel technique to non-invasively map the concentration of the major chromophores in human tissue, allowing 3-dimensional image reconstruction. We propose a tomographic system which is based on absorption contrast imaging, utilizing the absorbing properties of haemoglobin and melanin.

An interferometric method is employed using a broadband, white light source. The fringes obtained from a 'slice' of the material under test, indicate the chromophore content at that particular depth. This presentation details the workings of the method and outlines preliminary results of the calibration procedure of a system constructed from 'bulk' optics.

8222-25, Session 6

## Analysis of independent components obtained from functional near infrared data

I. Schelkanova, V. Y. Toronov, Ryerson Univ. (Canada)

One of the main issues of functional NIRS is the separation of functional signals from the contaminations by systemic and local physiological fluctuations. Various signal processing methods, including independent component analysis (ICA), were applied to the data acquired at the same wavelength and at multiple sites on the human or animal heads7 during functional activation. These signal processing procedures resulted in a number of independent components that could be attributed to functional activation but their physiological meaning remains unknown. Moreover, the best physiological specificity is provided by broadband NIRS5. A comparison with functional magnetic resonance imaging (fMRI) allows determining the spatial origin of fNIRS signals5. In this study, we applied ICA to broadband NIRS data to distill the components which might correspond to the breath hold activation paradigm and to correlate their time courses with the simultaneously acquired fMRI signals. Although the original signals were quite diverse, we found very few different components. The components correlated highly with fMRI BOLD signal at different locations in the brain. The analysis of the broadband spectra of the functional components reveals contributions of different chromophores into the dynamics of funtional cerebral response including water and cytochrome oxidase.

8222-26, Session 6

## Use of circular polarized light for tissue diagnostics: from optical clearing to cancer diagnostics

I. Meglinski, C. Macdonald, E. Avci, H. Yoon, M. Eccles, Univ. of Otago (New Zealand)

The interest in the applications of polarized light as well as other optical and laser-based system for biomedical diagnostics has been soared in the past. A number of studies involving the use of polarized light have been performed, including blood glucose sensing, analysis of the light back-scattered from cell suspensions to distinguish cancerous from healthy cells, Mueller matrix-based imaging of dermatological diseases, etc. In the current study circular polarized light has been applied to observe changes in biological tissues influenced by optical clearing. We demonstrate that optical clearing as well as cancer and non-cancer tissue samples in vitro can be clearly seeing as the polarization vector traverse at the Poincaré sphere.

8222-27, Session 6

## Single-wavelength imaging polarimeter based on liquid crystal technology

J. C. Gladish, D. D. Duncan, Portland State Univ. (United States)

The ability to detect changes in the structural organization of tissue has significant diagnostic value. A polarimeter has the ability to detect these changes as it can probe the tissue sub-wavelength structural organization through polarization effects. Here we present a single-wavelength (633 nm) imaging polarimeter that is based on liquid crystal technology. The system is comprised of two modules, a Stokes generator and a polarimeter. Each module employs a pair of Liquid Crystal Variable Retarders (LCVRs), which are computer-controlled birefringent devices. Additionally, the polarimeter utilizes a CCD camera to image the illuminated region, thus providing spatially resolved estimates of the complete Mueller matrix for the sample. Before the system can be employed, an overall system characterization involving all four LCVRs must be performed. This characterization defines a relationship between polarimeter measurements and the incident Stokes vectors. Here we briefly describe the calibration procedure and show Mueller matrix images of biological tissue.

8222-28, Session 7

## Using tissue mechanical properties to improve contrast and image quality in optical coherence tomography

B. F. Kennedy, K. M. Kennedy, R. A. McLaughlin, D. D. Sampson, The Univ. of Western Australia (Australia)

Exploiting mechanical properties is of significant utility in diagnosing diseased tissue, which often has different mechanical properties to surrounding healthy tissue. This has been exploited as a contrast mechanism, known as elastography, in ultrasound and magnetic resonance imaging (MRI). Ultrasound elastography is now available on commercial scanners. Initial steps have been taken to implement these techniques in optical coherence tomography (OCT), in a technique known as optical coherence elastography (OCE). Typically, a force is exerted on tissue, and the resulting tissue motion is used to determine its mechanical properties.

We will discuss the current status and challenges facing OCE. An important aspect of OCE is the method used to extract sample motion. Techniques have been proposed using both amplitude and phase. In OCE, the excitation can be quasi-static or dynamic. The impact of frequency on the mechanical properties measured will be discussed. The majority of techniques have focused on imaging the elastic strain. However, tissue is generally viscoelastic. We will present a new technique to perform viscoelastic contrast imaging. The development of OCE is critically dependent on availability of reproducible phantoms, with independently controllable optical and mechanical properties with controllable dimensions and features. Considering all of these factors, we will discuss the outlook for OCE.

We will also present two techniques to improve image quality by reducing speckle contrast in OCT using both the elastic and viscoelastic properties of tissue to decorrelate speckles between successive B-scans. These techniques achieve significant speckle reduction with minimal loss in spatial resolution.

8222-29, Session 7

## Measurement of mechanical properties of individual red blood cells from a sickle cell patient using quantitative phase microscopy

Y. Park, H. Byun, KAIST (Korea, Republic of); J. Higgins, Massachusetts General Hospital (United States) and Harvard Medical School (United States); T. R. Hillman, M. Diez-Silva, M. Dao, Massachusetts Institute of Technology (United States)

Sickle cell disease (SCD) is an inherited blood disorder characterized by sickle hemoglobin (HbS). Upon deoxygenation, HbS self-assembles in cytosol and significantly alters and damages the cell structures, resulting in a less deformable RBC (red blood cell). In SCD, ischemia and organ damage can result when microcirculation is impeded due to the poorly deformable RBCs.

Characterization of RBCs is crucial to understanding the pathophysiology of SCD, yet the mechanical properties of individual RBCs in SCD have not been fully assessed, largely due to the limitations of the measurement techniques. Micropipette aspiration, optical tweezers, microfluidics, and atomic force microscopy have been employed to study the biomechanics of SCD at the cellular level. Although these methods have significantly enhanced our understanding of sickle cell biomechanics, none of them can probe all of the major relevant mechanical parameters of individual RBCs simultaneously.

We non-invasively investigate the biomechanical properties of individual RBCs in SCD. We use quantitative phase microscopy to retrieve the material properties of single RBCs from their dynamic membrane fluctuations. We analyzed the measured fluctuations using a membrane model to retrieve four key mechanical properties of RBCs from a patient with SCD: bending modulus; shear modulus; area expansion modulus; and cytoplasmic viscosity. Our results show that high cytoplasmic viscosity at ambient oxygen concentration is mainly responsible for the significantly increased stiffness in RBCs in SCD, and that the mechanical properties of the membrane cortex of irreversibly sickled cells are different from those of the other types of RBCs in SCD.

8222-30, Session 7

## The study of collagen properties on cellular behavior and the mechanical strength of the formed hydrogel

Y. Yang, S. Wilson, Keele Univ. (United Kingdom); M. Guilbert, E. Millerot-Serrurot, P. Jeannesson, Univ. de Reims Champagne-Ardenne (France); J. Sule-Suso, Keele Univ. (United Kingdom); G. D. Sockalingum, Univ. de Reims Champagne-Ardenne (France)

Collagen is one of the most abundant proteins present in the body and constitutes approximately 25% of the human body protein content. Collagen type I is one of the five fiber-formation collagens present in most of the load-bearing tissues such as tendon, bone, muscle and blood vessel. Its chemical and physical properties dictate cellular behavior including cell migration, contraction, differentiation, adhesion, and mechanical strength. Collagen type I extracted from animal species is the most commonly used compound to generate in vitro connective tissue model for various studies. The chemical compositions of the extracted collagen depend on extraction methods and original tissue properties such as age. Consequently, the cells seeded in the collagen models will generate different cellular responses, which could provide very valuable information on the pathological situation in vivo. In this study, two non-destructive imaging systems, micro-indentation and optical coherence tomography, were used to study the effect of collagen type I composition variables on tumor cell invasion, fibroblast contraction, and related mechanical strength of the collagen hydrogels. The composition variation of type I collagen, extracted from rat tail tendons, was monitored by infrared spectroscopy. The preliminary data demonstrate that collagen hydrogels generated from old rats have low mechanical strength and the intact telopeptides in extracted collagen play a role on the mechanical properties. The non-destructive monitoring systems enable prolonged cellular behavior study for the same specimen in comparison to end point measurement.

8222-31, Session 8

## The influence of the hydrogen bonding on THz and Raman spectra of biological molecules

A. P. Shkurinov, M. Nazarov, Lomonosov Moscow State Univ. (Russian Federation); O. P. Cherkasova, Institute of Laser Physics (Russian Federation)

In the present work low-frequency vibrational spectra of bilogical molecules, such as, progesterone, 17α-hydroxyprogesteron (17-OP) and cortisone have been studied by terahertz time-domain and Raman spectroscopies in the temperature range of 17-300 K and in the spectral range 15 85 cm-1. All observed spectral features were interpreted by simulations of the crystalline structure and THz vibrational modes performed using solid-state density functional theory (DFT) (by DMol3). Evidence obtained by comparison of the experimental and calculated vibrational frequencies, for instance, for the steroid molecular crystals has demonstrated, that despite the weakness of intermolecular interactions, taking into account the nature of intermolecular bonds is required in computer modeling of crystalline structure and terahertz (THz) vibrational modes. In particular, the appearance of hydrogen bonds in the process of molecular crystals formation which considerably influences the topology and temperature dynamics of the Raman and THz absorption spectra. Besides, we have demonstrated that frequency localization of various types of vibrations and the number of external modes of THz range is largely determined by the character of intermolecular bonds.

8222-32, Session 8

## Characterization of nonmelanoma skin cancers using imaging in the optical and terahertz spectral ranges

C. S. Joseph, R. Patel, Univ. of Massachusetts Lowell (United States); V. A. Neel, Massachusetts General Hospital (United States); T. M. Goyette, R. H. Giles, A. N. Yaroslavsky, Univ. of Massachusetts Lowell (United States)

The goal of this work was to investigate the feasibility of combining continuous wave terahertz (CWT) and optical imaging for detecting nonmelanoma skin cancers. CWT shows promise for delineating skin cancers, but lacks resolution necessary to inspect tissue morphology. Imaging in the visible and near infrared spectral ranges yields resolution comparable to that of histology, but often lacks contrast for reliable detection of cancer. Thus, combination of optical and terahertz imaging has potential for accurate and sensitive skin tissue examination. Fresh skin cancer specimens were obtained immediately from Mohs surgeries and imaged within 24 hours. For CWT, a CO2 optically pumped far-infrared molecular gas laser at 584 GHz was used for illumination. The reflected signal was detected using liquid helium cooled silicon bolometer. For optical imaging, reflectance and fluorescence polarization images were taken in the range between 390 nm and 750 nm. After imaging, the specimens were processed for frozen histopathology. Histological slides were digitized and compared side-by-side with the CWT and optical images to evaluate correlation of tumor margins and tissue morphology, respectively. Our results indicate that combination of optical and terahertz imaging provides complimentary information and may offer a powerful tool for the detection of nonmelanoma skin cancers.

8222-33, Session 8

## Investigating the effects of terahertz radiation on Bacillus subtilis

J. P. Giles, B. J. Carney, C. S. Joseph, M. E. Hines, R. H. Giles, Univ. of Massachusetts Lowell (United States)

Medical and security sensing applications of Terahertz (THz) imaging are currently being developed. As a result, there is a need to further investigate the effects of THz radiation on biological systems. In this study, a 94 GHz mechanically tuned Gunn Oscillator and CO2 optically pumped FIR gas laser were used to irradiate Bacillus subtilis at 94 GHz, 584 GHz, and 1.4 THz. The bacteria was cultured in trypticase soy broth (TSB) and placed in polystyrene plates that had 96 wells each. The samples where irradiated during the exponential growth phase for differing exposure times of 1, 2, and 24 hours. Both the experimental and control plates were kept at room temperature (~32°C) and the experimental plate was monitored using an IRI 1011 Irisys thermal imager for the duration of the experiment. By evaluating the absorption of each well at 600nm immediately before and after irradiation, the population density within each well was assessed. Following this, the metabolic activity of each well was measured after irradiation by adding the tetrazolium dye XTT to the wells and evaluating the absorption of each well at 470nm after 2 hours of incubation. The instrumentation implemented and analysis techniques employed in this study will be presented.

8222-34, Poster Session

## Influence of uric acid on non-invasive blood glucose sensing studied with NIR spectroscopy

J. Jiang, L. Zhang, Tianjin Univ. (China); K. Zhang, Tianjin Chang Zheng Hospital (China); K. Xu, Tianjin Univ. (China)

It is reported that blood components are very complicated and in which glucose concentration is relatively low. This characteristic limits the practical application of NIR spectroscopy in in vivo blood glucose detection. And our previous study results demonstrate that cholesterol, which is one of the blood components, would influence the measurement result of noninvasive blood glucose sensing with NIR spectroscopy. In this talk, another factor-uric acid is taken as the study target and how it influences blood glucose sensing will be elucidated.

Spectroscopic measurements show uric acid appears the similar absorbance peaks to those of glucose within NIR range. Moreover, PLS modelling results demonstrate that there is a direct proportion relation between the measurement concentrations of glucose and the concentrations of uric acid. This correlation relationship reveals that uric acid has an influence on noninvasive blood glucose sensing studied with NIR spectroscopy. So, it is necessary to take steps to decrease the effect and improve the measurement precision of blood glucose sensing with NIR spectroscopy.

8222-35, Poster Session

## Mathematical modeling on experimental protocol of glucose adjustment for non-invasive blood glucose sensing

J. Jiang, X. Min, K. Xu, Tianjin Univ. (China)

Currently OGTT (Oral Glucose Tolerance Test) is a golden standard to diagnose diabetes in clinical laboratory. It is actually a way to adjust blood glucose artificially within a short period time by drinking a glass of glucose water. However, during the course of taking the OGTT, the testers must obey many strict rules. In this way, many influential factors have been ignored. These inherent limits make it hardly an effective method to provide more useful and complete backscattered light information caused by the change of blood glucose, so that OGTT is no longer the best experimental protocol for non-invasive blood glucose sensing.

In this talk, on the bases of physiological and mathematical knowledge, we establish a mathematical model of glucose metabolism system, with the final goal of providing a possible way to increase the accuracy of non-invasive blood glucose sensing. In this model, we get as much output as possible by setting different glucose input types (oral method, intravenous injection, or drip infusion) and adjusting parameters (such as parameters governing the rate of insulin injection, or individual differences, weight, age etc). The results show that by applying this kind of mathematical model, we could customize comparatively ideal experimental protocol of glucose adjustment for different groups of people, even individuals, with corresponding input type and parameters. Such a comprehensive data volume would makes PLS modeling more reliable. Therefore, it would be helpful to improve the accuracy of prediction model for noninvasive blood glucose sensing.

8222-36, Poster Session

## Investigation on how to choose measurement sites for non-invasive near-infrared blood glucose sensing

J. Jiang, D. Zou, K. Xu, Tianjin Univ. (China)

Detecting blood glucose noninvasively in human is of major importance clinically and commercially. In noninvasive near-infrared sensing, measuring precision varies significantly due to the different measurement sites. Many factors affect the final detected signals, such as the density and the depth of blood vascular, physiological lags between blood and interstitial fluid, the percentage of body fat within the probe region.

In this talk, we choose the diffuse reflectance mode according to physical conditions of the measurement sites, and then near-infrared glucose absorbance spectra of different measurement sites are collected in the fiber optic configuration for analysis. Skin structure features, including thickness of the epidermis and dermis layer, the localization of the blood plexus, are reviewed. Furthermore, blood flow properties and the change of tissue scattering quality are evaluated by measuring the delay correlation between the backscattered and the reference light since an increase of glucose concentration in the interstitial fluid would cause a decrease of scattering coefficient.

We concluded that the near-infrared diffuse reflectance performed on forearm and finger is of the first-class choice due to their high vascularization, little fatty tissue, homogeneous composition, limited temperature variations and the good correlation with the blood glucose signal. For individuals, comparisons between these two sites are still needed to choose the better measurement site specifically to indicate the blood glucose level.

8222-37, Poster Session

## Monte Carlo simulation on how cholesterol influences measurement of non-invasive blood glucose sensing with NIR spectroscopy

J. Jiang, L. Zhang, K. Xu, Tianjin Univ. (China)

Our previous experimental study shows that cholesterol has an influence on the measurement result of noninvasive blood glucose sensing with NIR spectroscopy, and the measurement concentrations of glucose are on the high side while containing cholesterol. However, for experiments, the cost and instrument accuracy limit concentration range and gradient of experimental samples. In this talk, Monte Carlo simulation will be used to estimate the influence level of cholesterol on non-invasive blood glucose sensing with NIR spectroscopy more accurately.

The main purpose is to simulate how glucose spectral change after being added into cholesterol with different concentrations. Serum is selected to simulate human blood, and it is set to be single layer structure. Glucose concentration is in the scope of 40-400mg/dl with the gradient of 20mg/dl. Cholesterol concentration changes between 0 and 300mg/dl and the gradient is 20mg/dl. Simulation results could find out the influence level of cholesterol on non-invasive blood glucose sensing within the range of 1200nm-1800nm. It would be helpful to reduce and remove the influence of cholesterol and improve the measurement precision.

8222-38, Poster Session

## Influence of hemoglobin on non-invasive Bilirubin measurement

J. Jiang, Q. Gong, K. Xu, Tianjin Univ. (China)

Since the abnormal metabolism of bilirubin could lead to diseases in the human body, especially the jaundice which is harmful to neonates. Traditional invasive measurement could cause the pain so that it is difficult to be accepted by people. Therefore, the real-time and non-invasive measurement of bilirubin is of great significance. However, the accuracy of current transcutaneous bilirubinometry(TcB) could be affected by many factors within the human skin, especially hemoglobin. In this talk, it is our aim to investigate how hemoglobin influences bilirubin measurement within the visible range by spectral measurement and Partial Least Squares (PLS) modelling. The results showed that Root Mean Square Error of Prediction(RMSEP) became larger when added hemoglobin into bilirubin solution. Therefore, hemoglobin has influence to non-invasive measurement of bilirubin concentration and it is necessary to reduce and remove this kind of influence by using the effective methods.

8222-39, Poster Session

## Characterization of liquid crystal variable retarder scatter

J. C. Gladish, D. D. Duncan, Portland State Univ. (United States)

Liquid Crystal Variable Retarders (LCVRs) are computer-controlled birefringent devices that contain nanometer-sized birefringent liquid crystals (LCs). The LCs impart retardance effects through a global, uniform orientation change based on a user-defined drive voltage input. These retardance effects, however, are less than ideal due to scattering by the LCs. This scattering ultimately determines the signal-to-noise ratio of a measurement system comprised of these LCVRs. For example, these LCVRS will ultimately be used in a spectral polarimeter for characterization of sub-wavelength structure of biological tissues. In this work, we characterize the LC scattering signature by making voltage-dependent goniometric measurements. From these measurements, we obtain the angular distribution of the light exiting the LCVR as a function of drive voltage and polarization state. Subsequently, the sub-wavelength spatial organization of the LCs is characterized in terms of a voltage-dependent structure factor. This same type of analysis can also be applied to biological tissue. However, the main difference here is that the LC characterization includes a well-controlled experiment in which there is a significant amount of a priori knowledge of the scatterer organization.

8222-40, Poster Session

## Wavelet-based analysis of gastric microcirculation in rats with ulcer bleedings

A. N. Pavlov, M. A. Rodionov, O. V. Semyachkina-Glushkovskaya, V. A. Berdnikova, Y. V. Kuznetsova, I. A. Semyachkin-Glushkovskij, N.G. Chernyshevsky Saratov State Univ. (Russian Federation)

Stress is related to the leading reasons of ulcer formation, however, its pathophysiological mechanisms in this process remain unclear. Abnormalities of microcirculation in a stomach have a clear connection with the stomach ulcer. It is also known that nitric oxide (NO) plays an important role in both, regulation of local microcirculation and in restriction of vascular effects of stress. Based on the given circumstances we assume that studying of NO-dependent mechanisms of regulation of microcirculation in a stomach can represent an important diagnostic marker of development of stress-induced ulcer bleedings. In our previous works, efficiency of wavelet-based analysis of microcirculation was demonstrated. Here, we use a multiscale analysis based on the discrete wavelet-transform to characterize a latent stage of illness formation. Experiments were performed in rats with stress-induced ulcer bleedings (n=37). The control group included healthy animals (n=52). Blockade of NO-synthesis was carried out using L-name (10 mg/kg, per os). Stomach microcirculation was studied by means of laser Doppler flowmetry. Analysis of experimental data was performed in a wide range of scales using different bases of Daubechies wavelets. The clearest distinctions between the analyzed groups of rats were revealed in high-frequency areas of power spectra. L-name provided a decrease of variability of wavelet-coefficients in 2 times ($p<0.05$) for healthy rats and in 4.5 times ($p<0.05$) for ill rats. The latter allowed us to conclude that sensitivity of stomach vessels to NO-level increased in rats with ulcer bleedings. The used approach represents a perspective method for diagnostics of ulcer injury.

8222-41, Poster Session

## Oxidase method for glucose determination using long-period grating waveguide

A. V. Malinin, A. A. Zanishevskaya, N.G. Chernyshevsky Saratov State Univ. (Russian Federation); Y. S. Skibina, N.G. Chernyshevsky Saratov State Univ. (Russian Federation) and LLC SPE Nanostructed Glass Technology (Russian Federation); V. V. Tuchin, N.G. Chernyshevsky Saratov State Univ. (Russian Federation) and Univ. of Oulu (Finland); I. Y. Silohkin, LLC SPE Nanostructed Glass Technology (Russian Federation)

Determination of glucose concentration in different physiological liquids is an aim of a big importance. Concentration of glucose in blood of healthy human does not exceed a value of 5,5 mmol/L in most cases. Therefore, quite sensitive methods have to be used for the purpose of detection of glucose in human blood or urine. Among the optical methods of glucose concentration determination in liquids there are two well known: refractometric and oxidase method. The first one is the most simple and reliable method, since glucose concentration have a significant impact to solution's refractive index. However this technique can be used for analysis of samples with high glucose (at least tenths of a percent). Glucose oxidase method is more precise and using this one can indicate glucose in liquid solution at physiological concentrations. Using photonic crystal fibers (PCFs) with a hollow core as a "smart cuvette" it is possible to combine both refractometric and oxidase methods in one measurement. Among many other unique properties, PCFs provide high sensitivity to the optical parameters of a medium, filling up a hollow core of the fiber, e.g. refractive index and absorption coefficient. In a purpose of making precise analysis of multicomponent liquid solutions, photonic crystal fiber may become a tool of a big efficiency.

8222-42, Poster Session

## VIS-NIR spectrum analysis for distinguishing malignant tumor, benign tumor and normal human breast tissue

Y. Zhang, Britton Chance Ctr. for Biomedical Photonics (China); Y. Yu, Huazhong Univ. of Science and Technology (China); X. Wen, C. Liu, J. Wang, Britton Chance Ctr. for Biomedical Photonics (China); X. Xue, Y. Chen, Huazhong Univ. of Science and Technology (China); V. V. Tuchin, N.G. Chernyshevsky Saratov State Univ. (Russian Federation) and Univ. of Oulu (Finland); D. Zhu, Britton Chance Ctr. for Biomedical Photonics (China)

The high incidence and mortality of breast cancer requires an effective method for early breast diagnosis. Here, a VIS-NIR spectral analysis method was developed to distinguish the malignant tumor, benign tumor, and normal human breast tissue. A commercial spectrophotometer combined with single integrating sphere was used to measure the absorption or scattering spectra of different types of breast tissue in vitro, and new analysis methods were proposed to find the optical markers. Furthermore, the sensitivity, specificity and accuracy for different analysis methods were calculated by comparing results of spectral analysis with the pathological examination. The results showed that the absorption or scattering spectral analysis can distinguish the type of samples to some extent, but the integrating spectral analysis method considering both absorption and scattering can significantly enhance the effectiveness. The integrating analysis method indicates that the normal breast tissue can be distinguished completely from all of samples, the sensitivity, specificity and accuracy are 100%, 87.82% and 87.50% for the benign tumor; and 81.82%, 100% and 87.5% for malignant tumor, respectively. This work is not only used for rapid optical diagnosis of bread diseases in vitro, but very helpful to develop innovative optical diagnosis of breast tumor in vivo.The high incidence and mortality of breast cancer requires an effective method for early breast diagnosis. Here, a VIS-NIR spectral analysis method was developed to distinguish the malignant tumor, benign tumor, and normal human breast tissue. A commercial spectrophotometer combined with single integrating sphere was used to measure the absorption or scattering spectra of different types of breast tissue in vitro, and new analysis methods were proposed to find the optical markers. Furthermore, the sensitivity, specificity and accuracy for different analysis methods were calculated by comparing results of spectral analysis with the pathological examination. The results showed that the absorption or scattering spectral analysis can distinguish the type of samples to some extent, but the integrating spectral analysis method considering both absorption and scattering can significantly enhance the effectiveness. The integrating analysis method indicates that the normal breast tissue can be distinguished completely from all of samples, the sensitivity, specificity and accuracy are 100%, 87.82% and 87.50% for the benign tumor; and 81.82%, 100% and 87.5% for malignant tumor, respectively. This work is not only used for rapid optical diagnosis of bread diseases in vitro, but very helpful to develop innovative optical diagnosis of breast tumor in vivo.

8222-43, Poster Session

## Non-invasive monitoring of vascularization of grafted engineered human oral mucosa

D. E. Wolf, M. Seetamraju, R. S. Gurjar, Radiation Monitoring Devices, Inc. (United States); S. Kuo, A. Fasi, S. E. Feinberg, Univ. of Michigan (United States)

Accident victims and victims of explosive devices often suffer from complex maxillofacial injuries. One of the most difficult areas of the face to reconstruct after an avulsion is the lips. Lip avulsion results in compromised facial esthetics and functions of speech and mastication. Reconstruction of the lips requires a composite tissue of mucosa, skin and muscles. Our (SEF) goal is to graft a human ex vivo produced tissue engineered muco-cutaneous epithelial construct grafted onto a prevascularized muscle flap, such as the latissimus dorsi muscle, to create a prelaminated flap that will be used in lip reconstruction. The process requires assessment of the vascularization of the grafted ex vivo engineered tissue while it is buried underneath the skin and overlying the latissimus dorsi muscle so that it can be harvested at the most optimal time. We describe the design and animal testing of a hand-held surgical probe based upon diffuse correlation spectroscopy to assess vascularization Distinct features that reflect graft vascularization are identified and correlated with vascularization assessed histologically

8222-44, Poster Session

## Monitoring effect of dextran on whole blood sedimentation with a pulsed photoacoustic technique

M. Kinnunen, Univ. of Oulu (Finland)

The capabilities of a pulsed photoacoustic technique to monitor blood sedimentation and aggregation were tested in a cuvette in vitro. Whole blood as well as diluted blood concentrations of 40 %, 60 %, and 80 % were used as samples. In addition, the effect of dextran was investigated with blood concentrations of 40 % and 60 %. The results show that the acoustic pulse delay is a good indicator to follow the sedimentation process. Dextran greatly fastened the sedimentation process.

8222-45, Poster Session

## Laser-induced thermal dynamics and temperature localization phenomenon in tissues and cells doped with nanoshells

A. N. Yakunin, Institute of Precision Mechanics and Control (Russian Federation); Y. A. Avetisyan, Institute of Precision Mechanics and Control (Russian Federation) and N.G. Chernyshevsky Saratov State Univ (Russian Federation); V. V. Tuchin, N.G. Chernyshevsky Saratov State Univ. (Russian Federation) and Institute of Precise Mechanics and Control RAS (Russian Federation) and Univ. of Oulu (Finland)

The localized selective hyperthermia of tissues and cells are associated with the use of functionalized nano-sized particles of different shape, such as nanorods, nanoshells, or nanocages. Their unique properties to be bound to the surface of cancer cells and to absorb selectively laser irradiation are used. Pulsed laser radiation is typically used to achieve optimal thermal effects.

This paper presents and discusses the features of laser-induced thermal dynamics of the gold nanoshells, which is associated with their relatively large size and layered structure. Unlike bulk nanoparticles the existence of a novel thermal phenomenon hoop-shaped narrow hot zone on the nanoshell surface is predicted. It is caused by spatial-temporal inhomogeneities of light field diffracted by a nanoshell and corresponding absorbed laser radiation. The numerical solution of time-dependent heat conduction equation accounting for corresponding spatially inhomogeneous distribution of heating sources is presented.

Effects of the metal layer thickness, laser light intensity, wavelength, pulse duration and duty cycle on the degree of the temperature localization are investigated. Conditions are found under which the process of local hyperthermia is optimal. The significance and perspectives of possible applications of the observed effect in medicine are discussed.

8222-46, Poster Session

## Temporal change of adipose tissue refractive index at photodynamic treatment: in vitro study using OCT

I. Y. Yanina, N.G. Chernyshevsky Saratov State Univ. (Russian Federation); V. V. Tuchin, N.G. Chernyshevsky Saratov State Univ. (Russian Federation) and Institute of Precise Mechanics and Control RAS (Russian Federation) and Univ. of Oulu (Finland)

Temporal changes in the refractive index of adipose tissue at photodynamic treatment were studied with OCT. The 100-150 μm fat tissues slices were used in in vitro experiments. Water-ethanol solutions of indocyanine green (ICG) and brilliant green (BG) of 1 mg/ml and 6 mg/ml concentration, respectively, were used for fat tissue staining. CW laser diode (ACCULASER, 810 nm) and dental diode irradiator Ultra Lume Led 5 (442 and 597 nm) were used for irradiation of tissue slices. Laser irradiation time was 1 min, and the diode lamp 5 min. The studies were conducted at room temperature.

It was found that relative refractive index of the scatterers decreased with time elapsed after treatment that indicated the immersion optical clearing. These data support the hypothesis that photodynamic treatment induces fat cell lipolysis for some period after treatment.

8222-47, Poster Session

## Assessment of transcutaneous vaccine delivery by optical coherence tomography

T. Kamali, A. Doronin, E. Avci, T. Rattanapak, S. Hook, I. Meglinski, Univ. of Otago (New Zealand)

Immunization is one of the most efficient and cost-effective means for the prevention of diseases, but most vaccines have to be administered invasively. A novel strategy of inducing an immune response is topical application of vaccines to intact skin. Apart from being a non-invasive route of drug delivery, skin delivery also offers an advantageous mode of immunization due to the unique ability of skin immune cells to present antigens to the immune system. Topical vaccines penetration through the outermost layers of skin is based on the percutaneous diffusion of lipid-based nano-particles. In the current paper, by applying Optical Coherence Tomography, we investigate transcutaneous delivery of the peptide vaccine into the skin in vivo.

# Conference 8223: Photons Plus Ultrasound: Imaging and Sensing 2012

Sunday-Tuesday 22-24 January 2012
Part of Proceedings of SPIE Vol. 8223 Photons Plus Ultrasound: Imaging and Sensing 2012

8223-01, Session 1

## Fast deep-tissue multispectral optoacoustic tomography (MSOT) for preclinical imaging of cancer and cardiovascular disease

A. Taruttis, D. Razansky, V. Ntziachristos, Technische Univ. München (Germany) and Helmholtz Zentrum München GmbH (Germany)

Optoacoustic imaging has enabled the visualization of rich optical contrast at high resolutions in deep tissue. By adding the wavelength dimension, multispectral optoacoustic tomography (MSOT) allows specific imaging of chromophores of interest, resolving tissue-intrinsic absorbers of light such as hemoglobin in its separate oxygenation states, or exogenous dyes and light-absorbing nanoparticles. Recent developments in the field of small animal MSOT imaging have culminated in a platform of instrumentation and quantitative reconstruction techniques that allows real-time imaging (10 frames/s) of transverse (cross-sectional) slices through living mice at a spatial resolution of ~150 microns. Our MSOT imaging results reveal internal tissue heterogeneity, for example in the case of tumor imaging, where the underlying distribution of fluorescent agents, as well as oxy- and deoxyhemoglobin concentrations, can be resolved in detail, giving a more complete picture of non-uniform tumor parameters than the near-infrared fluorescence methods commonly used in tumor studies. Technical advances in cardiac imaging now allow motion-resolved multispectral measurements of intrinsic contrast and molecular agents in the heart, opening the way for studies of cardiovascular disease. We further demonstrate the noninvasive characterization of the pharmacokinetic profiles of light-absorbing agents in the circulation and multiple organs at rates of 10 samples-per-second in single-wavelength mode and 3.5 samples-per-minute in high-SNR multispectral operation. Overall, our in vivo MSOT findings indicate new possibilities in fast, high resolution imaging of functional and molecular parameters in deep tissue.

8223-02, Session 1

## In vivo imaging of stents using an integrated intravascular ultrasound and photoacoustic imaging catheter

A. B. Karpiouk, B. Wang, J. L. Su, D. E. Yeager, The Univ. of Texas at Austin (United States); J. H. Amirian, R. W. Smalling, The Univ. of Texas Health Science Ctr. at Houston (United States); S. Y. Emelianov, The Univ. of Texas at Austin (United States)

Intravascular photoacoustic (IVPA) imaging has been successfully used to image lipid, macrophages, or stent in ex vivo tissue experiments. In this study, combined intravascular ultrasound (IVUS) and IVPA imaging of a coronary stent deployed inside a rabbit aorta was performed in vivo using integrated IVUS/IVPA imaging catheter. Although IVUS imaging can depict the morphology of the aorta, IVUS alone cannot reliably image stent because of poor acoustic contrast between stent struts and tissue. As previously shown in an ex vivo study, IVPA imaging can reliably image stent due to the strong optical absorption of its metal struts. Here, using integrated IVUS/IVPA imaging catheter, IVUS/IVPA imaging in vivo was achieved. The integrated catheter consists of a commercially available 40-MHz IVUS catheter incorporated with a custom light delivery system. For in vivo imaging, the catheter was inserted into the rabbit aorta through an 8F introducer. IVPA imaging of a commercially available coronary stent deployed into the thoracic aorta of a New Zealand White rabbit was performed without flushing using 5-ns duration laser pulses at 1064 nm wavelength. The delivered laser energy per pulse was 2.5 mJ, and the repetition frequency was 20 Hz. Imaging results indicate that combined IVUS/IVPA imaging can reliably image the struts of the stent and the stent apposition relative to the blood vessel. The advantages and limitations of stent imaging using integrated IVUS/IVPA imaging catheter are analyzed. Further improvements to the integrated IVUS/IVPA imaging catheter and real-time combined IVUS/IVPA imaging system are also discussed.

8223-03, Session 1

## Spectroscopic molecular photoacoustic imaging of sentinel lymph node metastases

G. P. Luke, The Univ. of Texas at Austin (United States); A. Papagiannaros, The Univ. of Texas M.D. Anderson Cancer Ctr. (United States); J. O. Tam, The Univ. of Texas at Austin (United States); K. Sokolov, S. Y. Emelianov, The Univ. of Texas M.D. Anderson Cancer Ctr. (United States)

Identifying the sentinel lymph node (SLN) is necessary for staging and treatment planning for many types of cancer. However, an invasive biopsy is needed to determine if cancer cells are present in the SLN. We have developed a non-invasive method to detect the SLN and cancer cells in the SLN using ultrasound-guided spectroscopic photoacoustic (sPA) imaging and targeted gold nanospheres. An oral cancer model with high likelihood of metastasis was used. Primary (oral cancer) tumors comprised of FaDu cells, which overexpress the epidermal growth factor receptor (EGFR), were grown in the tongues of nude mice for 2 to 4 weeks. Gold nanospheres were conjugated to a monoclonal EGFR antibody and injected in the tongue near the tumor. After 1 day the mice were imaged with sPA and ultrasound imaging at 9 wavelengths ranging from 520 nm to 690 nm with a Vevo 2100 high frequency ultrasound system. The nanospheres which aggregate in the endosomes of EGFR expressing cells exhibit a significantly different spectrum than either free nanospheres or endogenous absorbers in the region (predominantly blood). We developed a novel image processing algorithm that utilizes this unique spectrum to identify the regions of aggregated nanospheres (i.e., regions where micrometastases are present). The findings were confirmed with hyperspectral imaging and histology of the excised lymph nodes. These results suggest that photoacoustic imaging, when coupled with gold nanospheres, can be used to noninvasively detect micrometastases in the SLN.

8223-04, Session 1

## Simultaneous in vivo imaging of melanin and lipofuscin in the retina with multimodal photoacoustic ophthalmoscopy

X. Zhang, The Univ. of Southern California (United States); H. F. Zhang, Northwestern Univ. (United States); S. Jiao, The Univ. of Southern California (United States)

Melanin and lipofuscin are two major pigments in the retinal pigment epithelium (RPE). RPE is a monolayer of pigmented cells located between the choriocapillaris and light-sensitive outer segments of the photoreceptors. Melanin protects RPE cells from oxidative damage. Unfortunately, melanin may lose its protective function with aging. On the other hand, lipofuscin is a byproduct of phagocytosis of the photoreceptor outer segments, which accumulates with aging of the retina. Excessive levels of lipofuscin accumulation could compromise essential RPE functions and contribute to the pathogenesis of age-related macular degeneration (AMD). Hence, in vivo imaging of melanin and lipofuscin can provide important aging information of the retina, which is important for AMD research and clinical diagnosis.

We combined photoacoustic ophthalmoscopy (PAOM) with autofluorescence imaging for simultaneous in vivo imaging of dual molecular contrasts (melanin and lipofuscin) in the retina using a single light source, which provides perfectly registered images of melanin and lipofuscin. We successfully imaged the retina of pigmented and albino rats at different ages. Results showed that the distribution of the AF intensity increased significantly with aging. For the same age the AF intensity of albino rats is stronger than that of pigmented rat. When the rats became older the increase of the AF intensity is obvious especially in the albino rats. The experiments showed the evidence of increased lipofuscin concentration with aging. Possibly due to the protective functions of RPE melanin in the pigmented rats the increase of lipofuscin concentration is not as significant as in the albino rats.

8223-05, Session 1

## Photoacoustic imaging of chemotherapy-induced apoptosis in squamous cell carcinoma

Q. Yang, H. Cui, S. Cai, M. L. Forrest, X. Yang, The Univ. of Kansas (United States)

Anti-cancer drugs typically exert their pharmacological effect on tumors by inducing apoptosis, or programmed cell death, within the cancer cells, with PCD occurring as soon as 4 hours after treatment. Detection of apoptosis in patients could decisively report a response to treatment days or even weeks before MRI, CAT, and ultrasound indicate morphological changes in the tumor. Here we developed a novel near-infrared dye based imaging probe to directly detect apoptosis with high specificity in cancer cells by utilizing a non-invasive photoacoustic imaging technique. Nude mice bearing head and neck tumors received cisplatin chemotherapyand were imaged by PAI after tail vein injection of the contrast agent. In vivo PAI indicated a strong apoptotic response to chemotherapy on the peripheral margins of tumors, whereas untreated controls showed no contrast enhancement by PAI. The apoptotic status of the mouse tumor tissue was verified by immunohistochemical techniques staining for cleaved caspase-3 p11 subunit. The results demonstrated the potential of this imaging probe to guide the evaluation of chemotherapy treatment.

8223-06, Session 1

## In vivo photoacoustic imaging of breast cancer cellular receptors using multiplex contrast agents

C. Bayer, Y. Chen, I. Graf, G. P. Luke, The Univ. of Texas at Austin (United States); K. Sokolov, The Univ. of Texas M.D. Anderson Cancer Ctr. (United States); S. Y. Emelianov, The Univ. of Texas at Austin (United States)

Distinction between cells over-expressing different receptors within a cancerous tumor would provide important information about tumor prognosis and treatment potential. To concurrently and non-invasively image multiple cell receptors in vivo, we have developed an approach based on combined photoacoustic and ultrasound imaging of targeted silica-coated gold nanorods. Silica-coated gold nanorods were synthesized and bioconjugated to monoclonal antibodies to create contrast agents with distinguishable absorption spectra, and therefore different wavelength-dependent photoacoustic signals. Breast cancer xenografts, consisting of two tumors several millimeters apart, were inoculated in the mammary pad of female nude mice with HER2 over-expressing BT-474 cells, and $\alpha v\beta 3$ integrin over-expressing MDA-MB-231 cells. When tumor volumes reached approximately 50mm3, tumors were 3D imaged using a Vevo 2100 small animal ultrasound imaging system combined with a tunable SpectraPhysics OPO laser before and after the injection of the two targeted contrast agents in the 640-930 nm range. The spectroscopic photoacoustic signals were analyzed and fit using a mean squared error analysis to identify the two different cell types. Images of the locations of the targeted contrast agents were overlaid on the ultrasound image of the tumors to positively identify the cell type each tumor contained. Histological analysis was performed to verify the cell receptors which were over-expressed and confirm the photoacoustic imaging results. This work demonstrates in vivo photoacoustic imaging to identify regions within a tumor which are over-expressing receptors of relevance to breast oncology, using tunable gold nanorods with a silica coating for enhanced photoacoustic signal and improved thermal stability.

8223-07, Session 1

## Photoacoustic imaging of functional domains in primary motor cortex in Rhesus Macaques

J. Jo, The Univ. of Kansas (United States); H. Zhang, P. Cheney, The Univ. of Kansas Medical Ctr. (United States); X. Yang, The Univ. of Kansas (United States)

Functional detection in primate brains has particular advantages because of the similarity between non-human primate brain and human brain and the potential for relevance to a wide range of conditions such as stroke and Parkinson's disease. In this research, we used photoacoustic imaging (PAI) technique to detect functional changes in primary motor cortex of awake rhesus monkeys. We observed strong increases in photoacoustic signal amplitude during forelimb movement, which indicates an increase in total hemoglobin concentration resulting from activation of primary motor cortex. Further, with PAI approach, we were able to obtain depth-resolved functional information from primary motor cortex. The results show that PAI can reliably detect primary motor cortex activation associated with forelimb movement in rhesus macaques with a minimal-invasive approach.

8223-08, Session 1

## Photoacoustic and thermoacoustic imaging with a multichannel breast scanner

B. Huang, K. I. Maslov, L. V. Wang, Washington Univ. in St. Louis (United States)

Photoacoustic and thermoacoustic phantom images obtained with a multiple channel breast scanner designed for breast cancer screening are presented here. A Q-switched Nd:YAG laser (PRO-350-10, Newport), combined with a tunable dye laser (NS, Sirah) with a pulse duration of 6.5 ns was used for photoacoustic irradiation, and a 3.0 GHz microwave source with a pulse width of 0.5 μs was used for thermoacoustic tomography. Multiple (>=16) 2.25 MHz single-element unfocused ultrasonic transducers at different heights were scanned simultaneously for a full 360° to obtain a full data set for three-dimensional (3D) tomography. Negative acoustic lens were attached to these unfocused transducers to increase their acceptance angles. An ultrasound receiving system with 64 parallel receive channels (Verasonics Inc.) was used for data acquisition. A filtered backprojection algorithm was used to reconstruct two-dimensional (2D) and 3D images. Different phantoms were imaged to evaluate the performance of the scanner. A lateral resolution of less than 1 mm and an elevational resolution of less than 5 mm were achieved.

The phantom studies demonstrate that this scanner can potentially provide high-resolution, dual modality three-dimensional images and can potentially be used for human breast cancer screening.

8223-09, Session 2

## Two-dimensional optoacoustic imaging combined with B-mode ultrasound: system evaluation for application in breast cancer detection and diagnostics

J. Zalev, B. Clingman, D. Herzog, T. Miller, Seno Medical Instruments, Inc. (United States); P. Otto, The Univ. of Texas Health Science Ctr. at Houston (United States); K. Kist, N. C. Dornbluth, The Univ. of Texas Health Science Ctr. at San Antonio (United States); S. Ermiliov, R. Su, V. Nadvoretsky, A. A. Oraevsky, TomoWave Labs., Inc. (United States)

Two-dimensional opto-acoustic (OA) imaging with a handheld probe operated in backward mode is being developed for diagnostic imaging of breast cancer. The purpose of this study was to evaluate the feasibility of a dual modality opto-acoustic plus ultrasonic system, which provides contrast associated with molecular optical absorption of hemoglobin and oxyhemoglobin in tumor angiogenesis while simultaneously mapping anatomical tissue structures with ultrasonic resolution. The opto-acoustic system uses laser pulses at two different wavelengths in the near-infrared spectral range (757 nm and 1064 nm) to illuminate tissues and detect the resulting ultrasonic signals using a custom-made hand-held probe. Molecular optical contrast provides differentiation between hypoxic blood of breast carcinomas and normally oxygenated blood in benign masses. Noninvasive diagnosis from the two coregistered images is compared with the gold standard of core biopsy. After the system was optimized and calibrated in well-defined phantoms, a pilot clinical study in patients with breast masses suspected for malignancy has been initiated. Capability of the combined system to improve detection and diagnosis of breast tumors will be reported.

8223-10, Session 2

## PAT of the breast using a hemispherical array and rectilinear scanning

R. A. Kruger, R. B. Lam, D. Reinecke, S. P. DelRio, OptoSonics, Inc. (United States)

We have developed a 3D-PAT scanner that acquires photoacoustic data over a hemispherical aperture. Recently, we successfully imaged the vasculature within a human breast in vivo over a volume of 6 x 6 x 3.5 cm. While those imaging results demonstrated submillimeter vessels with good endogenous contrast, the field of view was limited by the angular sensitivity of the transducer elements that we employed. We have developed a data acquisition strategy that will allow us to increase the lateral field of view by employing a rectilinear scan of our hemispherical array during data acquisition.

To demonstrate how the field of view of our PAT scanner can be increased using rectilinear scanning, we imaged an 80-mm diameter “uniformity” phantom, which was fabricated by printing an array of 1-mm dots on a sheet of transparent plastic, and embedding the phantom in a flat-bottomed imaging bowl filled with 6% Liposyn-20%. This phantom was imaged with our current PAT scanner in two ways. First, a single PAT image was acquired with the phantom centered over the light beam. Next, four PAT images of the same phantom were acquired with the phantom shifted off center from the light beam in one of four quadrants. A composite PAT image was formed by shifting and adding the four component images to compensate for the lateral offsets of the phantom from the center of the light beam. In this case the field of view was increased by a factor of two and uniformity throughout the volume was improved.

8223-11, Session 2

## Imaging breast lesions using the Twente Photoacoustic Mammoscope: ongoing clinical experience

M. Heijblom, Univ. Twente (Netherlands) and Medisch Spectrum Twente (Netherlands); D. Piras, W. Xia, J. van Hespen, Univ. Twente (Netherlands); F. van den Engh, J. Klaase, Medisch Spectrum Twente (Netherlands); T. G. van Leeuwen, Univ. Amsterdam (Netherlands) and Univ. Twente (Netherlands); W. Steenbergen, S. Manohar, Univ. Twente (Netherlands)

Current imaging modalities are often not able to detect early stages of breast cancer with high imaging contrast. Visualizing the malignancy-associated increased hemoglobin concentrations might significantly improve early breast cancer diagnosis. Since photoacoustic imaging can visualize hemoglobin in tissue with optical contrast and ultrasound-like resolution, it is potentially an ideal method for breast imaging.

The Twente Photoacoustic Mammoscope (PAM) has been designed specifically for breast imaging. Based on a successful pilot study in 2007, a large clinical study using PAM has been started in December 2010. Within a period of 2 years, up to 100 patients with different kind of breast lesions will be included in this study.

PAM uses a Q-switched Nd:YAG laser to illuminate a region of interest on the breast with 1064 nm pulses. Photoacoustic signals are detected with a 1MHz ultrasound detector array at the opposite side of the breast. Three dimensional data are reconstructed using an acoustic backprojection algorithm. Those reconstructed images are compared with conventional imaging and histopathology.

In the first phase of the study, ten measurements on malignancies and two measurements on cysts have been performed. In the reconstructed volumes of all ten malignancies, a confined high contrast region could be identified at the expected lesion depth. Such confined regions were absent in the photoacoustic images of the cysts. In the current and coming phases of the study the focus will gradually shift towards the less suspicious breast lesions in order to find the photoacoustic markers that best discriminate benign from malignant breast tissue.

8223-12, Session 2

## Optoacoustic angiography of peripheral vasculature for disease detection and staging

M. P. Zamora, S. Ermiliov, A. A. Oraevsky, TomoWave Labs., Inc. (United States)

We developed a new optoacoustic angiography system intended for diagnostic imaging of peripheral vasculature in the human foot. The system incorporates a Q-switched Ti:Saph laser tuned to 765 nm; a submerged 128-channel linear array of ultrasonic transducers combined with optical fibers for illumination and imaging in the backward mode; and custom electronics and software to collect, process, and reconstruct 3D optoacoustic images. The imaging subject, a human foot, is submerged in a temperature-controlled water bath and scanned from beneath. The scanning proceeds as an automated, linear translation, orthogonal to the imaging plane of the probe. To demonstrate capabilities of the optoacoustic system in foot angiography, we present images of the plantar arterial network from 3 volunteers representing healthy, aged, and diabetic conditions. We propose that this system be used for vascular mapping and diagnostics, and specifically, for screening of peripheral arterial disease (PAD).

8223-13, Session 2

## Real-time detection of exhaled human breath using quantum cascade laser based sensor technology

F. K. Tittel, R. Lewicki, L. Dong, Rice Univ. (United States); T. H. Risby, The Johns Hopkins Bloomberg School of Public Health (United States); S. Solga, T. Schwartz, St. Luke's Hospital (United States)

The development and performance of a cw, TE-cooled DFB quantum cascade laser based sensor for quantitative measurements of ammonia (NH3) concentrations present in exhaled breath will be reported. Human breath contains ~ 400 different chemical species, usually at ultra low concentration levels, which can serve as biomarkers for the identification and monitoring of human diseases or wellness states. By monitoring ammonia concentration levels in exhaled breath a fast, non-invasive diagnostic method for treatment of patients with liver and kidney disorders, is feasible.[1]

The NH3 concentration measurements are performed with a 2f wavelength modulation quartz enhanced photoacoustic spectroscopy (QEPAS) technique [1], which is very suitable for real time breath measurements, due to the fast gas exchange inside an ultra compact QEPAS gas cell. A compact Hamamatsu air-cooled high heat load (HHL)packaged CW DFB-QCL is operated at 17.5oC, targeting the NH3 absorption line at 967.35 cm-1 (λ~10.34 μm), with ~ 20 mW of optical power. The sensor architecture includes a reference cell, filled with a mixture of 2000 ppmv NH3 and N2 at 130 Torr, which is used for absorption line-locking. A minimum detection limit ($1\sigma$) for the line locked NH3 sensor is ~ 6 ppbv (with a $1\sigma$; 1 sec time resolution of the control electronics). This NH3 sensor was installed in late 2010 and is being clinically tested at St. Luke's Hospital in Bethlehem, PA.

References

[1] T. Risby and F. K. Tittel, "Current Status of Mid-Infrared Quantum and InterbandCascade Lasers for Clinical Breath Analysis", SPIE Optical Engineering 49 111123-1 - 111123-14 (2010).

8223-14, Session 2

## Noninvasive optoacoustic system for rapid diagnostics and management of circulatory shock

R. O. Esenaliev, I. Y. Petrov, Y. Y. Petrov, M. Kinsky, D. S. Prough, The Univ. of Texas Medical Branch (United States)

Circulatory shock is lethal, if not promptly diagnosed and effectively treated. Typically, circulatory shock resuscitation is guided by blood pressure, heart rate, and mental status, which have poor predictive value. In patients, in whom early goal-directed therapy was applied using central venous oxygenation measurement, a substantial reduction of mortality was reported (from 46.5% to 30%). However, central venous catheterization is invasive, time-consuming and often results in complications. We proposed to use the optoacoustic technique for noninvasive, rapid assessment of central venous oxygenation. In our previous works we demonstrated that the optoacoustic technique can provide measurement of blood oxygenation in veins and arteries due to high contrast and high resolution. In this work we developed a novel, portable optoacoustic system for noninvasive, automatic, real-time, and continuous measurement of central venous oxygenation. We performed clinical tests of the system in human subjects with different central venous oxygenation. Highly-sensitive optoacoustic probes developed in our laboratory and a special algorithm for central venous signal extraction allowed for monitoring of central venous oxygenation with minimal influence of overlying tissue. The data demonstrate that the system provides precise measurement (<2%) of central venous oxygenation continuously and in real time. Both current value of the central venous oxygenation and trend (in absolute values and for specified time intervals) are displayed in the system. In some studies, the system was used with standard clinical ultrasound imaging systems (GE Healthcare and C.R. Bard, Inc.) as well as with a novel hand-held ultrasound imaging system developed by GE.

8223-15, Session 3

## Small-animal whole-body imaging using a photoacoustic full-ring array system

J. Xia, M. R. Chatni, R. Sohn, J. M. Arbeit, M. A. Anastasio, Washington Univ. in St. Louis (United States); Q. Zhu, Univ. of Connecticut (United States); L. V. Wang, Washington Univ. in St. Louis (United States)

We report herein a novel 3D photoacoustic computed tomography (PACT) system for small-animal whole-body imaging. The PACT system, based on a 512-element full-ring transducer array, was cylindrically focused and capable of forming a 2D image in 1.6 seconds. The illumination source was a tunable pulsed laser, and the light could either illuminate directly from the top or be reshaped to illuminate the sample from the side, using a conical lens and an optical condenser. Top illumination was mainly used for functional mouse brain imaging, where the hemodynamics within the entire cerebral cortex were studied. Side illumination provided in vivo anatomical images of an adult mouse. The dark-field illumination technique was utilized by shifting the illumination area away from the focal plane to minimize surface signals. By translating the mouse along the elevational direction, the system provided serial cross-sectional images of the mouse heart, liver, and kidney. With the help of near-infrared dye, the mouse bladder was also clearly imaged. The system was utilized to image mice with kidney tumors and A431 subcutaneous tumors.

A 3D focal-line image reconstruction algorithm was developed for the array. Compared with conventional 2D reconstruction, we found 3D reconstruction improved the elevational resolution by 30% and the signal-to-noise ratio by two times. An iterative reconstruction algorithm was also introduced to mitigate image artifacts due to the heterogeneous acoustic properties of mouse organs.

8223-16, Session 3

## High-resolution imaging of mouse anatomy and molecular probes by means of multispectral optoacoustic tomography (MSOT)

A. Buehler, Technische Univ. München (Germany) and Helmholtz Zentrum München GmbH (Germany); S. Morscher, iThera Medical GmbH (Germany); D. Razansky, Helmholtz Zentrum München GmbH (Germany); V. Ntziachristos, Technische Univ. München (Germany) and Helmholtz Zentrum München GmbH (Germany)

Multispectral optoacoustic tomography (MSOT) is a modern imaging modality which can resolve optical contrast in tissue with high spatial ultrasonic resolution at real-time frame rate. The technique is based on a physical phenomenon called the optoacoustic effect, i.e. the generation of acoustic waves due to thermoelastic expansion caused by absorption of ultra-short optical pulses. Recently, we have developed a small animal scanner comprising a highly-sensitive multi-element ultrasound detector array for parallel signal detection and optimized light delivery to avoid the need of signal averaging in order to enable cross-sectional imaging in real-time. In addition the system features multiwavelength illumination for spectroscopic applications. For imaging, the animal is placed in horizontal position in an animal holder comprising a transparent water-proof membrane to avoid direct contact of the animal with the surrounding coupling medium. Further, the animal holder can be translated to obtain three-dimensional scans of the entire body. Herein, we showcase the systems potential by resolving structural, dynamic and molecular information. Specifically, we will show anatomical whole body scans and resolve dynamic processes capitalizing of the real-time operation mode. Since the volumes considered by MSOT can significantly attenuate light and consequently pronounce structures close to the animal's surface at the expense of deeper inside lying structures, we also present a simple method that correct for the depth dependent light intensity for quasi-quantitative reconstructions. Moreover we present methods to detect extrinsically administered contrast agents (e.g. fluochromes) by multispectral means and apply them on whole body scans to resolve their 3D biodistribution. To validate our reconstructions we will use photographs of cross-sectional post-portem cryoslices of the same mouse.

8223-17, Session 3

## In vivo imaging with GRIN-lens optical resolution photoacoustic micro-endoscopy

P. Hajireza, W. Shi, P. Shao, A. Forbrich, R. J. Zemp, Univ. of Alberta (Canada)

For the first time optical resolution photoacoustic micro-endoscopy (OR-PAME) with the capability of focusing light into tissue is demonstrated. Previously the feasibility of OR-PAME in contact mode for both in vitro and in vivo images was demonstrated by our group. Only highly superficial structures could be visualized with this approach. However, in this paper using a pair of GRIN lenses we refocused light into tissue in order to improve the penetration depth and resolution of our earlier reported system. Using a sensitive transducer, optimized image guide and optical components we significantly improved the signal-to-noise ratio of the system. This real-time imaging system takes advantage of an image guide fiber consisting of 30,000 individual single-mode fibers in a 800-μm-diameter bundle, and a 532-nm fiber laser with repetition-rates as high as 600 KHz. The system offers <7 μm lateral spatial resolution, and frame-rates of several volumetric/C-scans per second. The setup keeps many of the powerful properties of previous top-table OR-PAM systems but adds high flexibility due to the nature of the image guide and micron-scale footprint of the apparatus. We demonstrate imaging of capillary networks in several anatomical locations of live Swiss Webster mice. The GRIN-lens assembly at the image-guide tip is ~2mm in diameter, small enough for many hand-held, intra-cavity, laparascopic, and endoscopic procedures, and could offer an alternative to intra-vital microscopy in cases where optical absorption contrast is desired.

8223-18, Session 3

## Photoacoustic ophthalmology in mouse eyes

W. Song, Northwestern Univ. (United States); S. Jiao, The Univ. of Southern California (United States); H. F. Zhang, Northwestern Univ. (United States)

We developed a multimodal ophthalmic imaging system that combines photoacoustic ophthalmoscopy (PAOM) and spectral-domain optical coherence tomography (SD-OCT), providing comprehensive anatomic and functional information of the retina based on complementary contrast mechanisms. The multimodal imaging capabilities were previously demonstrated in rats and, here, we further demonstrate in mice. Mouse models are widely used in understanding mechanisms and monitoring the therapeutic effects of several ocular diseases. Mouse models offer a uniquely useful combination of affordable cost, rapid reproduction and maturation, well-established platforms for genetic manipulation, and a wide availability of recombinant proteins and antibodies. However, there are several challenges in imaging mouse eyes, which include the very small pupil size, the rapid cataract formation, the large aberration of mouse eye, and the smaller retinal vessels. In this report, we present the simultaneously in vivo imaging of mouse retina using a modified PAOM and SD-OCT for mice. In a pigmented C57BL/6 mouse, retinal vessels and retinal pigment epithelium (RPE) were imaged by PAOM as a result of the strong optical absorption of hemoglobin and melanin. In an albino Swiss Webster mouse, in addition to retinal vessels, the densely-packed choroidal vasculature network was also clearly delineated because of lacking melanin in the RPE. The high-quality images suggested that the integrated PAOM and SD-OCT is a potential invaluable tool to study various ocular diseases in mice models.

8223-19, Session 3

## Optoacoustic 3D visualization of changes in physiological properties of mouse tissues from live to postmortem

R. Su, S. Ermiliov, A. Liopo, V. Nadvoretsky, T. Hernandez, A. A. Oraevsky, TomoWave Labs., Inc. (United States)

In this work we studied the postmortem autolysis of tissues in nude mice as it is manifested via 3D optoacoustic tomography. The studies provide necessary baseline for optoacoustic imaging of the necrotizing tissue, acute or chronic hypoxia, and reperfusion. They also establish a new optoacoustic model of early postmortem conditions of the whole body. In experiments, we used 6-7 week old nude mice with a body mass of 22-26 g. Animals were scanned in a 37C water bath using a three-dimensional optoacoustic tomography system, which was previously shown to provide high contrast maps of vasculature and organs based on changes in the optical absorbance. The scans were performed right before, 1 hour and 1 day after the lethal injection of KCl. Two laser wavelengths (765 nm and 1064 nm) were used to evaluate spectral features of postmortem changes. Our data shows that optoacoustic imaging is well suited for visualization of postmortem tissues. The images revealed changes of optical properties in mouse organs and tissues. Specifically, at 765 nm we observed improvements in contrast of the vascular network and organs after the death of an animal associated with reduced optical scattering, while optoacoustic images at 1064 nm degraded significantly due to lack of oxyhemoglobin.

8223-20, Session 3

## Photoacoustic tomography of the monkey brain using virtual point detectors: experiment

L. Nie, C. Huang, Z. Guo, M. A. Anastasio, L. V. Wang, Washington Univ. in St. Louis (United States)

Human brain imaging can benefit greatly from the development of photoacoustic tomography (PAT). In this report, a PAT system using virtual point ultrasonic transducers was developed and applied to image monkey brains. The virtual point transducers at 2.25 MHz provided a 10 times greater field-of-view (FOV) than finite-aperture unfocused transducers, which enables large animal imaging. Also it supplied an improved signal-to-noise ratio (SNR) and reduced artifacts rather than negative-lens transducers. Our PAT system can achieve high uniformity in resolution (<1 mm) within a FOV of 6 cm diameter, even when the imaging objects are enclosed by a monkey skull. The cerebral cortex of a monkey brain was accurately mapped transcranially, through one or even two skulls ranging from 4 to 8 mm in thickness. The speed of sound and boundary of the skull can be measured by optically focused photoacoustic measurements, a corresponding time-reversal algorithm was employed to correct the imaging distortion induced by the skull aberration. The oxygenation saturation (SO2) in blood phantoms through a monkey skull was also imaged and quantified, with results consistent with measurements by a gas analyzer. Our experimental results demonstrate that PAT can overcome the optical and ultrasound attenuation of a thick skull and can potentially be applied to functional human brain imaging.

8223-21, Session 4

## In vivo functional and molecular photoacoustic imaging of endogenous and exogenous chromophores using quantitative spectroscopic techniques

J. G. Laufer, B. T. Cox, Univ. College London (United Kingdom); B. E. Treeby, The Australian National Univ. (Australia); E. Zhang, P. Beard, Univ. College London (United Kingdom)

The potential of photoacoustic imaging to recover absolute concentrations of tissue chromophores from multiwavelength images is perhaps its most powerful attribute and is crucial to functional and molecular imaging capabilities. An important application is preclinical studies of tumour pathophysiology and the development of novel anti-cancer therapies where photoacoustic imaging would enable, for example, 3D maps of the distribution of the blood oxygenation, targeted exogenous contrast agents or genetically expressed labels to be obtained. This is likely to provide new information about the disease progression and the efficacy of new drugs. To achieve this goal, multiwavelength imaging and spectral unmixing methods are typically required. However, generally applicable and computationally feasible methods for in vivo 3D imaging are still in development. Model-based inversion schemes have shown great promise but in order to enable their widespread use practicable computational techniques are needed. This study will explore methods for quantitative imaging of blood oxygenation or contrast agents in subcutaneous tumours in mice. The main challenge of model-based inversions is their scale, as the large number of variables that make them computationally expensive. Different computational techniques are investigated to develop practicable quantitative methods. For example, to reduce the number of variables, image segmentation methods based on vessel filtering algorithms are employed to parameterise the space into vascular and non-vascular regions. The methods are evaluated on tissue phantom measurements and in vivo multiwavelength images of tumours to establish their suitability for recovering blood oxygenation and the spatial distribution of exogenous contrast agents or genetically expressed biomarkers.

8223-22, Session 4

## Functional photoacoustic microscopy of pH

M. R. Chatni, J. Yao, A. Danielli, C. P. Favazza, K. I. Maslov, L. V. Wang, Washington Univ. in St. Louis (United States)

pH is a tightly regulated indicator of metabolic activity. In mammalian system, imbalance of pH regulation may result from or cause serious illness. Even though the regulation system of pH is very robust, tissue pH can be altered in many diseases, such as cancer, osteoporosis and diabetes mellitus. Traditional high-resolution optical imaging techniques, such as confocal microscopy, routinely image pH in cells and tissues using pH sensitive fluorescent dyes, which change their fluorescence properties with the surrounding pH. Since strong optical scattering in biological tissue blurs images at greater depths, high-resolution pH imaging is limited to penetration depths of less than 100 μm. Here, we report photoacoustic microscopy (PAM) of commercially available pH-sensitive fluorescent dye in tissue phantoms. Using both optical-resolution photoacoustic microscopy (OR-PAM), and acoustic resolution photoacoustic microscopy (AR-PAM), we explored the possibility of recovering the absolute value of pH in tissue phantoms. Using two-wavelength PAM and linear spectral separation, we demonstrate that PAM is capable of recovering absolute pH values up to a depth of 2 mm, greater than possible with other forms of optical microscopy.

8223-23, Session 4

## Photoacoustic correlation spectroscopy for in vivo blood flow speed measurement

S. Chen, Univ. of Michigan (United States); Z. Xie, P. L. Carson, X. Wang, Univ. of Michigan Medical School (United States); L. J. Guo, Univ. of Michigan (United States)

Photoacoustic (PA) imaging has been widely used in structural and functional imaging. Because of its safety, high resolution, and high imaging depth, it has great potential for a variety of medical studies. Recently, there has been a growing interest in PA velocimetry, such as PA Doppler effect, M-mode PA flow imaging, and PA correlation spectroscopy (PACS). Compared with current techniques such as laser Doppler velocimetry and optical/ultrasound particle image velocimetry employing the detection of scattering property of tracer particles to provide imaging contrast, PA methods use the endogenous absorbing properties of red blood cells (RBCs), enabling high sensitivity and high depth because the RBCs can absorb light 100 times more than the background. Noninvasive flow speed measurement of blood speeds provides a unique perspective on disease diagnosis because physiologic activity such as tumor growth and angiogenesis is closely related to blood flow speeds. Previously we proposed PACS, inspired by fluorescence correlation spectroscopy, and shown a proof-of-concept experiment to measure the particle flow speed. In this work, in vivo measurement of blood speeds by PACS is demonstrated. The laser-scanning photoacoustic microscopy system is used, and the probe beam volume is calibrated by flow measurement of dye-doped beads. The measured speeds in vivo are similar to those found in the literatures, which confirm the feasibility of PACS in blood velocimetry. This technique could find applications in disease diagnosis and treatment.

8223-24, Session 4

## Blood flow measurements using a pulsed time correlation photoacoustic Doppler technique: accuracy, resolution, and velocity range

J. Brunker, P. Beard, Univ. College London (United Kingdom)

The feasibility of making spatially resolved measurements of blood flow using pulsed photoacoustic Doppler techniques has been investigated. Doppler time shifts were quantified via cross-correlation of pairs of photoacoustic waveforms generated within various blood-simulating phantoms using pairs of laser light pulses. The photoacoustic waves were detected using an ultrasound transducer. Each flow measurement involved cross-correlation of at least 25 waveform pairs, and the velocity value and resolution were calculated from the mean cross-correlation function. Refinement and characterisation of the experimental setup has enabled greater control over experimental parameters such as the time separation between the laser pulses and the transducer acoustic response. These parameters were evaluated in terms of their effect on the accuracy, resolution and range of measurable velocities. Development of a LabVIEW interface has made it possible to acquire real-time measurements. Flow rates less than 50 mms-1 were measured for various fluids flowing along an optically transparent tube. Several different suspensions of carbon and phenolic resin microspheres of various micron-scale diameters were explored; experiments were also performed with red blood cell suspensions and whole blood. The homogeneity of the suspensions and the diameter of the tubing were varied, and the effect on the quality of the measurements was evaluated. The distinguishing advantage of pulsed rather than continuous-wave excitation is that spatially resolved velocity measurements can be made. This offers the prospect of mapping flow within the microcirculation and thus providing insights into the perfusion of tumours and other pathologies characterised by abnormalities in flow status.

8223-25, Session 4

## Investigations into soft tissue discrimination obtainable in thermoacoustic imaging

O. Ogunlade, P. Brennan, P. Beard, Univ. College London (United Kingdom)

The dielectric contrast mechanism exploited for any microwave based imaging modality is known to be due to the water and ionic content of tissues. When comparing adipose dominated tissues with soft tissues, the amount of contrast can be as much as ten times. However, for two different tissues with high water content, the contrast is often very small, in the region of a few percent. This therefore sets a limit on the tissue discrimination that can be obtained with thermoacoustic imaging.

We show by simulation, the power loss density distribution for three cylindrical phantoms having small dielectric contrast between them. Both the dielectric constant and conductivity of the phantoms are varied and they are illuminated with a uniform plane wave.

We also conduct phantom experiments imaging dielectric tubes of the same cross section, containing tissue mimicking liquids. A resonant cavity perturbation method which is very sensitive to small changes in permittivity is used to measure the permittivity of the phantoms, which are created using solutions of varying concentrations of salt and sugar in water. The thermoacoustic signal amplitudes as well as the reconstructed images are presented giving a quantitative indication of the specificity that can be expected in thermoacoustic imaging of soft tissue.

8223-26, Session 4

## In vivo imaging of inducible tyrosinase gene expression with an ultrasound array-based photoacoustic system

T. Harrison, R. J. Paproski, R. J. Zemp, Univ. of Alberta (Canada)

Tyrosinase, a key enzyme in the production of melanin, has shown promise as a reporter of genetic activity. While green fluorescent protein has been used extensively in this capacity, it is limited in its ability to provide information deep in tissue at a reasonable resolution. As melanin is a strong absorber of light, it is possible to image gene expression using tyrosinase with photoacoustic imaging technologies, resulting in excellent resolutions at multiple-centimeter depths. While our previous work has focused on creating and imaging MCF-7 cells with doxycycline-controlled tyrosinase expression, we have now established the viability of these cells in a murine model. Using an array-based photoacoustic imaging system with 5 MHz center frequency, we capture interleaved ultrasound and photoacoustic images of tyrosinase-expressing MCF-7 tumors both in a tissue mimicking phantom, and in vivo. Images of both the tyrosinase-expressing tumor and a control tumor are presented as both coregistered ultrasound-photoacoustic B-scan images and 3-dimensional photoacoustic volumes created by mechanically scanning the transducer. We find that the tyrosinase-expressing tumor is visible with a signal level 12dB greater than that of the control tumor in vivo. Phantom studies with excised tumors show that the tyrosinase-expressing tumor is visible at depths in excess of 2cm, and have suggested that our imaging system is sensitive to a transfection rate of less than 1%.

8223-27, Session 4

## Temperature mapping using photoacoustic and thermoacoustic tomography

H. Ke, Washington Univ. in St. Louis (United States); T. N. Erpelding, L. Jankovic, Philips Research North America (United States); L. V. Wang, Washington Univ. in St. Louis (United States)

Photoacoustic (PA) and thermoacoustic (TA) effects are based on the generation of acoustic waves after tissues absorb electromagnetic energy. The amplitude of the acoustic signal is related to the temperature of the absorbing target tissue. A combined photoacoustic and thermoacoustic imaging system built around a modified commercial ultrasound scanner was used to obtain an image of the target's temperature, using reconstructed photoacoustic or thermoacoustic images. To demonstrate these techniques, we used photoacoustic imaging to monitor the temperature changes of methylene blue solution buried at a depth of 1.5 cm in chicken breast tissue from 12 to 42 °C. We also used thermoacoustic imaging to monitor the temperature changes of porcine muscle embedded in 2 cm porcine fat from 14 to 28 °C. The results demonstrate that these techniques can provide non-invasive real-time temperature monitoring of embedded objects and tissue.

8223-28, Session 4

## In vivo photoacoustic tomography of total blood flow and Doppler angle

J. Yao, K. I. Maslov, L. V. Wang, Washington Univ. in St. Louis (United States)

As two hallmarks of cancer, angiogenesis and hypermetabolism are closely related to increased blood flow. Volumetric blood flow measurement is important to understanding the tumor microenvironment and developing new means to treat cancer. Current photoacoustic blood flow estimation methods focus on either the axial or transverse component of the flow vector. Here, we propose a method to compute the total flow speed and Doppler angle by combining the axial and transverse flow measurements. Both the components are measured in M-mode. Collating the A-lines side by side yields a 2D matrix. The columns are Hilbert transformed to compare the phases for the computation of the axial flow. The rows are Fourier transformed to quantify the bandwidth for the computation of the transverse flow. From the axial and transverse flow components, the total flow speed and Doppler angle can be derived. The method has been verified by flowing bovine blood in a plastic tube at various speeds from 0 to 7.5 mm/s and at Doppler angles from 30 to 330°. The measurement error for total flow speed was experimentally determined to be less than 0.3 mm/s; for the Doppler angle, it was less than 15°. In addition, the method was tested in vivo on a mouse ear. The advantage of this method is simplicity: No system modification or additional data acquisition is required to use our existing system. We believe that the proposed method has the potential to be used for cancer angiogenesis and hypermetabolism imaging.

8223-29, Session 4

## Hemoglobin oxygen saturation measurement in rat retinal vessels by multiwavelength laser-scanning photoacoustic ophthalmoscopy

Q. Wei, Northwestern Univ. (United States); S. Jiao, The Univ. of Southern California (United States); H. F. Zhang, Northwestern Univ. (United States)

Hemoglobin oxygen saturation (sO2) in rat retinal vessels was measured by a multimodal system that combines laser-scanning photoacoustic ophthalmoscopy (PAOM) and spectrum-domain optical coherence tomography (SD-OCT). Output of a tunable dye laser at three optical wavelengths (570 nm, 578 nm, and 588 nm) were used as the irradiate source for PAOM. At each optical wavelength, a total 32 B-scan images of retinal vessels along a circular path around the optical disc were averaged at an A-line rate of 6 kHz. The sO2 value of each vessel was then calculated by averaged photoacoustic vessel intensity acquired under all three optical wavelengths.

In the reported experiment, the sO2 values of 17 retinal vessels, including 9 arteries and 8 veins, were measured non-invasively using multi-wavelength PAOM and the averaged sO2 values in artery and vein were 83±6% and 70±6%, respectively. To verify the measured sO2 results qualitatively, Doppler phase shifts of each vessel were further measured by SD-OCT, which showed the blood flow directions in all the 17 vessels. The veins and arteries were distinguished by the imaged blood flow direction and agreed with the PAOM results well. The total metabolic rate of oxygen of the retina may be calculated in the future if Doppler angle of each vessel can be resolved and the absolute blood can be measured.

8223-81, Poster Session

## Compact fiber-Bragg-grating detector for high-sensitivity ultrasound measurements

A. Rosenthal, D. Razansky, V. Ntziachristos, Helmholtz Zentrum München GmbH (Germany)

Piezoelectric sensors constitute the method of choice in most applications of optoacoustic imaging. One of the main drawbacks of these sensors is their sensitivity, which is proportional to detection area. As a result, when small detectors are required the sensitivity offered by piezoelectric technology may not be sufficient.

In this work we demonstrate a sensitive compact hydrophone based on a pi-phase shifted fiber Bragg grating. The grating exhibits a sharp resonance, whose central wavelength is pressure sensitive. The resonance is monitored by a continuous-wave laser to measure ultrasound-induced pressure variations within the grating. In contrast to standard fiber sensors, the high finesse of the resonance - which is the reason for the sensor's high sensitivity - is not associated with a long propagation length. Light localization around the phase shift reduces the effective size of the sensor below that of the grating and is scaled inversely with the resonance spectral width. In our system, an effective sensor length of 270μm, pressure sensitivity of 440 Pa, and effective bandwidth of 10MHz were achieved. This performance makes our design attractive for medical imaging applications, such as optoacoustic tomography, in which compact, sensitive, and wideband acoustic detectors are required.

8223-82, Poster Session

## The study of quantitative optical absorption imaging by using Monte Carlo simulation of combined photoacoustic tomography and ultrasound-modulated optical tomography

C. Kim, Y. Li, Univ. at Buffalo (United States); L. V. Wang, Washington Univ. in St. Louis (United States)

In this poster presentation, we show the potential ability of quantitative mapping of optical absorption coefficients by using a Monte Carlo (MC) simulation of combined photoacoustic and ultrasound-modulated optical tomography. W. Steenbergen has recently reported MC simulation results for this purpose. By labeling all photons in the ultrasound zone with a simple Doppler shift, the author measured the amount of tagged photons, and these values were used to compensate for the fluence variation in the initial PA stress distribution. Our approach, based on the temporal correlation transfer equation (CTE), calculated the three-dimensional distribution of the power spectra of light without and with a focused ultrasound field in an optically scattering medium with a heterogeneous optical distribution. Our simulation results prove that the fluence map obtained from UOT accurately compensates for the optical fluence on initial PA pressure distributions and permits recovery of relative optical absorption coefficients. Further, although the optical heterogeneities of the sample varied, the optical absorption coefficients from a target, recovered by using the ratio of between PAT and UOT signals, remained constant, whereas PA amplitudes fluctuated. Practically speaking, these two ultrasound-aided optical tomography systems can easily be integrated.

8223-83, Poster Session

## A method for simultaneously estimating acoustic and optical properties of heterogeneous absorber using focused photoacoustic imaging based on Hilbert transform

Z. Li, Z. Zeng, H. Li, Fujian Normal Univ. (China)

It is known that there exist significant differences in acoustic and optical properties between normal and tumor tissues. In this paper, we report on experimental demonstration of focused photoacoustic (PA) imaging for simultaneous recovery of the acoustic and optical properties of strong absorber in homogeneous media. Some experiments based on focused PA imaging were developed. We used ink to simulate the strong absorber in the sample. In this PA system, a pulse light from an Nd:YAG laser at the wavelength of 830 nm, 6-ns pulse-width is used at a repetition rate of 10 Hz. A wideband focused ultrasonic transducer is used to receive the photoacoustic signals. The central frequency of the ultrasonic transducer is 3.5 MHz. The transducer is connected to a pulse amplifier. After a pre-amplifier, the detected signals are recorded and averaged 512 times by an oscilloscope and then collected by a personal computer. We used the Hilbert transform (HT) of PA signal to extract the acoustic and optical properties of absorber. The results demonstrate that the HT-based PA signal occurs at the edge of sample. And the average acoustic velocity could be obtained by the size dividing the traveling time. In addition, the absorption coefficient of heterogeneous absorber could be reconstructed by the intensity of the HT-based PA signal at the edge of sample based on the theoretical analysis. Thus, the results show that the HT-based PA signals are quantitative in terms of the location, acoustic and optical properties of the heterogeneities.

8223-84, Poster Session

## 3D digital acousto-optical coherence tomography

E. Benoit, S. Farahi, E. Bossy, F. Ramaz, Ecole Supérieure de Physique et de Chimie Industrielles (France)

Acousto-optic tomography is a technique that couples ultrasound and light in order to measure local optical properties through thick and highly scattering media, e.g. human breast tissues. Thanks to the acousto-optic effect, we can get the optical contrast information given by light and get the spatial localization from the ultrasound longitudinal waves.

The accuracy of localization is typically 2 mm perpendicularly to the ultrasound propagation axis, which corresponds to the diameter of the ultrasound focus spot. In order to get the same millimetre resolution along the ultrasound direction of propagation, we implement the Acousto-Optical Coherence Tomography (AOCT) technique. AOCT consists in applying a stochastic phase modulation on light and ultrasound. By this way, we get a short coherence length ultrasound source that explores the sample. A time delay between ultrasound and light modulation enables to select the active zone along the ultrasound column, where the acousto-optic interferometric signal remains coherent in time.

The detection of the ultrasound modulated light is performed with an interferometric setup. We use off-axis digital holography on a high speed CMOS camera. This technique enables us to make a tunable spatio-temporal filter with a high signal to noise ratio.

Moreover, this system works around 780 nm which is an appropriate wavelength for biological imaging since it is where light has its maximum penetrating depth in tissues.

We image in 3 dimensions optically contrasted objects embedded within several-centimetre thick media (phantoms or chicken breast). Our technique represents an interesting approach to multimodal imaging for breast cancer detection.

8223-85, Poster Session

## Photoacoustic spectral characterization of liquid perfluorocarbon droplets

E. Strohm, M. Rui, Ryerson Univ. (Canada); I. Gorelikov, N. Matsuura, Sunnybrook Health Sciences Ctr. (Canada); M. C. Kolios, Ryerson Univ. (Canada)

Liquid perfluorocarbon droplets are currently being investigated as contrast agents and for cancer therapy. Droplets loaded with optical absorbing nanoparticles can be used as photoacoustic contrast agents to enhance vessel and tumour visualization. Alternatively, droplets can be vaporized to gas bubbles under laser irradiation for cancer therapy by vessel occlusion and targeted drug delivery.

Micron-sized perfluoropentane droplets containing 10 nm diameter silica-coated lead sulphide nanoparticles were characterized using a scanning photoacoustic/acoustic microscope. Individual droplets were measured using pulse echo ultrasound and photoacoustics under optical guidance. For ultrasound measurements, droplets were probed with 200, 400 and 750 MHz transducers. For photoacoustic measurements, droplets were irradiated with 532 and 1064 nm laser pulses focused to a 4-10 µm spot size with an energy up to 450 nJ per pulse.

The photoacoustic signal from droplets was compared to theory where some discrepancies were found in both the time and frequency domain. The sound velocity of the perfluorocarbon liquid was calculated using a modified insertion method and was found to increase by a 2-5% over the frequencies used. Better agreement was found when accounting for sound dispersion. The measured photoacoustic signal increased with increasing laser energy, until droplet vaporization occurred (200-450 nJ). The large range could be due to variations of the nanoparticle concentration within the droplets.

This research demonstrates a method to selectively image or vaporize droplets based on the laser energy or wavelength. In addition, the droplet size in a region can be estimated by comparing the signal to photoacoustic theory.

8223-86, Poster Session

## Photoacoustic microscopy of myocardial sheet architecture in unfixed and unstained mammalian hearts

C. Zhang, Y. Cheng, D. Yao, Washington Univ. in St. Louis (United States); S. A. Wickline, Washington Univ. School of Medicine in St. Louis (United States); L. V. Wang, Washington Univ. in St. Louis (United States)

The laminar myocardial sheet architecture and its dynamic change play a key role in myocardial wall thickening. Histology, confocal optical microscopy (COM), and diffusion tensor MRI (DTI) have been used to unveil the structures and functions of the myocardial sheets. However, histology and COM require fixation, sectioning, and staining processes, which dehydrate and deform the sheet architecture. Although DTI can delineate sheet architecture nondestructively in viable hearts, it cannot provide cellular-level resolution. Here we show that photoacoustic microscopy (PAM), with high resolution (~1 um) and label-free detection, is appropriate for imaging 3D myocardial architecture. The endogenous photoacoustic contrast of the saline-perfused blood-free heart originated mainly from lipofuscin and melanin in myocytes, which was demonstrated by photoacoustic spectroscopy of heart samples within the wavelength range of 440 nm to 560 nm. PAM of an unstained dog heart section was shown to have a higher image contrast than either wide field optical microscopy or phase contrast optical microscopy. Perfused half-split mouse hearts were also imaged by PAM in vitro without fixation, dehydration, nor staining. The laminar myocardial sheet architecture was clearly visualized within a 0.15 mm depth range. Two populations of oppositely signed sheet angles were observed, and the distance between adjacent sheets was quantified to be ~5 um in undehydrated hearts for the first time to the best of our knowledge. In summary, PAM reveals myocardial architectures with endogenous contrast but without unwanted dehydration artifacts, thereby promising to access dynamic changes of myocardial architectures in ex vivo perfused-viable hearts.

8223-87, Poster Session

## Photoacoustic sensing of exogeneously delivered contrast agents using high-frequency ultrasonic transducers

P. V. Subochev, R. V. Belyaev, A. R. Katichev, A. N. Morozov, A. G. Orlova, I. V. Turchin, Institute of Applied Physics (Russian Federation)

This work is devoted to the development of photoacoustic system tuned by high frequency acoustic transducers for high resolution imaging of exogenously delivered contrast agents in small animals. LOTIS LT-2214-PC tunable laser was used in preliminary experiments which finite laser pulse length 18 ns corresponds to 28 μm spatial resolution blurriness or 55MHz maximum ultrasonic transducer frequency limit. To provide high spatial resolution at 50MHz ultrasonic frequency, impulse responses of two LiNbO3-based 50MHz and PVDF-based 30MHz transducers were analyzed and compared to impulse responses of V383, XMS-310, and V316-N Panametrics transducers given at paper [G. Ku , X. Wang, G. Stoica, and L.V. Wang, Phys. Med Biol., 2004, 49, 1329-1338]. Preliminary experiments allow to conclude, that due to better opportunities on high mechanical damping PVDF-based transducer has the greater potential on high spatial resolution than LiNbO3-based transducer or common commercial Panametrics transducers, while it has comparable with LiNbO3-based transducer maximum diagnostic depth. Therefore, at the moment we find PVDF to be the better transducer base material for photoacoustic imaging applications that require high resolution. A direct comparison of diagnostic depth versus spatial resolution for 30MHz V-series Panametrics transducer with LiNbO3 and PVDF transducers is planned for 2011. Based on the developed photoacoustic system a number of model experiments on photoacoustic sensing of fluorescent proteins and gold nanoparticles is planned.

8223-88, Poster Session

## Developing a stochastic model for acousto-optic tissue imaging

S. G. Resink, W. Steenbergen, MIRA Institute for Biomedical Technology and Technical Medicine (Netherlands)

Direct optical measurements in scattering media offer poor resolution due to the high scattering. Ultrasound is scattered orders of magnitude less in tissue compared with light and therefore offers great resolution. Photoacoustics and acousto-optics are both relatively new hybrid techniques that enable measurements of optical optical properties in scattering media by combining ultrasound and light. Quantified measurements of the fluence and absorption coefficient however are desired and can not be performed directly by these techniques. A new approach to achieve this goal is to combine both hybrid techniques. By combining photoacoustic and acousto-optic measurements there is sufficient information to calculate the absorption coefficient and fluence at the ultrasound focus used for the acousto-optics. The theory requires knowledge on the interaction of light and sound inside tissue, so the size of the so called tagging volume can be determined. This tagging volume is defined by the size and shape of the ultrasound focus used in the acousto-optic measurements. A stochastic model for acousto-optics is under development to gain more insight in the interaction between light and sound. By separating light transport and the interactions of light and sound and writing this interaction as a probability density function it is possible to find the effective geometrical properties of the tagging volumeMultiple interaction mechanisms of sound and light are added to this model. This model will be validated in Monte-Carlo simulations and in a later stage in phantoms and biological tissue.

8223-89, Poster Session

## Measuring tissue blood flow using ultrasound modulated diffused light: a preclinical study

I. Breskin, A. Ron, N. Racheli, C. Metzger, Z. Silman, M. Kamar, A. Nini, M. Balberg, R. Shechter, Ornim Medical Ltd. (Israel)

Monitoring Tissue Blood Flow is vital during states of decreased or increased flow. However, there are currently no non-invasive devices that measure microcirculatory blood flow in tissue continuously. The CerOx monitor (Ornim Medical Ltd.) is a novel device that uses Ultrasound Modulation of Diffused Light to perform non-invasive monitoring of blood flow in the microvascular level underneath its sensor.

We demonstrate the ability of the CerOx to monitor tissue blood flow on anesthetized swine model during different manipulations. Increased Blood flow manipulations were performed by systemic Epinephrine injection. Decreased flow manipulations were performed by arterial occlusion. Measurements were done on the calf muscle of the animal and compared with Laser Doppler (LD) (Moor Instruments. UK).

Results from 6 animals demonstrate a good response of the CerOx readings to all of the flow manipulations. Receiver Operator Curves (ROC) analysis was performed as a test for the discriminative power of the measurements to accurately identify these manipulations. For detecting decrease in flow during arterial occlusion, or increase in flow following Epinephrine injection, CerOx flow readings provide a ROC curve with an area under the curve (AUC) of 0.95. The results demonstrate a high sensitivity for measuring the relative increase or decrease of blood flow during the manipulations. In addition, results show a significant correlation with Laser Doppler reading from a proximal location, with correlation of $r = 0.81$, $p<0.001$.

8223-90, Poster Session

## Drug delivery monitoring by photoacoustic tomography with an ICG encapsulated double emulsion

X. Wang, J. Rajian, M. Fabiilli, J. B. Fowlkes, P. L. Carson, Univ. of Michigan Medical School (United States)

The absorption spectrum of indocyanine green (ICG), a nontoxic dye used for medical diagnostics, depends upon its concentration as well as the nature of its environment, i.e., the solvent medium into which it is dissolved. We have successfully encapsulated ICG in an ultrasound-triggerable perfluorocarbon double emulsion (W1/PFC/W2) that prevents ICG from binding with plasma proteins. The emulsion was found to be stable in both plasma and whole canine blood, thus hindering the ability of ICG - contained in the W1 phase - to bind with plasma proteins. Also, it was found that the photoacoustic spectrum of the free (non-emulsified) or emulsified ICG in blood was a linear combination of the spectra of the individual respective components. Photoacoustic measurements on a point target as well as 2-D images of phantom vessels revealed that the photoacoustic spectrum changes significantly in blood when the ICG-loaded emulsion undergoes acoustic droplet vaporization (ADV). This ADV-induced spectral change of the ICG-emulsion in blood and the linearity of the spectral dependence suggest that the amount of ICG released is proportional to the degree of the spectral change. Since the spectral change can be used to measure the amount of ICG released, the same technique can be used to monitor drug release in targeted treatments, such as cancer therapy, where the desired drug is solubilized in the W1 phase of the emulsion. Moreover, the spectral change due to ADV might be exploited as contrast from a focally targeted vascular bed in differential photoacoustic imaging to obtain a background-free photoacoustic image.

8223-91, Poster Session

## An optical resolution photoacoustic dermoscope for port-wine stain imaging

B. Rao, Washington Univ. in St. Louis (United States); W. Jia, J. S. Nelson, Beckman Laser Institute and Medical Clinic (United States); L. V. Wang, Washington Univ. in St. Louis (United States)

One long-standing problem in port-wine stain (PWS) treatment is the “blindness” of the current laser treatment procedure: It is difficult to image PWS vasculature transcutaneously. The major technical barriers of imaging resolution and imaging contrast limit the usefulness of many imaging modalities in PWS clinics. Previously published photoacoustic PWS imaging approaches suffer from low resolution and low imaging speed. Due to the strong background signal of surrounding tissues, optical coherence tomography (OCT), which is based on optical scattering contrast, cannot identify small PWS capillaries. When Doppler OCT (DOCT) and optical microangiography (OMAG) are used to image PWS lesions, they suffer from the inherent motion artifacts of surrounding bulk tissues and from reduced contrast due to fringe washout. Based on the recently invented optical resolution photoacoustic microscopy (OR-PAM), an innovative prototype PWS imaging dermoscope has been developed to overcome the above limitations. The miniature, confocal, fiber optics based OR-PAM imaging probe (27 grams), translated by a fast scanning voice-coil stage, allows simultaneous real time PWS imaging (20 frames/second) at a high signal-to-noise ratio. The combination represents the first step in a continuum of research that is expected to lead to solving the long-standing PWS clinical problem.

8223-92, Poster Session

## Photoacoustic speckles: boundary dependence and experimental validation

Z. Guo, Z. Xu, L. V. Wang, Washington Univ. in St. Louis (United States)

Photoacoustic tomography (PAT) suppresses speckles by prominent boundary buildups. We theoretically study the dependence of PAT speckles on the boundary roughness, which is quantified by the root-mean-squared (RMS) value and the correlation length of the height. The speckle visibility and the correlation coefficient between the reconstructed and actual boundaries are quantified as a function of the boundary roughness. The statistics of PAT speckles is studied experimentally.

8223-93, Poster Session

## Photoacoustic molecular imaging on ferritin as a reporter gene

S. Ha, A. Carson, Univ. of Pittsburgh Medical Ctr. (United States); K. Kim, Univ. of Pittsburgh Medical Ctr. (United States) and Univ. of Pittsburgh (United States)

Photoacoustic (PA) molecular imaging (PMI) of ferritin expressed in human melanoma cells (SK-24) was performed in-vitro. Ferritin is a ubiquitously expressed iron-storage protein, which can be detected by PA imaging and utilized as a reporter gene. To overexpress ferritin, SK-24 cells were cotransfected with plasmid expressing ferritin (pCDNA3.1-ferritin) and plasmid expressing enhanced green fluorescent protein (pEGFP-C1) using LipofectamineTM 2000. Nontransfected SK-24 cells served as a negative control. Flourescent imaging of EGFP confirmed transfection and transgene expression in cotransfected cells. To detect iron accumulation in SK-24 cells, a focused high frequency ultrasonic transducer (60 MHz, f/1.5), synchronized to a pulsed laser (<20mJ/cm2), was used to scan the PA signal from 680 nm to 950 nm (in 10 nm increments) from the surface of the 6-well culturing plate. PA signal intensity from ferritin transfected cells was close to equal that of nontransfected cells at wavelengths less than 850 nm, but more than 4dB higher than nontransfected cells at 850 ~ 950 nm. Flourescent microscopy also indicates significant accumulation of iron in ferritin transfected SK-24, with no significant iron accumulation observed in the non-transduced control cells. PA spectral analysis at 680 ~ 950 nm clearly detected increased iron levels, and these levels were associated with transfection of ferritin plasmid. As such, the feasibility of ferritin as a reporter gene for PMI has been demonstrated in-vitro.

8223-94, Poster Session

## Photoacoustic tomography of the monkey brain using virtual point detectors: theory

C. Huang, R. W. Schoonover, L. Nie, Z. Guo, L. V. Wang, M. A. Anastasio, Washington Univ. in St. Louis (United States)

Because of its portability, the information it can yield, which is complementary to that produced by existing brain imaging methods, its safety, and low cost, photoacoustic tomography (PAT) brain imaging deserves great attention and investigation. A major challenge in PAT brain imaging is to compensate for the distortion introduced into the measurement data by the skull. By use of information regarding the skull morphology and composition obtained from adjunct X-ray CT image data, we developed a patient-specific imaging model that accounts for the relevant wave physics and other physical factors related to the measurement process. A frequency power law describes acoustic attenuation in the skull. To reconstruct cross-sectional brain images, we employed a time-reversal-based reconstruction algorithm to invert the developed image model. The developed image reconstruction methodology has been systematically evaluated in computer-simulation studies and experimental studies involving phantoms and monkey heads. The results establish that our reconstruction methodology can effectively compensate for skull-induced acoustic aberration and attenuation, which represents a significant step toward human PAT brain imaging.

8223-95, Poster Session

## Compensation of shear waves in photoacoustic tomography with layered acoustic media

R. W. Schoonover, M. A. Anastasio, Washington Univ. in St. Louis (United States)

Almost all known analytic reconstruction algorithms for photoacoustic computed tomography (PCT) are based on the assumption that the optical absorber is embedded in an acoustically homogeneous and fluid background. Variations in the speed of sound, density, and the conversion of longitudinal and shear waves at fluid-solid interfaces are not accounted for in such reconstruction algorithms.

In this work, we develop a PCT reconstruction formula for applications in which a planar detection surface is employed and the to-be-imaged optical absorber is embedded in a planar-layered acoustic medium in which at least one of the layers is assumed to be an elastic solid. Elastic solids support a second type of ultrasonic waves - shear waves - whose effects have not yet been accounted for in PCT imaging algorithms. The modeling of solids in PCT is an important step towards quantitative transcranial PCT.

The reconstruction formula is exact in a mathematical sense and accounts for multiple reflections of the induced photoacoustic wavefield between the layers of the medium, shear waves in the solid layers, and absorptive and dispersive effects in the layers. The reconstruction formula establishes a mapping that relates the 3D Fourier components of the sought-after optical energy density distribution to the 2D Fourier transform of the measured pressure data that correspond to propagating wave modes. Computer-simulation studies are conducted to demonstrate and investigate the proposed method.

8223-96, Poster Session

## Ultrasound-modulated optical tomography using slow light in spectral-hole burning materials

H. Zhang, Harvard Univ. (United States); M. Sabooni, L. Rippe, S. Kröll, Lund Univ. (Sweden); L. V. Wang, Washington Univ. in St. Louis (United States); P. R. Hemmer, Texas A&M Univ. (United States)

Ultrasound-modulated optical tomography is a hybrid non-invasive imaging modality which combines the advantages of ultrasound resolution and optical contrast. To achieve reasonable signal to noise ratio (SNR) ultrasound 'tagged' photons (signal) must be separated from 'un-tagged' photons (background noise) to very high degree. So far spectral hole burning (SHB) in rare earth crystals has demonstrated the most encouraging preliminary results, but residual leakage of untagged photons is still a problem. Slow light based on SHB can provide an addition temporal degree of freedom that enhances the spectral filtering sufficient to permit short ultrasound pulse detection in deep tissue phantoms and real chicken breast tissue. This might open an opportunity for the development of a clinically applicable deep tissue high resolution optical imaging modality.

8223-97, Poster Session

## Imaging the ultrasound field and shear-wave propagation using acousto-optic laser speckle contrast analysis (AO-LASCA)

L. Song, Y. Cheng, R. Li, M. Tang, D. S. Elson, Imperial College London (United Kingdom)

In this paper, we present a new method to image the ultrasound field in a single shot and to image the propagation of the shear wave based on acousto-optic laser speckle contrast analysis. For imaging the acoustic field a laser beam (532 nm) was transmitted through an optically transparent phantom (2% agar) and was modulated by a continuous focused ultrasound beam (5 MHz, 200 mVpp). The output light was imaged onto a CCD camera such that the field of view contained the central propagation axis of the ultrasound. For capturing the propagation of the shear wave, a 10% intralipid suspension was added to the ultrasound modulated part of the agar phantom as an acoustic and optical scatterer and a shear wave was generated when a 2 ms acoustic burst was applied to the phantom. The CCD camera acquired a sequence of speckle images during and after the burst at a delay time increment of 1 ms. The calculated speckle contrast image showed characteristic features in the near field, far field and central region of the ultrasound. The pressure profile fits with that measured with a hydrophone. The sequence of contrast images illustrates the propagation of the shear wave. This method is fast and may be used to study the propagation of the shear wave and the effects of variations in mechanical properties. This signal is important for understanding how ultrasound mediated optical tomography signals vary in the presence of shear waves and may be used to guide experiments on biological tissue.

8223-98, Poster Session

## Passive acoustic radiometer for non-invasive monitoring of internal temperature during local laser hyperthermia

P. V. Subochev, Institute of Applied Physics (Russian Federation); M. A. Sirotkina, Nizhny Novgorod State Medical Academy (Russian Federation); V. V. Klin'shov, A. D. Mansfel'd, Institute of Applied Physics (Russian Federation)

Internal thermodynamic temperature of the human body is an important parameter for measurement and monitoring. By measurements of internal temperature one can draw the conclusions about various physiological processes, provide monitoring of inflammatory diseases, etc. Measurements of the internal temperature are also required during certain therapeutic procedures based on local heating of biological tissues (hyperthermia, HIFU-therapy).

Among the existing technics, passive and non-invasive methods of temperature sensing are of most interest for medicine since such methods are not based on irradiation of the body by external fields and do not require surgical intervention. One of such methods is passive acoustic thermometry which is based on the broadband registration of the intrinsic thermal acoustic radiation of investigated tissue.

Intensity of thermal acoustic radiation of each individual deep-sited area of a tissue is proportional to the temperature of this area and has Planck spectrum (in analogy with the electromagnetic radiation). However, while generated radiation travels through the tissue with frequency-dependent coefficient of acoustic absorption (in soft biological tissues $y(f)=y0*f$, where f is frequency) the initial spectrum becomes distorted with decreased intensity of high-frequency components. Therefore, having known the acoustic absorption coefficient in tissue and providing broadband measurements of passive acoustic radiation on its surface it is possible to reconstruct internal temperature of the tissue passively and noninvasively.

We developed passive acoustic radiometer that implements the described principle of passive multi-frequency acoustic thermometry real time. The results of internal temperature measurements in laboratory animals during their laser hyperthermia in vivo will be presented.

8223-99, Poster Session

## Conjugate gradient preconditioning methods with symmetric algebraic reconstruction technique in photoacoustic imaging

X. Liu, Northeastern Univ. (China); J. Tian, D. Han, G. Li, Institute of Automation (China); W. Guo, Beijing Univ. of Technology (China); C. Qin, X. Ma, X. Yang, Institute of Automation (China)

Photoacoustic imaging (PAI) is a fast-developing biomedical imaging technology suitable for noninvasive structural and functional imaging. Image reconstruction in PAI requires the solution of an inverse source problem, where the source represents the optical energy absorption distribution in the object. PAI in spherical or circular geometry gives good image resolution yet is slow in signal acquisition and image formation. Reducing the number of detection angles can ameliorate such issues. Besides, it is almost impossible to cover the entire surface of tissue. This will restrict it in the medical application. To resolve such limiting factors, in this thesis, a preconditioned conjugate gradient method is applied to an Algebraic Reconstruction Technique (PCGART) method for reconstructing the absorption distribution. A computer simulated has been used for the evaluation. Under the common assumption, a zero-mean Gaussian noise is added to the projection signals. This algorithm works well in rectification of the measurement and converges quickly onto an accurate estimate of the distribution of absolute absorption. It not only runs much faster than the ART algorithm, but also shows stronger robustness in that it provides better image quality with detection data from limited view angles. We observed that diagonal precondition offer some improvement in convergence rate for image reconstruction, and preconditioning with relaxation parameter greater than zero makes the method faster than that equal zero. In addition, a physical experiment that will be done with our experiment equipment system further demonstrates the potential of the proposed algorithm in practical applications.

8223-100, Poster Session

## Ultrafast ultrasound and photoacoustic co-registered imaging system based on FPGA parallel processing

U. S. Alqasemi, H. Li, A. Aguirre, Q. Zhu, Univ. of Connecticut (United States)

Co-registered photoacoustic tomography (PAT) and ultrasound (US) images map tumor vasculature distributions superimposed on lesion anatomic landmarks provided by ultrasound. Both tumor vasculature and tumor morphology are important for diagnosis of cancers and assessment of treatment response. Last year, we have developed a co-registered near real-time PAT/US 64-channel system with up to 1 frame per second (fps) ultrasound pulse-echo imaging, 5 fps photoacoustic imaging, and 0.5 fps co-registered imaging. This year, we have dramatically improved the data acquisition and processing speed such that it acquires data from 128 channels and displays up to 15 fps co-registered ultrasound and photoacoustic images limited by the laser pulse repetition rate. The system architecture is original and unique, and it provides the ability of acquiring the RF channel data for both modalities and the flexibility of adjusting every parameter involved in the imaging process.

The system frontend consists of combined commercial and customized circuits of eight 16 channel modules. Each 16-channel module consists of two commercial 8-channel receiving circuitry boards and one FPGA board from Analog Devices. The receiving board contains an IC that combines 8-channel low-noise amplifiers, variable-gain amplifiers, anti-aliasing filters, and ADCs in a single chip with sampling frequency of 40MHz. The FPGA board captures the LVDS Double Data Rate (DDR) digital output of the receiving board and performs data conditioning and sub-beamforming. A customized 16-channel transmission circuitry is connected to the two receiving boards and controlled by the module FPGA for US pulse-echo (PE) mode data acquisition. An advanced FPGA-based PCIe card is used to interface with the eight 16-channel modules through a customized adaptor board of ultrafast LVDS tracks. The FPGA on the PCIe card transfers the data from the modules FPGAs to the onboard DDR2 memory, then through the x8 PCIe link to the PC where the images are stored, post-processed, and displayed by a C++ interfacing code. The C++ code pre-calculates the delay coefficients used for transmission focusing and receiving dynamic focusing based on the imaging parameters and transducer type, then it transfers them before the imaging process starts to the PCIe card, which eventually distributes them to the modules FPGAs.

Initial in vivo experiments were performed on mice tumor models to map out tumor vasculature and tumor hypoxia, which were superimposed on co-registered US images. The real-time system allows capturing co-registered US/PAI images free of motion artifacts and also provides ultrafast dynamitic information during cardiac cycle when a contrast agent is used.

8223-101, Poster Session

## DVD pickup head based optical resolution photoacoustic microscopy

P. Wang, M. Li, National Tsing Hua Univ. (Taiwan)

Optical resolution photoacoustic microscopy (OR-PAM) has been shown as a promising tool for label-free micro-vascular and single-cell imaging in clinical and bioscientific applications. However, most OR-PAM systems are realized by using a bulky laser for photoacoustic excitation. The large volume and high price of the laser may restrain the popularity of OR-PAM. In this study, we develop a low-cost and compact OR-PAM system based on a commercially available DVD pickup head. We showed that the DVD pickup head have the required laser energy and focusing optics for OR-PAM. The firmware of a DVD burner was modified to enable its laser diode to provide a 13-ns laser pulse with 1.3-nJ energy at 650 nm. Two excitation wavelengths at 650 and 780 nm were available. The laser beam was focused onto the target after passing through a 0.6-mm thick DVD transparent polycarbonate coating, and then aligned to be confocal with a 50-MHz focused ultrasonic transducer in forward mode. To keep the target on focus, a scan involving auto-tracking procedure was performed. The lateral resolution was verified via cross-sectional imaging of a 6-um carbon fiber. The measured -6 dB width of the carbon fiber was 6.66 um which was in agreement with optical diffraction limit. The proposed OR-PAM has potential as an economically viable and compact blood screening tool available outside of large laboratories due to its low cost and portability. Furthermore, a better spatial resolution could be provided by using a blue ray DVD pickup head.

8223-102, Poster Session

## Influence of laser pulse width to the photoacoustic temporal waveform and the image resolution with a solid state excitation laser

K. Irisawa, K. Hirota, K. Tsujita, FUJIFILM Corp. (Japan); T. Hirasawa, M. Ishihara, National Defense Medical College (Japan)

Properties of excitation laser are the important parameters that affect the photoacoustic image quality. As for the pulse width, it is closely related to signal strength and image resolution, which reported as a result of an experiment using a laser diode that can control the pulse width relatively easily [1]. However, though a solid-state laser is promising for a medical application due to its high pulse energy creating high photo acoustic signal, its influence on waveform or the image quality has not been discussed in detail because the pulse width is hardly changeable in a solid-state laser.

We use two kinds of solid-state lasers, i.e., Q-switched Nd:YAG and Ti-Sapphire Laser, in this study and create different pulse width between 4.2ns and 45ns by changing wave length and excitation energy. These laser pulses are entered into a silicon tube composed of carbon-particle suspension as absorber whose wavelength dependence for absorption is small. We detect the generated laser-induced photoacoustic waves by hydrophone.

The photoacoustic temporal waveform shows sharper as the pulse width is shorter, which also indicates high frequency signal components increase. The width of the first peak on the temporal waveform is corresponding to the pulse width. Additionally, as a result of the photoacoustic imaging experiment preformed with 192-channel PZT linear array probe to image a thin wire, the modulated transfer function shows that the narrower the pulse width, the better the image resolution.

[1] T. J. Allen and P. C. Beard, Opt. Lett. 31, 3462-3464 (2006).

8223-103, Poster Session

## New adaptive beamforming with spatially smoothed coherence factor for photoacoustic imaging

J. Kang, J. H. Chang, Y. Yoo, T. Song, Sogang Univ. (Korea, Republic of)

In photoacoustic imaging, an adaptive beamforming method with coherence factor (ABF-CF) was previously introduced for improving spatial resolution and signal-to-noise ratio (SNR) over a conventional delay-and-sum beamforming method (DAS). However, the ABF-CF method is not suitable for being used in practical diagnosis due to a significant amount of artifacts (e.g., irregular speckle patterns) caused by inter-channel interferences.

In this paper, a new adaptive beamforming method with spatial-smoothed coherence factor (ABF-SSCF) is presented for photoacoustic imaging to enhance the spatial resolution while preserving the regular speckle patterns by applying a spatial-smoothing technique into CF values from multiple sub-arrays within an array probe. To evaluate the proposed ABF-SSCF method, the in vitro experiments were conducted where 64-channel pre-beamformed radio-frequency (RF) data were captured from a 0.5-mm diameter graphite-lead-injected PVC phantom with a commercial ultrasound system equipped with a research package by using a 7-MHz linear array probe (SonixTouch, Ultrasonix Corp., BC, Canada) and an Nd:Yag laser excitation system (LS-2132U, LOTIS Ltd., Belarus).

From the in vitro experiments, the proposed ABF-SSCF method provides the 0.9-mm improvement in -20-dB lateral resolution compared to the DAS method, and this improvement is comparable to the ABF-CF method (i.e., 2.8 mm, 1.8 mm, and 1.9 mm for DAS, ABF-CF, and ABF-SSCF, respectively) while potentially avoiding image distortions in terms of a degree of preservation of the speckle patterns compared to the ABF-CF method.

These results indicate that the proposed ABF-SSCF method can effectively enhance the spatial resolution for photoacoustic imaging without artifacts such as irregular speckle patterns.

8223-104, Poster Session

## Model-based image enhancement in optoacoustic tomography of the mouse brain

A. Rosenthal, T. Jetzfellner, X. L. Deán Ben, D. Razansky, V. Ntziachristos, Helmholtz Zentrum München GmbH (Germany)

In optoacoustic tomograophy, detector geometry plays an important role in determining the image quality. When image reconstruction is performed without accounting for the effect of detector geometry, the resolution of the image may be degraded. This is often the case when flat acoustic detectors with relatively large size are used. When reconstruction is performed without accounting for the geometry of these detectors, the resolution in the tangential direction is degraded.

In this work we developed a model-based reconstruction method which accounts for detector geometry. The model is composed of two steps: First, the relation between the detected signals and the optoacoustic image is discretized under the assumption of point detectors. Then, the effect of the detector is taken into account by temporally convolving its response with the signals obtained in the first step. The results are saved in a matrix which is subsequently inverted to obtain the optoacoustic image. Regularization is applied in the matrix inversion to enable stable reconstruction.

The method is demonstrated in an ex vivo experiment, where the brain of a mouse was imaged using cylindrically focused transducers. Significant resolution enhancement is obtained using the new technique as compared to the reconstruction obtained by model-based inversion that does not account for the detector geometry. In the enhanced images, the contrast of some anatomical features was increased by over a factor of 3.

8223-105, Poster Session

## An algorithm for sensing venous oxygenation using ultrasound-modulated light enhanced by microbubbles

J. E. P. Honeysett, E. Stride, T. S. Leung, Univ. College London (United Kingdom)

Optical spectroscopy can provide an estimate of the mean oxygen saturation in tissue. This technique is limited by optical scattering, which reduces the spatial resolution of the measurement, and by absorption, which makes the measurement insensitive to oxygenation in larger blood vessels. Combining focused ultrasound (US) with optical spectroscopy has been shown to improve the spatial resolution as a result of US-modulation of the light signal. However this technique still suffers from a low signal-to-noise ratio when detecting a signal from regions of high optical absorption such as blood vessels. Combining an US contrast agent with this hybrid technique has been proposed to amplify an US-modulated light (UL) signal. Microbubbles are a clinical contrast agent used in diagnostic US for their ability to resonate in a sound field: in this work we also make use of their optical scattering properties (modelled using Mie theory). A Monte Carlo model of light transport in a highly absorbing blood vessel containing microbubbles surrounded by tissue is used to calculate the UL signal which can be detected on the top surface of the tissue. An algorithm based on the modified Beer-Lambert law is derived which expresses intravenous oxygen saturation in terms of an UL signal. This is used to determine the oxygen saturation in the blood vessel from the measured UL, when this signal is enhanced by intravenous microbubbles.

8223-106, Poster Session

## Real-time imaging of renal clearance using multispectral optoacoustic tomography

S. Morscher, N. C. Burton, A. Taruttis, N. C. Deliolanis, D. Razansky, V. Ntziachristos, Helmholtz Zentrum München GmbH (Germany) and Technische Univ. München (Germany)

Multi-Spectral Optoacoustic Tomography (MSOT) offers real time imaging that simultaneously exploits high ultrasound resolutions and strong optical contrast. It allows the resolution of absorbers in tissue using their distinct spectral absorption profiles, enabling a rich portfolio of functional applications in the regime of pre-clinical biomedical imaging with clinical applications in reach.

This work presents a pioneering, non-invasive in vivo study of mouse kidney physiology that utilizes a real time MSOT imaging system on which our group previously reported. Using excitation wavelengths in the near infrared, the kinetics involved in the renal clearance of IRdye800CW (Li-Cor Biosciences) were imaged using continuous acquisition, providing 45 measurement time points equally spaced over 28 minutes. 20nmol of the agent were injected into the tail vein of 8 week old nude CD1 mice.

Multi-spectral processing of the motion corrected data set reveals the biodistribution of the injected fluorescent probe in the kidneys. Time-domain analysis of regions of interest in both renal cortex and renal pelvis reveals the kinetics of the clearing process. The resulting curve for the cortex region of interest features a steep increase, reaching a plateau after 15 minutes. Conversely, the region in the pelvis shows a similar, but delayed behavior that is consistent with known renal clearance pathways.

These results prove MSOT as a very powerful imaging modality that has the potential of revolutionizing the field of biomedical imaging, enabling a large variety of applications in monitoring therapeutic efficacy and drug development.

8223-107, Poster Session

## Elasticity characterisation in turbid tissue mimicking phantoms by optical tracking of shear waves

Y. Cheng, R. Li, D. S. Elson, M. Tang, Imperial College London (United Kingdom)

Ultrasound has been used to track shear wave propagation in tissue for the estimation of tissue elasticity. In this study we propose an alternative non-invasive technique using optical tracking of shear waves. A 5 MHz focused ultrasound transducer was stimulated by 1 ms burst cycles to generate shear waves in tissue mimicking phantoms. This resulted in the phase modulation of photons comprising a 532 nm Nd:YAG laser beam that was positioned perpendicular to the ultrasound axis and a few millimetres from the ultrasound focus. The photons were detected using a CCD camera and the resulting speckle pattern was processed to obtain the speckle contrast. This parameter has been shown to allow the modulation due to the shear wave to be tracked as a function of time. Shear wave propagation in homogenous phantoms with different stiffness (0.8% Agar, 1.0% Agar and 1.2% Agar, all with 4% intralipid) has been studied. The speeds of the shear waves were estimated by processing the speckle contrast signals and found to be 2.5 m/s (0.8% agar), 3.2 m/s (1.0% agar), and 3.7 m/s (1.2% agar). Furthermore, shear wave propagation in an inhomogeneous phantom (a 5 mm 1.2% agar inclusion was embedded in a 0.8% agar phantom) has also been investigated. With speckle contrast analysis, the inclusion could be distinguished from background by scanning. To conclude, as a non-invasive sensing method, the proposed optical technique provides a novel way to investigate shear wave propagation in tissue, and the elasticity of tissue can be estimated from the shear wave speed.

8223-108, Poster Session

## On laser-induced ultrasound generated in a thin semi-transparent layered polymer structure

E. Svanström, T. Löfqvist, J. Delsing, Luleå Univ. of Technology (Sweden)

In this study, we investigate laser-induced ultrasound generated in a plane semi-transparent layered polymer structure. The scope of the investigation is to study the relations between frequency spectra of the generated ultrasound, as e.g. bandwidth, center frequency and amplitude, and properties of the polymer layers, like thickness, absorption and elastic properties. The influence of laser pulse length end pulse energy is also studied. This knowledge can then be used when designing polymer film based, semi-transparent ultrasonic devices specifically for photoacoustic applications.

The experimental study is set-up as a factorial experiment with completely randomized design. The experiments are backed up by simulations of laser-induced ultrasound from first order principles. In the experiments, the light source is a diode-pumped, Q-switched, Nd:YAG laser with pulse length 9 ns and wavelength 532 nm. As absorber a semi-transparent non-conductive 50 micron thick polymer film in a plane layered structure of one or more layers on a glass substrate is used. The frequency of the ultrasound generated is 2 to 10 MHz, and recorded by a broadband PVDF ultrasonic transducer.

The results show that an increased number of polymer film layers relate to a lower center frequency, a higher optical absorption gives higher ultrasound amplitude and ultrasound bandwidth is sensitive to the stacking of the film layers. The experimental findings in this study correlates with simulations.

8223-109, Poster Session

## Continuous wavelet-transform analysis of photoacoustic signal waveform to determine optical absorption coefficient

T. Hirasawa, M. Ishihara, National Defense Medical College (Japan); K. Tsujita, K. Hirota, K. Irisawa, FUJIFILM Corp. (Japan); M. Kitagaki, M. Fujita, M. Kikuchi, National Defense Medical College (Japan)

In photo-acoustic (PA) imaging, valuable medical applications based on optical absorption spectrum such as contrast agent imaging and blood oxygen saturation measurement have been investigated. In these applications, there is an essential requirement to determine optical absorption coefficients accurately. In present, PA signal intensities have been commonly used to determine optical absorption coefficients. This method achieves practical accuracy by combining with radiative transfer analysis. However, time consumption of radiative transfer analysis and effects of signal generation efficiencies were problems of this method.

In this research, we propose a new method to determine optical absorption coefficients using continuous wavelet transform (CWT). We used CWT to estimate instantaneous frequencies of PA signals which reflects optical absorption distribution.

We demonstrated an experiment to validate the effectiveness of CWT in determination of optical absorption coefficients. In the experiment, planar shaped samples were illuminated to generate PA signal and its optical properties were adjusted by changing the concentration of dye solution. The PA signal was measured by our fabricated PA probe in which an optical fiber and a ring shaped P(VDF-TrFE) acoustic sensor were coaxially aligned. Tunable Ti:Sapphire laser (680 - 900 nm) was used as illumination source.

As a result of experiment, strong correlation between optical absorption coefficients of samples and the instantaneous frequency of PA signal obtained by CWT were confirmed. Advantages of this method were less interference of light transfer and signal generation efficiency

This work was partially supported by Health and Labour Sciences Research Grants for Research on Medical Device Development.

8223-110, Poster Session

## Functional photoacoustic micro-imaging of rat cerebral hemodynamic response function in single vessels during forepaw electrical stimulation

L. Liao, National Chiao Tung Univ. (Taiwan); Y. Chen, National Yang Ming Univ. (Taiwan); C. Lin, J. Chang, National Chiao Tung Univ. (Taiwan); M. Li, National Tsing Hua Univ. (Taiwan)

The specificity of the hemodynamic response function (HRF) is determined spatially by the vascular architecture and temporally by the evolution of hemodynamic changes. Here, we used functional photoacoustic microscopy (fPAM) to investigate the spatiotemporal evolution of the HRFs of hemoglobin concentration (HbT), cerebral blood volume (CBV) and hemoglobin oxygen saturation (SO2) in single cerebral vessels to rat left-forepaw stimulation. The HRF changes in specific cerebral vessels responding to different stimulation intensities and durations were bilaterally imaged with 36 × 65-um spatial resolution. Various electrical stimulations were applied with stimulation intensities at 1, 2, 6 and 10-mA combined with 5-s and 15-s stimulation durations, respectively. Our main findings were as follows: 1) the functional HbT and SO2 increased sub-linearly (i.e. compressed) with increasing stimulus intensities; 2) the results suggested that the CBV changes are more linearly correlated with arterioles than HbT and SO2 within a limited dynamic range of stimulation intensities and duration and 3) time to the peak for HbT, CBV and SO2 was lower in the bigger arterioles than that in the smaller arterioles. The findings in this study indicate that the regulation of hemodynamic changes in single vessels can be reliable studied by the fPAM technique without the use of contrast agents.

8223-111, Poster Session

## Photoacoustic array imaging of calcifications: phantom study

Y. Cheng, T. Hsiao, National Tsing Hua Univ. (Taiwan); W. Tien, S. Luo, D. Chiou, Industrial Technology Research Institute (Taiwan); M. Li, National Tsing Hua Univ. (Taiwan)

Breast calcification is one of the most important indicators for early breast cancer detection. In our previous study, we have demonstrated the feasibility of visualization of calcifications using photoacoustic microscopy setup. In this study, based on a medical ultrasound array imaging platform, we attempt to develop a real-time and high penetration photoacoustic (PA) array imaging system for visualization of breast calcifications. Phantom studies were used to verify the imaging capability and penetration depth of the developed PA array system for calcification imaging. Intralipid gelatin phantoms with different-sized hydroxyapatite (HA) particles - major chemical composition of the breast calcification associated with malignant breast cancers - embedded were imaged. Laser at 750 nm was used for photoacoustic excitation and a custom-made 5-MHz photoacoustic array transducer with linear light guides was applied for photoacoustic signal detection. To obtain better image contrast, coherence weighting was applied in addition to delay and sum beamforming. Experimental results demonstrated that this system is capable of calcification imaging of 300-500 um HA particles. For the 500-um HA particles, the imaging contrast was about 34 dB and the achievable penetration was 20 mm where the axial, lateral, and elevational resolution of this PA array imaging system is 0.39 mm, 0.38 mm, and 1.25 mm, respectively. The highest frame rate was 10 frames/sec limited by the laser pulse rate. Future work will focus on optimization of the photoacoustic transducer to further improve the penetration depth and development of photoacoustic and ultrasound dual-modal imaging to enhance the calcification imaging capability.

8223-112, Poster Session

## Signal recovered from a photoacoustic imaging based on a long-focal-zone transducer

W. Xie, Z. Zeng, L. Li, Z. Li, H. Li, Fujian Normal Univ. (China)

The photoacoustic (PA) signal attenuation was affected by many factors in an imaging system. In this presentation, the factors lead to the signal attenuation and their characters were discussed based on tissue optics, acoustic transport and detection in a long-focal-zone PA imaging system. A method to recover the detected PA signals was presented and employed to image a thyroid sample in vitro. The experimental results demonstrated that the method could be used to improve the imaging depth and quality in the PA system.

8223-113, Poster Session

## Single-mode polymer fiber line detector for photoacoustic tomography

H. Grün, T. Berer, K. Felbermayer, RECENDT GmbH (Austria); G. Paltauf, Karl-Franzens-Univ. Graz (Austria); P. Burgholzer, RECENDT GmbH (Austria)

Photoacoustic imaging provides optical contrast at ultrasonic resolution. To avoid the trade-off between spatial resolution and sensitivity of point-like, broadband detectors, our group introduced integrating detectors - special detectors for photoacoustic imaging which integrate the pressure at least along one dimension (e.g. line detectors). Several types of integrating line detectors have been presented up to now. Since for medical applications high sensitivity and good spatial resolution are important, we present a new fiber-based integrating line detector made of a single mode polymer optical fiber. Compared to glass optical fibers, polymer fibers are much better impedance matched to the surrounding water (coupling medium), provide better elasto-optic coefficients and a lower Young's modulus. Therefore integrating line detectors made of polymer fibers are more sensitive than glass fibers, as we have shown in previous work. However, up to now only multimode polymer fibers have been available, which yield limited spatial resolution due to their relatively large diameter. Furthermore, when the fiber is used in a Fabry-Perot interferometer, the multiple modes make stabilization of the device difficult. Consequently, single mode polymer fibers, which have not been commercially available up to now, combine many favourable properties: high resolution, higher sensitivity than glass fibers, and good stability. In this paper we present measurements involving this new detector and give a comparison with previous fiber-based line detectors to show the enhancement in sensitivity. The better stability of operation point compared with multimode fibers is also demonstrated.

8223-114, Poster Session

## Optical detection of photoacoustic waves using phase sensitive low-coherence interferometry

B. Hermann, M. Gabriele Sandrian, B. Považay, B. Hofer, W. Drexler, Medizinische Univ. Wien (Austria)

Detection of acoustic waves is the cornerstone of photoacoustic tomography (PAT). Detection has conventionally been performed mechanically using ultrasonic transducers, or optically by interferometric techniques. We propose an interferometric detection scheme using low coherence interferometry (LCI) and discuss the challenges, advantages and limitations of applying this technique to photoacoustics.

The main advantages of using LCI for photoacoustic detection is depth selectivity due to coherence gating, which permits noncontact measurements of surface displacement, such as those caused by a photoacoustic wave. With the coherence gate set at the surface, only displacements from the surface contribute to the phase change. To demonstrate this approach, we compared interferometric measurements (with a long coherence length) and LCI measurements of an ultrasound transducer. LCI detection was achieved using a 50 MHz dual balanced detector (Thorlabs Inc.). A superluminescent diode (SLD, Superlum) light source centered at 840 nm ($\Delta\lambda$ = 107nm) was used. The corresponding 3μm axial resolution is not sufficient to visualize the small surface displacements connected with PAT, but the phase of the LCI signal enables the visualization of much smaller changes. A phase change of $2\pi$ corresponds to 420 nm, which theoretically enables the visualization of surface vibrations generated by photoacoustic signals.

8223-115, Poster Session

## Ultrasound-guided photoacoustic image reconstruction

P. Kruizinga, F. Mastik, Erasmus MC (Netherlands); N. de Jong, A. F. W. van der Steen, Erasmus MC (Netherlands) and Interuniversity Cardiology Institute of The Netherlands (Netherlands); G. van Soest, Erasmus MC (Netherlands)

A small in-homogeneity in the initial photoacoustic pressure distribution will act as a source producing a weak photoacoustic signal. This weak signal can be obscured by the background signal originating from the larger homogenous part. In image reconstruction this unwanted 'swamping' effect becomes even more pronounced. To reveal these small in-homogeneities we propose a method where the expected background signal is removed from the actual recorded signals. The expected background signal is calculated using a simulation of the photoacoustic field originating from the structure(s) as they appear in a complementary ultrasound image. To validate this method experimentally we fabricated a polyvinylalcohol vessel phantom containing three optical absorption irregularities within the vessel wall. We imaged this phantom with a 128 element linear ultrasound array, operating at 6 MHz, using plane wave ultrasound imaging. The ultrasound image, showing the vessel geometry, was used to assign the pressure distribution geometry for the k-Wave Matlab® photoacoustic simulation toolbox. The simulated field was then correlated with the actual recorded field that was obtained using the same ultrasound array at the same position and sideways laser light illumination. The residual of the correlation was used for image reconstruction and compared with the normal photoacoustic image. The resulting image clearly shows all three inclusions, whereas in the original photoacoustic image only one of the inclusions could be discerned well. We therefore think that our method of 'expected background subtraction' can be helpful to identify the presence of small sources that are 'swamped' in a strong photoacoustic background.

8223-116, Poster Session

## Photoacoustic imaging of the near-infrared fluorescent protein iRFP in vivo

A. Krumholz, Washington Univ. in St. Louis (United States); G. S. Filonov, Albert Einstein College of Medicine (United States); J. Xia, J. Yao, Washington Univ. in St. Louis (United States); V. V. Verkhusha, Albert Einstein College of Medicine (United States); L. V. Wang, Washington Univ. in St. Louis (United States)

Although many contrast agents, including nanoparticles and organic dyes, have been used with photoacoustic tomograophy (PAT), genetically encoded probes are particularly powerful because they can be targeted to specific tissues, cells, and subcellular locations noninvasively and with high spatial and temporal precision. iRFP is a novel near-infrared fluorescent protein with low quantum yield whose absorption and fluorescence maxima are located at wavelengths longer than the Q-band of hemoglobin absorption, making it ideal for PAT. Here, we report the PA imaging of the iRFP probe in a mouse tumor xenograft model. iRFP was selected after comparison with all other currently available far-red fluorescent proteins: as E2-Crimson, mNeptune, mKate2, TagRFP657, and eqFP670. To test the maximum imaging depth achievable with the protein, a phantom was constructed from sections of laboratory tubing later embedded in chicken breast tissue, with purified protein in one tube and blood in the other for comparison. Subsequent depths were simulated by stacking sections of chicken on the sample. iRFP was then stably transfected into MTLn3 adenocarcinoma cells and injected into the mammary fat pad of female SCID/NCr mice. The resulting tumors were imaged two and three weeks post injection. The contrast increase achieved was high enough to clearly separate the tumor region from the rest of the animal.

8223-155, Poster Session

## Image quality assessment using different types of optical diffusers for photoacoustic tomography

D. Kim, U.S. Food and Drug Administration (United States); S. Ryu, D. Shin, C. Song, Chonbuk National Univ. (Korea, Republic of)

We have investigated different types of optical diffusers for the image quality assessment of photoacoustic tomography (PAT). PAT has been adapted in many biomedical researches for the past decade, however, studies on image quality of PAT have not been performed as much as that for photoacoustic microscopy. We developed a simple imaging phantom using strings of red plastic embedded in gelatinous base. Using a 531 nm Nd:YAG laser and focused/unfocused transducers, we reconstructed PAT images of the phantom with various types of optical diffusers. Our initial results showed that the uniformity of the diffuser did not affect the PAT image quality, while the degree of light scattering contributed relatively more to the image quality. Image quality of biological samples will be presented and discussed.

8223-30, Session 5

## 3D high-resolution pure optical photoacoustic microscopy

Z. Xie, Univ. of Michigan Medical School (United States); S. Chen, T. Ling, L. J. Guo, Univ. of Michigan (United States); P. L. Carson, X. Wang, Univ. of Michigan Medical School (United States)

The concept of pure optical photoacoustic microscopy(POPAM) was proposed based on optical rastering of a focused excitation beam and optically sensing photoacoustic signals using a microring resonator fabricated by nanoimprinting technique. The featured high sensitivity allowed the microring resonator to detect weak photoacoustic signals from micro- or submicroscale objects. The current POPAM system provides comparable optical resolutions on both lateral and axial dimensions with unique contrast of optical absorption complementing other optical modalities. The 3D structure of microvasculature, including capillary networks, and even individual red blood cells has been discerned successfully in the proof-of-concept experiments on mouse bladders ex vivo and mouse ears in vivo. The potential of approximately GHz bandwidth of the microring resonator also might allow much higher resolution than shown here at depths in unfrozen tissue specimens or thicker tissue sections not now imageable with current optical or acoustic microscopes of comparable resolution.

8223-31, Session 5

## In vivo imaging of small animal models by photoacoustic microscopy

S. Ye, R. Yang, J. Xiong, Peking Univ. (China); K. K. Shung, Q. Zhou, Univ. of Southern California (United States); C. Li, Peking Univ. (China); Q. Ren, Peking Univ. (China) and Shanghai JiaoTong Univ. (China)

Several animal larvae, such as larvae of zebrafish, drosophila, caenorhabditis elegans, are important animal models in biomedical researches. For instance, researches using zebrafish larvae to study gene expression, nervous and circulatory systems, heart disease and angiogenesis in cancer have been always receiving intense attention for a long time. Traditional imaging methods of studying of larvae primarily employ several optical microscopic imaging modalities that rely on optical scattering or exogenous fluorescence. As we known, optical absorption properties also contain essential biological functional information. Photoacoustic (PA) microscopy (PAM) is an emerging biomedical imaging method that combines optical contrast with ultrasonic detection, which is highly sensitive to the optical absorption contrast of living tissue, such as pigments, the vasculature and other optically absorbing organs. Using zebrafish larvae as a sample, we report the whole body label-free imaging of larvae by PAM. Based on endogenous optical absorption contrast, high resolution images of pigments, microvasculature and several other major organs have been obtained in vivo and non-invasively, and compared with their optical counterparts. Our results demonstrated that PAM has the potential to be a powerful non-invasive imaging method for studying larvae of animal models.

8223-32, Session 5

## Imaging dynamic processes using fiber laser optical-resolution photoacoustic microscopy

W. Shi, P. Hajireza, A. Forbrich, R. J. Zemp, Univ. of Alberta (Canada)

Recently we have reported in vivo near-realtime volumetric optical-resolution photoacoustic microscopy (OR-PAM) using a high pulse-repetition-rate (PRR) nanosecond fiber-laser to realize 2 volumetric image frames per second within 1mm x 1mm field of view. However, the imaging of dynamic process was limited by the amount of data required for each frame (nearly 100 Mbytes/frame), the total on-board storage capacity of data acquisition (DAQ) card and the data transfer rates between the DAQ card and the PC RAM. We demonstrate an OR-PAM system to overcome these drawbacks by decreasing the number of data channels, storing only peak-to-peak values by using on-board FPGA-based peak-detection firmware, which also permits sustained data transfer to PC at > 1 million maximum-amplitude-projection (MAP) pixels per second. Thus, frame-rate is no longer limited by acquisition hardware or PCI-bus transfer rates, but by the laser PRR of 600 kHz. Much higher PRR than this may be complicated by deep-tissue signals from previous pulses interfering with those due to superficial structures. Using a nanosecond-pulsed 532-nm fiber laser combined with fast-scanning mirrors, our proposed system is capable of sustained imaging at several frames per second. We demonstrate the dynamic process imaging capabilities of our system by imaging capillary-scale microvasculature in a live Swiss Webster mouse ear with ~6-μm optical lateral spatial resolution at close-to-video speed. Realtime positioning and occlusion reperfusion experiments are demonstrated. It is anticipate that the realtime nature of the system should prove important in clinical and preclinical adaptation, and may prove useful for functional brain imaging studies.

8223-33, Session 5

## Optoacoustic microscopy system based on an off-axis parabolic reflector

D. Tsyboulski, A. Conjusteau, A. A. Oraevsky, TomoWave Labs., Inc. (United States)

We introduce a novel experimental design for non-invasive scanning optoacoustic microscopy which utilizes an off-axis parabolic mirror. Such reflector provides an ideal and lossless conversion of a spherical wavefront into a plane wave and enables diffraction-limited ultrasound focusing. We have designed and build a custom and broadband polyvinyledene fluoride (PVDF) transducer with 0-19 MHz bandwidth and measured sensitivity of 4 Pa. Using our optoacoustic microscopy system based on a parabolic mirror with NA of 0.52, we have achieved resolution of 130 micrometers and depth of imaging greater than previously reported. Further improvements of transducer bandwidth and numerical aperture of the imaging system are underway. The achieved resolution limits and in vivo imaging depth of our optoacoustic microscopy system will be presented and discussed.

8223-34, Session 5

## Multiparameter photoacoustic microscopy of tumor micro-environment

S. Hu, Washington Univ. in St. Louis (United States); R. Sohn, Z. Lu, Washington Univ. School of Medicine in St. Louis (United States); B. T. Soetikno, Q. Zhong, J. Yao, K. I. Maslov, Washington Univ. in St. Louis (United States); J. M. Arbeit, Washington Univ. School of Medicine in St. Louis (United States); L. V. Wang, Washington Univ. in St. Louis (United States)

A growing tumor possesses a complex microenvironment that facilitates its growth, neovascularization, invasion, and metastasis. Incomplete understanding of the tumor microenvironment, including malignant tissue-vascular interaction and therapeutic responses, impedes effective treatments. Clinically, tumors either do not respond to therapies or resume growth after transient shrinkage. Thus, detailed preclinical studies of the tumor microenvironment can potentially provide insight into mechanisms of therapeutic evasion, resistance, or relapse. However, most current optical microscopy techniques involve invasive procedures such as tissue window construction and fluorescent probe injection, which alter the tumor microenvironment and thereby obfuscate interpretation of longitudinal imaging data. Thus, there is a strong demand for a new imaging tool that can noninvasively interrogate the tumor microenvironment with minimal perturbation.

We have developed multi-parameter photoacoustic microscopy (PAM) for noninvasive, label-free, high-resolution, and wide-field imaging/monitoring of the spontaneous growth and therapeutic responses of renal carcinoma, a paradigm model for elucidation of tumor neovascularization and microenvironmental regulation. We have also developed a robust xenograft technique to grow renal tumors at a precise anatomic location in nude mouse ears that is optimized for multi-parameter PAM analysis. We longitudinally determined tumor vascular morphology (e.g., vessel length, diameter, and tortuosity), blood flow, total concentration and oxygen saturation of hemoglobin, oxygen extraction fraction, and regional metabolic rate of oxygen, at scales down to the capillary level. We demonstrate distinct and diametric differential tumor vascular responses to inhibitors for mammalian target of rapamycin (mTOR) and vascular endothelial growth factor (VEGF).

8223-35, Session 5

## Mosaicing for fast wide-field-of-view optical-resolution photoacoustic microscopy

P. Shao, R. Chee, A. Forbrich, R. J. Zemp, Univ. of Alberta (Canada)

The acquisition speed of previous mechanically-scanned Optical-Resolution Photoacoustic Microscopy (OR-PAM) systems has been limited by both laser pulse repetition rate and mechanical scanning speed. Recently, Hu et al. reported that with their second generation OR-PAM system, 70 minutes is needed to scan an area of 7.8 × 10 mm. While image quality of their system was outstanding, the long-scan times may preclude practical adaptation by a wider community. Recently we reported a fiber-laser-based laser-scanning system providing mm-scale field-of-view (FOV) volumetric images at frame-rates of several frames per second, ~100x faster than previous systems. While our system used a low-loss probe with a focused ultrasound transducer for high sensitivity, our FOV was highly limitedTo remedy the FOV deficiency of our system, yet maintain sensitivity, we introduce a mosaicing scheme wherein a grid of small sub-mm-scale FOV patches are acquired in 0.5s per patch (or less), and a 3-axis stepper-motor system is used to mechanically move from patch-to-patch in less than 1s. To overcome the limitation of PCI data transfer rate, we use the on-board FPGA-based peak-detection firmware to sustain only maximum-amplitude-projection (MAP) data. Patch images are aligned and stitched to generate a large FOV image. This system retains the SNR-advantages of focused-transducer OR-PAM systems, and is a hybrid approach between laser-scanning and mechanical scanning. With this strategy we reduce the data acquisition time of previously reported large-FOV systems by a factor of nearly 30. Ears and cortical surface of Swiss Webster mice are imaged.

8223-36, Session 5

## A fast multiwavelength-scanning photoacoustic microscope based on a digital mirror device

Y. Wang, K. I. Maslov, L. V. Wang, Washington Univ. in St. Louis (United States)

Based on optical absorption contrast, photoacoustic microscopy (PAM) has demonstrated utility in imaging fine structures in biological tissues. Using optical excitation at multiple wavelengths, PAM spectroscopically measures the optical absorption properties of tissue chromophores. We have developed a fast wavelength-switching PAM system using a digital mirror device. The imaging system can quickly tune the wavelength at the laser pulse repetition rate, providing functional photoacoustic images consisting of A-line signals at multiple wavelengths acquired at several kHz. The multiwavelength PAM image stack, combined with a spectral fitting approach, is able to resolve different optical absorption contrast mechanisms at high spatial resolution. The wavelength-scanning PAM system has the potential of rapidly visualizing functional and molecular characteristics of physiological and pathological conditions in tissue.

8223-37, Session 6

## Optoacoustic temperature monitoring during HIFU impact on biological tissues: ex-vivo study and numerical simulation of 2D temperature reconstruction

I. M. Pelivanov, S. M. Nikitin, Lomonosov Moscow State Univ. (Russian Federation); T. Khokhlova, Univ. of Washington (United States)

Preliminary study of the possibility of the optoacoustic (OA) method application in dynamic monitoring of high intensity focused ultrasound (HIFU) impact on biological tissues is performed. The proposed OA method is based on the temperature dependence of the efficiency of light-to-sound transformation in tissues and organs. Layered samples consisted of healthy and thermally coagulated tissues as well as the samples with HIFU lesions inside were studied experimentally to prove the OA method applicability in monitoring of a lesion location. The next stage of this work was focused in the experimental study of the dependence of the OA signal amplitude on temperature in different ex-vivo tissues, in the temperature range of 20°C - 75°C. We used chicken breast as a model of muscle, porcine liver as a model of richly perfused tissue, and porcine lard as a model of fatty tissue. Characteristic features of the temperature dependencies in tissues under study were described in terms of the difference of its structures. Finally we performed the numerical simulation of the 2-D OA image dynamics during HIFU impact. It is shown that the temperature dependence of the OA image maximum coincides within a constant factor with the measured calibration dependence, justifying thus the possibility of real-time temperature reconstruction.

8223-38, Session 6

## Combined optoacoustic and high-frequency ultrasound imaging of live mouse embryos

P. V. Chitnis, Riverside Research Institute (United States); O. Aristizábal, New York Univ. School of Medicine (United States); E. Filoux, A. Sampathkumar, J. Mamou, Riverside Research Institute (United States); D. H. Turnbull, New York Univ. School of Medicine (United States); J. A. Ketterling, Riverside Research Institute (United States)

The cell differentiation and proliferation of the central nervous system (CNS) are closely related to vascular development. An imaging protocol that integrated optoacoustics (OA) with high-frequency ultrasound (HFU) was developed for in vivo imaging of brain ventricles and vasculature in mouse embryos. A 40-MHz, co-polymer, 5-element annular-array transducer with a geometric focus of 12 mm was modified to accommodate a coaxial fiber-based optical delivery system for collimated illumination. Three-dimensional (3-D) data sets were acquired by raster scanning the transducer-optics assembly in 50-μm increments. A single intact conceptus from an anesthetized mouse was surgically exposed into PBS-filled Petri-dish. A 250-μm spot illumination from a pulsed, 532-nm, Nd-YAG laser was synchronized with a high-voltage impulse excitation of the central array element to facilitate simultaneous and spatially co-registered OA and HFU data acquisition. All datasets were gated to the resting phase of the respiratory cycle. The resulting OA and HFU signals from each scan location were recorded on all five array channels and post-processed using a synthetic-focusing algorithm to enhance the depth of field (DOF). Dual-modality images were acquired from mouse embryos at E11.5, E12.5, and E13.5 days of gestation. The extended DOF allowed morphologically accurate visualization of the embryonic head. The brain ventricles were segmented from the HFU data and rendered in 3-D. The OA data provided visualization of the vascular plexus as well as individual blood vessels. Feasibility of real-time, spatially co-registered, low-cost dual-modality in vivo imaging of mouse embryos was demonstrated.

8223-39, Session 6

## In vivo combined photoacoustic and Doppler ultrasound imaging

Y. Jiang, T. Harrison, A. Forbrich, R. J. Zemp, Univ. of Alberta (Canada)

In this work, our goal is to develop photoacoustic and Doppler ultrasound imaging methods for non-invasive estimation of the oxygen consumption rate (MRO2) in vivo. Previously, we have demonstrated a combined photoacoustic and high-frequency Doppler ultrasound system with single element transducer and shown the feasibility of MRO2 estimation using flow phantoms in the visible light range. However, when implementing this technique in vivo, the blood flow velocity is hard to be accurately estimated using traditional color Doppler algorithm due to the lack of Doppler angles. Thus we use ultrasound Doppler bandwidth broadening to estimate the transverse flow velocity. This technique has been validated using a flow phantom with 860μm vessel positioned 90o angle to the transducer, and the results show improvements over the color Doppler algorithm. In vivo experiments have been performed on a human finger to provide co-registered photoacoustic and Doppler flow images with image depth of ~2mm. The diameter of the blood vessel is ~1mm and the mean flow velocity is 30mm/s. To obtain more imaging depth and higher frame rate, we also implement combined photoacoustic and Doppler ultrasound imaging based on a clinical array system from Verasonics Inc. which enables flexible pulse-sequence programming and parallel channel data acquisition. An interlaced photoacoustic and flash-Doppler pulse-sequence was generated and the photoacoustic and Doppler images are co-registered. In vivo experiments have been performed on a 250g SD rat using NIR light. We demonstrate imaging of blood vessels to depths of ~1.5cm with both modalities. We are working towards blood oxygen saturation estimation in vivo and 3D oxygen consumption imaging of tumors of both systems at depths beyond OR-PAM.

8223-40, Session 6

## Functional dual-modality photoacoustic and ultrasonic endoscopy in vivo

J. Yang, C. P. Favazza, Washington Univ. in St. Louis (United States); R. Chen, The Univ. of Southern California (United States); J. Yao, X. Cai, K. I. Maslov, Washington Univ. in St. Louis (United States); Q. Zhou, K. K. Shung, The Univ. of Southern California (United States); L. V. Wang, Washington Univ. in St. Louis (United States)

Photoacoustic endoscopy is a promising tomographic endoscopic modality that can provide a unique combination of functional optical contrast and high spatial resolution at clinically relevant depths, far exceeding the penetration depths of conventional high-resolution optical imaging modalities. Another technical merit is that photoacoustic endoscopy systems are compatible with conventional ultrasound imaging, enabling multi-modality imaging with complementary contrast. Hence, this dual-modality imaging can provide unprecedented physiological information and promote morphologic and functional understanding of the target tissue. In this study, we developed simultaneous photoacoustic and ultrasonic dual-mode endoscopy, which can provide spatially coincident photoacoustic and ultrasonic volumetric images, and demonstrated its in vivo endoscopic imaging capability. Specifically, we performed in vivo imaging of the upper and lower gastrointestinal tracts of rabbits and rats, and successfully produced 3D images with complementary contrasts and functional information from the target organs. In addition, we demonstrated the molecular and trans-enteric imaging ability of this integrated endoscopic technique. In this talk, we will discuss the benefits of the integrated dual-modality endoscopic technique and will highlight possible clinical applications.

8223-41, Session 6

## Optoacoustic generation of high-amplitude focused ultrasound by using carbon-nanotube polymer composite films

H. W. Baac, A. Maxwell, J. G. Ok, K. Lin, Z. Xu, L. J. Guo, Univ. of Michigan (United States)

High-intensity focused ultrasound (HIFU) has been used extensively as a noninvasive modality for therapeutic applications as well as a promising approach to promote drug delivery through biological membranes. Currently, the HIFU is obtained by using piezo-based transducers. However, these transmitters are bulky and operated normally around 1~5 MHz frequency range. As this makes focal spot size large (typically a few mm in width and ~10 mm in length), it is difficult to satisfy needs for high-resolution applications.

Laser-generated ultrasound is known as an efficient way to easily obtain broadband and high-frequency ultrasound. However, due to poor energy conversion efficiency (output acoustic energy/incident optical energy is 10-6~10-8), the optoacoustic pressure could not reach to the HIFU amplitude.

In this work, we introduce HIFU that is optoacoustically generated by using the carbon-nanotube (CNT) polymer composite films. The composite film was made on a concave surface which generates focused ultrasound under laser excitation. Depending on the applications, the design of the focused transmitters could be easily modified in terms of focal distance and numerical aperture of lens. Due to highly efficient optoacoustic conversion in the composite[Baac et al., Appl. Phys. Lett. 97, 234104 (2010)], we could successfully obtain the HIFU amplitude on the order of several tens of MPa. We characterized focal spot profiles and waveforms by using a fiber-optic hydrophone. High-resolution aspects and potential applications are discussed.

8223-42, Session 6

## Combined optical-resolution photoacoustic and fluorescence micro-endoscopy

P. Shao, P. Hajireza, W. Shi, R. J. Zemp, Univ. of Alberta (Canada)

We present a new microendoscopy system combining realtime C-scan optical-resolution photoacoustic microscopy (OR-PAM), giving optical absorption contrast for label-free capillary-network visualization and a high-resolution fluorescence microendoscopy system for visualizing fluorescently labeled cellular components. With a diode-pumped 532-nm fiber laser, it is capable of imaging with a resolution of ~ 7μm with an acquisition frame rate of 4 frames per second (fps) or higher. The fluorescence sub-system consists of a high power LED with 447.5 nm-centered emission as the light source, an objective lens and a CCD camera. Proflavine, a FDA approved drug for human use, is used as the fluorescent contrast agent by topical application. The fluorescence system does not require any mechanical scanning. The scanning laser and the LED light source share the same light path within an optical fiber bundle containing 30,000 individual single mode fibers. The absorption of Proflavine at 532 nm is low, which mitigates absorption bleaching of the contrast agent by the photoacoustic excitation source. We imaged cultured MCF-7 cells, and demonstrate imaging in live murine models. The system is able to provide cellular morphology with sub-cellular resolution co-registered with the structural and functional information given by OR-PAM. Therefore, the system has the potential to serve as a virtual biopsy technique, helping researchers and clinicians visualize angiogenesis, effects of anti-cancer drugs on both cells and the microcirculation, as well as aid in the study of other diseases.

8223-43, Session 6

## Real-time intravascular ultrasound/ photoacoustic imaging system with omni-directional light excitation

B. Hsieh, P. Li, National Taiwan Univ. (Taiwan)

Photoacoustic imaging has been explored for intravascular applications (IVPA), and integration with intravascular ultrasound (IVUS) is highly desirable. One of the main challenges is that the imaging frame rate is limited by the laser pulse repetition frequency (PRF). Conventionally, a laser pulse is required for each scan line, and there are up to hundreds of scan lines per image frame. On the other hand, many solid-state pulsed lasers have a PRF of 10-20Hz, which makes real-time intravascular imaging difficult. Although higher PRF lasers are available, they are often more expensive and with a lower pulse energy. Thus, the goal of this study is to develop new imaging strategy for real-time intravascular imaging. Specifically, we propose to combine omni-directional optical excitation with a ring array transducer. With this, only a single laser pulse is needed for an image frame. In the preliminary study, we developed a real-time integrated IVUS/IVPA imaging system by combining omni-direction light excitation, Nd:YLF pulsed laser and a clinical IVUS system. The optical fiber with axiconlike distal tip can e directly combined with the IVUS imaging catheter. The imaging frame rate of this integrated imaging system is 19 fps. Both US and PA images are recorded and co-registered so that a fusion image can be formed. The IVUS/IVPA images of tungsten wire, black tube and rabbit's atherosclerotic aorta were acquired with this integrated system to evaluate the imaging performance. The lateral/axial resolution of US image is 2.56°/62.4μm at -6 dB. The resolution of PA image is 3.76°/91.5μm. In ex-vivo study, the imaging system was used to acquire IVUS/IVPA images of atherosclerotic rabbit's aorta. The images can be used to demonstrate 360° view without rotating the optical fiber. In the future, with an ultrasound ring array on receive, the imaging frame rate can be as high as the laser PRF.

8223-44, Session 7

## New photoacoustic cell with diamond window cover for mid-infrared investigations on biological samples

J. Kottmann, J. M. Rey, M. W. Sigrist, ETH Zurich (Switzerland)

We present a new photoacoustic (PA) cell which is sealed on the sample side with a 163 μm thick chemical vapor deposition (CVD) diamond window. If samples containing volatile compounds are investigated with an open-ended PA cell varying conditions in the PA chamber (changing light absorption or relative humidity) cause unstable signals. In contrast a diamond cover ensures stable conditions in the PA chamber and thereby enables sensitive measurements. This is particularly important if biological samples with a high water content are investigated. Due to the high thermal conductivity of CVD diamond (1800 W/mK) strong PA signals are generated and the broad optical transmission (250 nm to THz) renders the cell useful for various applications. The performance of the cell is demonstrated by tracking glucose in aqueous solutions and in epidermal skin phantoms with an external-cavity quantum-cascade laser (1010-1095 cm-1). These measurements yield a current detection limit of 100 mg/dl (SNR=3). Furthermore the temporal spectral changes of glucose dissolved in water caused by mutorotation have been monitored. Although glucose measurements within the physiological range (30-500 mg/dl) are feasible, further improvements are needed for non-invasive glucose monitoring of diabetes patients. First in vivo measurements at the human forearm show an additional PA signal induced by blood pulsation at a frequency around 1 Hz. Furthermore a steadily increasing relative humidity in the PA chamber due to transpiration is observed when measuring with an open-ended cell yet not when employing the closed cell. First results on non-invasive glucose monitoring will be presented.

8223-45, Session 7

## Time-reversed ultrasonically encoded (TRUE) optical focusing in reflection mode: demonstrations in tissue mimicking phantoms and ex vivo tissue

P. Lai, X. Xu, H. Liu, Y. Suzuki, L. V. Wang, Washington Univ. in St. Louis (United States)

The problem of how to effectively deliver light dynamically to a tight region inside turbid media has been intensively investigated for imaging and therapeutic purposes. Most recently, a new modality termed Time-Reversed Ultrasonically Encoded (TRUE) optical focusing was proposed by integrating the concepts of ultrasound (US) modulation of diffused light with optical phase conjugation. In this work, the diffused photons that travel through the US focal region are "tagged" with a frequency shift due to the US modulation. Part of the tagged light is collected in reflection mode and transmitted to a photorefractive crystal (PRC), forming there a stationary hologram through interference with a coherent reference optical beam. The hologram is later read by a conjugated optical beam, generating a phase conjugated wavefront of the tagged light. It is conveyed back to the turbid medium in reflection mode, and eventually converges to the US focal zone. Optical focusing effects from this system are demonstrated experimentally in tissue-mimicking phantoms and ex vivo chicken breast tissue, achieving effective round-trip optical penetration pathlengths (extinction coefficient multiplied by round-trip focusing depth) exceeding 160 and 70, respectively. An example of imaging optical inclusions with this system is also reported.

8223-46, Session 7

## Non-contact photoacoustic tomography and ultrasonography for biomedical imaging

G. Rousseau, D. Lévesque, A. Blouin, J. Monchalin, National Research Council Canada (Canada)

Photoacoustic tomography (PAT) and ultrasonography (US) of biological tissues usually rely on ultrasonic transducers for the detection of ultrasound. For an optimum sensitivity, transducers require a physical contact with the tissue using a coupling fluid (water or gel). Such a contact is a major drawback in important potential applications such as surgical procedures on human beings and small animal imaging in research laboratories. On the other hand, laser-ultrasonics (LU) is a well established optical technique for the non-contact generation and detection of ultrasound in industrial materials. In this paper, the remote optical detection scheme used in industrial LU is adapted to allow the detection of ultrasound in biological tissues while remaining below laser exposure safety limits. Both non-contact PAT (NCPAT) and non-contact US (NCUS) are considered experimentally using a high-power single-frequency detection laser emitting suitably shaped pulses and a confocal Fabry-Perot interferometer in differential configuration. It is shown that an acceptable sensitivity is obtained while remaining below the maximum permissible exposure (MPE) of biological tissues. Results were obtained ex vivo on chicken breast and calf brain specimens with embedded inclusions simulating blood vessels optical properties. Sub-mm inclusions are readily detected at depths exceeding 1 cm. The method is expected to be applicable to living tissues.

8223-47, Session 7

## Flow-dependant photothermal modulation of the photoacoustic response

A. Sheinfeld, A. Eyal, Tel Aviv Univ. (Israel)

The efficiency of photoacoustic (PA) excitation is described by the dimensionless Grüneisen coefficient. Previous studies investigated its temperature dependence and utilized it for in-vivo temperature monitoring. In this study we used this temperature dependence for modulating the PA response of blood in a phantom vessel. Simultaneously with the PA excitation, oscillatory temperature variations at low frequencies were induced in the medium via the photothermal (PT) effect. These variations modulated the amplitude of the PA response, and gave rise to two sidelobes on both sides of the PA carrier frequency. Frequency scan of the PT excitation yielded the system's modulation frequency response. It featured negative slope with a cutoff (modulation peak at noise level) at ~10Hz. Initiating flow in the vessel (in the range of 1-10mm/sec) had a dramatic effect on the frequency response making it lower at the peak but broader. The experimental setup comprised a pair of fiber-coupled directly-modulated 830nm laser diodes with CW powers of 200mW each. One diode was modulated at 1MHz to generate the PA response and the second diode induced PT temperature oscillations at frequencies in the range 0.1-10Hz. The phantom vessel was a blood-filled transparent tube immersed in water with one end attached to a syringe pump. The detection was made using a piezoelectric ultrasonic transducer. The significant dependence of the modulation frequency response on flow, which is attributed to its effect on the thermal constants of the probed volume, can find important applications in noninvasive measurements of blood flow and blood perfusion.

8223-48, Session 7

## Multispectral photoacoustic coded excitation using pseudorandom codes

M. F. Beckmann, C. Friedrich, M. P. Mienkina, N. C. Gerhardt, M. R. Hofmann, G. Schmitz, Ruhr-Univ. Bochum (Germany)

Photoacoustic imaging using semiconductor laser diode systems is desirable, as it reduces the size and the cost of the laser system. However, using such a system is challenging, as its optical power is strongly reduced compared to solid state lasers commonly used in this field. To overcome this limitation, we introduced photoacoustic coded excitation (PACE), exploiting the greatly increased PRF of lasers diodes. In order to further improve SNR compared to time equivalent averaging (coding gain), consecutively we introduced orthogonal Golay codes for simultaneous multi wavelength use. As an alternative for multiple wavelengths, we compare pseudorandom sequences to orthogonal Golay codes. Pseudorandom sequences, such as maximally connected sets of m-sequences, Gold codes or Kasami sequences are more simple to use than orthogonal Golay codes. Their asymptotic coding gain is equal. For finite code lengths, pseudorandom sequences always yield a slightly better coding gain, which is an inherent result of the simplification. This can be several dB depending on the code lengths and number of wavelengths used, e.g. for 2cm maximum depth and 128 bit at 500kHz the gain is improved by 0.2dB for two wavelengths, by 0.6dB for four wavelengths and by 1.8dB for six wavelengths. Since the auto- and cross correlation properties are not perfect, side lobes may be introduced into the images. However, these may remain invisible depending on SNR and sequence length. The coding gain scales linearly with the number of wavelengths used. Overall, pseudorandom codes are a suitable alternative to orthogonal Golay codes for PACE.

8223-49, Session 7

## Acoustic reflector combined with optical detection for photoacoustic section imaging

R. Nuster, S. Gratt, K. Passler, G. Paltauf, Karl-Franzens-Univ. Graz (Austria)

Recently, it has been shown that integrating line detectors can be used for photoacoustic imaging. Differently to "point-like" detectors the procedure to obtain the initial pressure distribution from line detector signals is a combination of back projection and the inverse Radon transform. Optical line detectors, such as a focused laser beam in an interferometer, combine high resolution (due to the small beam diameter and the high bandwidth of optical detection) and complete optical and acoustic transparency, leading to very accurate three-dimensional (3D) images. However, when using a single integrating detector it is very time-consuming to record the data, making the method ill-suited for in-vivo experiments.

As a less time-consuming alternative to full 3D imaging, various techniques have been employed that use single detectors with cylindrically focusing elements for imaging of selected sections. The method proposed in this work combines the advantages of optical detection with 2D slice imaging, using an optical interferometer combined with an acoustic reflector. The latter is a concave mirror that forms an acoustic image of the initial pressure distribution. By probing the temporal evolution of the image pressure distribution with an optical beam perpendicular to the acoustic axis and simultaneously rotating the object, data for reconstruction of a slice are acquired. Image reconstruction from the recorded signals requires only the application of the inverse Radon transform. The resolution and sensitivity of the detection system were investigated by simulations and experiments on phantom samples. Furthermore, the imaging system was tested on a real biological sample.

8223-50, Session 7

## Contactless photoacoustic imaging of biological samples

T. Berer, A. Hochreiner, H. Grün, P. Burgholzer, RECENDT GmbH (Austria)

In this paper we acquire photoacoustic signals remotely by using a two-wave mixing interferometer (TWMI). The TWMI allows measurement of ultrasonic displacements on sample surfaces without the need of coupling agents or a water bath. We demonstrate contactless photoacoustic imaging on porcine skin phantoms and on a human forearm. The porcine phantoms consist of porcine skin with subcutaneous fat and artificial blood vessels, filled with human blood. Furthermore imaging on tissue-mimicking phantoms is shown. These phantoms consist of artificial blood vessels or hair bristles immersed in water/Intralipid or water/milk solutions.

Photoacoustic signals are generated by pulses from a Nd:YAG laser at a wavelength of 1064nm. The TWMI utilizes a frequency doubled cw-YAG laser and a bismuth silicon oxide photorefractive crystal. The photorefractive crystal is operated in drift regime. To keep the laser power at the tissue low a Pockels cell and a polarizing beam splitter are used to direct the detection laser to the tissue only during measurement. After the measurement the initial pressure distribution is reconstructed using a Fourier domain synthetic aperture focusing technique.

In summary we show remote contactless photoacoustic imaging. By using a two-wave mixing interferometer we acquire photoacoustic signals without the need for a water bath or a coupling agent, e.g. directly on skin. This allows measurements on regions where immersion into a water bath is a limitation or which are difficult to access otherwise.

8223-51, Session 7

## Miniature fiber optic photoacoustic imaging probes for micro-endoscopic applications

E. Z. Zhang, P. Beard, Univ. College London (United Kingdom)

Miniature ultrasound sensor probes are required for a number of important clinical applications of photoacoustic imaging in which the target tissue can only be accessed by introducing an endoscopic probe percutaneously or through a natural orifice. Among these are the assessment of coronary artery disease, prostate cancer and gastrointestinal pathologies. The design of a photoacoustic probe for these applications poses several challenges. These include the question of how to integrate the delivery optical fibre with the ultrasound receiver to avoid obscuring the excitation laser pulses, obtaining the necessary level of miniaturisation and achieving low unit cost for single use applications. To address these challenges, we have developed a miniature all-optical photoacoustic probe which employs a transparent Fabry Perot ultrasound sensor at the tip of a 250µm delivery optical fibre. There are several advantages of this all-optical approach over conventional piezoelectric based photoacoustic probes. It offers a high level of miniaturisation, inexpensive batch fabrication using vacuum deposition techniques and can readily be combined with other imaging modalities such as OCT and pulse-echo ultrasound. The concept also offers flexibility in its configuration allowing the implementation of forward and sideways looking probes and multielement imaging devices. We have also demonstrated that ultra high acoustic sensitivity (<10Pa NEP) is achievable by using a concave FP interferometer cavity design. A number of new probe designs and fabrication methods have been implemented with a view to improving the sensitivity and acoustic frequency response. To evaluate the imaging performance of these probes, a variety of phantoms designed to simulate vascular and other tissues have been imaged.

8223-52, Session 7

## Vibrational photoacoustic microscopy for deep tissue bond-selective imaging

J. Cheng, Purdue Univ. (United States)

Signals from molecular vibration permit chemical imaging without labeling. However, the limited penetration depth of c.a. 100 micron in linear and nonlinear vibrational microscopy prevents deep-tissue molecular imaging. To overcome this limitation, vibrational photoacoustic microscopy is demonstrated based on excitation of molecular overtone vibration and acoustic detection of the resultant pressure transients in tissues (Phys Rev Lett 2011, 106: 238106). In this new approach overtone excitation with a near-infrared nanosecond laser provides label-free chemical selectivity and undetectable photodamage to tissues. Acoustic detection eliminates the tissue scattering problem encountered in near-infrared spectroscopy and enables depth-resolved signal collection. We demonstrate three-dimensional vibrational photoacoustic imaging of lipid-rich atherosclerotic plaque with millimeter-scale penetration depth from from the artery lumen, and of intramuscular fat with a penetration depth of over 1 mm into the muscle tissue. Selective imaging of fat and collagen is also shown based on the VPA signals arising from overtone transitions of CH2 and CH3 groups, respectively.

8223-54, Session 7

## Real-time photoacoustic imaging with optical ultrasound detection

R. Nuster, G. Paltauf, Karl-Franzens-Univ. Graz (Austria)

Optical ultrasound detection has become an attractive alternative to piezoelectric ultrasound detection for photoacoustic imaging. The favorable properties of optical detection are high resolution, complete optical and acoustical transparency. Nevertheless, optical detection devices are less common because of the difficulty to realize optical parallel detection. Consequently, a single detector is commonly used to record the data. Due to the huge scanning effort, full 3D imaging becomes quite time-consuming and impracticable for in-vivo applications.

Recently, it has been shown that optical phase contrast full field detection in combination with a CCD-camera can be used to record acoustic fields. Depending on whether the detection system is used with or without an acoustic imaging device (acoustic lens or reflector), an acoustic image of the initial pressure distribution or an image of the acoustic wave pattern is observed at a certain time in the imaging volume of the optical detection system. This allows to record photoacoustic projection images directly from the measurement system in real-time.

The reconstruction of the initial three dimensional pressure distribution is a two step process. First of all, projection images of the initial pressure distribution are acquired. This is done either by back propagating the observed wave pattern in frequency or Radon space or by using the acoustic imaging device as acoustic processor. In the second step the inverse Radon transform is applied to the obtained projection dataset to reconstruct the initial three dimensional pressure distribution.

Simulations and experiments are performed to show the overall applicability of this technique in photoacoustic imaging.

8223-55, Session 7

## Novel optoacoustic system for noninvasive, continuous monitoring of cerebral venous blood oxygenation

Y. Y. Petrov, I. Y. Petrov, D. S. Prough, R. O. Esenaliev, The Univ. of Texas Medical Branch (United States)

Traumatic brain injury (TBI) and spinal cord injury are a major cause of death for individuals under 50 years of age. In the USA alone, 150,000 patients per year suffer moderate or severe TBI. Moreover, TBI is a major cause of combat-related death. Monitoring of cerebral venous oxygenation (CVO) is critically important for management of TBI patients because CVO below 50% results in death or severe neurologic complications. At present, there is no technique for noninvasive, accurate CVO monitoring. We proposed to use optoacoustic technique for noninvasive CVO monitoring by probing cerebral veins such as the superior sagittal sinus (SSS) and validated it in animal studies. In this work, we developed a novel optoacoustic system for continuous, real-time CVO monitoring and tested it in human subjects at normal conditions and during hyperventilation to simulate changes in the CVO that may occur in patients with TBI. We designed and built a highly-sensitive optoacoustic probe for SSS detection. First, we scanned the probe over the head to obtain the SSS signal. Then, continuous, multi-wavelength measurements were performed in the near infrared spectral range and the SSS oxygenation absolute values were automatically calculated in real time using a special algorithm developed by our group. Continuous measurements performed at normal conditions and during hyperventilation demonstrated that hyperventilation resulted in approximately 10% decrease of CVO. Within next few months, we are planning to test and validate the system performance in patients with TBI in whom invasive measurements of CVO are performed using catheterization.

8223-56, Session 7

## Noninvasive, optoacoustic monitoring of cerebral venous blood oxygenation in newborns

I. Y. Petrov, K. E. Wynne, Y. Y. Petrov, R. O. Esenaliev, C. J. Richardson, D. S. Prough, The Univ. of Texas Medical Branch (United States)

Cerebral ischemia after birth and during labor is a major cause of death and severe complications such as cerebral palsy. In the USA alone, cerebral palsy results in permanent disability of 10,000 newborns per year and approximately 500,000 of the total population. Currently, no technology is capable of direct monitoring of cerebral oxygenation in newborns. This study proposes the use of an optoacoustic technique for noninvasive cerebral ischemia monitoring by probing the superior sagittal sinus (SSS), a large central cerebral vein. We developed and built a multi-wavelength, near-infrared optoacoustic system suitable for noninvasive monitoring of cerebral ischemia in newborns with normal weight (NBW), low birth-weight (LBW, 1500 - 2499 g) and very low birth-weight (VLBW, < 1500 g). The system was capable of detecting SSS signals through the open anterior and posterior fontanelles as well as through the skull. We tested the system in NBW, LBW, and VLBW newborns (weight range: from 675 g to 3,000 g) admitted to the neonatal intensive care unit. We performed single and continuous measurements of the SSS blood oxygenation. The data acquisition, processing and analysis software developed by our group provided real-time, absolute measurements and visualization of the SSS blood oxygenation. The SSS blood oxygenation ranged from 60% to 80%. Optoacoustic monitoring of the SSS blood oxygenation provides valuable information because adequate cerebral oxygenation would suggest that no therapy was necessary; conversely, evidence of cerebral ischemia would prompt therapy to increase cerebral blood flow.

8223-57, Session 7

## Impulse-based near-field thermoacoustic tomography of small animals

S. Kellnberger, D. Razansky, V. Ntziachristos, Helmholtz Zentrum München GmbH (Germany)

Thermoacoustic tomography (TAT) is a non-invasive hybrid imaging technique that combines ultrasound with microwave imaging, providing high resolution images with good intrinsic contrast. Conventional thermoacoustic systems so far relied on carrier frequency amplification with long pulse durations in the order of 500ns, increasing signal to noise ratio on the one hand but also mitigating demands for high spatial resolution. In order to overcome these limitations, we developed a new thermoacoustic system which utilizes ultrahigh energy electromagnetic impulses at hundreds of mJoule with short excitation times of ~20ns. Our novel near-field radiofrequency thermoacoustic (NRT) tomography modality delivers high resolution images without loosing SNR since biological tissue dissipates a considerable amount of electromagnetic energy when placed in the near-field of a microwave or radiofrequency source. Herein we experimentally validate the NRT performance by means of highly dissipative media, consisting of copper wires with a characteristic diameter of 100µm. In addition, we imaged an ex-vivo mouse at the pelvic region. Tomographic images show a spatial resolution of 150µm, being mainly determined by the finite detection bandwidth of the transducers. Images from the mouse showcase clear anatomical details like the urinary bladder or the hindlimb together with a subcutaneously inserted copper wire for control means. Providing high resolution images, NRT is a new thermoacoustic imaging modality that goes beyond conventional TAT thresholds, offering a compact and simple setup along with economic technology. Furthermore, NRT has versatile applications since it can be scaled for small animal as well as human imaging because radiowaves have high penetration depth in biological tissue.

8223-58, Session 7

## Near-field radio-frequency thermo-acoustic imaging based on transmission lines for optimized performance

M. Omar, S. Kellnberger, Technische Univ. München (Germany) and Helmholtz Zentrum München GmbH (Germany); G. Sergiadis, Aristotle Univ. of Thessaloniki (Greece); D. Razansky, V. Ntziachristos, Technische Univ. München (Germany) and Helmholtz Zentrum München GmbH (Germany)

Near-field Radio-frequency Thermoacoustic Imaging (NRTI) is an imaging modality that was recently introduced to generate thermoacoustic signals using ultra-short high energy impulses. Because it allows for a higher energy coupling within an ultra-short time, it can achieve higher resolutions and higher signal to noise ratio, compared to traditional thermoacoustic tomography based on radiating sources at single frequencies. As for traditional thermoacoustic imaging the contrast comes from the conductivity and the dielectric properties of the tissues, while the resolution depends on the measured acoustic waves. Since NRTI depends on the efficient generation of high energy short pulses, the ability to control their time width and pulse shape is of high importance. We present here a methodology for generating such pulses based on transmission lines. We characterize the basic performance of such a pulser in terms of pulse width and energy generated, we show their ability to generate ultra-short impulses in the range of several nano-seconds to tens of nano-seconds, which allows for a resolution in the range of tens of microns to hundreds of microns. Finally the pulser is used to generate high resolution images of small absorbing insertions, of phantoms with different conductivities and of ex-vivo mouse images. From the phantoms with different conductivities it is possible to see how the signal scales with the conductivity, from ex-vivo mouse images it is possible to see several anatomical characteristics, such as the mouse boundary, the heart muscle, the lungs, the spinal cord and some muscles from the back of the mouse in the thorax region.

8223-142, Session 7

## Frequency domain photoacoustic correlation imaging: novel methodology for non-invasive imaging of biological tissues

S. A. Telenkov, R. Alwi, Univ. of Toronto (Canada); W. Shi, E. Chen, A. I. Vitkin, Ontario Cancer Institute (Canada); A. Mandelis, Univ. of Toronto (Canada)

It was demonstrated that spatially-resolved photoacoustic (PA) imaging can be accomplished using relatively long intensity-modulated laser excitation as opposed to the conventional nanosecond pulsed mode. Although this technique is very attractive for designing portable clinical instrumentation, it requires more complex signal detection and image reconstruction methods. The concept of PA sonar (or radar) was introduced to take advantage of the high signal-to-noise ratio provided by coherent signal processing and the high spatial resolution obtained as a result of signal compression. In this talk, we will show further developments of the PA sonar technology including phased array imaging and discuss possible optimization methods through coherent signal integration and design of custom modulation waveforms. Application of the novel PA imaging technology will be demonstrated using tissue phantoms and an in-vivo animal model with induced cancer lesion.

8223-53, Poster Session

## Photoacoustic and ultrasonic image co-registration using a phased array probe and frequency domain correlation processing

S. A. Telenkov, R. Alwi, Univ. of Toronto (Canada); W. Shi, E. Chen, A. I. Vitkin, Ontario Cancer Institute (Canada); A. Mandelis, Univ. of Toronto (Canada)

We present a biomedical imaging system that combines the frequency-domain photoacoustic (PA) modality and a conventional ultrasound system for hybrid image co-registration of biological tissues. We demonstrate that the same 64-element phased array probe can be used for both photoacoustic and standard ultrasound imaging. Custom designed software consisting of multi-channel matched filter processing and a digital frequency-domain beamforming algorithm is employed for reconstruction of PA images similar to the conventional B-mode ultrasound. Potential advantages and problems of dual-mode co-registration will be discussed using preliminary imaging data obtained using tissue phantoms and in-vivo animal model (immunodeficient rats) with induced intramuscular tumors.

8223-117, Poster Session

## Photoacoustic tomography of breast phantoms based on a custom-made linear array transducer

W. Xia, D. Piras, J. Van Hespen, W. Steenbergen, T. G. van Leeuwen, S. Manohar, Univ. Twente (Netherlands)

A photoacoustic tomographic system based on a custom-made linear array transducer for breast imaging is presented. 1 MHz, large area transducer elements (5 mm x 5 mm) are chosen because of their relatively high sensitivity. Acoustic lenses are used to enlarge the narrow acceptance angle of such transducer elements. The noise equivalent pressure, frequency bandwidth and angular sensitivity of the transducer elements are characterized. Different light delivery approaches are investigated to improve the image quality of the system. A back-projection algorithm is used as the imaging reconstruction. Results on breast phantoms show that the system can detect deeply embedded objects with around 1.5 mm resolution. This study also provides an insight into the capability of the system for beast cancer detection when upgraded to a 2-D array system in the future.

8223-118, Poster Session

## Detection and characterization of red blood cell (RBC) aggregation with photoacoustics

E. Hysi, R. K. Saha, M. Rui, M. C. Kolios, Ryerson Univ. (Canada)

RBCs form aggregates during periods of increased fibrinogen concentration and reduced shear rates. This phenomenon is observed in circulatory disorders such as myocardial infarction and cerebral ischemia. Currently, the only non-invasive modality assessing RBC aggregation is ultrasound. Photoacoustics combines the molecular specificity of optical methods with ultrasound resolution to provide excellent functional information. In this work, we demonstrate the potential of photoacoustics for detecting and characterizing RBC aggregation.

Non-aggregated RBCs were simulated using a Monte Carlo method. Aggregates were formed through hexagonal packing. Photoacoustic signals were computed by employing a frequency domain solution to the wave equation for fluid spheres [1]. In-vitro human RBCs measurements were conducted using the Imagio photoacoustic imaging system (Seno Medical Instruments Inc.) at 1064 and 750nm. Varying degrees of aggregation were achieved by altering the concentration of Dextran-70. The effect of hematocrit and aggregate size was investigated on time and frequency domain signal properties.

Theoretical photoacoustic signals for non-aggregating RBCs monotonically increased with increasing hematocrit. Photoacoustic signal amplitude of aggregated samples along with their spectral intensity at 15.6MHz, increased significantly as the aggregate size increased (11dB for 10.13μm). Experimental results show good agreement with the predicted increase in signal amplitude with increasing hematocrit. For the most aggregated RBCs a ~10dB enhancement at 4MHz compared to the non-aggregated case was observed.

The photoacoustic method discussed here has never been applied to RBC aggregation. It demonstrates the feasibility of using photoacoustics for the clinical detection and assessment of RBC aggregation.

[1] Saha et al, JASA, 129(5), 2011.

8223-119, Poster Session

## Optimising the excitation and detection parameters for deep-tissue photoacoustic imaging applications

T. J. Allen, E. Zhang, P. Beard, Univ. College London (United Kingdom)

For photoacoustic tomography of large tissue volumes such as the breast, ultrasound detectors made of PVDF or PZT materials with large element size (>1mm) and narrow bandwidth (<5MHz) are generally used, as they can provide the required high sensitivity to achieve imaging depths of several centimeters. However, these detectors are generally not optimised in terms of bandwidth and element size. Furthermore it is not always obvious which piezoelectric material provides the highest sensitivity. For example, piezoelectric PVDF provides a higher receiving constant (1.74mVmN-1) than PZT (0.26mVmN-1) suggesting a higher intrinsic sensitivity. However the resonant nature of PZT detectors can provide a higher sensitivity over a narrow bandwidth that coincides with the spectral content of the photoacoustic wave leading in some circumstances to a higher overall SNR. Also, when imaging relatively deep anatomical features, spatial resolution is likely to be limited by the effects of frequency dependent acoustic attenuation of tissue. It may therefore be possible to increase the SNR of the detected photoacoustic signal by using long excitation pulses to downshift the acoustic frequency content of the generated photoacoutic signal in order to reduce the effect of acoustic attenuation of tissue, without degrading the spatial resolution.

In this study, the optimum bandwidth and element size of the detectors were deduced by investigating their effects on the SNR and spatial resolution of photoacoustic images. To achieve this, the generation, propagation and detection of photoacoustic signals in a 2D cylindrical imaging geometry were simulated and an image reconstructed. The effects of varying the excitation pulse durations (10ns to 1μs) on the reconstructed photoacoustic image were also investigated, in order to determine the optimum pulse duration which would provide the highest SNR without degrading the spatial resolution. The impulse responses of a range of detectors were also modeled to establish which piezoelectric material (PVDF, PZT, piezo-composites) would provide the highest sensitivity for the desired bandwidth and element size. A range of piezoelectric detectors and an optical ultrasound sensor were also compared experimentally. To achieve this, single point measurements were made in a tissue mimicking phantom allowing the maximum imaging depth to be determined. These detectors were also incorporated within a 2D cylindrical scanner to image a breast tissue mimicking phantom. These results provide a new framework for optimising the design of photoacoustic scanners for breast and other deep tissue imaging applications.

8223-120, Poster Session

## 3D photoacoustic imaging via staring, sparse approach at 0.7 FPS

M. B. Roumeliotis, J. J. L. Carson, Lawson Health Research Institute (Canada)

Photoacoustic imaging is a hybrid modality that serves to combine the benefits of the strong contrast inherent to optical imaging with the enhanced penetration depth and resolution from ultrasound imaging. One approach to 3D photoacoustic imaging is to utilize a separate data acquisition and storage channel on each acoustic transducer. With this approach, a staring, sparse array of transducers (30 transducers in a hemispherical arrangement) was recently used to produce photoacoustic images of optically-absorbing objects in 3D at 0.7 frames per second [Opt. Express 19, 13405 (2011)]. The reconstruction technique utilized an experimentally measured imaging operator that was applied to a linear system model. An estimate of the object in the field of view of the transducer array was computed directly by multiplying the pseudoinverse of the imaging operator with the acquired transducer data. Due to the limited number of transducers, simple objects such as point and line sources were used to test the system capabilities. Here, we report 3D photoacoustic imaging via a similar system and reconstruction technique of a variable number and orientation of line objects in a backward mode illumination scheme. The results provide insight into the system limitations as the number of line sources (object complexity) is systematically increased in object space. In the future, these results will provide context and restrictions on biologically relevant imaging tasks that can be successfully completed.

8223-121, Poster Session

## Laser-diode based 10MHz photoacoustic Doppler flowmetry at 830 nm

A. Sheinfeld, A. Eyal, Tel-Aviv Univ. (Israel)

Photoacoustic Doppler Flowmetry (PDF) has several potential advantages over its purely ultrasonic counterpart. The key ones are better inherent contrast and the useful molecular information it can provide. It is therefore highly desired to continue developing this modality into a viable complimentary tool alongside with Doppler Ultrasound flowmetry. Working towards this goal we have constructed a PDF setup based on a combined pair of laser diodes at 830nm and a 10MHz focused acoustical transducer. To allow depth resolved spectral analysis we directly modulated the diodes with a long coherent series of tone-bursts and analyzed the received PA signal via the short time Fourier transform. To characterize the PDF system we used a polymer tube attached to a syringe pump which infused into it either a suspension of graphite micro-particles or blood. Our measurements resulted with high quality spectrograms at axial and spectral resolutions of ~300 micron and 1Hz respectively in the case of the graphite suspension. The measurement of blood, on the other hand, was significantly less repeatable and while flow-induced spectral contents could be observed occasionally, reliable spectrograms could not yet be obtained. The difference between the behaviors of the two fluids is attributed mainly to their significantly different heterogeneity. We also performed a k-space based simulation of moving random spatial distributions of red blood cells. Using the theory of linear time-varying systems to estimate the frequency response we compared the spectra of different particles concentrations and observed a decrease in the normalized Doppler signal with increased concentration.

8223-122, Poster Session

## Wide-spectral range quantitative photoacoustic spectroscopy to measure non-linear optical absorption of hemoglobin

A. Danielli, K. I. Maslov, L. V. Wang, Washington Univ. in St. Louis (United States)

Functional photoacoustic microscopy (PAM) is a valuable tool for quantifying hemoglobin oxygenation within single vessels. Recently, optical-resolution PAM was developed to achieve higher resolution by reducing the laser beam diameter, which increased the light intensity. As intensity increases, saturation of the optical absorption and multi-photon/multi-step absorption can occur, which, together with the temperature dependence of thermal expansion, result in a nonlinear dependence of the photoacoustic signal on the excitation pulse fluence. For hemoglobin, the major absorber in tissue for photoacoustic imaging, these non-linear phenomena have strong wavelength dependence. To enable quantitative photoacoustic measurements at different wavelengths in the presence of nonlinearity, a careful wide range analysis of the intensity-dependent absorption should be performed. Here, we built a photoacoustic spectrometer, using a tunable nanosecond optical parametric oscillator that operates between 410 nm and 2400 nm as our light source. To reduce uncertainty in our measurements due to inhomogenous spatial distribution of the optical fluence, we used a flat-top beam illumination and a flat transducer which was mounted in reflection mode, effectively reducing quantitative measurements to a one dimensional problem. The intensity-and concentration-dependent non-linear spectra of the photoacoustic signals of oxy- and deoxy-hemoglobin were obtained. These measurements have the potential to contribute significantly to quantitative functional PAM.

8223-123, Poster Session

## Monitoring of streptozotocin-induced diabetes in a mouse model by photoacoustic microscopy

A. Krumholz, J. Yao, L. V. Wang, Washington Univ. in St. Louis (United States)

Diabetes, characterized by excess glucose in the blood stream, is a risk factor increasing retinopathy, renal failure, and cardiovascular disease. Photoacoustic microscopy can provide a new tool for measuring parameters associated with diabetes-induced damage to the microvasculature. To produce an animal model for Type 1 diabetes, streptozotocin (STZ) is particularly toxic to the insulin-producing beta cells of the pancreas in mammals, has been widely used. In this work, ND4 Swiss Webster mice received intraperitoneal injections of an STZ solution for five consecutive days at a concentration of 50 mg/kg. Most mice developed a very significant rise in blood glucose level (>500 mg/dL) within three weeks of administration of STZ. Changes in vasculature and hemodynamics were tracked for six weeks, with each mouse's baseline acting as its own control. The left ear of each mouse was imaged with an optical resolution photoacoustic microscope at a third order branch of the main vasculature. Blood glucose level, body weight, vessel diameter, total hemoglobin, hemoglobin oxygen saturation, and blood flow speed were monitored. From these measurements it was possible to estimate the oxygen consumption in the tissue, and therefore the metabolic rate. Changes associated with the disease included vessel occlusion and increased flow speed.

8223-124, Poster Session

## Image quality improvement for photoacoustic imaging systems employing linear transducer arrays

A. Petschke, P. J. La Rivière, The Univ. of Chicago Medical Ctr. (United States)

Traditionally, photoacoustic imaging systems have used simple one-step reconstruction algorithms such as backprojection and filtered backprojection. Recently, in an effort to improve image quality, there has been interest in potentially more accurate algorithms such as iterative reconstruction algorithms. However, most of these require increases in computation time which preclude them at present from real-time imaging, or at least increase the cost of the imaging system. In addition, these algorithms are not compatible with existing ultrasound systems, which may prevent their use in combined ultrasound and photoacoustic imaging systems. In this paper we perform a systematic study of image quality for the backprojection and filtered backprojection reconstruction algorithms for different sampling rates, apodization functions, and deconvolution filters. For this study we use a 38 mm, 3.5 MHz linear transducer array in the 3D forward model and include a cylindrical lens in the elevation direction. The image reconstruction is 2D, and for the filtered backprojection reconstruction we use a ramp filter. To quantify image quality of this linear, shift-variant system we define the signal-to-noise ratio (SNR) as the volume under the local noise equivalent quanta (LNEQ) curve. This SNR is a measure of the signal detectability of an ideal observer when the signal and background are known exactly. We find that the image quality in terms of the SNR, resolution, and streak length can be significantly improved by oversampling to prevent time quantization errors and applying an apodization function and deconvolution filter. These improvements are applicable to real-time imaging systems, and oversampling and apodization with backprojection are applicable to existing ultrasound beamformers.

8223-125, Poster Session

## Photoacoustic imaging of RF ablations in cardiac tissue

R. R. Bouchard, The Univ. of Texas M.D. Anderson Cancer Ctr. (United States); L. Di Base, A. Natale, St. David's Medical Ctr. (United States); S. Y. Emelianov, The Univ. of Texas at Austin (United States) and The Univ. of Texas M.D. Anderson Cancer Ctr. (United States)

Radiofrequency (RF) ablation procedures are used to destroy abnormal electrical tissue in the heart that can cause cardiac arrhythmias. Current methods relying on echocardiography and electrical conduction mapping are unable to accurately assess ablation lesion size. In an effort to better visualize RF lesions, photoacoustic (PA) and ultrasonic (US) imaging were utilized to obtain co-registered images of ablated porcine cardiac tissue. The left ventricular free wall of fresh (i.e., never frozen) porcine hearts was harvested within 24 hours of the animals' sacrifice. A THERMOCOOL® Ablation System (Biosense Webster, Inc.) operating at 40 W for 30-60 s was used to induce ablations through the endocardial wall of the cardiac samples. Following lesion creation, the ablated tissue samples were cast into 8% gelatin to allow for acoustic coupling while helping preserve the samples during multi-wavelength PA imaging. Samples were imaged with a Vevo® 2100 system (VisualSonics, Inc.) using a modified 20-MHz array that could provide laser irradiation to the sample from a Pro-290-10 pulsed tunable laser (Newport Corp) to allow for co-registered PA and US imaging. PA imaging was conducted from 720-1020 nm with a surface fluence of approximately 15 mJ/cm^2 maintained during imaging. With PA imaging, the ablated region could be well visualized, with contrasts of 25 dB achieved at 750 nm. Although imaging penetration depth is a concern, PA imaging shows promise in being able to reliably visualize RF ablation lesions.

8223-126, Poster Session

## Photoacoustic microscopy imaging of spheroids with endogenous and exogenous contrast

M. Rui, M. C. Kolios, Ryerson Univ. (Canada)

Photoacoustic microscopy can be used to generate images of cells and cells constructs with high spatial resolution and contrast. Here we demonstrate photoacoustic microscopy with micron-level axial and lateral resolution for the imaging of spheroids with endogenous and exogenous contrast. For the endogenous contrast spheroids, breast cancer MCF-7 cells and B16F1 melanocytes were made by the hanging-drop method at a cell ratio of 2:1. For the exogenous contrast spheroids, MCF-7 cells were incubated with gold nanorods (780nm absorption) for 24 hours and mixed with native MCF-7 cells (number ratio of 6:1). The spheroids were ~0.5 mm in diameter. Imaging was performed with a high-resolution photoacoustic microscope based on the SASAM acoustic microscope (Kibero GmbH, Germany). A 200MHz transducer (0.5mm aperture and focal length) was used for the detection of the photoacoustic waves, and all spheroids were illuminated with short laser pulses (700 ps, 1064nm) from a diode pumped passively Q-switched Nd:YAG at a laser fluence of 3.57 J/cm2. Strong photoacoustic signals were detected for both spheroids (signal to noise typically > 20). Images of the MCF7-B16F1 spheroid showed the formation of a speckle patterns, whereas the MCF7-nanorod spheroid showed distinct locations of strong photoacoustic signals, smaller than the size of fully developed speckle. The signals from the MCF7-nanorod spheroid is thought to coincide with the intracellular aggregates of gold nanorods, as occurs when imaging single nanorod-loaded MC7 cells. In summary, photoacoustic microscopy with micron-level lateral and axial resolution is demonstrated for spheroids with endogenous and exogenous contrast.

8223-127, Poster Session

## 2.5-mm outer diameter photoacoustic endoscopic mini-probe based on highly sensitive PMN-PT ultrasonic transducer

J. Yang, Washington Univ. in St. Louis (United States); R. Chen, The Univ. of Southern California (United States); C. P. Favazza, J. Yao, Washington Univ. in St. Louis (United States); Q. Zhou, K. K. Shung, The Univ. of Southern California (United States); L. V. Wang, Washington Univ. in St. Louis (United States)

Development of a photoacoustic endoscopic “mini-probe” for use in an instrument channel of a conventional video endoscope probe is an important strategy for realizing the benefits of photoacoustic endoscopy. Standard video endoscope instrument channels are 2.8 or 3.7 mm in diameter. In this study, we developed a 2.5-mm outer diameter photoacoustic endoscopic mini-probe with a highly-sensitive PMN-PT ultrasonic transducer. The 2.5-mm diameter includes the entire outer sheath. The PMN-PT ultrasonic transducer has a ~1.8-mm aperture and ~40-MHz center frequency (~40% fractional bandwidth). The new endoscopic probe employs the same scanning mirror and micromotor-based, built-in actuation mechanism described in our previous reports; however, the length of the rigid distal section of the new probe was also further reduced to ~35 mm. We performed several experiments to quantify the new transducer’s imaging resolution and signal-to-noise ratio (SNR), and compared the SNR to other types of transducers. Despite a much smaller aperture size, the SNR of the PMN-PT ultrasonic transducer is ~1.6 times higher than our previously used LiNbO3 crystal-based transducers with apertures around 2.6 mm. The presented experimental results validate the PMN-PT transducer’s improved performance over previous transducers and demonstrate the photoacoustic endoscopic mini-probe’s in vivo imaging capability.

8223-128, Poster Session

## A hand-held, low-cost photoacoustic microscopic probe

B. Huang, K. I. Maslov, W. D. Richard, L. V. Wang, D. M. Zar, Washington Univ. in St. Louis (United States)

We report on the development of a portable, low-cost photoacoustic microscopy system, primarily for cutaneous imaging of skin lesions. We have developed imaging techniques for this application that use large, non-portable ultrasonic scanning equipment. The recent development of low-cost, Universal Serial Bus (USB) based ultrasound probes that connect to laptops provides an opportunity to significantly lower the cost of photoacoustic microscopy systems. We have combined a traditional laser source with a low-cost USB probe and produced images of rabbit tissue using through transmission photoacoustic imaging. Our latest work on an integrated probe for in-vivo imaging of human skin lesions is described in detail.

8223-129, Poster Session

## Tissue-mimicking phantoms for photoacoustic and ultrasonic imaging

R. R. Bouchard, The Univ. of Texas M.D. Anderson Cancer Ctr. (United States); J. Cook, The Univ. of Texas at Austin (United States); S. Y. Emelianov, The Univ. of Texas at Austin (United States) and M.D. Anderson Cancer Ctr. (United States)

In combined photoacoustic (PA) and ultrasonic (US) imaging, both the optical and acoustical properties of an imaged medium play an important role in image formation. Consequently, with the increased use of combined PA and US imaging in pre-clinical and clinical applications, the ability to design and fabricate a phantom that is capable of mimicking the optical and acoustical scattering/absorption properties of biological soft tissue will be crucial. To this end, gelatin-based phantoms were constructed with various additives to provide realistic levels of tissue scattering and absorption. Forty-micron silica particles were added to induce acoustic scattering, Intralipid 20% IV fat emulsion was added to cause optical scattering, while India ink, Direct Red 81, and Evans blue dyes were added to set the optical absorption of the phantoms. The following parameters were then measured in each phantom formulation: speed of sound, acoustic attenuation, acoustic backscatter coefficient, optical absorption, and optical attenuation. Results from these measurements were then compared to similar measurements, which are offered by the literature, for various soft tissue types. Based on these comparisons, it was shown that a reasonably accurate tissue-mimicking phantom can be constructed using a gelatin base with the aforementioned additives. Thus, it is possible to construct a phantom that mimics specific tissue acoustical/optical properties for the purpose of combined PA and US imaging studies.

8223-130, Poster Session

## In vivo quantitative evaluation of gold nanocages' kinetics in sentinel lymph nodes by photoacoustic imaging

X. Cai, W. Li, Washington Univ. in St. Louis (United States); C. Kim, Univ. at Buffalo (United States); Y. Yuan, Y. Xia, L. V. Wang, Washington Univ. in St. Louis (United States)

As a new class of sentinel lymph node (SLN) tracers for photoacoustic (PA) imaging, Au nanocages offer the advantages of noninvasiveness, strong optical absorption in the near-infrared region (for deep penetration), and accumulation in higher concentrations than the initial injected solution. By monitoring the amplitude changes of PA signals in an animal model, we quantified the accumulations of nanocages in SLNs over time. Based on this method, we quantitatively evaluated the kinetics of gold nanocages in SLN in terms of concentration, size, and surface modification. We could detect the SLN at an Au nanocage injection concentration of 50 pM and a dose of 0.1mL in vivo. This concentration (50 pM) is about 40 times less than the previously reported value. We also investigated the influence of nanocages' size (50 nm and 30 nm in edge length), and the effects of surface modification (with positive, or neutral, or negative surface charges). The results are helpful to develop this AuNC-based PA imaging system for noninvasive lymph node mapping, providing valuable information about metastatic cancer staging.

8223-131, Poster Session

## Multiphoton photoacoustic microscopic imaging of fluorescently labeled neuron populations

G. Sela, H. Dana, I. Brosh, Technion-Israel Institute of Technology (Israel); D. Razansky, Helmholtz Zentrum München GmbH (Germany); S. Shoham, Technion-Israel Institute of Technology (Israel)

Optical resolution photoacoustic microscopy (OR-PAM) is the only imaging modality capable of imaging absorption contrasts non-invasively with cellular and sub-cellular resolution, however, the optical resolution deteriorates rapidly in the highly scattering environment of biological tissues. To maintain microscopic resolution deeper within biological tissue, photoacoustics based on multi photon absorption may be advantageous, because multiphoton excitation essentially occurs only in a small focal volume while avoiding bleaching and thermal damage to the tissue above the focal plane. Moreover, because multiphoton excitation provides optical axial sectioning, axial resolution will be independent of the US probe's frequency and bandwidth, as well as relatively independent of imaging depth.

In this work, we demonstrate microscopic femtosecond photoacoustic imaging of mammalian cortical neurons labeled with organic and genetically encodable calcium sensitive fluorescent indicators. Our imaging system uses a laser-scanning microscope with a low repetition rate (150KHz) 800nm femtosecond laser source and unfocused ultrasonic transducers. We find that the photoacoustic neuron images measured by the system are highly correlated with the underlying reference fluoresence images. Femtosecond photoacoustic microscopic imaging of fluorescent dyes can provide complementary structural and functional biological information, and has the potential for enabling deeper and/or more rapid high resolution in vivo functional imaging than possible with multiphoton fluorescence imaging.

8223-132, Poster Session

## Design of an optimum ultrasound pattern to minimize multiple-scattered light reflected from inhomogeneous tissue

P. Pereira, S. S. Sherif, Univ. of Manitoba (Canada)

The refractive index of tissue is closely related to its density. Therefore pressure changes caused by an ultrasound pattern inside tissue will modify both its density and its refractive index. It has been demonstrated previously that the presence of ultrasound in tissue can reduce the negative effect of multiple-scattered light on imaging. We present an approach to generate a standing wave based ultrasound pattern inside inhomogeneous tissue that would result in an optimum modulation of its refractive index to minimize multiple-scattered reflected light at a detector. We design the desired ultrasound pattern using COMSOL Multiphysics and verify its performance using our fast simulator of multiple-scattered optical field in tissue. We use COMSOL Multiphysics's acoustics package to simulate the effect of different ultrasound standing waves on the density of tissue and then relate it to the change in refractive index using the well-known Lorentz-Lorenz model. This optimum ultrasound pattern could be used to design and implement an integrated- computational optical coherence tomography (OCT) system with extended depth of imaging.

8223-133, Poster Session

## Modeling comparison of optical-resolution photoacoustic microscopy and optical coherence tomography

Y. Liu, C. Zhang, S. Hu, Y. Suzuki, Z. Xu, S. L. Ferradal, L. V. Wang, Washington Univ. in St. Louis (United States)

The penetration depth achievable with ballistic optical imaging technologies is limited by scattering of light. To study the effect of scattering on signal degradation and localization, we classified the signals in optical-resolution photoacoustic microscopy (OR-PAM) and optical coherence tomography (OCT) into two categories (Class I and II). The Class I signal carries the information of the optical property in the target volume, which is defined by the system resolution, while the Class II signal does not carry such information and degrades the desired signal. Through Monte Carlo simulation, we found that the Class I signal of both modalities decays at a rate close to the extinction coefficient of the medium in the case of low objective NA, while the Class II signal decays much more slowly due to multiple scattering. In OCT, the decay rate of the Class II signal decreases with increasing depth, until it almost reaches a plateau within the depth of one transport mean free path. This result shows a poor capability of OCT to reject unwanted signal, which leads to degradation of resolution and contrast, and ultimately limits the penetration depth. Because of the acoustic detection, the axial resolution of OR-PAM is not degraded by light scattering and OR-PAM can reject most of the unwanted signals generated outside the acoustic focal zone.

8223-134, Poster Session

## Dichroic photoacoustic microscopy of amyloid plaques in a transgenic mouse model

K. I. Maslov, S. Hu, P. Yan, J. Lee, L. V. Wang, Washington Univ. in St. Louis (United States)

A widely used diagnostic for amyloidosis is based on Congo red (CR) staining of amyloid fibrils, wherein the CR molecules are oriented along the long fiber axis and exhibit strong linear birefringence and dichroism. The principal diagnostic criterion of amyloidosis is the detection of so-called apple-green birefringence from CR-stained tissue sections using polarized light microscopy. Strong linear dichroism of CR-stained amyloid fibrils implies polarization-dependent optical absorption, which can be differentiated from non-dichroic background optical absorption. Moreover, in contrast to birefringence, dichroism can easily be detected in reflection mode and hence has potential for in vivo imaging of amyloid plaques. Here, we report our very recent development of dichroic photoacoustic microscopy (D-PAM), where brain sections from APP/PS1 mice (an Alzheimer's disease mouse model) stained with CR are illuminated alternatingly by laser pulses of two orthogonal linear polarization states. Differential images acquired from two polarization states show greatly enhanced contrast of amyloid deposits. Validation using conventional fluorescence microscopy shows that D-PAM has sufficient sensitivity and spatial resolution to identify amyloid plaques.

8223-135, Poster Session

## Time-resolved transient absorption ultrasonic microscopy measurements of the ground state recovery time

R. L. Shelton, B. E. Applegate, Texas A&M Univ. (United States)

Transient Absorption Ultrasonic Microscopy (TAUM) is a recently developed hybrid imaging modality that uses photoacoustic microscopy to exploit transient absorption, a two-photon, molecular process. TAUM enables ultrahigh-resolution photoacoustic imaging, attributed to the squared intensity dependence of the point spread function, equivalent to confocal microscopy. The amplitude of the TAUM signal is a function of the interpulse delay between the pump and probe pulses. Varying the interpulse delay and plotting the amplitude of the TAUM signal against the delay measures the ground state recovery time of the chromophore. Physically, the ground state recovery time is the time it takes for the ground state to repopulate after photoexcitation. It is an exponential function of time and analogous to the fluorescence lifetime. Likewise, it may be used in much the same way to differentiate signals from multiple chromophores, such as oxy- and deoxy- hemoglobin. As a proof of concept experiment, the ground state recovery time of R6G was measured using two 532 nm laser sources (pulse duration < 1 ns) and a programmable pulse delay generator. The measured recovery time was ~ 3 ns, which is consistent with the known fluorescent lifetime of R6G. We would expect close agreement between the fluorescence lifetime and ground state recovery time when the dominant path back to the ground state is fluorescence emission. Measurements on whole blood where hemoglobin is the dominant absorber yielded a recovery time of ~ 8 ns, which is also consistent with previously published pump-probe based measurements.

8223-136, Poster Session

## Photoacoustic microscopy of intestinal hemodynamics following massive small bowel resection

J. Yao, Washington Univ. in St. Louis (United States); K. J. Rowland, Washington Univ. School of Medicine in St. Louis (United States); L. Wang, K. I. Maslov, Washington Univ. in St. Louis (United States); B. W. Warner, Washington Univ. School of Medicine in St. Louis (United States); L. V. Wang, Washington Univ. in St. Louis (United States)

Massive small bowel resection (SBR) results in villus angiogenesis and intestinal adaptation. The exact mechanism that causes intestinal villus angiogenesis remains unknown. We hypothesize that hemodynamic changes within the remnant bowel after SBR will trigger intestinal angiogenesis. To validate this, we used photoacoustic microscopy (PAM) to image the microvascular system of the intestine in C57B6 mice and to measure blood flow and oxygen saturation (sO2) of a supplying artery and vein. Baseline measurements were made 6 cm proximal to the ileal-cecal junction (ICJ) prior to resection. A 50% proximal bowel resection was then performed, and measurements were again recorded at the same location immediately and 7 days following resection. The results show that arterial and venous sO2 were similar prior to SBR. Immediately following SBR, the arterial and venous sO2 decreased by 14.3 ± 2.7% and 32.7 ± 6.6%, respectively, while the arterial and venous flow speed decreased by 62.9 ± 17.3% and 60.0 ± 20.1%, respectively. Such significant decreases in sO2 and blood flow indicate a hypoxic state after SBR. Within one week after SBR, both sO2 and blood flow speed had gradually recovered. By 7 days after SBR, arterial and venous sO2 had increased to 101.0 ± 2.9% and 82.7 ± 7.3% of the baseline values, respectively, while arterial and venous flow speed had increased to 106.0 ± 21.4% and 150.0 ± 29.6% of the baseline values, respectively. Such increases in sO2 and blood flow may result from angiogenesis following SBR.

8223-137, Poster Session

## Molecular probes for imaging of enzyme activity by photoacoustic lifetime imaging (PALI)

E. Morgounova, Q. Shao, S. Abdo, M. Wilson, G. Barany, S. Ashkenazi, Univ. of Minnesota, Twin Cities (United States)

Photoacoustic lifetime imaging (PALI) is a technique that combines photoacoustic imaging with the high robustness of probing excitation lifetime of molecules. Fusing PALI with exogenous agents provides high contrast molecular imaging in tissues due to large differences in lifetime between contrast agents and tissue components. Methylene Blue (MB) is an FDA approved dye that exhibits long intrinsic lifetime (70 µs). Energy transfer between a dimer pair, however, quenches MB inter-system crossing resulting in a short lifetime. This contrast allows for the in-vivo imaging of molecular processes by an enzyme specific probe consisting of two MB molecules bound by a enzyme-specific, cleavable, peptide link. Upon cleavage, the two molecules will diffuse separately and recover their long lifetime, enabling their detection by PALI.

We have tested a model system comparing PALI signals generated by both forms of MB. The ratio of dimers to monomers in our model system is controlled by adding sodium sulfate in solution. The dimers-to-monomers ratio is verified by spectroscopy. Our measurements show that increasing sodium sulfate concentration from 0 to 0.75 M reduces the photoacoustic lifetime contrast by half. This suggests that dimers are strongly quenched during the excitation and do not reach a triplet state. Contrarily, monomers present a high quantum yield in inter-system crossing and high photoacoustic constrast.

The translation of this technique to clinical applications and the gain in depth and resolution compared to current fluorescence imaging methods can bring substantial improvements in areas as varied as inflammation-related disease diagnosis, drug tailoring and cancer screening.

8223-138, Poster Session

## Modeling optical phase conjugation of ultrasonically encoded signal utilizing finite-difference time-domain simulations

J. L. Hollmann, C. A. DiMarzio, Northeastern Univ. (United States)

Strong scattering of light propagating through tissue limits the maximum focal depth of an optical wave, inhibiting the use of light in medical diagnostics and therapeutics. However, turbidity suppression has been demonstrated utilizing phase conjugation with an ultrasound (US) generated guide star. We analyze this technique utilizing a Finite-Difference Time-Domain (FDTD) simulation to propagate an optical signal in a synthetic skin model. The US beam is simulated as perturbing the indicies of refraction proportional to the acoustic pressure for four equally spaced phases. By the Nyquist criterion, this is sufficient to capture DC and the fundamental frequency of the US. The complex optical field at the detector is calculated utilizing the Hilbert transform, conjugated and ``played back" through the media. The resulting field travels along the same scattering paths and converges upon the US beam's focus. The axial and transverse resolution of the system are analyzed and compared to the wavelength of the optical and US beams. The source geometries are varied and the effect of a finite etendue is modeled and studied to aid in system design.

8223-139, Poster Session

## Inducible expression of photoacoustic reporter gene tyrosinase in cells using a single plasmid

R. J. Paproski, R. J. Zemp, Univ. of Alberta (Canada)

We have previously demonstrated that tyrosinase is a reporter gene for photoacoustic imaging since tyrosinase is the rate-limiting step in the synthesis of melanin, a pigment capable of producing strong photoacoustic signals. We previously created a cell line capable of inducible tyrosinase expression (important due to potential toxicity of melanin) by stably transfecting tyrosinase in a specialized MCF-7 Tet-On cell line from Clontech which expresses a doxycycline-controlled transactivator. Sensitive in-vivo molecular imaging has been demonstrated using this system. Unfortunately, there are few available Tet-On advanced cell lines. In order to simplify the creation of cell lines with inducible expression of tyrosinase, we created a single plasmid that encodes both the doxycycline-responsive transactivator as well as tyrosinase. The transactivator sequence within the Tet-On Advanced plasmid was amplified by polymerase chain reaction (PCR) using 5′ and 3′ primers containing XhoI and HindIII restriction enzyme sites, respectively. The tyrosinase sequence from the pTRE-Tight-TYR plasmid was amplified by PCR using 5′ and 3′ primers containing SacII and PstI restriction enzyme sites, respectively. Both PCR products were cloned into the pEGFP-N1 plasmid using the above restriction enzymes. The newly created plasmid was transfected in HEK293 cells using lipofectamine and cells were cultured in medium containing 1 µg/mL doxycycline. After several days, brown melanin was observed in some of the HEK293 cells, suggesting that the newly created plasmid should allow inducible tyrosinase expression in many different cells lines, simplifying the use of this photoacoustic reporter gene for other researchers.

8223-140, Poster Session

## Characterization of dual-contrast microbubbles for photoacoustic and ultrasound imaging

R. F. Castelino, Univ. of Toronto (Canada) and Sunnybrook Health Sciences Ctr. (Canada); A. L. Martin, Sunnybrook Health Sciences Ctr. (Canada); F. S. Foster, Univ. of Toronto (Canada) and Sunnybrook Health Sciences Ctr. (Canada)

Contrast agents (CA) that permit multiple imaging/therapy applications using a single agent is beneficial as it can provide the ability for simultaneous imaging from different modalities while also possibly improving intracellular deposition and detection sensitivity.

In this work, a dual contrast agent that allows both ultrasound (US) and photoacoustic (PA) imaging by incorporating gold nanorods (AuNRs) to the surface of microbubbles (MB) will be discussed. PA imaging utilizes light to generate US and thus can exploit optical absorption of the AuNRs that are undetectable using a purely ultrasonic technique. While using non-linear acoustic techniques, it is possible to image and track the dual agent deeply in tissue with sound alone.

These dual agents are constructed of MBs composed of a perfluorocarbon gas core encapsulated by a positively charged lipid shell, on which negatively charged AuNRs are attached via an electrostatic interaction. Imaging and characterization of these particles was performed using a high frequency linear array (Vevo2100, VisualSonics), equipped with a 20 MHz center frequency probe. Imaging these particles show an in increase in image contrast in both non-linear and PA modes when compared to conventional B-mode imaging without compromising cell viability. Further acoustic and PA characterization of the particles are studied in vitro to demonstrate their feasibility as dual contrast agents.

8223-141, Poster Session

## Signal-to-noise-ratio scaled coherence weighting for photoacoustic array imaging

Y. Wang, P. Li, National Taiwan Univ. (Taiwan)

Ultrasound array systems with conventional delay-and-sum beamformers are often adopted for high frame rate photoacoustic imaging. In this report, we propose a coherence factor (CF) based imaging approach to further improve the image contrast of such array systems by suppressing sidelobes of the acoustic diffraction pattern. Specifically, minimum variance based coherence factor (CFMVDR) is used. Furthermore, because CF-based weighting is susceptible to variations in signal-to-noise-ratio (SNR), we also adopt a Wiener filter approach to alleviate this problem so that the method can perform well under all SNR conditions. This is of particular interest as the SNR in photoacoustic imaging is typically low. To test this method, a human hair and a graphite phantom were used as test subjects. The imaging system consisted of a 523nm pulsed laser, and a 128-channel linear array (bandwidth from 5 to 10MHz) for photoacoustic signal detection. It is demonstrated that the beam widths (i.e., lateral resolution) can be effectively improved and the noise background is suppressed by 20 dB. The contrast improvement is also evident.

8223-143, Poster Session

## Optoacoustic signal characterization of laser heated tissues

A. Ladéroute, Univ. of Prince Edward Island (Canada); M. P. Patterson, Univ. of Prince Edward Island (Canada) and Atlantic Veterinary College (Canada); M. C. Kolios, Ryerson Univ. (Canada); W. M. Whelan, Univ. of Prince Edward Island (Canada) and Atlantic Veterinary College (Canada)

Laser thermal therapy involves heating tissue using light to temperatures between 55°C and 95°C for several minutes resulting in coagulation and cell death. This treatment method has been under investigation for use as a minimally invasive method for treating solid tumors and cancer cells. Heating tissues results in highly variable outcomes and challenges; for example, ensuring complete coagulation of the target tissue while avoiding damage to surrounding healthy tissues. Overcoming such challenges requires precise and real-time monitoring. Optoacoustic (OA) imaging has been proposed as a real-time, noninvasive method for monitoring laser thermal therapy providing an optical solution to treatment delivery and assessment. In this study, 6 mm diameter surface lesions were generated in ex-vivo porcine muscle using a 1000 µm core optical fiber coupled to an 810 nm diode laser. Lesions were scanned using a prototype reverse-mode optoacoustic system consisting of a pulsed laser which operates at 1064 nm and 775 nm coupled to a bifurcated fibre bundle, and an 8 element annular array wideband ultrasound transducer with a central frequency of 4MHz. OA detection was performed across lesions and axially within the lesions with a pulse energy of 6.5 mJ. Optoacoustic contrast values (i.e. coagulated vs native tissues) of 4.9 and 2.2 across lesions and 2.0 and 1.4 axially were observed for 775 nm and 1064 nm illuminations respectively. These results demonstrate that optoacoustic signals increase with tissue thermal damage and suggests that 775 nm illumination may offer improved OA contrast compared to 1064 nm illumination for detecting tissue coagulation.

8223-144, Poster Session

## Measuring metabolic rate of oxygen with combined photoacoustic microscopy and optical coherent tomography in small animals

T. Liu, Northwestern Univ. (United States); S. Jiao, The Univ. of Southern California (United States); H. F. Zhang, Northwestern Univ. (United States)

In this report, we demonstrate the feasibility of measuring metabolic rate of oxygen (MRO2) at the microvascular level in vivo without extrinsic contrast agent using a combined laser-scanning optical-resolution photoacoustic microscopy (LSOR-PAM) and spectral-domain optical coherence tomography (SD-OCT). Firstly the flow rate in a phantom made by two connected capillary tubes with different diameters was measured to verify the flow volume measurement. Then we imaged two parallel vessels selected from a mouse ear. The hemoglobin oxygen saturation (sO2) and the vessel diameter were measured by the LSOR-PAM, the blood flow velocity was measured by the Doppler SD-OCT, and the total concentration of hemoglobin was measured by drawing blood from the animal after the experiments. Blood flow rate and MRO2 were further calculated based on the above experimental values. Four wavelengths (570nm, 578nm, 588nm, and 590nm) were used in LSOR-PAM to measure sO2. We verified the self-consistence in the multimodal imaging system by comparing the measured flow rates in the two-tube phantom and the in the selected pair of vessels.

8223-145, Poster Session

## High-sensitivity polymer inverted-rib optical waveguide interferometric sensor for optoacoustic imaging

D. C. Gallego, H. Lamela, Univ. Carlos III de Madrid (Spain); M. Wang, Univ. of Oulu (Finland); J. Hiltunen, VTT Technical Research Ctr. of Finland (Finland); R. Myllylä, Univ. of Oulu (Finland)

Optoacoustic tomography (OAT) is a non-invasive and non-ionizing imaging technique to visualize biological soft tissues. It takes the superior contrast based on the optical absorption and the spectroscopy capacity from the optical tomography and its high spatial resolution from the ultrasonic imaging. These features make it suitable in many medical imaging applications.

Optoacoustic signals require broadband detectors to image the different sizes of absorption regions inside the body. The detection technology traditionally used in ultrasonic imaging is based on piezoelectric transducers. The detectors based on thin piezoelectric polymer films can be made sensitive within an ultrawideband, but their sensitivity decreases as their size is reduced. Optical detection techniques have some advantages over traditional electrical methods such as, large detection bandwidth and immunity to electrical perturbations. Polymer optical channel waveguide sensors, which has been used in a resonator configuration for OAT, present some particular advantages such as the fabrication method is simple and potentially can be manufactured in industry and it is non-metallic, thus can be combined with MRI in a multimodality imaging technique.

The acoustic sensitivity of an interferometric optical waveguide sensor depends strongly of the material which is composed of. In the case of optical fiber sensors, it has been demonstrated that a single-mode polymer (SMPOF) optical fibers, at 633nm, has 12 times more sensitivity detecting ultrasonic waves in the 1 MHz frequency range than a single-mode silica optical fiber. However, these SMPOF are still under development and present high loss and difficulties to coupling light into. In this paper we introduce a straightforward interferometric polymer inverted-rib optical waveguide sensor (IPOWS). It is single-mode at a wavelength of 633nm and shows low attenuation. This sensor has an acoustic sensitivity of 26.1mrad/kPa at 1MHz, what doubles the sensitivity of the SMPOF sensor. In this work we present an experimental comparison between the two fiber optic sensors, based on silica and PMMA, and the new IPOWS. All the sensors are designed for detection of optoacoustic wave sources with dimensions between 15mm and 0.15mm what corresponds to ultrasonic frequencies in the range from 100 kHz to 10 MHz. This will be done based on the comparison of sensitivity, dynamic range, frequency bandwidth, spatial resolution and compactness.

8223-146, Poster Session

## PEG-coated gold nanorods conjugated with monoclonal antibodies for preclinical research in optoacoustic imaging and sensing

A. Liopo, A. Conjusteau, A. A. Oraevsky, TomoWave Labs., Inc. (United States)

In this report, gold nanorods (GNR) with a peak absorption wavelength of 760 nm were prepared using a seed-mediated method. A novel protocol has been developed to replace hexadecyltrimethylammonium bromide (CTAB) on the surface of GNR with 16-mercaptohexadecanoic acid (MHDA) and metoxy-poly(ethylene glycol)-thiol (mPEGt or PEG), and the monoclonal antibodies: HER2 and CD33. The physical-chemical properties of the conjugates were monitored through optical and zeta-potential measurements to confirm surface chemistry. In the process of conjugation, the plasmon resonance maximum was kept intact in the near-infrared area, and changes from strong positive charge for GNR-CTAB to slightly negative for GNR-PEG-mAb conjugates were observed. The toxicity of the conjugates was investigated for different cells lines: breast cancer cells, human chronic and acute leukemia lines, prostate and liver carcinomas, and normal kidney and fibroblast cells. These results demonstrate successful in vivo accumulation of our modified conjugates in mouse tumors made of human breast cancer cells overexpressing HER2/neu cellular receptors. We also demonstrated sensitive detection of human leukemia cells in vitro using optoacoustic biosensor. Although the new synthesis has not enhanced accumulation of conjugates on cancer cell as compared with published data (Eghtedari M., 2009), we have developed a much easier method of commercial production of conjugates for optoacoustic molecular imaging and sensing.

8223-147, Poster Session

## Vessel segmentation analysis of ischemic stroke images acquired with photoacoustic microscopy

B. T. Soetikno, S. Hu, Washington Univ. in St. Louis (United States); E. Gonzales, Washington Univ. School of Medicine in St. Louis (United States); Q. Zhong, K. I. Maslov, Washington Univ. in St. Louis (United States); J. Lee, Washington Univ. School of Medicine in St. Louis (United States); L. V. Wang, Washington Univ. in St. Louis (United States)

Brain ischemia results from the lack of blood flow to a region of the brain, which may lead to permanent neurological disability. Studying cerebral metabolism during ischemia has been limited by imaging modalities that have either good tissue penetration but low spatial resolution, or high resolution requiring invasive preparations (open-skull windows).

We have applied optical-resolution photoacoustic microscopy (OR-PAM) to longitudinally monitor cerebral metabolism through the intact skull of Swiss Webster mice before, during, and up to 72 hours after a 1-hour transient middle cerebral artery occlusion (tMCAO). Oxygen extraction fraction (OEF) was calculated based on cerebrovascular hemoglobin oxygen saturation (sO2) determined by OR-PAM in combination with vessel segmentation techniques. Brain regions with the lowest OEF levels 72 hours after tMCAO delineated eventual infarction identified by postmortem triphenyltetrazolium chloride (TTC) staining. Moreover, longitudinal OEF measures behaved differently in brain regions that eventually infarcted compared to regions that did not. During the 1-hour tMCAO, veins within brain regions that eventually infarcted had more significant decreases in sO2 than in non-infarct regions, suggesting a greater increase in OEF during acute ischemia. After reperfusion, venous sO2 in infarcted regions gradually increased to above the baseline value and approached the arterial sO2, suggesting a lack of oxygen consumption. In contrast, venous sO2 in the non-infarct region progressively recovered back to baseline values after reperfusion, suggesting recovery to baseline OEF.

In conclusion, OR-PAM is capable of minimally invasive, logitudinal imaging of oxygen metabolism in rodent models of ischemia at the microscopic level.

8223-148, Poster Session

## Numerical simulation based photoacoustic design parameter optimization for deep tissue imaging

Z. Wang, S. Ha, Univ. of Pittsburgh Medical Ctr. (United States); K. Kim, Univ. of Pittsburgh Medical Ctr. (United States) and Univ. of Pittsburgh (United States)

Finite element (FE)-based numerical simulation was developed and evaluated for deep tissue photoacoustic (PA) imaging. In this silico simulation using a commercially available FE simulation package (COMSOL MultiphysicsTM, ), a short-pulsed laser point or array source (fluence of 4 mJ/cm2, pulse length of 5 ns) was placed in water, 20 mm above the skin. Overall, four sets of simulation models were integrated to describe the physical principles of photoacoustic imaging. Light energy transmission through background tissues from the laser source to the target tissue or contrast agent was described by diffusion equation. The absorption of light energy and conversion to heat by target tissue or contrast agent was described by bioheat equation. The heat then causes the stress and strain change, producing acoustic pressure. The created wide-band acoustic pressure will propagate through background tissues to the ultrasound detector, being described by acoustic wave equation. Both optical and acoustical parameters such as scattering, absorption, and attenuation are incorporated in tissue models. PA imaging performance with different design parameters of a laser source, including pulse duration, power, and spatial arrangement of the laser array source were investigated. The optimized parameters through simulation will guide the design of PA system for deep tissue imaging, and help to form the base protocols of in vivo experiments.

8223-149, Poster Session

## Application of laser pulse stretching scheme for efficiently delivering laser energy in photoacoustic imaging

T. Wang, P. D. Kumavor, Q. Zhu, Univ. of Connecticut (United States)

High-energy outputs from lasers are desirable to improve the photoacoustic image quality when imaging deeply-seated lesions. In many clinical applications, the high-energy pulses are coupled to tissue using optical fibers. These high peak intensity pulses can damage an optical fiber input face if the fiber damage threshold is exceeded. While keeping the total energy under the FDA limit for avoiding tissue damage, it is necessary to reduce the peak intensity to minimize the fiber damage and to delivery sufficient light for imaging. In this paper, a laser pulse stretching technique is introduced to reduce the peak intensity of laser pulses.

To demonstrate the technique, an initial 17ns pulse was stretched to 27ns and 37ns by a ring-cavity laser-pulse-stretching system. For the 37ns stretched pulse, the laser peak power reduced to 42% of the original pulse while trading off 8% optical cavity loss. The stretched pulse increased the fiber damage threshold by 1.5-fold. Three ultrasound transducers centered at 1.3MHz, 3.5MHz, 6MHz frequencies of 80-120% bandwidth were simulated and the results showed that the photoacoustic signal of 0.5mm-diameter target obtained with 37ns pulse was about 98%, 91% and 80% respectively of the same energy of that obtained with the 17ns pulse. Simulations were validated using a broadband hydrophone with a frequency response of 1-10MHz. The received photoacoustic signals after applying corresponding bandpass filters agreed well with the simulations. Quantitative comparisons of photoacoustic images obtained with three corresponding ultrasound transducers showed that the image quality was not affected by stretching the pulse.

8223-150, Poster Session

## Photoacoustic imaging using Porphyrin derivatives as exogeneous contrast agents

A. Abuteen, S. Zanganeh, J. Akhigbe, N. C. Biswal, A. Aguirre, C. Brückner, Q. Zhu, Univ. of Connecticut (United States)

Photoacoustic tomography (PAT) is a promising non-invasive in vivo diagnostic method. It provides optical contrast at ultrasonic imaging resolution. To further improve the optical contrast, researchers are investigating varies exogenous contrast agents for PAT imaging. We introduce here a class of novel porphyrin-derived photoacoustic contrast agents that exhibits a broad near-infrared absorption in the therapeutic window of tissue (~700-850 nm). The contrast agents tested belong to the group quinoline-annulated porphyrins, synthesized from readily available meso-tetraphenylporphyrin by fusion of the meso-phenyl group into co-planarity with the porphyrinoid chromophore using an imine-type nitrogen. This reaction may be followed by an N-oxidation. These structural features are responsible for their bathochromic spectra, and their low (<1%) fluorescence quantum yields, both physical characteristics responsible for their large photoacoustic response.

The feasibility of these materials to serve as PAT contrast agents was tested using a photoacoustic measurement system. Tubings filled with different porphyrin-based and benchmark indocyanine (ICG) contrast agents were used as targets. An Nd:YAG laser pumped at 745 nm was used to illuminate the targets. Photoacoustic measurements were taken for each target using a single element ultrasound transducer connected to a Panametrics 5073PR for amplification and filtering. Two of the four porphyrin-based dyes have shown enhanced photoacoustic measurements over the ICG benchmark used. The monoquinoline-fused dye diluted at 500 uM resulted in 1.8-fold higher signal than that of ICG; while the bis-quinoline-fused N-oxide dye diluted at 400 uM resulted in 1.8-fold higher signal than that of ICG under the same measurement conditions.

8223-151, Poster Session

## Investigation of a quantitative photoacoustic tomography fitting procedure on multiple targets in reflection geometry with diffuse optical measurement assistance

C. Xu, P. D. Kumavor, Q. Zhu, Univ. of Connecticut (United States)

We report the experimental investigation of an improved fitting procedure which can quantitatively characterize optical absorption coefficients of multiple targets. The original fitting procedure was proposed by us and used for a single target. Using the target information from the PAT images and the background information from diffuse optical measurements (DOM), the fitting method minimizes the photoacoustic measurements and forward model data and recovers the target absorption coefficient quantitatively. The fitting errors in the absorption coefficients can reach 20% to 50% if the original fitting procedure is directly used on multiple targets. In our improved fitting method, an extra calibration procedure is introduced to quantify the photoacoustic intensities from different targets, and the ratios between the intensities serve as extra inputs to the fitting procedure. As a result, the total number of unknown parameters is reduced and fitting accuracy is improved. The hybrid system used in the experiment combines a 64-channel photoacoustic system with a frequency-domain diffused optical system. The experiment was performed in the reflection geometry suitable for breast imaging. Phantom experiments include the combination of high contrast and low contrast targets with absorption coefficients ranging from 0.07 to 0.28 cm-1 and with different spatial separations. The phantoms were inserted into a chicken breast tissue. The fitting errors of multiple targets were reduced to less than 10% for both high and low contrast targets. These results illustrate the potential application of this quantitative DOM-assisted photoacoustic fitting procedure to image and diagnose breast cancer having multiple and complex tumor distribution.

8223-152, Poster Session

## Optoacoustic monitoring of cerebral venous blood oxygenation in rats with traumatic brain injury

K. E. Wynne, D. S. Dewitt, Y. Y. Petrov, I. Y. Petrov, M. A. Parsley, R. O. Esenaliev, D. S. Prough, The Univ. of Texas Medical Branch (United States)

Monitoring of cerebral venous blood oxygenation is critically important for the management of life-threatening illnesses including traumatic brain injury (TBI). The existing technique for monitoring cerebral venous blood oxygenation is invasive. Near-infrared spectroscopy (NIRS) is the only noninvasive method for monitoring blood oxygenation, but it provides no information about cerebral venous blood oxygenation. In contrast to NIRS, using the optoacoustic technique allows for spatial localization of blood vessels and it has the ability to monitor cerebral venous blood oxygenation. Our previous studies demonstrated the capability of this technique to monitor cerebral oxygenation in large animals and humans. This work demonstrates optoacoustic monitoring of cerebral oxygenation in a new animal model for blast-induced TBI. Blast-induced TBI (mild, moderate or severe injuries) were obtained in anesthetized rats using a specially developed blast device. The optoacoustic system was modified for measurements of rat SSS blood oxygenation through an intact scalp and skull using a wide-band optoacoustic probe. Arterial blood pressure, heart rate, temperature, and other physiologic variables were recorded simultaneously as the optoacoustic measurements were taken. The optoacoustic signals were continuously measured before and after the blasts from the SSS at different near-infrared wavelengths. The system hardware and software provided continuous, real-time measurements of the SSS blood oxygenation in a wide range: from 40% to 100%. The data indicate that optoacoustics can be used for monitoring cerebral blood oxygenation in a rodent TBI model and may become a valuable tool for studying TBI.

8223-153, Poster Session

## Integrated scanning confocal photothermal-lens and photoacoustic microscopy

D. A. Nedosekin, E. I. Galanzha, R. J. S. Reis, V. P. Zharov, Univ. of Arkansas for Medical Sciences (United States)

Light absorption contrast imaging has long been shadowed by fluorescence based methods. In the recent years, photothermal microscopy demonstrated significant advances including imaging of individual nanoparticles and even single molecule detection. However, the most sensitive PT detection schemes are not optimal for natural biological specimens due to a strong absorption and high scattering background. Fixed wavelength laser sources limit possible applications of the method. Here, we report a significant progress in photothermal microscopy which now integrates confocal imaging optimized for biological tissues, time-resolved detection, spectral identification in a wide 420 - 2400 nm range and multispectral imaging. The capabilities of the new platform were tested for high-resolution 3D imaging and identification of multiple (up to 4) chromophores and fluorophores in bacteria, live cells and C. elegans. Examples include cytochrome c, green fluorescent protein, fluorescent dyes, and drug-induced or genetically engineered melanin, 3D-mapping of nanoparticles distribution on a cell surface. Thermal lens schematics featuring nanosecond pump lasers provided a unique opportunity for close integration of photothermal microscopy with photoacoustic method. An integrated confocal photothermal-lens and photoacoustic platform extends the range of possible applications from bacteria to a small animal level. Light absorption contrast could provide a valuable supplement to fluorescence microscopy, for imaging of nonfluorescent chromophores and fluorophores, respectively.

8223-154, Poster Session

## Quantification of optical absorption coefficient from acoustic spectra in the optical diffusive regime using photoacoustic microscopy

Z. Guo, C. P. Favazza, L. V. Wang, Washington Univ. in St. Louis (United States)

Photoacoustic (PA) tomography (PAT) can image optical absorption contrast with ultrasonic spatial resolution in the optical diffusive regime. Multi-wavelength PAT can noninvasively monitor hemoglobin oxygen saturation (sO2) with high sensitivity and fine spatial resolution. However, accurate quantification in PAT requires knowledge of the optical fluence distribution, acoustic wave attenuation, and detection system bandwidth. We propose a method to circumvent this requirement using acoustic spectra of PA signals acquired at two optical wavelengths. We quantify the sO2 of shallow blood vessels (~100 μm in depth) in a live mouse using the traditional amplitude method as the gold standard. We then cover the imaging region with scattering medium (1 mm chicken breast layer), and then quantify the sO2 of the same vessels again from acoustic spectra. By comparing the quantification results, we validate our method in vivo.

8223-59, Session 8

## Ultrasound guided spectroscopic photoacoustic imaging for in vivo monitoring of mesenchymal stem cells labeled with nanotracers

S. Y. Nam, L. M. Ricles, L. J. Suggs, S. Y. Emelianov, The Univ. of Texas at Austin (United States)

Monitoring stem cells provides valuable information relating to their migration and participation in tissue regeneration, leading to improved therapies and treatments. While effective stem cell imaging requires capabilities in various aspects such as sensitivity, long-term ability, biocompatibility, high resolution, and deep penetration depth, current imaging methods have not satisfied those requirements simultaneously. Ultrasound and photoacoustics (US/PA) can be an effective stem cell imaging technique due to the capability of visualizing morphological, functional, and molecular properties with high spatial resolution and deep penetration depth. Our group previously performed an in vitro study to verify that the US/PA imaging is able to visualize mesenchymal stem cells (MSCs) labeled with gold nanotracers (Au NTs) with high sensitivity and good cell viability. In this study, in vivo monitoring of MSCs labeled with Au NTs was demonstrated using ultrasound guided spectroscopic photoacoustic imaging. Specifically, Au NT labeled MSCs injected intramuscularly in the lower limb of the Lewis rat were longitudinally monitored over a one week time period. After imaging, the acquired photoacoustic signals were spectrally analyzed to distinguish Au NT labeled MSCs and blood vessels from background tissue. The results suggest that US/PA imaging can be a novel alternative for noninvasive longitudinal monitoring of MSCs as well as neovascularization.

8223-60, Session 8

## Intravascular photoacoustic imaging of gold nanorod-labeled atherosclerotic plaques

D. E. Yeager, B. Wang, A. B. Karpiouk, The Univ. of Texas at Austin (United States); J. H. Amirian, The Univ. of Texas Health Science Ctr. at Houston (United States); K. Sokolov, The Univ. of Texas M.D. Anderson Cancer Ctr. (United States) and The Univ. of Texas at Austin (United States); S. Y. Emelianov, The Univ. of Texas at Austin (United States) and The Univ. of Texas M.D. Anderson Cancer Ctr. (United States)

The ability to image atherosclerotic plaques using combined intravascular photoacoustic (IVPA) and intravascular ultrasound (IVUS) imaging of both endogenous and exogenous contrast has been previously demonstrated. However, continued translation of initial results to clinical application will benefit if IVPA signals and images can be obtained in the presence of luminal blood. In the present study, PEGylated gold nanorods (AuNR) were used to selectively label atherosclerotic lesions. AuNRs, tuned to absorb light in the near-infrared region, provide a high magnitude IVPA signal at wavelengths with decreased absorption and scattering coefficients of blood relative to those previously used for imaging plaques with exogenous contrast absorbing primarily within the visible range.

Specifically, AuNR with an aspect ratio of 4.0 were conjugated with 5 kDa molecular weight PEG. The particles were injected into a balloon injured New Zealand white rabbit and allowed to circulate for 26 hours, at which time the animal was sacrificed for ex-vivo imaging and analysis of AuNR biodistribution. Combined IVUS/IVPA imaging was performed on rabbit aorta sections using a commercially available 40-MHz IVUS catheter in conjunction with an optical fiber-based light delivery system emitting 5 ns, 1 mJ pulses from a tunable laser. IVPA imaging at the AuNR peak absorbance revealed localized high photoacoustic signal, further determined to originate from AuNR by spectroscopic analysis. Histological cross-sections confirmed the presence of AuNR preferentially located at atherosclerotic regions and correlate with IVPA signal. These results indicate the potential for IVPA imaging of atherosclerotic plaques through blood.

8223-61, Session 8

## Trapping and dynamic manipulation with magnetomotive photoacoustic imaging of targeted microspheres mimicking metastatic cancer cells trafficking in the vasculature

C. Wei, J. Xia, Univ. of Washington (United States); I. M. Pelivanov, Univ. of Washington (Russian Federation); X. Hu, X. Gao, M. O'Donnell, Univ. of Washington (United States)

Trapping and manipulation of micro-scale objects in a flow field have been demonstrated with magnetomotive photoacoustic (mmPA) imaging. Coupled contrast agents combining gold nanorods (10 nm x 30 nm; absorption peak around 730 nm) with 15 nm diameter magnetic nanospheres (MNP) were targeted to 10 μm polystyrene beads recirculating in a 1.6 mm diameter tube mimicking metastatic cancer cells in the human vasculature. The targeted beads were then trapped by an external magnetic field produced by a dual magnet system consisting of two disc magnets separated by 5 cm to form an polarizing field (0.04 Tesla in the tube region) to magnetize the magnetic contrast agents, and a custom designed cone magnet array with a high magnetic field gradient (about 0.15 Tesla/mm in the tube region) producing a strong trapping force to the magnetized contrast agents. A tunable pulsed OPO laser (Surelite OPO plus, Continuum, CA) operating at 730 nm was used for optical illumination. The excited PA signals were detected with a linear array transducer (AT8L12-5 50mm, Broadsound, Taiwan) interfaced with an imaging system (Verasonics, WA). Results show that the MNP-Au nanocomposites linked to polystyrene beads can be trapped and manipulated by changing the position of the cone magnets with respect to the tube at flow speeds up to 100 mm/sec. This experiment strongly suggests that mmPA imaging is very promising for differential visualization of metastatic cells trafficking within the vasculature.

8223-62, Session 8

## Dual-contrast photoacoustic nanodroplets: in vivo imaging results

K. E. Wilson, A. Hannah, K. Homan, S. Y. Emelianov, The Univ. of Texas at Austin (United States)

Photoacoustic nanoDroplets (PAnDs), optically triggered dual contrast agents containing encapsulated superheated liquid and plasmonic nanoparticles, have been previously shown to enhance both ultrasound and photoacoustic imaging simultaneously. The contrast enhancement mechanisms are not only through impedance mismatch for ultrasound and thermal expansion for photoacoustic imaging, but also through a stronger photoacoustic phenomenon, vaporization. In this study, the efficacy of PAnDs is demonstrated in an in vivo murine model. PAnDs were directly injected under ultrasound guidance into the mouse liver, a highly optically absorbing tissue due to its large blood content. The PAnDs were remotely activated using a 10 Hz pulsed (7 ns pulse duration) Nd:YAG laser tuned with an optical parametric oscillator to 780 nm at an energy of 10 mJ/cm2. Photoacoustic and ultrasound signals were collected using a Vevo® 2100 ultrasound imaging system (VisualSonics, Toronto, CA) with a 40 MHz, 256 element array transducer. After laser activation, the ultrasound signal in the region of the injection showed increased contrast. Furthermore, strong photoacoustic signal due to vaporization of the nano-sized, perfluorocarbon droplets was demonstrated, followed by a slightly lower amplitude signal resulting from thermal expansion around the expelled plasmonic, gold nanorods in the injection site. Both types of photoacoustic signal were stronger than the endogenous contrast of the liver. Overall, this experiment shows the feasibility of PAnDs as a useful contrast agent in vivo, and highlights the ability of PAnDs to provide this contrast deep in blood-laden tissues.

8223-63, Session 8

## In vivo photoacoustic flow cytometry in plants: direct study of nanomaterials uptake and accumulation

D. A. Nedosekin, Univ. of Arkansas for Medical Sciences (United States); M. V. Khodakovskaya, A. S. Biris, Univ. of Arkansas at Little Rock (United States); E. I. Galanzha, V. P. Zharov, Univ. of Arkansas for Medical Sciences (United States)

Nanotechnology transformed modern science, industry and medicine. However, potential release of nanomaterials to the environment and the development of nanotechnology based solutions for the agriculture industry demand comprehensive understanding of the nanoparticles interactions with plants. Possible accumulation of such materials in plants, especially, in edible ones suggests that potential harm includes impact on humans.

Herewith, we present an integrated platform combining photoacoustic and photothermal detection techniques for in vivo real-time detection of nanomaterials transported by xylem and phloem flow in live plants and for imaging of nanomaterials accumulated in various plant tissues including leaves, roots, seeds and fruits.

Using this approach, we discovered penetration of carbon nanotubes into tomato plant tissues with detection sensitivity down to a single cell level. First of a kind studies of carbon nanotubes uptake demonstrated ultra-fast penetration of carbon nanotubes through roots of tomato plant into the xylem flow and further throughout the plant. Confirmed was a presence of nanomaterials in the tissues of tomato fruits. Accumulation of nanomaterials in these plants was correlated with the previously unknown changes in gene expression in tomato leaves and roots, particularly with up-regulation of the stress-related genes.

8223-64, Session 9

## Photoacoustic cystography

C. Kim, M. Jeon, Univ. at Buffalo (United States); L. V. Wang, Washington Univ. in St. Louis (United States)

Vesicoureteral reflux (VUR), the retrograde flow of urine from the bladder into the upper urinary tract, is commonly diagnosed after patients (typically children) have a urinary tract infection. By transporting bacteria from the bladder, VUR causes renal scarring. Severe renal scarring may reduce renal function and produce severe side effects. Therefore, early detection and treatment of VUR are essential. Two main methods have been used to evaluate VUR: fluoroscopic voiding cystourethrography (VCUG) and direct radionuclide voiding cystography (DRNC). Although radiation dose reduction has been achieved in VCUG, this method is still ionizing. Further, despite the smaller radiation dose of DRNC, this technique suffers from low spatial resolution, and patients are still exposed to radiation. The pediatric VUR guidelines panel of the American Urological Association strongly urges the development of techniques with less radiation exposure. Echo-enhanced urosonography has been recently applied to monitor VUR, and it offers the advantages of nonionizing, real-time, and portable imaging capability. However, ultrasound (US) imaging suffers from low image contrast because of speckle artifacts. Therefore, US imaging alone cannot be used for VUR tracking. We describe the feasibility of a novel and safe approach for VUR monitoring using PAT. As the first step, a healthy rat bladder filled with methylene blue was photoacoustically and spectroscopically imaged in vivo without any ionizing radiation. When combined with a clinical US scanner, this technique can potentially supply an accurate, safe, cheap, portable, and real-time imaging capability for VUR monitoring, completely avoiding radiation exposure to children.

8223-65, Session 9

## Photoacoustic imaging of oxygen release from hemoglobin in single red blood cells in vivo

L. Wang, L. V. Wang, Washington Univ. School of Medicine in St. Louis (United States)

Real-time in vivo imaging of oxygen release from red blood cells (RBCs) is of fundamental importance in understanding oxygen transport and consumption in tissue, and in studying many diseases and physiological functions. We present a novel approach to image oxygen release from single RBCs in vivo by using a high resolution photoacoustic microscope. The photoacoustic microscope has multiple advantages providing this imaging capability. First, sub-cellular lateral resolution is achieved by utilizing optical focusing. Second, high temporal resolution provides video-rate functional imaging ability by using a fast voice-coil scanning mechanism and a micro-second laser wavelength switching. Third, acoustic/optical confocal alignment provides high a signal-to-noise ratio for in vivo quantitative study. Fourth, intrinsic optical absorption contrast was employed to quantify the oxygen release, which enabled label-free imaging and minimized perturbations during in vivo quantitative imaging. Oxygen release under hypoxia, hyperoxia, and vasomotion was imaged on single RBCs. Other parameters were also quantified from the real-time imaging, including total hemoglobin concentration, blood flow speed, and local oxygen metabolic rate. These results demonstrate that high-resolution, fast-scanning photoacoustic microscopy can successfully image oxygen release from single RBCs, and quantify local oxygen transport and consumption in vivo.

8223-66, Session 9

## Label-free photoacoustic microscopy of cytochrome C in mitochondria

C. Zhang, K. I. Maslov, L. V. Wang, Washington Univ. in St. Louis (United States)

Mitochondria, important cellular energy sources and metabolism regulators, utilize cytochrome c for many of their functions, such as electron transport. Because cytochrome c is a weakly fluorescent and low-scattering protein, it requires labeling for functional imaging in cell biology studies. However, labeling can affect its normal function. Here, by exciting cytochrome c at the Soret peak, we demonstrate label-free functional photoacoustic microscopy (PAM) of mitochondria for the first time. The PAM system employed a tunable diode-pumped OPO laser for spectral measurements. Mitochondria in fixed fibroblast cells were clearly imaged by PAM with pulse energy of ~100 nJ at 422 nm wavelength. Both fluorescent labeling and photoacoustic spectroscopy confirmed the identity of the contrast signals detected by PAM as originating from mitochondria. The ratio of the reduced to the oxidized form of cytochrome c was quantified by the measured absorption spectrum. The results suggest that PAM has broad potential label-free applications in cell biology.

8223-67, Session 9

## In vivo imaging of cell nuclei by photoacoustic microscopy without staining

D. Yao, Washington Univ. in St. Louis (United States); R. Chen, The Univ. of Southern California (United States); K. I. Maslov, Washington Univ. in St. Louis (United States); Q. Zhou, The Univ. of Southern California (United States); L. V. Wang, Washington Univ. in St. Louis (United States)

Invasive histologic imaging of cell nuclei plays an important role in cancer diagnosis. Cell nuclei in tissues have been imaged by reflectance confocal microscopy and fluorescence confocal microscopy with staining, and by multiphoton microscopy with negative contrast. Without staining and with positive contrast, cell nuclei have also been imaged with high contrast and resolution noninvasively by ultraviolet photoacoustic microscopy (UVPAM), which uses 266 nm wavelength light for excitation of DNA and RNA to produce photoacoustic waves. In order to optimize UVPAM for in vivo cell nucleus imaging, we set up a UVPAM system which used UV light at wavelengths ranging between 210-310 nm. The light was emitted by a tunable laser system with a pulse width of 5 ns. The laser pulse (22-25 nJ) was focused on the object by a 0.1 NA objective lens, and the photoacoustic waves were detected by a 40-MHz focused ring ultrasonic transducer. Time-resolved photoacoustic signals were collected during raster scanning to reconstruct tomographic images. We applied the UVPAM to in vivo imaging of cell nuclei in the skin of nude mice, and obtained UVPAM images of the unstained cell nuclei at wavelengths of 250, 260, 266, 270, 280, and 282 nm. However, the UVPAM did not produce identifiable images of cell nuclei at wavelengths of 210, 220, 230, 240, 290, 300, and 310 nm. We found that the images of cell nuclei at a 250 nm wavelength had the largest ratio of contrast to noise, two times larger than that at 266 nm.

8223-68, Session 10

## Application of iterative image reconstruction algorithms to three-dimensional optoacoustic tomography

K. Wang, Washington Univ. in St. Louis (United States); A. A. Oraevsky, TomoWave Labs., Inc. (United States); M. A. Anastasio, Washington Univ. in St. Louis (United States)

Filtered backprojection (FBP) algorithms are commonly employed for image reconstruction in optoacoustic tomography (OAT). A limitation of FBP algorithms is that they require the measured data to be densely sampled, which necessitates expensive ultrasound arrays that possess a large number of elements or increased data-acquisition times if mechanical scanning is employed. Additionally, FBP algorithms are based on idealized imaging models that do not accurately model the response of the transducers and fail to exploit the statistical characteristics of noisy measurement data to minimize noise levels in the reconstructed image. Iterative image reconstruction algorithms can circumvent these difficulties. However, to date, iterative reconstruction algorithms have not been successfully applied to three-dimensional (3D) OAT. One reason for this is the intense computational burden associated with 3D iterative image reconstruction.

In this work we implement and investigate the use of iterative image reconstruction methods in 3D OAT. Accurate image models that incorporate the transducer response are utilized and the reconstruction algorithms are implemented using graphics processing units (GPUs) to alleviate the computational burden involved. Three iterative reconstruction algorithms for limited-data reconstruction are implemented: the penalized least-squares (PLS) algorithm, the algebraic reconstruction technique (ART), and the constrained, total variation (TV) minimization algorithm. The algorithms are applied to experimentally measured data and evaluated by use of task-specific image quality metrics. These results, for the first time, demonstrate the computational feasibility of iterative algorithms for 3D OAT and their ability to mitigate artifacts due to incomplete data. Implications for future system designs are also discussed.

8223-69, Session 10

## Adapted directivity approach for photoacoustic imaging reconstruction

D. Piras, W. Xia, M. Heijblom, W. Steenbergen, Univ. Twente (Netherlands); T. G. van Leeuwen, Univ. Amsterdam (Netherlands) and Univ. Twente (Netherlands); S. Manohar, Univ. Twente (Netherlands)

In Photoacoustic imaging, upon short laser pulse irradiation, absorbers generate N-shaped pulses which are detected by Ultrasound transducers. Radio frequency signals from multiple spatial locations are reconstructed taking into account the Ultrasound transducer's angular response. Usually, directivity is part of the "a priori" characterization of the transducer and it is assumed constant in the reconstruction algorithm.

This approach is valid in pure ultrasound, where any echo resembles the transducer's frequency response. The center frequency and bandwidth of any echo stays approximately the same, and the ultrasound transducer collects signals from a "fixed" acceptance angle region. In photoacoustics, instead, absorbers generate echoes for which the time duration is proportional to the absorber size: this means that large absorbers generate low frequency echoes, whereas small absorber echoes are centered at higher frequencies. For different absorber sizes, different pulse center frequencies are obtained and, because of the frequency dependent angular response of the detector, different directivities need to be applied in the reconstruction algorithm.

For this purpose once a radio-frequency signal is aquired, it is pre-processed with a sliding window: every segment is Fourier transformed to extract the central frequency. Then a proper directivity can be estimated for each time segment. Finally signals can be reconstructed via a backprojection algorithm. According to the system geometry, echoes are backprojected on spherical arcs with angular extension being adapted to the frequency content of the photoacoustic sources.

Simulation and experimental validation of this approach are discussed showing promising results in image contrast and resolution.

8223-70, Session 10

## Analysis of the role of shear waves in transcranial photoacoustic tomography

R. W. Schoonover, L. V. Wang, M. A. Anastasio, Washington Univ. in St. Louis (United States)

Transcranial photoacoustic tomography (PAT) holds great potential for human brain imaging applications. A major technical challenge in PAT brain imaging is to compensate for the distortion induced in the PAT measurement data by the skull. Although our preliminary studies are highly encouraging, there is a need for the further development, characterization, and validation of this technology. One important issue that remains to be investigated is the role that shear waves play in transcranial PAT image formation. Although conversion of longitudinal pressure waves to shear waves and vice-versa occurs at the skull-tissue interfaces, conventional PAT reconstruction methods assume a fluid medium and therefore neglect such wavefield interactions.

In this work we report on an investigation of the role of shear waves in transcranial PAT brain imaging. By use of a recently developed PAT image reconstruction method for use with elastic, planar, layered media, we will quantify the extent to which properly accounting for shear waves in the reconstruction method can improve image quality. Specifically, through extensive computer-simulation studies, the impact of accounting for or neglecting shear waves on image resolution, artifact level, and signal-to-noise ratio will be quantified. The studies will incorporate realistic models of the measurement process, including the response of the ultrasonic transducers. These results will clarify the role of shear waves in transcranial PAT image formation and indicate whether further research is warranted to develop reconstruction algorithms for more general imaging geometries that account for shear wave physics.

8223-71, Session 10

## Spatial resolution and sensitivity in photoacoustic tomography taking noise into account: from point-like detectors to large integrating detectors

P. Burgholzer, RECENDT GmbH (Austria); T. Berer, RECENDT GmbH (Germany); H. Grün, RECENDT GmbH (Austria); R. Nuster, G. Paltauf, Karl-Franzens-Univ. Graz (Austria)

As for any other imaging technique spatial resolution and sensitivity are important features for a photoacoustic imaging device. It is already well known that spatial resolution depends on the size and the bandwidth of the detectors. Therefore for photoacoustic image reconstruction usually small point-like and broadband detectors are assumed, which measure the pressure as a function of time on a detection surface around the sample. But in reality point-like detectors are not ideal at all: because of the small detector volume the thermodynamic fluctuations (= noise) get high and the signal amplitude is low, which results in a bad signal-to-noise ratio (SNR). For a bigger detector volume the fluctuations are less and the signal amplitude is better, which gives a better SNR. But on the other hand the photoacoustic pressure signal is averaged over the whole detector volume, which results in blurring and a reduced spatial resolution if reconstruction algorithms for point-like detectors are used. To characterize this trade-off between spatial resolution and sensitivity for a varying detector volume in a quantitative way the pressure is described by a random variable having the measured pressure as a mean value and noise as random fluctuations around that mean value ("stochastic process"). We have numerically compared reconstructions from four idealized concepts of detectors for the photoacoustic pressure wave: a small membrane and a small piece of a PVDF foil as two realizations of point-like detectors and two realizations of integrating line detectors: a piezoelectric line and an optical fiber.

8223-72, Session 10

## Sparsity regularized data-space restoration in optoacoustic tomography

K. Wang, Washington Univ. in St. Louis (United States); A. A. Oraevsky, TomoWave Labs., Inc. (United States); M. A. Anastasio, Washington Univ. in St. Louis (United States)

In optoacoustic tomography (OAT), also known as photoacoustic tomography, a variety of filtered backprojection (FBP) image reconstruction algorithms have been developed. FBP algorithms are computationally more efficient than many iterative image reconstruction algorithms but possess disadvantages that include: (1) Assumption of point-like ultrasonic transducers that have an idealized (Dirac delta) acousto-electric impulse response (EIR); (2) Requirement that the optoacoustic data be densely sampled with respect to transducer location; (3) Failure to optimally exploit the statistical characteristics of noisy measurement data to minimize image variance. While all of these shortcomings can be circumvented by use of appropriate iterative image reconstruction methods, 3D iterative reconstruction is computationally burdensome.

We will present a novel data-restoration method that seeks to recover an accurate and densely sampled estimate of the pressure data with reduced noise levels from knowledge of the experimentally acquired data. From knowledge of the "restored" pressure data, an FBP algorithm is applied for image reconstruction. This approach combines the advantages of an iterative reconstruction algorithm with the computational efficiency of an FBP algorithm. The restored pressure data correspond to the solution of a constrained optimization problem that is inspired by compressive sampling methods. Innovative characteristics of this method include: (1) exploitation of sparsity of the pressure data in a suitably defined transform domain; (2) exploitation of the continuous wavefront of the pressure signal in the measured data space; and (3) optimal suppression of data noise for certain classes of objects. The method is comprehensively evaluated using simulated and experimental data sets.

8272-12, Session 11

## Creating filters for shot-noise-limited Ultrasound Optical Tomography (UOT)

M. Sabooni, Lund Univ. (Sweden); H. Zhang, Texas A&M Univ. (United States); L. Rippe, Lund Univ. (Sweden); C. Kim, Washington Univ. in St. Louis (United States); S. Kroll, Lund Univ. (Sweden); P. Hemmer, Texas A&M Univ. (United States)

Large depth imaging in strongly scattering media using UOT relies on collecting the small fraction of light frequency-shifted by ultrasound and assuring that this weak signal is not hidden in the noise from the (non frequency-shifted) carrier light wave. Conveniently any filter with a spectral transmission window will both suppress the carrier wave and delay radiation within its transmission window. This talk will describe filters, where the transmitted light (shifted by the ultrasound) arrives at the detector at a time much later than the scattered carrier radiation and thus is detected on a zero background enabling deep tissue imaging.

8272-13, Session 11

## Rare-earth-doped materials with application to optical signal processing, quantum information science, and medical imaging technology

R. L. Cone, C. W. Thiel, Montana State Univ. (United States); Y. Sun, The Univ. of South Dakota (United States); T. Böttger, Univ. of California, San Francisco (United States); R. M. Macfarlane, Montana State Univ. (United States)

Unique spectroscopic properties of rare earth ions in solids enable a variety of recent applications. Within rare earth optical absorption transitions which are already regarded as sharp at room temperature, optical decoherence times as long as 4.2 msec have been measured in our laboratory at 1.6K, equivalent to homogeneous optical linewidths as narrow as 75 Hz. This linewidth reduction of nine orders of magnitude gives linewidths rivaling those of isolated trapped single atoms used at the frontiers of atomic physics.

We design rare-earth-doped crystals, ceramics, and fibers with persistent or transient “spectral hole” recording properties for applications including high-bandwidth optical signal processing where light and our solids replace electronics, quantum cryptography and information science including the goal of storage and recall of single photons, and medical imaging technology for the 700-900nm therapeutic window.

Ease of optically manipulating rare-earth ions in solids enables capturing and processing complex spectral information in 105 to 108 frequency bins. Combining spatial holography and spectral hole burning provides a capability for capturing and processing high-bandwidth RF and optical signals with sub-MHz spectral resolution and bandwidths of tens to hundreds of GHz. Applications include range-Doppler radar and high bandwidth RF spectral analysis, where systems demonstrated in Montana exceed the capabilities of state-of-the-art electronics. Simply stated, one can think of these crystals as holographic recording media capable of distinguishing 105 to 108 different colors.

Ultra-narrow spectral holes also serve as a vibration-insensitive sub-kHz frequency references for laser frequency stabilization to a part in 1013 over tens of ms.

8223-73, Session 11

## Signals, noises, and detection schemes in ultrasonically modulated optical imaging

F. Ramaz, Ecole Supérieure de Physique et de Chimie Industrielles (France); M. Gross, Univ. Montpellier 2 (France); A. C. Boccara, Ecole Supérieure de Physique et de Chimie Industrielles (France)

Compared to purely optical diffuse tomography that aims to reveal the spatial distribution of optical properties (absorption and scattering) hybrid techniques that combine light and ultrasounds provide a much better resolution: typical results are of the order of 1/100 of the targeted depth. In ultrasonically modulated optical imaging (also called Acousto Optical Tomography), the part of the light that overlaps the acoustic field is modulated by an ultrasonic beam focused inside the biological tissue. 2-D or 3-D images are generated by scanning the acoustic field across the sample volume. The so-called tagged-photons (created at the position of the focused ultrasonic beam) can be discriminated from background of unmodulated photons. The difficulty of the coherent detections (heterodyning using cameras or photorefractive crystals) that rely on the speckle field modulation is that they are sensitive to its fast (< 1 ms) decorrelation time due to blood flow. Inversely the techniques that use a narrow band pass filter (Fabry Perot or Hole Burning) do not suffer from such decorrelation. When optimized Hole Burning offers the larger optical etendue and should be the best detection technique. We will discuss the performances of each detection scheme in term of signal to noise ratio and illustrate their potential for a realistic bedside experiment.

8223-74, Session 11

## Ultrasound-modulated optical tomography of biological tissue using spectral-hole burning

X. Xu, H. Liu, Washington Univ. in St. Louis (United States); S. Kothapalli, Stanford Univ. (United States); P. Lai, Y. Suzuki, L. V. Wang, Washington Univ. in St. Louis (United States)

In ultrasound-modulated optical tomography, coherent detection of the optical signal is difficult because of the multiple scattering of light through a turbid medium. To improve the signal-to-noise ratio in UOT, spectral-hole burning has been proposed as a front end absorptive filtering method, based on its narrow linewidth as well as its immunity to speckle-induced spatial incoherence and speckle decorrelation. Experimental implementation of SHB with a Tm3+:YAG crystal has shown a 13.5 dB transmission improvement of the UOT signal. Images of biological tissues and tissue mimicking phantoms of various thicknesses have been acquired using SHB-UOT. The effect of a finite suppression of the background light on the final SNR is investigated, and further improvement of SHB-UOT is proposed.

8223-75, Session 11

## Recent progress in ultrasound-mediated fluorescence

B. Yuan, Y. Liu, The Univ. of Texas at Arlington (United States)

Invited Talk:

Fluorescence imaging techniques can provide unique tissue physiological information and is sensitive to tissue microenvironments. Unfortunately, the highly scattering property of tissue to light has limited most fluorescence measurements either in excised sample slices or superficial in vivo tissues. When detecting fluorescence from deep tissue, the spatial resolution significantly deteriorates. To improve the spatial resolution and maintain the unique functional information of the fluorescence signal, ultrasound-mediated fluorescence (UMF) techniques have been developed recently. Like ultrasound-modulated optical tomography, a highly focused ultrasound beam is usually employed to tag fluorophores. By detecting UMF signal, the functional information of the fluorophore may be quantified with ultrasonic spatial resolution. Recent studies have shown that UMF is experimentally detectable and a fluorescent target can be visualized in a turbid medium with ultrasonic resolution. However, significant challenges for developing UMF techniques exist, such as unclear modulation mechanisms, relatively low signal-to-noise ratio (SNR), and less developed imaging contrast agents, etc. In this talk, the potential modulation mechanisms will be discussed. Methods for improving SNR will also be discussed based on three strategies: (1) increase the sensitivity of the detection system, (2) improve the modulation efficiency via microbubbles, and (3) suppress unwanted background fluorescence emission (via the detection system and imaging contrast agents). To bring UMF techniques to any practical biomedical applications, further improvement of SNR has to be achieved. Development of UMF imaging contrast agents is a promising direction, which will be introduced in this talk based on our recent results.

8223-76, Session 11

## The potential of ultrasound-modulated optical sensing in clinical monitoring

T. S. Leung, Univ. College London (United Kingdom)

Near infrared spectroscopy (NIRS) is a widely adopted technique to measure tissue oxygenation non-invasively in human tissues such as the brain and muscle. A number of commercial NIRS clinical monitors have emerged over the past twenty years and they are gaining popularity with many clinical applications. However, in many situations, the region of interest is beneath a superficial layer, e.g., muscle overlaid by a superficial layer of skin and fat, which can affect the accuracy of the NIRS measurement. By applying focused ultrasound in the region of interest, ultrasound-modulated optical (UMO) techniques can potentially provide a measurement less susceptible to physiological changes in the superficial layer. In this talk, we will explore the potential of UMO techniques for clinical monitoring. We will present and compare the depth sensitivity of the NIRS and UMO measurements based on a series of absorption and scattering perturbation experiments. Our results show that in the reflection mode with a source detector spacing of 3 cm, the UMO measurement is more sensitivity to its NIRS counterpart when the ROI is more than 14 mm deep into the tissue in one realistic scenario. However, the most sensitive region of an UMO measurement does not always coincide with the focused ultrasound location. We will also show that by incorporating ultrasound microbubbles as contrast agents, UMO techniques can potentially provide a non-invasive venous oxygen saturation measurement in a vein which is something conventional NIRS techniques cannot achieve because of the high absorption of blood inside the vessel.

8223-14, Session 12

## Atom like centers in solids for nanophotonic and quantum devices

Z. U. Hasan, Temple Univ. (United States)

Devices working with a few atoms at the core of their operation not only set the limit of miniaturization, but also define a new level of exploitation of matter, the quantum regime. Therefore, nano-photonics and quantum devices for computing and communication have been vigorously pursued for the last one and a half decade. The practical realization of most of these devices faces challenges mainly on three fronts: i). Implementing the desired quantum mechanical operation on an ensemble of atoms considering their interaction with each other and with the surrounding. ii). Fabrication of such devices with a minimum number of atoms performing the desired operation. iii). The control of these devices with external photons to demonstrate their successful operation.

This presentation will review the progress in tailoring the materials for single atom or at most few atoms based devices. Three different classes of materials have emerged that can be exploited for designing such devices: color centers particularly in the diamond crystal, the traditional rare earth based systems where localized 4fn electronic states are used for quantum manipulation, and lastly rare earth based f-d systems. The focus of our studies is on solids lightly doped with f-d rare earths in the form of nanoparticles and multi-layer thinfilms.

f-d rare earths can be considered as the hybrid of the transition metal (dn electrons) system and the rare earth (fn electrons) systems. These materials provide for the maximum atomic scale tailoring of solids: d-states allow the tunability of pertinent electronic transitions from UV to IR. f-d transitions are strongly electric dipole allowed and therefore maximize the electron photon interaction. Also, in such systems f-d rare earth centers can be tailored to enhance or eliminate the electron-lattice coupling.

With such intricate and extensive tailoring possible, these systems demonstrate the highest density of spectral storage; up to 1000 channels, optical holes, can be made(burned) using the zero phonon line of a single rare earth center. In multi-layer structures this number is multiplied by the number of layers. Such channels can be used in frequency selective wide-band communication and ultra-dense memory. Strongly interacting atomic centers that can be efficiently addressed by photons have the potential to provide systems for quantum computing, single atom devices, single photon sources, and single atom based nano-sensors. For biological applications such nano-probes could potentially provide efficient fluorescent markers and tags in living cells.

8223-15, Session 12

## Spectral-hole burning techniques for ultrasound-modulated optical tomography

H. Zhang, Texas A&M Univ. (United States); M. Sabooni, L. Rippe, Lund Univ. (Sweden); C. Kim, Washington Univ. in St. Louis (United States); S. Kroll, Lund Univ. (Sweden); L. V. Wang, Washington Univ. in St. Louis (United States); P. R. Hemmer, Texas A&M Univ. (United States)

Large depth imaging in strongly scattering media using UOT relies on collecting the small fraction of light frequency-shifted by ultrasound and assuring that this weak signal is not hidden in the noise from the (non frequency-shifted) carrier light wave. Conveniently any filter with a spectral transmission window will both suppress the carrier wave and delay radiation within its transmission window. This talk will describe filters, where the transmitted light (shifted by the ultrasound) arrives at the detector at a time much later than the scattered carrier radiation and thus is detected on a zero background enabling deep tissue imaging.

8223-16, Session 12

## Organic materials for spectral hole burning and non-hole burning narrowband optical filters

A. Gorokhovsky, College of Staten Island (United States)

An overview of properties and applications of organic materials for narrowband spectral hole burning (SHB) and non- hole burning optical spectral filters will be presented. Main focus will be on the properties important for the filters applications in ultrasound -modulated optical tomography (UOT). In UOT these filters may be used to improve image quality in tandem with the more narrowband SHB filters made of RE ions doped inorganic crystals. The following issues will be reviewed: optical spectra of organic molecules at low temperatures, electron -vibrational spectral structure, zero-phonon lines and phonon sidebands, mechanisms of homogeneous and inhomogeneous broadening, optical dephasing in crystals and glasses, spectral hole burning, mechanisms of transient and persistent photochemical, photophysical and gated SHB, kinetics and quantum efficiency of SHB, SHB in optically thick samples. Organic materials for SHB in red and NIR spectral regions, spectral band engineering, applications for narrowband spectral filtering and comparison with narrowband interference filters will be discussed. In addition, non- hole burning organic materials as secondary absorption optical filters to reduce phone-mediated fluorescence from inorganic SHB crystals in UOT applications will be considered.

8223-17, Session 12

## Efficient high-etendue four-wave mixing in a spectral hole-burning medium

B. S. Ham, Inha Univ. (Korea, Republic of); P. R. Hemmer, Texas A&M Univ. (United States)

Real time holography has been used in ultrasound modulated optical tomography demonstrations to extract weak ultrasound tagged light from the intense scattered light emerging from tissue samples. Phase conjugation has also been used to more efficiently direct light to the ultrasound focus in tissue. For both these applications, a high etendue (produce of acceptance angle and area) must be as large as possible. Unfortunately, until now photorefractives demonstrated for such experiments have slow response times, relatively low photon efficiency, and limited acceptance angle due to the small range of allowed grating vector magnitudes. Wavemixing in spectral hole-burning materials promises to have a higher etendue because it supports large grating vectors (signal and reference beam counterpropagating). It can also have relatively fast response times and a high photon efficiency. In a rare-earth Pr3+ doped spectral hole-burning crystal, three orders of magnitude higher photon echo efficiency was observed using ultraslow light. In the photon echoes the signal's amplitude and phases of signal light are recorded in a form of a large enetendue phase grating. Resonant optical transition of Pr3+ ions doped Y2SiO5 at ~606 nm was used for both photon echoes and ultralslow light, where the ultraslow light functions enhanced data absorption and reduced echo reabsorption. Here we discuss potential applications of the controlled photon echoes for high etendue, high resolution bio-imaging applicable to the time-reversed ultrasonically encoded optical focusing.

8223-77, Session 12

## Acoustic radiation force assisted ultrasound modulated optical tomography

M. Tang, R. Li, Y. Cheng, C. W. Dunsby, R. J. Eckersley, D. S. Elson, Imperial College London (United Kingdom)

Acoustic radiation force (ARF) is generated when momentum transfers from the propagating acoustic wave to the medium. As it can cause large (but slow) particle displacement and is closely related to tissue mechanical properties, it has potential in assisting ultrasound modulated optical tomography (UOT) by improving the system SNR and bringing additional information about tissue mechanical properties. A mechanical scanning UOT system has been developed including a 532nm laser, an ultrasound system with a 5MHz focused transducer, and a CCD camera. Tissue mimicking phantoms with heterogeneous inclusions of different optical and mechanical properties were exposed to the laser and ultrasound bursts which generated ARF and subsequent shear wave. The CCD camera was positioned on the side of the phantom opposite to the laser to measure the transmitted photons. The phantom was scanned and the image contrast was calculated based on CCD measurements. Both the timing and the length of CCD exposure were adjusted. It has been shown that by using a short CCD exposure time, the optical measurements were not affected by ARF and shear wave. By increasing and optimising CCD exposure time, the SNR of the measurement can be significantly improved by the ARF without losing spatial resolution. At the same time it is shown that our measurements are sensitive to tissue mechanical properties. By acquiring with multiple CCD exposure times, or multiple CCD trigger delay times to track the shear wave propagation, tissues of different stiffness can be detected and quantified.

8223-78, Session 12

## Improving signal-to-noise ratio and spatial resolution in ultrasound modulated optical tomography

S. P. Morgan, H. Ruan, N. T. Huynh, M. L. Mather, D. He, J. Crowe, F. R. Rose, B. R. Hayes-Gill, The Univ. of Nottingham (United Kingdom)

(Invited)

Ultrasound modulated optical tomography can reduce the effects of light scattering and improve the resolution of optical imaging systems by 'tagging' light that passes through the ultrasound column.

Ultrasound imaging has benefited from non-linear approaches to improve image resolution and reduce the effects of side-lobes. A system for performing second harmonic ultrasound modulated optical tomography is demonstrated which incorporates both pulsed optical illumination and acoustic excitation. A pulse inversion scheme is employed which involves exciting the ultrasound transducer consecutively with a pulse and then an inverted pulse. Summing the detected pulses allows the second harmonic signal to be extracted. The advantage of this approach is that the second harmonic signal can be obtained while still maintaining a short pulse length of the acoustic excitation. A speckle detection algorithm tailored to this configuration has been developed to optimise signal to noise ratio. Images of absorbing objects embedded in tissue phantoms demonstrate that the method can provide an improvement in image resolution.

The use of ultrasound modulated optical tomography in imaging fluorescent targets is also discussed. This is challenging because the modulated light signal is much smaller than when coherent light is detected. A system is described based on pulsed acoustic excitation and optical detection with a photomultiplier tube. Simple experiments show that by changing the length of the acoustic pulse the image contrast can be optimised. Applications in imaging in regenerative medicine are discussed where tissue is grown in three dimensions within scaffolds and non-destructive evaluation is beneficial.

8223-79, Session 12

## Sound light: rendering photoacoustics fluence-independent by adding acousto-optic modulation

W. Steenbergen, A. Hussain, K. Daoudi, Univ. Twente (Netherlands)

A major challenge of photoacoustic imaging is to measure absolute absorption coefficients associated with the concentration of chromophores in tissue. In normal photoacoustics this is not possible because of the unknown optical excitation levels within the tissue. This limitation can be overcome by 'Sound Light', which is a tailored combination of photoacoustic imaging and acousto-optic tissue modulation. In the latter, ultrasound modulates the phase of the light crossing the ultrasound focus, which can be observed in the dynamics of an externally measured speckle pattern. We also have developed a theoretical framework for recombining results of photoacoustics and acousto-optics into absolute absorption coefficients, without the need for calibration. Specific aspects of the method are subsequent injection of light for photoacoustics at two tissue locations, and use of these points as optode location for the acousto-optic part of the method. Included in this strategy is a pure reflection mode implementation in which the points of injection and detection coincide. We will particularly focus on reflection mode Sound Light and on the effects of the size of the injection beam and detection window. Our results will shed light on the potential and limitations of Sound Light to render absolute absorption coefficients, and on the background of the found deviations in terms of the beam size, size of the ultrasound labeling volume and the distance to the tissue surface in relation to the scattering properties of the tissue.

8223-80, Session 12

## Non-invasive blood flow measurements using ultrasound modulated diffused light

N. Racheli, A. Ron, C. Metzger, I. Breskin, M. Balberg, R. Shechter, Ornim Medical Ltd. (Israel)

Capillary blood flow is a critical parameter for determining tissue vitality.

Existing optical methods for measuring blood flow such as Diffuse Correlation Spectroscopy (DCS), Laser Doppler, spatial-temporal image correlation spectroscopy (NIR-STICS) and Speckle Imaging suffer each from drawbacks, such as shallow sampling volumes, complexity and expense of apparatus.

Ultrasound based methods such as Ultrasound Doppler are used for monitoring directional flow in relatively big blood vessels and are problematic when applied to capillary flow.

We present a novel non-invasive method for measuring blood flow based on the acousto-optic effect. Blood flow within the sampled volume disturbs the photons' temporal correlation and therefore the spectral component of light fluctuating at the Ultrasound frequency decreases as flow increase, while the spectral width around the ultrasound frequency broadens. A cross correlation of the sampled light with the emitted ultrasound pattern provides a measure of flow within the sampled volume.

The benefits of the presented method are: localized measured volumes, continuous real time measurement, simplicity of apparatus and ease of operation.

We demonstrate the ability of the method to detect flow of scattering fluid using a calibrated flow phantom model. Fluid flow was generated by a calibrated syringe pump and the phantom's sampled volume contains millimeter size flow channels (10% fluid by volume). Results demonstrate linear dependence of flow as measured by the presented technique (FI) to actual flow values with $r=0.97$, $p<0.001$.

# Conference 8224: Biophotonics and Immune Responses VII

Monday 23 January 2012

Part of Proceedings of SPIE Vol. 8224 Biophotonics and Immune Responses VII

8224-01, Session 1

## Expression of damage-associated molecular patterns in tumors treated by photodynamic therapy

M. Korbelik, The BC Cancer Agency Research Ctr. (Canada)

Trauma inflicted through oxidative stress in tumors treated by photodynamic therapy (PDT) elicits a strong host reaction that mobilizes major protective effector processes dominated by inflammation, acute phase response and immune response. A key role in orchestrating this host response is played by molecular signals called damage-associated molecular patterns (DAMPs) or alarmins consisting of endogenous molecules becoming expressed on or released from PDT-treated tumor tissue. The injury to targeted cancerous lesion induced by PDT is manifested as a massive rapidly formed cellular damage with loss of local homeostasis. Such type of insult is promptly detected by sensors of evolutionary highly organized system for detection, containment and repair. These sensors, known as pattern recognition receptors (PRRs), are dedicated for detection of DAMPs whose presence alerts to the appearance of danger as a consequence of injury to endogenous structures and cell death. The recognition of DAMPs by PRRs prompts the activation of innate immune signaling pathways securing production of pro-inflammatory mediators and mobilizing phagocytes and other host effector cells. These events ensure the restoration of homeostasis by phagocytic removal of damaged cells and debris followed by healing. However, the events associated with innate immune system activation focused on the tumor also lead to the development of adaptive immune response recognizing the antigens of PDT treated cancerous tissue. It has become increasingly evident that PDT is particularly effective in generating an abundance of DAMPs. Prominent representatives include expressed heat shock proteins and calreticulin becoming expressed on the cell surface, and high-mobility group box-1 (HMGB1) released into circulation.

8224-02, Session 1

## Photodynamic therapy can induce non-specific protective immunity against a bacterial infection

M. Tanaka, National Defense Medical College (Japan); P. Mroz, T. Dai, Massachusetts General Hospital (United States); M. Kinoshita, Y. Morimoto, National Defense Medical College (Japan); M. R. Hamblin, Massachusetts General Hospital (United States)

Photodynamic therapy (PDT) for cancer is known to induce an immune response against the tumor, in addition to its well-known direct cell-killing and vascular destructive effects. PDT is becoming increasingly used as a therapy for localized infections. However there has not to date been a convincing report of an immune response being generated against a microbial pathogen after PDT in an animal model. We have studied PDT as a therapy for bacterial arthritis caused by Staphylococcus aureus infection in the mouse knee. We had previously found that PDT of an infection caused by injection of MRSA (5X10(7) CFU) into the mouse knee followed 3 days later by 1 microg of Photofrin and 635-nm diode laser illumination with a range of fluences within 5 minutes, gave a biphasic dose response. The greatest reduction of MRSA CFU was seen with a fluence of 20 J/cm2, whereas lower antibacterial efficacy was observed with fluences that were either lower or higher. We then tested the hypothesis that the host immune response mediated by neutrophils was responsible for most of the beneficial antibacterial effect. We used bioluminescence imaging of luciferase expressing bacteria to follow the progress of the infection in real time. We found similar results using intrarticular methylene blue and red light, and more importantly, that carrying out PDT of the non-infected joint and subsequently injecting bacteria after PDT led to a significant protection from infection. Taken together with substantial data from studies using blocking antibodies we believe that the pre-conditioning PDT regimen recruits and stimulates neutrophils into the infected joint which can then destroy bacteria that are subsequently injected and prevent infection.

8224-03, Session 1

## Study of post-PDT markers of topical photosan-mediated photodynamic therapy on DMBA-induced hamster buccal pouch precancerous and cancerous lesions

Y. Hsu, Chung Yuan Christian Univ. (Taiwan)

Several post-PDT markers of topical photosan-mediated PDT (topical photosan-PDT) using a 640-nm light-emitting diode Wonderlight were studied. Western blots and assays were examined on the specific markers were examined on specimens to study induced apoptotic mechanisms on topical photosan-PDT hamster precancerous and cancerous lesions. The normal side is examined as control in vivo. The major finding is apoptotic enzyme activity reached peak activity at 48 and 72 hrs on precancerous and cancerous lesions respectively. Our findings indicate that suitable marker could serve as a good biomarker for monitoring post-PDT effectiveness for personalized PDT treatment for DMBA-induced hamster buccal pouch precancerous and cancerous lesions.

8224-04, Session 1

## Induction of immune responses and prevention of UV-induced skin carcinoma by topical photodynamic therapy

X. Wang, T. Lv, H. Wang, F. Miao, J. Li, Shanghai Skin Diseases and STD Hospital (China); Z. Huang, Univ. of Colorado Denver (United States)

Objective: To investigate preventive effect of topical photodynamic therapy (PDT) on UV-induced skin carcinomas. Materials and Methods: Female SKH-1 hairless mice were used as a model animal. UV irradiation was delivered through a solar simulator to the back area at a minimal erythema dose (MED) four-day a week. At the mean time, low dose topical PDT mediated with 2% ALA cream was applied to the same area once a week. Effects of PDT on histological change, tumor number and cytokine expression were examined. Results: Low dose ALA-PDT could delay UV-induced histopathological change and prolong tumor-free survival. ALA-PDT could induce cytokine expression and significantly reduce UV-induced carcinogenesis. Conclusion: This in vivo study demonstrated that ALA-PDT could delay and inhibit UV irradiation-induced skin carcinomas. Immune responses may play a role in this process.

8224-05, Session 2

## Long-term effects of laser-imiquimod combination in the treatment of late-stage melanoma patients

M. F. Naylor, Dermatology Associates of San Antonio (United States); H. Le, Univ. of Central Oklahoma (United States); H. Liu, The Univ. of Oklahoma (United States); R. E. Nordquist, Wound Healing of Oklahoma, Inc. (United States); T. Hode, Immunophotonics, Inc. (United States); W. R. Chen, Univ. of Central Oklahoma (United States)

Topical application of a potent immunological modulator, imiquimod, followed by laser irradiation has been used for the treatment of late-stage melanoma patients. We started a phase I clinical trial in 2006 with promising initial outcomes. The laser-imiquimod combination showed significant palliative effects for these patients with multiple treatment cycles. For the returning patients, we found that the recurrent tumors were less aggressive than usually seen in untreated patients. Now we report the five-year follow-up of this phase I trial. The overall 5-year survival rate is close to 50% for the stage III and stage IV patients. The current protocol uses a light-absorbing dye for selective laser photothermal interaction for non-pigmented melanoma nodules. To avoid the complications of the light-absorbing dye, particularly when the tumors are big or deep, we recently tried interstitial laser irradiation with a cylindrical active tip to provide a laser irradiation over a large area. The initial results of the interstitial laser irradiation, together with the application of imiquimod showed great local response, with more effective thermal damage to the target tumor and less skin damage. More follow-ups are needed to see the long-term immunological responses of the interstitial intervention for melanoma patients.

8224-06, Session 2

## Laser immunotherapy for the treatment of human breast cancer: 2-year follow-up results

T. Hode, Immunophotonics, Inc. (United States); O. Adalsteinsson, International Strategic Cancer Alliance (United States); G. L. Ferrel, Hospital Nacional Edgardo Rebagliati Martins (Peru); J. A. Lunn, International Strategic Cancer Alliance (United States); M. Guerra, Immunophotonics, Inc. (United States); X. Li, Chinese PLA General Hospital (China); R. E. Nordquist, Immunophotonics, Inc. (United States); W. R. Chen, Univ. of Central Oklahoma (United States)

Laser immunotherapy (LIT) is an in situ therapeutic cancer vaccine for the treatment of metastatic cancer. The fundamental reasoning behind LIT is to activate dendritic cells (DC) in situ, and subsequently expose the activated DCs to tumor antigens in vivo through a simple local procedure so that a tumor-specific T-cell response is induced. Here we report the initial results and two-year survival data from a human breast cancer pilot trial with laser immunotherapy. The immediate goal of the trial was to determine the patient tolerance and the toxicity of the therapy, the optimal dose for the alteration of the course of the disease, and the reduction of the tumor burden. Ten stage III and IV cancer patients were treated, all of which were considered to be out of all other options. Two patients withdrew prematurely for unrelated reasons, leaving eight evaluable patients. Each patient was individually evaluated for toxicity tolerance through physical exams and by appropriate supplemental and routine laboratory tests. No toxicity or significant adverse reactions were observed, and the treatment was very well tolerated by all patients. 12-month objective response rate (RECIST) was 62.8%, and clinically favorable response was 75%.

8224-07, Session 2

## Interstitial laser irradiation for the treatment of metastatic mammary tumors in combination of intratumoral injection of immunoadjuvant

W. R. Chen, C. Joshi, D. Figueroa, K. Le, H. Liu, Univ. of Central Oklahoma (United States); R. E. Nordquist, Wound Healing of Oklahoma, Inc. (United States); T. Hode, Immunophotonics, Inc. (United States)

Interstitial laser irradiation using a cylindrical diffuser was applied to treat metastatic mammary tumors in rats. To enhance the interstitial irradiation induced photothermal interaction, an immunological modifier, glycated chitosan (GC), was injected around the tumor after the laser treatment. A cylindrical diffuser with an active length of 1 cm was used to treat tumors of sizes approximately 1 to 1.5 cm size. Different laser powers (1 to 3 watts) and different irradiation durations (10 to 30 minutes) were used to test the thermal effects. Different doses of the GC (1.0%, 0.1 to 0.6 ml per rat) were also used to determine the effect of the immunological stimulation. Our results showed that the animal survival depends on both the laser dose and GC dose. A dose of 0.2 ml per tumor appeared to result in the highest survival rate with 2.5 watts and 20 minutes. While the study is still ongoing, our preliminary results indicate that interstitial laser irradiation can be combined with immunotherapy to treat metastatic tumors. Furthermore, our results suggest that an optimal combination of laser dose and GC dose can be obtained as a basis for future clinical protocols using interstitial laser immunotherapy.

8224-08, Session 3

## Visualizing the mediators of innate and adaptive host response to photodynamic therapy

S. Mitra, S. M. Hupcher, T. H. Foster, Univ. of Rochester Medical Ctr. (United States)

Optical imaging strategies together with molecular biology tools have made it possible to visualize in living mice some of the photodynamic therapy (PDT)-induced inflammatory and molecular responses. A hallmark of the inflammatory response is the arrival of neutrophils into the treated tumor, and this influx is associated with the increased expression of adhesion molecules. We have established means of labeling and visualizing various cell types in the tumor using intradermal injection of small (~30 microliters) volumes of fluorophore-conjugated antibodies. Data from in vivo confocal fluorescence imaging of EMT6 tumors subjected to HPPH-PDT show significantly increased cell-surface expression of intercellular adhesion molecule-1. This expression is not limited to the vascular endothelium and appears to extend throughout the tumor. PDT-mediated induction of heat shock proteins (HSPs) and its extracellular release is a molecular response that could assist an effective adaptive host response. Using tumors grown from EMT6 cells transfected with a plasmid in which GFP is placed under the control of an hsp70 promoter, we examined a range of mTHPC-PDT conditions that result in the hsp70 promoter activation and HSP70 extracellular release. We observe a strong correlation between PDT doses that result in tumor cure and those that cause high levels of extracellularly-released HSP70s. Studies have shown that macrophages have higher capacity than tumor cells to accumulate photosensitizers. To examine this phenomenon further, we explore the uptake by phagocytic host cells in the tumor of photosensitizer molecules and their counterpart packaged inside lipid nanoparticles, and their transport to draining lymph nodes.

8224-09, Session 3

## Magnetic resonance thermometry using proton resonance frequency method to monitor photothermal effects of interstitial laser irradiation

J. Goddard, J. Jose, D. Figueroa, K. Le, Univ. of Central Oklahoma (United States); H. Liu, The Univ. of Oklahoma (United States); R. E. Nordquist, Wound Healing of Oklahoma, Inc. (United States); T. Hode, Immunophotonics, Inc. (United States); W. R. Chen, Univ. of Central Oklahoma (United States)

Selective photothermal interaction using dye-assisted non-invasive laser irradiation has limitations when treating deeper tumors or when the overlying skin is heavily pigmented. We developed an interstitial laser irradiation method to induce the desired photothermal effects. An 805-nm near-infrared laser with a cylindrical diffuser was used to treat rat mammary tumors by placing the active length of the fiber inside the target tumors. Three different power settings (1.0 to 1.5 watts) were applied to treat animal tumors with an irradiation duration of 10 minutes. The temperature distributions of the treated tumors were measured by a 7.1-Tesla magnetic resonance imager using proton resonance frequency (PRF) method. Three-dimensional temperature profiles were reconstructed and assessed using PRF. This is the first time a 7.1-Tesla magnetic resonance imager has been used to monitor interstitial laser irradiation via PRF. This study provides a basic understanding of the photothermal interaction needed to control the thermal damage inside tumor using interstitial laser treatment. It also shows that PRF can be used effectively in monitoring photothermal interaction during interstitial laser irradiation. Our long-term goal is to develop a PRF-guided laser therapy for cancer treatment.

8224-10, Session 4

## Circulation times of cancer cells by in vivo flow cytometry

X. Wei, J. Guo, Fudan Univ. (China)

In metastasis, the cancer cells that travel through the body are capable of establishing new tumors in locations remote from the site of the original disease. To metastasize, a cancer cell must break away from its tumor, invade either the circulatory or lymphatic system, which will carry it to a new location, and establish itself in the new site. Once in the blood stream, the cancer cells now have access to every portion of the body. Here we have used the “in vivo flow cytometer” to study if there is any relationship between metastatic potential and depletion kinetics of circulating tumor cells. The in vivo flow cytometer has the capability to detect and quantify continuously the number and flow characteristics of fluorescently labelled cells in vivo. We have improved the counting algorithm and measured the depletion kinetics of cancer cells with different metastatic potential. Interestingly, more invasive PC-3 prostate cancer cells are depleted faster from the circulation than LNCaP cells. In adddition, we have measured the depletion kinetics of two related human hepatocellular carcinoma (liver cancer) cell lines, high-metastatic HCCLM3 cells and low-metastatic HepG2 cells. Interestingly, the low-metastatic HepG2 cells possess noticeably slower depletion kinetics. The differences in depletion kinetics might provide insights into early metastasis processes.

8224-11, Session 4

## In vivo high-speed photoacoustic flow cytometry of immune-related cells

E. I. Galanzha, M. Sarimollaoglu, D. A. Nedosekin, V. P. Zharov, Univ. of Arkansas for Medical Sciences (United States)

We have developed high-speed clinically relevant photoacoustic flow cytometry (PAFC) for ultrasensitive detection of immune-related cells (e.g., leukocytes) in blood circulation in vivo. Among various biomedical applications, we propose the integration of PAFC and nanotechnology-based cell labeling with antibodies to CD45 for detection and counting of rolling and fast moving leukocytes in blood flow. The dynamic measurements of PA signals were performed using fast signal acquisition algorithms which are most accurate and sensitive. As demonstrated on a mouse model, PAFC has potential to distinguish linear velocity, size, and concentration of leukocytes by analyzing PA signal width, shapes and rate. The presence of leukocyte in the detected volume was controlled by optical imaging. Since immune-related cells are pivotal players of almost all human diseases at their early stages, our clinically relevant technology may be potentially used for advanced diagnosis, prognosis and for real-time assessment of therapeutic efficacy of pharmacologic compounds by quantifying leukocytes before, during, and after therapy.

8224-12, Session 4

## In-plane Spatial Resolution Measurements of X-ray Tomosynthesis Prototype

D. Wu, H. Miao, Y. Li, The Univ. of Oklahoma (United States); X. Wu, The Univ. of Alabama at Birmingham (United States); H. Liu, The Univ. of Oklahoma (United States)

The objective of this project is to investigate the in-plane spatial resolution of an x-ray tomosynthesis prototype. Experimentally, a 3D phantom is assembled with 2 standard resolution patterns placed in parallel but at different depth. Tomosynthesis images are acquired and reconstructed. The two in-plane slices corresponding to each of the resolution patterns are viewed by observers, and the in-plane limiting resolutions are determined. For comparison, the resolution patterns are also imaged by single projections. Under single x-ray projection, with only one resolution pattern, the limiting resolution of the system is 17 lp/mm; with 2 resolution patterns superimposed, the image of the resolution patterns is blurred for distinguishing line pairs. The tomosynthesis in-plane images showed that the limiting resolution of the system is about 13 lp/mm. As expected, the tomosynthesis prototype studied in this project reveals superimposed fine structures of the object. The in-plane resolution of the tomosynthesis system can be further improved by optimizing the system alignment, and the reconstruction algorithms.

8224-13, Session 4

## An Automatic Scanning Method for High Throughput Microscopic System to Facilitate Medical Genetic Diagnosis: An Initial Study

Y. Qiu, The Univ. of Oklahoma (United States); X. Chen, Tianjin Univ. (China); Z. Li, The Univ. of Oklahoma (United States); W. R. Chen, Univ. of Central Oklahoma (United States); B. Zheng, Univ. of Pittsburgh Medical Ctr. (United States); S. Li, The Univ. of Oklahoma Health Sciences Ctr. (United States); H. Liu, The Univ. of Oklahoma (United States)

The purpose of this paper is to report a new automatic scanning scheme for high throughput microscopic systems, to facilitate clinical genetic diagnosis. To minimize the impact of the random vibration and mechanical drifting of the scanning stage in microscopic image acquisition, auto-focusing operations are usually applied repeatedly during scanning process. Such methods ensure the acquisition of well focused images for clinical diagnosis, but are time consuming. The technique investigated in this preliminary study applies the auto-focusing operations at a limited number of locations on the slide. For the rest of the imaging field, the focusing position is quickly adjusted through linear interpolation. In this initial validation study, a blood pathological slide containing both metaphase and interphase cells is scanned. For a selected area of 10mm×6.9mm, a number of 4, 12, 21, and 33 positions are evenly sampled for auto-focusing operations. Respectively, 15, 20, 25, and 25 clinically meaningful cells are identified for each sampling scheme. The results suggest that even with a 4 position auto-focusing scheme, one could obtain the adequate number of clinically required cells/features for the diagnosis, for the specific case investigated. The schemes with more auto-focusing operations provide an option for high reliability diagnosis when clinically necessary. More comprehensive research is planned, and that may lead to optimal design trade-off for developing the scanning scheme of the high throughput microscopic system.

8224-14, Session 5

## Effect of near-infrared lasers on myofibroblast differentiation and contraction

M. B. Vaughan, C. Spencer, J. Goddard, W. R. Chen, Univ. of Central Oklahoma (United States)

Lasers employed in wound healing have shown increased ability to heal wounds by affecting fibroblast proliferation and migration. Other studies have shown that certain intensities and wavelengths increase DNA damage and oxidative stress antagonistic to proliferation and migration. All of these effects, at different times, are known to increase wound healing by the myofibroblast. Our objective was to determine whether either of two laser wavelengths, 805nm and 980nm, affect the presence of myofibroblasts and cellular contractility using an attached collagen lattice model. Fibroblasts were cast into type I collagen lattices and allowed to generate tension for 5 days in the presence or absence of laser light stimulation. Presence of myofibroblasts was determined by immunostaining lattices; tension generation was determined indirectly by releasing and measuring diameter change over time. Total number of cells per lattice was determined by solubilizing lattice after contraction and counting with a hemocytometer. The results will be reported and discussed. The ability to modulate the myofibroblast phenotype will have important implications in wound healing, aging and cancer development.

8224-16, Session 6

## Cellular internalization of a membrane binding two-photon probe by forming a nanostructure composed of anionic diblock copolymer and cationic surfactant

O. K. Nag, W. R. Chen, Univ. of Central Oklahoma (United States)

A plasma membrane binding water-soluble two-photon (TP) probe, 1,4-bis(4'-(N,N-bis(6"-(N,N,N-trimethylammonium)hexyl)amino) styryl)benzene tetrabromide (C1) is spatially confined into a vesicular nanostructure composed of anionic diblock copolymer, poly[(ethylene oxide)-block-(sodium-2-acrylamido-2-methyl-1-propane sulfonate)] (Em-An) and cationic surfactant, hexadecyltrimethylammonium bromide (C16), and its linear and nonlinear optical properties are studied. Electrostatic interaction between cationic C16 and anionic Em-An is used to form a self-assembled nanostructure with a hydrophobic core. Incorporation of C1 into the nanostructre modulates its optical properties as compared to those in water. The fluorescence quantum yield ($\eta$) of C1 (0.32 in water) was measured to increase up to 0.56 accompanied with ~40 nm PL spectral shift in the vesicular nanostructure. Furthermore, C1 exhibited ~2-fold increase of two-photon action cross section(in GM) in the nanostructure. Two-photon Microscopy (TPM) images suggest the successful internalization of the encapsulated probe C1 into the cytosol, which itself is stained only in the plasma membrane. This technique not only highlight a simple way to develop two-photon properties of the probe but also demonstrated the possibility of using this type of the nanostructure as a vehicle for intracellular target delivery of hydrophilic and hydrophobic therapeutics.

8224-17, Session 6

## Applications of frequency up-converting "rare-earth" nanoparticles in activating photodynamic agents through near-infrared induced visible luminescence: An in-vitro study.

D. B. Tata, U.S. Food and Drug Administration (United States)

Background and Objective: Photodynamic agents such as Photofrin II utilized in cancer therapy possess two important properties: (i) to become preferentially retained within tumors and the tumor's immediate micro-vascular environment and (ii) a long lived meta-stable state enabling interactions with triplet state molecular oxygen. Upon the photo-agent's activation through visible light photon absorption, photo-agents exert their cytotoxicity through extensive generation of singlet oxygen 1O2, O2-, and H2O2 within the intratumoral environment. Unfortunately, the visible light penetration depth in tissue is shallow (~ 2mm to 5mm). In this investigation we formulated a strategy for visible light production into deep seated cancers through near infra-red light and engineered frequency up-converting nano-particles.

Materials and Methods: In view the fact that near infra-red penetration depths are significantly deeper than visible light, we utilized a 980nm wavelength laser irradiation to induce visible light luminescence from engineered NaYF4:Yb,Tm "rare-earth" nano-particles. Quantification of reactive oxygen species (ROS) generation was made through the change in absorbance of un-oxidized Vitamin C at 265 nm wavelength.

Results: Robust ROS generation from Photofrin II was detected due to the visible light emission from frequency up-converting "rare-earth" based nanoparticles.

Conclusion: The positive in-vitro findings herein provide the basis for future in-vivo studies, in determining the therapeutic efficacy of photodynamic agents indirectly activated through infra-red induced luminenscence from rare-earth particles.

8224-18, Session 6

## Imaging caveoale-mediated transport of nanoparticles using super-resolution microscopy

Z. Wang, C. Tiruppathi, R. Minshall, A. B. Malik, Univ. of Illinois at Chicago (United States)

Caveolae are membrane invaginations of 50-100 nm in diameter that bud from the membrane to form vesicles. Caveolar structures in endothelium might be exploited to efficiently transport therapeutic nanoparticels across endothelial barrier, but it remains determined. Recently, we designed bovine serum albumin (BSA)-conjugated fluorescent nanoparticles that can bind to the receptors in the caveolae in bovine lung endothelial cells. Co-localization of caveolin-1, a protein associated with caveolae, with the internalized BSA-conjugated nanoparticles indicates BSA-conjugated nanoparticles are internalized in caveolae. To determine the caveolar size and dynamics in live endothelial cells, we developed the super-resolution microscopy using a dual-color nanoparticle pair. Using this method, we optically measured the caveolar size based on the combination of different size of the nanoparticle pair. The result is consistent with the TEM measurement. In addition, we measured the transport of BSA-conjugated nanoparticles across a monolayer of endothelial cells using Transwell, and found that the transcytosis of 20nm-sized nanoparticles is more efficient than 100nm nanoparticles. This finding is consistent with our observations that caveolar size is a key determinant of the uptake of nanoparticles in endothelial cells. We also studied caveolae-mediated transport of albumin-conjugated nanoparticles in microvessels using intravital microscopy. The result shows that caveolin-1 knockout mice reduce the internalization of nanoparticles in vessel walls, suggesting that caveolar structures in endothelium play a role in transporting nanoparticles across endothelial barrier. In summary, we have demonstrated the potential of exploiting caveolae to efficiently deliver therapeutic nanoparticles across endothelial barrier using advanced microscopy (super-resolution microscopy and intravital microscopy).

8224-19, Session 6

## Thermo responsive polyelectrolyte-gold nanorod composite for NIR-light-triggered controlled release of doxorubicin

X. Chi, J. Cao, S. Wan, C. Du, Y. Gu, China Pharmaceutical Univ. (China)

In this paper, we use a near-infrared (NIR) light responsive polyelectrolyte-gold nanorod composite (Au NRs/DOX/PE) to control the release of a small-molecule chemotherapeutic drug doxorubicin (DOX). Au NRs with aspect ratio of 3.9 and a longitudinal absorbance peak at 765nm were prepared using seed-mediated method where the cationic surfactant cetyltrimethylammonium bromide (CTAB) used as a soft template and structure-guiding agent. Furthermore, we used layer-by-layer (LbL) technique to prepare Au NRs/DOX/PE by the sequential deposition of polyanions (sodium polystyrene sulfonate (PSS)) and polycations (poly diallyldimethylammonium chloride (PDADMAC)). The release of DOX from the swelling polyelectrolyte composite Au NRs/DOX/PE was induced by the heat which was generated from gold nanorods under NIR light irradiation. Finally, we tested the tumor inhibition rate of Au NRs/DOX/PE in vitro. The results indicated that the composite Au NRs/DOX/PE possessed obviously inhibition rates to breast cancer cells (MCF-7) when exposed to NIR light, compared to results of either Au NRs or DOX alone. Moreover, the tumor inhibition rate was largely dependent on the output power of the NIR laser, irradiation time and the concentration of Au NRs. Overall, our studies have showed a potential drug release system to achieve the purpose of hyperthermia and chemotherapy treatment of breast cancer in the future.

8224-20, Poster Session

## Direct laser light enhancement of susceptibility of bacteria to gentamicin antibiotic

Y. Reznick, E. Banin, A. Lipovsky, R. Lubart, Z. Zalevsky, Bar-Ilan Univ. (Israel)

In the past 50 years, antibiotics have been critical in the fight against many diseases and infections. As the use of antibiotics became more widespread, the prevalence of antibiotic resistant bacteria increased and the pace at which new antibiotics are being produced is slowing down. One possible alternative treatment against bacteria that are resistant to antibiotics is Photodynamic Therapy (PDT). In the present study, we investigated the possibility to increase the effectiveness of existing antibiotics (not photosynthiszer) by combining it with exposure to laser light.

Objectives: To test the effect of pulsed (Q-switched) and continuous wave (CW) laser light at wavelength of 532nm on the viability of free-living stationary phase bacteria with and without gentamicin treatment.

Methods: Free living stationary phase gram negative bacteria (Pseudomonas aeruginosa strain PAO1) was immersed in Luria broth (LB) solution and exposed to Q-switched and CW lasers with and without the addition of the antibiotic gentamicin. Cell viability was determined at different time points.

Results: Laser treatment alone did not reduce cell viability compared to untreated control and as expected the gentamicin treatment alone only resulted in a 0.5 log reduction in the viable count for P. aeruginosa. The combined laser and gentamicin treatment, however, resulted in a synergistic effect and viability was significantly reduced by 8 log's for P. aeruginosa PAO1.

Conclusions: Combination of laser light with gentamicin shows significantly improved efficacy against P. aeruginosa.

8224-21, Poster Session

## SB203580 enhances the RV-induced loss of mitochondrial membrane potential and apoptosis in A549 cells

H. Li, X. Wang, Jinan Univ. (China); T. Chen, South China Normal Univ. (China)

Resveratrol (RV), a naturally occurring phytoalexin, is known to possess a wide spectrum of chemopreventive and chemotherapeutic effects in various stages of human tumors. There are increasingly evidences showing that apoptotic pathway plays an important role in anti-cancer effect of RV. p38 is a member of the mitogen-activated protein kinase (MAPK) superfamily, it is always activated by some extracellular stimulus to regulate many cellular signal transduction pathway, such as apoptosis, proliferation, inflammation and so on. In this report, we assessed the effect of SB203580, pyridinyl imidazole compound which is known as a specific inhibitor of p38 MAPK signaling pathway, on the RV-induced apoptosis in human lung adenocarcinoma (A549) cells. CCK-8 assay was used to assess the cell viability, and we found that treatment of cells with 1 or 10 μM SB203580 alone didn't show inhibitory effect of cell growth, but pretreatment with 10 μM SB203580 significantly enhanced the cytotoxicity of RV after treatment for 48 h, which was verified by flow cytometry analysis by using Annexin and propidium iodide staining. In order to confirm further that SB203580 accelerated apoptosis via the intrinsic pathway, we stained the cells with rhodamine 123 to detect the dysfunction of mitochondria and anslyzed by flow cytometry. This result for the first time reported that p38 inhibitor SB203580 enhanced the RV-induced apoptosis via a mitochondrial pathway.

8224-22, Poster Session

## Artesunate induces AIF-dependent apoptosis in A549 cells

C. Zhou, T. Chen, South China Normal Univ. (China)

Artesunate (ART), a semi-synthetic derivative of the sesquiterpene artemisinin extracted from the Chinese herb Artemisia annua, exerts a broad spectrum of clinical activity against human cancers. It has been shown ART-induced cancer cells death through the apoptosis pathway. This study was investigated in human lung adenocarconoma A549 cell line and aimed to determine whether the proapoptotic protein apoptosis inducing factor (AIF) is involved in ART-induced apoptosis. We used rhodamine 123 to probe the level of mitochondrial membrane potential by flow cytometry. Immunofluorescence staining was utilized here to study the release of AIF from mitochndria in single cells. In order to determine the role of AIF in ART-induced apoptosis, we silenced AIF by transfection of shAIF plasmid in cells. Overall, the result showed that (1) ART could induced A549 cell death in the apoptosis pathway, which was assayed by Cell Counting Kit (CCK-8) and Hoechst 33258 staining. Cells treated with ART exhibit typical apoptotic morphology as chromatin condensation, margination and shrunken nucleus, the chromatin of control cells was evenly present in whole nuclear; (2)ART induced a loss of mitochondrial membrane potential and then AIF to release from mitochndria. We used confocal microscope to monitor the spatial distribution of AIF inside cells with specific antibodies for AIF. Control cells showed a granular staining pattern (mitochondrial localization) of AIF, whereas ART-treated cells presented significant translocations of AIF to the nucleus; (3) AIF plays a central role in ART-induced A549 cells apoptosis. CCK-8 analysis showed that shAIF did not harm cells and remarkably attenuated ART-induced cell death.

Keywords: Artesunate; Apoptosis; AIF release; A549 cells

8224-23, Poster Session

## Low-power laser irradiation enhance macrophage phagocytic capacity through Src activation

F. Zhou, South China Normal Univ. (China)

Phagocytosis and subsequent degradation of pathogens by macrophages play a pivotal role in host innate immunity in mammals. Laser irradiation has been found to produce photobiological effects with evidence of interference with organic functions. In this study, we focused our attention on the effects of He-Ne laser on the phagocytic activity of macrophages, the regulation mechanism of phagocytosis was also discussed. Our results indicated that Low-power laser irradiation can enhance the phagocytosis of macrophage through activation of Src.

8224-24, Poster Session

## Nanoscopy of Protein-protein Interaction in Living Cells by Combination of Bimolecular Fluorescence Complementation

L. Qin, Z. Huang, S. Zeng, Z. Zhang, Britton Chance Ctr. for Biomedical Photonics (China)

In past decade, super-resolution imaging methodologies such as PALM, STROM and STED, bring cell biological research via protein labeling and visualization to a brand new level. While we got impressive progress in realm of single molecular imaging and tracking, there are no appropriate technology, just like Fluorescense Resonance Energy Transfr (FRET) or Bimolecular Fluorescence Complementation (BiFC) which widely used in normal fluorescence imaging, to investigate protein-protein interactions in super-resolution condition, which play key roles in most cellular protein-related events. Here, we report a novel BiFC System based on a far-red fluorescent protein (fRFP) with significant photoconversion, and combine this photoconversionable BiFC system with photoactivated localization microscopy (PALM) to study protein-protein interactions at the nanoscale. Our results demonstrate that fRFP-based BiFC can be successfully used to investigate bFos-bJun protein interaction pairs with PALM imaging.

8224-25, Poster Session

## Time-delayed mathematical model of nonlinear dynamics of interleukin-2 immunotherapy

G. S. Terentyuk, T. S. Kondaurva, N. M. Ryskin, I. L. Maksimova, N.G. Chernyshevsky Saratov State Univ. (Russian Federation)

Modeling of immune response is among the most intriguing problems of modern mathematical biophysics. There have been several attempts to develop a mathematical model of immune response. In particular, a well-known time-delayed model has been suggested by G.I. Marchuk et al. [G.I. Marchuk, Mathematical Models in Immunology. Nauka, Moscow, 1980. (in Russian)]. This model consists of four differential equations for concentrations of antigens, antibodies and plasma cells. The delayed term appears in the equation for plasma cells describing the effect of the immune system delayed response to antigen invasion. One of the most interesting features of the Marchuk's model is prediction of self-oscillatory dynamics for sufficiently large antigen growth rate.

In this paper we have modified the Marchuk's model for account of interleukin-2 (IL2) immunomodulator impact. In the suggested model the speed of antibodies production from plasma cells becomes function of the IL2 concentration. This function attains maximum at a certain value of IL2 which corresponds to healthy organism. Also, an equation describing dynamics of the IL2 concentration is added. We perform numerical simulation of the model for various parameters. In particular, we simulate the process if IL2 immunotherapy, i.e. decease treatment by injection of IL2 in the case of suppressed immunity. It is shown that increase of IL2 up to the level of healthy organism results in enhance of production of antibodies and suppression of anigen. We investigate connection of optimal period of injection with period of oscillations.

8224-26, Poster Session

## Neutrophils of the patient s with cervical cancer after femtosecond laser radiation in vitro

T. Abakumova, Ulyanovsk State Univ. (Russian Federation); A. Sysolyatin, A. M. Prokhorov General Physics Institute (Russian Federation); V. Svetukhin, I. Antoneeva, D. Arslanova, S. Gening, Ulyanovsk State Univ. (Russian Federation)

The cytochemical analysis of the aerobic and anaerobic bactericidal, phagocytic activity, phagocytosis completeness, as well as membrane topology and rigidity has been performed with the Atomic -force microscopy (SolverPro, NT-MDT, Russia) in neutrophils of the patients with cervical carcinoma treated with the Erbium laser radiation of different intensity.

The obtained data reveal a significant effect of the femtosecond laser radiation on morphofunctional state of the neutrophils of the patients with cervical cancer. The efficiency of the femtosecond radiation depends on its intensity and clinical stage of the cervical cancer.

8224-27, Poster Session

## Comparsion of light dose on topical ALA-mediated photodynamic therapy for DMBA-induced hamster buccal pouch premaligant lesions

Y. Hsu, D. Yang, M. Tseng, Chung Yuan Christian Univ. (Taiwan)

Oral cancer has becomes the most prominent male cancer disease due to the local betel nut chewing habit combing with smoking and alcohol-drinking lifestyle. In order to minimize the systemic phototoxic effect of 5-aminolevulinic acid (ALA), this study was designed to use a topical ALA-mediated PDT for treatment of DMBA-induced hamster buccal pouch cancerous lesions. DMBA was applied to one of the buccal pouches of hamsters thrice a week for 8 to 10 weeks. Precancerous lesions were induced and proven by histological examination. These DMBA-induced cancerous lesions were used for testing the efficacy of topical ALA -mediated PDT. Before PDT, fluorescence spectroscopy was used to determine when ALA reached its peak level in the lesional epithelial cells after topical application of ALA gel. We found that ALA reached its peak level in cancerous lesions about 2.5 hrs after topical application of ALA gel. The precancerous lesions in hamsters were then treated with topical ALA -mediated PDT with light exposure dose of 75, 100 and 150 J/cm2 using LED 635 nm Wonderlight device. Visual examination demonstrated that the given light dose does make drastic therapeutic difference for DMBA-induced hamster buccal pouch precancerous lesions. It is suggesting that optimization of the given light dose is critical to the success of PDT results.

8224-28, Poster Session

## Combination therapies in adjuvant with topical ALA-mediated photodynamic therapy for DMBA-induced hamster buccal pouch premaligant lesions

Y. Hsu, D. Yang, Chung Yuan Christian Univ. (Taiwan)

In Taiwan, oral cancer has becomes the fastest growth male cancer disease due to the betel nut chewing habit combing with smoking and alcohol-drinking lifestyle of people. In order to eliminate the systemic phototoxic effect of 5-aminolevulinic acid (ALA), this study was designed to use a topical ALA-mediated PDT for treatment of DMBA-induced hamster buccal pouch precancerous lesions. DMBA was applied to one of the buccal pouches of hamsters thrice a week for 10 to 12 weeks. Cancerous lesions were induced and proven by histological examination. These DMBA-induced cancerous lesions were used for testing the efficacy of topical ALA -mediated PDT. Before PDT, fluorescence spectroscopy was used to determine when ALA reached its peak level in the lesional epithelial cells after topical application of ALA gel. We found that ALA reached its peak level in precancerous lesions about 2.5 hrs after topical application of ALA gel. The cancerous lesions in hamsters were then treated with topical ALA -mediated PDT with light exposure dose of 100 J/cm2 using LED 635 nm fiber-guided light device. Visual examination demonstrated that adjuvant topical ALA -mediated PDT group has shown effective therapeutic results in compared to those of non-adjuvant topical ALA-mediated PDT group for DMBA-induced hamster buccal pouch precancerous lesions.

8224-29, Poster Session

## Synthesis of dimeric cyclic RGD based near-infrared probe for in vivo tumor diagnosis

J. Cao, S. Wan, J. Tian, X. Chi, C. Du, D. Deng, Y. Gu, China Pharmaceutical Univ. (China)

Cell adhesion molecule integrin $\alpha v\beta 3$ is an excellent target for tumor interventions because of its unique expression on the surface of several types of solid tumor cells and on almost all sprouting tumor vasculatures. In this manuscript, we describe the synthesis of near-infrared (NIR) fluorochrome ICG-Der-02-labeled dimeric cyclic RGD peptides (ICG-Der-02-c(RGDyK)2) for in vivo tumor integrin targeting. The optical properties and structure of the probe were intensively characterized. Afterwards, the integrin specificity of the fluorescent probe was tested in vitro for receptor binding assay and fluorescence microscopy and in vivo for subcutaneous MDA-MB-231 and U87MG tumor targeting. The results indicated that after labled the RGD peptide, the optical properties of ICG-Der-02 showed no obvious change. Besides, in vitro and in vivo tumor targeting experiment indicated that the ICG-Der-02-c(RGDyK)2 probe with high integrin affinity showed excellent tumor activity accumulation and strong tumor-to-normal tissue contrast. This uptake is integrin specific as the signal accumulated in the tumor can be effectively blocked by unconjugated RGD peptide antagonist of integrin $\alpha v\beta 3$. Noninvasive NIR fluorescence imaging is able to detect tumor integrin expression based upon the highly potent RGD peptide probe.

8224-30, Poster Session

## ER$\beta$ regulates miR-21 expression and inhibits invasion and metastasis in cancer cells

J. Tian, Y. Gu, Z. Tu, China Pharmaceutical Univ. (China)

In human, estrogens play important roles in many physiological processes, and is also found to be connected with numerous cancers. In these diseases, estrogen mediates its effects through the estrogen receptor (ER), which serves as the basis for many current clinical diagnosis. Two forms of the estrogen receptor have been identified, ER$\alpha$ and ER$\beta$, and show different and specific functions. The two estrogen receptors belong to a family of ligand-regulated transcription factors. Estrogen via ER$\alpha$ stimulates proliferation in the breast, uterus, and developing prostate, while estrogen via ER$\beta$ inhibits proliferation and promotes differentiation in the prostate, mammary gland, colon, lung, and bone marrow stem cells. MicroRNAs (miRs) are small non-coding RNA molecules that occur naturally and downregulate protein expression by translational blockade of the target mRNA or by promoting mRNA decay. MiR-21 is one of the most studied miRNAs in cancers. MiR-21 is overexpressed in the most solid tumors, promoting progression and metastasis. The miR-21 gene is located on the chromosome 17, in the 10th intron of a protein-coding gene, TMEM49. While, the function of TMEM49 is currently unknown. Our experiment is designed to identity the relationship between miR-21 and ER$\beta$ in cancer progression. The human cancer cells were transfected with ER$\beta$. Real-time PCR analysis showed that the expression level of miR-21 was significantly inhibited down by ER$\beta$ treatment. As MTT assay showed the tumor cell survival rate was also inhibited significantly. Go/Gl phase cell cycle arrest was founded and tumor cell apoptosis was induced in ER$\beta$ group.

8224-31, Poster Session

## Surface modification of upconversion nanoparticles with amphiphilic chitosan for cancer cell imaging

S. Cui, H. Zhu, J. Tian, X. Chi, H. Chen, Y. Gu, China Pharmaceutical Univ. (China)

Upconversion nanoparticles (UCNPs) as a new kind of biological luminescence materials have many advantages comparing with organic fluorescence probes and semi-conductive quantum dots, such as sharp fluorescence emission, long emission lifetimes, high optical and chemical stability and low toxicity, especially low auto-fluorescence background and deep tissue penetration under near-infrared excitation for bioimaging. In common, oleic acid and oleylamine capped UCNPs with excellent upconversion luminescence are widely synthesized in past five years. However, these UCNPs are not suitable to be used in biological application without surface modification, due to their poor solubility in physiological solution and the lack of functional groups.

Herein, we demonstrate a facile approach to transfer UCNPs from hydrophobic to hydrophilic and the use of these UCNPs for cell imaging. Oleic acid-capped UCNPs based on NaYF4 were synthesized and modified with amphiphilic chitosan derivative through hydrophobic interaction. The resulting chitosan-based UCNPs were characterized by transmission electron microscopy (TEM), X-ray diffraction (XRD), Fourier transform infrared spectroscopy (FTIR) and photoluminescence spectroscopy. Cell viability was assessed by MTT assays and in vitro cell imaging was investigated using confocal fluorescence microscope with near-infrared excitation. The results indicate that the produced chitosan-based UCNPs possess good monodispersibility, excellent optical properties and low cytotoxicity after surface modification. Our work suggests a feasible method to modify OA-UCNPs with amphiphilic polymer and the promise of chitosan-based UCNPs for bioimaging application.

8224-32, Poster Session

## Preliminary study of PDT-1O2 dosimetry in vitro using Singlet Oxygen Sensor Green

H. Lin, H. Zheng, D. Chen, B. Li, S. Xie, Fujian Normal Univ. (China)

Singlet oxygen (1O2) is a highly oxidative reactive oxygen species that plays an important role in photodynamic therapy (PDT). Singlet Oxygen Sensor Green (SOSG) is a newly developed 1O2 specific fluorescence probe. In the presence of 1O2, SOSG can react with 1O2 to produce SOSG endoperoxides (SOSG-EP) that are strongly fluorescence emission at 525 nm. In this study, we investigated the feasibility of monitoring 1O2 generation during PDT using SOSG. The human nasopharyngeal carcinoma CNE1 cells were sensitized with Protoporphyrin IX (PpIX), and the sensitized cells in SOSG solution were irradiated with a power adjustable 643 nm light-emitting diode (LED) based illumination system. SOSG fluorescence before and after PDT treatment was measured by LP 940 multimode reader, while the intracellular PpIX concentration was monitored by FLS 920. The survival rate of treated cells was assessed by 3-(4,5-dimetnyl-thiazol-2-yl)2,5-diphenyl tetrazolium bromide (MTT) method. The obtained results show that the survival rate of CNE1 cells is correlated well with the enhancement of SOSG fluorescence. This preliminary study demonstrates the potential utility of SOSG fluorescence probe as an indicator for PDT-1O2 dosimetry in vitro.

# Conference 8225: Imaging, Manipulation, and Analysis of Biomolecules, Cells, and Tissues X

Saturday-Monday 21-23 January 2012

Part of Proceedings of SPIE Vol. 8225 Imaging, Manipulation, and Analysis of Biomolecules, Cells, and Tissues X

8225-01, Session 1

## Testing the behavior of microorganisms in combinatorial microfluidics

D. V. Nicolau, Univ. of Liverpool (United Kingdom)

No abstract available

8225-02, Session 1

## Light scattering of individual erythrocytes from a sickle cell anemia patient

Y. Kim, Korea Advanced Institute of Science and Technology (Korea, Republic of); J. Higgins, Massachusetts General Hospital (United States); Y. Park, Korea Advanced Institute of Science and Technology (Korea, Republic of)

Sickle cell disease (SCD) is characterized by sharp- and elongated-shaped erythrocytes upon exposure to deoxygenated condition. Pathophysiological aspect of SCD is largely determined by biomechanical properties of erythrocytes and their hemodynamics in circulatory system. Here, to understand the pathophysiology of erythrocyte with SCD, we present static and dynamic light scattering signals of erythrocytes from a patient with SCD using Fourier transform light scattering (FTLS) technique.

In order to retrieve elastic light scattering signals from individual erythrocytes, we quantitatively measured the electric field from erythrocytes by using diffraction phase microscopy (DPM). All the experimental measurements were performed under room temperature and oxygenated condition. According to the morphological characteristics, we classified erythrocytes with SCD into three different groups; echinocytes, discocyte, and irreversibly sickled cells. We present anisotropic FTLS to analyze the scattering signal associated with long and short axes for the elongated erythrocytes in SCD. Using anisotropic FTLS analysis, we demonstrate that the static and dynamic light scattering signals of erythrocytes are significantly altered in SCD.

In conclusion, we report the both static and dynamic light scattering signals of individual erythrocytes with SCD based on anisotropic FTLS technique. We demonstrates a novel methodology to study the erythrocytes in SCD. The anisotropic FTLS technique potentially would provide a useful noninvasive optical method to study pathophysiology of SCD at the single-cell level, as well as other erythrocyte-related diseases.

8225-03, Session 1

## Imaging caveolae-mediated transport of nanoparticles using superresolution microscopy

Z. Wang, C. Tiruppathi, R. Minshall, A. B. Malik, Univ. of Illinois at Chicago (United States)

Caveolae are membrane invaginations of 50-100 nm in diameter that bud from the membrane to form vesicles. Caveolar structures in endothelium might be exploited to efficiently transport therapeutic nanoparticels across endothelial barrier, but it remains determined. Recently, we designed bovine serum albumin (BSA)-conjugated fluorescent nanoparticles that can bind to the receptors in the caveolae in bovine lung endothelial cells. Co-localization of caveolin-1, a protein associated with caveolae, with the internalized BSA-conjugated nanoparticles indicates BSA-conjugated nanoparticles are internalized in caveolae. To determine the caveolar size and dynamics in live endothelial cells, we developed the super-resolution microscopy using a dual-color nanoparticle pair. Using this method, we optically measured the caveolar size based on the combination of different size of the nanoparticle pair. The result is consistent with the TEM measurement. In addition, we measured the transport of BSA-conjugated nanoparticles across a monolayer of endothelial cells using Transwell, and found that the transcytosis of 20nm-sized nanoparticles is more efficient than 100nm nanoparticles. This finding is consistent with our observations that caveolar size is a key determinant of the uptake of nanoparticles in endothelial cells. We also studied caveolae-mediated transport of albumin-conjugated nanoparticles in microvessels using intravital microscopy. The result shows that caveolin-1 knockout mice reduce the internalization of nanoparticles in vessel walls, suggesting that caveolar structures in endothelium play a role in transporting nanoparticles across endothelial barrier. In summary, we have demonstrated the potential of exploiting caveolae to efficiently deliver therapeutic nanoparticles across endothelial barrier using advanced microscopy (super-resolution microscopy and intravital microscopy).

8225-04, Session 1

## Heavy metal stress detection and monitoring via LED-induced chlorophyll fluorescence analysis of Zea mays L. seedlings aiming polluted soil phytoremediation

A. S. Gouveia-Neto, E. Arcanjo da Silva, A. J. da Silva, C. W. A. Nascimento, Univ. Federal Rural de Pernambuco (Brazil)

There has recently been a widespread scientific and technological interest in laser-induced sensing techniques to investigate the status of terrestrial vegetation. The techniques rely upon the light generated in the photosynthesis process which occurs mostly in the red(680-690 nm) and far-red(730-740 nm) wavelength regions and is called Chlorophyll Fluorescence(ChlF). ChlF spectral analysis permits detection, monitoring, and evaluation of abiotic stresses upon healthy plants. Plant stress caused by heavy metal soil contamination is of great interest motivated by environmental and economical issues. Overabundance of metal in soil causes harm to human, animal and plant health and is an environment problem that requires effective and affordable remediation techniques. The metal contamination study examines stress aiming phytosanity and/or evaluate tolerance of certain plant spieces to high heavy metal concentrations for application in soil phytoremediation. For optimal concentrations some heavy metals are essential for plant nutrition, and when the concentrations reach supraoptimal values, toxic effects and metabolic desorder occurs. Nevertheless, plants capable of retaining high heavy metal concentrations in their shoots are potential candidates for soil remediation through phytoextraction. LED-induced chlorophyll fluorescence is employed to detect and study the time evolution of metal(Pb, Cd, Zn) stress of Zea mays L. seedlings aiming polluted soil phytoremediation. The ChlF spectra of intact leaves were analyzed using 405 nm excitation. Red(Fr) and far-red (FFr) emissions around 685 nm and 735 nm, respectively, were examined as a function of the heavy metal concentration. The fluorescence ratio Fr/FFr was employed to monitor the effect of heavy metal upon the physiological state of the plants before signs of visual stress became apparent. The ChlF analysis permitted detection and evaluation of the damage caused by heavy metal soil contamination in the early stages of the plants growing process, which is not feasible using conventional in vitro spectral analysis

8225-05, Session 1

## Interferometric measurement of traveling waves in the mammalian cochlea in vivo combined with photo-deactivation of prestin: a cellular force-generating protein

J. A. N. Fisher, F. Nin, T. Reichenbach, A. J. Hudpeth, The Rockefeller Univ. (United States)

Sensorineural hearing loss affects millions of Americans. In many cases, the symptoms of such hearing loss are consistent with a loss of “active” hearing, a process by which hair cells of the inner ear nonlinearly amplify their own mechanical stimuli. Prestin, a voltage-sensitive membrane protein, causes electrically evoked length changes in the inner ear’s mechanosensory hair cells, and may serve as the dominant force underlying active hearing. Using a scanning heterodyne interferometer, we measured sound-evoked traveling waves in the cochlear partition in vivo. The amplitude of the waves scaled nonlinearly as a function of sound stimulus intensity, consistent with previous work. To determine prestin’s role in this nonlinear response, we combined our interferometric measurements with targeted photo-deactivation of prestin’s motor properties using scanning ultraviolet (UV) photolysis of 4-azidosalicylate, a compound that binds covalently to prestin upon UV irradiation. The scanning photolysis enabled us to affect the motor protein in selected hair cells. We then re-measured the traveling waves after targeted photolysis of selected regions along the cochlear partition. We observed a shift in peak location and reduced amplitude. Despite these changes, nonlinear amplification in the traveling waves remained after prestin’s contribution was optically compromised. The results suggest a nuanced role for prestin, and that the motor protein is not solely required for nonlinear amplification in the cochlea.

8225-07, Session 1

## Effects of cross-linkers on optical spectral properties and nano/microstructure of collagen hydrogels

Y. J. Hwang, J. Granelli, J. Larsen, J. G. Lyubovitsky, Univ. of California, Riverside (United States)

Non-enzymatic cross-linking of collagen hydrogels with glyceraldehyde, 1-Ethyl-3-(3-dimethylaminopropyl)carbodiimide (EDC) and N-hydroxysuccinimed (NHS) mixed with EDC was followed by multiphoton microscopy, transmission electron microscopy and Raman spectroscopy. The non-zero cross-linker glyceraldehyde induced strong auto-fluorescence within the collagen hydrogels. The two-photon fluorescence emission maximum of the fluorescent adducts formed by glyceraldehyde was observed at about 460 nm (l=720 nm). The emission peak shifted to 480 nm when we used 800 nm light. The glyceraldehyde remodeled both the initial nano- and microstructure of collagen hydrogels as detected with transmission electron and multi-photon microscopy respectively. Raman spectroscopy showed elevated areas for the peaks at 854, 879 and 928 cm-1 that were assigned to the C-C stretch of the proline and hydroxyproline ring and for the peaks at 821 and 938 cm-1 assigned to C-C stretch of the protein backbone. The zero cross-linker EDC alone or in combination with NHS had no appreciable effect on the collagen microstructure as detected with multiphoton microscopy. However, the fibrils, which represent collagen nanostructures, became smaller and more homogeneous in diameters as detected with transmission electron microscopy. The areas under the 1642 cm-1 peak (C=O stretch) and 2067 cm-1 peak (C-N stretch) increased indicating an increase in the content of amide bonds as a result of cross-linking.

8225-09, Session 1

## In vivo imaging of microglia response to ionizing radiation

C. Alt, J. M. Runnels, C. P. Lin, Wellman Ctr. for Photomedicine (United States)

Whole body irradiation (WBI) is routinely performed in cancer patients and bone marrow transplant recipients. The gamma radiation ablates hematopoietic cells, but can potentially cause collateral damage, for example, in the central nervous system (CNS). Moreover, accidental exposure to radiation can occur in a variety of settings and can pose a long-term threat to human health. Here, we investigated cellular and vascular effects of WBI by non-invasive in vivo imaging of the retina as an optically accessible compartment of the CNS.

We have set up a confocal scanning laser ophthalmoscope (SLO) that allows the detailed visualization of murine retinal microstructure, such as vasculature and retinal microglia. Using three laser sources with multiband dichroic beamsplitters allows observation of up to three cell populations simultaneously. Mice were exposed to lethal and sublethal doses of gamma radiation; some mice were protected with a head-shield. The integrity of the blood retinal barrier was evaluated by fluorescein angiography. To longitudinally track turnover of microglia populations, bone marrow cells from universal DsRed donor mice were transplanted in CX3CR1-GFP mice that express GFP in microglial cells. The populations of native (GFP) and engrafting (DsRed) cells were followed by live imaging for four months after WBI.

Increased vascular leakage was detected after sublethal irradiation. We quantified dose dependent loss of native GFP+ microglia and concomitant but delayed engraftment of bone marrow derived DsRed+ cells.

Our results suggest that even sub-therapeutic, exposure to gamma radiation compromises the integrity of the neural barrier and affects microglial turnover in the CNS.

8225-10, Session 1

## Evaluation of atherosclerotic plaque development by texture analysis of multimodal CARS images of rabbit arteries

L. Mostaço-Guidolin, A. C. T. Ko, D. P. Popescu, M. S. D. Smith, E. Kohlenberg, National Research Council Canada (Canada); M. Shiomi, Kobe Univ. School of Medicine (Japan); A. Major, Univ. of Manitoba (Canada); M. G. Sowa, National Research Council Canada (Canada)

Atherosclerotic plaques and plaque development are complex systems where the composition and structure vary greatly with respect to age, the location along and within the vessel. A multimodal approach based on a single-platform TPEF (two-photo excited fluorescence), SHG (second-harmonic generation) and CARS (coherent anti-Stokes Raman) microscope has recently demonstrated its strength in imaging arterial structures, in particular tracing the morphological changes within the extracellular components of the vessel wall [1]. Several other studies have also demonstrated the use of nonlinear optical (NLO) microscopy to image arterial tissue [2,3]. However, few of these studies have provided quantitative descriptors of the images and related these metrics to the development of atherosclerosis or vascular wall anatomy and pathology. Tonal and texture parameters from nonlinear optical images have the potential to provide objective metrics that correspond to structural and biochemical changes that occur within the vessel wall in early and late stage atherosclerosis. Textural features [4] extracted from nonlinear optical images were investigated for their utility in providing quantitative descriptors of structural and compositional changes associated with plaque development. Texture parameters were derived from the image histogram and gray level co-occurrence matrix and evaluated according with the ability to classify differences between plaques at different locations along the aorta, in particular at the aorta arch and the external iliac aorta. Tonal-texture parameters can be linked to key histological features that characterize vulnerable plaque: the thickness and density of the fibrous cap, size of the atheroma, and the level of inflammation indicated through lipid deposition.

[1] Ko A C-T, Ridsdale A, Smith M S D, Mostaço-Guidolin L B, Hewko M D, Pegoraro A F, Kohlenberg E K, Schattka B, Shiomi M, Stolow A and Sowa M G Multimodal nonlinear optical imaging of atherosclerotic plaque development in myocardial infarction-prone rabbits J. Biomed. Opt. 15 020501, 2010.

[2] Lilledahl M B, Haugen O A, de Lange Davies, C and Svaasand L O Characterization of vulnerable plaques by multiphoton microscopy J. Biomed. Opt. 12 044005, 2007

[3] Le T T, Langohr I M, Locker M J, Sturek M and Cheng J X Label-free molecular imaging of atherosclerotic lesions using multimodal nonlinear optical microscopy J. Biomed. Opt. 12 054007, 2007

[4] Haralick R M, Shanmugam K and Dinstein I H Texture features for image classification IEEE Trans. Sys. Man Cybernet. SMC-3 610-21,1973.

8225-11, Session 1

## Long-term measurement of spontaneous membrane fluctuations over a wide-dynamic range in the living cell by low-coherent quantitative phase microscopy

T. Yamauchi, H. Iwai, Y. Yamashita, Hamamatsu Photonics K.K. (Japan)

The spontaneous fluctuations of the plasma membrane have been studied as an intrinsic indicator of the cell's physical properties in the field of biology. In order to measure spontaneous membrane fluctuations in three dimensions, we demonstrate reflection-phase imaging of live cultured cells by the low-coherent quantitative phase microscope (LC-QPM), which is a reflection-type interference microscope employing the digital holographic technique with a low-coherent light source. Owing to the low-coherency of the light-source, only the light reflected from a specific sectioning height of the sample generates an interference image on the CCD camera. Because the digital holographic technique enables us to quantitatively measure the intensity and the phase of the optical field, a nanometer-scale surface profile of living cells can be obtained by capturing the light reflected by the cell membrane. The lateral and the vertical spatial resolutions were 0.56 microns and 0.93 microns respectively, and the mechanical stability of the phase measurement was better than 2 nanometers. The measurements were made at fast (20 frames/sec) and slow (0.2 frames/sec, time-lapse) frame rates and the slow measurements were performed over a period of 10 minutes. The temporal fluctuations of the cell membrane were analyzed by the mean-square-displacement (MSD) as a function of time-difference tau. By merging the fast and slow data, the MSDs from tau = 50 msec to tau = 300 sec were obtained and the wide-dynamic-range measurement of the MSDs from 2 nm^2 to over 10000 nm^2 were demonstrated.

8225-12, Session 2

## Rotation of microscopic objects in fiber optic trap

B. Black, S. K. Mohanty, The Univ. of Texas at Arlington (United States)

Due to easy integration with microfluidic devices, fiber optical trapping is finding increasing use to immobilize microscopic objects for physical and spectroscopic analysis of samples in solution. However, in most cases, microfluidic actuation in these optofluidic chips is carried out by mechanical pumps. Though conventional microscope objective based laser spanners (based on transfer of spin or orbital angular momentum) are being employed to drive fluid flow in microfluidic channels, the working distance inside microfluidic channel is limited in depth. Recently, we have demonstrated fiber optic tweezers for in-depth trapping of microscopic objects. Here, we demonstrate the development of a fiber optic spinner for rotation of microscopic objects. This single-mode fiber optics based method does not require special structure or optical properties of the sample to be rotated. Trapping and simultaneous rotation of microscopic objects (pinwheel as well as cell) around axis perpendicular to optic axis could be achieved. The microfluidic flow (monitored by a tracer particle) was controlled by rotation speed of the trapped object, which could be changed by adjusting the laser beam power coupled to the fiber optic trap. Since the fiber optic spinner could be easily integrated onto a microfluidic platform, the proposed configuration can find potential applications in lab-on-a-chip devices.

8225-13, Session 2

## Multispectral optical tweezers for molecular diagnostics of single biological cells

S. Fardad, A. Sincore, M. Baudelet, M. Richardson, CREOL, The College of Optics and Photonics, Univ. of Central Florida (United States)

Biological and medical diagnostics at the single cell level have seen an impressive increase of interest thanks to the introduction of optical trapping by laser and the introduction of readily available kits on the market. Nevertheless, the adaptation of such systems for efficient optical interrogation of the single cells is still in development. Molecular diagnostic of biological samples by fluorescence is the most common spectroscopic approach but doesn't provide enough discriminative diagnostics of samples where small modification of the cell structure or composition contributes in a small proportion to the emission signal. In order to improve the information on the molecular content of the cell, more than the electronic transitions, a molecular spectroscopy such as Raman is really adapted. The combination of both spectroscopies can bring a clear picture of the nature and state of the cell. Furthermore, this fusion is advantageous when combined to optical tweezers: (i) the use of visible/near-infrared lasers can be used for trapping and excitation, (ii) compact and rugged laser sources are available, (iii) industrial silicon detector can be used for both techniques. This paper shows the integration of both fluorescence and Raman spectroscopies in a modular arrangement for molecular diagnostics of single optically trapped biological cells. The study of basic systems such as yeast and blood cells will be shown, in addition to more complicated cells (functionalized as well as cancerous cells). Discussion supported by experimental validation on the modular integration of more advanced Raman spectroscopies (CARS and SERS) will be given.

8225-14, Session 2

## Compact cell stretcher for RBC quantitative phase information

M. C. Potcoava, D. W. M. Marr, R. Jimenez, JILA (United States)

A desire to investigate the dynamics and mechanical characteristics of living cells using microfluidic devices has led to significant challenges in developing appropriate detection technologies. Using a linear source, we present a novel instrument for quantitative measurement of stretched red blood cells (RBC) profile and membrane characteristics across the whole cell surface. In this, a single element diode laser optical trap is imaged at the sample plane of a diffraction setup. Diffraction patterns of the cells passing along the line trap are recorded using a CMOS detector at 1000 fps. Cells height profile fluctuation and elastic deformation parameters are quantified with nm sensitivity from processed phase information of each recorded image. Mechanical properties are characterized by out-of-the-plane bending modulus and in-plane shear modulus. Two-dimensional devices were fabricated using micromolding methods with polydimethylsiloxane (PDMS).

8225-15, Session 2

## Fluorescence enhancement with glancing angle deposited nanostructured surfaces

S. Suran, H. J. Singh, V. S. Goudar, A. Ghosh, M. M. Varma, A. Ghosh, Indian Institute of Science (India)

We describe a novel method of enhancing the strength of the fluorescence signal using a one step fabrication process utilizing nanostructured SiO2 surfaces. The substrates were fabricated using shadow-evaporation techniques, and were found to have significantly high surface area enhancement. By using a physical vapor deposition source at oblique incidence to a rotating sample, which is a glass slide, results in the formation of a columnar thin film of SiO2 with approximately two orders of surface area enhancement for a mean SiO2 layer thickness of 200 nm. The enhanced surface area leads to increased loading of fluorophore conjugated bio-molecules which enhances the signal compared to an unstructured surface. We measured the fluorescent enhancement factor of these substrates by physically adsorbing fluorescein conjugated Bovine Serum Albumin (FITC-BSA). The signal enhancement factor obtained on the nanostructured surface compared to unstructured glass slide varies between 7 and 10. Unlike the multilayer thin film based approach for fluorescence enhancement which requires the deposition of 15-20 layers, this approach is a single step process and is simpler. Also, unlike plasmonic enhancement of fluorescence which requires gold or preferably silver nanoclusters, this technique provides a glass surface which is the preferred material for most commercially available functionalized slides.

8225-16, Session 2

## Amplification of the signal per background in microarrays modulated by micro/nano-structures

D. V. Nicolau, Univ. of Liverpool (United Kingdom)

No abstract available

8225-17, Session 3

## Phase resolved and coherence gated en-face reflection imaging of multilayered embryonal carcinoma cells

T. Yamauchi, T. Fukami, H. Iwai, Y. Yamashita, Hamamatsu Photonics K.K. (Japan)

Embryonal carcinoma (EC) cells, which are cell lines derived from teratocarcinomas, have characteristics in common with stem cells and differentiate into many kinds of functional cells. Similar to embryonic stem (ES) cells, undifferentiated EC cells form multi-layered spheroids. In order to visualize the three-dimensional structure of multi-layered EC cells without labeling, we employed full-field interference microscopy with the aid of a low-coherence quantitative phase microscope, which is a reflection-type interference microscope employing the digital holographic technique with a low-coherent light source. Owing to the low-coherency of the light-source (halogen lamp), only the light reflected from a specific sectioning height of the sample generates an interference image on the CCD camera. P19CL6 EC cells, derived from mice, form spheroids that are about 50 to 200 micrometers in diameter. Since the height of each cell is around 10 micrometers, it is assumed that each spheroid has 5 to 20 cell layers. The P19CL6 spheroids were imaged in an upright configuration and the horizontally sectioned reflection images of the sample were obtained by sequentially and vertically scanning the zero-path-length height. Our results showed the three-dimensional structure of the spheroids, in which plasma and nuclear membranes were distinguishably imaged with lateral and vertical resolutions of 0.56 micrometers and 0.93 micrometers, respectively. The results imply that our technique is further capable of imaging induced pluripotent stem (iPS) cells for the assessment of cell properties including their pluripotency.

8225-18, Session 3

## Label-free multiphoton fluorescence imaging monitors metabolism in living primary human cells used for tissue engineering

L. Chen, W. R. Lloyd III, S. Kuo, C. L. Marcelo, S. E. Feinberg, M. Mycek, Univ. of Michigan (United States)

Multiphoton fluorescence imaging was employed to noninvasively characterize metabolic function in living primary human cells, a necessary precursor to studying the viability of engineered constructs for repairing damaged tissues. Primary human oral keratinocytes were harvested from patients with Institutional Review Board approval and cultured at 37°C under varying chemical stimuli, resulting in differing cellular morphologies, growth rates, and metabolic activity. Label-free multiphoton fluorescence microscopy was employed to noninvasively study endogenous fluorescence of thin optical sections (<1 micron) from cells with reduced out-of-focus photobleaching. Multiphoton imaging measured intrinsic fluorescence from two important metabolic biomarkers predominating in mitochondria, cellular nicotinamide adenine dinucleotide (NADH) and flavin adenine dinucleotide (FAD). Fluorescence images were acquired with a 40x and 63x oil immersion lenses (spatial resolution up to 0.1 micron) in ~40 seconds with a 200 Hz line scanning speed. To increase signal-to-noise ratio, a line average of 8 was employed. At each measured sample site, the NADH and FAD images were post-processed for denoising and image enhancement. A redox ratio was calculated at each image pixel and redox ratio mapping was employed as a novel noninvasive technique with high sensitivity to reduce the prominence of instrumentation signal artifacts and quantitatively evaluate cellular metabolic change and spatial distribution. Our results show that fluorescence redox ratio imaging may be a useful tool to monitor human keratinocyte growth and development. Translation of multiphoton fluorescence imaging to study cellular metabolism and viability in thick tissue-engineered constructs will be discussed.

8225-19, Session 3

## Targeting of engineered Mesenchymal stem cells to sites of inflammation as monitored using multicolor mixed mode intravital imaging

L. J. Mortensen, Massachusetts General Hospital (United States) and Harvard Medical School (United States); D. Sarkar, Brigham and Women's Hospital (United States) and Harvard Medical School (United States); J. A. Phillips, Brigham and Women's Hospital (United States); J. A. Spencer, Massachusetts General Hospital (United States) and Harvard Medical School (United States) and Tufts Univ. (United States); R. Sridharan, Massachusetts General Hospital (United States) and Harvard Medical School (United States); S. K. Sankaran, Brigham and Women's Hospital (United States) and Harvard Medical School (United States); W. Zhao, Brigham and Women's Hospital (United States) and Harvard Medical School (United States) and Harvard Stem Cell Institute (United States); P. K. Vemula, Brigham and Women's Hospital (United States) and Harvard Medical School (United States); R. Karnik, Massachusetts Institute of Technology (United States); J. M. Karp, Brigham and Women's Hospital (United States) and Harvard Medical School (United States); C. P. Lin, Massachusetts General Hospital (United States) and Harvard Medical School (United States)

Mesenchymal Stem Cells (MSC) are multi-potent progenitor cells that have been demonstrated to improve disease prognosis after intravenous infusion by homing to sites of injury and secreting therapeutic factors in animal models, such as osteogenesis imperfecta, graft versus host disease, and myocardial infarction. Therefore, a large number of clinical trials testing the safety and efficacy of intravenous MSC administration have begun. Although MSC have been shown to be safe, recent late stage trials have failed to meet primary endpoints. This lack of efficacy can be attributed in part to loss of MSC phenotype through extended culture expansion, which is caused by variation or loss of surface homing receptors and cytokine expression. To overcome these limitations, researchers use a number of approaches including cell surface engineering techniques, cell transfection, and cytokine pretreatment of cells. Our approach utilized Sialyl Lewisx (SLeX) cell surface modification to increase MSC homing to sites of inflammation in an in vivo murine inflammation model. SLeX modified MSC exhibited increase homing to LPS-inflamed ears with single cell resolution using intravital multi-channel confocal and multiphoton microscopy, and population biodistribution alteration using whole-animal bioluminescence imaging. Our results indicate that SLeX surface modification increases the in vivo inflammatory homing potential of MSC and increases the length of time that cells remain viable in the host. These results suggest future directions in the application of pre-treated MSC to target and treat inflammatory-based diseases, and may provide alternate routes to maximizing MSC therapeutic potential.

8225-20, Session 3

## Investigation for the differentiation process of mouse ES cells by Raman spectroscopy

Y. Yamaguchi, M. El-Hagrasy, E. Shimizu, M. Saito, E. Tamiya, Osaka Univ. (Japan)

The arrangement of differentiated pluripotent embryonic stem cells into three-dimensional aggregates, that are known as embryoid bodies (EBs), is a main step for progressing the ES cells differentiation. In this work, EBs, that were directly produced from the hanging drop step (HD) as a three-dimensional structure with no further two- dimensional differentiation, were diagnosed with Raman spectroscopy as a non-invasive and label-free technique. Raman spectroscopy was employed to discriminate between mouse embryoid bodies of different degrees of maturation. EBs were prepared applying the hanging drop method. The Raman scattering measurements were obtained in vitro with a Nanophoton RAMAN-11 micro-spectrometer (Japan) (URL: www.nanophoton.jp) equipped with an Olympus XLUM Plan FLN 20X/NA= 1.0 objective lens (Japan). Spectral data were smoothed, baseline corrected and normalized to the a well-defined intense 1003 cm-1 band (phenylalanine) which is insensitive to changes in conformation or environment. The differentiation process of ES cells is initiated by the removal of LIF from culture medium. 1, 7 and 17-day-old EBs were collected and investigated by Raman spectroscopy. The main differences involve bands which decreased with maturation such as: 784 cm-1 (U, T, C ring br DNA/RNA, O-P-O str); 1177 cm-1 (cytosine, guanine) and 1578 cm-1 (G, A). It was found that with the progress of differentiation the protein content was amplified. The increase of protein to nucleic acid ratio was also previously observed with the progress of the differentiation process. Raman spectroscopy has the potential to distinguish between the Raman signatures of live EBs with different degrees of maturation.

8225-21, Session 3

## Sensing end enumeration of rare circulating cells with diffuse fluorescence light in mice in vivo

M. J. Niedre, E. W. Zettergren, Northeastern Univ. (United States); J. M. Runnels, C. P. Lin, Wellman Ctr. for Photomedicine (United States)

Sensing and enumeration of rare circulating cells in the bloodstream is important in many areas of biomedical research including study of cancer metastasis and the immune system. Normally this is achieved by drawing small blood samples which are later analyzed using a number of analytical techniques, or more recently non-invasively using microscopy-based in vivo fluorescence flow cytometry. In both cases, the blood sampling volume is relatively small so that rare cells may escape detection entirely. In this presentation, we describe a new instrument for sensing rare circulating cells in vivo by detection of diffuse fluorescence light with a miniaturized optical ring placed around a mouse limb, thus allowing interrogation of relatively large blood vessels and blood volumes. The instrument uses two modulated diode lasers and array of six optical detection fibers coupled to a photomultiplier tube array operating in photon counting mode to detect weak fluorescence signals from individual cells. We first validated this instrument using a limb-mimicking optical flow phantom with similar size, optical properties, autofluorescence and flow speeds as a mouse limb. We show that we can robustly detect circulating cells at concentrations less than 103 cells per mL. Analysis of multi-optode data sets also allowed localization cells in the cross-section of the phantom with a resolution of about 0.5 mm. Finally, we demonstrate that our instrument can detect circulating multiple myeloma cells in mice in vivo. We anticipate that our instrument will have many uses in the preclinical study of rare circulating cell types in vivo.

8225-08, Session 4

## A new diagnostic tool based on diffusion reflection measurements of gold nano particles

R. Ankri, D. Fixler, R. Popovtzer, Bar-Ilan Univ. (Israel)

Diffusion reflection measurements have been proved as a noninvasive simple tool that can correlate between the reflected light profile and the structure and optical properties of an irradiated tissue. The physiological condition of a tissue can influence its structure and, consequently, its optical properties. Thus, the reflected light intensity profile varies from one physiological condition to another.

Gold nano particles have unique size and shape-dependent optical properties, therefore, their insertion into an irradiated tissue might cause a significant change in its optical properties. These gold nano particles can be targeted toward a tissue presenting a specific physiological condition. Thus, by their intravenously injection, the targeted tissue will present optical properties that differ from its surrounding tissue.

We present a new utilization of the diffusion reflection measurements that distinguish between different physiological conditions, based on the insertion of gold nano particles. Experimental set-up for diffusion reflection measurements was built and tissue-like phantom, as well as in vivo measurements, were performed. Our diffusion reflectance measurements presents high efficiency and sensitivity resulting from the insertion of the gold nano particles that specifically targets damaged cells and significantly changes their absorption. The diffusion reflection method presents a non-invasive and non-ionizing optical detection method to provide a highly sensitive, simple and inexpensive tool for diagnostic purposes.

8225-22, Session 4

## MEM-FLIM: all-solid-state camera for fluorescence lifetime imaging

Q. Zhao, I. T. Young, R. Schouten, B. Schelen, Technische Univ. Delft (Netherlands); R. Leenen, H. van Kuijk, I. Peters, F. Polderdijk, J. Bosiers, Teledyne DALSA (Netherlands); K. Jalink, Netherlands Cancer Institute (Netherlands); S. de Jong, L. van Geest, K. Stoop, Lambert Instruments BV (Netherlands)

Fluorescence lifetime imaging microscopy (FLIM) is an intrinsically quantitative tool to image the lifetime of molecular fluorescence. The current generation of frequency-domain FLIM systems requires an image intensifier, the use of which is necessary for low light levels and MHz demodulation frequencies. We propose improving frequency-domain FLIM instrumentation by replacing the image intensifier with an application-specific CCD design.

We have designed, built, and tested such a CCD image sensor and camera that can be modulated at the pixel level. Incoming light is captured by modulated pixels, recording two phase images at once. This is in contrast to an image intensifier with a duty cycle of about 50% when recording a single phase image. This all-solid-state FLIM camera is designed for shorter image acquisition times because of higher photon efficiency and does not need high voltage sources and RF amplifiers. By removing the intensifier and the fiber/lens coupling to the camera, possible sources of distortion-noise and geometric-are significantly reduced.

We will describe the performance of this all-solid-state FLIM camera: its linearity, noise characteristics, sensitivity, and the accuracy and precision of lifetime measurements made with this system. At the time of this writing we have measured a sensitivity of 0.6 ADU/e- with a 14-bit ADC, a SNR = 19.3 dB with 100 ms integration, a readout noise of 5.7 ADU, and for two different fluorophores a lifetime measurement accuracy based upon phase modulation of about 2%. Our lifetime measurement precision, however, averages about 35%; this is currently being worked upon.

8225-23, Session 4

## MB-FLIM: model-based fluorescence lifetime imaging

I. T. Young, Q. Zhao, R. Schouten, S. Stallinga, Technische Univ. Delft (Netherlands); K. Jalink, Netherlands Cancer Institute (Netherlands); S. de Jong, Lambert Instruments BV (Netherlands)

Frequency-domain FLIM is based upon the magnitude and phase changes that occur in fluorescence emission induced by sinusoidally-modulated excitation light. A single frequency, f1, is sufficient to determine a single lifetime t1 assuming that there is only one lifetime in a pixel. With a mixture of two lifetimes, t1 and t2, in a pixel then two frequencies are needed and, in general, the analysis is sequential. We have developed a parallel procedure where multiple frequencies are present in a single excitation signal. Modeling the entire fluorescence and measurement process produces an analytical ratio of polynomials in the lifetime variables and the mixing parameter p. A non-linear model-fitting procedure is then used to estimate {p, t1, t2}. We have analyzed this model-based approach by simulating, for example, a 2 μM rhodamine solution (t1 = 4 ns) and all relevant noise sources. We have used data from a real LED excitation source to drive the simulation. Using 7 phase steps, a 20 MHz “square-wave” LED signal with a 25% duty cycle, and 1000 pulses, we estimate t1 as 4.01 ns, an error of 0.30%. The computation time per pixel is 6.0 ms. When a mixture of two lifetime components is presented (p=0.40, t1=4, t2=2}, a two-component model produces the excellent values {0.41, 4.02, 1.99}. The computation time per pixel is 25.5 ms. We are currently implementing this model-based approach in our laboratory and will be testing the results under a variety of settings such as concentrations, lifetime mixing percentages, and lifetime differences.

8225-24, Session 4

## Quality testing of an innovative cascade separation system for multiple cell separation

A. Pierzchalski, A. Moszczynska, Univ. Leipzig (Germany); J. Heinrich, pluriSelect GmbH (Germany); A. Tarnok, Univ. Leipzig (Germany)

Isolation of different cell types from mixed samples in one separation step by FACS is feasible but expensive and cheaper but still challenging by magnetic separation. An innovative bead-based cascade-system (pluriSelect GmbH, Leipzig, Germany) relies on simultaneous physical separation of different cell types. It is based on antibody-mediated binding of cells to beads of different size and isolation with sieves of different mesh-size.

We validated pluriSelect system for simultaneous separation of CD4 and CD8 cells from EDTA blood-samples. Results were compared with those obtained by MACS (Miltenyi-Biotech) magnetic separation. pluriSelect separation was done in whole blood, MACS on Ficoll gradient isolated leukocytes, according to the manufacturer's protocols.

Isolated and residual cells were immunophenotyped (7-color 8-antibody panel (CD3;CD16/56;CD4;CD8;CD14;CD19;CD45;HLADR) on a CyFlowML flow cytometer (Partec GmbH). Cell count (Coulter), purity, yield and viability (7-AAD exclusion) were determined.

There were no significant differences between both systems regarding purity (85-90%), yield (50-60%) and viability (92-98%) of isolated cells. However, pluriSelect separation was significantly faster than MACS (1h versus 2.5h). Moreover, no pre-enrichment steps were necessary. In addition, pluriSelect isolation of two cell types was done in one step but had to be done in two steps with MACS (first isolation of CD4, then restaining of residual suspension with CD8 and second isolation).

In conclusion, pluriSelect is a fast, simple and gentle system for efficient simultaneous cell separation of two cell subpopulation directly from whole blood and can provide a simple alternative to FACS. The isolated cells can be used for further research applications.

8225-25, Session 4

## An optical platform for in vivo cell tracking and quantification in adult zebrafish

L. Zhang, Wellman Ctr. for Photomedicine (United States) and Fudan Univ. (China); C. Alt, Wellman Ctr. for Photomedicine (United States); P. Li, R. M. White, L. I. Zon, Harvard Medical School (United States); X. Wei, Shanghai Jiaotong Univ. (China) and Fudan Univ. (China); C. P. Lin, Wellman Ctr. for Photomedicine (United States)

Zebrafish has become a powerful vertebrate model organism for drug discovery, cancer and stem cell research. A recently developed transparent adult zebrafish using double pigmentation mutant, called casper, provides unparalleled imaging power in in vivo longitudinal analysis of biological processes at an anatomic resolution not readily achievable in murine or other systems.

Here we describe an integrated optical system that combines a laser scanning confocal microscope (LSCM) and an in vivo flow cytometer (IVFC) for visualization and cell quantification. The system was set up specifically for non-invasive tracking of both stationary and circulating cells in transparent adult zebrafish, casper, under physiological conditions in the same fish over time, without drawing blood samples or sacrificing animals. Confocal imaging in this instrument serves the dual purpose of visualizing fish tissue microstructure and as an image-guidance tool to locate a suitable vessel for quantitative analysis of circulating cells by IVFC. The multi-color, multi-channel instrument allows the detection of multiple cell populations or different tissues or organs simultaneously. We demonstrate initial testing by imaging and quantification thrombocytes in transgenic CD41-GFP casper zebrafish injected with Texas Red Dextran for blood vessel visualization. Circulating fluorescent cell incidents were recorded and counted in different types of vessels, and over time.

This novel instrument provides great opportunities of tracing stem cells in vivo in adult zebrafish that have previously not been possible, including following up in competitive transplantation experiments with zebrafish mutants hematopoietic stem cells (HSCs) and chemicals to test for effects on homing, engraftment, and self-renewal.

8225-26, Session 4

## Optofluidic tomographic microscopy: a new tool for optofluidics

S. O. Isikman, W. Bishara, H. Zhu, A. Ozcan, Univ. of California, Los Angeles (United States)

Opto-fluidics is a rapidly emerging field that aims to complement microfluidic chips with optical functionalities such as sensing and imaging, paving the way toward building lab-on-a-chip devices with e.g., enhanced sensitivity and better throughput. Among these devices, opto-fluidic microscopy (OFM) in specific presents an important example of how the fluidic-flow could be used to bring a new function to lab-on-a-chip devices, while still keeping the entire platform compact and cost-effective. Existing opto-fluidic microscopy/imaging modalities, however, have so far lacked the ability to achieve 3D sectioning of micro-objects within a micro-channel. For this need, here we present an opto-fluidic tomographic microscope that achieves depth sectioning of specimen, flowing through microfluidic-channels, without using any lenses or bulky optical components. In opto-fluidic tomography, a micro-channel is placed on a digital sensor-array, such as a CMOS chip, and lensfree in-line holograms of the flowing objects within the micro-channel are recorded at different viewing angles by rotating a partially-coherent light source, e.g. a light-emitting-diode. At each illumination angle, multiple lensfree holograms that are slightly shifted with respect to one another are recorded utilizing the flow of the sample above the sensor-chip, which enables synthesizing pixel super-resolved (SR) holograms at each illumination angle. These SR holograms can then be tomographically reconstructed to compute 3D images of objects achieving volumetric structural information with microscopic spatial resolution, both laterally and axially. With its lensfree and simple on-chip architecture that is seamlessly integrated with micro-fluidic chips, opto-fluidic tomographic microscopy could be a promising tool for micro-total-analysis platforms.

8225-27, Session 4

## Structural imaging of cell membranes using polarimetric fluorescence microscopy

S. Brasselet, P. Ferrand, X. Wang, A. Kress, H. Ranchon, H. Rigneault, Institut Fresnel (France)

Biomolecular orientational organization is a crucial factor in biological processes where func-tions (such as cell motility, vesicular trafficking, signalling, protein interactions, etc.) are closely related to orientation and ordering. The investigation of structural behaviors of bio-molecular assemblies is today a determining factor towards the better understanding of the fundamental mechanisms governing the cell membrane.

One-photon fluorescence microscopy provides a convenient and powerful tool towards this goal. Indeed, both absorption and emission of light are strongly dependent on the orientation of the fluorescence dipole with respect to the polarization of the excitation and emission fields. We have developed a general polarimetric fluorescence microscopy technique which relies on the analysis on the fluorescence image recorded for a tuneable incident exciting field polarization. We show that this technique permits to give a picture of the angular distribution of an ensemble of molecules present in the confocal volume without a priori knowledge of its average orientation, which is particularly relevant for the study of cell membranes of complex shapes.

The potentiality of this method will be illustrated on the monitoring of structural changes of the cell membrane at the sub-diffraction scale, using lipid probes under different pharmaco-logical treatments affecting the membrane mechanical tension. We will extend the analysis to the investigation of the MHC Class I protein ordering in the plasma and endo-membranes.

8225-28, Session 4

## Optical coherence phase microscopy with a dual beam allows intracellular phase imaging

F. Helderman, M. de Groot, J. F. de Boer, Vrije Univ. Amsterdam (Netherlands)

Optical Coherence Phase Microscopy can image biological tissue with excellent phase stability by using a common path configuration with the microscope slide as a phase reference. For intracellular studies a large numerical aperture (NA) objective is needed to obtain the required resolution. Unfortunately, this also means that the depth of field becomes too small to obtain sufficient power from the microscope slide as a reference if the beam is focused deep into the sample. Therefore, we designed a dual beam sample arm. A polarizing beam splitter divided the beam into s- and p-polarized states that travelled the same path but in opposite direction through a Sagnac interferometer. A telescope in the Sagnac enlarged one beam while narrowing the other. Both beams followed a common path to the microscope. A 1.2 NA water immersion objective focused the broad beam for high resolution imaging. The other beam had a larger depth of field and could detect the microscope slide as a reference. Phase stability was quantified by monitoring the top and bottom of the microscope slide. The width (FWHM) of the axial point spread function was smaller than the diameter of a typical cell (0.8 vs. 10 μm). The monitored phase had a standard deviation of 3.7 nm. In conclusion, a dual beam, common path design is an elegant way to create high resolution depth resolved phase contrast images in reflection of cells and tissues.

8225-29, Session 4

## Monitoring protein-protein interactions in vivo: FLIM and FIDSAM as powerful time-resolved fluorescence techniques for quantitative FRET-analysis

F. Schleifenbaum, Eberhard Karls Univ. Tübingen (Germany); K. Elgass, La Trobe Univ. (Australia); S. Peter, A. J. Meixner, K. Harter, Eberhard Karls Univ. Tübingen (Germany)

The identification of the interaction between proteins by Förster resonance energy transfer (FRET) is a key research field in proteomics. While intensity-based FRET protocols are straight forward, they are error-prone due to photobleaching or donor emission leaking into the acceptor channel. A more sophisticated technique uses the reduced donor fluorescence lifetime (FLT) in presence of an acceptor to identify FRET. We show that this FRET-FLIM technique allows for mapping the packing density of DNA in isolated nuclei of mitotic cells as well as the identification of interaction partners and even their relative orientation of two target proteins in living plant cells.

Although quantitative, the FRET-FLIM approach is limited for great chromophoric distances in large interacting proteins, the determination of significant FRET activity is often not univocal or possible at all. We present a novel approach based on fluorescence intensity decay shape analysis microscopy (FIDSAM). Here, a monoexponential decay function is fit to the intensity decay histograms of a FLIM image and the deviation from fit to measured data is calculated. Whereas label dyes, which exhibit a reduced FLT due to environmental impact, still show a monoexponential fluorescence decay, the decay becomes intrinsically multiexponential if FRET occurs and the FIDSAM-error value increases for increasing FRET activity. Accordingly, FIDSAM can be used to distinguish FRET-active sample areas from false-positives, even in a quantitative manner. The FIDSAM-FRET technique is even more sensitive than conventional FRET-FLIM studies as even small FRET efficiencies give rise to a significant change in the FIDSAM-error value.

8225-30, Session 4

## Delay time spectroscopy: a novel method for measuring nanoscale disorder in a biological cell and its application to early cancer detection

P. Pradhan, D. Park, H. Subramanian, D. Damania, L. Cherkezyan, V. Backman, Northwestern Univ. (United States)

We developed delay time spectroscopy of a photon travel through or reflect from a weakly disordered medium such as a biological cell. The delay time (optical) is the extra time spent by a photon to travel through or reflect from an optical medium. Real delay time for the reflection is defined as $\tau=d\theta/d(ck)$, where $\theta$ is the associated phase of the reflectance, k is the wave vector, and c is the speed of light. Time delay is related to phase delay. We found a symmetry between the real delay time ($\tau$) and the imaginary delay time ($\tau_i$) that is derived from the reflectance, where $\tau_i=id\theta_i/d(ck)$ and the reflectance $r = \exp( -i\theta_i)$. This delay time symmetry has important experimental consequences. For example, to establish the delay time or its statistics, one has to measure the phase of the reflected or transmitted wave. However, if the delay time symmetry is utilized by measuring the imaginary delay time from the reflectance without phase information, we can predict the real delay time or its statistics in the media. For a fixed probing light, the optical delay time depends on the degree of disorder and size of the sample, where more delay time is for more disordered or longer sample. We have used the delay time spectroscopy to distinguish between nanoarchitectural disorder in cancerous and normal cells. Our results show that cancerous cells have more delay time than normal cells. Use of the technique for early cancer detection is addressed.

8225-31, Session 4

## Chemometric analysis of multispectral FLIM data based on nonnegative matrix factorization methods

P. Pande, J. A. Jo, Texas A&M Univ. (United States)

Several methods for the estimation of fluorophore concentrations from FLIM data, including global analysis, have already been proposed. However, all these methods are limited by its inability to handle non-monoexponential fluorescence decays, to resolved more than two fluorophores, and/or to analyze multispectral data. We proposed the application of Nonnegative Matrix Factorization (NMF) to a novel treatment of the multispectral FLIM data defined as a sequence of fluorescence decays acquired at different emission bands. The NMF method is a multivariate data analysis technique that is aimed at extracting nonnegative profiles of "pure components" and their nonnegative abundances from an additive mixture of components. Since no assumptions are made in NMF about the number and the functional form of the component profiles, this approach will overcome the main limitations of most global analysis methods. One major limitation of NMF, however, is the scaling ambiguity of the estimated component profiles, which can lead to biased estimation of the relative concentrations. Few attempts to find the right scaling factors have been proposed and are based on matching the estimated profiles to some a-priori profiles. This is, however, an extremely hard requirement to meet in the context of multispectral FLIM. We thus propose a data-driven post-unmixing algorithm to resolve the scaling ambiguity, based on much milder assumptions about the dataset. The proposed method was successfully validated in both synthetic and experimental multispectral FLIM data and is allowing accurate estimation of both the profiles and the relative concentration of "pure fluorescence components" from multispectral FLIM data.

8225-32, Session 5

## Quantitative FRET measurements in live cell by fluorescence lifetime excitation-emission matrix imaging

M. Zhao, R. Huang, L. Peng, College of Optical Sciences, The Univ. of Arizona (United States)

Fluorescence resonance energy transfer (FRET) is a versatile tool for the study of molecular interactions in biological systems. Hetero-FRET signal in live cells are often buried by signals from free donor and acceptor, as well as homo-FRET signal caused by intra-molecular interaction, polymerization or oligomerization. Full quantification of FRET requires the separation of all three mechanisms. In this paper, we developed a method that uses fluorescence intensity and lifetime excitation-emission matrices (EEM) to obtain quantitative hetero-FRET measurements in the presence of free donor/acceptor and homo-FRET in vitro and in vivo. An EEM represents properties of the fluorophores as a function of both the excitation and emission wavelengths. Intensity and lifetime EEMs provide complimentary information for the quantification of FRET measurements. A measurement method based on Fourier transform fluorescence lifetime spectroscopy [1] was used to measure the intensity and lifetime EEM simultaneously within 46 microseconds. We first demonstrated the method with EEM measurements of FRET interaction in dsDNA during melting. As the population of free ssDNA increased and more donor and acceptor became dissociated, the FRET efficiency of the remaining dsDNA stayed constant and was accurately determined by lifetime EEM despite an increasing free fluorophore background. We then performed quantitative FRET imaging of a FRET aptamer reporter for RNA expression in live yeast cells. By combining EEM measurements with acceptor photobleaching, both hetero-FRET and homo-FRET were precisely quantified.

[1] M. Zhao and L. Peng, Optics Letters 35(17), p2910

8225-34, Session 5

## Lensfree incoherent color imaging using compressive decoding

I. Sencan, A. F. Coskun, T. Su, D. G. Herman, Y. Suh, A. Ozcan, Univ. of California, Los Angeles (United States)

Lensfree computational imaging techniques provide opportunities to replace bulky and expensive designs of conventional microscopes with much simpler, compact and cost-effective on-chip imaging architectures, which can achieve a decent spatial resolution over a significantly larger imaging area. One example of such an emerging computational microscopy technique involves lensfree fluorescent imaging on a chip using sparse signal recovery. In this approach, an opto-electronic sensor-array (e.g., a CCD or CMOS chip) records lensfree diffraction images of incoherent objects located on e.g., a bio-chip that is placed at less than ~0.5mm away from the active area of the sensor-chip. With the knowledge of the point-spread function of this lensfree imaging platform (which can be experimentally measured), the object distribution on the chip can be rapidly reconstructed using sparse signal recovery algorithms based on compressive sampling/sensing theories. Here we demonstrate multi-color imaging performance of this lensfree incoherent microscopy technique achieving a spatial resolution of ~1μm in each color channel (i.e., red, green and blue) over a wide field-of-view of ~60mm2. Having a decent multi-color resolution and a large imaging field-of-view within a compact and cost-effective imaging architecture is especially valuable for e.g., high-throughput cytometry, microarray imaging and rare cell detection applications involving large-area micro-fluidic channels.

8225-35, Session 5

## A cost-effective analog method to produce time-gated luminescence images

R. C. Leif, S. Yang, Newport Instruments (United States); Y. Lu, D. Jin, Macquarie Univ. (Australia); S. Chambers, Artemis CCD Ltd. (United Kingdom)

Time-gated luminescence images were obtained by summation of a series of sequential images that were taken with 3 different interline CCD cameras and a fluorescence microscope modified to use a UV LED for illumination. The 3 CCD interline cameras were 1) research grade cooled that digitally summed sequential images, 2) an inexpensive room temperature camera, and 3) a modified astronomy camera. Cameras 2 and 3 performed analog summations. An interline CCD camera obtains an analog sum of a multi-frame image by not reading out the storage line after each frame is acquired; instead, the charges from the acquisition pixels are transferred to the storage pixels, which adds them to those previously stored and subsequently, the sum of the images is readout from the storage pixels and digitized. The length of the exposure is limited by the capacity of the storage pixels and the rate of background (noise) generation. In the case of the scientific grade, cooled CCD camera, the data acquisition rate of approximately 10 one millisecond exposure images per second was too slow for standard research and clinical use. An unwanted undulating background was also present, which could not be totally removed by subtraction of an unexposed, control image. Similarly the quality of the images obtained with the room temperature camera was degraded by the buildup of thermal noise. The interline transfers, electronically shuttered, cooled astronomy CCD camera, which was modified for analog summation rapidly produced low noise images. The past problems with lanthanide dyes of low extinction coefficients and equipment cost have now been solved.

8225-36, Session 5

## Toward a colony counting system using hyperspectral imaging

B. Masschelein, IMEC (Belgium); A. Robles-Kelly, National ICT Australia (Australia); S. Liu, N. Tack, A. Lambrechts, IMEC (Belgium); B. Simpson-Young, National ICT Australia (Australia); F. Pessolano, IMEC (Belgium)

Colony counting is a procedure used in microbiology laboratories for food quality monitoring, environmental management, etc. Its purpose is to detect the level of contamination due to the presence and growth of bacteria, yeasts and molds in a given product. Current automated counters require a tedious training and setup procedure per product and bacteria type and do not cope well with diversity. Microbiology laboratories for food safety testing, however, have to test different types of food for different types of contaminations. This induces additional variations of color and shape which render the actual counting a manual step in an otherwise fully automatable procedure.

To overcome the limitations of current automated counters, we propose the use of hyperspectral imaging technology. Our training and test data consists of specific colonies grown on different types of agar and food samples. After collection, the data is processed by simultaneously recovering the illuminant power spectrum and reflectance via a statistical approach which imposes consistency over the data and allows for small compositional variations across the imagery. The recovery of the illuminant minimizes the variations in the spectra due to reflections, shadows, etc, whereas imposing consistency prevents the break-up of regions that, despite corresponding to the same materials, present small variations in reflectance. The colonies can then be counted making use of classical segmentation and classification algorithms combined with watersheds so as to extract and count the targeted colonies. Our results show that the proposed system has the ability to exceed the limitations of RGB-based systems.

8225-37, Session 6

## The effects of different gold standards on the assessment of the accuracy of different resampling techniques for optical coherence tomography

C. Copeland, A. K. Ellerbee, Stanford Univ. (United States)

Fourier domain optical coherence tomography (FD-OCT) uses interferometry and a spatially coherent, polychromatic light source to acquire cross-sectional images of scattering media like biological tissue. Reconstruction of FD-OCT images requires taking the Fourier Transform of the raw data; the accuracy of the reconstruction depends on the choice of processing algorithms used, system noise, calibration and quantization errors. To decrease the processing time, the robust and popular Fast Fourier Transform algorithm is preferred over the traditional Discrete Fourier Transform when the data are evenly sampled in wavenumber. Unfortunately, most OCT systems are designed for constant wavelength sampling, leaving researchers to apply hardware- or software-based methods to resample the data accordingly. While there is general agreement on the qualitative superiority of some resampling methods over others, to the best of our knowledge there has been no detailed study that compares these methods quantitatively for OCT data in theory and in practice. Moreover, while there are choices for gold standard datasets (which amounts to different choices for assigning the sampled wavelengths), there have been no investigations on the effect of these differences on the assessment of the accuracy of reconstructions generated from resampled data. We first compare different options for gold standard datasets and then examine the effects of various resampling techniques on reconstructed OCT data in terms of accuracy, SNR, axial resolution and susceptibility to system errors.

8225-38, Session 6

## Comparison of measured and calculated quantitative flow cytometric data provided by panels with lower and increased color number

J. Bocsi, Univ. Leipzig (Germany) and Leipzig Research Ctr. for Civilization Diseases (Germany); A. Mittag, A. Pierzchalski, A. Baumgartner, I. Dähnert, A. Tarnok, Univ. Leipzig (Germany)

To date the flow cytometry (FCM) industry is booming with new generations of commercial clinical instruments. Long-term clinical studies have the dilemma that moving to new instruments being capable of more complex cell-analysis makes it difficult to compare new data with those obtained on older instruments with less complex analysis panels. Since 15 years we conduct follow-up studies on children with congenital heart disease. In this period we moved from 2- to 3- and now to 10-color FCM immunophenotyping panels. Questions arise how to compare and transfer data from lower to higher level of complexity.

Two comparable antibody panels for leukocyte immunophenotyping (15-tube 2-colors, and 9-tube 4-colors) were measured on a BD FACScalibur FCM (calibration: Spherotech beads) in 15 blood samples from children with congenital heart disease. This increase of colors was accompanied by moving antibodies that were in the 2-color panel either FITC or PE labeled to red dyes such as PerCP or APC. Algorithms were developed for bridging data for quantitative characterization of antigen expression (mean fluorescence intensity) and frequency of different cell subpopulations in combination with rainbow bead standard data. This approach worked for the most relevant antibodies (CD3, CD4, CD8 etc.) well, but rendered substantial uncertainty for activation markers (CD69 etc.).

Our techniques are particularly well suited to the analysis in long-term studies and have the potential to compare older and recent results in a standardized way.

8225-39, Session 6

## Diffusion properties of single FoF1-ATP synthases in a living bacterium unraveled by superlocalization microscopy

T. Rendler, Univ. of Stuttgart (Germany); M. Renz, Jena Univ. Hospital (Germany); S. Ernst, Jena Univ. Hospital (Germany) and Univ. of Stuttgart (Germany); A. Zappe, Univ. of Stuttgart (Germany); M. Börsch, Jena Univ. Hospital (Germany) and Univ. of Stuttgart (Germany)

FoF1-ATP synthases in Escherichia coli bacteria are membrane-bound enzymes which use an internal proton-driven rotary double motor to catalyze the reaction of adenosinetriphosphate (ATP) synthesis. According to the “chemiosmotic hypothesis”, a series of proton pumps generate the necessary pH difference plus an electric potential across the bacterial plasma membrane. These proton pumps are redox-coupled membrane enzymes which are possibly organized in supercomplexes, as shown for the similar enzymes in the mitochondrial inner membrane. We apply diffusion measurements of single fluorescent FoF1-ATP synthases in living E. coli by superlocalization microscopy and single enzyme tracking to distinguish a monomeric enzyme from a supercomplex-associated form in the bacterial membrane. For quantitative mean square displacement (MSD) analysis, the confinement in a small membrane (the bacterial cells have a diameter of about 500 nm and a length of 2 microns) with a significant membrane curvature was taken into account. Because the surface coordinate system yielded different localization precision, we developed a sliding region-of-interest approach to obtain a diffusion constant for FoF1-ATP synthase in E. coli and to disciminate free diffusion from anomalous diffusion expected for protein supercomplexes.

8225-40, Session 6

## Sparsity reconstruction for bioluminescence tomography based on an augmented lagrangian method

W. Guo, K. Jia, Beijing Univ. of Technology (China); J. Tian, D. Han, Institute of Automation (China); X. Liu, Northeastern Univ. (China); K. Liu, Q. Zhang, C. Qin, Institute of Automation (China)

Bioluminescence imaging (BLI) is an optical molecular imaging modality for monitoring physiological and pathological activities at the molecular level. The information of bioluminescent probe distribution in small animals can be three-dimensionally and quantitatively obtained by bioluminescence tomography (BLT). Due to ill-posed nature, BLT may bear multiple solutions and aberrant reconstruction in the presence of measurement noise and optical parameter mismatches. Among different regularization methods, L2-type regularization strategy is the most popular and commonly-applied method, which minimizes the output-least-square formulation incorporated with the l2-norm regularization term to stabilize the problem. However, it often imposes over-smoothing on the reconstruction results. In contrast, for many practical applications, such as early detection of tumors, the volumes of the bioluminescent sources are very small compared with the whole body. In this paper, L1 regularization is used to fully take advantage of the sparsity prior knowledge and improve both efficiency and stability. And then a reconstruction method based on the augmented lagrangian approach is proposed, which considers the BLT problem as the constrained optimization problem and employs the Bregman iterative method to deal with it. By using “divide and conquer” approach, the optimization problem can be exactly and fast solved by iteratively solving a sequence of unconstrained subproblems. To evaluate the performance of the proposed method in turbid mouse geometry, stimulate experiments with a heterogeneous 3D mouse atlas are conducted. In addition, physical experiments further demonstrate the potential of the proposed algorithm in practical applications.

8225-41, Session 7

## Raman imaging of alkyne as a small tag for biological molecules

K. Fujita, Osaka Univ. (Japan); H. Yamakoshi, Japan Science and Technology Agency (Japan); K. Dodo, RIKEN (Japan); A. Palonpon, Japan Science and Technology Agency (Japan); M. Okada, Osaka Univ. (Japan); J. Ando, Japan Science and Technology Agency (Japan); S. Kawata, Osaka Univ. (Japan); M. Sodeoka, RIKEN (Japan)

Unraveling the complex chemical reactions inside living cells is a very important area of research especially in the field of chemical biology. Usually, the role of small molecules such as drugs or metabolites in cells is studied by attaching a fluorescent label to the molecule and using a fluorescence microscope to trace its location inside the cell. However, fluorescent labels are usually large that often interfere with the normal cellular function of the molecule. To avoid the use of bulky fluorescent labels, we introduce a new technique that uses a simple small chemical tag called alkyne consisting of just two carbons connected by a triple bond. The alkyne-tagged molecule is then imaged using a Raman microscope that takes advantage of the strong Raman signal from CC triple bond stretching vibration (~2120 cm-1). Because the alkyne peak is located at the so-called silent region of the cell (1800-2700 cm-1), it does not interfere with any intrinsic cellular Raman signals. Here, we demonstrate this novel imaging technique by showing Raman images of an alkyne-tagged component of DNA called EdU using a specially developed Raman microscope. We constructed a slit-scanning confocal Raman microscope that achieves rapid imaging times practical for bioimaging of alkynes. This fast imaging technique is based on a line-shaped focus illumination and simultaneous detection of the Raman spectra from multiple points of the sample. Using this microscope, we obtained time-series Raman pictures of the incorporation of EdU into the DNA of replicating HeLa cells in just several tens of minutes.

8225-42, Session 7

## Two-photon cryomicroscope

K. König, K. Köhler, H. G. Breunig, JenLab GmbH (Germany)

We report on a compact two-photon laser scanning microscope with a motorized cryostage. Samples can be frozen down to -196°C with a maximum freezing speed up to 150K/min. The thawing process can be realized with the same speed.Studies have been performed in dependence on the cryobehavior of immersion oils, glass carriers, and objectives. Frozen tissue samples including fish eyes and human skin as well as fluorescent microbeads have been investigated regarding the NAD(P)H autofluorescence behaviour and the formation as well as disappearence of SHG. Two-photon cryomicroscopes have the potential to optimize freezing and thawing procedures as well as to evaluate the viability of frozen cells and tissues.

8225-43, Session 7

## Extraction of masked fluorescence peaks through polarized synchronous fluorescence spectroscopy

M. Mozumder, S. Devi, Indian Institute of Technology Kanpur (India); N. Ghosh, Indian Institute of Science Education and Research Kolkata (India); A. Pradhan, Indian Institute of Technology Kanpur (India); A. Agarwal, K. Pandey, Ganesh Shanker Vidhyarthi Memorial Medical College (India)

Fluorescence spectroscopy has been demonstrated as a viable tool for noting subtle biochemical changes that occur during early-stage cervical cancer progression. Due to multiple fluorophore contributions, the individual fluorophore activities often get masked due to overlapping spectra of neighbouring fluorophores. Recently synchronous fluorescence spectroscopy has been demonstrated as an efficient technique for investigation of such non-dominant fluorophores. With synchronous fluorescence spectroscopy individual fluorophore responses are highlighted as sharp peaks by choosing appropriate offsets during signal acquisition. Such peaks may, however be missed due to absorption effects. In our earlier work, we demonstrated the use of polarized fluorescence spectroscopy for non-invasive detection of cervical dysplasia progression. Polarized synchronous fluorescence spectroscopy extracts the missing peaks of the unpolarized synchronous spectra. Synchronous fluorescence spectra corresponding to 20,40,55,90 and 120nm were studied in detail to note the differences with unpolarized and polarized light. By dividing elastic scattering data it was observed that the masked fluorophores are highlighted while the broader bands are sharpened. Interestingly, fluorophore activities of protoporphyrin, collagen, NADH, FAD and porphyrin can now be studied using this technique, as compared to only collagen and NADH seen earlier. The results have been verified using tissue phantoms with known fluorophores and scatterers. Use of normalized polarized synchronous spectra has led to enhancement of several fluorophore responses. It was also observed that among the different offsets, the lower ones show sharper features, whereas the larger offsets show a broadband response. Among the different offsets 40nm is found optimal for further investigation.

8225-44, Session 7

## Water's contribution and enzyme's work: a KITA study

B. P. Born, Ruhr-Univ. Bochum (Germany) and The Weizmann Institute of Science (Israel); I. Sagi, The Weizmann Institute of Science (Israel); M. Havenith, Ruhr-Univ. Bochum (Germany)

Functional motions of enzymes control myriads of metabolic processes of which many are well characterized, yet understanding the role of the surrounding aqueous reaction matrix remains a goal beyond the horizon of most experimental approaches. By kinetic THz absorption (KITA) spectroscopy, we have studied in real-time the complex dynamic interplay between water and an enzyme at work. In our KITA setup we combined a THz-time domain spectrometer (THz-TDS) with a stopped-flow mixing apparatus. Using picosecond THz pulses which directly probe hydrogen bond forming and breaking in the water network and with protein surfaces, we followed enzyme-water interactions upon the enzymatic reaction with millisecond time resolution. We observed a strong perturbation of coupled enzyme-water network dynamics during productive binding of a peptide substrate to the enzyme active site, forming a Michaelis complex. By employing complementary, real-time biophysical techniques and molecular dynamics simulations sensitive to the local active site and to the whole enzyme-water ensemble, we analyzed water's contribution to enzyme catalysis. Our results show a gradient of water dynamics at the remote active site of the enzyme slowing down hydration water dynamics in direction of the active site, a long-range collective mechanism which might facilitate productive binding of substrate molecules. During substrate binding, the conserved water motions gradient at the enzyme active site is being perturbed resulting in a pronounced change of the KITA signal. Further KITA experiments shall quantify water's contribution to enzyme function.

8225-45, Session 7

## Chloroplast fluorescence excitation and emission spectroscopy in live plant cells

S. Peter, Eberhard Karls Univ. Tübingen (Germany); M. Zell, Univ. zu Köln (Germany); C. Blum, Univ. Twente (Netherlands); K. Elgass, La Trobe Univ. (Australia); V. G. Maurino, Univ. zu Köln (Germany); A. J. Meixner, Eberhard Karls Univ. Tübingen (Germany); V. Subramaniam, Univ. Twente (Netherlands); F. Schleifenbaum, Eberhard Karls Univ. Tübingen (Germany)

Leaf cells exhibit strong fluorescence from Chloroplasts, the center of photosynthesis. The fluorescence spectra show two major bands that are assigned to the two photosystems PSI and PSII. Changes in a plant's environmental conditions are reflected by an altered efficiency of photosynthesis and therefore a changed extent of energy transferred between PSII and PSI. Fluorescence spectroscopy of plant photosystems is commonly carried out at 77K for freezing energy transfer between the photosystems which strongly affects fluorescence spectroscopy at room temperature.

We show that statistical analysis of chloroplast fluorescence spectra recorded at room temperature enables for drawing conclusions about the relative PSI/PSII ratio in wild type and carbon deficient plant cells. Furthermore, we were able to record fluorescence excitation spectra with a confocal microscope, which enables for spatially resolved reading out light collection efficiency recorded over a range of 100 nm. For this purpose, we combined a supercontinuum laser with a grating spectrograph as dispersive element and a confocal microscope. Fluorescence excitation spectra of plants grown under different conditions show three peaks assigned to different carotenoids. The spectra not only differ in the intensity ratios between different pigments but also in the broadth of the respective distributions revealing a higher flexibility to adapt to local conditions in wildtype plants than in carbon-deficient mutants.

Therefore, fluorescence excitation and emission spectroscopy at room temperature enables for live read-out of the photosynthesis adaption to external conditions without generating artifacts from extensive sample preparation and low temperatures.

8225-46, Session 7

## Examining aortic valvular interstitial cells live utilizing Raman spectroscopy

K. Cloyd, I. El-Hamamsy, P. Sarathchandra, E. Gentleman, M. H. Yacoub, A. H. Chester, M. M. Stevens, Imperial College London (United Kingdom)

Calcified aortic valves experience a significant loss in functionality due to thickening, leaflet fusion and a loss of flexibility. Obstruction to natural flow produces pressure hypertrophy, diastolic dysfunction, myocardial ischemia and without repair or replacement ultimately death. Valvular interstitial cells (VICs) are critical to understanding this phenomenon as they populate the valves and may play a direct role in calcification. When VICs are cultured in vitro they produce nodule like formations staining positive for Alizarin red, a stain commonly used to identify calcium in bone matrices. The question then remains as to the similarity of the matrix composing these nodules and that of bone or naive heart valve calcified legions. Bio-Raman micro-spectroscopy is a rapid, non-invasive, label free method of detecting the molecular content of living systems1. Information rich Raman spectra were collected from VICs nodules at various time points in both control and osteogenic media. These spectra are then analysed using univariate and multivariate techniques. Our results show that porcine VICs nodules at 7,14 and 21 days, which stain and are morphologically similar to those previously reported, demonstrate a biomolecular matrices varying greatly from bone nodules grown in vitro tested at similar time points and calcified human aortic cusps.

The nodules formed by VICs may provide information on the calcification happening in vivo however the relationship between these nodules and of other mineralizing tissues and especially calcified naïve valves must be thoroughly investigated using sensitive techniques such as bio-Raman micro-spectroscopy.

1. Gentleman, E. et al. Comparative materials differences revealed in engineered bone as a function of cell-specific differentiation. Nat. Mater. 2009. 8(9): p. 763-770.

8225-47, Session 7

## Inhomogeneous Monte Carlo simulations of dermoscopic spectroscopy

D. S. Gareau, T. Li, S. Jacques, J. Krueger, Oregon Health & Science Univ. (United States)

Clinical diagnosis of skin lesions is aided by dermoscopy: 10X epiluminescence microscopy. The appearance of skin lesions range from black to white and include blue, red, gray and orange. Uneven coloration is an important diagnostic criteria for skin diseases including melanoma. The content of chromophores (melanin & blood considered here) and their distribution both contribute to the diffuse remittance in the 300-1000nm spectral range. Multiple axial layers (compartments) such as the immersion medium, stratum corneum, spinous epidermis, basal epidermis and dermis as well as laterally asymmetric features such as the undulation of the basal layer and invasion of melanocytic cell nests were modeled in a inhomogeneous Monte Carlo simulation of photon transport. Each compartment was assigned homogeneous optical properties based on a weighted sum of the cromophores typical for its anatomy. Simulations run at various wavelengths were initiated with the optical properties specified by the absorption spectra of the chromophores. Scattering was approximated as A(fMie(λ/λo)-B1 + fRayleigh(λ/λo)-B2) where λo=reference wavelength, and the A and B coefficients were compartment-specific and fMie, fRayleigh represent the fractions of scattering that, based on the local scattering particle size, were Mie (B1 ≈ 1) or Rayleigh (B1 ≈ 4) type. The spectral remittance output results were integrated over the tri-stimulus RGB functions to produce maps of simulated lesions in background normal skin. These results serve as an interesting prediction of morphometric hue and a look-up table that may specify anatomical architecture based on clinical observation.

8225-48, Session 7

## Raman spectroscopic study of keratin 8 knockdown oral squamous cell carcinoma derived cells

S. P. Singh, H. Alam, C. Dmello, M. M. Vaidya, C. M. Krishna, Advanced Ctr. for Treatment, Research & Education in Cancer (India)

Keratins are cytoplasmic intermediate filament proteins expressed in tissue specific and differentiation dependent manner. Alterations in pattern of keratin expression are often observed in various pathological conditions including cancer and are being widely used as diagnostic markers. Aberrant expression of keratin 8 and 18 is commonly seen in oral cancer. Optical spectroscopic methods are sensitive to biochemical changes and being projected as novel diagnostic tools for cancer. Aim of this study was to evaluate potentials of Raman spectroscopy in detecting minor changes associated with depletion of keratin expression in tongue cancer derived AW13516 cells. K8-knockdown-clones derived from AW13516 cells were grown and synchronized by serum starvation. Cell pellets of three independent experiments in duplicate were used for recording Raman spectra with fiberoptic-probe coupled HE-785 Raman instrument. A total of 123 and 96 spectra from knockdown clones and vector controls, respectively were recorded. Differences in 1200-1800 cm-1 region were successfully utilized for classification using LDA. Two separate clusters with classification efficiency of ~95% were obtained. Leave-one-out cross-validation yielded ~63% efficiency which could be attributed to spectral range employed the study. Due to fiber interference we have restricted analysis to this region. Therefore Raman signals of keratin and changes associated with loss of keratin expression could not be fully explored. However, findings of the study demonstrate the potentials of Raman spectroscopy in detecting even subtle changes such as variations in keratin expression levels. Future studies towards identifying Raman signals from keratin in oral cells can help in precise cancer diagnosis.

8225-49, Session 7

## Multiphoton spectroscopy in human skin in vivo

H. G. Breunig, K. König, JenLab GmbH (Germany)

We report on spectral in vivo data from volunteers and patients with dermatological disorders using certified multidimensional multiphoton tomography. A tunable femtosecond laser source was applied to induce two-photon excited autofluorescence,second harmonic generation,and CARS signals from different skin tissue layers with submicron resolution. Fluorescence lifetimes, emission spectra, exciation spectra, and chemical fingerprints were obtained using time-resolved single-photon counting modules, polychromators,and white light generation.

8225-50, Session 8

## A non-iterative exact solution to the phase problem in optical imaging

A. Lewis, The Hebrew Univ. of Jerusalem (Israel)

No abstract available

8225-51, Session 8

## Multimodal in-vivo MRI and NIRF imaging of bladder tumors using peptide conjugated glycol chitosan nanoparticles

J. Key, D. Dhawan, D. K. Knapp, Purdue Univ. (United States); K. Kim, I. C. Kwon, K. Choi, Korean Institute of Science and Technology (Korea, Republic of); J. F. Leary, Purdue Univ. (United States)

Exact detection and complete removal of tumors is a key point to minimize cancer recurrence. However, it is currently very difficult to find small tumors inside human body and continuously monitor tumors using a non-invasive imaging modality. Presently, positron emission tomography (PET) can provide the most sensitive cancer images in the human body. However, PET imaging has very limited imaging time because they typically use isotopes with short half-lives. PET imaging cannot also visualize anatomical information. Magnetic resonance imaging (MRI) can provide high-resolution images inside the body but it has a low sensitivity, so MRI contrast agents are necessary to enhance the contrast of tumor. Near infrared fluorescent (NIRF) imaging has a good sensitivity to visualize tumor using optical probes, but it has a very limited tissue penetration depth. Therefore, we developed multi-modality nanoparticles for MRI based diagnosis and NIRF imaging based surgery of cancer. We utilized glycol chitosan of 350 nm as a vehicle for MRI contrast agents and NIRF probes. The glycol chitosan nanoparticles were conjugated with NIRF dye, Cy5.5 and bladder cancer targeting peptides to increase the internalization of cancer. For MR contrast effects, iron oxide based 22 nm nano-cubes were physically loaded into the glycol chitosan nanoparticles. The nanoparticles were characterized and evaluated in bladder tumor bearing mice. Our study suggests the potential of our nanoparticles by both MRI and NIRF imaging for tumor diagnosis and real-time NIRF image-guided tumor surgery.

8225-52, Session 8

## Optical dry mass measurement in live cells: phase delay versus Raman scattering

J. W. Kang, N. Lue, Y. Sung, I. Barman, N. C. Dingari, C. Kong, R. R. Dasari, M. S. Feld, Massachusetts Institute of Technology (United States)

Recently, we have developed a novel multimodal microscopy system that incorporates confocal Raman, confocal reflectance and quantitative phase microscopy (QPM) into a single imaging entity. Confocal Raman provides detailed chemical information from the sample while confocal reflectance and quantitative phase offer a detailed morphological understanding. By combining these intrinsic contrast imaging modalities, both morphological and chemical information can be acquired quantitatively without exogenous staining.

The dry mass of a cell is an important parameter in order to understand cell development and cell cycle. QPM techniques have been successfully applied to measure dry mass in its natural state by integrating phase delays caused from the cell. However, QPM-based dry mass measurement has limitations due to the lack of chemical information. Variation of intra cellular chemical composition is not considered in QPM-based dry mass measurement which does not accurately represent the real picture.

To overcome this problem, we have applied the new multimodal microscopy system for dry mass measurements. Comparison between QPM and Raman images from the same cells show the relation between optical phase delays and intra cellular chemical composition. QPM image can be understood in terms of chemical distribution which is acquired by Raman imaging. The correlation between phase delays and chemical composition, arising from the presence of nucleic acids, proteins and lipids, is studied.

Furthermore, from the statistical studies, QPM-based dry mass is compared to the Raman-based measurement from whole cell. The refractive indices for major chemical components can be inversely estimated from this process.

8225-53, Session 8

## Dual imaging with fluorescence and full-field optical coherence microscopy

E. Auksorius, Y. Bromberg, E. Coron, L. Liu, J. A. Gardecki, B. E. Bouma, G. J. Tearney, Massachusetts General Hospital (United States)

Full-field optical coherence microscopy (FFOCM) is a wide field interferometric technique that can record reflectance images with better than 1 μm resolution in all three dimensions. The interferometric nature of the microscope also allows deep imaging in the scattering sample making it an ideal tool for tissue imaging. However, the FFOCM signal lacks cellular specificity. To this end, it is advantageous to add fluorescence channel to the FFOCM microscope and co-register FFOCM and fluorescence images.

We have implemented a wide-field fluorescence imaging modality on FFOCM setup by adding appropriate filters and a separate CCD camera for fluorescence imaging. Further to that a structured illumination technique was implemented to provide optical sectioning in fluorescence images. A Ronchi grating on a piezo based translation stage was used to create structured illumination on a sample, which could be moved across it.

The performance of FFOCM and fluorescence imaging was measured and compared in terms of resolution and imaging depth. We used the system to study various samples ex-vivo that had administered fluorescent contrast dye or label and it showed that in many cases fluorescence may provide additional contrast mechanism. Finally we have explored if tissue autofluorescence can provide additional information to FFOCM. This could potentially be useful for in-vivo imaging as both techniques are minimally invasive and do not require any labeling.

8225-54, Session 8

## Multimodal optical setup for nonlinear and fluorescence lifetime imaging microscopies: improvement on a commercial confocal inverted microscope

V. B. Pelegati, J. F. Adur, A. A. de Thomaz, D. B. Almeida, M. O. Baratti, H. F. Carvalho, C. Lenz Cesar, Univ. Estadual de Campinas (Brazil)

In this work we proposed and built a multimodal optical setup that extends a commercially available confocal microscope (Olympus FV300) to include nonlinear optical (NLO) microscopy and fluorescence lifetime imaging microscopy (FLIM). The NLO microscopies included two-photon fluorescence (TPFE), Second Harmonic Generation (SHG) and Third Harmonic Generation (THG). The whole system, including FLIM, used only one laser source composed of an 80 MHz femtosecond laser. The commercial Ti:sapphire lasers can be tuned up to 1040-1064 nm bringing the THG signal to the 350 nm region where most microscopy optics do not work. However, the third harmonic is only generated at the sample, meaning that we only have to take care of the collection optics. To do that we used a remote photomultiplier to acquire the THG signal at the 310-350 nm wavelength window. After performing the tests to guarantee that we are observing actually SHG/THG signals we than used this system to acquire multimodal images of several biological samples, from epithelial cancer to vegetables. Juxtaposition of different modality images shows how complementary they are. The ability to see the collagen network together with the cell nuclei proved to be important for cancer tissues diagnosis. Moreover, FLIM provides information about the cell metabolism, also very important for cancer cell processes.

8225-55, Session 9

## Multivariate optical computing using a digital micromirror device for Raman and fluorescence spectroscopy

Z. J. Smith, S. Strombom, S. Wachsmann-Hogiu, UC Davis Medical Ctr. (United States)

A multivariate optical computer has been constructed that utilizes an imaging spectrograph with a digital micromirror device placed in the image plane to act as a programmable optical filter, with the length of the DMD chip corresponding to wavelength and the height to position within the spectrometer slit. Pixels of the DMD that are turned on direct light to a point detector, while off pixels send light to a beam dump. By rapidly varying binary patterns, 8-bit greyscale patterns can be displayed on the chip at 60 Hz. The measurement at the point detector represents the projection of the source spectrum onto the axis defined by the pattern displayed on the DMD. Assuming the sample spectrum can be represented as a linear model of component spectra (principal components, pure reference spectra, vertex components, etc.), such measurements can provide quantification of absolute concentrations of these components with a signal-to-noise advantage over standard detection utilizing a spectrograph and CCD array. Experiments have been performed on ternary mixtures using fluorescence and Raman spectroscopy showing accurate quantification of absolute concentrations. Simulations have been performed using Raman spectra of cancerous and noncancerous T-cells, showing that computing the first two principal component scores (which are diagnostic for disease) directly using the optical computer provides greater robustness to noise compared to computing them from detected spectra. This could have important implications for the feasibility of Raman-activated cell sorting. These and continuing results will be presented.

8225-56, Session 9

## Realization of an endoscope equipped with microprojection system for optogenetics

R. Pashaie, Univ. of Wisconsin-Milwaukee (United States)

Abstract- Optogenetics is the science where recent progresses in the field of photonics are combined with the techniques in molecular genetics to develop a methodology for modulation of neural activities. Despite enormous enthusiasm in using optogenetics for brain studies, little has been done on the engineering side such as technology development for light delivery or realization of reliable systems for optical monitoring of the induced activities.

In this project, we have implemented a Digital Micromirror Device based microprojection system capable of delivering illumination patterns through a high-resolution imaging fiber bundle that guides the pattern to the region of interest on the surface or within the brain tissue. The system is also equipped with an imaging path for detection of calcium signals and monitoring the induced patterns of cellular activities.

A very interesting application of the system is extracting topographic computational maps of cortex or cellular receptive fields in-vivo. It is known that such maps are the engine of information processing in the cortex. Better understanding of the structure of such maps will help to unravel the mysteries of brain higher level computations. Another application of this system is related to the high-resolution stimulation patterns that cannot be produced with electrode arrays. Production of high-resolution patterns is important in the study of specific modes of brain activities.

We report the details of our optical design, preliminary results produced by testing the system on tissue phantoms, and we discuss our strategy to extract new data from the brain tissue.

8225-57, Session 9

## Design and development of a wide-field structured illumination fluorescence imaging system for breast tumor margin assessment

H. L. Fu, N. Ramanujam, J. Q. Brown, Duke Univ. (United States)

Cancer is associated with specific morphological changes at the cellular level, such as increased nuclear size and crowding due to rapidly proliferating cells. In situ imaging of these hallmarks may be useful for microscopic detection of residual cancer in breast tumor margins. We have previously presented a contact-based high resolution micro-endoscope system for imaging microanatomy in situ in combination with topically-applied fluorescent nuclear stains. However, breast tumor margins are often large (~4.5x4.5cm) and difficult to cover with the small single-shot field of view (FOV = 0.3 mm2) afforded by micro-endoscopy.

We have developed a custom wide-field fluorescence microscope system with a single-shot FOV of 2.1x1.6 mm (3.36 mm2). The ability to resolve cell nuclei in thick tissues in situ is achieved by rejecting out of focus fluorescence via structured illumination microscopy (SIM). The system is designed to image a 20 cm2 tissue sample at sub-cellular resolution within 10 minutes. Using a supercontinuum fiber laser and bandpass filters, the system can excite a variety of fluorescent contrast agents, and the LCTF allows collection of spectral emission images.

The system was tested on solid phantoms consisting of 10 μm fluorescent spheres (to simulate cell nuclei) embedded in a PDMS matrix and TiO2 spheres to yield a reduced scattering coefficient of 10 cm-1 (at 630 nm). The 10 μm spheres were clearly resolved with a 13 dB SNR increase from the non-sectioned to sectioned images. We are currently evaluating the tool for detection of microscopic residual disease in a transgenic murine cancer model.

8225-58, Session 9

## Investigation of in situ fluorescence optical detection based on a programmable spatial light modulator

J. Choi, K. Kim, D. Kim, Yonsei Univ. (Korea, Republic of)

Microfluidic 3D cell culture systems have received tremendous attention because they provide an in vitro microenvironment in which cellular dynamics can mimic those obtained in in vivo conditions. In this study, we investigated enhancement of imaging resolution for in situ fluorescence optical detection of 3D cell cultures using a digital micro-mirror device (DMD) as a programmable binary-intensity spatial light modulator. The fluorescence optical detection system was designed for various architectures of 3D microfluidic cell-based assays to be measured in situ in a conventional incubator. Through the combination of DMD-based multiple-pinhole scanning and fast axial scanning by a motorized stage, the optical detection system was developed to provide 3D fluorescence imaging. The performance was initially tested by the measurement of an USAF target and fluorescent microbeads (diameter: 10 μm; emission λ = 515 nm) that are similar in size to stained mammalian cells. Furthermore, we studied cellular dynamics of 3D cultured cells embedded in an alginate-based extracellular matrix and stained by Celltracker Green, which is a fluorescence indicator representing cell viability. Preliminary results indicate objective-dependent enhancement of imaging resolution by at least 2.5 times. Further improvements in 3D fluorescence images are under way based on multiple approaches including programmable structured illumination and optimized image reconstruction algorithm. The in situ fluorescence optical detection system that employs a programmable spatial light modulator is expected to offer a simple and useful analytical tool for measuring cellular dynamics in diverse 3D cell assays while maintaining dynamic culture environments.

8225-59, Session 10

## Distributed light delivery system (DLDS) for optogenetics

R. Pashaie, Univ. of Wisconsin-Milwaukee (United States)

Abstract- Manipulation of neuronal activities at multiple locations in the brain would help us to better understand the neural circuitry as well as to provide possible cures or treatments for some neurological disorders such as Parkinson or Autism. Using optical energy and photosensitive proteins such as channelrhodopsin, optogenetics provides the ability to alter neural activities with excellent cell specificity and high temporal resolution in the brain. In this approach, an optical fiber has been commonly used as a waveguide to deliver light into the brain. However, an optical fiber is capable of delivering light only into the tip of the fiber.

A DLDS, capable of delivering light to multiple sites alongside of the fiber axis, provides the ability to manipulate neural activity in different layers or regions of the brain. In this work, we introduce two different techniques to implement a DLDS, which facilitate more versatile optical control of neurons by accurately delivering light to various layers of cortex or multiple deep brain objects. The first technique includes the design of a fiber consisting of multiple tilted gratings. When such a fiber is connected to a spectrally programmable light source, each of these gratings efficiently radiates light out of the fiber at a specific wavelength and in a desired location. The second technique comprises a custom designed micro motor assembly. The assembly, with a weight limit of 2grams, includes a piezoelectric motor capable of moving a side-firing fiber along a glass-made capillary over 4.5mm travel distance.

8225-66, Session 10

## Multimodal intravital microscopy for studying cellular dynamics of wound healing in mouse skin

B. W. Graf, M. C. Valero, E. J. Chaney, M. Marjanovic, M. D. Boppart, S. A. Boppart, Univ. of Illinois at Urbana-Champaign (United States)

We present methods for imaging cellular dynamics in living mouse skin using an integrated optical coherence (OCM) and multiphoton (MPM) microscope. OCM allows structural features of the skin to be observed while MPM enables visualization of fluorescently labeled cells. With time-lapse imaging, the dynamic behavior of single cells can be observed over a period of several hours. Utilizing a novel image registration algorithm, the same skin site is observed repeatedly to track long term dynamics of cell populations and structural changes in the skin.

We utilize this multi-modal, intravital imaging system to study wound healing dynamics in mouse skin following bone-marrow transplants from GFP donors into species-matched wildtype hosts. The bone-marrow derived GFP-labeled cells in the skin of these mice are a heterogeneous population which includes lymphocytes, dendritic cells and mesencyhmal stem cells. Various methods are employed to extract quantitative parameters from the time lapse OCM and MPM data. Parameters of interest include the density and migration patterns of the GFP cells as well as structural repair of the skin as visualized by OCM. The ability to directly observe the dynamic behavior of these cells and their interactions with the tissue environment enables a clearer understanding of the roles of these different cells during normal conditions and during wound healing.

8225-60, Poster Session

## LED-induced chlorophyll fluorescence signatures from leaves of saccharum officinarum seedlings under water deficit stress

A. S. Gouveia-Neto, E. Arcanjo da Silva, P. C. Cunha, R. A. Oliveira-Filho, E. B. Costa, T. J. R. Câmara, L. G. Willadino, Univ. Federal Rural de Pernambuco (Brazil)

Chlorophyll fluorescence(ChlF) is an intrinsic signal emitted by plants under UV-visible light illumination that conveys information on their physiological state, state of health, and response to stress events. Abiotic stresses impose damage to crop and provokes reduction of yield productivity, and water deficit is one of the most commonly investigated owing to the worldwide extent of cultivated area affected by water shortage. Water scarcity and increase competition for water resources involving several sectors of the production segment(agriculture, industry, hydroelectric energy) and also for human basic necessities, imposes the study of new concepts of irrigation, in order to adapt crops to water shortage maintaining satisfactory levels of productivity. Nowadays, a major technological goal of the energy production is the replacement of fossil-based fuel to biofuel, mainly due to environmental issues. So, it is compulsory to study the effects of water deficit upon plant species used in mass production of nonfossil based fuels, such as Saccharum officinarum based ethanol. Our interest is to employ LED-induced ChlF signatures from Saccharum officinarum leaves to evaluate the effect of water deficit upon the plant growing process. The ChlF is a nondestructive and nonintrusive indicator of the chlorophyll content of leaves, and was used to monitor the time evolution of the effect of water deficit stress upon plants physiological state. Red(Fr) and far-red (FFr) ChlF emission signals around 685 nm and 735 nm, respectively, were observed and examined as a function of irrigation amount. The Fr/FFr ratio allowed one to detect signs of damage in the early stages of the plants growing process, and before traces of visible stress became apparent. The results indicated an unusual behavior of the Fr/FFr ratio for water stress that can potentially be used as a discriminator amongst several abiotic stresses

8225-61, Poster Session

## Hydrogen peroxide induces a rapid loss of mitochondrial membrane potential and apoptosis in chondrocytes

Z. Caiping, X. Wang, The First Affiliated Hospital Of Jinan Univ. (China); T. Chen, South China Normal Univ. (China)

The degenerative joint disease such as osteoarthritis (OA) is closely associated with the death of chondrocytes by apoptosis. Hydrogen peroxide (H2O2), higher expression following acute damage in OA patients, has been shown to be up-regulated during apoptosis in a bulk of experimental models. This study was aimed to explore the mechanism of H2O2-induced rabbit chondrocytes apoptosis. Articular cartilage was biopsied from the joints of 6 weeks old New Zealand rabbits. Cell Counting Kit (CCK-8) assay was used to assess the inhibitory effect of H2O2 on cell viability.. H2O2 treatment induced a remarkable reduction of cell viability. We used flow cytometry to assess the form of cell death with Annexin-V/PI duble staining, and found that H2O2 treatment induced apoptosis in a dose-and time-dependent manner. Exposure of chondrocytes to 0.3 mM of H2O2 for 2 h induced a burst apoptosis that can be alleviated by N-acetyl cysteine (NAC) pretreatment, an anti-oxidant amino-acid derivative. Loss of mitochondria membrane potential ($\Delta\Psi$m) was evaluated using confocal microscopy imaging and flow cytometry (FCM). H2O2 treatment induced a marked reduction of $\Delta\Psi$m, and the abrupt disappearance of $\Delta\Psi$m occurred within 5 minutes. These results indicate that H2O2 induces a rapid apoptosis via a mitochondrial pathway in rabbit chondrocytes.

8225-62, Poster Session

## Combining nanoscale optical phenomena with atomic force microscopy for cellular studies

S. Amini, Texas A&M Univ. (United States); Z. Sun, G. A. Meininger, Univ. of Missouri-Columbia (United States); K. E. Meissner, Texas A&M Univ. (United States)

Nanoscale imaging and sensing capabilities of evanescent waves (EW) and Förster resonance energy transfer (FRET) techniques are combined with nanoscale spatial resolution of a microsphere-modified atomic force microscopy (AFM). Mounting the probe on AFM also provides the ability to mechanically stimulate the cell and characterize the cellular response at the pN force level. The hybrid system is being investigated for imaging and sensing at the cellular level. In both cases, quantum dot (QD)-modified microspheres are mounted on AFM cantilevers. In the case of EWs, luminescence from embedded QDs couples to the whispering gallery modes in the periphery of the polystyrene microsphere (~10 μm diameter). This results in EWs which extend on the order of 100 nm from the surface of the microsphere. This EW decays exponentially and is used to excite fluorescent labeled trans-membrane and near-membrane proteins. In the case of FRET, QDs coated on silica microspheres are conjugated with fibronectin. Moving the microsphere down to the surface of the RFP-$\alpha$v integrin tagged cells, the microsphere binds to the cell surface and FRET is observed between the QDs (donor) and RFP (acceptor). The FRET interaction is limited to approximately 10 nm and, therefore, only excites fluorescent labeled trans-membrane proteins. These innovative imaging and sensing systems provide nanoscale axial resolution from 10 nm to 100 nm and enable the collection of unique dynamic data from living cells to improve understanding of cell adhesion and mechanobiology in cells.

8225-63, Poster Session

## Analysis of time-gated FLIM data by means of the phasor approach

F. Fereidouni, D. van den Heuvel, J. Voortman, E. Hofman, H. C. Gerritsen, Utrecht Univ. (Netherlands)

Fluorescence lifetime imaging is a versatile tool which can be utilized to distinguish or identify the molecular environment. Both time correlated single photon counting (TCSPC) and time gating methods are used for lifetime imaging but to obtain high accuracies high signal-to-noise ratios are required.

The phasor approach is a graphical global analysis method that increases the S/N ratio of the analysis. This method simplifies the analysis of FLIM data and avoids difficulties of nonlinear regression fitting.

It has been successfully employed for analyzing both frequency domain and time domain lifetime images. Time gating detection methods run at very high count rates (~10 MHz) but use of the phasor approach to analyze the data is complicated by truncation and under sampling of the decay curve due to the limited number of gates. In this paper we present a modification to the phasor analyses method that takes into account the cut-off and sampling problem. This approach is tested on both simulated lifetime images and on real data. We demonstrate that this method can be applied to retrieve two lifetimes from time gating data that can not be resolved using standard (non global) fitting techniques.

8225-64, Poster Session

## A study of the characteristics of the analog mean delay (AMD) method for fluorescence lifetime measurements

Y. J. Won, D. Y. Kim, Gwangju Institute of Science and Technology (Korea, Republic of)

The analog mean-delay (AMD) method is a new alternative method used in determining the lifetime of a fluorescence molecule. Due to its powerful advantages of accurate lifetime determination, photon economy and a high photon-detection rate, the AMD method is very suitable for the realization of high-speed confocal fluorescence lifetime imaging microscopy (FLIM). For a proper use of the AMD method in various FLIM applications, we present a study of the characteristics of the AMD method. The optimum integration window size that satisfies accurate lifetime extraction was estimated in a simple simulation and was experimentally demonstrated using Cy5 and Alexa fluor 633. Photon economy for lifetimes of 1, 3.2, 5 and 8 ns was also evaluated via a Monte-Carlo simulation (MCS). We confirmed that the photon economy of the AMD method is not degraded for longer lifetimes even when the applied integration window size is increased. By an extension of MCS, the photon economy with respect to different designs of the Gaussian low-pass filter (GLPF) used in the AMD setup was also studied. When a GLPF with the highest cutoff frequency of 100 MHz is applied, the most effective photon economy performance is achieved for lifetimes of 1, 3.2, 5, and 8 ns.

8225-67, Poster Session

## The relationship between metabolic activity and collagen deposition during osteoblastic differentiation of mesenchymal stem cells

K. P. Quinn, R. S. Hayden, D. L. Kaplan, I. Georgakoudi, Tufts Univ. (United States)

Tissue engineering requires the optimization of complex culture protocols through biochemical and microstructural assessments of the tissue. Although traditional histological techniques can provide tissue characteristics at specific time points, non-destructive approaches are needed to understand the dynamic changes that occur during in vitro development. Using two-photon excited fluorescence (TPEF) microscopy and second harmonic generation (SHG), the objective of this study was to quantify the relationship between the cellular redox state and collagen fiber deposition during the osteoblastic differentiation of human mesenchymal stem cells (hMSCs) over 28 days. A redox ratio of the fluorescence contribution of the coenzymes FAD and NADH was computed for each cell, which is inversely proportional to metabolic rate. The redox ratio in the differentiating cells significantly decreased between days 1, 7, and 21 ($p<0.0002$), but increased between days 21 and 28 ($p<0.0001$). More collagen fiber deposition was detected from SHG images of the differentiating cells at days 21 and 28 compared to undifferentiated hMSCs ($p<0.0001$). During the first 7 days of differentiation, the redox ratio and SHG signal were negatively correlated ($R=-0.9286$; $p<0.0001$). However, between days 21 and 28, redox ratio and SHG signal were positively correlated ($R=0.6043$; $p=0.0005$). These findings suggest that TPEF is sensitive to a transient increase in metabolism produced during the onset of osteogenic differentiation. Once differentiation has occurred, cell metabolism decreases and collagen deposition becomes more visible in SHG images. Collectively, these findings demonstrate the diagnostic utility of non-linear microscopy to assess differentiation status and functional tissue development.

8225-69, Poster Session

## Milk phospholipid's protective effects against UV damage in skin equivalent models

L. H. Laiho, A. A. Russell, Z. Achay, C. Dargitz, M. Bingham, California Polytechnic State Univ., San Luis Obispo (United States)

Exposure of skin tissue to UV radiation has been shown to cause DNA photodamage. If the damaged DNA is allowed to replicate, carcinogenesis may occur. Damage can be prevented by upregulation of the protein p21. p21 halts the cell cycle allowing the cell to undergo apoptosis or repair its DNA before replication. Preliminary work involving confocal reflectance and fluorescence microscopy implies that milk phospholipids may possess protective properties against UV damage. In this study, we observed cell morphology, cell apoptosis, and p21 expression in tissue engineered epidermis through the use of Hematoxylin and Eosin staining, confocal microscopy, and western blot, respectively. Tissues were divided into four treatment groups including: a control group with no UV and no milk phospholipid treatment, a group exposed to UV alone, a group incubated with milk phospholipids alone, and a group treated with milk phospholipids and UV. All groups were incubated for twenty-four hours after treatment. Tissues for histology and immunofluorescence were then fixed, processed, and embedded in paraffin. Performing western blots on whole tissue lysates resulted in visible p21 bands for the UV group only, indicating that in the other groups, p21 expression was less. The percentage of apoptotic cells was determined by staining the tissues with Hoechst dye and imaging with a confocal microscope. We found a decrease in apoptotic cells in tissues treated with milk phospholipids and UV compared to tissues exposed to UV alone indicating milk phospholipids may protect against UV damage.

8225-70, Poster Session

## High-density microarrays using lithographically patterned polelectrolytes

G. R. Prashanth, V. S. Goudar, S. Suran, M. M. Varma, Indian Institute of Science (India)

We report a substrate-independent strategy to fabricate bio-microarrays (protein/DNA or cells) on virtually any substrate using lithographically patterned polyelectrolyte films. Polyelectrolytes are ionizable polymers which can electrostatically adsorb on charged surfaces. We created laterally patterned polyelectrolyte multilayers by sequentially spin coating a cationic polymer Poly-allylamine hydrochloride (PAH) and an anionic polymer Poly-acrylic acid (PAA) on glass slides containing a photoresist pattern obtained by photolithography. Stripping off the photoresist layer with extended sonication (~ 10 minutes) results in a well defined microarray pattern of polyelectrolytes. The native pH dependent surface charge present in biological entities is used to attach them to the polyelelctrolyte microarray. We used this strategy to create an avidin microarray with 10 micron size spots and demonstrated the activity of the attached protein by performing an avidin-biotin assay using fluorescently labeled biotin and obtained a limit of detection around 0.1 ng/mL. Electrostatic assembly of polyelectrolytes onto glass and proteins onto polyelectrolytes are fast reactions with saturation times around 30 - 45 seconds unlike covalent surface functionalization procedures which typically take several hours for completion. Electrostatic attachment depends only on the sign of the substrate surface charge and not on the chemical nature of the surface. Therefore this approach can be used with a variety of substrates such as glass, plastics and metals unlike covalent functionalization schemes which are very specific to the substrate used. Finally, this approach enables orders of magnitude increase in array densities compared to piezo-electric printing, the most dominant microarray manufacturing technology currently.

8225-71, Poster Session

## Biological imaging with high-dynamic range using compressive imaging technique

M. Abolbashari, F. Farahi, A. S. Gerges, G. Babaie, The Univ. of North Carolina at Charlotte (United States); F. Magalhães, M. V. Correia, F. M. Araújo, INESC Porto (Portugal)

Scenes in real world have dynamic range of radiation that cannot be captured by conventional cameras. High dynamic range imaging (HDRI) is a technique to capture detail images where, in the field of image, intensity variation is extreme. This technique is very useful for biological imaging where the samples have very bright and very dark regions and both parts have useful information. In this article we propose a novel high dynamic range imaging technique based on compressive imaging that uses one single detector instead of camera (array of detectors) to capture an image. Combination of high dynamic range imaging and compressive imaging benefits from both imaging with high dynamic range of radiation and advantages of compressive sampling; namely, imaging in wavelength that conventional cameras are not readily available and single detectors are available. Additionally, as its name suggests, this technique requires less number of samples (compared to raster scanning). Our experimental results show that high dynamic range compressive imaging system is capable of capturing images with large intensity contrast.

8225-72, Poster Session

## Measurement of depth-dependent elastic properties of breast tissue phantoms by holographic imaging of surface waves

K. D. Mohan, W. W. Sanders, A. L. Oldenburg, The Univ. of North Carolina at Chapel Hill (United States)

Elastography is a promising method for the early detection of breast cancer, since tumors exhibit an elastic modulus 3-10x greater than healthy tissue. We report on results utilizing image plane digital holography to measure the elastic properties of silicone phantoms that are mechanically similar to real breast tissue. Surface acoustic waves (SAWs) generated by a piezo-electric transducer are mapped over a 16mm x 16mm area in real-time using a high-speed CMOS camera at frame rates of 1-5kHz, and an appropriate phase-shifting algorithm. The measured SAW velocities are found to be proportional to the square root of elastic modulus, as expected. Phantoms with elastic moduli varied between 3-35 kPa are investigated, simulating elasticity variations in real breast tissue. Furthermore, SAWs are generated at various frequencies between 50-500 Hz, resulting in wavelengths between 2.5-25mm. As penetration of the waves is approximately one wavelength, we utilize the dependence of penetration depth on frequency to detect variations in elasticity as a function of depth. In phantoms composed of multiple layers with different elastic moduli, SAWs at a lower frequency (longer wavelength) exhibit velocities corresponding to the elastic modulus of the lower layers, and vice versa. This depth-dependence on frequency is further applied to detect the presence of tumor-like inclusions. The nanoscale sensitivity of holography allows for measurement of surface waves generated by a very small excitation, thus making the method minimally invasive. Holographic Elastography represents a novel optical sensing method for soft tissues, which may be particularly relevant for the detection of breast cancer.

8225-73, Poster Session

## Single optical fiber probe for optogenetics

R. Pashaie, Univ. of Wisconsin-Milwaukee (United States)

Abstract- With the advent of optogenetics, all optical control and visualization of the activity of specific cell types is possible. We have developed a fiber optic based probe to control/visualize neuronal activity deep in the brain of awake behaving animals. In this design a thin multimode optical fiber serves as the head of the probe to be inserted into the brain. This fiber is used to deliver excitation/stimulation optical pulses and guide a sample of the emission signal back to a detector. The major trade off in the design of such a system is to decrease the size of the fiber and intensity of input light to minimize physical damage and to avoid photobleaching/phototoxicity but to keep the S/N reasonably high. Here the excitation light, and the associated emission signal, are frequency modulated. Then the output of the detector is passed through a time-lens which compresses the distributed energy of the emission signal and maximizes the instantaneous S/N. By measuring the statistics of the noise, the structure of the time lens can be designed to achieve the global optimum of S/N. Theoretically, the temporal resolution of the system is only limited by the time lens diffraction limit. By adding a second detector, we eliminated the effect of input light fluctuations, imperfection of the optical filters, and back-reflection of the excitation light. We have also designed fibers and micro mechanical assemblies for distributed delivery and detection of light.

8225-74, Poster Session

## Fast and efficient phase extraction method for real-time quantitative phase imaging

S. K. Debnath, Y. Park, KAIST (Korea, Republic of)

Quantitative phase imaging (QPI) has gain rapid importance in the field of biophysics and cell biology. QPI quantitatively measures the shape and its dynamic change of biological samples without using any exogenous labeling agents. In QPI, spatially modulated interferograms are typically recorded and the quantitative phase images are extracted using an appropriate algorithm. There are two main algorithms for extraction quantitative phase image from a spatially modulate interferogram: Fourier Transform (FT) technique and Hilbert Transform (HT) technique. In the FT method, the interferogram is Fourier transformed, the positive spatial frequency is translated to zero frequency. Then, an inverse Fourier transform with an appropriate spatial filtering gives a complex field image, from which the phase is extracted. In the HT method, applying Hilbert transform in the interferogram will directly result in a complex field image. Both the techniques are computationally intensive as they require multiple Fourier transforms which prevents from real time quantitative phase imaging. We propose a faster and simpler quantitative phase extraction method based on spatial phase shifting (SPS). In the spatially modulated interferogram there is a fixed amount of phase shift between the adjacent pixels. This phase shift can be calculated using phase shifting algorithms. In SPS method this phase shift value is used for the calculation of unknown phase using phase shifting algorithm. The present method improves the computation speed by six-fold, compared to the conventional FT method. The SPS method is capable of extracting quantitative phase in 37 ms in a typical desktop computer which will enable us for 28 Hz dynamic quantitative phase imaging. The present method may offer an effective and sufficiently general method for quantitative phase imaging of dynamic phenomena of biological samples

8225-75, Poster Session

## Validating novel melanoma treatments via S100 protein

A. A. Russell, C. Dargitz, A. Rowley, Z. Achay, M. Bingham, R. Jimenez, L. H. Laiho, California Polytechnic State Univ., San Luis Obispo (United States)

Mitotic inhibitors for cancer treatments target rapidly dividing cancer cells to diminish growth and stop mitosis. One method to validate novel treatments in vitro is by studying the S100 protein, a marker for melanoma. Angiostatin biomolecules in combination with milk phospholipids are thought to be a potential treatment against melanoma. In this study, tissue engineered melanoma tissue constructs were treated with angiostatin biomolecules, as well as milk phospholipids, to inhibit the growth of the melanoma cells. The angiostatin was produced from the interaction of bacillus polymyxa protease (BPP) and plasminogen (PG), in which BPP cleaves PG to create an angiostatin fragment. It is believed that the angiostatin element that was created acts like an angiogenesis inhibitor. Immunofluorescence using confocal microscopy, traditional histopathology with hematoxylin and eosin, and western blots were performed to verify the potential of the different therapies. Preliminary results show that the angiostatin fragments created by BPP/PG, as well as a 0.1% milk phospholipid solution, noticeably decreased the presence of s100. This suggests that these treatments may inhibit melanoma progression.

8225-76, Poster Session

## Dual coupled radiative transfer equation and diffusion approximation for the solution of the forward problem in fluorescence molecular imaging

D. S. Gorpas, Technological Educational Institute of Messolonghi (Greece); S. Andersson-Engels, Lund Univ. (Sweden)

The accurate solution of the forward problem in fluorescence molecular imaging is among the most important premises for the successful confrontation of the inverse problem. To date the most typical approach has been the diffusion approximation of the radiative transfer equation as the forward model. This model is basically a first order angular approximation for the radiative transfer equation, and thus it has limitations. The scope of this manuscript is to present the dual coupled radiative transfer equation and diffusion approximation model for the solution of the forward problem in fluorescence molecular imaging. Towards the solution of the forward problem with utilization of the proposed model, the spatial region was discretized, resulting in the development of a discretization matrix, and the integro-differential equations of the weak formalism were solved via the finite elements method. Algorithmic blocks with cubature rules and analytical solutions of the multiple integrals have been constructed for the solution. Furthermore, since the solution was per element of the discretized region, mapping matrices have been developed to assembly the finite elements matrix. Additionally, the integration over the angular discretization, which was performed over polar and azimuthal angles, was implemented mainly analytically, while quadrature rules were applied whenever required. Finally, this model has been evaluated on numerous virtual phantoms and compared against the widely used diffusion approximation model. The results of these tests validate the accuracy of the proposed model, as they present over 90% relative accuracy when compared to the radiative transfer equation, with increased time efficacy.

8225-77, Poster Session

## Spectrally resolved visualization of fluorescent dyes permeating into skin

U. Maeder, T. Bergmann, S. Beer, J. M. Burg, T. Schmidts, F. Runkel, M. Fiebich, Technische Hochschule Mittelhessen (Germany)

Evaluating the capability to transport drugs into the skin is a common task in the development of pharmaceutical drug carrier systems. There is a strong demand for a reliable, easy to use and standardized method to compare different systems.

We present a method to visualize the permeation depth of fluorescent dyes using spectrally resolved confocal microscopy. The confocal microscope used in this study was a Leica TCS SP5 II that allows measuring fluorescence emission spectra of the samples without using filter cubes with a maximal spectral resolution of about 5 nm. Thereby high spectral resolution images with the common confocal spatial resolution can be acquired.

In our experiments the surface of porcine skin samples is treated for different periods of time with a submicron emulsion enriched with the fluorescent dye Nile Red. The topically applied dye permeates into the skin supported by the submicron emulsion. It is expected to reach deeper skin layers with increasing experiment duration. After this step the skin sample is cut vertically into small thin sections and placed on the cutted edge onto coverslips. In this way all skin layers can be imaged in the xy-plane of the microscope. After performing spectral imaging it is possible to evaluate the permeation depth of the dye by looking at the recorded spectra. The spectral measurements help separating the light emissions caused by the dye from the skin autofluorescence which usually disturbs the direct assessment of the permeation depth of external dyes. It is planned to perform these experiments with fluorescent labeled drugs.

8225-78, Poster Session

## Live cardiomyocyte imaging via hybrid SHG-TPEF microscopy

W. Qin, H. Liu, Clemson Univ. (United States); Y. Shao, Shenzhen Univ. (China); Q. Liu, Z. Ma, Clemson Univ. (United States); T. K. Borg, Medical Univ. of South Carolina (United States); B. Gao, Clemson Univ. (United States)

Second harmonic generation (SHG) has displayed its potential application in the study of myofibrillogenesis through providing high-resolution, high-contrast, and three-dimensional images of sarcomere structure of cardiomyocytes. However, the dynamic process of myofibril's construction and deconstruction is sensitive to the microenvironments. We have developed a hybrid SHG-TPEF imaging system combined with an onstage incubator for long time live cell imaging while the temperature, humidity and the concentration of CO2 are well controlled (e.g., 5% CO2 with 95% air and 95% humidified at 37°C). With the excitation beam from an fs Ti:Sappire laser being bi-directionally raster scanned across the focal plane using a pair of orthogonal galvanometers, signal of second harmonic generation from the sarcomere structure and two photon excitation from the DiO-stained cell membrane of live neonatal cardiomyocytes are collected by two PMTs in the forward and backward direction respectively. The developed system provides the ability to observe the sarcomere dynamics of cardiomyocytes for a prolonged period of time. It is found that 2.8mW incident power of the laser beam is the preferred incident power to keep the cells free from laser damage while acquiring sarcomere image with satisfied quality. Under 2.8mW incident laser beam, sarcomere structures of single cells are acquired up to 10 hours with a snap of the sarcomere structure at a one hour interval. The sarcomere dynamics of in vitro cultured cardiomyocytes are recorded while the cells are undergoing dedifferentiating and redifferentiating process.

8225-79, Poster Session

## Quantitative measurements of dielectrophoretic forces using a single-beam optical tweezer

S. H. Park, E. Lee, Korea Univ. (Korea, Republic of); S. Jung, S. W. Lee, D. S. Yoon, Yonsei Univ. (Korea, Republic of); B. Kim, Korea Univ. (Korea, Republic of)

Optical tweezers have been applied to a variety of biological studies to investigate the mechanical/chemical properties of biomolecules. Many research groups have trapped and manipulated small particles including bacteria, polymers and cells. These techniques are based on the principle of generating pico-newton forces due to momentum changes arising from the refractive index mismatch between dielectric particles and the medium in a tightly focused beam.

In this study, we combined a single beam optical trap with a precise photodiode position detector for quantitative measurements of absolute dielectrophoretic (DEP) forces acting on micro-particles. When DEP force is applied to a micron-sized particle trapped by an optical trap, the object is displaced from the center of the trap by an amount proportional to the external forces. The stiffness of the optical tweezer was calibrated with power spectrum method and then we converted each particle displacements into absolute forces approximated by Hook's law.

The experimental system was applied to polystyrene beads as sizes of beads, coating status, and medium pH were varied. The experimental results showed consistency with theoretical expectation or previous studies. The setup was then applied to both live and dead yeast cells to observe how the living status affects DEP forces. As expected by a previous simulation, the live yeast cells exhibit two crossover frequencies while dead ones show only one. They show opposite polarity at very low frequencies, and live cells experienced relatively strong DEP force at intermediate frequencies.

8225-80, Poster Session

## Quantification and classification of retinopathic injury using image cytometry and vasculature feature extraction

K. Staniszewski, R. Sepehr, C. Sorenson, N. Sheibani, M. Ranji, Univ. of Wisconsin-Milwaukee (United States)

Retinal vasculopathies are a common symptom of many eye diseases. However, if detected early, much of the damage caused by various injuries can be prevented, or in some cases reversed. In this study, images of wholemount retinal trypsin digests were classified as normal or injured by measuring multiple quantitative markers. Each image was taken in either differential interference contrast (DIC) or fluorescence microscopy to allow for cellular and vasculature identifications, respectively. The DIC images are then automatically segmented to allow for cell cytometry, whereas the following features are extracted from the fluorescence images: total power spectrum, relative low frequency content, fractal dimension, tortuosity, branching frequency, and vessel caliber. To model retinal vasculopathies, two types of retinas were analyzed, the first consisting of retinas from mice with the bcl-2 gene partially or completely inactivated to be compared to their corresponding wild type. Bcl-2 plays a critical role in the development of retinal vasculature, impacting apoptosis and angiogenesis. Therefore, the knockout mice exhibit different number of vascular cells and a vasculature with differing degree of complexity compared to the wild type retinas. These qualities agree with the pathology of retinopathy in that retinopathic injuries are characterized by vascular cell death and abnormal vessel growth. When the aforementioned features were extracted from the images, classification was performed using a majority vote between a linear classifier, k-nearest-neighbors classification, and a support vector machine. This resulted in a classification accuracy of 92% using the "leave one out" error determination method.

8225-81, Poster Session

## Multiplexed fluorescence detection using joint spectral and temporal data sets for small animal molecular imaging

D. A. Weinberg, M. Niedre, Northeastern Univ. (United States)

Small animal fluorescence imaging is an important biomedical research tool for studying biological processes in vivo. Multiplexed imaging with four or more fluorophores is potentially highly useful for observing multiple molecular targets, but the overlap of their wide emission spectra in the red and near-infrared regions makes simultaneous imaging ("demixing") a challenging problem. Since fluorophores have both unique spectral and temporal (lifetime) properties, the goal of this research is to improve the accuracy of fluorophore demixing by jointly acquiring and analyzing temporal and spectral data.

Our instrument consists of a pulsed supercontinuum laser and a fiber-coupled spectrograph adjoined to a 16-channel photomultiplier tube array operated in time-correlated single photon counting mode. This was configured to acquire full-time data in the range of 650-850 nm with 13 nm resolution. Initially, four fluorophores in various combinations were placed into multiple tubes in a 1.5 cm imaging chamber filled with tissue-mimicking intralipid. The imaging chamber was scanned in transmission mode using an X-Y translation stage. We were able to analyze temporal and spectral data using a classical least-squares approach at each position to produce a 2-D image of the component fluorophores. Preliminary results show that the combination of temporal and spectral data results in an 8.3% decrease in the mean error of the relative concentrations compared to spectral data alone. Second, as a more realistic model we performed imaging in euthanized mice with implanted fluorescent tubes filled with fluorophore combinations. Future work will extend this approach to multiplexed fluorescence tomographic imaging in vivo.

8225-82, Poster Session

## Imaging of Protoporphyrin IX (PPIX) in neural cell culture

B. Lai, C. J. Fisher, Y. Chen, L. Lilge, Ontario Cancer Institute (Canada)

ALA induced Protoporrphyrin IX (PPIX) mediated Photodynamic therapy (PDT) is under investigation by various groups as therapeutic approach for intracranial neoplasms. The ability of PPIX to generate sufficient cytotoxic substances is related more to its cellular concentration, and its overall efficacy on its subcellular localization. While most studies considered only bulk tumor versus normal distal brain, the effects of PPIX synthesis due to physiological and co-treatment impact have received little attention. This study examines the synthesis and localization of PPIX in a neuronal co-culture system in a variety of conditions. The conditions under investigation are temperature (normothermia and hypothermia), in the presence/absence of NOS 2 inhibitors, EPO/IGF cytokines and cortical steroids. The co-culture systems used comprised of astrocytes and neurons, glioma and neurons, neurons only, glioma only, and astrocytes only. The location and production levels of PPIX in the cell cultures is determined via the co-localization of PPIX and Mitotracker Green fluorescence under confocal fluorescence microscopy. PDT is performed thereafter using the microscope's light source as the excitation source to measure the production and localization of reactive oxygen species (ROS) in these cells. The purpose of the study is to determine whether the investigated conditions can improve the differential mitochondrial concentrations of PPIX and the production of ROS between neurons and glioma cells to increase the therapeutic index of intracranial PDT. Any increase in the therapeutic index is beneficial in that it would either allow higher light doses to be used in vivo, or potentiate PDT in glioma cells and thus achieve the high resection rates needed for significant increase in the survival times of glioma patients.

8225-83, Poster Session

## Threshold-free method for three-dimensional segmentation of organelles

Y. M. Chan, W. F. Marshall, Univ. of California, San Francisco (United States)

An ongoing challenge in the field of cell biology is to how to quantify the size and shape of organelles within cells. Automated image analysis methods often utilize thresholding for segmentation, but the calculated surface of objects depends sensitively on the exact threshold value chosen, and this problem is generally worse at the upper and lower z-boundaries because of the point spread function. We present here a threshold-independent method for extracting the three-dimensional surface of vacuoles in S. cerevisiae whose limiting membranes are labeled with a fluorescent fusion protein. These organelles typically exist as a clustered set of 1-10 sphere-like compartments. Vacuole compartments and center points are identified manually within z-stacks taken using a spinning disk confocal microscope. A set of rays is defined originating from each center point and radiating outwards in random directions. Intensity profiles are calculated at coordinates along these rays, and intensity maxima are taken as the points the rays cross the limiting membrane of the vacuole. These points are then fit with a set of basis functions to define the surface of the vacuole, and then parameters such as volume and surface area are calculated. This method is able to determine the volume and surface area of spherical beads (0.8 to 2 micron diameter) with less than 10% error, and validation using model convolution methods produce similar results. Thus, this method provides an accurate, automated method for measuring the size and morphology of organelles and can be generalized to measure cells and other objects on biologically relevant length-scales.

8225-84, Poster Session

## Optical cryo-imaging of kidney mitochondrial redox state during diabetes

S. Maleki, R. Sepehr, K. Staniszewski, N. Sheibani, C. Sorenson, M. Ranji, Univ. of Wisconsin-Milwaukee (United States)

Diabetic nephropathy is the most common cause of established chronic kidney disease and is a major risk factor for cardiovascular disease. Oxidative stress (OS), which increases during diabetes, exacerbates the development and progression of diabetes complications such as renal vascular and proximal tubule cell dysfunction. The objective of this study was to investigate the change in the metabolic state of the tissue in diabetic mice kidneys using fluorescence imaging. Akita mice develop diabetes at 4-weeks of age. Mitochondrial metabolic coenzymes NADH (Nicotinamide Adenine Dinucleotide), and FADH2 (Flavin Adenine Dinucleotide) are autofluorescent and can be monitored without exogenous labels by optical techniques. The ratio of these fluorophores, (NADH/FAD), called the redox ratio (RR), is a marker of metabolic state of a tissue. Here RR was used as a quantitative marker of OS in Akita diabetic mice. A total of four groups of mice, including Akita (8-week-old), Akita (12-week- old) and their wild type controls were studied. Mice were sacrificed and kidneys were harvested and frozen rapidly for low temperature (cryogenic) imaging. The cryoimager is an automated image acquisition system for 3D fluorescence imaging of tissue slices. Average intensity and histogram of maximum projected images of FAD, NADH, and RR were calculated for each group. Our results indicated a significant difference in the mean NADH RR of kidneys from 8- and 12-week-old diabetic mice compared to controls. The RR showed a 31% decrease in reductive state of kidneys from 8-week-old and a 30% decrease in reductive state of kidneys from12-week-old diabetic mice compared to control mice. These results demonstrate that RR can be used as a hallmark of OS in diabetic kidney allowing spatiotemporal identification of oxidative state.

8225-85, Poster Session

## Investigation of shape memory of red blood cells using optical tweezers and quantitative phase microscopy

N. Cardenas, S. K. Mohanty, The Univ. of Texas at Arlington (United States)

The unique viscoelastic property of red blood cell (RBC) allows it to regain its shape after passage through narrow capillaries. The resting shape of the RBC is determined by the elastic properties of the membrane, its surface area, and the enclosed volume. RBC has been shown to possess shape memory subsequent to shear-induced shape transformation. However, this property of RBC may not be generalized to all kinds of stresses. Here, we report our observation on the action of radiation pressure forces upon RBC using quantitative phase imaging (QPI). QPI, based on Mach-Zehnder interferrometry, allowed dynamic changes of shape of RBC in optical tweezers at different trapping laser powers. In high power near-infrared optical tweezers (>200mW), the RBC was found to deform (squeeze) significantly due to optical forces from all directions. Upon removal of the tweezers, hysteresis in recovering its original resting shape was observed. In very high power tweezers or long-term squeezing events, shape memory was almost erased. This irreversibility of the deformation may be due to temperature rise or stress-induced phase transformation of lipids in RBC membrane. Preservation of shape memory of RBC under long-term physiological (e.g. high osmolarity, temperature) and/or pathological (e.g. malaria parasite infection) stresses needs further investigation.

8225-86, Poster Session

## Multispectral angular domain imaging with a tunable pulsed laser light source

E. Ng, F. Vasefi, The Univ. of Western Ontario (Canada) and Lawson Health Research Institute (Canada); J. J. L. Carson, The Univ. of Western Ontario (Canada)

Angular Domain Imaging (ADI) is an imaging technique that is capable of generating three dimensional images of attenuating targets embedded in a scattering medium. In ADI, an angular filter is positioned between the sample and the detector to discriminate between quasi-ballistic photons and scattered photons. Quasi-ballistic photons have undergone a few forward directed scattering events, and can be used to generate a projection image representative of the imaging target. Scattered photons contain little information regarding the imaging target, and decrease image contrast. Our implementation of ADI utilizes a silicon microtunnel array to reject scattered photons based on the angle at which they exit the sample. The objective of this work was to collect ADI images with a tunable pulsed laser light source in the visible range. Samples were illuminated at 5 wavelengths between 600 nm and 700 nm. An angular filter array of 80 μm x 80 μm tunnels 2 cm long was used to select the quasi-ballistic photons. Images were detected with a linear 16-bit CCD. The phantom consisted of a 0.7 mm attenuating target submerged in an Intralipid dilution (0.25%) at 1 cm path length. Image contrast ranged from 0.1 at 600 nm to 0.42 at 700 nm and increased with longer wavelengths. Resolution varied minimally with wavelength. The results suggest that multispectral ADI is feasible with a tunable pulsed laser source, and is suitable for imaging thin tissue samples.

8225-87, Poster Session

## 3D high-resolution visualization of the biodistribution of fluorescence with multispectral cryosection imaging and unmixing

N. C. Deliolanis, A. Sarantopoulos, N. Terziyska, I. Jeremias, V. Ntziachristos, Helmholtz Zentrum München GmbH (Germany)

In the past years there is an increasing availability of diagnostic and therapeutic agents used in pre- and clinical applications. However, the accuracy and the sensitivity of various small animal imaging systems is limited. We demonstrate a cryosectioning multispectral imaging method to visualize the biodistribution of fluorescent contrast agents and reporter genes in mouse decease models with ultra-high resolution and sensitivity.

We use a modified Leica cryotome that we have installed with a multispectral illumination and a multispectral imaging system with a CCD camera to capture the fluorescence from the sample as well as an RGB color image. The fluorescence z-stack is acquired by imaging the complete series of slices throughout the sample to render a 3D volume with 10x10x50 microns (x,y,z) voxel size. The specific fluorescence is spectrally unmixed from the food and tissue autofluorescence using “guided” independent component analysis (ICA). Simultaneous ICA of multiple adjacent slices enhances the robustness of the component unmixing.

We demonstrate the performance of the imaging and unmixing method on a NOD/SCID mouse model of pediatric leukemia, where the leukemic cells express GFP and fLuc. The whole body 3D fluorescence biodistribution has revealed the development of leukemia in the bone marrow and the spleen, as well as micro-metastases, beyond the sensitivity of macroscopic reflectance fluorescence and bioluminescence imaging.

8225-88, Poster Session

## Tissue imaging with a stigmatic mass microscope using laser desorption/ionization

K. Awazu, H. Hazama, Osaka Univ. (Japan) and JST, CREST (Japan); T. Hamanaka, Osaka Univ. (Japan); J. Aoki, M. Toyoda, Osaka Univ. (Japan) and JST, CREST (Japan); Y. Naito, The Graduate School for the Creation of New Photonics Industries (Japan) and JST, CREST (Japan)

Imaging mass spectrometry (IMS) with matrix-assisted laser desorption/ionization (MALDI) has been intensively used for molecular imaging. However, the spatial resolution of MALDI-IMS has been still limited to about 10 μm and inadequate for cellular-scale imaging. Therefore, we have developed a stigmatic MALDI mass microscope equipped with a multi-turn time-of-flight mass spectrometer, in which the spatial distributions of ions at the sample surface are magnified and projected onto a position- and time-sensitive ion detector.

An eye of a mouse was sliced to a thickness of 2 μm and attached onto a slide glass coated with indium tin oxide. The section was stained with an aqueous solution of crystal violet (CV) and methylene blue (MB). The third harmonic of a Nd:YAG laser was irradiated to the sample at a beam diameter of about 0.8 mm. Ions were accelerated by a voltage of 20 kV and the ion distribution at the sample surface was magnified and projected with an einzel lens onto a microchannel plate phosphor screen assembly and recorded with a cooled CCD camera.

Stigmatic ion images of the ions of CV and MB produced from the stained section of the eye were observed at an ion optical magnification of about 20-fold. The ion images of the section were in good agreement with the photomicrograph of the same part in the section. Especially, a fine layer structure was clearly observed in the stigmatic ion images of the retina. The stigmatic mass microscope should be suitable for high-spatial resolution and high-throughput IMS.

8225-89, Poster Session

## Novel florescent scaffolds to study embryonic stem cell behaviors

J. Larsen, Y. J. Hwang, N. zur Nieden, J. G. Lyubovitsky, Univ. of California, Riverside (United States)

We are developing fluorescent hydrogels to non-invasively elucidate the complex mechanisms that govern embryonic stem cell (ESC) proliferation and differentiation in real time. We chemically modified a gelatin scaffold through glyceraldehyde crosslinking. Excitation of our modified materials with 360 nm light generates fluorescence at 430 nm and creates a dark field background that contrasts with the ESCs. Preliminary data of ESC cultures exhibited an inhibition of differentiation while maintaining proliferation capabilities. Further analysis of the ESC proliferation and differentiation potential is being investigated through RT PCR.

8225-90, Poster Session

## Validating novel melanoma treatments via cancer stem cells

A. A. Russell, C. Dargitz, A. Rowley, M. Bingham, Z. Achay, R. Jimenez, L. H. Laiho, California Polytechnic State Univ., San Luis Obispo (United States)

Current treatments on the market today tend to target the rapidly dividing cells to diminish growth and stop mitosis. It is crucial to remove all tumor cells during the patient's treatment or else the cancer will relapse. The cell population responsible for the return of the tumor is thought to be caused by the cancer stem cells (CSCs). Many recent findings in primary literature demonstrate that the CSC population within metastatic tumors typically divide at a much slower rate than that of the actual tumor itself and therefore are more resistant to current therapies. Novel treatments can easily be validated in vitro by identifying these subpopulations. Tissue engineered skin constructs were treated with angiostatin biomolecules as well as milk phospholipids in vitro to demonstrate potential treatments in the battle against melanoma. Confocal microscopy and western blots were used to verify the potency of the each therapy.

8225-91, Poster Session

## Image-based analysis of cell death by metabolic stress-induced autophagy

F. Chuang, A. Changou, H. Kung, NSF Ctr. for Biophotonics Science and Technology (United States)

Autophagy is an evolutionarily conserved intracellular process, which allows cell to degrade organelles and proteins, and autophagy can be induced when cells are under different type of stress. Numerous reports have shown that autophagy can promotes cellular survival under adverse environmental conditions, such as metabolic stress or genotoxic damage. Although autophagy is generally considered as a pro-survival mechanism; however, prolonged and/or over-stimulated autophagy have been shown to induce a programmed cell death, also known as autophagic cell death, that is different from apoptosis.

We have recently shown that some prostate cancers undergo metabolic stress and caspase-independent cell death following arginine deprivation by arginine deiminase (ADI, an enzyme that degrades arginine). Our current investigation into the application of ADI as a novel therapy has two general amis: 1) to identify the components mediating tumor cell death, and 2) to characterize the effect of autophagy (stimulated by ADI and/or rapamycin) on cell death.

Using advanced 3D fluorescent imaging methods to quantify and characterize the morphological changes associated with autophagic cell death - we obtained data suggesting that ADI-induced, but not rapamycin-induced, autophagy may cause damage to DNA, which may later contribute to the cell death. Although the detailed mechanism is still unclear, these results provide a possible mechanism for cell death by metabolic stress induced autophagy. Therefore, targeting autophagy may be a valid strategy for improving the efficacy of therapeutic strategies in prostate cancer, which initiate cell death through metabolic stress.

8225-92, Poster Session

## Dry-matter follow-up and mitotic index determination from quantitative phase imaging

P. Bon, B. F. Wattellier, PHASICS S.A. (France); S. Monneret, J. Savatier, Institut Fresnel (France); D. Marguet, C. Billaudeau, Ctr. d'Immunologie de Marseille-Luminy (France)

Mitotic index is one way to measure the aggressiveness of a malign tumour. It is defined as the fraction of dividing cells in the whole cell population. Objective and automatic ways to measure this index is crucial in oncology to diagnose and make a prognostic about a tumour.

Since a long time, it is known that optical path difference (OPD) in a cell is proportional to its dry matter. We have followed cells during several cell divisions with a Quadri-Wave Lateral Shearing Interferometer wave front sensor [1], located in the image plane of a microscope. This technique is compatible with time-lapse growth conditions such as the use of plastic dishes and incubators. The method can be considered as "plug and play" when used with a conventional microscope: its native bright-field illumination system is used as the light source, and the wavefront sensor has only to be mounted on one of its video port.

We observed cell divisions in time using an automated segmentation algorithm, and determined criteria mixing OPD and morphology to qualify the cell state during the division cycle. Then we made a study of hundreds of cells at a given time to determine the population mitotic index. Different cell lines have been studied and their behavior statistically compared.

[1] Bon, Maucort, Wattellier, and Monneret, "Quadriwave lateral shearing interferometry for quantitative phase microscopy of living cells," Opt. Express 17, 13080-13094 (2009)

8225-93, Poster Session

## Dynamic focus optical coherence tomography for improved investigation of basal cell carcinoma

M. R. N. Avanaki, Univ. of Kent (United Kingdom) and Barts and the London NHS Trust (United Kingdom); A. Aber, Barts and the London NHS Trust (United States); S. A. Hojjatoleslami, Univ. of Kent (United Kingdom); M. Sira, Hermitage Lane Maidstone Hospital (United Kingdom); J. Schofield, Preston Hall Hospital (United Kingdom); C. Jones, Barts and the London NHS Trust (United Kingdom); A. G. Podoleanu, Univ. of Kent (United Kingdom)

Objectives: Basal cell carcinoma (BCC) is the most common form of skin cancer. To improve the diagnostic accuracy, additional non-invasive methods of making a preliminary diagnosis have been sought. With the emergence of optical coherence tomography (OCT), capturing three-dimensional tomograms from microstructures within the skin with both high resolution and penetration depth has become possible.

Methods and Materials: We have implemented an En-Face OCT for this study in which the dynamic focus was integrated into it. With the dynamic focus scheme, the coherence gate moves synchronously with the peak of confocal gate determined by the confocal interface optics. The transversal resolution is then conserved throughout the depth range and an enhanced signal is returned from all depths. The Basal Cell Carcinoma specimens were obtained from the eyelids of three patients. The specimens under went analysis by DF-OCT imaging and histologically. Histology sections were photographed and compared with the OCT images. We searched for remarkable features that were visualized by OCT and compared these findings with features presented in the histology slices.

Results and conclusion: In the imaging of the skin specimens containing basal cell carcinoma there was an excellent correlation between the features seen in OCT imaging and those identified in histological sections. Due to using the dynamic focus, a more distinct border for BCC regions was found, and deeper levels of the specimen was seen. Dynamic Focus OCT imaging has the potential to identify tumour tissue from healthy tissue. It also showed correlation with corresponding histopathologic findings.

8225-94, Poster Session

## Kynetic resazurin assay (KRA) for bacterial quantification of foodborne pathogens

Y. Arenas, A. Mandel, Theralase, Inc. (Canada); L. Lilge, Ontario Cancer Institute (Canada)

Fast detection of bacterial concentrations is important for food industry as for health care. Since earlier detection of infections and appropriate treatment is essential. The delay of treatment for bacterial infections tends to be associated with higher mortality rates. In the food industry and in health care standard procedures required the count of colony-forming units to test bacterial quantifications, this method is time consuming and reports require 3 days to be completed. Alternative metabolic-colorimetric assays provide time efficient in vitro bacterial quantifications. A colorimetric assay based on Resazurin was developed as a time kinetic assay (KRA) suitable for bacterial concentration measurements. An optimization was performed, finding excitation and emission wavelengths for fluorescent acquisition. Comparison of Listeria monocytogenes and Escherichia coli was performed in 96 well plates, form part of this study. A metabolic and clonogenic dependence was established for fluorescent kinetic signals.

8225-95, Poster Session

## Chemically etched axicon fiber for cell trapping without physical contact

K. Taguchi, S. Hirota, J. Sugiyama, Ritsumeikan Univ. (Japan)

In this paper, chemically etched axicon fiber was proposed for cell trapping. We fabricated axicon micro lenses on a single-mode bare optical fiber by selective chemical etching technique using an etching solution of buffered hydrofluoric acid(BHF), a mixture of 50% weight hydrofluoric acid (HF) and 40% aqueous solution of ammonium fluoride (NH4F). By varying the concentration and mixture ratios of etching solutions, we could make axicon micro lenses with different apex angles. We also studied the laser beam profiles emanating from the axicon lens by objective-lens imaging experiments. A semiconductor laser module at 980nm, which had a SMF (Single-Mode Fiber) pig-tailed connector, was used for experiments. The output of laser light was coupled into an optical fiber which had an optical connector at the fiber end. The trapping fiber was attached to an xyz manipulator and the fiber was introduced into a sample chamber at an angle. The laser beam from fiber axicon microlens was strongly focused and optical forces were sufficient to move a microorganisms and biological cells without physical contact. Furthermore we could levitate biological cells without physical contact using plural chemically etched axicon fibers. The apex angle of the chemically etched fiber axicon microlens was very important parameter for laser trapping. From these experimental results, it was found that our proposed method was a promising tool for the isolation of microorganisms. Furthermore we investigated the wavelength dependence of cell cloning efficiency after optical trapping.

8225-96, Poster Session

## Cell manipulation and isolation using dynamically etched fiber tip

K. Taguchi, J. Okada, Ritsumeikan Univ. (Japan)

In biology, optical tweezers has been applied in researches on cells, viruses, bacterias and DNA molecules. In traditional optical tweezers, a high N.A. microscope objective is necessary to focus the laser beam, which is the disadvantage of this method. For this reason, fiber optical tweezers has been developed: this system is simpler and more flexible than conventional optical tweezers. However, these fiber optical tweezers cannot form a Three-Dimensional optical trap by using just single one optical fiber due to the weakly focused laser beam from the polished tapered fiber with spherical lens.

In this paper a novel tapered single fiber optic tweezers was proposed for cell manipulation and isolation. Optical fiber tips were fabricated by dynamic chemical etching method. Compared with traditional static chemical etching, this method has advantages such as reproducibility, controllability, convenience, less cost, and making tip surface smooth. The mechanically cleaved bare single mode fiber was dipped into Hydrofluoric (HF) acid containing a protective layer of Toluene at the top. By moving the fiber at variable speeds, a variety of tip shapes could be created. In our experiments, tip angle could be adjusted from 7deg to 37deg. From our experimental results, it was found that a Three-Dimensional optical trap of yeast cell dispersed in water solution could be formed by the fiber tip with 7deg tip. So it was easy to trap and isolate cell for obtaining pure cultures of bacteria. Furthermore we could see the clonal growth of yeast cell trapped and isolated using 980nm laser.

8225-97, Poster Session

## Spectral Imaging of Brain Cancer by Using Terahertz Waves

S. J. Oh, Y. Huh, S. Kim, J. Yang, K. Jeong, M. H. Hwang, Yonsei Univ. College of Medicine (Korea, Republic of); J. Son, The Univ. of Seoul (Korea, Republic of); J. Suh, Yonsei Univ. College of Medicine (Korea, Republic of)

Terahertz spectroscopic imaging has received a great attention as new feasible medical imaging modality due to many advantages points such as high sensitivity of interstitial water and non-ionizing characteristics. Among the various medical applications, the cancer imaging has been studied for the skin, breast, tongue and liver cancer. However, THz imaging technique has not yet been adopted for diagnosing brain cancer. In this paper, we obtained the spectral images of the fresh whole brain of rats with and without the glioma by using the terahertz time-domain spectroscopic imaging method. The brain tumor model was a rat glioma model. The rat brain tumors were allowed to grow for 3-4 weeks, and then, the brains of rats were extracted after killing the mice. We showed the visible, THz images and magnetic resonance imaging (MRI) images for fresh brain with and without tumor. The region of tumor was quiet distinct from the normal region and the THz intensity of the region of tumor was larger than that of a normal region. We also found bright and dark areas in the normal region, and these areas corresponded to the grey matter and white matter in the brain. This difference in brightness was attributable to the protein and lipid contents of myelin. The MRI findings were similar to those of THz spectroscopic images. These results show that the THz imaging technique is useful for diagnosing brain cancers and for studying the structure of the brain.

8225-02, Session 11

## Hyperspectral imaging in the operating room: what a surgeon wants

S. L. Best, Univ. of Wisconsin School of Medicine and Public Health (United States)

Visualization is the key to surgery, but limiting one's "vision" to visible light images received by the human eye ignores a lot of available data. Imaging technology such as hyperspectral and infrared imaging can greatly expand the amount and type of information available to the surgeon. We propose several areas in which this type of technology can be useful in medicine, paying particular attention to the way in which this technology might be best integrated into current operating room setups.

8225-03, Session 11

## Evaluation of a novel laparoscopic camera for characterization of renal ischemia in a porcine model using DLP® hyperspectral imaging

E. O. Olweny, S. L. Best, N. Jackson, E. F. Wehner, S. K. Park, Y. K. Tan, A. Thapa, J. A. Cadeddu, K. J. Zuzak, The Univ. of Texas Southwestern Medical Ctr. at Dallas (United States)

Introduction: Digital light processing hyperspectral imaging (DLP® HSI) has previously been used to characterize renal ischemia during open partial nephrectomy in pigs and humans. By incorporating a light guide, 0-degree laparoscope, customized digital CCD camera (DVC, Austin, TX), and a DLP-based Agile Light source (OL490; Gooch & Housegro, Orlando, FL), we adapted DLP® HSI for use during laparoscopic surgery.

Methods: Laparoscopic DLP® HSI was performed in 5 adult female pigs (Group 1). 3 pigs that were previously imaged using the open system (Group 2) were selected for comparison. In Group 1, spectra were recorded at several intervals before, during and after clamping the renal hilum for 90 minutes. In Group 2, similar measurements were obtained, but the renal ischemic period was 60 minutes. Spectra obtained over common imaging intervals for each group were analyzed. The relative percentage of oxygenated hemoglobin (relative %HbO2) at each time interval was determined using previously described methodology, and compared for the groups using the Student's t-test.

Results: For Lap vs. Open respectively, relative %HbO2 was 74.2 vs. 72.8% pre-clamp, dropping by an average of 22% vs.19% during the initial 10 minute interval post hilar occlusion, and rapidly rising to baseline after clamp removal. There were no statistically significant differences between the groups in the relative %HbO2 measured for any of the imaged intervals.

Conclusion: The laparoscopic DLP® hyperspectral imaging system performs similarly to the open system and has excellent spectral imaging capabilities. Preliminary clinical application during minimally invasive partial nephrectomy is currently underway.

8225-04, Session 11

## Instrument validation and applications of a clinic-friendly spatial frequency domain imaging (SFDI) device

D. J. Cuccia, Modulated Imaging, Inc. (United States)

Quantitative characterization of tissue structure and function is one of the most challenging problems in Medical Imaging. We are advancing the Modulated Imaging (MI) technique, toward its application as a clinical research device to provide objective parameters for in-vivo tissue status determination. MI is a spatial frequency domain imaging (SFDI) method, which employs spatially-patterned illumination to non-invasively obtain subsurface images of biological tissues. This non-contact approach enables rapid quantitative determination of the absorption and scattering optical properties of tissues over a wide field-of-view. When combined with multi-spectral imaging, the optical properties at several wavelengths can be used to quantitatively determine the in-vivo concentrations of chromophores that are relevant to tissue health, namely, oxy- and deoxy-hemoglobin.

We present the design, fabrication, testing, can clinical deployment of a robust, user friendly MI instrument appropriate for deployment at clinical sites. This instrument is compatible with a plurality of light sources, provides a wide field of view (~180x135mm), and is sufficiently compact and robust for human subject measurements. It possesses sufficient spatio-temporal resolution to study both fast (<1s) and localized (<1mm) events at depths of several millimeters in thick tissues. The device performance was characterized in a laboratory setting in terms of linearity, dynamic range, reproducibility, and drift. A turnkey software interface was developed facilitating clinical deployment for real-world testing and evaluation. Ultimately, we envision that this platform will enable quantitative insight into disease progression and therapeutic response in areas such as wound healing, dermatology, skin cancer and reconstructive surgery.

8225-05, Session 11

## Advances in optical tomography using spatial frequency domain imaging

S. D. Konecky, T. B. Rice, A. Lin, A. Mazhar, R. B. Saager, Beckman Laser Institute and Medical Clinic (United States); D. J. Cuccia, Modulated Imaging, Inc. (United States); A. J. Durkin, B. Choi, B. J. Tromberg, Beckman Laser Institute and Medical Clinic (United States)

Diffuse optical spectroscopy and imaging are rapidly growing fields with applications including human breast, human brain, and small animal imaging. Typically, a collimated beam or optical fiber is used to inject light into biological tissue, and the amount of light remitted from the tissue is measured at several locations. While this approach is useful for determining the average properties of large volumes of tissue, it is not ideal for imaging. Recently, we have begun projecting spatially extended patterns of light on tissue and detecting the remitted light with a CCD array, eliminating the need to use large arrays of optical fibers or raster scan a collimated beam. The spatially varying optical properties of the tissue are determined by measuring the attenuation (or fluorescence) of sinusoidal patterns of light projected onto the sample at varying spatial frequencies and phases. Using this technique, called Spatial Frequency Domain Imaging (SFDI), we image the absorption, scattering, and fluorescence properties of biological tissues. SFDI is wide-field, non-contact, inexpensive, and it eliminates the need for detectors with a wide dynamic range. By combining diffuse optical methods with CCD imaging, SFDI allows one to acquire high resolution images with quantitative spectroscopic information. In this presentation, I will review the underlying physics of SFDI, and then show our recent advances extending SFDI to reconstruct three-dimensional images, determine the orientation of microscopic structures, and image rates of blood flow.

8254-06, Session 12

## Digital micromirror device based confocal 4D-microscopy

W. Neu, M. Schellenberg, Fachhochschule Oldenburg/Ostfriesland/Wilhelmshaven (Germany)

Any approach to understand the dynamics of living cells and cell clusters requires time resolved sufficiently fast 3D sampling at high spatial resolution. Confocal microscopy using a digital micromirror device (DMD) realizes both the illumination and the confocal sectioning through a single DMD-array. Making use of the fast modulating frequency DMDs offer, the inherent multifocal sample illumination and simultaneously utilization of each micromirror as a virtual pinhole allows to reduce volume sampling times to a seconds time scale. An electronically intensified CCD-camera synchronized to the DMD takes the images of each single optical slice. Due to the high DMD-frequency (8000 frames/s), each complete measurement plane is recorded within a single frame of the electron multiplying CCD-camera. The z-scan is realized by a piezo-driven microscope objective.

Through purpose designed scan patterns for a particular object, regions of the specimen can be protected from an excess of excitation light intensity, e.g to alleviate fluorophore bleaching. Furthermore, adaptive illumination scenarios are possible such as the tracking of objects within a cell. Through flexible illumination and a system easily adaptable to a standard microscope, conventional microscopy techniques can be implemented, such as Dark Field Microscopy and Phase Contrast Microscopy. In this way non-fluorescent structures within the sample can be imaged and the data can be combined with the fluorescent confocal acquisition.

Objects can be imaged with a diffraction limited spatial resolution of approx. 300 nm laterally and approx. 1000 nm axially @ 405 nm. High temporal resolution of 1 s to 4 s for 50 layers at ca. 1 µm optical slicing distance enables one to visualize and analyse in vivo and in realtime e.g. physiological processes within living cells in a 3D-film.

8254-07, Session 12

## A pico projector source for confocal fluorescence and ophthalmic imaging

M. Muller, Aeon Imaging, LLC (United States)

Small, flexible, and low cost, pico digital light projectors (DLPs) incorporate high power LEDs with a digital micromirror array. DLPs can be driven directly from a PC video card to create a versatile and programmable display. In this paper, the pico projector is used in a novel confocal imaging system as both an illumination and scanning element.

Confocal imaging systems traditionally scan light across a target, then descan and spatially filter the light return before detection. An alternative design avoids descanning and instead synchronizes the illumination of the target to the rolling shutter read-out of a CMOS sensor placed in a conjugate plane (US Patents 7,331,669 and 7,831,106). By detecting light sequentially across the 2D sensor array, the rolling shutter creates a linear confocal aperture that is electronically adjustable in width and position. When the illumination and scanning element are replaced with a pico projector, continuous scanning can be approximated by rapidly projecting a series of lines onto the target.

The use of a DLP as an integrated source and scanning element not only reduces the cost and size of traditional confocal imaging devices, but readily allows frame-to-frame software control over the target illumination pattern, timing, and wavelength. With a barrier filter inserted into the detection pathway, the system can switch from standard confocal imaging using the red or green channels (631 or 516nm) to fluorescent imaging using the blue channel (476nm) via software in real-time. With additional optical components, retinal plane images have been acquired using a 2.5mm pupil.

8254-08, Session 12

## Medical devices in dermatology using DLP™ technology from Texas Instruments

F. Lüllau, Lüllau Engineering GmbH (Germany)

Medical Devices in Dermatology using DLP™ Technology from Texas Instruments:

The market of medical devices is growing continuously worldwide. With the DLP™ technology from Texas Instruments Lüllau Engineering GmbH in Germany has realized different applications in the medical discipline of dermatology.

Especially a new digital phototherapy device named skintrek® PT5 is revolutionizing the treatment of skin diseases like Psoriasis, Vitiligo and other Eczema. The reason is that this device treats fully automated skin lesions with high contour precision and exactly with the right dose of UVA or UVB rays without damaging surrounding healthy skin. Healthy skin will not be irradiated with UV-light and therefore compared with the traditional phototherapy the risk of skin cancer is minimized and other side effects are avoided.

The functions of the new phototherapy device can only be realized through the use of DLP™ technology which is not only be used for the selective irradiation process. In combination with other optical systems DLP™ technology undertakes also other functionalities like 3D-topology calculation und patient movement compensation.

But digital phototherapy is not the sole DLP™ application for dermatology devices. E.g. the supportive diagnostic of skin cancer or inflammatory skin diseases can also be realized. Special optical systems in combination with DLP™ technology and sophisticated software algorithms are the base for such medical devices.

8254-09, Session 12

## Implementation of an LED based clinical Spatial Frequency Domain Imaging (SFDI) system

A. Mazhar, S. A. Sharif, Beckman Laser Institute and Medical Clinic (United States); S. Saggesse, D. J. Cuccia, Modulated Imaging, Inc. (United States); B. Choi, A. J. Durkin, Beckman Laser Institute and Medical Clinic (United States)

Spatial Frequency Domain Imaging (SFDI) is a non-contact imaging method that uses multiple frequency spatial illumination to generate two dimensional maps of tissue optical properties (absorption and reduced scattering). We present phantom validation and pilot clinical data of a deployed LED-based system. The system employs four wavelengths (658 nm, 730 nm, 850 nm, 970nm) of light-emitting diodes (LED) to quantitatively assess tissue health by measurement of common tissue constituents (oxy-hemoglobin, deoxy-hemoglobin, and water). The system is compact (10cm x 10cm x 10cm) and light-weight (~ 12 lbs). The projection optics are optimized for the near infrared and typical exposure times (~20 ms) reduce typical acquisition time to seconds making the system twenty times faster than the SFDI system that we have described previously while minimizing the effect of motion artifacts in the clinic. The system is designed for large field of view applications (13.5 cm x 10.5 cm) and integrates a tissue surface profile measurement to correct for errors caused by height variations seen in large fields of view when imaging tissue. An important component of this system as designed is that a co-registered color camera has been integrated to record a simultaneous clinical impression of the sample for every pass of SFDI data. Finally, we have deployed the instrument in the clinic for pilot studies assessing burn severity and efficacy of port wine stain treatment. Maps of oxy-hemoglobin, deoxy-hemoglobin, water content, reduced scattering, and surface topography will be presented for each of these applications areas.

# Conference 8226: Multiphoton Microscopy in the Biomedical Sciences XII

Sunday-Tuesday 22-24 January 2012

Part of Proceedings of SPIE Vol. 8226 Multiphoton Microscopy in the Biomedical Sciences XII

8226-04, Session 1

## Polarized fluorescence correlation spectroscopy (pFCS): a single-molecule method for simultaneously measuring homo-FRET, brightness, and the diffusion of protein complexes in living cells

T. Nguyen, P. Sarkar, National Institutes of Health (United States); J. V. Veetil, National Institutes of Health (USA); S. V. Koushik, C. Thaler, National Institutes of Health (United States); A. Seeman, National Institutes of Health (USA); S. S. Vogel, National Institutes of Health (United States)

No abstract available

8226-05, Session 1

## Monitoring nuclear protein interactions using FRET-FLIM

A. P. Siegel, N. Hays, R. N. Day, Indiana Univ. (United States)

The discovery and engineering of novel fluorescent proteins (FPs) from diverse organisms is yielding fluorophores with exceptional characteristics for live-cell imaging. In particular, the development of FPs for Förster resonance energy transfer (FRET) microscopy is providing important tools for monitoring dynamic protein interactions inside living cells. Fluorescence lifetime imaging microscopy (FLIM) is among the most accurate methods to measure FRET because it maps the spatial distribution of fluorescent probe lifetimes inside living cells, quantifying the shorter donor lifetimes that result from FRET. Here, we use FRET-FLIM to investigate the interactions between transcription factors and chromatin modifying proteins that function in anterior pituitary gene regulation. The heterochromatin protein 1 (HP1) plays a key role in the establishment and maintenance of heterochromatin through its interactions with histone methyltransferases. More recent studies, however, have highlighted the importance of HP1 as a positive regulator of active transcription in euchromatin as well. Intriguingly, we observed that the transcription factor CCAAT/enhancer-binding protein alpha (C/EBP$\alpha$) interacts with HP1 in regions of pericentromeric heterochromatin in mouse pituitary cells. These observations prompted us to investigate how these protein interactions involving HP1 might function to specify pituitary specific gene regulation.

8226-06, Session 1

## Spatially resolved recording of transient fluorescence-lifetime effects by line-scanning TCSPC

W. Becker, B. Su, Becker & Hickl GmbH (Germany)

We present a technique that records transient effects in the fluorescence lifetime of a sample with spatial resolution along a one-dimensional scan. The technique is based on building up a photon distribution over the distance along the scan, the experiment time after a stimulation of the sample, and the arrival times of the photons after the excitation pulses. The maximum resolution at which lifetime changes can be recorded is given by the line scan time. With repetitive stimulation and triggered accumulation, transient lifetime effects can be recorded at a resolution of about one millisecond. We demonstrate the use of the technique for recording fluorescence transients of chloroplasts in live plants.

8226-07, Session 1

## Phasor FLIM metabolic mapping of stem cells and cancer cells in live tissues

C. Stringari, P. Donovan, E. Gratton, Univ. of California, Irvine (United States)

Here we present a novel label-free method for deriving metabolic maps of cells and living tissues in vivo. We use the phasor approach to fluorescence lifetime imaging and intrinsic biochemical fluorescence biomarkers in conjunction with image segmentation and the concept of cell phasor. In live tissues we are able to identify and separate intrinsic fluorophores such as collagen, retinol, retinoic acid, porphyrin, flavins, free and bound nicotinamide adenine dinucleotide (NADH). Metabolic signatures of living tissues are obtained by calculating the phasor fingerprint of cells and by mapping the relative concentration of metabolites. This method can detect small changes in metabolic signatures and redox states of cells. Phasor fingerprints of stem cells cluster according to their differentiation state in a living tissue such as the C. elegans germ line and the crypt base of small intestine and colon. Phasor FLIM provides a label-free, fit-free and sensitive method to identify different metabolic states of cells and to classify stem cells, normal differentiated cells and cancer cells both in vitro and in a live tissue. Our method could identify symmetric and asymmetric divisions, predict cell fate and identify pre-cancer stages in vivo. This method is a promising non-invasive optical tool for monitoring metabolic pathways during differentiation and carcinogenesis, for cell sorting and high throughput screening.

8226-08, Session 1

## Fluorescence lifetime imaging microscopy (FLIM) studies of living primary human cells for applications in tissue regeneration

W. R. Lloyd III, L. Chen, S. Kuo, C. L. Marcelo, S. E. Feinberg, M. Mycek, Univ. of Michigan (United States)

This study investigates the ability of fluorescence lifetime imaging microscopy (FLIM) to noninvasively characterize function in living primary human cells, a necessary preliminary step toward the goal of developing functional engineered tissues for implantation. With Institutional Review Board approval, primary human oral keratinocytes were harvested from patients and cultured at 37°C until 70-80% confluence. Controlled culture conditions were then varied to create differing levels of cellular function and viability.

Cells were imaged using nonlinear optical microscopy via two-photon excitation of endogenous molecular fluorophores associated with metabolic activity. 100 fs laser pulses (80 MHz) at excitation wavelengths 705 and 900 nm were employed to excite preferentially cellular NAD(P)H and FAD, respectively. Optical sectioning with multiphoton excitation was employed to minimize out-of-focus fluorophore photobleaching. Time-resolved fluorescence emission decays were measured at each image pixel via time-correlated single-photon counting (TCSPC) to create FLIM maps of the cellular endogenous fluorescence. TCSPC data acquisition time was ~5 minutes and temporal resolution was 52 ps.

To the best of our knowledge, this is the first report of employing FLIM to characterize primary human oral keratinocytes. Fluorophore lifetime is known to be sensitive to microenvironmental conditions (including molecular associations, pH, and oxygen) and can therefore serve as a novel reporter of live cell function. Novel post-processing algorithms were developed and tested for cellular FLIM data analysis. Results suggest that endogenous FLIM may provide useful information about live cell function and viability. Translation of the label-free optical molecular imaging method to characterization of tissue-engineered constructs will be discussed.

8226-09, Session 1

## High speed 3D-resolved fluorescence and phosphorescence heterodyned wide field lifetime imaging

H. Choi, D. Tzeranis, J. Cha, P. T. C. So, Massachusetts Institute of Technology (United States)

Fluorescence and phosphorescence lifetime can provide an additional contrast mechanism to complement excitation and emission spectra for structural determination of biological specimens. Lifetime can also be used to probe the local environment near the fluorophores since its lifetime is dependent on its chemical interactions. So far, lifetime microscopy technique was limited to either 2D or is relatively slow for 3D mapping of an entire sample. The fastest 3D-resolved fluorescence lifetime resolved microscopes are either based on multi-foci excitation or on spinning-disc confocal detection as demonstrated by Paul French and Robert Clegg groups. To further improve upon these approaches, we have developed high speed 3D resolved fluorescence(FLIM) and phosphorescence(PLIM) lifetime imaging microscopy. This combines the temporally focused wide field two photon microscopy for depth resolved 3D imaging and the heterodyne frequency domain technique to measure the lifetime. For the heterodyne frequency domain detection, the femtosecond pulsed laser is modulated with acousto optic modulator (AOM) and the resulting phase shift and demodulation of fluorescence and phosphorescence are measured by gating the image intensifier that is coupled to the CCD camera. Depending on the modulation frequency of the light source it can measure either fluorescence or phosphorescence. For fluorescence, we have verified that the lifetimes of RhodaminB in different solvents are in excellent agreement with literature values and we have shown that the lifetimes of fluorescent labels of cells in 3D collagen matrix can be accurate measured. Most importantly, this system reduce the data acquisition time significantly for the case of PLIM compared to existing techniques because of the parallelism of our approach. We have verified the Stern-Volmer relationship of phosphorescence quenching by measuring the Ruthenium phosphorescence at different concentration of the oxygen. We have further demonstrated the measurement of 3D resolved oxygen concentration in cell seeded matrix.

8226-10, Session 2

## Multiwavelength FLIM: new concept for fluorescence diagnosis

A. C. Rueck, Univ. Ulm (Germany)

Fluorescence guided tumor resection is very well accepted in the case of bladder cancer and brain tumor, respectively. However, false positive results are one of the major problems, which will make the discrimination between tumor tissue and inlammation difficult. In contrast fluorescence lifetime imaging (FLIM) and especially spectral resolved FLIM (SLIM) [1] can significantly improve the analysis.

The fluorescence decay of a fluorophore in many cases does not show a simple monoexponential profile. A very complex situation arises, when more than one compound has to be analyzed. This could be the case when endogenous fluorophores of living cells and tissues have to be discriminated to identify oxidative metabolic changes. Other examples are PDT, when different photosensitizer metabolites are observed simultaneously. In those cases a considerable improvement could be achieved when time-resolved and spectral-resolved techniques are simultaneously incorporated.

Within this presentation the principles of spectral and time-resolved fluorescence imaging and new algorithms [2] will be discussed together with a short overview on successful applications reported in the literature.

Literature: [1] A. Rück, C. H. Hülshoff, I. Kinzler, W. Becker and R. Steiner SLIM: A new method for molecular imaging, Micr. Res. Techn., 70, 485-492 (2007).

[2] D. Strat, F. Dolp, B. von Einem, C. Steinmetz, C.A.F. von Arnim and A. Rueck “Spectrally resolved fluorescence lifetime imaging microscopy (SLIM): FRET Global Analysis with a one- and two-exponential donor model”, JBO 16(2), 026002 (February 2011).

8226-11, Session 2

## Clinical multiphoton FLIM tomography

K. König, JenLab GmbH (Germany)

An overview on current clinical multiphoton fluorescence lifetime imaging in volunteers and patients is provided. FLIM Microscopy in Life Sciences was introduced in Jena/Germany 23 years ago. Some years later time-gated cameras were employed to detect dental caries in volunteers. First two-photon FLIM images in humans were generated with the introduction of the certified multiphoton femtosecond laser tomograph DermaInspect nearly 10 years ago. Nowadays, multiphoton tomographs with FLIM modules as approved medical products are used to detect intradermal sunscreen nanoparticles and different melanin types, for the early diagnosis of dermatitis and malignant melanoma, as well as the measurement of therapeutic effects.

8226-12, Session 2

## Monitoring transient elastic energy storage within the rotary motors of single FoF1-ATP synthase by DCO-ALEX FRET

S. Ernst, Jena Univ. Hospital (Germany) and Univ. Stuttgart (Germany); M. G. Düser, N. Zarrabi, Univ. Stuttgart (Germany); M. Börsch, Jena Univ. Hospital (Germany) and Univ. Stuttgart (Germany)

The enzyme FoF1-ATP synthase provides the 'chemical energy currency' adenosine triphosphate (ATP) for living cells. Catalysis is driven by mechanochemical coupling of subunit rotations within the enzyme with conformational changes in the three ATP binding sites. Proton translocation through the membrane-bound Fo part of ATP synthase powers a 10-step rotary motion of the ring of c subunits. This rotation is transmitted to the gamma and epsilon subunits of the F1 part. Because gamma and epsilon subunits rotate in 120° steps, we aim to unravel this symmetry mismatch by real time monitoring subunit rotation using single-molecule Förster resonance energy transfer (FRET). One fluorophore is attached specifically to the F1 motor, another one to the Fo motor of the liposome-reconstituted enzyme. Photophysical artifacts due to spectral fluctuations of the single fluorophores are minimized by a previously developed duty cycle-optimized alternating laser scheme (DCO-ALEX). We report the detection of reversible elastic deformations between the rotor parts of Fo and F1 and estimate the maximum angular displacement during the load-free rotation measurement.

8226-13, Session 2

## Three-color FRET expands the ability to quantify the interactions of several proteins involved in actin nucleation

H. K. Wallrabe, Y. Sun, A. Periasamy, X. Fang, G. S. Bloom, Univ. of Virginia (United States)

Traditional 2-color Förster Resonance Energy Transfer (FRET) microscopy yields valuable quantitative analyses based on correlations of donor (D), acceptor (A) and their ratios (D:A) with energy transfer efficiency (E%) to measure changes between control and interventions and to differentiate clustered vs. random interactions. 3-color FRET uses the same parameters, but exponentially expands the opportunities to quantify interrelationships among 3 cellular components. We investigated a number of questions based on the results of a triple combination (F1-F2-F3) of TFP-NWASP/Venus-IQGAP1/mCherry-Actin - all involved in the nucleation of Actin - to apply the extensive analysis assay possible with 3-color FRET. For example, how does NWASP or NWASP:IQGAP1 ratio affect E% IQGAP1-Actin or Actin level of fluorescence? Since IQGAP1 affects NWASP upstream of Actin, what is the correlation between them in the presence or absence of Actin? The proteins of interest may all interact at some stage, but not all the time in a particular Region of Interest (ROI). 4 cases are compared based on bleed-through corrected FRET: (1) all 3 interact, (2) only F1-F3 and F2-F3 interact [not F1-F2], (3) only F1-F2 and F2-F3 interact [not F1-F3], (4) only F1-F2 and F1-F3 interact [not F2-F3]. Other than describing the methodology in detail, several biologically relevant results are presented showing how E% (i.e. distance), fluorescence levels and ratios are affected in each of the cases. These correlations can only be observed in a 3-fluorophore combination. 3-color FRET will greatly expand the investigative range of quantitative analysis for the life-science researcher.

8226-14, Session 2

## New detection and analysis FLIM and FCS techniques for confocal laser scanning microscopes

S. Fore, PicoQuant Photonics North America, Inc. (United States); B. Krämer, F. Koberling, M. König, V. Buschmann, M. Wahl, U. Ortmann, S. Orthaus, R. Erdmann, PicoQuant GmbH (Germany)

The compact FLIM Upgrade Kit for Confocal Laser Scanning Microscopes (CLSM) allows Fluorescence Lifetime imaging (FLIM) by applying Time-Correlated Single Photon Counting (TCSPC). Based on a network interface, the FLIM and FCS data acquisition can be directly accessed from the CLSM computer. This unique integration enables a seamless work flow.

The new Hybrid photomultiplier detector PMA Hybrid allows for a high detection efficiency together with an excellent timing performance and nearly afterpulsing free photon detection. The PMA Hybrid can also be used for non-descanned detection (NDD) together with two-photon excitation. An advantage for FCS measurements is a nearly afterpulsing free detection, which avoids artifacts in the FCS curve common to SPAD detectors.

A newly developed polarization beamsplitter for CLSMs allows to split the fluorescence light into its two linear polarization components in front of the detection fibers guiding the light to the detectors. This technique enables rotational diffusion measurements for the study of the rotational behavior of dye molecules inside e.g. membranes.

The unambiguous separation of multiple dye labels or their separation from autofluorescent background is often a problem in modern biology. With lifetime imaging, the lifetime information can be utilized to overcome this problem. However, standard TCSPC fitting techniques are not optimally adapted for the separation of different dye molecules, especially when they exhibit a bi - or more exponential lifetime decay behavior.

In order to overcome this problem, we have developed a pattern-matching technique which can be applied to separate dye molecules independent of their decay pattern.

8226-15, Session 2

## In vivo, high resolution measurement of cerebral oxygen tension and NADH using phosphorescence- and fluorescence- lifetime imaging

M. A. Yaseen, S. Sakadžic, J. Lee, Athinoula A. Martinos Ctr. for Biomedical Imaging (United States); S. Vinogradov, Univ. of Pennsylvania (United States); W. Becker, Becker & Hickl GmbH (Germany); D. A. Boas, Athinoula A. Martinos Ctr. for Biomedical Imaging (United States)

Thorough characterization of energy metabolism is crucial to better understand how the brain functions. Additionally, as impaired mitochondrial function is symptomatic of several pathological disorders, understanding brain metabolism at a cellular level is important for developing effective diagnostic and therapeutic strategies for neurodegenerative disorders such as Alzheimer's and Parkinson's disease, stroke, and to counteract the general physiological decline associated with the aging process. Here we present minimally-invasive, in-vivo measurements of two markers of cerebral metabolism, oxygen partial pressure (pO2) and reduced nicotinamide adenine dinucleotide (NADH), collected from the rat cortex. We incorporated commercially available time-correlated single photon counting (TCSPC) equipment into our custom-built multimodal imaging system to allow for simultaneous, multiphoton phosphorescence lifetime imaging (PLIM) and fluorescence lifetime imaging (FLIM). We simultaneously measured phosphorescence-lifetime of Ptp-C343, a novel oxygen-sensitive nanoprobe, and fluorescence lifetimes of autofluorescent NADH. Measurements were performed in both neurons and astrocytes during baseline conditions and in response to physiological perturbations such as hypoxia and cortical spreading depression (CSD). Cerebral pO2 was found to vary with proximity to vasculature. Multi-exponential fits for NADH fluorescence lifetimes indicate multiple, distinct enzyme-bound formulations, or 'species.' Each NADH specie was found to respond differently to hypoxia and CSD. Our results indicate that lifetime imaging of NADH provides more comprehensive information over traditional intensity-based NADH measurements, enabling better distinction of anaerobic from aerobic activity. Correlating the NADH measurements with pO2 will ultimately lead to a deeper understanding of cerebral energetics and its pathology-related alterations

8226-16, Session 3

## An automated approach for the analysis of multispectral multiphoton FLIM data and its application to the diagnosis of skin cancer

Y. Alexandrov, R. Patalay, C. B. Talbot, S. Warren, I. Munro, Imperial College London (United Kingdom); H. G. Breunig, K. König, JenLab GmbH (Germany); M. A. A. Neil, P. M. W. French, Imperial College London (United Kingdom); A. Chu, Imperial College Healthcare NHS Trust (United Kingdom); G. W. Stamp, The Royal Marsden Hospital NHS Trust (United Kingdom); C. W. Dunsby, Imperial College London (United Kingdom)

We present an analysis of multispectral fluorescence lifetime imaging (FLIM) data obtained from autofluorescence of human skin using two-photon excitation. 33 pre-cancerous and cancerous lesions were imaged ex vivo and normal skin was imaged from 14 patients in vivo.

Data was acquired using a commercially available clinically licensed optical tomography system (DermaInspect®) equipped with a 4-channel time-correlated single photon counting (TCSPC) fluorescence lifetime module and a CCD based module providing hyperspectral imaging.

Our analysis method is based on measurements of physiologically meaningful regions of interest (ROI) within the FLIM images. For the main dataset, ~9000 ROIs were defined manually to select individual cells. A second dataset was produced by an automatic image segmentation approach.

For each ROI, a bi-exponential decay fitting algorithm was utilized that accounted for the effects of dark noise, PMT after-pulsing and incomplete fluorescence decays. We also investigate the use of a phasor analysis approach. ROIs were characterized by morphological, spectral intensity, and fluorescence lifetime (FL) based descriptors.

Statistical techniques, including significance tests and supervised and unsupervised multivariate machine learning, were applied to assess the possibility of an automated diagnosis based on our FL/spectral/morphology measurements. We found that a high inter-patient variability strongly influenced the outcome of these approaches. The study is concluded by a comparison of ROIs generated by manual versus automatic segmentation. The results demonstrate the significant diagnostic potential of spectrally resolved FLIM.

8226-17, Session 3

## Multiphoton fluorescence lifetime imaging of cleared mouse organs

S. Vesuna, R. Torres, M. J. Levene, Yale Univ. (United States)

Multiphoton microscopy of cleared tissue has previously been demonstrated to generate large 3D volumetric image data with sub-cellular resolution using only intrinsic fluorescence. By combining multiphoton (MPM), second-harmonic generation (SHG), and fluorescence lifetime imaging (FLIM), we provide unique morphological information. We demonstrate the use of FLIM in cleared mouse testicle and knee to achieve molecular contrast that reveals morphologically distinct structures that, in some cases, are unobservable in traditional histological analysis, even in the absence of knowledge of the underlying molecular source. Moreover, in cleared mouse brain, we demonstrate that our tissue clearing protocol is compatible with exogenous fluorescent proteins such as YFP. Cleared and imaged organs were then processed as routine pathology specimens without any recognizable artifacts making them available for traditional stains such as H&E. This research demonstrates the feasibility of this technique for performing "virtual biopsies" as an adjunct to traditional histologic analysis, maximizing informational content in research and clinical pathology samples.

8226-18, Session 3

## Ion-beam sputtered (IBS) thin-film interference filters for nonlinear optical imaging

N. Anderson, P. Prabhat, T. Erdogan, Semrock Inc. (United States)

Multimodal nonlinear optical (NLO) microscopy is emerging as a powerful technique for the study of biological samples. By combining several different imaging modalities such as multiphoton fluorescence, second harmonic and third harmonic generation (SHG and THG), and coherent Raman scattering (CARS & SRS), it is possible to combine the best practices of label and label-free imaging into a single platform capable of imaging structures within single cells and elucidate the health of biological tissue samples, at the submicron level. Ion-beam sputtered (IBS) thin-film interference filters are a key enabling technology in laser-based optical microscopy and play a critical role in multimodal NLO imaging. In microscopy applications, optical filters are used to select and discriminate exactly which wavelengths of light are to be transmitted, reflected and suppressed. In this talk we will discuss various important characteristics of hard-coated thin film filters, such as high light throughput (i.e., transmission), edge steepness and out-of-band blocking, all of which that require careful consideration when designing and manufacturing dichroic, excitation and emission filters for NLO imaging applications. Furthermore, we will discuss how these optical filters are designed to work in unison within a single multimodal NLO microscopy platform to permit high fidelity imaging of biological samples.

8226-19, Session 3

## Recent development in ultrafast lasers for multimodal nonlinear imaging

M. F. Arrigoni, D. Armstrong, Coherent, Inc. (United States)

New trends in non-linear microscopy includes combining different techniques like MPE, SHG and femtosecond SRS microscopy to obtain deep images with minimum damage to enable long-term in-vivo imaging of animals and - ultimately - can enable diagnostics in humans. Additional emerging microscopy requirements involve the use of longer wavelengths and of multiple excitation wavelengths at the same time. In this presentation we will describe new commercially available laser devices that satisfy these requirements. While mainstream Titanium Sapphire laser technology provides access to only the “classical” wavelength range of 700-1050 nm, the addition of automated non-linear conversion devices extend this range to cover wavelengths from the UV to the mid-IR, providing also multiple, independently tunable outputs. These tools enable the production of information-rich images

8226-20, Session 3

## Latest advances in ultrafast laser sources for multiphoton microscopy

P. G. Smith, Spectra-Physics®, a Newport Corp. Brand (United States)

The advent of compact, fully automated, and widely wavelength-tunable ultrafast oscillators has triggered an explosive growth in their use in a broad array of multiphoton imaging techniques. Over the past decade laser manufacturers have constantly improved the performance characteristics of these sources to meet the requirements of the user community. We will review the latest advances at Newport / Spectra-Physics in this field and discuss new ways of optimizing key parameters for efficient deep-tissue fluorescence generation, including turn-key, automated second order dispersion compensation that allows for optimization of the pulse width at the sample over a wide wavelength range, without compromising beam pointing and other critical beam parameters.

8226-21, Session 3

## Pulse shaping multiphoton FRET microscopy

M. H. Brenner, Univ. of Michigan (United States); S. R. Nichols, Whitman College (United States); S. W. Straight, Univ. of Michigan Medical School (United States); A. D. Hoppe, South Dakota State Univ. (United States); J. A. Swanson, Univ. of Michigan Medical School (United States); J. P. Ogilvie, Univ. of Michigan (United States)

Fluorescence Resonance Energy Transfer (FRET) microscopy is a commonly-used technique to study problems in biophysics that range from uncovering cellular signaling pathways to detecting conformational changes in single biomolecules. Unfortunately, the results of standard FRET measurements are signal intensities in arbitrary units, and it can be difficult to obtain quantitative results. FRET stoichiometry has resolved this for one-photon FRET microscopy, but similar rapid and quantitative methods for multiphoton microscopy are lacking. Here we present a novel multiphoton FRET microscopy technique using pulse shaping to provide quantitative information about the concentrations of donor and acceptor molecules and their temporal dynamics in cellular processes. This multiphoton FRET stoichiometry technique overcomes the limitation of conventional tuneable femtosecond lasers to allow rapid switching between selective excitation of donor and acceptor fluorophores. Pulse shaping via multiphoton intrapulse interference tailors the excitation pulses to achieve selective excitation using a single broadband pulse, thus permitting multiphoton FRET stoichiometry. This technique will permit subcellular imaging with improved penetration depth into tissues, while also causing less photobleaching and photodamage than single-photon imaging. We apply the method to imaging live cells expressing fluorescent proteins such as mCerulean and mCherry, demonstrating selective excitation of fluorophores via pulse shaping and the detection of multiphoton FRET.

8226-22, Session 3

## Analysis of human aorta using fluorescence lifetime imaging (FLIM)

G. Vieira-Damiani, J. F. Adur, D. Peixoto Ferro, R. L. Adam, V. B. Pelegati, A. A. de Thomaz, C. Lenz Cesar, K. Metze, Univ. Estadual de Campinas (Brazil)

The use of photonics has improved our understanding of biologic phenomena. For the study of the normal and pathologic architecture of the aorta the use of Two-Photon Excited Fluorescence and Second Harmonic Generation showed interesating details of morphologic changes of the elastin-collagen architecture during aging or development of hypertension. In this study we tried to apply the fluorescence lifetime imaging (FLIM) for the morphologic analysis of human aortas. In this work our aim is to use FLIM in non-stained samples of the aorta ascendens in hypertensive and normotensive patients of various ages, examining two different topographical regions.

The FLIM-spectra of collagen and elastic fibers were clearly distinguishable, thus permitting an exact analysis of unstained material on the microscopic level. Moreover the FLIM spectrum of elastic fibers revealed variations between individual cases, which indicate modifications on a molecular level and might be related to age or diseases states and reflect modifications on a molecular level.

8226-23, Session 3

## Fluorescence lifetime and fluorescence correlation spectroscopy in colloidal quantum dots

A. A. de Thomaz, D. B. Almeida, Univ. Estadual de Campinas (Brazil); E. Jimenez Villar, Univ. de València (Spain); V. B. Pelegati, Univ. Estadual de Campinas (Brazil); J. F. Adur, Univ. Estadual de Campinas (Brazil) and Univ. Nacional de Entre Ríos (Argentina); H. F. Carvalho, C. Lenz Cesar, Univ. Estadual de Campinas (Brazil)

The unique physical and chemical properties of colloidal semiconductor quantum dots (QDs), specially the high photostability, but also the size-dependent fluorescence emission, broad excitation spectra, etc have made them a good alternative to organic dyes in the past two decades. Even the usually undesired blinking has been used nowadays to perform super resolution microscopy. Improvements in their surface chemistry and the conjugation to other bio-molecules allowed the specific labeling of cells organelles and structures. However, QDs studies with Fluorescence Lifetime Imaging (FLIM) and Fluorescence Correlation Spectroscopy (FCS) are rare compared with organic dyes, where they provide rich information about the chemical environment around the molecules and the co-localization of bio-molecules. We believe this is due to the fact that the physics of interaction between the QDs with external media, mediated by the cap-layer and the conjugation, is not well understood. In this work we show FLIM, and FCS measurements in colloidal QDs in different solutions and stained biological tissue. FCS measurements give us information about the QDs hydrodynamic radius, including the cap or conjugation layer. Compared with the optical radius obtained with spectroscopy or Electron Microscopy we can then evaluate the thickness of the cap layer. The thickness of the cap layer is very important to control the energy transfer processes between the QDs and the external media.

8226-46, Poster Session

## In vivo multiphoton imaging of the cornea: polarization-resolved second-harmonic generation from corneal collagen

G. Latour, I. Gusachenko, Ecole Polytechnique (France); L. Kowalczuk, Ecole Nationale Supérieure de Techniques Avancées (France); I. Lamarre, M. Schanne-Klein, Ecole Polytechnique (France)

Multiphoton microscopy provides specific and contrasted images of unstained collagenous tissues such as tendons or corneas. Polarization-resolved second harmonic generation (SHG) measurements have been implemented in a laser-scanning multiphoton microscope. Distortion of the polarimetric response due to birefringence and diattenuation during propagation of the laser excitation has been shown in rat-tail tendons. A model has been developed to account for these effects and correct polarization-resolved SHG images in thick tissues. This new modality is then used in unstained human corneas to access two quantitative parameters: the fibrils orientation within the collagen lamellae and the ratio of the main second-order nonlinear tensorial components. Orientation maps obtained from polarization resolution of the trans-detected SHG images are in good agreement with the striated features observed in the raw images. Most importantly, polarization analysis of the epi-detected SHG images also enables to map the fibrils orientation within the collagen lamellae while epi-detected SHG images of corneal stroma are spatially homogenous and do not enable direct visualization of the fibrils orientation. Depth profiles of the polarimetric SHG response are also measured. Comparison with modelling that accounts for orientation changes of the collagen lamellae within the focal volume show a good agreement. Finally, in vivo polarization-resolved SHG is performed in rat corneas and structural organization of corneal stroma is determined using epi-detected signals. To conclude, polarization-resolved SHG is a new modality that can be used for in vivo epi-imaging of collagenous organizations in tissues and opens great opportunities for biomedical studies.

8226-82, Poster Session

## Rapid volumetric temporal focusing multiphoton microscopy of neural activity: theory, image processing, and experimental realization

H. Dana, A. Marom, N. Farah, S. Shoham, Technion-Israel Institute of Technology (Israel)

Systems based on laser-scanning multiphoton microscopy are widely used both in vivo and in-vitro for cellular-resolution imaging of distributed neural activity patterns using calcium-sensitive and other functional dyes. However, point scanning inherently limits the image acquisition speed, and rapid functional imaging is currently largely tackled by rapid hopping systems that require trajectory planning and are not robust to tissue motion. An alternative to point scanning or hopping that can significantly enhance data acquisition rates is to use temporal focusing, a simple strategy for achieving optically sectioned wide-field excitation in nonlinear microscopy, photo-manipulation and photo-stimulation.

In this work, we demonstrate rapid volumetric imaging of distributed neural activity in scattering and transparent media using a new line-scanning temporal focusing system based on a microjoule ultrafast amplifier source. The system can image a field of at up to 200 frames/sec (limited by the camera's acquisition rate) and can axially scan up to several millimeters at 10Hz. An algorithm developed for efficient analysis of the functional volumetric data is introduced. Finally, we systematically study the system's sectioning performance for different configurations of temporal focusing geometries and at varying scattering tissue depths experimentally and using a model that combines geometrical optics considerations with Monte-Carlo scattering simulations. The implications of this approach will be discussed in the context of different physiological applications, including functional activity imaging in bio-engineered neural networks, retinas and cortical networks.

8226-83, Poster Session

## In-vivo pump-probe microscopy of melanoma and pigmented lesions

J. W. Wilson, T. E. Matthews, S. Degan, J. Y. Zhang, M. J. Simpson, W. S. Warren, Duke Univ. (United States)

A growing number of dermatologists and pathologists are concerned that the rapidly rising incidence of melanoma reflects not a true 'epidemic' but an increasing tendency to overdiagnose melanoma. Addressing this problem requires a better understanding of early-stage melanoma and new diagnostic criteria based on more than just cellular morphology and architecture.

Here we present a method for in-vivo optical microscopy that utilizes near-infrared ultrafast pump-probe spectroscopy to image the microscopic distribution of the two forms of melanin found in skin: eumelanin and pheomelanin. Previously we have shown this microscopic distribution to be of clinical significance with biopsy slides. In-vivo images are acquired with a sensitive modulation transfer technique by directing an RF-modulated pump pulse train (at 720 nm) and an unmodulated probe pulse train (at 810 nm) into a scanning microscope. Scattered probe light, detected episcopically, is analyzed with a lock-in amplifier, and a stack of images is acquired as a function of pump-probe delay.

In-vivo, non-invasive pump-probe microscopy is performed on a human skin xenografted mouse model, seeded with cultured melanoma cell lines. Individual melanocytes, with and without dendrites, have been observed, in addition to pigmented keratinocytes. Combining the pump-probe images simultaneously with a multiphoton autofluorescence and second harmonic generation image (acquired with a photomultiplier tube) allows visualization of the skin architecture, framing the functional image in a structural context.

8226-84, Poster Session

## Carcinogenic risk from nonlinear optical imaging: comparison between skin and internal organs tissues

G. Thomas, Erasmus MC (Netherlands); O. Nadyarnykh, J. van Voskuilen, Utrecht Univ. (Netherlands); A. van der Ploeg, Erasmus MC (Netherlands); H. C. Gerritsen, Utrecht Univ. (Netherlands); H. J. C. M. Sterenborg, Erasmus MC (Netherlands)

Nonlinear optical imaging has immense potential in biomedical diagnostics due to high resolution, deeper tissue penetration and minimal photobleaching. However, imaging in vivo with high peak intensity could generate cyclic pyrimidine dimers (CPDs) in DNA leading to mutations and thence carcinogenesis. CPDs are normally prevalent in sun exposed skin resulting from UV radiation absorption. In skin, the latter is attenuated by the presence of stratum corneum and melanin, while cells repair these lesions by Nucleotide Excision Repair. Meanwhile, CPDs are uncommon in internal organs which never receive UV exposure. Hence, the ability to repair CPDs in these tissues is not known. Besides lack of the aforementioned protective features of skin could make these tissues more vulnerable to radiation induced CPDs. Thus it would be important to compare the carcinogenic risk arising from nonlinear imaging between internal organ tissues and skin based on their susceptibility for CPD formation.

In this study we compared the incidence of CPD formation between murine skin as opposed to other murine tissues like stomach, colon and liver after being irradiated by pulsed NIR laser. The different tissue types exposed to UV radiation served as the respective positive controls. CPDs were quantified based on fluorescence intensity obtained from immunofluorescence experiments performed on the irradiated tissue. The recorded CPD level values were later used as input in the theoretical risk model we developed from literature. The carcinogenic risk for different tissues was then calculated and compared accordingly.

8226-85, Poster Session

## Second-harmonic generation and fluorescence lifetime imaging microscopy through a rodent mammary imaging window

P. A. Young, P. J. Keely, K. W. Eliceiri, Univ. of Wisconsin-Madison (United States)

Specific Tumor-Associated Collagen Signatures (TACS) were identified that manifest in specific ways during breast tumor progression and that correspond to patient outcome. In addition to the stromal environment, there are compelling data demonstrating metabolic changes in carcinoma cells. Invasive cells are known to undergo an angiogenic switch that is associated with hypoxia which may lead to the glycolytic switch known as the Warburg Effect. We have characterized the difference in the autofluorescent properties of metabolic co-factors, NADH and FAD, between normal and carcinoma breast cell lines. Also, we have shown in vitro that increased collagen density alters metabolic genes which are associated with glycolysis and leads to a more invasive phenotype. Establishing the relationship between collagen density, cellular metabolism, and metastasis is crucial for developing cancer therapies.

To study cellular metabolism with respect to collagen density, we use multiphoton fluorescence excitation microscopy (MPM) in conjunction with a rodent mammary imaging window implanted in defined mouse cancer models. These models are ideal for the study of collagen changes in vivo, allowing determination of corresponding metabolic changes in breast cancer invasion and progression. To measure cellular metabolism, we collect fluorescence lifetime (FLIM) signatures of NADH and FAD, which are known to change based on the microenvironment of the cells. Additionally, MPM systems are capable of collecting second harmonic generation (SHG) signals which are a nonlinear optical property of collagen. Therefore, MPM, SHG, and FLIM are used to characterize key features of carcinoma in vivo.

8226-86, Poster Session

## Vibrational molecular interferometry

E. T. Garbacik, J. P. Korterik, C. Otto, J. L. Herek, H. L. Offerhaus, Univ. Twente (Netherlands)

Nonlinear vibrational microspectroscopy techniques such as coherent anti-Stokes Raman scattering (CARS) and stimulated Raman scattering (SRS) are becoming widely used for applications. However, both CARS and SRS suffer some drawbacks that can make it difficult to accurately interpret the data. The presence of a persistent non-resonant background in CARS measurements can preclude the detection of small concentrations of the resonant molecule of interest, and the interference of this background with the resonant component warps the spectral features. While SRS is free from this non-resonant background, other nonlinear processes---photothermal lensing, two-photon absorption, self-phase modulation---can be difficult to distinguish from the resonant vibrational signal. To solve these problems we have developed a new technique that features a pair of Stokes Raman pathways interfering in the same molecular level. Slightly shifting the frequency of one pathway relative to the other induces an amplitude modulation in the molecular state. This amplitude modulation appears on all of the optical fields in the experiment, and is detected in a manner similar to that used in traditional SRS measurements. Subtraction of the amplitudes of two of the fields yields a vibrational signal that is free of any non-resonant background. In addition to being background-free, this technique also allows us for the first time to distinguish between vibrational and electronic resonances in a single measurement by monitoring the relative gain and loss in each field.

8226-87, Poster Session

## Stimulated-Raman scattering microscopy by spectral focussing and fiber-generated Stokes pulse

E. R. Andresen, P. Berto, S. Saint-Jalm, H. Rigneault, Institut Fresnel (France)

Stimulated-Raman scattering (SRS) microscopy is - along with coherent anti-Stokes Raman scattering (CARS) microscopy - at present the most acclaimed method of vibrational microscopy. Here, we demonstrate an alternative, simplified, yet efficient and flexible implementation of SRS microscopy which incorporates the advantages of the “spectral focussing” scheme while retaining the known advantages of SRS.

In our contribution [1], we experimentally demonstrate the proficiency of our light source based on a fs-laser at 1 um (pump pulse) and a photonic-crystal fiber (PCF) that generates a fs-pulse (Stokes pulse), frequency-shifted through the Raman self-frequency shift (RSFS) and tunable within 1-1.4 um, giving access to the vibrational frequency range 0-2000 cm-1. The generated pump and Stokes average powers, 200 and 4 mW respectively are sufficient to saturate a photodiode and permit lockin-detection at the shot-noise limit. The spectral focussing is effectuated by imposing equal chirps on the pump and Stokes pulses. The spectroscopic signal generation by these chirped pulses is equivalent to that by transform-limited pulses with identical envelopes. In a series of imaging experiments, we demonstrate the imaging capabilities and the rapid (in seconds) acquisition of Raman spectra.

Our relying on fs- rather than ps-pulses enables us to employ the RSFS in a PCF to impose a tunable frequency-shift on a part of the laser pulse. The effect is particularly strong for fs-pulses with conversion factors approaching unity, even for weak pulses in the 10 pJ-range. This conversion efficiency achieved by a 1 m-long PCF essentially eliminates the need for bulk frequency conversion systems. The method is feasible with any fs-laser with center wavelength in the anomalous dispersion region of the employed PCF.

[1] E.R. Andresen, P. Berto, H. Rigneault, “Stimulated-Raman scattering microscopy by spectral focussing and fiber-generated soliton as Stokes pulse”, Opt Lett 36, 2387-2389 (2011)

8226-88, Poster Session

## MPTflex®: a flexible clinical multiphoton tomograph for early melanoma detection, skin analysis, testing of anti-age products, and in situ nanoparticle tracking

M. Weinigel, H. G. Breunig, P. Fischer, M. Kellner-Hoefer, R. Bückle, K. König, JenLab GmbH (Germany)

Multiphoton imaging systems are capable for high-resolution 3-D image acquisition of deep tissue. A commercially available CE-certified biomedical system for subcelluar resolution of human skin has first been launched by JenLab company with the DermaInspect® in 2002. Six years later the demand for more flexibility caused the development of the MPTflex®. Equipped with flexible articulated arms, it provides an increased flexibility and accessibility especially for clinical and cosmetic examinations.

8226-89, Poster Session

## Custom-made Cr: LiCAF laser for a nonlinear microscope

S. Pratavieira, C. Grecco, A. Cosci, V. Bagnato, L. Misoguti, C. Kurachi, Univ. de São Paulo (Brazil)

We present the design and the assembly of a custom-made two-photon microscope for in-vivo and ex-vivo fluorescence imaging of biological tissues and organs. By means of the microscope it is possible to have a three dimensional reconstruction of tissues with cellular resolution. Construction involves both the assembly of a Cr:forsterite pulsed laser system (100 fs pulses, 80 MHz repetition rate @ 800nm) and of the two-photon microscope using two galvo-mirrors relayed by two spherical mirrors as scanners.

8226-90, Poster Session

## Quantifying colonic cancer progression with multiphoton microscopy

S. Zhuo, Fujian Normal Univ. (China)

Real-time histology or virtual biopsy for the diagnosis of colonic cancer is of great medical significance. In this work, we show that label-free multiphoton imaging is feasible and effective in monitoring colonic cancer progression by providing cellular and subcellular details in fresh, unfixed, unstained colonic specimens. Our results also demonstrate the capability of using tissue quantitative analysis of the redox ratio for quantifying colonic cancer progression. These results suggest that multiphoton microscopy has potential to become an in situ histological tool, which is free from the labeling requirement of conventional methods, for the early diagnosis and detection of malignant lesions in the colon.

8226-91, Poster Session

## Recommendations for the design and the installation of large laser scanning microscopy systems

P. J. Helm, Univ. of Oslo (Norway)

Laser Scanning Microscopy (LSM) has since the inventions of the Confocal Scanning Laser Microscope (CLSM) and the Multi Photon Laser Scanning Microscope (MPLSM) developed into an essential tool in contemporary life science and material science.

The market provides an increasing number of small turn-key and hands-off commercial LSM systems, un-problematic to purchase, set up and integrate even into minor research groups.

However, the successful definition, financing, acquisition, installation and effective use of one or more large laser scanning microscopy systems, possibly of core facility character, often requires major efforts by senior staff members of large academic or industrial units.

Here, a set of recommendations is presented, which are helpful during the process of establishing large systems for confocal or non-linear laser scanning microscopy as an effective operational resource in the scientific or industrial production process.

Besides the description of technical difficulties and possible pitfalls, the article also illuminates some seemingly “less scientific” processes, i.e. the definition of specific laboratory demands, advertisement of the intention to purchase one or more large systems, evaluation of quotations, establishment of contracts and preparation of the local environment and laboratory infrastructure.

8226-92, Poster Session

## The use of microstructures for high-resolution axial axis imaging

S. H. McIntyre, J. M. Cooper, G. Smith, Univ. of Glasgow (United Kingdom)

It is known that the lateral resolution of a one or two-photon confocal microscope is superior to the axial resolution by a factor of 2-3. Therefore of this structures in the axial plain cannot easily be resolved. Micromirrors have been manufactured that circumvents these problems by allowing a secondary image of the specimen to be obtained at a steep angle to the original axis through the same high NA objective. This approach allows conventional laser scanning confocal systems achieve superior axial resolution.

The mirror is fabricated by spinning the polymer SU1818 onto a 500  m silicon wafer and patterning a sharp edge. This photoresist is then developed and the silicon is etched through in a 80oC potassium hydroxide etch. An oxide layer of 100-800nm is grown on the surface then silicon oxide is removed with hydrofluoric acid. Finally the surface is coated with 100nm of silver.

This creates a micro mirror at 55 degrees to a coverslip base. The mirror is placed next to a specimen and once a conventional image of the specimen is acquired using laser scanning confocal imaging, the mirror image of the specimen is located and imaged. It is then possible to deconvolve these images and merge to make a high resolution 3-D image.

Because the mirror deflects excitation light toward the objective, there is a sensitivity benefit to this method so that only very low levels of laser excitation light are required, thereby increasing the signal-to-noise ratio of fast scans and/or allowing longer acquisition times.

8226-93, Poster Session

## Comparison of calcium imaging in dorsal root ganglion neurons by using laser scanning confocal and two-photon microscopy

Y. Huang, H. Yang, J. Chen, X. Shen, L. Zheng, Y. Wang, S. Xie, Fujian Normal Univ. (China)

As one of the most important second messengers, calcium in nerve cells plays a critical role in neuronal processes, including excitability, neurotransmitter release, synaptic plasticity. Modulation of the calcium concentration is an important means of regulating diverse neuronal functions. To evaluate the role of calcium, quantitative measurement of cytosolic free calcium concentrations is required. Laser scanning confocal microscopy, combined with calcium fluorescence probes, has been used to measure the concentration of calcium in living cells. The low efficient of photon collection in laser scanning confocal microscopy due to the limitation of pinhole would induce photobleaching and phototoxicity, which might restrict its application in long-term investigation. In this paper, two-photon microscopy was introduced to study the calcium concentration in rat dorsal root ganglion neurons with fluorescence probe. Photobleaching and phototoxicity of two-photon microscopy were compared with that of laser scanning confocal microscopy. The results showed that the two-photon microscopy had an advantage over the laser scanning confocal microscopy in photobleaching and phototoxicity.

8226-94, Poster Session

## Development of photon detectors for picosecond resolution, high rate, multi-channel life science applications

T. Conneely, Photek Ltd. (United Kingdom) and University of Leicester (United Kingdom); J. Lapington, Univ. of Leicester (United Kingdom); J. Milnes, Photek Ltd. (United Kingdom)

Photek, in collaboration with the University of Leicester space research centre, are pursuing a number of R&D projects aimed at developing systems for parallel detection of single photon events with time resolution of the order of 25 ps using Microchannel plate detectors. This includes three detector systems utilising similar readout electronics, the NINO amplifier/discriminator and HPTDC time-to-digital convertor developed at CERN. These electronics allow a timing resolution of 25 ps, at event rates in excess of 10 MHz.

The first detector, HiContent, is a 8x8 multi-anode MCP-PMT for parallel acquisition of data. The timing jitter of the detector has been demonstrated to be better than 40 ps RMS, with a maximum rate approaching 10 MHz. The HiContent detector is also a prototype for the IRPICS project, which increases the channel density to a 256x256 array of anodes, which is currently under development. Finally, the C-DIR (Capactive Division Readout) detector is a wide-field imaging device currently in development, which uses a charge division technique for imaging single photon events, and recording a timestamp better than 25 ps.

8226-95, Poster Session

## Characterization of optical properties of ZnO nanoparticles for quantitative assessment of transdermal transport

Z. Song, T. A. Kelf, Macquarie Univ. (Australia); W. H. Sanchez, M. S. Roberts, The Univ. of Queensland (Australia); M. Frenz, J. Ricka, Univ. Bern (Switzerland); A. V. Zvyagin, Macquarie Univ. (Australia)

ZnO nanomaterial is widely used in sunscreen formulations to protect against the UV radiation damage to skin. The application is generally regarded safe, provided the material is mainly accumulated in the top layer of human skin, stratum corneum, which provides superior protection against environmental assault. Quantitative evaluation of the distribution of ZnO nanoparticles in skin layers including stratum corneum and viable epidermis provides important information for safety assessment [1, 2], and it has been assayed by a number of techniques. Among these, non-linear optical microscopy (NLOM) is a promising imaging modality capable of assaying ZnO NP absorption in skin in vivo [3]. ZnO NP appeared to exhibit high NLOM-imaging contrast on the intense autofluorescence background due to skin endogenous fluorophores, explained by its enhanced two-photon absorption across-section of the nanomaterial.

We report on systematic study of ZnO NP nonlinear optical properties, which aims to addressing two characterization techniques suitable for determination of the two-photon action across-section. Using two-photon absorption across-section and quantum yield values, nonlinear optical microscopy images of the excised human skin topically treated with ZnO nanomaterial were processed which yield nanoparticle concentration map in skin layers. A correspondence between the nonlinear optical microscopy signal of ZnO NP and its distribution in skin was established, which paves a way for quantitative in vivo nanotoxicology studies.

References:

1. Zvyagin et al. , “Imaging of zinc oxide nanoparticle penetration in human skin in vitro and in vivo,” J Biomed. Opt., 13 (2008).

2. Cross et al. , “Human skin penetration of sunscreen nanoparticles: in-vitro assessment of a novel micronized zinc oxide formulation,” Skin Pharm. Physiol, 20 (2007).

3. Masters et al. , “Confocal microscopy and multi-photon excitation microscopy of human skin in vivo,” Opt. Express, 8 (2001).

8226-96, Poster Session

## Multifocus nonlinear optical microscopy based on SLM and AO deflector

W. Qin, Clemson Univ. (United States); Y. Shao, Shenzhen Univ. (China); H. Liu, Clemson Univ. (United States); J. Qu, X. Peng, H. Niu, Shenzhen Univ. (China); B. Gao, Clemson Univ. (United States)

Laser scanning microscopes generally have poor temporal resolution, caused by the serial scanning of each pixel. Multifocus microscopes have been shown to be particularly suitable for dynamic cell imaging with high recording speeds. We present a high-speed, light-efficient, nonscanning, second harmonic generation and multiphoton excitation fluorescence hybrid microscope that provides three-dimensional imaging with high resolution. Our system does not contain mechanically moving parts. Using a diffractive spatial light modulator (SLM), we shape the near-infrared light of a mode-locked Ti-sapphire laser into a matrix of beams that are transformed into a matrix of high-aperture foci at the object. NA of each focused beam of the beam matrix is the same as that of the original beam. In order to further increase the imaging speed, we scan the foci matrix by scanning the incident beam to the SLM using an acousto-optic deflector (AOD). For a 512 by 512 image with a 3 by 3 excitation foci matrix, we can achieve a image acquiring rate of 20k frames per second. A cooled CCD camera with high sensitivity is used for record the SHG signal or two-photon fluorescence image. Compared with the Galvo scanner-based multifocus microscope, our system presents about 1000-fold increase in imaging speed. This increase of imaging speed is critical for recording very fast process of live samples, such as the contraction of a cardiomyocyte. In addition, the SLM is also used in our system to create arbitrary, computer controlled excitation pattern to image the special interesting area of the sample with even higher temporal resolution.

8226-97, Poster Session

## Two-photon excited fluorescence spectroscopy and imaging of melanin in vivo

T. B. Krasieva, Beckman Laser Institute and Medical Clinic (United States); F. Liu, Univ. of California, Irvine (United States); M. Balu, C. Sun, Beckman Laser Institute and Medical Clinic (United States); F. L. Meyskens, Univ. of California, Irvine (United States); B. J. Tromberg, Beckman Laser Institute and Medical Clinic (United States)

The ability to detect early melanoma non-invasively would improve clinical outcome and reduce mortality. Recent advances in two-photon excited fluorescence (TPEF) in vivo microscopy offer a powerful tool in early malignant melanoma diagnostics.

The goal of this work was to develop a TPEF optical index for measurement determining relative concentrations of eumelanin and pheomelanin since ex-vivo studies show that changes in this ratio have been associated with malignant transformation. We acquired TPEF emission spectra ($\lambda$ex=900 nm) of melanin and keratin from several specimens, including human hair, normal melanocytes and malignant melanoma cell lines, and different skin layers (epidermis, papillary dermis) in five healthy volunteers in-vivo. We found that the pheomelanin emission peaks at around 600 nm and is blue-shifted from the eumelanin maximum at 635-640 nm.

We defined “melanin index” (MeI) as a ratio of fluorescence signal intensities measured at 640 nm and 600 nm. The measured MeI for a melanoma cell line MNT-1 was 1.4±0.05. The MNT-46 and MNT-62 lines (Mc1R gene knock-out) showed an anticipated increase in pheomelanin production and had MeI of 1.2±0.05 and 1.05±0.05, respectively, which strongly correlated with HPLC data obtained for these lines. MeI measured for basal cells layers (melanocytes and keratinocytes) in normal human skin type II, IV and VI in vivo was 1.2, 2.3 and 2.5, respectively. These data suggest that changes in a non-invasive TPEF index could indicate potential for malignant melanocyte transformation.

8226-98, Poster Session

## Long-distance fluorescence lifetime imaging with stimulated emission

P. Lin, T. Dellwig, F. Kao, National Yang-Ming Univ. (Taiwan)

Fluorescence lifetime imaging is a powerful tool in elucidating molecular interaction and changes of the fluorophores’ nanoenvironment. Stimulated emission, on the other hand, has been used to shape the point spread function (PSF) to achieve spatial resolution beyond the diffraction limit and to detect dark fluorophores with low quantum yield by competing with non-radiative decay. In this study, we further adopt the spatial coherence resulting from stimulated emission and demonstrate long-distance fluorescence lifetime imaging (LDSEI). We also apply LDSEI to image dark fluorophores, with malachite green as an example, and probe its fluorescence lifetime in long-distance configuration. The dark fluorophores usually possess very short lifetime (sub- ns), which is difficult to measure with conventional lifetime techniques, such as time correlated single photon counting (TCSPC). The stimulated emission based probe-pump technique provides unique opportunity to detect these dark molecules and measure the corresponding fluorescence lifetimes. The sample is excited by pulse diode laser (635 nm) and stimulated by a synchronized mode-locked Ti:sapphire laser operating at a wavelength of 735 nm. The stimulated emission signal is discriminated with a lock-in amplifier, with the excitation beam modulated by a mechanical chopper. The initial results indicate that stimulated emission is a powerful tool in visualizing dark fluorophores as well as their fluorescence lifetime at extended distance.

(The author will participate the students poster session competition)

8226-99, Poster Session

## Investigating nucleation, growth, and structural diversity of self-assembled nanomaterials

N. R. Anthony, A. J. Bisignano, D. G. Lynn, K. M. Berland, Emory Univ. (United States)

We use Fluorescence Lifetime Imaging Microscopy (FLIM) and Second Harmonic Imaging Microscopy (SHIM) to investigate the fundamental molecular mechanisms responsible for nucleation and growth of amyloidogenic-derived nanomaterials. In this case the nanomaterials are predominantly composed of Amyloid-ß(16-22), specifically Ac-KLVFFAE-NH2, the nucleating core of the Alzheimer’s Amyloid-ß protein. Understanding the self-assembly pathways of these materials will provide key insights towards both a top down understanding of amyloidogenic diseases and a bottom up control of functional nanomaterials. Continued application of these techniques to peptide self-assembly could allow for real time structural indicators during nanofabrication. We describe how FLIM and SHIM can be used to follow different nucleation pathways and to quantify structural heterogeneities within these complex nanomaterials. In addition, new evidence from these microscopy techniques suggests that different structures emerge from distinct nucleation pathways. We discuss our recent findings and the insights they provide to understanding peptide self-assembly mechanisms.

8226-100, Poster Session

## Multiphoton ultraviolet microscopy reveals dopamine dynamics in live brain tissue

B. Sarkar, Tata Institute of Fundamental Research (India); A. Bandyopadhyay, Cold Spring Harbor Lab. (United States); S. Nag, Tata Institute of Fundamental Research (India); S. K. Kaushalya, Max-Planck-Institut für medizinische Forschung (Germany); A. K. Das, S. Maiti, Tata Institute of Fundamental Research (India)

Intracellular dopamine dynamics is a prelude to the sensation of reward and to motor control, and also a key to understanding substance addiction and Parkinson's disease. Yet there has been no optical method to probe it in live neurons. Dopamine neurotransmission has been investigated extensively, yet direct optical probing of dopamine has not been possible till now. Here we image intracellular dopamine with sub-micron three-dimensional resolution, by harnessing its autofluorescence with two-photon ultraviolet excitation (using a femtosecond optical parametric oscillator with output at 540 nm) and non-epifluorescent detection. The technique is established by first imaging dopamine in the dopaminergic cell line MN9D. Dopamine content and drug-induced dopamine release in these cells is quantified in parallel by HPLC and mass spectrometry. The results confirm that the observed images are indeed from dopamine. We then show that individual dopamine vesicles in the substantia nigra region can be imaged inside cultured brain slices. Our technique can follow the intracellular events preceding dopamine release induced by depolarization and amphetamine exposure in these slices. This provides a unique assay for following any neurophysiological process which affects the intracellular dopamine dynamics.

8226-101, Poster Session

## Non-invasive monitoring of redox state to assess cell differentiation in engineered adipose tissues

K. P. Quinn, E. Bellas, N. Fourligas, D. L. Kaplan, I. Georgakoudi, Tufts Univ. (United States)

The use of engineered adipose tissue in reconstructive surgery has been limited by insufficient biocompatibility and rapid scaffold degradation. Non-invasive optical imaging approaches to quantify biochemical changes in tissue would aid in optimizing tissue development and in vivo integration. The goal of this study was to quantity endogenous cellular fluorescence through two-photon microscopy in order to monitor the metabolic status of cells undergoing adipogenesis in silk scaffolds. Three-dimensional porous silk scaffolds (n=8) were seeded with either adipose-derived mesenchymal stem cells (hASCs) undergoing adipogenic differentiation or a co-culture of hASCs and human microvascular endothelial cells (HMVEC). Images isolating the fluorescence contribution of the coenzymes FAD and NADH were acquired at a range of depths within the scaffold over 14 weeks. A redox ratio of FAD/(NADH+FAD) was computed for each cell, which is inversely proportional to its metabolic rate. The average redox ratio in both tissue groups significantly decreased between Weeks 1 and 2 ($p=0.0464$), corresponding to the onset of differentiation and the formation of lipid droplets. Significant increases in redox ratio were also detected between Weeks 8 through 14 ($p<0.0037$). The average redox ratio significantly increased with increasing depth in the hASC scaffold group ($p=0.0056$) but not the co-culture group, suggesting the potential formation of lumens by HMVECs may help to maintain cell metabolic activity deeper within the tissue. These findings are consistent with the enhanced development of vascularized engineered adipose tissue and provide an important step in developing non-invasive optical biomarkers to evaluate the biochemical status of three-dimensional engineered tissues.

8226-102, Poster Session

## Investigation of laser-induced cyclobutane-pyrimidin-dimers damage to cellular DNA in nonlinear optical imaging

O. Nadyarnykh, Utrecht Univ. (Netherlands); G. Thomas, Erasmus MC (Netherlands); J. van Voskuilen, Utrecht Univ. (Netherlands); H. J. C. M. Sterenborg, Erasmus MC (Netherlands); H. C. Gerritsen, Utrecht Univ. (Netherlands)

Nonlinear optical imaging modalities (multi-photon excited fluorescence, second and third harmonic generation) are increasingly promising for clinical diagnostics and monitoring of cancer and other disorders, as they probe tissue structure in vivo with high diffraction-limited resolution (0.3μm) at near-IR wavelengths (700-1000nm). Autofluorescence in tissues originates from NADH, FAD, melanin, and lipoproteins, while non-centrosymmetric protein arrays (collagen, myosin) give rise to second harmonic generation. However, high peak intensity of femtosecond laser pulses required for multi-photon processes is sufficient to excite UV absorption band of cellular DNA and form cyclobutane-pyrimidin-dimers (CPDs) similar to damage from exposure to solar UV light. Malfunctioned repair of subsequent mutations might cause carcinogenesis.

Here, we investigated CPD damage recorded in Chinese Hamster Ovary cells in vitro by imaging them with two-photon excited autofluorescence, where CPD levels were quantified by immunofluorescent staining. Then we evaluated CPD damage severity with respect to varied laser parameters: wavelength (690 to 810nm), pulsewidth at focal plane (150 to 450 μm), and pixel dwell time as compared to regular one-photon damage from UV source.

While three-photon absorption has been considered as the source of CPD damage, our study revealed that CPDs are induced by competing two- and three-photon absorption processes corresponding to UVA and UVC absorption bands, respectively.

This finding is independently verified by nonlinear dependencies of damage on laser power, wavelength and pulsewidth. We observed different distribution of CPDs within the nuclei resulting from two-photon imaging as compared to UVC source. Finally, relatively safe imaging parameters can be identified as damage is undetectable below still acceptable excitation peak intensity.

8226-103, Poster Session

## Low cost laser system generating 26 fs pulse duration, 30 kW peak power, and tunability from 800 to 1200 nm for multiphoton microscopy

B. Resan, F. Brunner, A. Rohrbacher, H. Ammann, K. J. Weingarten, Time-Bandwidth Products AG (Switzerland)

There is a need for ultrashort pulse laser sources covering the IR part of the spectrum around and beyond 1 micron. A biomedical tissue exhibits less absorption and scattering in this wavelength region, enabling deeper tissue penetration. Currently available ultrashort pulse tunable lasers are mainly Ti:sapphire based lasers, which are limited in wavelength tuning range up to 1 micron, and tunable versions are limited in pulse duration down to 100 fs. In addition, Ti:sapphire based lasers are costly owing to the need for an additional pump laser. Laser systems generating even shorter then 100 fs pulses are highly desirable for multiphoton imaging and nanosurgery owing to minimized heat deposition to living cells resulting in prolonged cell viability.

A tunable, high peak power, ultrafast laser system is developed based on a SESAM modelocked solid-state Yb tungstate seed laser, spectral broadening via a microstructured fiber, and pulse compression. The spectral selection, tuning, and pulse compression are performed with a simple prism compressor. The long-term stable output pulses are tunable from 800 to 1200 nm, with a peak power up to 30 kW, and a pulse duration down to 26 fs. The generation of an output beam with fs pulsewidth and multiple colours in infrared will be discussed. The compact, low cost system is ideally suited for multiple biomedical applications including multiphoton (TPE, SHG, THG, CARS) and multimodal microscopy, nanosurgery, biomaterial nanostructuring, and optical coherence tomography (OCT).

8226-104, Poster Session

## Correlation scanning microscopy techniques to quantify DNA repair protein kinetics using confocal microscopy and two-photon microscopy

S. Abdisalaam, The Univ. of Texas at Arlington (United States)

Two-photon microscopy have been tool of choice compare to single-photon microscopy due to inherent advantage of reducing photobleaching. There are two distinct pathways of repairing DSBs, homologous recombination and non-homologous end joining (NHEJ). In the NHEJ repair pathway the DNA dependent protein kinase (DNA-PK) complex, consisting of the catalytic subunit (DNA-PKcs) and a DNA-binding Ku70/80 protein heterodimer, plays a major role in orchestrating the sequence of molecular interactions at DSBs. The kinetics of these proteins involved in DNA repair following ionizing radiation cannot be quantified by standard live cell fluorescence microscopy methods. This is because a high fluorescence background from freely moving and immobile fluorescent proteins that exists in the nucleus masks the aggregation of proteins at sparse DNA damage sites.

8226-105, Poster Session

## Photodamage in whole living organisms under imaging conditions as a function of pulse duration

M. M. Dantus, I. Saytashev, N. S. Winkler, K. L. Zuraski, S. N. Arkhipov, V. V. Lozovoy, Michigan State Univ. (United States)

We report on the photodamage caused by femtosecond laser pulses as a function of peak intensity for short (37 fs) and long (100 fs) pulses on Drosophila melanogaster as a whole- body model of multicellular eukaryotic organism. This study is intended to better understand photodamage under conditions that mimic the application of femtosecond lasers in multiphoton imaging in living tissues. Measurements on the level of entire organism allow us to quantitatively characterize different mechanisms for damage. The organisms, in their larvae stage, were irradiated with 800 nm pulses of different pulse duration and peak intensities. The larvae were then allowed to mature to the pupae and fly stage, where the changes in basic parameters, such as lethality, phenotype, physiological functions, and development were scored. TUNEL assay has been applied to examine photodamage shortly after irradiation on the level of cellular DNA. Imaging of tissues from irradiated larvae was accomplished by two-photon microscopy to reconstruct three-dimensional structures of the imaginal disks. Our results show that for fixed peak intensity the larvae irradiated with longer pulses (100 fs) had a lower survival rate as well as more DNA damage in comparison with the larvae irradiated with the shorter femtosecond pulses (37 fs).

8226-106, Poster Session

## Design and performance of a wide field-of-view multiphoton microscope

G. J. Kintz, Laser Biopsy, Inc. (United States); W. R. Zipfel, Cornell Univ. (United States)

An easy to use, high throughput, low cost, robust multiphoton imaging system is required for clinical applications of rapid examination of biopsy samples in the operating room. The system should be low cost, but ideally with the performance parameters of a high end commercial system. In this paper we will describe the fundamental optical design of a low cost imaging system together with the performance characteristics. The optical system is capable of optimizing signal levels over a wide FOV view without sacrificing resolution to enable rapid imaging of an entire endoscopic biopsy specimen without the need for “tiling” many images together. Further, by optimizing the signal levels, the required power levels and ultimately the cost of the laser system can be reduced. The optical performance characteristics are: Numerical Aperture = 0.63, Design wavelength = 780 nm, Field of View = 2.1 mm diameter, and Strehl ratio > 0.85 for 100% of the field. The wide Field of View results in some residual field curvature in the image plane. The optical design consists of 7 spherical optical elements, one spherical mirror element and two diamond turned aspheres. The system uses a pair of galvo scanners where the scan angles: +/-16.9° which allows for enough scan range for acceleration/deceleration profiles in the scan. The Numerical Aperture = 0.6 which results in a ~0.600 µm lateral and ~1 µm axial resolution. A 3200 x 2400 pixel image contained within the Field of View. Measured performance characteristics and images of animal tissue will be presented.

8226-107, Poster Session

## Real-time action potential recording from multiple neurons

L. Sacconi, J. Lotti, Univ. degli Studi di Firenze (Italy); P. Yan, L. M. Loew, Univ. of Connecticut Health Ctr. (United States); F. S. Pavone, Univ. degli Studi di Firenze (Italy)

The central nervous system can process a tremendous amount of information, which is encoded in terms of action potetnial and transmitted between neurons at synapses. A central question in neuroscience is how simple processes in neurons can generate cognitive functions and form complex memories like those experienced by humans and animals. In principle, if one were able to record from all the neurons in a network involved in a given behavior, it would be possible to reconstruct the related computations. This is not possible with current techniques. Here we set up a random access multi-photon microscope (RAMP) capable of optically recording fast membrane potential events occurring in a wide-field of view. The RAMP microscope, in combination with a novel voltage sensitive dye, was used to simultaneously record action potential in real time from clusters of Purkinje cells in acute cerebellar slices. These results show the strength of this technique in describing the temporal dynamics of neuronal assemblies, opening promising perspectives in understanding the computations of neuronal networks.

8226-108, Poster Session

## Random access multiphoton (RAMP) microscopy for investigation of cerebral blood flow regulation mechanisms

D. J. Christensen, Univ. of Rochester (United States); M. Nedergaard, Univ. of Rochester Medical Ctr. (United States)

The processes by which blood flow is regulated at the capillary network level in the brain has been a source of continual debate. It is generally accepted that cerebral blood flow regulation occurs primarily at the arteriolar level. It has been recently suggested, however, that the capillary network is likewise under dynamic regulation. The exact mechanisms of capillary regulation remain unknown.

Previously, the limiting factor in determining how the cerebrovascular network is regulated has been the speed at which multiphoton images of large (~ 100um^3) capillary and arteriole systems can be acquired in three dimensions. Conventional laser scanning microscopy systems are temporally limited in two dimensions by the scan speeds of physical mirrors and in three dimensions by the speed of a physically moving stage or microscope nosepiece along the optical axis. We have developed a Random Access Multiphoton (RAMP) microscope, which operates on the principles of Acousto-optic beam scanning and therefore has no moving parts, specifically for the purpose of imaging blood flow virtually simultaneously throughout the 3D capillary network. The instrument will be discussed and current results will be presented.

8226-109, Poster Session

## Effect of pulse duration on photodamage in living organisms

M. M. Dantus, I. Saytashev, N. S. Winkler, K. L. Zuraski, S. N. Arkhipov, V. V. Lozovoy, Michigan State Univ. (United States)

We report on differences in the photodamage observed in Drosophila melanogaster treated with femtosecond laser pulses with the same peak intensity [W/cm2] but different pulse durations. These findings are relevant to multiphoton imaging, where 100-200 femtosecond laser pulses are used, and where the major contributors towards photodamage in cells are multiphoton absorption processes that trigger formation of free electrons, reactive oxygen radicals, and direct DNA damage. In our experiments, the living specimens, in their larvae stage, were irradiated and then allowed to mature to the pupae and fly stages. Lethality as well as possible changes in morphology, physiological functions, and development have been scored. We found statistically significant differences between longer and shorter pulses. For a fixed peak intensity shorter pulses (37 fs) caused less detrimental effects and correlated with higher survival rates for all three stages (larvae, pupae and fly) than longer pulses (100 fs).

8226-110, Poster Session

## Toward nonlinear microscopy with few-cycle laser pulses

G. Tempea, FEMTOLASERS Produktions GmbH (Austria); S. Gomes da Costa, H. Wan, A. Volkmer, Univ. Stuttgart (Germany)

With the advent of high-dispersion mirrors, the delivery of tightly focused laser pulses with sub-20-fs durations became feasible with compact, user-friendly compressors. For tightly focused sub-10-fs pulses in the visible and near infrared region, typically active pulse-shaping techniques have been employed. Here, we report on pushing the limits of pure passive dispersion management in nonlinear optical microscopy with few-cycle pulses. 6.4-fs laser pulses generated from an all-dispersive-mirror Ti:Sapphire oscillator were coupled into a standard Olympus IX71 inverted microscope. The pulse spectrum spans 500 nm (174 nm FWHM, 303 nm width at the 1/e^2 level) in the visible and near infrared spectral range. We demonstrate the pre-compensation of the group delay dispersion in two high-numerical aperture water-immersion objectives commonly used in multi-photon bio-imaging applications (Olympus LUMPLFLIR 40x 0.8W and Olympus UPLSAPOIR 60x 1.2W). By using ultra-broadband dispersive mirrors that cover the full pulse spectrum along with thin glass wedges, in-focus pulse durations of 9.8 fs and 9.9 fs, respectively, have been achieved. Further shortening of the pulse duration at the sample was limited by the bandwidth and phase characteristics of the microscope's dichroic beamsplitter that separates the fundamental beam from the nonlinear signal generated by the sample. Consequently, a tailored dichroic filter that supports the full bandwidth of the laser pulse and introduces negligible dispersion upon its reflection has been designed and manufactured. The implementation of this novel filter is expected to enable the delivery of pulses closely approaching the sub-7-fs bandwidth limit at the focus.

8226-111, Poster Session

## Sensitive fluorescence detection using a camera from the gaming industry

B. L. Van Hoozen, Jr., J. P. Korterik, Univ. Twente (Netherlands); K. de Bruin, Netherlands Forensic Institute (Netherlands); W. Nagengast, Univ. Medical Ctr. Groningen (Netherlands); J. L. Herek, H. L. Offerhaus, Univ. Twente (Netherlands)

The detection limit for linear (fluorescence) and nonlinear (stimulated fluorescence or Raman) imaging can be improved by reducing noise. One way to reduce the noise in these types of imaging is to modulate the signal at a certain frequency and only detect signals at that frequency. Since most noise sources have a 1/f dependence, higher modulation frequencies result in less noise. Typically cameras used for imaging have frame rates of 50 or 100 Hz; however, a new time-of-flight camera developed for the gaming industry has a modulation frequency of 20 MHz, allowing for a substantial reduction in noise. In this study, the improved detection limit of this camera was applied to three different experiments: the detection of fluorescent dyes used for tracing cancer cells, the detection of biological material (e.g. saliva) using autoflorescence which has applications in forensics, and the detection of otherwise non-fluorescent materials (e.g. hemoglobin) using stimulated fluorescence.

8226-112, Poster Session

## Three-photon fluorescence imaging of melanin with a CW laser and a dual-wedge scanning system

Y. J. Mega, C. A. DiMarzio, Northeastern Univ. (United States)

Confocal microscopy offers high resolution optical imaging with sectioning capability. This imaging modality is being developed as a practical tool in non-invasive applications in medical diagnostics and evaluation. In particular, it is being used in the early detection of skin cancer to identify pathological cellular components and, potentially, replace conventional biopsies. Previous work in the field has shown that the detection of melanin and its spatial location and distribution is important in the detection of skin cancer. Melanin absorbs UV and visible light strongly and appears black in images. This strong absorption can be observed in the darker cancerous skin lesions which contain much higher melanin concentration than the surrounding tissue. However, melanin can also appear bright in confocal images since it can scatter the laser light efficiently. This dual contrast mechanism can complicate the detection or identification of melanin by confocal imaging. Earlier, our group has shown that the melanin fluorescence can also be used to detect melanin. The visible emission is strong and can be easily observed with a near-infrared CW laser using low power. This is due to the unique step-wise three photon excitation signature of melanin. This paper shows that the same step-wise three photon fluorescence can also be achieved with an inexpensive continuous-wave laser using a dual prism scanning system. The results are in agreement with images obtained with the larger and more expensive femtosecond laser system used earlier. This finding is important since it shows that our low-cost configuration, which is portable and can be miniaturized, can be extended for practical non -invasive skin cancer detection.

8226-114, Poster Session

## Improvement of the spatial resolution in two-photon excitation fluorescence microscopy by saturated excitation (SAX)

M. Yamanaka, Y. Yonemaru, N. I. Smith, S. Kawata, K. Fujita, Osaka Univ. (Japan)

Two-photon excitation fluorescence (2PEF) microscopy enables three-dimensional imaging of biological samples due to the quadratic intensity dependence in 2PEF. However, because of the use of longer excitation wavelength, achievable resolution is similar to that in confocal microscopy using visible excitation wavelength. Here, we report the improvement of the spatial resolution in 2PEF microscopy by saturated excitation (SAX). Since the saturation effect produces high-order nonlinear fluorescence responses, extraction of the nonlinear fluorescence signal can be used for high spatial resolution imaging. Using SAX in 2PEF microscopy, we demonstrated fluorescence imaging of mitochondria in HeLa cells, which was stained with Rhodamine 6G. The excitation light source was femtosecond pulsed laser at the center wavelength of 820 nm and the repetition rate of 80 MHz, and the pulsed laser was focused into the samples with a water-immersion objective lens (NA=1.2). The excitation intensity was modulated at 10 kHz and the fluorescence signals were demodulated at 30 kHz. The fluorescence images show the improvement of the spatial resolution of 2PEF microscopy in 3 dimensions by using SAX.

8226-115, Poster Session

## Totally integrated linear and nonlinear optics multimodal microscopy platform to understand single cell processes

V. B. Pelegati, A. A. de Thomaz, D. B. Almeida, J. F. Adur, M. O. Baratti, H. F. Carvalho, C. Lenz Cesar, Univ. Estadual de Campinas (Brazil)

A process is a sequence of events in time in which the order of events matters and can lead to different results. Cell biology relies upon spatial and time organized events where biochemistry and biomechanics play important roles. To understand cell biology working it is necessary to use tools capable of real time non-destructive observations in space and time. This show the importance of one integrated multimodal platform capable to gather all available information during each one cell process, contrary to sequential observations that require the cell process to be restart at each modality imaging. All tools must be integrated in one instrument with the capability to acquire images simultaneously. We built such a totally integrated multimodal instrument including the following microscopy techniques: multi/single photon spectral confocal, Coherent AntiStokes Raman Scattering (CARS), confocal Micro-Raman spectroscopy, Second/Third Harmonic Generation (SHG/THG), Fluorescence Lifetime Imaging (FLIM), Fluorescence Correlation Spectroscopy (FCS), Multiple Optical Tweezers/Laser Microdissection and, finally, a tip-enhancement/Atomic Force Microscopy near field optical microscopy. Optical Tweezers and tip-enhancement/AFM are somehow different from the other techniques because they allow us to directly interfere on the cell processes, and not only to observe them. They also open the way to perform bio-mechanical measurements, while near field allowed us to perform super resolution 10-20 nm spatial resolution microscopy. This paper will describe how to set up such a system, from the excitation laser circuits to the detection circuits, and provide examples of the use of this multimodal integrated tool.

8226-116, Poster Session

## Automated control of optical polarization for nonlinear microscopy

C. Brideau, I. Micu, P. K. Stys, Univ. of Calgary (Canada)

Laser-scanning non-linear optical techniques such as multi-photon fluorescence excitation microscopy (MPM), Second/ Third Harmonic Generation (SHG/THG), and Coherent Anti-Stokes Raman Scattering (CARS) are being utilized in research laboratories worldwide. The efficiencies of these non-linear effects are dependent on the polarization state of the excitation light relative to the orientation of the sample being imaged. In highly ordered anisotropic biological samples this effect can become pronounced and the excitation polarization can have a dramatic impact on imaging experiments. Therefore, controlling the polarization state of the exciting light is important; however this is challenging when the excitation light passes through a complex optical system. In a typical laser-scanning microscope, components such as the dichroic filters, lenses, and even mirrors can alter the polarization state of a laser beam before it reaches the sample. We present an opto-mechanical solution to compensate for the polarization effects of an optical path, and to precisely program the polarization state of the exciting laser light. The device and accompanying procedures allow the delivery of precise laser polarization states at constant average power levels to a sample during an imaging experiment. We are able to compensate for perturbations of the microscope system by pre-adjusting the polarization state of the laser prior to the microscope. This pre-compensated input polarization state is modified by the microscope to achieve the desired polarization at the sample. A suite of control and calibration software allows for synchronization between image acquisition and polarization and maintains reliable calibration of the excitation polarization.

8226-117, Poster Session

## Oxygen-glucose deprivation (OGD) induced changes in the microtubules structure of cultured rat cortical neurons' axons studied using polarization SHG imaging

S. Psilodimitrakopoulos, ICFO - Institut de Ciències Fotòniques (Spain); V. Petegnief, N. de Vera, IBIB, Consejo Superior de Investigaciones Científicas (Spain); O. Hernandez, ICFO - Institut de Ciències Fotòniques (Spain); D. Artigas, ICFO - Institut de Ciències Fotòniques (Spain) and Univ. Politecnica de Catalunya (Spain); A. M. Planas, IBIB, Consejo Superior de Investigaciones Científicas (Spain); P. Loza-Alvarez, ICFO - Institut de Ciències Fotòniques (Spain)

In this study, we develop and use polarization sensitive second harmonic generation imaging microscopy (PSHG) to experimentally retrieve submicron structural information from cultured cortical neurons. The technique is used to estimate the effective orientation of the supramolecular SHG source in axons before and after simulating ischemia (using the oxygen-glucose deprivation (OGD) model) to the cultured neurons. For that purpose, the PSHG images of axons after OGD were processed pixel-by-pixel using a novel FFT based algorithm. The algorithm is based on a biophysical model that extracts the orientation of the dominant hyperpolarizability inside the axons microtubules, (the SHG source in neurons). For a selected region of interest we then retrieved the pixels' values distributions of the microtubules' hyperpolarizability effective orientations, θe, for 0, 30, 60, 90 and 120min of OGD. The hyperpolarizablity orientation is directly correlated to the geometrical characteristics of the tubulin heterodimmers forming the microtubules. We found that the center of the distributions for the effective orientation shifts to higher θe values for long exposure times under the OGD condition (>60min). For shorter periods of deprivation (30-60 min), the primary cultures appeared somewhat resistant and no changes on the PSHG analysis was found. This suggests that by observing the SHG effective orientation, θe, in axons of cultured neurons it is possible to monitor OGD induced modifications on tubulin dimers.

8226-118, Poster Session

## Probing live samples in secondhHarmonic generation microscopy using specific markers and fluorescent proteins

E. De Meulenaere, Katholieke Univ. Leuven (Belgium); R. Paesen, M. M. Ameloot, Univ. Hasselt (Belgium); P. Loza-Alvarez, ICFO - Institut de Ciències Fotòniques (Spain); J. Vanderleyden, K. Clays, Katholieke Univ. Leuven (Belgium)

Two-photon excited fluorescence (TPEF) is a nonlinear optical process that can be used in microscopy, for simultaneous imaging with second-harmonic generation (SHG). Both techniques exhibit the advantages of other nonlinear techniques using near-infrared light, e.g. a longer penetration depth combined with reduced photodamage. In TPEF, one needs a fluorophore to create contrast, while SHG will arise from non-centrosymmetrically, but highly ordered structures.

In previous work, we have characterized the second-order nonlinear optical properties of fluorescent proteins, more precisely, we determined the first hyperpolarizability (β) of several frequently used fluorescent proteins both experimentally and by quantumchemical calculations. We found that the red-shifted proteins possess a much higher β than regular GFP or eGFP, due to the more extended conjugated system typical for these red fluorescent proteins.

On the other hand, we have also shown the applicability of several carbazole-based fluorescent dyes as selective markers for SHG imaging of live cell lines. SHG microscopy is mostly performed on structures exhibiting intrinsic SHG, where no additional selectivity can be created. The introduction of specific markers for SHG microscopy can help to unravel structural properties of interactions in biochemical pathways. The highest achievable selectivity for proteins is to genetically fuse the proteins of interest with fluorescent proteins, also eliminating the need to stain the cells. Our recent experiments enable us to compare the imaging using the carbazole-based dyes with the use of red fluorescent proteins in live cells as contrast markers for SHG imaging of biological systems.

8226-119, Poster Session

## The structural origin of second-harmonic generation in fascia

M. Rivard, M. Laliberté, A. Bertrand-Grenier, C. Harnagea, Institut National de la Recherche Scientifique (Canada); C. P. Pfeffer, Harvard Medical School (United States); M. Vallières, Y. St-Pierre, A. Pignolet, M. A. El Khakani, F. Légaré, Institut National de la Recherche Scientifique (Canada)

Fascia tissue is made of collagen type I proteins and can be imaged using second harmonic generation (SHG) microscopy technique. SHG is a coherent process that strongly depends of the tridimensional structure of the medium in which it occurs. The SHG images of fascia contain long structures aligned together that reveal the direction of the collagen fibrils in the tissue. It was originally thought that those structures were individual fibrils, but after comparison of forward and backward SHG images and with a careful analysis of the forward radiation pattern in which variations are observed, it appears that this assumption is wrong and that fascia has a heterogeneous noncentrosymmetric (piezoelectric) structural arrangement at the sub-micron level. Additionally, piezoresponse force microscopy (PFM: a scanning probe technique that measures the piezoelectricity of a surface with a nanoscale spatial resolution) images of an individual collagen fibril show that is has a noncentrosymmetric structural organization along the fibrillar axis that is preserved over tens of microns. PFM images of fascia reveal that fibrils are densely packed in collagen sheets and form nano-domains in the tissue. The phase of the second order nonlinear susceptibility is Pi shifted between adjacent nano-domains of fibrils. The features found in the SHG images of fascia tissue can be explained by the coherent addition of the SHG light generated in the noncentrosymmetric nano-domains1. The structural arrangement of collagen in fascia tissue could be compared to a nanometric randomly poled crystal. [1] M. Rivard et al., Biomed. Opt. Express 2, 26-36 (2011).

8226-120, Poster Session

## Application of second-harmonic generation microscopy for in vivo observation of structural change in human dermal collagen fiber caused by aging and/or UV exposure

T. Yasui, Univ. of Tokushima (Japan); M. Yonetsu, R. Tanaka, S. Fukushima, Osaka Univ. (Japan); T. Yamashita, Y. Ogura, T. Hirao, Shiseido Co., Ltd. (Japan); T. Araki, Osaka Univ. (Japan)

Aging is an irreversible, physiological phenomenon that cannot be avoided. In skin, mechanical properties such as tension and elasticity decline gradually with age, resulting in the appearance of wrinkles and sagging. This is because fibroblast loses power to produce renewal collagen fiber due to its declined activity. Furthermore, repeated exposure of ultraviolet B (UVB) rays in sunlight to the skin often accelerates skin aging and causes changes in the skin, such as mottled pigmentation, leathery texture, laxity, sallowness, and deep wrinkle. Therefore, the need exists for an in vivo assessment technique for the degree of skin aging for studies in fields such as skin cosmetics and anti-aging dermatology.

Recently, second-harmonic-generation (SHG) microcopy has emerged as a new mode to visualize collagen fiber in biological tissues because the SHG light is specifically generated by collagen molecules due to its structural asymmetry. In this paper, a reflection-type SHG microscope equipped with a 1250-nm mode-locked Cr:Forsterite laser was applied to observe dermal collagen fiber in human cheek skin in vivo. We measured cheek skin of subjects within the age range from twenties to sixties, who give consent to serve as a subject in this experiment. The resulting SHG images visualized structual change of dermal collagen fiber caused by aging and/or UV exposure, indicating that density of fine collagen fibers was largely decreased while thickly growong collagen fibers remained. Experimental protocol was approved by Bioethics Committee for Human Experiment at Osaka University.

8226-121, Poster Session

## Second harmonic generation microscopy differentiates collagen Type I and Type III in diseased lung tissues

M. Suzuki, W. M. Elliott, The Univ. of British Columbia (Canada); J. C. Hogg, St. Paul's Hospital (Canada); T. Abraham, The Univ. of British Columbia (Canada)

The structural remodeling of extracellular matrix macromolecules is an important feature of the remodeling of the peripheral lung in chronic obstructive pulmonary disease [Abraham, T., Hogg, J. (2010) J. Struct. Biol. 171,189-196]. Multiphoton microscopy, which uses ultra-short femto-second laser pulses as an excitation source, is efficient in the induction of a highly specific second harmonic generation (SHG) signal from non-centrosymmetric macromolecules such as fibrillar collagens. Although the pioneering work of Cox et al. [(2003) J. Struct. Biol. 141, 53-62] indicated the the capability of SHG microscopy in discriminating the fibrillar collagen Type I and Type III in diseased liver tissues, this unique capability of SHG microscopy has never been exploited further [Source: PubMed]. In this study, SHG microscopy method was used to examine structural remodeling of the fibrillar collagens in human lung alveolar walls undergoing emphysematous destruction. The SHG signals originating from these diseased lung thin sections were captured simultaneously in both forward and backward scattering directions to understand the collagen structural differences and to generate a comprehensive understanding of collagen matrix remodeling. Non-descanned detectors in both reflection and transmission geometries, as well as the spectral scanning mode in the reflection geometry, were employed for generating the 3D images and SHG spectral information, respectively. An infrared ultra -short pulse laser tuned to 880-nm was used for generating SHG images. We found that spectrally clean SHG signal peaked at 440-nm with an excitation wavelength of 880-nm. The SHG images detected in the forward direction showed well developed and well structured collagen fibers while the SHG images detected in the backward direction showed striking different morphological features which included the diffused pattern of forward detected structures plus other forms of collagen structures. Comparison of these images with the well established immunohistochemical methods indicated that the structures detected in the forward direction are primarily the well developed collagen Type I fibers and the structures identified in the backward direction are diffusive structures of forward detected collagen Type I plus collagen Type III. Thus by taking advantages of both the directional pattern of SHG signals and the dynamic range of the PMT detectors, collagen Type I and Type III can be selectively visualized and subsequently quantified in the forward and backward directions respectively.

8226-122, Poster Session

## Second-harmonic generation microscopy used to evaluate the effect of the Dimethyl sulfoxide in the cryopreservation process of collagen fibers to differentiated chondrocytes

M. F. Andreoli-Risso, A. S. S. Duarte, T. B. Ribeiro, P. Bordeaux-Rego, A. Luzo, M. O. Baratti, J. F. Adur, A. A. de Thomaz, V. B. Pelegati, H. F. Carvalho, C. Lenz Cesar, F. F. Costa, S. T. Olalla-Saad, Univ. Estadual de Campinas (Brazil)

The aim of this work is to observe the effect of the usual Dimethyl Sulfoxide (DMSO) cryopreservation process on the growth of collagen fibers of chondrogenic cells from mesenchymal stem cells by Second Harmonic Generation (SHG) microscopy. Cartilaginous lesions are a significant public health problem and the use of adult stem cells represents a promising therapy for this condition. To perform this study we used Mesenchymal Stem Cells (MSC) derived from adipose tissue, which presents the capacity to differentiate into other lineages such as osteogenic, adipogenic and chondrogenic lineages. After the Approval of the Ethic Committee and written informed consent the mesenchimal stem cells obtained after a liposuction were isolated in a flow cytometry. The characterization of mesenchymal stem cells was carried out by differentiation of mesodermic lineages, and flow cytometry using specific markers. The isolated MSCs were cryopreserved by the DMSO technique and the chondrogenic differentiation was carried out using the micromass technique. We then compared the cryopreserved vs non-cryopreserved collagen fibers which are naturally formed during the differentiation process. We observed that non-cryopreserved MSCs presented a directional trend in the collagen fibers formed which was absent in the cryopreserved MSCs. We confirmed this trend quantitatively by the aspect ratio obtained by Fast Fourier Transform which was 0.76 for cryopreserved and 0.52 for non-cryopreserved MSCs, a statistical significant difference.

8226-123, Poster Session

## Three-dimensional analysis of muscle fiber orientation in a single-shot through polarization-resolved second-harmonic generation holography

D. Smith, P. Schlup, R. Bartels, Colorado State Univ. (United States)

Second harmonic generation (SHG) occurs from many native tissues and structures in un-labeled biological organisms. The most common sources of intrinsic SHG emission include Myosin filaments in muscle tissues and collagen fibrils. As second harmonic generation requires non-centrosymmetric organization from a molecular to a mesoscopic level, polarization analysis can isolate tensor components of the second order nonlinear optical susceptibility that reports on the orientation of fibers (e.g., myofibrils and collagen fibrils). In addition, anomalous values of the ratios second order optical susceptibility tensor components can be predictive of disease in some tissues. A drawback of the standard laser-scanning SHG microscopy is that raster scanning of the images in 3D typically takes several minutes to acquire a full image. With SHG holography, we have demonstrated 3D imaging in as short as 1 ms exposure times. In this work, we take a sequence of polarization-resolved SHG holographic images and reconstruct them in three dimensions. Because the SHG holography provides access to both amplitude and phase information, the data can be readily processed to provide information regarding not only in-plane fibril orientation, but also the out-of-plane orientation of the fibers. This is clearly advantageous in tissue where fibers are not carefully aligned to be perpendicular to the direction of propagation. The theoretical analysis for processing the polarization-resolved second harmonic field in three dimensions and its application to obtaining the tensor component ratios and 3D fiber orientation will be presented.

8226-124, Poster Session

## Hilbert-transform phase shifting second-harmonic generation holographic imaging

D. Smith, P. Schlup, R. Bartels, Colorado State Univ. (United States)

Second harmonic generation (SHG) occurs from many native tissues and structures in un-labeled biological organisms. The most common sources of intrinsic SHG emission include Myosin filaments in muscle tissues and collagen fibrils. The majority of SHG microscopy images have been taken with by scanning a tightly focused ultrafast laser pulse in a sample. Rapid raster scanning allows for two-dimensional images to be taken in less than a second; however, imaging in three dimensions takes much longer as the depth of focus must be scanned. This serial acquisition of SHG image voxels typically requires at least several minutes to acquire a three dimensional image of an object. Many biological processes occur at rates vastly exceeding the fraction of a Hertz update rate possible with current laser scanning SHG microscopies. With SHG holography, we have demonstrated 3D imaging in as short as 1 ms exposure times. In this work, we demonstrate phase shifting SHG holographic microscopy. This configuration provides for higher spatial resolution than for off-axis holographic configurations. We have experimentally demonstrated phase shifting SHG holography and have used it to image un-labeled biological specimens. In addition, we have developed an improved algorithm that allows for simultaneous extraction of both the reference and object intensities in addition to the phase difference from a set of four phase-shifted holographic interferograms. Further, we demonstrate a simplified phase-shifting holographic approach using Hilbert transform processing that requires only two hologram measurements. Experimental results elucidating the advantages of phase-shifting SHG holography for 3D imaging will be presented.

8226-125, Poster Session

## Nonlinear optics for the study of human scar tissue

D. Peixoto Ferro, G. Vieira-Damiani, R. L. Adam, A. A. de Thomaz, V. B. Pelegati, C. Lenz Cesar, K. Metze, Univ. Estadual de Campinas (Brazil)

Collagen fibers are important components of the dynamic process of scarring, which accompanies various diseases. Scar tissue may reveal different morphologic expressions, such as hypertrophic scars or keloids. Collagen fibers can be visualized by fluorescent light when stained with eosin.

Second Harmonic Generation (SHG) is a non linear signal that occurs only in molecules without inversion symmetry and is particularly strong in the collagen fibers arranged in triple helices. The aim of this paper is to describe the methodology for the analysis of the distribution of collagen in keloids, hypertrophic scars and conventional scars.

Samples were examined in the National Institute of Science and Techonology on Photonics Applied to Cell Biology (INFABIC) at the State University of Campinas. The images were acquired simultaneamente in a multifoton microscopy LSM 780-NLO Zeiss 40X and both signals, Two-phtoton excitaded fluorescence (TPEF) and SHG, were excited by a Mai-Tai Spectra Physics, 940nm (Ti:Sapphire laser). We used a NDD filter to filter (LP490/SP485) to SHG. For fluorescence NDD filter BP565-610. For analyses of density of collagen we used software Cell Sociology.In each case, ten images were acquired serially (512x512µ) in Z-stack.

Keloids, hypertrophic scars and normal scar tissue show different collagen architecture. Inside an individual case differences of the scar process may be found between central and peripheral parts.

In summary, the use of nonlinear optics is a helpful tool for the study of scars tissue.

8226-126, Poster Session

## Multiphoton imaging with 10 fs pulses: comparing signal strength and photo damage

L. Krapf, R. Orzekowsky-Schröder, N. Koop, H. Diddens-Tschoeke, G. Hüttmann, Univ. zu Lübeck (Germany)

Multiphoton imaging typically uses pulse widths between 100 fs and 200 fs with a corresponding spectral width of around 10 nm. Intra-cavity dispersion control enables Ti:Saphir laser with emission spectra more than 200 nm wide and corresponding sub-10 fs pulse width. With these laser parameters tissue autofluorescence of a larger number of chromophores, like NADH, flavins, and lipoproteins as well as SHG can be exited in parallel. However, the higher peek irradiance may cause additional phototoxic effects. In order to assess photodamage of ultra-short pulses, we imaged of different tissues with 10 fs and 150 fs pulses and quantified photodamage to cultured CHO cells at varying irradiances and dispersion compensation. With 10 fs pulses, skin imaging was possible with good quality at a radiant flux of 30 mW for 100 µm imaging depth. In contrast to the excitation with the Mai Tai, autofluorescence of the epidermis and SHG of collagen could be imaged together in a single scan. Imaging of the small intestine was possible with a 5.6 fold reduced radiant flux. At longer irradiance times, the 10 fs pulse showed an “inverse bleaching”, i. e. the fluorescence increased.

Additional damage to CHO cells was observed for 10 fs pulses compared to 150 fs pulse width. By introducing some dispersion to stretch the pulses no additional photodamage compared to the 150 fs pulses was observed.

In conclusion, ultra-short pulses with 200 nm spectral width can be used for simultaneous excitation of different chromophores and of SHG in autofluorescence based multiphoton imaging. Additional photodamage can be avoided by not fully compensating the dispersion of the microscope.

8226-127, Poster Session

## Breast pathology assessment using two-photon microscopy

Y. K. Tao, O. A. Ahsen, Massachusetts Institute of Technology (United States); P. Fendel, Idesta Quantum Electronics (United States); A. E. Cable, Thorlabs Inc. (United States); D. Shen, J. L. Connolly, Beth Israel Deaconess Medical Ctr. (United States); J. G. Fujimoto, Massachusetts Institute of Technology (United States)

Two-photon microscopy (TPM) has advantages of high resolution, molecular-specificity, and improved imaging depth and contrast over conventional white-light and fluorescence microscopes, enabling endogenous and exogenous contrast imaging in both in vivo and ex vivo specimens. TPM is particularly well-suited for visualizing subcellular-resolution biomarkers of disease progression, such as nuclear size and shape, and morphological changes, such as reorganization of collagen, which are markers of dysplastic and metastatic tissues. The advantage of TPM versus standard histological processing is that it can rapidly assess specimen surfaces and cut-faces in real-time, eliminating time-consuming formalin fixation and paraffin embedding processes. TPM would also be faster than frozen-section preparation and enables non-destructive broad tissue coverage. Therefore, TPM could potentially enable intraoperative assessment of tumor margins. In this project, we investigate the utility and advantages of using 10 femtosecond pulses for two-photon microscopy imaging of breast tumor margins.

Second harmonic generation (SHG), intrinsic NADH two-photon fluorescence, and exogenously stained human breast specimens, both in normal tissue and regions suspected for invasive carcinoma and carcinoma in situ, were imaged using TPM. Exogenously stained specimens showed terminal ductal lobular unit (TDLU) epithelial cell nuclei and surrounding adipocytes and collagenous stroma, imaged using SHG. At higher magnification, sub-nuclear features in the epithelial cells were also visible. Stained specimens of lobular carcinoma in situ (LCIS) showed regions of atypical lobular hyperplasia (ALH). In addition, specimens imaged using intrinsic NADH fluorescence and SHG showed TDLU in collagenous stroma, demonstrating the capacity for contrast-free two-photon microscopy in human breast.

8226-128, Poster Session

## SHG microscopy of articular cartilage to image osteoarthritis

M. Houle, Institut National de la Recherche Scientifique (Canada); C. P. Brown, Univ. of Oxford (United Kingdom); M. Nicklaus, Institut National de la Recherche Scientifique (Canada); A. Price, Univ. of Oxford (United Kingdom); A. Ruediger, Institut National de la Recherche Scientifique (Canada); H. Gill, Univ. of Oxford (United Kingdom); F. Légaré, Institut National de la Recherche Scientifique (Canada)

Osteoarthritis is a painful and debilitating condition involving the dysfunction and degeneration of joint tissue. The irreversible stage of this degeneration is thought to be damage to the collagen meshwork, which leads to a cascade of degradation. Recent studies have shown that SHG microscopy has considerable potential for imaging this degradation [1]. Here, we use SHG to probe the modification of the collagen structure in the deep cartilage matrix. In thin sections of human tissue, we have measured the polarisation dependence of the SHG signal in the forward and in the backward direction. For tissues with early-stage disease, we found regions (20×20microns) of high forward SHG signal in which the polarization angle at maximum amplitude differs from elsewhere in the tissue. In the forward direction, it appears that SHG reveals clearly the appearance of osteoarthritis in terms of collagen bundling and microcracking. Images acquired in the backward direction show changes to the helices within the fibrils, indicating degradation in the extracellular matrix and synthesis of new collagen by the cells. Considering backscattering as a process that will redirect forward SHG signal in the backward direction for thick tissue samples, SHG microscopy may provide a very useful imaging modality to understand the collagen meshwork modification of osteoarthritis.

[1]. C.P. Brown, M-A Houle et al. (2011, submitted to Journal of the Mechanical Behaviour of Biomedical Materials), Damage initiation and progression in the cartilage surface probed by nonlinear optical microscopy.

8226-129, Poster Session

## Second-harmonic generation microscopy used to evaluate chondrogenic differentiation of mesenchymal stem cells for cartilage repair

P. Bordeaux-Rego, M. F. Andreoli-Risso, A. S. S. Duarte, T. B. Ribeiro, M. O. Baratti, B. de Campos Vidal, J. B. Miranda, J. F. Adur, A. A. de Thomaz, V. B. Pelegati, F. F. Costa, H. F. Carvalho, C. Lenz Cesar, A. Luzo, P. Kharmadayan, S. T. Olalla-Saad, Univ. Estadual de Campinas (Brazil)

Articular cartilage injury remains one of the major concerns in orthopedic surgery. Mesenchymal stem cell (MSC) transplantation has been introduced to avoid some of the side effects and complications of current techniques. MSCs retain both high proliferative multipotentiality, including chondrogenic differentiation potential. With the aim to evaluate the chondrogenic differentiation of mesenchymal stem cells, we used Second Harmonig Generation (SHG) microscopy to analyze the aggregation and orientation of collagen fibrils in the hyaline cartilage of rabbit knee. The experiment was performed using implants with type II collagen hydrogel (a biomaterial that mimics the microenvironment of the cartilage), one implant containing MSC and the other without MSC (control). After 10 weeks, the rabbit's knees were dissected and fibril collagen distribution and spatial organization in the extracellular matrix of the lesions were verified by SHG. The result shows significant differences, while in histological sections of the cartilaginous lesions with MSC the collagen fibers are organized and regular; in the control sections the collagen fibers are more irregular, with absence of cells. A macroscopic analysis of the lesions confirms this difference, showing more percentage of lesions filling in knees treated with MSC than knees controls. This study demonstrates the SHG microscopy will be an excellent tool to help in the evaluation of the effectiveness of MSC-based cell therapy for cartilage repair

8226-130, Poster Session

## In vivo multiphoton microscopy associated to 3D image processing for human skin characterization

T. Baldeweck, L'Oréal Recherche et Innovation (France); E. Tancrède, L'Oréal Recherche et Innovation (France) and Service de dermatologie Hôpital St. Louis (France); P. Dokladal, S. Koudoro, V. Morard, F. Meyer, E. Decencière, Ecole Nationale Supérieure des Mines de Paris (France); A. Pena, L'Oréal Recherche et Innovation (France)

Multiphoton microscopy has emerged as a promising non-invasive skin imaging technique as it allows the characterization of normal skin, photoaging as well as dermatological disorders. The aim of this study was to assess whether multiphoton microscopy coupled to specific 3D image processing tools could provide new insights into the organization of different skin components and their modifications due to skin aging.

For that purpose, we performed a clinical trial on 15 young and 15 aged human female volunteers on the ventral and dorsal side of the forearm using the DermaInspect® medical imaging system. We visualized the skin by taking advantage of intrinsic multiphoton signals from collagen (SHG), cells and elastic fibers (2PEF).

We also developed 3D image processing algorithms adapted to in vivo multiphoton images of human skin in order to extract quantitative parameters on the different skin components. The processing contains two main steps. The first one consists in separating the different skin layers (3D segmentation) and the second one in applying adequate filtering to be able to measure quantitative parameters (3D quantification) in both epidermis and superficial dermis.

The results show that in vivo multiphoton microscopy is able to evidence several skin modifications due to skin aging: morphological changes in the epidermis and modifications in the quantity, organization and orientation of the collagen and elastic fibers network.

In conclusion, the association of multiphoton microscopy with specific image processing allows visualizing and quantifying the three-dimensional organization of skin components and offers a powerful tool for cosmetic and dermatological investigations.

8226-131, Poster Session

## Quantitative second-harmonic generation imaging to detect osteogenesis imperfecta in human skin samples

J. F. Adur, Univ. Estadual de Campinas (Brazil) and National Univ. of Entre Rios (Argentina); A. Ferreira, L. D'Souza-Li, V. B. Pelegati, A. A. de Thomaz, D. B. Almeida, M. O. Baratti, H. F. Carvalho, C. Lenz Cesar, Univ. Estadual de Campinas (Brazil)

Osteogenesis Imperfecta (OI) is a genetic disorder that leads to bone fractures due to mutations in the Col1A1 or Col1A2 genes that affect the primary structure of the collagen I chain with the ultimate outcome in collagen I fibrils that are either reduced in quantity or abnormally organized in the whole body. The molecular genetics characterization of the disease would be overwhelmed by the heterogeneities of the phenotypes related to this disease. A quick test screening of the patients would largely reduce the sample number to be studied by the time consuming molecular genetics techniques. For this reason an assessment of the human skin collagen structure by Second Harmonic Generation [SHG] can be used as a screening technique to speed up the correlation of genetics/phenotype/OI types understanding.

In the present work we have used quantitative second harmonic generation (SHG) imaging microscopy to investigate the collagen matrix organization of the OI human skin samples comparing with normal control patients. By comparing fibril collagen distribution and spatial organization, we calculated the anisotropy and texture patterns of this structural protein. The analysis of the anisotropy was performed by means of the two-dimensional Discrete Fourier Transform and image pattern analysis with Gray-Level Co-occurrence Matrix (GLCM), both computed with free ImageJ software. From these results, we show that statistically different results are obtained for the normal and disease states of OI. We suggest that our results provide a framework to use SHG as a clinical diagnostic to classify human OI accordingly to severity types.

8226-132, Poster Session

## Applications of second-harmonic (SHG) and third-harmonic generation(THG) in diagnostic cytology and histology

D. Peixoto Ferro, G. Vieira-Damiani, J. F. Adur, R. L. Adam, I. Lorand-Metze, V. B. Pelegati, A. A. de Thomaz, C. Lenz Cesar, K. Metze, Univ. Estadual de Campinas (Brazil)

Routine cytologic and histologic examinations of human tissues, blood or effusions are still the gold standard for the diagnosis of neoplasias and other diseases all over the world. These procedures are mainly based on simple laboratory staining procedures, which date from the 19th century or the early 20th century and use the standard light microscope.

Nonlinear optical microscopy allows the creation of images of high resolution and the detection of various types of structures due to their physicochemical properties.

The aim of this study was to apply nonlinear optical microscopy for the analysis of specimens in cytology and histology and to look for possible advantages for the diagnostic process..

We used frozen sections and cytologic smears and applied second-harmonic generation (SHG), and third-harmonic generation (THG). We examined material from patients with leukemia, multiple myeloma, adenocarcinomas and fibromas We found very strong THG signals in the nuclei of leukemias, multiple myelomas, and parasites stained with acridine orange. A similar strong signal was seen in cells and tissues stained with MGG, but the cells were easly destroyed by overheating Frozen sections of tumors stained with haematoxylin-eosin showed always a clear signal for SHG in collagen and THG in the nuclei. The information of the presence of collagen (THG) and the precise design of the nuclear chromatin structure were always an additional help for diagnosis.

In conclusion, the application of nonlinear optical methods in diagnostic cytology and frozen section pathology can give additional clues for the correct diagnosis.

8226-133, Poster Session

## A study on the spectral dependence of SHG generation from collagen tissues

M. Shen, The Univ. of British Columbia (Canada); H. Wang, A. M. D. Lee, J. Zhao, H. Zeng, The BC Cancer Agency Research Ctr. (Canada); S. Tang, The Univ. of British Columbia (Canada)

Second harmonic generation (SHG) imaging has emerged as a powerful tool for imaging biological tissues with submicron resolution. Since the first practical SHG imaging on fiber bundle in rat tail tendon in 1986, imaging collagen fibers in a variety of connective tissues and acto-myosin complexes in muscle have constituted the majority of applications of SHG. Besides qualitative visualization, many efforts in the past decades have shown the promise of SHG in characterizing the optical properties of tissues quantitatively. For example, the spectral dependence of SHG intensity is an optical property that is not fully understood so far. A few published results have shown a sine-like shaped curve having peak excitation wavelength around 800 nm. In this paper, we will investigate this problem in detail through experiments. Some standard second harmonic generators such as nonlinear optical crystals were excited by multiple wavelengths under the tight focusing condition. The SHG excitation spectrum was compared with theoretical prediction and good match was obtained. Proper calibration is found to be critical because from shorter to longer wavelength, the transmission efficiency of the measurement instrument could vary as much as 10 times. Through further examining different types of biology tissues, it is found that our experimental results are different from previously published ones. For crystals, a curve fitting according 1/ 2 was observed. For biology samples, depending on the thickness or tissue type, the trend can vary according to 1/ n (n>4). Several wavelength dependant factors such as focal area variation, phase matching and scattering are attributed to the measured results.

8226-134, Poster Session

## Two-photon imaging and spectroscopy of fresh human colon biopsies

R. Cicchi, A. Sturiale, G. Nesi, F. Tonelli, F. S. Pavone, Univ. degli Studi di Firenze (Italy)

Two-photon fluorescence (TPEF) microscopy is a powerful tool to image human tissues up to 200 microns depth without any exogenously added probe. TPEF can take advantage of the autofluorescence of molecules intrinsically contained in a biological tissue, as such NADH, elastin, collagen, and flavins. Two-photon microscopy has been already successfully used to image several types of tissues, including skin, muscles, tendons, bladder. Nevertheless, its usefulness in imaging colon tissue has not been deeply investigated yet. In this work we have used combined two-photon excited fluorescence (TPEF), second harmonic generation microscopy (SHG), fluorescence lifetime imaging microscopy (FLIM), and multispectral two-photon emission detection (MTPE) to investigate different kinds of human ex-vivo fresh biopsies of colon. Morphological and spectroscopic analyses allowed to characterize both healthy mucosa, polyp, and colon samples in a good agreement with common routine histology. Even if further analysis, as well as a more significant statistics on a large number of samples would be helpful to discriminate between low, mild, and high grade cancer, our method is a promising tool to be used as diagnostic confirmation of histological results, as well as a diagnostic tool in a multiphoton endoscope or colonoscope to be used in in-vivo imaging applications.

8226-135, Poster Session

## Investigating protein-protein interactions in living cells

## with FRET, FLIM, FCCS and ICCS

Y. Sun, A. Periasamy, Univ. of Virginia (United States)

Abstract: The development of non-invasive fluorescence microscopy imaging techniques, used in combination with the genetically encoded fluorescent proteins (FPs), provides the tools necessary for the direct visualization of protein interactions inside living cells. For example, Förster resonance energy transfer (FRET) microscopy, fluorescence cross-correlation spectroscopy (FCCS) and image cross-correlation spectroscopy (ICCS) have been used to study protein-protein interactions in living cells. Here, all three techniques are employed to investigate the association between the Phosphatase inhibitor-2 (I2) and the prolyl isomerase Pin1 (Pin1) in living cells. For FRET, both intensity-based and time-resolved measurements were carried out. The strength and limitation of each technique are discussed based on the study.

Key Word: Protein-protein interaction, Fluorescence proteins (FPs), Förster resonance energy transfer (FRET) microscopy, Fluorescence lifetime imaging microscopy (FLIM), Fluorescence correlation spectroscopy (FCS), Fluorescence cross-correlation spectroscopy (FCCS), Image correlation spectroscopy (ICS), Image cross-correlation cpectroscopy (ICCS), Phosphatase inhibitor-2 (I2), prolyl isomerase Pin1 (Pin1).

8226-136, Poster Session

## Spectral FLIM detection and new analysis schemes for confocal laser scanning microscopes

F. Koberling, B. Krämer, M. König, V. Buschmann, M. Wahl, H. Rahn, U. Ortmann, R. Erdmann, PicoQuant GmbH (Germany); S. Fore, PicoQuant Photonics North America, Inc. (United States); G. Weiß, PicoQuant GmbH (Germany); I. Gregor, J. Enderlein, Georg-August-Univ. Göttingen (Germany)

Confocal laser scanning microscopes (CLSM) are an essential tool in biological and biomedical research. Their functionality can be further enhanced by adding sensitive time-resolved data acquisition capabilities, enabling for Fluorescence Lifetime Imaging (FLIM). Complete upgrade packages allow the user to apply these techniques easily to all modern CLSMs from major manufacturers.

Many state-of-the-art confocal microscopes have the ability to obtain spectrally resolved images. The separation of multiple dye molecules in biological samples, however, remains often a problem. The combination of spectrally resolved detection together with fluorescence lifetime measurements allows for the simultaneous detection of spectral AND lifetime parameters which dramatically improves the separation capability. In addition, FLIM FRET can be performed with excellent suppression of autofluorescent background. A newly developed 32 channel spectral FLIM (sFLIM) detection module is utilized for this purpose.

However, conventional tail-fitting or re-convolution fitting techniques are not optimally adapted for the separation of different dye molecules, especially when they exhibit a bi- or higher exponential lifetime decay behavior.

In order to overcome this problem, we have developed a pattern-matching technique which can be applied to separate dye molecules due to their decay pattern.

In addition to lifetime, also spectral absorption and emission properties of the dye molecules can be utilized for the separation of different fluorescent species. For this aim, the fluorescence is excited by pulsed interleaved excitation with multiple wavelengths and detected with two or more spectrally separated detectors.

8226-137, Poster Session

## Fluorescence lifetime imaging microscopy with acousto-optic deflectors

K. Wang, J. Qi, Y. Shao, J. Qu, H. Niu, Shenzhen Univ. (China)

Fluorescence Lifetime Imaging Microscopes generally employ inertia-limited galvanometer-driven mirrors to scan the laser beam across the field of view, which limits its efficacy, particularly for fast functional fluorescence imaging. Both the achievable frame rates and signal integration time at sites of interest are limited. In this paper, we developed a fluorescence lifetime imaging microscope which uses a pair of acousto-optic deflectors (AODs) to scan the laser beam, which provides inertia-free beamsteering. The AODs employ high-frequency sound waves in a crystal, which acts as a tunable diffraction grating. By adjusting the acoustic frequency, the grating constant varies, which changes the beam deflection angle. By employing two orthogonal AODs, multiple sites of interest on the sample can be selected and sampled at very high frame rate. The emitted fluorescence from the sample is detected by a Time-Correlated Single Photon Counting (TCSPC) imaging module. We control the AOD devices, TCSPC module and image acquisition using LabView. The sites of interests on the sample can be addressed and sampled for lifetime measurement. In addition, the integration time can also be controlled. Therefore high-speed fluorescence lifetime imaging can be achieved.

8226-138, Poster Session

## A simple laser Ti:Sapphire system upgrade for multimodal nonlinear optical microscopy

M. Laliberté, A. Bertrand-Grenier, Institut National de la Recherche Scientifique (Canada); Y. Kim, B. Burgoyne, A. Villeneuve, Jr., Genia Photonics Inc. (Canada); F. Légaré, Institut National de la Recherche Scientifique (Canada)

Coherent anti-Stokes Raman scattering (CARS) microscopy is a label-free imaging technique that is capable of real-time, non-pertubative examination of living cells and organisms based on molecular vibrational spectroscopy with a sub-micron spatial resolution. For many applications, CARS microscopy is used with other nonlinear imaging techniques, like 2-photon fluorescence (2PF), fluorescence lifetime (FLIM), second harmonic generation (SHG) and third harmonic generation (THG). These techniques are typically using a femtosecond laser oscillator to generate the images, in contrast with the picosecond optical parametric oscillator (OPO) used for CARS microscopy. In addition of not being optimal for 2PF, FLIM, SHG and THG, an OPO is difficult to handle for non-expert with optics. Thus, to have a platform for multimodal nonlinear optical microscopy, it may look necessary to have a femtosecond laser oscillator and a picosecond OPO, which turns to be an expensive investment.

Considering that multimodality is the key to image tissues, we have in collaboration with Genia Photonics built a laser system to make multimodal nonlinear microscopy, consisting of a femtosecond laser oscillator synchronized electronically with a fiber-based picosecond Master Oscillator Power Amplifier (MOPA). The MOPA system clock is used to control the repetition rate of the Spectra-Physics Tsunami. Recent results show that this system offers superior stability to the system using two synchronized picosecond Ti-Sa oscillators, and equivalent to using picosecond parametric oscillator, in a system friendly to use for a fraction of the cost.

8226-139, Poster Session

## Integrated multimodality microscope for functional imaging of engineered and natural tissues

Y. Zhao, B. W. Graf, R. Devolder, H. Kong, Z. Mahmassani, M. D. Boppart, S. A. Boppart, Univ. of Illinois at Urbana-Champaign (United States)

A highly integrated microscope, which embodies multimodal imaging capabilities on a single laser source platform, is demonstrated for in vivo imaging of engineered and natural tissues. The instrument combines the complimentary imaging functions of optical coherence (OCM), multi-photon (MPM, including two-photon excitation fluorescence (TPE) and second harmonic generation (SHG)), and fluorescence lifetime imaging microscopy (FLIM). In addition, extended optical coherence tomography (OCT) methodologies, including spectroscopic analysis, Doppler measurement, magnetomotive OCT, and optical coherence elastography (OCE) are embedded, which enhance either the functional detection specificity or contrast capability of the OCM modality. While utilizing a single-laser dual-spectrum light source, which consists of a widely tunable (~ 300 nm), Ti-sapphire femtosecond laser with a portion of its output specially broadened via supercontinuum generation in a photonic crystal fiber, this multimodal imaging instrument has the capability to simultaneously reveal complimentary information of multiple properties of biological tissues. These properties include cell morphology and dynamics (by OCM), physiological functions of specific molecules and proteins (by MPM), cell metabolism and viability (by FLIM), tissue biomechanical parameters (by OCE), flow dynamics (by Doppler OCM), among others. The system is applied to in vivo imaging of un-treated human skin and engineered bilayer skin equivalents which consists of green fluorescent protein (GFP)-expressed fibroblasts and keratinocytes seeded on three dimensionally structured scaffolds. Full characterization of these samples are realized by this multimodality imaging microscope which demonstrates potential applications in numerous areas such as tissue engineering, cell biology, and other biomedical studies.

8226-141, Poster Session

## Building an “affordable” coherent Raman scattering (CRS) microscope

C. W. Freudiger, Harvard Univ. (United States); K. Q. Kieu, College of Optical Sciences, The Univ. of Arizona (United States); G. R. Holtom, Harvard Univ. (United States); N. Peyghambarian, College of Optical Sciences, The Univ. of Arizona (United States); X. S. Xie, Harvard Univ. (United States)

Coherent Raman scattering (CRS) microscopy allows biomedical imaging based on vibrational spectroscopy without the need for dye staining or fluorescent labeling. In contrast to spontaneous Raman scattering, the CRS sample is excited with two pulsed laser beams. This stimulated excitation of molecular transition results in greatly improved sensitivity and imaging speed. However, CRS microscopy systems have traditionally been expensive and challenging to align. We present the implementation of a robust CRS microscope based on an all-fiber laser and inexpensive beam-scanning systems. This is an essential step toward implementation of a clinical CRS system. To demonstrate that this “affordable” CRS microscope does not compromise performance, we present sensitive tissue imaging with contrast from lipids, protein, blood and water with acquisition speeds of 1 frame per second.

8226-142, Poster Session

## Multicolor stimulated Raman scattering (SRS) microscopy

F. F. Lu, D. Fu, M. Ji, C. W. Freudiger, X. Zhang, X. Ni, G. R. Holtom, X. S. Xie, Harvard Univ. (United States)

Stimulated Raman scattering (SRS) microscopy has been successfully demonstrated for video-rate label-free chemical imaging with high sensitivity using the lock-in detection scheme. However, the narrowband (1-5 picoseconds pulses) excitation makes it difficult to distinguish mixed chemical species with overlapping Raman bands. High sensitivity broadband SRS is hard to realize due to the lack of lock-in array detectors with both large dynamic range and high spectral resolution. Frequency modulation and tailored-spectra excitation techniques are well suited for accurate measurement of one species in the presence of interfering species. Unfortunately, it can only measure one species at a time. In some of the biological applications, the relative concentration or the ratio between different chemical species could be more significant than the absolute concentration of one species. Here we present a multicolor excitation scheme which can be used to simultaneously measure the relative concentrations or the ratios of a few chemical species in a complicated environment. A broadband femtosecond pump beam is manipulated into a few narrow peaks (FWHM 1-2 nm, a spectral comb) by the spectral-tailoring using a spatial light modulator (SLM). Mathematical processing is used to calculate, in real-time, the relative concentrations or ratios of different targeted components. The mixture of oleic acid, cholesterol and ethanol is measured for system characterization and calibration. Simultaneous lipid and protein imaging in a mouse ear is also demonstrated. Multicolor SRS microscopy offers new potential for multiple chemical selective imaging and high throughput screening.

8226-143, Poster Session

## Evaluation of atherosclerotic plaque development by texture analysis of multimodal CARS images of rabbit arteries

A. C. T. Ko, National Research Council Canada (Canada)

Atherosclerotic plaques and its development are complex systems where the composition and structure vary greatly with respect to age, the location along and within the vessel. A multimodal approach based on a single-platform TPEF, SHG and CARS has recently demonstrated its strength in imaging arterial structures, in particular tracing the morphological changes within the extracellular components of the vessel wall [1]. Several other studies have also demonstrated the use of NLO microscopy to image arterial tissue [2,3]. However, few of these studies have provided quantitative descriptors of the images and related these metrics to the development of atherosclerosis or vascular wall anatomy and pathology. Tonal and texture parameters from nonlinear optical images have the potential to provide objective metrics that correspond to structural and biochemical changes that occur within the vessel wall in early and late stage atherosclerosis. Textural features [4] extracted from nonlinear optical images were investigated for their utility in providing quantitative descriptors of structural and compositional changes associated with plaque development. All studied texture parameters are derived from the image histogram and gray level co-occurrence matrix and are evaluated according with its ability to classify differences between plaque developed at different aorta locations, in particular at the aorta arch and the external iliac aorta. Tonal-texture parameters can be linked to key histological features that characterize vulnerable plaque: the thickness and density of the fibrous cap, size of the atheroma, and the level of inflammation indicated through lipid deposition.

[1] Ko et al, Multimodal nonlinear optical imaging of atherosclerotic plaque development in myocardial infarction-prone rabbits J. Biomed. Opt. 15 020501

[2] Lilledahl M B et al 2007 Characterization of vulnerable plaques by multiphoton microscopy J. Biomed. Opt. 12 044005

[3] Le et al 2007 Label-free molecular imaging of atherosclerotic lesions using multimodal nonlinear optical microscopy J. Biomed. Opt. 12 054007

[4] Haralick at al 1973 Texture features for image classification IEEE Trans. Sys. Man Cybernet. SMC-3 610-21

8226-144, Poster Session

## Application of hyperspectral coherent anti-Stokes Raman scattering microscopy to pharmaceutics

A. L. Fussell, E. T. Garbacik, Univ. Twente (Netherlands); S. Gueres, Heinrich-Heine-Univ. Düsseldorf (Germany); C. Strachan, Univ. of Otago (New Zealand); P. Kleinebudde, Heinrich-Heine-Univ. Düsseldorf (Germany); H. L. Offerhaus, Univ. Twente (Netherlands)

Chemical selectivity and spatial resolution are important factors in imaging. Hyper-spectral coherent anti-Stokes Raman scattering (CARS) microscopy is a novel technique applied for rapid spectrally and spatially resolved analysis of pharmaceutical oral dosage forms. Active pharmaceutical ingredients (APIs) can exist in different solid state forms such as various crystalline and amorphous forms. The conversion between the different solid state forms can occur during production and storage, sometimes leading to unpredictable solid state forms in the oral dosage form. This can lead to unpredictable and incomplete API dissolution resulting in uncontrollable bioavailability and therapeutic efficacy of a medicine. There is thus a need to identify and visualize different solid state forms and API distribution on the surface of pharmaceutical oral dosage forms. In this study hyper-spectral CARS microscopy was used to rapidly image the different spatial distribution of indomethacin (Biopharmaceutics Classification System class two model API) and its solid state forms on the surface of an oral dosage form. The hyper-spectral CARS microscopy results give a diffraction limited spatial resolution of about 400 nanometers and spectral resolution of a few wavenumbers. Hyper-spectral stacks containing 256x256 pixels covering 200 wavenumbers are acquired in less than 90 seconds.

8226-145, Poster Session

## The use of two-photon microscopy to study the biological effects of focused ultrasound on the brain

A. Burgess, E. E. Cho, L. Shaffaf, T. Nhan, C. Poon, K. H. Hynynen, Sunnybrook Health Sciences Ctr. (Canada)

Focused ultrasound (FUS) has been used to successfully disrupt the blood-brain barrier (BBB), aiding in the delivery of therapeutic agents to the brain and leading to improvements in disease pathology. Although significant progress has been made in the development of FUS technology, there is still a lack of understanding of the biophysical mechanisms of the BBB disruption and the microscopic effects of this disruption on brain cells. In this study, we combine a custom built ultrasound transducer with two-photon microscopy to conduct real time monitoring of BBB disruption in vivo. We have manufactured and tested a single element and a multi-element piezoelectric transducer with frequencies ranging from 1.15 to 1.30 MHz. Sonications were performed using 0.07-0.25 MPa estimated in situ pressure, 10 ms pulses, 1Hz pulse repetition frequency for a total duration of 120 s in the presence of microbubbles. BBB disruption was observed through a cranial window created in the rat skull after intravenous injection of dextran conjugated-Texas Red (MW: 10,000 - 70,000 Da). Using this experimental setup, we have observed and characterized 3 different leakage patterns following BBB disruption. Our results indicate that varying the acoustic power may allow us to control the mechanism of BBB disruption. Furthermore, we have labelled astrocytes and pericytes in vivo in order to visualize the effects of FUS on these cell populations. Combination of our custom transducers with two-photon microscopy will allow significant advancement in evaluating the applicability of FUS as a potential treatment for brain disorders.

8226-146, Poster Session

## Dynamic nuclear protein interactions investigated using FRET-FLIM and FCS

A. P. Siegel, N. Hays, R. N. Day, Indiana Univ. (United States)

The discovery and engineering of novel fluorescent proteins (FPs) from diverse organisms is yielding fluorophores with exceptional characteristics for live-cell imaging. In particular, the development of FPs for Förster resonance energy transfer (FRET) microscopy and fluorescence correlation spectroscopy (FCS) provide important tools for monitoring dynamic protein interactions inside living cells. Fluorescence lifetime imaging microscopy (FLIM) quantitatively maps changes in the spatial distribution of donor FP lifetimes that result from FRET with acceptor FPs. FCS probes dynamic protein associations through its capacity to monitor localized protein diffusion. Here, we use FRET-FLIM combined with FCS in living cells to investigate changes in protein mobility due to protein-protein interactions involving transcription factors and chromatin modifying proteins that function in anterior pituitary gene regulation. The heterochromatin protein 1 (HP1) plays a key role in the establishment and maintenance of heterochromatin through its interactions with histone methyltransferases. Recent studies, however, also highlight the importance of HP1 as a positive regulator of active transcription in euchromatin. Intriguingly, we observed that the transcription factor CCAAT/enhancer-binding protein alpha (C/EBP$\alpha$) interacts with HP1 in regions of pericentromeric heterochromatin in mouse pituitary cells. These observations prompted us to investigate the relationship between HP1 dynamic interactions in pituitary specific gene regulation.

8226-150, Poster Session

## Monitoring changes in endogenous fluorophores through FLIM and spectral imaging

V. Jyothikumar, Y. Sun, A. Periasamy, Univ. of Virginia (United States)

Changes in energy metabolism, mitochondrial functions and of reactive oxygen species are often supposed to induce alterations in cellular activity. NADH and FAD are among the brightest endogenous fluorophores inside biological tissue and they can be used to image tissue architecture without any exogenous probe. Their fluorescence can be excited by multi-photon microscopy using NIR laser wavelengths [Zipfel WR et al, 2003;]. Moreover, they are the main electron donor and acceptor in the biochemical process of oxidative phosphorylation, which is the main metabolic pathway used by biological tissues to produce energy. This important feature enables the use of NADH and FAD fluorescence not only to investigate tissue morphology, but also to provide functional information about cellular metabolism which can in turn be related to disease conditions, for example cancerous or pre-cancerous. Further to investigate the changes in endogenous fluorophores, the cellular metabolic activity was altered on addition of different substrates at the time of imaging.

8226-24, Session 4

## Multiphoton tomography in animal research

K. König, JenLab GmbH (Germany) and Saarland Univ. (Germany)

The novel multiphoton tomograph MPTflex with its flexible articulated arm provides high-resolution optical biopsies. One favorite application is the investigation of fluorescent proteins, in particular green and red emitting proteins, in living mice. Nestin-expressing stem cells have been tracked over hours in the hair follicles of nude mice with 300 nm lateral resolution and 1 µm axial resolution non-invasivily. Furthermore, the SHG pattern in tumors have been investigated. Combined with microsurgery the pharmacokinetics of fluorophores in the liver of small animals has been studied.

Multiphoton tomographs with flexible arms may become interesting nonlinear imaging tools in animal research.

8226-25, Session 4

## Looking stem cells at work with a flexible multiphoton tomograph

A. Uchugonova, Univ. des Saarlandes (Germany); R. M. Hoffman, Anticancer Inc. (United States); M. Weinigel, K. König, JenLab GmbH (Germany)

We report on the finding of nestin-GFP expressing stem cells in their native niche in the bulge of the hair follicle of living mice by using high-resolution in-vivo multiphoton tomography. The 3D imaging with submicron resolution was based on two-photon induced fluorescence and second harmonic generation (SHG) of collagen. Migrating stem cells from the bulge to their microenvironment have been detected inside the skin during optical deep tissue sectioning.

8226-26, Session 4

## Spectral phasor analysis allows rapid and easy unmixing of fluorescence microscopy spectral images

F. Fereidouni, A. Bader, H. C. Gerritsen, Utrecht Univ. (Netherlands)

Global analysis algorithms based on the phasor representation have been demonstrated to be very powerful for the analysis of lifetime imaging data. Here, we present the analogous approach for spectral imaging data. In spectral phasor analysis the fluorescence spectrum of each pixel in the image is Fourier transformed. Next, the real and imaginary components of the first harmonic of the transform are employed as X and Y coordinates in a scatter (spectral phasor) plot. Importantly, the spectral phasor representation allows for rapid (real time) semi-blind spectral unmixing of up to three components in the image. This is demonstrated on a specimen containing fluorescently labeled DNA, actin and tubilin. In addition the method is used to analyze autofluorescence of grass halm cells. The spectral phasor approach can be used on spectral imaging data recorded with 8 or more spectral channels.

8226-27, Session 4

## Photon reassignment for structured light imaging based microscopy

V. R. Singh, Singapore-MIT Alliance (Singapore); J. Rajapakse, Nanyang Technological Univ. (Singapore); P. T. C. So, Massachusetts Institute of Technology (United States)

In this paper, we report a new method for 3D visualization of biological tissues utilizing single-photon and two-photon structured light wide-field microscopic imaging systems. This new method provides the capability to image deeper into biological tissue by reassigning fluorescence photons generated from off-focal plane excitation. Recently, novel methods for 3D resolved imaging based on structured light illumination has been developed by several groups (Wilson et al, Gustasson et al, and Mertz et al) allowing wide-field visualization of the focal plane while rejecting out-of-focus background “haze”. While these methods improve image contrast, the loss of out-of-focal plane fluorescent photons limits image signal-to-noise ratio (SNR). Our new method seeks to better utilize these “lost” photons by using the ‘prior knowledge’ about the optical transfer function of the structured light illumination. Utilizing a maximum likelihood approach, we identify the most likely fluorophores distribution in 3D that will produce the observed image stacks under structured and uniform illumination using an iterative maximization algorithm. The accuracy of the reconstruction partly depends on the smoothness of initial estimate chosen and the constrained parameters for convergence of the algorithm. It should be noted that this approach is different from typical deconvolution methods. The fluorophores distribution in 3D is already known from using existing structured light reconstruction algorithms although with limited SNR. This known distribution is used as the prior for the maximization algorithm that iteratively improves the SNR of this distribution. The proposed approach is first validated with the simulation data where the results show the significant improvement in SNR compare to existing methods and then it further applied for experimentally recorded data of tissue sample. Our results show the significant optical sectioning capability of tissue sample while preserving the photons count, which is usually not achievable with other existing structured light imaging methods.

8226-28, Session 4

## Single-shot 3D multi-photon microscopy

E. Y. S. Yew, Singapore-MIT Alliance (Singapore); P. T. C. So, Massachusetts Institute of Technology (United States)

Temporal focusing is the basis for performing wide-field two-photon microscopy that is axially resolved. This is accomplished through controlling the pulse width of the excitation pulse such that it is the narrowest at the focal plane resulting in localized high photon flux in the object space. In order to generate a three-dimensional image volume, it is necessary to scan the focal plane through the volume of interest. This can be done either by scanning the object or the objective. In principle, the latter is equivalent to adding a quadratic phase to the spectrum (i.e a chirp) as demonstrated previously (Durst et al, 2006). In principle, it is possible to generate multiple planes each separated at some distance and, as such, either create a system wherein volume of interest in 3D may be observed simultaneously. This is of importance in biological systems where organs and tissues extend in the third dimension. We present a system wherein we are able to generate multiple images at different depths thereby paving the way for simultaneous 3D volume imaging.

8226-29, Session 4

## Multimodal polarimetric nonlinear microscopy in tissues

S. Brasselet, H. Rigneault, J. Duboisset, P. Ferrand, D. Ait-Belkacem, S. Brustlein, F. Bioud, F. Munhoz, Institut Fresnel (France)

Polarization resolved microscopy is a powerful method to probe orientation and structural properties in molecular assemblies. Such “molecular order” information can advantageously complete the understanding of a large number of biological functions and events at different spatial scales, from proteins - lipids interactions to cell and bio-filaments mechanics in tissues. In this work, we show that measuring molecular order in a complex sample (such as in tissues) requires a full polarimetric approach where the incident optical polarization is controlled and tuned at the focal spot of a microscope objective. We have developed a multimodal polarimetric nonlinear microscopy technique, able to probe orientational order in molecular assemblies of sub-wavelength scales in cells and tissues, based on different optical contrasts: Second Harmonic Generation (SHG), Two Photon Fluorescence (TPF), Four Wave Mixing (FWM), Coherent Anti-Stokes Raman Scattering (CARS), and Stimulated Raman Scattering (SRS). Each of these contrasts is complementary to the others, in particular SHG being specific to non-centrosymmetry (such as in collagen type I), FWM to high order symmetries, CARS and SRS to vibrational information. We show that the order of symmetry of the orientational distribution probed by a polarization resolved nonlinear contrast is closely related to the order of nonlinearity of the contrast used, which makes them highly complementary.

This approach finally provides new insights into the mechanical interaction between cells and the extracellular matrix in tissues, which plays a crucial role in cell migration properties or cancerous tissues development.

8226-30, Session 5

## Ray-tracing study on the post-scanner variable beam expansion optics of a two-photon microscopy system

D. Kim, C. Welle, V. Krauthamer, U.S. Food and Drug Administration (United States)

Due to the low signal level from two-photon excitation fluorescence in biological samples, optimization of optics in two-photon microscopy (2PM) system is critical. One of the most important factors to ensure the operation of 2PM in optimal optical condition is to overfill the back aperture of the objective lens. A variable beam expander is commonly placed before the scanning mirrors to achieve this goal, however, it also introduces additional degradation of optical quality due to the increased dispersion by beam expanding optics. Also, the scanning mirror size restricts the degree of expansion, which prevents the overfilling of objective lens back aperture under certain conditions.

We investigated the variable beam expansion optics placed after the scanning mirrors. Ray-tracing study confirmed that the post-scanner beam expansion has multiple advantages over the conventional beam expansion before the scanner: (1) Reduced number of optical element reduces pulse dispersion; (2) Reduced size of the scanning mirror enables faster scanning speed. Resolution and aberration of a 2PM with post-scanner beam expansion optics were identical to that of a system with pre-scanner beam expansion. A few two-photon images using the 2PM based on this beam expansion scheme are also presented.

8226-31, Session 5

## Scanning fiber optic two-photon excitation endomicroscopy with reduced photo damage and precision focal position localization

W. Liang, Y. Y. Zhang, K. Murari, Y. Chen, The Johns Hopkins Univ. (United States); M. Li, Corning Incorporated (United States); X. D. Li, The Johns Hopkins Univ. (United States)

We present a fiber-optic scanning two-photon fluorescence endomicroscopy with reduced photo damage, a stable scanning pattern, and precision focal position localization. The system comprises a customized double-clad fiber (DCF) for light delivery as well as fluorescence collection, a miniature objective lens and a compact tubular PZT actuator that vibrates the DCF cantilever in two orthogonal directions and thus enables two dimensional scanning and imaging. The commonly used spiral scanning pattern, though easy to implement, concentrates excitation power in the center of the imaging area which causes accelerated photo-bleaching and potential laser-induced damage to the imaged tissue. To overcome this deficiency, we demonstrated a stable Lissajous scanning pattern, by slightly modifying the PZT scanner design, in which more uniform illumination throughout the field of view (FOV) was realized, and thus photo damage subsided effectively. To verify these benefits, A431 squamous carcinoma cells incubated with both live-cell and dead-cell indicator dyes (SYBR-14 and PI respectively) were imaged for visual assessment of photo damage and cell viability. Fluorescence signals emitted from both dyes were collected simultaneously using dual-channel detection, and real-time position-accurate images were reconstructed using our newly-devised method for precision focal position localization. The accurate position calibration/restoration method is easy to perform and the details will be discussed at the presentation. Initial studies show that cells in the center of the FOV under spiral scanning started losing viability after ~7 minutes of two photon excitation, while cells throughout the FOV under Lissajous scanning remained alive even after 15 minutes of illumination.

8226-32, Session 5

## Two-photon imaging based on both tryptophan autofluorescence and exogenous fluorescence

H. Nam, K. H. Song, B. Jeong, T. Wang, M. S. Jang, J. Doh, B. G. Yang, K. H. Kim, Pohang Univ. of Science and Technology (Korea, Republic of)

We explored feasibility of tryptophan fluorescence. Tryptophan is an essential amino acid, and fluoresces at the excitation/emission wavelengths of 280 nm/ 340 nm. Different from other autofluorescence molecules, the level of tryptophan fluorescence is strong and comparable to that of exogenous fluorephores. Therefore, tryptophan may be used as additional contrast in conjunction with other exogenous fluorephores. This combination will be useful to study cell-cell interactions which may need multiple labeling. We made our custom two-photon microscope(TPM) to image both tryptophan and typical exogenous fluorephores in the same sample by using two laser sources: Ti-Sapphire laser to excite ordinary fluorephores and OPO laser with second harmonic crystal to generate 580 nm light for two-photon excitation of tryptophan. Using OPO is advantageous in that UV excited tryptophan can be excited by visible light. We will apply this TPM to study the interaction of immune cells. First we will image the cell-cell interaction within collage scaffolds in 3D. Second, we will image tissues such as the skin and small intestine both ex-vivo and in-vivo. Different types of cells are distinguished based on different fluorephores. We expect to be able to image at least three different types of cells with this method.

8226-33, Session 5

## Targeted nanosensor aided three-dimensional pH mapping in tumor spheroids using two-photon microscopy

A. Ray, Y. L. Koo, R. Elbez, R. Kopelman, Univ. of Michigan (United States)

Tumors are generally characterized by lower pH compared to the surrounding tissues. The mapping of tumor pH is of great importance as it plays a critical role in drug delivery and its effectiveness. Here we present a ratiometric, fluorescent, pH nano-sensor that is based on two-photon excitation. The nanosensor consists of 8-Hydroxypyrene-1,3,6-trisulfonic acid(HPTS), a pH sensitive dye, encapsulated in polyacrylamide hydrogel matrix. The nanosensor has an average size of 68nm and contains approximately 0.5% dye by weight. The fluorescence intensity ratio at two-photon excitation wavelengths of 900nm and 810nm increases linearly in the pH range from6.0 to 8.0 and is used to determine the pH of the local environment. These nanosensors are biocompatible and can be targeted to any type of tumors by surface modification with proper targeting moieties. We have used the targeted nanoparticles to map the pH of the human breast cancer and rat brain tumor cells and also spheroids. Spheroids are micro-tumors that are widely used as an in-vitro three dimensional tumor model to study the different properties of the tumor for the purpose of drug delivery, therapy etc. Our study reveals the pH distribution inside the spheroids (of different sizes) during the various stages of its formation. This information can be used to develop efficient drug delivery mechanisms. The two-photon excitation used for this purpose is especially useful as it minimizes the photobleaching and autofluorescence drastically, leading to an increase in the signal-to-noise ratio. It also enables deep tissue imaging due to higher penetration depth.

8226-34, Session 5

## Implementation and characterization of an axicon-based nonlinear digital line-scanning microscope

O. E. Olarte, ICFO - Institut de Ciències Fotòniques (Spain); J. Licea-Rodriguez, Ctr. de Investigación Científica y de Educación Superior de Ensenada (Mexico); J. A. Palero, E. J. Gualda, ICFO - Institut de Ciències Fotòniques (Spain); D. Artigas, ICFO - Institut de Ciències Fotòniques (Spain) and Univ. Politecnica de Catalunya (Spain); P. Loza-Alvarez, ICFO - Institut de Ciències Fotòniques (Spain)

Recently, we presented for the first time the practical implementation of the Two-Photon Single Plane Illumination Microscopy (2p-SPIM) technique. We showed that such technique provides with intrinsic optical sectioning and fast acquisition rates. In this work, we present other alternative implementations based on the Digital Line Scanning Microscopy (DLSM) technique working in the nonlinear regime. In particular, we have implemented and characterized two different DLSM techniques over the same optical setup: DLSM and 2p-DLSM. Furthermore, we study the use of quasi-non-diffractive (QND) focal lines (generated by an axicon), to produce the excitation sheet for both implementations of DLSM.

We show that the combination of the use of QND beams in a 2p-DLSM (A-2p-DLSM) improves: i) the contrast, ii) the sheet's uniformity and iii) the field of view of the image.

In this case, a 6x larger field of view (FoV) is generated when compared with 2p-DLSM and 1.4x larger when compared with conventional single photon DLSM. In the case of DLSM produced with QND beams (A-DLSM), a FoV 1.16x larger is generated when compared to that of the A-2p-DLSM. However, this is at the expenses of a reduced contrast in the image due to the fluorescence excited by the side-lobes in the QND beams. We present results on the complete system characterization and show preliminary results of the technique applied for imaging living C. elegans.

8226-35, Session 5

## Chronic, simultaneous multiphoton imaging of cortical layers I to V with microprism implants

N. B. Gilfoy, R. N. S. Sachdev, D. A. McCormick, M. J. Levene, Yale Univ. (United States)

Neocortical circuits are organized in columns and layers that span ~ 1.5 mm, even in mice. Traditional multiphoton imaging methodologies are restricted to only the top few hundred microns. Here we used multiphoton microscopy and implanted microprisms for studying activity in identified excitatory and inhibitory neurons, and blood flow, in layers 1-5 over more than 4 weeks in anesthetized animals. Genetically modified mice were implanted with 1.5 mm by 1.5 mm fused silica microprisms. In order to study excitatory and inhibitory circuits both Thy1-YFPH and PvCre-ZSGreen adult mice were used for experiments. Headposts and chambers were surgically attached to the skull, and microprisms were implanted caudal to and within primary somatosensory "barrel" cortex of adult mice. The effects of implantation on the surrounding cortex were studied using multiphoton microscopy, electrophysiology, and conventional histology. Using a custom built multiphoton microscope, anesthetized mice were imaged immediately after prism implantation and for more than 30 days after the implant to track the changes in the neuropil and the tissue surrounding the prism. Layer 5 pyramidal cell bodies, interneurons, and blood vessels were clearly visible through the microprism and could be tracked on the day of the implant and in subsequent days post-implantation. Damage studies, including extracellular recording in response to whisker stimulation and conventional histology, reveal normal tissue in the area surrounding the implant.

8226-36, Session 6

## Polarization resolved SHG as a robust means to quantify changes in collagen in fibrotic diseases

P. J. Campagnola, V. Ajeti, K. B. Tilbury, K. Campbell, S. Mathur, N. Jarjour, S. M. Ponik, P. J. Keely, K. W. Eliceiri, Univ. of Wisconsin-Madison (United States)

We show that characteristic changes in the architecture of collagen (concentration, fibril/fiber structure) in diseases such as cancer and asthma can be probed quantitatively by Second Harmonic Generation (SHG) imaging microscopy using both 3D and polarization resolved metrics. In one class of measurements SHG 3D responses of directionality was utilized to show changes in the fibril assembly in self-assembled gel models for extracellular matrix (ECM) structure consisting of mixtures of type I and type V collagen, where up-regulation of the latter has been implicated in carcinogenesis but not found in normal breast. The F/B and SHG intensity results are consistent with electron microscopy analysis, demonstrating that SHG is sensitive to sub-resolution changes in structure (~50-100 nm). In a second study we use SHG to investigate the role of ECM remodeling in asthma. We found that tissues from asthmatics were characterized by significant fibrosis, where the SHG is significantly brighter than that from normal airway tissues. Additionally, complete polarization analysis of the SHG signal reveals quantitative differences in the collagen assembly, where the diseased tissues were found to have a higher degree of organization, similar case to that we have observed in both ovarian and breast cancer. The use of polarization-resolved SHG will also be discussed for the human connective tissue disorder osteogenesis imperfecta. All these findings point to the applicability of SHG as a diagnostic optical biopsy tool with broad relevance to a variety of diseases involving remodeling of collagen.

8226-37, Session 6

## Analysis of collagen structure changes in ovarian tumor development

J. M. Watson, P. F. Rice, S. L. Marion, The Univ. of Arizona (United States); M. Brewer, Neag Cancer Ctr. (United States); J. Davis, U. Utzinger, P. B. Hoyer, J. K. Barton, The Univ. of Arizona (United States)

More than 80% of ovarian cancers are diagnosed after metastasis has occurred, making treatment more difficult. We hope to detect the microscopic changes preceding metastasis in order to develop a screening test for high risk patients. A mouse ovarian cancer model has been developed by treating mice with 4-Vinylcyclohexene Diepoxide to induce ovarian failure and 7, 12-Dimethylbenz[a]anthracene to induce ovarian tumors. Ovaries were imaged ex vivo, using second harmonic imaging to visualize the collagen structure from the surface of the ovary up to 200μm deep in 10μm increments. Thirty ovaries were imaged successfully with diagnoses as follows, 12 normal, 4 atretic, 6 benign tumors, 4 malignant tumors and 4 unknown. We have performed analysis using gray level co-occurrence matrices and Fourier transforms and found that the collagen structure of malignant tumors generally has lower frequency content than the collagen structure of benign tumors and normal tissue. By comparing energy in three regions of frequency space we have been able to separate malignant from non-malignant images. After implementing a support vector machine we have automated the classification of unknown images using a training set of 12 normal images and 12 malignant images. Using this classifier on a test set of 38 malignant images and 46 normal images we have obtained diagnoses with 95% specificity and 89% sensitivity. This automated classifier brings us a step closer to a semi-automated diagnostic system for ovarian cancer. We will continue to work on optimizing our analysis method and complete analysis on all images.

8226-38, Session 6

## In vivo characterization of organizational and orientation changes in precancerous submucosal collagen via polarization SHG

K. Edward, T. Shilagard, J. Yang, S. Qiu, G. Vargas, The Univ. of Texas Medical Branch (United States)

Numerous morphological and structural changes are associated with oral dysplasia. Specifically, it has been reported that alterations in stromal biology may precede and facilitate neoplastic progression in precancerous pathology. Thus carefully monitoring of stromal changes may provide additional non-invasive adjunctive biomarkers of dysplasia. Image-based optical techniques have confirmed that reduced autofluorescence intensity is detected from precancerous and cancerous tissue compared to normal tissue. This change is not specific since a similar intensity reduction is observed for non-malignant inflammation. However, improved specificity may be achieved by analyzing the organization and orientation alterations of sub-mucosal collagen via SHG imaging using a linearly polarized source with adjustable polarization. Although this approach has been used to study collagen orientation in diseased tissue, it is yet to be applied to discrimination between normal and precancerous tissue.

In this investigation, linearly polarized incident light at 840 nm was exploited for SHG imaging of stromal collagen in normal and precancerous mucosa. In the case of the latter, oral dysplasia was induced in the buccal pouch of Syrian Golden hamsters by tri-weekly topical application of 9,10-dimethyl-1,2-benzanthracene (DMBA). Images were recorded at 10 degree polarization angle intervals at three separate depths in the stroma. Investigated sites were immediately marked for biopsy, processed for histology and H&E staining, and graded by a pathologist.

Our results revealed both structural and orientation differences between the normal and DMBA treated hamsters and the technique shows promise as an adjunctive diagnostic tool for monitoring the early physiological changes associated with the progression oral dysplasia.

8226-39, Session 6

## Polarization-resolved SHG microscopy of collagenous tissues with controlled mechanical strain

I. Gusachenko, Y. Goulam Houssen, G. Latour, S. Bancelin, V. Tran, J. Allain, M. Schanne-Klein, Ecole Polytechnique (France)

Collagen is the main protein of the extracellular matrix. It forms highly structured 3D assemblies that are specific for every tissue and are responsible for their biomechanical properties. In that respect, rat-tail tendon is a model tissue since it exhibits a unidirectional hierarchical organization: collagen molecules form fibrils of around 200 nm diameters that assemble into fibers and further form fascicles with a crimped pattern.

This study aims to determine the relationship between microscopic macromolecular organization and macroscopic biomechanical properties of collagenous tissues. For that purpose, we implemented a new biomechanical device combining polarization-resolved multiphoton microscopy and mechanical assays. We monitored simultaneously the fibrillar collagen architecture at microscopic scale using endogenous second harmonic generation (SHG) signals, and the strain-stress relationship at macroscopic scale during multiple loading cycles. We observed a straightening of the crimps followed by a sliding of the fibrils with increasing stretching of the tendon fascicles [1]. Polarization resolution of the SHG images provided complementary information about the orientation dispersion of collagen fibrils within the focal volume. We observed an increase of the linear birefringence of the tissue and a complex variation of the ratio of the 2 main tensorial components of the SHG response. We attributed this polarimetric response to collagen remodeling at the sub-micrometer scale. Our approach can be readily generalized to other tissues and should bring new valuable information about biomechanics of microstructured tissues.

[1] Goulam Houssen et al, J. Biomechanics 44, 2047-2052 (2011)

8226-40, Session 6

## Combined nonlinear laser imaging (two-photon excitation fluorescence, second and third-harmonic generation, and fluorescence lifetime imaging microscopies) in ovarian tumors

J. F. Adur, Univ. Estadual de Campinas (Brazil) and National Univ. of Entre Rios (Argentina); V. B. Pelegati, A. A. de Thomaz, F. Bottcher-Luiz, L. Andrade, D. B. Almeida, H. F. Carvalho, C. Lenz Cesar, Univ. Estadual de Campinas (Brazil)

In this work, we applied Two-photon Excited Fluorescence (TPEF), Second/Third Harmonic Generation (SHG and THG) and Fluorescence Lifetime Imaging (FLIM) Non Linear Optics (NLO) Laser-Scanning Microscopy within the same imaging platform to evaluate their use as a diagnostic tool in ovarian tumors. These microscopies have the triple advantage of offering high spatial resolution, high penetration depth, and low photodamage effects. The FLIM is an additional non-invasive microscopy technique useful to characterize endogenous fluorescence species and their surrounding medium by measuring the mean lifetime of fluorescent emission. We assess of applicability of this multimodal approach to perform a pathological evaluation of serous and mucinous tumors in human samples. The combination of TPEF-SHG-THG imaging provided complementary information about the interface epithelium/stromal, such as the transformation of epithelium surface (THG) and the overall fibrillar tissue architecture (SHG). The fact that H&E staining is the standard method used in clinical pathology and that the stored samples are usually fixed makes it important a re-evaluation of these samples with NLO microscopy to compare new results with a library of already existing samples. FLIM, however, depends on the chemical environment around the fluorophors that was completely changed after fixation; therefore it only makes sense in unstained samples. Our FLIM results in unstained samples demonstrate that it is possible to discriminate healthy epithelia from serous or mucinous epithelia. Qualitative and quantitative analysis of the different imaging modalities used showed that multimodal nonlinear microscopy has the potential to differentiate between cancerous and healthy ovarian tissue.

8226-41, Session 6

## Third-harmonic (THG) and four-wave mixing microscopy (FWM) of cells and biological tissues

P. Mahou, Ecole Polytechnique (France); N. Olivier, Ecole Polytechnique Fédérale de Lausanne (France); G. Labroille, M. Zimmerley, D. Débarre, E. Beaurepaire, Ecole Polytechnique (France)

Nonlinear microscopy can be used to probe the nonlinear optical properties of unstained samples, and provides relevant morphological and structural information. Third-harmonic generation (THG) imaging detects spatial variations of the electronic part of the third-order nonlinear susceptibility chi(3), and has proven useful in recent years for tissue imaging applications.

THG and four-wave mixing (FWM) signals can be efficiently produced and detected simultaneously, using pulsed excitation provided by a femtosecond Ti:Sapphire oscillator and a synchronously pumped optical parametric oscillator (OPO). Far from resonance, both signals probe the real part of chi(3). However their contrast mechanism results from different phase matching conditions. Combined imaging is therefore expected to provide more structural information on chi(3) variations than either modality alone.

We analyze theoretically the contrast mechanisms of THG and FWM imaging as a function of sample size and clustering in the half-wavelength regime, and present imaging examples from live tissues and embryos. We also show that combined THG-FWM imaging is compatible with simultaneous efficient detection of other nonlinear signals such as two-photon excited fluorescence and second-harmonic generation.

8226-42, Session 6

## Second-harmonic generation endomicroscopy imaging system for preterm birth imaging

Y. Y. Zhang, K. Murari, W. Liang, The Johns Hopkins Univ. (United States); M. L. Akins, K. Luby-Phelps, M. Mahendroo, The Univ. of Texas Southwestern Medical Ctr. at Dallas (United States); M. Li, Corning Incorporated (United States); X. D. Li, The Johns Hopkins Univ. (United States)

Approximately 500,000 babies a year in the U.S., which constitutes about 12.7% of all births, are born pre-term with associated significant monetary and societal costs. For diagnosis and prevention, a clinical tool for predicting preterm birth is critically needed. Here we present a fiber-optic second harmonic generation (SHG) endomicroscopy system that can detect the morphological changes in cervical collagen fiber during gestation with sub-micrometer resolution. The system consists of a customized double-clad fiber (DCF) with single-mode femtosecond pulse delivery through the core and a large inner-cladding diameter of 200 μm for SHG signal collection. A contact PZT actuator enables high-speed, two-dimensional spiral or Lissajous beam scanning. A miniature objective lens with a 0.8 NA and minimal chromatic aberration allows for tight focal excitation and efficient signal collection. The diameter of the probe head is only 2 mm. SHG images of collagen structural changes of murine cervical tissues during pregnancy were longitudinally taken with the endomicroscope. The images were also compared with SHG images obtained from a bench-top SHG microscope. Similar imaging quality shows the promise of the endomicroscopy system for high-resolution collagen fiber imaging. SHG images collected were analyzed quantitatively for changes in the mean intensity, collagen fiber size and fiber distance. All these parameters progressively increased from early to late pregnancy. The morphological features of cervical collagen assessed with the endomicroscope offer an opportunity to potentially detect abnormal cervical remodeling associated with preterm birth.

8226-43, Session 7

## Studies of human skin glycation by the use of multiphoton microscopy and spectroscopy

A. Ghazaryan, H. Hu, National Taiwan Univ. (Taiwan); S. Chen, National Cheng Kung Univ. (Taiwan); H. Tan, Chang Gung Memorial Hospital (Taiwan) and Department of Biomedical Engineering, National Taiwan University (Taiwan); C. Dong, National Taiwan Univ. (Taiwan) and Center for Quantum Science and Engineering, National Taiwan University, Taipei (Taiwan) and Biomedical Molecular Imaging Core, Div. of Genomic Medicine, Research Center for Med. Exc., NTU (Taiwan)

The accumulation of advanced glycation end products (AGEs) has been known as a pathogenic mechanism underlying diabetes-related complications. Quantification of the extent of skin AGEs proved to be useful for detection and diagnosis of these pathologies. In this regard an accurate, convenient and noninvasive screening test would be an attractive alternative to current tests. In the present study ex-vivo glycation-induced changes in optical properties of different constituents of human skin were studied and compared using multiphoton microscopy and spectroscopy. Specifically, the changes in the intensities of autofluorescence and second harmonic generation of the epidermis, collagen and elastin fibers of dermis were evaluated in relation to the extent of glycation. The results show that glycation of epidermis and dermal collagen is accompanied by linear increase of multiphoton autofluorescence intensity and decrease in second harmonic generation. Similar, but less prominent changes were found in dermal elastin. Our study suggests that the dermal collagen is the most sensitive skin tissue to be used in the in detecting changes in tissue glycation due to intrinsically weak autofluorescence.

8226-44, Session 7

## High-speed vibrational sum frequency generation microscopy

V. Raghunathan, Y. Han, N. Ge, E. O. Potma, Univ. of California, Irvine (United States)

Vibrationally resonant sum frequency generation (VR-SFG) microscopy is a useful multiphoton imaging technique which enables visualization of samples with simultaneous vibrational and second order nonlinear optical response. There have been few demonstrations of VR-SFG microscopy to image monolayers and biopolymers using high energy Hz-KHz repetition rate lasers, based on non-collinear geometries and loosely focused laser beams [1]. This existing approach results in low resolution, slow scanning speeds, and complex imaging geometries, which render these schemes incompatible with current nonlinear microscopy techniques. In this paper we demonstrate a new method to perform SFG microscopy that overcomes previous shortcomings.

Our implementation is based on a collinear geometry in which the mid-IR (3517/cm -2860/cm) and near-IR (850-765nm) beams extracted from a 76-MHz repetition rate optical parametric oscillator (Levante OPO) are combined and sent to an IX-71 Olympus microscope. The laser beams are focused on the sample using a reflective objective (Edmund optics 0.65NA), which produces tight focal spots for both incident beams. The SFG signal is collected in the epi-direction, while the SHG signal is simultaneously collected in the forward direction. The pixel dwell time is 1-ms, limited by scanning stage set-up; this is much faster than previous demonstrations. We measured the focal spot size of ~0.60 um by scanning 0.30 um sized BaTiO3 nanoparticles through focus. We applied this microscope to imaging collagen, an important bio-polymer which possesses a non-vanishing bulk X(2) along with strong vibrational signatures from the methylene backbone [2]. We show that the SFG images from collagen on-resonance (2945 /cm) and off-resonance (2866 /cm) shows ~15:1 contrast in SFG signal, confirming VR-SFG imaging. The capability to acquire simultaneous SHG and VR-SFG signals enables a direct correlation between electronic and vibrational nonlinearties of collagen biopolymers.

[1] D.M.P.Hoffmann et. al. Rev. Sci. Instru. v. 73, 3221-3226 (2002). K. Ciamatu et. al. J. Phys. Chem B v. 110, 1807-1813. K. Locharoenrat et. al. Phys. Stat. Sol.(c) v. 6, 304-306 (2009). [2] I.R-Mendoza et. al. Biophysical J. v.93, 4433-4444 (2007).

8226-45, Session 7

## Generic model for the biomolecular organization probed by second-harmonic generation polarization microscopy

J. Duboisset, P. Refregier, H. Rigneault, M. Roche, P. Ferrand, D. Ait-Belkacem, S. Brasselet, Institut Fresnel (France)

In the last few years SHG microscopy techniques have strongly evolved to become powerful imaging and spectroscopy tools that are nowadays ready to investigate the biological world. Furthermore, information on the molecular organization is becoming crucial for understanding biological processes and tissue organization. In this context, polarized SHG microscopy, which allows imaging orientation and order in non-centrosymmetric assemblies such as collagen, is a powerful investigative tool.

In this work we develop a generic method able to extract the information available by SHG about molecular orientations in biological samples. Molecular organization can be described as an angular distribution function of molecules in the sample plane, which can be decomposed onto different orders of symmetry. This decomposition permits to quantify molecular order without the need to infer an a priori model for the molecular distribution function. We show that the mean orientation of this distribution, as well as its first and third order of symmetry, can be estimated by monitoring SHG signals under a varying incident polarization. We use a fast method to estimate the symmetry orders based on serial Fourier decompositions of the polarized SHG intensity response. The accuracy of the method is also investigated and discussed as a function of the molecular distribution.

We apply this method to molecular order imaging in collagen isolated fibrils, and show the possibility to detect molecular disorder within fibrils assemblies at nanometer scales.

8226-47, Session 7

## Investigation of the wavelength dependence of SHG from various tissues

S. J. Matcher, H. Askew, The Univ. of Sheffield (United Kingdom)

The wavelength-dependent SHG emission efficiency in the epi-direction has been measured for equine tendon, bovine intervertebral disk, various polymer scaffolds and fixed human decellularized dermis. Whilst qualitative similarities are found for the biological tissues, quantitative differences exist also. The wavelength dependence of SHG from common polymer scaffolds is substantially different to that of bovine tendon. Whereas the latter tissue shows an increasing SHG efficiency as wavelength increases towards 1 micron the former material shows the opposite tendency, with SHG efficiency peaking at 800 nm. A comparison of bovine tendon with bovine articular cartilage, bovine intervertebral disk and fixed human decellularized dermis also reveal differences in the SHG efficiency spectra. It is also found that formaldehyde fixation of bovine tendon not only produces a large decrease in SHG intensity and increase in autofluorescence but also appears to change the wavelength-dependence of the SHG also, shifting the peak efficiency from 900 nm down towards 800 nm.

8226-49, Session 7

## The use of a sub-25 fs Yb fiber laser for multiphoton SHG and THG imaging

M. M. Dantus, I. Saytashev, B. Nie, S. N. Arkhipov, Michigan State Univ. (United States); A. Chong, H. Liu, F. W. Wise, Cornell Univ. (United States)

We report on multiphoton microscopy imaging using a new ultrafast Yb fiber laser source. The broadband laser spectrum is centered at about 1 um and supports sub-25 fs pulse duration. The laser average output power is 50 mW, and the repetition rate is 65 MHz. The pulses are compressed via Multiphoton Intrapulse Interference Phase Scan (MIIPS) and then used for second harmonic generation (SHG) and third harmonic generation (THG) microscopy imaging of polystyrene beads, fish tail, fly wings, mouse intestine, and flower pollens. The data confirms that the laser is appropriate for multiphoton microscopy, including multimodal imaging that delivers enhanced information about the sample structure. We believe that this Yb laser has a potential to become in the near future an ultrafast laser of choice for bio-imaging. Its fiber-based design offers compactness and ruggedness needed for biomedical applications. The red-shifted laser emission (when compared to a Ti:Sapphire laser output) is expected to provide higher penetration depth and reduced DNA damage, since the THG wavelength is shifted from 266 to about 350 nm. We currently explore ways to improve the laser performance characteristics and achieve shorten pulse duration and higher pulse energies.

8226-50, Session 7

## Video-rate, label-free second-harmonic generation holographic imaging of biological specimens

D. Smith, D. G. Winters, R. Bartels, Colorado State Univ. (United States)

Second harmonic generation (SHG) occurs from many native tissues and structures in un-labeled biological organisms. The most common sources of intrinsic SHG emission include Myosin filaments in muscle tissues and collagen fibrils. To date, the majority of SHG microscopy images have been taken by scanning a tightly focused ultrafast laser pulse in a sample. Rapid raster scanning allows for two-dimensional images to be taken in less than a second; however, imaging in three dimensions takes a much longer time as the depth of focus must be scanned. This serial acquisition of SHG image voxels typically requires at least several minutes to acquire a three dimensional image of an object. Observing biological specimens in three dimensions is essential to understand biological function. Further, many processes occur at rates vastly exceeding the fraction of a Hertz update rate possible with current laser scanning SHG microscopies. In this work, we demonstrate operation of recently developed label-free SHG holography at high speeds, supporting continuous video rate acquisition of an entire three-dimensional volume in a microscope. Efforts are advancing to improve the speed to exceed video rates to capture exceptionally fast biological dynamics. Experiments demonstrating video-rate 3D volume imaging on a number of biological specimens will be presented along with careful signal to noise investigations, and pulse duration optimization in an effort to minimize exposure times and optimize 3D imaging speed, and object tracking at high 3D imaging rates.

8226-51, Session 7

## Structure of collagen fibers revealed with polarization dependent second-harmonic generation microscopy

V. Barzda, A. E. Tuer, S. I. Kruglov, N. Prent, R. Cisek, D. Sandkuijl, Univ. of Toronto Mississauga (Canada)

Collagen fibers are readily visualized with second harmonic generation (SHG) microscopy. Structural properties of the fibers can be assessed by polarization in, polarization out (PIPO) measurements with the SHG microscope. The theoretical model is used to extract the triple-helix orientation angle with respect to the collagen fiber from the SHG microscopy of human lung tissue. The molecular origin of SHG from collagen is modeled using the time-dependent coupled perturbed Hartree-Fock calculations of the hyperpolarizibilities of glycine, proline and hydroxyproline. Two effective nonlinear dipoles are found to orient in-the-plane of the amino acids with one of the dipoles aligning close to the pitch orientation in the triple-helix, and providing dominant contribution to the SHG polarization properties. The calculated hyperpolarizability tensor elements ratios of collagen triple-helix models [(Gly3)n]3, [(Gly-Pro2)n]3, and [(Gly-Pro-Hyp)n]3 are used to predict the second-order nonlinear susceptibility ratios, and of collagen fibers. The study shows the dominant role of amino acids orientation in the triple-helix for determining the polarization properties of SHG and provides the method for determining the triple-helix orientation angle in the collagen fibers.

8226-147, Session 7

## Coupling two-photon excitation with optical nanoscopy and light-sheet illumination microscopy

A. Diaspro, P. Bianchini, Istituto Italiano di Tecnologia (Italy); F. Cella-Zanacchi, Univ. degli Studi di Genova (Italy); B. Harke, Istituto Italiano di Tecnologia (Italy); G. Vicidomini, Univ. degli Studi di Genova (Italy); S. Galiani, Istituto Italiano di Tecnologia (Italy); J. V. Chacko, Cochin Univ. of Science & Technology (India); Z. Lavagnino, Istituto Italiano di Tecnologia (Italy)

Coupling two-photon excitation (2PE) with two, comparatively young and successful optical methods specially realized for the improvement of resolution and 3D imaging of large samples, i.e. STED (stimulated emission depletion) and SPI (selective plane illumination) microscopy, would turn in some advantages. In the former case we aim to get a better resolution for 2PE microscopy while for the latter our goal is to obtain better penetration in scattering samples by shifting the light sheet wavelengths to the red in the non-linear domain. We show results obtained by adapting a commercial STED-CW microscope to 2PE and by implementing a 2PE-SPIM homemade system. We show results and related characterization obtained on subresolved and on thick samples using a commercial STED-CW set-up properly adapted and 2PE 3D imaging within the light sheet of cellular spheroids. A critical discussion will be conducted.

Work partially funded by IIT, IFOM (FIRC Institute of Molecular Oncology, Milan, Italy) and Italian PRIN 2008JZ4MLB grants.

8226-52, Session 8

## Lock-in free stimulated Raman microscopy

J. Cheng, M. N. Slipchenko, Purdue Univ. (United States)

Though being an essential component for heterodyne detected nonlinear optical microscopy based on stimulated Raman scattering, the lock in amplifier gives an electronic noise limiting the signal to noise ratio for low laser power applications. Additionally its lack of simplicity may hamper the wide use of stimulated Raman microscopy. To overcome such limitations, we developed a lock-in free scheme that improved the signal to noise ratio by an order of magnitude compared to conventional lock-in detection, as demonstrated through stimulated Raman imaging of live cells and tissues at the speed of 2 μs/pixel. The increased signal to noise ratio further allowed acquisition of high quality epi-detected images, where a much reduced local oscillator power reaches the detector

8226-53, Session 8

## High-speed spectral tuning CARS microscopy using AOTF laser

M. Hashimoto, J. Iwatsuka, H. Niioka, T. Araki, Osaka Univ. (Japan)

We have developed a high speed spectral tuning CARS microscopy system using a mode-locked Ti: Sapphire laser with an acousto-optic tunable filter (AOTF) in the cavity. Since the wavelength of the laser is tunable with the applied radio frequency to the AOTF, the wavelength is electrically tunable.The pulse duration of the laser is about 10 ps, tunable range is 820 nm to 920 nm, and the tuning speed is ms order.

The laser is synchronized with another mode-locked Ti: Sapphire laser laser our own method using a balance cross-correlator and phase lock loop technique. The synchronized lasers are used for light source of multi-focus CARS microscopy system using a microlens array scanner. The results using the system will be demonstrated.

8226-54, Session 8

## Ultra-broadband time-resolved coherent anti-Stokes Raman scattering microspectroscopy

J. Yin, Shenzhen Univ. (China); H. Niu, Shenzhen University (China)

In a broadband coherent anti-Stokes Raman scattering (CARS) microspectroscopy with supercontinuum (SC), the simultaneously detectable spectral range is limited by the spectral continuity and simultaneity of various spectral components of SC in an enough bandwidth. According to our theoretical analysis and experiments, the optimal experimental conditions are obtained. The broadband time-resolved CARS microspectroscopy based on the SC with required temporal and spectral distributions is achieved. The global CARS spectrum with well suppressed nonresonant background noise can be obtained in a single measurement and used as the imaging contrast. It will be more helpful to provide a complete and accurate molecular atlas, and to exhibit a potential to understand not only both the solvent dynamics and the solute-solvent interactions, but also the mechanisms of chemical reactions in the fields of biology, chemistry and material science.

8226-55, Session 8

## Broadband CARS microscopy: phenotypic and functional imaging for biology

M. T. Cicerone, Y. J. Lee, K. H. Aamer, National Institute of Standards and Technology (United States)

Broadband coherent Raman approaches such as broadband anti-Stokes Raman (bCARS) are promising methods for noninvasive imaging of biological systems and complex materials. We will show that bCARS can be used to very rapidly obtain linear Raman spectra from materials1 and biological samples.2 This allows us to utilize, now in an imaging mode, decades of spontaneous Raman bio-spectroscopy that has been focused in the “fingerprint” frequency range of (500 to 1800) cm-1. The ability to acquire images based on fingerprint spectra allows us to obtain spatially resolved functional and phenotypic information from cells and tissues. I will demonstrate applications of bCARS to questions regarding tumor growth as well as stem cell differentiation and normal tissue development. I will also discuss methods to greatly enhance imaging speed of this chemically specific imaging modality.

REFERENCES

1. Y.J. Lee, et al., Analytical Chemistry, 83 2733-2739 (2011).

2. S.A. Parekh, et al., Biophysical Journal, 99 2695-2704 (2010).

8226-56, Session 8

## High-resolution, high-speed tunable grating filter for stimulated Raman spectral imaging

W. Umemura, Y. Ozeki, K. Fujita, K. Sumimura, Osaka Univ. (Japan); N. Nishizawa, Nagoya Univ. (Japan); K. Itoh, Osaka Univ. (Japan)

Stimulated Raman scattering (SRS) microscopy can visualize molecular vibration with high sensitivity and high contrast, allowing label-free imaging of living cell. In order to specify molecules, it is important to obtain Raman spectrum at each pixel. High-speed wavelength scanning would allow such spectral imaging. Previously an acousto-optic tunable filter was used to filter out narrowband pulses from broadband pulses. However, it suffers from limited spectral resolution. Here, we demonstrate a tunable optical filter for spectral imaging with SRS microscopy. In the filter, an incident beam is reflected by a galvanometer scanner, and then imaged onto a Littrow grating by a 4f optical system. The diffracted beam is reflected back to the galvanometer scanner, and then launched into a fiber collimator. The transmission wavelength can be tuned because the Littrow angle is dependent on the angle of the galvanometer scanner. This configuration allows high spectral resolution of ~0.2 nm and high-speed wavelength scanning with a period of milliseconds. Furthermore, the optical path length is kept constant when the wavelength is scanned. In the experiment, broadband pulses from a 38-MHz ytterbium fiber laser is filtered out by the optical filter, and then amplified to obtain 7-ps pulses. The wavelength is tunable from 1020 to 1040 nm. The pulses are synchronized with a 76-MHz 5-ps Ti:sapphire laser. By using this system, the SRS spectrum of aromatic CH stretching mode of a polystyrene bead is successfully obtained.

8226-57, Session 8

## A spectrally modulated stimulated Raman scattering microscope

D. Zhang, M. N. Slipchenko, D. E. Leaird, R. Wu, A. M. Weiner, J. Cheng, Purdue Univ. (United States)

We demonstrate a new method of stimulated Raman scattering imaging using modulation at the spectral domain. The intensity modulation of either pump beam for stimulated Raman loss or Stokes beam for stimulated Raman gain has been a dominating scheme for stimulated Raman imaging since its emergence. However, other pump-probe contrasts induced by the intensity modulation, such as cross-phase modulation, transient absorption, remain inevitable along with the stimulated Raman scattering process. We modulate the broadband femtosecond pulse in frequency domain to switch between on- and off-Raman resonance while retain the intensity constant. We show that those unfavorable pump-probe signals could be reduced more than one order of magnitude. Spectrally modulated stimulated Raman imaging of molecules in highly pigmented samples such as human hair is demonstrated.

8226-58, Session 8

## From coherent Raman microscopy to quantitative coherent Raman spectral imaging

D. Fu, F. F. Lu, X. Zhang, G. R. Holtom, C. W. Freudiger, M. Ji, X. Ni, X. S. Xie, Harvard Univ. (United States)

Recent developments in Stimulated Raman Scattering (SRS) microscopy offers exciting new opportunities in studying biological samples with high spatial and temporal resolution based on intrinsic molecular contrasts. It overcomes a decade-old problem in Coherent Anti-Stokes Scattering (CARS) microscopy: eliminating non-resonant background, which causes image artifacts, limits sensitivity and distorts vibrational spectra. Highly sensitive video-rate SRS imaging has been achieved and applied to many different areas of study such as drug delivery, lipidomics and cancer diagnosis.

However, most previous implementations of SRS microscopy employ synchronized picosecond laser sources, which probes one specific Raman band at a time. Imaging at different Raman bands requires tuning the laser cavity, which is both slow and unreliable. To extend the use of SRS microscopy in imaging of complicated biological samples, where Raman bands from multiple species have significant overlap, we developed two new methods of SRS spectral imaging exploiting the rich Raman spectral feature and concentration linear dependence nature of SRS microscopy. One method employs a picosecond-femtosecond laser system and modulation multiplexing technique to probe a few selected Raman bands simultaneously. It allows quantitative study of biochemical systems with relatively simple composition. The other method utilizes two synchronized femtosecond laser sources and spectral focusing to achieve fast Raman spectra sweeping. The entire lipid/protein band of biological samples can be easily mapped out and used for quantitative chemical analysis. We will present these technological advances as well as applications of these new developments.

8226-59, Session 9

## CARS for catalysis

M. Bonn, FOM Institute for Atomic and Molecular Physics (Netherlands)

There are many processes throughout nature and industry that rely on efficient catalysis. However, schemes for optimizing these processes generally rely on trial-and-error approaches. Determining the precise mechanisms and kinetics is nontrivial, as few techniques can access the time- and length-scales at which these reactions occur. Broadband coherent anti-Stokes Raman scattering (CARS) microscopy is particularly suited to address these systems, being quantitative and having sub-micron spatial resolution. We present the first broadband CARS studies of two classes of industrial catalysts: homogenous and heterogeneous catalysts. We expect that the success of CARS with these industrial catalysis processes will extend to the study of enzymes and bio-catalysis.

The rapid reaction rates that can be achieved with homogenous catalysts preclude the use of conventional techniques to probe the reaction kinetics. We have employed broadband CARS with microfluidic devices to access sub-ms timescales in the hydrosilylation reaction between alkenes and silanes catalyzed by organo-platinum complexes.

Zeolites are heterogeneous catalysts that are used in the petrochemical and fine chemical industries as super-acids and ion exchange. We have employed broadband CARS to investigate the etherification reaction between alkenes and glycols in situ within the zeolite crystal. Using both the chemical specificity and spatial resolution of CARS, we have identified both the critical protonation step of the alkene and the location of the acidic sites within the zeolite crystal. The results reveal surprising inhomogeneity of the reactivity within micron-sized catalysts particles

These insights are expected to aid in the design of next generation catalysts.

8226-60, Session 9

## CARS spectro-microscopy of cell patterns in Drosophila melanogaster wing imaginal disc

M. Bonn, G. Rago, FOM Institute for Atomic and Molecular Physics (Netherlands); F. Marty, Univ. of Zürich (Switzerland); G. Eijkel, J. P. R. Day, R. M. A. Heeren, FOM Institute for Atomic and Molecular Physics (Netherlands); K. Basler, E. Brunner, Univ. of Zürich (Switzerland)

At the basis of developmental biology lies the understanding of how the development of the size and shape of organs is regulated during the growth process. There is evidence of a strong connection in embryogenesis between the appearance of clusters of specific cells and the proliferation of these cells into a specific tissue. Despite extensive efforts to understand how the fate of cells is determined during organ development, little is known about the relationship between the chemical composition of cells and their function in the growth process.

We present here the application of broadband Coherent anti-Stokes Raman Scattering (CARS) hyperspectral microscopy to the study of cell morphology and local chemical composition in the developing wing of Drosophila melanogaster larvae. Broadband CARS is a third order multiphoton microscopy that acquires a Raman-like vibrational spectrum at each location of the sample. Hence, CARS is the ideal tool for the non-invasive imaging of complex samples as it allows label-free, chemically specific, quantitative determination of the local concentration of the various. Here, the chemical information contained in the CARS spectra is extracted by principal component analysis. This combination of CARS and PCA allows us to visualize directly the occurrence of cell clusters in the developing wing that exhibit common chemical features. We also relate these clusters to regions of the developing organ that are known from biology to give rise to specific parts of the adult wing.

8226-61, Session 9

## Coherent Raman scattering microscopy for label-free imaging of live amphioxus

T. Chen, Z. Yu, X. Zhang, J. Shen, Peking Univ. (China); J. Chen, Nanjing Univ. (China); Y. Huang, Peking Univ. (China)

Label-free imaging techniques hold clear advantages over other approaches because many staining procedures and widely used fluorescent proteins are not practical to many applications. However, current optical imaging techniques face difficulties to allow label-free detection for most biological samples especially living samples because of the lack of specific contrast. In contrast with these widely used biomedical imaging methods such as encodable fluorescence, confocal imaging, and multi-photon imaging, coherent anti-Stokes Raman scattering (CARS) and stimulated Raman scattering (SRS) doesn't require staining. CARS/SRS imaging detects molecular vibrations with great specificity. Intrinsic molecular contrast with no dyes or other labels can be directly employed for in vivo studies. CARS/SRS microscopy allows visualization of living (or unfixed) biological specimens without overheating or destroying the inherent molecular signal, is chemically selective and highly sensitive.

We built a CARS/SRS microscope using a picosecond pulsed laser, an OPO, and an Olympus laser scanning microscope. With this system, we have studied the lipid distribution inside the living animal Branchiostoma belcheri. We found that in amphioxus, a Cephalochordata, both the structure and the chemical distribution of the lipid inside the amphioxus notochord are different from vertebrates, such as zebra fishes. The notochord of amphioxus is lipid and protein rich, with highly ordered notochordal plates stacking along the body. This unique structure and chemical distribution in notochord provide unique functions for amphioxus to swim and to get into the sand.

8226-62, Session 9

## Neuronal cell growth on polymeric scaffolds studied by CARS microscopy

A. M. Enejder, H. Fink, M. Jonsson, C. Brackmann, P. Gatenholm, A. Ewing, Chalmers Univ. of Technology (Sweden); H. Kuhn, Univ. of Gothenburg (Sweden)

Major efforts are presently made to develop polymeric scaffold materials for guided integration, protective support and signal stimulation of neurons in order to treat damages in the neuronal system causing e.g. vision-, hearing- and motor impairments. This requires deep insights into the mechanisms behind cell-substrate interactions in a full three-dimensional scaffold. Stiff, fibrous scaffolds possess the important capability to guide the neurites, though here primarily forming a two-dimensional superficial network. In contrast, soft materials have shown to promote increased outgrowth and three-dimensional branching of the neurites. By means of CARS microscopy we have studied and compared neuronal cell adhesion, differentiation and neurite outgrowth on scaffolds of different character. Detailed visual information on the adhesion points formed between the cells and the scaffold components could be obtained by simultaneous CARS microscopy at the CH-stretch vibration characteristic of membrane lipids and SHG microscopy of the fibrous scaffold components. Different cell interaction and integration characteristics were observed depending on the micro-chemical and micro-mechanical properties of the materials.

8226-63, Session 9

## Study of signal relay and chemotaxis of neutrophils using broadband CARS microscopy

Y. J. Lee, National Institute of Standards and Technology (United States); P. Afonso, C. A. Parent, National Institutes of Health (United States); K. H. Aamer, M. T. Cicerone, National Institute of Standards and Technology (United States)

Neutrophils are the most abundant leukocytes in the blood stream and the first cells recruited to an inflammation site. We study cell signaling for chemotaxis of neutrophils, in particular, signal amplification of primary chemoattractants from the inflammation site by releasing secondary chemoattractants from neutrophils. By using broadband CARS microscopy, we obtained chemical images of neutrophils stimulated with a primary chemoattractant (fMLP) and measured the locations of the production of a secondary attractant (LTB4), which leads to better understanding of the signal relay mechanism for efficient chemotaxis of neutrophils.

8226-64, Session 9

## Live animal nervous system imaging with video-rate multimodal coherent anti-Stokes Raman scattering microendoscopy

E. Bélanger, J. Crépeau, S. Laffray, R. Vallée, D. Côté, Univ. Laval (Canada)

Coherent anti-Stokes Raman scattering (CARS) has been extensively used to study myelin, a lipid-rich membrane wrapped around axons. It has an excellent molecular and label-free sensitivity for lipids at a high time resolution and provides intrinsic sectioning. However, little has been done for in vivo longitudinal imaging, partly because of the need for surgery and the problems with animal movement.

The use of a micro objective does minimize surgery invasiveness, but advances in this field have been hampered by the difficulty to guide two powerful picosecond pulses at different wavelengths, to have them superposed temporally and spatially at the sample and to collect the diffuse signal at a third wavelength.

We report the use of a microendoscope to obtain high quality myelin images from coherent anti-stokes raman scattering (CARS) lipid contrast in live mice spinal cord. A combination with two-photon excitation and second harmonic generation is also shown to illustrate multimodality. Finally, techniques to alleviate animal movement, enabling morphometric data extraction, are described. The technique is sensitive to small variations of the myelin thickness, as would be observed in demyelinating pathologies. In addition, fluorescence images of microglia and axons can be obtained with the same endoscope.

The small diameter of microendoscope (1,4mm) enables in vivo time-lapse CARS imaging in the spinal cord at cellular resolution with minimal surgery. In particular, the course of demyelinating disorders such as experimental autoimmune encephalomyelitis (EAE) model will be followed through a longitudinal study of myelin degeneration, microglial activation and loss of blood brain permeability.

8226-65, Session 9

## Surface-mediated four-wave mixing microscopy

E. O. Potma, Y. Wang, X. Liu, Univ. of California, Irvine (United States)

The use of the strong surface fields associated with surface plamon excitations holds promise as an efficient mechanism for generating nonlinear four-wave mixing (FWM) signals from structures and molecules adhered to metal surfaces. The practical implementation of surface plasmons for boosting the FWM response of surface bound structures is, however, far from trivial. Complications arise because of unfavorable heating kinetics and unwanted FWM background contributions from the metal substrate. Therefore, a better understanding of the surface-mediated FWM response along with the development of optimized probing techniques are highly desirable. In this contribution, we demonstrate several successful strategies for acquiring background-free, surface-mediated FWM of surface bound structures. Our approach is based on traveling surface plasmon porlaritions (SPP) in a so-called remote excitation scheme. In this scheme, the target is exposed only to the surface field and not to illuminating photons. We show several applications of surface-mediated FWM microcopy and draw some general conclusions on the applicability of surface plasmon excitations in coherent Raman microscopy.

8226-148, Session 9

## Toward a tunable fiber source for coherent Raman imaging

F. W. Wise, S. Lefrancois, Cornell Univ. (United States)

Applications of coherent anti-Stokes and stimulated Raman scattering microscopies will benefit greatly from the development of convenient, inexpensive, and compact sources of the required picosecond light pulses. Fiber lasers and amplifiers offer major practical advantages, but fiber sources have not been able to compete with the performance of solid-state lasers and parametric oscillators. We will report a fiber laser and frequency converter that generates synchronized pulses that will be valuable for Raman microscopy. Transform-limited few-picosecond pulses at wavelengths around 800 and 1030 nm are generated, with energies of at least several nanojoules. These proof-of-concept experiments show the feasibility of generating the widely-spaced but narrowband near-infrared pulses desired for Raman imaging, and the process offers some wavelength tunability. The route to integrated instruments with the parameters needed for video-rate imaging will be discussed.

8226-66, Session 10

## Early demyelinating lesions of the nervous system: a multimodal approach with CARS imaging

D. Côté, Ctr. de Recherche de l'Univ. Laval Robert-Giffard (Canada)

No abstract available

8226-67, Session 10

## Chemically selective spectral imaging of bone mineral density and the collagen manifold in bulk bone using CARS and SHG

A. D. Slepkov, National Research Council Canada (Canada) and Trent Univ. (Canada); A. F. Pegoraro, A. Ridsdale, D. J. Moffatt, A. Stolow, National Research Council Canada (Canada)

Coherent anti-Stokes Raman scattering (CARS) microscopy has garnered widespread interest as a label-free and chemically-specific nonlinear optical imaging modality. In particular, newer schemes that seek to utilise femtosecond laser based CARS imaging are allowing for integration with established nonlinear optical microscopes, and provide for true multimodal imaging. Because CARS signal intensities scale quadratically with concentration, CARS microscopy is best suited to condensed and aggregated phases. Bone tissue is such a sample. The ability to spatially measure bone mineral density, and to furthermore correlate it in three dimensions to other bone components such as collagen is vitally important for studying diseases such as osteoporosis and osteosarcoma. We utilize a single-source femtosecond-laser-based multimodal nonlinear optical CARS microscope to image bulk bone samples, with strong contrast at the 950 cm^-1 phosphate vibrational peak. The CARS spectrum of the fresh bone matrix across the 850 cm^-1-1700 cm^-1 frequency range is collected, and is used to demonstrate variations in bone mineral density in 3D. The use of fs pulses further permits simultaneous imaging of the collagen matrix with SHG and of structures such as the Haversian canal with endogenous TPEF.

8226-68, Session 10

## Clinical multiphoton CARS

H. G. Breunig, K. König, M. Weinigel, JenLab GmbH (Germany)

We report on clinical CARS with the certified hybrid multiphoton tomograph DermaInspect-CARS for intradermal lipid and water imaging. The novel imaging system consists of an 80 MHz titanium:sapphire laser system combined with an OPO and a white-light generating PCF fiber. CARS signals were obtained in the red, autofluorescence in the green, and SHG signals in the blue spectral range from pateints with dermatological disorders.

8226-69, Session 10

## In vivo monitoring specialized hepatocyte-like cells in Drosophila by coherent anti-Stokes Raman scattering (CARS) and two-photon excitation fluorescence (TPE-F) microscopy

C. Chien, W. Chen, Academia Sinica (Taiwan); J. Wu, National Taiwan Univ. (Taiwan); T. Chang, Academia Sinica (Taiwan)

A group of specialized cells in Drosophila called oenocyte, sharing certain similar properties of hepatocytes in mammals, is known to play an important role in lipid metabolism. During starvation, the lipids are released from the fat body, and oenocytes then would accumulate lipid droplets and probably further oxidize them into shorter fatty acids chain as an energy source. Any genetic defect in lipid metabolism may result in different responses of oenocytes to starvation. To investigate this process in vivo, we used coherent anti-Stokes Raman scattering (CARS) and two-photon excitation fluorescence (TPE-F) microscopy to monitor oenocytes in living Drosophila larvae during starvation. We identified oenocytes by their intrinsic fluorescence and visualized lipid droplets by CARS signals at ~2845 cm-1 without any labeling. Compared with the wild-type, mutants with defects in lipid metabolism show different accumulation curves of lipid droplets in oenocytes. While some mutants accumulate much less lipid droplets in oenocytes during starvation, some have many lipid droplets in oenocytes even though they were fed with plenty of foods. Unlike traditional tissue staining, in vivo imaging allows us to specifically monitor the changes in individual, and provides us more information on the dynamic process of lipid metabolism in Drosophila.

8226-70, Session 10

## An integrated coherent anti-Stokes Raman scattering and multiphoton imaging technique for liver disease diagnosis

J. Lin, F. F. Lu, W. Zheng, National Univ. of Singapore (Singapore); H. Yu, National Univ. of Singapore (Taiwan); C. Sheppard, Z. Huang, National Univ. of Singapore (Singapore)

Liver steatosis and fibrosis are two prevalence liver diseases and may eventually develop into hepatocellular carcinoma (HCC) Due to their prevalence and severity, much work has been done to develop efficient diagnostic methods and therapies. Nonlinear optical microscopy has high sensitivity and chemical specificity for major biochemical compounds, making it a powerful tool for tissue imaging without staining. In this study, three nonlinear microscopy imaging modalities are applied to the study of liver diseases in a bile duct ligation rat modal. CARS shows the distributions of fats or lipids quantitatively across the tissue; SHG visualizes the collagens; and TPEF reveals the morphology of hepatic cells. The results clearly show the development of liver steatosis and fibrosis with time, and the hepatic fat and collagen fibrils are quantified. This study demonstrates the ability of multimodal nonlinear optical microscopy for liver disease diagnosis, and may provide new insights into the understanding of the mechanisms of steatosis/fibrosis transformations at the cellular and molecular levels.

8226-71, Session 11

## All-fiber tunable picosecond laser source for coherent Raman scattering microscopy

K. Q. Kieu, College of Optical Sciences, The Univ. of Arizona (United States); C. W. Freudiger, G. Holtom, Harvard Univ. (United States); N. Peyghambarian, College of Optical Sciences, The Univ. of Arizona (United States); X. S. Xie, Harvard Univ. (United States)

We will present our progress on the development of fiber-based tunable picosecond sources for Coherent Raman Scattering (CRS) Microscopy.

Our approach features all-fiber design and scalable output power - a challenge that has been the main drawback of fiber-based sources for CRM. It is based on jitter-free, optical synchronization of Yb- and Er-based fiber lasers and has full tunability over full CH- and OH-region of vibrational spectra.

8226-72, Session 11

## Active and passive photonic crystal fibers for compact coherent Raman scattering (CRS) microscope and endoscopes

H. Rigneault, S. Brustlein, Institut Fresnel (France); A. Muir, Univ. of Bath (United Kingdom); P. Berto, E. R. Andresen, P. Ferrand, Institut Fresnel (France); C. Billaudeau, D. Marguet, CIML, Univ. de la Méditerranée (France); J. Knight, Univ. of Bath (United Kingdom)

Photonic crystal fibers (PCF) appear nowadays as powerful components in the experimentalist optical toolbox as being able to guide light with unprecedented properties. Namely, solid core PCF can exhibit extremely high nonlinearity to generate new frequencies with low input power whereas hollow core PCF can guide ultra-short pulses without any significant spectral and temporal alteration. In this talk we will investigate the assets and constrains of PCF to perform coherent Raman scattering (CRS) in microscope and endoscope.

Performing label free coherent anti-Stokes Raman scattering (CARS) and stimulated Raman scattering (SRS) in endoscope imaging is a challenge, with huge potential clinical benefit. To date, this goal has remained inaccessible because of the inherent coherent Raman noise that is generated in the fiber itself. By developing double-clad hollow core photonic crystal fiber, we demonstrate here CARS and SRS in an endoscope scheme. Both the excitation beams and the collected CARS and SRS signals travel through the same fiber. No CARS and SRS signals are generated within the hollow core fiber even for temporally overlapping pump and Stokes beams, leading to excellent image quality.

Another interest of solid core PCF lies in its ability to generate new wavelengths with low input power. Whereas super continuum (SC) can be advantageously used as a broad source to generate the pump and Stokes pulses required for CRS, we focus here on the more controlled soliton generation that red shift while propagating down the fiber. CARS and SRS are demonstrated in the fs regime using soliton, the spectral resolution being achieved through spectral focusing scheme.

8226-73, Session 11

## Fiber delivered two-color picosecond source for coherent Raman scattering imaging

K. Wang, C. Xu, Cornell Univ. (United States)

We demonstrate two-color, fiber delivered picosecond source for coherent Raman scattering (CRS) imaging. The wavelength tunable picosecond pump is generated through nonlinear spectral compression of a prechirped femtosecond pulse from a mode-locked femtosecond Titanium:Sapphire (Ti:S) laser. The 1064 nm Stokes pulse is generated by an all-fiber time-lens source that is synchronized to the Ti:S laser. The pump and Stokes are combined in an optical fiber coupler, which serves not only as the delivery fiber for the two-color picosecond source but also as the nonlinear medium for spectral compression of the femtosecond Ti:S pulse. The temporal overlap of the two pulses is electronically adjusted without any mechanical optical delay line, greatly facilitating the temporal alignment of the excitation beams for CRS. CARS imaging of mouse skin at CH2 stretching frequency (2845 cm-1) are performed to demonstrate the practicality of this source. The combination of the all-fiber time-lens source and the nonlinear spectral compression of a femtosecond source in an optical fiber has the potential to make CRS imaging practical to any researcher with a wavelength tunable femtosecond source.

8226-74, Session 11

## A novel multimodal CARS miniaturized microscope

B. D. W. Smith, M. Naji, S. Murugkar, Univ. of Ottawa (Canada); C. Brideau, P. K. Stys, Univ. of Calgary (Canada); H. Anis, Univ. of Ottawa (Canada)

We demonstrate for the first time, a completely portable multimodal coherent anti-Stokes Raman scattering (CARS) microscope based on an integrated scanning microelectromechanical system (MEMS) mirror and custom miniature optics. This is in contrast to our previous work where we demonstrated a bench-top version of the microscope in which the beam delivery to the miniature microscope was in free space and only forward collection was possible. A single Ti:sapphire femtosecond pulsed laser at 800nm is used to produce the CARS, two photon excitation fluorescence (TPEF) and second harmonic generation (SHG) images. For CARS, the Stokes beam at 1030nm is created by using a photonic crystal fibre (PCF) with 2 zero dispersion wavelengths and filtering the generated supercontinuum. The pump beam (and Stokes beam for CARS) is delivered to the miniaturized microscope by a large mode area PCF that is connected to the body of the microscope using standard FC/PC connectors. This excitation light is collimated within the microscope, reflects off the MEMS mirror, passes through a dichroic mirror, and is focused onto the sample by means of custom miniaturized optics corrected for chromatic aberration. Light generated in the epi (backward) direction in the sample is collected by the same custom miniaturized optics and reflected off the dichroic mirror to a separate multi-mode fibre for detection. We demonstrate the operation of this miniaturized microscope by imaging a variety of unlabeled and labeled samples including myelin in a rat nerve, yellow fluorescent protein stained mouse lung tissue, and fluorescein stained vasculature in the epi and forward direction.

8226-75, Session 12

## SLM-aided wide-field CARS microscopy

A. Jesacher, C. Roider, S. Khan, S. Bernet, M. A. Ritsch-Marte, Innsbruck Medical Univ. (Austria)

SLM-aided widefield CARS microscopy

A. Jesacher, C. Roider, S. Khan, S. Bernet and M. Ritsch-Marte

Division for Biomedical Physics, Innsbruck Medical University, Müllerstraße 44, 6020 Innsbruck

We show how the functionality of a widefield CARS microscope can be greatly extended by the implementation of a liquid crystal spatial light modulator (SLM). Such a device is capable of modulating light by the generation of flexible dynamic diffraction patterns.

When integrated into the excitation beam path, it provides accurate control over the beam incidence angles and thus the phase-matching condition. This allows to optimize the image contrast between objects of different size and to strongly suppress the undesired signal from the solvent which embeds small target specimens. We show results from experiments where this technique allowed highlighting the signal of submicron polystyrene beads against the solvent background by about 20 dB.

Another option is to place an SLM into the CARS signal pathway. There it can act as adaptive darkfield mask for enhancing image contrast or can be used to measure the phase of the CARS signal. This opens up the possibility to retrieve the according Raman-spectra from measured CARS-spectra.

8226-76, Session 12

## Computational optimization of phase shaped CARS

A. C. W. van Rhijn, A. S. Jafarpour, M. Jurna, J. L. Herek, H. L. Offerhaus, Univ. Twente (Netherlands)

We explore strategies for optimizing selectivity, specificity, and sensitivity in broadband CARS by precalculating pulse shapes using an evolutionary algorithm. The particular implementation of coherent anti-Stokes Raman scattering that we consider uses a spectrally broadband pump and probe source in combination with a spectrally narrowband Stokes source, resulting in a broadband CARS signal that contains non-resonant background and contributions from different pathways and interferences between vibrational resonances. We present spectral phase shaping approaches that take advantage of these different pathways by exploiting both constructive and destructive interferences. As a result the presence of molecules of interest can be inferred from the spectrally integrated output pulse intensity.

We show the possibility of selective excitation of a single constituent in a test case of a mixture of five resonant compounds. The obtainable contrast ratio ranges from 100:1 up to 2200:1, depending on the uniqueness of the complex vibrational response of the compound of interest compared to that of the surrounding molecules. Furthermore we investigate how the effects of homodyne mixing in the focal volume affect the obtainable contrast ratio and how noise affects the optimization.

8226-77, Session 12

## Stimulated Raman scattering based multimodal nonlinear optical microscopy

D. Li, Hong Kong Univ. of Science and Technology (Hong Kong, China)

The endogenous nonlinear optical (NLO) signals of coherent Raman scattering, two-photon excitation fluorescence (TPEF) and harmonic generation (SHG, SFG and THG) have been widely used to image a variety of biological samples. Different nonlinear optical signals could convey complementary morphological and biochemical information. Therefore, it is desirable to integrate multiple NLO signals together for biomedical imaging. Specifically, the recently demonstrated stimulated Raman scattering (SRS) microscopy provides the chemical imaging capability and overcomes the major drawbacks associated with CARS. Moreover, the TPEF signals of tryptophan and hemoglobin excited by visible femtosecond light augment the capability of conventional TPEF microscopy by label-free imaging the distributions of proteins and microvasculature in tissues, respectively. In this work, we instrument a multimodal NLO microscopy system which integrates the SRS of C-H stretching, TPEF of tryptophan and hemoglobin and SFG of collagen together. The excitation sources are the combination of the Ti:sapphire femtosecond laser and its pumped OPO system. The time- and spectral-resolved detection system could precisely separate different NLO signals and extracts more information about the microenvironment of the fluorophore from the TPEF signals. We demonstrate the multimodal imaging capability by implementing the noninvasive optical biopsy in mouse ear skin in vivo. Very rich morphological and biochemical information from the stratum corneum down to stroma including sebaceous gland, microvasculature and fat tissue can be label free conveyed. Furthermore, we observe the acetic acid (AA) induced protein aggregations in living cells using different NLO signals. That may help to explain the mechanisms of AA induced acetowhitening in tissue level.

8226-78, Session 12

## In-vivo SRS microscopy in biomedical applications by using longer wavelength excitation

M. Ji, Harvard Univ. (United States); T. Ito, Sony Corp. (Japan); G. Holtom, Harvard Univ. (United States); M. Misra, Unilever HPC USA (United States); X. S. Xie, Harvard Univ. (United States)

Intrinsic optical imaging in-vivo with chemical specificity is highly desirable in biomedical imaging. Stimulated Raman scattering (SRS) microscopy has been proven to have sig

# Conference 8227: Three-Dimensional and Multidimensional Microscopy: Image Acquisition and Processing XIX

Tuesday-Thursday 24-26 January 2012

Part of Proceedings of SPIE Vol. 8227 Three-Dimensional and Multidimensional Microscopy: Image Acquisition and Processing XIX

8227-01, Session 1

## Measuring aberrations in the rat brain by a new coherence-gated wavefront sensor using a Linnik interferometer

J. Wang, Ecole Supérieure de Physique et de Chimie Industrielles (France) and Institut Langevin, ESPCI ParisTech, CNRS UMR 7587, ESPCI, 10 rue Vauquelin, 75005 Paris, France (France); J. Leger, Ecole Normale Supérieure (France); J. Binding, Ecole Supérieure de Physique et de Chimie Industrielles (France) and Institut Langevin, ESPCI ParisTech, CNRS UMR 7587, ESPCI, 10 rue Vauquelin, 75005 Paris, France (France); A. C. Boccara, S. Gigan, Ecole Supérieure de Physique et de Chimie Industrielles (France); L. Bourdieu, Ecole Normale Supérieure (France)

Wavefront aberration due to refractive index mismatch and tissue inhomogeneity may limit the resolution, signal intensity and achievable imaging depth of microscopy. Traditional Shack-Hartmann wavefront sensors (SHWS) can't be used in strongly scattering biological samples. In contrast, coherence-gated wavefront sensing (CGWS) allows the fast measurement of aberrations in tissues and therefore the implementation of adaptive corrections. We have implemented a new CGWS scheme based on a Linnik interferometer with Super Luminescent Emission Diode (SLED) as low temporal coherence light source. Compared to a previously described CGWS system based on a femtosecond laser, its main advantages are the cost, the automatic compensation of dispersion between the two arms and its possible implementation on any microscope. Using a mirror as sample, the system was calibrated with a real SHWS. In fresh rat brain slices, we successfully measured up to a depth of about 400 µm a known defocus aberration, obtained by axially displacing the coherence gating (CG) with respect to the actual focus in the sample. At different depths, we investigated the dependency of the speckle size in the pupil plane and the measurement precision on the CG positions. We have shown that the speckle size was limiting the maximal depth of measurement. At shallow layer, the speckle size was maximum when the CG was located at the actual focus, which was in consistent with previous publications. When the depth was greater than about 160µm, the speckle size monotonically decreased when the CG was moved deeper into the sample.

8227-02, Session 1

## Performance evaluation of point-spread function engineering to reduce the impact of depth-induced aberrations on extended depth-of-field microscopy

S. Yuan, C. Preza, The Univ. of Memphis (United States)

In 3D extended depth-of-field (EDOF) microscopy, information from the whole range of specimen depths is displayed simultaneously. This is accomplished by placing a phase mask at the pupil plane to encode the wave front emerging from the imaging system and using computations to decode the information in the recorded intermediate image [1]. To achieve high resolution in microscopy, high NA lenses are used and thus spherical aberration (SA) introduced by refractive index mismatch could impact the EDOF feature [2]. In this study, we evaluated different wave front encoding (WFE) designs for their suitability to reduce the impact of SA on the 3D PSF and thereby facilitate the image processing required for EDOF for high NA microscopy in the presence of SA. Design parameters in a family of cubic phase masks (CPM, generalized CPM and sinusoid CPM) were varied resulting in different WFE PSFs. In addition, depth-variant WFE PSFs were computed by including SA at different imaging layers [3, 4]. Mean square errors computed between the Z layers of 3-D depth-variant PSFs and also between 3-D PSFs with increasing amounts of SA, were used to evaluate the potential performance of each WFE design. Optimal parameters were determined for each design and forward model images from these optimal designs were computed and compared to images from original designs published in the literature for EDOF [1, 5, 6].

1. E. R. Dowski and W. T. Cathey, "Extended Depth of Field through Wave-Front Coding," Applied Optics 34, 1859-1866 (1995)

2. M. R. Arnison, C. J. Cogswell, C. J. R. Sheppard and P. Török, "Wavefront Coding Fluorescence Microscopy Using High Aperture Lenses," in Optical imaging and microscopy- Techniques and Advanced Systems, P. Török and F. J. Kao eds., Springer-Verlag,, p.143 (2003)

3. S. F. Gibson and F. Lanni, "Experimental Test of an Analytical Model of Aberration in an Oil-Immersion Objective Lens Used in 3-Dimensional Light-Microscopy," Journal of the Optical Society of America a-Optics Image Science and Vision 9, 154-166 (1992)

4. http://cirl.memphis.edu/COSMOS

5. H. Zhao, Y. C. Li, H. J. Feng, Z. H. Xu, and Q. Li, "Cubic sinusoidal phase mask: Another choice to extend the depth of field of incoherent imaging system," Optics and Laser Technology 42, 561-569 (2010).

6. G. Carles, A. Carnicer, and S. Bosch, "Phase mask selection in wavefront coding systems: A design approach," Optics and Lasers in Engineering 48, 779-785 (2010).

8227-03, Session 1

## Imaging sharper and deeper in a spinning disk microscope by using adaptive optics

J. Andilla, Imagine Optic SA (France); V. Fraisier, T. Piolot, Institut Curie (France); J. Ballesta, Imagine Optic Inc. (United States); X. Levecq, Imagine Optic SA (France); J. Salamero, Institut Curie (France)

Three dimensional confocal microscopy has become a basic element in the bio-cellular and bio-molecular researches. A particular case of confocal microscopy, the spinning disk technology, allows the confocal 3D imaging in high frame rates by multiplexing the scanning of the laser. High numerical aperture optics allows imaging objects in 3D with lateral and axial resolution down to hundreds of nanometers. However, as other optical techniques of microscopy, optical aberrations present in the optical path reduce the performances of the system. Because the high numerical aperture of the system, this reduction can be especially dramatic when doing 3D imaging and going deep into a sample. The index mismatch of the objective immersion medium and the sample can create strong aberrations which increase proportionally with the penetration depth. As it has been shown in previous publications, the introduction of adaptive optics can compensate this effect and improve the quality of the image.

In this communication, we show the application and the improvements obtained by using adaptive optics in a spinning disk microscope. We will show the implementation of the experimental setup and we will discuss about the different strategies used to improve the quality of the measurement depending on the nature of the sample. In order to quantify the benefits and the efficiency of using adaptive optics in spinning disk systems, we will show and discuss about the comparison between the images obtained in traditional conditions, without the adaptive optics system, and the images obtained when using with the adaptive optics system.

8227-04, Session 1

## Real-time 3D microscopy made possible through PSF engineering designs that simultaneously record depth locations while extending the depth of focus of live cell features

R. N. Zahreddine, R. H. Cormack, C. J. Cogswell, Univ. of Colorado at Boulder (United States)

Abstract not available.

8227-06, Session 1

## Measurement and correction of spatially dependent aberrations in adaptive optical microscopy

M. Booth, Univ. of Oxford (United Kingdom)

Specimen-induced aberrations are frequently encountered in high resolution microscopy, particularly when high numerical aperture lenses are used to image deep into biological specimens. These aberrations distort the focal spot causing a reduction in resolution and, often more importantly, reduced signal level and contrast. The techniques of adaptive optics (AO) have been used to measure and correct the aberrations, restoring image quality.

AO systems normally use a wave front sensor to measure aberrations, which are in turn corrected using an adaptive element, such as a deformable mirror. In microscopes, however, direct wave front sensing is not straightforward and wave front sensor-less schemes are often employed. In these systems, the adaptive element is reconfigured in order to maximise an image quality metric, such as total intensity. Most implementations have used image averages for determination of the aberrations and hence a single correction aberration is derived for each image. However, for many specimens aberrations vary across the image field, so an averaged measurement leads to a compromise correction where some image regions are improved and others may become worse. This limits the applicability of current AO microscopes. We develop sensorless aberration measurement schemes to cope with spatial variations in aberrations. Furthermore we investigate practical methods that vary the aberration correction across the microscope's field of view.

8227-36, Session 1

## Comparison of varying pupil configurations in line-scanning confocal reflectance microscopy

Y. G. Patel, Northeastern Univ. (United States); M. Rajadhyaksha, Memorial Sloan-Kettering Cancer Ctr. (United States); C. A. DiMarzio, Northeastern Univ. (United States)

Confocal point-scanning microscopy has shown success in imaging human skin in vivo. However, current point-scanning systems are large, complex, and expensive. A confocal line-scanning microscope, utilizing a CMOS-linear array detector can be simpler, smaller, less expensive, and may accelerate the translation of confocal microscopy into the clinic. A confocal line-scanner may have a divided pupil or full pupil configuration. In a divided pupil configuration, half of the pupil is used for transmission and half for detection, while, in a full pupil, the entire pupil is used for coaxial transmission and detection. To progress toward clinical application, a study to explain resolvability of in vivo skin images, with morphology of varying index-of-refractions, is important.

We present a Fourier optics model for a confocal line-scanning microscope, using divided pupil and full pupil configurations, to evaluate spherical aberrations and field-curvature effects due to index-of-refraction mismatch. We theoretically determined the axial and lateral resolution using a variable detector slit of 5, 10, 25, 50μm, which corresponds to 0.59,1.18,2.95,and 5.90 Airy units, respectively. Axial resolution measurements for an index-matched line-scanning full pupil configuration are 1.6, 2.1, 2.5, and 3.6μm, respectively. For index-mismatch, computed axial resolutions measurements degrade by ~15%. For a line-scanning divided pupil configuration, axial resolution measurements from index-matching to index-mismatch degraded by ~12%. As the detector slit increases, speckle and background noise degraded resolvability in both pupil configurations.

8227-07, Session 2

## Calibration of an adaptive microscope using phase diversity

D. Débarre, T. Vieille, E. Beaurepaire, Ecole Polytechnique (France)

Adaptive optics has proven a powerful tool for improving the quality of images obtained within thick aberrating biological samples, in particular in the case of nonlinear microscopy [1,2]. Setting up an adaptive microscope however requires particular care since the effect of the adaptive element (usually a deformable mirror (DM)) on the transfer function of the microscope has to be carefully calibrated. Indeed, errors in this calibration critically affect the quality of subsequent corrections. Here we present a simple, versatile and scheme for characterising the electric field modulation by an active element, such as a DM, in the pupil plane of a high NA microscope. Using a flat mirror in the vicinity of the focal plane of the objective to record images of the focal spot on a camera, we show that reliable measurement of the influence function of the DM actuators in the pupil plane of the objective can be obtained using an iterative electric field retrieval algorithm. The setup permits the use of a variety of objectives with different NA and pupil size, requires minimal space inside the microscope, and can be used with pulsed sources such as used for multiphoton microscopy. To check the accuracy of our method, we compare our data to results obtained with a Shack-Hartmann sensor (SHS), and show that comparable precision is achieved with reduced cost and complexity.

[1] Débarre et al, Opt. Lett. 34 (2009).

[2] Olivier et al, Opt. Lett. 34 (2009).

[3] Débarre et al, J. Microsc. (2011, to be published)

8227-08, Session 2

## Correction precision in image-based adaptive optics for nonlinear microscopy

D. Débarre, A. Facomprez, E. Beaurepaire, Ecole Polytechnique (France)

Aberration correction has proven useful to improve the quality of nonlinear images when focussing inside thick biological samples. In image-based adaptive optics, a metric (such as brightness or sharpness) is calculated from images acquired with a series of aberration applied, and the initial amount of aberration is then estimated using a simple maximization algorithm. This approach has been shown to significantly improve the quality of images in two-photon fluorescence microscopy and third-harmonic generation microscopy[1-3].

Here we investigate experimentally the precision of the achieved correction as a function of the algorithm parameters, such as the number of measurements per corrected aberration mode, the amount of aberration corrected, the number of photons per image, etc. We show that the optimal parameters for precise correction depend on the initial amount of aberration that needs be corrected for, and propose optimized algorithms for various practical situations.

Using appropriate parameters, we subsequently show that we can quantify aberrations in various biological samples with 3D resolution. This permits to precisely estimate the gain that can be obtained with adaptive optics in various tissues. Examples include embryonic tissue, brain slices and ex-vivo skin samples.

[1] Débarre et al, Opt. Lett. 34 (2009).

[2] Olivier et al, Opt. Lett. 34 (2009).

[3] Jesacher et al, Opt. Lett. 34 (2009).

[3] Débarre et al (in preparation).

8227-09, Session 2

## Real-time visualization of cardiomyocytes contractions resolved with multidepth nonlinear optical microscopy

M. Samim, Univ. of Toronto (Canada); I. Tretyakov, N. Prent, R. Cisek, D. Sandkuijl, S. Musikhin, V. Barzda, Univ. of Toronto Mississauga (Canada)

Real-time volume imaging allows for studying muscle cell contraction, microorganisms motility, neuronal activity, and other fast cellular processes. We present video-rate investigations of structural dynamics in heart muscle tissue with the multicontrast third- and second-harmonic generation. The multidepth scanning is achieved by two combined laser beams with staggered femtosecond pulses. Each beam is independently equipped with a deformable mirror for dynamic wavefront manipulation, enabling multidepth refocusing with simultaneous corrections for optical aberrations. Combined, more than 250 frames per second lateral scanning with fast axial refocusing have enabled the microscope of video-rate multi-depth imaging of rapidly moving structures. All data acquisitions are performed by a Xilinx Virtex-5 FPGA. In addition, combination of two laser beams is accomplished at two perpendicular polarizations making possible live imaging of sample anisotropy. Anisotropy is important for structural studies particularly with the second harmonic generation microscopy. Investigations of beating chick embryo hearts with the 3D video-rate scanning microscope revealed multidirectional cardiomyocyte contraction dynamics in myocardial tissue. Intricate synchronization of contractions between different layers of myocytes in the tissue will be presented. The video-rate 3D microscopy opens new possibilities of imaging fast biological processes in living organisms.

8227-10, Session 2

## A new calibration tool for fluorescence microscopy

A. Royon, P. Legros, G. Papon, T. Cardinal, L. S. Canioni, Argolight (France)

Confocal fluorescence microscopes equip many laboratories and platforms, not only in biology and medicine, but also in materials science. More and more, these laboratories and platforms want to pursue a quality approach. To achieve this goal, the performances of the microscopes must be guaranteed. However, these instruments are not sold as “measurement tools”, because the different devices composing the microscope cannot be calibrated altogether.

We have developed a new process that enables the inscription of fluorescent patterns with sub-micrometer sizes in three dimensions inside photosensitive glass. In this paper, we present, based on this new process, a fluorescent multi-dimensional (space, intensity, spectrum, lifetime) ruler adapted for the control and the calibration of fluorescence microscope components (usual, confocal, epi).

Non-exhaustively, this new tool enables the measurement of:

- The repositioning of the translation stages with a resolution higher than the optical one.
- The dynamics of the detectors, thanks to nine well-discriminated fluorescence intensity levels.
- The field homogeneity of the microscope objective.
- The XY and Z resolutions of the microscope objective with an uncertainty of 200 nm and 1 µm, respectively.
- The spectral response (spectrum, intensity and lifetime) of the system.

This device is guaranteed not to photo-bleach, it can be used for a long period of time (> 5000 hours), and can be stored without any particular precaution. Thus, measurements can be carried out at different times and can be compared, to follow, for example, the performances of a microscope in time and/or detect any malfunction.

8227-11, Session 3

## Comparison of 3D imaging of the blood drops and splatters using multiframe microscopy and structured light profilometry

W. Walecki, F. Szondy, P. S. Walecki, Sunrise Optical LLC (United States)

We have constructed a system employing an accelerated Richardson Lucy algorithm for three dimensional mapping of small dry and liquid blood splatters and drops. The system collects data at several wavelength bands. Several frames representing image of the device allow combining multi-frame spectral and spacial information. Our algorithm uses this information together with prior information about optical properties of the blood to recover the shape, thickness, and volume of dry and liquid blood splatters. We compared results of our measurements with results obtained using 3D structured multicolor light profilometry.

Our tool investigates several image frames taken at various working distances from the sample. We have developed proprietary algorithms that take advantage of the de-focus information in conjunction with the Richardson-Lucy (RL) iterative procedure involving regularization steps incorporating penalties for salt and pepper noise. In this we have reduced noise amplification inherent to RL algorithm.

We have found that spectroscopic and hyperspectral data alone cannot provide information easily about topography and the internal structure of dry splatter samples.

The presentation contains photographs of the tool itself, and results obtained using animal blood models. We expect that this new technology will find applications in forensic studies.

8227-12, Session 3

## Hyperspectral fluorescence microscopy based on compressed sensing

V. Studer, Interdisciplinary Institute for NeuroScience (France); J. Bobin, Commissariat à l'Énergie Atomique (France); M. Chahid, H. Mousavi, Interdisciplinary Institute for NeuroScience (France); E. J. Candes, Stanford Univ. (United States); M. Dahan, Lab. Kastler Brossel (France)

In fluorescence microscopy, one can distinguish two kinds of imaging approaches, wide-field and raster scan microscopy, differing by their excitation and detection scheme. In both imaging modalities the acquisition is independent of the information content of the image. Rather, the number of acquisitions N, is imposed by the Nyquist-Shannon theorem. However, in practice, many biological images are compressible (or, equivalently here, sparse), meaning that they depend on a number of degrees of freedom K that is smaller that their size N. Recently, the mathematical theory of compressed sensing (CS) has shown how the sensing modality could take advantage of the image sparsity to reconstruct images with no loss of information while largely reducing the number M of acquisition.

Here we present a novel fluorescence microscope designed along the principles of CS. It uses a DMD to create structured wide-field excitation patterns and a sensitive point-detector to measure the emitted fluorescence. On sparse fluorescent samples (beads, and cultured cell), we could achieve compression ratio N/M of up to 64, meaning that an image can be reconstructed with a number of measurements of only 1.5 % of its pixel number.

Furthemore, we demonstrate how CS acquisition schemes can be extended to an hyperspectral imaging system. We could acquire fluorescence images, with 128 different spectral channels, with a compression ratio of up to 128. We finally discuss strategies to further reduce the number of acquisition by taking into account the sample sparsity, not only in the spatial but also in the spectral domain.

8227-13, Session 3

## Optimisation of the diffractive optical element for snapshot spectral imaging used in fluorescence microscopy

R. Leitner, M. De Biasio, T. Arnold, G. McGunnigle, Carinthian Tech Research AG (Austria); R. Rogojanu, G. E. Steiner,

Snapshot approaches address various possibilities to acquire the spectral and spatial information of a scene within a single camera frame. One advantage over the classical push broom or staring imager approaches is that the temporal inconsistency between consecutive scan lines in first case or between the acquired monochromatic images in the second case is avoided. However, this has to be paid by some effort to rearrange or reconstruct the explicit spectral cube from the raw data in the single camera frame. Besides others, the utilisation of a diffractive optical element (DOE) is one such snapshot approach (CTIS - computed tomography imaging spectrometer). The DOE is used

to create an optical transfer function that projects both the spectral and spatial information of a scene onto a sensor array and a reconstruction algorithm that inverts this projection. The design of the DOE is intricate as the absolute transmission efficiency of the 0./1. order versus the relative efficiency over the required wavelength range are difficult to optimise if the camera's dynamic range is considered additionally. We describe the optimisation of such a 2D DOE for the wavelength range 400 - 780nm and the required reconstruction algorithm. The described approach has been evaluated using experiments to assess the spatial and spectral resolution (colour standards, LEDs). Additionally the results achieved using the described setup for multi-colour in-situ fluorescence hybridised preparations (MFISH) are discussed.

This work was funded within the research project 820116 of the BRIDGE funding program of the Austrian Funding Agency FFG and TissueGnostics (Vienna, Austria) and IPAC (Villach, Austria).

8227-14, Session 3

## Double helix PSF engineering for computational fluorescence microscopy imaging

S. Ghosh, The Univ. of Memphis (United States); S. A. Quirin, G. Grover, R. Piestun, Univ. of Colorado at Boulder (United States); C. Preza, The Univ. of Memphis (United States)

Point spread function engineering with a double helix (DH) phase mask is part of a joint computational-optical approach to extract depth and intensity information from fluorescence images. In this study, simulated DH-PSFs computed with different amounts of depth-induced spherical aberration are evaluated through a comparison to empirically determined DH-PSFs measured from quantum dots. The simulated DH-PSFs show a trend that captures the main effects observed in the empirically-determined DH-PSFs.

8227-15, Session 3

## Three-dimensional refractive index imaging with differential interference contrast microscopy

H. Aung, J. Buckley, P. Kostyk, B. Rodriguez, S. Phelan, M. Xu, Fairfield Univ. (United States)

Differential interference contrast (DIC) microscopy is well known for its ability to image transparent phase objects that otherwise produce very little contrast in conventional brightfield microscopy. Its particular advantages over other phase imaging techniques include applicability at high numerical apertures, high contrast, and its ability to image phase objects embedded within a transparent material. Additionally, the differential shear of DIC microscopy makes it very sensitive to small phase gradients. At the same time it is a full-field imaging technique and therefore does not require scanning. Although the advantages of DIC microscopy are useful in a large range of applications, it is fundamentally a qualitative imaging method because the complex transmission function of the specimen is recorded as an intensity measurement. As a result, there is a nonlinear relationship between image intensity and the magnitude and phase gradient of the object. Past decade has witnessed active development in extracting quantitative phase information from the qualitative intensity maps recorded by a DIC microscope via, for example, phase shifting DIC microscopy, the approach based on the transport of the intensity equation, and tomographic approaches.

We report here a new approach based on an extension of the transport of the intensity equation to generate three dimensional refractive index map from a series of images recorded by a DIC microscope (Axiovert 40cfl PlasDIC) at different focus (z-stack). Our method is first validated by imaging polystyrene spheres of various sizes (4.19 micron and 8.31 micron). We then apply this method to image human breast MCF7 epithelial cell. The sub-cellular feature identified from the reconstructed refractive index map is verified by fluorescence microscope image of the cell stained by Alexa Fluor 488 dye and Propidium Iodide. The potential applications and the efficacy of our approach are assessed at the end.

8227-16, Session 3

## Performance evaluation of an image estimation method based on principal component analysis (PCA) developed for quantitative depth-variant fluorescence microscopy imaging

S. Yuan, C. Preza, The Univ. of Memphis (United States)

In 3D wide-field computational microscopy, the image formation process is depth variant due to depth-induced aberrations that increase with the imaging depth and the refractive index mismatch between the imaging layers [1]. In a previous study, an image estimation method based on a principle component analysis (PCA) model for the representation of the depth varying point spread function (DV-PSF) was presented [2]. The performance of the PCA-based method was demonstrated using noiseless simulations. In this study, we further evaluated the performance of the PCA-based image estimation method using noisy simulations and by applying it to measured data acquired from a test sample that consists of a 15 um in diameter spherical shell of fluorescence. We first investigated the noise influence using a synthetic object that resembles the test sample, and theoretically-determined depth-variant PSFs approximated by the PCA approach and different noise levels. We then compared findings from the simulation study to results obtained from the 3D fluorescence bead image acquired using a 3D wide-field optical-sectioning fluorescence microscope.

1. C. Preza and J. A. Conchello, “Depth-variant maximum-likelihood restoration for three-dimensional fluorescence microscopy,” Journal of the Optical Society of America a-Optics Image Science and Vision, 21(9), 1593-1601 (2004)

2. S. Yuan and C. Preza, “3D fluorescence microscopy imaging accounting for depth-varying point-spread functions predicted by a strata interpolation method and a principal component analysis method,” Proceedings of SPIE Vol. 7904, 79040M (2011).

8227-17, Session 4

## Multicolor focal modulation microscopy

G. Gao, S. P. Chong, N. Chen, National Univ. of Singapore (Singapore)

A spatial-temporal phase modulator (STPM) is the critical component in focal modulation microscopy (FMM). The configuration and implementation of the STPM affect the performances of the FMM system in a significantly way. The desirable properties of STPM include high-speed, compatibility with multiple wavelengths, and the ease to implement. We have developed an EOM (Electro-optic modulator) based modulator to meet these requirements. The EOM is operated at around 10 MHz and works with a spatial polarizer and other general-purpose polarization components to achieve a high modulation depth. Such a modulator is inserted into an Olympus FV300 confocal system for multi-color FMM.

8227-18, Session 4

## Melanin fluorescence spectra by step-wise three photon excitation

Z. Lai, J. Kerimo, C. A. DiMarzio, Northeastern Univ. (United States)

We present photothermal images of melanin using modulation with two laser beams. The melanin from several samples including Sepia officinalis, black human hair, live zebra fish, and human tissue were imaged with a high signal-to-noise ratio. Two laser beams with different wavelengths (one with amplitude modulation) were focused collinearly on the sample and the scattering of one of the beams, at the modulation frequency, was detected. Strong step-wise excited state absorption (ESA) of the modulated beam by melanin leads to an increase in temperature with changes in the refractive index and the scattering of the second laser beam. Although the dual-beam photothermal method has been used to image single metal nanoparticles and semiconductor nanocrystals, this method appears to be practical for imaging and detecting melanin. Important benefits of this method are that the melanin can be detected without interference from the background scattering since the background is suppressed efficiently by the modulation, and that low laser power can be used for an extended period of time without photoactivation or photodamage to the melanin in the imaging. Furthermore, the signal is stable and does not suffer from any photobleaching effects normally seen in fluorescence. The nature of the photothermal image is discussed including the image resolution, dependence on the laser power, wavelength, and modulation frequency. The new photothermal imaging method is promising and can be easily implemented with low-cost CW lasers to accurately map the melanin content.

8227-19, Session 4

## Holographic linear imaging with a single-pixel using spatial frequency modulated microscopy

D. Higley, D. G. Winters, R. Bartels, Colorado State Univ. (United States)

Recently, we introduced a technique demonstrating high-speed line scan imaging with a single pixel detector. Spatial information is encoded into the electronic frequency domain of the signal from a single-element photodiode by modulating the intensity at each point of an illumination beam at a distinct and linearly varying frequency. With this modulation, both absorptive and fluorescent line images can be recorded. Two-dimensional images are readily obtained by scanning the line image, or by expanding the beam and performing tomographic reconstruction on a sequence of relative rotations of the modulated beam and the object. The SPIFI modulation mask imparts a sinusoidal intensity modulation at each spatial point with a binary transmittance mask with a square amplitude transmission grating whose spatial frequency sweeps linearly in time. The SPIFI images obtained to date have provided the intensity response of the object, that is the intensity transmission or the fluorescent intensity. In this work, we demonstrate that in SPIFI line imaging, holographic detection with a single-element detector can recover full amplitude and phase information in a technique strongly analogous to conventional off-axis holography. Numerical back-propagation of this field gives line images as a function of back propagation distance, and produces a 2D sheet image from a single stationary single-element photodetector. Experiments and theory demonstrating SPIFI holography in an absorptive and fluorescent SPIFI microscope will be presented.

8227-21, Session 5

## Tomographic phase microscopy combined with light scattering measurements to investigate the structure and light scattering properties of live epithelial cells for early cancer detection

J. Su, W. Hsu, K. Sung, National Taiwan Univ. (Taiwan)

The progression of epithelial dysplasia, a precursor of many epithelial cancers, is accompanied by changes of sub-cellular structures which alter the light scattering properties of the cells. Tomographic phase microscopy (TPM) is a powerful technique for measuring the refractive index distributions in live biological cells. To gain more knowledge about the structural changes and associated light scattering properties of precancerous and caner cells, we develop a TPM combined with the light scattering technique for simultaneous acquisition of quantitative 3D refractive index maps and 2D light backscattering patterns from live epithelial cells. The proposed TPM system is based on generalized phase shifting interferometry with Mach-Zehnder configuration. Nanometer-scale stability, up to 1 nm, in transmission mode quantitative phase images is achieved without actively stabilizing the instrument or precisely controlling the amount of phase shift. With the application of optical diffraction tomography and a prior knowledge of the cells, high-resolution quantitative refractive index distributions of live and unstained cells can be reconstructed from a set of angle-dependent phase and amplitude images. Furthermore, the 2D backscattering patterns contributed from the living biological cells can be detected simultaneously. We use the proposed method to investigate the structures and light scattering properties of squamous epithelial cells of the skin and oral cavity. The characteristics and changes of the sub-cellular structures in normal and cancerous cells exposed to acetic acid are also studied.

8227-22, Session 5

## Dynamic phase imaging and processing of biological processes and moving organisms

K. Creath, G. Goldstein, 4D Technology Corp. (United States) and College of Optical Sciences, The Univ. of Arizona (United States)

This paper describes recent work utilizing an interference Linnik microscope system and presents images and data of live biological samples. This system enables instantaneous 4-dimensional video measurements of dynamic motions within and among live cells without the need for contrast agents. This “label-free”, vibration insensitive imaging system enables measurement of biological objects in reflection using harmless light levels with a variety of magnifications and wavelengths with fields of view from several hundred microns up to a millimeter. At the core of the instrument is a phase measurement camera (PMC) enabling simultaneous measurement of multiple interference patterns utilizing a pixelated phase mask taking advantage of the polarization properties of light. Utilizing this technology enables the creation of phase image movies in real time at video rates so that dynamic motions and volumetric changes can be tracked. Objects are placed on a reflective surface in liquid under a coverslip. Phase values are converted to optical thickness data enabling volumetric, motion and morphological studies. Data from a number of different organisms such as paramecium, flagellates and rotifers will be presented, as will measurements of human breast cancer cells with the addition of various agents that break down the cells. Our latest data will be presented highlighting examples of monitoring different biological processes and motions. The live presentation features 4D phase movies of these examples.

8227-23, Session 5

## Low-coherence reflection tomography

Y. Sung, Massachusetts Institute of Technology (United States); D. Fu, Harvard Univ. (United States); W. Choi, Korea Univ. (Korea, Republic of); R. R. Dasari, Z. Yaqoob, Massachusetts Institute of Technology (United States)

Tomographic phase microscopy (TPM) is a field-based 3-D imaging technique that uses 3-D refractive index contrast for stain-free monitoring of transparent biological specimens. TPM can provide twice higher resolution than the diffraction limit in transverse direction, while its axial resolution remains the same as the diffraction limit. The so-called reflection tomography can provide higher axial resolution, but its application has been limited to highly scattering samples. For weakly scattering biological cells, major impediments have been the noise, either coherent speckle or scattered light from the optical elements in the setup, overwhelming the weak reflection signal. Here, we report the development of a low coherence reflection tomography system for imaging transparent biological specimens with high axial resolution. Our system is built on the wide-field single-shot reflection phase microscope. We use a light source with relatively long coherence length to selectively collect the reflection signals from the cells, while rejecting those from other locations within the setup. The coherence gating, together with angular scanning, provides high axial resolution that is otherwise not achievable in stain-free imaging of transparent biological samples. The angular scanning is achieved via a 2-D galvanometer mirror in an intermediate image plane conjugate to the sample plane. We record both the phase and amplitude of the back-scattered light from the specimen while changing the illumination angle of the incident beam. A regularized inversion algorithm is developed to reconstruct the 3-D reflection tomographic image of the sample from the collected data.

8227-24, Session 5

## Low-coherence quantitative phase microscopy with a rapidly tunable broadband source

M. T. Rinehart, F. E. Robles, Y. Zhu, M. G. Giacomelli, A. P. Wax, Duke Univ. (United States)

Quantitative phase microscopy (QPM) enables label-free visualization of cellular structure using local variations in refractive index as contrast, thereby allowing direct measurement of morphological changes. Current methods of transmission geometry QPM utilize laser light sources and thus suffer from coherent noise (speckle) and degradation of image quality by reflections from system components. Therefore we have developed a novel microscope that uses broadband light with low temporal coherence to reduce both noise and coherent artifacts. Using a supercontinuum light source in combination with an acousto-optic tunable filter, the illumination center wavelength may be tuned at kHz rates across the visible region of the spectrum (450nm to 700nm) with bandwidths of 5 nm to 30 nm to probe spectral features of the samples. By acquiring high visibility interferograms in an off-axis geometry with a high speed CMOS camera, full field quantitative phase images are captured in a single shot at up to 1000 frames per second. With this novel instrument, we have achieved sub-nanometer temporal stability across a full field of view. Furthermore, this scheme can sequentially acquire quantitative phase maps at varying spectral points at high speeds to study temporally-resolved changes in spectral features of individual and populations of cells. We validate the utility of this approach by measuring wavelength dependent refractive index changes in various fluorescent microspheres and also investigate absorption features of hippocampal neurons in vitro.

8227-25, Session 5

## Polarimetric microscopy of Si:Ga nanostructures

M. Theisen, B. McIntyre, T. G. Brown, Univ. of Rochester (United States)

Polarization-sensitive nanostructures are interesting and useful in creating unconventional polarization states and as calibration targets for polarimetric microscopy under epi-illumination. We report on the results from a polarimetric microscopy study of freestanding nanowire structures formed from heavily implanted Gallium doped Silicon.

Starting with a commercial grade silicon wafer, we used a focused ion beam system (Zeiss Auriga dual beam SEM/FIB) to implant wire patterns surrounded by a scaffold structure to support the wires following an under-cutting etch. The etch was done with a SF6-Ar reactive ion etch (South Bay Technology Inc. RIE-2000); gallium doped regions remain unaffected by the etch, thus leaving the Si:Ga nanowires suspended in air. Support wires were anchored to a square pad surrounding the structure allowing the nanowire to be suspended off the substrate once the RIE process is completed. Typical suspended wires are 200 nm wide and less than 50 nm thick; they can be suspended over 1 micon above the substrate.

When viewed in green laser illumination, the nanowires show substantial retardance on reflection with regions of relatively low diattenuation, a feature that is potentially useful as a calibration target for quantitative polarization microscopy.

8227-26, Session 5

## Point spread function polarimetry using stressed engineered optical elements

R. Ramkhalawon, A. M. Beckley, T. G. Brown, Univ. of Rochester (United States)

It has previously been shown that stressed engineered optical elements have potential applications in ‘snapshot polarimetry’, in which a single irradiance image is used to deduce the polarimetric properties of a beam. In this paper, we present a correlation-based method to perform polarization retrieval of isolated scatterers. With a symmetrically stressed window placed at the pupil plane of an imaging system, a single frame point spread function can be analyzed to recover the Stokes parameters of the incident beam. In this scheme, one polarization component of the point spread function is compared to a database of known point spread functions to identify the polarization with the highest correlation. We will present the basic approach, along with an analysis of sensitivity to defocus and general considerations of how the method might be applied to systems of high numerical aperture and images containing many scatterers.

8227-27, Session 6

## Lensless holographic volume imaging using a pseudo-random phase mask

W. H. Harm, A. Jesacher, S. Bernet, M. A. Ritsch-Marte, Innsbruck Medical Univ. (Austria)

We demonstrate three-dimensional imaging in the visible optical regime with high axial sectioning capability from a single recorded diffraction pattern. A scalar electromagnetic wave is fully described if its complex amplitude is known in one transverse plane or if either the phase or the intensity is known in two different planes. In our approach to lensless imaging the latter condition applies, where one or more samples are located at a variable axial position between a spatial light modulator (SLM) and a CMOS camera chip. The phase of the illuminating HeNe laser beam is modulated with a pseudo-random phase mask displayed by the SLM and the scattered speckle pattern, i.e. the intensity distribution, is captured by the CMOS chip in the Fresnel regime. Image reconstruction in the image sensor plane is performed by multiplying the calculated Fresnel transform of the pseudo-random phase mask by the measured intensity distribution. For three-dimensional image acquisition the reconstructed complex amplitude is axially propagated over the entire volume between the SLM and the CMOS chip.

The basic principle is related to on-axis holography though here, instead of employing interference, the intensity of the complex amplitude is represented by the difference between the speckle pattern and a pre-recorded undisturbed reference speckle pattern, thus being inherently stable against vibrations and phase fluctuations. Furthermore the diffusive sample illumination prevents the formation of other diffraction orders such as the overlapping twin image that appears in conventional on-axis holography. Once the reference speckle pattern is recorded, this method enables real-time image reconstruction with a resolution of about 20 micrometer.

8227-28, Session 6

## Digital holographic microscopy for the cytomorphological imaging of cells under zero gravity

M. F. Toy, Ecole Polytechnique Fédérale de Lausanne (Switzerland); S. Richard, ETH Zurich (Switzerland); J. Kühn, Ecole Polytechnique Fédérale de Lausanne (Switzerland); A. Franco-Obregón, M. Egli, ETH Zurich (Switzerland); C. Depeursinge, Ecole Polytechnique Fédérale de Lausanne (Switzerland)

Digital holographic microscopy (DHM) has been gaining interest from cell biology community because of its label free nature and quantitative phase signal output. Besides, fast shutter time, image reconstruction by numerical propagation of the wave fields, and numerical compensation of the aberrations are other intrinsic advantages of this technique that can be explored for harsh imaging conditions. In the frame of this work, a transmission type DHM is developed with a decoupled epifluorescence microscopy mode for cytomorphological monitoring under zero gravity and hyper gravity. With the implemented automatic post processing routines, real time observation of the cell morphology is proven to be feasible under the influence of mechanical disturbances of zero gravity platforms. Post processing of holograms is composed from dynamic numerical compensation of holograms, robust autofocusing and phase image registration. Experiments on live myoblast cells are carried out on two different platforms; random positioning machine (RPM), a ground base microgravity simulation platform, and parabolic flight campaign (PFC), a fixed wing plane flight providing short durations of alternating gravity conditions. Results show clear perinuclear phase increase with accelerated membrane protrusion activity and actin network reorganization in the case of minutes of microgravity exposure. During seconds scale microgravity exposure, measurable scale morphological modifications are observed with the accumulated effect of repetitive exposures and short breaks. Intracellular calcium observations via fluorescent calcium indicators also indicate to variation of intracellular ionic concentration with the level of net gravitational force.

8227-29, Session 6

## Lensless holographic microscopy with high-resolving power for 4D measurement of micro-organism swimming in water

M. Otani, K. Sato, Univ. of Hyogo (Japan)

There is the holographic microscope in one of various fields where digital holography has been applied. Holographic microscopes with microscope objectives have already been studied previously. These holographic microscopes, however, lost the advantage of the holography, that is, the recording of 3-D images with no distortion and with a large depth, because the object beam is recorded through the imaging lens in their optical systems. Lensless configurations have been proposed for holographic microscopy using in-line Gabor holography. The holographic microscope by in-line Gabor holography does not provide quantitative phase information, because the real and conjugate wavefronts are all spatially overlapped in the hologram and the illumination beam is attenuated or perturbed by the objects.

A purpose of the present paper is to develop a lensless 4-D (spatio-temporal) holographic microscope with a high resolving power. An off-axis hologram with a large numerical aperture is recorded, and a complex-amplitude in-line hologram is extracted from the recorded off-axis hologram by applying the one-shot digital holography. A new angular spectrum method is developed for fast and precise numerical reconstruction of 3-D image from the in-line hologram with a large numerical aperture. A small complex-amplitude in-line hologram is generated for the reconstruction of microscopic high-resolution images by dividing the large hologram into a number of small sections and by superimposing them. 3-D images with no distortion, with a resolution higher than 1μm, and with a depth larger than 1mm are recorded and reconstructed by the present holographic microscopy. 4-D (spatio-temporal) images are also observed microorganisms swimming in water.

8227-30, Session 6

## Resolving 3D trajectories of sperms on a chip using multi-angle lensfree digital holography

T. Su, A. Ozcan, Univ. of California, Los Angeles (United States)

Monitoring the dynamics of sperm trajectories in three-dimensional (3D) space is quite important to understand the delivery paths of genetic material to female eggs. However, most of the studies on sperm dynamics so far were only limited to 2D analysis due to the limited depth-of-field ( 5mm^2 and a depth-of-field of 0.5-1mm. Within this sample volume of ≥2.5uL, hundreds of 3D sperm trajectories are analyzed all in parallel to provide not only the dynamics of individual sperms, but also the statistical behavior of a population. Such a simple, cost-effective, and yet high-throughput 3D sperm tracking platform could be especially useful for resolving infertility issues, improving animal breeding, as well as for tracking cells inside 3D microfluidic structures.

8227-31, Session 7

## Lensfree optical tomographic microscopy: from bench-top to field use

S. O. Isikman, W. Bishara, O. Yaglidere, U. Y. Sikora, J. Yeah, A. Ozcan, Univ. of California, Los Angeles (United States)

Recent advances in three-dimensional (3D) microscopy enable volumetric investigation of micro-organisms. Nevertheless, existing 3D microscopy modalities have relatively complex, bulky and costly architectures, hampering their use in lab-on-a-chip platforms as well as in low-resource settings. Toward this need, here we present lensfree optical tomography (LOT) that offers micron-scale 3D resolution over a large imaging volume. In LOT, the sample is placed on an optoelectronic-sensor-array, and is illuminated with partially-coherent light along different directions to record its lensfree holograms at different viewing angles within a range of ±50°. To increase the numerical aperture of these holograms, multiple holograms with sub-pixel shifts with respect to each other are also recorded at each angle. Once pixel super-resolved (SR) holograms are obtained, digital holographic reconstruction of these SR holograms followed by filtered back-projection yields the tomograms of the objects over a large imaging volume.

In our bench-top demonstration, the necessary sub-pixel hologram shifts and multi-angle illumination are both obtained using a source mounted on motorized translation/rotation stages, achieving <1μm x<1μm x<3μm x-y-z resolution over a large sample volume of e.g., ≥15mm3. Owing to its simple architecture, LOT also lends itself to cost-effective and simple designs. Therefore, by devoting separate light-emitting-diodes that are butt-coupled to individual multi-mode fibers for each illumination direction, we also demonstrated, without the use of any mechanical scanning, 3D imaging using a field-portable tomographic microscope (weighing ~110g). Providing a decent 3D resolution in optical part of the spectrum, LOT could provide a useful toolset for lab-on-a-chip platforms and for field-use in resource-limited environments.

8227-32, Session 7

## A quantitative analysis of the effects of different resampling techniques for optical coherence tomography

C. Copeland, A. K. Ellerbee, Stanford Univ. (United States)

Fourier domain optical coherence tomography (FD-OCT) uses interferometry with a spatially coherent, polychromatic light source to acquire cross-sectional images of scattering media like biological tissue. Phase-sensitive derivatives of FD-OCT, such as spectral domain phase microscopy (SDPM), can perform quantitative phase imaging of cellular dynamics with sub-Angstrom sensitivity. Reconstruction of FD-OCT and SDPM images requires taking the Fourier Transform of the raw data; the accuracy of the reconstruction depends on the choice of processing algorithms used, system noise, calibration and quantization errors. To decrease the processing time, the robust and popular Fast Fourier Transform algorithm is preferred over the traditional Discrete Fourier Transform when the data are evenly sampled in wavenumber. Unfortunately, most OCT systems are designed for constant wavelength sampling, and leaving researchers to apply hardware- or software-based methods to resample the data accordingly. While there is general agreement on the qualitative superiority of some resampling methods over others, to the best of our knowledge there has been no detailed study that compares these methods quantitatively for OCT data in theory and in practice, or that has investigated the effects of different methods on the accurate recovery of phase information for SDPM. We examine the effects of various resampling techniques on phase and amplitude data in terms of accuracy, SNR, axial resolution and susceptibility to system errors. Given the trend towards high-speed imaging with OCT, the choice of resampling methods is critical as one need balance processing time and image accuracy - not merely quality - when analyzing medical image data.

8227-33, Session 7

## Multi-angle view of lung using optical coherence tomography(OCT)

A. Golabchi, C. A. DiMarzio, Northeastern Univ. (United States)

Lung imaging, visualization and measurement of alveolar volume has great importance in determining lung health. However, the heterogeneity of lung tissue complicates this task. In this paper multi angle Optical Coherence Tomography (OCT) is used in order to overcome this problem.

One of the limitations of utilizing OCT in lung is the speckle noise and artifacts that originate from the refraction at the tissue-air interface inside the lung. Multi angle view of lung using OCT is incoherent summation of multiple angle-diverse images. Utilizing image registration of multi angle OCT scans of the lung helps reduce the speckle noise and refraction artifacts. This technique helps to extract more information from the images which improves visualization and the ability to measure of the geometry of alveoli. The other difficulty of utilizing OCT is interpreting the images due to the low numerical aperture (NA) on the OCT. The multi angle view of the lung increases NA, which increase the imaging resolution through synthetic aperture imaging. Inflated excised lung tissue and lung phantom will be presented.

8227-34, Session 7

## Optical projection tomography for imaging zebrafish vascular network in vivo

A. Bassi, L. Fieramonti, C. D'Andrea, G. Valentini, Politecnico di Milano (Italy)

Optical Projection Tomography (OPT) is a powerful three dimensional imaging technique for whole biological organisms and samples that range in the millimeter scale.

Similarly to x-ray computed tomography, OPT is based on the acquisition of a sequence of optical transmission images through the sample at several angles. The acquired projections are mathematically combined to image the tissue in 3D.

We describe our OPT system designed for in-vivo imaging of juvenile zebrafish (Danio-Rerio), a widely used model organism. The system is based on white light LED illumination and camera detection. Telecentric lenses are used to uniformly illuminate the sample and to select the light which primarily travels through the sample parallel to the optical axis of the camera. A stepper motor is used to rotate the sample over 360°.

We present the protocol for in- vivo imaging of the zebrafish. Firstly, the sample is anesthetized and mounted in a low melting point agarose gel. Then, it is included in a fluorinated ethylene propylene tube, which is immersed in water.

We show that it is possible to visualize the vasculature of the zebrafish, by detecting the movement of the cells present in the bloodstream, without the need for a fluorescent probe. We therefore demonstrate a label free, in vivo, three dimensional imaging technique that can be used to reconstruct the vascular network of transparent and weakly scattering living specimens.

8227-20, Poster Session

## Two-photon scanned light sheet microscopy reveals spatio-temporal organization of cells and proteins in developing embryos

T. V. Truong, X. Cui, S. E. Fraser, California Institute of Technology (United States)

Light sheet microscopy uses the novel sheet-illumination, orthogonal to the detection direction, to achieve higher acquisition speed and lower photodamage than conventional imaging techniques. We recently applied 2-photon excitation to light sheet microscopy to increase the penetration depth, allowing long-term imaging of cells deep inside of live embryos. Here we show the application of this imaging technology to record the cellular and gene expression dynamics in developing embryos. The combined subcellular resolution, high acquisition speed, and high penetration depth allows study of the spatio-temporal organization and control of cells and proteins that are critical in the development of an organism.

8227-44, Poster Session

## Generalized pulse spectrum technique for diffuse optical tomography based on the third-order spherical harmonics approximation to radiative transfer equation

W. Ma, F. Gao, L. Wu, X. Yi, H. Zhao, Tianjin Univ. (China)

Diffuse optical tomography (DOT) has become an indispensable imaging modality in preclinical research. It is extensively applied and is an efficient tool for in vivo small animal research. The diffusion-approximation (DA) theory is commonly used in this modality as the theoretical basis of image reconstruction. However, this methodology has several limitations for small animal applications, where small geometries and high absorption or low scattering areas are encountered. A three-order spherical harmonics (P3) approximation of Radiative Transfer Equation in two-dimensional tissue geometries is presented in this paper, which improves the three-order equation for ignoring anisotropic factor in previous papers. To evaluate the performance of the P3 approximation, we compare its solution with Monte Carlo (MC) simulation. The validation results show that this method significantly improve the solution of diffusion approximation (DA) equation in near-source region and domains with high absorption geometries. On this bases, the paper presented a image reconstruction method of generalized pulse spectrum technique based on the P3 equation (P3- GPST), and it is an extent to generalized pulse spectrum technique based on the diffusion equation (DA- GPST). Simulation results show that P3- GPST performs better than DA- GPST.

8227-45, Poster Session

## Time-resolved single-molecule microscopy coupled with atomic force microscopy

S. Fore, PicoQuant Photonics North America, Inc. (United States); M. Sackrow, U. Ortmann, F. Koberling, R. Erdmann, PicoQuant GmbH (Germany)

Confocal microscopy is a well established technique to study spectral and spatial properties, providing detailed insight into processes and the structure of samples in biology and material science. Modern time-resolved fluorescence detection expands these analysis properties towards an even better species identification, separation and quantification and allows to follow fluorescence dynamics from the sub-ns regime up to seconds and beyond.

Of course not all properties of interest can be adressed optically or are hidden by the diffraction limited optical resolution, for example the size and shape of nanometer sized particles. At this point atomic force microscopy is a handy tool to get a better picture of the sample, its surface and the physics happening there.

We present a straight forward combination of single molecule sensitive time-resolved confocal microscopy with different commercially available atomic force microscopes (AFM). Besides an extra of information about for example a cell surface, the AFM tip can also be used to nanomanipulate the sample and to change the optical response from the detection volume. This opens a path to influence the sample on a nanometer scale down to the single molecule level. The influence of the tip can manifest itself in a fluorescence quenching of the single molecule approaching the tip (see figure). One can notice the shortened lifetime and reduced fluorescence intensity when the tip is in close proximity to the molecule. This allows to measure the position of individual emitters with a resolution far below the diffraction limit.

8227-46, Poster Session

## Restoration of high-resolution AFM images captured with broken probes

Y. f. Wang, Trinity College Dublin (Ireland)

This paper introduces a solution to an artefact in Atomic Force Microscope (AFM) images caused by damage of the scanning probe. When the AFM operates at high resolution (e.g. amyloid fibrils at nanoscale), the reaction of the scanning probe will not be fast enough to avoid collision with sharp edges of the surface. Therefore, several asperities will be developed due to the collision and each asperity will operate as an individual sharp probe. As a result, instead of a single clear fibril feature in the image, there are a number of confusing echos. The proposed deblurring algorithm in this paper is developed based on existing blind deconvolution algorithms in the natural image domain. It involves a novel Hough Transform kernel estimation technique and a Bayesian deblurring algorithm. The Hough Transform technique generates a rough estimation of the blur kernel which is used as the initial input to the Bayesian deblurring process. The Bayesian framework employs novel priors that capture image gradient information as well as constrain the blur kernel. The result is a much improved image as well as information about the broken probe shape. To our knowledge, the restoration of this artefact has never been successfully addressed before.

8227-47, Poster Session

## A novel, fast approach to light-sheet microscopy to perform scattering-free, high-resolution fluorescence imaging on whole brains

L. Silvestri, L. Sacconi, Univ. degli Studi di Firenze (Italy); A. Bria, G. Iannello, Univ. Campus Bio-Medico (Italy); F. S. Pavone, Univ. degli Studi di Firenze (Italy)

Light-sheet based microscopy (ultramicroscopy), coupled with optical tissue clearing, has been recently proposed (Dodt et al. Nat Met 2007) to reconstruct whole mouse brains with microscopic resolution. In this technique the sample is illuminated by a sheet of light and the fluorescence is observed from an axis perpendicular to the illumination plane.

This approach seems well-suited for high resolution whole brain imaging because it doesn't require mechanical slicing of the specimen, as in electronic or confocal microscopy. However, this technique is limited because of residual scattering inside cleared tissues, which degrades the quality of both excitation and emission light, leading to a global blur of the acquired images, and preventing scattering-free whole-brain imaging with microscopic resolution.

To overcome this limitation several methods have been proposed, such as structured illumination (Kalchmair et al. Opt Lett 2010), but all these strategies share the same drawback, i.e. long acquisition times, as many images has to be acquired to produce a single final one.

We propose a novel optical filtering method, based on spatial filtering, to reduce drastically scattering artefacts in light-sheet optical architecture. This approach allows imaging at the same frame rate of conventional ultramicroscopy.

With this technique we were able to reconstruct whole mouse brains with quasi-diffraction-limited resolution. We have also compared our technique with structured illumination, showing that we obtain a slightly better contrast with much faster acquisition times.

8227-48, Poster Session

## Determination of cellular mass, volume, and density using differential interference contrast microscopy

K. G. Phillips, Oregon Health & Science Univ. (United States); A. Koltkar, The Scripps Research Institute (United States); C. Loren, A. McClain, W. Potter, S. L. Jacques, Oregon Health & Science Univ. (United States); P. Kuhn, The Scripps Research Institute (United States); O. J. T. McCarty, Oregon Health & Science Univ. (United States)

A label-free imaging modality capable of quantifying cellular organization would have widespread application in the physical understanding of cellular structure and function. We introduce a theory of differential interference contrast (DIC) imaging based on the unification of the transport of intensity formalism with phase tomography to yield a diffusion-type equation relating the transverse Laplacian of the refractive index to the derivative of the measured DIC intensity along the optical axis. This procedure enables high-resolution measurements of cellular density, mass, and volume from through-focus DIC imagery. We present measurements of cellular volume, mass, and density of blood cell sub-populations including platelets, erythrocytes, leukocytes, and circulating tumor cells from breast and prostate cancer patients.

8227-49, Poster Session

## Depth aberrations characterization in linear and nonlinear microscopy schemes using a shack-Hartmann wavefront sensor

R. Aviles-Espinosa, ICFO - Institut de Ciències Fotòniques (Spain); J. Andilla, R. Porcar-Guezenec, X. Levecq, Imagine Optic SA (France); D. Artigas, ICFO - Institut de Ciències Fotòniques (Spain) and Univ. Politècnica de Catalunya (Spain); P. Loza-Alvarez, ICFO - Institut de Ciències Fotòniques (Spain)

The development of fluorescence based imaging tools such as linear and nonlinear microscopy (NLM), has offered biologists powerful means for visualizing micron-sized structures in living organisms. However, the optical performances of these instruments as well as the optical properties of the sample limit its imaging quality. Such an important aspect has already been described using different theoretical models. The most studied aberration correction methodologies are based on sensor-less implementations where aberrations are iteratively corrected trough an image related parameter or merit function (aberrations are not measured). This has been carried out due to the difficulties of implementing a direct wavefront sensing scheme in fluorescence microscopy.

In this work, we perform a practical implementation of a Shack-Hartman wavefront sensor and demonstrate its application in linear and nonlinear microscopy. We perform an extensive analysis of aberration effects through different depths employing phantom samples (having similar refractive indices to deep epidermis and basal layers of skin). Aberration effects originated by the refractive index mismatch and depth are quantified performing a single measurement inside the sample. Employing both excitation modalities, spherical aberration increases a factor of 37 at depth of 100 µm. More over we analyze off-axis aberrations in NLM (an important aspect that is commonly overlooked). In this case spherical aberration behaves similarly to the wavefront error compared with the on-axis case.

Finally we give an example of spherical aberration compensation induced by 60 µm of glass having an air refractive index mismatch in a bovine pulmonary artery endothelial cells sample using epi-fluorescence microscopy.

8227-50, Poster Session

## Phase-sensitive optical coherence reflectometer using a supercontinuum source

H. Song, D. Kim, S. B. Cho, S. Jeong, Gwangju Institute of Science and Technology (Korea, Republic of); D. Y. Kim, Yonsei Univ. (Korea, Republic of)

We report a high-speed phase-sensitive optical coherence reflectometer with a stretched supercontinuum source. Supercontinuum source has been generated by injecting an amplified fiber laser pulse into a highly nonlinear optical fiber. The repetition rate and pulse duration of the generated supercontinuum source are 10 MHz and 30 ps, respectively. The supercontinum pulses are stretched into 70 ns pulses with a dispersion-compensating fiber. The relation of time-wavelength (group delay) has been measured by modified time-of-flight method. We have built a phase-sensitive optical coherence reflectometer with this stretched pulse source and a 2-dimensional scanning system. By using the linear relation between the wavelength and the temporal position in a linearly chirped pulse, high-speed spectrum measurement can be obtained in the time domain. We have demonstrated two-dimensional surface profiling for a standard image target and high-speed single point monitoring for a fixed point under vibrational motion of piezoelectric transducer. The measurement speed for a single position and sensitivity of proposed system are 2.5 MHz and 4.49 nm, respectively.

8227-51, Poster Session

## A custom-built two-photon microscope based on a mode-locked Yb3+ doped fiber laser

D. Kim, H. Song, W. Song III, H. Kwon, Gwangju Institute of Science and Technology (Korea, Republic of); D. Y. Kim, Yonsei Univ. (Korea, Republic of)

Two-photon microscopy is a very attractive tool for the study of the three-dimensional (3D) and dynamic processes in cells and tissues. One of the feasible constructions of two-photon microscopy is the combination a confocal laser scanning microscope and a mode-locked Ti:sapphire laser. Even though this approach is the simplest and fastest implementation, this system is highly cost-intensive and considerably difficult in modification. Many researcher therefore decide to build a more cost-effective and flexible system with a self-developed software for operation and data acquisition. We present a custom-built two-photon microscope based on a mode-locked Yb3+ doped fiber laser and demonstrate two-photon fluorescence imaging of biological specimens. The mode-locked fiber laser at 1064 nm delivers 320 fs laser pulses at a frequency of 36 MHz up to average power of 80 mW. The excitation around 1 µm can be more suitable in thick, turbid samples for 3D image construction as well as cell viability. The system can simply accomplish confocal and two-photon mode by an additional optical coupler that allows conventional laser source to transfer to the scanning head. The normal frame rate is 1 frames/s for 400 × 400 pixel images. The measured full width at half maximum resolutions were about 0.44 µm laterally and 1.34 µm axially. A multi-color stained convallaria, rat basophilic leukemia cells and a rat brain tissue were observed by two-photon fluorescence imaging in our system.

8227-52, Poster Session

## Quantifying fluorescence signals in confocal image stacks deep in turbid media

S. Beer, U. Maeder, T. Bergmann, J. M. Burg, M. Fiebich, Technische Hochschule Mittelhessen (Germany); F. Runkel, Fachhochschule Giessen-Friedberg (Germany)

When confocal depth stacks are taken, the collected signal (normally the fluorescence signal), decays dependent of the depth of the confocal slice in the turbid medium. This decay is caused by scattering and absorption of the exciting light and of the fluorescence light. As the attenuation parameters, i.e. scattering and absorption coefficients, are normally unknown when observing a new sample, a method is proposed to compensate for the attenuation of the involved light by correcting the fluorescence signal using the attenuation behavior of the sample measured directly on the spot where the fluorescence stack is taken. Using this self-reference technique, a confocal fluorescence depth stack can be achieved where the signal intensity is not dependent on scattering and absorption caused intensity decay.

Hydrogel phantoms, consisting of agarose as a gelling agent, lipid droplets as scatterers, melanin as absorber and 5µm fluorescent beads are created. Depth stacks are taken with a confocal microscope. Alongside the fluorescence stack, two reflection stacks, one at the exciting wavelength and one well within the spectral region, where the fluorescence signal is collected. Using the reflection stacks, the attenuation of the observed part is estimated and the fluorescence stack is corrected using this parameter.

Using this technique, confocal depth stacks can be produced where the signal intensity is only dependent on the fluorophore concentration. Future developments include testing the method on heterogeneous, multilayer systems like the skin. This targets the application of observing and quantifying the penetration of fluorescent labeled drugs into the skin.

8227-53, Poster Session

## Multimodal light-sheet microscopy for fluorescence live imaging

Y. Oshima, Ehime University (Japan) and National Institute for Basic Biology (Japan); H. Kajiura, S. Nonaka, National Institute for Basic Biology (Japan)

Laser scanning confocal microscopy is a valuable tool for fluorescence imaging analysis in cells and tissues with high contrast visualization at high spatial resolution. It allows us to obtain live cell images in vivo and in vitro. However point-by-point image construction affects a living sample in phototoxicity and it takes image acquisition time. Light-sheet microscopy for developmental biology, it is known as single plane illumination microscope (SPIM), is a fluorescence imaging technique which can overcome these problems by optical sectioning with light-sheet illumination and CCD detector. Thus the light-sheet microscopy enables live cell imaging and three-dimensional image construction by manipulating the sample. We have been developed a high speed and stable imaging system using electrically focus-tunable lens to collect z-stack image rapidly and simultaneously without any mechanical movement. We also performed that the light-sheet based microscopy was equipped a spectrometer and applied to fluorescence unmixing analysis and Raman imaging. Slit of the spectrometer was placed on conjugate plane of imaging plane of the optical system. In the result, it was successful to obtain high resolution in wavelength and high throughput hyperspectral images of biological samples. In addition, femtosecond pulse infrared laser will be installed for multiphoton fluorescence, second-harmonic generation (SHG) and third-harmonic generation (THG) imaging.

8227-54, Poster Session

## Cell morphology classification in phase contrast microscopy image reducing halo artifact

M. Kang, S. Song, H. Lee, M. Kim, Ewha Womans Univ. (Korea, Republic of)

Tumor cell morphology is closely related to its invasiveness characteristics and migratory behaviors. Invasive tumor cell has highly irregular shape where as sphere-like cell is non metastatic. Thus, quantitative analysis of cell feature is crucial to determine tumor malignancy or efficacy test of anticancer treatment.

For analyzing single cell's morphology and monitoring its change, we use phase contrast microscopy image because it enables observation of long-term activity of living cells without photobleaching and phototoxicity which is common in other fluorescence-labeled microscopy. Nevertheless of this strength, it has drawbacks at image level such as local light effect, contrast interference ring, and etc.

Thus, first of all, we apply rolling-ball filter to compensate non-uniform illumination. Then, we use intensity distribution information to detect cell boundary. In phase contrast microscopy image, cell is normally appeared as dark region surrounded by bright halo ring. Due to halo artifact is minimal around the cell body and has non-symmetric diffusion pattern, we calculate cross sectional plane which intersects center of each cell and orthogonal to first principal axis. Then, we extract dark cell region by analyzing intensity profile curve considering local bright peak as halo area.

However, dense population of cultured cells still makes single cell analysis difficult. To separate touching cells, we adjust cross section image smaller if bright peak is detected more than two and iterate previous step. Finally, we measure roundness to classify tumor cells into malignant and benign group. And we validate segmentation accuracy by comparing result manually done by biologists.

8227-55, Poster Session

## Full-field OCT combined with optical tweezer

W. J. Choi, K. S. Park, T. J. Eom, B. Lee, Gwangju Institute of Science and Technology (Korea, Republic of)

We present new full-field optical coherence tomography (FF-OCT)system combined with optical tweezer technique. The proposed scheme enables ultrahigh-resolution OCT imaging of a floating object optically trapped by single-beam gradient force in medium. The set up consists of a Linnik type white light interference microscope combined with an optical tweezer system. The optical trap is formed by tightly focusing a 1064 nm Q-switching pulsed laser beam with a water-immersion microscope objective lens of high numerical aperture (1.0 NA) in the OCT system. The trapping power onto the sample was 12.4 mW. Thus, en-face OCT imaging is performed for the optically-seized object using a white light illuminator having spectral bandwidth (FWHM) of 220 nm, where the sample incident beam is co-channelled with the trapping beam. Axial resolution and later resolution of the systme were measured to be 0.8 um and down to 1.0 um in water, respectively. Optical slicing of the sample in depth is made by moving the focal position of the trapping beam in Z-axis. With the system, a micron-sized dielectric particle in solution could be trapped in space and depth-resolved imaged.

8227-56, Poster Session

## Three-dimensional imaging of the mouse pituitary: reconstructing a mammalian organ at cellular resolution

E. J. O'Reilly, F. Molino, Institut de Génomique Fonctionnelle (France); T. E. Keyes, Dublin City Univ. (Ireland); P. Mollard, C. Lafont, Institut de Génomique Fonctionnelle (France)

The aim of this work was to develop a framework towards the quantitative histology of a whole mammalian organ. Using high-throughput 3D imaging on transgenic animals and an integrated modelling environment, the mouse anterior pituitary gland has been reconstructed at cellular resolution. The reconstructed 3 dimensional structure is known to be related to the neuroendocrine function of the gland.

This has been demonstrated using traditional qualitative histology to image portions of the gland at different stages of development and functionally using electrophysiology and calcium imaging. To date there has been no development of tools to quantitatively describe the 3D structural organisation of the different cell types, their consequent integration in space and the relationship of this to cellular function. Cells exhibit correlated behaviour dependent on their organisation in networks, which are varying, depending on changing physiological needs. A striking example is the remodelling of the growth hormone cell network in aggregated cluster-like structures at puberty in the male mouse, resulting in an increased correlation of cellular response to stimulation

This work documents the novel methods used to obtain a first map of the complete pituitary whereby in excess of 95% of cells can be correctly identified, as well as the use of high throughput data gathering techniques used to create a 3D image for each gland.

8227-57, Poster Session

## Spatial coherence and transfer function analysis of structured illumination superresolution microscopy

S. Chowdhury, A. Z. Dhalla, J. A. Izatt, Duke Univ. (United States)

Lateral structured illumination microscopy is a technique that achieves super-resolution by illuminating the sample with structured patterns with known frequencies and phase shifts to alias higher, normally inaccessible, frequencies into the system's passband. This technique has been typically applied to fluorescence microscopy, where the sample characteristically emits incoherent light. However, many biologically relevant samples are either not fluorescent or cannot be fluorescently tagged easily, and thus do not emit completely incoherent light. Here, we provide an analysis describing how spatial coherence of the light from the source as well as at the light scattered from the sample affects the super-resolution capabilities of structured illumination. We start with a theoretical review of the conventional theory of structured illumination and extend it to include considerations for the spatial coherence of the illuminating and detected light. Using our models, we simulate the modulation transfer functions (MTFs) of the patterned illumination and the final reconstructed image under both coherent and incoherent conditions and discuss the differences in the coherent and incoherent reconstruction procedures for obtaining super-resolution. We follow through with a proof of principle experiment, where we set up an optical system to coherently and incoherently image a test chart illuminated with varying spatial frequencies. We obtained experimental MTF plots of the illumination pattern and reconstructed image that are in good agreement with the simulations.

8227-58, Poster Session

## Optical sectioning properties of single-pixel line imaging with spatial frequency modulated microscopy

D. G. Winters, D. Higley, R. A. Bartels, Colorado State Univ. (United States)

Recently, we introduced a technique demonstrating high-speed line scan imaging with a single pixel detector. Spatial information is encoded into the electronic frequency domain of the signal from a single-element photodiode by modulating the intensity at each point of an illumination beam at a distinct and linearly varying frequency. With this modulation, both absorptive and fluorescent line images can be recorded. Two-dimensional images are readily obtained by scanning the line image, or by expanding the beam and performing tomographic reconstruction on a sequence of relative rotations of the modulated beam and the object. In this work, we demonstrate that this new technique of spatial frequency modulation imaging (SPIFI) exhibits optical sectioning properties. The SPIFI modulation mask imparts a sinusoidal intensity modulation at each spatial point with a binary transmittance mask with a square amplitude transmission grating whose spatial frequency sweeps linearly in time. When this mask is demagnified and reimaged in an optical microscope, the intensity modulation is localized along an axial position to near the focal plane. This can be understood by noting that away from the focal region, the modulation mask is defocused, reducing the modulation depth that transfers object spatial information in the electronic frequency spectrum. As a result, when an object is moved away from the focal plane, the image is no longer resolved, and image information is limited to a region localized near the focal plane. Experiments and theory demonstrating optical sectioning in an absorptive and fluorescent SPIFI microscope will be presented.

8227-59, Poster Session

## High-speed single-pixel line-scan imaging with a time sequence of intensity masks reconstructed through compressed sensing

W. Dang, D. G. Winters, D. Higley, A. Pezeshki, R. A. Bartels, Colorado State Univ. (United States)

Recently, we introduced a technique demonstrating high-speed line scan imaging with a single pixel detector. Spatial information is encoded into the electronic frequency domain of a single-element photodiode signal by modulating the intensity at each point of an illumination beam with a linear varying frequency. With this modulation, both absorptive and fluorescent line images can be recorded. Two-dimensional images are readily obtained by scanning the line image, or by expanding the beam and performing tomographic reconstruction on a sequence of relative rotations of the modulated beam and the object. The original SPIFI work made use of an intuitive modulation mask design, with a linear chirp in modulation frequency across the excitation beam. The number of resolved points is set by Nyquist sampling considerations, determined by the modulation bandwidth and the time window of observation. These considerations have restricted image update rates to once per disk. Compressed sensing takes advantage of rigorous findings that for objects that are sparse, full image information can be obtained with many fewer measurements than suggested by Nyquist sampling requirements. Consequentially, image information can be obtained with fewer samples, and thus requires a smaller number of modulator mask patterns. The advantage of this approach is that sparse objects can be imaged at faster update rates than conventional SPIFI. Improved speed comes at a cost, and for compressed imaging SPIFI, image recovery occurs through an optimization routine, rather than a simple Fourier transform. Experiments and theory demonstrating compressed SPIFI with absorptive and fluorescent objects will be presented.

8227-60, Poster Session

## A wavelet-SVM based Bayesian framework for 3D object segmentation in microscopy

K. Pan, A. C. Kokaram, M. Ramaswami, J. Hillebrand, Trinity College Dublin (Ireland)

Formation of long term memory requires new protein synthesis at specific synapses. The investigations of the formation process require the knowledge of the 3-D shape of the synapses from the stacks of 2-D image slices captured at different depth of the specimens by the confocal microscopes. However, due to physical limit of the microscopes, the images may contain objects that are out-of-focus at the corresponding observing depth level. Consequently, the segmentation of the synapses is heavily reliant on manual evaluation of the biologists. In this paper, we propose a Bayesian framework for segmenting the 3-D synaptic object from the observed 2-D image stack. This Bayesian framework employs a novel likelihood derived from a support vector machine (SVM) using dual-tree complex wavelet transform (DTCWT) for feature extraction. The wavelet transform provides a time-frequency representation of a signal and satisfies multi-resolution analysis. Also, since DTCWT has overcome the 'shift variant' and 'lack of directional information' problems of the classic discrete wavelet transform (DWT), the wavelet transform has conducted powerful tools for extracting the luminance -, rotation- and scale-invariant features of 'target' objects, which is more advance from the image domain. Furthermore, the combination of DTCWT and the well-known supervised learning tool-SVM is a novel technique which has recently applied to object classification and face recognition, where several publications have shown solid results to prove the superiority of wavelets while comparing to traditional SVM techniques. By injecting the advantage of DTCWT-SVM to a maximum a posterior (MAP) estimation model with a smoothness prior, our proposed algorithm provides excellent segmenting results of the synapses.

8227-61, Poster Session

## Localization accuracy in single-molecule microscopy using electron-multiplying charge-coupled device cameras

J. Chao, The Univ. of Texas at Dallas (United States); E. S. Ward, The Univ. of Texas Southwestern Medical Ctr. at Dallas (United States); R. J. Ober, The Univ. of Texas at Dallas (United States)

The electron-multiplying charge-coupled device (EMCCD) is a popular technology for imaging under extremely low light conditions. It has become widely used, for example, in single molecule microscopy experiments where few photons can be detected from the individual molecules of interest. Despite its important role in low light microscopy, however, little has been done in the way of determining how accurately parameters of interest (e.g., location of a single molecule) can be estimated from an image that it produces. Here, we develop the theory for calculating the Fisher information matrix, and hence the Cramer-Rao lower bound-based limit of the accuracy, for estimating parameters from an EMCCD image. An EMCCD operates by amplifying a weak signal that would otherwise be drowned out by the detector's readout noise as in the case of a conventional charge-coupled device (CCD). The signal amplification is a stochastic electron multiplication process, and is modeled here as a geometrically multiplied branching process. In developing our theory, we also introduce a "noise coefficient" which enables the comparison of the Fisher information of different data models via a scalar quantity. This coefficient importantly allows the selection of the best detector (e.g., EMCCD or CCD), based on factors such as the signal level, and regardless of the specific estimation problem at hand. We apply our theory to the problem of localizing a single molecule, and compare the calculated limits of the localization accuracy with the standard deviations of maximum likelihood location estimates obtained from simulated images of a single molecule.

8227-62, Poster Session

## Comparison of analysis methods for fluorescence lifetime imaging

T. Hall, D. Dorroh, E. Robertson, D. Schaafsma, California Optical Engineering, Inc. (United States)

Numerous methods have been proposed and employed for lifetime analysis, and several proprietary algorithms are now in the public domain. We compare various time-gated and discrete-time methods for extracting the decay constant from an exponential signal, typical of fluorescence lifetime imaging (FLIM) instruments, as well as a host of other physical phenomena. Analytical methods are evaluated for accuracy and precision as well as for computational and sampling efficiency. Effects of different noise sources, such as spurious clocking and 60-cycle noise, as well as non-signal effects, such as system threshold or baseline nonlinearity and multi-component decays, are also examined. While gated and time-spectral methods are advantageous for their ease of implementation, we have found that the specifics of using various gating methods can have a large impact on the robustness and accuracy of results.

8227-64, Poster Session

## Modeling the effect of refraction on OCT imaging of lung tissue: a ray-tracing approach

F. N. Golabchi, D. H. Brooks, A. Gouldstone, C. A. DiMarzio, Northeastern Univ. (United States)

Determining the structure and mechanical behavior of lung tissue is notoriously difficult in ex-vivo samples. For example, alveolar volume change with stress, which is of potentially clinical importance for lung re-inflation, cannot be measured directly. Optical coherence tomography (OCT) offers a non-invasive real-time methodology to image up to several layers of alveoli. The OCT imaging model however does not model optical effects in lung tissue that cause distortion in the resulting images. For example, OCT assumes backscattered returns come from directly beneath the detector, and that distance measured in the reference arm in air matches distance traveled in tissue. However in lung, due to air in alveoli, light refracts at the alveolar surface and travels at different speeds in tissue and air.

We employ a ray-tracing approach to model changes in alveolar shape and volume in OCT images due to these distortion effects. Both directional and speed changes are included. We study a variety of eccentricity and angles of elliptical alveolar shapes. Results show, for example, apparent thickening of inter-aveolar walls consistent with our group's previously published FDTD modeling of OCT in lung, as well as changes in both shape and depth of the first alveolar layer. Our approach suggests a direct method to correct for these effects by combining the implications of the model with image processing based analysis of the acquired images. Accurate correction of these distortions will be important to infer tissue mechanical properties and in imaging deeper alveolar layers.

8227-65, Poster Session

## Common-path, wide-field reflection phase microscopy

Y. Sung, T. R. Hillman, N. Lue, R. R. Dasari, P. T. C. So, Z. Yaqoob, Massachusetts Institute of Technology (United States)

Field-based microscopy techniques use optical phase as the intrinsic contrast mechanism to study the dynamics and physiological activity of various structures in living cells with high (e.g., nanometer scale or better) measurment sensitivity. Depending on the application, one can adopt different kinds of sources, modulation techniques, and system geometries to extract the phase information of biological cells. Recently, we have developed a wide-field reflection phase microscope for single-shot phase imaging of plasma membrane in eukaryotic cells with complicated 3-D internal structures [1]. The wide-field reflection phase microscope used a separate reference arm with an appropriate diffractive optical element for off-axis interferometry. A region of the measured interferogram with no sample was used to determine the reference phase to remove temporal noise. This approach, however, can easily introduce phase noise to regions which have reduced fringe contrast.

In the past, a number of techniques with a varying levels of complexity have been proposed [2-5] for reducing phase noise. Here, we report the development of a simple phase-stabilized wide-field reflection phase microscope in which both the sample and reference beams follow a common-path configuration, thus canceling the common-mode noise in phase imaging. The optical design also guarantees the desired wavefront tilt of the reference beam in order to perform single-shot, off-axis interferometry. The interferograms are processed to determine the optical phase of the returning sample beam and hence sub-nanometer motions associated with the sample under study. The new setup will be used to study plasma and nuclear membrane fluctuations in eukaryotic cells.

References:

1. Yaqoob Z, Yamauchi T, Choi W, Fu D, Dasari RR, Feld MS. Single-shot Full-field reflection phase microscopy. Opt Express. 19, 7587-95 (2011). PMID: 21503067.

2. Hitzenberger CK, Fercher AF. Differential phase contrast in optical coherence tomography. Optics Letters. 24, 622-4 (1999).

3. Dave DP, Milner TE. Optical low-coherence reflectometer for differential phase measurement. Optics Letters. 25, 227-9 (2000).

4. Koliopoulos CL, editor. Simultaneous phase-shift interferometer1992: SPIE.

5. Zhao C, Burge JH. Vibration-compensated interferometer for surface metrology. Appl Opt. 40, 6215-22 (2001).

8227-66, Poster Session

## A reflection-mode configuration for enhanced light delivery through turbidity

Y. Choi, T. R. Hillman, N. Lue, Y. Sung, R. R. Dasari, Massachusetts Institute of Technology (United States); W. Choi, Korea Univ. (Korea, Republic of); Z. Yaqoob, Massachusetts Institute of Technology (United States)

The phenomenon of multiple scattering severely degrades the performance of reflection-based imaging modalities such as optical coherence tomography (OCT), confocal reflectance & fluorescence microscopy, and two-photon microscopy. If treated as a stochastic phenomenon, multiple scattering is a source of noise that limits the achievable imaging depth in turbid media. However, modern turbidity suppression techniques treat it deterministically, utilizing it to achieve a sharp point focus or form an image via wavefront control [1-3]. Here, we report an OCT-based, reflection-mode wavefront control method for enhancing light delivery to any point of interest within a turbid medium. The incident wavefront is repeatedly modified using a spatial light modulator (SLM) and the corresponding depth-resolved backscattered signals measured for a stationary sample. The set of measurements is used to determine the linear transformation between the SLM-induced wavefront and the backscattered signal. Based on this knowledge, we can exert spatiotemporal control over the incident wavefront to maximize the signal arising from any particular location in the sample. In fact, we can enhance this detected signal by several orders of magnitude. We thereby demonstrate that sample turbidity suppression can be achieved in reflection mode, without any external contrast mechanism, and without directly imaging the optical signal at the target light-delivery location. We propose that our approach can benefit alternate imaging modalities such as two-photon microscopy, which require a high concentration of optical power within a turbid tissue sample in order to achieve high signal-to-noise ratio and penetration depth.

[1] M. Wenner,"The most transparent research,"Nature Medicine, vol. 15, pp. 1106-1109, 2009.

[2] S.Popoff, G.Lerosey, M. Fink, A. C.Boccara, and S.Gigan,"Image transmission through an opaque material," Nature Communications, vol. 1, art. 81, 2010.

[3] I. Vellekoop, A. Lagendijk, and A. P. Mosk, "Exploiting disorder for perfect focusing," Nature Photonics, vol. 4, pp. 320-322, 2010.

8227-67, Poster Session

## Image registration and refractive index measurement based on combined optical coherence tomography and multiphoton microscopy

Y. Zhou, The Univ. of British Columbia (Canada)

Optical coherence tomography (OCT) and multiphoton microscopy (MPM) are two emerging optical imaging techniques. In this paper, an integrated microscope system that combines OCT and MPM using a femtosecond broadband (120-nm) laser source is demonstrated. The microscope enables spectral domain OCT based on optical back scattering, and MPM for the detection of two-photon fluorescence and second harmonic generation signals. The unique configuration of this integrated microscope allows for the successive acquisition of OCT cross-sectional images with 2.35um source limited axial resolution and MPM 3D images with 0.6um experimental lateral resolution and 1.6um axial resolution. Fish cornea is chosen as the sample to evaluate the integrated system since it has multilayer and can generate strong second harmonic signal. In our experiment, OCT and MPM images of fresh fish cornea at the same location are acquired successively. A 2D cross-sectional image is reconstructed from the 3D MPM data stack and then registered with OCT image. OCT has a larger image depth (up to 611um in air) and relatively lower resolution while MPM has a smaller image depth (up to 400um) but higher lateral and axial resolution. The registration of these two image modalities provide us with a large field-of-view (OCT) and high resolution (MPM) image of tissue. This system can be used to measure the refractive index of tissue. Since OCT image is generated based on optical path length while MPM can be used to get the physical thickness of tissue, the refractive index can be computed by directly comparing the thickness of tissue in OCT and MPM images.

8227-68, Poster Session

## Manipulating and visualizing non-adherent cells in four dimensions

D. L. Thompson, NSF Ctr. for Biophotonics Science and Technology (United States); G. P. McNerney, Univ. of California, Davis (United States); M. P. Persson, M. Goksör, Göteborg Univ. (Sweden); T. R. Huser, Univ. Bielefeld (Germany)

Fluorescence microscopy is one the most widely used tools for visualizing cells in the biological sciences. However, the relevance of in vitro imaging experiments relies heavily on the microenvironment surrounding the cell. The majority of cellular-level microscopy experiments necessarily rely on the attachment of cells to a substrate to reduce errors induced by drift or cell movement, but the function and properties of many important cell types (such as immune cells) change dramatically when encountering a surface. In order to visualize suspension cells in a biologically-relevant environment, we have combined a spinning disk confocal microscope (SDCM) with spatial light modulator-based holographic optical tweezers (HOT). The SDCM captures 2D optical sections with near-diffraction limited resolution at a frame rate of ~30 Hz, in up to three channels. The HOT allows us to manipulate multiple cells simultaneously in three dimensions to promote or discourage interactions with other objects. This combined system provides a four-dimensional method to initiate, study, and track cellular interactions in a biologically-relevant environment, both dramatically increasing experiment throughput and enabling a more active approach to investigation.

8227-37, Session 9

## Background and speckle suppression with a divided pupil and Nomarski prism for reflectance line-scanning confocal microscopy of human tissues

C. Glazowski, Memorial Sloan-Kettering Cancer Ctr. (United States); J. M. Zavislan, Univ. of Rochester (United States); M. Rajadhyaksha, Memorial Sloan-Kettering Cancer Ctr. (United States)

The line-scanning confocal microscope (LCM) is simpler, smaller and consequently less-expensive to manufacture than a point-scanning confocal microscope (PCM). A relatively simple optical configuration and inexpensive linear CCD/CMOS arrays can be employed. This makes it an attractive candidate to accelerate reflectance confocal microscopy into widespread clinical use, particularly for in-vivo diagnostic imaging. However, compared to the PCM, the sectioning performance is degraded by ~20% due to the line being confocal in only one dimension. Improving sectioning requires the use of narrower slits in front of the detector array. This increases speckle noise when imaging human tissue, which degrades resolution and contrast. We will present a design of an LCM for reduced speckle and improved sectioning performance by the use two pupil-modification techniques. The first is a divided-pupil configuration in which the illumination and detection paths are separate in object space except in the focal (optical sectioning) plane. The second technique is a novel implementation of a Nomarski prism and quarter-wave retarder to coherently suppress out-of-focus background. This polarization-based suppression has shown good results in PCM and we will present its translation to LCM. A stable turbid phantom that simulates the background-driven speckle was used for quantitative characterization. Initial results show 100% and 50% improvements, respectively, in image fidelity for the two pupil modifications tested. Preliminary imaging in human skin and oral mucosa in-vivo demonstrates the reduction in speckle.

8227-38, Session 9

## Real-time quantitative differential interference contrast microscopy implemented using novel liquid crystal prisms

R. N. Zahreddine, Univ. of Colorado at Boulder (United States); S. V. King, H. Masterson, Boulder Nonlinear Systems (United States); R. H. Cormack, C. J. Cogswell, Univ. of Colorado at Boulder (United States)

A phase shifting differential interference contrast (DIC) microscope, which provides quantitative phase information and is capable of imaging at video rates, has been constructed. Using a combination of phase shifting and bi-directional shear the microscope captures a series of eight images which are then integrated in Fourier space. In the resultant image, the intensity profile linearly maps to the phase differential across the object. The necessary operations are performed by specialized liquid crystal devices (LCDs), recently developed by the co-authors, which can operate at high speeds. A set of four liquid crystal prisms shear the beam in both the x and y directions. A liquid crystal bias cell delays the phase between the e- and o-beams providing phase shifted images. The liquid crystal devices are then synchronized with a CCD camera in order to provide real time image acquisition. Previous implementation of this microscope utilized Nomarski prisms, a rotation stage and a manually operated Sernamont compensator to perform the necessary phase shifting operations. It was only capable of fixed sample imaging due to the slow image acquisition rate. A series of comparison images were taken using both the new LCD prism based microscope and the previously implemented Sernamont compensator based system. Results show that the new LCD prism microscope achieves equal and in some cases superior results to that of the old system, with the added benefit of real-time quantitative DIC imaging of living cells.

8227-39, Session 9

## Dynamic quantitative microscopy and nanoscopy of red blood cells in sickle cell disease

N. T. Shaked, Tel Aviv Univ. (Israel) and Duke Univ. (United States); L. L. Satterwhite, Duke Univ. (United States); M. J. Telen, Duke Univ. Medical Ctr. (United States); G. A. Truskey, A. P. Wax, Duke Univ. (United States)

Sickle cell disease is a genetic disorder that affects the structure and mechanical properties of red blood cells (RBCs). RBCs abnormalities during sickle cell disease include deformation, dehydration, and increased adhesivity, which cause multisystem dysfunctions associated with the disease. We have applied, for the first time to our knowledge, wide-field digital interferometric techniques to quantitatively image sickle RBCs in a noncontact label-free manner, and measure the nanometer-scale fluctuations in their thickness as an indication of their stiffness. The technique is able to simultaneously measure the fluctuations for multiple spatial points on the RBC and thus yields a map describing the stiffness of each RBC in the field of view. Using this map, the local rigidity regions of the RBC can be evaluated quantitatively. Since wide-field digital interferometry is a quantitative holographic imaging technique rather than one-point measurement, it can be used to simultaneously evaluate cell transverse morphology plus thickness in addition to its stiffness profile. Using this technique, we examine the morphology and dynamics of RBCs from individuals who suffer from various conditions associated with sickle cell disease, and find that RBCs from individuals with sickle cell disease are significantly stiffer than healthy RBCs. Furthermore, we show that the technique is sensitive enough to distinguish various classes of sickle RBCs, including sickle RBCs with visibly-normal morphology, compared to the stiffer crescent-shaped sickle RBCs. We expect that this approach will be useful for diagnosis of sickle cell disease, identification of carriers of sickle cell trait, and determining efficacy of therapeutic agents.

8227-40, Session 9

## Analyze fluorescent characteristic of cancer cell using hyperspectroscopic imaging system (HIS)

Y. Hsieh, National Central Univ. (Taiwan); O. Mang, National Chiao Tung Univ. (Taiwan); J. Duann, China Medical Univ. (China); C. Chen, J. Chiou, National Chiao Tung Univ. (Taiwan); Y. Lin, China Medical Univ. (United States); M. Tsai, China Medical Univ. (China); S. Wu, National Taiwan Normal Univ. (Taiwan)

Currently, the cancer was examined by diagnosing the pathological changes of tumor. If the examination of cancer can diagnose the tumor before the cell occur the pathological changes, the cure rate of cancer will increase. This research develops a human-machine interface for hyper-spectral microscope. The hyper-spectral microscope can scan the specific area of cell and records the data of spectrum and intensity. These data is helpful to diagnose tumor. This study finds the hyper-spectral imaging have two higher intensity points at 550nm and 700nm, and one lower point at 640nm between the two higher points. For analyzing the hyper-spectral imaging, the intensity at the 550nm peak divided by the intensity at 700nm peak. Finally, we determine the accuracy of detection by Gaussian distribution. The accuracy of detecting normal cells achieves 89%, and the accuracy of cancer cells achieves 81%.

8227-41, Session 10

## Parallel depth resolved spectral encoded high-speed reflectometry of biological tissue

B. Považay, A. Kumar, D. Fechtig, A. Unterhuber, Medizinische Univ. Wien (Austria); T. Le, FEMTOLASERS Produktions GmbH (Austria); J. R. Fergusson, Cardiff Univ. (United Kingdom); M. Eibl, W. Drexler, Medizinische Univ. Wien (Austria)

Interferometric encoding of depth-utilizing wavelength diversity has been a very successful concept for three-dimensional imaging of tissue morphology for clinical application. Raster scanning optical coherence tomography (OCT) permits the acquisition of volumes from reflective specimen at clinically relevant measurement speeds with extremely high sensitivity. OCT devices have now surpassed the level where power on the sample in a single spot can be safely increased. Therefore, parallel imaging schemes that can bridge the gap between microscopic resolution imaging and applicability in a mechanically dynamic environment are being developed. However, the simple addition of multiple independent confocal OCT channels with current technology is a technical challenge. Other approaches, which utilize the intrinsically parallel illumination and detection from digital holography, confocal imaging and structured illumination, have been proposed, but suffer from their individual limitations.

In this presentation we will examine the options and challenges of developing a parallel OCT-type imaging system and investigate the limitations imposed by sample motion, scattering and optical aberrations and discuss the possible countermeasures. Different encoding schemes using multiple beams or wide-field illumination and detection replacing current detector and source technology will be assessed in terms of their ability to increase imaging speed, resolution and specificity while suppressing speckle, crosstalk and distortions caused by motion artifacts. Specifically, a novel scanner-less, high resolution imaging ( 120 nm) together with dual camera phase detection for motion control, and structured illumination via a micro optical array for cross-talk and speckle suppression.. Volumetric images of skin are compared to an existing confocal scanning OCT device to quantify the effect of crosstalk and parasitic reflections.

8227-42, Session 10

## Deep-focus compound-eye camera with polarization filters for 3D endoscopes

K. Kagawa, Shizuoka Univ. (Japan); E. Tanaka, Panasonic Electronic Devices Co., Ltd. (Japan); K. Yamada, Osaka Univ. (Japan); S. Kawahito, Shizuoka Univ. (Japan); J. Tanida, Osaka Univ. (Japan)

A deep-focus three-dimensional endoscope based on a compact compound-eye camera called TOMBO (thin observation module by bound optics) with polarization filters and polarized illuminations is presented. TOMBO is a very compact multi-camera system, which is composed of a single image sensor, a lens array, and a crosstalk barrier. The features of TOMBO is compactness of the camera system, and additional functionality achieved by attaching optical filters to lenses. In this paper, to observe shallow and deep structure of biological tissues separately, polarization filters, which are parallel and vertical to the polarized illumination, respectively, are attached to a part of lenses. To achieve extended depth of focus, a wavefront coding technique based on the spherical aberration is introduced. A prototype TOMBO with 3x3 lenses and a 2.2-μm-pixel color CMOS image sensor was fabricated. The focal length and diameter were 1.5 mm and 1.0 mm, respectively. Lens pitch was 1.1 mm. About 400×400 pixels were accommodated in each lens. To estimate the shape of subject from both parallel and vertical polarization images, the lens in the center of the lens array is not equipped with a polarization filter. With this configuration, the depth can be retrieved by minimizing an evaluation function of no-filter image minus vertical and parallel polarization images because the non-filter image is expressed by a linear combination of vertical and parallel polarization images.

8227-43, Session 10

## Improved contrast by modal illumination in scanning reflectance confocal microscopy

C. Glazowski, J. M. Zavislan, Univ. of Rochester (United States)

Scanning reflectance confocal microscopy (SRCM) has a firm foothold in clinical, in-vivo and ex-vivo imaging environments. As a platform, it provides cellular resolution images of tissue morphology with tailored resolutions and fields of view. Contrast derived from structural and chemical components can be optimized across a wide optical spectrum. However, how accurately an object is represented is critical in medical imaging and is not represented simply by optical resolution. The correlation of an image to the object properties is described by image fidelity. In this work we consider the back scatter from the object as a source of morphological contrast, and we characterize the SRCM image fidelity within turbid tissue. When imaging within a turbid environment, the detected signal is a coherent superposition of light from the desired in-focus plane as well as regions out-of-focus. Reducing the out-of-focus contributions enable images that better represent the true object's state. We present theoretical and experimental results showing improved fidelity when using modal illumination. In particular we investigated the use of TEM10 and a novel implementation of Nomarski differential-interference-contrast (DIC). Both of these modes of illumination present two separated focal spots in the object and provide coherent suppression of the out-of-focus background. Using a repeatable, stable turbid phantom the system fidelity was characterized against these illumination and pupil modifications. The theoretical model is also parameterized against potential optical configurations and novel imaging modes enabled by DIC imaging are described theoretically and experimentally.

8227-63, Session 10

## Prospective gating for 3D imaging of the beating zebrafish heart in embryonic development studies

J. M. Taylor, J. M. Girkin, G. D. Love, Durham Univ. (United Kingdom)

Techniques such as spinning disc confocal microscope and in particular selective plane illumination microscopy (SPIM) can be used for sectioned fluorescence imaging of living tissue. 3D image stacks are particularly useful for understanding the structural function and growth of heart tissue.

We demonstrate the use of prospective gating from continuously acquired brightfield images to trigger the acquisition of fluorescence images with the heart at a precisely selected position in its cycle. By avoiding the need to acquire many separate fluorescence images for each section before selecting the most appropriate ones to build up a consistent 3D image stack, the laser exposure of the sample is reduced by an order of magnitude while retaining an extremely high quality dataset.

We will present results obtained using our SPIM system including 3D reconstructions of the living, beating heart, acquired using optical gating without the need for any pharmacological or electrophysiological intervention. We will describe the optical solution we have used in order to maintain correct synchronization while the illuminating light sheet is scanned through the sample.

The new method will be described in detail and results using the novel system will be discussed in a range of biologically interesting situations.

# Conference 8228: Single Molecule Spectroscopy and Superresolution Imaging V

Saturday-Sunday 21-22 January 2012

Part of Proceedings of SPIE Vol. 8228 Single Molecule Spectroscopy and Superresolution Imaging V

8228-02, Session 1

## Fluorescence antibunching microscopy

O. Schwartz, J. Levitt, D. Oron, Weizmann Institute of Science (Israel)

It has long been recognized that quantum properties of light can be utilized for superresolution imaging. However, due to conceptual and technical difficulties, sub-diffraction limited quantum imaging has not been realized yet. We experimentally demonstrate a superresolution microscopy technique enabled by the non-classical emission statistics of regular fluorophores. Specifically, we utilize photon antibunching, i.e. the property of fluorescence photons to arrive one by one rather than in bursts. Unlike many quantum phenomena, antibunching is a very robust effect, generically exhibited by most fluorophores at room temperature. On the other hand, it is a distinctively quantum phenomenon, implying reduced quantum fluctuations (squeezing) of light and sub-poissonian photon statistics. Studying photon statistics at the image plane, we find that the antibunching-induced lack of pair coincidence events with respect to classical light decays in space proportionally to the square of the optical point spread function (PSF). Similarly, the lack of higher order coincidence events decays as higher powers of the PSF. Thus antibunching gives rise to spatial correlations that encode high spatial frequency information on the distribution of fluorescent emitters. We detect these correlations in a standard fluorescence microscope setting using photon counting instrumentation and obtain superresolved images of the fluorophores. Our technique allows for signal to noise limited resolution enhancement in three dimensions, and is compatible with various modalities of fluorescent microscopy. It provides a quantum alternative to the established superresolution tools and lends the emerging field of quantum imaging a new degree of relevance to practical microscopy.

8228-03, Session 1

## Giant unilamellar vesicle (GUV) as model system in advanced 3D orientation determination

R. Börner, Univ. zu Lübeck (Germany); N. Ehrlich, Univ. of Copenhagen (Denmark); C. G. Hübner, Univ. zu Lübeck (Germany)

One of the unique features of single molecule absorption/emission is their anisotropy due to the well-defined transition dipoles for both processes allowing the determination of the molecule's 3d orientation. Therefore, several techniques have been proposed in order to determine the full three-dimensional orientation of dipole emitters on a single molecule level. We recently demonstrated a technique that combines emission distribution and polarization detection [1,2,3]. As the method is an intensity distribution technique and based on single photon detection in principle, one can extend the 3d orientation determination to fluorescence correlation spectroscopy (FCS) as well as dynamical anisotropy measurements. This allows for the determination of the dynamics in 3d orientation of single molecules down to a nanosecond timescales. The 3d orientation is particularly interesting in non-isotropic environments. A lipid membrane is such a non-isotropic environment of enormous importance in biological systems. We therefore use giant unilamellar vesicle (GUV) labeled with dyes like DiO as a model system. Due to the defined curvature of such vesicles all possible dipole orientations can be achieved. This allows us to show the capabilities of our method on different timescales and to quantify the error in determination of 3d orientation dynamics in lipid membranes. Furthermore Monte Carlo simulations of rotational dynamics taking into account the excitation/emission characteristics of dipoles incorperated in the lipid membrane in conjunction with the 3D orientation determination complement our experiment.

[1] J. Hohlbein & C. G. Hübner, APL, 86, 121104 (2005)

[2] J. Hohlbein & C. G. Hübner, JCP, 129, 094703 (2008)

[3] R. Börner et al., Proc. SPIE, 7905, 79050D (2011)

8228-04, Session 1

## Monitor single-lipid dynamics during ligand-induced signaling in living cells with FCS and STED nanoscopy

C. Hsieh, L. Yang, Academia Sinica (Taiwan); Y. Lin, National Taiwan Univ. (Taiwan); J. Shen, Y. Chang, Academia Sinica (Taiwan); Y. Chang, National Changhua Univ. of Education (Taiwan); C. Chou, Academia Sinica (Taiwan)

Lipid raft serves as a platform for recruiting signaling components of effective signal transduction. However, the dynamics of sub-200 nm rapidly aggregated lipid rafts are still not elucidated in living cells. In our studies, we use ligand-coated Qdot to trigger slow lipid-raft aggregation in living cells. Moreover, the slow ligand-induced lipid-raft aggregation was monitored with the combination of fluorescence correlation spectroscopy (FCS) and stimulated emission depletion microscopy (STED), which provide high temporal and spatial resolution, respectively. We then investigated and compared the dynamics of lipid raft in supported bilayers and living cells with milli-second temporal and 10's nm spatial resolution.

8228-05, Session 2

## Conformational dynamics of single G protein-coupled receptors in solution

S. Bockenhauer, A. Fuerstenberg, X. J. Yao, B. Kobilka, W. E. Moerner, Stanford Univ. (United States)

G Protein-Coupled Receptors (GPCRs) comprise a large family of seven-helix transmembrane proteins which regulate cellular signaling by sensing light, ligands, and binding proteins. The GPCR activation process, however, is not a simple on-off switch; current models suggest a complex conformational landscape in which the active, signaling state includes multiple conformations with similar downstream activity. The present study probes the conformational dynamics of single β2-Adrenergic Receptors (β2ARs) in the solution phase by Anti-Brownian ELectrokinetic (ABEL) trapping. The ABEL trap uses fast electrokinetic feedback in a microfluidic configuration to allow direct observation of a single fluorescently-labeled β2AR for hundreds of milliseconds to seconds. By choosing a reporter dye and labeling site sensitive to ligand binding, we observe a diversity of discrete fluorescence intensity and lifetime levels in single β2ARs, indicating a varying radiative lifetime and a range of discrete conformational states with dwell times of hundreds of milliseconds. We find that binding of agonist increases the dwell times of these states, and furthermore, we observe millisecond fluctuations within states. The intensity autocorrelations of these faster fluctuations are well-described by stretched exponential functions with stretching exponent β ~ 0.5, suggesting protein dynamics over a range of timescales.

8228-07, Session 2

## Biological structure from precise and accurate estimation of fluorophore orientations and distances: proof-of-principle using internally labeled dsDNA

K. I. Mortensen, J. Sung, Stanford Univ. (United States); H. Flyvbjerg, Technical Univ. of Denmark (Denmark); J. A. Spudich, Stanford Univ. (United States)

Structure and structural transitions are at the heart of the molecular basis of biological function. In super-resolution microscopy and single-molecule biophysics, such information is probed using fluorophores. The emitted light gives rise to diffraction-limited spots whose centers are routinely localized with nanometer precision when spots are isolated. Thus, distances shorter than the diffraction limit may be assessed by filtered imaging of differently colored fluorophores. Popular approaches assume rotational freedom of the fluorophore emission dipole moment hence fit a 2D Gaussian intensity distribution to the image of a fluorophore using least-squares methods. However, when the dipole moment is resolved in time or deliberately fixed, the resulting intensity pattern is highly anisotropic and depends radically on the dipole orientation. We recently showed that the optimal analysis to extract simultaneous orientations and positions from focused images of fixed fluorophores uses the theoretical point spread function in conjunction with maximum likelihood estimation. Here we show that this approach is mature as a structural tool able to determine real, physical distances and orientations of intra- and inter-molecular domains. As proof-of-principle, we use dsDNA strands with two differently colored probes doubly attached to the double-helix backbone. Relative orientations and distances between probes are controlled by the number of base pairs separating them. We demonstrate that estimates of orientation and distance are accurate and precise: they scatter tightly around their true values known from structural information with a standard deviation that achieves the ultimate precision possible according to Fisher's information limit.

8228-08, Session 2

## Novel bimolecular fluorescence complementation (BiFC) protein complexes as innovative tools for in vivo interaction studies and their characterization by single-molecule spectroscopy

S. zur Oven-Krockhaus, S. Peter, A. J. Meixner, K. Harter, F. Schleifenbaum, Eberhard Karls Univ. Tübingen (Germany)

The visualization of protein-protein interaction networks in living organisms is of major importance in proteomics. Two methods play a dominant role in the field of modern microscopy: Foerster Resonance Energy Transfer (FRET), which is the most commonly employed tool, and Bimolecular fluorescence complementation (BiFC).

The latter utilizes two fragments of different fluorescent protein mutants as labels for putative interaction partners. These label fragments will only re-combine to a functional, fluorescent protein complex if their protein carriers are at very close quarters. The fluorescence signal as a primary effect usually results in much better signal-to-noise ratios compared to FRET. It could be shown that differently matched BiFC-complexes show a significant diversity in their spectroscopic properties, even though they only differ in few mutations of their amino acid sequence. As of now, the structure and properties of those complexes are only insufficiently documented. However, a competent knowledge of their photophysical properties is essential for a significant use in scientific applications. As many photophysical features stay hidden in bulk measurements, for the first time a single molecule approach has been used to characterize model systems of these BiFC complexes. The main focus was placed on spectral dynamics and differences in the characteristic blinking behavior of eight selected complexes. Based on statistics in single molecule spectra and intensity trajectories three amino acid mutations could be identified which seem to be especially pivotal for the spectroscopic properties. Moreover, the single molecule data allow for the typification of the mechanical flexibility of the protein shells.

8228-09, Session 2

## New tools for discovering the role sRNA plays in cell regulation

D. P. Shepherd, N. Li, E. Hong-Geller, B. Munsky, J. Werner, Los Alamos National Lab. (United States)

Small RNA (sRNA, [1]) represent an important class of regulatory molecules of cellular dynamics. Direct study of sRNA dynamics within living cells faces two important challenges. First, the functional role of sRNA can be difficult to discern, as a given cell response or observable phenotype could have produced from a variety of possible regulatory network motifs. Second, the small size of sRNA makes it difficult to attach enough fluorescent probes to achieve a measurable signal without perturbing the system dynamics. To address these challenges, we have used single molecule fluorescence in situ hybridization (smFISH, [2]) to study cell-to-cell heterogeneity of mRNA copy numbers for human host cells in the presence and absence of bacterial sRNA. These experimental distributions of mRNA are used to refine and down-select regulatory models, using the Finite State Approach [3] along with other techniques. A large number a cells are subjected to varying conditions such as nutrient concentration, salt content, and pathogen infection to eliminate incorrect regulatory models. The models, in turn, provide feedback and guidance to our experimental work to better understand the roles that sRNA plays in the cellular response.

[1] Fire et al., "Potent and specific genetic interference by double-stranded RNA in Caenorhabditis elegans", Nature (1998)

[2] Raj et al., "Imaging individual mRNA molecules using multiple singly labeled probes", Nature Methods (2008)

[3] Munsky et al., "Listening to the noise: random fluctuations reveal gene network parameters", Molecular System Biology (2009)

Young Investigator best paper competition BO403

8228-10, Session 2

## Fluorescent saxitoxins for live cell imaging of single voltage-gated sodium ion channels beyond the optical diffraction limit

H. D. Lee, A. Ondrus, Stanford Univ. (United States); S. Iwanaga, Sysmex Corp. (Japan); J. Dubois, W. E. Moerner, Stanford Univ. (United States)

Neuronal function is shaped by the proper expression, distribution, and operation of voltage-gated sodium ion channels (NaVs). A desire to better understand the role of NaVs in signal conduction and their dysregulation in specific disease states motivates the development of high precision tools for their study. Nature has evolved a collection of small molecule nerve blocking agents, including the paralytic shellfish poison (+)-saxitoxin, that bind with low nanomolar affinity and exquisite fidelity to the extracellular pore of select NaV isoforms. De novo chemical synthesis enables the preparation of fluorescently labeled derivatives of (+)-saxitoxin, STX-Cy5 and STX-DCDHF, which display rapidly reversible binding to endogenous NaVs in live cells. Fluorescence colocalization studies with a pan-NaV antibody confirm that binding of these STX-based dyes is highly selective to NaVs. The utility of these probes is underscored in single-molecule and super-resolution imaging experiments, which reveal NaV distributions well beyond the optical diffraction limit in subcellular features such as neuritic spines and filopodia. Collectively, these data establish STX-Cy5 and STX-DCDHF as selective molecular probes that offer a dynamic view of native NaVs in living cells with unprecedented visual detail.

8228-11, Session 3

## Stepsize of the rotary proton motor in single FoF1-ATP synthase from a thermophilic bacterium by DCO-ALEX FRET

E. Hammann, A. Zappe, Univ. Stuttgart (Germany); S. Keis, Univ. of Otago (New Zealand); S. Ernst, Jena Univ. Hospital (Germany) and Univ. of Stuttgart (Germany); G. M. Cook, Univ. of Otago (New Zealand); M. Börsch, Jena Univ. Hospital (Germany) and Univ. of Stuttgart (Germany)

The ATP-producing enzyme FoF1-ATP synthase from thermophilic bacillus sp. strain TA2.A1 is driven by an Fo motor consisting of a ring of 13 c-subunits. The thermophilic enzyme can be genetically modified and expressed in other bacteria for purification. In contrast to the Escherichia coli FoF1-ATP synthase, ATP hydrolysis is suppressed in the TA2.A1 enzyme at room temperature, but is activated at higher temperatures and in the presence of the detergent LDAO. We applied a single-molecule Förster resonance energey transfer (FRET) approach using duty cycle optimized alternating laser excitation (DCO-ALEX) to monitor the expected 13-stepped Fo motor at work. Two fluorophores were atttached specifically, one to the static a-subunit and another to one of the rotating c-subunits in Fo. A new FRET transition histogram was developed to identify the smaller step sizes compared to the 10-stepped Fo motor of the Escherichia coli enzyme. Dwell time analysis and Monte Carlo simulations revealed the temperature and the LDAO dependence of the Fo motor on the single molecule level. The elastic properties of the rotor of this thermophilic enzyme will be discussed.

8228-12, Session 3

## Parallel multispot smFRET analysis using an 8-pixel SPAD array

A. Ingargiola, Univ. of California, Los Angeles (United States) and Politecnico di Milano (Italy); R. Colyer, Univ. of California, Los Angeles (United States); D. Kim, Nesher Technologies, Inc. (United States); R. Lin, Univ. of California, Los Angeles (United States); A. Gulinatti, I. Rech, M. Ghioni, Politecnico di Milano (Italy); S. Weiss, X. Michalet, Univ. of California, Los Angeles (United States)

Single-molecule Förster resonance energy transfer (smFRET) is a powerful tool for extracting distance information between two fluorophores (a donor and acceptor dye) on a nanometer scale. This method is commonly used to monitor binding interactions or intra- and intermolecular conformations in biomolecules freely diffusing through a focal volume or immobilized on a surface. The diffusing geometry has the advantage to not interfere with the molecules and to give access to fast time scales.

However, separating photon bursts from individual molecules requires low sample concentrations. This results in long acquisition time (several minutes to an hour) to obtain sufficient statistics. It also prevents studying dynamic phenomena happening on time scales larger than the burst duration and smaller than the acquisition time.

Parallelization of acquisition overcomes this limit by increasing the acquisition rate using the same low concentrations required for individual molecule burst identification.

In this work we present a new two-color smFRET approach using multispot excitation and detection. The donor excitation pattern is composed of 4 spots arranged in a linear pattern. The fluorescent emission of donor and acceptor dyes is then collected and refocused on two separate areas of a custom 8-pixel SPAD array. We report smFRET measurements performed on various DNA samples synthesized with various distances between the donor and acceptor fluorophores.

We demonstrate that our approach provides identical FRET efficiency values to a conventional single-spot acquisition approach, but with a reduced acquisition time. Our work thus opens the way to high-throughput smFRET analysis on freely diffusing molecules.

8228-13, Session 3

## Development of time-resolved Mueller polarization microscopy through time-correlated single-photon counting

J. Qiu, N. Mazumder, T. Kuo, P. Lin, H. Tsai, C. Hu, F. Kao, National Yang-Ming Univ. (Taiwan)

In this work, we have established a time-resolved Stokes-Vector-Mueller-Matrix polarization microscopy. A four-channel time correlated single photon counting setup is integrated into the Stokes vector polarization state analyzer for highly sensitive time-resolved measurements. The validity of the setup is demonstrated firstly through experiments using air as the standard sample since its Mueller matrix is expected to be unit matrix. Furthermore, we mixed 1mM R6G ethanol solution into water, ethanol and glycerol with 1:1 volume ratio respectively to prepare three sample fluorescence liquids with different viscosities. The viscosity of the sample fluorescence liquids is determined by resolving the polarization status of the emitted fluorescence. The results show that depolarization depends critically on viscosity. It is a function of both viscosity and time-delay. Linear retardance and optical rotation, in contrast, are independent of either viscosity or time-delay. Such simultaneous determination of fluorophores' multiple polarization parameters in both temporal and spatial domains is unprecedented and is a powerful tool in elucidating molecular dynamics.

8228-14, Session 3

## Multiplexing and confinement in fluorescence correlation spectroscopy with an array of optical fibers

F. Quinlan-Pluck, L'Institut Langevin (France) and CNRS (France); Q. Wilmart, L'Institut Langevin (France); E. Fort, L'Institut Langevin (France) and Univ. Denis Diderot (France); S. Leveque-Fort, Univ. Paris-Sud 11 (France) and CNRS (France); N. Sojic, Univ. Bordeaux 1 (France) and ENSCBP (France); S. Gresillon, L'Institut Langevin (France) and Univ. Pierre and Marie Curie (France)

The impact of fluorescence correlation spectroscopy (FCS) on life science is ever widening, with recent advances for the measurement of transport properties within the living cell or in the membrane. The technique itself has also improved, combining FCS to lifetime fluorescence or cross-correlation. However, improving both resolution and speed together is still a challenge. Here we present fluorescence correlation spectroscopy with multiple volumes using an electron multiplying charge coupled device camera, a microscope and an ordered array of etched optical fibers. An independent observation volume is created at the end of each optical fiber. The sub-wavelength aperture of the etched fibers confined light in the near-field. The lateral size of the correlation volume is given by the aperture diameter. Using this camera, the bundle of fibers allows the discrimination of the fluorescence coming from each observation volume. Moreover, physical separation of the observation volume on the sample side avoids unwanted cross talk between the correlation signals. Multiplexed correlation with a well defined localization of the observation volume is demonstrated on fluorescent beads. With fast acquisition modes on the camera, we perform fluorescence correlation with a time resolution better than 0.1 milliseconds and lateral resolution below 250 nanometers. By reducing the output of the fiber down to 100 nanometers, improvement of the resolution of our FCS set-up can be obtained. Comparison with standard FCS is also shown. Thanks to the use of these fiber bundles, this system is easily adaptable above a confocal microscope or in standard FCS configuration.

8228-15, Session 4

## Next-generation TCSPC detection

F. Koberling, U. Ortmann, H. Rahn, B. Kraemer, M. König, P. Kapusta, M. Wahl, R. Erdmann, PicoQuant GmbH (Germany)

More than 20 years ago single photon counting based single molecule detection started with cooled photomultiplier tubes (PMT). Already 5 years later the single photon avalanche photodiode (SPAD) starts to replace the PMT especially due to its higher detection efficiency and became the workhorse in confocal single molecule microscopy. In the last decade step by step SPAD technology improvements enabled to meet most of the requirements of modern Time-Correlated Single Photon Counting (TCSPC) for ultrasensitive detection.

Recently a new detector module became available which allows to merge the still remaining timing performance advantages of the PMT with the photon processing efficiency of the SPAD. We incorporated this novel hybrid photomultiplier detector module (PMA hybrid) in a cooled, self-contained housing and will present its outstanding performance like narrow and ultrastable IRF, low darkcounts and almost negligible afterpulsing. Our experiments will demonstrate the advantages for several applications like FLIM and FCS.

Beneath this new single point detector we will show recent results for different types of TCSPC detector arrays for highly parallel and / or spectrally resolved detection together with high throughput counting electronics and new approaches towards a robust and efficient multidimensional data analysis.

8228-16, Session 4

## Multiplex tumor marker quantification with spectrally-resolved fluorescence lifetime imaging

I. Gregor, Georg-August-Univ. Göttingen (Germany); A. Loman, F. S. Wouters, Univ. Medicine Göttingen (Germany); J. Enderlein, Georg-August-Univ. Göttingen (Germany); G. Bunt, Univ. Medicine Göttingen (Germany)

The development of single-molecule fluorescence techniques has led to an enormous progress in quantitative cellular biophysics. However, the precise absolute quantification of concentrations, or even relative numbers, of several proteins at the same time within a single cell remains difficult. For many biomedical studies, this information can provide insight into intracellular correlations of protein levels. Such information is the key to understand e.g. cancer development and finding possible strategies for therapeutic intervention. Using spectrally-resolved Fluorescence Lifetime Imaging Microscopy (sFLIM) in combination with new highly efficient quantitative data analysis algorithms we are able to simultaneously quantify the relative levels of three important tumor-associated proteins within a single cell from immunofluorescence signals. The incorporation of lifetime information reports the state of specific genetically expressible FRET sensors that are based on fluorescent proteins (FPs).

The quantitative analysis of sFLIM data is usually time consuming and prone to errors if the lifetime decay patterns are complex (multi-exponential). Of central importance, therefore was the development of a new approach to quantify multiplex sFLIM data. Our method is fast and quantitatively precise even in the case of complex fluorescence decays. We present its working principles and several of its applications.

8228-17, Session 4

## Ultrasensitive fluorescence correlation spectroscopy of highly parallelized microfluidic devices

B. K. Canfield, W. N. Robinson, J. K. King, W. H. Hofmeister, L. M. Davis, The Univ. of Tennessee Space Institute (United States)

Preliminary drug library screenings and related assays currently require relatively large amounts of both time and candidate materials, in addition to the costly technology necessary to perform the screenings. In order to lower material needs and processing costs while increasing throughput, we are developing an ultrasensitive, fluorescence-based detection system in highly parallel microfluidic channels with kHz readout rates. Highly parallelized prototype microfluidic devices have been fabricated by direct femtosecond laser machining of multiple micron-scale channels (~ 150) in fused silica substrates, which are subsequently bonded to coverslips. A custom-built, wide-field microscope epi-illuminated by a line-generating red diode laser provides a uniform excitation region just a few microns wide over the field of view of 500 microns. We approach single-molecule level detection sensitivity by introducing very dilute aqueous solutions (~ pM) of fluorescently labeled molecules into the microchannels. Fluorescence signals from molecules that flow through the illuminated microchannel sections are detected with an electron-multiplying CCD camera. Limiting the excited region of the CCD to only a few rows of pixels at most and exploiting its frame transfer capability allows readout rates of several kHz. Fluorescence correlation spectroscopy is used to analyze the data from each separate microchannel. Once the prototype methods have been optimized, devices could easily be mass-fabricated in low-cost, low-autofluorescence polymer substrates using imprint lithography.

8228-18, Session 4

## High-performance SPAD array detectors for parallel photon timing applications

I. Rech, A. Gulinatti, C. Cammi, M. Ghioni, Politecnico di Milano (Italy)

Over the past few years there has been a growing interest in monolithic arrays of single photon avalanche diodes (SPAD) for spatially resolved detection of faint ultrafast optical signals. SPADs implemented in planar technologies offer the typical advantages of microelectronic devices (small size, ruggedness, low voltage, low power, etc.). Furthermore, they have inherently higher photon detection efficiency than PMTs and are able to provide, beside sensitivities down to single-photons, very high acquisition speeds.

In order to make SPAD array more and more competitive in time-resolved application it is necessary to face problems like electrical crosstalk between adjacent pixel, high detection efficiency in the red spectral range, large area, low dark counting rate. Moreover to develop array with high number of pixel became more and more important to develop all the TCSPC electronics with picosecond resolution to create a new family of detection system for TCSPC applications. Recent advances in our research on single photon time resolved array is here presented.

8228-01, Session 5

## Fluorescence intensity fluctuations in single-molecule polarization sensitive measurements

L. Turgeman, D. Fixler, Bar-Ilan Univ. (Israel)

A general framework to include fluctuations in single molecule fluorescence intensity (FI) signal due to random changes in molecule dipole orientation was introduced by Foreman and co-workers (Optics Express 21, 2007). By assuming continuous changes in dipole orientation described by Brownian rotational diffusion, this research derives the probability density function equation that governs single molecule FI fluctuations as a result of molecule dipole reorientation in single molecule measurements. Solution of the proposed equation for several limiting cases and different correlation times yields the short time behavior of FI fluctuations. For extremely low FI - long integration time is needed. In some fluorescence fluctuation spectroscopy techniques, however, it is essential that the chosen integration time is sufficiently short in order to follow the fluctuations. In a typical Photon counting histogram experiment the integration time that is used might be in the order of tens of microseconds. During this time some rotational diffusion is likely to occur (based on typical diffusion coefficient for small molecules in solution). Applying our suggested model in these cases should yield accurate expectation values of photon counts for a very short integration time. Monte Carlo simulations results, in accordance with those found in theory will be presented during our talk.

8228-19, Session 5

## ‘Sizing’ the oligomers of Azami green fluorescent protein with FCS and antibunching

J. Temirov, St. Jude Children’s Research Hospital (United States); J. Werner, P. Goodwin, A. Bradbury, Los Alamos National Lab. (United States)

Fluorescent proteins are invaluable molecules in fluorescence microscopy and spectroscopy. Some of the important features of fluorescent proteins are size and brightness. While it is desirable to have monomeric proteins, often proteins tend to form oligomers (dimers and tetramers) at which state they are actually more stable. However, photophysical properties of monomers do not necessarily multiply by their number when they form oligomers. In this work we studied oligomerization status of the Azami Green (AG) proteins [1,2] with FCS and Photon antibunching. With FCS we compared the hydrodynamic sizes of the proteins and with antibunching we counted the number of emitters. The results showed that the dimers of AG protein were single emitters and the tetramers were dual-emitters. This indicated dipole-dipole interaction and energy transfer between the monomeric units. We also applied this approach to estimate the number of fluorescent proteins displayed on T7 phage molecules [3].

[1] S. Karasawa, T. Araki, M. Yamamoto-Hino, and A. Miyawaki, J. of Bio. Chem., v.278, #36, p3467-3471, 2003.

[2] M. Dai, H.E.Fisher, J. Temirov, C. Kiss, M.E.Phipps, P. Pavlik, JH. Werner and A.R.M.Bradbury, PEDS, v.20, #2, p69-79, 2007.

[3] M. Dai, J. Temirov, E. Pesavento, C. Kiss,N. Velappan, P. Pavlik, J.H. Werner and A.R.M. Bradbury, PEDS, v.21, #7, p413-424, 2008.

8228-20, Session 5

## A designed DNA probe to evaluate counting single molecules by photon antibunching

A. Kurz, Univ. of Heidelberg (Germany); H. Ta, Max-Planck-Institut für biophysikalische Chemie (Germany) and Univ. of Göttingen (Germany); D. Herten, Univ. of Heidelberg (Germany)

“Young Investigator best paper competition BO403”

Typical problems in molecular biology, like Oligomerization of proteins, appear on non resolvable length scales. Therefore a method which can observe numbers of fluorescent emitters beyond this barrier can help to answer some of these questions. E.g. this can be achieved by exploiting the photon antibunching effect (PAB). Most fluorophores are, due to their quantum nature, single photon emitters, therefore a molecule can only emit one single photon per exciting laser pulse. By analyzing coincident events of photon detections (Coincidence Analysis, CCA ) in many excitation cycles the number of observed fluorophores in the confocal volume can be estimated.

In simulations was shown that up to 40 fluorophores can be distinguished with reasonable error. In following experiments up to five bleach steps could be identified by CCA. We will present in this work a new probe design, which is based on oligomerization of labelled DNA strands. By careful design we can address different numbers of dyes. Therefore simulations can be compared with experimental results and capabilities of CCA can be examined. CCA is critical to several parameters like photo stability, background, label efficiency and photopysic properties of the dye label, like brightness and blinking. These topics and their influence will be addressed in this publication.

8228-21, Session 5

## Fluorescence correlation spectroscopy and scanning correlation spectroscopy techniques to quantify dynamics and kinetics of EGFR in vivo before and after γ-irradiation

S. Abdisalaam, The Univ. of Texas at Arlington (United States)

In this study, Fluorescence Correlation Spectroscopy and scanning correlation spectroscopy techniques are employed to demonstrate the nuclear translocation of EGFR in living cells under a variety of experimental conditions Wild type epidermal growth factor receptor (EGFR) modulates the repair of IR induced DNA damage by translocating to the nucleus in response to γ-irradiation. WT EGFR translocated to the nucleus after γ-irradiation while the mutants did not. Then, the effects of γ-irradiation together with cetuximab were monitored simultaneously for different cell lines. Stable transfectants of WT, L858R and ΔE746-E750 were treated with cetuximab and then irradiated with different doses of gamma-irradiation. Raster scan images then were taken for different time points for one hour. The result shows EGFR concentration in stable HBEC WT cells increases in the nucleus after one hour of 4 Gy of γ-irradiation while concentration of mutants L858R and ΔE746-E750 remains constant.

8228-22, Session 5

## Understanding the synapse at nanoscale using hyperresolved molecular interaction imaging

C. Tardif, H. Dufour, D. Côté, P. De Koninck, Laval Univ. (Canada)

Studying the spatial distribution of protein interactions is of great interest in neurons, particularly at their connexion sites, the synapses, and because of the complexity of signaling pathway involved in neuronal communication. We are therefore developing a super resolution microscope based on stimulated emission depletion (STED) capable of measuring protein-protein interactions using Förster resonant energy transfert (FRET) and Fluorescent lifetime imaging (FLIM) approaches. We present our system, which includes a supercontinuum laser to both excite and deplete fluorescence and a time-correlated single photon counting (TCSPC) card to perform a time gating acquisition and fluorescence lifetime measurements. We show distribution of protein interactions between synaptic components in neuronal culture with a high spatial resolution using immunostaining approach. We chose the signaling cascade that involves the protein kinase “CaMKII”, an enzyme that is involved in learning and memory and that undergoes dynamic activity-dependent relocation in neurons. We are studying the interaction between CaMKII and other partners in various neuronal compartments. Using antibodies conjugated with FRET pairs of fluorophore (Atto 594 and 647N) respectively targeted to those proteins, we will localize with high resolution these interactions. Learning more about the spatial distribution of CaMKII and its interactions with other partners such as synaptic receptors, motor or scaffolding proteins should help us understand the cellular and molecular basis of neuronal plasticity.

8228-23, Session 6

## Nanoscopy with focused light

S. W. Hell, Max-Planck-Institut für biophysikalische Chemie (Germany)

For more than a century, it has been generally accepted that the resolution of a lens-based optical microscope is limited to about > 200 nm in the focal plane and > 500 nm along the optic axis, with NA denoting the numerical aperture of the lens and the wavelength of light. The discovery in the 1990’s that elementary transitions between the states of a fluorophore can be used to eliminate the limiting role of diffraction has led to light microscopy concepts with resolution on the nanometer scale(1, 2). Currently, all existing and successfully applied nanoscopy methods share a common enabling element: they switch fluorescence on or off, so that adjacent features are registered sequentially in time (3, 4).

For example, in a typical Stimulated Emission Depletion (STED) microscope(1), the fluorophores are switched off (=kept dark) by overlapping the excitation beam with a de-exciting (STED) beam which effectively confines the fluorophores to the ground state everywhere in the focal region except at a tiny area where the STED beam is close to zero. Fluorophores that are located in this subdiffraction-sized smaller area are registered. Scanning the beams further in space registers those fluorophores that had been switched off. An image of the whole object is assembled by sequential registration. The resolution is now given by the smaller diameter of this area in which the fluorophores are still fluorescent. I is the intensity of the STED beam, which, for I >> Is, entails d→0, meaning that the resolution is conceptually no longer limited by .

STED microscopy has been used to investigate the fate of synaptic vesicle proteins after exocytosis(5), thus demonstrating the potential of emerging ‘fluorescence nanoscopy’ for the life sciences. A video-rate STED microscope was used to describe the mobility of vesicles inside the axons of cultured living neurons(6). Live-cell STED microscopy has also been used to image activity-dependent morphological plasticity of dendritic spines(7), while in another study, it revealed that single sphingolipids, but not phospholipids, are transiently ( >1 detectable photons in a row before returning to a dark state, allowing the calculation of their position. These single fluorophore switching concepts(10-14) require only a single switching cycle(3, 4) per fluorophore, which greatly extends the power of the switching concept for subdiffraction separation. Altogether, lens-based optical nanoscopy is an unexpected and fascinating development in the physical sciences that is poised to impact several areas of science, in particular the life sciences, in the near future.

8228-24, Session 6

## Full-field stimulated emission depletion (STED) imaging by surface plasmon resonance (SPR) enhancement

H. Zhang, M. Zhao, L. Peng, College of Optical Sciences, The Univ. of Arizona (United States)

Nonlinear structured illumination microscopy (SIM) allows fast full-field imaging at resolutions <100 nm. We report that it is feasible to apply STED in nonlinear SIM, and achieve better resolution than saturated SIM (SSIM). STED requires intense laser field, which is usually generated locally with a focused laser. Nonlinear SIM requires strong full-field nonlinear effects. To generate strong full-field STED at low laser intensity, we used SPR enhancement of evanescence field near a dielectric-metal-dielectric interface. Guided by optical field calculation, we optimized a glass-silver-glass-water planar structure that experimentally gave 17 times STED enhancement in comparison to plain glass substrate. The enhancement factor matches the theoretical prediction from field calculations. Over 10 times of STED saturation intensity in a 17 × 10 μm area was achieved. We further conducted signal to noise analysis and imaging performance simulation of STED-SIM under the measured STED field strength. Our analysis showed that STED-SIM will reach 30nm resolution over a field of 17 × 10 μm, and single molecule imaging is possible under current conditions. In comparison to SSIM, STED-SIM will have better resolution, higher sensitivity and less photon toxicity to live cells. STED-SIM may serve as a better super-resolution alternative when coupled to conventional total internal reflection microscopy, and allow evaluate membrane resident or near membrane structure at super-resolution over time in live cells. Instrument building of the STED-SIM microscope is under way.

8228-25, Session 6

## Superresolution imaging of diffusing analyte in surface-enhanced Raman scattering hotspots

K. A. Willets, S. M. Stranahan, M. L. Weber, The Univ. of Texas at Austin (United States)

Single molecule surface-enhanced Raman scattering (SM-SERS) is characterized by fluctuations in the measured SERS intensity from an analyte adsorbed on a metal nanoparticle surface. In this paper, we use super-resolution imaging techniques to resolve the centroid of the SERS emission and track how its position changes with time. SM-SERS samples are imaged onto a CCD camera, and the resulting point spread function is fit to a 2-dimensional Gaussian function to extract the centroid of the SERS emission. The SERS centroid position provides an indirect measurement of the location of the analyte on the nanoparticle surface. The mean-square-displacement of the SERS centroid is calculated as a function of time lag and reveals a non-linear relationship, indicative of non-Brownian analyte diffusion. Signatures of sub-diffusion and confinement are apparent in the data, and are related back to nanoparticle structure obtained via electron microscopy. By analyzing these diffusion trajectories, we are able to determine how single analytes move on the surface of metal nanoparticle aggregates and how this is related to the observed SERS signals. (Young Investigator best paper competition BO403).

8228-26, Session 6

## Optimal acquisition schemes for superresolution localization microscopy of bleachable fluorophores

A. R. Small, E. Shore, California State Polytechnic Univ., Pomona (United States)

Superresolution localization microscopy (e.g. PALM, STORM) requires the acquisition of many frames containing sparse, non-overlapping single-fluorophore images. In any given frame, only a fraction of the fluorophores in the sample are actually activated to emit light, and the user typically controls the fraction of fluorophores activated in each frame. Two competing considerations determine the fraction of fluorophores that the user should activate: Activating a large fraction of the fluorophores increases the rate at which information is acquired, but also increases the probability of nearby fluorophores activating simultaneously, producing overlapping images. Further complicating the analysis is bleaching, which decreases the number of fluorophores present over time and thus reduces the probability of overlaps.

We have performed a mathematical analysis, using variational calculus, that takes into account the effects of bleaching and overlaps, to determine the optimal time-dependent activation probability per molecule that maximizes the number of single-molecule images acquired in a given time interval. When the experiment is controlled by two wavelengths (one for activating molecules, the other for exciting fluorescence) the optimal scheme is one with a constant error rate, and is insensitive to the detailed kinetics of the bleaching process. However, when the experiment is controlled by a single wavelength, activation and excitation are coupled variables, and the optimal scheme depends quite sensitively on the details of the bleaching process, particularly whether the ground state of the fluorophore is dark or activated. We also analyze robustness, to determine how error rates are affected by deviations from the optimal scheme.

8228-27, Session 7

## Recent developments in GSDIM microscopy

M. Dyba, J. Fölling, Leica Microsystems CMS GmbH (Germany)

GSDIM Microscopy (Ground State Depletion with Individual Molecule return) is a superresolution method which makes use of intrinsic dark states of standard fluorophores to break the diffraction barrier. The fluorophores are pumped to metastable dark states (such as radical states) and individual dye molecules, which are spontaneously returning to the fluorescing state, are localized, yielding a superresolution image. No special switchable markers are needed as in the related techniques PALM and STORM. Instead a large variety of standard dyes can be used. We present new developments in GSDIM Microscopy including solutions for practical imaging problems such as sample drift and image visualization during acquisition.

Drifting presents a major problem for this type of imaging. Due to the fact that the image acquisition can take on the order of several tens of minutes or longer, even slow and slight drifting results in an image which is smeared out and thus limits the image resolution.

8228-28, Session 7

## SIM and PALM as tools to study protein structural organization, numbers, interaction and dynamics

K. Weisshart, Carl Zeiss MicroImaging GmbH (Germany)

Lately quite a plethora of concepts have been successfully developed, which take resolution beyond the classical limits of a light microscope. Among these structured illumination microscopy (SIM) and photo activated localization microscopy (PALM) hold the promise to provide biologists with unprecedented insights into sub-cellular organizations. A combination of these methods seems particularly attractive as it allows adapting to the required resolution and enables to map single molecules or molecule ensembles in the context of highly resolved structures. SIM achieves two fold resolution enhancements in both lateral and axial directions, so structures can be highly resolved in 3D. Adapting the structuring to the wavelength opens up the avenue for multi-colour staining. Hence the distribution of one protein and its associated structure can be viewed in the context of others. Since all common fluorescent dyes can be used sample preparation is straightforward. Besides the classical approach to obtain highly resolved structures with up to 10 times the classical resolution, the power of PALM lies additionally in its ability to count and observe single molecules. As such clustering of molecules can be studied as well as many molecules tracked simultaneously to study their diffusion. New strategies open up the possibility to obtain resolution enhancement in the axial direction as well. These applications start already to have an impact on our view how a cell is organized and how different proteins contribute to its make-up.

8228-29, Session 7

## Optimization of precision localization microscopy using CMOS camera technology

E. Toda, T. Takahashi, T. Maruno, J. Yamashita, Hamamatsu Photonics K.K. (Japan); S. M. Fullerton, Hamamatsu Corp. (United States)

Light microscopy imaging is being transformed by the application of computational methods that permit the detection of spatial features below the optical diffraction limit. Successful localization microscopy (STORM, dSTORM, PALM, PhILM, etc.) relies on the precise position detection of fluorescence emitted by single molecules using highly sensitive cameras with rapid acquisition speeds. Electron multiplying CCD (EMCCD) cameras are the current standard detector for these applications. Here, we challenge the notion that EMCCD cameras are the best choice for precision localization microscopy and demonstrate through simulated and experimental data, that certain CMOS detector technology achieves better localization precision of single molecule fluorophores. It is well-established that localization precision is limited by system noise. Our findings show that the two overlooked noise sources relevant for precision localization microscopy are the shot noise of the background light in the sample and the excess noise from electron multiplication in EMCCD cameras. At low light conditions (< 200 photons/fluorophore) with no optical background, EMCCD cameras are the preferred detector. However, in practical applications, optical background noise is significant, creating conditions where CMOS performs better than EMCCD. Furthermore, the excess noise of EMCCD is equivalent to reducing the information content of each photon detected which, in localization microscopy, reduces the precision of the localization. Thus, new CMOS technology with 100fps, <2 e- read noise and high QE is the best detector choice for super resolution precision localization microscopy.

8228-30, Session 7

## Advances in super resolution technology and application in biomedical research

S. Ross, Nikon Instruments Inc. (United States)

There have been many advances in Super Resolution Imaging instrumentation over the last decade. Although these powerful tools are emerging in the market, such as Nikon's advanced N-SIM and N-STORM Structured Illumination and Localization Imaging systems, it is only recently that such technologies have been applied to investigate key questions in Biomedical Research. This talk will focus on some of those advances and applications.

8228-31, Session 8

## Superresolution imaging using fluctuations

F. Koberling, V. Buschmann, R. Erdmann, M. König, PicoQuant GmbH (Germany); T. Dertinger, Univ. of California, Los Angeles (United States); S. van de Line, Julius-Maximilians-Univ. Würzburg (Germany); S. Fore, PicoQuant Photonics North America, Inc. (United States); M. Sauer, Julius-Maximilians-Univ. Würzburg (Germany); J. Enderlein, Georg-August-Univ. (Germany)

The interest in superresolution microscopy techniques has dramatically increased in the last years due to the unprecedented insight into cellular structure which has become possible. All superresolution techniques rely on probes which can be switched between a bright and a dark state. For all camera-based techniques, such as STORM, dSTORM, GS-DIM or PALM, it is crucial to have perfect control over these 'on' and off' states. This photoswitching can be induced and controlled in most fluorophores using the dyes' oxidation and reduction behaviour by adding oxidizers and reductors (ROXS, Never2FADE [1]).

A recently developed superresolution technique, namely Superresolution Optical fluctuation Imaging (SOFI) [2] offers the possibility to record superresolved images within short acquisition times, while allowing switching rates of the probes to be almost arbitrary.

SOFI is based on the evaluation of stochastic signal fluctuations stemming from a single emitter by means of higher-order statistics. Even though in the experiment the fluctuations of many emitters might overlap in a pixel, the algorithm is designed in such way that it is able to extract superresolution information based on these stochastic fluctuations. An experiment consists of taking a movie of these fluctuations and afterwards subject this movie to the SOFI algorithm. Note that this algorithm works completely 'blindly', i.e. no assumptions / fitting of any kind have to be made on sample structure, emitter properties etc.

[1] M. Heilemann et al, Ang. Chem. Int. Ed. 48, 37, 6903 (2009)

[2] T. Dertinger et al, PNAS 106, 22287 (2009)

8228-32, Session 8

## Latest advances in commercially available STED microscopy

W. Fouquet, A. Giske, Leica Microsystems CMS GmbH (Germany)

STimulated Emission Depletion (STED) microscopy enables imaging of biological samples combining significantly improved optical resolution with all benefits of a confocal microscopy. Especially, by combining multi-channel image acquisition with high spatial resolution opens up a new understanding of co-localization experiments on nanoscales. Such a microscope provides new insights in various fields of biology, such as cell and membrane biology, neurobiology and physiology. We present new developments and a variaty of biological examples for STED microscopy, showing structural details on scales well below 70nm and give an overview of possible field of applications, mainly focussed on live cell imaging.

8228-33, Session 8

## Improvement of 3D localization in PALM, STORM, and single particle tracking by using adaptive optics

J. Andilla, Imagine Optic SA (France); I. Izeddin, Lab. Kastler Brossel (France); P. Clemenceau, Imagine Optic Inc. (United States); X. Levecq, Imagine Optic SA (France); X. Darzacq, Ecole Normale Supérieure (France); M. Dahan, Lab. Kastler Brossel (France)

Fluorescent microscopy is widely being used in biology as a basic tool to investigate cellular and molecular processes. Nowadays, super-resolution microscopy is unveiling new information beyond the diffraction limit. However, super-resolution techniques, as all the other optical techniques, are affected by the optical aberrations of the system which reduce the performance of its point spread function. In PALM/STORM or single particle tracking techniques the accuracy of the system is directly related with the number of collected photons by the detector. Because of this, the optical aberrations of the system degrade the precision of the detection. In microscopy techniques like two photon microscopy or confocal microscopy, adaptive optics has already been demonstrated as a suitable technique to compensate the effects of the optical aberrations improving the obtained signal and optimizing the systems.

In this communication we present the application of adaptive optics in pointillist super-resolution techniques (PALM/STORM/SPT). We will show how the adaptive optics system is installed in the emission path of the microscope in a very simple way. We will also show the improvement obtained after correcting the optical aberrations. Finally, we will demonstrate the capability of the adaptive optics system to realize beam shaping in order to introduce the third dimension information as in the PALM3D/STORM3D/3D-SPT techniques. We will discuss about the accuracy of using these capabilities in comparison with previous strategies. We will also show how dynamical properties of this approach allow the arbitrary adaptation of the shape as a function of the particular experimental conditions.

8228-34, Session 8

## From single-molecule chemistry to superresolution microscopy

D. Herten, A. Rybina, A. Seefeld, J. Balbo, M. Schwering, T. Erhard, K. Lymperopoulos, Ruprecht-Karls-Univ. Heidelberg (Germany)

Detection of single fluorescent molecules has contributed with the development of various methods to modern spectroscopy in the past 20 years and wide spread applications ranging from material to life sciences. A key element of a reasonable single molecule experiment and at the same time a limitation are the probes which requires the fluorescent label to undergo a change in its emission properties in order to indicate associated molecular processes. Therefore, we have a strong interest in photo-physical properties of fluorophores that could get connected to molecular transitions of interest and we try to combine photo-physical processes, like photo-induced electron transfer, to molecular transitions that can then be sensed with the tools of single-molecule fluorescence spectroscopy. In that context we developed dye conjugates for protein labelling that show an increase fluorescence intensity when they get attached to the protein tag allowing background free fluorescent labelling. In a similar way we study the influence of various quenching moieties on different fluorophores to sense elementary chemical processes like metal ion complexation or redox reactions on the single-molecule level. A side-effect of the interesting properties of such probes sometimes lead to surprising developments, like a novel super-resolution method based on chemical switching. However, our ultimate goal is to study catalytic processes in metal complexes on the single molecule level.

8228-35, Session 8

## Complementation activated light microscopy for nanometer accuracy single-molecule targeting and tracking in cells and living animals

F. Pinaud, C. Stigloher, Ecole Normale Supérieure (France); I. Gregor, J. Enderlein, Georg-August Univ. (Germany); M. Dahan, J. Bessereau, Ecole Normale Supérieure (France)

Limitations for studying the biomolecules in their native environment by single molecule fluorescence include the need to express them at low concentration or to target them specifically with a small number of probes. In cells, both conditions are hard to meet. The task is even more challenging in living tissues. Indeed, in animals, issues associated with variable protein expression levels or inadequate intravital probe delivery strongly complicate the specific detection of single biomolecules within the complex and highly auto-fluorescent environments of living tissues. To circumvent these limitations, we recently developed a methodology named Complementation Activated Light Microscopy (CALM), in which proteins of interest are fused to dark split-fluorescent proteins (split-FP) which are stochastically activated into bright FPs by irreversible complementation with exogenous synthetic peptides. We will describe how we use CALM to specifically target, image and track individual proteins with nanometer accuracy in living cells and in living C. elegans nematodes, independently of protein expression levels and at micromolar probe concentrations.

8228-36, Poster Session

## A SPAD array detector for spectrally and lifetime resolved microscopy

F. Koberling, B. Kraemer, R. Erdmann, PicoQuant GmbH (Germany); M. Ghioni, I. Rech, A. Gulinatti, Politecnico di Milano (Italy); G. Buller, A. McCarthy, A. J. Waddie, M. R. Taghizadeh, Heriot-Watt Univ. (United Kingdom); I. Gregor, J. Enderlein, Georg-August-Univ. Göttingen (Germany)

Time-resolved single molecule detection techniques are state-of-the-art. In order to obtain as much information as possible, parallel detection of several polarization and spectral channels is necessary. In addition, parallelization of the measurement overcomes many of the limitations due to the inherently long measurement times.

Fluorescence lifetime measurements are indispensable for many single molecule measurements. The optimal detector type, combining an excellent timing resolution together with very high quantum efficiency, is the Single Photon Avalanche Diode (SPAD). Therefore SPAD detector arrays would be an ideal detection tool for either spectral or parallelized time-resolved single molecule measurements.

We investigated a prototype of a silicon based SPAD array featuring eight detection channels. The array, designed by the Politecnico in Milano, Italy, achieves a detection efficiency of around 30% measured at 470 nm and 670 nm. The timing resolution is 170 ps and 80 ps respectively. Due to a novel electronic architecture, the crosstalk is reduced and reaches a value below 1%. The sensitive areas have a diameter of 50 µm and there is a pitch of 250 µm between each detection pixel.

A special optical layout was developed in order to illuminate the different SPAD areas after spectral splitting minimizing the loss of fluorescence light. To this aim a set of relay lenses and an array of micro-lenses were designed, which focus the light after the spectral separation onto the different sensitive areas of the SPAD array.

Preliminary results demonstrate the feasibility of the planned setup.

8228-37, Poster Session

## Camera simulation engine enables efficient system optimization for superresolution imaging

T. Takahashi, T. Maruno, J. Yamashita, Hamamatsu Photonics K.K. (Japan); S. M. Fullerton, Hamamatsu Corp. (United States)

Quantitative fluorescent imaging requires optimization of the complete optical system, from the sample to the detector. Such considerations are especially true for precision localization microscopy such as PALM and (d)STORM where the precision of the result is limited by the noise in both the optical and detection systems. Here, we present a Camera Simulation Engine (CSE) that allows comparison of imaging results from CCD, CMOS and EMCCD cameras under various sample conditions and can accurately validate the quality of precision localization algorithms and camera performance. To achieve these results, the CSE incorporates the following parameters: 1) Sample conditions including optical intensity, wavelength, optical signal shot noise, and optical background shot noise ; 2) Camera specifications including QE, pixel size, dark current, read noise, EMCCD excess noise; 3) Camera operating conditions such as exposure, binning and gain. A key feature of the CSE is that, from a single image (either real or simulated “ideal”) we generate a stack of statistically realistic images. We have used the CSE to validate experimental data showing that current CMOS technology outperforms EMCCD in most super-resolution scenarios. Our results support using the CSE to efficiently and methodically select cameras for quantitative imaging applications. Furthermore, the CSE can be used to robustly compare and evaluate new algorithms for data analysis and image reconstruction. These uses of the CSE are particularly relevant to super-resolution precision localization microscopy and provide a faster, simpler and more cost effective means of system optimization, especially camera selection.

8228-38, Poster Session

## Structured illumination confocal scanning microscope with enhanced optical resolution and acquisition speed

Y. D. Kim, M. Ahn, D. Gweon, KAIST (Korea, Republic of)

There was a previous research that proposed the structured illumination confocal scanning microscope (SICSM) so as to improve the lateral resolution of the confocal microscope. However, the image acquisition speed of the SICSM was very slow and also an alignment error due to the mechanical rotation of a grating and a slit can easily occur. As a theoretical study, in this paper we propose a new SI method, the cross SI method, which improves lateral resolution and image acquisition speed. Performances of the conventional SI and the proposed SI methods are compared by analysis of the modulation transfer function. The proposed SI method shows similar lateral resolution and can shorten the image acquisition time compared to the conventional SI method. The cross structured illumination confocal microscope (CSICM) is combined with the cross SI pattern optics and the line scanning confocal microscope. We have introduced a 2-D diffractive grating in order to create the cross SI pattern. The effects of the cross SI pattern, intensity and visibility, on the system performance are analyzed. The CSICM has double the lateral resolution of the conventional microscope, an optical sectioning ability and a fast image acquisition speed.

8228-39, Poster Session

## Accurate single-molecule localization of superresolution microscopy images using multiscale products

V. A. Ngo, Biopolis Shared Facilities, A*STAR Singapore (Singapore); Y. N. Law, Bioinformatics Institute (Singapore); H. Srivats, A*STAR Institute of Medical Biology (Singapore); H. K. Lee, Bioinformatics Institute (Singapore); S. Ahmed, A*STAR Institute of Medical Biology (Singapore)

Recently, a class of Single-molecule based localization techniques such as the Photoactivated Localization Microscopy (PALM) or the Stochastic Optical Reconstruction Microscopy (STORM) has ingeniously brought light-microscopy beyond the diffraction limit. However, as the Single-molecule images contain point source objects (which have no clear edges, alignment and usually superimposed to the background), traditional restoration techniques used for industrial vision images do not give satisfactory result on the PALM/STORM dataset. In this work, we apply the multi-scale product of sub-band images resulting from the wavelet transformation, a technique originally used for astronomical image restoration, for the noise filtering and single-molecule detection in the Superresolution images. This is an extension of the work by J.C Olivo-Marin [Pattern Recognition 35 (2002)] on spot detection in biological images. Experimental results on real and synthetic datasets with ground-truth show that our approach achieves very good detection rates as compared to other PALM/STORM analysis software such as the QuickPALM or rapidSTORM.

8228-40, Poster Session

## Two-fold enhancement of optical resolution in laser scanning microscopy

H. Dehez, Y. De Koninck, M. Piché, Univ. Laval (Canada)

Laser scanning microscopy is usually preferred to wide-field microscopy for its z-sectioning ability. However the transverse resolution of laser scanning microscopy, limited by the diffraction barrier, remains similar to that of wide-field microscopy.

For biomedical applications, high resolution is needed and a large variety of techniques have been developed to overcome the diffraction limit. Most of them are probe dependent (PALM/STORM) or require a complete modification of the microscope (STED). We present here a procedure independent of the probe, laser, or objective being used, that can easily be retrofitted in conventional laser scanning microscopes to improve the transverse resolution by a factor of two.

We proceed by subtracting two specific images: a positive image recorded with a laser beam having a maximum of intensity at its center and a negative image taken with a laser beam having null intensity at its center. By doing so the dimension of the PSF is strongly reduced, and resolution is enhanced. With an appropriate choice of the positive and negative beams, a circular PSF without side lobes is obtained. The beam switching device is composed of achromatic components to preserve versatility. Switching can be done faster than the line scanning dwell-time, allowing the user to record the two images line-by-line to avoid artefacts due to motion of the specimen.

Results on neuronal growth cones in confocal microscopy will be presented where details were revealed by immunohistochemistery labeling of tubulin and calmodulin-dependent kinase beta protein. Preliminary results in two-photon microscopy will also be presented.

8228-41, Poster Session

## Optical extinction spectroscopy of a single gold nanorod by using a fast camera

S. B. Cho, H. Song, Y. Bae, Gwangju Institute of Science and Technology (Korea, Republic of); C. Park, Gwanju Institute of Science and Technology (Korea, Republic of); D. Y. Kim, Yonsei Univ. (Korea, Republic of)

We report a digital lock-in detected spatial modulation spectroscopy (SMS) technique using a fast line camera instead of a lock-in amplifier. It is composed of a manufactured supercontinuum source (SC) part, a confocal microscopy part and a spectrometer part using a fast line camera. The sample is mounted on the piezoelectric stage and its position is modulated by means of a piezoelectric element. The transmitted light power is detected by a fast line camera in the spectrometer part and we could apply to a digital lock-in detection by using digital frequency filtering and amplification of camera lines as the modulate frequency directly. The used SC source has a wide range spectrum from 750 nm to 1550 nm (> 10dB). In order to construct a correct spectroscopic system when using a broadband light source we have constructed using reflective components as much as possible to remove a chromatic aberration. We present optical properties of absorption and scattering spectrums of single particles like gold nanorods which have the surface plasmon resonance (SPR) wavelength longer than 1 um center wavelength which is seldom present. We can obtain light-polarization dependent measurements to identify the source of the absorption due to the analysis of longitudinal and transverse SPR.

8228-42, Poster Session

## Nano-aperture design and characterization for subdiffraction-limited fluorescence imaging

W. Lee, K. Kim, D. Kim, Yonsei Univ. (Korea, Republic of)

Optical nanoantennas have recently been widely investigated to create a dramatically amplified and highly localized electromagnetic field, a. k. a. hot spot, for many applications such as surface enhanced-Raman spectroscopy, extraordinary transmission, single-molecular sensing and imaging, high-resolution imaging, optical trapping, and nanolithograpy. In these applications, an optimum nanoantennas design has been often sought for the enhancement of maximum field intensity. In fluorescence imaging, the size of a hot spot can be as critical as the field intensity, so that a nanoantenna can be used to excite subwavelength hot spots and to reconstruct fluorescence images at nanoscale resolution.

In this paper, we report results of nanoaperture designs and characterization for sub-diffraction limited total internal reflection fluorescence imaging. Properties of a hot spot such as size, intensity, and shape depends on various geometric factors of nanoapertures that are used for excitation, eg., apertures size, period, thickness, height, and the overall structure of nanoapertures.

We have analyzed how these parameters influence hot spot shape and size. Three aperture shapes have been considered based on the ease of fabrication: circular, rhombic, and square nanoholes. The results suggest that rhombic nanoapertures can be close to an optimum that produces the smallest and most symmetric hot spots among the considered. This is manifested by the efficient localization of near-fields at the vertex of rhombic nanoapertures, as a result of lightning rod effect, rather than at the sides of circular and square apertures. Effects of other geometrical parameters will also be discussed.

8228-43, Poster Session

## Diamond particles as nanoantennas for nitrogen-vacancy color centers: consequences in STED imaging of fluorescent nanodiamonds

J. Greffet, J. Hugonin, M. Besbes, Lab. Charles Fabry (France); M. Adam, P. Spinicelli, X. L. Le, N. D. Lai, F. Treussart, J. Roch, Ecole Normale Supérieure de Cachan (France)

The negatively charged nitrogen-vacancy (NV–) color center in diamond is a solid-state artificial atom with unique room-temperature properties: a perfectly stable photoluminescence and an optically detectable electron spin resonance.

When recorded from a set of nanodiamonds spincoated on a coverglass the NV luminescence decay time exhibits a broad statistical distribution and the lifetime is on average longer than the value measured in a bulk diamond [1]. This lengthening has been qualitatively attributed to modifications of the dielectric environment [1,2]. It has also been noted that the lifetime distribution is not correlated to the brightness of the emitter [1]. Finally, although a 6 nm resolution was reached in bulk diamond with Stimulated Emission Depletion (STED) imaging, the image of a single NV center in a 30 nm nanodiamond was limited by the size of the hosting particle [4].

We show that the differences between emission by a NV center in a bulk or in a nanoparticle can be understood by considering that the dielectric nanoparticle acts as a dielectric nanoantenna [4]. Furthermore, we demonstrate that the optical resolution of STED imaging is intrinsically limited to the nanodiamond size when considering particle dimension smaller than the emission wavelength.

References

[1] J. Tisler, et al. ACS Nano 3, 1959 (2009).

[2] A. Beveratos, R. Brouri, T. Gacoin, J.-P. Poizat, and P. Grangier, Phys. Rev. A 64, 061802 (2001)

[3] K. Y. Han, et al. Nano Lett. 9, 3323 (2009).

[4] J.-J. Greffet et al., “Diamond particles as nanoantennas for nitrogen-vacancy color centers”, arXiv:1107.0502

8228-44, Poster Session

## Visualization of neuron cells using surface plasmon enhanced randomly activated fluorescence microscopy

Y. Oh, K. Kim, W. Lee, N. Han, R. Lee, D. Kim, Yonsei Univ. (Korea, Republic of)

Recently, super-resolution imaging has drawn tremendous interests in optical microscopy for the detection of bio-molecular events in cellular environments. One of the approaches that have been attempted to enhance imaging resolution is the use of nanoantennas that can excite highly localized near-fields below diffraction limit. Previously, we proposed use of metallic nanoislands, which can be easily synthesized in a large area, as random nanoantennas for surface plasmon enhanced randomly activated (SUPRA) microscopy.

In this study, we report demonstration of nanoisland based nanoplasmonic SUPRA imaging for imaging live neuron cells. Nanoislands were synthesized by temperature annealing with varying thickness of silver films. For comparison, periodic nanoantenna structures based on gratings and nanoholes were also fabricated. Near-field distribution formed by random nanoislands were calculated using rigorous coupled-wave analysis to understand the effects of film thickness and island parameters, such as size and separation, and also for image reconstruction. Primary cultured hippocampal neuron cells were collected and fixed on the metal structure and cells were stained with TUJ1 marker. Experimental results generally confirm the imaging resolution on the order of 100 nm below diffraction limited resolution. Issues related to image reconstruction algorithm by pseudorandom deconvolution will also be presented.

SUPRA microscopy is expected to be useful as a convenient way of achieving far-field imaging of near-field events using facilitated construction of nanoisland substrates.

8228-45, Poster Session

## Stoichiometry quantification of DNA-dependent protein Kinase-catalytic subunit and Ku70/80 heterodimer using fluorescence correlation spectroscopy (FCS)

S. Abdisalaam, The Univ. of Texas at Arlington (United States)

Fluorescence Correlation Spectroscopy (FCS) and Fluorescence Cross-Correlation Spectroscopy (FCCS) techniques have the potential to give information about the stoichiometry and binding kinetics of DNA-protein and protein-protein interactions at the single-molecule level. DNA double-strand breaks (DSBs) are one of the most lethal DNA damage occurs in eukaryotic cells. There are two distinct pathway of repairing DSBs, homologous recombination (HR) and non-homologous end joining (NHEJ). In NHEJ repairing pathway, the DNA dependent protein kinase (DNA-PK) complex play a major role; DNA-PK complex consist of the catalytic subunit (DNA-PKcs) and DNA-binding subunit Ku70/80 heterodimer. We are interested in how these different DNA DSBs proteins play role in DNA repair together with stoichiometry information about these proteins.

8228-46, Poster Session

## Dielectric and SM measurements in polymer PMA and PVAc above glass transition temperature

S. Adhikari, M. Selmke, F. Cichos, Univ. Leipzig (Germany)

No abstract available

8228-47, Poster Session

## Monitoring protein-protein interactions in vivo: FLIM and FIDSAM as powerful time-resolved fluorescence techniques for quantitative FRET analysis

F. Schleifenbaum, Eberhard Karls Univ. Tübingen (Germany)

No abstract available

8228-48, Poster Session

## Probe size dependent rotational dynamics in polymer by single molecule spectroscopy

S. Adhikari, Univ. of Leipzig (Germany); F. Cichos, Univ. Leipzig (Germany)

We study the rotational dynamics of four different perylene dimide molecules in polymer poly (methylacrylate) (PMA) and poly (vinylacetate) (PVAc) close to glass transition temperature. Two of them are rigid molecules and others are flexible molecules. The temperature dependence of mean relaxation times for all the molecules is similar in both polymer and most importantly they follow the Debye-Stokes-Einstein (DSE) law for polymer viscosity. For PMA it is exactly same as the DSE prediction and for PVAc it is 5 times faster than DSE prediction. For flexible molecules the rotational dynamic is faster than rigid molecules and the only rigid part of the molecules takes role in the rotational dynamics. The change in distribution width of rotational times and stretching exponents cannot be explained as Cierone et.al [2] or Mackowial et.al [3] explained but we explain it by change in dynamical heterogeneity time scale.

A wealth of new information on the heterogeneous dynamics and structure is further expected from an extension of two point michrorheology to SM optical studies based on fluorescence resonance energy transfer(FRET).We have therefore synthesized bi-labeled(Alexa488 & Alexa594) polystyrene polymer and have been characterized by absorption and emission spectra.First SM FRET measurements are reported.

Reference:

(1 ) S. Adhikari, M. Selmke and F. Cichos ,Phys. Chem. Chem. Phys. 2011, 13, 1849-1856

(2) Marcus T.Cierone, F.R. Blackburn, M.D. Ediger,J. Chem. Phy. 1995, 102, 471-479.

(3) S.A.Mackowiak, L.M. Leone, L.J. Kaufman, Phys. Chem. Chem. Phys. 2011, 13, 1786 - 1799.

# Conference 8229: Optical Diagnostics and Sensing XII: Toward Point-of-Care Diagnostics

Wednesday-Thursday 25-26 January 2012

Part of Proceedings of SPIE Vol. 8229A Optical Diagnostics and Sensing XII: Toward Point-of-Care Diagnostics

8229A-26, Poster Session

## Determination of melamine of milk based on two-dimensional correlation infrared spectroscopy

R. Yang, R. Liu, K. Xu, Tianjin Univ. (China)

The adulteration of milk with harmful substances is a threat to public health and beyond question a serious crime. In order to develop a rapid, cost-effective and high-throughput analysis method for detecting of adulterants in milk, the discriminative analysis of melamine is established in milk based on the two-dimensional (2D) correlation infrared spectroscopy in this paper. Pure milk samples and adulterated milk samples with added different content of melamine were prepared. Then the absorption spectra of all samples were measured at room temperature. The characteristics of pure milk and adulterated milk were studied by one-dimensional spectra. The 2D correlation spectrum in the 400-10000cm-1 was generated from concentration-dependent spectral variation of melamine in milk. Both 2D NIR and 2D IR correlation spectra have greatly enhanced spectral resolution. The spectral feature of trace melamine in milk has become clear by the 2D correlation analysis not readily accessible by one-dimensional spectra. Therefore, accroding to the 2D correlation characteristic spectrum of melamine, we can discriminate whether melamine was included in milk. 2D NIR-IR heterospectral correlation analysis was also attempted for the same NIR and IR data. The heterospectral correlation map has provided new insight into the correlation between NIR and IR bands, confirming their band assignments. The results demonstrate that the adulterant can be discriminated correctly by 2D correlation infrared spectroscopy. This analytical method is highly rapid, effective, visual and accurate for adulterant in dairy products without pre-treatment. At the same time, this method can also be applied to other food safety detection areas.

8229A-27, Poster Session

## Sensing cocaine in saliva with attenuated total reflection infrared (ATR-IR) spectroscopy combined with a one-step extraction method

K. M. C. Hans, S. Müller, M. E. Gianella, ETH Zürich (Switzerland); M. W. Sigrist, ETH Zurich (Switzerland)

Consumption of illicit drugs like cocaine or heroin is a worldwide concern. Detection methods preferentially directly applicable in body fluids like saliva are therefore of great interest. Common techniques include liquid chromatography combined with mass spectrometry often in connection with solid-phase extraction. Other methods use immunoassays to detect, e.g., cocaine via fluorescence. Although highly sensitive, such techniques are either sophisticated and time consuming or often not sufficiently quantitative or selective. We are developing an easy-to-use optical sensor based on ATR-IR spectroscopy. To avoid the strong water absorbing in the IR region, different approaches were investigated. The simplest method consists in drying the sample on the ATR crystal without any extraction yielding a detection limit of 0.02 mg/ml for cocaine in saliva. This is a concentration encountered in real-life situations. Another approach is a one-step liquid-liquid extraction. Here, saliva samples are first mixed with an organic solvent that is immiscible with water. In this process the substance of interest is efficiently extracted from the saliva to the organic solvent. We measured ATR-IR spectra of cocaine including many of its metabolites, but also of potentially interfering compounds such as alcohol, caffeine, mouthwash, medication, diluents, etc. Survey spectra to explore the most appropriate spectral region were recorded with a common FTIR spectrometer whereas the selected spectral window around 1750 cm-1 is accessed with a quantum cascade laser.

Further steps to enhance the sensitivity include an improved configuration or an alternate concept for the layout of the interaction zone between laser beam and sample.

8229A-28, Poster Session

## The wide-field Fourier spectroscopic-imaging of the radiation heat from the object itself in the middle infrared region for the health monitoring

W. Qi, T. Takuma, A. Inui, R. Tsutsumi, T. Yuzuriha, H. Kagiyama, D. Kojima, A. Nishiyama, I. Ishimaru, Kagawa Univ. (Japan)

We are aiming at the realization of the wide-field spectroscopic-imaging-sensor that is available for the health monitoring or the plant factory. Conventionally, the body temperature is measured by the thermography as a total intensity of the middle infrared radiation. We are trying to analyze the spectroscopic characteristics of the radiation heat from the human body in detail to measure the blood glucose or the moisture-retaining properties of the human skin. The proposed imaging-type 2-dimensional Fourier spectroscopy can measure the radiation heat from the object itself with the wide field of view and the wide wavelength-band. In this proposed method, we install the phase-shifter on the optical Fourier-transform-plane of the imaging optics to give the arbitrary phase-shift to the half flux of the object beams. Thus, the interferogram can be formed on the imaging plane in each bright point by the phase-shift interference-phenomena between the object beams that are emitted from the each corresponding bright point on the objective surface. So, even if the radiation heat from the object itself is the spatially incoherent light, the interferogram can be formed in each bright point on the imaging plane. And because we correct the phase-shift value in accordance with the angle of field to secure the accuracy of the spectrum, the wide-field Fourier spectroscopic-imaging can be realized. In this report, we mention the feasibility results of the wild-field spectroscopic-imaging using the black body for the basic optical evaluation and the house plants for measuring the glucose distribution with the infrared camera(wavelength: 8μm-14μm).

8229A-29, Poster Session

## Study of specificity for non-invasive glucose measurements based on two-dimensional correlation mid-infrared spectroscopy

W. Zhang, Y. Cao, R. Liu, K. Xu, Tianjin Univ. (China)

Glucose specificity is the premise of spectroscopic measurements for blood glucose concentration, and it is also paramount for feasibility study of a spectral measurement method. Two-dimensional correlation spectroscopy technology is widely used in many fields such as inter-/intra-molecular reaction, material phase transition and information extraction because of its high resolution and the effective "sequential order" rules(Noda's rule). By using 2D correlation spectroscopy analysis, we aimed at exploring glucose specificity for noninvasive glucose measurements from mid-infrared spectra collected from human beings. The study is mainly divided into two parts. The first part is to prove the realizability of the method by 2D correlation analysis of in vitro solutions which all contain glucose. And the second part is validating feature information of glucose from mid-infrared ATR spectra of human fingers by use of the 2D correlation spectroscopy technology. The conclusion is that glucose specific spectral information is really present in noninvasive mid-infrared in vivo spectra. So the feasibility of mid-infrared spectroscopy in noninvasive measurements of blood glucose concentration is demonstrated fundamentally.

8229A-30, Poster Session

## A fluorescence polarization based assay for glucose sensing

B. M. Cummins, G. L. Coté, Texas A&M Univ. (United States)

A fluorescence polarization (FP) assay was developed to determine concentrations of glucose using the C-type lectin, concanavalin A (ConA), as the receptor and fluorescently-labeled dextran as the competing ligand. According to mathematical modeling that combined competitive binding theory, Perrin's equation, and the additivity characteristic of FP, predictive FP responses to glucose were elicited for different assay configurations and displayed herein. We chose the labeled ligand for this work to be 4 kDa FITC-dextran because of its ideal combination of intrinsic polarization, fluorescence lifetime, molecular weight, and association constant to ConA. Using experimentally determined FP values for 4 kDa FITC-dextran and FITC-ConA to serve as the FP for bound and unbound populations, the model predicted a change of 50 mP units from 0 mg/dL glucose to 500 mg/dL for an optimized assay configuration. As competitive binding theory typically relies on the assumption that the binding interactions are singular in nature, this FP assay was also used to determine the validity of those assumptions for a multivalent ConA/dextran sensing chemistry by determining its ability to follow the predicted responses from the model. Experimental FP data then was collected for the identical optimized assay configuration and showed a change of 48 mP units from 0 mg/dL glucose to 500 mg/dL which agreed well with the modeled response. This indicates that a homogenous, reproducible FP assay can be engineered to measure glucose concentrations using tetrameric ConA and 4k kDa FITC-dextran, and that such an assay appears to generally follow competitive binding assumptions.

8229A-31, Poster Session

## Raman spectroscopy of blood in vitro

A. E. Villanueva-Luna, J. Castro-Ramos, Instituto Nacional de Astrofísica, Óptica y Electrónica (Mexico); A. Flores-Gil, Univ. Autónoma del Carmen (Mexico); S. Vazquez-Montiel, C. M. Ortiz-Lima, J. A. Delgado-Atencio, Instituto Nacional de Astrofísica, Óptica y Electrónica (Mexico)

There are several types of sensors to determine glucose, cholesterol and triglycerides. The variety ranges from fiber optic sensors to spectroscopic techniques. Some of them take into consideration the blood type of people. In this work, we subtracted out samples from 10 volunteers that thoughtless have different types of blood. We extract a drop of blood and then place in a glass slice. The excitation wavelength used for this work was 785 nm, an ocean optics spectrometer of 6 cm-1 resolution and the spectral region used ranges from 300 to 1800 cm-1.

Literature related blood spectroscopic signature with contain of fluorescent background, hemoglobin and fibrin as principal components. We found vibrational lines at 1000, 1368, 1542 and 1620 cm-1 that are related with hemoglobin and its derivatives. Vibrational lines at 967, 1248 and 1342 cm-1 are correlated to pure fibrin. We made a classification of the influence of blood type in the results obtained, this was done using the principal components analysis. Finally, we found vibrational lines of cholesterol, glucose and triglycerides that are reported in literature.

8229A-32, Poster Session

## Snapshot hyperspectral imaging to measure oxygen saturation in the retina using fiber bundle and multislit spectrometer

B. Khoobehi, LSU Health Sciences Ctr. (United States); A. Khoobehi, LSU School of Medicine (United States)

We developed a snapshot fiber bundle technique. In this technology, 458 individual fibers are assembled in a two-dimensional array where each fiber represents a portion of the image. These fibers are redistributed into two fiber rows interfaced into a two-slit spectrometer. The light from each fiber is decomposed into its spectral components by the spectrometer. We detected the whole spectrum of hemoglobin with 0.5 nm spectral resolution using the single light exposure capabilities of a fundus camera. The hemoglobin signature of the retinal arteries, veins, and retina tissue can be recorded. The final result is a complete, 3-dimensional representation of the spectral and spatial information. Using the algorithm developed in our lab, we constructed oxygen saturation maps of the optic nerve head.

By adjusting the field of view on the imaging portion of the fundus camera, the fiber optic cable may encompass a larger area with decreased spatial resolution. Due to the specific spectral band necessary to analyze oxygen levels, it is possible to insert multiple slits (and increase the number of fibers) at the entrance of the spectrometer while maintaining the spectral and spatial resolution for a larger image area. To further increase the field of view without sacrificing spatial resolution, we designed a novel spectrometer. We increased the area of the fiber array by increasing the number of the fibers from 458 to 648, increasing the size of each individual fiber from 10 µm to 20 µm, and increasing the number of spectrometer slits from two to four.

8229A-33, Poster Session

## Quantitative determination of the human breast milk macro-nutrients by near-infrared Raman spectroscopy

E. C. M. Motta, L. Silveira, Jr., R. A. Zângaro, Univ. Camilo Castelo Branco (Brazil)

Raman Spectroscopy has been proposed as a rapid and nondestructive tool for quality control. This work proposes the evaluation of the macro-nutrient constitution of human breast milk based on the spectral information provided by near-infrared Raman spectroscopy. Human breast milk from a subject was collected during the first two weeks and after 4 to 6 months of breast-feeding. 10 mL of milk were collected daily and stocked in -20oC freezer in sterile plastic vessels for Raman measurements. After passive unfreezing, 1 mL of each milk sample was put in an aluminum holder and the spectra were collected in triplicate. The Raman spectra were measured using a Raman spectrometer (830 nm excitation) coupled to a fiber-optic based probe (Lambda Solutions, Inc.). Integration time was set to 20 s and laser power adjusted to 300 mW. The background fluorescence was further removed by baseline correction. Spectra of human milk were dominated by bands of lipids and carbohydrates in the spectral region of 600 to 1800 cm-1. It was developed a model based on least-squares fitting to quantify the relative amount of selected macro-nutrients: casein, lactose, linoleic acid, triolein, cholesterol, etc., in each spectrum of milk. Raman spectroscopy revealed differences in the biochemical constitution of human milk depending on the time of mother's milk production, being rich in proteins and carbohydrates in the first week of feeding and rich in lipids in the 4th to 6th months. This technique could be employed to classify the milk in human milk banking according to the child's metabolic needs.

8229A-34, Poster Session

## An noncontact pulse oximeter with two-laser diode

J. Choi, Honam Univ. (Korea, Republic of)

This paper presents a prototyped noncontact laser-based Pulse Oximetry system, and reports on test results from comparative trials with a commercially available fingerbased Pulse Oximetry system using several human subjects.

Pulse oximeter operate by comparing scattered light of red and infrared laser diode light from a patient's skin with a photosensor, which provides information on what proportion of the hemoglobin in the blood is dark red and deoxygenated versus bright red and oxygenated. The modulation of the oximeter signal with arterial diameter due to blood pressure variations in between heartbeats helps separate blood transmission characteristics from the unmodulated tissue background.

This work is significant and timely as it provides compelling evidence that SpO2 measurements from the scattered light of skin offer an ambulatory vital-signs monitoring.

8229A-35, Poster Session

## Effect on glucose monitoring of pressure exerted by fiber optic probe: skin model and simulation

C. Li, H. Zhao, Z. Shi, K. Xu, Tianjin Univ. (China)

In the research of optical diagnosis, such as noninvasive measurement of blood glucose by near-infrared diffuse-reflectance spectroscopy, the fiber-optic probe were widely used to deliver light to the tissue site of interested and collect the reflectance light. In order to minimize the motion artifacts within in the measurement, the fiber-optic probe were contact to tissue site with certain pressure. Under local pressure, the spacing between tissue components decreased due to water displacement, while the volumes of cells and elastic fibers were reduced. However, local pressure reduced tissue thickness, which in turn increase the scatter and absorber's concentration inside the tissue. This effect is considered to be dominant that lead to increase the scattering and absorption coefficient of tissue. In this paper we mainly focused on how the pressure of fiber-optic probe influenced the measurement of diffused-reflectance spectroscopy. The three-layer skin model was established. The thickness, mechanical parameters and optical properties of each layer were determined by the anatomy and in vivo measurement results of other researchers. Based on the skin model, the Finite Element Method was employed to simulation the compression of skin tissue by fiber-optic probe with different pressure. The changes of thickness of each layer after compression were determined. Based on the skin model, the change of water volume inside the tissue as well as the concentration and scattering cross section of scatters were considered. Then the optical properties of each layer after compression were calculated. The Monte Carlo simulation was utilized to establish the diffuse-reflectance spectroscopy of three-layer skin model before and after compression. The result indicated that we should control the external pressure less the 50kpa to reduce the influence on measurement accuracy.

8229A-36, Poster Session

## Novel commercial nanostructured thin films for ultra-sensitive POC diagnostics

D. Gerion, LamdaGen Corp. (United States)

We present an optical platform for rapid point-of-care diagnostics based on a nanostructured thin film that exhibits an enhanced Localized Surface Plasmon Resonance (LSPR). The optical biosensor is composed of a stable thin gold film that displays a color visible to the naked eye. The color of the film changes when a bioassay is performed on its surface and the change can be measured and quantitated with simple hardware. The color shift is dependent on the bioanalyte concentration, and this color change can be very large, i.e. surfaces can migrate from burgundy to dark-blue or even green. Further, these color changes can be precisely quantified. The precise quantification allows us to build dose-response curves and titrate unknowns. The LSPR thin films are also compatible with various media - cell lysates, sera and whole blood - while also being impervious to extreme acidic or alkaline conditions.

The LSPR technology has been quantitated against ELISA in a series of models and has been shown to be more sensitive and faster, in the order of minutes vs. hours. We will discuss the physics behind the technology, its sensitivity and limits of detection. We will illustrate the films performance in various evolving diagnostic fields, such as predictive assays for cervical cancer, cardiac biomarkers, and the detection of low level toxins.

In conclusion, we will discuss how commercially available LSPR film technology can be integrated into economical multi-panel POC handheld devices for broad adoption in diagnostics.

8229A-01, Session 1

## Fetal oxygenation measurement using wireless near-infrared spectroscopy

B. Shadgan, The Univ. of British Columbia (Canada) and Ctr. for International Collaboration on Repair Discoveries (Canada); A. J. Macnab, P. Janssen, D. Rurak, B. Molavi, The Univ. of British Columbia (Canada)

Fetal wellbeing is determined in large part by how well the placenta is able to supply oxygen and nutrients, but current technology is unable to directly measure how well a placenta functions. Near-infrared spectroscopy (NIRS) utilizes optical methods to measure tissue oxygenation

This pilot project evaluated the feasibility of NIRS for fetal monitoring through the maternal abdominal wall using a sheep model.

The miniature wireless 2 wavelength NIRS device has 3 paired light emitting diodes and a single photodiode detector. This spatial geometry allows measurement of an index of oxygen saturation (Tissue Saturation Index - TSI%). The device was placed on the abdominal skin over the placenta of a pregnant ewe whose fetus had been cannulated to allow arterial sampling for measurement of oxygen saturation in real time. Fetal breathing movements decrease arterial oxygen saturation in fetal lambs; correlation was made during these events between arterial values and TSI%.

The correlation between NIRS derived TSI% and direct arterial oxygen saturation was very high (R2= 0.86). This result suggests that NIRS in spatially resolved configuration is sensitive enough to detect changes in fetal tissue oxygenation non-invasively through the maternal abdominal wall in real time. If validated by further study this optical methodology could be applied as means of monitoring fetal wellbeing.

8229A-02, Session 1

## Non-invasive gas monitoring in newborn infants using diode laser absorption spectroscopy: a case study

P. Lundin, E. Krite Svanberg, L. Cocola, S. Andersson-Engels, J. Jahr, V. Fellman, K. Svanberg, S. Svanberg, Lund Univ. (Sweden)

Assessing lung function is of prime importance in preterm children intensive care, since lack of surfactant in very premature children leads to respiratory distress syndrome (RDS). Development of non-invasive methods for lung function monitoring is of great importance in the management of preterm babies. Following successful monitoring of gas contents in human paranasal sinuses, using diode laser spectroscopy applied to scattering media (the so called GASMAS method), a feasibility study was earlier performed on preterm baby thoracic phantoms. These were made up of animal lung tissue covered by gelatin layers with scattering particles and absorbing ink, mimicking the chest wall of a small child. Oxygen as well as water vapor could be detected in such phantoms of realistic sizes using modulated diode laser sources around 760 and 935 nm, respectively. We have now made a case study on a two week old baby weighing about 4 kg - thus, almost a factor of 10 heavier than the smallest premature children who can still be saved in specialist clinics. Light injection and detection locations were separated by about 6 cm. Clear water vapor signals could be detected from the belly, while oxygen signals, as expected, were lacking. Lungs, below a thicker tissue layer, exhibited signals only close to the noise level for both oxygen and water vapor. The study indicates that the method will function for preterm baby monitoring.

8229A-03, Session 1

## In vitro performance of a perfusion and oxygenation optical sensor using a unique liver phantom

T. J. Akl, T. J. King, R. Long, Texas A&M Univ. (United States); M. N. Ericson, Oak Ridge National Lab. (United States); M. A. Wilson, Univ. of Pittsburgh (United States) and U.S. Dept. of Veterans Affairs (United States); M. J. McShane, G. L. Coté, Texas A&M Univ. (United States)

Between the years 1999 and 2008, on average 2,052 people died per year on the waiting list for liver transplants. Monitoring perfusion and oxygenation in implanted organs in the 7 to 14 days period post transplant can enhance graft and patient survival rates and increase the availability of organs. In this work, we present in vitro results using a unique liver phantom that support the ability of our sensor to detect perfusion changes in the portal vein at low levels (50 mL/min ≈ 4.5% of normal level). Our sensor measures diffuse reflection from three wavelengths (735, 805 and 940 nm) around the hemoglobin isobestic point (805 nm) to determine perfusion and oxygenation separately. To assess the sensitivity of our sensor to flow changes in the low range, we used two peristaltic pumps to pump a dye solution mimicking the optical properties of oxygenated blood, at various rates, through a PDMS based phantom mimicking the optical properties of liver tissue. The collected pulsatile signal increased by 120% (2.2X) for every 100 mL/min flow rise for all three wavelengths in the range 50 to 500 mL/min. In addition, we used different dye mixtures to mimic oxygenation changes at constant perfusion/flow levels. The optical properties of the dye mixtures mimic oxygen saturations ranging between 0 and 100%. The sensor was shown to be sensitive to changes in oxygen saturations above 40%.

8229A-04, Session 1

## Measuring hemoglobin amount and oxygen saturation of skin with advancing age

S. Watanabe, Chiba Univ. (Japan); S. Yamamoto, Keio Univ. (Japan); M. Yamauchi, N. Tsumura, Chiba Univ. (Japan); T. Akiba, AKIBA Clinic of Traditional Medicine (Japan); K. Ogawa-Ochiai, Kanazawa Univ. Hospital (Japan)

We measured hemoglobin concentration and oxygen saturation of skin for various ages using our previously proposed method which can simulate the skin spectral reflectance fast with high accuracy. Oxygen saturation is commonly measured by pulse oxymeter to evaluate oxygen delivery for monitoring the current functions of heart and lung. On the other hand, oxygen saturation of the skin is expected to assess peripheral conditions. Our previously proposed method which was named as optical path-length matrix method (OPLM) is based on a Monte Carlo for multi-layered tissue (MCML) but can simulate skin spectral reflectance 27,000 times faster than MCML. To use this for estimating hemoglobin concentration and oxygen saturation from measured skin spectral reflectance, in this research, we implemented iterative simulation of OPLM with non-linear optimization technique. Skin reflectance spectra of 86 outpatients ranged with 50.4 ± 19.2 years old were measured by the spectrophotometer in the experiments. Four points were measured for respective subject; forearm, thenar eminence, intermediate phalanx and tip of the middle finger. As the results, oxygen saturation of the skin showed constant value among the age at each point, despite diverse hemoglobin concentration. We could confirm that oxygen saturation of the skin is constant in subjects without serious illnesses. From the clinical point of the view, there are many patients suffering from symptoms which are difficult to objectively evaluate such as symptoms of neuropathy: numbness or pain. Oxygen saturation of the skin is expected to be used to help for determining such symptoms objectively.

8229A-05, Session 1

## Determination of oxygen saturation of the optic nerve head and overlying artery and vein using a snapshot multispectral imaging system

B. Khoobehi, LSU Health Sciences Ctr. (United States) and LSU Health Sciences Ctr. (United States); H. Wafapoor, A. Eaton, LSU Health Sciences Ctr. (United States); K. A. Firn, Tulane Univ. (United States) and LSU Health Sciences Ctr. (United States); M. Peters, LSU Health Sciences Ctr. (United States); E. Rodebeck, Tulane Univ. (United States) and LSU Health Sciences Ctr. (United States); B. Templet, Tulane Univ. (United States)

We have developed a snapshot optical imaging system capable of taking multiple images simultaneously and sending them to a CCD detector. Using an innovative lens array design, the beam obtained from the fundus camera is segmented into several different images passed through several different bandpass filters. Each bandpass filter defines a unique spectral region of imaging. The images are taken simultaneously into a large silicone chip with a dynamic range of 16 bits (highly sensitive) and are integrated with a single optical connection to a digital fundus camera.

Our algorithm maps blood oxygen saturation of the retina using several wavelengths. These wavelengths are capable of approximating the whole hemoglobin spectrum and have been found from a previously developed hyperspectral algorithm. They include four isosbestic points (522, 548, 569, and 586 nm) and three oxygen-sensitive points (542, 560, and 586 nm) where the difference between fully oxygenated and deoxygenated blood is at a maximum. Using MatLab code, color maps of oxygen saturation are produced.

The average value taken from all vein areas was 60.53%, assuming that the artery oxygen saturation value is 98%. Oxygen saturation of the tissue was 75.78%. Oxygen saturations of the temporal/inferior/nasal veins ranged from 61.86% to 63.37%; the superior vein was significantly lower (54.19%). Tissue oxygen saturations in different quadrants of the eye ranged from 74.17% to 76.74%.

Our algorithm has been developed for measuring oxygen saturation of the retina clinically. This was done for one subject only; further work can extend the measurements to different pigments.

8229A-06, Session 2

## MEMS-enabled hyperspectral imaging system for fast CTC screening

Y. Wang, The Univ of Texas at Austin (United States); S. F. Bish, Y. Huang, G. Bhave, J. W. Tunnell, X. Zhang, The Univ. of Texas at Austin (United States)

We demonstrate a MEMS based hyperspectral fluorescence imaging microsystem for circulating tumor cell (CTC) imaging, where 16 narrow-band images of captured CTC slides can be acquired simultaneously across the area under examination. This imaging system uses both a 405nm diode laser and a 488-514nm argon laser source. In addition to the advantages of both functional imaging and spectroscopy, the fast scanning over large field-of-view (FOV) is provided by a CMOS compatible 2-axis microelectromechanical system (MEMS) scanning mirror in the probe. The fluorescence from the quantum dot sample is simultaneously descanned by the MEMS mirror, reflected by the hot mirror onto the collection arm, coupled into a collection fiber out of the probe, and dispersed by a prism onto the surface of a 16 channel array PMT. A Labview based software acquires the multi-wavelength signal of the fluorescence from the 16 channel PMT simultaneously, and renders the hyperspectral image in a rate of 4 seconds per frame. Field-of-view up to 200um x 200um with 3μm lateral resolution are acquired. The imaging system tells the position and quantity of the tumor cells inside the blood sample by locating the different emission wavelength fluorophores. This fast screening system enables the on-site diagnosis for tumor cancer based on the imaging of CTC cells using hyperspectral imaging mode.

8229A-07, Session 2

## Biophotonic tool for sensing the dynamics of H2O2 extracellular release in stressed cells

G. Suarez, C. Santschi, S. Dutta Gupta, Ecole Polytechnique Fédérale de Lausanne (Switzerland); L. Juillerat-Jeanneret, Ctr. Hospitalier Univ. Vaudois (Switzerland); O. J. F. Martin, Ecole Polytechnique Fédérale de Lausanne (Switzerland)

Hydrogen peroxide (H2O2) is known to play a multifaceted role in cell physiology mechanisms involving oxidative stress and intracellular signal transduction. Therefore, the development of analytical tools providing information on the dynamics of H2O2 generation remains of utmost importance to achieve further insight in the complex physiological processes of living cells and their response to environmental stress. In the frame of the present work we developed a novel optic biosensor that provides continuous real-time quantification of the dynamics of the hydrogen peroxide release from cells under oxidative stress conditions. The biosensor is based on the ultra-sensitive dark field optical detection of cytochrome c (cyt c) that exhibits a narrow absorption peak in its reduced state (Fe(II)) at 550 nm. In the presence of H2O2 the ferrous heme group Fe(II) is oxidised into Fe(III) providing the spectroscopic information exploited in this approach. Extremely low limit-of-detection for H2O2 down to the subnanomolar range is achieved by combining scattering substrates (eg. polystyrene beads) able to shelter cyt c and an inverted microscope in dark field configuration. The developed biosensor was able to perform real-time detection of H2O2 extracellular release from human cells such as circulating neutrophil precursors (HL60) and adherent endothelial (HCEC) cells exposed to oxidative-stress inducing agents. This biosensing tool is currently being implemented to the real-time detection of several biomarkers such as dopamine, glutathione and superoxide in human cells. Multianalyte and dynamic information might bring new insights on the impact of potential toxicants such as nanoparticles on cells.

8229A-08, Session 2

## An in vivo optical imaging system for measuring lipid uptake, vessel contraction, and lymph flow in small animal lymphatic vessels

T. Kassis, M. J. Weiler, J. B. Dixon, Georgia Institute of Technology (United States) and Parker H. Petit Institute for Bioengineering and Bioscience (United States)

All postprandial dietary lipids are transported to the venous circulation through the lymphatic system, yet the underlying mechanisms lymphatics utilize to regulate this process remain unclear. Such understanding is important in the diagnosis and treatment of lipid and lymphatic related diseases such as obesity, hypercholesterolemia, and lymphedema.

Therefore, we sought to develop an in vivo imaging system that can quantify various parameters involved in lymphatic lipid transport. A custom-built optical set-up provides us with the capability of dual channel imaging of both high speed bright-field video and fluorescent images simultaneously. This is achieved through optically dividing the microscope light path into two bands, one for fluorescence (495-550nm) and the other for bright-field (> 550nm). Utilizing high-speed and back-illuminated CCD cameras and post-acquisition image processing algorithms, we use the system to study correlations between vessel contraction, lymph flow and lipid concentration in mesenteric lymphatic vessels in vivo after excising the mesentery and bathing it in a physiological solution to recapitulate the animal's internal environment and delivering a controlled infusion of lipid to the duodenum. Local flow velocity is measured through lymphocyte velocity tracking, vessel contraction through caliper measurements following edge detection on the two vessel walls and lipid uptake through tracking the intensity of a fluorescent long chain fatty acid analogue. All experiments are carried out on rats with the flexibility of using alternate small animals.

This system will prove to be an invaluable tool for both scientists studying lymphatic function in health and disease and those investigating strategies for targeting the lymphatic system with orally delivered drugs.

8229A-09, Session 2

## Sensitivity analysis of near-infrared functional lymphatic imaging

M. J. Weiler, T. Kassis, J. B. Dixon, Georgia Institute of Technology (United States)

Background - Near-infrared (NIR) imaging of lymphatic drainage of injected indocyanine green (ICG) has emerged as a new technology for clinical imaging of lymphatic architecture and quantification of vessel function, offering better spatial and temporal resolution than competing imaging modalities. While NIR lymphatic imaging has begun to be reported in the literature, the technology is still in its infancy and its imaging capabilities have yet to be quantitatively characterized. The objective of this study, therefore, was to characterize the parameters of NIR lymphatic imaging to quantify its capabilities as a diagnostic tool for evaluating lymphatic disease.

Methods - An NIR imaging system was developed using a laser diode for excitation, ICG as a fluorescent agent, and a CCD camera to detect emission. A tissue phantom with mock lymphatic vessels of known depths and diameters was used as an alternative to in vivo lymphatic vessels due to the greater degree of control with the phantom.

Results - When dissolved in an albumin physiological salt solution (APSS) to mimic interstitial fluid, ICG experiences shifts in the excitation/emission wavelengths such that it is maximally excited at 805nm and produces peak fluorescence at 840nm. Premixing ICG with albumin induces greater fluorescence intensity, with the ideal concentration being: 900μM (60g/L) albumin and 193.5μM (150μg/mL) ICG. ICG fluorescence can be detected as deep as 6mm, but spatial resolution deteriorates severely below 3mm, thus skewing vessel geometry measurements. ICG packet travel, a common measure of lymphatic transport, can be detected as deep as 5mm.

8229A-10, Session 3

## A miniaturized particle detection system

J. J. Dou, L. Chen, Univ. of Toronto (Canada); R. Nayyar, Cytoquest Corp. (Canada); J. S. Aitchison, Univ. of Toronto (Canada)

The enumeration of microscopic particles like white cells, bacteria and viruses in samples such as human body fluids are of primary importance in determining the state of human health. Examples of clinical importance include counting of CD4 T-cells in HIV positive subjects, platelets in patients undergoing chemotherapy and leukocytes in circulating blood samples. In this paper, we present a novel optical platform for particle detection and analysis that forms the basis of a handheld cytometer, as well as results obtained using this approach. The platform leverages recent advances in capillary microfluidics, combined with integrated fiber optics and a unique image acquisition and analysis algorithm. Using this approach, enumeration measurements were conducted on 8-um fluorescently labelled polymer microspheres and Immono-Trol (stabilized human whole blood sample), in which results obtained using our technique also agreed well with the flow cytometer benchmark.

Comparing with other reported cell/particle detection system, this approach further eliminates any additional moving components, such as mirrors, for laser scanning, or motion stages, for CCD sensor positioning, in order to measure a given amount of sample volume. In certain disease diagnosis and monitoring, a minimum amount of sample volume must be examined in order to obtain accurate analysis results. Due to physical limitations of optical imaging systems, a large area of samples must be imaged to meet this requirement. When the area to be imaged exceeds the size of the optical detector, moving optical sources or detectors to cover the entire sample field becomes inevitable.

8229A-11, Session 3

## A study of a self diagnostic platform for the detection of A2 biomarker for Leishmania donovani

P. J. R. Roche, M. C. K. Cheung, V. P. Chodavarapu, B. Ward, M. Ndao, A. G. Kirk, McGill Univ. (Canada)

Visceral leishmaniasis (L.donovani) is a protozoan infection that attacks mononuclear phagocytes and causes the liver and spleen damage that can cause death. The investigation presented is a proof of concept development applying a plasmonic diagnostic platform with simple microfluidic sample delivery and optical readout. An immune-assay method is applied to the quantification of A2 protein, a highly immunogenic biomarker for the pathogen. Quantification of A2 was performed in the ng/ml range, analysis by ELISA suggested that a limit of 0.1ng/ml of A2 is approximate to 1 pathogen per ml and the sensing system shows the potential to deliver a similar level of quantification. Significant reduction in assay complexity as further enzyme linked enhancement is not required when applying a plasmonic methodology to an immunoassay. The basic instrumentation required for a portable device and potential dual optical readout where both plasmonic and photoluminescent response are assessed is investigated including consideration of the application of the device to testing where non-literate communication of results is considered and issues of performance are addressed.

8229A-12, Session 3

## Complete urinary tract infection (UTI) diagnosis and antibiogram using surface enhanced Raman spectroscopy (SERS)

K. Hadjigeorgiou, E. Kastanos, A. Kyriakides, C. Pitris, Univ. of Cyprus (Cyprus)

There are three stages to a complete urinary urinary tract infection (UTI) diagnosis: (1) identification of a urine sample as positive or negative for an infection, (2) identification of the responsible bacterium, and (3) an antibiogram to determine the antibiotic to which the bacterium is most sensitive. Using standard conventional testing, UTI diagnosis requires bacterial cultures and approximately 48 hrs in order to provide results. This long delay in diagnosis causes a rise in ineffective treatments, chronic infections, health care costs, and antibiotic resistance. In this work, Surface Enhanced Raman Spectroscopy (SERS) is used as a point-of-care diagnostic to provide a complete UTI diagnosis within 2-4hrs. SERS spectra of serial dilutions of various gram negative bacteria, isolated from urine cultures, were classified as positive (10^5-10^8 cells/ml) or negative (10^3-10^4 cells/ml) for UTI after mixing the samples with silver nanoparticles and correlating the spectral intensity with concentration. For antibiotic sensitivity testing, SERS spectra of five species of gram negative bacteria were collected four hours after exposure to the antibiotics ciprofloxacin, amoxicillin, amoxicillin/clavulanate, norfloxacin, penicillin, cefuroxime, cefixime, and cefaclor. Spectral analysis revealed clear separation between bacterial samples exposed to antibiotics to which they were sensitive and samples exposed to antibiotics to which they were resistant. With the enhancement provided by SERS, this technique can be applied directly to urine samples, bypassing the need for urine cultures. This technology can become the basis for the development of a new, rapid method for UTI diagnosis and antibiogram.

8229A-13, Session 3

## Silica suspended waveguide splitter-based biosensor

M. C. Harrison, R. M. Hawk, A. M. Armani, The Univ. of Southern California (United States)

Label-free optical sensors enable real-time monitoring of water supplies, environmental contaminants as well as the detection of fundamental biological processes. One of the first sensors developed was based on evanescent detection from an optical fiber. This approach was quickly improved by integrating the waveguide onto a silicon wafer.

Recently, a novel integrated waveguide 50/50 splitter was developed. It is fabricated using standard lithographic methods, a pair of etching steps and a laser reflow step. However, unlike other integrated waveguide splitters, the waveguide is elevated off of the silicon substrate, improving its interaction with biomolecules in solution and in a flow field. Additionally, because it is fabricated from silica, it has very low optical loss, resulting in a high signal-to-noise ratio, making it ideal for biodetection.

To perform detection, the surface of the splitter was chemically modified using an amine terminated silane coupling agent to covalently attach biotin. A 1nM streptavidin solution was added to the coupling region to analyze the binding activity of streptavidin to biotin. Detection of the binding kinetics was performed by monitoring the coupling ratio, which is proportional to the amount of bound streptavidin.

By confining the protein solutions to the coupling region, we maximize the collection efficiency of the device, enabling highly efficient detection of streptavidin with only 0.001mL of solution. Therefore, the waveguide coupler sensor is representative of the next generation of ultra-sensitive optical biosensors, and, when combined with microfluidic capabilities, it will be an ideal candidate for a more fully-realized lab-on-a-chip device.

8229A-14, Session 3

## Low-level detection of cryptosporidium parvum in water using optical microfluidic biosensors

S. Angus, H. Kwon, J. Yoon, Univ. of Arizona (United States)

Cryptosporidium parvum is a difficult to detect protozoan that causes diarrhea in the healthy and can cause death in immunocompromised individuals. While it is easy to understand cryptosporidium transmission routes, it is currently difficult to identify low concentrations of cryptosporidium, especially when following EPA method 1623, which can easily require tens of liters of water to get a positive signal. Add to this high water requirement the time that goes into concentrating sample out of that much water and current detection limits are unacceptable. In this study I use a covalently bonded microbead-antibody suspension to cause agglutination of heat inactivated cryptosporidium oocysts. Both a normal concentration of 7.7 µg/mL and a concentration of 5 times normal at 38.5 µg/mL were tested using a filter with approximately 13 µm pore sizes using a microfluidic waveguide chip and a UV light source. The 5x concentration is more effective due to the large size of the cryptosporidium oocysts at roughly 5 µm in diameter. Field samples were also collected from a number of locations in Tucson, Arizona including: a farm Sump, a swimming pool, a Jacuzzi, an outdoor fish pond, and an outdoor fountain. A Coomassie (Bradford) protein assay was run on each sample to assess abhorrent protein concentrations from the sample.

8229A-15, Session 4

## A cellphone-based laser speckle imager

I. Remer, A. Bilenca, Ben-Gurion Univ. of the Negev (Israel)

Laser speckle imaging has proven to be a useful tool for the noninvasive assessment of tissue blood perfusion at high temporal and spatial resolution. In particular, laser speckle imaging of sub-skin blood has gained much interest in recent years due to its ability to detect anomalous alterations of peripheral blood flow, thereby providing an adequate indicator for various medical disorders such as diabetes. Typically, the instrumentation used for laser speckle imaging is based on high-speed CMOS/CCD cameras with large pixel size and therefore requires high-end cameras.

In this talk, we introduce a laser speckle imaging instrument based on standard camera-cellphone technology. This cellphone-based imager enables us to assess blood perfusion in vivo in healthy skin prior to and following occlusion across an area of about 1 - 5 square-cm with 480 × 640 - 720 × 1280 pixels-per-frame at a rate of 10 - 17 frames-per-second. In addition, we present further validations of the ability of the cellphone-based laser speckle imaging instrument to measure accurately microcirculatory perfusion using in-vitro models of healthy blood flow and malaria-infected blood flow.

Finally, potential application of the cell-phone based imager toward a point of care diagnostics of malaria will be discussed.

8229A-16, Session 4

## Spectral reflectance of the ocular fundus as a diagnostic marker for cerebral malaria

X. Liu, D. A. Rice, Tulane Univ. (United States); B. Khoobehi, LSU Health Sciences Ctr. (United States)

The difficulty of identifying malaria parasitization continues to impede efforts to control and treat this disease. Recent ophthalmological studies of malaria patients report retinopathy highly specific to severe malaria. To further explore the ocular manifestations of malaria, we used hyperspectral imaging to study retinal changes caused by Plasmodium berghei ANKA parasitization in a mouse model.

Spectral reflectances of the ocular fundus were extracted from hyperspectral images. The blood oxygen sensitive spectral region was normalized for variances in illumination, and used to calculate relative values that correspond to oxygenated hemoglobin levels. The relative values are markedly lower in parasitized mice, indicating that hemoglobin digestion by P. berghei may be detectable via spectral reflectance. Furthermore, the ocular reflectance spectrum of parasitized mice is abnormally elevated between 660nm and 750nm, suggesting fluorescence in this region. While the source of this fluorescence is not yet clear, its presence correlates strongly with P. Berghei parasitization, and may indicate the presence of hemozoin deposits in the retinal vasculature.

The pathology of severe malaria still poses many questions for clinicians and scientists, and our understanding of cerebral malaria has thus far been confined to clinical observation and post-mortem examination. As the retina is the only part of the central nervous system that can be imaged non-invasively, our technique may provide the basis for an automated tool to diagnose and evaluate severe malaria via retinal changes.

8229A-17, Session 4

## Lensfree pixel superresolution microscopy using thin wetting films on a chip

O. Mudanyali, W. Bishara, A. Ozcan, Univ. of California, Los Angeles (United States)

Microscopic screening of disease markers, parasites and other contaminants with fine morphological features is a challenging task to perform in resource-poor settings and field conditions. Toward this goal, we investigated the implementation of thin wetting films on lensfree pixel super-resolution holographic microscopy to improve its imaging performance. Formation of thin wetting films creates a micro-lens effect over individual micro-objects on a chip, providing up-to 4-fold improved signal-to-noise-ratio (SNR) and contrast in our lensfree reconstructed images.

In order to form these wetting films, the specimen of interest (e.g., bacteria) is initially dissolved within Tris-PEG (5%) buffer. A droplet of this suspension (<5μL) is carefully placed onto a glass cover-slip and randomly wiggled by gentle mechanical vibrations for ~60 seconds, forming the ultra-thin wetting film over the specimen. Finally, this wetting film sample is loaded onto a digital sensor-array (e.g., a CMOS chip) for lensfree pixel-super resolved holographic imaging.

We validated the performance improvement of lensfree holographic on-chip microscopy due to this micro-lens effect by imaging various micro-objects such as Giardia trophozoites, sperms, E. coli and red blood cells. Experimental results yielded up-to 4-fold SNR improvement, showing better recovery of submicron spatial-features such as flagella of parasites and sperm tails. This technique creates a long-term and repeatable micro-lens effect and allows lensfree imaging of deeply submicron morphological features and particles over a wide imaging-field-of-view of ~24 mm2. Therefore, it can be useful to carry out highly-sensitive and high-resolution microscopic measurements even in resource-limited environments and field settings.

8229A-18, Session 4

## Low-cost add-on microscope for cellphones for use in point-of-care diagnostics

H. Umesh Babu, S. Bogatscher, N. Heussner, L. Shinohara, W. Stork, Karlsruher Institut für Technologie (Germany)

A low cost add-on microscope for a cellphone is presented along with brightfield and trans-fluorescence illumination design. The add-on device is designed for any cellphone with a camera (resolution 2 mega pixels). In a true sense of miniaturization, this device resembles an infinity corrected objective which works in conjunction with a cellphone camera that captures, and bespoke software that analyzes the image.

The microscope objective combines custom and off-the-shelf optics. High refractive index material based lens, used as pick-up lens and achromat for color correction, constitutes the off-the-shelf component. The custom optics are entirely designed using plastics whereas conventional high performance objectives use variety of glasses. Aberration corrections are handled by custom optics using both aspheric and diffractive surfaces. The overall size of the microscope objective is around 30-35mm.

Currently only fixed focus objectives have been realized but we also present a low cost XY stage using Permanent Magnet Stepper motors having an accuracy of <50μm, with 18x18mm translation. The idea is to image the slide either as a high resolution video or as multiple shots and stitch them.

This device is not intended to replace the standard desktop microscope in labs but it serves as a handy diagnostic tool in the field especially for telemedicine. This device was primarily designed for fluorescence based detection of Mycobacterium tuberculosis but it can be extended to detection of other bacterial/fungal pathogens or other parasites in the range of 1μm-300μm.

8229A-19, Session 4

## Simple and affordable CD4 counting enabled by on-chip sample preparation and large-area image cytometry

M. Beck, N. van der Velde, S. Brockhuis, L. W. M. M. Terstappen, Univ. Twente (Netherlands)

The concentration of CD4+ T-cells in blood (CD4 count) is used to diagnose the disease progression of HIV. Rural areas in resource-limited countries often lack the required infrastructure for the standard method flow cytometry. We have developed a test which can potentially fulfill the need for an affordable test that provides immediate results and can be carried out with a portable instrument by non-professionals.

Whole blood from a finger prick is collected by capillary flow in a microfluidic chamber containing dried antibodies (anti-human CD4-PerCP and CD3-APC) inside a gelatin layer. After incubation for 10-30 min, the CD4+ count is obtained by fluorescence imaging and automatic image analysis. The fluorescence from APC and PerCP is imaged through the same emission filter, but can be distinguished easily by the fluorescence emission for red and blue excitation light, respectively. Thus, we can avoid any moving parts (e.g. filter changer) in our compact, battery-operated instrument. The image area of > 40 mm2 and the chamber height of 25 μm, correspond to more than 1 μl of whole blood, which is sufficient for CD4 counting.

A platform-independent ImageJ script automatically identifies the cells and distinguishes and counts different phenotypes based on the fluorescence intensities for the two excitation sources.

CD4 counts for undiluted whole blood (leukocyte-depleted to simulate low CD4 counts) from healthy donors, compare well over a wide range range of cell concentrations with reference values obtained with diluted, lysed blood and reference beads on a state-of-the-art flow cytometer.

8229A-20, Session 5

## A critical query into the basis of spectroscopic measurements in non-invasive blood glucose monitoring

N. C. Dingari, I. Barman, G. P. Singh, J. W. Kang, R. R. Dasari, M. S. Feld, Massachusetts Institute of Technology (United States)

Several non-invasive blood glucose detection studies have been carried out by quite a few research groups using near-infrared (NIR) absorption and Raman spectroscopy, but prospective prediction is still a challenging problem. The relationship between glucose concentration and spectral information is an important issue, particularly because of the intrinsic glucose signal is very small compared to that of the other analytes in blood-tissue matrix. Furthermore, other factors like tissue turbidity, time-dependent physiological processes will affect the relation between glucose concentration and spectral data. In this talk, we investigate chance correlations in Raman spectroscopy based calibration model for non-invasive glucose measurements for physical tissue models, animal models and human subjects. We assigned different spurious glucose concentration profiles to the Raman spectra obtained from physical tissue models, in which the actual glucose concentration is constant. Spurious and true concentration profiles are assigned to the datasets acquired from animal models during a glucose clamping study human subjects during oral glucose tolerance test. We show that the spurious concentration profile based calibration models are unable to provide prospective predictions, as compared to those based on actual concentration profiles, especially for physical tissue models. We also demonstrate that chance correlations infused by the calibration models are considerably less in Raman as compared to NIR absorption spectroscopy.

8229A-21, Session 5

## Spectroscopic tomography of biological tissues with the near-infrared radiation for the non-invasive measurement of the biogenic-substances

D. Kojima, T. Takuma, A. Inui, W. Qi, R. Tsutsumi, T. Yuzuriha, H. Kagiyama, A. Nishiyama, I. Ishimaru, Kagawa Univ. (Japan)

We are aiming at the realization of the non-invasive measurement of the biogenic substance, such as the blood glucose concentration, by the proposed imaging-type 2-dimensional Fourier spectroscopy. We had successfully obtained the spectroscopic tomography of the mouse's ear with the near-infrared radiation (wavelength: 900nm-1700nm). The proposed Fourier-spectroscopic imaging can limit the measuring depth into the focal plane. So, we can set the focal plane as the measurement plane near the skin surface that is not affected by the optical diffusion of the biological tissues. To analyze the absorbance index in the specific wavelength at the vessel area, we can expect to acquire the blood glucose concentration in high accuracy. In the proposed method, we install the variable phase-shifter into the optical Fourier transform plane of the imaging optics to give the arbitrary phase-shift to the half flux of objective beams. The proposed method can realize the phase-shift interferometer between the objective lights with the common path optics. Because of the imaging optics, only the rays from the focal plane can contribute the formation of the interferogram. Thus, we can obtain the 2-dimensional Fourier spectroscopic characteristics only on the focal plane. In this report, we mention the feasibility demonstration of the spectroscopic tomography of the mouse's ear obtained by the InGaAs camera. We had successfully obtained the distribution of the spectroscopic-absorption near the skin surface. We are trying to convert the absorption ratio into the glucose concentration by the quantitative spectroscopic image-processing.

8229A-22, Session 5

## A fiber loop ringdown glucose sensor

C. Wang, M. Kaya, Mississippi State Univ. (United States); C. Wang, Mississippi School for Mathematics and Science (United States)

Fiber loop ringdown (FLRD) evolved from cavity ringdown spectroscopy has become an emerging time-domain sensing technique for development of fiber optic sensors and sensor networks. The FLRD sensing scheme combined with various sensing mechanisms has been implemented to create different types of FLRD sensors for physical, chemical, and biological sensing. In this work, we report a new FLRD glucose sensor. Glucose Oxidase (GOD) is immobilized on the surface of a 16 cm long etched single mode fiber (the sensor head). When GOD is exposed to a glucose solution, GOD reacts with glucose and generates gluconic acid, resulting in a change in the refractive index around the surface of sensor head. When a laser beam passes through the sensor head and an evanescent field is excited in the interface between the etched fiber surface and the immobilized layer. Different optical losses are detected via the surface-index-based sensing and quantified by measuring different ringdown times. The sensor is tested in glucose sample solutions in the concentration range of 10 - 0.05% with a detection sensitivity of 0.05%. The sensor is also tested in standard artificial urine samples in different glucose concentrations and a detection sensitivity of 0.05%, which corresponds to the glucose renal threshold, is demonstrated. Fabrication of the sensor head, reproducibility, selectivity, response behavior, and potential applications of the sensor are discussed.

8229A-23, Session 5

## Polarimetric glucose sensing in an artificial eye anterior chamber

B. H. Malik, C. W. Pirnstill, G. L. Coté, Texas A&M Univ. (United States)

The application of optical polarimetry to glucose sensing in the anterior chamber of the eye has emerged as a potential technique to noninvasively ascertain blood glucose levels. One of the major limiting factors preventing the realization of such a device is the time varying corneal birefringence due to motion artifact in the eye. The varying birefringence confounds the optical activity of glucose, and thus, needs to be taken into account in order to successfully predict the glucose concentration in the aqueous humor of the eye. Our group has developed a multi-spectral optical polarimetric approach which can minimize the effect of corneal birefringence coupled with motion artifact by treating it as common mode noise to multiple wavelengths. Here, we present the application of a real-time closed-loop dual wavelength polarimeter to ex vivo glucose sensing in excised New Zealand White rabbits' corneas mounted on an artificial anterior chamber. Our PID control system can reach stability in less than 100 ms which is fast enough to overcome motion artifact due to heart beat and respiration. The system can predict the glucose concentration with a standard error of less than 25 mg/dL in the physiologic glucose range of 0 - 600 mg/dL. Our results indicate that dual-wavelength polarimetry has the potential to noninvasively probe glucose through the anterior chamber of the eye.

8229A-24, Session 5

## Fluorescence lifetime-based glucose sensor using NADH

A. von Ketteler, Kirchhoff Institute for Physics (Germany) and Roche Diagnostics GmbH (Germany); D. Herten, Heidelberg Univ. (Germany); C. Horn, Roche Diagnostics GmbH (Germany); W. Petrich, Roche Diagnostics GmbH (Germany) and Kirchhoff Institute for Physics (Germany)

In comparison to fluorescence intensity-based glucose sensing, fluorescence lifetime-based glucose sensing is independent of the power of the light source, light scattering, transmission properties of optical components and often also on photochemical properties such as photobleaching. We demonstrate a new technique for fluorescence lifetime-based glucose sensing based on the fluorescence lifetime properties of dihydronicotinamide adenine dinucleotide (NADH), which is created from NAD in the presence of glucose and glucose dehydrogenase. The fluorescence lifetime of NADH is enumerated by calculating a mean fluorescence lifetime, which arises from the two short lifetimes t_1=0.28ns and t_2=0.60ns (representing the free NADH) and the longer lifetime of t_3=2.9ns (for the protein-bound NADH). If the concentration of NADH is substantially larger than the concentration of the enzyme, the majority of the NADH molecules are free. Therefore the weighted average of the fluorescence lifetimes approximates the mean fluorescence lifetime of free NADH, i.e. t_av,free=0.42ns. If the concentration of NADH is low in comparison to the enzyme concentration the majority of the NADH molecules are protein-bound. Hence the mean fluorescence lifetime converges to the protein-bound fluorescence lifetime t_3. Since the production of NADH in this scheme directly depends on the concentration of glucose, no additional fluorescent dyes or mediators are necessary. It will be shown in how far the glucose concentration can thus be determined directly by measuring the mean fluorescence lifetime of NADH.

8229A-25, Session 5

## Loading of red blood cells with an analyte-sensitive dye for development of a long-term monitoring technique

S. Ritter, K. E. Meissner, Texas A&M Univ. (United States)

Measurement of blood analytes, such as pH and glucose, provide crucial information about a patient's health. Some such analytes, such as glucose in the case of diabetes, require long-term or near-continuous monitoring for proper disease management. However, current monitoring techniques are far from ideal: multiple-per-day finger stick tests are inconvenient and painful for the patient; implantable sensors have short functional life spans (i.e., 3-7 days). Red blood cells (RBCs) serve as an attractive alternative for carriers of analyte sensors. Once reintroduced to the blood stream, these carriers may continue to live for the remainder of their life span (120 days for humans). They are also biodegradable and biocompatible, thereby eliminating the immune system response common for many implanted devices. The proposed carrier system takes advantage of the ability of the RBCs to swell in response to a decrease in the osmolarity of the extracellular solution. Just before the membranes lyse, they develop small pores on the scale of tens of nanometers. While at low temperature, analyte-sensitive dyes in the extracellular solution diffuse into the perforated RBCs and become entrapped upon restoration of temperature and osmolarity. Because RBC membranes contain various analyte transporters, intracellular analyte levels rapidly equilibrate to that of the extracellular solution. Fluorescent dyes have been loaded inside of RBCs using various hypotonic techniques. The fluorescent signal from the entrapped dye then reports on changes in the analyte level of the extracellular solution. Alterations in preparation parameters affect physical characteristics of the dye-loaded RBCs, such as shape and fluorophore content.

# Conference 8229: Design and Performance Validation of Phantoms Used in Conjunction with Optical Measurement of Tissue IV

Saturday-Sunday 21-22 January 2012

Part of Proceedings of SPIE Vol. 8229B Design and Performance Validation of Phantoms Used in Conjunction with Optical Measurement of Tissue IV

8229B-37, Session 1

## Confocal reflectance microscopy to specify the scattering co-efficient and anisotropy of tissue phantoms

S. L. Jacques, Oregon Health & Science Univ. (United States)

Reflectance-mode confocal scanning laser microscopy (rCSLM) enables measurement of the superficial layers of a phantom in a non-perturbing manner. The focus of an objective lens is translated down into the phantom. The reflected light scattered from the focus that re-enters the objective lens is detected via a pinhole, yielding a signal R(z), where z is the depth position of the focus relative to the surface (z=0). The signal R(z) falls exponentially as z increases, since it becomes more difficult for light to reach the focus and successfully return to the lens: R(z) = rho exp(-mu z) , where rho is the local reflectivity [dimensionless] and mu [cm^-1] is an attenuation coefficient. The parameters rho and mu specify the scattering coefficient (mus) and the anisotropy of scattering (g). The rCSLM is calibrated such that reflectance from a mirror yields R(z) = 1.0. The relationships between the measurements (rho and mu) and the optical properties (mus and g) are rho = mus dz b(g), and mu = mus a(g) 2 G, where mus is the scattering coefficient, dz is the axial extent of the focus, b is the fraction of scattered light that backscatters into the solid angle of collection of the objective lens, a(g) is a factor between 0-1 that mitigates the effect of attenuation by mus, 2 accounts for the in/out path of photons, and G is a geometry factor accounting for the extra photon pathlength due to the numerical aperture of the objective lens. Examples of use are given.

8229B-38, Session 1

## Low abundances of synthetics lipids in phantoms

A. E. Villanueva-Luna, Instituto Nacional de Astrofísica, Óptica y Electrónica (Mexico); A. Santiago-Alvarado, B. I. G. Licona-Moran, Univ. Technológica de la Mixteca (Mexico); J. Castro-Ramos, Instituto Nacional de Astrofísica, Óptica y Electrónica (Mexico); A. Flores-Gil, Univ. Autónoma del Carmen (Mexico); S. Vazquez-Montiel, J. G. Aguilar-Soto, J. A. Delgado-Atencio, Instituto Nacional de Astrofísica, Óptica y Electrónica (Mexico)

Phantoms simulate optical characteristics of tissues commonly are used to mimic light distributions in living tissue. Tissue phantoms are designed and utilized for three purposes: a) to simulate light distributions with geometry of physical tissue, b) for the calibration of optical devices, and c) for recording a reference measurement with an optical device. Phantoms compositions of silicone, polyester, polyurethane, and epoxy resin have been described, but these have the problem of long time preservation. In this work is presented the fabrication and characterization of phantoms with low concentrations of synthetic lipid using Raman spectroscopy. We fabricate four phantoms that were made of Polydimethylsiloxane (PDMS), as well as we fabricate the same amount of phantoms with gelatin, these phantoms have synthetic lipid content of cholesterol and triglycerides. We use synthetic melanin in order to obtain rather similar results to those obtained when we study the skin. Our phantoms size is 1 cm x 1 cm and 5 mm of thickness, and they were mapped using the point-to-point mapping technique. Moreover, we use glucose and vitamin K with the aim of ensuring that is possible detect main spectral lines of synthetic cholesterol and triglycerides with low abundances. Finally, we compared advantages and performance of made PDMS and gelatin phantoms.

8229B-39, Session 1

## Possible diffusive reference standards for tissue phantoms based on fat emulsions

P. Di Ninni, Univ. degli Studi di Firenze (Italy); Y. Bérubé-Lauzière, Univ. de Sherbrooke (Canada); F. Martelli, Univ. degli Studi di Firenze (Italy)

The use of Intralipid 20% was recently suggested as a diffusive reference standard for tissue simulating phantoms. In this work, we extend previously obtained results to other fat emulsions, specifically Intralipid 10%, Intralipid 30%, Lipovenos 10%, Lipovenos 20%, Lipofundin 10%, and Lipofundin 20%. Of particular importance for practical applications, our measurements carried out at a wavelength of 751 nm show the following features. First, batch-to-batch variations for these products are less than 2 % similarly to Intralipid 20%. Second, measurements of the optical properties show that the reduced scattering coefficient of Intralipid 10% and Intralipid 30% can be scaled from that of Intralipid 20% with the same being possible for Lipovenous and Lipofundin. Further, concerning this second feature, it is of high interest to emphasize that our findings show that for these products, it is not the scattering coefficient itself that scales from one concentration to another, but rather its combination with the anisotropy factor leading to the reduced scattering coefficient. Finally, Lipovenos and Lipofundin show to have reduced scattering properties very close to those of Intralipid. Therefore, Intralipid 10, 20, 30%, Lipovenos 10, 20%, and Lipofundin 10% and 20% can be used interchangeably for tissue phantoms by adjusting proportionately the dilution ratio. The low variations between the optical properties of these products is most likely due to the highly stringent quality control and tight specifications used in the production process of pharmaceutical products such as fat emulsions for parenteral nutrition.

8229B-40, Session 1

## Characterization of an optical solid phantom for human skin fabricated by spin coating

Y. Bae, J. Lee, Y. Bae, E. Youn, B. Jung, Yonsei Univ. (Korea, Republic of)

To date, various types of optical phantoms have been developed in order for specific purposes such as calibration and performance test of optical devices and also mimicry of human skin for in vitro experiments. Among the number of types of optical phantoms, solid phantom has several advantages over other types of optical phantoms, gel and liquid types, in that it is semi-permanent, convenient for experimental purposes, and has improved storability. Despite the advantages of solid phantom, previous studies have revealed some limitations with solid phantom which made it less effective. One of the limitations is that it is difficult to make a single thin solid layer mimicking the epidermis (normally less than 100 μm in thickness). Also, it requires further cumbersome procedures to fabricate a multi-layered solid phantom by stacking the single thin solid layers. In order to address the problem, we suggested a spin coating method for making multi-layered phantom which has similar optical properties of both epidermis and dermis layers of human skin, and the thicknesses of each layer were determined by adjusting parameters for spin coating. The spin coating method made it possible to design thin-layered solid phantom that includes the essential parts of human skin with high degree of polarization (DOP). Moreover, a quantitative analysis of the parameters to control thicknesses of optical phantom layers has been conducted. In further studies, optimization of such parameters for fabrication of desired skin layers needs to be performed, which would be beneficial for both research and clinical purposes.

8229B-41, Session 1

## Fabrication and Characterization of a Multilayered Optical Phantom Using Buried Scattering Microspheres in Polymers

R. C. Chang, P. Johnson, C. Stafford, J. Hwang, National Institute of Standards and Technology (United States)

A multilayered optical tissue phantom fabrication methodology is reported as a known independently validated test target with general applicability for axial resolution and contrast in scattering measurements by depth-resolving optical coherent tomography (OCT) and confocal microscopy. We implement a combinatorial bottom-up approach to prepare alternating monolayers of light-scattering microspheres with intervening non-scattering polymer layers. Modifications of key parameters in the layer-by-layer polyelectrolyte multilayer deposition approach is applied to optimize particle transfer during elastomer-glass interfacial delamination while preserving the relative axial positioning as a polymer embedded monolayer. Judicious selection of the embedded scattering microsphere size and the thickness of the intervening polymer layers allows for the control of the inter-layer space of these phantoms. An interferometric microscope capable of measuring the axial dimension with XYZ nm resolution is used for independent verification of the spatial frequency of the periodically stacked layers. Ongoing efforts include the use of these calibrated phantoms to evaluate the axial resolution of a variety of 3D optical imaging platforms including OCT with sub-micron axial resolution.

8229B-42, Session 1

## Phantoms for performance assessment of optical co-herence tomography systems

M. R. N. Avanaki, A. G. Podoleanu, M. C. Price, S. A. Corr, Univ. of Kent (United Kingdom); R. M. Khoshki, Razi Univ. (Iran, Islamic Republic of); S. A. Hojjatoleslami, Univ. of Kent (United Kingdom)

In this paper, we have demonstrated the necessity for using different materials in phantom construction for different applications. We describe the procedures for making: (a) epoxy-resin dispersed homogeneous phantom composed of gold microspheres that can be used to find the point spread function of the system and longitudinal/transverse resolutions of an OCT system (b) epoxy-resin homogeneous phantoms composed of polystyrene microspheres that can be used to evaluate the optical properties extraction algorithm. Additionally, we discuss the relative merits of each of these types of phantom.

8229B-43, Session 1

## Absolute calibration of a steady-state trans-illumination breast spectroscopy device

E. J. Walter, Univ. of Toronto (Canada) and Univ. Health Network (Canada); L. D. Lilge, Univ. Health Network (Canada) and Univ. of Toronto (Canada)

A trans-illumination breast spectroscopy device is under investigation in our lab as a breast cancer risk assessment and pre-screening tool. The device measures steady-state transmission of red and near-infrared light and the spectrally-dependent attenuation is used to assess breast state. The device is capable of compensating for variations in signals over a range spanning ~2.5OD by varying the integration time and light source aperture. However since the signal ranges over >6.5OD due to variations in the breast tissue thickness and spectral variations in light source power and detector sensitivity and the minimum tissue attenuation is greater than OD1 in all cases, it is necessary to use an attenuator when calibrating the device. When relative measurements are sufficient, an Ultra high density polyurethane scattering phantom has utility as a calibration reference. However, to obtain device-independent, absolute attenuation spectra enabling studies employing different devices, it is necessary to have an absolute measurement of the light spectrum entering the tissue or the absolute phantom attenuation spectrum for each device. A tower with a pinhole was evaluated as a possible calibration system for the light source. The pinhole size and source-detector positioning were chosen to obtain 7 OD attenuation while avoiding speckle pattern generation smaller than the diameter of the detector fiber bundle elements. However, because the light source showed spectral variations across the beam profile, the pinhole, capturing only the center of the beam, did not capture the full spectrum coupled into scattering tissue. Alternatively, the spectral shape of the full beam is captured using an integrating sphere between the light source and detector fibers. The shape of the absolute attenuation spectrum of the phantom can be calculated from this full light source spectrum and the magnitude using power measurements with laser sources at several wavelengths spanning the spectral range.

8229B-44, Session 2

## Design of calibration slide for quantitative microscopy imaging in absorbance

C. E. MacAulay, The BC Cancer Agency Research Ctr. (Canada); M. Guillaud, British Columbia Cancer Agency (Canada)

With the explosive growth of whole slide imaging and commiserate growth in manufactures and types of scanning systems the need for a standard microscopy phantom/ calibration slide which can be used to calibrate, normalize and validate the imaging characteristics of these systems becomes critical. While the majority of these whole slide scanning systems are used for qualitative image assessment, more and more they are being used for semi quantitative and quantitative measures sometimes with clinical decision making intent. This makes it imperative to be able to establish that such systems are functioning within some specified set of performance metrics and that these conditions are continuously met over time or across multiple systems (system QA). This can be accomplished if slides with a multitude of objects with known morphological characteristics (size, shape, perimeter length, etc) and known optical photometric characteristics (optical density for specific NA imaging conditions) are available (such as the PRESS slide). These objects must be dispersed across the slide to enable the calibration across the entire field of the microscopy imaging system regardless of the scanning methodology. We will discuss use of such calibration slides for quantitative microscopy, the limitations of existing such slides and the design of enhanced versions of such phantoms and how they may be incorporated into QA processes and the statistical design of such processes.

8229B-46, Session 2

## Validating the LASSO algorithm for unmixing spectral signatures with application to multicolor phantoms

D. Samarov, M. Clarke, J. Y. Lee, D. Allen, M. Litorja, J. Hwang, National Institute of Standards and Technology (United States)

As hyperspectral imaging (HSI) sees increased implementation into the biological and medical fields it becomes increasingly important that the algorithms used to analyze these measurements be validated. While certainly important under any circumstances as this technology begins to see a transition from benchtop to bedside ensuring that the measurements being given to medical professionals are accurate and reproducible is critical. Recently work has been done creating a collection of datasets which could act as a testbed for algorithms to be validated against. Using a microarray spot printer a set of three dyes; acid red 1, brilliant blue R and erioglaucine are mixed together at different concentrations, proportions and locations on a microarray chip. With the concentration and mixture proportions known at each location, using HSI an algorithm should in principle be able to determine the concentrations and proportions of each dye at each location on the chip.

In this paper we present a novel algorithm for processing and analyzing HSI data based on the lasso algorithm. The lasso is a statistical method for simultaneously performing model estimation and variable selection. In the context of estimating abundances in an HSI scene these so called "sparse" representations provided by the lasso are appropriate as not every pixel will be expected to contain every endmember. The algorithm we present takes the general framework of the lasso algorithm a step further and incorporates the rich spatial information which is available in HSI to further improve the estimates of abundance.

8229B-47, Session 2

## Hyperspectral imaging of ischemic wounds

R. X. Xu, J. Melvin, J. X. Huang, H. Elgharably, S. Gnyawali, K. Huang, V. Bergdall, The Ohio State Univ. (United States); D. Allen, J. Hwang, M. Litorja, E. Shirley, National Institute of Standards and Technology (United States); C. Sen, The Ohio State Univ. (United States)

Chronic and acute wounds are among the most common tissue anomalies in clinical medicine. Accurate assessment and appropriate documentation of wound margin, oxygenation and vascular function will guide appropriate treatment and make significant clinical differences. Optical imaging has the potential to achieve high spatial resolution and high functional sensitivity in wound assessment. However, clinical acceptance of many optical imaging devices is hampered by lack of traceable standards for calibration and validation, poor reproducibility, low accuracy, and difficulty for biological interpretation. We developed an in vivo model of ischemic flap for non-contact assessment of wound tissue functional parameters and spectral characteristics. The model was created by elevating the bipedicle skin flaps of a domestic pig from the underlying vascular bed and inhibiting graft bed reperfusion by a silastic sheet. Hyperspectral imaging was carried out 2 days after the ischemic flap model was generated and compared with transcutaneous PO2 and perfusion measurements at different positions of the wound. Hyperspectral images have also been captured continuously during a post-occlusive reactive hyperemia (PORH) procedure. Tissue spectral characteristics obtained by hyperspectral imaging correlated well with cutaneous tissue oxygen tension, blood perfusion, and microscopic changes of tissue morphology. Our experiments not only demonstrated the technical feasibility for quantitative assessment of chronic wound but also provide a digital phantom platform for standardization and calibration of medical optical imaging devices in the future. This project is sponsored by National Institute of Standards and Technology (60NANB10D184) and US Army Medical Research Acquisition Act (W81XWH-11-2-0142).

8229B-48, Session 2

## Performance validation of EMCCD and ICCD based near-infrared fluorescence imaging systems on a fluorescence solid phantom

B. Zhu, E. M. Sevick-Muraca, The Univ. of Texas Health Science Ctr. at Houston (United States)

Near infrared (NIR) fluorescence imaging has been successfully applied for non-invasive assessment of both lymphatic architecture and function as well as potential disease markers of lymphatic dysfunction in clinical studies with intradermal injection of indocyanine green (ICG). For new "first-in-humans" NIR fluorescence imaging agents that need to be employed at far lower quantities, the NIR fluorescence imaging devices with high measurement sensitivity are most favorable. However, the measurement sensitivity of NIR fluorescence imaging device is limited by various parameters, including quantum efficiency of CCD chip, noise sources in the CCD camera and the leakage of excitation light through optical filters. In this contribution, we present a quantum dot-based fluorescence solid phantom and its use for characterization of excitation light leakage and measurement sensitivity in both the intensified CCD (ICCD) and Electron Multiplying CCD (EMCCD) based NIR fluorescence imaging devices. The stability of the constructed quantum dot-based fluorescence solid phantom was first demonstrated and used to demonstrate higher measurement sensitivity compared of the ICCD as opposed to the EMCCD based NIR fluorescence imaging device when integration time were maintained less than 1.0 s. The phantom was used to assess the calculated transmission ratio, R, to minimize noise owing to excitation light leakage and show optimized filtering capabilities. The constructed quantum dot based solid phantom and the methodology for measuring parameters of transmission ratio and SNR can be used as a standard and quantifiable metric for installation and operational qualification of all NIR fluorescence imaging devices.

8229B-50, Session 2

## Effects of physiological parameters in diffuse optical brain imaging

A. Hasnain, N. Chen, National Univ. of Singapore (Singapore)

Diffuse optical imaging (DOI) is an imaging technique which is sensitive to the changes in the blood haemoglobin level. As the DOI system is dependent on the changes in the haemoglobin concentration, therefore, any external factors, which can induce changes in the blood (e.g., flow, pressure, temperature etc), could result as an error in the system's output value. It is, therefore, important to study the behaviour of such changes in the imaging results.

The physiological parameters like heart-beat (frequency range: 0.6Hz to 1.4Hz) and respiration (frequency range: 0.125Hz to 0.3Hz) can give rise to systematic increase in the transient arterial blood volume and the modulation of venous blood volume respectively. These signals show significant spatial and temporal correlation.

We have developed a fast time-domain diffuse optical imaging system designed to image brain functions. To simulate the effects of heart-beat and respiration, we developed a liquid tissue phantom and a liquid blood phantom that runs into transparent narrow tubes. The tubes are attached to a motorized pump which can control the flow of blood-phantom liquid as desired. The phantom is imaged using multiple source-detector pairs and principal component analysis (PCA) method is used to determine the principal spatial-temporal covariance of the base line optical signal from the phantom.

8229B-45, Session 3

## Maximizing OCT image quality at depth using a 3D-structured phantom to optimize imaging parameters

A. Curatolo, B. F. Kennedy, D. D. Sampson, The Univ. of Western Australia (Australia)

We recently introduced a novel phantom with three-dimensional (3D) microstructure, comprising of two silicone castings, for use in optical coherence tomography (OCT). It is fabricated using a versatile lithographic method capable of producing a wide range of well-defined geometries of optical contrast introduced using known concentrations of titanium dioxide particles.

The well characterized 3D-features of the phantom, in terms of geometry and scattering properties, provide an unprecedented opportunity to study in detail image quality and its degradation in OCT.

In this paper, we explored the effect of overlaying scattering structures and system parameters on OCT image quality. We did this for a range of scatterer sizes and concentrations in the overlying layer, at two wavelengths (830nm and 1325nm), and over a range of sample illumination powers/detection times.

We observed that to attain similar penetration depths at 830nm and 1325nm we had to increase the sample illumination/detection time at 830nm. At the same time, the presence of multiple scattering became a problem at higher sample illuminations and scatterer concentrations and reduced the image quality. Similarly wavefront distortion and diffraction, taking place with increasing scatterer sizes at depths, had a deleterious effect on the image fidelity to the true probed phantom structure.

By quantifying the image quality degradation we were able to select the system parameters that maximized the image quality for a given combination of scattering tissue phantoms and 3D-structured phantom.

8229B-51, Session 3

## New developments in eye models with retina tissue phantoms for ophthalmic optical coherence tomography

T. S. Rowe, Rowe Technical Design (United States); R. J. Zawadzki, UC Davis Medical Ctr. (United States)

We show our latest work in developing eye models with solid-state retinal tissue phantoms ideal for demonstrating and comparing ophthalmic Optical Coherence Tomography (OCT) instruments. Eye models with retina tissue phantoms can serve a variety of purposes, including demonstrating OCT functionality and performance in both the clinic and exhibit hall, validation of retina layers thickness measurements from different commercial OCT instruments and as an aide for the R&D engineer and field service technician in the development and repair of instruments, respectively. The ideal eye model for OCT, the optical cross-sectional imaging modality, would have a volumetric morphology and scattering and absorption properties similar to that of normal human retina. These include multi-layered structure of equivalent thickness to nominal human retina layers, a foveal pit that can be used to orient the image, and a RPE/OS and choroid like layers to demonstrate the depth penetration of the OCT system. A solid state tissue phantom relieves the user of constant cleaning and maintenance associated with the more common water bath model eyes. Novel processes* have been developed to create retinal layers model that closely mimic the refractive index difference ($\Delta n$) and scattering coefficients of the real layers of the retina, as imaged by the OCT. Figure below compares OCT cross sections of human retina and our retina model.

8229B-52, Session 3

## Three-dimensional calibration targets for optical coherence tomography

M. Gabriele Sandrian, B. Považay, A. Alex, Medizinische Univ. Wien (Austria); P. Tomlins, Queen Mary, Univ. of London (United Kingdom); P. D. Woolliams, National Physical Lab. (United Kingdom); K. Sugden, Aston Univ. (United Kingdom); W. Drexler, Medizinische Univ. Wien (Austria)

The recent expansion of clinical applications for optical coherence tomography (OCT) is driving the development of approaches for consistent image acquisition. OCT parameters such as field of view, depth range, depth roll-off, distortion, linearity, axial and transverse resolution, resolution decay, and sensitivity must be considered in order to optimize system performance. Consequently, there is a specific need for cost-effective, easy-to-use imaging targets for calibration and standardization of OCT devices. We present calibration targets consisting of three-dimensional structures etched into BK7 glass (25mm$^3$) using commercial laser engraving techniques (point size 60µm lateral, 100µm axial). Our basic design incorporates geometric shapes and patterns of specified dimensions, while a second target is constructed using a Gallstrand reduced eye model with a plano-convex lens affixed to the cube surface to mimic the focusing power of the eye. A future design will merge these two concepts. In this work, we demonstrate that these three-dimensional scattering targets can be used to readily provide field of view, depth range, depth roll-off and distortion characteristics using a dual wavelength spectral-domain OCT system ($\lambda$=800nm, $\Delta\lambda$=180nm, and $\lambda$=1325nm, $\Delta\lambda$=100nm). We plan to merge this design with an existing phantom consisting of randomly dispersed scattering nanoparticles to measure the position-dependent point spread function and to use higher-precision femtosecond laser etching (point size of ~2µm) to evaluate resolution, depth range and sensitivity. We ultimately seek to develop a robust, low-cost, easy-to-use target that provides feedback on all OCT parameters and allows for standardization of system performance across a broad range of devices.

8229B-11, Session JS1

## Calibration and validation of chemical imaging spectrometry for clinical use

M. Litorja, National Institute of Standards and Technology (United States)

Multispectral and hyperspectral imaging of readily accessible health biomarkers such as hemoglobin oxygenation and bilirubin are currently being used in the clinic in a variety of devices. The different spectral deconvolution algorithms used to extract quantitative information about the concentration and distribution of these compounds in vivo cannot be evaluated properly without the use of laboratory-bench validation methods. This work describes standards currently used for laboratory medical devices such as blood oximeters and blood analyzers and how these can be extended towards in vivo imagers where sampling does not have the benefit of prior chemical purification methods. The differences in the optical configuration used in blood chemistry analyzers vs that by in vivo chemical imagers will be discussed and uncertainties that arise simply from this difference. In this work we describe the correlation of oxygen saturation values from spectral data with independent concurrent dissolved oxygen measurement. This also describes work on validation of spectra-based in vivo bilirubin assessment.

8229B-12, Session JS1

## Standard test methods for established medical imaging modalities and their implications for optical coherence tomography

J. Pfefer, A. Agrawal, A. Beylin, U.S. Food and Drug Administration (United States)

Standardized approaches for assessing device performance have a wide range of benefits such as improved ability to reliably and objectively compare device performance and provide quality assurance during research studies or clinical use. The adoption of field-wide consensus techniques can facilitate innovation and reduce the time and cost required for development, validation and regulatory approval. International standards documents detailing benchtop image quality assessment techniques are well established for imaging modalities such as MRI, CT and ultrasound, whereas few exist for optical diagnostic techniques. We have reviewed numerous standards for established medical imaging techniques and analyzed the general characteristics employed (e.g., resolution), as well as the specific, tissue-phantom-based test methods and figures of merit used to evaluate image quality. We have identified common themes from these documents that can be incorporated in development of tests for assessment of image quality in optical coherence tomography systems. This work also has relevance to a wide range of imaging techniques under development in biomedical optics which would benefit from standardized performance assessment methods.

8229B-53, Session JS1

## Challenges in manufacturing optical tissue phantoms: an industrial perspective

J. Bouchard, I. Noiseux, O. Mermut, INO (Canada)

Optical tissue phantoms can serve many needs encountered in the translation path between fundamental research and clinical acceptance. Each of these needs call for a different set of requirements on the phantom design. Earlier stage research will require the phantom to reproduce adequately the measurement challenges of the intended application. Phantoms used during the final verification and validation phase of a medical device seeking FDA clearance will focus more on stability, repeatability and traceability. Developing and producing phantoms meeting those quality requirement is a challenging task. Unlike MRI or CT, Optical technologies will not reach clinical practice as versatile multipurpose imaging platforms but as a collection of application specific instruments. This variety in the instrumentation and the way they will interact with the human body translates in very diverse requirements for phantoms. This presentation will illustrate the challenges imposed by this diversity of requirements with real life examples from a commercial phantom production. Solutions to overcome the diversity challenge through standardization will be proposed.

8229B-54, Session JS1

## Report on a recent workshop: Standards for Phantoms for the Performance Evaluation and Validation of Optical Medical Imaging Devices

J. Hwang, National Institute of Standards and Technology (United States); R. J. Nordstrom, National Cancer Institute (United States)

Phantoms for optical medical imaging provide a critical tool for independent assessment of biophotonic imaging systems for benchmarking performance and ensuring data consistency across multiple instruments, and their use as tools for the evaluation and validation of optical imaging devices has been demonstrated. For further use of phantoms for biomedical optical devices' regulatory clearance and quality assurance, their physical properties need to be accurately known and fabricated to the same quality according to the rigorous material and measurement standards. In a recent international workshop in November 2011, experts from government agencies (NIH, FDA, NIST, NPL, NRC etc.) and several universities and industries presented perspectives to address important issues on the material and measurement standards of phantoms such as phantom material composition, performance standards, and phantom-based test methods in the several key optical measurement platforms. This talk summarizes the key outcome of this workshop.

8229B-55, Poster Session

## Optical properties in simulated human skin at a wavelength of 633 nm

B. Morales, J. A. Delgado-Atencio, S. Vázquez y Montiel, Instituto Nacional de Astrofísica, Óptica y Electrónica (Mexico)

We report the construction and characterization at a wavelength of 633 nm of a polyurethane multilayered phantom with optical properties similar to a stratified model of human skin. During the construction of this phantom, integrating sphere technique was used to measure transmittance and reflectance, and using the inversion method GA-MCML, we ensure that the optical properties of each layer corresponds to those in the design, measuring an exact replica of each one. Using optical coherence tomography technique we characterized the optical phantom in the top layers. Also, a modified MCML code that includes the effects of lateral loss light and the spatial distribution of intensity at the entrance of the sample was used to compare the experimental transmittance and reflectance measurements of the whole phantom with the simulated ones obtained using the retrieved optical parameters in each layer.

8229B-56, Poster Session

## Influence of bubbles on the recovery of optical properties

B. Morales, J. A. Delgado-Atencio, S. Vázquez y Montiel, Instituto Nacional de Astrofísica, Óptica y Electrónica (Mexico)

In some vital organs of the human body, the air bubbles are indicative of the presence of disease. Pulmonary emphysema is characterized by permanent enlargement of airspaces distal to the respiratory bronchioles, with destruction of the alveolar wall. Therefore, it is important to know the effects introduced by the bubbles in an apparently homogeneous tissue. In order to study how change the optical properties of the tissue with bubbles, two phantoms were made of polyurethane with identical optical properties, a homogeneously cured and another with air bubbles. The distribution of bubbles into the phantom was observed with a microscope and optical properties were measured using integrating sphere technique.

# Conference 8230: Biomedical Applications of Light Scattering VI

Saturday-Monday 21-23 January 2012

Part of Proceedings of SPIE Vol. 8230 Biomedical Applications of Light Scattering VI

8230-01, Session 1

## Measuring intracellular motion using dynamic light scattering with optical coherence tomography in a mouse tumor model

G. Farhat, Univ. of Toronto (Canada); A. Mariampillai, V. X. D. Yang, Ryerson Univ. (Canada); G. J. Czarnota, Sunnybrook Health Sciences Ctr. (Canada); M. C. Kolios, Ryerson Univ. (Canada)

Speckle intensity in optical coherence tomography (OCT) images is dependent on the physical and optical properties of underlying scatterers. The motion of subcellular components within tissue introduces a dynamic variation in speckle intensity allowing the use of intracellular motion as an endogenous contrast mechanism. Previously, we used dynamic light scattering (DLS) adapted to OCT to measure changes in the rate of intracellular motion in cell aggregates undergoing apoptosis. We have since implemented this technique for the first time in an in vivo mouse model. Gliosarcoma cells (9L) were injected into a dorsal skinfold window chamber attached to female nude mice. Once tumors grew to a diameter of approximately 1 to 2 mm OCT imaging was conducted by acquiring 1600 consecutive frames of data from a single plane through the centre of the tumor, each consisting of 200 A-scans at a frame-rate of 70Hz. A map of speckle decorrelation times (DT) for each tumor cross section was generated by calculating, for each pixel, an intensity autocorrelation curve and measuring a DT based on a decay of the autocorrelation curve to 1/e of its maximum. Regions of the DT map corresponding to blood flow (vasculature) were removed by thresholding. The resulting DT maps indicated a significant difference between the tumor region and the surrounding normal tissue (137 ± 25 ms and 77.3 ± 12 ms, respectively). The ranges of DT measured were within those previously measured in tumor cell aggregates in vitro. Our preliminary results suggest in vivo feasibility of this technique.

8230-02, Session 1

## Biomechanical assessment of tissue using laser speckle rheology

Z. Hajjarian Kashany, S. K. Nadkarni, Harvard Medical School (United States)

In nearly all pathological conditions, alteration of tissue mechanical properties is a strong indicator of disease initiation and progression. Traditionally, mechanical properties are measured by loading a sample between the parallel plates of a rheometer and applying an oscillatory force to measure the frequency dependent viscoelastic modulus, $G^*(\omega)$. Here we describe a non-contact optical approach, termed Laser Speckle Rheology (LSR) that is capable of measuring the mechanical properties of tissue from laser speckle fluctuations.

In LSR, light from a Helium-Neon (632 nm) source is focused on the surface of a sample, and time-varying laser speckle patterns are captured using a high speed CMOS camera. Due to the Brownian motion of scattering particles within the sample, the speckle pattern is temporally modulated and the extent of this modulation is closely related to the viscoelastic properties of the sample. By processing the temporal statistics of speckle intensity fluctuations, and applying the Stokes-Einstein equation, linear frequency dependent viscoelastic modulus $G^*(\omega)$ is derived. The LSR approach is validated by measuring changes in $G^*(\omega)$ of test Polydimethylsiloxane (PDMS) substrates while curing over a 24 hour duration, and tissue samples obtained from swine aorta, myocardium muscle and fat. LSR measurements of sample $G^*(\omega)$ demonstrate a highly significant, strong correlation with conventional mechanical testing results for the PDMS ($R=0.91$, $p< 0.001$) and the swine tissue samples ($R=0.99$, $p < 0.0001$).

These results establish the validity of the new LSR approaches for the accurate assessment of the tissue mechanical properties and opens new avenues for the development of diagnostic tools to evaluate tissue biomechanics in situ.

8230-03, Session 1

## Eliminating the effect of bulk scattering when measuring skin surface roughness using speckle contrast imaging: a skin phantom study

L. Tchvialeva, D. I. McLean, H. Lui, The Univ. of British Columbia (Canada); T. K. Lee, The BC Cancer Agency Research Ctr. (Canada)

Light undergoes surface and bulk scattering when propagating through biological tissues. In some applications such as determining optical properties of biosamples or observing internal structures, bulk scattering provides useful signals while surface scattering is considered as noise. On the contrary, the roles of bulk and surface scattering are reserved when skin surface roughness is quantified. Based on speckle contrast imaging, we have developed a technique to measure skin roughness. Speckle contrast, being a measure of light coherence, decreases as coherence decays when low coherent light is reflected from a rough surface. However, bulk scattering also decays coherence and becomes a source of noise. To suppress bulk scattering, one can employ various techniques such as spectral, spatial and polarization filtering. However, these techniques cannot remove bulk scattering completely.

In this article we study the contribution of bulk signal in polychromatic speckle patterns. Solid silicone phantoms with known roughness and optical parameters are used to generate speckles. Comparison of the surface roughness determined by speckle contrast and the actual phantom roughness reveals an overestimation of roughness values. This systematic error is caused by the calibration curve which was calculated theoretically for non-transparent surfaces. We find that modification of the calibration curves according to the phantom experiments improves the accuracy and sensitivity of surface roughness. The new calibration curves reveal a weak dependence from phantom scattering coefficients in the range comparable to human skin.

8230-04, Session 1

## Optical histology of microvasculature in thick tissue sections

A. J. Moy, B. Choi, Beckman Laser Institute and Medical Clinic (United States)

The microvasculature is the network of blood vessels involved in delivering nutrients and gases for tissue survival. Visualization of the microvasculature is an important aspect of studying tissue disease state. Current methods, such as immunohistology, facilitate visualization of the microvasculature at limited spatial scales and tissue depths, resulting in information limited to superficial layers of the tissue. To use these methods to visualize the entire tissue microvasculature is time consuming, inefficient, and impractical. We have developed a method called "optical histology" that utilizes optical clearing of the tissue and optical imaging to rapidly produce high resolution, depth sectioned 3D images of the microvasculature.

Tissue microvasculature is stained in vivo via cardiac perfusion using DiI, a lipophilic carbocyanine dye. Tissues are then excised and sliced into ~1 mm slices. Tissue slices are then incubated in FocusClear (CelExplorer Labs, Hsinchu, Taiwan), a DMSO-based optical clearing agent, for 180 minutes and then visualized using a laser scanning confocal microscope. Sequential image z-stacks of the tissue are acquired and then reconstructed to produce a 3D image stack of the entire tissue slice. This data is used to calculate a maximum intensity projection image of the entire slice, functional vascular density in the tissue, and generate 3D maps of the tissue microvasculature.

We have successfully obtained high resolution, depth sectioned images of ~1 mm thick tissue slices using combined optical clearing and optical imaging techniques. Imaging of serial sections of tissue may facilitate visualization of the entire tissue microvasculature with potential depth sectioning capability.

8230-05, Session 1

## Tissue dynamics spectroscopy to detect cellular mitosis inside tissue

R. An, K. Jeong, J. J. Turek, D. D. Nolte, Purdue Univ. (United States)

Tissue Dynamics Spectroscopy (TDS) on depth-gated dynamic speckle from tumor spheroids captures the changes in the fluctuating frequency content of dynamic light scattering (DLS) as a function of time for tissue-based screening [1]. We have extended that work, by using time- and space-resolved spectral responses as functional finger-prints, to perform label-free mitosis event detection in tumor spheroids. Coherence-gated DLS gives us the ability to extract motility information from a specified depth of an optically thick target like a tumor spheroid. Frequency-versus-time spectrograms of speckle fluctuations provide a way to create functional spectral response fingerprints to identify complex cellular behavior like mitosis. For a proliferating tumor spheroid, mitosis is a statistically low probability event, and the characteristic signals can be easily obscurred by high backgrounds. To isolate the mitosis signal, instead of looking at an averaged spectrogram, we generate spatially-resolved spectrograms for voxels which contains limited numbers of cells. Mitosis is most dramatic during telophase and cytokinesis, when the cell shape, membrane and organelles have enhanced motions. These show specific mitosis finger-prints in the voxel spectrograms. We apply environmental perturbations such as serum starvation and different anti-mitotic cytoskeletal drugs to control the cell cycle. These results demonstrate the potential of TDS for cell proliferation studies and for malignancy diagnosis.

[1] David D. Nolte, Ran An, John Turek, Kwan Jeong, Tissue Dynamics Spectroscopy for Three-Dimensional Tissue-Based Drug Screening, Journal of the Association for Laboratory Automation June 2011, Vol. 16, No. 3

8230-06, Session 1

## Development of coherent Spatial Frequency Domain Imaging (c-SFDI) for simultaneous determination of optical and dynamical properties of tissue

T. B. Rice, S. D. Konecky, A. Mazhar, A. J. Lin, A. J. Durkin, B. Choi, B. J. Tromberg, Beckman Laser Institute and Medical Clinic (United States)

Laser Speckle Imaging (LSI) is a fast, noninvasive method to obtain relative flow changes in light scattering systems. LSI is not quantitative because it contains information from a mixture of scatterers in different concentrations and dynamic environments, as well as distortions from absorption changes that are characteristic of physiological systems. In order to address these limitations, we have developed an approach to project structured sinusoidal patterns of coherent light onto tissue and measure the remitted reflectance and speckle contrast. This allows us to perform coherent Spatial Frequency Domain Imaging (c-SFDI) to determine the tissue absorption coefficient, scattering coefficient, and rate of particle motion. We also combine c-SFDI with Multi-Exposure Speckle Imaging (MESI), which was developed to decouple speckle contrast images arising from dynamically and statically scattered photons. Performing c-SFDI at multiple exposures allowed us to determine optical properties and dynamics using light scattered primarily from moving particles. c-SFDI is validated through controlled phantoms containing static and dynamic scattering objects in different geometries. In addition, we test our method in-vivo using two wavelength spectroscopy to fit for the concentration and flow rate of oxy and deoxy-hemoglobin in a mouse brain during forepaw stimulation.

8230-07, Session 2

## Lasing modes in disordered media for single-nanoparticle quantitation: a new approach for biosensing

S. H. Choi, Y. L. Kim, Purdue Univ. (United States)

We demonstrate that random lasing in disordered nanostructures could potentially serve as an alternative yet superior biosensing mechanism to assess minute perturbations at single-nanoparticle levels. To numerically investigate random lasing modes induced by nanoscale alterations in disordered structures, we obtain eigenvalues of the system (i.e. resonant frequencies and the quality Q factors) using a finite element method, which can directly access individual modes of the passive system consisting of a large number of nanoparticles ($< \lambda$). Our visualization of random lasing modes shows dramatic amplification of subtle nanoscale perturbations to readily detectable states of resonant modes. This is possible because the spatial profile of self-formed optical cavity is strongly coupled with a new wave introduced by the perturbation. Moreover, changes in the output are multiple modes and thus can offer a "fine fishnet" effect to capture any of perturbations. This effect can provide additional advantage over other conventional biosensing methods that rely on single peaks or single modes to quantify input perturbations. Further, the existence of predictably behaving modes in both strongly and weakly scattering regimes supports our idea of random laser biosensors. Our current numerical experiments are also supported by our recent experimental studies, in which an extremely small number of nanoparticle attachment or extremely small strains were successfully detected using coherent random lasing phenomenon. These unique and intriguing characteristics of random lasers could potentially be applied to a wide range of multimodal sensing platforms (e.g. spectroscopy scheme, multiplexed scheme, or imaging scheme) for biological, chemical, and environmental applications.

8230-08, Session 2

## Time and wavelength resolved measurements of diffusive reflectance on electrically activated tissue phantom confirm depth selectivity of the method

M. Kacprzak, D. Milej, A. Gerega, N. Zolek, Institute of Biocybernetics and Biomedical Engineering (Poland); J. C. Hebden, S. Magazov, O. White, Univ. College London (United Kingdom); A. Liebert, Institute of Biocybernetics and Biomedical Engineering (Poland)

We present the results of time- and wavelength resolved measurements carried out on electrically activated dynamic tissue equivalent phantom. The phantom contains two electrically-activated inclusions whose absorption coefficient may be reduced by controlled heating. Both inclusions are cylinders 8 mm in diameter and 10 mm in length and are situated 10 and 15 mm below the surface of the phantom, 60 mm apart. The first series of measurements on the phantom were carried out using time resolved optical imager based on the time correlated single photon counting technique. The system was equipped with two semiconductor laser heads operating at 639 and 830 nm, emitting light pulses with full width at half maximum less than 100 ps, and set of fast photomultiplier tube detectors for collecting the diffusely reflected photons at 4 source-detector separations. The second series of measurements were carried out using the time- and wavelength resolved system equipped with the pulsed white light source and an integrated polychromator with photomultiplier tubes which allow for simultaneous observation of times of flight of photons in 16 spectral channels. Our results confirm the advantages of time resolved measurements for depth selective detection of absorption inclusions in the turbid media. The phantom may allow assessment of the time-resolved methodology for measurement of dynamic phenomena, such those simulating absorption changes due to haemodynamic activity in the head.

8230-09, Session 2

## Use of a radial angular filter array to estimate the position of an absorption target within in a turbid medium

Y. Zhang, Simon Fraser Univ. (Canada); F. Vasefi, Lawson Health Research Institute (Canada); M. Najiminaini, B. Kaminska, Simon Fraser Univ. (Canada); J. J. L. Carson, The Univ. of Western Ontario (Canada) and Lawson Health Research Institute (Canada)

The Radial Angular Filter Array (RAFA) is a novel optical filter consisting of a radially-distributed series of micro-machined channels, which converge upon a focal point several millimeters away from the edge of the device. It is designed to measure the angular distribution of light emitted from an object located at the focal point and has been shown to be useful for measuring the distribution of scattered light emitted from the surface of a turbid medium. Since the RAFA is most sensitive to light emitted from a source at the focal point of the device, we hypothesized that the device might be useful for examining optically absorbing features below the surface of a turbid medium. The experiment was performed with a laser diode (785 nm), a series of Intralipid™ sample solutions (0.1% to 1.0%), a 0.5 mm diameter graphite rod (absorber), and a RAFA optically coupled to a line camera. By scanning the position of the rod and comparing the light scattering profiles obtained by the RAFA at each scanning step, the location of the rod was successfully identified in regards to RAFA focal point. The RAFA-based detection system resulted in estimates of the depth of the object within 5 mm of the surface inside the turbid medium at a scattering level equivalent to 0.5% Intralipid™. Future work will be directed toward evaluating the imaging capability of the RAFA for detection of absorbers in a tissue mimicking phantoms.

8230-10, Session 2

## High-precision wide-bandwidth spectroscopy of turbid media

D. Khoptyar, Lund Univ. (Sweden); M. Saleem, National Institute of Lasers and Optronics (Pakistan); A. A. Subash, S. Andersson-Engels, Lund Univ. (Sweden)

Novel instrumentation and measurements techniques for diffused optical spectroscopy (DOS) of turbid (i.e. highly scattering) media are of paramount importance for the development in a wide range of highly important biophotonics, biomedical and industrial applications. The examples of advanced DOS applications range from non-invasive diagnostics and treatment monitoring of cancer till novel cost-effective analytical methods for pharmaceutical development and fabrication quality control.

Basing on the recent advances in source and detector technologies we developed ultra-broadband photon time-of-flight spectrometer that is capable to deliver continues absorption and scattering spectra of turbid media in an ultra broad wavelength range from 600 nm up to 1400 nm. The spectrometer is based on the broadband super-continuous source providing short (ca. 30 ps) optical pulses electronically tunable in measurement spectral range by acousto-optic tunable filters. Broadband single photon counting detectors operated in time correlated single photon counting mode enable precise monitoring of the photon time-of-flight (PTOF) distribution through the turbid sample. Evaluation of the PTOF distribution with either analytical or Monte-Carlo model for photon diffusion enables independent reconstruction of absorption and scattering coefficients of the sample.

In order to further improve accuracy and precision of the measures we have recently implemented double path measurement scheme that enables simultaneous recording of the timing calibration signal along with PTOF measurement. This enables drastic suppression of the temporal drifts and results in superior (ca. 0.5%) precision in determination of the absorption and scattering coefficients in the sample.

We illustrate outstanding performance of the instrument by reviewing numerous applications in precise analysis of pharmaceuticals and biomedical diagnostics.

8230-11, Session 3

## Experimental measurement of the optical properties of biological tissue using polarized enhanced backscattering (EBS) spectroscopy

A. J. Radosevich, N. N. Mutyal, J. D. Rogers, V. M. Turzhitsky, V. Backman, Northwestern Univ. (United States)

Enhanced backscattering (EBS) is a coherence phenomenon in which rays traveling time-reversed paths constructively interfere forming an angular intensity peak centered in the exact backscattering direction. The shape of the angular EBS peak forms a Fourier pair with the spatial backscattering impulse-response, and as a result EBS is highly sensitive to the scattering and absorbing properties of the specimen under investigation. The application of conventional EBS to measurements of biological tissue has been fairly limited due to difficult to resolve peaks which are masked by speckle noise, the inability to acquire spectroscopic information, and the lack of depth-resolution. However, with the introduction of affordable broadband lasers as well as improved experimental and theoretical methodologies these previous difficulties can be overcome. In this work we describe the methodologies used to acquire depth-resolved, spectroscopic, and polarization sensitive characterization of the EBS peak in biological media using an extremely simple backscattering instrument. We then present a model of polarized light scattering in biological media based on the Whittle-Mattérn family of correlation functions and demonstrate the extreme sensitivity of EBS to the shape of the scattering phase function. Finally, we apply this model to measure the scattering coefficient (μs), the absorption coefficient (μa), the anisotropy factor (g), and a higher order parameter of the phase function (D) for various tissue types without the need for sectioning or otherwise perturbing the sample.

8230-12, Session 3

## Optical phase measurements in red blood cells using low-coherence spectroscopy

I. Shock, U. Nevo, N. T. Shaked, Tel Aviv Univ. (Israel)

We propose a low-coherence spectroscopic system for accurate phase measurements in red blood cells (RBCs) for the prognosis and monitoring of various illnesses that manifest in mechanical and structural changes in RBCs. Spectroscopic phase measurements allow non contact, label free measurements with exquisite sub-nanometric scale sensitivities in living cells. Specifically in RBCs, a constant index of refraction assumption can be taken, so that the phase measurement is proportional to the thickness of the RBC. The spectroscopic system uses a low coherence super luminous diode (SLD) and is based on common path geometry. The SLD light passes through a 2X2 fiber coupler and is focused onto the sample by a lens system. The blood cells are encapsulated between two partially reflecting surfaces. The light reflecting from the top surface is combined with light reflecting from the bottom surface to form an interference pattern and is returned through the same optical path. This combined signal is then acquired by a compact spectrometer. A Fourier transform analysis is performed to determine the thickness of the sample which is monitored over time in a high frame rate. Using the system, we measured the cellular dynamics of healthy RBCs and RBCs ghosts for the study of RBC membrane mechanics. In particular, we looked at the membrane vibrational fluctuations in time to reflect a difference in membrane stiffness between the healthy RBC and abnormal RBCs.

8230-13, Session 3

## Characterization of the diffusion properties of light through scattering media with a femtosecond laser pulse

N. Curry, Ecole Supérieure de Physique et de Chimie Industrielles (France); P. Bondareff, Ecole Supérieure de Physique et de Chimie Industrielles (France) and Univ. Pierre et Marie Curie (France); M. Leclerc, Ecole Supérieure de Physique et de Chimie Industrielles (France); R. Sapienza, N. F. van Hulst, ICFO - Institut de Ciències Fotòniques (Spain) and ICREA - Institució Catalana de Recerca i Estudis Avançats (Spain); S. Gigan, Ecole Supérieure de Physique et de Chimie Industrielles (France); S. Gresillon, Univ. Pierre et Marie Curie (France)

Understanding how optical wave propagates in a scattering media is not only important from a fundamental point of view but also for very applied problems, such as light in skin and tissues. For instance the control of light in highly diffusing media could improve the focusing and the depth of focus. In the case of strongly scattering media, propagation is essentially governed by the transport mean free path and the diffusion constant. We propose a method to retrieve both parameters with a simple optical scheme (N. Curry et al, accepted for publication in Optics Letters). In this scheme a femtosecond laser pulse is transmitted trough a thin slab of scattering media. The interference pattern, called speckle, resulting from the multiple paths of light trough the medium, is recorded with a camera. The contrast of the recorded speckle is related to the broadening of the laser pulse and to the characteristic time of diffusion. Therefore controlling the bandwidth of the laser and measuring the speckle contrast gives access to the diffusion properties of the medium. The ability of our set-up to measure the diffusion constant is applied on thin slab of dielectric powder and compared to a total transmission measurement. Results obtained are in agreements with already published results. Our scheme does not require time measurements nor interferometry in contrast with previous methods. This is well adapted to the characterization of samples for pulse shaping, non-linear excitation through scattering media and biological imaging.

8230-14, Session 3

## The study of influence of radiation therapy on experimental tumor's oxygenation using diffuse optical spectroscopy

A. G. Orlova, Institute of Applied Physics (Russian Federation); A. Maslennikova, Nizhny Novgorod State Medical Academy (Russian Federation) and Institute of Applied Physics (Russian Federation) and N.I. Lobachevsky State Univ. of Nizhni Novgorod (Russian Federation); G. Golubjatnikov, Institute of Applied Physics (Russian Federation); T. Pryanikova, Institute of Applied Physics (Russian Federation) and N.I. Lobachevsky State Univ. of Nizhni Novgorod (Russian Federation); V. A. Kamensky, Institute of Applied Physics (Russian Federation); T. Smirnova, N.I. Lobachevsky State Univ. of Nizhni Novgorod (Russian Federation); N. M. Shakhova, I. V. Turchin, Institute of Applied Physics (Russian Federation)

The goal of the study was to investigate the capabilities of diffuse optical spectroscopy (DOS) for assessing and monitoring the oxygenation of experimental tumors and for studying the biological effects of the radiation therapy. The experiments were performed using two tumor models: Plis's lymph sarcoma (PLS) and rat mammary cancer (RMC-1) having different histological structure and functional characteristics. Experiments were performed by frequency-domain diffuse optical spectroscopy on the setup with single source-detector pair and parallel plane geometry (Institute of Applied Physics RAS, Russia). The results obtained by DOS were verified by immunohistochemical study of tissue samples marked with exogenous marker of hypoxia pimonidazole. PLS tumors were irradiated with single doses of 10 Gy and investigated by DOS daily for estimation of dynamics of tissue components, characterizing tumor oxygenation level. Additional direct measurements of pO2 of tumors were carried out using needle oxygen sensor. Differences of the distribution of total hemoglobin, oxygenated hemoglobin, deoxygenated hemoglobin, and blood oxygen saturation between PLS and RMC-1 were shown. DOS results obtained for both tumor models have shown good agreement with results of immunohistochemistry. After radiation therapy temporary increase of blood oxygen saturation as well as pO2 of tumor tissue was observed. Thereby, the capabilities of the method for estimation and monitoring of neoplastic oxygenation have been confirmed.

8230-15, Session 3

## Hyperspectral stray light imaging of chromosomes: a novel concept for label-free karyotyping

R. W. Kessler, Reutlingen Univ. (Germany); K. Rebner, Reutlingen Univ. (Germany) and BASF SE (Germany); D. Oelkrug, Eberhard Karls Univ. Tübingen (Germany)

The field of cytogenetic describes the study of chromosomes and disease states caused by chromosome defects. Staining techniques like G-banding are routinely used to identify metaphase chromosomes based on their unique banding pattern. Advanced molecular cytogenetic techniques like Fluorescence-In-Situ-Hybridization (FISH) provide a more sensitive tool for complex and small structural aberrations. In general, a broad expert knowledge is necessary to understand, diagnose and advise about diseases. We describe the design and performance of a Hyperspectral Imaging System (HSI) for label-free characterization of chromosomes. Chromosomes can be described by an "array of particles" with different size and refractive indices on a nanoscale. The globally or locally resolved spectral stray light pattern can be used to visualize and characterize unstained chromosomes due to the superposition of the interference spectra of the different layer thicknesses, the spectral interference of the band pattern, changes in refractive indexes along the chromosome axis as well as the absorption of chromophores in different spectral regions of the chromatin condensation. The spectra are explained using an extended Mie scattering theory and results are confirmed by FDTD simulations.

Mapping and imaging is carried out within the UV-VIS- and NIR range using pushbroom imaging technology which is integrated into a microscope. This measured spectral signature is then analyzed and classified by means of a principal component analysis (PCA) or multivariate curve resolution (MCR). Together with a Raman Microspectralphotometer, comprehensive information on the morphological and chemical structure of a chromosome can be obtained. The same concept can be applied to characterize cancer cells.

8230-16, Session 4

## Improved empirical models for extraction of tissue optical properties from reflectance spectra

K. Calabro, E. Aizenberg, I. J. Bigio, Boston Univ. (United States)

[note: INVITED talk by Dr. Adam Wax]

The use of empirical models for the extraction of optical and physiological properties from reflectance spectra is a relatively new approach, as compared to other techniques such as those based on the diffusion theory and inverse Monte Carlo algorithms. Empirical models are appealing for their ease of implementation and applicability to conditions for which analytical models are limited. Thus far, however, empirical models have been limited to only a handful of specific probe geometries. In this work, the relationship between reflectance and optical property values is explored for a wide range of geometry and tissue conditions. The influence of variation in tissue anisotropy factor, g, and numerical aperture of the optical fibers are investigated and incorporated into the empirical relationships for the first time. Reflectance data used in this work was simulated using an improved Monte Carlo model designed to run on a graphics processing unit (GPU). Improvements include a Mie theory-based phase function in place of the conventional Henyey-Greenstein phase function, and assignment of probe-specific reflectivity conditions to better model the tissue-probe tip interface. These improvements are particularly important for probe geometries with small source-detector separations. Probe geometries that offer the most stable relationships between reflectance and optical property values, and hence, the best accuracy and reliability in extraction of physiological properties from tissue, are presented.

8230-17, Session 4

## Determination of the scattering coefficient, the reduced scattering coefficient, and the anisotropy factor of tissue with differential interference contrast microscopy

B. DeAngelo, P. Shanley, G. Arzumanov, Fairfield Univ. (United States); Z. Xu, Wenzhou Medical College (China); M. Xu, Fairfield Univ. (United States)

Elastic light scattering (LSS) has long been shown to be sensitive to morphological structures of biological cells and tissues and has been extensively investigated to detect cancer and precancer using optical noninvasive probing. The accurate determination of the scattering property (the scattering coefficient, the reduced scattering coefficient, and the anisotropy factor) of heterogeneous tissue has been one fundamental problem in tissue optics. The most common approach is to use diffuse light to probe the scattering property of tissue. This approach does not yield the local property of the tissue due to the diffusion of light. There, however, exists a simple relationship between the bulk scattering properties of a random medium and the phase structure of the optical wave when light transmits through a thin slice of the same medium.

We report a new approach for determination of the scattering coefficient, the reduced scattering coefficient, and the anisotropy factor from the quantitative phase map measured by differential interference contrast (DIC) microscopy based on the above relationship. We show that accurate determination of the reduced scattering coefficient and the anisotropy factor requires also a proper account of light diffraction in the DIC microscope. The approach is first validated by showing the excellent agreement between the retrieved optical properties of Intralipid-20% suspension and the known values within the visible spectrum. The scattering coefficient, the reduced scattering coefficient, and the anisotropy factor of pathological prostate cancer slides and fresh cancerous and normal prostate tissue samples at probing wavelength from 450nm to 750nm are then investigated. The potential of the approach for tissue diagnosis is discussed at the end.

8230-18, Session 4

## Superresolution imaging for spatial light interference microscopy

K. Chu, NSF Ctr. for Biophotonics Science and Technology (United States)

Among many schemes for quantitative phase imaging, spatial light interference microscopy (abbreviated as SLIM and proposed by the group of Gabriel Popescu at University of Illinois at Urbana-Champaign) can offer images with very few artifacts (speckles, shadows). The system can be easily converted from existing phase contrast microscopes. The lateral resolution of the phase image is still diffraction limited.

At the same time, super-resolution (around 100nm) has been achieved in florescence microscopy. If resolution beyond the diffraction limit for quantitative phase imaging can be achieved, interest and efforts in developing the label-free phase microscopy will be unprecedented. Here we show that it is possible to achieve super-resolution phase imaging with the use of a grating. First we analyze the image formation of the SLIM, showing where the cutoff frequency is. Then a grating is added to the system. The new image exhibits a higher cutoff spatial frequency, thus demonstrating super-resolution. The principle is explained and images with super-resolved details are shown.

8230-19, Session 4

## Monte Carlo simulations of polarimetric response of healthy and cancerous human tissues

M. R. Antonelli, A. Pierangelo, T. Novikova, Ecole Polytechnique (France); P. Validire, A. Benali, B. Gayet, Institut Mutualiste Montsouris (France); A. De Martino, Ecole Polytechnique (France)

Full Mueller real-space imaging in the backscattering geometry is emerging as a powerful technique to identify and characterize anomalous regions of cervical and colon tissues. Understanding the origin of polarimetric contrasts between healthy and anomalous tissues is of high interest to optimize the method and help the detection of precancerous lesions and staging of cancerous ones. Monte Carlo simulations of polarized light propagation in multilayer tissue models were performed to reproduce these contrasts. In these models the uppermost layers are described as homogeneous media including spherical scatterers, while the deeper layers are “lumped” into a totally depolarizing lambertian backscattering surface. As a result, model parameters are layer thickness, scatter radius, volume fraction, refractive index contrast and the lambertian albedo. Bimodal populations of scatterers, with “large” and “small” (sub-wavelength) scatterers representing cell nuclei and collagen aggregates, respectively, were necessary to reproduce the systematically observed Rayleigh-like response, with larger depolarization for circular compared to linear incident polarization. We showed that small scatterers, even at low densities, stabilize the polarimetric response of the simulated structures in the Rayleigh scattering regime. In this work we use the bimodal population model and investigate the effect of parameters to reproduce the polarimetric response of cancerous tissues in connection to known histological trends such as the increase of size and number density of cell nuclei observed in budding cancerous regions with respect to healthy tissue.

8230-20, Session 4

## Numerical modelling and in vivo analysis of fluorescent and laser light backscattered from glial brain tumours

T. A. Savelieva, N. Kalyagina, M. Kholodtsova, A. M. Prokhorov General Physics Institute (Russian Federation); A. Potapov, S. Goryainov, N.N. Burdenko Neurosurgical Institute (Russian Federation); V. B. Loschenov, A. M. Prokhorov General Physics Institute (Russian Federation)

Brain glial tumours have peculiar features of the perifocal region extension, characterized by its indistinct area, which complicates determination of the borders for tissue resection. The combination of the measurements of fluorescent and diffuse-reflected light signals and their mathematical modelling can make it possible to characterize the optical properties of the tissue, and thus to determine the neoplasm grade and malignization level in the perifocal areas.

In the present study the fluorescent signals, excited at the wavelength of 632.8 nm, were measured in vivo on the white matter and analysed in order to determine the selective accumulation of the protoporphyrin-IX photosensitizer in the brain tissue at the wavelength 700±20nm. The filter-reduced back-scattered light signals compared to the data from mathematical modelling, were used for description of the tissue optical parameters for determination of the borders of astrocytoma perifocal area spread. The morphological characteristics of the brain tissues, examined in vivo by means of a fibre optic probe, were obtained from the histologic ex vivo studies. The simulations of the fluorescent and scattered light distributions were performed in a Monte Carlo program using scattering and absorption parameters of the different grades of the brain glial tumours. The parameters were obtained by the Mie calculations for different cellular organelles. Such numerical modelling of the light distribution was developed for the diagnostics improvement by taking into consideration the optical properties of a complex media and their micro-changes during the tumour formation. The presented method shows a good compliance of the results of the mathematical modelling with the clinical studies of the brain tissues.

8230-21, Session 5

## Cellular morphology measurement using high-speed two-dimensional angle-resolved low-coherence interferometry

M. G. Giacomelli, A. P. Wax, Duke Univ. (United States)

Angle-resolved low coherence interferometry (a/LCI) is a light scattering technique that has shown promise as a method of detecting neoplasia and analyzing cellular structure both in vivo and as a research tool. Combined with Mie theory and the T-matrix, a method for simulating scattered fields from non-spherical scatterers, we have previously demonstrated that a/LCI is capable of obtaining quantitative nuclear structural information from epithelial and sub-epithelial sites in studies of cells, animals and human tissues. Recently we have improved upon past techniques by developing a high speed line scan system that combines the depth resolution of optical coherence tomography with polar and azimuthal angle-resolved and polarization sensitive scattered field measurements. Using a custom imaging spectrometer, we have improved on our previous acquisition speed more than 1000 fold while also improving sensitivity and angular resolution.

By scanning over a wide range of solid angles and resolving polarization, a wealth of information is available for inverse analysis. To exploit this, we present a T-matrix based inverse analysis procedure that recovers the size, spheroidal aspect ratio, and orientation of both individual and ensemble scatterers. Initial studies using phantoms showed extremely unique size, shape and orientation fits. We extend previous experiments to live cells by exploiting the high speed and sensitivity of our improved system. With angle-resolved scattering, we measure the size and shape of cell nuclei as well as the orientation and organization of aggregates of cells.

8230-22, Session 5

## Determining the orientation of subsurface light scattering structures with spatial frequency domain imaging

S. D. Konecky, T. B. Rice, A. J. Durkin, B. J. Tromberg, Beckman Laser Institute and Medical Clinic (United States)

Many tissue types, including bone, muscle, skin, and white matter in the brain, have orientated internal structures such that the degree of optical scattering depends on the direction of light propagation. The scattering anisotropy of these tissues is determined by their microscopic structure. Imaging the directionality of light scattering provides a non-invasive way to interrogate this microscopic structure, and may aid in the early detection and diagnosis of disease. In this paper we investigate tissue anisotropy using Spatial Frequency Domain Imaging, a wide-field method in which the absorption and scattering properties of turbid media are determined by measuring the attenuation of sinusoidal patterns of light which are projected onto a sample at varying spatial frequencies. We derive analytic solutions in the spatial Fourier domain for the Greens functions of an anisotropic diffusion equation in the semi-infinite and slab geometries. These solutions predict the decay and phase shift of the sinusoidal patterns of light intensity as they propagate in anisotropic media. Based on our theoretical analysis we propose a contrast function which is sensitive to the direction and degree of anisotropy, but is relatively insensitive to changes in the overall absorption and scattering coefficients. We demonstrate that by rotating the orientation of the projected patterns, we can image the direction and degree of anisotropy in tissue. We validate the method experimentally in phantoms, as well as in muscle and brain.

8230-23, Session 5

## Direct and highly sensitive measurement of the spatial arrangement of microstructures within biological samples

N. N. Boustany, H. Sierra, R. M. Pasternack, B. Rabin, Rutgers, The State Univ. of New Jersey (United States)

Quantitative morphological assessment of biological cells and their subcellular environment is important to characterize cellular state in normal and diseased tissue and cellular response to various experimental treatments. Recently, we showed that optical Gabor-like filtering of light scattered by spheres yields an optical measurement which varies linearly with diameter. In addition, the sensitivity to changes in size was superior to post-processing of digital images. Here, we extend our previous results by showing that the linear relationship between Gabor filter period and particle size holds over a size range from 100nm to 2000nm. We also show that this relationship is independent of the particle's or medium's refractive index. Using simulations, we provide a theoretical basis for our findings. Unlike previous methods, this technique does not require the presence of single isolated particles and thus may be used to directly extract the characteristic size associated with the local texture of heterogeneous objects. We therefore discuss this applicability of our method in heterogeneous samples consisting of collagen and living cells.

8230-24, Session 5

## Correlating the light scattering pattern of a biological cell to its mitochondrial properties using a Gabor filter technique

M. Moran, X. Hu, J. Q. Lu, East Carolina Univ. (United States)

Traditional light scattering analysis of cells relies mostly on the one-dimensional distribution of the light scattering intensity, where only the cell size and some limited information regarding the internal structure can be obtained. More recent studies have attempted to analyze the two-dimensional diffraction images of cells using standard texture analysis techniques to extract additional intracellular information. We recently compared the effectiveness of several major methods that are often used in image texture analysis and found that the Gabor filter approach is more effective than most methods and is capable of providing information regarding the major structural features and mitochondrial properties of the cell. In this report we further our investigation by utilizing a Gabor filter technique to analyze light scattering patterns of cells and to correlate their changes to that of the mitochondrial properties of the cells. Numerical simulations of light scattering are performed using the discrete dipole approximation (DDA) on analytically generated biological cell models with various mitochondrial characteristics. A set of two-dimensional scattering images is produced corresponding to systematic variations in the size, shape, and distribution of mitochondria and is processed with a bank of Gabor filters. Selected mean values of the Gabor-filtered images are displayed in scatter plots, providing a novel approach to grouping the cell models according to mitochondria size, shape, and distribution.

8230-25, Session 5

## Light scattering based monitoring of leukemic cells in flowing in vitro blood samples

I. Georgakoudi, C. A. Greiner, M. Hunter, Tufts Univ. (United States)

The prognostic value of assessing minimal residual disease in leukemia has been established with flow cytometry and PCR. Nonetheless, these techniques are limited by high equipment costs, complex and costly cell processing and the need for highly trained personnel. Here, we demonstrate the potential of exploiting differences in the relative intensities of backscattered light at three wavelengths to detect the presence of leukemic cells in samples containing varying mixtures of white blood cells (WBCs) and leukemic cells flowing through microfluidic channels. We identify distinct light scattering intensity distributions for Nalm-6 leukemic cells, normal mononuclear (PBMC) and polymorphonuclear (PMN) white blood cells and red blood cells. We exploit these differences to develop cell classification algorithms, whose performance is evaluated based on simultaneous acquisition of light scattering and fluorescence data. When this algorithm is used prospectively for the analysis of samples consisting of mixtures of PBMCs and leukemic cells, we achieve an average specificity and sensitivity of leukemic cell detection of 99.6%, and 45.2%, respectively. Based on the performance of these algorithms, we estimate that 42 or 71 uL of blood would be adequate to confirm the presence of leukemia at an 80% power level in samples containing 0.01% leukemia cells to either PBMCs or PBMCs and PMNs, respectively. Therefore, light scattering based flow cytometry in a microfluidic platform could provide a low cost, highly portable, minimally invasive approach for detection and monitoring of leukemic patients. This could offer significant improvements especially for pediatric patients and for patients in developing countries.

8230-26, Session 6

## Digital Fourier holography for wide-field characterization of microstructures

D. D. Sampson, The Univ. of Western Australia (Australia)

Methods to improve the efficiency of the quantitative characterization of tissue microstructure, over large areas that require analysis or diagnosis, have the potential to impact on many areas, including medical point-of-care applications in the clinic and in the field, and pathology laboratory practice. We have employed holography in the development of such methods, with advantages which include: 1) the availability of the full complex amplitude of the scattered lightwave and not just its magnitude; 2) although the technique is not inherently optically sectioning, the availability of three-dimensional spatial information; 3) the ability to capture this information in a single, or at most a few, digital images; and 4) the great scope for subsequent computation and quantitation. Fourier holography, in particular, is convenient, because it records holograms directly in the spatial frequency domain, is amenable to large field-of-view geometries, and facilitates the use of digital imaging devices with limited dynamic range.

We have largely examined two methods employing digital Fourier holography. In the first method, we utilize the angular scattering "signature" of a sample, which is strongly correlated with its microstructure. If a spatially resolved angular scattering spectrum can be measured over a small region, it may not be necessary to resolve the underlying structures, such as cells, in order to classify them. We demonstrate the principles of the technique [1], its capacity to characterize such entities as red blood cells [2] and demonstrate an approach to extend its performance to three dimensions [3]. In the second method, a synthetic aperture is constructed in a wide-field-of-view Fourier holographic imaging system [4]. We show it is possible to determine quantitative sample information by acquiring data only from a selected sub-region of a large spatial frequency range - enjoying the benefits of low-numerical-aperture (NA) imaging but imaging structure that is commonly accessible only to high-NA microscopy techniques [5]. We demonstrate the effectiveness of this technique in imaging biological tissues [6].

We contrast such coherent approaches with an incoherent one that we have developed [7].

[1] S. A. Alexandrov, T. R. Hillman, and D. D. Sampson, "Spatially resolved Fourier holographic light scattering angular spectroscopy", Optics Letters, vol. 30, pp. 3305-3307, 2005.

[2] T. R. Hillman, S. A. Alexandrov, T. Gutzler, and D. D. Sampson, "Microscopic particle discrimination using spatially-resolved Fourier-holographic light scattering angular spectroscopy," Optics Express, vol. 14, pp. 11088-11102, 2006.

[3] T. Gutzler, T. R. Hillman, S. A. Alexandrov, and D. D. Sampson, "Three-dimensional depth-resolved and extended-resolution micro-particle characterization by holographic light scattering spectroscopy," Optics Express, vol. 18, pp. 25116-25126, 2010.

[4] S. A. Alexandrov, T. R. Hillman, T. Gutzler, and D. D. Sampson, "Synthetic aperture Fourier holographic optical microscopy," Physical Review Letters, vol. 97, 168102 (4pp), 2006.

[5] T. R. Hillman, T. Gutzler, S. A. Alexandrov, and D. D. Sampson, "High-resolution, wide-field object reconstruction with synthetic aperture Fourier holographic optical microscopy," Optics Express, vol. 17, pp. 7873-7892, 2009.

[6] T. Gutzler, T. R. Hillman, S. A. Alexandrov, and D. D. Sampson, "Coherent aperture-synthesis, wide-field, high-resolution holographic microscopy of biological tissue," Optics Letters, vol. 35, pp. 1136-1138, 2010.

[7] S. A. Alexandrov and D. D. Sampson, "Spatial information transmission beyond a system's diffraction limit using optical spectral encoding of the spatial frequency," Journal of Optics A - Pure and Applied Optics, vol. 10, 025304 (5pp), 2008.

8230-27, Session 6

## Speckle reduction using wavefront modulation for multifunctional optical coherence tomography

C. M. Oh, Univ. of California, Riverside (United States); C. Feng, Stanford Univ. (United States); Y. Wang, B. H. Park, Univ. of California, Riverside (United States); J. F. de Boer, Vrije Univ. Amsterdam (Netherlands)

The presence of coherent speckle in optical coherence tomography (OCT) images can obscure identification of small or thin tissue structures. We present a method of reducing the effect of speckle in a multifunctional spectral domain OCT system by modifying the wavefront and consequently the speckle pattern using a micro-deformable mirror (μDM) placed in the sample arm beam path. Our results indicate that by adjusting the wavefront modification between each depth profile acquisition and subsequently incoherently averaging small numbers of adjacent depth profiles, we can achieve a considerable reduction in both speckle contrast and standard deviation in phase retardation plots, without a significant increase in the phase noise floor. We demonstrate the results of our technique on in vivo and ex vivo samples including rat muscle and bovine retina.

8230-28, Session 6

## Detecting nanoparticles and cells with optical coherence microscopy

N. L. Bocchio, C. Pache, M. L. Villiger, A. Bouwens, C. Berclaz, C. Santschi, A. Grapin-Botton, T. Lasser, Ecole Polytechnique Fédérale de Lausanne (Switzerland)

Optical coherence microscopy (OCM) is an emerging technique in the field of functional cell imaging. The sectioning capabilities of the method combined with coherent signal amplification result in a very high sensitivity for backscattered light. In OCM, the contrast relies on variations of the optical properties of the sample under investigation.

When imaging tissue, inner structures cannot be identified if their backscattering does not differ from their surrounding environment. In order to add specificity to the images, it is necessary to adopt an appropriate labeling strategy. Gold nanoparticles are particularly interesting for this purpose, since they have, due to plasmonic excitation, tunable optical properties (absorption, scattering), can resist photo degradation, and their surfaces can be chemically functionalized for specific structure targeting.

This work combines the study of metal nanoparticles with a recently developed dark-field configuration for OCM (df-OCM), down to the single particle level. Dark-field illumination is known to enhance scattering contrast in microscopy and is, therefore, a suitable method for the study of weakly scattering entities like cells or particles. Using this approach we show cell imaging, the detection of single metal nanoparticles down to a few nanometers in size and explore contrast enhancement mechanisms (plasmon resonances, photothermal effects) for these labels.

8230-29, Session 6

## Probing biological tissue morphology and function with coherent light scattering imaging techniques

Y. Pan, H. Ren, Z. Yuan, Z. Luo, K. Park, C. Du, Stony Brook Univ. (United States)

Most biological tissue is highly scattering, which causes severely reduced image contrast/resolution and penetration depths of conventional optical (e.g., spectroscopy, fluorescence) techniques for detection of cancers and functional diagnoses. Imaging of scattering tissue under coherent illumination can be even more complicated due to overwhelming speckle nature in these images. For instance, both contrast and noise reside in the speckles of a coherent image like OCT and effective speckle handling to extract useful diagnostic information remains a technical challenging. Recent advances in dynamic light scattering approaches to effectively extract speckle contrast have shown great promise for probing biological tissue morphology and function. Here, we summarize our recent progresses on dynamic speckle characterizations (in both system development and image processing), which includes time-lapse ultrahigh-resolution OCT (TL-uOCT) to uncover subcellular details of epithelium, multi-channel laser speckle imaging (LSI) for brain functional studies, and Doppler OCT for 3D angiographic and quantitative subsurface blood flow imaging (DOCT), all of which are based on separation of static and dynamic speckle contrasts in either time domain or spatial domain. In addition, we present examples of these techniques for early epithelial cancer diagnosis (e.g., carcinoma in situ), functional brain imaging, and for detection of neurovascular dysfunction under interventions. Our results show that TL-uOCT enables subcellular imaging with low-NA optics (thus suitable for endoscopic diagnosis), LSI and DOCT together can provide high-fidelity blood flow and metabolic images that can potentially assist f-MRI BOLD for brain image studies.

8230-30, Session 7

## Recent progress in angle-resolved low-coherence interferometry and its application for detecting intestinal dysplasia

Y. Zhu, N. G. Terry, J. Thacker, J. Migaly, C. Guy, C. R. Mantyh, A. P. Wax, Duke Univ. (United States)

Angle-resolved low coherence interferometry (a/LCI) is a non-invasive, label-free “optical biopsy” technique which measures the angular intensity distribution of scattered light from tissues to quantify subcellular morphology as a function of depth in the tissue. For each depth layer, the collected angular scattering signal is processed to extract signatures from cell nuclei, which is then analyzed to produce measurements of average nuclear diameter with submicron accuracy. Using this depth-resolved information, a/LCI’s efficacy for assessing tissue health has been demonstrated in early studies of animal models and ex vivo human tissues. In a recent in vivo clinical pilot study, an endoscopic a/LCI system was used to identify the presence of dysplasia in Barrett’s esophagus patients with high sensitivity and specificity, showing great potential in assisting physicians in conventional biopsy procedures to improve detection accuracy and efficiency.

We present here the results of a pilot, ex vivo study of tissues from twenty-seven (27) patients undergoing partial colonic resection surgery, conducted to evaluate the ability of a/LCI to identify intestinal dysplasia. Performance was determined by comparing the nuclear morphology measurements with pathological assessment of co-located physical biopsies. A statistically significant correlation between increased average nuclear size, reduced nuclear density and the presence of dysplasia was noted at the basal layer of the epithelium, at a depth of 200 to 300 μm beneath the tissue surface. Using a decision line determined from a receiver operating characteristic, a/LCI was able to separate dysplastic from healthy tissues with a sensitivity of 92.9% (13/14), a specificity of 83.6% (56/67), and an overall accuracy of 85.2% (69/81). The study illustrates the extension of the a/LCI technique to the detection of intestinal dysplasia, and demonstrates the need for future in vivo studies.

8230-31, Session 7

## Subdiffractional differences in macromolecular density distribution detected in the field of esophageal cancer

L. Cherkezyan, Northwestern Univ. (United States); V. Konda, The Univ. of Chicago Medical Ctr. (United States); H. Subramanian, Northwestern Univ. (United States); K. Wroblewski, The Univ. of Chicago Medical Ctr. (United States); D. Damania, Northwestern Univ. (United States); L. Karl, The Univ. of Chicago Medical Ctr. (United States); M. J. Goldberg, NorthShore Univ. HealthSystem (United States); I. Waxman, The Univ. of Chicago Medical Ctr. (United States); H. K. Roy, NorthShore Univ. HealthSystem (United States); V. Backman, Northwestern Univ. (United States)

In America over fifteen thousand people are yearly diagnosed with esophageal cancer, of which 95% don't survive more than 5 years. In contrast, the prognosis for those diagnosed early is excellent. Screening practices often miss patients with dysplasia or esophageal adenocarcinoma until it's well spread. Analysis of proximal esophageal squamous epithelium with partial wave spectroscopic (PWS) microscopy may eliminate the need of finding and accessing the tumor location with current screening techniques. The sensitivity to subdiffractional length scales empowers PWS not only to sense the early dysplastic changes in cells that are microscopically invisible, but also to detect the field effect of esophageal cancer: the phenomenon of the tissue outside the tumor location that appears histologically normal having abnormalities at the molecular, nano-, scale. Sampled and validated as markers of risk, these structural changes in the field can lead to earlier diagnosis. In our study involving two medical centers, we established significant nanostructural differences in the field of esophageal cancer and dysplasia. Using PWS the heterogeneity of spatial intracellular mass distribution (Ld - the disorder strength) was quantified in the normal squamous epithelium of the proximal esophagus. We found that average Ld of 16 patients with esophageal cancer was 1.85 times higher than that of the 25 control patients ($p<0.01$); patients with dysplasia (6 high, 3 low grade) had a 1.68 times higher Ld than controls ($p<0.05$). Fourteen patient samples from the buccal mucosa were analyzed to determine the extent of the field effect and no difference was seen ($p=0.42$).

8230-32, Session 7

## Nanomorphology-based cancer diagnosis via spatial-domain low-coherence quantitative phase microscopy

Y. Liu, R. K. Bista, P. Wang, U. Shikhar, R. Bhargava, D. J. Hartman, S. Kevin, R. E. Brand, Univ. of Pittsburgh Medical Ctr. (United States)

Conventional pathology remains a gold-standard for cancer diagnosis, but it only detects structural alterations at the micron scale. Diagnoses may be missed when the sample is insufficient, is taken in the early course of the tumor development, or is not taken directly from the tumor. Further, due to the concern of missing cancer, patients with benign findings may still undergo aggressive treatment without subsequent finding of cancer. There is an urgent need for effective diagnostic tools with much better accuracy. Recognizing that nano-structures associated with molecular events during tumorigenesis may provide potentially diagnostic features, our group has developed an optical technique - Spatial-domain Low-coherence Quantitative Phase Microscopy (SL-QPM) - that adapts a low-coherence thermal light source and common light-path interferometric configuration to quantify the nano-structural changes within the cell nucleus (i.e., nano-morphology) with a sensitivity of 0.9 nm. Our SL-QPM system can be used in routine pathological specimens prepared with standard clinical protocol processing. We have demonstrated the feasibility of SL-QPM-derived nano-morphology characteristics from the cell nucleus to detect cancer in cells initially labeled as "negative" or "indeterminate" by expert pathologists that were subsequently confirmed to be cancerous; or to detect the presence of cancer in histologically normal cells distant from the tumor in multiple types of cancer (breast, pancreatic, esophageal, colorectal). We have also explored the potential biological mechanisms by characterizing the alterations of nuclear nano-morphology markers as a response to abnormal cell growth and genetic changes. Future studies are needed to validate this technique in a larger patient population.

8230-33, Session 7

## In vivo risk stratification of colon carcinogenesis by measurement of optical properties with novel lens-free fiber optic probe using low-coherence enhanced backscattering spectroscopy (LEBS)

N. N. Mutyal, A. J. Radosevich, J. D. Rogers, Northwestern Univ. (United States); M. J. Goldberg, L. Bianchi, N. Krosjnar, B. Jancan, H. K. Roy, NorthShore Univ. HealthSystem (United States); V. Backman, Northwestern Univ. (United States)

Colon cancer is the second-leading cause of cancer deaths in the United States. However, like most cancers, colon cancer is curable if detected and treated at an early stage. Optical spectroscopy is a promising technique for noninvasive detection of cancers and precancers. In our previous studies we have demonstrated that ex-vivo measurements of optical properties by LEBS taken from outside the spatial extent of lesion (rectal mucosa for colon cancer) were able to detect the advanced adenomas with 100% sensitivity, 80% specificity and area under ROC curve of 89%. Here we report the design, development and implementation of a novel lens-free fiber optic probe capable of measuring depth-resolved optical properties of tissue in-vivo. A scattering phantom consisting of polystyrene microspheres in water is used to characterize the performance of the probe. Monte Carlo simulations are performed to validate the capability to measure depth resolved optical properties. Finally, to evaluate the performance of the probe in-vivo we performed rectal measurements from 214 patients undergoing colonoscopy (160 No Dysplasia, 21 Diminutive adenomas, 22 adenomas & 11 advanced adenomas). The optical properties measured by the LEBS probe in-vivo were able to distinguish advanced adenomas with 87.5% sensitivity, 73.8% specificity and 87.10% AUROC. The dataset was validated by performing a blinded study on 128 patients which showed that the performance characteristics were similar to the training set, with minor degradation in AUROC to 82%.

8230-34, Session 7

## Measuring nanoscale refractive-index alterations in the field of ovarian cancer using partial wave spectroscopic microscopy

D. Damania, H. Subramanian, L. Cherkezyan, Y. Zhu, C. White, P. Pradhan, H. K. Roy, V. Backman, Northwestern Univ. (United States)

Currently, there is no minimally invasive early screening option available for the majority of cancer-types. Most of the available techniques are either sub-optimal in their efficacy, expensive or invasive. Moreover, cancer is an accumulation of several genetic/epigenetic changes leading to nanoscale alterations before apparent microscopic abnormalities (e.g., dysplasia). The conventional histopathology cannot visualize cell nano-architecture due to diffraction-limited resolution (~300nm). The novel imaging technique, partial wave spectroscopic (PWS) microscopy, can quantify cellular nano-architecture, corresponding to early morphological changes in cancer cells. PWS quantifies the nanoscale refractive-index (i.e., mass-density) fluctuations within a cell, termed as disorder strength (Ld). PWS has proven its sensitivity to early nanoscale changes in human colon, pancreas and lung (N = 300 subjects) based on concept of field-carcinogenesis (i.e., histologically normal tissue away from tumor location contains molecular,nanoscale abnormalities). Herein, we investigated similar field-effect changes in the ovarian cancer (which ranks fifth as cancer fatalities among American women) using PWS. We performed PWS on easily-accessible columnar epithelium from both, endometrium and endocervix regions of control (n = 10) and cancer (n = 10) patients. We observed statistically significant $\Delta$Ld between control and cancer patients in both, endometrium (Effect-size = 82%, P-value = 0.04) and endocervix (Effect-size = 108%, P-value = 0.007). These findings underscore the possibility of developing a minimally-intrusive and cost-effective “pre-screen” option for ovarian cancer based on PWS investigation while the existing screening options (CA-125, transvaginal ultrasound) have poor specificity. The biological mechanisms of nanoscale changes leading to disorder strength differences will also be discussed.

8230-35, Session 7

## Enhanced tumor contrast during breast lumpectomy provided by independent component analysis of localized reflectance measures

A. Eguizabal, Univ. de Cantabria (Spain); A. M. Laughney, Thayer School of Engineering at Dartmouth (United States); P. B. García-Allende, Helmholtz Zentrum München GmbH (Germany); V. Krishnaswamy, Thayer School of Engineering at Dartmouth (United States); W. A. Wells, Dartmouth Hitchcock Medical Ctr. (United States); K. D. Paulsen, B. W. Pogue, Thayer School of Engineering at Dartmouth (United States); J. M. Lopez-Higuera, O. M. Conde, Univ. de Cantabria (Spain)

A spectral analysis technique to enhance tumor contrast during breast conserving surgery is proposed. Surgically-excised breast tissues have been imaged in a local reflectance geometry. Measures of broadband reflectance are directly analyzed using principle component analysis (PCA), providing contrast maps to guide surgeons during lumpectomy without relying on approximations to light transport in tissue. PCA is directly applied, on a per sample basis, to broadband reflectance spectra to extract areas of maximal spectral variation. This process determines morphology-related features related to diagnosis. A dynamic selection threshold has been applied to obtain the final number of principal components on a per sample basis, accounting for inter-patient variability. A blind separation technique based on Independent Component Analysis (ICA) is then applied. Surgically resected breast tissues were imaged and classified by a pathologist and seven different tissue pathologies were identified, i.e. not-malignant (normal, benign and inflammatory epithelium and stroma), malignant (invasive and in situ cancers) and adipose. ICA application reveals that the behavior of just one independent component highly correlates with the pathologic diagnosis and it surpasses the contrast obtained using empirical models. Moreover, blind detection characteristics (no training, no comparisons with training reference data) and no need for parameterization makes the automated diagnosis simple and time efficient, favoring its translation to the clinical practice.

8230-36, Session 7

## Non-invasive detection of periodontal disease using diffuse reflectance spectroscopy: a clinical study

C. S. Prasanth, Ctr. for Earth Science Studies (India); J. Betsy, Government Dental College, Thiruvananthapuram (India); S. Narayanan, Ctr. for Earth Science Studies (India); J. Prasanthila, Government Dental College, Thiruvananthapuram (India)

The current clinical procedures for periodontitis diagnosis have several inherent draw backs due to obsolete technology and there is need develop techniques for noninvasive diagnosis and prognosis. A clinical trial was carried out in 28 healthy volunteers and 55 patients at Government Dental College, Trivandrum, Kerala, India to demonstrate the applicability of diffuse reflectance (DR) spectroscopy for quantification and discrimination of various stages of periodontitis. The DR spectra of diseased lesions recorded using a point monitoring system consisting of a tungsten halogen lamp and a fiber-optic spectrometer shows oxygenated hemoglobin absorption dips at 545 and 575 nm. Mean DR spectra on normalization shows marked differences between healthy, gingivitis and periodontitis. We have observed that using the DR intensity ratio R620/R575 gingivitis tissues could be discriminated from healthy with a sensitivity of 89% and specificity of 91%, and from periodontitis with a sensitivity of 90% and specificity of 100%. In order to screen the entire diseased area and its surroundings instantaneously, DR images were recorded with an EMCCD camera at 620 and 575 nm. The monochrome ratio image (R620/R575) was computed and color coded for visual discrimination. Marginal improvement is diagnostic accuracies were noticed.

This is the first time that DR spectral ratio/imaging systems were used for quantitatively discriminating healthy gingiva from diseased. In view of the diagnostic accuracies reported there is a great potential for further development of this non-invasive DR technique for periodontal disease screening and for monitoring of treatment efficacy during antimicrobial Photodynamic Therapy.

8230-37, Poster Session

## Polarized Monte Carlo simulation of blood vessel structure in colon tissue

W. Yip, A. Gomes, A. V. Sahakian, V. Backman, Northwestern Univ. (United States)

The purpose of this paper is to study the impact of blood vessel size and the depth of the vessel on polarization gating measurement using Monte Carlo simulation. The Monte Carlo method used in this work is adapted from combining the previous works of Chen et al. and Ramella-Roman et al. Chen's code allows the optical properties of each voxel in the simulation to be specified (scattering coefficient, absorption coefficient and anisotropy factor), and Ramella-Roman has developed a method for polarization of a photon to be tracked. Polarized light simulations in optical wavelengths are performed by simulating colon tissue using tissue parameters from the literature to define the structural and optical properties of mucosa, submucosa and muscle layer. The simulated cross-polarized and co-polarized signals will be used to resolve the blood vessel size at different depths. Furthermore, the effect of blood vessel size and density changes in different layers on polarization gating signal can be studied in order to better interpret experimental measurements. The results can be used to help differentiate measurements from healthy tissues and cancerous tissues. In addition, the penetration depths of photons are compared between homogeneous and vessel structure in order to determine the actual probe penetration depths in tissues.

8230-38, Poster Session

## Optimal attenuation of the unscattered light for spatial light interference microscopy

K. Chu, Univ. of Rochester (United States)

Among many schemes for quantitative phase imaging, the spatial light interference microscopy (abbreviated as SLIM and proposed by the group of Gabriel Popescu at University of Illinois at Urbana-Champaign) can offer images with very few artifacts (such as speckles and shadows). The interference in an SLIM is between the unscattered and scattered light, which is spatially separated in the fourier domain. The unscattered light is attenuated by a pupil mask and phase-modulated by a spatial light modulator. In the image plane, the unscattered light and scattered light are combined and interfere with each other. In

order to achieve the best contrasted interference, the amplitude of the unscattered and scattered light when arriving at the detector array should ideally be equal to each other. Due to the spatial variation of the scattered light, the attenuation (which is a constant) cannot satisfy this condition everywhere. We will report a scheme to find the optimized attenuation coefficient based on spatial averaging. The objects are simulated beads of different density, optimal attenuation is found for each case. This will provide a helpful look-up table for biological samples of different density. Quantitative phase images of the sample with optimal attenuation will be compared to images with non optimal attenuation.

8230-39, Poster Session

## Blind breast tissue diagnosis using independent component analysis of localized backscattering response

A. Eguizabal, Univ. de Cantabria (Spain); A. M. Laughney, Thayer School of Engineering at Dartmouth (United States); P. B. García-Allende, Helmholtz Zentrum München GmbH (Germany); V. Krishnaswamy, Thayer School of Engineering at Dartmouth (United States); W. A. Wells, Dartmouth Hitchcock Medical Ctr. (United States); K. D. Paulsen, B. W. Pogue, Thayer School of Engineering at Dartmouth (United States); J. M. Lopez-Higuera, O. M. Conde, Univ. de Cantabria (Spain)

A blind separation technique based on Independent Component Analysis (ICA) is proposed for breast tumor delineation and pathologic diagnosis. Tissue morphology is determined by fitting local measures of tissue reflectance to a Mie theory approximation, parameterizing the scattering power, scattering amplitude and average scattering irradiance. ICA is applied on the scattering parameters by spatial analysis using the fast ICA method. Only two independent components have been considered for diagnosis. Neither training, nor comparisons with reference parameters are required. Tissue diagnosis is provided directly following ICA application to the scattering parameter images. The time response of the diagnostic strategy is therefore enhanced, enabling near real-time assessment of pathology during breast-conserving surgery. Surgically resected breast tissues were imaged and identified by a pathologist. Seven different tissue pathologies were identified in 29 samples and classified as not-malignant (normal, benign, and inflammatory epithelium and stroma), malignant (invasive and in situ epithelium and stroma) and adipose. Contrast maps provided by the tissue's independent components highly correlate with the pathologic diagnosis. Moreover, the scatter plot analysis of the two ICA components provides results where diagnostic categories appear localized and highly concentrated in separated clusters favoring their classification. This fact makes the automatic diagnosis very simple and time efficient.

8230-40, Poster Session

## Development of a next-generation fully integrated hybrid FMT/XCT system

M. Koch, A. B. F. Ale, P. Mohajerani, V. Ntziachristos, Helmholtz Zentrum München GmbH (Germany)

Fluorescence Molecular Tomography (FMT) is a novel technology to provide volumetric information on fluorochrome distribution in biological tissue in vivo. Thus it is used to visualize and quantify functional processes and molecular distribution as in carcinogenesis, treatment efficacy and post-treatment cancer survival monitoring.

The development of a next generation fully integrated noncontact hybrid system of FMT and X-ray computed tomography (XCT) for small animals is shown.

A custom-made prototype ensures full access to all components of the optical and especially the X-ray imaging chain. This gives opportunities for advanced acquisition strategies to increase both temporal performance and accuracy.

The XCT volumetric data is used as prior information on optical parameters during the FMT reconstruction. It is in addition used for defining optimal acquisition parameters for the optical measurement and the respective region of interest. During the acquisition the parameters are adapted to ensure using the entire dynamic range of the optical imaging chain and therefore obtain the maximum possible signal to noise ratio.

Furthermore a nearly full automatic image-based method for a three-dimensional spatial calibration between the optical imaging- and X-ray imaging chain is presented. Higher degree optical aberrations such as tangential and radial distortions are modelled and corrected.

8230-41, Poster Session

## Optical reflectance spectroscopy with a double-clad fiber for measurements of blood oxygenation

R. d. P. Soto Astorga, E. Z. Zhang, J. G. Laufer, J. C. Hebden, A. E. Desjardins, Univ. College London (United Kingdom)

Monitoring of the cardiocirculatory function is of critical importance during cardiac surgery. Central venous oxygen saturation (ScvO2) provides an indication of tissue oxygenation to detect low cardiac output or sudden cardiovascular collapse. Endovascular measurements of ScvO2 can be performed with optical spectroscopy, with optical fibers integrated into a catheter. In many implementations, the delivery and collection of light is provided by separate fibers. In this study, we investigated the potential of performing blood oxygenation measurements with one double clad fiber. Broadband light from a superluminescent diode (790 to 870 nm) was delivered through the central core; a portion of light scattered by tissue was collected through the outer cladding and spectrally resolved. Monte Carlo simulations were used to estimate the mean of the maximum depth reached by photons relative to the distal end of the fiber, as a function of wavelength and oxygenation. Spectroscopic measurements of blood oxygenation were performed with extracorporeal circuit and a membrane oxygenator, and compared with measurements from blood gas analysis. Optical spectroscopy with a double clad fiber could allow for smaller optical catheters with simpler designs; as such, it is has potential applicability in broad range of probe designs and clinical procedures.

8230-42, Poster Session

## Generalized pulse spectrum technique for diffuse optical tomography based on the third-order spherical harmonics approximation to radiative transfer equation

W. Ma, F. Gao, L. Wu, X. Yi, H. Zhao, Tianjin Univ. (China)

Diffuse optical tomography (DOT) has become an indispensable imaging modality in preclinical research. It is extensively applied and is an efficient tool for in vivo small animal research. The diffusion-approximation (DA) theory is commonly used in this modality as the theoretical basis of image reconstruction. However, this methodology has several limitations for small animal applications, where small geometries and high absorption or low scattering areas are encountered. A three-order spherical harmonics (P3) approximation of Radiative Transfer Equation in two-dimensional tissue geometries is presented in this paper, which improves the three-order equation for ignoring anisotropic factor in previous papers. To evaluate the performance of the P3 approximation, we compare its solution with Monte Carlo (MC) simulation. The validation results show that this method significantly improve the solution of diffusion approximation (DA) equation in near-source region and domains with high absorption geometries. On this bases, the paper presented a image reconstruction method of generalized pulse spectrum technique based on the P3 equation (P3- GPST), and it is an extent to generalized pulse spectrum technique based on the diffusion equation (DA- GPST). Simulation results show that P3- GPST performs better than DA- GPST.

8230-43, Poster Session

## Polarized reflectance spectroscopy based on polarization maintaining single-mode optical fiber

V. A. Kamensky, A. N. Morozov, M. Y. Kirillin, Institute of Applied Physics (Russian Federation); M. Shakhova, Nizhny Novgorod Regional Hospital (Russian Federation); I. V. Turchin, Institute of Applied Physics (Russian Federation)

In the current paper we present an all-fiber optic-endoscope-compatible device for measuring the backscattered radiation and the effect of micro depolarization in biotissues – a subepithelial endoscopic polarized reflectance spectroscope. We sharply focus probing light on the basal membrane (focal distance 500 μm) to acquire maximum signal from the subepithelium and to remove background noise from the upper layer. The light intensity backreflected from healthy tissue in incident polarization depends on surface epithelium and underneath stromal layers. Intensity of the cross-polarization component is generally determined by the micro depolarization effect and scattering in stroma. In an incipient malignant tumor, cancer cells usually weakly depolarize probing light along basal membrane and the reflected depolarized intensity is much less than in normal tissue. Also, we acquire spectral information from backscattered radiation in orthogonal polarization. The shape of the reflectance spectra depends on tissue elementary scatterer type and orientation and gives additional diagnostic information. Our fiber-optic probe is compatible with biopsy channel of commercially available endoscopes and bronchoscopes so we can examine mucous membranes of hollow organs and serous cover of cavities. The principal possibility of creating a fiber probe for simultaneous detection of scattered radiation in two polarizations with one and the same fiber will make it possible to miniaturize the endoscopic probe, reducing its diameter, as a result of which the probe can be combined with any endoscopic equipment. Such an advantage has a potential as an in vivo puncture biopsy tool.

2. Optical system

To develop a device with a flexible probe we used a single-mode polarization maintaining PANDA type optical fiber to preserve polarization state of light during it propagation.

The choice of such a fiber allows using an optimal self-consistent system to illuminate biological tissue and at the same time receive scattered backscattered radiation. In this system, acquiring and subsequent separation of light scattered in both polarizations occurs simultaneously in one and the same fiber; as a result, it becomes possible to create an all-fiber optic instrument.

The radiation from a fiber pigtailed superluminescent diode (SLD) with 1310 nm central wavelength, FWHM, 45 nm and average optical power 20 mW (Inphenix, USA), passes through an all-fiber polarization controller, fiber polarizer and is linearly polarized with extinction ratio 28 dB. Optical power after PM beam splitter with extinction ratio 26 dB and custom made flexible fiber probe with 1.4 mm diameter and focal distance 500 μm , is focused on the object under investigation, scattered, and partially depolarized inside it.

8230-44, Poster Session

## Development and Eigenvalue calibration of an automated spectral Mueller matrix system for biomedical polarimetry

H. Purwar, Indian Institute of Science Education and Research Kolkata (India); S. Chandel, Ctr. of Excellence in Lasers and Opto-electronic Sciences (India); H. Lakhotia, C. Banerjee, J. Soni, N. Ghosh, Indian Institute of Science Education and Research Kolkata (India)

We present a novel spectral Mueller matrix measurement system for both elastic and inelastic scattering (fluorescence) polarimetric measurements. The system comprises of a Xe lamp as excitation source, a polarization state generator (PSG) and a polarization state analyzer (PSA) unit to generate and analyze polarization states required for 4x4 sample Mueller matrix measurements, coupled to a spectrometer for spectrally resolved (wavelength ~ 400-800 nm) signal detection. The PSG unit comprises of a fixed linear polarizer (polarization axis oriented at horizontal position) followed by a rotatable broadband quarter waveplate. The sample-scattered light is collected and collimated using an assembly of lenses, then passes through the PSA unit, and is finally recorded using the spectrometer. The PSA unit essentially consists of a similar arrangement as that of the PSG, but positioned in reverse order, and with the axis of the linear polarizer oriented at vertical position. A sequence of sixteen measurements are performed by changing the orientation of the fast axis of the quarter waveplates of the PSG unit (for generating the four required elliptical polarization states) and that of the PSA unit (for analyzing the corresponding polarization states). The orientation angles (35, 70, 105 and 140 deg.) were chosen based on optimization of the PSG and PSA matrices to yield most stable system Mueller matrices. The performance of the polarimeter was calibrated using Eigenvalue calibration method which also yielded the actual values of the system PSG and PSA matrices at each wavelength. The system has been automated and is capable of Mueller matrix measurement with high accuracy over the entire spectral range 400-800 nm (elemental error < 0.005). For recording the elastic scattering Mueller matrix of sample, the PSG and PSA matrices for each wavelength are used, while for fluorescence Mueller matrix measurements, the PSG for the excitation wavelength (chosen to be 405 nm) and PSA for varying emission wavelengths (450-800 nm) are used. The developed spectral Mueller matrix system has been initially used to record both elastic scattering and fluorescence Mueller matrices from normal and cancerous cervical tissues. The details of the polarimetry signal analysis for this specific scheme, Eigenvalue calibration results on standard optical elements, as well as initial results of quantitative elastic scattering and fluorescence polarimetry of biological tissues, will be presented.

8230-45, Poster Session

## A new imaging technique for the study of polarimetric properties using light polarization

I. C. Buscemi, S. Guyot, Univ. Paris 12 - Val de Marne (France)

This work is the first presentation of a new imaging technique which enables near real time multispectral acquisition of the so called “Degree Of Polarization” (DOP) in polarimetry, the normalized difference between two intensities of perpendicular polarization states.

Essentially it is used as the contrast element to study the optical properties of a medium and to determine the difference of light propagation in turbid media for different polarization input.

In this sense, it may be described according to the matrix formalism proposed by Jones, Poincaré and Mueller, which is the classical polarimetric approach to study several polarimetric properties like diattenuation, retardance or depolarization. Traditionally this approach is well known considering linear and/or circular polarizations, but beyond that the new improved method also permits the acquisition of DOP for all the possible elliptic ones. This is realized employing an incoherent input white light beam whose polarization is changed without perturbing the system since, using nematic crystals opportunely calibrated, no mechanical tools are necessary.

The aim is to demonstrate that the elliptical DOP degenerate in the linear and circular ones, furthermore the direct acquisition in a few seconds of a complete images’ set for different beam ellipticity and polarization orientation allows the complete dynamical characterization of a complex medium, already including the more traditional studies.

The biomedical application of this method suggests a simple, direct, fast and also easily exploitable future employment, as a desirable mean for clinical investigation. Moreover new elements to improve the model of light scattering will be acquired.

8230-46, Poster Session

## Investigation of diffusely backscattered Mueller matrix pattern of poly-disperse suspensions

P. Sun, X. Cao, Beijing Normal Univ. (China)

When particle size in a complex suspension consisting of a mixture of particle sizes, the Mueller matrix pattern of this suspension is more complex than that of a single-disperse suspension. Here, we investigated the pattern of complex mixtures of polystyrene spheres experimentally and theoretically. In theory, we simulated the Mueller matrices of single-disperse suspension with particle size of 100 nm using Rayleigh scattering theory, whereas we did for particle size of 2000 nm using Mie scattering theory. As a result, both of nine Mueller matrix elements Mij (i, j=1~3) were similar in structure. It can be inferred that the Mie theory is also feasible for the light-particle interaction where the particle size is of the same order as the wavelength. Therefore, we simulated the poly-disperse suspensions mixed with particle size of 100 nm and 2000 nm using Mie theory. The simulation results showed that the patterns of poly-disperse suspensions were more complicated than those of single-disperse suspensions. In experiment, we set up a Mueller matrix imaging system with oblique incidence and normal detection in order to avoid mirror reflection. The light source was a semiconductor laser with wavelength of 780 nm. We imaged the scattering media with particle size of 200 nm, 2000 nm and their mixture using 2D Mueller matrices. The experimental results were corresponding with the theoretical simulations. Especially, we imaged the chicken blood (6 m) added with Intralipid suspension (300 nm) regarded as a phantom of hyperlipidemia. Only four elements (Mij, i, j=1~2) showed clear patterns which similar to those of poly-disperse suspensions.

8230-47, Poster Session

## The reconstruction algorithm for endoscopic diffuse optical tomography based on effective detection area

Z. Qin, H. Zhao, X. Zhou, Y. Yang, F. Gao, Tianjin Univ. (China)

To reduce the cost of near-infrared endoscopic image equipment and the reconstruction time, a measurement method based on the effective detection area is proposed and the corresponding algorithm which simultaneously reconstructs the absorption coefficient and the reduced scattering coefficient is developed. First, the effective detection area is investigated with the Monte Carlo simulation. Secondly, the image reconstruction algorithm based on the effective detection area is studied. The Jacobian matrix is built by combining the adjoint method with the modified Generalized Pulse Spectrum Technique and calibrated by the maximum of its absolute value. The Generalized Minimal Residual Krylov method is used to obtain the iterative update factor. Finally, the impact of the number of measured points in the effective detection area on the reconstructed results is discussed, and the developed algorithm is verified by the simulation data and measured data. The results show that the reconstructed algorithm based on the effective detection area has equivalent accuracy to the traditional ones. The fidelity of reconstructed absorption and reduced scattering coefficient can be up to 80%, respectively. The scales and positions of the reconstructed lesions are both correspondent to the true and the reconstruction time is reduced by half. And the cross-talk between the absorption and reduced scattering images is small. The optimal number of sources and detectors is 16 depending on the scale of the simulation model. The detection using the effective detection area and the developed reconstruction algorithm will promote the development of diffuse optical tomography which is applied to cervical and other tubular organs.

8230-48, Poster Session

## Diffuse photon-pairs density wave for the detection of changes of glucose in highly scattering medium

L. Yu, C. Chou, Chang Gung Univ. (Taiwan); L. Su, J. Wu, National Central Univ. (Taiwan); Y. Wu, National Yang Ming Univ. (Taiwan); C. Lai, Chang Gung Univ. (Taiwan)

We proposed diffuse photon-pairs density wave to measure the glucose-induced scattering changes in a highly scattering medium. The range of changes of glucose in physiologically relevant level was measured. The results demonstrate the detection limit on changes of glucose can be archived to 4mM, which are distinct improvements compared with diffuse measurement of glucose by using standard diffuse photon density wave. Although the limit of detection of glucose (4mM) does not meet the clinically acceptable level (1mM), this method show a potential to develop a CGMS as a warning system to discriminate between hypoglycemia and hyperglycemia in patients with diabetes.

8230-49, Poster Session

## Nondestructive determination of absolute concentration of admixtures in turbid media by means of diffuse reflectance spectrophotometry without phantom calibration and preliminary measurements

A. V. Lappa, A. N. Kulikovskiy, A. Kulikovskiy, Chelyabinsk State Univ. (Russian Federation); V. A. Privalov, Chelyabinsk State Medical Academy (Russian Federation)

This paper presents a new method for distant determination of concentration of light absorbing admixtures in turbid media. It is supposed that there is a wavelength region where the absorbent has a narrow absorption peak and medium absorbance (without absorbent) varies smoothly. Main application of the method is photodynamic diagnostics where the turbid medium is biological tissue, and the absorbent is photosensitizer. The method uses a probe with 3 optical fibers: one illumination fiber for light delivery from white source to media, and two reading fibers for delivery of reflected light from media to spectrometer.

Determination of admixture concentration includes 2 stages (performed in one measurement-calculation procedure): evaluation of medium optical parameters at the edge of absorption peak, and calculation of concentration from spectra at the peak.

There are several features in the method:

the value to be determined is absolute concentration of admixtures;

the method needs no calibration measurements on phantoms with given admixture concentrations;

it needs no reference measurements on sample with zero admixture concentration;

it uses a new two parametric kinetic model for description of light propagation in medium and no questionable assumptions (diffusion approximation for light propagation, Bragg's rule for determination of mixture absorption coefficient, Mie theory for scattering coefficient and so on);

it uses original algorithms to resolve direct and inverse tasks of radiation transport theory, including Green function approach, the similarity transformation, and a special non-analog correlated technique of the Monte Carlo method.

Tests on tissue phantoms showed good performance of the presented method.

8230-50, Poster Session

## Experimental estimation of the sensitivity profile of time-resolved diffuse reflectance: experiments on cadavers

P. Sawosz, M. Kacprzak, Institute of Biocybernetics and Biomedical Engineering (Poland); W. Weigl, A. Borowska-Solonynko, P. Krajewski, Medical Univ. of Warsaw (Poland); N. Zolek, R. Maniewski, A. Liebert, Institute of Biocybernetics and Biomedical Engineering (Poland)

In near infrared spectroscopy the light penetration depth and spatial distribution of visiting probability of photons should be considered for proper interpretation of the acquired signals. The sensitivity of the measurement to the changes of absorption can be calculated with the use of numerical methods like Monte Carlo simulations or diffusion theory. In this study, we proposed a method for experimental estimation of distribution of light penetration probability in human head. Time-gated, intensified CCD camera was applied for imaging of a head of the cadavers. The top of the head was cut off and the brain was exposed together with overlaying extracerebral tissues (skin, skull). The camera was positioned above the head allowing for imaging of the brain in the plane perpendicular to the direction of the incident light. Two fibers were attached at the edge of the head in separation of 2 cm and 3 cm. The fibers delivered femtosecond light pulses from a Ti:Sapphire laser at 780 nm and 830 nm. The images were acquired for each fiber separately with recording of distribution of time of flight of photons (DTOF) for each voxel located on the surface of the phantom. Distribution of visiting probability of photons virtually travelling between source and detector was calculated by convolving the DTOFs recorded in each voxel for the two source positions. The experiments allowed to assess influence of inhomogeneities of the tissues of the head on the time-resolved distribution of light penetration probability.

8230-51, Poster Session

## Single-mode and subcellular fiber probes for cell scattering and density variation measurements

D. Kokkinos, R. Sullivan, N. Gadura, S. Dehipawala, G. Tremberger, Jr., T. Holden, P. Schneider, D. Lieberman, T. D. Cheung, Queensborough Community College (United States)

Cell density is an important parameter in the question of bio-variation and the studying of cell scattering could be a viable tool. The development of spatially resolved optical fiber probe would enable the characterization of optical scattering from cells within a colony. Single mode fiber probe would be budget friendly as compared to a 50-nm sub-cellular fiber probe. This project aims to develop a calibration procedure to correlate the optical scattering measured by a single mode fiber probe to that of a 50-nm sub-cellular fiber probe in the context of cell density variation. Data was modeled with Monte Carlo simulation for the observed non-Gaussian signals. Microscopy and centrifuge data were used as the density standards. Yeast, Staphylococcus aureus and breast cancer cell MDA-231 colonies were studied. The results show that the calibration procedure for yeast could be established in a single wavelength and the breast cancer MDA-231 would require spectral information. The use of a 50-nm sub-cellular fiber probe for detailed studies of breast cancer MDA-231 will be discussed.

# Conference 8231: Nanoscale Imaging, Sensing, and Actuation for Biomedical Applications VIII

Wednesday-Thursday 25-26 January 2012

Part of Proceedings of SPIE Vol. 8231 Nanoscale Imaging, Sensing, and Actuation for Biomedical Applications VIII

8231-33, Session

## Engineering nanodevices based on molecular motors

H. Hess, Columbia Univ. (United States)

Biomolecular motors can serve as biological components in engineered nanosystems, such as molecular shuttles. The development of this system has revealed a number of challenges in engineering at the nanoscale, particularly in the guiding, activation, and loading of these shuttles. A proof-of-principle application of the developed technologies is a “smart dust” biosensor for the remote detection of biological and chemical agents, which is enabled by the integration of recognition, transport and detection into a submillimeter-sized microfabricated device.

8231-35, Session

## From molecular motors to fungal intelligence

D. V. Nicolau, Univ. of Liverpool (United Kingdom)

Protein molecular motors are natural nano-machines that convert the chemical energy obtained from the hydrolysis of adenosine triphosphate (ATP) into mechanical work which is central to cellular motion, muscle contraction, cell division and a multitude of other critical biological processes. Remarkably, protein molecular motors differ fundamentally from artificial devices in that the conversion from chemical energy to mechanical energy is done directly, rather than via an intermediary state as in e.g., heat for thermal engines. This fundamental difference results in a far better efficiency (close to 100%, for both linear and rotary motors) of these natural mechanical devices compared to artificial ones. This exceptional efficiency, together with the small scale of protein molecular motors, has prompted an increasing number of studies focused on their integration in hybrid micro- and nanodevices. However, and despite tremendous progress in the engineering of molecular motors, much needs to be learnt from Nature, in particular regarding the cooperative behaviour of molecular motors in vivo, before coming even close to efficiency in in vitro devices.

Filamentous fungi are very successful in colonizing micro-confined maze-like networks (e.g., soil, wood, leaf litter, plant and animal tissues), suggesting that they may be efficient solving agents of geometrical problems. The growth behaviour and optimality of space-searching algorithms of several fungal species has been tested in microfluidic mazes and networks. First, it was found that the growth behaviour of all species was strongly modulated by the geometry of micro-confinement. Second, the fungi used a complex growth and space-searching strategy comprising two algorithmic subsets: (i) long-range directional memory of individual hyphae and (ii) inducement of branching by physical obstruction. Third, stochastic simulations using experimentally measured parameters showed that this strategy maximizes both survival and biomass homogeneity in micro-confined networks, producing optimal results only when both algorithms are synergistically used.

8231-01, Session 1

## Imaging caveolae-mediated transport of nanoparticles using superresolution microscopy

Z. Wang, C. Tiruppathi, R. Minshall, A. B. Malik, Univ. of Illinois at Chicago (United States)

Caveolae are membrane invaginations of 50-100 nm in diameter that bud from the membrane to form vesicles. Caveolar structures in endothelium might be exploited to efficiently transport therapeutic nanoparticels across endothelial barrier, but it remains determined. Recently, we designed bovine serum albumin (BSA)-conjugated fluorescent nanoparticles that can bind to the receptors in the caveolae in bovine lung endothelial cells. Co-localization of caveolin-1, a protein associated with caveolae, with the internalized BSA-conjugated nanoparticles indicates BSA-conjugated nanoparticles are internalized in caveolae. To determine the caveolar size and dynamics in live endothelial cells, we developed the super-resolution microscopy using a dual-color nanoparticle pair. Using this method, we optically measured the caveolar size based on the combination of different size of the nanoparticle pair. The result is consistent with the TEM measurement. In addition, we measured the transport of BSA-conjugated nanoparticles across a monolayer of endothelial cells using Transwell, and found that the transcytosis of 20nm-sized nanoparticles is more efficient than 100nm nanoparticles. This finding is consistent with our observations that caveolar size is a key determinant of the uptake of nanoparticles in endothelial cells. We also studied caveolae-mediated transport of albumin-conjugated nanoparticles in microvessels using intravital microscopy. The result shows that caveolin-1 knockout mice reduce the internalization of nanoparticles in vessel walls, suggesting that caveolar structures in endothelium play a role in transporting nanoparticles across endothelial barrier. In summary, we have demonstrated the potential of exploiting caveolae to efficiently deliver therapeutic nanoparticles across endothelial barrier using advanced microscopy (super-resolution microscopy and intravital microscopy).

8231-02, Session 1

## Tunable near-infrared dispersive quantitative phase microscopy

N. Cardenas, S. K. Mohanty, The Univ. of Texas at Arlington (United States)

Refractive index (RI) plays a major role in interaction of electromagnetic wave with matter. Further, dispersion of refractive index is an intrinsic optical property and highly-dependent on shape and phase of nanoparticles. Therefore dynamic measurement of dispersion at individual particle level can provide critical insight into shape and phase transformation. While conventional method such as ellipsometry requires isotropic sample and has limited spatial as well as temporal resolution, quantitative phase imaging (QPI) has proven to be a useful tool to estimate the RI from the sample-induced phase delay measurement at high spatio-temporal resolution. Here, we introduce near-infrared dispersive quantitative phase imaging (NIRD-QPI) of micro and nanoscopic objects. NIRD-QPI is achieved by integration of QPI with a tunable near-infrared laser source. In order to achieve QPI, digital holographic microscopy was employed using a modified Mach-Zehnder interferometer with digital recording of interference pattern of the reference and sample laser beams. High resolution refractive index spectroscopic measurement over a range from 690 to 1040nm in interval of 10nm was made to quantify dispersion. Thus, many types of nanoparticles and their allotropic forms can be differentiated by their dispersion measurement using the NIRD-QPI method.

8231-03, Session 1

## Multiprobe AFM bio-imaging: the next evolution in SPM

A. Lewis, Hebrew Univ. of Jerusalem (Israel); R. Dekhter, G. Fish, S. Kokotov, M. Kokotov, H. Taha, D. Lewis, Nanonics Imaging Ltd. (Israel)

Atomic force microscopy (AFM) with tuning fork feedback is the best method of AFM imaging known today. This presentation will describe the operation of this feedback mechanism in liquid. This allows for live cell AFM and NSOM operation in physiological media with high Q factors and without severe damping effects or any optical or mechanical constraints or interference. The extension of this frequency modulation feedback mechanism to tuning fork based liquid operation allows for scanned probe microscopy (SPM) cellular imaging fully integrated with any optical microscope including upright, 4 pi or standard Raman microprobes. It also will be shown that water immersion objectives can now be used with SPM and that these new directions allow for the first time live cell bioimaging with NSOM in spite of the stiff cantilevers that are generally associated with NSOM probes. The advances reported in this presentation, along with additional innovations in probe and scanner developments, allow for the dream of multiprobe NSOM/SPM to be implemented in physiological media. The results of these efforts portend important advances in the application of SPM in structural and functional bioimaging.

8231-04, Session 1

## Development of photonic force microscopy with chemical mapping function

S. Heo, K. Kim, Y. Cho, KAIST (Korea, Republic of)

Photonic force microscopy is an optical tweezers-based scanning probe microscopy, which measures the forces in the range of fN to pN. These low forces minimize mechanical deformations of soft biological samples.

We introduce an advanced photonic force microscopy to stably map various chemical properties as well as topographic information, utilizing weak molecular bond between probe and object's surface.

First, we constructed stable optical tweezers minimized instrumental noise, where an IR laser with 1064 nm wavelength was used as trapping source to reduce damage to biological sample and two-axis Galvano mirror were used for x, y directional probe scanning and a piezo stage was used for z directional probe scanning. We measured temporal fluctuation of probe's position to detect the moment of contact between probe and surface. The condition of probe scanning was optimized to image stable topographic map.

To test the chemical mapping, we designed oligo DNA pair with a fluorepore and measured the bonding strength of single pair, in which non-fluorescent oligo DNA was attached on probe and fluorescent oligo DNA was attached on surface. We measured the rupture force of molecular bond to measure chemical property on the surface placed the probe. The 2-dimansional image constructed by bond strengths was compared to the fluorescence imaging before probe scanning.

We expect this system can realize a high-resolution multi-functional imaging technique able to acquire topographic map of objects and to distinguish chemical difference between these objects simultaneously.

8231-07, Session 1

## Investigation of nanostructure scattering and absorption for combined optical diagnostic and therapeutic applications

M. Angelidou, C. Pitris, Univ. of Cyprus (Cyprus)

Medical applications of metal nanoparticles are the subject of intense research due to their unique properties which make them suitable for both diagnostic and therapeutic use. One such property is surface plasmon resonance which results in strong enhancement of the absorption and scattering of electromagnetic radiation. The combination of metal type, size, and shape characteristics provides unique tunability of a nanostructure's optical properties. Several types of nanoparticles have been explored for medical and biological applications. Here we present a theoretical investigation of novel metal nanostructures which have distinct absorption and scattering extinction maxima. This could be beneficial for combined diagnostic and therapeutic applications since the diagnostic and therapeutic laser wavelengths can be decoupled for increased efficacy and safety. For this purpose, it is desirable to have the most intense scattering, with minimal absorption, in the near-infrared for imaging and the opposite in the red, for therapy. The extinction efficiency of various metals, shapes and sizes was first calculated using the Discrete Dipole Approximation (DDA) method. From the results, nanostructures consisting of combinations of cubes and spheres were found to have the most appropriate scattering and absorption spectra and their optical properties were thoroughly investigated. The size, number and material (silver or gold) of the nanospheres and, to a lesser extent, the dimensions of the cubes were varied in order to obtain the optimum nanostructure with distinct absorption and scattering profiles. Given its properties, these nanostructures have the potential to be used for enhancement of various imaging and therapeutic methods.

8231-25, Session 1

## Multifunctional cell therapeutics with plasmonic nanobubbles

D. Lapotko, Rice Univ. (United States)

By exploiting the physical and optical properties of the newly discovered nano-phenomena, plasmonic nanobubbles we developed a new flow technology with single cell selectivity and high throughput for the multipurpose processing of cellular therapeutics. This technology is based on the controlled formation (in time, space and volume) of plasmonic nanobubbles around gold nanoshells and supports promising cellular and genetic therapies that are currently limited by the insufficient selectivity, safety and productivity of existing techniques. We show that the ability to genetically modify target cells and simultaneously eliminate other specific cells from a highly heterogeneous cell system (graft), with single cell selectivity and without compromising other important cellular components, increases the feasibility of ex vivo gene therapies and other cell-based interventions used for the treatment of human disease including cancer. High specificity, selectivity and speed of cell processing (including intracellular delivery of molecular cargo, gene transfection and elimination of target cells) was achieved with a new class of cellular nanoprobes we recently discovered, called plasmonic nanobubbles (PNB). A PNB is a nanosecond event (not a particle), and possesses the dual mechanical and optical properties of a vapor nanobubbles with precisely and dynamically tunable effects, allowing simultaneous optical detection and mechanical transmembrane injection or immediate ablation of individual specific cells. In this application we developed the methods required to use the PNB for ex vivo gene and cell therapy. The subsequent applications of the technology, however, will be much broader since it may be applied to processing any liquid tissues with targets such as cells, bacteria and viruses.

8231-05, Session 2

## Multimodal spatially resolved near-field scattering and absorption spectroscopy

E. Ostertag, T. Merz, R. W. Kessler, Reutlingen Univ. (Germany)

Several near-field techniques have been developed over the past years: tip - enhanced Raman spectroscopy is now well established, in transmission or reflectance spectroscopy usually aperture limited systems are used which generally suffer from a low light flux through the near-field probe. To increase the signal to noise ratio we have integrated a solid immersion lens (SIL) into an universal micro-spectrophotometer (Zeiss) or into a confocal Raman spectrometer (WiTec) by assistance of a scanning probe microscope. The SIL is a hemispherical lens with a conically sanded tip at the bottom and is placed between the sample and the microscope objective. The conical tip acts as an optical converter into the evanescent field on the sample surface. The evanescent field is then converted into the SIL to a propagating field, which can easily be measured through a monochromator and a photomultiplier, thus allowing optical spectroscopy with a high S/N ratio. We can show, that even with a tip radius of > 350 nm, the lateral resolution can be smaller than 30 nm. Further extensions to a multimodal near-field hyperspectral imaging system are the integration of additional detectors allowing besides Raman Spectroscopy also (UV), VIS, NIR and 2D-fluorescence and fluorescence lifetime imaging with the same sample. The combination of stray light spectroscopy and aborption spectroscopy allows a comprehensive characterization of e.g. chromosomes, cancer cells, macrophages, monocytes etc.

8231-06, Session 2

## Near-field coherent anti-Stokes Raman scattering microscopy using radially polarized light

K. Er, J. Lin, Z. Huang, National Univ. of Singapore (Singapore)

CARS is meritorious in its ability to perform chemical selective imaging, but its spatial resolution is limited by the diffraction limit of light; however, this limit can be broken by combining CARS and near-field scanning microscope. In this work, we report a novel radially polarized near-field coherent anti-Stokes Raman scattering microscopy (RP-NF-CARS), which uses radially polarized light as excitation to enhance the electric field enhancement under a metallic tip, and improves the signal to background ratio compared with that using linearly polarized excitations. We applied RP-NF-CARS to image nano-scale polystyrene beads and biological system.

8231-09, Session 2

## In vivo visualization of abnormal microvascular features in oral precancerous lesions by two-photon luminescence of gold nanorods

G. Vargas, S. Motamedi, K. Trahan, T. Shilagard, K. Edward, S. Qiu, The Univ. of Texas Medical Branch (United States)

Gold nanorods (GNRs) exhibiting two-photon induced photoluminescence are of great interest as contrast agents for in vivo imaging due to their ability to be excited with low incident powers and well-defined spectral properties. GNRs were used for intravital imaging of oral neoplasia. In particular GNRs provided contrast for visualization of the microvascular structure in oral precancerous lesions at low incident powers, revealing abnormalities. Quantitative image parameters describing vessel properties were qualitatively correlated to histology observations and temporal dynamics of the GNRs within the angiogenic regions were investigated.

Oral carcinogenesis was induced in the buccal pouch of Golden Syrian hamsters by thrice-weekly topical application of 0.5% 9,10-dimethyl-1,2-benzanthracene (DMBA). Hamsters received treatment for 12 weeks, when a variety of preneoplastic and neoplastic lesions were present. Dysplastic sites in DMBA hamsters and normal sites in control hamsters were imaged in vivo prior to i.v. delivery of GNRs, at 10 minutes, and up to 24 hours, after which a biopsy was obtained and samples stained with H&E and Verhoeff-Van Gieson (VVG) stain to confirm presence of vessels. To quantify vessel features, reconstructed 3D TPL images of the vascular network were evaluated for 1) number of vessel branch junctions and 2) distance between branch junctions. For each biopsy, a vessel count was performed on VVG stained single sections at 40x magnification

GNRs were >40 times brighter than surrounding tissue. Intravital imaging revealed 3D microvasculature, and in dysplasia, abnormal vessels (dense and tortuous) compared to normal. GNRs were diffusely distributed in lesions after 24 hours. Image based features of abnormal vessel structure correlated wel with histology and were consistent with recent finding of angiogenesis in dysplasia.

8231-10, Session 3

## Double resonance light scattering from gold nanoparticles on interferometric surfaces

K. Hayrapetyan, D. D. Nolte, C. A. Savran, K. M. Arif, Purdue Univ. (United States)

The detection and classification of nanoparticles is important for achieving high (efficient) contrast in biomedical imaging and sensing applications. Nanoparticle-based molecular assays have the advantages of fast analyte capture combined with low analyte depletion compared with micron-size bead-based assays. However, the advantages of the small nanoparticle size carries with it the disadvantage of low light scattering. This disadvantage can be alleviated by resonant enhancement of light scattering. In this paper, we identify a double resonance condition when gold nanoparticles are placed on an interferometric surface. The double-resonance condition for high-contrast detection is achieved when the resonance from an asymmetric Fabry-Perot condition of a substrate overlaps with the plasmon resonance of Mie scattering by the gold nanoparticles. The double resonance condition was predicted in the framework of a Modified Double Interaction Model (MDIM) and verified experimentally by studying the scattering of light by gold nanoparticles on thermal oxide on silicon using molecular interferometric imaging (MI2). An AFM scan of the sample was used to estimate the coverage and find clustering of nanoparticles on the surface. The spectrum of isolated and multiple nanoparticles was measured using MI2 and was in good agreement with the simulation of the MDIM model. The MDIM model explicitly includes multiple scattering between the particle and the substrate, including the phases of the partial scattered waves. Under resonance (and anti-resonance), the multiple scattering phases combine or cancel to provide the largest contrast for imaging and diffraction-based biosensor detection.

8231-11, Session 3

## Diffraction-based nanoparticle biosensors

H. Sun, K. Hayrapetyan, D. D. Nolte, C. A. Savran, Purdue Univ. (United States)

Detection of gold nanoparticles has important biomedical applications such as tracing biological objects and in molecular biosensors. For instance, nanoparticle-based molecular assays have the advantages of fast analyte capture combined with low analyte depletion. However, the advantages of the small nanoparticle size carries with it a distinct disadvantage for image-based detection compared with micron-size bead-based assays. This disadvantage can be alleviated by using diffraction-based detection that captures the combined scattered fields of all particles instead of the small scattered fields from each particle as in an imaging bead-counting system. The single-point diffraction detection also has considerably larger throughput than imaging approaches with considerably lower data storage requirements. In this paper, we compare diffraction-based vs. image-based detection of 100 nm radius gold nanoparticles. Dilute dispersions of gold nanoparticles are printed on silicon wafers in 50 micron stripes by nonspecific binding to bovine serum albumin (BSA) immobilized using physical adsorption. Diffraction measurements on the gold nanoparticle stripes are compared with both AFM measurements and imaging measurements performed using molecular interferometric imaging (MI2) on interferometric substrates. Numerical modeling of the two optical detection approaches is done using a Modified Double Interaction Model (MDIM) enabling numerical results to be compared with experiment. An interesting qualitative difference between diffraction and imaging arises because of the homodyne and heterodyne interferometric conditions, respectively. We find for the small 100 nm radius gold particles that diffraction is more reliable and faster than image-based approaches.

8231-12, Session 3

## Utilizing nonlinear optical properties of nanoparticles for imaging and sensing

B. G. Yust, N. Razavi, F. Pedraza, D. K. Sardar, The Univ. of Texas at San Antonio (United States)

Nonlinear optical properties of barium titanate (BaTiO3) nanoparticles, such as second harmonic generation and four wave mixing, are investigated as a function of size and shape. BaTiO3 is an attractive option as a nonlinear material because it can exhibit a high second and third order electronic susceptibility even at the nanoscale. The nonlinear response is first quantified by hyper-Rayleigh scattering as well as pump-power dependence of the nonlinear signals (second harmonic generation and optical phase conjugate). These particles are employed as contrast agents/biomarkers and phase conjugate nanomirrors in imaging, utilizing second harmonic generation for two-photon microscopy and four-wave mixing for scattering reversal image enhancement. Gold and silver are also used to create a shell around the BaTiO3 nanoparticle to see if a core/shell structure enhances any of the nonlinear effects. The practicality of these particles as markers, nanomirrors, and contrast agents will also be discussed.

8231-13, Session 3

## Toward the use of two-color emission control in upconverting $NaYF_4:Er^{3+},Yb^{3+}$ nanoparticles for biomedical imaging

C. F. Gainer, G. S. Joshua, M. Romanowski, The Univ. of Arizona (United States)

In the interest of generating new biomedical sensing techniques as well as improving those that currently exist, a great deal of attention has been given to upconverting lanthanide nanoparticles in recent years. In order to develop these nanoparticles for use in multiplexed and ratiometric sensing techniques, many recent studies have focused on experimental control of their emission wavelengths. Here we describe a new method for controlling the relative intensity of green and red emission bands in $NaYF_4:Yb^{3+},Er^{3+}$ nanoparticles via control of the excitation pulse repetition rate. Using this method, particles of the same composition may be tuned to produce red and green light in user-defined ratios. We discuss the mechanism behind this control as well as potential applications that could make use of this property, specifically in super resolution imaging techniques.

8231-14, Session 3

## Study on translating the nanoparticle-protein corona into microbubble contrast agents

W. Chuang, W. H. Chang, T. Huang, C. Chen, Chung Yuan Christian Univ. (Taiwan); W. T. Lai, Taipei Medical Univ. (Taiwan); C. J. Lin, Chung Yuan Christian Univ. (Taiwan)

In this study, a fast and easy way, capable of integration and multi-functionalization of nanoparticles was purposed. The albumin was be chosen because of its' abundant study and one of the most amount proteins in human serum. The albumin is adsorbs on nanoparticles or nano-clusters surface by static fore, in which nanoparticles are containing hydroxyl group on their surface. The corona shape was then performed, after the adsorption between nanoparticles and albumins. This kind of complex has been called nanoparticle-protein corona. The proteins' shell can be improved the biocompatibility and formed as protection media for nanoparticles. The nanoparticles within a corona-shaped shell was observed by transmission electron microscopy, and provided the information that nanoparticle-protein corona can be formed. Varies of nanoparticles, albumin and their protein corona were analyzed by spectra, finding the difference in protein structure, surface plasma resonance effect and photoluminescence between them. Micro-emulsion by sonication was utilized to fabricate the microbubbles, which was transformed from nanoparticle- protein corona. The microbubbles were exposed to ultrasound radiation of medical image system, confirming the microbubble has ability to increase the contrast of image. Herein, the study also observed and detected the morphology and optical feature of microbubbles by confocal laser scanning microscopy, in order to assure the microbubbles had been formed and nanoparticles were inserted in bubbles' shells. Acts as substrate between nanoparticles, albumin were transformed into microbubbles not only improved their performance when nanoparticles' centralization in bubble, but also rendered nanoparticle-protein corona has complexable potential.

8231-15, Poster Session

## Concentration and detection of bacteria in virtual environmental samples based on non-immunomagnetic separation and quantum dots by using a laboratory-made system

Z. Cheng, T. Wu, F. Chen, Y. Du, B. Gu, Z. Yang, Institute of Medical Equipment (China)

This study investigated a method that simultaneously detects three bacteria, Salmonella typhimurium, Escherichia coli, and Staphylococcus aureus in virtual environmental samples via an approach that combines un-immunized magnetic nanoparticles for the enrichment and antibody-conjugated quantum dots (QDs) as fluorescence markers, by using a laboratory-made system. In the enrichment procedure, the un-immunized Fe2O3 magnetic nanoparticles and the three bacteria formed "bead-cell" complex by the electrostatic attraction effect. Magnetic nanoparticles with different size(100nm, 180nm) were used and some interferents (soil,milk, biscuit and grass) were added into the bacteria suspension respectively to check the influence on concentration efficiency. In the immuno-fluorescence labeling procedure, QDs with different emission wavelenghs were immobilized with anti-E.coli antibody, anti-S. typhimurium antibody, and anti-S.aureus antibod, respectively. Anti-body conjugated QDs capture the bacteria selectively and specifically so that "sandwich" complex were formed. The suspension of the labeled bacteria was trickled onto a filter film. A 450nm semiconductor laser was used as a part of the laboratory-made system to excite the QDs. Three PMT detectors were utilized to detect the fluorescence intensity. In our method, we tested E.coli, S.aureus, and S.thphimurium, respectively from 10cfu/mL to 106cfu/ml. The un-immunized magnetic nanoparticles adsorbed more than 85% of all bacteria. The system could detect bacteria at 103cfu/ml. These un-immunized magnetic nanoparticles can be applied in nonspecific separation and enrichment of bacteria from environmental samples, and this method, of which the detection procedures are completed within 2 h, can be applied to the cost-effective and rapid detecting of bacteria contamination.

8231-16, Session 4

## Optical mapping by low-cost instrumentation and disposable chemically induced nanochannels

P. J. R. Roche, M. C. K. Cheung, McGill Univ. (Canada); L. Beitel, M. A. Trifiro, Lady Davis Institute, Jewish General Hospital (Canada); A. G. Kirk, V. P. Chodavarapu, McGill Univ. (Canada)

Elongation of DNA within nanochannels is becoming a popular academic approach in biophysical studies of DNA with envisaged applications ranging from the single molecule study of DNA binding proteins to genomic investigations of variance. An important consideration of single fragment DNA analysis is the potential to investigate the degree of variance in DNA extracted from cancerous cells in comparison to non-cancerous cells. To develop a rapid method of variance quantification would present clinicians and life scientists with a tool for both diagnosis and investigation of disease progression. A central issue with transitional technologies and particularly restriction digest optical mapping is the expensive optical instrumentation and multi-step fabrication of nanochannels via electron beam /focused ion beam lithography and etch processes. At present the cost of nanofluidic chips is limiting with regards to cost. A system is presented for the detection of YOYO-1 labelled linearized DNA within chemically formed nanochannels on a polystyrene chip. Elongation of the restriction digest fragments is accomplished by capillary driven flow through nanochannels. The inverted microscope developed is compact and of low cost but offers the sensitivity to detect individual fragments within channels down to a resolution of 265nm. Fragments ranging from 0.56Kb to 9.4Kb of the λ-phage genome were detected. Correlation between regions of YOYO-1 emission and fragment length was determined and non-linearity observed for the correlation between larger fragments and peak emission, indicative of a incomplete linearization of larger fragment or coiling under the de Gennes regime. Discussion includes applications for transcriptome and genomic analysis.

8231-17, Session 4

## Surface-enhanced biodetection on a CMOS biosensor chip

F. Belloni, F. Pippig, S. Contie, F. Vicaire, PixinBio SA (France); R. M. Owens, Ecole Nationale Supérieure des Mines de Saint-Étienne (France); H. Rigneault, Institut Fresnel (France)

Lab-on-a-chip devices are mainly characterized by miniaturization but are often complex and difficult to mass-product. Furthermore the often used far field optical detection proves to be far from optimal to detect the faint fluorescence signal emitted from the targeted bio-molecules. Here we present the development of a low-cost, simple, portable device based on CMOS photodiodes technology for the detection and quantification of biological targets through light detection, presenting high sensitivity, multiplex ability, and fast data processing. The key feature of our approach is to perform the analytical test directly on the CMOS sensor surface, improving dramatically the optical detection due to optical confinement of the molecule emitted light into the high refractive index semiconductor CMOS material. We compared the developed device with a commercial spectrophotometer and found similar intrinsic sensitivities in the fM range. Based on adequate surface chemistry modifications, we performed proof-of-concept bio-assays directed against typical immuno-makers such as inflammatory cytokines. The cytokine bio-assay is based upon an ELISA method and showed challenging sensitivity towards a reference ELISA kit. This promising type of device should be of great interest in the field of water quality monitoring and, through its versatility, may evolve towards a challenging clinical application.

8231-18, Session 4

## Porous polymer-based optically selective nanostructures

A. N. Cartwright, Univ. at Buffalo (United States)

No abstract available

8231-19, Session 4

## Bragg-grating air-slot optical waveguide for label-free sensing

A. S. Jugessur, J. J. Dou, M. Yagnyukova, J. S. Aitchison, Univ. of Toronto (Canada)

The development of miniature and label-free optical sensors is very critical for applications in a wide range of areas such as medicine, environment, forensic and food quality control. There is a growing demand for bio-medical diagnostics tools for rapid analysis of small samples volume. As a result, there have been several reports on different types of optical transduction and sensing mechanisms such as surface plasmon resonance [1, 2], refractive index change [3, 4, 5] and Raman scattering [6, 7]. Optical sensing using a photonic wire Bragg grating [4] and Bragg grating microcavity [8] structures have been demonstrated. In this work, a Bragg-grating air-slot waveguide is designed (using Finite Domain Time Difference modeling (FDTD)) and fabricated (using Electron beam lithography and Reactive ion etching) on silicon on insulator to develop a label-free optical sensor. Slot waveguides have recently received much interest for light guiding [9] and sensing [10]. The Bragg gratings constitute of recesses in the 120 nm air-slot waveguide. The grating structures generate a band-gap for certain frequencies and the spectral shift of the upper band-edge is used as the mechanism to sense fluids or bio-molecules in the air-slot. Based on the 3-D FDTD results, the sensitivity of our device is 620 nm/RIU, which is higher than other recently reported sensors [11]. Due to the high electric field intensity in the air slot, this area becomes very sensitive to index variations caused by bio-molecules or fluids in the air-slot. This device can also be potentially useful as a label-free optical sensor for DNA and RNA sensing.

[1] J. Homola, S.S. Yee, G. Gaugliz, Sens. Actuators, B 54, 3-15, 1999

[2] M. T. Flanagan, R. H. Pantell, Electron. Lett. 20, 968-970, 1984

[3] W. C. L. Hopman, P. Pottier, D.Yudistira, J. V. Lith, P. V. Lambeck, R. M. De La Rue, A. Driessen, H. J. W. M. Hoekstra, R. M. de Riddler, Select. Topics in Quant. Electron. 11, 11-16, 2005

[4] A. S. Jugessur, J. Dou, J. S. Aitchison, R. M. De La Rue and M. Gnan, Microelectron. Eng., 86, 1488-1490, 2009

[5] T. Xu, N. Zhu, M Y.-C. Xu, L. Wosinski, J. S. Aitchison and H. E. Ruda, App. Phys.

Let. 94, 241110, 2009

[6] A. Mahadevan-Jansen, Biomed. Phot. Handbook, in: T. Vo-Dinh (Ed.) CRC Press,

Boca Raton, 2003

[7] N.R. Isola, D.L. Stokes, T. Vo-Dinh, Anal. Chem. 70, 1352-1356, 1998

[8] A. S. Jugessur, M. Yagnyukova, J. Dou and J. S. Aitchison, OSA Integrated Photonics Research, Toronto, 2011

[9] Q. Xu et al., Optics Letters, 29, 14, 1626-1628, 2004

[10] C. A. Barrios, Sensor, 9, 4751-4765, 2009

[11] T. Claes et al., IEEE Photonics Journ., Vol. 1, No. 3, 197-204, 2009

8231-20, Session 4

## A nanorod polymer micro-array formed by microcontact printing

P. J. R. Roche, S. Wang, M. C. K. Cheung, V. P. Chodavarapu, A. G. Kirk, McGill Univ. (Canada)

In previous work, we demonstrate a simple approach to creating a plasmonic polymer microarray using a low cost tape methodology. Reflecting upon the need for greater spot density while still maintaining the objective of low cost analysis, the next generation of device is described where density up to 24000 sensing spots is achievable. A localised surface plasmon micro-array is described formed by single or multiple deposition of a nanorod plasmonic polymer by micro-contact printing. The structure of the polymer can be made micro-porous and thickness can be controlled by a cyclical deposition and rapid heat cure protocol. The consistency of feature deposition is assessed. The resulting micro-structure provides a large surface area for immobilisation of biomolecules for assay development. Dark-field analysis of the polymer demonstrates complex microstructure but intense Mie Scattering as expected from gold nanorods. Using fluorescence confocal analysis images of the polymer demonstrates two independent photo-luminescent emission spectra. The two independent emission spectra are linked to the positions of the localised surface plasmons of the nanorods, using a pump source of 543nm excites the transverse plasmon (peak at 550nm) and it's commensurate emission, but doesn't excite the longer emission that is linked to the longitudinal Plasmon around 737nm. The different emissions are demonstrated in the illumination of different portions of the polymer matrix under each pump source excitation. The potential for multiple spectroscopic biosensor analysis is discussed.

8231-21, Session 4

## Silicon cell culture templates with nanotopography: periodic nanostructures and random nanoporous topologies generated by high repetition-rate sub-15-femtosecond pulsed near-infrared laser light

M. H. Straub, A. Uchugonova, K. König, Univ. des Saarlandes (Germany)

In recent years a variety of studies has demonstrated that artificially generated microenvironments can exert a strong influence on cell development in the culture dish. In particular, cells tend to adapt themselves to elongated micro- and nanostructures. Thus, nanostructured substrates are of significant interest in the biological and biomedical sciences as adhesion and development of cells can be controlled via the topological surface properties. In contrast to earlier approaches relying on electron beam or nanoimprint lithography, in our contribution nanostructures were produced on Si(100) surfaces using sub-15 femtosecond high-resolution laser scanning microscopy. Laser processing was performed with the silicon surface immersed in water followed by hydrofluoric acid etching in order to remove silicon oxide residues. Rifts and ripples of 130-nm period as well as random nanoporous surface arrangements were generated by Ti:Sapphire laser light of centre wavelength 800 nm (bandwidth 120 nm, repetition rate 85 MHz) at picojoule pulse energies. Growth of Chinese hamster ovary (CHO) cells revealed good adhesion to the silicon substrates. Importantly, alignment of cells along the direction of ripples was observed, whereas random nanoporous surfaces did not induce any preference in cell orientation. Surface topologies generated at various levels of laser beam exposure were investigated in detail by scanning electron microscopy (SEM) as well as transmission electron microscopy (TEM) images recorded from focused ion beam sections. Adhesion and orientation of CHO cells on the laser-induced surface structures will also be illustrated by SEM images.

8231-22, Session 5

## Novel micro, nano, and meta structures for sensing

N. M. Litchinitser, A. Pandey, Univ. at Buffalo (United States); R. Biswas, The Univ. of Southern California (United States); T. Moein, J. Zeng, E. Furlani, A. N. Cartwright, Univ. at Buffalo (United States)

Compact, multimodal sensing capable of detecting four fundamental parameters of the electromagnetic radiation, such as intensity, phase, wavelength, and polarization is envisioned to have a plethora of applications in biology, medicine, and defense. We employ the unique transmission properties of micro- and nano-structured materials, including photonic bandgap structures, photonic crystal fibers and optical and plasmonic metamaterials to design and demonstrate several novel approaches to the realization of ultra-compact, multifunctional sensor arrays. In particular, we will discuss two new classes of sensors: i) antiresonant reflecting optical waveguide and fiber based refractometric and optofluidic devices and ii) polarization sensitive devices based on plasmonic and metamaterials structures.

8231-23, Session 5

## Studying split mesa photonic crystal gratings for self-referencing in microfluidic optical biosensing

R. Schilling, Univ. of Toronto (Canada)

Photonic crystal slabs (PCS) support in-plane guided resonances that easily couple to external radiation. Interaction between the evanescent field tail and the surrounding medium can be exploited to develop large surface area refractive index (RI) biosensors with a simple light coupling scheme. We propose a novel split-mesa self-referencing design incorporating two PCS lattices with shifted spectral resonances, to improve temperature stability.

We have designed and fabricated a split-mesa PCS biosensor with resonance peaks spaced 15nm apart and with a 1μm gap between mesas. Both spectral peaks are shifted equally by changes in RI of the bulk fluid, however selective functionalization of one lattice or use of a t-junction to flow different liquids over each mesa allows for a temperature insensitive differential measurement of the resonance shifts. To maximize sensing area the lattices should be as close together as possible while avoiding coupling effects.

To determine an appropriate gap length Fano lineshapes are fitted to resonances observed when both mesas or only a single mesa are excited. Quality factor (Q) and the shape parameter (q) are used to quantify the coupling effect. With a 1μm gap and TE-like resonances with experimental Qs of 500 and 990, we observe a 1.8x reduction of Q and 3.7x increase in q for the high-Q resonance, and negligible changes for low-Q. This demonstrates an observable coupling effect for the high-Q resonance. Current work involves determining the ideal gap length for self-referencing, using mode mixing to tailor coupling effects and exploring coupled self-referencing designs.

8231-24, Session 5

## Transmission characteristics of SWCNT-deposited microtapered long-period fiber gratings with the variation in O2 gas

Y. Han, N. Jun, W. Yi, Hanyang Univ. (Korea, Republic of)

Carbon nanotubes have attracted much attentions in photonics devices and sensors because of their superior advantages such as small size (diameter= 1~100 nm), good optical properties. Since single-walled carbon nanotubes (SWCNTs) have unique properties such as high nonlinearity, fast response time, and saturable absorption, optical fiber devices based on SWCNTs have been widely investigated, such as a mode locked fiber laser and an optical switch. SWCNT-deposited optical devices have been highly promising devices because of their many advantages such as fast response, low cost, and immunity to electromagnetic interference.

In this paper, we propose and experimentally demonstrate a micro-tapered long-period fiber gratings (MT-LPFGs) deposited with SWCNTS and discuss their transmission characteristics with the variation in O2 gas. The MT-LPFGs are fabricated by tapering a conventional single-mode fiber periodically. The fundamental core mode can be coupled to the cladding mode based on periodic refractive index modulation, which produces resonant peaks in the transmission spectrum. If gas molecules are adhered to SWCNTs, the variation in dielectric constant of SWCNTs changes the refractive index of SWCNTs. Since the MT-LPFGs are sensitive to the ambient index change, the transmission characteristics of MT-LPFGs can be changed by gas molecules. The gas detection was carried out in a vacuum chamber. Before the injection of the oxygen gas, the MT-LPFGs were heated up to 1300C for degassing the SWCNTs deposited on the MT-LPFGs. After the injection of oxygen gas, it took 80 minutes to finish the reaction. The total peak wavelength shift was measured to be 2.2 nm and the transmission loss of 1.3 dB was increased. The SWCNTs-based MT-LPFGs exhibit linear response and repeatability. Consequently, The SWCNTs-based MT-LPFGs will be useful for detecting the variation in O2 gas.

8231-26, Session 6

## Periodic two-dimensional nanobottle structures for SERS applications

H. M. Chen, L. Pang, Univ. of California, San Diego (United States); G. M. Hwang, The MITRE Corp. (United States); Y. Fainman, Univ. of California, San Diego (United States); L. Cambrea, Naval Air Warfare Ctr. Weapons Div. (United States)

Two-dimensional, large-area, periodic nanocavity ‘nanobottle’ structures have been simulated, fabricated, and characterized for biosensing applications. Three-dimensional simulations show high electrical field around the tips of the structure. The fabrication process consists of using holographic lithography to create 2-D periodic nanohole array. Subsequently, oblique metal deposition on the nanohole array as the sputtering stage is rotated results in large-area, periodic ‘nanobottle’ nanostructure when looking at its cross-section. The precise geometry of the nanobottle is dependent on the deposition time (thickness). The periodicity of the array was designed to excite propagating surface plasmon resonance (SPR) modes, while the geometric shape of the nanobottle nanostructure excites localized plasmons on its edges. The couplings between these two phenomena results in higher electric field and thus higher enhancement factor than conventional nanohole array over the whole substrate area ( > 4 cm^2). By analyzing the Raman mode of the adsorbed benezenethiol on the surface, the average surface enhanced Raman scattering (SERS) enhancement factor of greater than 10^7 has been measured over the whole array. Due to its moderately-high enhancement factor, large-area array, and low-cost fabrication method, the nanobottle structure is a promising candidate for future SERS biosensing applications.

8231-27, Session 6

## Raman spectroscopy hyperspectral imager based on volume Bragg gratings

S. Blais-Ouellette, M. Verhaegen, S. Marcet, Photon etc. Inc. (Canada); R. Martel, Univ. de Montréal (Canada)

We have developed a high efficiency unpolarized hyperspectral imager based on thick volume Bragg gratings for Raman spectroscopy.

Because the signal from Raman diffusion is much weaker than other optical characterization techniques, maximum efficiency is required from the imager. The standard methods increase dramatically the acquisition time because of the mechanical displacements of the sample (point-to-point measurements) or the low filter transmission (acousto-optic or liquid crystal tunable filters). The technology of volume Bragg gratings dramatically reduces the acquisition time and improves the spatial and spectral resolutions.

A narrow wavelength bandwidth of the entire field of view is diffracted and both polarizations are filtered by passing through a volume Bragg grating while other wavelengths are simply refracted and removed from the optical path. The beam is then focused on a CCD camera where a monochromatic image is formed. Wavelengths are scanned by continuously changing the angle of incidence of the incoming beam on the volume Bragg gratings.

The use spectral scanning rather than spatial scanning allows for reducing the acquisition time. The technology of volume Bragg gratings has an efficiency of 90%, allowing for non-destructive molecular analysis with high sensitivity and high spectral resolution of 0.2 cm-1. The transmission is continuous and tunable from 480 to 700 nm.

We present hyperspectral Raman images of carbon nanotubes taken with a spectral resolution of 0.2 cm-1 on the whole field of view of the microscope.

8231-28, Session 6

## Computer simulation of lipid bilayer detection using ion-sensitive field-effect transistors

S. Uno, Ritsumeikan Univ. (Japan)

Computer simulation of lipid bilayer detection using ion-sensitive field-effect transistors (ISFETs) is presented. Our previous work addressed DNA sensing using ISFETs, and impacts of DNA density, number of base pairs, salt concentration, and hybridization on output signal has been reported [1]. In this work, we extend our model for lipid bilayers on ISFET sensor surface to simulate experiments [2]. Our model consists of (a) sensor surface (Si3N4), (b) Stern layer, (c) thin electrolytic layer (3nm), (d) lipid bilayer (5nm), and (e) semi-infinitely-extended electrolyte domain. Poisson-Boltzmann equation is solved to determine electrostatics taking into account mobile ion charges in electrolyte and lipid charges. We successfully reproduced the experimental results of output signal change due to DOPC molar concentration and salt ion concentration. Our simulation has potential to include ion channels in lipid bilayer, which might be useful for ion channel research.

[1] S. Uno et al., Jpn. J. Appl. Phys., vol. 49, no. 1, p. 01AG07 (2010).

[2] C. Kataoka-Hamai et al., Langmuir, vol. 24, p. 9916 (2008).

8231-29, Session 6

## Selective surface functionalization of zero-mode waveguides to study membrane dynamics in living cells

C. Hsieh, C. Chen, S. Lai, Academia Sinica (Taiwan); Y. Lin, National Taiwan Univ. (Taiwan); K. Liao, S. Wang, P. Chiang, C. Chou, Academia Sinica (Taiwan)

Zero-mode waveguides (ZMWs) are optical nanostructures to confine fluorescent excitation within sub-diffraction volumes and commonly used for single-molecule analysis. In this study, we extend the applications of ZMWs from single-molecule analysis to membrane dynamics in living cells by selective functionalization of the bottom surface of the ZMWs with blocked ligands. The blocked ligands, serve as a “start” clock which enables us to monitor the dynamic process of ligand-induced lipid raft aggregation within the sub-diffraction excitation volume of the ZMWs.

8231-30, Session 6

## FDTD simulation on refractive index sensitivity of bow-tie metallic nanostructure

T. Luo, W. Zhang, Guangxi Univ. (China)

Optical biosensor based on localized surface plasmon resonance effect has become one of the hot point in the research due to its advantages including small volume, high sensitivity, free-label and so on. A comprehensive theoretical and experimental study has been performed on the refractive index sensitivity of different nanostructures such as nano-rods, nano-spheres, nano-triangles, nano-shells etc. With the ability to produce highly confined optical fields and the character of strong controllability , bowtie nanostructure has been applied to areas such as surface enhanced spectrum, near field scaning imaging, photoluminescence. Also, the resonant wavelength of this nanostructure is susceptible to the refractive index of external environment, which makes it be a sensor nanostructure. In this paper, we will study a bowtie system made of two identical Au-triangle.Near field optical responses of the system will be simulated by 3-D finite difference time domain(FDTD) method in the infrared region, and bulk refractive index sensitivity, surface refractive index sensitivity and substrate refractive index sensitivity of this system will be analysed.

# Conference 8232: Colloidal Nanocrystals for Biomedical Applications VII

Saturday-Sunday 21-22 January 2012
Part of Proceedings of SPIE Vol. 8232 Colloidal Nanocrystals for Biomedical Applications VII

8232-01, Session 1

## Interactions of gold nanoparticles and biological systems

A. G. Kanaras, D. Bartczak, O. L. Muskens, T. Sanchez-Elsner, T. M. Millar, Univ. of Southampton (United Kingdom)

Using sophisticated nanoparticles and controlling their interactions with biological systems can have numerous advantages in the development of new therapeutic methods. An important step for substantial progress in nanomedical applications is to understand how the different size, shape and functionality of advanced colloidal nanoparticles can be employed in order to control nanoparticle delivery and function in biological systems.

In this presentation we demonstrate our recent studies in understanding how gold nanoparticles of different size, shape and function interact at a fundamental level with advanced biological structures (i.e. blood vessels and skin) as well as their building units. We will address several questions such as a) why one should use nanoparticles as drug carriers, b) how the shape, functionality and size of particles affect the cell viability and the nanoparticle uptake, c) how the particles are exocytosed, d) how the number of particles, associated with biological systems, is correlated to the treatment by laser hyperthermia and e) how the development of biological structures depends on the nanoparticle functionality.

8232-02, Session 1

## Fluorescent diamond nanoparticle: a stable marker for the functional study of dendritic spines of mouse cortical neurons in culture

L. Le Xuan, Ecole Normale Supérieure de Cachan (France); A. Lepagnol-Bestel, Ctr. de Psychiatrie et Neurosciences (France) and Ctr. National de Génotypage (France); M. Adam, Ecole Normale Supérieure de Cachan (France); G. Dantelle, Ecole Polytechnique (France); H. Chang, Institute of Atomic and Molecular Sciences (Taiwan); M. Simonneau, Univ. Paris Descartes (France); F. Treussart, Ecole Normale Supérieure de Cachan (France)

Neurons display dendritic spines plasticity and morphology anomalies in numerous psychiatric and neurodegenerative diseases. These changes are associated to abnormal dendritic traffic that can be evidenced by fluorescence microscopy [1,2]. We use fluorescent diamond nanoparticles (fNDs) of size<50 nm to monitor this traffic.

Their fluorescence stems from embedded nitrogen-vacancy (NV) color centers, which are perfect photostable emitters, allowing for long-term cellular tracking [3]. It was shown that fNDs are spontaneously internalized by endocytosis [4] in various cell lines in culture and that their intracellular motion can be tracked on long-term scale [5].

Here we show that bare fNDs can be used to monitor dendritic traffic in mouse cortical neurons maintained in a primary culture.

The neurons are extracted from the cortex of mouse embryos (embryonic day 14), dissociated and incubated with a fNDs aqueous suspension. They are then placed in culture in LabTek dishes, and observed live about 24 hours after, using a home-made fluorescent microscope in a wide-field total internal reflection fluorescence (TIRF) configuration.

We recorded motion of fNDs along the dendrites proving that they are spontaneously taken in charge by molecular motors. We also transfected the cortical neurons to identify the compartments involved in this traffic.

References

[1] L. Davidovic et al., Hum Mol Genet. 16, 3047-3058 (2007).

[2] G. Maussion et al., Hum Mol Genet. 17, 2541-2551 (2008)

[3] H.-C. Chang, “Development and Use of Fluorescent Nanodiamonds as Cellular Markers,” in Nanodiamonds, Dean Ho, Ed., Springer, 2010, pp. 127-150.

[4] O. Faklaris et al., ACS Nano 3, 3955-3962 (2009).

[5] Y.-R. Chang et al., Nature Nanotech. 3, 284-288 (2008).

8232-03, Session 1

## Quantum-dots (QD) nanobiosensors for simultaneous dynamic measurements of multiple intracellular ions’ concentrations

L. B. Wong, H. Mao, Y. Wang, Cytoptics Corp. (United States)

Cells maintain their homeostatic functions by dynamically regulating the concentrations of intracellular ions via ionic channels. Using two recently Cytoptics developed QD-based nanobiosensors for Cl- and Na+ that emit separate wavelengths, herein we report the measurements of the concentrations of chloride ([Cl-]i) and sodium ([Na+]i) simultaneously in intact cells using 400 nm single excitation wavelength fluorescence microscopy. The Cl-QD525nm and Na-QD620nm were constructed by conjugating the chloride ion receptor, MEPTU, and sodium ion receptor, 12-crown-4, to the respective QD525nm and QD620nm within the FRET distances of the QD. This enables FRET energy transferred from the QD (donor) to the receptor complexes (acceptor). The fluorescence intensities of Cl-QD and Na-QD determined by photon counting were inversely proportional to the increased concentrations of the respective Cl- and Na+ according to Stern-Volmer. The quantum yields of these nanobiosensors were 0.6 compared to most organic-based fluorophores were ~0.1, well in the range of being robust sensors for cell applications. By co-loading Cl-$QD_{525}$ and Na-$QD_{630}$ into HEK-293F and T84 cells, we determined the dynamic responses of [Cl]i and [Na] i by pharmacologically-manipulated the chloride and sodium channels using five chloride channel blockers; two epithelial sodium channel inhibitors; and a C1C-2 chloride activator. The predictable physio-pharmacological responses of [Cl-]i and [Na+]i measurements have not heretofore been possible without these QD-based nanobiosensors. This assay is amendable to cell-based high throughput screening targeting translational ion channel drug discovery. (Supported by NIH DK084600-02)

8232-04, Session 1

## Differences in reactive oxygen species generation by quantum dots: core material and ligand comparisons

A. Nagy, A. Steinbrück, Y. Ghosh, A. M. Dennis, R. S. Iyer, J. A. Hollingsworth, Los Alamos National Lab. (United States)

Quantum dot (QD) toxicity may originate from the generation of reactive oxygen species (ROS) that damage cells or functional biomolecules therein. We characterized QD-derived ROS in a cell-free environment as a predictor of cellular toxicity due to oxidative stress. Superoxide and hydroxyl radical formation was examined in biochemical assays and cell studies, assessing the dose-dependent composition and size effects of CdSe, CdTe, and InP QDs. Furthermore, we investigated the influence of different coating ligands regarding electrostatic vs steric passivation in terms of stability in biologically relevant environments and possible effects on ROS generation. Appropriate controls distinguish between QD and ligand-induced effects. Preliminary in vitro results indicate that negatively charged CdSe QDs induce dose dependent increases in ROS, while minimal changes in intracellular ROS production were noted for cells exposed to CdTe and InP QDs. Electrochemical measurements correlate the electronic structure of each QD with the types of ROS produced. Collectively, these data can be useful to further understand the mechanisms of nanoparticle cellular toxicity and also provide insight into developing safer engineered nanomaterials.

8232-05, Session 1

## Aquatic organisms as new high-throughput systems for bio-non bio interactions

A. Ambrosone, V. Marchesano, L. Mattera, A. Tino, C. Tortiglione, Istituto di Cibernetica Eduardo Caianiello (Italy)

Although increasing efforts have been done to obtain new nanomaterials with minimal effects on the environment and human health, comprehensive toxicological evaluations are needed. The in vitro assays based on cell culture systems for rapid screening of bio-non bio interactions do not accurately address to the in vivo response complexity. We show here the feasibility of using two cnidaria species, the freshwater polyp Hydra vulgaris and the estuarine starlet sea anemone Nematostella vectensis, as new high throughput systems to study the interaction of new nanomaterials on living organisms, and to dissect the complexity of the evoked responses into multiple issues, such as biocompatibility, stability, internalization mechanisms, intracellular trafficking, toxicity, ecotoxicity. By using well established assays, spanning from in vivo evaluation of animal behaviour, morphological alteration, reproductive and regenerating capabilities, embryogenesis and development, we investigated, in vivo, the whole response elicited in these cnidaria by nanoparticle challenging, highlighting the differences due to the chemical composition, uptake efficiency, intracellular fate, and the those related to the animal species. As the need to deal with physical, chemical, and biological stressors has driven the animal evolution of an array of gene families and pathways that afford protection from challenges, cnidarian genomes harbor a variety of stressor genes. This allowed us to identify the genetic pathways leading to nanoparticle mediated cell death. In conclusion, by addressing multiple aspects of bio-non bio interaction, we provide a wide scenario of the possible effects displayed by nanoparticles on ecological key species, recommending Cnidaria as novel, fast time, cost effective biosensors for high-throughput evaluation of nanomaterials impact human and environment health.

8232-06, Session 1

## Optical sensing of small ions with colloidal nanoparticles

W. J. Parak, Philipps-Univ. Marburg (Germany)

Colloidal nanoparticles, in particular gold nanoparticles and quantum dots, can be used in a variety of different assays for optical sensing of small ions in solution. In this review different detection principles are introduced and their potential use for detection in biological samples (such as intracellular sensing) is discussed.

8232-07, Session 1

## Biodegradable polymer nanocarriers for therapeutic sense and antisense microRNA delivery in living animals

R. Paulmurugan, N. M. Sekar, T. V. Sekar, Stanford Univ. School of Medicine (United States)

MicroRNAs are endogenous regulators of gene expression, deregulated in several cellular diseases including cancer. Altering the cellular microenvironment by modulating the microRNAs functions can regulate different genes involved in major cellular processes, and has been considered as a promising new generation of molecularly targeted anti-cancer therapies. AntagomiRs (Antisense-miRNAs) are a novel class of chemically modified stable oligonucleotides used for blocking the functions of endogenous microRNAs which are overexpressed. A key challenge in achieving effective microRNA-based therapeutics is by developing an efficient delivery system, which can specifically deliver sense and antisense oligonucleotides to target cancer cells in living animals. Currently we are working on developing effective delivery system, which can selectively deliver antagomiR-21 and antagomiR-10b in triple negative breast cancer cells and revert tumor metastasis and invasiveness. The FDA-approved biodegradable PLGA-nanoparticles were used as a carrier for antagomiRs delivery. Chemically modified antagomiRs were co-encapsulated in PLGA-PEG-nanoparticles by using double-emulsification (W/O/W) solvent evaporation method with the average size of 150-200nm. The antagomiR encapsulated PLGA-nanoparticles were evaluated for in vitro antagomiR delivery, intracellular release profile, and functional effects, by measuring the endogenous cellular targets, and also by measuring the cell growth and metastasis. The xenografts of tumor cells in living mice were used for evaluating the tumor growth and metastasis, after treating the cells with antagomiR encapsulated PLGA-nanoparticles. The results found that the use of PLGA for antagomiR delivery is not only efficient in crossing cell membranes, it can also maintain functional intracellular antagomiRs level and achieve therapeutic effect in living animals.

8232-08, Session 2

## Photothermal microscopy of metallic and magnetic nanoparticles in cells

L. K. Bogart, Y. Cesbron, U. Shaheen, A. W. Taylor, R. Levy, Univ. of Liverpool (United Kingdom)

In recent years there has been an intense research effort to understand the behaviour of nanoparticles in cells. Biological applications demand that such nanoparticles are protected by a ligand shell, which not only shields the core from the harsh cellular environment but can also be functionalised to allow the nanoparticle to be targeted to specific locations within the cell. There are a variety of proposed applications that depend upon the core material of the nanoparticle, which ranges from targeted drug delivery for metallic nanoparticles to the in vivo tracking of stem cells for magnetic nanoparticles.

The realisation of these applications, however, requires thorough knowledge of the localisation and long term fate of nanoparticles within cells. Knowledge of the localisation and fate of nanoparticles has been achieved directly using photothermal microscopy; this is a technique based upon the absorption of light by the inorganic core, which results in the heating and subsequent change in refractive index of the local area that can be probed using a second laser at a higher wavelength. A systematic investigation into the intracellular behaviour of both metallic and magnetic nanoparticles within cells will be presented. Photothermal microscopy images are combined with electron microscopy images and fluorescence imaging of the ligand shell to provide a comprehensive study of metallic and magnetic nanoparticles. This work is an important preliminary step that is required for the optimisation of such particles in device based applications.

8232-09, Session 2

## Synaptosomes as a platform for loading nanoparticles into synaptic vesicles

D. T. Chiu, Univ. of Washington (United States)

No abstract available.

8232-10, Session 2

## Peptide-mediated cellular delivery of quantum dots

K. Boeneman, J. Delehanty, M. Stewart, K. Susumu, U.S. Naval Research Lab. (United States); J. B. Blanco-Canosa, P. Dawson, The Scripps Research Institute (United States); A. Huston, I. L. Medintz, U.S. Naval Research Lab. (United States)

The superior optical and photophysical properties of quantum dots make them ideal candidates for biological imaging and biosensing applications. Our laboratory has successfully shown FRET based in vitro sensing, as well as intracellular conjugation of microinjected QDs with the fluorescent protein, mCherry (1,2). These accomplishments indicate that intracellular biosensing with QD bioconjugates is possible in the near future. The caveat, however, is the current cellular delivery methods of the QDs. Microinjection is cumbersome and allows for examination of only a small population of cells. Other delivery methods have proven effective, but result in endosomal sequestration of the QDs after delivery.

We recently investigated an amphiphilic palmitylated peptide (Palm-1) which appeared to allow peptide-mediated intracellular delivery and endosomal escape of QDs (3). This peptide contains a palmitate group which is believed to facilitate entry through the cell membrane, positively charged lysines for interaction with the cell membrane and a polyproline helix which helps keep the peptide extended and accessible outside the QD's DHLA-PEG solubilizing layer. QD-peptide bioconjugates demonstrated escape from the endosome into the cytosol within 48 hours of delivery with limited apparent cytotoxicity to the cells. Recent work has followed up on this initial set of observations and focused on elucidating the peptide's mechanism of action by cellular delivery of numerous variants of the Palm-1 peptide in a semiquantitative manner. We also demonstrate cytosolic delivery of numerous dyes and proteins and co-delivery of QDs and other cargo using Palm-1.

1. Medintz et al. Nat Mater. 2006. 5(7):581-9.

2. Boeneman et al. J Am Chem Soc. 2010. 132(17):5975-7.

3. Delehanty et al. Integr Biol. 2010. 2(5-6):265-77.

8232-12, Session 2

## Effective silencing of a proto-oncogene through nanoparticle mediated RNA interference in hydra-vulgaris

C. Tortiglione, A. Ambrosone, V. Marchesano, Istituto di Cibernetica Eduardo Caianiello (Italy); J. M. de la Fuente, Instituto de Nanociencia de Aragon (Spain)

The widespread use of RNA interference (RNAi) therapeutics for disease prevention and treatment requires the development of clinically suitable, safe and effective drug delivery vehicles. Perhaps the most important issue to overcome is the effective delivery of small interfering RNAs (siRNA) to target tissues and cells, and the biological barriers standing between the newly administered siRNA and the cytoplasmic site of action. By using as model system a simple invertebrate, the freshwater polyps Hydra vulgaris, here we developed a nanoparticle mediated method for siRNA delivery, targeting the protooncogene myc. In vertebrates, this gene plays pivotal roles in the homeostasis of the stem cells, controlling both cell proliferation and differentiation pathways. Using two different strategies of myc-siRNA bioconjugation to gold nanoparticles (AuNP), several nanodevices were produced and tested in Hydra at whole animal, cellular, subcellular and molecular levels. A large scale screening of RNAi phenotype was possible leading to the selection of the most effective nanodevice, causing 80% of molecular downregulation. We provide multiple evidence of an unexpected function of Hydra myc in the homeostasis of stem cells, controlling the balance between stem cells self renewal/differentiation. The results showed in Hydra are in agreement with those obtained by the same multifunctional nanoparticle on other biological system (cell cultures, mouse), confirming the feasibility of using simple models to bridge from studies in cell lines through towards clinical reality.

8232-13, Session 2

## CdTe/CdS-AMP quantum dots as fluorescent probes to label yeast cells: synthesis, characterization, and conjugation with Concanavalin A

C. P. Sabino, C. Campos Santos, Instituto de Pesquisas Energéticas e Nucleares (Brazil); D. Azevedo, Univ. Federal de Pernambuco (Brazil); I. T. Kato, Instituto de Pesquisas Energéticas e Nucleares (Brazil); P. E. Cabral Filho, Univ. Federal de Pernambuco (Brazil); R. A. Prates, Instituto de Pesquisas Energéticas e Nucleares (Brazil); A. Fontes, B. S. Santos, Univ. Federal de Pernambuco (Brazil); M. Simões Ribeiro, Instituto de Pesquisas Energéticas e Nucleares (Brazil)

Candida albicans is the most frequent human opportunistic pathogenic fungus and one of the most important causes of nosocomial infections. In fact, diagnosis of invasive candidiasis presents unique problems. The aim of this work was to evaluate, by fluorescence image analysis, cellular labeling of Candida albicans with CdTe/CdS quantum dots conjugated or not to concanavalin A (ConA). Yeast cells were incubated with CdTe/CdS quantum dots (QDs) stabilized with mercaptopropionic acid (MPA) (emission peak at 560 nm) in phosphate saline buffer for 30 min. In the overall study we observed no morphological alterations. The fluorescence microscopic analysis of the yeast cells showed that the non-functionalized QDs do not label C. albicans cells, while for the QDs conjugated to ConA the cells showed a fluorescence profile indicating that the membrane was preferentially marked. This profile was expected since Concanavalin A is a protein that binds specifically to terminal carbohydrate residues at the membrane cell surface. The results suggest that the QD-labeled Candida cells represent a promising tool to open new possibilities for a precise evaluation of fungal infections in pathological determinations.

8232-14, Session 2

## Impact of nanomaterials on in vitro and in vivo systems: role of nanoscale features in nanotoxicology

P. P. Pompa, Istituto Italiano di Tecnologia (Italy)

The interactions between biological systems and nanostructured materials are attracting great interest, due to the possibility to open up novel concepts for the design of smart nano-biomaterials that actively play a functional biological role. On the other hand, the assessment of the potential toxic effects arising from such interactions is gaining increasing attention, and a new field known as nanotoxicology is strongly emerging. In this frame, we investigated the response of human neuroblastoma cell line to gold surfaces with different levels of nanoroughness, finding out that neurons are capable to sense and actively respond to these nanotopography features, with a surprising sensitivity to variations of few nanometers. By seeding cells onto micropatterned flat and nanorough gold surfaces, we demonstrated the possibility to realize substrates with cytophilic or cytophobic behavior, simply by fine tuning their surface topography at nanometer scale, inducing a clear self-alignment of neurons. These nanostructured substrates were also investigated to explore the impact of nanoscale topography on genomics and proteomics of adherent bacteria. A multidisciplinary approach (by means of AFM, SEM, real-time qPCR and 2D-DIGE) was exploited to characterize bacteria-nanostructured surface interactions, observing that type-1 fimbriae typically disappear in bacteria grown onto nanorough substrates, as opposed to E. coli onto reference glass or flat gold surfaces. We also show the results of several investigations of nanoparticle interactions with in vitro and in vivo biological systems. In particular, the toxic effect of a wide range of nanomaterials (AuNPs, QDs, SiO2 NPs) is presented, demonstrating the key role of size, shape, surface coating, and nanoscale surface features. Moreover, the peculiar behavior of nanorough and surface engineered nanoparticles is also discussed.

8232-15, Session 3

## Engineered nanoparticles for improved vasoactive intestinal peptide (VIP) applications in immune modulation

D. Pozo Perez, R. Klippstein, Ctr. Andaluz de Biologia Molecular y Medicina Regenerativa (Spain)

Nanotechnology can address key bottlenecks hindering successful bench to bedside translation of recent research in the development of neuropeptide-based drugs. This is the case for vasoactive intestinal peptide (VIP), where sustained interest in its therapeutic applications needs to devise new methodologies to improve its drugability or to convey innovation to diagnostics to identify cells that result from conditions such as carcinoid metastasis in which VPAC receptors are involved. Here we present our results covering the chemical synthesis and functional charectisation of VIP Au/Ag nanoparticles, the protective effects on protease-based degradation, and the specific target to dendritic cells as an approach to cell therapy.

8232-16, Session 3

## Quantum dots: aluminium phthalocyanine conjugates perform the photodynamic therapy to kill cancer cells by FRET

J. Y. Chen, Fudan Univ. (China)

Photodynamic therapy (PDT) has been established as a new treatment modality of cancers. The principle of this modality is that the photosensitizer (PS) can preferably accumulate in the tumor and produce reactive oxygen species (ROS) when excited with the light of appropriate wavelengths to destroy cancers. This is a typical light absorption dependent approach. However the light absorption of PSs is not high enough limiting the PDT efficiency. Since quantum dots (QDs) have one or two orders of magnitude higher light absorption coefficients than that of PSs, the conjugates of positively charged QDs with aluminum phthalocyanines (AlPcS), a common PS, were prepared with a way of electrostatic coupling in this work to study the PDT effect by fluorescence resonance energy transfer (FRET). The conjugates effectively fulfilled the FRET from QDs to AlPcS with the efficiency of 80%, and produce ROS as well. The conjugates can work as the carriers to take the AlPcS into cells and remain in the conjugate form in cells. With the irradiation of 532 nm, which can be absorbed by QDs but not AlPcS, the cellular conjugates destroyed most KB cancer cells with the typical way of FRET, whereas no damaging effect could be found when either AlPcS or QDs alone were used. Our results demonstrate that the FRET is a feasible way for QD-PS conjugates to perform PDT destroying cancer cells.

8232-17, Session 4

## Small NIR-to-VIS upconverting nanoparticles for photodynamic therapy

Y. Zhang, N. M. Idris, National Univ. of Singapore (Singapore)

Photodynamic therapy (PDT) involves two individually non-toxic components that are combined to kill cancer cells. The first component is photosensitizer, a photosensitive molecule that localizes to a target cell and/or tissue. The second component involves the administration of light of a specific wavelength that activates the sensitizer. The photosensitizer transfers energy from light to molecular oxygen, to generate reactive oxygen species which can kill cancer cells. However, the visible (VIS) light needed to activate most photosensitizers cannot pass through a thick tissue. For this reason, PDT is usually used to treat tumors on or just under the skin or on the lining of internal organs or cavities, and is less effective in treating large or deep seated tumors. Near infrared (NIR) light can penetrate into soft tissues for a few centimeters due to weak absorption in the optical window. In this study, a layer of porous silica is coated on the nanoparticles with NIR-to-VIS upconversion fluorescence emission and photosensitizers are incorporated into the porous silica shell. The nanoparticles are delivered to the tumors. After exposure to NIR light, the nanoparticles can convert the NIR light to visible light which will activate the photosensitizers to produce reactive oxygen species to kill cancer cells. The upconversion nanoparticles could be used for PDT in deep tissues, because NIR light can go much deeper in tissues than visible light.

8232-18, Session 4

## Photosensitization of InP/ZnS quantum dots for anti-cancer and anti-microbial applications

J. L. Nadeau, H. Chibli, L. Carlini, McGill Univ. (Canada)

Cadmium-free quantum dots (QDs), such as those made from InP, show similar optical properties to those containing toxic heavy metals and thus provide a promising alternative for imaging and therapeutics. The band gap of InP is similar to that of CdTe, so photosensitization of InP QDs with porphyrins or other dyes should lead to generation of reactive oxygen species, useful for targeted destruction of malignant cells or pathogenic bacteria. Here we show the results of measurements of singlet oxygen and superoxide generation from InP conjugates directly compared to Au nanoparticle conjugates and dyes alone. Reactive oxygen species are measured using colorimetric or fluorescent reporter assays and spin-trap electron paramagnetic resonance (EPR) spectroscopy. A set-up for direct measurement of singlet oxygen combined with time-resolved emission spectroscopy is also presented and preliminary results are discussed. Finally, the cytotoxic effects of InP/ZnS conjugates on melanoma cells are directly compared with those of drugs alone, Au nanoparticles, and CdSe/ZnS QDs. We find that the size of the InP QDs and the thickness of the ZnS shell both strongly influence ROS generation and especially cytotoxicity. Cytotoxicity is enhanced when QDs are delivered to cell nuclei, and is only slightly enhanced by light exposure. These results suggest future approaches to the design of therapeutic nanoparticles.

8232-19, Session 4

## Cells as factories for humanized encapsulation

D. Wang, Univ. of South Australia (Australia)

Biocompatibility is of paramount importance for drug delivery, tumour labelling and in vivo application of nanoscale bioprobes. Until now, biocompatible surface processing has typically relied on PEGylation and other surface coatings, which, however, cannot minimize clearance by macrophages or the renal system but may also increase the risk of chemical side effects. Cell membranes provide a generic and far more natural approach to the challenges of encapsulation and delivery in vivo. Here we harness for the first time living cells as “factories” to manufacture cell membrane capsules for encapsulation and delivery of drugs, nanoparticles, and other biolabels. Furthermore, we demonstrate that the built-in protein channels of the new capsules can be utilized for controlled release of encapsulated reagents.

8232-20, Session 4

## Antimicrobial properties of sub-nanometer silver clusters: a key to understand the biocide properties of silver?

M. A. Lopez-Quintela, Univ. de Santiago de Compostela (Spain); J. Calvo, Nanogap (Spain); F. Dominguez, J. Neissa, Univ. de Santiago de Compostela (Spain); J. M. Leal, B. Garcia, N. Busto, Univ. de Burgos (Spain); G. Barone, Univ. degli Studi di Palermo (Italy)

Although the use of noble metals, like silver, as antibacterial is known from ancient times, the effectiveness and mechanisms associated to such activities is relatively unknown. Scientific reports are very different from each other and the current major believe is that metal ions are responsible for such activities, so that metal particles provide only a reservoir to supply the active ions in the medium. But, the mechanisms by which such Ag ions are active still remain to be elucidated.

In this communication we will report the interaction of Ag (0) sub-nanometer clusters with biological relevant molecules. We will show that Ag clusters inhibit bacterial topoisomerase IV at very low concentrations, and represent a new family of substances based on metal (0) compounds having antibacterial activities. At the same time, our results yield a very different and simple explanation of the antibacterial properties of silver, which may explain the highly variability of the antimicrobial activities found with this noble metal.

8232-21, Session 5

## Synthesis and characterization of fluorescent dyes: magnetic nanoparticles for bioimaging applications

S. K. Yen, D. Janczewski, S. Bin Dolmanan, S. Tripathy, S. T. Selvan, A*STAR Institute of Materials Research and Engineering (Singapore)

Magnetic nanoparticles (MNPs) have been emerging as potential bioimagingprobes for early diagnosis of diseases and in therapeutics [1-3]. In recent years, there has been a great interest in the assemblies of quantum dots (QDs) with

MNPs [4]. The synergic combination of fluorophores and -MNPs would provide the real-time fluorescence imaging and magnetic resonance imaging (MRI). The synthesis and characterization of NIR fluorescent dyes and MNPs as magnetic-fluorescent bimodal probes remains a largely unexplored field.Conversely, the fluorophores with absorption and emission at longer wavelengths

(600-900 nm) are important for biolabeling applications. This presentation will highlight the tailor-designed synthesis, relationship of the molecular structure of NIR-organic dyes and the photophysical properties of NIR-MNPs, and their biomedical applications.

8232-22, Session 5

## Multifunctional superparamagnetic nanocrystals for imaging and targeted drug delivery to the lung

L. M. Armijo, Y. Brandt, The Univ. of New Mexico (United States); D. L. Huber, Sandia National Labs. (United States); N. J. Withers, J. B. Plumley, N. C. Cook, A. C. Rivera, G. A. Smolyakov, S. Yadav, The Univ. of New Mexico (United States); H. D. C. Smyth, The Univ. of Texas at Austin (United States); M. Osinski, The Univ. of New Mexico (United States)

Cystic fibrosis (CF) is one of the most common life-shortening, childhood-onset recessively inherited diseases, affecting 1 in 3,900 children in the US. CF is caused by a mutation in the cystic fibrosis transmembrane conductance regulator gene (CFTR) on chromosome 7, resulting in a chloride channel malfunction. The defective CFTR gene in the respiratory tract reduces the secretion of chloride ions, resulting in greatly increased thickness of respiratory mucus and leading to airway obstruction, chronic lung infection, and inflammatory reactions. The average lifespan of a CF patient today is approximately 32-37 years with intensive treatment.

Although inhalation aerosols have made a significant improvement in the life expectancy of CF patients, the bacterial production of extracellular biofilms has greatly reduced the efficacy of therapeutics due to the inability of the drug to penetrate the biofilm barrier and to reach the target bacterial pathogens.

We have prepared and characterized the Fe3O4 superparamagnetic nanoparticles (SPIONs) that can be loaded with the drug of choice (Tobramycin) to be transported to the affected area by a static external magnetic field (nanopulley function) in addition to hyperthermic mucus/biofilm disruption via application of an alternating magnetic field (nanoknife function). Multifunctional multishell SPIONs with fluorescent properties will allow monitoring of the SPIONs' passage through the mucus/biofilm barrier upon application of the magnetic field. The SPIONs will be further optimized to achieve maximum antibiotic delivery to the pathogenic bacteria via both modes of biofilm disruption.

8232-23, Session 5

## Nanoparticles: present and future towards molecular imaging

P. Padmanabhan, A. Asad, PWG Genetics Pte Ltd. (Singapore)

Preclinical disease model imaging is becoming increasingly important for biomedical research. The superparamagnetic iron oxide nanoparticles are conventionally used for magnetic resonance imaging (MRI) negative contrast agent due to its distinctive contrast effect in T2 sequence. On other hand, gadolinium (Gd) based chelates or oxides are used as positive contrast agents for T1 MR imaging. With high affinity magnetic nanoparticles, a detection and treatment of over expressing tumours on a molecular level by MRI is feasible. This talk would mainly focus on the recent development and application of nanoparticles in the context of multimodality imaging.

8232-24, Session 6

## Interaction of functionalized metallic nanoparticles with synthetic lipid membranes

K. Voitchovsky, M. Ricci, R. P. Carney, F. Stellacci, Ecole Polytechnique Fédérale de Lausanne (Switzerland)

Metallic nanoparticles present many biomedical applications, ranging from markers, to contrast agents, biosensors and drug delivery vessels. The metallic core can typically be coated with a self-assembled monolayer of ligand molecules in order to better control the nanoparticle's properties. Recent work has demonstrated that gold nanoparticles coated with a mixture of two dissimilar types of organic ligands can present highly unusual properties due to molecular structuring spontaneously occurring in the ligand shell under certain conditions [1]. This structuring gives rise to unforeseen effects, modifying in the way the particles interacts with their environment [2, 3]. In particular, it enables them to spontaneously traverse the membrane of cells without causing any permanent damage [4], thus opening new possibilities for drug delivery.

In order to better understand the membrane penetrating mechanism we have investigated the interaction between these nanoparticles and different types of supported synthetic lipid bilayers using atomic force microscopy in liquid environment. Our results highlight the importance of membrane structural defects, which act as primary nanoparticles uptake sites. Interestingly, the uptake appears strongly size-selective. Once inside the membrane, the particles tend to create organized 2D lattices, which rigidify the otherwise fluid membrane. The results are analysed from a thermodynamics perspective.

References

[1] R. P Carney et al, J. Am. Chem. Soc. 130, 798, (2008)

[2] A. Centrone et al, Proc. Natl. Acad. Sci. U.S.A. 105, 9886 (2008).

[3] J. J. Kuna et al, Nature Mat. 8, 837 (2009)

[4] A. Verma et al, Nature Mat. 7, 588 (2008)

8232-25, Session 6

## Stable gold nanocolloids with controllable surface modification and functionalization

W. Qian, M. Murakami, Y. Ichikawa, Y. Che, IMRA America, Inc. (United States)

For every biomedical application of gold nanoparticles, stability, biocompatibility, and targeting efficacy are the key requirements and surface modifications are essential for meeting these requirements. Although various surface modification strategies have been established, the fabrication of gold nanoparticles conjugated with a defined number of one or multiple types of ligands still presents a major challenge. In this presentation, we address this challenge by demonstrating highly efficient and controllable PEGylation of gold nanoparticles produced by femtosecond laser ablation. In the case of the gold nanoparticles prepared via the standard sodium citrate reduction of tetrachloroaurate (HAuCl4), for maintaining suspension stability of gold nanocolloids during the PEGylation, it is necessary to use a very large excess of poly(ethylene glycol) (PEG) over the amount required to form 100% surface coverage (sometimes over a 10 fold excess). In contrast, for the gold nanoparticles produced by femtosecond laser ablation, it is revealed that because of their unique surface chemistry, the PEGylation could be carried out with surface coverage of PEG being tunable between 0 and 100% and at the same time, the suspension stability of gold nanocolloids is perfectly maintained. The PEGylation process described here just serves as an example and the discussed strategies could be readily applied to construct other biologically important molecules onto surfaces of gold nanoparticles. Given the prominent importance of surface modification of gold nanoparticles in terms of their biomedical applications, our work represents a significant step forward in the ongoing effort to develop innovative gold nanoparticle-based diagnostic and therapeutic agents.

8232-26, Session 6

## Polymer coating of colloidal nanoparticles as a universal tool for tailoring properties toward biologically motivated experiments

F. Zhang, Inner Mongolia Agricultural Univ. (China)

Water solubilisation of nanoparticles is a fundamental pre-requisite for many biological applications. To date, no single method has emerged as ideal, and several different approaches have been successfully utilised. In the first part we review these “phase transfer” strategies indicating key advantages and disadvantages and also discuss conjugation strategies. In the second (experimental) part we then focus on one particular method, based on amphipathic polymers. Coating of hydrophobic nanoparticles with amphiphilic polymers provides a generic pathway for phase transfer of nanoparticles from non-polar to polar environments, including semiconductor, magnetic, metallic and upconverting nanoparticles. The polymers can be readily functionalized with chemical groups for specific applications. In the second part, we then demonstrate experimentally some of the new chemical features of such polymer capped nanoparticles. Nanoparticles to which a pH sensitive fluorophore has been attached are described and their use for intracellular pH-sensing. It is demonstrated that the properties of analyte-sensitive fluorophores can be tuned by using interactions with the underlying nanoparticles and thus the particles can be used for intracellular pH-sensing.

8232-27, Session 6

## Effects of LaF3:Ce nanoparticles capped with polyethylene glycol on human astrocytoma cells in vitro

N. J. Withers, Y. Brandt, A. C. Rivera, N. C. Cook, L. M. Armijo, M. Osinski, The Univ. of New Mexico (United States)

Cerium-doped lanthanum fluoride colloidal nanocrystals offer a way to improve radiation therapy through the enhanced absorption of high-energy photons at significantly lower cost than gold nanoparticles (NPs). In order to explore this possibility, multiple cytotoxicity assays need to be performed on mammalian cells in vitro to show satisfactory biocompatibility for future experiments. Lanthanum fluoride nanocrystals doped with 10% cerium and capped with polyethylene glycol (PEG) of varying molecular weight were synthesized in water as platelets 2-4 nm in diameter and 1-3 nm thick, and were suspended in deionized water. These batches of nanocrystals were characterized by transmission electron microscopy, muffle furnace ashing, absorbance spectroscopy, dynamic light scattering, zeta potential measurements, and photoluminescence spectroscopy. The five assays chosen are: Annexin V/SYTOX green and stain pairing of YO-PRO-1 with propidium iodide for detection of apoptosis with flow cytometry, the CytoTox96 Non-Radioactive assay, Caspase-3 enzyme activity detection assay, and neutral red for detection of intact lysosomes. All five tests were used, due to extensive problems in past literature with NPs chemically interfering with standard cytotoxicity tests, through either dye adsorption, ion depletion, or enzyme inhibition. The use of multiple cell viability assays allows cross checking in order to avoid incorrect readings. The cell line used in these cytotoxicity experiments was the human astrocytoma line U-87 MG, purchased from ATCC.

8232-28, Session 6

## Framing the nano-biointeractions by proteomics

S. Sabella, Istituto Italiano di Tecnologia (Italy)

Knowledge of the molecular mechanisms underlying the interactions between nanomaterials and living systems is fundamental for providing more effective products for nanomedicine and drug delivery. Controlling the response of cells/bacteria (such as activation of inflammatory processes or apoptosis/necrosis in tumor cells or pathogenic bacteria) by tuning specific properties of the nanomaterials is ultimately the challenging goal. Notably, this may also provide crucial information in the assessment of any toxic risks induced by nanoparticles on humans. However, in studying the nano-biointeractions, it is imperative to take into account the dynamic evolutions of the surface features of nanoparticles in the biological environments (in terms of protein corona formation, i.e. size and charge changes) in synergy with the dynamic events occurring in cells, including signal transduction, metabolic processes, homeostasis and membrane trafficking. In this context, we discuss the impact of analytical technologies, especially in the field of proteomics (cellular membranes and whole body proteomics), which can provide major insights into the processes affecting the NPs surface as well as the cells and bacteria functionalities. In particular, we show that a precise control of the chemical-physical characteristics of the interacting nanoparticles may impact the cells by inducing changes in the proteomic profiles with direct consequences on their viability.

8232-29, Session 7

## Oriented conjugates of monoclonal and single-domain antibodies with quantum dots for flow cytometry and immunohistochemistry diagnostic applications

A. Sukhanova, Univ. de Reims Champagne-Ardenne (France); K. Even-Desrumeaux, INSERM (France); J. Millot, Univ. de Reims Champagne-Ardenne (France); P. Chames, D. Baty, INSERM (France); M. Artemyev, Belarusian State Univ. (Belarus); V. A. Oleinikov, Shemyakin and Ovchinnikov Institute of Bioorganic Chemistry (Russian Federation); J. H. M. Cohen, I. Nabiev, Univ. de Reims Champagne-Ardenne (France)

Ideal diagnostic nanoprobes should not exceed 15 nm in diameter and need to contain on their surface high-affinity copies of homogeneously oriented capture molecules. Here, we have developed advanced procedure with the optimized critical steps of antibodies (Abs) reduction providing Abs reduced in two functional half-Abs: 75-kDa heavy-light fragments containing non-perturbed Ab binding site. Affinity purification of these half-Abs followed by coupling with the QDs generate oriented QD-Ab conjugates with largely improved functionality compared with those produced according to the standard procedures.

Additionally, we have engineered ultra-small diagnostic nanoprobes through oriented conjugation of QDs with 13-kDa single-domain antibodies (sdAbs) derived from llama IgG. sdAbs were tagged with QDs through an additional and single available for conjugation cysteine residue specifically integrated within the C-terminal of the sdAb. This approach allowed us to develop sdAbs-QD nanoprobes with <12 nm diameter and comprising four copies of sdAbs coupled with QD in a highly oriented manner. sdAbs-QD conjugates against carcinoembryonic antigen and HER2 demonstrated excellent specificity of flow cytometry quantitative discrimination of positive and negative tumor cells. Moreover, the quality of immunohistochemical labeling of biopsy samples with sdAb-QD conjugates was found to be comparable or even superior to that obtained with gold protocols of anatomo-pathology practice. sdAbs-QD oriented conjugates represent a new generation of ultra-small diagnostic probes for applications in high-through-put diagnostic platforms.

Developed approaches are very general and can be extended to conjugation of Abs with different semiconductor, noble metal or magnetic nanocrystals.

8232-30, Session 7

## Functionalized nanoparticles for binding ions from biological fluids

D. Jimenez de Aberasturi, I. Ruiz de Larramendi, T. Rojo, Univ. del País Vasco (Spain); J. M. Montenegro Martos, W. J. Parak, Philipps-Univ. Marburg (Germany)

Nowadays efforts are made to develop low-cost and selective materials which are able to bind ions for different applications such as metal recovery, treatment of hazardous and toxic wastes, medical diagnostics, etc. The use of colloidal nanoparticles is a promising approach for this purpose. Magnetic separation technology, using magnetic nanoparticles has been shown to be a useful technique for solid-solid phase separation as for biomedical applications, as a quick and easy method for sensitive and reliable capture of specific ions, proteins, genetic material and other biomolecules. Colloidal stability is a key requirement to keep the maximal binding capacity. The use of amphiphilic polymers to disperse originally hydrophobic nanoparticles in aqueous solution is a suitable approach in this direction. We demonstrate combination of magnetic cores with polymer shells with different integrated specific chelators. In this way selective ion binding was attempted.

8232-31, Session 7

## Intracellular delivery of water dispersed CdTe/CdS quantum dots by fusogenic liposomes

R. Lira, M. Seabra, J. Vasconcelos, D. Bezerra, Univ. Federal de Pernambuco (Brazil); R. Grillo, Univ. Estadual de Campinas (Brazil); N. Magalhães, O. Krasilnikov, Univ. Federal de Pernambuco (Brazil); E. de Paula, Univ. Estadual de Campinas (Brazil); B. S. Santos, A. Fontes, Univ. Federal de Pernambuco (Brazil)

The use of Quantum Dots (QDs) as fluorescent probes for understanding biological functions has emerged as an advantageous alternative over applying conventional fluorescent dyes. Intracellular delivery using QDs is currently a specific field of research. When QDs are tracking a specific target in live cells, they are mostly applied in extracellular membrane labeling and to study intracellular molecules and structures it is necessary to deliver free QDs into the cell cytosol. In this work, we present a new methodology for the encapsulation of water dispersed carboxyl-coated CdTe/CdS QDs using new cationic liposomes (with fusogenic properties) by using freeze-and-thaw cycles. We show, by conventional and confocal fluorescence microscopy, that the liposomes were able to fuse with live human stem-cells in an endocytic-independent way and we follow the delivery of the nanoparticles to the interior of the cell. The analysis of the images show that the QDs are not freely diffusing in the cytosol as it was expected and, on the contrary, we observe a co-localization of the QDs and the lipids suggesting a specific interaction. In this work, we also demonstrate that this methodology can be applied to a variety of lipids (neutral, positively and negatively charged) and liposome compositions and may be used as a general route of QD cell delivery.

8232-32, Session 7

## Multifunctional gold nanoparticles for gene silencing

V. Sanz Beltran, Univ. de Zaragoza (Spain); J. Conde, Univ. de Zaragoza (Spain) and Univ. Nova Lisboa (Portugal); Y. Hernandez, M. R. Ibarra, P. V. Baptista, J. Martinez de la Fuente, Univ. de Zaragoza (Spain)

The use of inorganic nanoparticles as drug release systems is nowadays gaining power. One of the most used nanoparticles for biomedical applications are gold nanoparticles (AuNPs). AuNPs provide non-toxic carriers and have been used in highly sensitive diagnostic assays, thermal ablation and as drug and gene delivery. Small interfering-RNAs (siRNA) show significant potential in new molecular approaches to down-regulate specific gene expression in cancerous or viral-infected cells. However, there are still significant obstacles to be overcome such as its short half-lives and degradation by RNases. We have developed effective conjugation strategies to combine, in a highly controlled way, biomolecules to the surface of AuNPs with specific functions such as cell penetrating peptides to overcome the cellular membrane barrier, quaternary ammonium to introduce stable positively charged in AuNPs surface and siRNA complementary to a master regulator gene, the proto-oncogene c-Myc. This gene is implicated in cell growth, proliferation, loss of differentiation and apoptosis. Two approaches were designed for the binding of all these molecules to the nanoparticles, the use of a thiolated siRNA for binding covalently to the surface of the nanoparticles; and by ionic interactions incorporation positive charge to the nanoparticles. These nanoparticles were characterized on their chemical functionalization, ease of uptake, cellular toxicity and knockdown of MYC protein expression in a cancer cell line. The results showed in human cells confirmed the high efficiency of these nanoparticles for silencing MYC expression. These results are in high concordance with the obtained results on other biological systems (Hydra and mice)

8232-33, Session 8

## Fighting cancer with magnetic nanoparticles and immunotherapy

L. Gutiérrez, Instituto de Ciencia de Materiales de Madrid (Spain); R. Mejias, D. F. Barber, Consejo Superior de Investigaciones Científicas (Spain); S. Veintemillas-Verdaguer, C. J. Serna, Instituto de Ciencia de Materiales de Madrid (Spain); F. J. Lázaro, Univ. de Zaragoza (Spain); M. d. P. Morales, Instituto de Ciencia de Materiales de Madrid (Spain)

Nanosized materials are already providing novel tools that are contributing to improve healthcare in the 21st century. We tested uniform dimercaptosuccinic acid (DMSA)-coated monodisperse magnetic nanoparticles as a delivery system for the anti-tumorigenic cytokine IFN-Gamma in mouse models of cancer. IFN-G-adsorbed DMSA coated magnetic nanoparticles were targeted to the tumor site by application of an external magnetic field. At the tumor site, we observed a high degree of nanoparticle accumulation and of cytokine delivery, which led to increased T cell and macrophage infiltration and promoted an antiangiogenic effect. The combined action led to a notable reduction in tumor size. Our findings indicate that IFN-G-adsorbed DMSA-coated magnetite nanoparticles can be used as an efficient in vivo drug delivery system for tumor immunotherapy. Magnetic nanoparticles were synthesized by thermal decomposition which leads to a high crystal quality and bulklike magnetic and electronic properties. Distribution of the magnetic nanoparticles in the body following systemic administration was also analysed before and after cytokine conjugation, in a mouse model by AC susceptibility measurements of the corresponding resected tissues. In general, only 10% of the total injected nanoparticles after multiple exposures were found in tissues.

8232-35, Session 8

## Photosensitizer-loaded magnetic vesicles as a new MRI-trackable biogenic nanoplatform for multimodal targeted cancer theranostics

A. Andriola Brun, Univ. Paris 7-Denis Diderot (France); S. Bonneau, Univ. Pierre et Marie Curie (France); N. Luciani, F. Gazeau, C. Wilhelm, Univ. Paris 7-Denis Diderot (France)

Iron oxide nanoparticles are responsible to magnetic field allowing them to be manipulated, tracked, imaged and remotely heated. Such key features open up a wide field of applications in medicine which includes cell separation, magnetic force-based tissue engineering, MRI tracking of transplanted cells, magnetic drug targeting and hyperthermia. We present here a pioneering strategy to design a biogenic nano-platform for multimodal therapy. Enclosing magnetic particles within biological vesicles could facilitate circulation in vivo and interaction with cells. Our approach consists of cell-derived magnetic vesicles which were loaded with a photosensitizer drug (m-THPC). In order to produce them, the first experimental step was the uptake of magnetic nanoparticles (8-nm maghemite particles stabilized by citrate ions) and the photosensitizer by macrophages derived from monocyte cell line. As a second step, the release of magnetic photosensitizer-loaded vesicles was triggered by culturing such cells in serum-deprived medium. A micromagnetophoresis experiment of the cell-released vesicles revealed both magnetophoretic mobility and red fluorescence emission due to photosensitizer. In vitro tests demonstrated that such vesicles were able to transfer their cargo into tumor cells. Transfer could be spatially modulated by a magnetic field gradient clearly indicating a magnetic targeting effect. Additionally, MRI detection was demonstrated in both in vitro and in TC1 tumor-bearing mice after intratumoral vesicle injection. In brief, photosensitizer-loaded magnetic vesicles derived from macrophages were successfully produced. Their properties enabled photosensitizer targeting and MRI detection. Besides, photodynamic therapy may be enhanced by magnetically induced hyperthermia.

8232-36, Session 8

## Stability of iron oxide nanoparticles in aqueous dispersions after laser irradiation in starch environment

A. I. Omelchenko, E. N. Sobol, Institute on Laser and Information Technologies (Russian Federation)

In spite of success of magnetic nanoparticles applications for drug delivery in human body by means of its motion in external magnetic field, the problem of control of nanoparticles transport in the viscoelastic biotissues is still unsolved. For example, solution of this problem is the aim of study of nanoparticles motion in low permeable cartilaginous tissues, thin capillary network and cell plasma membranes. Aim of this study is to enhance stability of aqueous dispersion of biofunctional nanoparticles of iron oxide used for laser engineering of cartilaginous tissue.

Laser treatment of iron oxides nanoparticles in starch aqueous solution is performed to obtain stable biofunctional nanoparticles. Optical properties of aqueous solution of these nanoparticles are investigated. By means of magnetic trap with axis-symmetric field, the nanoparticles with the size of 5-10 nm have been separated from their large scale agglomerates. It was shown that ultrasound fragmentation and demagnetizing field treatment do not allow obtaining stabile colloid without agglomeration. Laser treatment of nanoparticles of magnetite in starch aqueous solution makes stability of this colloid without agglomeration and sedimentation. This treatment helps solve problem of control of magnetic nanoparticles motion at the laser reshaping of cartilaginous tissue.

8232-37, Session 8

## Tailoring biocompatible $Fe_3O_4$ nanoparticles for applications to magnetic hyperthermia

M. Insausti, J. Salado, I. Castellanos, L. Lezama, I. Gil de Muro, T. Rojo, E. Garaio, F. Plazaola, Univ. del País Vasco (Spain)

Among the myriad of nanomaterials with high magnetic response to be applied to magnetic hyperthermia, magnetite has been widely used because of its active surface chemical functionality, biocompatibility and low cost. Nevertheless for medical purposes it is necessary to control not only the morphology and magnetic behavior, but also nanoparticles must be stable in physiological media, avoiding particle aggregation and interactions between proteins. In this way, we present a comparative study of different synthetic methods in order to obtain functionalized and hydrosoluble magnetite nanoparticles. The samples have been characterized by infrared spectroscopy, transmission electron microscopy and thermogravimetric measurements. Depending on the synthesis conditions and ligands employed nanoparticles with sizes between 5 - 50 nm and different distributions have been obtained. The specific absorption rate (SAR) was calculated to compare the efficiency of heating each sample for the various applied magnetic fields.

A complete magnetic study has been performed by means of a SQUID magnetometer and electron magnetic resonance (EMR), showing that organic matter recovering the nanoparticles enhances the superparamagnetic behaviour observed above 10 - 15 K in this kind of nanoparticles. The interaction with cells and cytotoxicity of some of the preparations were determined upon incubation on Hella cell line.

8232-38, Session 8

## Multifunctional fluorescent and magnetic nanoparticles for biomedical applications (Invited)

S. T. Selvan, A*STAR Institute of Materials Research and Engineering (Singapore)

Hybrid multifunctional nanoparticles (NPs) are emerging as useful probes for magnetic based targeting, delivery, cell separation, magnetic resonance imaging (MRI), and fluorescence-based bio-labeling applications. Assessing from the literature, the development of multifunctional NPs for multimodality imaging is still in its infancy state. This talk would focus on our recent work on quantum dots (QDs), magnetic NPs and bi-functional NPs (composed of either QDs or rare-earth NPs, and magnetic NPs - iron oxide or gadolinium oxide) for multimodality imaging based biomedical applications. The combination of MRI and fluorescence would ally each other in improving the sensitivity and resolution, resulting in improved and early diagnosis of the disease.

The challenges in this area will be discussed.

Recent Publications

1. D. Janczewski, Y. Zhang, G. K. Das, D. K. Yi, P. Padmanabhan, K. K. Bhakoo, T. T. Y. Tan and S. T. Selvan*, “Bimodal Magnetic - Fluorescent Probes for Bio-imaging”, Microscopy Research And Technique 2011, 74, 563-576. Invited Review Article.

2. S. T. Selvan*, Silica-coated quantum dots and magnetic nanoparticles for bioimaging applications, Biointerphases, 2010, 5 (3): FA110 - FA115. Invited Review Article.

3. S. T. Selvan*, T. T. Y. Tan, D. K. Yi and N.R. Jana, “Functional and Multifunctional Nanoparticles for Bioimaging and Biosensing”, Langmuir 2010, 26, 11631-11641. Invited Feature Article.

4. G. K. Das, B. C. Heng, S-C. Ng, T. White, J. S. C. Loo, L. D’Silva, P. Padmanabhan, K. K. Bhakoo, S. T. Selvan *, T. T. Y Tan *. Gadolinium oxide ultranarrow nanorods as multimodal contrast agents for optical and magnetic resonance imaging. Langmuir 2010, 26, 8959-8965.

5. C. Y. Ang, L. Giam, Z. M. Chan, A. W. H. Lin, H. Gu, E. Devlin, G. C. Papaefthymiou, S. T. Selvan*, and J. Y. Ying*, "Facile Synthesis of Fe2O3 Nanocrystals without Fe(CO)5 Precursor and One-Pot Synthesis of Highly Fluorescent Fe2O3-CdSe Nanocomposites", Advanced Materials 2009, 21, 869-873.

8232-39, Session 9

## Chirality sensing by metal nanoparticles

A. Guerrero-Martinez, L. M. Liz-Marzán, Univ. de Vigo (Spain)

The elaboration of artificial systems with controlled material properties has given rise to a rich set of fabrication techniques that allow a fine control over the morphology down to the nanoscale, though it often lacks the apparent effortlessness with which Nature has achieved complex structures, chiral in particular. A striking example of artificial structures that reach beyond naturally occurring substances is the emerging field of metamaterials [1], concerning in particular nanostructures displaying novel optical properties. More generally, many applications of nanoscale chirality can benefit from optical characterization; chiral nanostructured systems in particular are currently being investigated for their use as powerful probes and sensors upon interaction with chiral biomacromolecules (e.g. proteins) [2]. In this context, recent works have illustrated the potential of chiral metal nanostructures, which exploit the characteristic localized surface plasmon resonance of metal colloids, producing intense optical activity [3]. In this contribution, the concepts, synthetic methods, and theoretical predictions underlying the chirality of metal colloids, with a particular emphasis in chirality sensing of biological systems, will be analysed. The perspective of individual colloidal nanoparticles with a chiral morphology and a plasmonic response remains elusive; however, collective chirality and the associated optical activity in nanoparticle assemblies is a promising alternative that has seen a few recent experimental demonstrations.

[1] Liu, X. Zhang, Chem. Soc. Rev. 40 (2011) 2494.

[2] E. Hendry, T. Carpy, J. Johnston, M. Popland, R. V. Mikhaylovskiy, A. J. Lapthorn, et al., Nat. Nanotech. 5 (2010) 783.

[3] A. Guerrero-Martínez, J. Lorenzo Alonso-Gómez, B. Auguié, M. M. Cid, L. M. Liz-Marzán, Nano Today, in press.

8232-40, Session 9

## Optical properties and SERS enhancement of gold-silver alloy nanoparticles

D. Rioux, S. Vallières, Ecole Polytechnique de Montréal (Canada); P. A. Munoz, P. Peng, E. Mazur, Harvard Univ. (United States); M. Meunier, Ecole Polytechnique de Montréal (Canada)

SERS probes based on gold-silver alloy nanoparticles (NPs) are very promising for biomedical detection because they should have better SERS signal than pure gold as well as better biocompatibility than silver particles. Predicting the SERS signal intensity with theoretical modelling requires knowledge of the material's optical properties. In the case of gold-silver alloy, no exhaustive experimental study shows the relation between the complex refractive index and the alloy composition. Most theoretical studies simply use a composition average of the dielectric permittivities of gold and silver, which does not predict the correct plasmonic behaviour. We report the direct ellipsometric measurement of the dielectric permittivity of thin AuAg alloy films. We used a Drude-Lorentz model with 3 Lorentz functions to fit the experimental data. The position of the different Lorentz functions changes almost linearly with the alloy composition. However, the Lorentz widths follow a nonlinear behaviour. The Drude plasma frequency stays essentially the same for every composition, but the damping factor is much higher for alloys than for pure metals. This variation of the damping can be explained by the much smaller mean free path of the electrons in the alloys, since the ionic potential is not periodic anymore in a random arrangement of silver and gold atoms. Understanding the evolution of the different parameters enables us to predict the optical properties and SERS intensity of NPs with any composition. Both Mie modelling and experimental measurements show that alloy particles usually have stronger SERS signal, more than 10 times higher than pure gold NPs, depending on the excitation wavelength.

8232-41, Session 9

## Increased nucleic acid density on gold nanoparticles

T. A. Larson, D. Nguyen, K. Sokolov, The Univ. of Texas at Austin (United States)

Plasmonic metal nanoparticles are of great interest to the biomedical community due to their strong optical properties and their ease of conjugation. For example, gold nanoparticles have been explored as carriers for nucleic acids for molecular therapeutic and imaging applications. However, published protocols are lengthy and involve slowly increasing salt concentrations over a period of 24 - 48 hours. We have developed a rapid conjugation protocol that can be finished in 1 hour by separately heating a solution of gold nanoparticles and a solution of thiol-terminated oligonucleotide handles to 80 C and then mixing rapidly at 80 C. The kinetics of the thiol-gold interaction were explored and the reaction was found to be sufficient for gold nanoparticle stability in higher salt concentrations by 10 minutes. In addition to the faster kinetics of conjugation, this protocol resulted in more than 80 picomoles/cm2, more than 50% higher than has been reported in the literature. Dynamic light scattering and spectroscopic measurements demonstrate that the resulting DNA-nanoparticle conjugates are highly stable and monodispersed. These improvements and characterizations of DNA-nanoparticle conjugates are a necessary next step in applying these particles to in vivo delivery of nucleic acids for molecular specific therapeutic and imaging applications.

8232-42, Session 9

## Optically dense colloidal nanoparticles as discrete platforms for bio-SERS

R. A. Alvarez-Puebla, Univ. de Vigo (Spain)

There is currently a high demand for detection techniques that fulfil requirements relevant to extremely important social problems such as early stage diagnosis, environmental pollution, or terrorist threats, to name a few. These problems not only require extremely highly sensitive that allows detection of minute amounts of the relevant analyte, but also easy-to-handle devices and reduced (or ideally eliminated) sample preparation. Naturally, a universal detection technique would be highly preferred, so that various tests can be simultaneously run. Nanotechnology has been proposed as the perfect framework in which such techniques should be developed, and a number of nanostructured materials and devices have indeed been developed, including quantum dots, magnetic nanoparticles and plasmonic nanostructures, among others. In the context of nanoplasmonics (manipulation of light by metals with sub-wavelength dimensions), surface-enhanced Raman scattering (SERS) spectroscopy has been established as a true ultrasensitive, ultra-rapid and universal analytical technique, which can provide detection limits even down to the single molecule limit. A number of direct and label-free applications have been recently developed in fields as diverse as biomedicine, multiplex high-throughput screening, pollutant monitoring or molecular and materials characterization. The goal here is to summarize and discuss the rational design of plasmonic materials, with particular attention to those small and stable enough to be used in biological media for efficient analysis of low affinity target molecules and/or other analytes of interest, even under highly demanding circumstances such as those of real life samples.

8232-43, Session 9

## Highly organized complex plasmonic structures for biodiagnosis

N. Pazos Perez, A. Fery, Univ. Bayreuth (Germany)

Plasmonic nanoparticles are excellent candidates for their potential use in microelectronic, optical, biomedical applications or to develop new metamaterial properties. Their electromagnetic behaviour is for sure highly dependent on their specific particle size, shape, and surrounding environment. There are different methods which allow us to fine tune the control over the particle shape and size thus, the materials properties. However, the lack of capability to form reproducible organized structures is still a very important challenge to solve in order to control the plasmonic intercoupling between particles. Therefore, it is clear that their controlled organization in 2D and 3D structures is of key importance.

In this work we report novel methods to produce organized structures of plasmonic nanoparticles. These can be done either in a macroscale range, forming linear parallel arrays1 or, at the nanoscale regime through the controllable cluster formation with high coordination numbers. The plasmonic behaviour of these organizations was theoretically and experimentally investigated. Moreover, these structures, were effectively use for biodetection using Surface-enhanced Raman scattering (SERS) spectroscopy. Reaching enhancing factors up to 30 times higher to that observed for gold dimmers, one of the most efficient plasmonic materials known.

1. Chem. Sci., 2010, 1, 174; Soft Matter, 2011, 7, 4093

8232-44, Session 9

## Inorganic capsules for drug delivery: biocompatible open nanoboxes

V. F. Puntes, Institut Català de Nanotecnologia (Spain)

No abstract available

8232-56, Session 9

## Simplifying attachment chemistry for nanocrystal applications in life sciences

T. L. Jennings, S. G. Becker-Catania, R. C. Triulzi, G. Tao, eBioscience Inc. (United States); K. Sapsford, S. Spindel, E. Oh, V. Jain, J. Delehanty, D. E. Prasuhn, K. Boeneman, W. R. Algar, I. L. Medintz, U.S. Naval Research Lab. (United States)

The effective use of quantum dot nanocrystals (NC's) in many life science fields is often hindered by the lack of available biomolecular attachment chemistries that are both easily implemented and broadly applicable. Here, we report the development of two simple, small scale yet novel attachment chemistries that target the popular amine- and sulfhdryl- moieties found on most biomolecules. Further, by streamlining the conjugation/purification steps, the chemistries allow for the rapid conjugation and purification of NC conjugates in as little as 3 hours. The conjugates were tested and yielded positive results on flow cytometry, fluorescence immunoassays, cellular uptake, immunocytochemistry and 5-color multiplexed immunohistochemistry staining.

8232-11, Poster Session

## Characterization and bioactivity study of nanohydroxyapatite on superhydrophilic vertically aligned carbon nanotubes using optical techniques

A. O. Lobo, F. R. Marciano, Univ. do Vale do Paraíba (Brazil); A. M. E. Santo, Univ. Federal de São Paulo (Brazil); J. L. Rangel, Univ. do Vale do Paraíba (Brazil); U. A. Mengui, Instituto Nacional de Pesquisas Espaciais (Brazil); A. A. Martin, Univ. do Vale do Paraíba (Brazil); E. J. Corat, Instituto Nacional de Pesquisas Espaciais (Brazil)

Vertically-aligned multi-walled carbon nanotubes (VACNT) is of particular interest in regenerative medicine [1]. Template-induced hydroxyapatite (HA) has broad prospects in applied fields of bone regenerative medicine. Thus, it becomes very attractive a combination these two excellent materials to bone tissue engineering applications. In this were evaluated the in vitro biomineralization of HA/VACNT nanocomposites using optical techniques. Superhydrophilic VACNT films were obtained by CVD method and funcionalized by oxygen plasma. The fabrication of HA/VACNT nanocomposites was performed with a direct electrodeposition of the thin HA films on the VACNT films. The bioactivity and biomineralization in vitro process of superhydrophilic HA/VACNT nanocomposites were investigated using simulated body fluid (SBF) and optical techniques. The characterization of of HA/VACNT nanocomposites was performed before and after soaking 21 days in SBF and compared to superydrophilic VACNT films. XRD, Raman spectroscopy, FT-IR (ATR) and μEDX were employed to investigate the structural and chemical properties. The morphology was investigated by FEG-SEM analysis. After 21 days was identified that others biological apatites were formed only on HA/VACNT nanocomposites. Optical techniques showing as an powerful tool to characterizated and investigated the bioactivity in vitro process. These findings were very atractive to application of this new nanocomposites to bone tissue regeneration.

References

[1] V. Ramos, J.L. López-Lacomba, Biomaterials 29, 94 (2008).

[2] A.O. Lobo, M.A.F. Corat, E.F. Antunes, M.B.S. Palma, C. Pacheco-Soares, E.E. Garcia, E.J. Corat, Carbon, 48, 245 (2010).

[3] S.C. Ramos, G. Vasconcelos, E.F. Antunes, A.O. Lobo, V.J. Trava-Airoldi, E.J. Corat. Diam. Relat. Mater. 19, 752, (2010).

[4] A.O.Lobo, M.A.F. Corat, S.C. Ramos, J.T. Matsushima, A.E.C. Granato, C. Pacheco-Soares, E.J. Corat, Langmuir, 26, 18308 (2010).

8232-34, Poster Session

## Magnetic properties of functionalized PdFe-based nanoparticles: specific absorption rate (SAR) measurements

I. Gil de Muro, I. Castellanos, L. Lezama, M. Insausti, F. Plazaola, T. Rojo, Univ. del País Vasco (Spain)

Magnetic nanoparticles have attracted attention for their wide range of biomedical applications, such as drug delivery, contrast agents in magnetic resonance imaging (MRI), hyperthermia [1-2], or protein separation. Main properties of magnetic nanoparticles that are required for these biomedical applications are high magnetization value, monodispersity and narrow size distribution, good stability and biocompatibility. Surface functionalization is used to lead to good dispersibility and stability in aqueous solution [3]. The nanoparticles are generally composed of the magnetic core, water-dispersible biocompatible shell, and in some cases, a target biomolecule.

In this sense, oleic acid/oleilamine capped PdFe nanoparticles with sizes between 3 and 15 nm have been successfully synthesized using a diol as reducing agent. These particles have been characterized by infrared spectroscopy (IR), X-Ray Diffraction (DRX), thermogravimetry (TG) and Transmission Electron Microscopy (TEM) and their magnetic behavior has been studied by Electron Paramagnetic Resonance (EPR) and magnetization and Specific Absorption Rate (SAR) measurements. These last measurements are carried out in the aim of choosing the most appropriate particles to coat them with a biocompatible ligand and to carry out hyperthermia measurements “in vitro” and “in vivo”

References

[1] I. Hilger, R. Hergt y W.A. Kaiser, J. Magn. Magn. Mater., 293, 314-319 (2005)

[2] I. Hilger, E. Dietmar, W. Linß, S. Streck y W.A. Kaiser, J. Phys.: Condens. Matter, 18, S2951-S2958 (2008)

[3] W.C.W. Chan y S. Nie, Science, 281, 2016-2018 (1998)

8232-45, Session 10

## Are upcoverting $Ln^{3+}$ based nanoparticles any good for deep tissue imaging with retention of optical sectioning?

F. C. J. M. van Veggel, Univ. of Victoria (Canada)

One of the unique properties of the trivalent lanthanide ions (Ln3+) is their capacity to convert two or more low-energy photons into one of higher energy (upconversion). Another is their (para)magnetic properties, because of the partially filled 4f orbitals.

I will discuss the low quantum yield of upconversion, the slow photocycle and hence low brightness, and inefficient excitation efficiency as serious obstacles towards realisation of this promise. The issue of deep tissue imaging will be discussed with two-photon upconversion laser scanning microscopy (TPULSM) and two-photon upconversion wide field microscopy (TPUWFM) techniques, both using phantoms and sedated mice (brain imaging). The first is not practical, the second is.

I will also discuss our process on Gd3+ doped nanoparticles for MRI and show that the surface ions and the tumbling time at determine the T1 relaxivities. Is this approach is any better than low molecular chelates, dendrimers, liposomes, etc. that are loaded with Gd3+?

Finally, I will, if time permits, discuss claims, by us and others, that core-shell structures, e.g. NaGdF4-NaYF4 core-shell nanoparticles, have been synthesised. Many conclusions are mere inferences from TEMs and PL data and are, in my view, not sufficient proof. Advanced techniques, such as energy-dependent XPS, EELS and EDS in a STEM are needed to provide conclusive evidence for their (non-)formation.

8232-46, Session 10

## Glycine-coated photoluminescent silver nanoclusters

V. V. Kravets, K. Culhane, A. O. Pinchuk, Univ. of Colorado at Colorado Springs (United States)

We present the experimental results on the multicolor (blue and green) photoluminescence from glycine-coated silver nanoclusters which might be used as novel probes for bio-imaging. Glycine-coated silver nanoparticles were synthesized using a thermal reduction of silver nitrate in a glycine matrix, according to a modified procedure described in literature. According to the mass spectrometry, SEM and DLS characterization of the photoluminescent samples, sizes of silver particles vary from 0.5 nm to 17 nm. Extinction spectroscopy indicated that the absorption band of the small luminescent NP’s was blue-shifted when compared to non-luminescent larger nanoparticles. This effect indicates the well-known size dependence of the SPR in silver. The most pronounced photoluminescence peak observed around 410 nm (characteristic SPR wavelength for silver) which strongly suggests the enhancement of the photoluminescence by the SPR. The relative quantum yield of the photoluminescence of silver clusters was evaluated as 0.09.

In terms of their small size, brightness and photostability, noble metal nanoclusters hold the most promise as candidates for biological cell imaging, competing with commonly used semiconductor quantum dots, fluorescent proteins and organic dyes. When applied to the problem of intracellular imaging, the metal nanoclusters offer advantages over their much larger sized semiconductor counterparts in terms of ease of biological delivery. In addition, noble metal nanoparticles and nanoclusters are photostable. The high quantum yield (QY) of the photoluminescence emission signal enables the isolation of the cluster’s photoluminescence from the cellular autofluorescence in cell imaging, improving the image contrast.

8232-47, Session 10

## Rare earth-doped NaYF4 upconverting nanophosphors for tracking biological processes

D. J. Milliron, E. Chan, A. D. Ostrowski, B. E. Cohen, D. J. Gargas, P. J. Schuck, Lawrence Berkeley National Lab. (United States)

Optical upconversion gives rise to visible emission following near infrared excitation of rare earth dopants incorporated into large band gap host nanocrystals, such as NaYF4. The near infrared excitation light interacts little with cellular components, eliminating autofluorescence background and minimizing damage during imaging of biological processes in live cells. We have recently developed upconverting nanocrystals with diameters in the sub-10 nm range essential for typical tracking experiments. Brightness is enhanced by incorporating a thin, undoped shell that isolates the emission centers from the surrounding environment, thereby hampering non-radiative decay. Despite their small size, these nanophosphors are extremely photostable, showing no decrease in luminescence during hour-long single-particle optical measurements. In addition, doping levels are sufficiently high that each nanocrystal contains a statistical ensemble of emitting dopants so that no blinking is observed - crucial for tracking single tagged biomolecules.

While the narrow emission line-widths of rare earths are attractive, their utility has been limited by the fact that each species typically exhibits multiple emission lines, across the visible and infrared spectral ranges. To address this limitation, we have recently employed combinatorial screening of dopant compositions to uncover those that result in near single color emission. Simulation of the energy transfer processes occuring between dopants guides understanding of the mechanisms underlying these optical properties. Such color-pure upconverting nanophosphors will enable multi-color tracking with greatly simplified and more reliable signal discrimination.

8232-48, Session 10

## New synthetic route of CdTe/CdS quantum dot performed by electroreduction of Te0

R. T. Ribeiro, J. Dias, D. Freitas, M. Monteiro, A. Fontes, B. S. Santos, M. Navarro, G. A. Pereira, Univ. Federal de Pernambuco (Brazil)

Quantum confined semiconductor nanocrystals (quantum dots - QDs) have been extensively studied in the past two decades. These materials show great potential for application in different areas ranging from microelectronics to fluorescent labels. This is mainly due to their tunable optical properties which are achieved by size, composition, surface and morphological control of the particles. Usually, CdTe/CdS QDs water dispersed colloidal suspensions are obtained by reduction of metallic Te powder with NaBH4. However, this methodology leads to the reaction media a large excess of reducing agent that adds toxicity and reactivity to the system. In this context, in this work we are presenting a new synthetic route to obtain QDs of CdTe/CdS by electrochemistry process reduction under argon, where the Te0 is electroreduced at the electrode surface forming the Te2- in basic aqueous solution. CdTe/CdS are immediately formed, in a homogeneous and reducing agent free medium, after addition of solution containing Cd2+ and an appropriate amount of the thiol stabilizer under stirring. Spectroscopic and structural characterizations show that QDs obtained by this new electrochemical procedure are in agreement with those obtained by the conventional methods. The results support the possibility of use this new synthetic route for preparation of QDs in a cleaner medium where the reduction process is completely controlled and whole synthetic procedure is carried out in one step with great reprodutibility when compared with those that use chemical reducing agents.

8232-49, Session 10

## Colloidal upconverting Ln3+ doped nanoparticles: bio-imaging, cell tracking, and diagnostic medicine

J. A. Capobianco, Concordia Univ. (Canada)

A major challenge in medicine is to improve therapeutic efficiency by exerting effects at specific tissue sites. Nanoparticles hold great promise for achieving this goal. In particular, multifunctional nanoparticles are exciting agents for advanced biomedical intervention. Our group has worked with a novel family of lanthanide doped fluoride nanoparticles that have a unique ability to upconvert near-infrared (NIR) radiation, thereby allowing them to change low-energy excitation into higher energy emission via a multiphoton process. These upconverting nanoparticles are interesting alternatives to the readily studied quantum dots since they possess real intermediate states and thus could be excited with low power, low cost laser diodes. Furthermore, the use of NIR excitation light avoids some of the pitfalls associated with conventional UV excitation. NIR light possesses tissue penetration capabilities, avoids autofluorescence from fluorophores in the sample media, and photodamage of living tissue. As a result, the applications of these nanoparticles are broad and include cell targeting, cell imaging, diagnostic and delivery of therapeutic agents.

In this presentation we discuss the synthesis of lanthanide doped fluoride nanoparticles, the core/shell architecture, ligand exchange, silica coating, cellular uptake of the nanoparticles via endocytosis and imaging of cells.

8232-50, Session 10

## Bandgap engineering of InP nanocrystal quantum dots through shell thickness and composition

A. M. Dennis, Y. Park, B. D. Mangum, H. Htoon, J. A. Hollingsworth, Los Alamos National Lab. (United States)

Fields as diverse as biological imaging and communications utilize the unique photophysical and electronic properties of nanocrystal quantum dots (NQDs). The development of new NQD compositions promises new material properties optimized for specific applications, while addressing material toxicity. Indium phosphide (InP) offers a “green” alternative to the traditional cadmium-based NQDs, but suffers from an extreme susceptibility to oxidation. Coating InP cores with more stable shell materials significantly improves nanocrystal resistance to oxidation and photostability. We have investigated several new InP-based core-shell compositions, correlating our results with theoretical predictions of their optical and electronic properties. Specifically, we can tailor the InP core-shell QDs to a type-I, quasi-type-II, or type-II structure with emission wavelengths ranging from 500-1300 nm depending on the shell material used (ZnS, ZnSe, CdS, or CdSe) and the thickness of the shell. Thus, both the photophysical and electronic properties of InP NQDs can be tuned to a given application. Single molecule microscopy is being used to assess the photobleaching and blinking of single quantum dots with various shell thicknesses.

8232-51, Session 11

## Quantum dot barcode labels for high-throughput screening assays using droplet microfluidics

R. A. Sperling, A. R. Abate, P. Mary, T. Hung, D. A. Weitz, Harvard Univ. (United States)

Microfluidic droplets can be seen as the analogue of reaction tubes: They are small isolated compartments of a liquid, typically aqueous, separated by an inert outer phase, e.g. fluorinated oil. The droplets can be generated in a very controlled fashion at kiloherz frequency in a simple microfluidic device. Reagents can be added to droplets, the droplets can be manipulated on-chip or stored outside and reinjected at a later point. The contents of droplets can be optically detected by fluorescence. Taken together, generation, manipulation and detection of microfluidic droplets present a new approach to screening assays, where the reduction in sample size from microliters to picoliters offers a reduction of reagent cost of several orders of magnitudes, as it does in regard to processing time. We have developed a method for the parallel encapsulation of samples, allowing for the efficient generation of droplet libraries. By that, a large number of reagents can be encapsulated into droplets and stored for later use. Individual members of the library can labeled prior to encapsulation by fluorescent barcode labels, e.g. generated with different concentrations of quantum dots. For a screening assay, the samples to be screened are injected into each of the droplets of the pre-formed library, while all reactions are kept isolated inside the individual drops. The outcome of the reaction is read out optically for each individual droplet, while the library member is identified by its fluorescent barcode label. By this, the “expensive” droplet library containing all reagents has to be formed only once and can be used for many experiments. As eventually for each screened sample only sub-nanoliter droplets are needed, reagent cost will be greatly reduced. Possible applications include genotyping, DNA sequencing, or drug screening.

8232-52, Session 11

## Understanding "giant" II-VI nanocrystal quantum dots by synthetic manipulations, and spectroscopic and electrochemical methods

Y. Ghosh, B. D. Mangum, H. Htoon, J. A. Hollingsworth, Los Alamos National Lab. (United States)

Semiconductor nanocrystal quantum dots (NQDs) are considered as nearly ideal candidates for light-emission applications due to high quantum efficiencies and narrow-band and particle-size-tunable photoluminescence. However, they suffer from chemical-environment-dependent photo-instability at the ensemble level and intermittency in fluorescence intensity, or "blinking", at the single NQD level. Prior work in our research team showed for the first time that the growth of ultra-thick shells of the higher bandgap material, CdS, over CdSe NQD cores leads to remarkable photostability and significant suppression of blinking behavior.1,2 The new class of NQD, the so-called "giant" NQD (g-NQD), promises significant advantages for their application in novel light emitting devices (LEDs).

We now emphasize further improvements and tunability by manipulating the relative core-shell volume (by changing the overall core and shell diameter) and also the interfacial composition (by means of fine tuning the percent composition of shelling material). These variations lead to control over emission wavelength, single and multi-excitonic decay lifetimes, and fluorescence intermittency (blinking) at single NQD levels. We report syntheses of these novel CdSe/nCdS core-shell NQDs, and demonstrate their unique optical properties by ensemble and single quantum dot spectroscopy. We also utilize relatively unexplored field of electrochemistry, viz., cyclic voltammetry (CV) and differential pulse voltammetry (DPV) to accurately and directly determine the energy levels of the Highest Occupied Molecular Orbitals (HOMO) and Lowest Unoccupied Molecular Orbitals (LUMO) and conclusively comment on the electronic structures in solution dispersed semiconductor NQDs. This understanding of conduction and valence-band energy-level alignments allows us to design g-NQD based devices.

1. Chen, Y. et.al., J. Am. Chem. Soc., 2008, 130, 5026.

2. Vela, J. et.al., J. Biophotonics, 2010, 3, 706.

8232-53, Session 11

## Design and study of activatable ("OFF/ON") quantum dots (Qdots) for potential biomedical applications: Ligand selection for Qdot surface modification for controlling Qdot fluorescence quenching and restoration

S. Santra, S. Basumallick, R. N. Mitra, S. Banerjee, R. Shah, UCF NanoScience Technology Ctr. (United States)

Abstract: A number of Fluorescence Resonance Energy Transfer (FRET) based Qdot sensing probes have been reported for various applications including study of protease activity [1], study of interaction of maltose binding to maltose binding protein (MBP) [2], study of intracellular release of therapeutic drugs [3] and detection of 2,4,6-Trinitrotoluene (TNT) [4] and cocaine [5]. All these studies have successfully demonstrated that Qdots can be used as efficient FRET donors. In this direction of developing Qdot based sensing probes, we have designed and synthesized a series of CdS:Mn/ZnS Qdot based "OFF/ON" sensing probes for detection of toxic heavy metal ions [6], alkali metal ions [7] and intracellular glutathione [8]. Our basic Qdot sensing probe design involves selection of suitable ligands that will efficiently quench Qdot fluorescence upon attachment to Qdot surface. The Qdot quenching is believed to be governed by the electron transfer process. Qdot fluorescence restoration takes place when the electron transfer process is stopped. In my talk, I will discuss a series of ligands (small molecules to polymers), their efficacy in quenching Qdot fluorescence and insights about Qdot fluorescence restoration process. I will also briefly discuss design of activatable "OFF/ON" Qdot probes for tracking of intracellular release of active agents for potential biomedical applications.

References:

1. Shi, L., et al., Synthesis and Application of Quantum Dots FRET-Based Protease Sensors. Journal of the American Chemical Society, 2006. 128(32): p. 10378-10379.

2. Medintz, I.L., et al., Self-assembled nanoscale biosensors based on quantum dot FRET donors. Nat Mater, 2003. 2(9): p. 630-638.

3. Bagalkot, V., et al., Quantum Dot-Aptamer Conjugates for Synchronous Cancer Imaging, Therapy, and Sensing of Drug Delivery Based on Bi-Fluorescence Resonance Energy Transfer. Nano Letters, 2007. 7(10): p. 3065-3070.

4. Goldman, E.R., et al., A Hybrid Quantum Dot-Antibody Fragment Fluorescence Resonance Energy Transfer-Based TNT Sensor. Journal of the American Chemical Society, 2005. 127(18): p. 6744-6751.

5. Zhang, C.-y. and L.W. Johnson, Single Quantum-Dot-Based Aptameric Nanosensor for Cocaine. Analytical Chemistry, 2009. 81(8): p. 3051-3055.

6. Banerjee, S., S. Kar, and S. Santra, A simple strategy for quantum dot assisted selective detection of cadmium ions. Chemical Communications, 2008(26): p. 3037-3039.

7. Banerjee, S. and S. Santra, Semiconductor CdS:Mn/ZnS quantum dots for sensing applications. Vol. 7674. 2010: SPIE. 767403.

8. Banerjee, S., et al., Quantum Dot-Based OFF/ON Probe for Detection of Glutathione. The Journal of Physical Chemistry C, 2009. 113(22): p. 9659-9663.

8232-54, Session 11

## Optical spectroscopy of single semiconductor nanocrystals close to gold nanoparticles

A. Mews, X. Ma, T. Kipp, Univ. Hamburg (Germany); L. M. Liz-Marzán, Univ. de Vigo (Spain)

These observations are explained within a comprehensive physical picture. With the help of finite-difference time-domain simulations the PL enhancement can be predominantly attributed to a gold-nanoparticle induced local increase of the electric field of the excitation laser at the position of the NC. The lifetime reduction has its origin in the coupling of the excited NC to the metal-nanoparticle plasmon. This coupling increases both the radiative and non-radiative recombination rates of the hybrid NC-metal emitter as compared to the NC alone. Within the so-called fluctuating barrier model and with the help of Monte-Carlo simulations, we show that the blinking suppression has its physical reason in the increased recombination rates. The emission from gray-state is explained also by the increased radiative recombination rate that, in our system, becomes competitive to the fast and thus typically dominant non-radiative rate of the off-state.

8232-55, Session 11

## Facile synthesis of highly fluorescent metal nanoclusters and application in cellular imaging

L. Shang, R. M. Dörlich, S. Brandholt, N. Azadfar, Karlsruher Institut für Technologie (Germany); G. U. Nienhaus, Karlsruher Institut für Technologie (Germany) and University of Illinois at Urbana-Champaign (United States)

Conventional fluorophores for imaging applications include organic dyes and engineered fluorescent proteins, which suffer from poor photostability, restricting long-term experiments in live cells with high sensitivity. Semiconductor quantum dots (QDs) have been considered as a promising alternative owing to their excellent photophysical properties such as good photostability and high fluorescence brightness; therefore, they have been under intense investigation for various biological applications. However, these QDs have prompted potential safety concerns for in vivo use. In addition, their large physical size, usually comparable or larger than the size of most proteins, could possibly affect the function of attached ligand molecules. Recent advances in nanotechnology have given rise to a new class of fluorescent labels, metal nanoclusters, e.g., Au and Ag. Composed of a few to a hundred atoms, their sizes are comparable to the Fermi wavelength of electrons, resulting in molecule-like properties including discrete electronic states and size-dependent fluorescence. Fluorescent metal nanoclusters have an attractive set of features, such as ultrasmall size, good biocompatibility and large Stokes shift, thus making them attractive alternatives as fluorescent labels for biological applications. We have been devoted to developing facile, efficient methods for preparing fluorescent metal nanoclusters and further exploring their application in cellular fluorescence imaging. Particularly, uptake kinetics and intracellular tracking of these nanoprobes in living cells are pursued by virtue of advanced fluorescent microscopy techniques including spinning disk confocal microscopy, 4Pi microscope and fluorescence lifetime imaging.

# Conference 8233: Reporters, Markers, Dyes, Nanoparticles, and Molecular Probes for Biomedical Applications

Monday-Wednesday 23-25 January 2012

Part of Proceedings of SPIE Vol. 8233 Reporters, Markers, Dyes, Nanoparticles, and Molecular Probes for Biomedical Applications IV

8233-01, Session 1

## Targeting drug resistance mechanism for a rapid optical identification of specific antibiotic utility: photosensitizers as multifunctional molecular probes

T. Hasan, Wellman Ctr. for Photomedicine (United States)

Spectroscopic approaches applied problem-specific biological targets provide a unique opportunity of developing combined diagnostic and therapeutic opportunities. Photodynamic therapy (PDT), a photochemistry based modality is particularly well suited to this strategy as the photosensitizer molecules often have finite fluorescence quantum yields so that they can serve as multifunctional agents for both diagnostic and therapeutic applications. While this approach has been explored in the context of cancer therapeutics, there are significant non-cancer applications that have not received much attention. Enzyme-activated photosensitizers/fluorophores that are targeted to drug resistance mechanisms can serve dually as sensitive probes with utility in determining an effective antibiotic therapy and as targeted therapeutic agents. Our prototype construct, ß-lactamase enzyme-activated photosensitizer (ß-LEAP) and ß-lactamase enzyme-activated fluorophore (ß-LEAF) are examples where we have reported this approach for specifically targeting drug resistant bacteria for therapy and for the functional definition of the extended-spectrum ß-lactamases of multi-drug resistant bacteria. Progress in the development of this enzyme targeted approach in defining the appropriate antibiotic in a rapid optical assay will be presented.

8233-02, Session 1

## Electrospraying of multifunctional microparticles for image-guided delivery of anti-VEGF therapies

L. Zhang, J. Mena, A. Letson, C. Roberts, R. X. Xu, The Ohio State Univ. (United States)

Anti-VEGF therapies have been widely explored for the management of neovascular age-related macular degeneration (AMD). Loading these therapies in biodegradable microparticles may enable sustained drug release and improved therapeutic outcome. However, existing microfabrication processes such as double emulsification produce drug-loaded microparticles with low encapsulation rate and poor antibody bioactivity. To overcome these limitations, we fabricated multifunctional microparticles by an electrospraying process. The experimental setup includes a single axial stainless steel needle, two high voltage power supplies, two syringe infusion pumps, a particle collecting reservoir, illuminating light sources, and a CCD camera. Droplets encapsulating anti-VEGF antibodies and fluorescence dyes were formed by the electro-force between the needles and the ground electrode. By controlling the flow rate, the viscosity, and the interfacial tension of the fluid materials, we have successfully fabricated drug-loaded droplets with various sizes and morphologies. The droplets were further freeze dried to get drug-loaded microparticles. ELISA tests have demonstrated that electrospraying and lyophilization do not affect the antibody bioactivity significantly.

8233-03, Session 1

## Development of peptide multimers for improved endoscopic targeting of murine colonic dysplasia

B. Joshi, S. J. Miller, Z. Liu, S. Elahi, T. D. Wang, Univ. of Michigan (United States)

Currently, screening colonoscopy does not detect all polypoid or non-polypoid (flat and depressed) lesions. Colorectal cancer remains the third most common cause of cancer-related deaths in the U.S. Improved detection using highly specific molecular probes may improve diagnostic performance. We have previously developed a peptide specific for spontaneous colorectal dysplasia in a genetically-engineered CPC;Apc mouse using phage display technology. We aim to demonstrate that multimerization of this peptide can improve the binding affinity and detection sensitivity. A trilysine scaffold was utilized to develop the multimer peptide to mimic the presentation of peptides on the pIII phage protein by providing the same orientation as that of the displayed peptides. All peptides were synthesized using solid phase synthesis and labeled at C-terminus with either FITC or Cy5.5. A wide-field, small animal endoscope capable of fluorescence excitation at 450-475 and 671 nm was utilized to visualize adenomas in vivo. Quantitative analysis of the multimer binding to colonic adenomas revealed a target/background ratio (TBR) of 3.64+/-0.33 compared to 1.79+/-0.20 for the monomer peptide, $p<0.001$. Further validation of the multimer peptide on cultured human colorectal cancer-derived cells (HT29, SW480, and DLD1) demonstrated significantly higher binding on flow cytometry and fluorescence microscopy in comparison to the monomer peptide. Furthermore, the binding affinity for the multimer increased by a factor of 48 in comparison to that of the monomer on HT29 cells. Our results demonstrate that specific detection of dysplastic colonic mucosa on fluorescence endoscopy with monomer peptides can be significantly improved with use of multimer peptides.

8233-04, Session 1

## Cancer therapy utilizing molecular layer deposition (MLD) and self-organized lightwave network (SOLNET): proposal and theoretical prediction

T. Yoshimura, Tokyo Univ. of Technology (Japan)

Cancer therapy utilizing the Molecular Layer Deposition (MLD) and the Self-Organized Lightwave Network (SOLNET) is proposed. MLD is a growth method, in which different kinds of molecules are sequentially provided to a substrate to synthesize organic tailored materials with designated molecular arrangements. In the applications of MLD to cancer therapy, the liquid-phase MLD (LP-MLD) is used because the human is a kind of a liquid system. The human body is regarded as the MLD chamber and the cancer cells as the substrates.

The first proposal is the selective delivery of multi-functional materials, containing emissive molecules for imaging, sensitizers for photodynamic therapy, paramagnetic agents, and so on, to cancer cells by LP-MLD. The second proposal is the in-situ synthesis of drugs, especially large and toxic ones, at cancer cell sites by LP-MLD to deliver the drugs efficiently deep inside the cancer without attacking normal cells.

The third proposal is the SOLNET-assisted laser surgery. After stacks of emissive molecules are adsorbed in cancer cells by LP-MLD, a write beam is introduced from an optical fiber into the area containing cancer cells through photo-induced refractive index increase (PRI) materials to construct self-aligned optical waveguides of SOLNET connecting the optical fiber and the cancer cells. Surgery laser beams are selectively guided to cancer cells by SOLNET. We develop a SOLNET simulator based on the finite difference time domain method that can treat models involving emissive materials, and theoretically predict that SOLNET can guide the surgery laser beams to the cancer cells with high efficiency.

8233-05, Session 1

## Theranostic imaging guided target-specific photo-activatable immunotherapy (PIT)

H. Kobayashi, National Institutes of Health (United States)

Three modes of cancer therapy, surgery, radiation and chemotherapy, have been central to modern oncologic therapy. Molecular targeted cancer therapies have been introduced to target specific pathways, while minimizing side effects but have had limited success except in several notable cases. Here, we employ an activatable hydrophilic photosensitizer based on a near infrared (NIR) phthalocyanine dye, IR700, which is covalently conjugated to one of several humanized monoclonal antibodies (MAb) targeting cancer-specific cell-surface molecules. When exposed NIR light, the conjugate induces highly selective cell death in vivo, a process termed “photo-activatable immunotherapy” (PIT). MAb-IR700 bound target-specific cell death could be induced within 5 minutes of exposure to NIR light and resulted in cellular swelling, bleb formation, and rupture of vesicles indicating necrotic cell death. No phototoxicity was observed in co-cultured receptor-negative cells after incubation with MAb-IR700, even when MAb-IR700 was not removed from the medium during light exposure. Greater than 90% tumor shrinkage was observed in vivo within 3 days of the NIR irradiation, with no apparent side effects, only in target tumors. Furthermore, IR700 fluorescence produced by the MAb-conjugate permitted guidance of light delivery and allowed for monitoring after therapy. The MAb-IR700 PIT was most effective, when conjugates were bound to the cell membrane, but showed no phototoxicity, when unbound, suggesting a novel mechanism for PIT compared with conventional photodynamic therapies. In conclusion, theranostic image-guided target-selective PIT based on MAb-IR700 cell membrane binding enables selective treatment of cancer with no apparent side effects to normal cells or surrounding tissue.

8233-06, Session 2

## Novel water soluble NIR dyes: does charge matter?

G. Patonay, M. Henary, G. Beckford, A. Daube, Georgia State Univ. (United States)

Near-Infrared (NIR) dyes are used as reporters, probes or markers in the biological and medical field. NIR dyes can be useful for investigating and characterizing biomolecular interactions or imaging which is possible because biological mammalian tissue has a low absorption window in the NIR region. Biomolecules such as proteins are known to bind to NIR dyes. Upon binding NIR dyes often exhibit spectral changes that can be used for characterizing the binding event. Serum albumins may be responsible for in vivo transport of NIR dyes. The studies presented here use spectroscopic methods to investigate how NIR dyes that may be used in imaging, biological or bioanalytical applications bind to proteins, such as serum albumins. Our research group systematically synthesized several NIR dyes that have varying hydrophobicity, chromophore size and charge. During these investigations we developed novel NIR cyanine fluorophores having high water solubility even in buffers and a variety of net charges ranging from -4 to +4, including zero. The binding properties of the carbocyanines change when charged moieties are systematically varied. One of the properties we put a special emphasis on is what we call residual hydrophobicity of the NIR dye molecule which is defined as the unmasked (by the charged moieties) hydrophobicity of the molecule. Residual hydrophobicity may be responsible for binding to hydrophobic pockets of biomolecules. High residual hydrophobicity of an otherwise highly water soluble dye can be disadvantageous during biological, medical or similar applications. Bioanalytical utility of NIR dyes as tracers for measuring small molecule binding to biomolecules was also demonstrated via CE using NIR LIF detection. The results of these studies are useful in determining what NIR dye structures exhibit high binding constants and how to optimize detection of the biomolecule NIR dye complex as well as how to predict their in vivo behavior.

8233-09, Session 2

## Pyrrolopyrrole Cyanine (PPCy) dyes: A new class of near-infrared fluorophores

S. Wiktorowski, G. M. Fischer, E. Daltrozzo, A. Zumbusch, Univ. Konstanz (Germany)

Fluorescent dyes are the basis for a broad range of modern techniques in life and material sciences. Especially the possibility to detect individual fluorophores has stirred a lot of interest. Recently, much effort has been invested in the synthesis of near infrared (NIR) absorbing and emitting dyes due to two main reasons. Sample autofluorescence is significantly reduced under NIR excitation and deep penetration depths can be realized since NIR light is scattered less than visible light. Efficient long wavelength absorbing fluorophores are either cyanine or aromatic dyes. Cyanine dyes with absorption wavelengths above 700 nm, however, come along with the price of significantly reduced fluorescence quantum yields. Aromatic chromophores, by contrast, exhibit rather broad absorption bands with strong vibronic side bands, making their application in multicolour experiments difficult. Here, we describe Pyrrolopyrrole Cyanine (PPCy) dyes as a novel class of NIR chromophores. Their optical properties are marked by strong and narrowband NIR absorptions. Stiffening of the chromophore with BF2 or BPh2 groups leads to strong NIR fluorescence and hardly any absorption in the visible range. By varying the heterocyclic peripheral groups of the chromophore, the absorption spectra can be tuned between 684 nm and 864 nm while high fluorescence quantum yields are maintained. PPCys are attractive candidates for labeling applications or as selective NIR absorbers. Moreover, PPCys exhibit very high photostability. On a single molecule level, photostabilities of PPCys surpass that of terrylenediimide (TDI), the best single molecule fluorophore known to date.

8272-02, Session 3

## Rare-earth doped YAG nanoparticles for high- and super-resolution upconversion imaging

R. L. Kolesov, R. Reuter, K. Xia, R. Stoehr, A. Zappe, J. Wrachtrup, Univ. Stuttgart (Germany)

Rare-earth ion dopants can yield upconverted fluorescence whose wavelength is shorter than that of the excitation light.

In our work, we study upconverted fluorescence of rare-earth doped yttrium aluminium garnet (YAG) nanoparticles prepared by

sol-gel method. Three upconversion mechanisms are observed: two-step excitation, sensitized upconversion, and photon avalanche upconversion. Results of background-free upconversion microscopy of YAG nanoparticles doped with praseodymium, erbium,

and thulium are presented. Praseodymium ultraviolet fluorescence can be excited by two-step excitation in the visible. Erbium upconverted green fluorescence can be excited by a number of wavelengths in the red and infrared regions owing to either two-step or avalanche upconversion. Thulium-doped nanoparticles exhibit strong orange-to-blue avalanche upconversion. Upconverted fluorescence in all three species can be sensitized by co-doping with ytterbium. All three species of nanoparticles appear to be absolutely photostable and non-blinking. In addition, super-resolution microscopy similar to stimulated emission depletion (STED) microscopy was demonstrated on Pr:YAG nanoparticles yielding all-optical resolution of 50nm limited mostly by the nanoparticle size. Cytotoxicity tests performed on HeLa cells show harmlessness of YAG nanoparticles. The later fact makes them good candidates for background-free upconversion intracellular imaging. Apart from bio-applications, search for single rare-earth emitting centers in YAG is in progress. Particlularly interesting candidates are trivalent cerium and praseodymium ions. If detected, electron spin of cerium ion at room temperature and nuclear spin of praseodimuim at cryogenic temperature can be manipulated all-optically.

8272-03, Session 3

## Nanodiamonds pave the way for fluorescent quantum probes in biology

D. A. Simpson, L. P. McGuinness, Y. Yan, A. Stacey, L. T. Hall, D. Maclaurin, S. Prawer, P. Mulvaney, The Univ. of Melbourne (Australia); J. Wrachtrup, Univ. Stuttgart (Germany); F. Caruso, R. E. Scholten, L. Hollenberg, The Univ. of Melbourne (Australia)

Defect centres in diamond have long been identified as promising quantum systems for future communication and computation applications. However, in light of recent experimental demonstrations[1, 2] these single spin systems may find new applications in biology as fluorescent “quantum” probes[3]. The nitrogen-vacancy (NV) defect centre in diamond represents an ideal single spin system for use in biology. It has a broad absorption band from 512-560 nm, sustained fluorescence from 630-750 nm, is chemically inert and exhibits low cyto-toxicity [4]. These defects centres have been used as highly stable fluorescence beacons to track the position and diffusion of diamond nano-crystals in vitro and in vivo. In this work we explore the quantum properties offered by this unique fluorescent emitter in the biological context and demonstrate optically detected magnetic resonance (ODMR) of individual fluorescent nanodiamond nitrogen-vacancy centres inside living human HeLa cells. The ODMR spectrum from the nanodiamond is found to be a unique barcode which can be used for indentifying individual diamond nano-crystals of interest. The ODMR spectrum can also be used as an effective tool for probing the rotational dynamics of the nanodiamond. We demonstrate the successful orientation tracking of a single nanodiamond with acquisition times less than a second and an angular precision of less than a degree. The tradeoff between the ODMR acquisition time and angular resolution will be presented and discussed in terms of future biological applications.

1. Balasubramanian, G., et al., Nature, 2008. 455(7213): p. 648-651.
2. Maze, J.R., et al., Nature, 2008. 455(7213): p. 644-648.
3. Hall, L.T., et al., Proceedings of the National Academy of Sciences, 2010. 107(44): p. 18777-18782.
4. Schrand, A. M. et al., J. Phys. Chem. 111, 2, (2007).

8272-04, Session 4

## In vitro and in vivo applications of fluorescent nanodiamonds

H. Chang, Institute of Atomic and Molecular Sciences (Taiwan)

Fluorescent nanodiamonds (FNDs), containing negatively charged nitrogen-vacancy (NV-) centers as fluorophores, have recently emerged as a promising biomarker for in vitro and in vivo applications. The carbon-based nanomaterial is biocompatible, non-toxic, and can be easily conjugated with biomolecules. Uniquely, the built-in NV- centers can emit photostable far-red fluorescence ($\lambda$ = 600 - 800 nm) when excited by green-yellow light, making it well suited for long-term labeling/tracking of cancer and stem cells, not only in vitro but also in vivo. To prove the concepts, we have studied in detail the exocytosis of FNDs (size ~ 100 nm) from three different cell lines, HeLa cervical cancer cells, 3T3-L1 pre-adipocytes, and 489-2.1 multipotential stromal cells. No alteration in growth and proliferation of the FND-labeled cells was observed for up to 8 days and no substantial excretion of the endocytosed FND particles was found after 6 days of cell labeling. We have also applied the technique to whole model organisms such as C. elegans and nude mice. In vivo imaging of nude mice intradermally injected with FNDs revealed that most of the nanoparticles are accumulated in lymph modes, as confirmed by ex vivo imaging and biodistribution measurements. We acquired transverse section images of the lymph nodes by fluorescence lifetime imaging microscopy to visualize the individual particles in the tissues. We summarize in this talk our recent progress towards the development of FNDs for optical bioimaging with single particle sensitivity, long-term tracking capability, and nanometric resolution in cells as well as in whole organisms.

8272-05, Session 4

## Use of upconverting fluorescent nanoparticles for bioimaging

Y. Zhang, N. M. Idris, L. Ong, L. Ang, S. Alonso, National Univ. of Singapore (Singapore)

Lanthanide doped nanocrystals with near-infrared (NIR)-to-NIR and/or NIR-to-visible (VIS) upconversion fluorescence emission have been synthesized. The surface of these nanocrystals have been modified to render them water dispersible and biocompatible. Use of these nanocrystals for bioimaging introduces many advantages, for example, minimum photo-damage to biological samples, weak auto-fluorescence, high detection sensitivity, high light penetration depth, etc. The nanocrystals with small size and tunable multi-color emission have been developed. The emission can be tuned by doping different upconverting lanthanide ions into the nanocrystals. The nanocrystals with core-shell and multi-shell structure have also been prepared, to improve the upconversion efficiency and to tune the emission color. The NIR-to-NIR upconverting nanocrystals have been used for in vitro cell imaging and in vivo animal imaging and cancer cell detection because both the excitation and emission light are in the NIR range and can penetrate through thick tissues. Use of the NIR-to-VIS nanocrystals has also been explored for FRET based biodetection. Although these upconverting nanocrystals are very promising fluorescent materials, their applications in various areas are limited due to the low upconversion efficacy. There is an urgent need to develop new methods to solve this problem.

8272-06, Session 4

## Tailoring rare earth doped nano-particles for applications from biology to quantum computing

Z. U. Hasan, A. Konjhodzic, Temple Univ. (United States)

Ultra-small nano-sized fluorescent centers have found their applications in health sciences, sensor technology, nano-photonics and quantum computing. Their widespread use will undoubtedly demand a control over their physical, chemical and optical properties. Properties such as the size of the nanoparticle, toxicity to the environment, the fluorescence wavelength of operation and the duration for which they remain active in human or animal body are all very specific to an application. We have developed a robust and fast technique of producing nanoparticles doped with fluorescent impurity ions and we demonstrate tailoring of atomic properties of these ultrasmall nanoprobes to suit a variety of applications.

With our technique, pulsed laser ablation of a solid target, almost any solid can be used for producing the nanoparticles. The number fluorescent centers, or rare earth ions in the present case, in a particle has been controlled for different applications. We demonstrate doping of as low as one europium fluorescent ion per particle. We demonstrate the tailoring of the ionization state of the rare earth fluorescent ion inside the particle, for example, doubly or triply ionized europium. This photo-bleaching is fast and is accomplished in nanoseconds. This could allow a non-bleachable probe to become photo-bleachable.

The wavelength of fluorescence and its intensity have been tuned by atomic scale tailoring of symmetry and wavefunctions of the center. We show that fluorescence from doubly ionized europium, the fluorescent ion in our nanoparticles, can be tuned in discrete steps from 575-750nm. At the same time, compared to triply ionized europium, the fluorescence intensity has been increased by eight to ten orders of magnitude, approaching the theoretical limit for the strength of emission.

Such strongly fluorescing nanoparticles have uses as single particle single impurity probes in biological tissues and single photon on demand source in nano-photonics. Particles with larger number of fluorescent ions can be used for ultra-small fluorescent markers, IR-visible upconversion based tags, and hardware for quantum computing. The talk is aimed to show the possible atomic tailoring of ultrasmall fluorescent probes for a variety of applications in Health, Biological and Physical Sciences.

8233-53, Poster Session

## Interaction of 7-hydroxyquinoline with human serum albumin: revealing the mode of molecular recognition

N. Al-Lawatia, T. Steinbrecher, O. K. Abou-Zied, Sultan Qaboos Univ. (Oman)

Human serum albumin (HSA) plays an important role in the transport and disposition of endogenous and exogenous ligands present in blood. Its capacity to reversibly bind a large variety of drugs results in its prevailing role in drug pharmacokinetics and pharmacodynamics. In this work, we used 7-hydroxyquinoline (7HQ) as a probe to study the binding nature of one of the major drug binding sites of HSA (Sudlow I) and to unravel the local environment around the probe in the binding site. The interaction between 7HQ and HSA at physiological pH was investigated by steady-state and lifetime spectroscopic measurements and by molecular dynamics (MD) simulations. The fluorescence results indicate that a selective interaction between 7HQ and the Trp214 residue unmasks fluorescence from the Tyr263 residue. The reduction in both the intensity and lifetime of the Trp214 fluorescence upon binding of 7HQ indicates the dominant role of static quenching. MD simulations show that 7HQ is stabilized in the binding site through hydrophobic and electrostatic interactions. The experimental results reveal the existence of water inside the binding site, and the MD simulations unravel the role of water in molecular recognition and ligand binding.

8233-54, Poster Session

## Strain-hardening effect of graphene on a chain of the chitosan for the tissue engineering

O. E. Glukhova, I. V. Kirillova, N.G. Chernyshevsky Saratov State Univ. (Russian Federation); V. V. Nechaev, Saratov State Technology Univ. (Russian Federation); A. S. Kolesnikova, N.G. Chernyshevsky Saratov State Univ. (Russian Federation)

Already it is established that the composite nanomaterials containing chitosan and graphene are stronger that expands their field of application in the tissue engineering and biomedical technologies. We report the results of the investigations of the chitosan dimer, the mechanism of its interaction with the carbon nanostructures and also the study results of the mechanical properties of the complexes chitosan / graphene, chitosan / nanotube using the density functional (DFT) method and the molecular dynamic method.

The conformers of the chitosan dimer as the unit cells of the crystal chain were researched by the DFT method. The energy surface of the chitosan dimer with the different configurations of the dimer links relative to each other was constructed.

The formation mechanism of the nanocomposites of the chitosan / graphene and chitosan / nanotubes was researched by the molecular dynamics method. It was found that the physical adsorption of the chitosan on graphene is carried out by the Van der Waals interaction between the hexagonal links of the chitosan with the hexagonal cell of the atomic grid of graphene and nanotube. It is shown that the chitosan is adsorbed both on the external and internal surface of nanotube. The mechanical properties of composites on a basis of the chitosan were researched. The elastic modulus increases to ~8 GPa.

8233-55, Poster Session

## The observation research of the differences in cell death and reactive oxygen species in the process of infecting Arabidopsis with avirulent strains

W. L. Chen, H. B. Liu, South China Normal Univ. (China)

To observe the differences of cell death and accumulation of reactive oxygen species (ROS) in the process of infecting Arabidopsis with avirulent Pseudomonas syringae pv. tomato DC3000 (avrB, avrRps4), it will be of great importance to research the role of plant disease resistance and defense response. Using WT, AtrbohD and AtrbohF mutant as experimental materials, we discuss the impact of cell death and ROS on the leaves of Arabidopsis infected with avirulent Pst DC3000 (avrB, avrRps4), observed by spectral analysis and visualized by DAB and trypan blue stain. When infected with avirulent Pst DC3000, both WT and AtrbohF mutant line behaved resistance that exhibited burst of ROS and HR occur, limit senescence and pathogen induced chlorotic cell death. Paradoxically, AtrbohD mutant behaved susceptible characters that exhibited a small quantity of ROS accumulated and enhanced cell death. After infection of Arabidopsis with avirulent Pst DC3000, WT exhibited more ROS accumulation than AtrbohF, and AtrbohD eliminated the majority of total ROS production. Although both WT and AtrbohF mutant exhibited HR occur, enhanced cell death in AtrbohD mutant.

8233-56, Poster Session

## The observation of mitochondrial movement and ATG5 position in Arabidopsis during the process of infection with virulent and avirulent P. syringae strains

W. L. Chen, L. Yang, South China Normal Univ. (China)

Infection of plants with pathogens leads to programmed cell death (PCD) associated with the pathogen-triggered hypersensitive response (HR) during plant innate immunity. In this study, the effects of infection by virulent Pseudomonas syringae pv. tomato (Pst) DC3000 and strains harboring avirulence factors AvrRps4 and AvrB on the induction of HR-PCD were compared. There are some small molecules in cells before HR-PCD, such as salicylic acid (SA) and reactive oxygen species (ROS), which named Pro-PCD. Excessive ROS can cause mitochondrial damage. We found that ATG5 played a role in limiting pathogen growth at least during the early phase of bacterial infection in Arabidopsis. We used transgenic Arabidopsis (Arabidopsis thaliana) plants to study, which expressed green fluorescent protein labeled mitochondria (mito-GFP) and green fluorescent protein tagged ATG5 (atg5-GFP). We found AvrRps4 and AvrB can cause mitochondrial aggregation and overexpression of ATG5, but not by Pst DC3000.

8233-57, Poster Session

## Fluorescent nanodiamonds as highly stable biomarker for endotoxin verification

T. Bergmann, J. M. Burg, M. Lilholt, U. Maeder, S. Beer, D. Salzig, M. Ebrahimi, P. Czermak, M. Fiebich, Technische Hochschule Mittelhessen (Germany)

Fluorescent nanodiamonds (FND) provide advantageous properties as a fluorescent biomarker for in vitro and in vivo studies. The maximum fluorescence of FNDs occurs around 700 nm due to the negatively charged (N-V)- defect center. The defect centers can be generated by high-energy electron irradiation and annealing. This procedure increases the amount of fluorescence in comparison to untreated nanodiamonds.

The fluorescence of FND can be separated well from the autofluorescent background of biological samples due to the fluorescence spectra. FND do not show photobleaching or blinking and are assumed to be noncytotoxic. After a pretreatment with strong acid FND can be functionalized and coupled to biomolecules. FND tend to cluster which impede the coupling reaction. To avoid clustering a method was developed which can be controlled by IR-spectroscopy as well as by scanning-electron microscopy (SEM). For first investigations FND were coupled to endotoxin. Endotoxin is a decay product of bacteria and is found in almost all fluids even in those which are poor of nutrients. This is a huge problem for medical and pharmaceutical applications, because already small amounts of endotoxin cause strong immune reactions. Because of its size and stability the most effective removal procedure is membrane filtration. By coupling to FNDs, endotoxin can be visualized by using confocal fluorescence microscopy equipped with a spectral detection unit. The usage of highly photostable FNDs allows visualization and quantification of endotoxin seperation on investigated membranes. This enables a deeper understanding in the separation mechanisms of the filtration process within the membranes.

8233-58, Poster Session

## Real-time point-of-care measurement of impaired renal function in a rat acute injury model employing exogenous fluorescent tracer agents

R. B. Dorshow, R. M. Fitch, J. K. Wojdyla, A. R. Poreddy, J. N. Freskos, R. Rajagopalan, Covidien (United States)

Renal function assessment is needed for the detection of acute kidney injury and chronic kidney disease. Glomerular filtration rate (GFR) is now widely accepted as the best indicator of renal function, and current clinical guidelines advocate its use in the staging of kidney disease. The optimum measure of GFR is by the use of exogenous tracer agents. However current clinically employed agents lack sensitivity or are cumbersome to use. An exogenous GFR fluorescent tracer agent, whose elimination rate could be monitored noninvasively through skin would provide a substantial improvement over currently available methods. We developed a series of novel aminopyrazine analogs for use as exogenous fluorescent GFR tracer agents that emit light in the visible region for monitoring GFR noninvasively over skin. In rats, these compounds are eliminated by the kidney with urine recovery greater than 90% of injected dose, are not broken down or metabolized in vivo, are not secreted by the renal tubules, and have clearance values similar to a GFR reference compound, iothalamate. In addition, biological half-life of these compounds measured in rats by noninvasive optical methods correlated with plasma derived methods. In this study, we show that this noninvasive methodology with our novel fluorescent tracer agents can detect impaired renal function. A 5/6th nephrectomy rat model is employed.

8233-10, Session 5

## Excited-state prototropism-based fluorescent molecular probes for lipid bilayer membranes

A. K. Mishra, M. Mohapatra, Indian Institute of Technology Madras (India)

Excited state prototropism (ESPT) is observed in molecules having ionizable protons, whose proton transfer efficiencies are different in ground and excited states. ESPT based fluorescent molecules like naphthols and intramolecular ESPT (ESIPT) molecules like hydroxyflavones are efficient in probing structural and dynamical information on a variety of aggregated and organized systems, and ESPT as a probe concept has been gaining ground [1]. The fluorescence of different prototropic forms of such molecules, on partitioning to lipid bilayer membranes, often show sensitive response to the local environment with respect to the local structure, physical properties and dynamics. Our recent work using 1-naphthol as an ESPT fluorescent molecular probe has shown that the incorporation of monomeric bile salt molecules into lipid bilayer membranes composed from dipalmitoylphosphatidylcholine (DPPC, a lung surfactant) and dimyristoylphosphatidylcholine (DMPC), in solid gel and liquid crystalline phases, induce appreciable wetting of the bilayer up to the hydrocarbon core region, even at very low ($\leq$ 1 mM) concentrations of the bile salts. The interaction of fisetin, an ESIPT molecule having antioxidant properties, with lipid bilayer membranes could be sensitively monitored by its intrinsic fluorescence. The molecule appears to fulfil many essential criteria of a good fluorescence molecular probe with regard to the fluorescence parameters of its phototautomer form.

[1] Mishra, A. K. in Understanding and Manipulating Excited State Processes, Eds V. Ramamurthy and K. S. Schanze, Marcel Dekker, Inc., New York , Chapter 10, 2001, 577.

8233-11, Session 5

## Iridium complex probes for monitoring of cellular oxygen levels and imaging of hypoxic tissues

S. Tobita, T. Yoshihara, A. Kobayashi, K. Ichikawa, Gunma Univ. (Japan); M. Hosaka, Akita Prefectural Univ. (Japan); T. Takeuchi, Gunma Univ. (Japan)

We have recently reported that a red-emitting iridium complex Ir(btp)2(acac) (BTP) serves as a hypoxia-sensing probe for tumor imaging in living mice. BTP exhibits oxygen-sensitive phosphorescence that can be utilized to monitor oxygen levels in living cells and to visualize hypoxic tissues. In this study BTP was chemically modified to improve its optical and physicochemical properties as biological oxygen sensor. One of the great advantages of the iridium complexes as oxygen probe is that the optical and physicochemical properties (such as absorption and emission wavelengths, solubility to water, cellular uptake, etc.) can be improved by modifying the organic ligands. To improve the tissue penetrance of BTP, we designed and synthesized near-IR emitting iridium complexes according to two different approaches: extension of the -electronic system of benzothienyl-pyridinato ligand in BTP and introduction of substituents into suitable positions of ligands. The former approach was successful and near-IR emitting iridium complexes were obtained without reduction in emission quantum yield. Cellular uptake of BTP was greatly improved by introducing a dimethylamino group into the acetylacetonato ligand. Using these improved probes, in-vivo lifetime measurements were made to demonstrate the hypoxia of tumor tissues in SCC7 tumor-bearing mice. The second-harmonic (532 nm) of Nd3+:YAG laser was used to excite iridium complexes in tissues, and the phosphorescence lifetime was measured using the time-correlated single photon counting technique. The phosphorescence emitted from the tumor region actually gave longer lifetimes compared to those emitted from normal tissues, demonstrating the hypoxic nature of tumor tissues.

8233-12, Session 5

## Amyloid diagnostics: Probing protein aggregation and conformation with ultrasensitive fluorescence detection.

R. Abhyankar, B. Sahoo, N. K. Singh, L. Meijer, B. Sarkar, A. K. Das, S. Nag, Tata Institute of Fundamental Research (India); C. Muralidharan, Seth G. S. Medical College (India); D. Bhowmik, Tata Institute of Fundamental Research (India); S. Dandekar, Seth G. S. Medical College (India); S. Maiti, Tata Institute of Fundamental Research (India)

While dozens of human ailments are now identified as “protein aggregation diseases”, aggregation by itself does not seem to be a clear determinant of the toxicity. The structural transformation that accompanies the initial steps of aggregation may be an even more important aspect controlling the biological effects of these protein particles. For this, the key is to develop appropriate fluorescent biomarkers which can probe both aggregation and conformation at low physiological concentrations. Using Alzheimer’s amyloid beta (Aβ) as a model system, we have developed probes suitable for the application of Fluorescence Correlation Spectroscopy (FCS, which reports aggregation) and Förster Resonance Energy Transfer (FRET, which reports conformational changes) techniques. To diagnose these changes in the cerebrospinal fluid of Alzheimer’s patients, we are now designing better single molecule detection devices. Here we report a confocal device with a 4π collection geometry, which detects more than 0.5 million photons per second from a single rhodamine B molecule in aqueous solution, which to our knowledge is the highest sensitivity achieved so far with such devices. This allows us to perform quick and sensitive antibunching measurements which report the aggregate mass and fluorophore lifetime of Aβ oligomers.

8233-14, Session 6

## Targeted probes for fluorescence intensity and lifetime imaging exploiting a series of new nir dyes and ph-sensitive fluorophores

J. Pauli, Bundesanstalt für Materialforschung und -prüfung (Germany); J. Mathejczyk, Max-Planck-Institut für experimentelle Medizin (Germany); M. Grabolle, Bundesanstalt für Materialforschung und -prüfung (Germany); J. Berkemeyer, Freie Univ. Berlin (Germany); F. Alves, Max-Planck-Institut für experimentelle Medizin (Germany); K. Licha, mivenion GmbH (Germany); U. Resch-Genger, Bundesanstalt für Materialforschung und -prüfung (United States)

Fluorescence imaging relies on stable and water-soluble fluorescent reporters, strongly absorbing and emitting in the near infrared (NIR) that can be covalently coupled to biomarker-specific ligands like antibodies or peptides, thus yielding specific and sensitive molecular probes which respond to or target molecular species or processes. Here, we present different approaches to targeted fluorescent probes for in vivo imaging in the intensity and lifetime domain exploiting a series of new NIR dyes with controlled aggregation behavior and pH-sensitive fluorophores, spectrally resembling Cy5.5. Based upon these results, screening schemes for the fast identification of suitable fluorophores are derived and design criteria for different types of optical probes are presented.

8233-15, Session 6

## Measuring calpain activity in vivo using lifetime imaging of a far red biosensor

D. W. Stuckey, J. McGinty, R. Laine, Imperial College London (United Kingdom); V. Y. Soloviev, Univ. College London (United Kingdom); D. J. Wells, The Royal Veterinary College (United Kingdom); S. R. Arridge, Univ. College London (United Kingdom); J. V. Hajnal, P. M. W. French, Imperial College London (United Kingdom); A. Sardini, MRC Clinical Sciences Ctr. (United Kingdom)

Calpains belong to a family of calcium-dependant cysteine proteases that are ubiquitously expressed in mammals and have roles in numerous physiological processes. Inappropriate calpain activation, caused by a loss of calcium homeostasis, results in the unregulated proteolysis of structural and regulatory proteins. We have created a calpain-sensitive FRET biosensor (CSFB) and applied time-lapse FLIM to measure calpain activation in skeletal muscle in vivo. CSFB consists of the far red fluorophores TagRFP-T and mPlum, linked by a calpain-cleavable peptide. In the uncleaved state CSFB allows FRET. Upon calpain activation CSFB is cleaved and FRET ceases. Time-resolved FLIM was used to measure the proportion of cleaved versus uncleaved CSFB, as the fluorescence lifetime of TagRFP-T can be discriminated in the two states.

Plasmid DNA was electroporated into the tibialis anterior (TA) hind-leg muscle of mice. At the peak of protein expression mice were positioned on an imaging platform such that the TA could be imaged in reflection geometry. Calpains were activated by electrical stimulation of the leg muscle. The resulting eccentric contraction induced muscle damage and consequently raised intracellular calcium. A series of wide-field time-gated images were acquired allowing fluorescence decay profiles to be fitted and fluorescence lifetimes calculated over the course of calpain activation.

By multiplexing a calcium FRET sensor, TN-L15, with CSFB we will be able to record raised intracellular calcium and calpain activation simultaneously in live mice. This non-invasive methodology should allow a better understanding of calpain activation in vivo, enabling accurate assessment in translational studies.

8233-16, Session 6

## Monitoring tunable, pH responsive nanoprobes using Raster-scan Image Correlation Spectroscopy

S. Abdisalaam, The Univ. of Texas at Arlington (United States)

In this study we are using Raster scan Image Correlation Spectroscopy and Fluorescence Correlation Spectroscopy to study tunable, pH responsive micelle nanoprobes for selective activation in vivo and in vitro. Nanoscopic pH responsive imaging probes have been developed to help counter the complexity of modern diagnostic tools such as CAT, MRI, PET.

8233-17, Session 6

## Fast-responding and sensitive fluorescence in vivo imaging of cancer by using a novel protease probe for gamma-glutamyltranspeptidase

M. Sakabe, The Univ. of Tokyo (Japan); N. Kosaka, M. Mitsunaga, National Institutes of Health (United States); M. Ogawa, Hamamatsu Univ. School of Medicine (Japan); P. Choyke, National Institutes of Health (United States); D. Asanuma, M. Kamiya, T. Nagano, The Univ. of Tokyo (Japan); H. Kobayashi, National Institutes of Health (United States); Y. Urano, The Univ. of Tokyo (Japan)

Proteases play essential roles in cancer and immune disease. Sensitive and accurate protease detection systems become a crucial tool for the early diagnosis of diseases. To detect activity of protease, Rhodamine Green based fluorescence probes have been widely used. However, since they require two activation steps, they have low sensitivity compared to probes which can be activated by one-step.

Recently, we have reported that a series of rhodamine derivatives bearing a hydroxymethyl group instead of original carboxy group shows unique intramolecular spirocyclization. Among those derivatives, we found that new hydroxymethyl-Rhodamine Green (HMRG) was strongly fluorescent in aqueous solution at pH7.4, whereas singly acetylated HMRG was colorless and non-fluorescent. By utilizing this finding, we developed a novel protease probe (gGlu-HMRG) that can detect gamma-glutamyltranspeptidase (GGT) activity by one-step activation coupling with drastic fluorescence augmentation. It is known that GGT is a central player for glutathione metabolism and increased GGT activity has been implicated in human diseases including ovarian, lung and liver cancer. We then applied gGlu-HMRG for bioimaging. gGlu-HMRG showed a large fluorescence increase in GGT expressing cancer cell lines under microscope, but not in a normal cell line. Next, we performed imaging of cancer in a mouse model of peritoneal metastases. Cancer cells in peritoneal cavity were successfully visualized with gGlu-HMRG even at a few minutes after i.p.-injection. We anticipate that gGlu-HMRG will be a powerful tool as an imaging guidance for surgery operation.

8233-18, Session 6

## Time-domain Imaging with Quench-based Fluorescent Contrast Agents

W. J. Akers, M. Solomon, G. P. Sudlow, S. Achilefu, M. Y. Berezin, Washington Univ. School of Medicine in St. Louis (United States)

Quench-based probes utilize unique characteristics of fluorescence resonance energy transfer (FRET) to enhance contrast upon de-quenching. This mechanism has been used in a variety of molecular probes for imaging of cancer related enzyme activity such as matrix metalloproteinases, cathepsins and caspases. While non-fluorescent upon administration, fluorescence can be restored by separation of donor and acceptor, resulting in higher intensity in the presence of activator. Along with decreased quantum yield, FRET also results in altered fluorescence lifetime. Time-domain imaging can further enhance contrast and information yield from quench-based probes. We present in vivo time-domain imaging for detecting activation of quench-based probes. Time-domain diffuse optical imaging was performed to assess the FRET and quenching in living mice with orthotopic breast cancer. Tumor contrast enhancement was accompanied by increased fluorescence lifetime after administration of quenched probes selective for matrix metalloproteinases while no significant change was observed for non-quenched probes for integrin receptors. These results demonstrate the utility of time-domain imaging for detection of cancer-related enzyme activity in vivo.

8233-19, Session 7

## Pharmacokinetics of bioconjugated ICG-micellar nanocapsules for optical molecular imaging: preclinical and toxic studies

Y. Chen, T. Jabour, X. D. Li, The Johns Hopkins Univ. (United States)

Near infrared (NIR) fluorescence imaging is nowadays widely utilized to study pathologic and normal processes noninvasively with molecular sensitivity/specificity. The translation of this potentially powerful molecular imaging technology to clinical applications is hindered by the lack of biocompatible and disease specific fluorescent contrast agents. Indocyanine green (ICG) is the only NIR fluorescent dye approved by FDA for routine clinical use. However, it suffers from several shortcomings including optical and thermal instability, rapid clearance from the circulation system, and the lack of a functional group for bioconjugation and active targeting. Previously we demonstrated that the mentioned limitations of ICG could be effectively overcome by encapsulating ICG molecules into micelles that are formed by FDA approved polymers - Pluronic. This ICG-micellar nanocapsule approach dramatically improved the stability and yield of ICG fluorescence, and more importantly, enabled bioconjugation for molecular targeting. In this study, fluorescence molecular tomography and fluorescence reflectance imaging systems were utilized to study the pharmacokinetic profile of the bioconjugated ICG-micellar nanocapsules. The fluorescence signal from tumors could be observed with a high signal-to-background ratio only five hours post intravenous injection of the agent. Moreover, the strong signal from tumor lasts at least five days. To study the feasibility of utilizing this fluorescent probe made of only FDA approved materials in clinical practice, acute and chronic toxicity experiments are underway.

8233-20, Session 7

## Effect of capsid protein and ICG mass ratio on fluorescent quantum yield of plant virus-resembling optical nanomaterials

S. Gupta, G. Ico, P. Matsumura, Y. Guerrero, A. L. N. Rao, V. I. Vullev, B. Anvari, Univ. of California, Riverside (United States)

We recently reported on construction of a new type of optical nano-construct composed of genome-depleted plant infecting brome mosaic virus (BMV) doped with Indocyanine green (ICG),an FDA-approved near-infrared chromophore (ACS Nano, 5(2):1243-1252, 2011). We refer to these constructs as optical viral ghosts (OVGs) since only the capsid protein (CP) subunits of BMV remain to encapsulate ICG. To utilize OVGs as effective nano-probes in fluorescence imaging applications, their fluorescence quantum yield needs to be maximized. In this study, we investigate the effect of altering the CP to ICG mass ratio on the resulting fluorescent quantum yield of OVGs. Results of this study provide the basis for construction of OVGs with optimal amounts of CP and ICG to yield maximal flouorescence quantum yield.

8233-21, Session 7

## Selective detection of peritoneal ovarian cancer micrometastases by microendoscopic imaging of a photoimmunoconjugate

B. Q. Spring, X. Zheng, A. O. Abu-Yousif, T. Hasan, Massachusetts General Hospital (United States)

Metastatic ovarian carcinoma (OvCa) is characterized by nodular studding of the peritoneal cavity. There is a need for targeted imaging agents and therapies that enhance selectivity in such complex sites. Our laboratory is developing image-guided detection, monitoring and treatment of clinically occult peritoneal micrometastases. The multifocal nature and microscopic size of residual OvCa necessitates cellular resolution imaging with selective labeling of the neoplasms. Towards this goal we have developed a custom wide-field fluorescence microendoscope (FME) in conjunction with a photoimmunoconjugate that targets OvCa cells overexpressing the epidermal growth factor receptor (EGFR).

8233-22, Session 7

## Imaging B. anthracis heme catabolism in living mouse using the IFP1.4 gene reporter

B. Zhu, H. Robinson, N. Wilganowski, The Univ. of Texas Health Science Ctr. at Houston (United States); C. L. Nobles, Baylor College of Medicine (United States); E. M. Sevick-Muraca, The Univ. of Texas Health Science Ctr. at Houston (United States); A. Maresso, Baylor College of Medicine (United States)

B. anthracis is a gram-positive, spore-forming bacterium which likes all pathogenic bacteria, survive by sequestering heme from its host. To image B. anthracis heme catabolism in vivo, we stably transfect new red excitable fluorescent protein, IFP1.4, that requires the heme catabolism product. IFP1.4 reporter has favorable excitation and emission characteristics, which has an absorption peak at 685 nm and an emission peak at 708 nm. Therefore, IFP1.4 reporter can be imaged deeply into the tissue with less contamination from tissue autofluorescence. However, the excitation light “leakage” through optical filters can limit detection and sensitivity of IFP1.4 reporter due to the small Stoke’s shift of IFP1.4 fluorescence. To minimize the excitation light leakage, an Electron Multiplying CCD (EMCCD) based infrared fluorescence imaging device was optimized using two band pass filters separated by a focus lens to increase the optical density at the excitation wavelength. In this study, a mouse model (DBA/J2) was first injected with B. anthracis bacteria expressing IFP1.4, 150ul S.C, on the ventral side of the left thigh. Then mouse was given 250ul at 1mM of biliverdin IV. Imaging was conducted as a function of time after infection and after euthanasia, excised tissues were imaged and IFP1.4 fluorescence correlated with standard culture measurements of colony forming units. The work demonstrates the use of IFP1.4 as a reporter of bacterial utilization of host heme and may provide an important tool for understanding the pathogenesis of bacterial infection and developing new anti-bacterial therapeutics.

8233-23, Session 7

## Development of anti-HER2 conjugated ICG-loaded polymeric nanoparticles for targeted optical imaging of ovarian cancer

B. Bahmani, J. Tang, J. Crovisier, V. I. Vullev, B. Anvari, Univ. of California, Riverside (United States)

Targeted delivery of therapeutic and imaging agents using surface modified nanovectors has been explored immensely in recent years. The growing demand for site-specific and efficient delivery of nanovectors entails stable surface conjugation of targeting moieties. We have developed a polymeric nanocapsule doped with Indocyanine green (ICG) with potential for targeted and deep tissue optical imaging and phototherapy. Our ICG-loaded nanocapsules (ICG-NCs) have potential for covalent coupling of various targeting moieties and materials due to presence of amine groups on the surface. Here, we covalently bioconjugate PEG-coated ICG-NCs with monoclonal antibody against HER2 through reductive amination-mediated procedures. The irreversible and stable bonds are formed between anti-EGFR and aldehyde termini of PEG chains on the surface of ICG-NCs. We quantify uptake of anti-HER2 conjugated ICG-NCs by ovarian cancer cells using fluorescent confocal microscopy and flow cytometery. The proposed process for covalent attachment of anti-HER2 to PEGylated ICG-NCs can be used as a methodology for bioconjugation of various antibodies to such nano-constrcuts and provides the capability to use these optically active nano-probes for targeted optical imaging of ovarian and other cancer types.

8233-24, Session 7

## Variants of monomeric red fluorescent protein at residue 66: spectral and individual photophysical properties

A. A. Banishev, Institute on Laser and Information Technologies (Russian Federation); E. P. Vrzheshch, N. Usmanov, A. M. Saletsky, Lomonosov Moscow State Univ. (Russian Federation)

Fluorescent proteins (FPs) are a class of proteins that have a distinguishing property of forming an inner fluorescent (or absorbing, but not fluorescent) center (chromophore) without involvement of any additional cofactors and ferments (autocatalytic reaction), except for molecular oxygen. In recent years, FPs have gained enormous popularity as genetically encoded fluorescence markers. They enable the visualization of a broad range of biological processes in cells (protein translocation within cells and cell movement during development and etc) and tissue (primary tumor growth, tumor cell motility and invasion and etc).

The FPs with fluorescence in the red spectral range (red FPs) whose molecules are monomers are of particular interest. The application of red fluorescence allows reducing the influence of the background fluorescence of cell components on the total fluorescence signal and a monomeric property allows overcoming the tendency of red FPs to form large molecular aggregates.

At present active researches are being carried out to obtain new variants of red monomeric FPs with improved properties: with the fluorescence spectrum in a longer-wavelength range, a higher quantum yield of fluorescence, better photo- and pH-stability. In this report the influence of a single amino acid substitution in monomeric red FP mRFP1 on optical and individual photophysical properties of chromophore of fluorescent spectral form is presented. The 66th amino-acid residue (glutamine 66) has been chosen as a position to be replaced. The method of nonlinear laser fluorescence spectroscopy, along with conventional methods of spectroscopy, was used for photophysical properties of the proteins investigation.

8233-25, Session 8

## One-photon and two-photon fluorescence folate receptor bioimaging with an aggregation-enhanced emission silica nanoprobe

K. D. Belfield, X. Wang, A. R. Morales, Univ. of Central Florida (United States); T. Urakami, M. Komatsu, Sanford-Burnham Medical Research Institute (United States); L. Zhang, Univ. of Central Florida (United States)

A two-photon absorbing (2PA) and aggregation-enhanced near infrared (NIR) emitting pyran derivative, encapsulated in and stabilized by silica nanoparticles (SiNPs), is reported as a nanoprobe for two-photon fluorescence microscopy (2PFM) bioimaging that overcomes fluorescence quenching associated with high chromophore loading. The new SiNP probe exhibited aggregate-enhanced emission producing nearly twice as strong signal as the unaggregated dye, a three-fold increase in two-photon absorption relative to the DFP in solution, and approx. four-fold increase in photostability. The surface of the nanoparticles was functionalized with a folic acid (FA) derivative for folate-mediated delivery of the nanoprobe for 2PFM bioimaging. Surface modification of SiNPs with the FA derivative was supported by zeta potential variation and 1H NMR spectral characterization of the SiNPs as a function of surface modification. In vitro studies using HeLa cells expressing folate receptor (FR) indicated specific cellular uptake of the functionalized nanoparticles. The nanoprobe was demonstrated for FR-targeted one-photon in vivo imaging of HeLa tumor xenograft in mice upon intravenous injection of the probe. The FR-targeting nanoprobe not only exhibited highly selective tumor targeting but also readily extravasated from tumor vessels, penetrated into the tumor parenchyma, and was internalized by the tumor cells. Two-photon fluorescence microscopy bioimaging provided three-dimensional (3D) cellular-level resolution imaging up to 350 μm deep in the HeLa tumor.

8233-26, Session 8

## In vivo track the development of melanoma with the intrinsic third harmonic generation and two-photon fluorescence contrasts of melanin

P. Wu, T. Liu, Y. Chen, Y. T. Hsieh, H. Liu, W. Lin, National Taiwan Univ. (Taiwan)

The understanding of the interaction between tumors and surrounding microenvironment in vivo is an important first step and basis for pathway-targeting cancer therapy. To in vivo observe the dynamic development of tumor cells and validate the efficacy of therapy in microscopic scales, people commonly performed multi-photon fluorescence microscopy through an invasive window chamber setup. However, under such system, the cancer cells can't be identified and long-term tracked without a fluorescence labeling.

Exploiting the intrinsic third harmonic generation and two-photon fluorescence contrasts of melanin, we can in vivo identify melanoma and track its developmentwithout labeling. It was achieved with the least invasive femtosecond Cr:forsterite laser and a laser scanning nonlinear microscopy system with 3D sub-micron spatial resolution. Through this optical tomography platform, we caninvestigate the remodeling of collagens and evaluate the permeability of neovasculatures right around tumor sites. From second harmonic generation microscopy, tumor sites observe more cavities in extracellular matrices and more directivity of collagen fibers. Using intravenously injected fluorescence dextran, we also observed the enhanced permeation for melanoma-associated vasculatures. We anticipate thus developed platform with ongoing developments in molecular probes can be a powerful tool to reveal molecular insights of tumor microenvironments, enhance our understanding of tumor biology, and trigger new therapeutic approaches.

8233-27, Session 8

## Multiphoton fluorescence spectra and lifetimes of biliverdins and their protein-associated complex

C. Huang, C. Wu, T. Liu, National Taiwan Univ. (Taiwan)

Biliverdin is a down-stream metabolite of heme, which is a critical prosthetic group for many hemoproteins. It also plays a critical role for removing radicals in cytoplasm through the effective biliverdin/bilirubin redox cycle. However, the fluorescence yield of biliverdin is pretty weak compared with other endogenous fluorophores like NADH, flavins, and porphyrins. Therefore, biliverdin is rarely considered as a characteristic marker in the hyperspectral diagnosis on human tissues. Recently, it has been demonstrated that least invasive femtosecond Cr:forsterite laser can achieve deep tissue imaging and suppress most endogenous fluorophores. Only red-fluorophores like porphyrins can be selectively excited. Since the concentration of porphyrins is on the order of 10nM, the fluorescence yield of  M biliverdin in tissues could thus dominate the detected fluorescence signals and become a useful fluorescence marker.

In this report, with femtosecond Cr:forsterite laser, we measured the multiphoton fluorescence spectra and lifetimes of biliverdins and their protein-associated complex. Excited at 1230nm, the two-photon fluorescence of biliverdins peaks around 670nm. The corresponding lifetime (<100ps) is much shorter than those of porphyrins (~10ns). Further associated with proteins like human serum albumins, biliverdins reductase, or heme oxygenase, the yields of red fluorescences were increased and the corresponding lifetimes will be lengthened to 200~300ps. These spectral and temporal characteristics indicate biliverdin a potential marker fluorophore for hyperspectral diagnosis on human tissues.

8233-28, Session 8

## Detection of neurotransmitters by surface enhanced Raman scattering (SERS) within hollow-core photonic crystal fiber

V. S. Tiwari, A. Khetani, A. Momenpour, H. Anis, V. Trudeau, Univ. of Ottawa (Canada)

The present work demonstrates the feasibility of using surface enhanced Raman scattering (SERS) for detecting the neurotransmitters glutamate (GLU) and gamma-amino butyric acid (GABA) using hollow core photonic crystal fiber (HC-PCF). These amino acid neurotransmitters immediate fast excitatory and inhibitory neurotransmission in the brain, and are important for neuroendocrine control, and upsets are linked to epilepsy. GLU is converted to GABA in a single enzymatic step mediated by glutamic acid decarboxylase. We present an optical method for real-time monitoring of the concentration of GLU and GABA that may complement existing techniques such as High-Performance Liquid chromatography (HPLC) or mass spectrography for their characterization. SERS based detection has a number of known advantages which includes ease of sample preparation, molecular specificity and sensitivity, thus making it potentially useful in characterization of experimental brain extracts or clinical diagnostic samples of cerebrospinal fluid and saliva. The novelty of this work is in using HC-PCF to further improve the detection sensitivity of GLU and GABA. Our detection scheme facilitates strong light-matter interaction within the HC-PCF's that lead to the detection of low amount of glutamate and GABA in the range of 10-8 -10-9 M. The presence of one additional carboxylic group in GLU compared to GABA and the difference in their conformational structure presents unique spectral contrast in their respective SERS spectrum. This is evident in the relative broadening and shifting of SERS band ~1409 cm-1 (symmetrical stretching mode at COO-) which can be monitored for quantifying the relative concentration of GLU and GABA in their sample mixture.

8233-29, Session 9

## Design of peptide-conjugated glycol chitosan nanoparticles for near-infrared fluorescent (NIRF) in vivo imaging of bladder tumors

J. Key, D. Dhawan, D. K. Knapp, Purdue Univ. (United States); K. Kim, I. C. Kwon, K. Choi, Korean Institute of Science and Technology (Korea, Republic of); J. F. Leary, Purdue Univ. (United States)

Enhanced permeability and retention (EPR) effects for tumor treatment have been utilized as a representative strategy to accumulate untargeted nanoparticles in the blood vessels around tumors. However, the EPR effect itself was not sufficient for the nanoparticles to penetrate into cancer cells. For the improvement of diagnosis and treatment of cancer using nanoparticles, many more nanoparticles should specifically go inside cancer cells. Otherwise, they can leave the tumor area and not contribute to treatment. In order to enhance the internalization process, specific ligands on nanoparticles can help the specific internalization in cancer cells by receptor-mediated endocytosis. We previously developed glycol chitosan based nanoparticles that suggested a promising possibility for in-vivo tumor imaging using the EPR effect. The glycol chitosan nanoparticles showed a long circulation time beyond 1 day and they were accumulated predominantly in tumor. In this study, we evaluated two peptides for specific targeting and better internalization into bladder cancer cells. We conjugated the peptides on to the glycol chitosan nanoparticles; the peptide-conjugated nanoparticles were also labeling with near infrared fluorescent dye, Cy5.5, to visualize them by optical imaging in-vivo. Importantly real-time NIRF imaging can also be used for fluorescence-guided surgery of tumors beyond normal optical penetration depths. The peptide conjugated glycol chitosan nanoparticles were characterized with respect to size, stability and zeta-potential and compared with previous nanoparticles without ligands in terms of the internalization effect of bladder cancer cells. This study demonstrated the possibility of our nanoparticles for tumor imaging and emphasized the importance of specific targeting peptides.

8233-30, Session 9

## Plant virus-resembling optical nanoparticles conjugated with anti-EGFR for targeted cancer imaging

S. Gupta, H. Wilder, A. L. N. Rao, B. Anvari, Univ. of California, Riverside (United States)

Our group has recently constructed a new type of optically active nano-particles for biomedical applications, which is composed of genome-depleted plant infecting brome mosaic virus (BMV) doped with a FDA-approved near-infrared chromophore, Indocyanine green (ICG) (ACS Nano, 5(2):1243-1252, 2011). These nano-particles are referred as optical viral ghosts (OVGs) since only the capsid protein (CP) subunits of BMV are used to encapsulate ICG. Due to the presence of naturally available amine groups on CP subunits, OVGs can be functionalized with various targeting moieties including monoclonal anti-bodies. In this study, we covalently conjugated the surface of OVGs with anti-epidermal growth factor receptors (anti-EGFR) to target cancerous human bronchial epithelial cells (C-HBECs) in-vitro. Our preliminary results demonstrate that anti-EGFR conjugated OVGs are targeted more efficiently to C-HBECs in comparison with unconjugated OVGs or freely dissolved ICG for same incubation time.

8233-31, Session 9

## Active Brain Targeting of Hydrophilic Substances Using Polymeric Magnetic Nanoparticles

E. M. Sadoqi, B. Kirthivasan, M. M. Bommana, St. John's Univ. (United States); S. Raut, Univ. of North Texas Health Science Ctr. at Fort Worth (United States); D. Singh, Univ. of Nebraska Medical Ctr. (United States); E. Squillante III, St. John's Univ. (United States)

Oleic acid coated magnetic nanoparticles (OAMNP) were prepared by thermal decomposition of iron pentacarbonyl. Polymeric nanoparticles were prepared containing either NIR dye (ICG), or p-glycoprotein (p-gp) substrate Rh123 along with OAMNP in a matrix of PLGA and Met-PEG-PLA using single emulsion solvent evaporation. The prepared nanoparticles were preliminarily evaluated for morphology, particle size, dye content and magnetite content. The in vivo biodis-tribution study was carried out using three groups of six male Sprague Dawley rats each. Group I received a saline solution containing the dye, group II received dye-loaded polymeric magnetic nanoparticles without the aid of a magnetic field, and group III received dye-loaded polymeric magnetic nanoparticles with a magnet placed on the head of the rat. After a preset exposure period, the animals were sacrificed and dye concentration was measured in the brain, liver, kid-ney, lungs and spleen. Brain sections were fixed, cryotomed and visualized using fluorescence microscopy.

The particles were observed to be spherical and had a mean size of 220 nm. The encapsulation efficiency for OAMNP was 57%, while that for ICG was 56% and for Rh123 was 45%. In the biodistribution study, while the majority of the dose for all animals was found in the liver, kidneys and spleen, group III showed a significantly higher brain concentration than the other two groups ($p < 0.001$). This was further corroborated by fluorescence microscopy, which showed dye penetration into the brain parenchyma. This proves the potential use of polymeric magneti-cally-targeted nanoparticles in drug delivery & targeting to the brain and brain-imaging.

8233-33, Session 9

## Multi-modal in cellulo evaluation of NPR-C targeted C-ANF-peptide and C-ANF-comb nanoparticles

M. Shokeen, Washington Univ. School of Medicine in St. Louis (United States); E. Pressly, Univ. of California, Santa Barbara (United States); M. J. Welch, Washington Univ. School of Medicine in St. Louis (United States); C. J. Hawker, Univ. of California, Santa Barbara (United States); P. K. Woodard, S. Achilefu, Washington Univ. School of Medicine in St. Louis (United States)

Natriuretic peptides (NPs) are involved in homeostasis and have been used clinically as markers of heart failure. Of the 3 known NP receptors, the NP clearance receptor (NPR-C), is expressed during the growth and remodeling of vascular smooth-muscle cells (VSMCs) in atherosclerosis. In this study, we investigated the in cellular targeting potential of the C-type atrial natriuretic factor (C-ANF), a fragment of the C-type atrial natriuretic peptide, alone and when conjugated to novel comb nanoparticles for future use as effective optical molecular probes and PET radiopharmaceuticals. Well-defined amphiphilic graft copolymers and associated comb nanoparticles having a controlled number of targeting (C-ANF) peptides, fluorescent dyes, and diagnostic units (1,4,7,10-tetraazacyclododecane-1,4,7,10-tetraacetic acid (DOTA)) were prepared. The uptake of the particles in stably transfected NPR-C cell lines were studied. As a negative control, cellular uptake in NPR-A and NPR-B cell lines was investigated. The cellular associated fluorescence and radioactivity, which is the sum of the cell-internalized fraction and cell surface-bound fraction, was measured at 37 °C at 60 minute post incubation and normalized to protein content. Saturation Binding Assays were developed using a NPR-C transfected cell line to calculate the Kd and Bmax for the nanoparticles. The cellular uptake assays demonstrated that a significant reduction in percent cell associated activity for the 64-Cu-DOTA-CANF-comb nanoparticle in the presence of blocking agent (9.33±2.5 vs. 4.54±1.59, $p<.005$). Saturation binding study resulted in an average Kd: 1.12 and Bmax: 1201.5 (n=2). The results demonstrate that the internalization of nanoparticles using a multimodal imaging platform. These measurements allowed us to compare the binding affinities, cell internalization kinetics and specificities of the C-ANF functionalized comb nanoparticles with nanoparticles-functionalized C-ANF peptide.

8233-34, Session 10

## Plasmonic nanosensors for molecular photoacoustic imaging of regional micrometastasis

A. Papagiannaros, The Univ. of Texas M.D. Anderson Cancer Ctr. (United States); G. P. Luke, J. O. Tam, The Univ. of Texas at Austin (United States); S. Y. Emelianov, K. Sokolov, The Univ. of Texas M.D. Anderson Cancer Ctr. (United States)

Cancer metastasis is the premier cause of cancer mortality. Early detection of cancer cells in the sentinel lymph nodes can result in efficient treatment. Here we present combined photoacoustic/ultrasound imaging with molecular targeted plasmonic nanoparticles for specific detection of micrometastasis in sentinel lymph nodes.

We have synthetized 40nm gold nanoparticles conjugated with anti-EFGR antibody or 5k-PEG as molecular targeted and control nanoparticles, respectively. An orthotopic model of metastatic tongue cancer was created by injecting animals with FaDu cells.

Experiments have been carried out in three animal groups: tumor bearing mice injected with targeted or control nanoparticles at the site of the primary tumor and normal mice injected with targeted nanoparticles in the tongue. Ultrasound photoacoustic imaging was performed and mice were sacrificed. Tongue and lymph nodes were collected for ex-vivo hyperspectral analysis and histology examination for cancer cells (EGFR-staining), macrophages (RAM11) and gold (silver-staining).

Ultrasound and photoacoustic imaging exhibited a localized signal in lymph nodes of tumor bearing mice injected with EGFR targeted nanoparticles. Histology demonstrated co-localization of EGFR positive cancer cells and targeted gold nanoparticles. The hyperspectral optical imaging showed that molecular specific interactions between targeted nanoparticles and cancer cells resulted in strong shift of nanoparticle plasmon resonances to red-NIR region. These optical changes account for high contrast in detection of labeled metastatic cells using photoacoustics. Control PEG-coated nanoparticles also showed some accumulation in sentinel lymph nodes, but they were not co-localized with tumor cells. There were no detectable photoacoustic signals from control animal groups in the NIR region.

8233-35, Session 10

## Calibrating the imaging and therapy performance of magneto-fluorescent gold nanoshells for breast cancer

A. E. Dowell, N. C. Biswal, Baylor College of Medicine (United States); C. Ayala-Orozco, Rice Univ. (United States); M. Giuliano, W. Chen, R. Schiff, Baylor College of Medicine (United States); N. J. Halas, Rice Univ. (United States); A. Joshi, Baylor College of Medicine (United States)

Gold nanoshells with plasmon resonance in NIR can be modified to simultaneously enhance conjugated NIR fluorescence dyes and T2 contrast of embedded iron-oxide nanoparticles, and molecularly targeted to breast and other cancers. Herein, we calibrate the theranostic performance of magneto-fluorescent nanoshells, and a home-built visible-NIR in vivo imaging and NIR therapy device on MCF7L breast cancer cells which have been transfected with a dual GFP-firefly luciferase expression vector. Silica core gold nanoshells with Plasmon resonance on ~810 nm were doped with NIR dye Indocyanine Green and ~10 nm iron-oxide nanoparticles in a ~20 nm epi-layer of silica. Resulting nanocomplex exhibits strong NIR fluorescence properties and T2 MR contrast. MCF7L breast cancer cells were transduced with firefly luciferase reporter and GFP. Imaging was conducted in a home-built chamber equipped with visible to NIR light sources, an intensified CCD camera, and a 15W 810 nm therapeutic laser. Cell viability with varying laser power levels in presence and absence of nanoshells was assessed by bioluminescence imaging. Bioluminescent light intensity of MCF7L cells incubated with nanocomplexes was reduced from 9987 to 4111 (59%) after therapy with laser power of 1.5 W/cm2 for 3 minutes. The light emitted by luciferase from the MCF7L cells not treated with nanocomplexes was only reduced from 10088 to 9397 (6%) after treatment at identical laser exposure levels. This study demonstrates the capability of magneto-fluorescent nanocomplexes for imaging and therapy of breast cancer cells, and the advantages gained by bioluminescence imaging for sensitive calibration of photothermal therapy.

8233-37, Session 10

## Gold nanoparticles heated by x-rays for applications to cancer therapies

R. R. Letfullin, Rose-Hulman Institute of Technology (United States); B. Murphy, Radiological Technologies Univ.-VT (United States); C. W. Rice, Rose-Hulman Institute of Technology (United States)

The photothermal therapies of nanophotohyperthermia and nanophotothermolysis utilize the light absorptive properties of nanoparticles to create heat in a small localized region. Conjugating nanoparticles with various biomolecules allows for targeted delivery to specific tissues or even specific cells, cancerous cells being of particular interest. Previous studies have investigated nanoparticles at visible and infrared wavelengths where surface plasmon resonance leads to unique absorption characteristics. However, issues such as poor penetration depth of the visible light through biological tissues limits the effectiveness of delivery by noninvasive means. In other news, various nanoparticles have been investigated as contrast agents for traditional X-ray procedures, utilizing the strong absorption characteristics of the nanoparticles to enhance contrast of the detected X-ray image. Using X-rays to power photo-thermal therapies has three main advantages over visible-spectra wavelengths: the high penetration depth of X-rays through biological media makes non-invasive treatments very feasible, the high energy of individual photons means nanoparticles can be heated to desired temperatures with lower beam intensities, and X-ray sources are already common throughout the medical industry making future implementation on existing equipment possible. This paper uses Mie theory to investigate the light absorption properties of various size gold nanoparticles over photon energies in the 1-100 keV range. These absorption values are then plugged into a thermal model to determine the temperatures reached by the nanoparticles for X-ray exposures of differing time and intensity. The results of these simulations are then discussed in relation to the effective implementation of nanophotohyperthermia and nanophotothermolysis treatments.

8233-38, Session 10

## Silica-coated gold nanorods optimized for 1064-nm photoacoustic molecular imaging

Y. Chen, D. Xu, W. Frey, S. Y. Emelianov, The Univ. of Texas at Austin (United States)

We previously demonstrated that photoacoustic imaging of contrast agents at 1064 nm wavelength has enhanced contrast due to the low background photoacoustic signal from tissue. However, to absorb light at 1064 nm wavelength, traditional plasmonic nanoparticles including silica-coated gold nanorod become large (more than 100 nm in at least one of the linear dimensions) thus limiting the application of photoacoustic molecular imaging in vivo due to the possible decrease in vascular transportation, extracellular delivery and cell uptake. Therefore, there is a need to produce a photoacoustic contrast agent with strong optical absorption at 1064 nm, superior photothermal stability, efficient light-to-acoustic conversion, and the size of the nanoconstruct not to exceed 100 nm. In this study, we present a method to synthesize molecularly targeted silica-coated gold nanorods absorbing at 1064 nm wavelength while the size of the contrast agent remains below 100 nm. Specifically, the dye doped silica coated gold nanorods were prepared by a modified Stöber method using PEG-thiol as gold-to-silica coupling agents. Transmission electron microscopy images indicated that the length of the produced PEGylated gold nanorods was reduced to less than 60 nm and the average length of the nanoparticles after silica coating was within 100 nm. The silica surface was functionalized and then directionally bio-conjugated with anti-EGFR. The effects of size and surface charge of the anti-EGFR-conjugated silica-coated gold nanorods on the cellular uptake was investigated by targeting A431 cancer cells with various sizes of silica coated gold nanorods. The results confirm the size-reduced silica-coated gold nanorods are effective molecule-specific therapeutic agents and contrast agents for noninvasive photoacoustic molecular imaging.

8233-39, Session 11

## Self-illuminating nanoprobe for in vivo imaging of cancers over-expressing the folate receptor

S. C. Miller, Zymera, Inc. (United States); L. Beviglia, P. Yeung, OncoMed Pharmaceuticals (United States); S. Bhattacharyya, D. Sobek, Zymera, Inc. (United States)

Cancer metastases is responsible for most cancer deaths, yet despite extensive research the mechanisms involved remain to be elucidated. New in vivo imaging reagents with increased sensitivity and penetration depth are needed to advance our understanding of metastases and accelerate the development of therapeutics. The folate receptor (FR) is a promising imaging target that is up-regulated in many human carcinomas, including cancers of the ovary, breast, pancreas, endometrium, lungs, kidneys, colon, brain, and myeloid cells. Zymera has developed a self-illuminating Bioluminescence Resonance Energy Transfer Quantum Dot (BRET-Qdot) nanoprobe conjugated with folate (BQ-Folate) for in vivo imaging of cancers over-expressing FR. BQ-Folate is a novel nanoprobe formed by co-conjugating Renilla reniformis luciferase enzyme and folate to near-infrared (NIR) emitting quantum dots. The luciferase substrate, coelenterazine, activates the BQ-Folate nanoprobe generating luminescence emission in the near-infrared (NIR) region (655 nm) for increased sensitivity and penetration depth. Because BQ-Folate requires no external light source for light emission, it has significant advantages for challenging in vivo preclinical optical imaging applications, such as the detection of early stage metastases. Zymera and OncoMed Pharmaceuticals have demonstrated that in vivo imaging with the BQ-Folate nanoprobe detected the primary tumor and early stage metastases in an orthotopic mouse model of human pancreatic cancer. The BQ-Folate nanoprobe technology has both the sensitivity and the specificity needed for the in vivo detection of early stage peritoneal disseminated cancer metastases in the NOD/SCID mouse model of human pancreatic cancer.

8233-41, Session 11

## Dual modality photothermal OCT and magnetic resonance imaging with carbon nanotubes

J. M. Tucker-Schwartz, T. Hong, D. C. Colvin, Y. Xu, M. C. Skala, Vanderbilt Univ. (United States)

Preclinical molecular imaging of cancer has the potential to increase the understanding of fundamental cancer biology, elucidate mechanisms of cancer treatment resistance, and increase effectiveness of drug candidates. Optical and magnetic resonance imaging contain complementary strengths, suitable for gaining a wealth of knowledge when combined. Here, we demonstrate the inherent contrast sensitivity of single walled carbon nanotubes (~1nm X 100 nm) to absorption based photothermal optical coherence tomography (OCT), and magnetic resonance imaging spin dephasing contrast (T2, T2*). A spectral-domain OCT system was interfaced with an amplitude-modulated (50 Hz) titanium sapphire pump beam for photothermal OCT imaging. MRI was performed with a commercial 4.7 T animal scanner. With both imaging tools, contrast agent signal linearity ($r2 > 0.95$) and nanomolar sensitivity over tissue-like background ($p < 0.01$) was experimentally determined with serially dilute solutions of carbon nanotubes coated in amine-terminated polyethylene glycol. The surface functionalization chemistry for carbon nanotubes is well understood, and molecular targeting has been demonstrated in vitro and in vivo, making carbon nanotubes an attractive agent for molecular imaging in preclinical models. We have demonstrated the initial characterization steps for using carbon nanotubes for multi-modality imaging with OCT and MRI.

8233-42, Session 11

## Super-strong nanoindentors for biomedical applications based on the bamboo-like nanotubes

O. E. Glukhova, A. S. Kolesnikova, R. Zhnichkov, N.G. Chernyshevsky Saratov State Univ. (Russian Federation)

It is known that the increased requirements are imposed to flexibility and strength of nanoindentor. The hyperfine and durable structures such as carbon nanotubes of complex shapes can to use as nanoindentor. The results of quantum - chemical analysis of elastic and strength properties of the bamboo-like nanotubes are presented in this paper.

The different configurations of the bamboo-like nanotubes based on tubes (5,5), (10,10) and (30,30) are investigated. The internal jumpers were simulated by fragments of fullerenes, the sizes of which corresponded to a diameter of nanotubes. For the first time the configuration of the thinnest bamboo-like tube, which is a stable, was established. This configuration corresponds to the tube (30,30) of diameter 2.024 nm.

It is shown that the bamboo-like nanotube have a higher value of Young's modulus of ~ 1.2 TPa compared with a tube (30,30).

The parallel algorithms of the Hamiltonian formation, the calculation of atomic coordinates, the Hamiltonian diagonalization and the minimization of total energy of the bamboo-like nanotubes were used to simulate the process of stretching / compression, bending of nanotubes.

It is known that the tip plays a big role in the study of tissues. In this work the configuration of nanoindentor based on symmetric and streamlined tip of the tube (30.30) is an optimal. This configuration provides the perfect interaction between the nanoindentor tip and the tissue because the tip has no sharp protruding pieces. Therefore the tip does not destroy the tissue.

8233-43, Session 11

## Highly efficient phosphors in cancer sensing and PDT

B. G. Yust, L. C. Mimun, D. K. Sardar, G. A. Kumar, The Univ. of Texas at San Antonio (United States); P. J. Hornsby, J. Rocha, The Univ. of Texas Health Science Ctr. at San Antonio (United States)

Highly efficient upconverting phosphors (NaYF4) co-doped with erbium ions are bio-conjugated and used for cancer imaging and photodynamic therapy. These particles are fully characterized optically and morphologically, and the synthesis method is optimized to provide the most efficient fluorescence. Once they are conjugated, the particles are injected into mice to demonstrate that cancer imaging with a near-infrared excitation source is possible. Finally, the particles are also conjugated with a photosensitive molecule with strong absorption near the upconversion emission peak (~ 550nm). The upconversion energy causes the photosensitive molecule to create highly reactive oxidative species, which puncture and kill the cell to which it is attached. These particles are then used in a mouse model, and the size of the tumors is modeled as a function of the particle dosage and duration of the photodynamic therapy.

8233-44, Session 11

## Magnetomotive optical coherence elastography for monitoring tissue stiffness changes induced by magnetic hyperthermia

J. S. Kim, A. Ahmad, V. Crecea, B. M. Odintsov, S. A. Boppart, Univ. of Illinois at Urbana-Champaign (United States)

Some of the current tumor treatments available in clinical practice include surgery, radiotherapy, and chemotherapy. However, many of these treatments are not targeted at the cellular scale and side-effects are common, including harm to the surrounding healthy tissue. Magnetic hyperthermia in conjunction with tumor-targeted magnetic nanoparticles (MNPs) is a potential alternative treatment that can destroy tumor lesions while minimizing collateral damage to healthy tissue. MNPs made of iron-oxide can be modulated by an external high amplitude and frequency (> 50 kHz) magnetic field which can induce temperature increases due to the Brownian motion and/or Neel relaxation mechanisms. This localized thermal energy release is considered to be useful for therapeutic purposes. Magnetomotive optical coherence elastography (MM-OCE) is a functional extension of OCT (and MM-OCT) which utilizes MNPs that are modulated by an external magnetic field for contrast enhancement and for assessing the structural and viscoelastic properties of the surrounding tissues. We report our ongoing study results of assessing with MM-OCE the tissue stiffness changes induced by magnetic hyperthermia under different combinations of magnetic field parameters (i.e., modulation frequency, magnetic field strength, and duration of exposure). We expect these results to provide insight into the optimal parameters which maximize the efficacy of magnetic hyperthermia, and demonstrate the potential for using MM-OCE for dosimetric measurements during magnetic hyperthermia treatments. Ongoing studies are also being conducted to explore the possibility of extending these techniques to an in-vivo animal model.

8233-45, Session 12

## Metal-enhanced fluorescence improves the detection of reactive oxygen species in vivo

N. Murthy, Georgia Tech Research Institute (United States)

Reactive oxygen species (ROS) play a central role in biology and medicine and there is great interest in imaging them in vivo. A key challenge in imaging ROS is sensitivity, as ROS are speculated to exist at nanomolar concentrations in vivo. Hydrocyanines are a new family of fluorescent ROS dyes with great potential, but their efficacy would be improved by increased sensitivity. In this report we demonstrate that the sensitivity of the hydrocyanines to detect ROS increases by 1-2 orders of magnitude by conjugation to gold nanoparticles. Hydrocyanines are converted into cyanine dyes after reaction with ROS. Thus hydrocyanines conjugated to gold nanoparticles generate a cyanine-gold nanoparticle conjugate in the presence of ROS, which have dramatic metal enhanced fluorescence effects. We show here that hydrocyanines conjugated to gold can detect 50-100 picomolar concentrations of ROS in vitro and are approximately 10 fold better at detecting ROS in vivo than free hydrocyanines, in a mouse model of LPS induced inflammation. We anticipate numerous applications of hydrocyanine gold nanoparticle conjugates, given their high sensitivity.

8233-46, Session 12

## Autophagy plays a role in chloroplast degradation (chloropahgy) in Arabidopsis during the process of avirulent Pst DC3000(avrRps4) strain infection

W. L. Chen, J. Dong, South China Normal Univ. (China)

A increasing number of evidence suggests that the chloroplast plays an significant role during pathogen infection. Chloroplasts may be the primary source of reactive oxygen species (ROS) in the plant cells, as well as the pathogen-response signaling molecules salicylic acid (SA) and jasmonic acid (JA). But some evidence suggests that some pathogen effectors may targets and disrupts the plant chloroplasts and inhibit chloroplast-initiated defense signaling. While bulk degradation of the cytosol and organelles in plants is mediated by autophagy, its role in chloroplast degradation is mostly unknown. Autophagy may plays a significant role in chloroplast degradation (chloropahgy) during the process of pathogens infection, and it would give the pathogen an inhibition in the race to escape it is the site of infection and infiltrate distal host tissues. We have visualized the fate of stroma-targeted green fluorescent protein (CT-GFP) in order to investigate the involvement of autophagy in the mobilization of chloroplasts to the vacuole. It used the leaves cells of transgenic Arabidopsis(WT/CT-GFP; atg4a4b-1/CT-GFP) as experimental material to study the autophagy phenomenon of Arabidopsis chloroplast degradation induced by Pst DC3000 (avrRps4) by the LSCM technique. And we discuss the impact of photosynthetic function on detached leaves of Arabidopsis(WT and atg4a4b-1) infect with Pst DC3000(avrRps4), observed by analysis of chlorophyll fluorescence. Chloroplasts exhibiting chlorophyll fluorescence, as well as CT-GFP bodies, were also observed in the vacuole. No accumulation of bodies was observed in the vacuoles of the autophagy-defective mutant. And further

induced the decline of photosynthetic efficiency in mutant.

8233-47, Session 12

## Beta-galactosidase fluorescence probe with improved cellular accumulation based on spirocyclized rhodol scaffold

M. Kamiya, D. Asanuma, The Univ. of Tokyo (Japan); E. Kuranaga, RIKEN (Japan); M. Sakabe, The Univ. of Tokyo (Japan); M. Miura, The Univ of Tokyo (Japan); T. Nagano, Y. Urano, The Univ. of Tokyo (Japan)

Escherichia coli beta-galactosidase is well characterized and is extensively used as a marker enzyme in biology, because of its stability and high turnover rate, as well as the absence of endogenous beta-galactosidase activity in eukaryotic cells. A range of fluorogenic substrates has been developed, including our previous compounds based on the TokyoGreen scaffold (J. Am. Chem. Soc. 2005, 127, 4888-4894; J. Am. Chem. Soc. 2007, 129, 3918-3929). However, most of these substrates lack sufficient cellular permeability and accumulation to be able to specifically and clearly visualize beta-galactosidase activity in living cells and tissues. Here, we present a new class of fluorescence probe for beta-galactosidase based on the rhodol scaffold, which overcomes these problems. Our newly developed probe, HMDER-betaGal, was designed to utilize pH-dependent spirocyclization involving a hydroxymethyl group to control the fluorescence emission before and after reaction with the enzyme. We confirmed that HMDER-betaGal has sufficient cellular permeability, and that its hydrolysis product is well retained intracellularly, by using it to obtain well-defined images of beta-galactosidase activity in living cells and Drosophila melanogaster tissues. Since beta-galactosidase is one of the most widely used reporter enzymes in biological studies, the potential range of application of this new probe should be enormous.

8233-48, Session 12

## Tracking single cells in live animals using a photoconvertible near-infrared cell membrane label

A. L. Carlson, J. Fujisaki, Massachusetts General Hospital (United States); C. Lo Celso, Imperial College London (United Kingdom); J. Wu, J. A. Spencer, D. T. Scadden, Massachusetts General Hospital (United States); T. B. Strom, Beth Israel Deaconess Medical Ctr. (United States); C. P. Lin, Massachusetts General Hospital (United States)

We describe a novel photoconversion technique to track individual cells in vivo using a commercial lipophilic membrane dye, DiR. We show that DiR exhibits a permanent fluorescence emission shift (photoconversion) after light exposure and does not reacquire the original color over time. Ratiometric imaging can be used to distinguish photoconverted from non-photoconverted cells with high sensitivity. Combining the use of this photoconvertible dye with intravital microscopy, we tracked the division of individual hematopoietic stem/progenitor cells within the calvarium bone marrow of live mice. We also studied the peripheral differentiation of individual T cells by tracking the gain or loss of the FoxP3-GFP fusion protein, a marker of the immune suppressive function of CD4 T cells. With the near-infrared photoconvertible membrane dye, the entire visible spectral range is available for simultaneous use with other fluorescent proteins to monitor gene expression or to trace cell lineage commitment in vivo with high spatial and temporal resolution.

8233-49, Session 12

## Cellular preferential uptake of NIR fluorophore in tumor for lesion malignancy screening

K. Liao, National Chung Hsing Univ. (Taiwan)

The aim of this project is to develop a noninvasive fluorescent based 3-dimension tomography modality with near-infrared (NIR) fluorophore as contrast agent for breast cancer diagnosis and management. The system is desired to provide early screening of lesion malignancy and efficient evaluation of lesion size / boundary (indices of disease staging, chemotherapy efficacy and delineation for surgery) based on the spectral and temporal parameters.

The self-synthesized near-infrared fluorophore (diglucosamid-SIDAG) showed preferential uptake in tumor from both in vitro (cell-line) and in vivo (murine xenograft model) studies. It appeared in the time frame of hours after administration. Most of the biomedical imaging agents rely on the tissue level contrast of tumor due to the enhanced permeability from neovascularity and retention effect from lymphatic drainage, such as gadolinium compounds for MRI, liposome or microbubble for CT and US, and ICG for fluorescent image. We suspect that the contrast from diglucosamid-SIDAG in on the cellular level due to the time frame of preferential uptake in vivo and the result from the cell-line study, and plan to prove it by investigating the correlation between in vitro and in vivo fluorescent kinetics profiles. The mechanism (such as the route of endocytosis) behind the suspected cellular level contrast will be studied.

8233-50, Session 12

## Raman microscopy of ex vivo tissue culture reveals circadian rhythms in bone mineralization

J. P. McElderry, G. Zhao, R. T. Franceschi, M. D. Morris, Univ. of Michigan (United States)

Bone mineral formation is a complex process in which multiple proteins mediate formation of the collagen-based matrix and deposition of mineral. These include clock proteins whose expression is triggered by external light/dark stimuli. That periodicity suggests that mineralization should also follow a diurnal cycle. We show that Raman spectroscopy can detect periodicity in mineral deposition with chemical composition specificity. We use sections of murine calvaria harvested from neonatal mice. We use an inverted Raman microscope equipped with an X-Y-Z motorized stage and a stage incubator maintained at standard tissue culture conditions. Six-well plates are fitted with purpose-built immobilizers that stabilize tissue positions as the stage is moved from well to well. With this apparatus we can sample multiple specimens simultaneously. Time resolution varies from 5 to 60 minutes, depending on the number of specimens in the multi-well plate and the number of measurement sites per specimen. We will show kinetic Raman data (apatitic phosphate symmetric stretch) demonstrating pulsatile formation of bone mineral with approximate 24 hour periodicity. This work demonstrates the potential for kinetic Raman spectroscopic study of the normal mineralization process and of errors in bone mineralization resulting from genetic defects, metabolic disorders or other sources.

8233-51, Session 12

## Deep sample multiplexing using ratiometric rare earth optical encoding

R. C. Haushalter, R. W. Haushalter, K. J. Haushalter, S. Vetcha, J. Wang, A. Hill, Parallel Synthesis Technologies, Inc. (United States)

In order to deeply multiplex assays (i.e. perform many simultaneous assays in a single container) a wide variety of approaches have been tried to encode samples so that they can be easily differentiated when pooled together including shape encoding, reflectivity, physical barcodes and fluorescence. Although optical encoding is the most studied method for sample multiplexing, the substantial spectral overlap, photobleaching, synthesis/reproducibility and other issues has prevented sample multiplexing depths above about ~100 samples for optical encoding with organic dyes or quantum dots. By using multiple rare earth elements within a single host matrix, and exciting all of the rare earth emitters simultaneously using a single excitation wavelength, we can measure more than 100 different unique optical intensity ratios between two colors or more than one billion unique and resolvable optical signatures when using six colors. Importantly, we also show that there is no optical crosstalk between the rare earth optical encoding materials and the organic reporter dyes used to provide the extent of reaction so there are no limits on choosing which reporter color is required. By encoding properly surface-functionalized glass or agarose beads with these rare earth encoding materials, any assay may be readily multiplexed to any desired depth. After explaining how the optical encoded samples are prepared, how the beads are manipulated and optically characterized, we will provide examples of multiplexing PCR, DNA hybridization, antigen/antibody and other assays using the ratiometric rare earth encoding technology. Using this optical encoding technology is should be possible to perform a multiplex reaction for a similar cost to single, serially performed assays.

8233-52, Session 12

## The curvature influence of the graphene nanoribbon on its sensory properties

O. E. Glukhova, I. V. Kirillova, M. M. Slepchenkov, N.G. Chernyshevsky Saratov State Univ. (Russian Federation)

The results of the theoretical investigation of curvature influence of the deformed graphene nanoribbon on its sensory properties are presented in given work. The attachment mechanisms of atoms and molecules of various substances to the planar and the wave-like graphene nanoribbon are studied by the tight-binding method and molecular-mechanics modeling of adsorption process.

For the first time it is established that the sensory properties of nanoribbon improve with increase of surface curvature. It is revealed, that the potential well depth of interaction of the curved graphene with hydrogen atom is greater than the planar graphene. It is established, that the difference of the potential minima of Ñ-Í interaction energy increases exponentially with the curvature increase.

On the example of interaction of graphene with hydrogen atom is shown:

1) The physical and chemical adsorption of hydrogen atoms is more probable on the curved graphene structure. The potential barrier for the transition of the physical adsorption to chemisorption of the curved graphene on 1 eV less than the planar.

2) The energy of chemical interaction of the curved graphene with hydrogen atom is greater than the planar, i.e. the external factors will make smaller influence on the sensory properties.

8233-59, Session 12

## New cross-linking quinoline and quinolone based lanthanide ion probes for sensitive fluorescent labeling

S. Pillai, New Jersey Institute of Technology (United States)

A variety of contemporary analytical platforms in technical and biological applications take advantage of labeling the objects of interest with fluorescent tracers - compounds that can be easily and sensitively detected. Here we discuss the synthesis of new fluorescent quinoline and quinolone compounds whose light emission can be conveniently tuned by simple structural modifications. Developed probes represent high-quantum yield, large-Stokes shift fluorophores with amine-reactive and click-reactive groups convenient for conjugation. Some of these compounds can be used as sensitizers for lanthanide emission in design of highly sensitive luminescent probes. We also discuss efficient derivatization reactions allowing introduction of amine- or click-reactive crosslinking groups into the fluorophores. The reactivity of synthesized compounds is confirmed in reaction with low molecular weight nucleophiles as well as with click-reactive DNA-oligonucleotide counterparts. These reactive derivatives can be used for covalent attachment of the fluorophores to various biomolecules of interest including nucleic acids, proteins, living cells and small cellular metabolites. Obtained compounds are characterized using NMR, steady-state fluorescence spectroscopy as well as UV absorption spectroscopy.

# Conference 8234: Plasmonics in Biology and Medicine IX

Sunday-Tuesday 22-24 January 2012
Part of Proceedings of SPIE Vol. 8234 Plasmonics in Biology and Medicine IX

8234-02, Session 1

## Gold nanoparticle tags for SERS-based imaging of human glioblastoma cells

L. Fabris, B. J. Paladini, P. V. Moghe, D. J. Naczynski, Rutgers, The State Univ. of New Jersey (United States)

Early cancer detection is of fundamental importance to reduce morbidity and recurrence, especially for highly invasive cancers such as human glioblastoma. A great potential has been recognized for the use of nanoparticle (NP)-based imaging agents, capable of specifically visualizing only the targeted diseased cell. The additional advantage of NP-based systems is the ease of implementation to also carry therapeutic moieties, thus generating novel theranostic tools. Surface enhanced Raman spectroscopy (SERS)-based imaging tags are starting to attract increasing attention due to their brightness and the possibility of multiplexing. In this contribution I will report on the development of SERS-based imaging tags, composed of gold NP dimers held together by a Raman active small molecular linker. These systems are capable of specifically targeting and detecting in vitro U87 human glioblastoma cells, owing to the combined use of cyclic RGD peptides to target $\alpha v\beta 3$ integrins overexpressed on the surface of cancerous cells, and of Tat peptides, belonging to the family of cell penetrating peptides. This dual approach ensured an efficient targeting and binding of the SERS tags to the surface of the cells or their penetration into the cytoplasm. Combined analysis carried out via confocal and Raman microscopy demonstrated the efficient tagging and imaging of U87 cells via SERS-based Au NP dimers-based tags. Current studies are now targeting melanoma cells, to demonstrate the versatility of our systems and set the ground for versatile, SERS-based tagging systems relevant to a wide range of biomedical applications.

8234-03, Session 1

## SERS nanoprobes based on gold-silver alloy nanoparticles produced by femtosecond laser processing

D. Rioux, S. Osseiran, S. Besner, Ecole Polytechnique de Montréal (Canada); N. Tam, A. Albanese, A. Lee, C. M. MacLaughlin, G. C. Walker, E. Kumacheva, G. Zheng, W. C. W. Chan, Univ. of Toronto (Canada); M. Meunier, Ecole Polytechnique de Montréal (Canada)

The use of plasmonic nanoparticles based Surface Enhanced Raman Spectroscopy (SERS) probes is very promising for the detection of cancer. Most research is done on gold nanoparticles because of their high biocompatibility. However, it is well known that silver has better plasmonic properties than gold, but its use in biomedical applications is uncertain because of its potential cytotoxicity. We propose to use gold-silver alloy nanoparticles produced by femtosecond laser ablation and alloying. This approach should represent the better of two worlds with particles that have improved SERS signal than pure gold as well as better biocompatibility than silver. We report the fabrication of Au-Ag alloy nanoparticles by femtosecond laser ablation and alloying in liquid environment. The size of the nanoparticles (10 - 40 nm) depends on the laser parameters, the nanoparticle concentration and the use of stabilizing agents. The alloy composition is simply controlled by the amount of gold and silver nanoparticles used in the alloying process. Enhancement of the Raman signal of various dyes (Crystal Violet, Malachite Green, Rhodamine 6G) adsorbed on the nanoparticle surface was measured and we found that alloy particles usually have stronger signal, up to 10 times better than pure gold nanoparticles, depending on the excitation wavelength. In vitro cytotoxicity experiments were also performed to assess the biocompatibility of the nanoparticles.

8234-04, Session 1

## SERS enhancement of Ag nanoparticle patterns embedded in glass by two-step ion exchange

Y. Chen, L. Karvonen, Aalto Univ. (Finland); A. Säynätjoki, Aalto Univ. School of Science and Technology (Finland); A. Tervonen, S. K. Honkanen, Aalto Univ. School of Electrical Engineering (Finland)

Silver nanoparticles are widely studied for surface-enhanced Raman scattering (SERS). Silver nanoparticles embedded in glass are prepared by a two-step ion exchange process. Silver ions are introduced into glass in silver ion exchange, and reduced into metallic silver in subsequent potassium ion exchange with an aluminum mask. The galvanic replacement reaction takes place in potassium ion exchange to reduce silver ions into metallic silver, enhanced by the electrolytic deposition, which further promotes the formation of Ag nanoparticles uniformly under the metal mask. The method enables the patterning of the particle patterns when applying a photolithographic mask in either the Ag+ ion exchange or the K+ ion exchange process. The geometrical characteristics of the sensor areas, such as the shape and the dimensions, are totally determined by the mask pattern. In principle, any shape and dimensions are possible, which makes the development of integrated sensor chips much easier with increased flexibility in the integration of planar sensor devices. [1]

In this work, we demonstrated the fabrication of Ag nanoparticle patterns embedded in glass by two-step ion exchange and studied their SERS application. The Ag nanoparticles are exposed by etching the glass and incubated in Rhodamine 6G for studying their SERS properties. A Raman enhancement factor in the order of 109 was achieved. The optimal surface features in terms of SERS and fluorescence enhancements are also discussed.

[1] Y. Chen, L. Karvonen, A. Säynätjoki, C. Ye, A. Tervonen, and S. Honkanen, Opt. Mat. Exp. 1, 164 (2011).

8234-05, Session 1

## Plasmonic nanostructures on the basis of Ag covered PMMA gratings

M. Zeisberger, Institut für Photonische Technologien e.V. (Germany); K. Weber, Institut für Photonische Technologien e.V. (Germany) and Friedrich-Schiller-Univ. Jena (Germany); U. Hübner, H. Schneidewind, R. Mattheis, Institut für Photonische Technologien e.V. (Germany); D. Cialla, J. Popp, Institut für Photonische Technologien e.V. (Germany) and Friedrich-Schiller-Univ. Jena (Germany)

The aim of our work is the development of plasmonic chips for surface enhanced Raman spectroscopy (SERS). The technological approach we use bases on the patterning of a resist (PMMA) film on a quartz substrate by electron beam lithography and plasma etching. The usual pattern is a periodic array of square shaped dots with a lateral size from 200 x 200 nm2 to 400 x 400 nm2 and a height of 70 nm. This patterned surface is covered by an Ag film with 20-50 nm thickness using an evaporation technique. FEM simulations show that localized as well as propagating plasmons can be excited by laser irradiation from the top (air) side in this type of grating. The simulations allow to optimize the structures for a given excitation wavelength, e.g. 514 nm. A possible problem of the PMMA component is an unwanted contribution to the Raman signal. A solution of this problem is an intermediate layer of Al2O3 between Ag film and PMMA which can be deposited by ALD (atomic layer deposition). Our simulations show that a thickness of 20 nm Al2O3 is sufficient to achieve this. Within this contribution we present first results of the SERS characterization using crystal violet as model analyte.

Acknowledgement:

Funding of the research project “Photonic Nanomaterials (PhoNa)” within the framework “Spitzenforschung und Innovation in den Neuen Ländern” from the Federal Ministery of Education and Research, Germany (BMBF) is gratefully acknowledged.

8234-06, Session 1

## Optimization of SERS enhancement from nanostructured metallic substrate based on arrays of inverted pyramids, and investigation of effect of lattice non-symmetry

S. Z. Oo, M. D. B. Charlton, Univ. of Southampton (United Kingdom); D. Eustice, Renishaw plc (United Kingdom)

Surface-enhanced Raman scattering (SERS) can be used to amplify Raman signals by several orders of magnitude, by utilising plasmon polariton (photonic and surface plasmon mode) coupling to test molecules disposed on a textured metallo-dielectric surface.

Previously the ‘klarite™’ substrate consisting of an inverted array of pyramidal nanostructures patterned onto a Silicon substrate has been demonstrated to afford highly reproducible SERS signals. In this paper, we investigate a new rectangular lattice arrangement and investigate the effect of lattice pitch and pit geometry on SERS enhancement factor. We also investigate effect of aspect ratio for the rectangular pits and effect of pit density on SERS enhancement factor. A test chip is fabricated for the purpose of performing a matrix experiment, allowing deconvolution of geometrical variables: lattice pitch (1000nm-3000nm), pit size (500nm-2500nm), pit aspect ratio [1:1.0 (square) to 1:1.3 (rectangular)] and pit density.

Nanostructured test substrates are coated with gold by thermal evaporation, followed by a monolayer of benzenethiol which provides a stable test molecule for signal enhancement comparison. SERS signals are analyzed with Invia Raman Spectrometer (RENISHAW) at a wavelength of 785nm. The resulting SERS enhancement was found to be highly dependent on Pitch, Pit size, and spacing between pits. The derived optimal design is shown to give an improvement in signal level of 524% compared to standard Klarite.

8234-07, Session 2

## Surface-enhanced Raman scattering for label-free protein detection and identification

M. Culha, S. Keskin, Yeditepe Univ. (Turkey)

Proteins are the end products of gene expression and they undertake many vital processes in living world. Their detection has critical importance in many fields ranging from biotechnology to medicine. The current approaches involve a separation step followed by a detection scheme based on fluorescence or mass spectroscopy. When an antibody-antigen interaction is employed as a separation step, the detection step requires labeling procedure. Both immunoassay based and mass spectroscopic approaches have certain drawbacks such as false readings and issues with quantification with the former and cost and necessity of having a trained personnel with the later. Although the sensitivity of the technique is proven, surface-enhanced Raman scattering (SERS) of proteins is always difficulty due to complex, flexible and diverse structures of proteins. This difficulty is one of the major obstacles hindering the applicability of the technique for the protein detection and identification. In this study, we have employed several sample preparation approaches involving the packing AgNPs or AuNPs with protein molecules in a proper manner to allow the polarization of the electron system of proteins in coherence with the nanostructured noble metal system. The applicability of heat denaturation kinetics, which protein molecules expose their electron rich hydrophobic moieties such as phenyl hidden inside to nanostructured noble metal surface, is perused for the detection and identification of protein in protein mixtures. We demonstrate the experimental conditions where the power of the technique for protein detection and identification is exploitable.

8234-08, Session 2

## Deep-UV surface-enhanced resonance Raman scattering for ultrasensitive detection of biomolecules

S. K. Jha, ETH Zurich (Switzerland); Y. Ekinci, ETH Zurich (Switzerland) and Paul Scherrer Institut (Switzerland); M. Agio, J. Löffler, ETH Zurich (Switzerland)

Surface-enhanced Raman scattering (SERS) is an important technique for detecting low concentrations of molecules from their vibrational fingerprints. Here, molecules placed in the close proximity of metal nanostructures experience highly enhanced optical near-fields associated with the excitation of localized surface plasmon resonance. Most often visible and near-infrared (NIR) lasers are used for excitation since traditionally used Au and Ag SERS substrates support strong plasmon resonances in the visible and NIR.

In addition to the general increase in Raman scattering at lower wavelengths due to its inverse wavelength dependence, the use of deep-UV (DUV) excitation could be advantageous especially for detecting biomolecules since most of them have absorption bands in the UV and therefore have larger Raman cross-sections resulting from resonance Raman effect. Moreover, with DUV excitation the fluorescence background and Raman peaks are well separated leading to increased signal to noise ratio.

We report experimental and theoretical studies of deep-UV surface-enhanced resonance Raman scattering (DUV-SERRS) which combines the advantages of DUV excitation and SERS effect in order to realize a highly-sensitive, large-area, and reproducible detection platform for biomolecules. We used Al nanostructures as SERRS substrates which exhibit strong plasmon resonances in DUV. We fabricated well-defined Al nanoparticle arrays over large areas using extreme-ultraviolet interference-lithography and performed DUV-SERRS from DNA bases. Using 257.2 nm laser excitation, we measured reproducibly sub-attomoles of DNA bases sublimated onto Al nanoparticle arrays. FDTD simulations were carried out in order to understand and optimize the near-field and far-field optical properties of the Al nanostructures.

8234-09, Session 2

## Controllable cavity rim opening of up-right nanocrescents leading to repeatable SERS measurements

H. M. Chen, L. Pang, Univ. of California, San Diego (United States); G. M. Hwang, The MITRE Corp. (United States); A. King, Renishaw Inc. (United States); Y. Fainman, Univ. of California, San Diego (United States)

Nanocrescents are one of the most structurally and optically tunable anisotropic nanostructure used for biological applications such as surface enhanced Raman scattering (SERS) where its plasmonic resonance can be tuned within the important biological window in the near-infrared regime. Unlike structures that rely on a few nanometer gap inter-particle plasmon coupling to achieve high electrical field, nanocrescents are fabricated on hundreds of nanometer template sacrificial nanoparticles, where intra-particle plasmon coupling between the cavity modes and the tip edges are utilized to achieve high electrical field. Unlike previous efforts, our new fabrication approach creates three dimensional (3-D) up-right oriented nanocrescent structures with controllable cavity rim opening. First, randomly-distributed silica nanoparticles are spun onto a substrate coated with a photoresist layer. Reactive ion etching is then used to etch into the photoresist to create small narrow pedestal with the nanoparticles serving as etching masks. The etching recipe and time will determine the diameter of the pedestal and ultimately, the cavity rim opening of the nanocrescents. 3-D simulations show that a smaller rim opening will yield a higher electrical field and thus a higher SERS enhancement factor. We have fabricated and measured these randomly-distributed up-right oriented nanocrescent structures with as smaller as ~50 nm cavity rim opening to achieve an enhancement factor greater than 10^7. Moreover, the repeatability of the enhancement factor (EF) from one nanocrescent to the next within the same substrate is better than 80%. We attributed the measurement consistency to the up-right orientation of the nanocrescent structures and the high enhancement factor to the small rim opening.

8234-10, Session 2

## Surface-enhanced Raman scattering and microwave absorption in silver nanoparticle inks

M. A. Figueroa, Drexel Univ. (United States); S. A. Schraer, Villanova Univ. (United States); K. Pourrezaei, S. D. Tyagi, Drexel Univ. (United States)

Nanoparticle inks are colloidal suspensions of silver or gold nanoparticles in water or some other suitable organic solvent. These nanoparticles can be sintered at relatively low temperatures (70 - 200oC) to fabricate circuit elements on a variety of flexible substrates. Recently we have shown that if the inks are heated at temperatures at which the formation of robust connections between nanoparticles over large areas does not take place, a sample is obtained containing particle clusters of varying sizes and with a distribution of interparticle distances. Such substrates exhibit relatively high (10^8 - 10^9) surface enhanced Raman scattering (SERS) amplification factors (AFs). The high AFs in these clusters stem from a lack of translational symmetry which do not support propagating electromagnetic (em) waves and thus leads to localization of em excitations to very small regions that can create SERS hot spots. Here we report that microwave absorption (~10GHz) as a function of isothermal annealing in dry-drop substrates can be used to monitor the sintering process in metallic nanoparticle inks. The predominant contribution to microwave absorption - which is sensitive to the interparticle separation - comes from weak links that are formed between nanoparticles as a result of the thermal treatment. Such nanoparticle pairs are also the ones that make a major contribution to the SERS AFs. This leads to a correlation between the observed microwave absorption and the SERS signal intensities. We also present a simple model that describes the microwave absorption as a function of the isothermal annealing treatment.

8234-63, Session 2

## Fluorescence enhancement using silver-gold nanocomposite substrates

S. D. Choudhury, R. Badugu, K. Ray, J. R. Lakowicz, Univ. of Maryland School of Medicine (United States)

For the past several years, we have been extensively investigating the use of plasmonics to increase the capabilities of fluorescence technology. Metal enhanced fluorescence (MEF) is a methodology wherein the near-field interaction of fluorophores with the plasmons in metallic nanostructures leads to substantial fluorescence enhancements. To realize the potential of plasmon controlled fluorescence, it is essential to construct robust and reproducible metallic substrates with controlled geometry and tunable optical properties, in an easy and cost effective manner. We present a simple, one-step strategy for the fabrication of silver-gold nanocomposite (Ag-Au-NC) substrates based on the galvanic replacement reaction of silver with gold. The motivation for this work is to manipulate the plasmonic properties of the substrate by combining the optical properties of gold and silver and to improve the stability and biocompatibility of silver, one of the most widely used metallic substrate for MEF, by coating it with gold nanoparticles. We anticipate that this approach will make the surfaces more suitable for biophysical studies or bio-sensor applications. With the present Ag-Au-NC substrates we have achieved a significant enhancement in the fluorescence of ATTO655, a dye that is commonly used for bio-imaging and single molecule fluorescence based studies. We observe that the increase in the fluorescence intensity of the dye is accompanied by a considerable reduction in its fluorescence lifetime, indicating that the fluorophore-plasmon coupling mechanism is at play. Both ensemble and single molecule fluorescence studies of the MEF using the fabricated Ag-Au-NC substrates will be discussed.

8234-11, Session 3

## Nanobiophotonics for molecular imaging of cancer

L. Lucas, K. Hewitt, Dalhousie Univ. (Canada)

Our research aims to image the Epidermal Growth Factor receptor (EGFR, HER1) distribution in cancer cells. Many cancers and pre-cancers over-produce the cell surface receptor, EGFR. EGFR over-expressing A431 cancer cells are targeted through a biocompatible nano-probe. This probe is formed by attaching modified EGF protein, an EGFR specific ligand, to 5 nm diameter gold or silver nanoparticles (Au/AgNPs). By linking a molecule to the protein, EGF is altered to give stronger bonds to noble metals. Normal human bronchial epithelial (NHBE) cells are used as controls. By tuning the 632.8 nm He-Ne laser excitation frequency to the surface plasmon of metal nanoparticles, we enhance Raman to get an effect called Surface Enhanced Raman spectroscopy (SERS). Raman spectroscopy (Horbia Jobin Yvon T64000) measurements are obtained with a point-mapping scheme (0.3 µm step size, ~40 x 40 µm map) to chart the nanoparticle, and thus the EGFR, distribution. The small EGF-coated nanoparticles should avoid detection by the immune system. As EGFR is engulfed through endocytosis, we expect to visualize the aggregated nano-probes attached to EGFR in endosomes and lysosomes when imaging through cells. Previous research showed signal intensities of 850:1 at 1583 cm-1 and 107 orders of magnitude enhancement with anti-EGFR antibody tagged 30 nm AuNPs on A431 cells. We report on our efforts to synthesize the biocompatible EGF-NPs, and to gain enhancement with SERS in cells. This yields a simple and effective way to map EGFR over-expression in cancers.

8234-12, Session 3

## Intravital confocal Raman microscopy with multiplexed SERS contrast agents

P. McVeigh, Univ. of Toronto (Canada); B. Wilson, Univ. of Toronto (Canada) and Univ. Health Network (Canada)

Nanoparticle contrast agents which take advantage of Surface Enhanced Raman Scattering (SERS) to generate an optical signal have the potential to improve in-vivo detection of target tissues as a result of their uniquely bright and narrow SERS spectral features. Their potential for multiplexing outstrips that of any fluorescence-based platform, and spectroscopic detection allows for the removal of broad in-vivo autofluorescent background signals and greatly improves their detection limit. Many fundamental studies have been carried out which have demonstrated that SERS-active nanoparticles can successfully be targeted to specific tissues through the addition of targeting moieties such as antibodies, affibodies, or peptides, however these works have primarily relied on either point monitoring spectroscopy or ex-vivo microscopy to study their biodistribution kinetics.

Here we present the results from high resolution intravital Raman microscopy using a dorsal skinfold window chamber model of human lung adenocarcinoma. SERS-active gold nanoparticles were functionalized with an anti-Epidermal Growth Factor Receptor (EGFR) antibody and made biocompatible through the addition of a PEG coating. The nanoparticles were then administered IV or topically to mice bearing A549 or H460 xenograft tumours growing in the window chamber, and images were recorded using a high-speed confocal Raman microscope. We have compared the uptake kinetics between EGFR overexpressive (A549) and low-expressing (H460) cell lines growing concurrently in the same window chamber, as well as the clearance times from the key compartments (blood, extracellular space, host tissue, tumour tissue) as determined through long-term microscopic evaluation in our unique in-vivo model system.

8234-13, Session 3

## Molecular imaging with surface-enhanced CARS on nanostructures

S. Mahajan, J. J. Baumberg, C. Steuwe, Univ. of Cambridge (United Kingdom)

Raman spectroscopy is a molecular finger-printing technique; however, its feebleness prohibits fast imaging applications. Non-linear coherent anti-Stokes Raman scattering (CARS) transitions can be stimulated by using pulsed (ps or fs) lasers. Hence, in CARS, higher signals (up to 10^6) compared to normal Raman spectroscopy are generated. Although this permits better imaging with CARS than normal Raman yet reduction in photo damage, faster acquisition and prolonged monitoring ability especially in biological applications is much desirable. Therefore higher sensitivity is needed and we achieve this by combining CARS with plasmonic enhancement on metal nanostructured surfaces. Here we present our work on development of surface-enhanced CARS (SECARS) on nanostructured surfaces and its application in bio-molecular imaging. Over the past several years we have developed nanovoid surfaces which are fabricated by colloidal templated electrodeposition. They have unique plasmonic properties, which are easily tuned as a function of their geometry, and are ideal for producing plasmon-enhancement in SERS. Using nanovoid surfaces we are able to show that resonance matching with plasmons is essential for obtaining maximal SECARS enhancements. We have also established that SECARS shows an enhancement of >10^5 over conventional CARS. By careful measurement we find an additional enhancement of >10^3 in SECARS over SERS. Further we have been able to demonstrate the chemical selectivity of SECARS. Having established its sensitivity and chemical selectivity we have employed SECARS for molecular imaging and for studying the interaction of lipid layers and cellular structures with biomolecules. Our work paves the way for reliable single molecule spectroscopy and fast biomolecular imaging with SECARS.

8234-14, Session 3

## Intracellular multiplex detection and imaging of stable chemisorbed labels by SERS

N. M. Sirimuthu, C. D. Syme, J. M. Cooper, Univ. of Glasgow (United Kingdom)

Surface-enhanced Raman scattering (SERS) spectroscopy is gaining wider acceptance in biological research due to its high sensitivity, narrow spectral bands and minimal interference from aqueous media. Narrower spectral features compared to fluorescence spectroscopy makes SERS superior for multiplexed detection. Many types of substrate are available for SERS experiments, but nanoparticles remain the most commonly used. Nanoparticles are especially useful for intracellular studies due to their size, shape and plasmonic properties, as well as their ability to enter cells via endocytosis. Nanoparticles can be functionalised with a reporter molecule (such as a dye or thiol) or a ligand binding molecule to create a nanosensor. SERS nanosensors are useful for an increasingly wide range of bioanalytical applications, such as DNA detection, immunoassays, in vivo imaging in animals and multiplexing. As the applications of SERS nanosensors expands and the demand for reproducibility and reliability grows, it is becoming increasingly necessary to describe the physical properties and behaviour of the most commonly used types of SERS nanosensors, especially in biological environments. We have tested the stability of two general types of label molecule, chemisorbed and physisorbed, in order to assess their suitability for SERS measurements over prolong periods of time within live cells. We also demonstrate the use of multiple chemisorbed labels for intracellular multiplexed detection using SERS. Chinese Hamster ovary (CHO) cells were infused with a mixture of differently labelled stable nanosensors and were detected using SERS imaging. We show that multiple species can be detected in a single SERS spectrum without spectral deconvolution.

8234-16, Session 4

## Plasmonic gold nanorods as nanorheology probes in diffusion-sensitive optical coherence tomography

R. K. Chhetri, The Univ. of North Carolina at Chapel Hill (United States); K. A. Kozek, A. C. Johnston-Peck, J. B. Tracy, North Carolina State Univ. (United States); A. L. Oldenburg, The Univ. of North Carolina at Chapel Hill (United States)

The ability to image viscoelastic properties of optically-thick biological systems extends the biomedical applications of microrheology, and provides a new window into the biophysical properties of tissues. We employ optical coherence tomography as a platform for depth-resolving dynamic light scattering from diffusive plasmonic nanorods that act as nanorheology probes. In previous work, we demonstrated the ability to depth-resolve the viscosity of a simple (molecular) fluid using polarization-sensitive OCT to monitor the rotational diffusion of gold nanorods (GNRs) nominally 15 x 53nm in size. To extend this technique for use on complex, biological fluids such as mucus, we have developed a generalized method to extract the frequency-dependent, complex shear modulus of the medium. We have validated our method in polyethylene oxide (PEO) solutions of varying concentration. We have also compared diffusion-sensitive OCT of both polystyrene microspheres and GNRs, and show the expected dependence of the co- and cross-polarized light scattering signals on the rotational and translational diffusion rates of the probes. Importantly, we also validate our results against standard particle-tracking microrheology using microspheres in the same PEO medium.

The anisotropic plasmon-resonant properties of GNRs are particularly favorable for nanorheology because they provide a strong cross-polarized dynamic light scattering signal that is specific to rotational diffusion and insensitive to translational motion. GNRs are also detectible at a considerably smaller size than non-resonant microspheres, which enables study of rheological properties on both a smaller size scale and a faster time scale.

8234-17, Session 4

## A magnetic-field enriched surface-enhanced resonance Raman spectroscopy strategy towards the early diagnosis of malaria

Y. Clement, Q. Liu, Nanyang Technological Univ. (Singapore)

Human malaria disease is a worldwide disease. Early diagnosis is critical to reducing morbidity and mortality rates because effective malaria drugs have not been developed. Raman spectroscopy for the detection of a malaria biomarker, i.e. hemozoin, has shown great potential for malaria diagnosis. Compared to blood smear examination, which is the current "gold standard" method, Raman diagnosis is faster and less labor-intensive; moreover, it requires minimal expertise for data interpretation. However, one significant disadvantage of Raman spectroscopy is the intrinsically weak Raman signal, which is aggravated by the low concentration of the malaria diagnosis biomarker at the early stage of malaria infection.

In this paper, we present a magnetic field-enriched surface-enhanced resonance Raman spectroscopy (SERRS) strategy for the sensitive detection of β - hematin crystals, which is equivalent to hemozoin in the characteristics of Raman spectra, by using magnetic nanoparticles. Several orders of enhancement in the SERRS signal of magnetic field-enriched β - hematin can be realized by this hybrid method, in comparison to the cases of SERRS alone or magnetic enrichment alone in phantoms that mimics hemozoin in erythrocytes infected by malaria disease. The strategy of optimizing the enhancement factor will also be discussed. These results show the potential for integrating SERRS and magnetic enrichment for the sensitive detection of hemozoin towards early malaria diagnosis.

8234-18, Session 4

## Characterisation of individual microdroplets by multiplex SERRS spectroscopy

C. D. Syme, N. M. Sirimuthu, C. Martino, R. Yusvana, J. M. Cooper, Univ. of Glasgow (United Kingdom)

Raman spectroscopy and its various derivatives continue to offer the analyst fast, powerful, non-invasive and non-destructive means by which to identify multiple analytes simultaneously and in real time. By virtue of the huge enhancements possible in Raman scattering, generated by both surface enhancement and the resonance Raman effect, or when coupled with other techniques such as confocal microscopy, Raman spectroscopy is becoming more and more applicable to the types of assay being conducted in lab-on-a-chip applications, such as flow cytometry, cell patterning and trapping, and microarrays, all of which often involve the detection of extremely low quantities of analyte. Surface enhanced Raman scattering (SERS, or when coupled with the resonance Raman phenomenon, SERRS) spectroscopy has proven to be of particular use as a robust optical detection method in microfluidic environments. In this paper, we demonstrate the use of SERRS multiplex detection to quantitatively characterize individual microdroplets in a continuous stream whose contents are gradually varied using a bespoke pump control algorithm.

8234-19, Session 4

## Experimental investigation of droplet biosensing by multiwavelength plasmonic

C. Desfours, S. Habraken, J. Hastanin, C. Lenaerts, K. Fleury-Frenette, Univ. de Liège (Belgium)

Surface Plasmons Resonance (SPR) architectures involving multi-wavelength interrogation is an attractive alternative for micro-sized liquid droplet biosensing. In this work, we describe and experimentally investigate two detection concepts.

The first one involves the SPR Coupler and Disperser (SPR_CD) spectroscopic sensor principle, where the reflected light spectrum analysis is performed directly on each SPR detector pixel using the same diffraction grating that is employed for the optical coupling of the incident light wave with the surface plasmons. The considered sensor configuration includes a polychromatic light wave source, a grating structure and an imaging system. The main advantage of the described sensor design is that the diffracted light wave to be detected propagates entirely in the grating substrate. Consequently, the wavelength spectrum is perturbed neither by the light absorption in the droplet sample, nor by the reflection from its inner walls. The experimental setup implementing this architecture enables the spectroscopic detection in both transmitive and reflective modes.

The second instrumental concept is based on an angular scanning combining one near-IR and one visible light probes simultaneously. This two-wavelength SPR method is used to increase the number of parameters for numerical fitting, which improves the precision of measurement. Moreover, this architecture gives access to sensing at different penetration depths and the system is able to detect potential gradients in the analyzed solution with a sub-micron resolution. Results are shown for in situ SPR measurements of biological molecules (transferrin) and demonstrate the feasibility of this promising approach.

8234-20, Session 4

## Ultrasensitive system for the real-time detection of H2O2 based on strong coupling in a bioplasmonic system

S. Dutta Gupta, G. Suarez, C. Santschi, Ecole Polytechnique Fédérale de Lausanne (Switzerland); L. Juillerat-Jeanneret, Ctr. Hospitalier Univ. Vaudois (Switzerland); O. J. F. Martin, Ecole Polytechnique Fédérale de Lausanne (Switzerland)

In the past few decades, plasmonic structures have been used for enhancing different optical phenomena like Raman emission, IR absorption, second harmonic generation, etc.. Here we present a detection scheme based on the enhancement of the absorption of Cytochrome c molecules in the visible range using plasmonic resonances supported by gold nanoparticles. In the presence of H2O2, Cytochrome c is converted from the reduced to the oxidized state, both of them exhibiting different optical absorption spectra. H2O2 is an important biomolecule since its concentration in a biological environment generally gives an indication of the oxidative stress on the nearby biological entity like mammalian or plant cells. Since the enhancement of the absorption is strictly through the near field, it is necessary to control the distance between the Cytochrome c molecules and the gold nanoparticle. In this work, chemical routes are used to bind the Cytochrome c to the gold surface with a linker molecule in between in order to control the absorption enhancement of the Cytochrome c molecule. The absorption enhancement of Cytochrome c molecules can be easily tuned by optimizing the linker chain length. Furthermore by acquiring the spectra of gold nanoparticles at different locations simultaneously it is possible to get an estimate of the spatial dependence of H2O2 evolution from cells.

8234-55, Session 4

## Development of LSPR and SPR sensor for the detection of an anti-cancer drug for chemotherapy

S. S. Zhao, O. R. Bolduc, D. Y. Colin, J. Y. Pelletier, J. Masson, Univ. de Montréal (Canada)

The anti-cancer drug, methotrexate (MTX) as a strong inhibitor of human dihydrofolate reductase (hDHFR) has been studied in localized surface plasmon resonance (LSPR) and surface plasmon resonance (SPR) competitive binding assays with folic acid stabilized gold nanoparticles (FANP). The latter with a diameter of 15 nm were prepared in a simple step with sequential characterization using UV-Vis, FTIR, and Raman. A LSPR competitive binding assay between different concentrations of MTX and FANP for hDHFR in solution was designed to quantify MTX by using UV-Vis spectroscopy. Sensitivity of the assay was optimized with respect to both concentrations of the enzyme and FANP. The detection and quantification of spiked MTX was demonstrated in phosphate buffer saline and in fetal bovine serum accompanied by solid-phase extraction treatment of the serum. In addition, this assay could also provide as a screening tool for potential inhibitors of hDHFR. In another perspective, MTX was measured in a competitive binding assay with FANP for histidine-tagged hDHFR immobilized on a SPR sensitive surface. In this case, FANP provide a secondary amplification of the analytical response which is indirectly proportional to the concentration of MTX. This alternative approach could contribute to the realization of direct detection of MTX in complex biological fluids. A comparison of characteristics and analytical parameters such as sensitivity, dynamic range and limit of detection between the LSPR and SPR sensing platforms will also be presented. Both assays offer potential in tackling real biological samples for the purpose of monitoring and validating anti-cancer drug levels in human serum during chemotherapy.

8234-21, Session 5

## Plasmon-controlled fluorescence and single DNA strand sequencing

J. R. Lakowicz, Univ. of Maryland School of Medicine (United States)

No abstract available

8234-22, Session 5

## Surface plasmon resonance detection enhancement using colocalization of near-fields and target molecules

Y. Kim, Y. Oh, W. Lee, D. Kim, Yonsei Univ. (Korea, Republic of)

Surface plasmon resonance (SPR) detection technique has been extensively utilized for sensing biomolecules and biomolecular interactions. However, because of the label-free nature of SPR detection technique, it suffers from moderate detection limit. Numerous approaches have been proposed to overcome the limit and enhance the sensitivity. In this paper, we demonstrate the sensitivity enhancement by colocalization of near-fields and target molecules. The enhancement was strengthened through conjugation of gold nanoparticle with target molecules. Near-field hot spots were produced by sub-wavelength nanostructure that was numerically modeled and fabricated using e-beam lithography. Angled deposition of a dielectric film on the nanostructures made possible the colocalization of hot spots and target molecules. When a dielectric film was deposited on the nanostructure, a small opening was formed at the side of the nanostructure ridge. We studied the correlation between overall detection enhancement and diverse nanostructures by measuring the opening gaps with various deposition angles and evaluating the sensitivity dependent upon different opening gap area. DNA hybridization was tested for SPR detection and the results of resonance shift due to colocalization were compared to non-colocalized measurements. Preliminary results indicate that sensitivity enhancement per molecule by colocalization was at least two orders magnitude improved than that of thin-film-based conventional detection. These results may open a new approach to molecular detection based on SPR.

8234-23, Session 5

## Localized surface plasmonic resonant based on bow-tie type metallic nanostructure

T. Luo, L. Pang, W. Zhang, Guangxi Univ. (China)

optical biosensor based on localized surface plasmon resonance effect has attracted a great attention due to its advantages including small volume, high sensitivity and label-free. A comprehensive theoretical and experimental study has been performed on the refractive index sensitivity of different nanostructures such as nano-rods, nano-spheres, nano-triangles, nano-shells etc. With the ability to produce highly confined optical fields and the character of strong controllability, bowtie type nanostructure has been applied to areas such as surface enhanced spectrum, near field scanning imaging, photoluminescence and so on. In this presentation, with 3-D finite difference time domain (FDTD) method, we investigate the effect of the geometry parameters, near field distribution on sensitivity of the bowtie type nanoresonator biosensor in terms of refractive index, and overlayer thickness variations. The effect of the substrate is also investigated in terms of optical near field. Optimal designs are performed to address the co-localization of the maximal optical field and biological targets for maximal detection.

8234-24, Session 5

## Hybrid nanoparticle and thin film SPR biosensor with a high figure of merit

A. Farhang, B. Abasahl, O. J. F. Martin, Ecole Polytechnique Fédérale de Lausanne (Switzerland)

Due to their extreme sensitivity to refractive index changes, surface plasmon resonance (SPR) sensors have long been established as extremely valuable tools for biosensing. In the past few years researchers have begun investigating various other metallic nanostructures as candidates for localized SPR (LSPR) sensing. These structures, though not nearly as sensitive to bulk refractive index changes as standard SPR sensors, have the advantage in being extremely sensitive to local refractive index changes, thereby providing detection on the level of a single molecule. In practice such sensitivity criterion is of paramount importance since the analyte layer under investigation is often only a few nanometers thick and deposited directly on the surface of the metal. Most desirable, however, would be a sensor that combines the sensitivity of local refractive index changes given by an LSPR sensor with the high figure of merit (FOM) given by a traditional SPR sensor. For this reason, we are investigating hybrid structures of nanoparticle arrays coupled to a metallic film. In such structures, the excitation and use of propagating modes is generally achieved through coupling of incident light via scattering off the nanoparticles. Standard SPR sensing owes its high FOM to the excitation of propagating modes via total internal reflection (TIR). To this end, we study a metallic nanoparticle array and film system excited via TIR illumination. The resulting hybrid system exhibits both a strong localization of the electromagnetic field and a high FOM.

8234-25, Session 5

## Label-free biosensing based on multilayer plasmonic nanocomposites and a cationic polymeric transducer

D. Brouard, F. Lavoie, O. Ratelle, D. Boudreau, Univ. Laval (Canada)

This study describes the development and application of a DNA sensing architecture combining the molecular recognition capabilities of a cationic conjugated polymer (CCP) transducer with highly fluorescent core-shell nanoparticles (NPs).

This novel plasmonic- and FRET-based sensing scheme features a unique amplification mechanism based on the multilayer structure of probe-labeled core-shell NPs combined with polymer-induced aggregation, which maximize the proximity between donors and acceptors that is required for optimal RET. Plasmonic coupling with the NPs' metal core enhances the luminosity of the fluorophores and increases the range and efficiency of RET, allowing several acceptors to be excited by one polymer donor and promoting energy distribution through the aggregated system.

This plasmon-mediated amplification mechanism is exploited in a highly selective and sensitive detection of target nucleic acids. Without any labelling of amplification of the nucleic acids, a limit of detection in the femtomolar range was demonstrated when measuring 20-mer target oligonucleotides sequences specific to the C. Albicans yeast. Also, results from genotyping experimentations using genomic DNA extracted from actual human blood samples will be presented.

8234-26, Session 5

## Radiative-SPR platform for the detection of small proteins

B. Sciacca, A. Francois, P. Hoffmann, J. Brazzatti, M. Klingler-Hoffmann, T. Monro, The Univ. of Adelaide (Australia)

Surface Plasmon Resonance (SPR) based sensors enable the rapid, label-free and highly sensitive detection of a large range of biomolecules. We have previously shown that, using silver coated optical fibres with an high surface roughness, a re-scattering of the surface plasmons is possible, turning SPR into a radiative process. This approach overcomes many limitations associated with current SPR technologies such as the tight tolerance on the metallic coating thickness, and results in a more compact, versatile, robust and cost-effective approach. However, the specific detection of small molecules is a challenge in SPR systems, regardless of the SPR architecture that is used. This new sensing platform, that we proved effective for the detection of large molecules such viruses, is now demonstrated to be able to detect small proteins thanks to an improved surface functionalization, which is the key point for reliable and robust immunosensors. Avidin, a tetrameric biotin-binding protein, was used to link biotinylated antibodies to the biotinylated surface, with a given orientation, to enable efficient sensing of the analyte. This approach may offer significant advantages compared to protein A functionalization strategies such as limited cross reactivity with free IgG antibodies in clinical samples.

We demonstrate that by bringing together this novel emission-based fibre SPR platform, with the appropriate surface functionalization, is possible to detect rapidly and specifically human apolipoprotein E, a low molecular weight protein (~39kDa) known to be involved in cardiovascular diseases and in Alzheimer's disease. The results obtained clearly show that this new sensing platform has the potential to serve as a tool for point-of-decision medical diagnostics.

8234-27, Session 6

## Controlled fluorescence emission via surface modes on dielectric and metallo-dielectric multistack

E. Descrovi, M. Ballarini, F. Frascella, Politecnico di Torino (Italy); F. Michelotti, Univ. degli Studi di Roma La Sapienza (Italy); N. De Leo, E. Enrico, National Institute of Metrological Research (Italy); F. Giorgis, Politecnico di Torino (Italy)

An alternative/complementary route to Plasmon-Controlled Fluorescence [1] for improving the detection of fluorescence is proposed. In place of, or in addition to a metallic layer, a suitable multilayer [2] is used to generate a surface mode-coupled emission from a thin polymeric layer decorated with fluorescent dyes.

The multi-layered photonic crystal has been obtained by PECVD deposition of alternated layers of Low refractive index and High refractive index a-Si based materials.

The polymeric layer consists in a functional PolyAcrylic Acid (PAA) film deposited by Plasma Polymerisation process, with a thickness accurately controllable.

The fluorescent dye is conjugated to Protein A molecule and stably anchored to the -COOH groups exposed at PAA surface through a covalent bond (amidic bond).

In an additional layout, a gold thin layer is deposited on the dielectric multilayer provides the opportunity of coupling hybrid surface plasmon polaritons -BWS modes.

Fluorescent radiation coupled to surface modes is strongly polarized and directional, with an angular divergence of 0.3 degrees corresponding to a spectral bandwidth of 3 nanometres. An overall signal enhancement of more than 500 is obtained as compared to a glass substrate [4]. Calculation have been also carried out to be compared with the experimental results.

Preliminary results concerning the surface patterning by Plasma Polymerization Deposition assisted by photolithographic procedures have been also obtained.

References

[1] J.R. Lakowicz, Principles of Fluorescence Spectroscopy, 3rd ed. Springer; New York, 2006.

[2] E.Descrovi et al. Nano Lett. 10, 2087 (2010).

[3] M. Ballarini et al., Appl. Phys. Lett., accepted (2011)

8234-28, Session 6

## Green CdTe/CdS quantum dots fluorescence enhancement by core-shell silver nanoparticles

L. S. de Melo, C. R. Chaves, Univ. Federal de Pernambuco (Brazil); S. Saska, K. Nigoghossian, S. J. L. Ribeiro, Y. Messaddeq, Univ. Estadual Paulista (Brazil); A. S. L. Gomes, B. S. Santos, R. E. de Araujo, A. Fontes, Univ. Federal de Pernambuco (Brazil)

Metallic colloidal nanoparticles have been increasingly used on spectroscopic applications enhancing the radiative emission of organic fluorophores. In particular, metallic nanoparticles scatter optical light elastically with remarkable efficiency due to the collective resonance of the conduction electrons in the metal (i.e., the dipole plasmon resonance). Moreover, fluorescent nanopaticles as Quantum Dots (QDs) has emerged as powerful probes to the understanding of biological systems. However chemical changes of QDs surface such as conjugation with molecules or pH variation of biological medium can decrease or suppress their fluorescence. The aim of this research was to study the interaction of silver nanoparticles with water dispersed green fluorescent CdTe/CdS QDs. Colloids of 13nm diameter silver nanospheres and silver core-pectin shell nanoparticles were used in this work. The 11 nm thicker monolayer of pectin, a complex carbohydrate found in plants primary cell walls, isolates the silver nanosphere increasing the biocompatibility of the colloid. Fluorescence analysis of CdTe/CdS QDs-silver was performed by exciting the suspension with a 375nm light source. We observed 100% increase of CdTe/CdS emission due to the interaction of the silver-pectin nanoparticles and the QDs. The metallic nanoparticle-QDs distance is an important parameter on the fluorescence enhancement process. Therefore, the QD interaction with silver nanospheres without pectin shell was also investigated, and a very small enhancement of the semiconductor emission was detected. Silver enhancement of QDs solution-base platform fluorescence was purposed and demonstrated.

8234-29, Session 6

## Non-centrosymmetric metallic nanoparticles as new efficient nonlinear nanoemitters

S. Brasselet, Institut Fresnel (France); H. Shen, N. Nguyen, Univ. de Technologie Troyes (France); V. Maillard, D. Gachet, Institut Fresnel (France); T. Toury, Univ. de Technologie Troyes (France)

Linear optical responses from metallic nanoparticles used for biological imaging and manipulation are essentially governed by plasmons, which result in the confinement of optical fields within sub-wavelength size regions. This confinement can result in significant enhancements of their nonlinear responses, which involve higher powers of the incident optical fields. Nonlinear fields enhancements can lead to interesting applications such as efficient generation of optical harmonics in new types of nano-emitters for imaging, ultra-sensitive detection of molecules at the surface of metals, active optical fields nano-manipulation for sub-diffraction scale imaging.

In this work, we study non-centrosymmetric gold nanoparticles of about 100nm size, in order to enhance second harmonic generation (SHG) signals, which are by essence primarily efficient in structures exhibiting no center of symmetry. We show that resonant structures with a third order symmetry can lead to SHG responses of two orders of magnitude higher than in centrosymmetric nano-structures which have been more extensively studied. We have developed a polarization resolved nonlinear microscopy technique to understand the fundamental processes producing SHG signals in such nanoparticles. We evidence in particular the possibility to tune optical fields localization at the nanometer scale in such structures, using polarization control and SHG read-out. These properties make these particles interesting candidates for nonlinear nano-emitters and near field scanning nano-devices.

8234-30, Session 6

## Surface plasmon enhanced-field fluorescence biosensor for point-of-care testing using fluorescent nanoparticles

K. Horii, T. Kimura, H. Ohtsuka, N. Kasagi, T. Oohara, T. Matsuno, M. Hakamata, A. Komatsu, T. Sendai, FUJIFILM Corp. (Japan)

We have developed an optical biosensor system using surface-plasmon field-enhanced fluorescence spectroscopy (SPFS), which allows high sensitivity and fast measurement available. Intensity of fluorophores in SPFS is highly dependent upon the distance from metal surface. The resonant evanescent electric field excites fluorophores within the penetration area. On the other hand, fluorescence quenching in close proximity to a metal surface interfere with the excitation. We have developed a new technology for fluorescent nanoparticles that could receive the energy from metal surface effectively. This enables technology of detecting strong and stable SPFS signals, as well as homogeneous assay method that allows us to eliminate binding/free separation process for unreacted fluorescent particles. We also have employed a rate measurement, which resolves affect from diffusion-limited access, in order to realize a fast surface immunoreaction in a microchannel. Taking advantage of these two developments, as eliminating an enzyme response process such as CLEIA, our system reaches much faster reaction time of 2 minutes to detect thyroid stimulating hormone (TSH) of canine serum sample at 0.1ng/mL. We believe our system with these new technologies is a powerful tool for in-vitro diagnosis which meets various clinical requirements.

8234-31, Session 7

## Fluorescence enhancements and spectral modifications near the cut-off frequency of plasmonic structure

K. Elsayad, Research Institute of Molecular Pathology (Austria); A. Urich, Technische Univ. Wien (Austria); M. Nemethova, J. V. Small, Institute of Molecular Biotechnology GmbH (Austria); K. Unterrainer, Technische Univ. Wien (Austria); K. Heinze, Research Institute of Molecular Pathology (Austria) and Univ. of Würzburg (Germany)

Enhanced radiative emission of fluorophores near plasmonic structures is receiving much interest in regards to biomedical/sensing applications. In Surface Enhanced Fluorescence (SEF) sub-wavelength features of the substrate produce local field enhancements and an effective outcoupling mechanism for the Surface Plasmons. For structures with smooth metallic interfaces excitation of Surface Plasmon Polaritons (SPPs) and outcoupling of the SPPs excited by the emitters requires a sufficiently high refractive index medium (Surface Plasmon Coupled Emission). Here we show there is an additional regime for enhancing fluorescence near “smooth” structures if a supported SPP mode is localized weakly enough in the emitter medium, such that emitter-SPP coupling over a wide range of distances from the substrate becomes significant. We show that the finite energy width associated with the coupling, results in an increased excitation rate near the substrate which can over-compensate the (non-radiative) decay rate for sufficient emitter densities. Spectral modifications -which for SEF are usually proportional to the spectrum of the radiative transition rates- are governed by the total non-radiaitve decay rate. Since this is strongly dependent on the emitter-substrate separation an axial fluorophore density profile can be generated by spectral analysis. The resolution of this can be more than an order of magnitude better than the classical axial diffraction limit. We present a theoretical analysis of the effect, results of proof of principle experiments, and studies on the axial density distributions of several fluorescently labeled proteins associated with cell migration found in the adhesion sites of fibroblasts on metal/dielectric coated substrates.

8234-32, Session 7

## Superresolution axial sensitivity in plasmonic fluorescence cellular assays of protein internalisation

N. I. Cade, G. O. Fruhwirth, T. C. Ng, D. R. Richards, King's College London (United Kingdom)

We present a novel imaging technique with super-resolution axial sensitivity, exploiting the changes in fluorescence lifetime above a plasmonic substrate. In particular, we demonstrate that the changes in lifetime can be used to monitor the position of a membrane receptor during endocytosis in carcenoma cells expressing of enhanced green fluorescent protein (eGFP), providing a novel assay suitable for screening protein internalization.

Measurements have been performed using silver island films (SIF) manufactured over large continuous areas. Using fluorescence lifetime imaging (FLIM) of a calibration sample deposited on these films, we have quantified the reduction in fluorescence lifetime as a function of separation of fluorophores from the film: within 50 nm of the SIF we observe a two-fold reduction in radiative lifetime, with a commensurate enhancement in fluorescence intensity. From this it is possible to determine changes in the axial position of a fluorophore with a sensitivity of ~3nm.

We demonstrate this phenomenon using fluorescence lifetime imaging of endocytosis in carcinoma cells expressing fluorescently labeled proteins. We show that the lifetime of eGFP expressed in a cellular membrane is greatly reduced in close proximity to the SIF, resulting in a distance-dependent lifetime distribution throughout the cell, while changes in fluorescence lifetime are insensitive to changes in fluorescence intensity, either from variations in expression levels or from photobleaching. In particular, we have shown that using a plasmonic substrate, FLIM is sensitive to redistribution of proteins in a cell during endocytosis.

8234-33, Session 7

## Optical transmission study of fractal iterate nano-apertures made by direct-focused ion beam milling of metallic thin films

Y. Yuen, L. Hesselink, Stanford Univ. (United States)

We evaluate the use of fractal shaped nano-structured metallic thin films to concentrate light energy for use in single molecule fluorescence detection and surface enhanced Raman spectroscopy. Light confinement and enhancement of local fields using metallic nano-apertures allows for high concentration single molecule studies which allows for faster reaction rates and faster detection times. Traditionally, the Bethe limit constrains the maximum power throughput of small single apertures to diminish as the fourth power of the aperture dimension. In Ebbesen's work, the period arrangement of single nano-apertures and dimples can increase the power throughput. Here, we explore the use of deterministic fractal arrangements. In particular, we focus on the transmission of light through small square shaped apertures with dimension on the order of 35 to 50nm arranged in a Purina fractal topology. Preliminary FDTD studies using PEC boundary conditions reveal strong multiple resonances in the infrared and in the visible range with local enhancements of field intensities up to 1000x in hot spots in well defined and controllable locations. In the present study, we compare the real metal Drude model FDTD simulation results to the experimental white light spectra. In particular, the details of the local field enhancements and the frequency spectrum will be discussed.

8234-34, Session 7

## Multifunctional gold nanorods for detection and photothermal therapy of cancer

C. Barriere, P. B. García-Allende, J. Qi, D. S. Elson, Imperial College London (United Kingdom)

Nanoparticles are viewed as a promising tool for numerous medical applications, for instance gold nanorods have been proposed for imaging and photothermal therapy (PTT). We are developing multi functional gold nanorods (m-GNRs) which have potential for image guided endoscopic surgery and therapy/localisation of tumour tissue with a modified laparoscope system. A new synthesis method potentially allows any useful acid functionalised molecule to be bonded at the surface. We have created fluorescent m-GNRs which are targeted using folic acid to accumulate above and beyond the well-known nanoparticle retention effect in diseased tissue. The same nanoparticles can also be used for therapy as they absorb light in the infrared, which may penetrate deep into the tissue and produce localised heating.

We have performed a tissue based experiment to demonstrate the feasibility of fluorescence guided PTT using m-GNRs. Ex-vivo tests were performed using sheep heart. We were able to localise the m-GNRs with a white light DRS probe by detecting the absorption of the m-GNRs at 800 nm. This measurement, correlated with the fluorescence signal of the m-GNRs measured by the laparoscope allows the clear discrimination of the artery system containing m-GNRs. A laser diode (ThorLabs, L808P1WJ) was used to heat the m-GNRs and a thermal camera was able to record the heat distribution. These images were compared to the fluorescence images for validation.

Further study involves small animal work and these results demonstrate the potential of those multifunctional nanoconstructs for both spectroscopic and image guided detection and therapy of tumours.

8234-35, Session 7

## Plasmonic sensing in crude biofluids with microhole arrays

J. Masson, L. S. Live, J. Breault-Turcot, D. Y. Colin, J. Y. Pelletier, Univ. de Montréal (Canada); M. T. Canva, Institut d'Optique Graduate School (France); A. Dhawan, T. Vo-Dinh, Duke Univ. (United States)

Methods capable of improving the SPR response are actively researched to lower detection limits for biomolecules. We exploit the enhanced sensitivity of Au microhole arrays, which can improve the detection of biomolecules by at least a factor of 3. This improvement of the sensitivity of SPR sensors is a factor of the geometry of the microhole arrays: the periodicity, diameter of the hole and thickness of the metal layer all influence the sensitivity. In addition, the enhanced SPR sensing occurs for a small range of incident angle of the light beam and refractive index of the solution. Microhole arrays of 3.2 microns periodicity, 1.8 micron diameter and 70 nm depth are optimal to achieve maximal sensitivity for bioassays with SPR sensors. Experimental evidence and RCWA simulations supporting the influence of these parameters on SPR sensing will be presented and applied to IgG sensing. By blocking nonspecific adsorption to the SPR sensor, a peptide monolayer allows biosensing in crude biofluids. The peptide monolayer also favors immobilization of highly active antibodies, further contributing to attaining low detection limits. These advances will be demonstrated to detect the cancer biomarkers PSA and HER-2. Preliminary results will be presented on the performance of these substrates in surface enhanced Raman scattering (SERS) and surface plasmon coupled fluorescence.

8234-36, Session 8

## Fabrication method for controlling surface plasmon resonance wavelength and improving bio-conjugation yield of Au nanoring

H. Tseng, Y. Jung, Y. Kiang, C. Yang, National Taiwan Univ. (Taiwan)

Because the localized surface plasmon (LSP) resonance wavelength of an Au nanoring (NRI) can be more easily extended to the range of 1000-1300 nm in tissue, which corresponds to the deepest light penetration range into tissue, Au NRI has certain advantages in the biomedical application over Au nanorod and nanoshell. Due to its unique geometry, Au NRIs cannot be fabricated with chemical synthesis. They have to be fabricated with nano-process procedure, usually including nanosphere lithography and metal secondary sputtering. In this paper, we demonstrate a modified method of first fabricating nanopillars on a substrate. Au is then sputtered onto the sidewalls of nanopillars. After removing the nanopillars and liftoff, we can have Au NRIs in water solution. By controlling the height of nanopillar, one can determine the height of an Au NRI. Also, by controlling the deposited Au thickness, the thickness of Au NRI can be controlled. With different NRI heights and thicknesses, the LSP resonance wavelength can be adjusted. On the other hand, it is found that by adding the linker for bio-conjugation when the Au NRIs are still on the substrate, the yield of bio-conjugated Au NRIs after they are lifted off can be significantly enhanced, when compared with the methods of chemical synthesis. The fabrication procedure of Au NRIs of various LSP resonance wavelengths and their LSP behaviors will be demonstrated.

8234-38, Session 8

## Properties and commercial applications of mass-produced LSPR films

D. Gerion, LamdaGen Corp. (United States)

We present a commercial platform for both label-free and labeled bioanalyses based on Localized Surface Plasmon Resonance (LSPR). The platform utilizes mass-produced nanostructured thin films with robust and reproducible plasmon resonances. The physical properties (optical, structural, etc.) of these films, as well as their stability, noise level, and intrinsic detection limits, will be discussed. We will also illustrate the performance and reproducibility of the platform in real-life assays. For example, we will review application of the LSPR chip in therapeutic antibody purification in a bioprocessing plant where the sensitivity barrier was lowered from the ng/mL range to the fg/mL range using the very same chip under different implementations. This process and data from this application will demonstrate that the platform is rich, fast, simple and reliable as compared to existing alternative technologies such as ELISA and HPLC.

We will conclude by discussing investigations into promising new applications for these films, from SERS detection to surface enhancements in fluorescence detection.

8234-37, Poster Session

## Surface-enhanced Raman spectroscopy of pterins

C. Smyth, I. Mirza, J. G. Lunney, E. M. McCabe, Trinity College Dublin (Ireland)

Raman spectroscopy is a useful technique in the identification and characterisation of compounds, but in terms of sensitivity its application is limited. With respect to this the discovery of the surface-enhanced Raman scattering (SERS) phenomenon has proved monumental, and much research has been carried out over the past 30 years developing the technique.

Pterins are biological compounds that are found in nature in colour pigmentation and in mammalian metabolic pathways. Moreover, they have been identified in abnormal concentrations in cancer patients, suggesting potential applications in cancer diagnostics.

SERS is an ideal technique to identify these compounds, and both nanoparticle suspensions and laser-ablated nanoparticle substrates have been used to examine the spectra of xanthopterin and isoxanthopterin. Quantification of the SERS data can be problematic so methods of addressing this issue, such as the incorporation of an internal standard or the analysis of relative concentrations, have also been examined.

8234-50, Poster Session

## Integrated waveguide sensor platform utilizing organic photodiodes

B. Lamprecht, E. Kraker, P. Hartmann, G. Jakopic, M. Sagmeister, S. Köstler, JOANNEUM RESEARCH Forschungsgesellschaft mbH (Austria); T. Abel, T. Mayr, Technische Univ. Graz (Austria); H. Ditlbacher, N. Galler, Karl-Franzens-Univ. Graz (Austria)

We present a novel waveguide sensor platform, combining monolithically integrated ring-like sensor waveguides together with ring-shaped thin-film organic photodiodes on one substrate. The organic photodiodes serve as integrated light detectors, simplifying the detection system by minimizing the number of required optical components. The waveguide structures, including a means of coupling light in and out of the waveguides, serve as sensing elements. Aiming at the parallel detection of multiple parameters in a single sensor chip different sensing principles can be applied in the same basic sensor platform. Utilizing absorbance as sensing principle is demonstrated by an integrated carbon dioxide sensor. Utilizing fluorescence as sensing principle is demonstrated by an integrated oxygen sensor. The feasibility of this integrated waveguide platform is further demonstrated by employing surface plasmon resonance (SPR) as sensing principle, enabling real-time and label-free detection of a wide range of analytes. The SPR sensing principle is based on a surface plasmon mode at the surface of a 50 nm thin gold layer, deposited directly on the sensor waveguide. The guided light in the waveguide is exciting a plasmon mode in the gold layer, whereas the light-plasmon coupling strongly depends on the refractive index at the surface of the metal film which in turn is changed by the analyte. Thereby the transmission through the gold coated region of the waveguide, and consequently the signal at the organic photodiode, is dependent on the analyte-induced refractive index change at the surface of the metal film.

8234-51, Poster Session

## Nucleic acid sequencing with tip-enhanced Raman spectroscopy: toward single-base resolution

N. J. Kolodziejski, R. S. Gurjar, Radiation Monitoring Devices, Inc. (United States); J. Hwang, National Institute of Standards and Technology (United States)

We adapted commercial AFM instrumentation for Tip-Enhanced Raman Spectroscopy (TERS), to the end of developing a new DNA/RNA sequencing modality, sensitive to sequencing information and cancer-relevant lesions. Immobilization of DNA on TERS-compatible substrates, optical designs for optimal efficiency, and tip production methods will be discussed in terms of base sensitivity and sequencing capability for immobilized DNA. Sensitivity to mid-sequence lesions and base modifications such as 8-oxoguanosine and/or CpG methylation, and other cancer-relevant polynucleotide modifications will be disseminated. Current limits of detection will be discussed, as well as methods to increase sensitivity to achieve single-base resolution.

8234-52, Poster Session

## Single-cell targeting using plasmon resonant gold-coated liposomes

S. J. Leung, M. Romanowski, The Univ. of Arizona (United States)

We have developed an experimental system with the potential for the delivery and localized release of an encapsulated agent with high spatial and temporal resolution. We previously introduced liposome-supported plasmon resonant gold nanoshells (Troutman et al., Adv. Mater. 2008, 20, 2604-2608); in this composite structure, the liposome allows for the encapsulation of substances, such as therapeutic agents, neurotransmitters, or growth factors, and the plasmon resonant structure facilitates the rapid release of encapsulated contents upon laser light illumination. More recently, we demonstrated that these gold-coated liposomes are capable of releasing their contents in a spectrally-controlled manner, where plasmon resonant nanoparticles only release content upon illumination with a wavelength of light matching their plasmon resonance band (Leung et al., Adv. Funct. Mater. 2011, 21, 1113-1121). We now show that this release mechanism can be used in a biological setting to deliver a peptide derivative of cholecystokinin (CCK8) to HEK293 cells overexpressing the CCK receptor. We also demonstrate that these liposome-supported gold nanoshells can be used in conjunction with optical trapping and use computational modeling to present a general scheme for modulating the trapping laser to enable the optical trapping of and subsequent localized release from gold-coated liposomes to enable accurate perturbation of cellular functions in response to released compounds; this system may have possible applications in signaling pathways and drug discovery.

8234-53, Poster Session

## Visual detection of cancer biomarkers with naked eye using plasmonic Fano resonances

A. A. Yanik, A. E. Çetin, M. Huang, A. Artar, Boston Univ. (United States); S. H. Mousavi, A. Khanikev, The Univ. of Texas at Austin (United States); J. H. Connor, Boston Univ. (United States); G. B. Shvets, The Univ. of Texas at Austin (United States); H. Altug, Boston Univ. (United States)

We report a breakthrough development allowing visual detection of cancer biomarkers without the use of fluorescent labels or enzymatic reactions. The introduced ultrasensitive label free biodetection platform is based on asymmetric Fano resonances in optofluidic/plasmonic nanoholes with far reaching implications for point-of-care diagnostics. Our sensors bring a number of advantages: (i) ultrasensitive detection limits surpassing the gold standard surface plasmon resonance sensors, (ii) visual detection capability allowing seeing biomarker molecules with “the naked eye” without using any labeling agents or electronic instrumentation (such as spectrometer or a camera), (iii) massive multiplexing capabilities.

Normal excitation of surface plasmon polaritons (SPPs) by grating-coupling mechanisms in nanohole arrays offers massive multiplexing and lab on chip integration capabilities. However, nanohole sensors have not been widely adapted as result of lower sensitivies reported in literature during the last decade. To overcome this sensitivity limitation, we developed a radiative engineering approach utilizing subradiant dark resonance modes. We showed that strongly dispersive Fano profile combined with sub-radiant dark modes can be exploited for ultrasensitive label free biosensing. We have shown an ultrasensitive sensor platform with figure of merits (FOMs~162) surpassing that of the gold standard SPR biosensors. We get extremely sharp optical resonances as narrow as a few nanometers (~4nm) in resonance line-widths leading to nearly an order of magnitude improvement in FOMs than the previously reported nanohole biosensors as well as metamaterial structures. As a spectacular demonstration of the extraordinary sensitivity and the quality of our biosensors, we show direct detection of a single monolayer of biomolecules with naked eye.

8234-54, Poster Session

## Nano-optical conveyor belt

Y. Zheng, J. Ryan, P. Hansen, Y. Cheng, Y. Yuen, L. Hesselink, Stanford Univ. (United States)

Conventional optical tweezer (COT) has a growing role in the manipulation of bio-molecules through tethered microspheres, but the gradient force is inadequate for the manipulation of particles far below 1 micron at reasonable laser powers because of the diffraction limit. Near-field optics can overcome the diffraction limit by exploiting deeply subwavelength field distributions near structured metal-dielectric interfaces, such as nanoapertures and nanoantennas. Our theoretical study and numerical simulations show that a C-shaped nano-aperture in a metal film concentrates light to a 50nm hot spot and increases the intensity by about 200x at its resonance peak. Thus, the C-shaped apertures can enable a higher trapping efficiency of nano-scale objects than COT. We present force maps obtained through FDTD simulations and Brownian motion dynamics calculations to show that a 10kT potential well depth can be achieved for trapping 100nm polystyrene spheres under normal focused laser intensity (~10mW/um^2), which is about 10 times lower than the power requirements for COT. Moreover, the resonance wavelength of the C-aperture can be engineered by adjusting its size or orientation. These apertures have strongly localized resonances which allow their close placement in linear arrays while maintaining independent trap control. Therefore, we present a nano-optical conveyer belt (NOCB) consisting of a chain of periodically arranged C-apertures, with wavelength or polarization selective activation. Nano-particles can be transported in a peristaltic manner with a step size of about 150nm. The NOCB is integrated with a PDMS microfluidic sample delivery system and initial experimental results will be represented.

8234-56, Poster Session

## Thermal contrast measurement of gold nanoparticle biodistribution

Z. Qin, T. Akkin, Univ. of Minnesota, Twin Cities (United States); W. C. W. Chan, Univ. of Toronto (Canada); J. C. Bischof, Univ. of Minnesota, Twin Cities (United States)

With increasing interest in the use of nanomaterials for nanomedicine (e.g. photothermal cancer treatment and drug release), it is important to understand the interactions between the nanomateials with biological systems (i.e. molecules, cells and tissue). One of the basic interactions is the quantity and distribution of the nanomaterial in the biological system. Traditional methods, such as atomic emission spectroscopy (AES) and radioactive labeling, have been applied to determine this quantity. However, these methods are either expensive or requires additional labeling, both limiting large scale usage. Here we present a thermal contrast method for measuring gold nanoparticle biodistribution in cancer cells and tissue. It is based on the plasmonic heat generation of gold nanoparticles and directly related with the ability of photothermal treatment. The results are compared with the current standard (AES) and show promising correlation. It is hoped that this will enable fast and inexpensive determination of highly absorbing nanomaterials in biological systems.

8234-57, Poster Session

## Surface plasmon resonance sensing using index-matched metallic nano-hole array structures

M. Najiminaini, F. Vasefi, Simon Fraser Univ. (Canada) and Lawson Health Research Institute (Canada) and Univ. of Western Ontario (Canada); B. Kaminska, Simon Fraser Univ. (Canada); J. J. L. Carson, Lawson Health Research Institute (Canada) and Univ. of Western Ontario (Canada)

An array of sub-wavelength holes in an opaque metal film exhibits Extraordinary Optical Transmission (EOT) and is applicable to many photonic applications such as Surface Plasmon Resonance (SPR) sensing and Surface Enhanced Raman Spectroscopy (SERS). The EOT properties (e.g. resonance wavelength) of nano-hole arrays depend highly on the characteristics of the dielectrics above and below the metal film. For example, a change in the composition of the dielectric material on top of the nano-hole array can be detected as a change in one or more optical parameters thereby providing a means to detect a variety of chemical and biological agents. We present an approach to improve SPR sensing performance by incorporating SP energy matching into a nano-hole array structure.

We designed and fabricated a nano-hole array structure that provides for Surface Plasmon (SP) energy matching on the top and bottom of the perforated gold film. The SP energy matching properties originate from the presence of the same dielectric material on both sides of the nano-hole array. We performed experimental analysis on this novel nanostructure and compared its SPR sensitivity to a conventional nano-hole array. Optical transmission spectra were measured for both devices when various bulk refractive index materials were applied to the top surface. Consequently, we observed 2-fold better sensitivity during SPR sensing with the new structure compared to a conventional nano-hole array. The novel SP energy-matched nano-hole array structure could potentially improve the sensitivity of multiplexed SPR sensors for detection of bio-molecules.

8234-58, Poster Session

## A feasibility study on plasmon coupled whispering gallery mode biosensors

K. Kim, Y. Oh, W. Lee, D. Kim, Yonsei Univ. (Korea, Republic of); F. Vollmer, Max-Planck-Institut für die Physik des Lichts (Germany)

Surface plasmon resonance (SPR) and whispering gallery mode (WGM) biosensors are widely investigated to detect various biological phenomena without the need for labels. Both techniques are based on evanescent fields near surface and are sensitive to changes of refractive index or polarizability. More specifically, SPR biosensor measures the shift of resonance conditions with changing refractive index values. In contrast, a WGM biosensor measures a shift of resonance frequency induced by a polarizable particle such as a molecule or virus. In terms of implementation, SPR uses metal films on dielectric substrates; WGM on the other hand often uses spherical resonators such as microcavity and microtoroid.

In this study, we focus on improving the sensitivity of SPR and WGM biosensors towards detection of molecular interactions. We achieve such improved sensitivity by combining these two methods by way of metallic nanostructures for efficient coupling of photonic and plasmonic modes. When electromagnetic excitation fields couple to well-defined plasmonic nanostructure, the fields are redistributed and localized. Intensity of these localized fields, or hot spots, is significantly increased compared with the evanescent fields of plain WGM or SPR sensors, whereby sensitivity for molecular detection can be substantially enhanced.

In this paper, we compare the sensitivity enhancement by the coupling of photonic and plasmonic modes with different metallic nanostructures and confirm the sensitivity enhancement experimentally. To this end, we fabricated periodic gold nanostructure samples on thin gold films using electron beam lithography. For the coupling with photonic WGM modes, the distance between the plasmonic nanostructure samples and the resonating WGM microcavity was adjusted for optimum coupling and sensitivity enhancement.

8234-59, Poster Session

## SPR prism sensor using laser line generator

B. L. Chan, S. Jutamulia, Univ. of Northern California (United States)

A Kretschmann prism configuration using a laser line generator is disclosed. The laser line generator includes a laser diode and a line generator lens, which has different optical powers in x- and y-direction. A thin metal layer is directly coated on one side of the prism. The line generator determines the width of the laser line and the angle of the fan-shaped laser light. The length of the laser line on the metal layer is determined by the separation of the focus position of the laser light from the metal layer. Although a linear detector array is technically sufficient, an off-the-shelve commercially available 2D image sensor may be used. The system is designed so that the prism coated with the metal layer is disposable. Similar to other SPR sensors, for detecting analyte concentration, immobilized recognition elements or molecules are coated on the metal layer. When the immobilized elements are exposed to a liquid or gaseous sample, the analyte in the sample are captured and bound with the immobilized recognition elements. The amount of the captured analyte changes the refractive index of the dielectric medium adjacent to the metal layer. Thus, one may obtain the amount of the captured analyte or the concentration of analyte by detecting the incident angle of the incident light in the prism that is converted to surface plasmon wave. The coupling incident angle is indicated by a dark band in the intensity pattern of the internally reflected light detected by the image sensor.

8234-60, Poster Session

## Surface plasmon resonance imaging (SPRI) sensor chips based on gold and silver nano- and microstructures

A. Dhawan, Duke Univ. (United States); J. Moreau, A. Duval, M. T. Canva, Institut d'Optique Graduate School (France); T. Vo-Dinh, Duke Univ. (United States)

Conventional Surface Plasmon Resonance Imaging (SPRI) systems are based on Kretschmann configuration and employ CCD cameras and uniform gold or silver thin film layers to monitor the evolution of reflectivity on the surface of the sensor chip - as chemical or biological molecules are flowed over or adsorbed on the sensor chip surface. Numerical simulation of the generation of surface plasmons in a nano- and micro- structured gold layer have shown that the sensitivity of the whole biochip could be enhanced compared to a uniform metallic surface with the use of nano- and micro- structuration. In this presentation, we describe our experimental and theoretical studies of the effect of micro- and nano- structuration on the sensitivities of SPRI sensor chips as well as the development of novel SPRI sensor chips that are not based on Kretschmann configuration. We fabricated novel SPRI sensor chips consisting of arrays of plasmonics-active (gold and silver) nano- and micro- structures and deep-groove plasmonic nano-gratings by employing several nano- and micro- lithography techniques such as deep UV lithography and Electron beam lithography. Several nano- and micro- structures investigated include Au and Ag nanoline and nanopillar arrays as well as nanohole arrays in metallic films (Au and Ag). We are carrying out measurements of reflectivity maps, using a spectro-angular SPRI setup, on the sensor chips (containing the metallic nano- and micro- structures) and studying the dependence of plasmon resonance wavelengths and angle of incidence on the nano- and microstructure size and spacing. Moreover, we are employing Rigorous Coupled Wave Analysis (RCWA) and Finite Difference Time Domain (FDTD) calculations to obtain transmission and reflectance spectra from these films containing the metallic nano- and microstructures. Comparison between numerical simulation and experimental results is being carried out.

8234-62, Poster Session

## Three-dimensional gold nanorods-doped multicolor microstructures

C. Lien, W. Kuo, C. Lin, K. Cho, S. Chen, National Cheng Kung Univ. (Taiwan)

In this study, three-dimensional (3D) crosslinked bovine serum albumin (BSA) microstructures containing gold nanorods (AuNRs) at different absorption wavelengths were fabricated via multiphoton excited photochemistry using Rose Bengal (RB) as the photoactivator. After the processing, a higher laser power, greater than the threshold of the AuNR photothermally damage at the matched wavelength for the longitudinal plasmon resonance of AuNR, is adopted to reshape the AuNRs into gold nanospheres at a specific position of the 3D structure. As a result, 3D BSA microstructures containing different designated wavelength AuNRs can be successfully fabricated. The AuNRs-doped BSA multicolor microstructures not only can be applied in biomedical scaffolds with plasmonic properties such as two-photon luminescence imaging and photothermal therapy but also can be a specific 3D biomaterial mirodevice for plasmonic field.

8234-15, Session 9

## Plasmonic nanobubbles for cell theranostics

D. Lapotko, Rice Univ. (United States)

Theranostic applications require coupling of diagnosis and therapy, a high degree of specificity and adaptability to delivery methods compatible with clinical practice. The tunable physical and biological effects of selective targeting and activation of plasmonic nanobubbles (PNB), not nanoparticles but transient nano-event, were studied in a heterogeneous biological microenvironment of prostate cancer and stromal cells. All cells were targeted with conjugates of gold nanoparticles (NPs) through an antibody-receptor-endocytosis-nanocluster mechanism that produced NP clusters. The simultaneous pulsed optical activation of intracellular NP clusters at several wavelengths resulted in higher optical contrast and therapeutic selectivity of PNBs compared with those of gold nanoparticles alone. The developed mechanism was termed "rainbow plasmonic nanobubbles." The cellular effect of rainbow PNBs was tuned in situ in target cells, thus supporting a theranostic algorithm of prostate cancer cell detection and follow-up guided destruction without damage to collateral cells. The specificity and tunability of PNBs is promising for theranostic applications and we discuss a fiber optic platform that will capitalize on these features to bring theranostic tools to the clinic.

8234-39, Session 9

## Multimodal gold nanoshells for simultaneous imaging and therapy of cancer

A. Joshi, Baylor College of Medicine (United States); N. J. Halas, Rice Univ. (United States)

No abstract available

8234-40, Session 9

## Copper/gold and silver/gold composites as sensing surface for high-performance spectral phase surface plasmon resonance sensors

H. A. Ho, The Chinese Univ. of Hong Kong (Hong Kong, China); C. Wang, Tsinghua Univ. (China); S. Wu, The Chinese Univ. of Hong Kong (Hong Kong, China); P. Shum, Nanyang Technological Univ. (Singapore); S. Kong, The Chinese Univ. of Hong Kong (Hong Kong, China)

Until now the material of choice for surface plasmon resonance (SPR) sensors is gold because of its stability and well-established surface chemistry. In this paper, we show that copper and silver offer much better performance in the spectral SPR detection mode. A dual-layer design based on copper/gold and silver/gold configurations, in which the top gold layer continues to take benefit of established surface functionalization chemistry, while the bottom layer made from copper or silver provides high SPR shifts upon immobilization of target molecules. We have focused our efforts in the measurement of spectral SPR phase shift, i.e. measuring relative phase change between the s- and p-polarization across a range of wavelengths. Our result indicates that it is possible to achieve a refractive index sensing resolution at the level of ~10-9 refractive index unit (RIU) across a wide range of sample refractive index (1.3330-1.3505), thus demonstrating that the spectral-phase detection approach enables extremely high resolution in measuring phase change with almost no limit in the excitation wavelength.

8234-41, Session 9

## LSPR sensing with Ag nanodisk arrays fabricated using nanospherical-lens lithography

H. Chung, J. Huang, Y. Chang, National Cheng Kung Univ. (Taiwan)

Localized surface plasmon resonance (LSPR) is collective electron oscillation within a noble metal nanoparticle, whose light scattering spectrum is very sensitive to the dielectric environment and is widely used in ultrasensitive chemical and biological sensing applications. The sensitivity of LSPR is defined by a parameter, which is referred as figure-of-merit and defined as the resonance shift upon a change in the refractive index of the surrounding dielectric normalized by the resonance line width, which means narrow LSPR peak imply better sensitivity. The periodicity effect of one- or two-dimensional array was reported to be able to produce very narrow LSPR shape.

In this study, fabrication of Ag nanodisk array was demonstrated using Nanospherical-Lens Lithography (NLL). A close-packed single-layered nanosphere array was assembled on top of an unexposed photoresist. Nanospheres with diameters of between 500 and 1000 nm were used as nanoscale spherical lens to focus the incident UV light from a commercial exposure aligner. The focus UV light exposed the underneath photoresist thin film and revealed cylindrical hole arrays after developing. Ag nanodisk arrays were fabricated using Ag lift-off process. Localized Surface Plasmon Resonance (LSPR) of the nanodisk arrays were analyzed by transmission spectroscopy. The linewidth of the LSPR was found to be strongly affected by the size of the nanodisks and the periodicity of the nanodisk arrays. Optimization of the linewidth by controlling the size and periodicity can produce ultrasensitive LSPR sensors with high figure-of-merit, which should lead to more important results in plasmonic biosensing applications.

8234-43, Session 9

## Specific cell fusion using femtosecond pulses and gold nanoparticles

D. Yeheskely-Hayon, L. Minai, L. Golan, G. Bisker, D. Yelin, Technion-Israel Institute of Technology (Israel)

Cell fusion is a naturally occurring, fundamental biological process in which two or more cells merge by fusing their plasma membranes. Numerous biomedical applications require the production of fused hybrid cells with desired properties, including tumor-dendritic cell fusion for cancer therapy, myeloma-B cells hybrids for monoclonal antibody production and reprogrammed progenitors for stem cell therapy. Current fusion methods are based on compromising the plasma membrane by using chemicals such as polyethylene glycol, electric fields, viral fusogens, and focused laser beams. These methods are often inadequate due to high toxicity, low efficiency and the lack of means for specific fusion of only selected cell population.

Here we present a novel technique for selective cell fusion using femtosecond pulse irradiation and gold nanoparticles, and experimentally demonstrate fusion between cancer cells targeted by antibody-conjugated nanoparticles with high efficiency and low toxicity. The technique was studied using a variety of cell types, including skin carcinoma cells, lymphoma B cells, dendritic cells and myeloma cells, and a range of laser illumination parameters. A fusion efficiency of up to 35 % of irradiated B cells was obtained using 20 nm diameter gold particles and irradiation of sixteen 50-fs pulses at peak intensity of approximately 5x1011 W/cm2 and wavelength which was tuned to the particles' plasmonic resonance.

Owing to its high specificity, high efficiency and low toxicity, the technique would be useful for various cancer-related applications and drug development, and with its wide array of controlling parameters, may open new possibilities in biological research and technology.

8234-44, Session 9

## Infrared surface plasmon spectroscopy and biosensing

D. Davidov, V. Yashunsky, V. Lirtsman, A. Zilbershtein, T. Marciano, M. Golosovsky, B. Aroeti, The Hebrew Univ. of Jerusalem (Israel)

We report a label-free biosensing system based on the surface plasmon wave excited by the FTIR source and propagating along the 12-18 nm thick Au film in contact with analyte. This system combines spectroscopic capabilities offered by the Fourier-transform infrared source and the extreme sensitivity of the surface plasmon resonance to refractive index changes. Together with extended probing depth of the infrared surface plasmon wave (in comparison to its visible range counterpart) this allows studying living cell morphology with submicron precision. This broadband surface plasmon infrared spectroscopy is used for label-free and real-time sensing of live cells on substrate. The surface plasmon senses the real and imaginary parts of the cell refractive index and yields (i) structural information on cells and (ii) information on molecular vibrational modes associated with different cellular components. This is used to track in real time and label-free manner the structural and chemical modifications in living cells, in particular:

- cell spreading on substrate,
- cell-cell adhesion,
- opening and closure of cell junctions under Ca2+ depletion, or pathogenic bacteria,
- monitoring cholesterol concentration in cell membrane,
- cell reaction on drugs.

The SPR sensor can be used to characterize cell assays and for drug discovery.

1.V.Yashunsky, V.Lirtsman, M.Golosovsky, D.Davidov, and B.Aroeti, Biophysical J. 99, 4028 (2010).

2.M.Golosovsky, V.Lirtsman, V.Yashunsky, D.Davidov, B.Aroeti, J. Appl. Phys. 105, 102036 (2009).

8234-45, Session 9

## Dynamical sequence of Au nanopore formation for genome sequencing using high-electron beam exposure

S. S. Choi, Sun Moon Univ. (Korea, Republic of); M. J. Choi, Korea Military Academy (Korea, Republic of); T. Yamaguchi, Sun Moon Univ. (Korea, Republic of)

Recently there has been a tremendous interest about the solid state nanopore fabrication due to ultra fast genome sequencing capabilities. In this report, the Au nanopore on top of the pyramidal structure was fabricated using electron beam exposure. The dynamic sequence of Au nanopore formation from 100 nm to 1.5 nm is observed. Low energy SEM imaging at 3 keV along with the 200 keV TEM imaging is utilized to examine the nanopore structure. Depending upon the electron beam current density, the size reduction or enlargement of the nanopore was observed. This phenomenon can be attributed to high temperature rise of the Au thin film due to the electron beam exposure. In addition, the gigantic transmission spectra of 1000 fold increase at the peak for the fabricated nanopopre with its diameter ranging from 50 nm to 1.5 nm are observed using Nikon TE inverted microscope with Princeton Acton spectrophotometer. The proper plasmonic force with high transmission is great enough to control the speed of DNA translocation through the Au nanopore.

8234-46, Session 9

## Single-step injection of gold nanoparticles through phospholipid membranes

A. S. Urban, T. Pfeiffer, A. A. Lutich, J. Feldmann, Ludwig-Maximilians-Univ. München (Germany)

We propose and demonstrate a new method of an all-optical, contactless, one-step injection of single gold nanoparticles through phospholipid membranes. The method is based on the combination of strong optical forces acting on and simultaneous optical heating of a gold nanoparticle exposed to laser light tuned to the plasmon resonance of the nanoparticle. A focused laser beam captures single nanoparticles from the colloidal suspension, guides them towards a phospholipid vesicle and propels them through the gel-phase membrane, resulting in the internalization of the nanoparticle within the vesicle. Localized resonant optical heating of the gold nanoparticle causes a pore to form in the membrane, a few hundred nanometers in size, which remains open for several minutes. This approach offers great promise as a new method for drug-delivery and can be made more efficient by using gold nanoparticles with plasmon resonances tuned to the biological near-infrared window.

8234-47, Session 9

## Novel biosensor for detecting Hemoglobin and its oxygenation state based on nonreciprocity in a coupled waveguide system

S. Dutta Gupta, O. J. F. Martin, Ecole Polytechnique Fédérale de Lausanne (Switzerland); S. Dutta Gupta, Univ. of Hyderabad (India)

We exploit the nonreciprocity relations for a lossy near-symmetric coupled waveguide system to propose a novel type of biosensor which can distinguish the different oxygenation states of Hemoglobin and detect the concentration of Hemoglobin present. The sensor contains two empty identical 100 nm channels (to be filled by the bio-sample and the reference) enclosing a symmetric coupled waveguide system. The resonant tunneling geometry has the advantage that coupled guided mode resonances are supported and their location can be controlled by the spacer layer between the guides. The structure is symmetric except for the difference in the dielectric constants of the samples in the two channels. Both the amplitude and the phase (through the Goos-Hanchen shift) of the reflection coefficient are monitored from both ends of incidence through two identical high-index prisms. The spatial asymmetry with broken time reversal symmetry (due to losses) can have two-fold effect in the different responses for the amplitude and the phase for illumination from the two ends. The tiny difference in losses due to different oxygenation levels or concentration between the sample and the reference is shown to lead to different reflectivities, or even in the Goss-Hanchen shift, for illumination from opposite ends.

8234-48, Session 9

## Microwave hyperthermia of tumor in combination with gold nanorods

M. V. Shirmanova, N.I. Lobachevsky State Univ. of Nizhni Novgorod (Russian Federation); M. A. Sirotkina, V. Elagin, Nizhny Novgorod State Medical Academy (Russian Federation); A. Strikovsky, D. Yanin, Institute of Applied Physics (Russian Federation); A. Kordyukova, N.I. Lobachevsky State Univ. of Nizhni Novgorod (Russian Federation); V. Nadtochenko, N.N. Semenov Institute of Chemical Physics (Russian Federation); E. Zagaynova, Nizhny Novgorod State Medical Academy (Russian Federation)

Nanoparticles are supposed to enhance an efficacy of tumor treatment. But one of the problems is in vivo detection of nanoparticles accumulation in a tumor node.

The aim of the research was to design a method of a local microwave hyperthermia of a tumor with plasmon-resonant gold nanorods under noninvasive examination of the time of nanoparticles accumulation in the tumor.

The research was performed on CBA mice bearing with a cervical carcinoma transplanted subcutaneously. The gold nanorods with size 70/30 nm had a plasmon resonance peak at 750 nm. The nanoparticles surfaces were coated with polyethylene glycol with 6000 D molecular weight.

The animals were divided into three groups of five mice: one untreated group and two treated by microwave energy. One of the treated groups was in combination with gold nanorods. The nanorods were injected intravenously.

Verification of tumor cells death after hyperthermia was carried out by morphological analysis in different time points.

Control of the nanoparticles accumulation in the tumor was carried out in vivo by means of a near-field microwave probing technique.

Two regimes of the microwave radiation were applied: 50 J and 150 J. The anti-tumor impact of the microwave hyperthermia is confirmed by an inhibition of a tumor growth.

The time of nanorods accumulation in the tumor was found to be maximal in 4-6 hours after intravenous injection. Heating of the tumor with nanoparticles occurred locally. The significant damage of the tumor with nanorods was obtained after microwave hyperthermia. Tumor growth inhibition coefficient was 64.7%.

8234-49, Session 9

## Gold nanorods-doped membranes for laser-activated drug delivery

P. Matteini, F. Ratto, F. Rossi, L. Luconi, G. Giambastiani, Istituto di Fisica Applicata Nello Carrara (Italy); L. Dei, G. Caminati, Univ. degli Studi di Firenze (Italy); R. Pini, Istituto di Fisica Applicata Nello Carrara (Italy)

Gold nanorods are cylindrical gold nanoparticles with effective absorption bands in the near infrared region (NIR) of principal interest in biomedical optics. The excitation of these particles with a laser source matching their NIR band can be conveniently employed for selective conversion of light into heat in a number of minimally invasive laser therapies such as laser tissue bonding and hyperthermia of tumors. Here we are proposing the development of hybrid membranes composed of a biopolymeric matrix of high porosity and gold nanorods for the laser-activated delivery of small molecules and drugs. These membranes are resistant and stable in physiological conditions over time, while the biopolymer matrix provides excellent control over the distribution and stability against aggregation of the nanoparticles, which translates into a dependable optical response and photothermal conversion. A locally produced temperature enhancement beyond the physiological value triggers the release of the molecules entrapped in the porous matrix, which is proportional to the duration of the laser treatment. Thanks to the possibility to remotely and reversibly trigger the process with a highly penetrating NIR light, this technology may be exploited for the in-vivo on-demand delivery of drugs in a number of applications including selective chemotherapy for advanced tumor treatment.